

IN SEARCH OF THE
PHYSICAL BASIS OF COET

PLenum

IN SEARCH OF THE PHYSICAL BASIS OF LIFE

IN SEARCH OF THE PHYSICAL BASIS OF LIFE

GILBERT N. LING

*Pennsylvania Hospital
Philadelphia, Pennsylvania*

PLENUM PRESS · NEW YORK AND LONDON

Library of Congress Cataloging in Publication Data

Ling, Gilbert, 1919-

In search of the physical basis of life.

Bibliography: p.

Includes index.

1. Cell physiology. 2. Life (Biology) I. Title. [DNLM: 1. Biochemistry. 2. Physics. 3. Cells—Physiology. QH 631 L755i]

QH631.L56 1984

574.87

83-26919

ISBN 0-306-41409-0

©1984 Plenum Press, New York
A Division of Plenum Publishing Corporation
233 Spring Street, New York, N.Y. 10013

All rights reserved

No part of this book may be reproduced, stored in a retrieval system, or transmitted,
in any form or by any means, electronic, mechanical, photocopying, microfilming,
recording, or otherwise, without written permission from the Publisher

Printed in the United States of America

Dedicated to
“Gee” and Frank Elliott

Acknowledgments

It is with much appreciation that I thank two government research-funding agencies whose support has made my scientific efforts of the last twenty years possible.

The Office of Naval Research supported my work between 1953 and 1957 through a contract award to Prof. R. W. Gerard (ONR 110-128). Later, after I settled down at the Pennsylvania Hospital, ONR continued its funding and it has, without a single interruption, supported my work for the last 18 years under Contract N0014-71C-0178. In particular I take pleasure in thanking Dr. Arthur B. Callahan, who had both the scientific insight and the courage to support my work through the years when many considered it highly controversial.

The National Institutes of Health, primarily through the Institute of General Medical Science and later also the National Cancer Institute, have provided vitally needed funds for the continued efforts of my laboratory. I feel particularly indebted to dedicated scientist-administrators like Dr. Ruth Kirschstein and Dr. Stephen Schiaffino for their continued efforts to make possible the support of scientists like myself who have long been disputing the validity of the view of cell physiology held by most of our peers.

I thank the John A. Hartford Foundation for supporting my work between 1961 and 1977, first through a research grant awarded to my friend, Dr. Frank Elliott, and then through another one awarded directly to me.

Pennsylvania Hospital (the nation's first, founded by Thomas Bond and Benjamin Franklin in 1755) has been the home of my laboratory for the last twenty years. I owe a debt of gratitude to its President, Mr. H. Robert Cathcart, to its Vice Presidents, Harry Heston and Gary Aden, and to many other helpful and sympathetic friends.

It gives me great pleasure that the support of the ONR, the NIH, the Hartford Foundation, Pennsylvania Hospital, and my friends has already borne practical fruits,* directly benefiting mankind.

*NMR scanning, which allows continued quantitative investigations and monitoring of normal and diseased human body parts without surgery or X-ray irradiation, was invented by Dr. Raymond Damadian, the patent holder, who wrote me on November 9, 1977:

On the morning of July 3, 1977, at 4:45 A.M. . . . we achieved with great jubilation the world's first NMR image of the live human body.

The achievement originated in the modern concepts of salt water biophysics [introduced by] your treatise, the association-induction hypothesis.

For the gifts of their photographs, I am indebted to Professors M. Barbacid; M. C. Chiang; K. S. Cole; R. Damadian; S. Ebashi; L. Edelmann; (the late) E. Ernst; J. B. Gurdon; Sir A. L. Hodgkin, Nobel laureate; Sir A. Huxley, Nobel laureate; H. Huxley; T. Kanazawa; F. Lipmann, Nobel laurete; P. Mitchell, Nobel laureate; E. Racker; J. C. Skou; (the late) B. Steinbach; A. Szent-Gyorgyi, Nobel laureate; T. C. Tai; I. Tasaki; A. S. Troshin; H. H. Ussing; J. D. Watson, Nobel laureate; and R. W. Weinberg.

I thank Prof. E. Michaud, Conservateur du Musée Pasteur, Institut Pasteur, Paris, for the photograph of Prof. J. Monod, Nobel laureate; Prof. A. S. Troshin, for the photograph of D. N. Nasonov; Prof. H. L. Booij, Rijksuniversiteit te Leiden, Leiden, for the photograph of H. G. Bungenberg de Jong; Dr. L. Barth, for her photograph and that of her late husband, Dr. L. C. Barth; Prof. K. Sollner, NIH, Bethesda, for the photographs of J. Bernstein and L. Michaelis; Prof. R. P. Kernan for the photograph of E. J. Conway; and Mrs. F. Gerard and Charlotte (Bell) Taylor (his former secretary) for the photograph of R. W. Gerard.

I thank Magnus Verlag GmbH, Kempten/Allgäu, West Germany, for permission to reproduce the portraits of the Abbé Nollet, E. DuBois-Reymond, T. Schwann, and H. Spemann published in the *Handbuch der Biologie*; The American Physiological Society, Bethesda, for permission to reproduce the portraits of L. Caldani and L. Galvani published in the *Handbook of Physiology*, and that of A. V. Hill published in *History of the International Congress of Physiological Sciences 1889–1968*; the American Association for the Advancement of Science, Washington, D.C., for permission to reproduce the portrait of R. A. Gortner published in *The December Scientific Monthly*, 1942; British Information Services, London, for permission to publish the portrait of A. Huxley; Springer-Verlag, Heidelberg, for permission to reproduce the portraits of H. von Helmholtz and Carl Ludwig published in the *Lehrbuch der Physiologie in Einzeldarstellungen* and in *Geschichte der Physiologie*, 1953; Georg Thieme Verlag, Stuttgart, for permission to reproduce the portrait of L. Oken published in *Deutschen Medizinischen Wochenschrift*; Dr. Dietrich Steinkopff Verlag, Darmstadt, for permission to reproduce the portrait of M. H. Fischer published in *Kolloid-Zeitschrift und Zeitschrift für Polymere*, 1962; Masson S.A., Paris, for permission to reproduce the portrait of F. Dujardin published in *Archives de Parasitologie*, 1901; Wissenschaftliche Verlagsgesellschaft mbH, Stuttgart, for permission to reproduce the portrait of O. Warburg; the National Cancer Institute, Bethesda, for permission to reproduce the portrait of J. Greenstein published in *Contrary to Nature*. For the portraits of T. Graham, M. Traube, W. Pfeffer, W. Ostwald, and J. H. van't Hoff I am indebted to Longmans, Green and Company, London.

At a personal level, I must begin by acknowledging the influence of my professor at the National Central University, Chungking, the late Prof. C. Oh Yang, and of Prof. P. S. Tang of the National South West University, Kuming, whose unwavering encouragement and support prepared me for my future in biological research.

It was the late Prof. Ralph W. Gerard of the University of Chicago who set the direction for the cell physiology research described in this volume. To him I give my most sincere thanks. To my great sadness, he is no longer with us to write a Preface for my second book, as he did for my first.

Dr. Frank Elliott, who brought me to Pennsylvania Hospital, has been a real friend in many ways; without his generous support my life in the last twenty years would have been a great deal less easy and productive.

Two young scientists who have, each in his own unique way, contributed greatly to this volume are Drs. William Negendank and Ludwig Edelmann. Those who read through this book will readily understand the crucially important contributions they have been steadily making. To Bill I owe special thanks for the enormous amount of time and energy that he has spent in improving the manuscript, suggesting better ways of presentation and writing up a number of the summary statements at the ends of the chapters. I also thank Ludwig for helping me in the by no means easy task of finding many of the portraits of scientists displayed throughout the volume.

Other scientists whose unwavering friendship and support and endless discussions I dearly treasure include Drs. George Karreman, Carleton Hazlewood, Raymond Damadian, and the late Freeman Cope, who—feeling despondent over the loss of his research support—committed suicide on October 10, 1982.

It is difficult to thank adequately my assistant and colleague, Miss Margaret Ochsenfeld, who as my coauthor has been turning out some of the most meticulous and accurate studies that have come out of this laboratory for more than twenty years. In addition she has been performing many of the administrative duties in running the laboratory. Randy Murphy, John Greenplate, and Zhenglian Zhang from the Peking Institute of Biophysics are all highly capable young scientists whose dedication, skill, and high productivity have made it hard to resist the temptation to add more and more of the latest findings to this volume.

Among the long list of other able assistants and colleagues who have unwaveringly placed the search for truth above personal comforts and advantage and to whom I owe thanks are Dr. Ignacius Reisin, Dr. Victor Smolen, Andy Fischer, Grace Bohr, Cheryl Walton, Marianne Tucker, Diane Graham, Dee Zodda, and the late Sandy Wills.

This book would not have become a reality without the efforts of my secretary, Jean Brogan, and her able helpers, Theresa Bonner and Eileen Bryson, whose skill and dedication have pulled together what was at one time a hopeless mass of tangled yellow pads and incomplete reference lists.

At Plenum Press, I thank Mr. Kirk Jensen, whose broad knowledge about and enthusiasm for our work got the publication of this volume off to an early start, and Mr. Peter Strupp, whose perceptive and constructive suggestions and meticulous efforts have done much to improve the book.

Finally I must say a word of loving thanks to my wonderful and talented concert pianist wife Shirley, whose love, energy, and talents have permitted me to devote the needed extra attention and time to the writing of this book and made possible a struggling but charmed life, which we share with our three wonderful children, Mark, Timothy, and Eva.

G.N.L.

Contents

Introduction	xxv
--------------------	-----

I. Opposing Concepts in Cell Physiology: History and Background

1. The Early History of Cell Physiology	3
1.1. The Evolution of Physiology as the Physics and Chemistry of Living Phenomena	3
1.2. The Cell Theory	5
1.3. The Discovery of Protoplasm	7
1.4. Colloidal Chemistry and the Concept of Bound Water	8
1.5. Traube's Semipermeable Copper Ferrocyanide Gel Membrane and the Introduction of the van't Hoff Equation	9
1.6. Pfeffer's Membrane Theory	12
1.7. Summary	13
2. Evolution of the Membrane and Bulk Phase Theories	15
2.1. Concepts of the Nature of the Plasma Membrane	15
2.1.1. The Lipoidal Theory of Overton	15
2.1.2. Mosaic Membranes with Pores	16
2.1.3. Membranes with Charged Pores and Selective Ionic Permeability	17
2.1.4. The Paucimolecular Membrane of Davson and Danielli	18
2.2. Cellular Electrical Potentials and Swelling in the Context of the Membrane Theory	18
2.2.1. Early History of Cellular Electrical Potentials	18

2.2.2. Bernstein's Membrane Theory and the Diffusion Potential	21
2.2.3. The Cremer–Haber–Klemensiewicz Theory for Glass Electrodes	22
2.2.4. Phase Boundary Potentials and the Baur–Beutner Controversy	24
2.2.5. Michaelis's Theory of the Cation-Permeable Collodion Membrane	25
2.2.6. The Donnan Theory of Membrane Equilibrium	28
2.3. Cellular Ionic Distribution in the Context of the Membrane Theory	32
2.3.1. Boyle and Conway's Theory of Membrane Potentials, Ionic Distribution, and Swelling	33
2.4. Early Criticisms of and Experimental Evidence against the Membrane Theory	35
2.5. Inquiries into the Nature of Protoplasm	36
2.5.1. Protoplasm as a Structural Substance	36
2.5.2. Fischer's Theory of Protoplasm	38
2.5.3. Lepeschkin's Vitaid Theory	39
2.5.4. Nasonov's Phase Theory of Permeability and Bioelectric Potentials	40
2.5.5. Bungenberg de Jong's Concept of Protoplasm as a Coacervate	41
2.6. Early Inquiries into the Physical State of Water and Ions in Living Cells	43
2.6.1. Bound Water	43
2.6.2. Bound K ⁺	46
2.7. Rejection of the Bulk Phase Theories	47
2.7.1. Evidence against the Bulk Phase Theories	47
2.7.2. Evidence against the Concepts of Bound K ⁺ and Bound Water	48
2.8. Summary	51
 3. The Emergence of the Steady-State Membrane Pump Concept	53
3.1. Major Developments Providing the Background for the Acceptance of the Membrane Pump Theory	53
3.1.1. The Disproof of the Original Equilibrium Membrane Theory	53
3.1.2. The Concept That the Constituents of Living Beings Are in a State of Dynamic Equilibrium	57
3.1.3. The Hill–Embden Controversy and “A-lactic Acid” Muscle Contraction	57
3.1.4. The High-Energy Phosphate Bond as the Immediate Source of Energy for Biological Work Performance, Including Ionic Pumping	58
3.2. The Postulation of the Na ⁺ Pump	60
3.3. Arguments and Evidence in Support of the Na ⁺ Pump Theory	61
3.3.1. The Dependence of Ionic Distribution on Continued Metabolic Activities and Normal Temperature	61

3.3.2. The Energy Requirement of the Na^+ Pump Appears to Be Adequately Met by Cell Metabolism	61
3.3.3. Active Solute Transport by Epithelial Tissues and Giant Algal Cells	64
3.4. The Further Development of the Membrane Theory of Cellular Electrical Potential in the Context of the Membrane Pump Theory: The Ionic Theory of Hodgkin, Katz, and Huxley	64
3.4.1. The Hodgkin-Katz-Goldman Equation	65
3.4.2. The Hodgkin-Huxley Theory of the Action Potential	74
3.4.3. The Hodgkin-Huxley Theory of Permeability Changes during the Action Potential	77
3.4.4. Experimental Confirmation of the Membrane Theory of the Resting and Action Potentials	78
3.5. Summary	79
4. The Reemergence of the Bulk Phase Theories	81
4.1. Kamnev's Study of Sugar Distribution in Frog Muscle	81
4.2. Troshin's Sorption Theory	82
4.2.1. Osmotic Behavior of Living Cells	83
4.2.2. Cells as Colloidal Coacervates	84
4.2.3. Solute Exclusion and Accumulation	84
4.3. Rekindled Doubts about the Revised Membrane Pump Theory	88
4.3.1. Discovery of the Non-Donnan Distribution of Many Permeant Substances	88
4.3.2. Reinvestigation of the Question of Whether or Not Cells Have Enough Energy to Operate the Postulated Na^+ Pump	89
4.4. Ling's Fixed-Charge Hypothesis	91
4.4.1. A New Molecular Mechanism for the Selective Accumulation of K^+ over Na^+ in Living Cells	93
4.4.2. Some Distinctive Features of Ling's Fixed-Charge Hypothesis	95
4.5. Molecular Mechanisms of Selective Ionic Permeability	97
4.5.1. The Membrane Carrier Model	98
4.5.2. Ling's Fixed-Charge Hypothesis	99
4.6. The Surface Adsorption Theory of the Cellular Resting Potential	104
4.6.1. Three Historical Models: Glass, Oil, and Collodion	104
4.6.2. The Surface Adsorption Theory of Cellular Electrical Potentials	109
4.7. Summary	110
5. Experimental Tests of the Alternative Theories	113
5.1. Evidence Supporting the Membrane Pump Theory	113
5.1.1. Full Ionic Dissociation of K^+ Salts in Water at Ionic Strengths Similar to Those in Living Cells	113

5.1.2. High Mobility of K^+ in Living Cells	113
5.1.3. High K^+ Activity in Living Cells	115
5.1.4. Genetic Control of Permeases or Sugar Pumps	115
5.1.5. Na^+,K^+ -Activated ATPase as the Na^+ Pump	118
5.1.6. “High Energy” Contained in the Phosphate Bonds of ATP Provides the Immediate Source of Energy for Na^+ Pumping	119
5.2. Evidence against the Pump Hypothesis	122
5.2.1. There Is Not Enough Energy to Operate the Na^+ Pump	122
5.2.2. Reassessment of the High Energy of the “High-Energy Phosphate Bond”	126
5.2.3. Failure to Demonstrate Selective K^+ Accumulation and Na^+ Exclusion by a Cytoplasm-Free Squid Axon Membrane Sac	127
5.2.4. Failure to Prove Selective Ion Pumping in Membrane Vesicles	128
5.2.5. Studies of the Red Cell Ghost	128
5.2.6. Ouabain-Sensitive Selective Accumulation of K^+ over Na^+ in an Effectively Membrane (Pump)-less Open-Ended Muscle Cell (EMOC) Preparation	133
5.3. Summary	140

II. The Association-Induction Hypothesis

6. The Association-Induction Hypothesis I. Association of Ions and Water with Macromolecules	145
6.1. The Living State	145
6.1.1. The General Concept of a High-Energy Resting State	145
6.1.2. The Major Components of Living Systems	147
6.1.3. Protoplasm and the Living State	147
6.2. Association of Ions	148
6.2.1. Enhanced Counterion Association in a Fixed-Charge System	148
6.2.2. The Theory of Selective Ionic Adsorption and Its Variation with the Electron Density or c -Value of the Fixed Anionic Sites	154
6.2.3. Reversal of Ionic Selectivity Ratios: Comparison of Theory with Experiment in Ion Exchange Resins	159
6.2.4. Generalized Relations between c -Value and Adsorption Constants	162
6.2.5. Salt Linkages, c -Value, and the <i>in Vitro</i> Demonstration of Selective Na^+ and K^+ Adsorption on Isolated Proteins	163
6.3. Association of Water	163
6.3.1. Historical Background	163
6.3.2. The Polarized Multilayer Theory of Cell Water	167

6.3.3. Theory of Solute Exclusion from Water Existing in the State of Polarized Multilayers	170
6.3.4. <i>In Vitro</i> Experimental Testing of the Polarized Multilayer Theory of Cell Water in Model Systems	172
6.4. Summary	180
7. The Association–Induction Hypothesis II. The Inductive Effect and the Control of Physiological Activities	183
7.1. The Inductive Effect	183
7.1.1. Early Theories of the Molecular Inductive Effect	183
7.1.2. Chiang and Tai's Theory: A Quantitative Relation between Molecular Structure and Chemical Reactivity	185
7.1.3. Functional Groups Affected by the Inductive Effect	190
7.2. The Direct F-Effect and the Molecular Mechanisms of Physiological Control	198
7.2.1. Association of Protons and Adsorption of Cations	199
7.2.2. Changes in H-Bonding	199
7.3. Modulation and Control of Physiological Activities	200
7.3.1. The One-Receptor-Site System as a Model for Competitive Interaction	201
7.3.2. The Two-Receptor-Site System as a Model for Noncompetitive Facilitation and Inhibition	203
7.4. Cooperativity: Molecular Basis for Controlled and Coordinated Physiological Activities	204
7.4.1. The Indirect F-Effect: The Propagated Inductive Effect	206
7.4.2. The Yang–Ling Cooperative Adsorption Isotherm	208
7.4.3. The Control of Shifts between Discrete Cooperative States by the Adsorption and Desorption of Cardinal Adsorbents	219
7.4.4. An Analysis of the Theoretical Model of Controlled Cooperative Interaction	222
7.5. Summary	224
8. The Physical State of K⁺ and Na⁺ in Living Cells	227
8.1. A Reassessment of the Critical Experiments of Hill and Kupalov	227
8.2. Experimental Proof That the Bulk of Muscle K ⁺ Is in an Adsorbed State	228
8.2.1. Early Work on Localization of K ⁺	228
8.2.2. Electron Microscopic Demonstration of Localization of K ⁺	230
8.2.3. Autoradiographic Demonstration of Localization of K ⁺	231
8.2.4. Energy-Dispersive X-Ray Microanalysis	235
8.2.5. Laser Microprobe Mass Spectrometric Analysis	237
8.2.6. Implications of the Adsorbed State of K ⁺ in Muscle Cells	238
8.3. X-Ray Absorption Edge Fine Structure of K ⁺ in Frog Erythrocytes	241

8.4. Secondary Evidence for K ⁺ Adsorption in Living Cells	242
8.4.1. K ⁺ Mobility in Living Cells	242
8.4.2. K ⁺ Activity in Living Cells Measured with an Ion-Specific Microelectrode	250
8.4.3. NMR Relaxation Times of ²³ Na ⁺ and ³⁹ K ⁺ in Living Cells	257
8.5. Summary	268
9. The Physical State of Water in Living Cells	271
9.1. Introduction	271
9.2. Solvent Properties	272
9.2.1. Inanimate Models	272
9.2.2. Biopolymers and Viruses	275
9.2.3. Living Cells	277
9.3. Freezing Points	278
9.3.1. Theoretical Expectations	278
9.3.2. Behavior of Models	279
9.3.3. Freezing Pattern of Living Cells	282
9.4. Vapor Sorption Isotherms	283
9.5. Infrared and Raman Spectra	289
9.6. Dielectric Dispersion	291
9.6.1. Model Systems	294
9.6.2. Living Cells	295
9.7. NMR Relaxation Times of Water Protons and Other Nuclei	298
9.7.1. NMR Theories	299
9.7.2. NMR Studies of Water in Solutions of Native Globular Proteins	301
9.7.3. NMR Studies of Water in Living Cells	301
9.7.4. Concluding Remarks on the Current Status of NMR Studies	307
9.8. Quasielastic Neutron Scattering	308
9.9. Summary	309
10. ATP and the Source of Energy for Biological Work Performance	311
10.1. The General Question of the Energization of Biological Work	311
10.2. The Heat Engine Theory	311
10.3. The High-Energy Phosphate Bond Concept	311
10.4. The Energy Source for Biological Work Performance According to the AI Hypothesis	314
10.4.1. The Immediate Source of Energy for Biological Work Performance	314
10.4.2. The Source of Energy for Cyclic Work Performance	315
10.5. Summary	315

III. Applications of the Association-Induction Hypothesis to Traditional Problems in Cell Physiology

11. Selective Distribution of Ions, Sugars, and Free Amino Acids	319
11.1. The General Theory of Solute Distribution	319
11.1.1. Equation Describing Solute Distribution	321
11.1.2. Control of Solute Distribution by Cardinal Adsorbents	323
11.1.3. The Effect of Temperature on Solute Distribution	326
11.2. Experimental Testing of the Theory	326
11.2.1. Basic Patterns of Solute Distribution: Free and Adsorbed Fractions	327
11.2.2. Cooperativity in Solute Adsorption	345
11.2.3. Effect of Temperature on Solute Distribution	353
11.2.4. Control of Solute Distribution by Cardinal Adsorbents	358
11.3. Summary	375
12. Permeability	377
12.1. Evidence against the Conventional Lipoidal Membrane Theory	379
12.1.1. K^+ -Specific Ionophores Do Not Increase the Permeability of Living Cell Membranes to K^+	379
12.1.2. There Is Not Enough Lipid in Many Membranes to Provide a Continuous Bilayer	380
12.1.3. Removal of Membrane Lipids from the Liver Mitochondrion Inner Membrane Does Not Alter the Trilayer Structure	382
12.2. What Is the Rate-Limiting Step for the Entry of Water into Living Cells?	386
12.3. Polarized Water as the Semipermeable, Selective Permeability Barrier	391
12.4. Permeability of Cells to Ions	396
12.4.1. Influx of Ions	397
12.4.2. Efflux of Ions	404
12.5. Sugar Permeation and Its Control by Insulin	426
12.6. Amino Acid Permeation and Its Dependence on External Na^+	428
12.6.1. The Saturable and Nonsaturable Fractions in the Uptake and Exodus of Amino Acids	428
12.6.2. Permeation of Glycine and Other Neutral Amino Acids into Ehrlich Ascites Cells	429
12.6.3. The Saturable Fraction	430
12.7. Surface Protein Adsorption Sites as the Seat of the Selective Adsorption-Desorption Route for Entry of Amino Acids	434
12.8. Summary	435

13. Swelling, Shrinkage, and Volume Control of Living Cells	437
13.1. The Refutation of the Membrane Theory of Cell Volume Regulation	437
13.2. Polarized Water in Lieu of Free Intracellular K ⁺ in the Maintenance of Osmotic Pressure of Living Cells	438
13.3. What Does the Vapor Sorption Isotherm Tell Us about the Osmotic Behavior of Living Cells?	442
13.4. Swelling of Living Cells in Isotonic KCl and Other Salt Solutions ..	443
13.5. The Variable Number of K ⁺ , Rb ⁺ , and Cs ⁺ Adsorption Sites: The Role of Salt Linkages	454
13.6. The Mechanism of Cell Swelling Caused by the Depletion of ATP and the Role of NaCl in the Medium	455
13.7. Classification of Cell and Tissue Swelling	460
13.8. Summary	461
14. Electrical Potentials	463
14.1. Evidence against the Membrane Theory of Cellular Electrical Potentials	463
14.1.1. The Indifference of Resting Potential in Frog Muscle to External Cl ⁻ Concentration	463
14.1.2. Do the Resting and Action Potentials Depend on the Intracellular Concentrations of K ⁺ and Na ⁺ ?	465
14.1.3. The Electrogenic Na ⁺ Pump Hypothesis	467
14.1.4. All-or-None Opening and Closing of Na ⁺ and K ⁺ Gates ..	468
14.1.5. The Independence Principle	469
14.1.6. The Significance of the Demonstration of the Localization of the Bulk of Intracellular K ⁺ in Frog Muscle	469
14.2. Evidence for the Surface Adsorption Theory of Cellular Resting Potentials	470
14.2.1. Collodion-Coated Glass Electrode	470
14.2.2. Colacicco's Experiment on Oil Membranes	472
14.2.3. Edelmann's Experiment on Guinea Pig Heart Trabecular Muscle	473
14.3. Experimental Observations Not Explicable by the Membrane Theory but in Harmony with the Surface Adsorption Theory	475
14.3.1. The Adsorbed State of Cell K ⁺	475
14.3.2. The Lack of a Relation between External Cl ⁻ and ψ	475
14.3.3. The Contradictory Reports on the Relation between ψ and Intracellular K ⁺	475
14.4. The Molecular Mechanism of the Resting and Action Potentials ..	477
14.4.1. The New Equation for the Cellular Resting Potential	477
14.4.2. The Control of the Resting Potential by Cardinal Adsorbents According to the AI Hypothesis	481
14.4.3. Changes of the Resting Potential of Toad Oocytes during the Maturation Process	484

14.4.4. Effect of Mechanical Puncturing of the Cell Surface on Oocyte Activation	488
14.5. Molecular Events Underlying Excitation	489
14.5.1. Basic Molecular Structure and Properties of the Cell Surface of Muscle and Nerve According to the AI Hypothesis	491
14.5.2. The Molecular Basis of the Sudden, Transient Permeability Increase during Excitation	493
14.6. Summary	499
 IV. A Reevaluation of Current Concepts in Physiology and Biochemistry	
15. Oxidative Phosphorylation, ATP Synthesis, and Other Aspects of Mitochondrial Physiology	503
15.1. The Central Role of ATP in Biological Work Performance	503
15.2. The Sources of ATP	503
15.2.1. Creatine Phosphate and Arginine Phosphate	503
15.2.2. Glycolysis or Fermentation	504
15.2.3. Respiratory Chain	504
15.3. Theories of the Mechanism of Oxidative Phosphorylation and Their Critiques	507
15.3.1. The Chemical Coupling Hypothesis	507
15.3.2. The Conformation Coupling Hypothesis	509
15.3.3. The Chemiosmotic Hypothesis	509
15.4. A Tentative Model of the Inductive-Associative Coupling Mechanism for Electron Transport and Oxidative Phosphorylation	517
15.4.1. The Coupling Mechanism	517
15.4.2. Comparison with Model Systems	519
15.5. New Interpretations of Observations in Mitochondrial Physiology	521
15.5.1. Swelling and Shrinkage	521
15.5.2. "Transport" of ATP	524
15.5.3. Uncouplers, Ionophores, Ca^{2+} , Mg^{2+} , ATP, and Other Cardinal Adsorbents	525
15.5.4. Synchronous Oscillatory Changes in Properties of Mitochondria	534
15.6. Summary	537
16. Muscle Contraction and Related Phenomena	539
16.1. Early Theories of Muscle Contraction	539
16.1.1. Engelmann's Heat Engine Theory	540
16.1.2. The Osmotic Theories of McDougall and MacDonald	541
16.1.3. The Lactic Acid Theory	541
16.1.4. The Engelhardt-Ljubimova Theory	542

16.1.5. The Actin–Myosin Association Theory of Szent-Györgyi	543
16.1.6. The Active Relaxation Theory	545
16.1.7. The Electrostatic Extension–Entropic Contraction Theory	545
16.1.8. The Earlier Association–Induction Model	546
16.2. Current Views of the Mechanism of Muscle Contraction	549
16.2.1. The Sliding Filament Theories	549
16.2.2. The Kinetics of the Unregulated Actin–Myosin–ATP System	557
16.2.3. The Control Mechanism	558
16.2.4. Other Recent Theories of Muscle Contraction	563
16.3. Critique of the Sliding Filament Model	564
16.3.1. The Energy Problem	564
16.3.2. The Number, Duration, and Synchronization of Cycles of Cross-Bridge Formation and Breakage	565
16.3.3. What Keeps the Filaments from Tangling Up?	565
16.3.4. Why Should the Bulk of Water in the I Bands Move with the Telescoping Thin Filaments?	566
16.4. A Tentative Model of Muscle (and Nonmuscle Cell) Contraction: An Updated Theory According to the AI Hypothesis	566
16.4.1. The Resting, Relaxed Muscle	568
16.4.2. Contraction	570
16.4.3. Relaxation	571
16.5. Agreements and Disagreements with Relevant Existing Knowledge	571
16.5.1. Electron Microscopic and X-Ray Diffraction Evidence of the Continuing Existence of Thin Filaments	571
16.5.2. A Key Role of Cell Water in Muscle Contraction	572
16.5.3. A Mechanism That Prevents the Filaments from Tangling Up	572
16.5.4. A Key Role of K ⁺ Adsorption and Desorption in Muscle Contraction	574
16.5.5. The Source of Energy and Force in Muscle Contraction	578
16.6. Summary	583
17. Active Transport across Intestinal Epithelia and Other Bifacial Cell Systems	585
17.1. Unifacial and Bifacial Cells	585
17.2. Concepts of Active Solute Transport Based on the Membrane Pump Theory	586
17.2.1. The “Two-Membrane Theory” of Koefoed-Johnson and Ussing	586
17.2.2. The Standing Osmotic Gradient Theory of Diamond and Bossert	588
17.2.3. The Pericellular Pump Theory of Cereijido and Rotunno	588
17.2.4. The Na ⁺ Gradient Hypothesis of Sugar and Amino Acid Transport	588

17.3. Cooperative Adsorption-Desorption Model of Active Transport across Epithelia and Other Bifacial Cell Systems	588
17.4. Application of the Model to Experimental Findings	591
17.4.1. Cyclic Changes of Adsorption-Desorption as the Basis for Active Transport	591
17.4.2. Location of the Pumping Mechanism	591
17.4.3. The Source of Energy for Active Transport	593
17.4.4. Coupling of Ion and Water Transport	593
17.4.5. The Relation between "Homocellular" Regulation of Cell K ⁺ and Na ⁺ Composition and "Homoepithelial" Na ⁺ Transport	595
17.4.6. Coupling of Na ⁺ Transport with Sugar and Amino Acid Transport	595
17.5. Summary	598

V. A Tentative Approach to Some Unsolved Problems in Biology and Medicine

18. The Control of Protein Synthesis	603
18.1. Transcription and Translation in Prokaryotes	603
18.1.1. The lac Operon and the Control of Gene Transcription	603
18.1.2. The Role of K ⁺ , Na ⁺ , Glycerol, and DMSO in DNA Transcription	608
18.1.3. The Role of K ⁺ in mRNA Translation	610
18.2. The Control of Gene Function in Eukaryotes	611
18.2.1. Gene Transcription	613
18.2.2. mRNA Translation and Protein Synthesis	624
18.3. Summary	633
19. Growth and Differentiation	635
19.1. Mosaic and Regulative Eggs	635
19.2. Maturation of Amphibian Eggs	636
19.2.1. Ca ²⁺ and the Depolarization of the Electrical Potential	638
19.2.2. Maturation-Promoting Factor	640
19.2.3. A Key Role of Adsorbed Na ⁺ in the Control of Maturation	640
19.2.4. An Attempt to Provide a Consistent Theoretical Framework for Future Investigation	641
19.2.5. Other Cytoplasmic Factors in Maturing Oocytes: Cytostatic Factor and Chromosome-Condensing Activity	641
19.3. Fertilization (or Activation) of Sea Urchin Eggs	642
19.3.1. Alteration of Surface Proteins Accompanying Activation	642
19.3.2. Electrical Potential Changes Accompanying Activation	644
19.3.3. Ca ²⁺ Release Accompanying Activation	645
19.3.4. Requirement of External Na ⁺ in Egg Fertilization	647

19.4. Differentiation	650
19.4.1. Brief Historical Sketch	650
19.4.2. Classical Transplantation Experiments of Spemann and Mangold	652
19.4.3. In Search of the Evocator	655
19.4.4. Barth and Barth's Experiments and Theory of Differentiation	657
19.4.5. Landström and Løvtrup's Work on Differentiation	660
19.4.6. Concluding Remarks on Differentiation	660
19.5. The Cell Cycle	660
19.5.1. The Transition Probability Model	662
19.5.2. The Control of Entry into the C Phase	663
19.5.3. Control of Chromosome Condensation	669
19.5.4. The Promotion of Differentiation of Enucleated Eggs by Nuclear Transplantation	671
19.6. The Stem Cells: "Immortal" Queen Bees of the Society of Renewing Cells	674
19.7. Some Molecular Mechanisms According to the AI Hypothesis	676
19.7.1. Migration of Proteins (and RNA) between the Nucleus and the Cytoplasm	676
19.7.2. Nuclear Swelling during DNA Replication	679
19.8. Amphibian Metamorphosis	681
19.8.1. Thyroid Hormones	682
19.8.2. Prolactin	682
19.9. Summary	684
20. Cancer	687
20.1. General Theories of Cancer	687
20.1.1. The Somatic Mutation Theory: Historical Background	687
20.1.2. Dramatic Recent Confirmation of the Somatic Mutation Theory	688
20.1.3. The Mal differentiation Theory	690
20.2. Physiological Theories of Cancer	697
20.2.1. Szent-Györgyi's Theory of Cancer	698
20.2.2. Cone's Theory of Cancer	699
20.3. What Distinguishes Cancer from Normal Tissues?	700
20.3.1. The Morphological Generalization	700
20.3.2. The Warburg Generalization	701
20.3.3. The Greenstein Generalization	701
20.3.4. The Roberts-Frankel Generalization	703
20.3.5. The Damadian Generalization	703
20.3.6. The Ling-Murphy Generalization	708
20.4. Another Apparent Paradox and the Bright Future of Cancer Research	710

Appendices

A. Nuclear Magnetic Resonance Spectroscopy	715
A.1. NMR Relaxation Time, T_1	715
A.2. Proton Resonance Spectrum, Linewidth, and T_2	717
A.2.1. Chemical Shift	718
A.2.2. Linewidth and T_2	718
A.3. The Relation of T_1 and T_2 to the Rotational Correlation Time, τ_c	719
A.4. Orientation-Dependent Doublet Structure on NMR Spectral Line Shape	719
 B. Infrared and Raman Spectra	 721
 References	 723
 Abbreviations	 759
 Notation List	 763
 Index.....	 773

Introduction

It is highly probable that the ability to distinguish between living and nonliving objects was already well developed in early prehuman animals. Cognizance of the difference between these two classes of objects, long a part of human knowledge, led naturally to the division of science into two categories: physics and chemistry on the one hand and biology on the other. So deep was this belief in the separateness of physics and biology that, as late as the early nineteenth century, many biologists still believed in vitalism, according to which living phenomena fall outside the confines of the laws of physics. It was not until the middle of the nineteenth century that Carl Ludwig, Hermann von Helmholtz, Emil DuBois-Reymond, and Ernst von Brücke inaugurated a physicochemical approach to physiology in which it was recognized clearly that one set of laws must govern the properties and behavior of all matter, living and nonliving..

The task of a biologist is like trying to solve a gigantic multidimensional crossword puzzle: to fill in the right physical concepts at the right places. The biologist depends on the maturation of the science of physics much as the crossword solver depends on a large and correct vocabulary. The solver of crossword puzzles needs not just a good vocabulary but a special vocabulary. Words like *in ee* and *o ke* are vitally useful to him but are not part of the vocabulary of an English professor. Similarly, the physicist and the chemist may find themselves using the same language but different vocabularies. For example, the physicists James and Coolidge in 1933 used very elaborate wave-mechanical methods to predict almost exactly the properties of hydrogen molecules. It seemed that all of chemistry could be completely understood in terms of physics. But only in principle. The reality is that after another fifty years, one still cannot use wave-mechanical or other sophisticated methods to predict correctly even the prominent differences between the acid dissociation constants of the simple organic compound acetic acid ($pK_a = 4.76$) and its derivative trichloroacetic acid ($pK_a < 1$). Instead, less elegant methods, first entirely empirical ones and later deductive ones (see Section 6.3), were developed by chemists to provide very useful ways of predicting the behavior of many organic chemical compounds. Undoubtedly, biologists also must evolve their own special branch and vocabulary of physics. Yet they must do so within the confines of the basic language of physical laws.

One of the most useful ways for a biologist to evolve his own kind of physics is to study appropriate nonliving models. These models are much more complex than what physicists usually study, but a great deal less complex than what biologists must contend with. The models can be analyzed vigorously with dependable physical methods. Physical knowledge derived from studies of models can then serve as the foundation for the formulation of hypotheses that have predictable and hence testable traits. Indeed, many examples in the following chapters will show how major progress in mechanistic biology invariably parallels the development and study of good models.

Both the biologist and the crossword solver need to keep constantly in mind the past history and current state of the "whole map," to erase ideas once considered attractive and reasonable but now proven untenable, and to replace them with better ones more compatible with the big picture.

Without this constant awareness of past history, the same mistakes will be made again and again. Worse still, such repeated failure saps the strength and will of the investigator and creates the false impression that certain problems are too difficult to understand and therefore that the crossword puzzle is in fact insoluble.

At the end of the Second World War, the government of the United States embarked on a history-making new enterprise: government funding of basic scientific research. The Office of Naval Research (ONR), the National Science Foundation (NSF), and the National Institutes of Health (NIH) have since then been providing billions of dollars annually for crash programs to foster and accelerate the development of science. The results of this new enterprise have been spectacular, as illustrated by the brilliant progress made again and again in the understanding of the branch of cell physiology called genetics—progress that has led from the deciphering of the genetic code to the evolution, as a by-product, of a major industry, genetic engineering.

Yet a careful scrutiny of the accomplishments, even within the confines of molecular genetics, reveals vastly unequal speeds of progress in the different directions pursued. As an example, let us choose the concept of bacterial permeases or sugar pumps, introduced in the 1950s by one of the brightest and most capable microbiologists, the Nobel Laureate Jacques Monod of the Pasteur Institute of Paris, and his colleagues (see Cohen and Monod, 1957). Almost thirty years later the study of permeases has slowed down alarmingly. In contrast, the rest of molecular genetics continues to expand at dazzling speed, accented by the spectacular discovery of cancer-creating genes, the oncogenes (see Section 20.1.2). Why has one area stopped growing while others continue to shake the world with ever more spectacular achievements? In my opinion, the basic concept of genetics, i.e., the physiology of what the German biologist August Weismann called "germ plasm," has been developed in the right direction all along, while the theory of the somatic living cell, Weismann's "soma," is seriously faulty. So when Monod and his colleagues attempted to extend his earlier brilliant genetic findings and wed them to the framework of the conventional theory of the (somatic) living cell, he and others following his lead ran into trouble.

I shall next give a brief account of how I came to the conclusion that the widely accepted membrane pump theory of the living cell is incorrect. In 1943 I had the good fortune of graduating from college at exactly the right time to win the (last) competitive examination for the Boxer Biology Scholarship, a scholarship financed by the Boxer

Rebellion Indemnity Funds returned by America to China. Under Prof. Ralph W. Gerard in the Department of Physiology at the University of Chicago, I began to study the resting potential of frog muscle with the glass capillary electrode—a technique that had been introduced by Prof. Gerard and his pupil, Dr. Judith Graham (Graham and Gerard, 1946). I improved the way of preparing the electrode and the method of filling the electrode in such a way that it could yield quantitatively reproducible results (Ling and Gerard, 1949a). My graduate studies went on smoothly; by and large my findings seemed to complement the work of many others. It was only after my Ph.D. thesis was completed that I began to observe more and more frequently behaviors of the frog muscle that were unexpected within the context of the then evolving membrane pump theory. As time went by I began to suspect that Prof. Gerard and I might have been wrong in supporting the membrane pump theory, which was by no means universally accepted at that time but which had been the basis for both my Ph.D. thesis and the papers which I had written with Prof. Gerard (Ling and Gerard, 1949a-d, 1950).

One of the most fundamental problems in biology is to understand what, in physicochemical terms, is a living cell. What keeps a cell from being dispersed in the external medium? Why are virtually all cells loaded with K^+ and why do they remain loaded with K^+ for as long as a hundred years while being constantly bathed in a solution containing little K^+ but a great deal of the closely similar Na^+ ? In the membrane pump theory, this asymmetrical distribution of K^+ and Na^+ is due to a constant outward pumping of Na^+ by pumps postulated to be located in the microscopically thin cell membrane. According to this theory, the rate of Na^+ flux outward should be reduced by metabolic poisons, which block the energy supply of the pump. Yet I could not detect any such expected change (Ling, 1952) (see Chapter 5 for details). If the Na^+ pump idea is not correct, the theory of cellular electrical potentials built on the membrane pump concept cannot be correct either.

The realization that the membrane pump theory might be wrong came from a variety of observations that contradicted the predictions of this theory. The most outstanding was that certain functions of muscle cells, such as their “pumping” of Na , often were indifferent to suppression of their energy-yielding metabolic reactions. These early “negative” findings were most unwelcome to me at that time. They were made right after I had received an invitation from the editor of *Physiological Reviews* to write a review on the subject of membrane potentials and Na^+ pumps, to be published synchronously with one being prepared by Prof. Alan Hodgkin of Cambridge University for the English journal *Biological Reviews* (Hodgkin, 1951). I requested five postponements, and with great reluctance finally declined the offer! I knew for sure that something was wrong but I had neither decisive experimental proof nor an alternative explanation for the unexpected observations.

In searching for answers I was astonished to find that there was already a rich literature on the subject by scientists whose names I had not even heard of, even though I thought that I had already earned my Ph.D. Given a great deal of freedom as a Seymour Coman Postdoctoral Fellow at the University of Chicago, and then as an instructor in Dr. Stephen Kuffler’s laboratory at Johns Hopkins University, I spent a great deal of time browsing in the libraries and brooding over the only clue that I felt was relevant: The hydrated Na^+ is larger than the hydrated K^+ . Eventually I suggested a new molecular mechanism for the preferential accumulation of K^+ over Na^+ in living cells: selec-

tive electrostatic adsorption on negatively charged sites of cytoplasmic proteins (Ling, 1951, 1952). In the next ten years this concept became the seed for a general theory of the living cell, an account of which was published in 1962 under the title *A Physical Theory of the Living State: The Association-Induction Hypothesis*. The eighth chapter of that book dealt exclusively with the minimal energy requirement of the postulated Na^+ pump and compared it with the much lesser total energy available to the cell under specified conditions. The writing of that book took about five years; for most of that time I was a senior research scientist at the Eastern Pennsylvania Psychiatric Institute.

In 1961 I was invited by Dr. Frank Elliott to start a new research laboratory as part of his Department of Neurology at Pennsylvania Hospital. An old storage building, at one time a part of St. Joseph's Catholic Orphanage, was converted into a research laboratory with the aid of a research grant from the John A. Hartford Foundation to Dr. Elliott, and Pennsylvania Hospital has provided my laboratory ever since.

The concept of cooperative ion adsorption and its role in the control of cellular processes, a part of the original association-induction hypothesis (Ling, 1962, Chapter 5) was further developed in the early 1960s. In this effort I benefited much from the help of my friend, the Nobel Laureate physicist Dr. C. N. Yang, now at New York University at Stony Brook. Further development of this concept was achieved by my colleague, Dr. George Karreman, who has been a long-time supporter of the hypothesis.

In 1965, to the association-induction hypothesis was added the polarized multilayer theory of cell water. According to this theory, virtually all the water in living cells exists in the state of polarized multilayers as a result of interaction with a matrix of protein chains existing in an extended conformation throughout the cell. A decreased solubility in this polarized water, rather than the action of Na^+ and other pumps, maintains the low level of Na^+ as well as of many other solutes found in living cells. These theories generated much interest, and among new friends and supporters were Drs. Carlton Hazlewood, Freeman Cope, and Raymond Damadian. Each had his own reasons to reject the membrane pump theory, and their contributions will be discussed in the following pages.

One of the greatest threats to the long-range future of the biological sciences is their increasing fragmentation. This fragmentation came naturally with the establishment of the crash research programs. In the unaccelerated course of scientific development, as it actually happened in the past, there were few financial rewards for one's efforts. Driven only by intellectual curiosity, a few scientists chose, observed, and studied an interesting subject open to attack. There was plenty of time to test and weed out incorrect hypotheses. The more successful ones that stood the test of time then provided the trunks and boughs of the magnificent tree of knowledge that we now have.

On the other hand, a crash research program, a deliberate effort to speed up further scientific progress, involves the enlistment of many scientists to solve all kinds of problems at once. No time is allowed to eliminate what may be popular but incorrect basic concepts. Instead the system tends to insulate and preserve such concepts against negative evidence. At the same time, many centers of attack or beachheads are established. As time passes, each of these specified areas develops its own terminology, its own preferred method of operation, its own specialized journals, and so forth. In due time each of these areas will spawn still more specialized areas. The result is the fragmentation of the

coherent, indivisible crossword puzzle into a collection of smaller and often incoherent pieces. From a long-range viewpoint, this is clearly an undesirable trend that will lead nowhere unless effective corrective measures are taken.

Fragmentation of science also inadvertently coerces young scientists more and more into the roles of engineers and technicians. An antidote to this adverse effect on the development of future generations of scientists is to teach fewer so-called "facts"—many of which are really unproven hypotheses, presented as unqualified truths by textbook writers more concerned with clarity than veracity—and instead to use the precious impressionable years to communicate the salient features of the big picture and the habits and skills needed to extend this broad knowledge as time goes by. With this sound background, later specialization will not create "dinosaurs," helpless and useless when a particular field dries up. Instead, sharing the strengths of the primitive little mammals, the investigators thus trained will be able to meet the new challenges that the unknown future will bring.

An engineer-technician's time scale of operation is very short. A failure is a failure. The kinds of scientists who deserve the greatest encouragement are those who operate on a much longer time scale. In this case, a failed hypothesis is as important as a successful one to achieve the higher level of understanding essential for the true progress of science.

It was with all these thoughts in mind that I undertook the writing of this volume more than five years ago. It is a story centered around my view of the living cell, but is, in fact, the creation of all those scientists, living and long dead, whose work I have cited.

To the readers of this volume, I therefore play three different roles: first, as a guide to a comprehensive history of cell physiology that has not been told before; second, as a proponent of the association-induction hypothesis; and last, as an ambassador of good will to admire and review the progress made in diverse areas of cell physiology which deserve far more attention than they have received but in which I have little direct experience. It is to be hoped that this book will help to initiate the building of more and more bridges—a task that has been sadly neglected with the increasing fragmentation of the recent past.

As a guide, I shall take the reader through the first five chapters of the book. It will be shown how, as soon as the theory of living cells as the basic units of life was presented, two divergent views of the cell emerged: In the membrane theory, the cell interior is regarded as merely a dilute solution and it is a microscopically thin membrane that sets the cell interior apart from the external environment. In what may be called the protoplasmic or bulk phase theory of the living cell, the entire cell substance, the protoplasm, has unusual properties owing to its colloidal attributes, and it is the nature of this protoplasm that keeps the cell apart from its environment. The first three chapters emphasize the decisively dominant role assumed by the membrane theory in the early 1940s. In the form of Boyle and Conway's masterful theory, the four major subjects of cell physiology—selective ion accumulation and exclusion, selective ionic permeability, cell swelling and shrinkage, and cellular electrical potentials—were put into a simple framework describable by simple quantitative equations. It was at this time that the critical events of the establishment of the research funding agencies occurred.

The process of fragmentation continued. More and more textbooks described the

concepts of the membrane pump theory as proven facts. These are some of the underlying reasons that major developments in the years following, described in Chapters 4–14, were little known to most students of biology and medicine.

Chapter 4 describes the reemergence of new bulk phase theories. In this and the following chapters, it is shown that what for some time has been regarded as evidence in support of the membrane theory has, after more careful investigations, turned out to be just the opposite.

In Chapters 6 and 7 I take on my second role, as the proponent of the association-induction hypothesis, and a fuller version of this hypothesis, including the results of extensive model studies, is presented. Chapters 8 and 9 present the decisive experiments of the recent past, which leave no doubt in my mind at least about the essential correctness of the bulk phase theory in general and the association-induction hypothesis in particular.

Chapter 10, a very brief one, reevaluates the role of ATP as a cardinal adsorbent controlling the electronic and steric conformation of the protein–water–ion system, rather than delivering a package of captured energy in the so-called high-energy phosphate bonds.

Chapters 11–14 review the extensive data collected over the last twenty-five years on the four classical subjects of cell physiology mentioned above: selective solute accumulation and exclusion, selective solute permeability, cell and subcellular particle swelling and shrinkage, and cellular resting and action potentials. These results are then compared with the theoretical predictions of the association-induction hypothesis, with favorable conclusions.

The following six chapters deal respectively with mitochondrial physiology and oxidative phosphorylation, muscle and nonmuscle contraction, active transport across bifacial cells, protein synthesis, growth and differentiation, and cancer. In each case, the most exciting recent developments are described and a few tentative hypotheses are suggested to bring them into line with the now established adsorbed state of the major cell cation, K^+ , and cell water. In the process, a number of key contradictions are reconciled. However, the detailed writing in these last six chapters is aimed primarily at restoring in the mind of the reader an appreciation of how inseparable and how coherent are all the behaviors and properties of the living cell. As a good detective, no future research scientist in cell physiology can afford to close his or her eyes to any one of these specialized areas of research, nor to other areas into which the writer's limited time and space did not permit him to delve. Indeed each and every one of them is an inseparable part of the whole.

This book is at once a monograph, a science history tract, and a textbook. Yet it differs from a conventional monograph in that it does not deal with a specific subject. It is instead more like a collection of monographs made coherent by the single framework of the association-induction hypothesis. It differs from a conventional history tract in that it chronicles the actual events of science, not just dates and names. It differs from a conventional textbook in that it presents knowledge, not in the form of a finished product, but rather in an account of where we are, how we have gotten here, and where we may go in the near future. In other words, it is the latest story of man's search for the physical basis of life, as seen from the viewpoint of one investigator.

I

Opposing Concepts in Cell Physiology: History and Background

The Early History of Cell Physiology

1.1. The Evolution of Physiology as the Physics and Chemistry of Living Phenomena

It was not until the early nineteenth century that physiology was thought of as the knowledge of the physics and chemistry of living functions. Aristotle (384–322 B.C.) used the term *physiology* in a broad sense to mean “knowledge about nature” (Rothschuh, 1973). Thales of Miletos (ca. 640–548 B.C.) tried to explain all natural phenomena in terms of variations of one single principle: water. Empedocles of Agrigentum (ca. 495–435 B.C.) believed that the world was formed from four basic elements—fire, water, air, and earth—operated upon by two opposing forces: love that unites them and hate that separates them. Both he and Hippocrates (ca. 460–377 B.C.), who founded Western medicine, considered the human body to be a microcosmos embodying the same four elements as the macrocosmic world. These, and the four opposing qualities of warmth or coldness, dryness or moisture, combine to form four humors: blood, which is warm and moist; phlegm, cold and moist; black bile, cold and dry; and yellow bile, warm and dry.

Galen (ca. 130–201) adapted the humoral doctrine of Hippocrates into a theory of health and disease. Health depends on the proper balance of the humors and is maintained by a fire burning in the empty left ventricle of the heart. Heat generated by this fire is dissipated by respiration. Galen’s philosophy dominated until the sixteenth century (C. Singer, 1959; Rothschuh, 1973).

The year 1543 witnessed the publication of two major works: *Opus de Revolutionibus Coelestibus* by Nikolaus Copernicus (1473–1543) and *De Humani Corporis Fabrica* by Andreas Vesalius (1514–1564). The first book initiated a major development in the physics of the inanimate world; the second marked the beginning of an accurate study of anatomy. The middle of the sixteenth century saw the gradual replacement of the classical doctrine of humors by chemistry, through efforts like those of Paracelsus (1493–1541). This prepared the way for the great discoveries of the seventeenth century,

one of the most outstanding of which was the explanation of the circulation of the blood by William Harvey (1578–1657).

At that time, knowledge of physiology was limited to phenomena that could be seen by the naked eye. Vesalius's anatomy offered an adequate basis for the understanding of the circulation of the blood by Harvey. However, the final proof of Harvey's scheme came with the development of the microscope and discovery by Marcello Malpighi (1628–1694) of direct capillary connections between the arterial and the venous systems in the frog lung (Rothschuh, 1957). Malpighi noted that blood is not a mixture of four humors but consists of “almost an infinite number of particles, white serum and red atoms.” The development of the microscope by Malpighi, Anton van Leeuwenhoek (1632–1723), and others opened the door to the recognition and study of living cells.

Georg E. Stahl (1659–1734), a deeply religious, brilliant physician and chemist, was the champion of an *animistic* or vitalistic view of living phenomena (King, 1963), in which all body parts are passive and their movements are controlled entirely by the soul. Stahl also developed a theory in which combustion, respiration, and fermentation cause the release of a substance called *phlogiston*—a theory defended by Joseph Priestley (1733–1804). Its disproof by the French chemist Antoine Lavosier (1743–1794) marked a major change of paradigm in the history of science. Nevertheless, Stahl's vitalistic view exercised a profound influence on physiologists well into the early years of the nineteenth century, including the German physiologist Johannes Müller (1801–1858).

Müller's great influence on physiology was exercised through his many illustrious students, including Schwann, Schultze, DuBois-Reymond, Brücke, von Helmholtz, Hermann, Bernstein, Kühne, Bethe, and Starling. An even greater German physiologist, Carl Ludwig, has been called the founder of modern physiology (Bauereisen, 1962). Ludwig also trained a large number of brilliant students, including Fick, Pavlov, Rub-



Carl Ludwig (1816–1895)



Hermann von Helmholtz (1821–1894)

ner, Loeb, Krogh, and Höber. Ludwig's American students, Bowditch and Welch, played major roles in the development of the physiological and medical sciences in the United States (Sewall, 1923; Fleming, 1954; Flexner and Flexner, 1941).

Ludwig, DuBois-Reymond, von Helmholtz, and Brücke were good friends, united in their belief in a physical direction of physiology and their opposition to the vitalistic view held by many of their contemporaries.

Ivan Pavlov's (1849–1936) famous experiment on the conditioned reflex opened the door to physiological psychology. He exerted a great influence on the development of Russian physiology (Cuny, 1965). In 1897 he wrote

The path of modern organ physiology is straight and clear, and we are not far from a complete understanding of life as an association of organs. But the organ is an assembly of cells and its properties and activities are dependent on the properties and activities of its component cells. Organ physiology has therefore so to speak, begun the study from the midst of life: the beginning, the basis of life, is in the cell. [cited by Heilbrunn, 1937]

1.2. The Cell Theory

The Latin word *cella* describes a small “room” such as one sees in a honeycomb. In 1665 Robert Hooke (1635–1703) noted the similarity between the fine structure of cork seen under a magnifying glass and that of a honeycomb and called these small units *cellula*. Later he extended this name to describe similar units he saw in living tissues (Hooke, 1665). In the 1830s Matthias Schleiden (1804–1881) and Theodor Schwann formally presented the *cell theory*, according to which cells are the basic units of all life. Schleiden and Schwann's concept was not entirely new. By means of a maceration technique, René J. H. Dutrochet (1776–1847) had demonstrated in 1824 that single cells were the structural and physiological units in plant and animal tissues and that these



Theodor Schwann (1810–1882)

cells were not inseparably bound in sheets of tissues, as had up to then been believed (see A. Chambers and Chambers, 1961), but were held together by simple adhesive forces.

Even earlier, in 1805, the German biologist Lorenz Oken wrote in his monograph, *Die Zeugung (The Creation)*,

All organic beings originate from and consist of vesicles or cells. These when detached and regarded in the original process of production are the infusorial mass or Urschleim, whence all larger organisms fashion themselves or are evolved. . . . [cited by C. Singer, 1959]



Lorenz Oken (1779–1851)

Not only did Oken lucidly enunciate the basic concept of cell theory 25 years ahead of Schleiden and Schwann, but he also clearly recognized "protoplasm" 30 years before its description by Dujardin.

1.3. The Discovery of Protoplasm

Felix Dujardin of Paris, a contemporary of Schleiden and Schwann, has been credited as the discoverer of protoplasm. He observed a jellylike substance exuding from crushed infusoria, a class of ciliated protozoa. To this living jelly (*gelée vivante*) he gave the name *sarcode* (Dujardin, 1835). Dujardin described sarcode as gelatinous, diaphanous, and water-insoluble. Sarcode tends to form globules and attach to dissecting needles; it stretches like mucus. Though not miscible with water, isolated sarcode suspended in water diminishes in volume until eventually it leaves only a faint irregular residue. Nitric acid and alcohol rapidly coagulate sarcode, turning it white and opaque. Dujardin noted that one of its most distinguishing characteristics is the tendency to form vacuoles spontaneously inside its mass.

Johann E. Purkinje (1787–1869), a physician and anatomist from Prague, described the substance of embryonic animal tissues as *protoplasm* and compared this substance to the material within cambian cells of plants (1840). Independently, Hugo von Mohl (1846), a botanist, used the term *protoplasm* to describe the living substance in plant cells. Von Mohl pointed out that Schleiden had previously referred to this living matter as *Schleim*, a term which von Mohl found insufficiently distinctive, since the word had already been used in various other contexts; he apparently was unaware of Oken's name for protoplasm, *Urschleim*. Cohn in 1850 proposed that the sarcode of zoologists and the protoplasm of botanists "if not identical, must be at any rate in the highest degree analogous substance" (see Hall, 1969). The exhaustive efforts of Schultze (1863) and de Bary established beyond doubt that Dujardin's sarcode from lower forms of organisms and the protoplasm in the cells of higher plants and animals are identical.



Felix Dujardin (1801–1860)

Max Schultze (1825–1874), a disciple of Müller, has been called the father of modern biology. His *protoplasm doctrine* described living cells as small masses of protoplasm surrounding a nucleus. The full significance of protoplasm in living phenomena was elegantly paraphrased by Thomas Huxley (1825–1895) as “the physical basis of life” (1853). Looking back on the period between 1840 and 1860, Locy in 1908 wrote

Let us picture to ourselves the consequence of the acceptance of this idea [the protoplasm doctrine]. Now for the first time physiologists began to have their attention directed to the actually living substance; now for the first time, they saw clearly that all future progress was to be made by studying the living substance—the seat of vital activity. This was the beginning of modern biology.

1.4. Colloidal Chemistry and the Concept of Bound Water

Thomas Graham, a contemporary of Oken and Dujardin, was a truly remarkable scientist. His life-long work was devoted to the study of diffusion. To him we owe Graham's law, according to which the diffusion rate of a gas is inversely proportional to the square root of its density. From a large number of studies he recognized that substances seemed to fall into two classes: salts, sugars, and alcohols diffuse rapidly; hydrated silicic acid, alumina, starch, the gums, tannin, albumin, and gelatin diffuse slowly. He called the first class of substances *crystalloids* and referred to the second class in the following words: “As gelatine appears to be its type it is proposed to designate substances of the class as *colloids* (*κολλα*, glue) and to speak of their peculiar form of aggregate as the *colloidal condition of matter*” (T. Graham, 1861). He pointed out that slowness of diffusion is only one of the characteristics of colloids. They tend to be gelatinous and mutable in form and were believed to be involved in the organic process of life. Graham



Thomas Graham (1805–1869)

invented dialysis and showed that it is the gelatinous starch in parchment paper that causes its impermeability to colloids. Graham believed that

the water of the gelatinous starch is not directly available as a medium for the diffusion of either sugar or gum, being in a state of true chemical combination, feeble although the union of water with starch may be. . . . Sugar, however, with all other crystalloids, can separate water, molecule after molecule, from any hydrated colloid, such as starch.

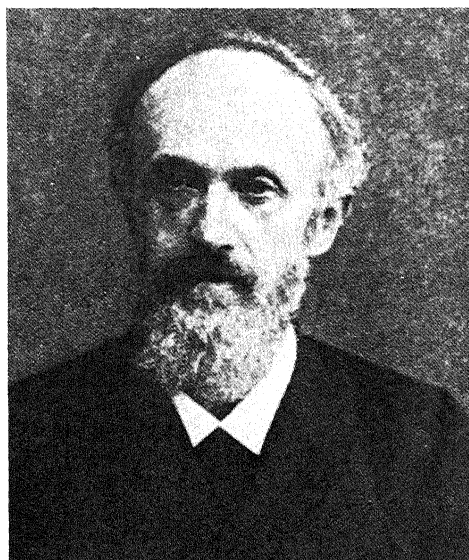
Among the large collection of materials he studied was the gelatinous precipitate of copper ferrocyanide formed when copper sulfate was mixed with potassium ferrocyanide, a colloid that played a major role in the subsequent development of a major theory of cell physiology.

1.5. Traube's Semipermeable Copper Ferrocyanide Gel Membrane and the Introduction of the van't Hoff Equation

In 1748, the Abbé Nollet performed the first recorded study of osmosis (cited in Glasstone, 1946). When alcohol and water were separated by an animal bladder membrane, the water passed through the membrane into the alcohol-containing side, but alcohol did not pass through the membrane into the water-containing side. Eighty years later René J. H. Dutrochet (1776–1847) studied the flow of water through animal membranes and introduced the terms *endosmosis* and *exosmosis*, describing the movement of water in opposite directions. This later was reduced to the simpler term *osmosis* (Dutrochet, 1827). Dutrochet emphasized the great importance of osmosis in physiological phenomena and introduced the manometric method for the quantitative measurement of osmotic pressure.



The Abbé Nollet (1700–1770)



Moritz Traube (1826–1894)

Graham's discovery that colloids cannot pass through parchment paper greatly intrigued Moritz Traube, a German-Jewish tradesman living in Berlin. Traube was interested in artificial membranes and their relation to the study of osmosis in biology. He discovered a *precipitation membrane* of copper ferrocyanide gel which is permeable to water but not to ions like Cu^{2+} or to ferrocyanide, sucrose, and other solutes. Traube



Wilhelm F. Pfeffer (1845–1920)

TABLE 1.1. Pfeffer's Data (1877) on the Influence of Concentration of Sucrose (A) and of Temperature (B) on the Osmotic Pressure Recorded across a Copper Ferrocyanide Membrane^a

A	Sucrose concentration (C) (g/100 g water)	Osmotic pressure (π) (mm Hg)	π/C
1		535	535
2		1016	508
2.74		1518	554
4		2082	521
6		3075	513

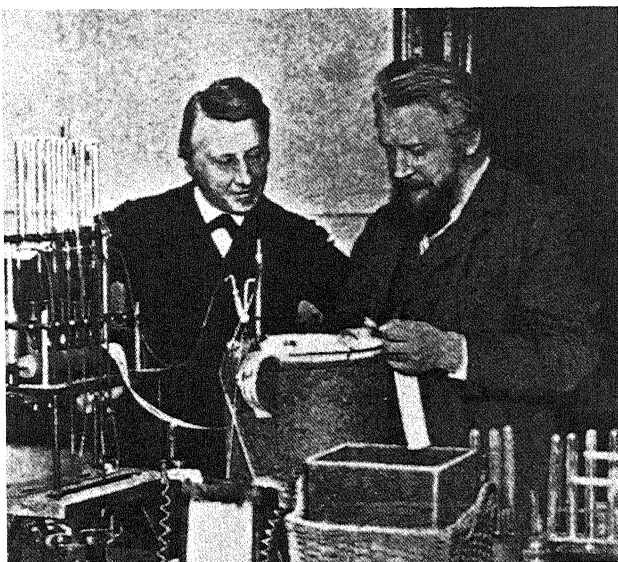
B	Absolute temperature (T) (K)	Osmotic pressure (π) (mm Hg)	π/T
280.0		505	1.80
286.9		525	1.83
295.2		548	1.85
305.2		544	1.79
309.2		567	1.83

^aIn (A) the temperature was 15°C. In (B) the sucrose concentration was 1%.

(1867) suggested that this semipermeability of the gel membrane is due to its behaving like an atomic sieve, with pores large enough to allow passage of water but too small to allow passage of solutes. [This idea, which was to appear again and again in the literature, was eventually disproved by X-ray and electron diffraction studies which showed that copper ferrocyanide gel exists in the form of a crystalline lattice whose interstices are many times larger than the solutes which cannot penetrate the membrane (Fordham and Tyson, 1937; for review, see Glasstone, 1946).] By precipitating the fragile copper ferrocyanide gel onto the wall of a porous pot, the botanist Wilhelm F. Pfeffer (1877, 1921) prepared semipermeable membranes strong enough to lend themselves to long-term precise studies. With this membrane and an enclosed manometer, he measured the osmotic pressure of sucrose solutions. Osmotic pressure (π) is the pressure that must be applied to a solution in order to prevent the passage of solvent into it when the solution is separated by a semipermeable membrane from a pure solvent or a more dilute solution. Part of Pfeffer's results are reproduced in Table 1.1. The approximate constancy of π/C (where π is the osmotic pressure and C is the sucrose concentration) shows that π is directly proportional to the molar concentration of sucrose. π/T , where T is the absolute temperature, is also constant.

While the physical chemist J. H. van't Hoff was studying problems of gas equilibrium, the botanist Hugo de Vries (1848–1935) brought Pfeffer's findings to his attention. van't Hoff recognized that since the concentration C (in moles per liter) is the reciprocal of the volume V (in liters) containing 1 mole of solute, the first part of Pfeffer's data would indicate that

$$\pi V = \text{constant} \quad (1.1)$$



J. H. van't Hoff (1852–1911) and Wilhelm Ostwald (1853–1932)

which is analogous to Boyle's law for gases. Furthermore, the second part of Pfeffer's data,

$$\pi/T = \text{constant} \quad (1.2)$$

is analogous to Gay-Lussac's law for gases. Combining the two laws, he obtained

$$\pi V = RT \quad (1.3)$$

By comparing the osmotic pressure of a sucrose solution with the pressure exerted by hydrogen gas, van't Hoff found that R for 1 mole of solute had the same value as the gas constant for one mole of gas. Equation (1.3) bears van't Hoff's name but is also known as the Boyle-van't Hoff law.

Equation (1.3) holds only for a nondissociating solute like sucrose at low concentration. The complete equation introduced by van't Hoff is

$$\pi V = iRT \quad (1.4)$$

where i is a coefficient which may be higher than 1 in the case of dissociating electrolytes.

1.6. Pfeffer's Membrane Theory

In 1855, the Swiss botanist Carl von Nägeli described *plasmolysis*—the shrinkage of a plant cell protoplast in solutions of anthocyanin, to which protoplast is not perme-

able—as an osmotic withdrawal of water from the cell sap. Von Nägeli's work, described in his monograph *Pflanzenphysiologische Untersuchungen* (1855), included some of the earliest and most important experimental research in cell physiology. Twelve years later W. Hofmeister (1867) found that the protoplasts of the beet root remain shrunken for several weeks in a concentrated NaCl solution. This observation led H. de Vries (1888a) to conclude that these cells are impermeable to NaCl. It is important to note that in plasmolysis the loss of water from the plant cell is primarily from the water-filled central vacuole. That is why von Nägeli, Hofmeister, and de Vries regarded the entire protoplast as the equivalent of a semipermeable membrane. Indeed both von Nägeli and de Vries clearly recognized that the protoplasm, and not just the cell wall, is impermeable to salts and pigments. Pfeffer's theory, however, was quite different.

Following his studies of membrane models, Pfeffer proposed the membrane theory of cell physiology, in which he postulated the existence of a thin *plasma membrane* surrounding the entire protoplast (another membrane, the *tonoplast*, lines the central vacuole). He postulated that the resistance to diffusion of solutes like sugars and salts is in the plasma membrane, and that the cytoplasm or protoplasm is essentially a simple solution of both organic and inorganic solutes. Pfeffer's theory was published in his monograph *Osmotische Untersuchungen* (1877, 1921). Pfeffer stressed that permeability depends not only on the size of the permeating molecule relative to the size of the membrane pores, but also on the solubility of the molecule in the membrane material. Although Pfeffer has been widely recognized as the founder of the membrane theory, he was not the first to suggest that cells are covered by a membrane barrier or that the cytoplasm represents in essence a simple solution. Indeed, these concepts were expressed by Schultze (1863) and by Kühne (1864).

In addition to plasmolysis in plant cells, the hemolysis of red blood cells was widely used for studying osmotic behavior. This method, invented by Hartog J. Hamburger (1859–1924) (1889, 1904), used hemolysis to determine the permeability of a particular solute. Hamburger believed that there is a critical volume of the red blood cells beyond which the cell will burst open, releasing its hemoglobin content (see, however, Section 5.2.5) and that this critical volume is created by immersing the cell in a solution of lower osmotic pressure. He believed that this would occur at a given critical osmotic pressure, regardless of the chemical nature of the solute, provided the solute does not permeate and enter the cell. A variant of the plasmolysis method was used to measure the relative *permeability rates* of different substances (Klebs, 1887; H. de Vries, 1888b). This method followed the rate of recovery of cell volume after initial shrinkage when the cell is plunged into an aqueous solution containing an excess of the solute under investigation.

1.7. Summary

Following the enunciation of the cell theory in the early nineteenth century, two major concepts developed. One, based on the protoplasm doctrine and colloidal chemistry, implied a uniqueness, in a physical-chemical sense, of the entire cell substance. The other, the membrane theory, focused attention on a hypothetical thin surface, or plasma membrane. Concepts of osmotic pressure and of the permeability of cells or their

membranes to solutes were felt to be closely related. According to the membrane theory, cell water and solutes like K^+ dissolved in the cell water exist in a physical state like that of the dilute aqueous solution of their environment. The next chapter traces the development of these two opposing concepts—the protoplasm doctrine and the membrane-osmotic theory—within the context of studies of osmosis, of permeability, and of the electrical properties of cells and of model membranes.

Evolution of the Membrane and Bulk Phase Theories

2.1. Concepts of the Nature of the Plasma Membrane

2.1.1. The Lipoidal Theory of Overton

Charles E. Overton, a distant cousin of Charles Darwin, investigated the permeability of a variety of living animal and plant cells (e.g., muscle, erythrocytes, root hair, and algal filaments) to some 500 compounds. He found that the introduction of polar groups (e.g., carboxyl, hydroxyl, and amino groups) into a chemical substance decreases its permeability into cells, while lengthening of the carbon chain, or esterification of carboxyl or hydroxyl groups, increases it. These observations became a part of Overton's Rules. A specific example is the series of hydroxylic compounds, which follow this order of decreasing permeability: monohydric alcohol (ethanol and methanol) > dihydric alcohol (e.g., ethylene glycol) > trihydric alcohol (e.g., glycerol) > tetrahydric alcohol (e.g., erythritol) > hexahydric alcohol (e.g., mannitol) > hexoses and di- and trisaccharides. This observation appeared to indicate a positive correlation between the lipophilic nature of the compounds and their permeability.

On the basis of these and other findings, and with the acceptance of Pfeffer's concept that the barrier to diffusion in living cells lies in a thin plasma membrane covering the cell surface, Overton postulated that this plasma membrane is primarily lipid in nature (Overton, 1899). The relative solubility of a substance in lipid compared to its solubility in water determines the permeability of a particular substance through the plasma membrane. (It should be pointed out that Quincke (1898) had expressed a similar view.)

Overton died before publishing all of his work, and undoubtedly much of his data was lost. The best experimental support for Overton's theory came from Collander (Collander, 1959; Collander and Bärlund, 1933), who analyzed chemically the amount of a substance that appeared in the cell sap of the central vacuole of a giant plant cell like

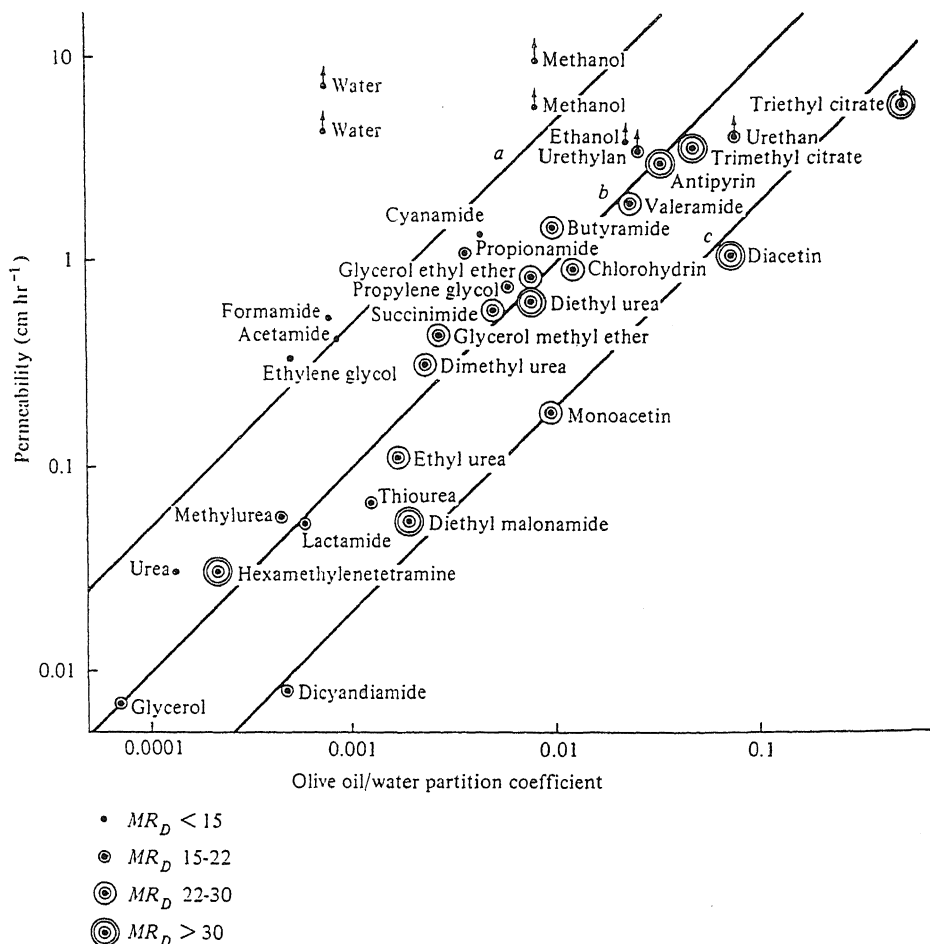


FIGURE 2.1. Relation between the permeability constants of penetration into *Nitella* and the olive oil/water partition coefficients of 35 compounds. MR_D is the molar refraction coefficient, which is proportional to the size of the molecule. The data also indicate that small molecules with low MR_D tend to fall above the limits where the larger molecules are found. [From Dowben (1969), by permission of Harper and Row.]

Nitella, after adding the substance to the external medium. Collander's data are reproduced here as Fig. 2.1.

Since lipids have no ability to dissolve a variety of compounds, including sugars and amino acids, that are essential for the survival of the cell, Overton attributed their movement across the plasma membrane to a secretory or "adenoid" process. He stressed that his *lipoidal theory* accounted only for the passive permeability of the membrane to solutes.

2.1.2. Mosaic Membranes with Pores

A major weakness of Overton's lipoidal membrane theory is that it fails to explain why the cells are permeable to water, urea, and many other substances that are insoluble

or poorly soluble in lipids. In Nathansohn's *mosaic theory* (Nathansohn, 1904), the cell membrane is not a pure lipid layer but a mosaic of areas with lipid and areas with properties similar to Traube's precipitation membrane (described in Section 1.5). Such a mosaic membrane would offer different routes of entry to lipid-soluble and lipid-insoluble materials. Ruhland (1908, 1913), on the other hand, developed an *ultrafilter theory* in which the semipermeable membrane is considered to act as a molecular sieve. Ruhland and Hoffman (1925) showed that the rate of permeation of nonelectrolytes into the sulfur bacterium, *Beggiatoa mirabilis*, shows an inverse relation to the molar refraction (MR_D), which is proportional to the size of these compounds. The ultrafilter theory is in fact Traube's atomic sieve theory (Section 1.5) applied to living cells, and thus subject to the same criticism. Moreover, the copper ferrocyanide membrane has an almost ideal semipermeability, i.e., it is permeable to water but not to many ions or to sucrose, while living cell membranes are as a rule much more permeable (see Figs. 4.1 and 9.5).

Collander and Bärlund's data, reproduced in Fig. 2.1, show a general agreement with Overton's lipoid theory. The data also show that those compounds with MR_D smaller than 15 (i.e., smaller size) all appear to permeate at a rate faster than one can expect from their olive oil/water distribution coefficients. To explain this discrepancy these authors also combined the lipoid theory of Overton and the ultrafilter theory of Ruhland into a mosaic membrane theory in which small pores allow additional passage of small molecules. This theory is in essence the same as Nathansohn's mosaic theory. Like all the other mechanical sieve theories, it suffers from the same drawbacks discussed above and in Section 1.5 in relation to Traube's original concept.

2.1.3. Membranes with Charged Pores and Selective Ionic Permeability

From studies of a variety of artificial membranes (gelatin, coagulated egg white, agar, pig bladder, collodion, parchment paper, charcoal, and clay), Bethe and Toropoff (1914, 1915) concluded that permeability to ions originates from electrical charges in the pores of these membranes. They thought that these fixed charges may be due to ion adsorption onto the walls of the pores (which will make this type of charged ion immobile, leaving the oppositely charged ions free to move) or, in the case of protein, a H^+ -concentration-dependent ionization of ionic side chain functional groups. (The reader is reminded that the Zwitterion theory of protein ionization had not yet been discovered.) Later, Michaelis (1925; Michaelis and Fujita, 1926) studied the ionic permeability of collodion membranes and concluded that the adsorption of anions onto the walls of pores makes the membrane less permeable to anions because of electrostatic repulsion, and that this membrane shows selective permeability toward cations because they have different frictional resistances owing to their different degrees of hydration. Thus an ion with a thicker hydration shell has a higher frictional resistance because its "sphere of attraction" for water molecules extends to those already adhering on the walls of the pores. With these concepts, Michaelis and his co-workers were able to explain the low permeability of the collodion membrane to anions in general, as well as its higher permeability toward the smaller, less hydrated K^+ , than toward the larger, more hydrated Na^+ . Similarly, A. Fujita (1926) showed that dried collodion is permeable to urea, which is small, but not to glucose, which is larger.

It is interesting to note that Michaelis was firmly convinced that the collodion is itself electrically neutral, and he emphatically pointed out that "If the wall [of the pores

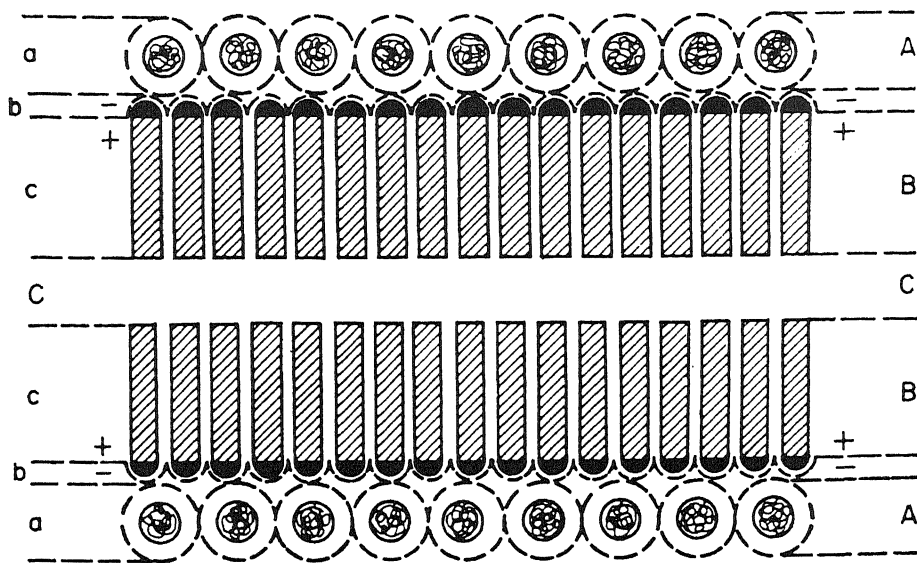


FIGURE 2.2. Diagram showing the structure of the semipermeable membrane according to Harvey and Danielli. A, layer of globular proteins; B, layer of oriented lipid molecules; C, unoriented layer of lipid molecules; a, hydrated protein molecules; b, ionized ends of lipid molecules; c, unionized ends of lipid molecules; a + b, hydrophilic zone; C + c, lipophilic zone. [From Höber (1945), by permission of McGraw-Hill (Blakiston).]

in collodion] is negative, this charge can only be brought about by adsorbing negative ions" (Michaelis, 1925, p. 37). This point will be brought up again in Section 2.2.5.

2.1.4. The Paucimolecular Membrane of Davson and Danielli

The interfacial tension at the surface of a lipid layer directly exposed to water is high (20 to 30 dynes/cm) and is incompatible with the surface tension of the living cell, which is in the realm of 0.1–0.2 dyne/cm (Cole, 1932; E. N. Harvey and Collander, 1932). This discrepancy led E. N. Harvey and Danielli (1939) to suggest that the lipid layer postulated by Overton is not directly exposed to water but is covered on each side with a layer of protein. This then led to the development of the *paucimolecular model* of the cell membrane shown in Fig. 2.2 (see Davson and Danielli, 1943).

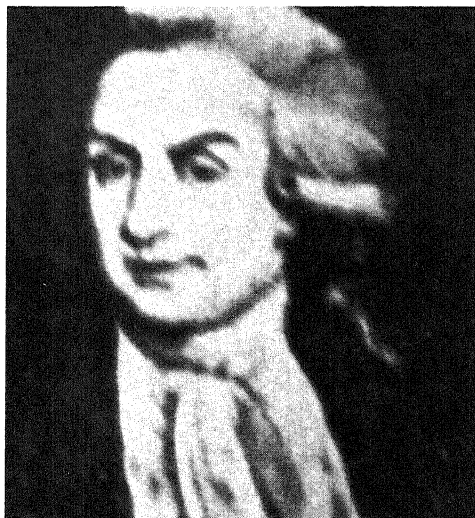
2.2. Cellular Electrical Potentials and Swelling in the Context of the Membrane Theory

2.2.1. Early History of Cellular Electrical Potentials

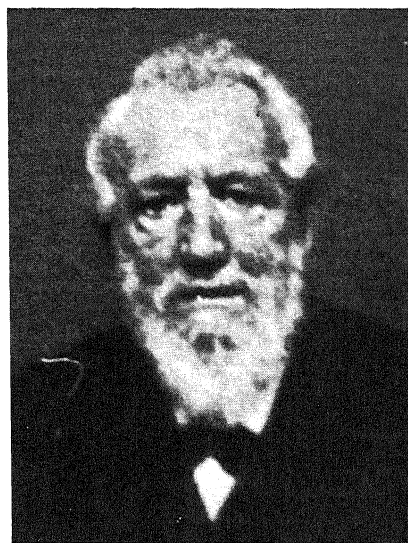
In 1757, Leopoldo M. A. Caldani found that sparks from a discharging Leyden jar elicit muscle contraction, but the physiological importance of electricity was brought forth only after extensive study of the phenomenon by Aloisius Galvani. In 1786 Galvani



Leopoldo M. A. Caldani (1725–1813)



Aloisius Galvani (1737–1798)



Emil DuBois-Reymond (1818–1896)

discovered that, when a brass hook inserted into the spinal cord of a frog touched the iron plate on which the frog was lying, the muscles twitched. He postulated that the electricity was generated in the brain. This "animal electricity" was stored in the muscle as in a Leyden jar; the surface of muscle was considered to be negatively charged, the inside of the muscle positively charged (see Galvani, 1953; Hoff, 1936; Rothschild, 1963).

In 1841 Matteucci found that the intact surface of muscle is electrically positive with respect to the cut end. An isolated muscle stimulated directly, or indirectly through its nerve, goes into a sustained contraction (tetanus). Emil DuBois-Reymond (1843, 1848, pp. 49–88) discovered that the *Muskelstrom* (current measured between the surface of muscle and its tendon) decreased during tetanus and he referred to this as *die negative Schwankung* or *negative variation*. It was later found that this negative variation also occurs in response to a single stimulation. DuBois-Reymond discovered a similar electrical potential in nerve. Since the muscle and nerve currents are largest after cutting or injury, they were called the *demarcation current* (or injury current) and their electrical potentials, the *demarcation potential* (or injury potential). The negative variation which propagates along the length of the cell is now called the *action potential*.

Galvani's suggestion that the outer surface of muscle was negatively charged and the muscle interior positively charged was incorrect, as later studies showed. DuBois-Reymond thought that muscle and nerve contain *electromotive molecules* which are arranged in an orderly fashion at the cell surface. This was known as the *preexistence theory*—that the potential was present in the intact muscle or nerve cell. DuBois-Reymond's student, Hermann (1879), on the other hand, thought that the demarcation potential originated from the cut surface of the cell. Hermann's theory was known as the *alteration theory*—that the demarcation current did not exist in the normal resting cell but was caused by injury.

2.2.2. Bernstein's Membrane Theory and the Diffusion Potential

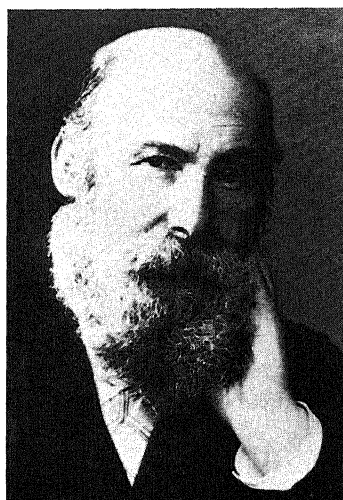
In 1890, Ostwald studied the selective ionic permeability of and the electrical potential across the copper ferrocyanide membrane; he suggested that muscle and nerve cell potentials, as well as the activity of the electric eel, might be due to similar semipermeable membranes at the surface of cells. This suggestion played an important role in the development of theories of the cellular potential.

In 1900 MacDonald, in his thesis "The Demarcation Current Considered as a Concentration Cell," presented the view that the internal structure of the nerve "is to all intents and purposes a stronger aqueous solution of electrolytes than is found in its superficial parts. . ." This thesis was supported by demonstrating an inverse relation between the magnitude of the demarcation potential and the logarithm of the external concentration of salt, since a similar relation exists in concentration cells. MacDonald showed that, if the initial potential in nerves is represented as ψ_0 , the potential measured in the presence of a salt of concentration $[p_n]$ is ψ_n . His data follow the equation

$$\psi_n = \psi_0 - k_1 \cdot \log \frac{k_2}{[p_n]} \quad (2.1)$$

where k_1 and k_2 are constants. MacDonald apparently was unaware of Ostwald's suggestion. Julius Bernstein, a student of von Helmholtz, took Ostwald's idea and developed it into a major theory of the cellular potential.

In his article "Untersuchungen zur Thermodynamik der bioelektrischen Ströme," published in 1902, Julius Bernstein proposed the *membrane theory* of the cellular electrical potential. Based on Pfeffer's observation of the semipermeability of plant cell membranes, Bernstein postulated a similar ionic semipermeability of the intact membranes of muscle and nerve. If the intact cell membrane (but not the cut end) is assumed



Julius Bernstein (1839–1917)

to be impermeable to anions, the demarcation potential becomes the algebraic sum of the two separate potentials. The diffusion potential at the injured end, ψ_{inj} , is, according to Nernst (1889),

$$\psi_{\text{inj}} = \frac{RT}{\mathcal{F}} \frac{u - v}{u + v} \ln \frac{C_{\text{in}}}{C_{\text{ex}}} \quad (2.2)$$

where R is the gas constant, T is the absolute temperature, \mathcal{F} is the Faraday constant, and u and v are the mobilities of cations and anions of salts whose concentrations inside and outside the cell are represented as C_{in} and C_{ex} , respectively. Assuming that the salt involved is a K salt (e.g., KH_2PO_4) one may replace $C_{\text{in}}/C_{\text{ex}}$ by $[\text{K}^+]_{\text{in}}/[\text{K}^+]_{\text{ex}}$ (where $[\text{K}^+]_{\text{in}}$ and $[\text{K}^+]_{\text{ex}}$ are the intracellular and extracellular K^+ concentrations, respectively), since these two ratios may be taken as equal:

$$\psi_{\text{inj}} = \frac{RT}{\mathcal{F}} \frac{u - v}{u + v} \ln \frac{[\text{K}^+]_{\text{in}}}{[\text{K}^+]_{\text{ex}}} \quad (2.3)$$

Assuming that the normal cell membrane is impermeable to anions, $v = 0$. The normal resting potential at the intact surface is

$$\psi = \frac{RT}{\mathcal{F}} \ln \frac{[\text{K}^+]_{\text{in}}}{[\text{K}^+]_{\text{ex}}} \quad (2.4)$$

The measured demarcation potential, ψ_d , is the sum of equations (2.3) and (2.4),

$$\psi_d = \frac{RT}{\mathcal{F}} \frac{2v}{u + v} \ln \frac{[\text{K}^+]_{\text{in}}}{[\text{K}^+]_{\text{ex}}} \quad (2.5)$$

In arriving at this equation, Bernstein assumed that the normal cell surface is impermeable to intracellular anions (and to Na^+). If u and v have approximately the same temperature coefficients, ψ_d should vary linearly with the absolute temperature. Within limits, Bernstein found this to be true. He later suggested (Bernstein, 1912) that the action potential during excitation originated from a propagated local increase of the membrane permeability due to a chemical change in the plasma membrane. Bernstein was, therefore, in favor of what was then known as the preexistence theory, i.e., that the electrolyte corresponding to $[\text{K}^+]$ existed in the intact cell.

2.2.3. The Cremer–Haber–Klemensiewicz Theory for Glass Electrodes

The copper ferrocyanide gel membrane was by no means the only model membrane that had played a role in the evolution of the theories of bioelectric potentials. Others included the glass membrane, the collodion membrane, and the oil layer.

Von Helmholtz (1881) studied the electrical potential generated by a glass membrane when it separates two aqueous solutions. Cremer (1906), citing Helmholtz's work, used glass as a model for the semipermeable living cell membrane and the generation of

of cellular electric potentials. Haber and Klemensiewicz (1909, 1911) combined the then well known observation that an activated region of a muscle cell is electrically negative in reference to the inactive parts and that acid is produced during muscle activity, and suggested that the plasma membrane of Pfeffer may indeed behave like a glass membrane, generating the cell resting and action potentials because of the differences in H^+ concentration between the intra- and extracellular phases. However, Haber and Klemensiewicz's main efforts were directed at understanding the mechanism of the glass electrode. They considered the glass to be a neutral insulator and the electric current to pass through the glass only via the water that the glass has imbibed. They considered three theoretical alternatives: In the first case the H^+ concentration in the glass is constant. Varying external H^+ concentration would affect the potential, ψ , according to the theory of Haber (1908):

$$\psi = \frac{RT}{\mathcal{F}} \ln \frac{[H^+]_I}{[H^+]_{II}} \quad (2.6)$$

where $[H^+]_I$ and $[H^+]_{II}$ are the H^+ concentrations in the acidic and alkaline phases. In the second case, the product of H^+ and OH^- concentration is constant; ψ persists but is much smaller. In the third case, the ionic mobility of H^+ in the glass phase and the diffusion potential generated within the glass are taken into consideration; the theoretical relation would predict deviation from the logarithmic relationship and the potential would exhibit maxima and minima with variation of H^+ concentration.

To test these theories Haber and Klemensiewicz experimented with bulbs made of soft Thüringer glass. Typically they filled the inside of the glass bulb with HCl or KCl solution and immersed the bulb first in HCl. NaOH (1 N) was then added drop by drop and the electrical potential recorded. The curves shown in Fig. 2.3 agree with the theoretical equation (2.6) derived on the assumption that the H^+ concentration in the glass is constant and that a diffusion potential inside the glass is nonexistent or trivial. Haber and Klemensiewicz also experimented with hard Jena glass, which exhibited a much smaller ψ than equation (2.6) predicted. They concluded that the chemical composition of the glass determines whether or not the full value of ψ is obtained.

It is also important to note that, although equations (2.6) and (2.4) are formally identical, they were based on different experimental events. In arriving at equation (2.4),

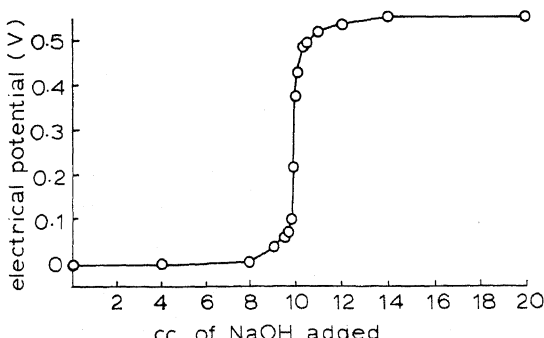


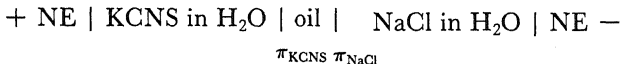
FIGURE 2.3. Changes of the glass electrode potential initially in HCl with the addition of increasing amounts of 1 N NaOH. [After Haber and Klemensiewicz (1909), by permission of *Zeitschrift fuer Physikalische Chemie*.]

ionic diffusion through the membrane is of foremost significance; in arriving at equation (2.6), diffusion through the membrane is of no importance. Nevertheless, the rationale behind equation (2.4) came to dominate physiologists' approach to the cell potential.

2.2.4. Phase Boundary Potentials and the Baur-Beutner Controversy

Nernst (1892) postulated that at the interface between two contiguous phases containing ions each ion (from the dissociation of a salt) has a *partition coefficient* between the two phases. Since the dissociated ions have different charges, the ion which has a higher partition coefficient between Phase 1 and Phase 2 will endow Phase 1 with its charge, positive or negative as the case may be. Nernst pointed out that the law of electroneutrality dictates that there be no net electric charge in either phase; in other words, in each phase the positive ions and negative ions occur in equivalent amounts. It is only at the phase boundary that a spatial separation of charges occurs, generating an electric double layer.

Beutner (1914, 1920, 1944) tried to apply Nernst's concept in his *phase boundary potential theory*, in which the cell membrane was considered to be in harmony with Overton's model of the cell membrane. An example of Beutner's oil-water phase boundary potential chain was

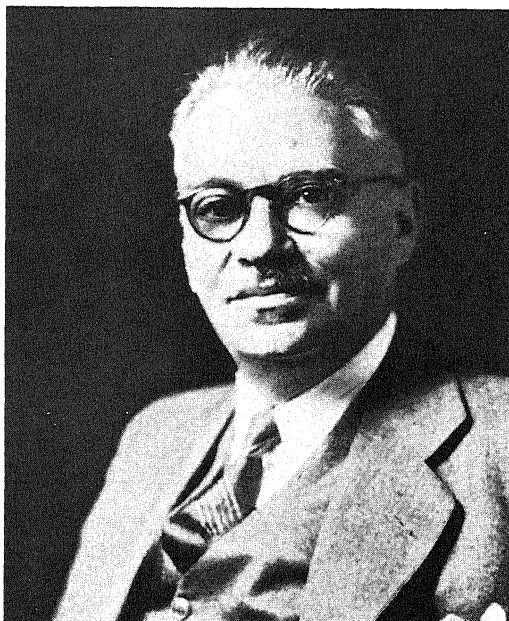


where +NE and NE— refer to the positive and negative nonpolarizable electrodes respectively. In this chain, there are two potential sources, π_{KCNS} and π_{NaCl} , at the two interfaces of the oil layer, each determined by the ionic partition coefficients postulated by Nernst. Beutner then wrote the equation for the total potential difference as

$$\pi_{\text{KCNS}} - \pi_{\text{NaCl}} = \frac{RT}{\mathcal{F}} \ln \frac{\alpha' C_{\text{KCNS, oil}}}{\alpha C_{\text{NaCl, oil}}} \quad (2.7)$$

where $C_{\text{KCNS, oil}}$ and $C_{\text{NaCl, oil}}$ are the concentrations of KCNS and NaCl in the oil phases and α' and α are their respective ionization constants. Thus, if KCNS has a greater partition coefficient in oil than does NaCl and if ionization constants are such that $\alpha' C_{\text{KCNS, oil}} > \alpha C_{\text{NaCl, oil}}$, the potential difference observed, $\pi_{\text{KCNS}} - \pi_{\text{NaCl}}$, would be positive.

It is my opinion that Beutner did not correctly understand and apply the concepts of Nernst and of Haber, even though Beutner's phase boundary potential theory has been cited as being derived from their work. For example, neither Nernst nor Haber concerned himself with the partition coefficients of the whole salt molecules—to which the terms C_{KCNS} and C_{NaCl} refer—or with the postulated high degree of ionization of the salt dissolved in the oil as the criterion for the creation of the potential. Yet this was the main theme of Beutner's theory. Thus in 1949 Beutner and Barnes argued that the structural specificities of the actions of drugs "are nothing more than additional factors determining lipid solubility and degree of ionization in the oil" (T. C. Barnes and



Leonor Michaelis (1875–1949)

Beutner, 1949). [Criticisms of Beutner's theory included those of Baur and Kronmann (1917) and Michaelis and Perlzweig (1927).]

Baur also used an oil phase as a model of the cell membrane, in this case as a "model of the electric organ of the fish" (Baur, 1913). Baur correctly extended the theory of Nernst and Haber in the sense that the key notion is the relatively higher uptake of one species of the ion over another by the oil phase, but only at the phase boundary. Baur referred to this as "adsorption." Baur's work will be discussed again in Section 4.6.1.2.

2.2.5. Michaelis's Theory of the Cation-Permeable Collodion Membrane

The collodion membrane was investigated extensively as a model of living membranes by Leonor Michaelis and his students in the 1920s. One recalls that by this time it had been clearly shown that K^+ plays a major role in the creation of the cellular resting potential (MacDonald, 1900). It also was known that the ionic concentrations inside and outside cells are roughly equal, though they exist largely as K^+ salts in the cell and as Na^+ salts outside the cell (J. A. Katz, 1896).

Table 2.1A, taken from Michaelis (1926), shows how a dried collodion membrane generates a transmembrane potential difference of 44–55 mV when there is a tenfold difference in concentration of a mono-, monovalent salt across the membrane. Since the side containing the lower concentration of salt is electrically positive, the membrane is, according to Michaelis, more permeable to the cations. The equation for this electrical

TABLE 2.1. Potential Difference (PD) across a Collodion Membrane Separating Solutions of Two Fixed but Tenfold Different Concentrations of the Same Salt (A) and of the Same Concentration (0.1 N) of Two Different Salts (B)^a

	A	B		PD (mV)
	PD (mV)	Solution I	Solution II	
HCl	54.8	KCl	HCl	-93
KCl	47	KCl	RbCl	-8
KI	48	KCl	NH ₄ Cl	-6
KBr	47	KCl	KCl	0
KNO ₃	45	KCl	NaCl	+48
K ₂ SO ₄	44	KCl	LiCl	+74
K ₂ CO ₃	48	HCl	RbCl	+87
K ₂ C ₂ O ₄	48	HCl	NaCl	+140
K ₂ Fe(CN) ₆	49	HCl	LiCl	+165
LiCl	45			
RbCl	49	KCl	KBr	-2
NH ₄ Cl	47	KCl	KI	0
		KCl	K ₂ SO ₄	-2
		KCl	K ₂ C ₂ O ₄	0
		KCl	K ₂ Fe(CN) ₆	0
		KCl	KOH	-2

^aFrom Michaelis (1926), by permission of *Naturwissenschaften*.

potential reduces to one equivalent to equation (2.4) if the membrane is permeable only to cations; in that case, for a tenfold difference in C_1 and C_2 at 25°C, a potential difference of 58 mV is predicted. Table 2.1B shows a collodion membrane separating different salt solutions of equal concentration. A potential difference appears only if the salts on the two sides have different cations but not if they have different anions, and seems especially relevant because a segregation of K⁺ and Na⁺ exists across living cell membranes.

Michaelis believed that the observed difference in potential in Table 2.1B arose from differences in the mobilities of the cations in the dried collodion membrane, which is permeable to cations but not to anions.

Based on these assumptions, Michaelis calculated the relative mobilities of cations in reference to that of K⁺. As shown in Table 2.2, these follow the same order as in dilute solution, but the differences between them become greatly exaggerated. The significance of the data in Table 2.2 rests upon the correctness of the underlying assumption, i.e., the potential arises from the different rates of diffusion of the ions through the membrane. Table 2.3, taken from Michaelis and Fujita (1926), shows actual measurements of the diffusion rate of H⁺, K⁺, and Cl⁻ through the dried collodion membrane. The results qualitatively confirmed Michaelis's assumption: H⁺ diffused faster than K⁺; both H⁺ and K⁺ diffused faster than Cl⁻. However, one also notes that it took many days for a minute amount of K⁺ to diffuse across the membrane, while the electrical potential measurements in the same membrane took no more than 15 min to reach a steady equilibrium value. This difference suggests that the relation between potential

TABLE 2.2. Ionic Mobilities in Collodion Membrane and in Free Solutions^{a,b}

	Li ⁺	Na ⁺	K ⁺	Rb ⁺	H ⁺
Relative mobility inside the membrane	0.048	0.14	1	2.8	42.5
Relative mobility of the same ions in free diffusion	0.52	0.65	1	1.04	4.9

^aMobilities in the membrane are calculated from the potentials, as measured in Table 2.1, assuming the potentials to arise from different mobilities of the ions through the membrane.

^bFrom Michaelis (1926), by permission of *Naturwissenschaften*.

and permeability is much less direct than Michaelis envisaged; this subject will be brought up again in Section 4.6.1.

Michaelis compared his dried collodion membrane with the glass membrane of Haber and Klemensiewicz, pointing out that both were impermeable to anions and both had their greatest permeability to H⁺. He concluded that the difference between Haber's soft glass, with ideal behavior toward H⁺, and hard glass, with less than ideal behavior, is that the soft glass has the narrowest pores, making the soft glass selectively permeable to H⁺ only, and not to anions, while the hard glass with larger pores is less selective.

Another important finding was that of Mond and Hoffman (1928). After exposure of collodion to the positively charged basic dye rhodamine B, the collodion membrane potential became selectively sensitive toward anions, in agreement with Michaelis's theory. However, the agreement is not complete, because the relative sensitivity of the potential to a series of anions did not follow the rank order of their mobilities, as the Michaelis theory predicted. Rather, the effectiveness of the anions in changing the potential followed the familiar Hofmeister lyotropic series, decreasing in the order SCN⁻ > NO₃⁻ > I⁻ > Br⁻ > Cl⁻ > CH₃COO⁻ > SO₄²⁻ (Table 2.4). The mobilities of these anions in water, however, follow the rank order Br⁻ > I⁻ > Cl⁻ > NO₃⁻ > SCN⁻ > CH₃COO⁻ (see *International Critical Tables*, 1929, p. 230, and *Tables Annuelles*, 1930, p. 837). Mond and Hoffman concluded that it was not possible to clarify this discrepancy, but their findings were ignored in the subsequent development of concepts of cell potentials until much later (see Section 4.6).

TABLE 2.3. High Permeability of Fully Dried Collodion Membrane to H⁺, Moderate Permeability to K⁺, and No Demonstrable Permeability to Cl⁻^{a,b}

Duration (days)	0.1 N HCl on side a			0.1 N KCl with methyl orange on side b			0.1 N HCl on side a			Distilled water with methyl orange on side b		
	1	2	3	1	2	3	1	2	3	1	2	3
1	Reddish	Reddish	Reddish	Yellow	Yellow	Yellow	Yellow	Yellow	Yellow	Yellow	Yellow	Yellow
2	Very clearly red	Very clearly red	Very clearly red	Yellow	Yellow	Yellow	Yellow	Yellow	Yellow	Yellow	Yellow	Yellow
8	Very clearly red	Very clearly red	Very clearly red	Trace of red	Somewhat red	Somewhat red	Yellow	Yellow	Yellow	Yellow	Yellow	Yellow
10	Very clearly red	Very clearly red	Very clearly red	Somewhat red	Somewhat red	Somewhat red	Yellow	Yellow	Yellow	Yellow	Yellow	Yellow
20	Very clearly red	Very clearly red	Very clearly red	Somewhat red	Somewhat red	Somewhat red	Trace of red	Trace of red	Trace of red	Trace of red	Trace of red	Trace of red
24	K demonstrable in HCl	K demonstrable in HCl	K demonstrable in HCl	Cl not demonstrable in water	Cl not demonstrable in water	Cl not demonstrable in water	Cl not demonstrable in water	Cl not demonstrable in water	Cl not demonstrable in water	Cl not demonstrable in water	Cl not demonstrable in water	Cl not demonstrable in water

^aPermeation to H⁺ was monitored by the change of color of methyl orange in the side (b) opposite from the compartment to which HCl was added (a). Results for experiments 1–3 in two triplicate series are given.

^bFrom Michaelis and Fujita (1926), by permission of *Biochemische Zeitschrift*.

TABLE 2.4. Dependence of the Electric Potential across a Rhodamine-Treated Collodion Membrane on the Anions in the Solutions on the Two Sides of the Membrane ^a

Solution 1	Solution 2	Potential difference (mV)
0.1 N NaCl	0.1N NaSCN	+ 60
0.1 N NaCl	0.1N NaNO ₃	+ 51
0.1 N NaCl	0.1N NaI	+ 33
0.1 N NaCl	0.1N NaBr	+ 20
0.1 N NaCl	0.1N NaCl	0
0.1 N NaCl	0.1N Na acetate	- 8

^aFrom Mond and Hoffman (1928), by permission of *Pflügers Archiv*.

2.2.6. The Donnan Theory of Membrane Equilibrium

Donnan (1911, 1924) analyzed the effect of a membrane which is impermeable to one ion (B^+) on the pattern of distribution of other permeant ions in the two phases (1 and 2) which are separated by the membrane.

In the case where the membrane is permeable to K^+ and Cl^- , he showed that, at equilibrium,

$$\frac{a_{K^+}^I}{a_{K^+}^{II}} = \frac{a_{Cl^-}^{II}}{a_{Cl^-}^I} = r \quad (2.8)$$

where $a_{K^+}^I$ and $a_{Cl^-}^{II}$ are, respectively, the activity of K^+ in Phase I and the activity of Cl^- in Phase II. The term r is referred to as the *Donnan ratio*. When the concentration of the ions is sufficiently low, the activity ratios can be replaced by the concentration ratios:

$$\frac{[K^+]^I}{[K^+]^{II}} = \frac{[Cl^-]^{II}}{[Cl^-]^I} = r \quad (2.9)$$

For the permeant i th cation (C_i) of valency n and the j th anion (A_j) of valency m , the more general expression is

$$\left(\frac{[a_{C_i}]^I}{[a_{C_i}]^{II}} \right)^{1/n} = \left(\frac{[a_{A_j}]^{II}}{[a_{A_j}]^I} \right)^{1/m} = r \quad (2.10)$$

The equation for the membrane potential in the Donnan model is

$$\psi = \frac{RT}{\mathcal{F}} \ln r \quad (2.11)$$

This equation is formally the same as equations (2.4) and (2.6).

The copper ferrocyanide membrane experiments of Donnan and his co-workers, as well as those of Ostwald, showed that these membranes are not impermeable to all

solutes, but are permeable to K^+ and Cl^- , for example. This corrected the prior misinterpretation that such membranes were perfectly semipermeable (i.e., permeable only to water). Like J. Bernstein's, Donnan's theory was inspired by the same work of Ostwald (1890).

The presence of the impermeant ion B^+ on one side of the membrane also demands an unequal number of diffusible ions in the two phases separated by the membrane so that electrical neutrality can be maintained. As a result, the side containing B^+ contains more osmotically active particles and movement of water into this phase will occur unless it is balanced by some other force, such as a hydrostatic pressure exerted by the elastic force of the semipermeable membrane.

2.2.6.1. *The Procter-Wilson Theory of Swelling*

Procter (1914) and Procter and Wilson (1916) explained the swelling of gelatin gel and collagen, which do not have a semipermeable membrane, on the basis of a broadened version of the Donnan membrane equilibrium. In this case electrically charged protein, immobilized by intermolecular bonds, serves as the equivalent of the impermeant ion. Net positive charges of the protein could be generated or, more correctly, liberated after treatment with HCl and after some H^+ combines with the negatively charged β - and γ -carboxyl groups of the protein. To balance the concentration of these (net) positive charges (equal to z), an equal concentration of Cl^- must remain in the collagen. As a result, the total Cl^- concentration is equal to $z + y$, where y is the concentration of free H^+ in the protein-containing phase. The concentrations of external H^+ and Cl^- must be equal and are represented as x .

At equilibrium, the chemical potentials of H^+Cl^- in the protein-containing phase and in the outside solution must be equal. One derives

$$y(y + z) = x^2 \quad (2.12)$$

In equation (2.12) the product of unequals is equated with the product of equals. It follows that the sum of the unequals is greater than the sum of the equals:

$$y + y + z > 2(x) \quad (2.13)$$

The excess of diffusible ion in the protein-containing phase is

$$e = 2y + z - 2x \quad (2.14)$$

This excess of anion produces a force, which J. A. Wilson (Wilson and Wilson, 1918) considered to be the basis for acid-induced swelling. In this theory, the increase in volume, V , is directly related to e by the relation

$$e = CV \quad (2.15)$$

where C is a constant, corresponding to the bulk modulus of the protein system.

The attractiveness of the Procter-Wilson concept can be seen from its ability to explain three well-recognized characteristics of acid-induced swelling:

1. As the acid concentration is increased, the net positive charge z increases, and as a result swelling increases. This continues until all the titratable groups are exhausted. Further increase of HCl can no longer increase z , but does increase x , which in turn reduces e . This predicts a maximum in the swelling of proteins. Experiments show that the increased volume of gelatin in HCl as a function of the external concentration of HCl (x) compares well with the theoretical curves presented by Procter and Wilson (1916).
2. The depressing effect of neutral salt on swelling is explained by an increase of x , which decreases e [equation (2.14)] and hence swelling.
3. The much greater swelling produced by monobasic acids (e.g., HCl, HNO₃) as compared with dibasic acids (e.g., H₂SO₄) also can be explained. Since the concentration of the sulfate ion is only one-half that of the monobasic acid, its concentration in the external solution is only $z/2$, and the concentration in the collagen is only $(y + z)/2$. The value of e [equation (2.14)] decreases, and hence less swelling is brought on by sulfuric acid than by HCl of equal pH.

Although Procter and his co-workers have treated the problem of gelatin swelling with considerable rigor and insight, several observations cannot be explained by their theory; only two of these will be discussed:

1. The first observation was definitely known to Procter and Wilson (1916): In the last paragraph of their paper, they raised the issue of the ability of neutral salt to suppress swelling in acid. They considered this to be due to a decrease in the value of e . But the lowest limit of e is zero, and, from equation (2.15), the change in volume, V , then is also zero. A swollen gel should remain unchanged in volume. Yet, as Procter described in his "method," high concentrations of salts actually dehydrate the gelatin and shrink it into "horny plates."
2. As pointed out by Kuntzel (1944) (see also Stiasny, 1931), neutral salts such as NaCl, effective in suppressing the swelling of gelatin (and collagen) in acid, fail to suppress the swelling of collagen in alkali. However, Na₂SO₄ markedly depresses this swelling.

2.2.6.2. Loeb's Studies of Swelling

Like Procter, Loeb extensively studied gelatin (and other proteins) as a solid gel, which was either enclosed in a collodion membrane bag or directly exposed to an external aqueous solution (J. Loeb, 1920–1921a,b). He showed that the H⁺ concentrations inside and outside the bag alone determine the measured electrical potential difference between the inside and outside of the gelatin-containing phase.

His extensive studies of swelling, osmotic pressure, viscosity, and membrane potentials were coordinated efforts that in broad outline supported Donnan's theory of membrane equilibrium, which can explain most if not all of these behaviors of protein systems. Nevertheless, a more careful study of his publications reveals discrepancies:

1. If swelling and membrane potentials both originate from the same cause, it is

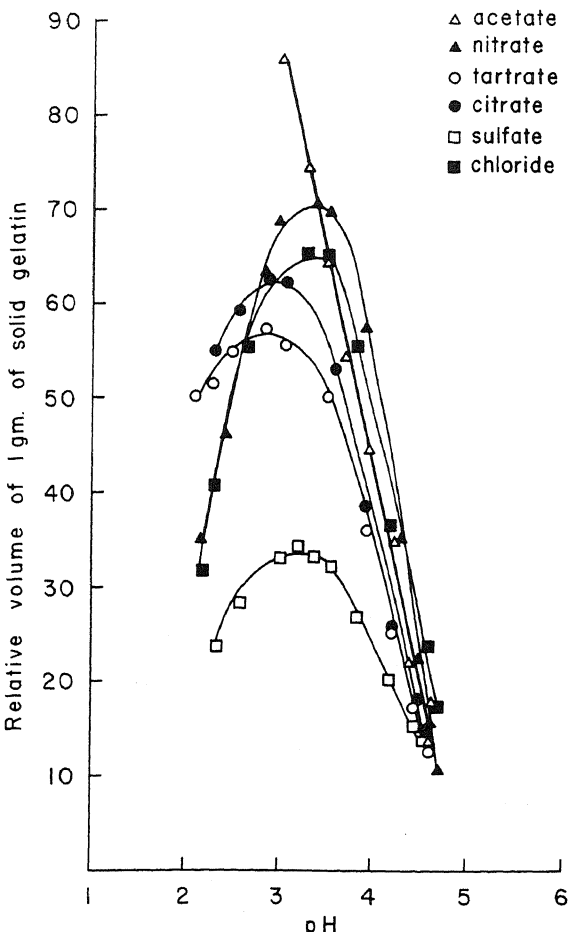


FIGURE 2.4. Influence of HCl, HNO₃, H₂SO₄, acetic acid, tartaric acid (divalent), and citric acid (trivalent) on the swelling of gelatin. [Data from J. Loeb (1920–1921a), by permission of *Journal of General Physiology*.]

difficult to see how the pH maxima of the membrane potential (3.7–4.1) and of swelling (3.2–3.3) (Fig. 2.4) differ considerably in the same gelatin preparation described in the same paper.

2. Loeb vigorously advocated the view that swelling of gelatin is dependent only on the valency of the anion of the acid used and that Hofmeister's series of specific ion effects on swelling is "erroneous and has never been confirmed." Yet if Loeb's own data, which were presented in separate graphs, are combined into one, as in Fig. 2.4, it is difficult to reach his conclusion. It would seem that a considerable specific anion effect does indeed exist (see also Table 2.4 from Mond and Hoffman, 1928, and Section 2.5.2).

2.2.6.3. Meyer and Sievers's Formulation of Charge-Selective Permeability

Meyer and Sievers (1936a,b) pointed out that a collodion membrane, such as that studied by Michaelis, contains fixed negative charges and an equivalent amount of free

cations. The interior of the membrane, therefore, satisfies the condition of a Donnan system. Meyer and Sievers derived a variety of interesting relationships. As an example they found that, if N_K and N_A are what they call "passage numbers" of a membrane, or the percentage of current carried by the cation and anion, respectively, and if u_K and u_A represent the mobility of the free cation and anion, then

$$\frac{N_K}{N_A} = \frac{u_K}{u_A} \cdot R \quad (2.16)$$

and

$$R = \frac{\sqrt{4C^2 + A^2} + A}{\sqrt{4C^2 + A^2} - A} \quad (2.17)$$

where C is the salt concentration outside the membrane and A is the concentration of fixed anion in the membrane. Equation (2.17) shows that R increases sharply with decrease of C and increase of A , as found experimentally. These theoretical considerations explain the high cation permeability and low anion permeability in the collodion membrane that was dried (high A), especially at low external salt concentrations. Meyer and Sievers noted that other factors would help determine the selectivity in the effect of ions on the membrane potential, including the size of the meshes of pores and the solubility of the ion in the membrane. Mesh size determines the relatively small effect of the large hydrated Li^+ , while the greater solubility of SCN^- in the membrane gives this anion its high rate of permeability through organic membranes (an observation they attributed to R. Höber).

2.3. Cellular Ionic Distribution in the Context of the Membrane Theory

Through the work of J. A. Katz (1896) and others (Urano, 1908; Fahr, 1909), it was recognized that living cells in general are rich in K^+ but poor in Na^+ . This phenomenon, and striking physiological actions of K^+ not shared by Na^+ , led Bayliss (1918, p. 217) to suggest a possible relation of these phenomena to the higher mobility of K^+ than of Na^+ . Mitchell, Wilson, and Stanton (1922) showed that Rb^+ and Cs^+ can replace K^+ in frog muscles; they suggested that K^+ uptake could be related to the fundamental electronic structure of K^+ and its hydration (see Lorenz, 1920; Born, 1920).

From studies of perfused frog legs, Mond and co-workers (Mond, 1927; Mond and Amson, 1928) concluded that resting frog muscle fibers are impermeable to all anions and to the cations Ca^{2+} , Li^+ , and Na^+ , but are permeable to K^+ and Cs^+ . They interpreted these data by postulating that the muscle fibers have membranes with narrow pores carrying fixed negative charges like Michaelis's dry collodion membranes, which, as mentioned in Section 2.2.5, are impermeable to anions in general and are much more permeable to K^+ , Rb^+ , and Cs^+ than to Li^+ and Na^+ .

Two other important contributions from the University of Kiel were: (1) Netter's recognition that K^+ (and H^+) distribution in muscle cells should follow the rules of the Donnan membrane equilibrium (Netter, 1928) and (2) Mond and Netter's theory

(1930) that the cell membrane is permeable to K^+ and other cations that are equal in size to or smaller than (hydrated) K^+ , but impermeable to ions equal in size to or larger than (hydrated) Na^+ .

2.3.1. Boyle and Conway's Theory of Membrane Potentials, Ionic Distribution, and Swelling

In 1941 the *Journal of Physiology* (London) published, as the opening article in its 100th volume, Boyle and Conway's "Potassium Accumulation in Muscle and Associated Changes." This paper dealt coherently with all three of the central problems of cell physiology: ion permeability and distribution, electrical potential, and volume regulation.

Boyle and Conway began with the observation that, in a high concentration of KCl, frog muscle gains large quantities of K^+ and Cl^- , without at the same time losing its ability to exclude Na^+ . The maintenance of the low Na^+ concentration in the muscle cell assures that the membrane remains physically intact. It was assumed that the membrane normally is not permeable to Na^+ . They clearly established that the frog muscle cell membrane is permeable to Cl^- , contrary to the universal assumption that it is not (Fenn, 1936; Mond and Amson, 1928). This finding made seemingly unnecessary, at least in its original form, the suggestion of Michaelis (1925) and Netter (1928) that the muscle cell membrane has negatively charged pores and therefore is impermeable to anions. Consequently, Boyle and Conway eliminated the idea of electric charges in the membrane pores but retained the sievelike property of the membrane. A single critical pore size would seem to explain not only the permeability to K^+ and H^+ , and the impermeability to Na^+ , Ca^{2+} , and Mg^{2+} , as Mond and Netter had earlier proposed, but also the permeability to some anions (e.g., Cl^-) but not to others (Table 2.5).



Edward J. Conway (1894–1968)

TABLE 2.5. Boyle-Conway Theory of the Segregation of Permeant and Impermeant Ions According to the Mobilities and Relative Diameters of Cations and Anions^a

	Velocities of ions under gradient of 1 V/cm or 0.5 V/cm for divalent ions				Relative ion diameters (diameter of K ⁺ = 1.00)			
	Cations		Anions		Cations		Anions	
Permeant ions	H ⁺	315.2	OH ⁻	173.8	H ⁺	0.20	OH ⁻	0.37
	Rb ⁺	67.5	Br ⁻	67.3	Rb ⁺	0.96	Br ⁻	0.96
	Cs ⁺	64.2	I ⁻	66.2	Cs ⁺	1.00	I ⁻	0.97
	NH ₄ ⁺	64.3	Cl ⁻	65.2	NH ₄ ⁺	1.00	Cl ⁻	0.98
	K ⁺	64.2	NO ₃ ⁻	61.6	K ⁺	1.00	NO ₃ ⁻	1.04
Impermeant ions	Na ⁺	43.2	CH ₃ COO ⁻	35.0	Na ⁺	1.49	CH ₃ COO ⁻	1.84
	Li ⁺	33.0	SO ₄ ²⁻	34.0	Li ⁺	1.95	SO ₄ ²⁻	1.89
	Ca ²⁺	25.5	HPO ₄ ²⁻	28	Ca ²⁺	2.51	HPO ₄ ²⁻	2.29
	Mg ²⁺	22.5			Mg ²⁺	2.84		

^aAfter Boyle and Conway (1941), by permission of *Journal of Physiology*.

Having theoretically sorted out the permeant ions from the impermeant ones, Boyle and Conway extended Donnan's theory of membrane equilibrium to explanations of the resting potential (ψ) and the cell volume (V). Their equation for the resting potential was simply Donnan's membrane potential equation [equation (2.11)]. Their equation for the volume of cell water, V , was based on the maintenance of macroscopic electro-neutrality, osmotic balance, and the basic equation of Donnan's membrane equilibrium. Taking into account the known concentrations of ions in frog muscles, various colloids, and colloidal ions and nonelectrolytes, they gave this simplified equation for the case where a wide variation of cell volume (V) accompanies a constant intracellular K⁺ concentration:

$$V = \frac{211}{c - 2[K^+]_{\text{ex}}} \quad (2.18)$$

where c is the total ionic concentration (in millimoles) in the external solution. As an approximation,

$$[K^+]_{\text{in}} = \frac{1}{2}c \quad (2.19)$$

Their results showed a fair concordance between theory and experiment in the cell water content, which rose with increasing substitution of NaCl in the Ringer solution by an isoosmotic equivalent of KCl. Since c is constant, their equations also predicted a constancy of [K⁺]_{in}; again the data appeared to be in agreement with theory.

Boyle and Conway also considered another case in which increasing external K⁺ is achieved by adding KCl while maintaining a normal concentration of NaCl. In this case, the cell volume should remain constant, and again [K⁺]_{in} = $\frac{1}{2}c$. At sufficiently high KCl concentration in the external fluid the other ions, like Ca²⁺ and Mg²⁺, can be ignored, and equation (2.19) simplifies to

$$[K^+]_{in} = [Na^+]_{ex} + [K^+]_{ex} \quad (2.20)$$

A plot of $[K^+]_{in}$ against increasing $[K^+]_{ex}$ should yield a straight line with a slope of unity and an intercept equal roughly to the constant $[Na^+]_{ex}$. This expectation was also confirmed. For intracellular Cl^- , Boyle and Conway derived the relation

$$[Cl^-]_{in} = \frac{2[K^+]_{ex}[Cl^-]_{ex}}{c} \quad (2.21)$$

Again at sufficiently high KCl concentration the concentration of external Cl^- is equal to $\frac{1}{2}c$, since the bulk of the extracellular anion is Cl^- due to KCl and NaCl. Therefore

$$[Cl^-]_{in} = [K^+]_{ex} \quad (2.22)$$

A plot of $[Cl^-]_{in}$ against increasing $[KCl]_{ex}$ should yield a straight line with a slope of unity and an intercept at the origin. Boyle and Conway again showed essential agreement of the experimental data with theoretical predictions.

Boyle and Conway's thesis dealt quantitatively with ion distribution, ion permeability, cell volume, and the cell potential, and was the final synthesis of all the knowledge that had accumulated by 1940 and been mustered under the basic heading of the membrane theory. It incorporated into a single, coherent theme the historical development of cell physiology since the observations of the Abbé Nollet and Galvani, and it is a landmark in man's quest to understand living things.

More important, however, is that their analysis justified the assumptions on which the membrane theory was based—that the interior of the cell, and the physical states of its water and ions, are essentially those of a dilute aqueous solution. Before describing the next dramatic development in the evolution of the membrane theory in Chapter 3, I will outline the bulk phase theories of the cell that existed in the early twentieth century, and then the reasons for their rejection by physiologists.

2.4. Early Criticisms of and Experimental Evidence against the Membrane Theory

In 1906 and in the years following, Moore, Roaf, and others (B. Moore, 1906; Moore and Roaf, 1908; Moore *et al.*, 1912) attacked the idea, propounded in Pfeffer's theory and experimentally supported by Hamburger's work on red blood cells (Hamburger, 1904), that the cell membrane is completely impermeable to ions like K^+ , Na^+ , PO_4^{3-} , and Cl^- . It was well known that these ions are asymmetrically distributed across the cell surface (J. A. Katz, 1896). Moore and his colleagues found it difficult to understand how a cell can contain a constant high concentration of K^+ and yet be covered by a membrane impermeable to this ion. Citing the accumulation of oxygen in erythrocytes and the selective accumulation of K^+ over Na^+ in soil colloids, Moore and Roaf suggested that "cell protoplasm combines or fixes in some chemical or physical way the potassium and phosphatic ions, while the plasma similarly holds the sodium and chlorine ions" (B. Moore and Roaf, 1908, p. 59).

M. H. Fischer and Suer (1935, 1938, 1939) also rejected the membrane theory in general and the lipoid membrane theory in particular, in these terms:

Overton's hypothesis of the lipoid element as an enveloping membrane of cells, too, falls away. Such a surface layer has never been seen, is not demonstrable analytically (tissues do not "grease" but "wet" a bibulous paper) and makes the life of all cells impossible (by preventing ingress or egress of water, of most of their foods, and of many of the products of their metabolism). [Fischer and Suer, 1938]

Lepeschkin's doubt about the validity of the membrane theory as proposed by Pfeffer was based on observations including the following:

Moreover, my experiment on *Bryopsis plumosa* showed that the surface of protoplasm can be increased 1,000 times without any change of the sharpness of its outlines.

As the movement of granules, near the surface of protoplasm, shows that the thickness of the liquid film covering the protoplasm could not be greater than 0.1 micron, the thickness of the liquid layer on the 1,000 times increased surface could not be greater than 0.0001 micron, that is the diameter of one hydrogen atom. [Lepeschkin, 1930, p. 275]

Kite (1913) microinjected solutions of different osmotic strengths, and a large variety of vital dyes, into many types of animal cells (various eggs, striated muscle, epidermal cells) and plant cells (five species of *Spirogyra*, *Hydrodictyon*, manubrial cells of *Chara*, leaves of *Elodia*, roots of *Vicia faba*, parenchyma cells of *Tradescantia*, yeasts). He discovered that distilled water or seawater injected into a variety of cells forms vacuoles which slowly disappear. A vacuole of hypertonic solution, however, grows in size, showing that the *naked* protoplasm exhibits osmotic activity in a way that the membrane theory sees as only the result of the presence of a semipermeable membrane. Kite also found, by puncturing and cutting *Asteria* eggs with fine glass needles, that acid dyes penetrate the swollen area near the cut to varying depths but never enter the normal unswollen cytoplasm. In his summary, Kite concluded that "impermeability or partial permeability to water, dyes, and crystalloids is a property of all portions of protoplasmic gels." Kite's finding reaffirmed a great deal of older observations by de Vries, von Nägeli, and others.

2.5. Inquiries into the Nature of Protoplasm

That the physical basis of life is protoplasm and that protoplasm, whether in plant or animal cells, is gelatinous in nature was universally acknowledged in the middle of the nineteenth century. While Pfeffer and others were propounding the membrane theory, stressing the microscopic plasma membrane, other biologists were more directly concerned with the study of protoplasm, often in the context of a colloidal material.

2.5.1. Protoplasm as a Structural Substance

If the surface envelope of a plant or protozoan is broken, the protoplasm can often flow or be squeezed out (Fig. 2.5). Furthermore these protoplasmic droplets respond to hypotonic solution by swelling (Lepeschkin, 1924), and to hypertonic solution by shrinking, an observation that led von Nägeli, de Vries, and others to conclude that protoplasm

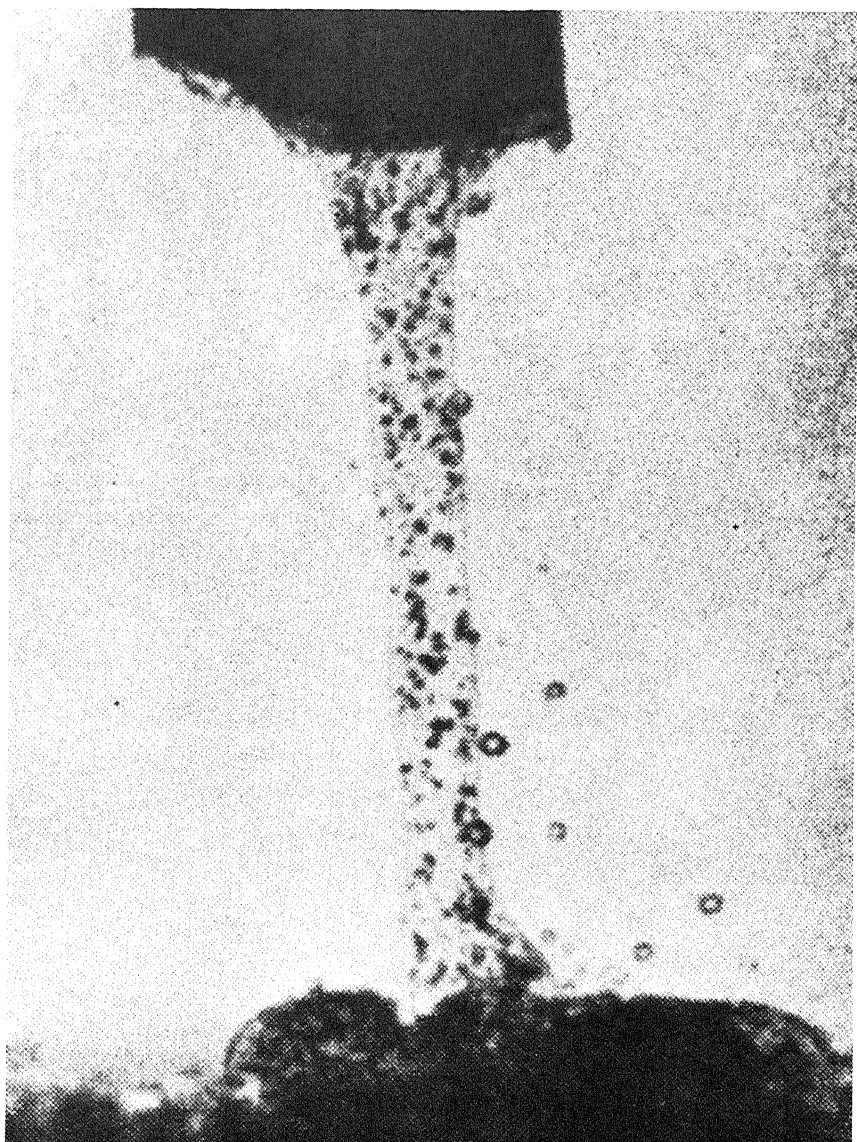


FIGURE 2.5. Outflow of cytoplasm from the cut end of a *Nitella* cell into an aqueous medium 5 min after amputation. Note air bubbles in the water. [From Kuroda (1964), by permission of Academic Press.]

is impermeable to salts (H. de Vries, 1871, 1885; Kite, 1913). The protoplasm thus isolated did not mix with the surrounding water but remained as discrete droplets (von Nägeli, 1855; Kühne, 1864; Pfeffer, 1877, 1921).

Otto Bütschli (1894), a contemporary of Pfeffer, was the first to propose that the apparently homogeneous protoplasm may have an underlying structure. In this view,

the physical separateness of the living cell from its environment is not due to the presence of a plasma membrane barrier, a barrier which in the days of light microscopy was not visible. Rather, Bütschli believed that living protoplasm was like a foam in which the more liquid components were dispersed in many microcells of a heavier consistency. Flemming (1882) suggested that protoplasm is a tangle of minute fibrils lying in a fluid matrix. Both Bütschli's foam theory and Flemming's fibrillar theory received what was then widely believed to be a fatal blow from the finding that albumin fixed in various fixatives can assume all sorts of artifactual filamentary or foamlike structures like those Bütschli and others had described (Hardy, 1899; A. Fischer, 1899).

2.5.2. Fischer's Theory of Protoplasm

Martin H. Fischer was a student and collaborator of W. Ostwald. Fischer and his co-workers (Fischer and Moore, 1907; Fischer, 1909, 1921; Fischer and Suer, 1935, 1938, 1939) believed that protoplasm is a hydrated colloidal system. Water in the protoplasm is not free but in a chemically combined form. Salts in protoplasm cannot be easily leached out and they too must be held in combination. Indeed Fischer and Suer (1938) suggested that protoplasm represents "a union of protein, salt and water in a giant molecule" and wrote that "this compound when made synthetically actually repeats the physical properties of living matter (its gelatinous feel, high electrical resistance, nonmiscibility with water and neutrality)." The "synthetic protoplasm" to which these authors referred is derived from casein (Fischer and Suer, 1935). Pure casein is hardly soluble in water or dilute salt solution. But if casein reacts with a small amount of alkali or acid, the acid- or base-caseinate formed is a homogeneous gel which on titration to neutrality will not precipitate out but remain in the transparent gel state



Martin H. Fischer (1879–1962)

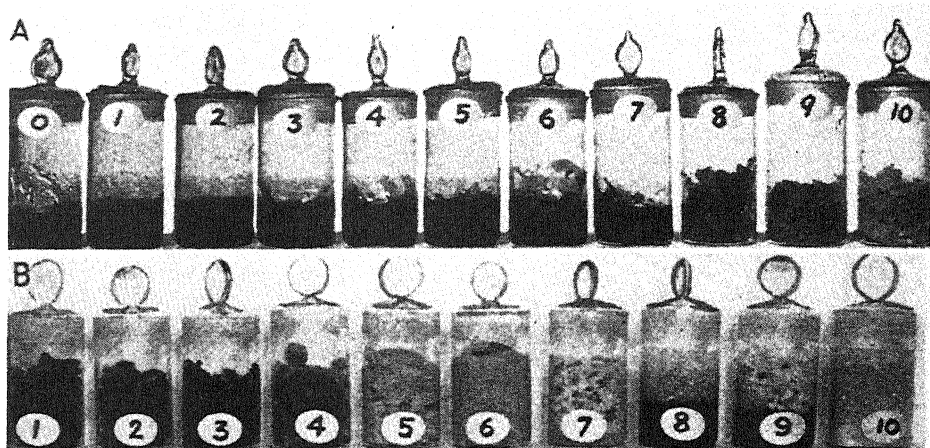


FIGURE 2.6. (A) Standard sodium caseinate to which increasing increments of hydrochloric acid have been added up to the point of complete neutralization of the base. (B) Standard potassium caseinate to which increasing increments of water have been added and then hydrochloric acid to the point of complete neutralization. Casein is definitely precipitated only in vessels 8, 9, and 10. [From M. H. Fischer and Suer (1935), by permission of *Archives of Pathology*.]

with the properties described above. Figure 2.6, from Fischer and Suer (1935), shows that, in the absence of an increase of total water content, progressive neutralization of casein does not cause precipitation. However, if neutralization is carried out in the presence of a large volume of water, casein does precipitate out. In the absence of excess water, therefore, the protein system exists as a triple compound of acid-casein-base.

Fischer's study stressed the basic similarity of the swelling of living tissues in water and salt solutions and the swelling of fibrin and gelatin (Fischer, 1908, 1909). The characteristics of swelling that Fischer found to be shared by both living and nonliving systems include the following:

1. They both swell more in acid than in distilled water; they swell more in some acids (e.g., HCl, HNO₃) than in others (e.g., H₂SO₄). Like the data shown in Fig. 2.4, Fischer's data indicate that the specific nature of the anionic component of acids with the same valency is very important in contradiction to the concept of swelling derived from the theory of Donnan.
2. Addition of salts reduces the degree of swelling produced by acid. The effectiveness of a salt in reducing swelling is the sum of the effectiveness of each of its ionic components.
3. Nonelectrolytes have much less or no ability to suppress the swelling induced by acid.

2.5.3. Lepeschkin's Vitaid Theory

In an address delivered at the dedication of a new botanical building at Wellesley College in 1928, Lepeschkin stated,

As is well known, living protoplasm possesses the so-called selective permeability. . . . the well-known German botanist, Pfeffer [proposed] twenty years ago that the surface of protoplasm is covered by a membrane, by the so-called "plasma membrane," which only possesses the selective permeability while the inside of protoplasm is as permeable to all substances as gelatine jelly. According to recently published investigations, Pfeffer's theory proved to be wrong; it was based on an incorrect interpretation of experiments. Protoplasm has no "plasma membrane" and all its parts possess the selective permeability.

Lepeschkin placed emphasis on lipoids as a major constituent of living protoplasm or *vitaid* (Lepeschkin, 1936) on the basis of experimental observations that included those made by Meyer (1901). Meyer noted that lipid-soluble and water-insoluble narcotics are readily taken up by living cells and suggested that lipoids must be present in them. M. H. Fischer and Suer (1938), on the other hand, did not accept lipoids as an important component of protoplasm, pointing out that many living cells contain hardly any lipoids at all.

2.5.4. Nasonov's Phase Theory of Permeability and Bioelectric Potentials

For a long time, owing to the language barrier, very little of the work of Dimitri N. Nasonov and his Russian co-workers was known to cell physiologists in other parts of the world. Nasonov began his career as a cytologist and once studied with E. B. Wilson at Columbia University. In his pursuit of understanding of cell physiology, he rarely wavered from a position in which he dealt with the cell as a whole, using simple, direct, and often highly original methods.

Nasonov opposed the membrane theory of cell permeability as well as the membrane theory of the cellular electric potential. Instead, like Fischer, Lepeschkin, and others, he believed that it is the bulk phase cytoplasm that is the seat of many physio-



Dimitri N. Nasonov (1895–1957)

logical phenomena. His *denaturation theory of excitation* emphasizes proteins as the central components in both physiological and nonphysiological activities of living cells (Nasonov, 1962). In support, he presented results from many interesting studies in which in response to electrical or other stimuli different parts of living cells exhibit changes in their vital dye-staining characteristics.

Nasonov and Aleksandrov (1944) compared the origins of the electrical potential according to the membrane theory and according to Nasonov's phase theory. Thus Nasonov states, "In the first place, the membrane theory assumes a difference in potential found in the resting cells. . . . According to our theory, the electromotive force arises only at the moment of injury or excitation. . . . In this respect our theory resembles the alteration theory of Hermann. . . ." (Nasonov, 1962, p. 178).

Nasonov also believed that "the main reason for the appearance of both action currents and resting currents is the release of electrolytes bound to proteins, and the loss of phase properties of protoplasm" (Nasonov, 1962, p. 194).

2.5.5. Bungenberg de Jong's Concept of Protoplasm as a Coacervate

It had been known for a long time that, under certain conditions in a mixture of hydrophobic colloids, a colloid-rich fluid layer separates out from the rest of the solution. This phenomenon was first observed in gelatin in response to neutral salt at 30°C by Pauli and Rona in 1902 (see also Spiro, 1903; McBain and Kellogg, 1928). H. G. Bungenberg de Jong and Kruyt (1929) gave this layer the name *coacervate* (Latin, *acer-vus* = aggregation), and divided coacervates into two large categories, simple and complex.

Figure 2.7, taken from Bungenberg de Jong's review article of 1932, shows complex coacervates of gelatin with both negatively charged gum arabic and negatively charged nucleic acid. The pH was kept low so that the gelatin would carry a net positive charge. Note that two kinds of coacervates are formed, and that only the gelatin-nucleic acid coacervate stains with the dye methyl green. Similar complex coacervates are formed between positively charged proteins and negatively charged proteins, lecithin, and carbohydrates.

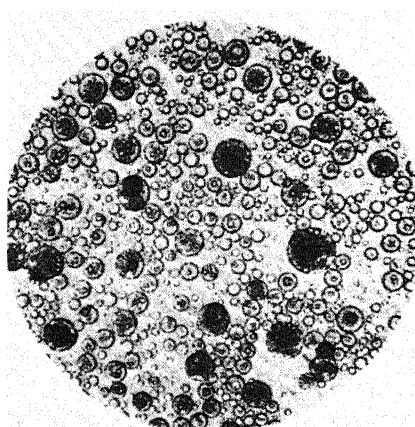


FIGURE 2.7. Complex coacervate of gelatin and gum arabic plus yeast nucleic acid. Two complex coacervates are formed: One contains gelatin and gum arabic; the other contains gelatin and nucleic acid. Only the latter stains with methyl green. Magnification 75 \times . [From Bungenberg de Jong (1932), by permission of *Protoplasma*.]



H. G. Bungenberg de Jong (1893–1977)

Bungenberg de Jong was not certain whether coacervates similar to these models constitute the entire cell or only a part of the living cell. Nevertheless he believed that coacervates must play an important role in biology. In support he quoted the following evidence:

1. Coacervates and living protoplasm are both fluid and yet immiscible with the surrounding fluid medium.
2. Vacuolization in coacervates can be brought about by a variety of circumstances (see Fig. 2.8). Vacuolization also is a common feature of living substances. (Indeed, as mentioned earlier, Dujardin recognized that the propensity for vacuolization is a main distinctive feature of protoplasm, or, in his terms, sarcode.)
3. Both living protoplasm and coacervates can take up oil droplets.
4. When coacervates are vigorously shaken, an air bubble appears in many of the droplets. The same was described for living protoplasm (see Verworn, 1922).
5. Coacervates have a tendency to engulf solid particles (e.g., coal, indigocarmine); cells have the same tendency.
6. Under certain circumstances coacervates can engulf pollen, erythrocytes, and *Euglena*. Similar behavior of certain types of living cells is of course well known.
7. The movement of living cells in a constant-current electric field resembles that of coacervates.

Bungenberg de Jong regarded coacervates as static models of living cells. He believed that the static models represent equilibrium models but that living cells represent states of "nonequilibrium." To maintain this state of nonequilibrium, the cells rely

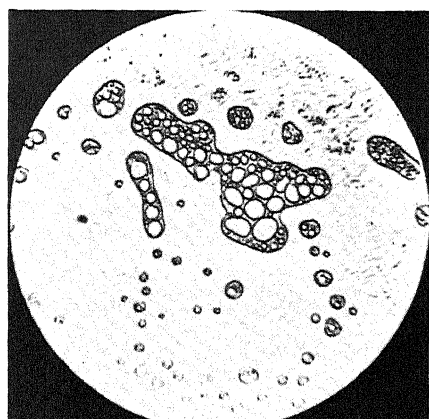


FIGURE 2.8. Vacuolization of a coacervate of iso-electric gelatin and resorcin. Magnification 110 \times . [From Bungenberg de Jong (1932), by permission of *Protoplasma*.]

on their membranes. Indeed this firm belief in the membrane theory distinguished Bungenberg de Jong throughout his career.

Bungenberg de Jong's view of the mechanism of coacervation is shown in Fig. 2.9: Sol particles form a dense shell of layers of solvent and then fuse to form a coacervate containing many sol particles within a common dense solvent shell.

2.6. Early Inquiries into the Physical State of Water and Ions in Living Cells

2.6.1. Bound Water

In Section 1.4, it was pointed out that Thomas Graham attributed the selective permeability of membranes of, for example, gelatin and parchment to water chemically bound within the substance and thus without normal solvent properties. Fischer and Suer and also Lepeschkin regarded protoplasmic water as bound in some way. The knowledge that biological materials strongly react with water could be traced to ancient

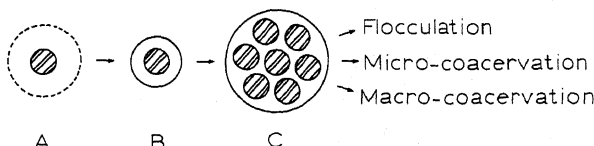


FIGURE 2.9. Schematic illustration of the mechanism of coacervation. (A) Sol particle with diffuse solvent shell. (B) Sol particle with dense solvent shell. (C) Sol particles with dense solvent shells fuse into a coacervate. The concrete boundary is only present at the boundary of the coacervate and its surrounding liquid. [From Bungenberg de Jong (1932), by permission of *Protoplasma*.]

times. The reaction of water with dried wood produces strong forces of expansion. Rocks used to build the pyramids in ancient Egypt were split in the quarries along the Nile Valley by hammering fire-dried wood into holes drilled into the rock and wetting the wood with water.

Colloid chemists called pressure created by water interaction of this kind *Quellungsdruck* (swelling pressure or *imbibition pressure*). It was repeatedly shown that imbibition pressure could far exceed osmotic pressure in magnitude. Examples include the following:

1. Seeds of the plant *Xanthium glubatum*, containing 8–9% of water, will take up water from a saturated solution of LiCl which has an osmotic pressure of 965 atm (Shull, 1913, 1924), although the salt content of the seed (if considered as totally free) is sufficient to account for only a few atmospheres of pressure.
2. Dried pig's bladder imbibes water from a saturated solution of NaCl, causing the salt to crystallize out (Ludwig, 1849).
3. Similarly, if a sheet of dried gelatin is placed in a saturated NaCl solution, NaCl will also crystallize out of solution (Gortner and Gortner, 1949, p. 237).

2.6.1.1. *Quellungsdruck and Quellungswasser*

It is interesting to note that the originator of the membrane theory, Wilhelm Pfeffer (1881, 1897), did not believe that the inside of a living cell is entirely filled with a simple aqueous solution. Indeed he was among the first to point out that *Quellungswasser* or swelling water could have accounted for the departure from osmotic behavior in plant materials that he and others had observed. F. Hofmeister (1891), Höber (1906, pp. 61, 62, and 70), and Overton (1902a) expressed similar views. In 1902, Overton concluded from his studies of osmotic behavior of frog muscle that the inside of the cell is not a simple solution but at least in part contains swelling water.

On the basis of this supposition, Overton explained the failure of muscle to swell in hypotonic solution to a level demanded by the Boyle–van't Hoff Law (Section 1.5) ($\pi V = \text{constant}$).

2.6.1.2. *The Nonsolvent Volume*

Hamburger (1904) found that red blood cells transferred from 0.9% to 1.5% NaCl became only 17.5% smaller. If this volume were inversely proportional to the external osmotic pressure, they should have become 40% smaller. However, if a certain volume of the cell occupied by lipids, proteins, and nucleic acids is not involved in the volume changes, then the Boyle–van't Hoff equation [equation (1.3)] should be modified to read

$$\pi(V - b) = \text{constant} \quad (2.23)$$

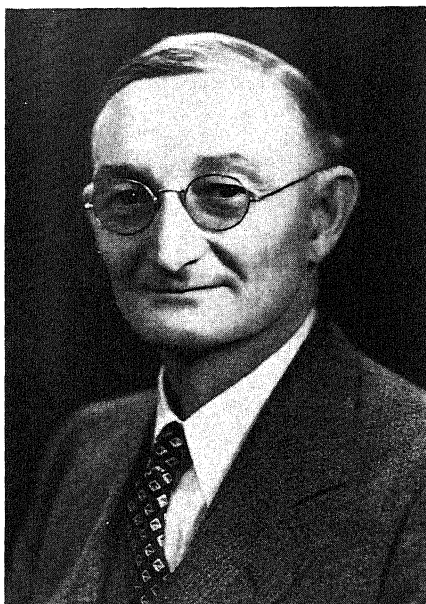
where b is the *nonsolvent volume* (its German equivalent expression *Nichtlösender Raum* was first introduced by Polanyi, 1920). Hamburger's calculation gave a value of b equal to 50–55% of the total cell volume, a figure not too different from the total solid

volume of the red blood cells. Kunitz (1927), however, suggested that the nonsolvent volume must also include water of hydration. Indeed, Overton (1902a) showed that, when frog sartorius was moved from 0.30% NaCl solution to 0.15% NaCl solution, the volume did not double. It increased by only one-third of its original value. This difference cannot be resolved by subtracting the dry matter, which is only 20% of the total volume. To explain the swelling actually observed b must include 50% of the cell water. It should also be noted that the extension of nonsolvent volume to include water implies that this water in effect behaves like lipids and other nonaqueous substances, occupying volume but not behaving like normal water in its interaction with solutes.

The physical basis of water having the property of complete solute exclusion was not addressed adequately by authors at that time, and the postulation of nonsolvent water remains an *ad hoc* one.

2.6.1.3. Demonstration of Bound Water by Measuring Colligative Properties of Colloidal Systems

In the 1920s and 1930s, a number of methods were developed in order to determine the amount of bound water in colloidal systems, including living cells (for review, see I. D. Jones and Gortner, 1932). In one, the amount of water that does not freeze at -20°C was considered to be bound water. In another, a known amount of a reference substance such as sucrose was added to the system and the vapor pressure or freezing point determined. Assuming that sucrose will not dissolve in the bound water, the freezing point or vapor pressure depression in excess of what could be expected if the entire



Ross A. Gortner (1885–1942)

system were simple liquid water then yields the volume of bound water (Newton and Gortner, 1922). A third, dilatometric method relied on the expansion of water during freezing (I. D. Jones and Gortner, 1932).

At a meeting of the Faraday Society, attended by some of the most prominent physical chemists of the time, Ross A. Gortner (1930) elaborated briefly on the possible mechanism of bound water. Citing the work of Keyes and Marshall (1927) on water vapor adsorption on charcoal and that of Nutting (1927) on water sorption on silica, Gortner pondered the possibility that the water bound by colloids may be in the form of multilayers. He added: "Unfortunately the properties of water in oriented adsorption films have not been sufficiently characterized to enable us to state whether or not this may be the type of water which the biologist is coming to call bound water." Most attending scientists were favorably impressed by Gortner's presentation. One notable exception was A. V. Hill, whose work will be presented subsequently.

2.6.2. Bound K⁺

Moore, Roaf, Fischer, Suer, and their co-workers did not believe that membrane impermeability could account for the pronounced accumulation of K⁺ and the exclusion of Na⁺ in living cells (Section 2.4). They envisaged some sort of chemical or physical binding of K⁺ in the protoplasm. Others shared this view.

Meigs and Ryan (1912; Meigs, 1912) studied the osmotic behavior of both voluntary and smooth muscle of the frog. They found that, while the voluntary muscle cells behaved as if they were covered with a semipermeable membrane impermeable to NaCl and sugars, the smooth muscle cells from the stomach exhibited no such impermeability.



E. Ernst (Ernst Jeno) (1895–1981)

TABLE 2.6. Potassium Content of Gastrocnemius Muscles Perfused with Solutions Containing 13.4 or 40 mM K⁺ and Stimulated Electrically to Contract^{a,b}

[K ⁺] in perfusion fluid (mM)	Weight of muscle (g)		K ⁺ content of muscle (mg)	
	U	S	U	S
13.4	2.34 ± 0.08	2.12 ± 0.07	6.33 ± 0.13	4.50 ± 0.39
40	2.39 ± 0.02	2.09 ± 0.04	8.89 ± 0.32	6.22 ± 0.14

^aU, unstimulated; S, stimulated (means ± SE).

^bData from Ernst (1963).

On the contrary, these cells appeared to be highly permeable to both sugars and salts. They concluded that smooth muscles are not covered with semipermeable membranes. To explain the continued selective accumulation of K⁺ in smooth muscle, they suggested that along with phosphorus, sulfur, and magnesium, K⁺ exists in the cell in a "nondiffusible form." In support of this idea they demonstrated that frog stomach muscles cut into small slices lose only a small fraction of their K⁺ (e.g., 5%).

Between 1924 and 1926 Neuschloss (1925, 1926) published a series of papers in which he showed that a fraction of K⁺ in muscle cannot be extracted with isotonic NaCl after the muscle has been minced. E. Ernst and his co-workers, beginning as early as 1925, strongly advocated the view that in resting frog muscle cells the major portion of K⁺ exists in an "indiffusible," "undissociated instead of ionic form." He also believed that during muscle activity potassium ions are released. Ernst and his co-workers presented a long list of evidence for indiffusible K⁺ both from their own work and that of others. This is well documented in Ernst's monograph, *Biophysics of the Striated Muscle* (1963). The earlier evidence included Ernst and Sheffer's (1928) finding that perfusion of frog gastrocnemius muscle with high-K⁺ Ringer solution caused the muscle to gain K⁺ if it was not stimulated. On the other hand, in the same environment, the muscle lost K⁺ to the perfusion fluid if it was stimulated directly (Table 2.6). Ernst and Sheffer argued that the bulk of the muscle K⁺ is nondiffusible but becomes diffusible in response to functional activity.

Thus far almost all the evidence suggested the possibility that K⁺ binding existed in muscle tissues. However, observations in other cell types led to a similar conclusion. Thus, Peters (1935), in order to account for the osmotic behavior of red blood cells, suggested that the potassium "salt" of hemoglobin in red blood cells probably exists largely in an unionized form.

2.7. Rejection of the Bulk Phase Theories

2.7.1. Evidence against the Bulk Phase Theories

The theories of Bütschli, Lepeschkin, and Fischer were directed against Pfeffer's membrane theory, in which the postulated cell membrane was considered to be *perfectly* semipermeable—permeable to water but not at all to electrolytes, sugars, or amino acids.

In their monograph *The Permeability of Living Cells* (1941) Brooks and Brooks dismissed the theories of Fisher, Lepeschkin, and others on the ground that water-soluble dyes and salts diffuse freely and rapidly within the cell. They argued for the spontaneous formation of a new semipermeable membrane on freshly exposed protoplasmic surface which prevents free intermixture of cytoplasm and surrounding solution (Heilbrunn, 1928; Costello, 1932; Reznikoff and Chambers, 1925). Some of the findings of Kite (Section 2.4), which contradicted these statements, were not mentioned. At that time, it was widely believed that the cut and exposed surface of cytoplasm rapidly regenerates a new cell membrane. However, it was not until many years later that methodology had evolved to a point that a definite experiment could be carried out to test this postulation (see Section 5.2.6).

That Brooks and Brooks were expressing a view that was widely accepted can be seen in the literature some 20 years later when R. Chambers and Chambers (1961) expressed their support of the membrane theory in these words:

At the protoplasmic surface is a water-immiscible surface film. . . . It separates the protoplasm aqueous phase from the external environment. . . . The presence of this film may be demonstrated by the fact that when non-coagulating aqueous solutions of the dyes which do not penetrate from outside the cell are micro-injected, they diffuse rapidly through the interior of the protoplasm, but, on coming into contact with the surface film, do not pass out into the external medium. [R. Chambers and Chambers, 1961, p. 9]

These observations are certainly true for a variety of cells. However it is worth noting that Kite (1913) and Ruhland (1912) both observed that many other cells were in fact readily permeable to externally added lipid-insoluble acid dyes.

2.7.2. Evidence against the Concepts of Bound K⁺ and Bound Water

From the foregoing, one realizes that the concepts that cell K⁺ and cell water are in some way bound have been repeatedly suggested but that they were not part of a coherent theory in the sense that the opposing membrane theories of Pfeffer, Overton, and Boyle and Conway were. It is therefore not altogether surprising that these bound K⁺ and bound water ideas, alongside the bulk phase or protoplasmic theories of the living cell, became all but extinct after the 1940s. It is recognized that, in clearing the way for the broad acceptance of the membrane theory, one scientist, Archibald V. Hill, wielded a most powerful influence through work published by him and his co-worker in two papers in 1930 (A. V. Hill, 1930; Hill and Kupalov, 1930).

In the first paper, "The State of Water in Muscle and Blood and the Osmotic Behavior of Muscle," Hill (1930) defined "free" water as the weight of water in 1 g of fluid or tissue which can dissolve substances added to it with a normal depression of vapor pressure. Hill pointed out that this is analogous to Gortner's definition (Gortner, 1929), substituting *vapor pressure* for *freezing point*.

To measure the "free" fraction of water in a fluid, a weighed quantity of urea was added to the fluid and its vapor pressure depression measured and compared with the vapor pressure depression produced by the same quantity of urea added to a similar volume of isotonic NaCl. With this method Hill showed that the "free" water is equal to virtually all the water in whole blood or separated red blood cells. Hill also studied



Archibald V. Hill (1886-1977)

casein (15% protein) and egg white (21% protein) and found that in these substances, too, the free water is virtually equal to the total water.

To determine the free water of muscle, Hill used two methods. In one he and his collaborators determined the equilibrium concentration of urea in muscle and compared it with that of the external solution; the data suggested that all water in muscle is free. In a second method, muscles were stirred in a double-strength Ringer solution ($2 \times R$) equal in weight to the water in the muscle. After equilibrium was reached, the vapor pressure of the outside solution was measured and was close to $1.5 \times$ that of normal Ringer solution. Again Hill concluded that little if any of the water is bound.

In these studies, however, Hill confirmed the finding of Overton that osmotic swelling or shrinkage does not agree with the assumption that all the water in muscle cells is free (Section 2.6.1.2). Hill explained this phenomenon by assuming that after prolonged soaking about 20% of the muscle cells have lost their semipermeable properties. Since dead cells could no longer respond to a change in osmotic activity, the behavior of these partially dead tissues gave the impression that a part of the water was osmotically inactive.

Having presented a strong argument that virtually all the cell water is free, Hill and Kupalov (1930) then turned to the question of whether or not intracellular K^+ is bound. To answer it they simply measured the vapor pressure of normal resting frog muscles. The value obtained was almost exactly equal to that of a simple salt solution containing all the ingredients of the muscle cells in their free state. Since the major component of this mixture is K^+ , they concluded that all or nearly all the muscle K^+ must be free. However, Hill and Kupalov also measured the vapor pressure of fatigued muscle and muscle in rigor. In each case, the measured vapor pressure was much higher

than anticipated on the basis of known chemical changes. This point was not further pursued.

In 1938, Otto Weismann presented a penetrating and objective analysis of the evidence cited for and against the bound water concept. The four basic colligative methods that Gortner, D. R. Briggs (1932), and co-workers had used were the freezing method, the calorimetric method, the dilatometric method, and the cryoscopic method, and all four involved freezing of water. Yet Weismann pointed out that ice formation varies not only with how low the temperature is, but also with the speed of the cooling process. Since these factors were not uniformly controlled, a large scatter and inconsistency were present in the data obtained, making it difficult to use these data to establish a difference between free and bound water. The Jones-Gortner cryoscopic method involved the addition of rather high concentrations of sugars and the complications and uncertainty concerning the amount of "bound" water of hydration due to these sugars made it difficult to either confirm or disprove that a certain fraction of water in plant cells is bound.

Weismann (1938) also criticized the chemical analysis method used by Walter (1923), whose data are reproduced here in Table 2.7. In these experiments, Walter added dry agar to solutions containing glucose, $MgSO_4$, or KSCN. Weismann pointed out that the data may indeed support the notion that there is bound water, since the concentrations of glucose and $MgSO_4$ went up as a result of interaction with agar. However, results with KSCN would indicate that there is a quantity of bound water less than zero, since the KSCN concentration in the solution actually went down! In hindsight, I want to point out that this high uptake of KSCN could very well be due to its adsorption onto agar (see Chapters 4 and 11)—a possibility that Weismann did not consider.

Ten years after Hill's paper, in a review entitled "Water, Free and Bound," Blanchard (1940) cited the work of Greenberg and Cohn (1934), who found that neither a 4% gelatin solution nor a 6% casein solution shows any significant tendency to exclude glucose from its water. Blanchard also cited the work of MacLeod and Ponder (1936), who showed that another molecular "probe," ethylene glycol, was equally distributed between erythrocytes and their external environment. These two sets of data confirmed Hill's main finding, reported earlier in muscle.

Blanchard pointed out that much of the freezing point depression data cited in support of the bound water concept could be more readily explained by a failure to reach equilibrium. In particular he noted that the criterion of failure to freeze at -20°C , used

TABLE 2.7. Influence of the Addition of Dry Agar on the Concentration of Various Solutes, as Measured by Freezing Point Depression^a

Dissolved materials	Influence on the swelling of agar according to Walter	Concentration (M)	Agar:water	Freezing point depression ($^{\circ}\text{C}$)	
				Before	After
Glucose	—	1.0	1:10	2.076	2.190
$MgSO_4$	—	0.5	1:10	0.884	0.980
KSCN	+	1.0	1:20	3.116	3.079

^aData from Walter (1923).

by Rubner (1922), Thoenes (1925), and others, cannot be cited as evidence that the water is in any way abnormal, since normal water in a volume as large as 8 cc can be supercooled to as low a temperature as -21°C (Dorsey, 1940).

Some thirty years later, Ernst, in his monograph *Biophysics of the Striated Muscle* (1963), recalled that Höber abruptly changed from a view in which he recognized and elaborated on the significance of *Schwellungswasser* (Höber, 1914) to one in which he considered the equilibrium water content of fresh muscle to be due to simple osmosis alone (Höber, 1945). Similarly Fenn (in Höber, 1945) and Buchthal (1947) abruptly changed their views in favor of the notion that muscle is "a simple osmotic system." Höber, Fenn, and Buchthal, major opinion-makers of the day, explicitly stated that their decisions were based on Hill's findings.

2.8. Summary

The first forty years of the twentieth century saw the development of a large number of model membranes with permeability and electrical properties having certain characteristics in common with cells. At the same time, a large number of workers developed concepts of protoplasm and believed that water and K^+ within it are more or less "bound." However, the evidence against bound cell water and K^+ , and especially the work of A. V. Hill, led to the widespread acceptance of the membrane theory.

Although Hill's experiments played a critical role in the rejection of the bulk phase or protoplasmic theories, one must emphasize that Hill only triggered a decision that was probably inevitable because of the much more primitive state of development of the bulk phase theories when compared with the membrane theory. In the form of Boyle and Conway's comprehensive model, the membrane theory and the Donnan equilibrium offered sophisticated quantitative explanations of many major cell functions, including selective ionic accumulation and exclusion, swelling and shrinkage, and the electrical potential.



The Emergence of the Steady-State Membrane Pump Concept

3.1. Major Developments Providing the Background for the Acceptance of the Membrane Pump Theory

3.1.1. The Disproof of the Original Equilibrium Membrane Theory

As outlined in Section 2.3.1, Boyle and Conway further developed the basic concepts of Traube and Donnan, but especially those of Netter and Mond, and offered for the first time a general theory for the asymmetrical ionic distribution of living cells. In this theory, small ions like K^+ and Cl^- distribute across the cell membrane according to a Donnan ratio r [equation (2.10)]; large ions like Na^+ are permanently and completely barred from entering or leaving the cell (Table 2.5). This absolute impermeability to Na^+ was in accord with a similar belief derived from studies in erythrocytes (Koeppen, 1897; Ege, 1922).

It was ironic that Boyle and Conway's theory should appear in print immediately following the development of the radioactive tracer technique, which, for the first time in history, permitted direct and accurate measurements of cellular permeability to ions. Almost simultaneously five independent studies proved that the cell membrane is not impermeable to Na^+ at all, thereby shaking the very foundation on which the Boyle-Conway theory was built.

Cohn and Cohn (1939) injected radioactive Na^+ -containing saline into dogs and assayed the labeled Na^+ content of the erythrocytes. Their data showed that the red cell membrane is permeable to Na^+ (Fig. 3.1). Hahn *et al.* (1939) found similar results in rabbits. Completely taken by surprise (see Brooks and Brooks, 1941, Preface), Brooks (1940) found that radioactively labeled Na^+ was very rapidly taken up by *Spirogyra* cells from a 5 mM NaCl solution, reaching a level in the cells ten times higher than that in the surrounding medium within only 15 sec (Fig. 3.2). Rapid accumulation of Na^+ (and K^+) was also demonstrated by Brooks (1940) in *Nitella* and in *Arbacia* eggs and *Amoeba proteus*. [The much slower entry of labeled ion into the sap in the central

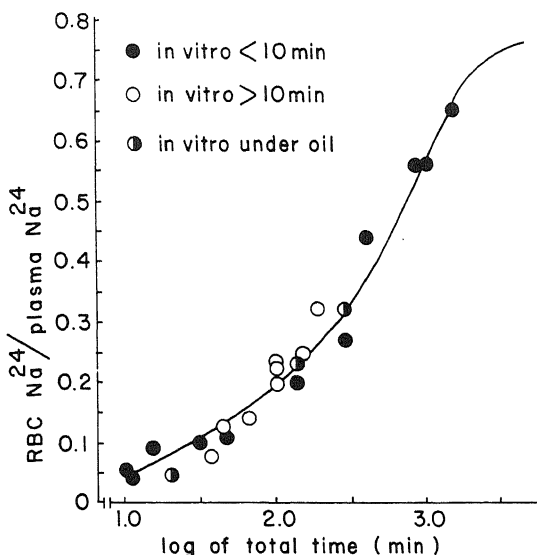


FIGURE 3.1. Permeation of $^{24}\text{Na}^+$ into dog red blood cells. [From Cohn and Cohn (1939), by permission of *Proceedings of the Society for Experimental Biology and Medicine*.]

vacuole of *Nitella*, also reported by Brooks, again pointed out the much lower permeability of the tonoplast compared to that of the outer surface of the cell, or plasma membrane, thus confirming the earlier conclusion that the osmotic behavior of plant cells reflected a semipermeability property of the tonoplast and not the plasma membrane (Section 1.6).]

Heppel (1939) found that the muscle of rats fed a K^+ -deficient diet lost a large amount of K^+ and at the same time underwent a twofold increase in Na^+ concentration. He showed that the gain of Na^+ in muscle must be intracellular since the total concentration of Na^+ far exceeds the total tissue Cl^- concentration, which sets the upper limit on extracellular space. Heppel (1940) then assayed the radioactive tracer $^{24}\text{Na}^+$ in muscle tissue. The time it took for the $^{24}\text{Na}^+$ content in muscles to reach a level such that its ratio to that in the plasma equaled a similar ratio for the total Na^+ was only 60 min (see Table 3.1). That K^+ deprivation and gain of cell Na^+ did not involve cell damage was shown by the complete reversibility of the process: When K^+ -deprived rats were fed a normal- K^+ diet, the muscles readily regained their usual concentrations of K^+ and Na^+ .

While Heppel was pursuing his *in vivo* studies of rat muscles, Burr Steinbach (1940a) carried out *in vitro* studies of isolated frog muscles. In these experiments Steinbach quite conclusively showed that muscles incubating in a low- K^+ Ringer solution

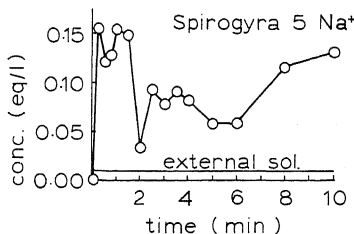


FIGURE 3.2. Concentration of radioactively labeled Na^+ in *Spirogyra* cells during the first 10 min of immersion in 0.005 M NaCl . [From Brooks (1940), by permission of *Cold Spring Harbor Symposia on Quantitative Biology*.]



Burr Steinbach (1905-1981)

lost K^+ and gained Na^+ . On being returned to a normal- K^+ Ringer solution, the muscles regained the K^+ and extruded the accumulated Na^+ (Table 3.2).

The experiments of Cohn and Cohn, Hahn *et al.*, Brooks, Heppel, and Steinbach left no doubt that the long-held belief that cell membranes are in general impermeable to Na^+ is wrong, thus undermining the membrane theory of selective ionic distribution, of volume control, and of cellular electrical potentials.

Equally important to recognize is the fact that, although all cells studied are permeable to Na^+ , the rate of exchange, as measured by the half-time of isotopic exchange,

TABLE 3.1. Penetration and Equilibration of $^{24}Na^+$ into K^+ -Depleted Muscles of Rats Fed a Low- K^+ Diet for 34-44 Days^a

Time between injecting ^{24}Na solution and sacrifice of animal (min)	$\frac{^{24}Na \text{ in muscle}}{^{24}Na \text{ in serum}}$	$\frac{Na^+ \text{ in muscle}}{Na^+ \text{ serum}}$
	$(\frac{\text{cpm/g}}{\text{cpm/g}} \times 100)$	$(\frac{\text{mmoles/kg}}{\text{mmoles/kg}} \times 100)$
5	14	39.2
10	17	23.5
10	15	26.8
20	23	36.4
31	31	34.4
60	33	32.7
60	28	35.0
182	38	31.1
187	38	41.2
215	32	30.2
260	33	32.6

^aData from Heppel (1940).

TABLE 3.2. Exchange of K^+ and Na^+ in Frog Muscle, Showing its Ability to Gain Na^+ and Then Replace it with K^+ ^{a,b}

Condition	Ion concentration (mEq % wet weight)	
	Na^+	K^+
In K^+ -free Ringer solution for 17 hr	5.04 (4)	3.44 (8)
In K^+ -free Ringer solution for 17 hr, then in K^+ -containing Ringer solution (0.01 N K^+) for 6-8 hr	4.04 (4)	4.99 (8)

^aMeans of indicated number of separate analyses.

^bData from Steinbach (1940a).

varied from seconds to many hours. This great divergence in ionic permeability is not readily compatible with a belief that all living cells share a very similar membrane—an assumption implicit in Overton's lipoidal membrane theory, already extant, and in Robertson's unit membrane concept, yet to come (Section 12.1).

Before discussing the immediate responses of those intimately associated with these new discoveries, it is worthwhile to ask what alternative hypotheses may have existed. Indeed, to explain the unequal distribution between two contiguous phases of a solute that, like Na^+ , does not follow a Donnan electrochemical equilibrium, there are only three basic mechanisms: (1) the presence of an insurmountable energy barrier between the two phases, (2) a difference in the bulk phase physicochemical environments in the two phases, and (3) the continual operation of a pump. Pfeffer's original interpretation, now disproven, was based on mechanism (1). So only two general categories were left; one or both must offer the right answer. Donnan's theory of equilibrium ionic distribution, described in Section 2.2.6, represents one variant of mechanism (2); other variants of mechanism (2) include those suggested by Moore, Roaf, Fischer, and Suer, as described in Sections 2.4 and 2.5.2.

Brooks (1940) suggested that the phenomena observed are ion exchange phenomena. He was therefore definitely leaning toward mechanism (2) (see also Brooks and Brooks, 1941), in spite of his criticism of similar views expressed earlier by Fischer, Moore, and others. Unfortunately Brooks died not too long afterward. Steinbach also was explicitly in favor of the bulk phase mechanism, pointing out that selective ionic accumulation probably has little to do with cell membranes but more to do with cytoplasm (Steinbach, 1940b). In 1946, Conway too presented calculations suggesting that muscle cells do not have enough energy to operate a Na^+ pump. This conclusion, though not the details of the data that led to the conclusion, was later confirmed (Ling, 1952). Yet, in less than 10 years, Conway went ahead and produced the theory of just such a Na^+ pump (Conway, 1955). He never gave an explicit explanation for abandoning his earlier view of 1946. Nor did Steinbach's turn toward a bulk phase mechanism long survive his 1940 publication. Powerful forces soon propelled the membrane pump model based on mechanism (3) mentioned above to a status of dominance. While I realize that probably no one can accurately tell the whole story, I believe that the events described on the following pages were likely to have played key roles.

In addition to these events, the then widely held opinion that the colloidal concepts of bound K⁺ and bound water had already been disproven (Section 2.7) also had a strong impact. Still other scientific developments provided fertile soil for the concept that cells are kept alive by some sort of continual metabolic effort to forestall their tendency toward increasing entropy.

3.1.2. The Concept That the Constituents of Living Beings Are in a State of Dynamic Equilibrium

What am I, Life? a thing of watery salt,
Held in cohesion by unresting cells....

—MASEFIELD

These lines decorated the front page of R. S. Lillie's monograph, *Protoplasmic Action and Nervous Action* (1923). They also might have inspired the title of R. W. Gerard's popular book, *The Unresting Cell* (1940). It was this book that first introduced me to Gerard's broad concepts of cell physiology and played a role in my coming to the United States to study with him as a graduate student. The ceaseless activity of the living process was then a central theme of cell physiology, and a concept that received great support from work like that of Schoenheimer.

The availability of both radioactive and nonradioactive isotopes brought new dimensions to biochemical methodology. Using ¹⁵N labels Schoenheimer (1942) and co-workers demonstrated how the elemental compositions of body parts are not stable but are in a state of constant flux or *dynamic equilibrium*. A dramatic and picturesque illustration of this concept was the comparison of living systems with the flame of a candle in a quiet atmosphere. The flame maintains a characteristic shape and other distinctive properties just as living beings do, even though the elemental composition of the flame at any one moment is different. These findings favored the introduction of the pump concept, according to which ions, being also constituents of living cells like nitrogen, must also be in a state of dynamic flux, sustained by energy-yielding metabolic activities.

3.1.3. The Hill–Embden Controversy and “A-lactic Acid” Muscle Contraction

A. V. Hill's powerful influence in the rejection of the concepts of bound water and K⁺ has already been discussed. In addition, Hill had long advocated the concept that muscle contraction is initiated by the production of lactic acid. In 1922, Hill and Otto Meyerhof received the Nobel prize for physiology and medicine “for the discovery of the fixed relation between the consumption of oxygen and the metabolism of lactic acid in muscle” (Nobel Foundation, 1965). Gustav Embden, a student of the Czech physiologist Franz Hofmeister, strongly objected to Hill's lactic acid theory of muscle contraction because Embden believed that he could demonstrate that lactic acid production actually followed rather than preceded muscular contraction (Emden *et al.*, 1926).

Then Einar Lundsgaard (1930) appeared on the scene. He claimed that, under the action of the poison iodoacetic acid, frog muscle could continue to contract many times in the total absence of lactic acid production. Hill and Meyerhof promptly repeated and

confirmed Lundsgaard's finding. In an article entitled "The Revolution in Muscle Physiology," Hill (1932) conceded his error with grace and generosity in the following words:

I admit that a page or two of theory in the text books will have to be rewritten: most, however, of the facts can remain. And in casting out the old Vorstellungen, whosoever they are, let us treat them kindly, for they deserve our gratitude for leading us, perhaps by a devious road and over unexpected obstacles, to the new knowledge.

The completion of this important transition—with a minimum of wasted energy and time, largely due to A. V. Hill's generosity and dedication to science—heralded one of the most brilliant phases of biochemistry—the recognition of the key role of the final metabolic product, adenosine triphosphate.

3.1.4. The High-Energy Phosphate Bond as the Immediate Source of Energy for Biological Work Performance, Including Ionic Pumping

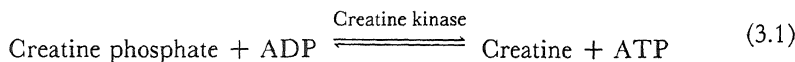
The discovery of "a-lactic acid" contraction not only clearly established that lactic acid production does not initiate muscle contraction, but also made clear the important role of creatine phosphate. After the independent discovery of this compound in muscle tissue by Fiske and Subbarow (1929) and by P. Eggleton and Eggleton (1927), these workers found that after an intensive burst of contraction the level of phosphocreatine in muscle dropped to a low level. In the presence of oxygen, the normal level of phosphocreatine is soon restored by oxidative metabolism. Nachmansohn (1928) demonstrated that creatine phosphate can be regenerated in the absence of oxygen by anaerobic glycolysis, a process which (instead of converting glucose or glycogen to CO_2 and H_2O , as in aerobic metabolism) produces lactic acid, as Fletcher and Hopkins demonstrated in 1907.

Blocking of respiration is easily achieved by anoxia, i.e., exposure of cells to pure nitrogen. Lundsgaard's discovery that iodoacetate (IAA) blocks glycolysis permitted an effective suppression of both potential sources of regeneration of creatine phosphate by the combined actions of IAA and pure nitrogen. Under these conditions, Lundsgaard showed that muscle could still undergo perfectly normal contractions. But with each contraction a certain amount of the limited store of creatine phosphate is used up, until its level finally approaches zero. As this state is approached, the muscle becomes less and less able to go back to the normal relaxed state after each contraction, until finally it enters a permanent state of shortening or rigor mortis.

These findings provided the background for the introduction of the concept of the high-energy phosphate bond. Mechanical work performed by the muscle during its reversible contractions must ultimately derive its energy from the food materials the animal consumes. The contraction of muscle under anoxia and IAA shows that a more immediate source of energy is creatine phosphate. Since, to perform its role, each creatine phosphate molecule splits into its constituent parts, one creatine and one phosphate, it seemed most reasonable to suppose that it was the bond that holds these two components together that "contains" and "stores" the energy originally derived from glucose or other food materials. And so the high-energy phosphate bond concept was launched.

After the recognition of the role of creatine phosphate in muscle contraction, Loh-

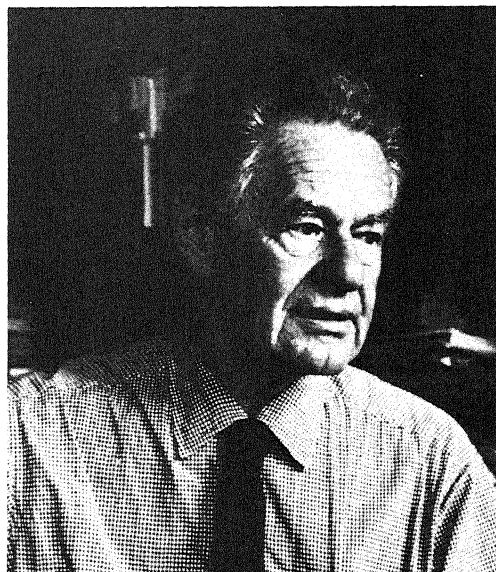
mann (1935) discovered adenosine triphosphate (ATP) and the important reaction which was to bear his name, catalyzed by the enzyme creatine kinase:



The Lohmann reaction is the only way for creatine phosphate to be synthesized, and also the only way for it to break down in living cells. This knowledge pointed to ATP as an even closer source of energy for muscular contraction. Indeed energy stored in its "high-energy" phosphate bonds was suggested to be the immediate source of energy for biological work performance, including "osmotic" work or ionic pumping (Lipmann, 1941).

The high-energy phosphate bond concept was elaborated by Fritz Lipmann (1941). This theory proposes that free energy made available in metabolic reactions is stored in the form of energy-rich phosphate bonds, represented as $\sim\text{P}$ to distinguish them from ordinary low-energy phosphate bonds, $-\text{P}$. $\sim\text{P}$ was believed to be present in, for example, polyphosphate esters, acetyl phosphate, enol phosphate, and amine phosphate, and its free energy could be released and utilized upon the hydrolysis of these bonds.

The initial experimental foundation of this theory was the calorimetric measurements of the heat of hydrolysis of ATP and other phosphates by Meyerhof and his co-workers in the 1920s-1930s. The enthalpy (ΔH) measured for ATP and creatine phos-



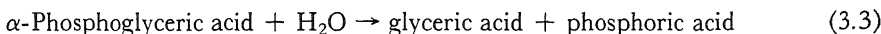
Fritz Lipmann

phate was about -12 kcal/mole. Assuming the entropy of hydrolysis (ΔS) to be small, Meyerhof concluded that the free energy of hydrolysis (ΔF), where

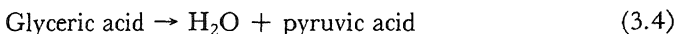
$$\Delta F = \Delta H - T\Delta S \quad (3.2)$$

is also about -12 kcal/mole.

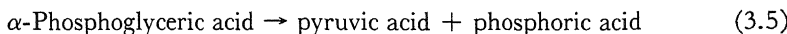
In later years a second approach was taken to assess the free energy change associated with the hydrolysis of $\sim P$, that of choosing appropriate sets of reactions, which, when added together, produced the ΔF being sought. One such reaction pair is that shown as equations (3.3) and (3.4). When the reactions are added together "algebraically," a reaction accompanied by a single $\sim P$ hydrolysis is obtained [equation (3.5)]. Thus,



and



combined to yield



The experimentally measured ΔF of reaction (3.3) was employed, while ΔF for reaction (3.4) was calculated indirectly from bond combustion values and the standard entropies of contributing atoms. The value of ΔF for the $\sim P$ bond thus calculated was approximately -11 kcal/mole, in good agreement with the expectation that the phosphate bond in α -phosphoglyceric acid would be "energy-rich."

3.2. The Postulation of the Na^+ Pump

Overton (1907) suggested that the operation of an "adenoid" or secretory activity within the cell membrane transported essential ingredients that are not soluble in the lipid membrane into the cells. Lillie, in his monograph *Protoplasmic Action and Nervous Action* (1923), discussed specifically how Na^+ could be kept at such a low concentration in muscle cells. He suggested that "either the salts do not diffuse across the membrane, or some active physiological factor is at work which opposes or compensates the effect of diffusion and maintains the salt content of the protoplasm at a certain norm" (p. 117).

In 1932, Steward more explicitly expressed the view of a metabolism-driven energy-consuming accumulation of salt ions in plant cells. Lundegårdh also proposed a respiration-driven anion-pumping mechanism (see Lundegårdh and Burström, 1935).

In 1941, in an article entitled "Theories of Electrolyte Equilibrium in Muscle," R. B. Dean discussed the theories of Mond and Netter and of Boyle and Conway, both of which rested on the by then disproven assumption of an absolute impermeability of

the muscle cell membrane toward Na^+ . Dean then said what must have been on minds of many scientists, including Lillie—that the difficulty generated by this new knowledge could be resolved by a Na^+ pump which continually pumps Na^+ out of the cells. K^+ in this case would still accumulate in the cells according to the Donnan equilibrium as specifically adapted to living cells by Netter (1928) and Boyle and Conway (1941).

3.3. Arguments and Evidence in Support of the Na^+ Pump Theory

3.3.1. The Dependence of Ionic Distribution on Continued Metabolic Activities and Normal Temperature

If ion accumulation and exclusion depend on continual pumping, the levels of ions in the cell should be dependent on metabolism. Evidence confirming this expectation was found in a number of cells and tissues (Lundegårdh and Burström, 1935; Steward and Harrison, 1939; R. B. Dean, 1940; J. F. Harris, 1941; Wilbrandt, 1940; Mullins, 1942; Scott and Hayward, 1953a; Hoagland and Broyer, 1942). Sensitivity of ion accumulation and exclusion to cooling also would be expected on the basis of the pump model, because inward leakage, a diffusion process, has a low temperature coefficient, while metabolic pumping, a chemical process, may be expected to have a high temperature coefficient. In agreement with this hypothesis, cooling causes loss of K^+ and gain of Na^+ in a variety of plant and animal tissues (Hoagland *et al.*, 1926; Steward, 1932; Hoagland and Broyer, 1936; Brues *et al.*, 1946; Scott and Hayward, 1953b) (see also Section 11.2.3).

3.3.2. The Energy Requirement of the Na^+ Pump Appears to Be Adequately Met by Cell Metabolism

In 1946, Conway published a brief article attacking the Na^+ pump concept because it would consume too much energy (Section 3.1.1). However, the rate of Na^+ pumping that Conway used in his calculation was subject to criticism. Two years later, Levi and Ussing (1948) reported for the first time a study of labeled Na^+ efflux from an isolated normal frog sartorius muscle at room temperature. Their results (Fig. 3.3) showed that the Na^+ efflux curves can be resolved into two fractions. The faster fractions, with a half-time of exchange ($t_{1/2}$) of about 2 min, was assigned to labeled Na^+ trapped in the extracellular space; the slower fraction, with $t_{1/2}$ equal to about 34 min, was assumed to be intracellular Na^+ whose efflux is rate-limited by cell membrane permeability. Based on these assumptions, Levi and Ussing made an estimate of the energy requirement of the Na^+ pump. They noted that the electrical potential is negative inside, so that both it and the Na^+ concentration gradient are oriented in such a direction that free outward diffusion of Na^+ is negligible. Therefore, in their subsequent calculations, they could assume that the entire outward flux, F_{outw} , in moles/kg·hr, is due to pumping, and

$$F_{\text{outw}} = -k_{\text{outw}}[\text{Na}^+]_{\text{in}} \quad (3.6)$$

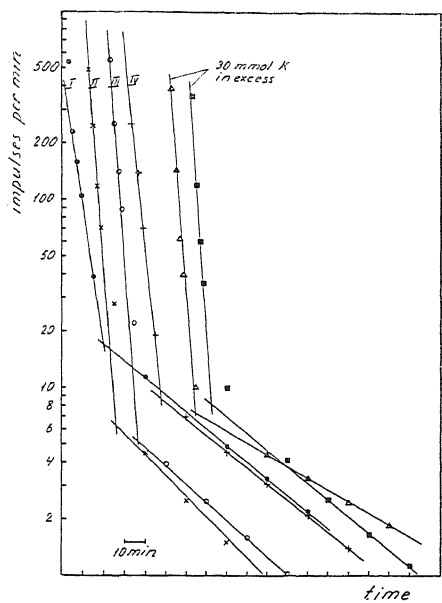


FIGURE 3.3. $^{24}\text{Na}^+$ efflux from an isolated frog sartorius muscle. Medium K^+ was 2.5 mM except in the two experiments marked "30 mmol K in excess." [From Levi and Ussing (1948), by permission of *Acta Physiologica Scandinavica.*]

where k_{outw} in hr^{-1} is the outward exchange constant that can be calculated from the $t_{1/2}$ by the relation

$$k_{\text{outw}} = \frac{\ln 2}{t_{1/2}} \quad (3.7)$$

The $t_{1/2}$ of Na^+ efflux averaged 34 min in cells incubated both in normal Ringer solution (containing 2.5 mM K^+) and in K^+ -rich Ringer solution (containing 32.5 mM K^+) (Fig. 3.3), so that under both conditions $k_{\text{outw}} = 1.22 \text{ hr}^{-1}$.

The rate of energy consumption by the Na^+ pump is then the outward flux rate (F_{outw}) multiplied by the electrochemical potential difference, $\Delta\bar{\mu}_{\text{Na}}$. The electrical potential is given by $[\text{K}^+]_{\text{in}}/[\text{K}^+]_{\text{ex}}$, and the concentration potential by $[\text{Na}^+]_{\text{ex}}/[\text{Na}^+]_{\text{in}}$, so that

$$\Delta\bar{\mu}_{\text{Na}} = RT \ln \left(\frac{[\text{K}^+]_{\text{in}}}{[\text{K}^+]_{\text{ex}}} \cdot \frac{[\text{Na}^+]_{\text{ex}}}{[\text{Na}^+]_{\text{in}}} \right) \quad (3.8)$$

where $\Delta\bar{\mu}_{\text{Na}}$ is in cal/mole. R , the gas constant, is equal to 1.987 cal/deg·mole and T , the absolute temperature, is equal to 293 K at 20°C. The energy consumption rate of the Na^+ pump is therefore

$$E_{\text{Na}} = F_{\text{outw}} \cdot \Delta\bar{\mu}_{\text{Na}} \quad (3.9)$$

From Levi and Ussing's data for cells in 32.5 mM K⁺, equations (3.8) and (3.9) give

$$E_{\text{Na}} = 1.22 \times 0.012 \times 1.987 \times 293 \times 2.3 \log \left(\frac{125 \times 115}{32.5 \times 12} \right)$$

or 30.7 cal/kg cell water·hr. (Note that this is less than the 51 cal/kg·hr given by Levi and Ussing, who made an error in their calculation.) From their data for cells in 2.5 mM K⁺,

$$E_{\text{Na}} = 1.22 \times 0.023 \times 1.987 \times 293 \times 2.3 \log \left(\frac{71 \times 115}{2.5 \times 23} \right)$$

or 80.9 cal/kg cell water·hr.

Levi and Ussing took Conway's (1946) figure for the metabolic rate of resting frog muscle as 175 cal/kg·hr and arrived at an energy consumption rate of the Na⁺ pump relative to the total energy production rate of the muscle. For cells in 32.5 mM K⁺, this would be 18% of total energy, and for cells in 2.5 mM K⁺, it would be 46%. Levi and Ussing (who calculated a 30% ratio) felt that this rate of energy consumption would be too high for the cell to cope with. This, however, did not lead them to reject the Na⁺ pump concept. Rather, they concluded that much of the observed efflux of ²⁴Na⁺ is not due to the Na⁺ pump but to some other mechanism. Ussing postulated a Na⁺-Na⁺ "exchange diffusion" carrier within the membrane that shuttles Na⁺ back and forth without expending energy and without contributing to net Na⁺ movement in or out. This subject will be taken up in Section 5.2.

E. J. Harris and Burn (1949) subsequently suggested a minor correction which reduced the energy consumption rate of the Na⁺ pump. They also used a higher figure for the total energy delivery derived from the resting heat production, i.e., 240 cal/kg·hr instead of the 170 cal/kg·hr given by Conway. Based on the recalculated value of 46%, this would reduce the minimal energy need of the Na⁺ pump to 46% × 175/240 = 33.5%. Keynes and Maisel (1954) made similar estimates of the energy need of the Na⁺ pump in muscle. They varied the external K⁺ concentration from 0 to 10 mM and measured the rates of oxygen consumption and the rates of Na⁺ efflux. Taking the resting potential data from the literature, they calculated a minimum energy consumption rate of the Na⁺ pump of 15% for muscle in a Ringer solution containing its normal 2.5 mM K⁺. Lower figures of from 6 to 12% were obtained for muscles in 0 or 10 mM K⁺. The significance of these values is somewhat questionable because very low external K⁺ concentrations as well as above-normal K⁺ concentrations artificially increased oxygen consumption rates (Fenn, 1930, 1931).

In all the above estimates, Levi and Ussing's original assumption that the slow fraction of Na⁺ efflux represents the membrane-limited portion of exchange was accepted. Indeed, at that time, it seemed to be an eminently reasonable assumption. Taken as a whole but ignoring some dissenting opinion (Ling, 1952) the consensus seemed to favor the view that the cell has at its disposal enough energy to operate the postulated Na⁺ pump.

TABLE 3.3. Ionic Composition of Cell Sap of Some Giant Algal Cells^a

Species and external solution	Ion concentration (mM)						
	Na ⁺	K ⁺	Ca ²⁺	Mg ²⁺	Cl ⁻	NO ₃ ⁻	SO ₄ ²⁻
Seawater	494	10.4	10.6	55	575	0.01	29
<i>Valonia macrophysa</i>	195	431	1.0	1.1	600	45	0.3
<i>Codium decorticatum</i>	302	368	11	21	568	—	74
<i>Halicystis parvula</i>	415	9.2	42	65	579	8.6	0.6
<i>Chaetomorpha linum</i>	68	697	4	27	754	—	20
Freshwater	0.2	0.1	0.8	1.7	1.0	—	0.3
<i>Nitella clavata</i>	28	80	10	20	136	—	8

^aFrom Gutknecht *et al.* (1978), by permission of Springer-Verlag.

3.3.3. Active Solute Transport by Epithelial Tissues and Giant Algal Cells

Tissues like frog skin and intestinal epithelium clearly can pump ions and other solutes from one aqueous solution to another against electrochemical gradients (see Chapter 17). This process, called *active transport*, is a function of the intact tissue, but must be a property of the cells making up the tissue. That a single cell can perform active transport is shown by the pattern of ionic distribution in some giant algal cells. These cells contain a large central vacuole filled with a dilute aqueous solution (the sap) much like that bathing the outside of the cells. Yet the concentration of K⁺ in the cell sap is many times higher than that in the surrounding water, while the Na⁺ concentration in the sap is many times lower (Table 3.3).

3.4. The Further Development of the Membrane Theory of Cellular Electrical Potential in the Context of the Membrane Pump Theory: The Ionic Theory of Hodgkin, Katz, and Huxley

The brilliant success of Hodgkin, Huxley, and Katz in the development of the membrane theory of cellular potentials provided even more support for the membrane pump model.

In Section 2.2.2, I described in some detail a particular theory of the cellular resting potential—the membrane theory of Bernstein. This theory was by no means universally accepted at that time, and among the alternatives that have already been mentioned was the phase theory of Nasonov and Aleksandrov (1944). Lund (1928), G. Marsh (1935), Korr (1939), and Lorente de Nó (1947) thought that the cellular electrical potential is not ionic but electronic in origin and considered it to be like an oxidation-reduction potential. The most important support for this idea was the great sensitivity of some bioelectrical potentials to oxygen deprivation. However, rigorous dependence on oxygen is by no means universal. Thus frog muscles can sustain a normal resting potential for long periods of time in pure nitrogen (Ling and Gerard, 1949a). Although early versions of the oxidation-reduction potential theory did not long survive their postulation, a variant of this view, called the *chemiosmotic theory*, was suggested by Mitchell to explain

behavior of the mitochondrion, a subcellular particle of central importance in the oxidative activities of the cell. This subject will be taken up in detail in Chapter 15.

3.4.1. The Hodgkin-Katz-Goldman Equation

Bernstein's theory of the cellular resting potential was based on the implicit assumption that cell membranes are absolutely impermeable to Na^+ . The disproof of this assumption made equation (2.4) no longer tenable as a description of the resting potential because Na^+ could no longer be ignored. However, since Na^+ does not follow the Donnan ratio, r , the potential should be described by a modified version of the equation, i.e.,

$$\psi = \frac{RT}{\mathcal{F}} \ln \left(\frac{[\text{K}^+]_{\text{in}} + [\text{Na}^+]_{\text{in}}}{[\text{K}^+]_{\text{ex}} + [\text{Na}^+]_{\text{ex}}} \right) \quad (3.10)$$

where $[\text{Na}^+]_{\text{in}}$ and $[\text{Na}^+]_{\text{ex}}$ refer to the intracellular and extracellular Na^+ concentrations. Since the sum of the intracellular K^+ and Na^+ concentrations is roughly equal to the sum of the extracellular K^+ and Na^+ concentrations, the ratio of these sums is approximately equal to 1 and the predicted potential ψ is then zero—contrary to fact: In frog muscles, ψ is about 90 mV (Ling and Gerard, 1949a). Therefore, the discovery of Na^+ permeability not only forced a revolution in the theory of the mechanism of selective ionic accumulation and volume control (see Chapter 13), it also forced a revolution in the theory of the cellular electrical potential.



Alan L. Hodgkin

The new theory, first put forward by Alan L. Hodgkin and Katz (1949a), was described by an equation similar to one earlier published by Goldman (1943):

$$\psi = \frac{RT}{\mathcal{F}} \ln \left(\frac{P_K[K^+]_{in} + P_{Na}[Na^+]_{in} + P_{Cl}[Cl^-]_{ex}}{P_K[K^+]_{ex} + P_{Na}[Na^+]_{ex} + P_{Cl}[Cl^-]_{in}} \right) \quad (3.11)$$

where P_K , P_{Na} , and P_{Cl} are the membrane permeability constants for K^+ , Na^+ , and Cl^- , while $[Cl^-]_{in}$ and $[Cl^-]_{ex}$ are the intracellular and extracellular chloride ion concentrations. This equation is referred to as the *Hodgkin-Katz-Goldman equation*, or simply the *Hodgkin-Katz equation*. It should be pointed out that P_K , P_{Na} , and P_{Cl} are not independent parameters; they vary with ψ (see Section 14.2.3).

One recalls that, up to the time this new theory was introduced, the electrical potential had been regarded primarily as an ionic equilibrium phenomenon. Bernstein's theory, Donnan's theory, and Boyle and Conway's version of the Donnan theory all had described it as such. It is interesting that Hodgkin and Katz named their theory the *ionic theory of electrical potential*, suggesting that in these authors' minds the alternative theories from which their theory was to be differentiated were more like the oxidation-reduction or electronic theories of the electrical potential.

The ionic theory of Hodgkin and Katz closely harmonized with the biochemical view of the living cell as being in a state of dynamic equilibrium, or, more correctly, in a *steady state*. As is well known, the maintenance of an equilibrium state does not call for a continual energy expenditure while a steady state, by definition, is maintained only by a continued supply of energy. The ionic theory gained rapid and wide acceptance partly because of the accumulation of experimental evidence in support of the theory and partly because from this theory was derived an elegant explanation of the *action*



Ralph W. Gerard (1900–1974)

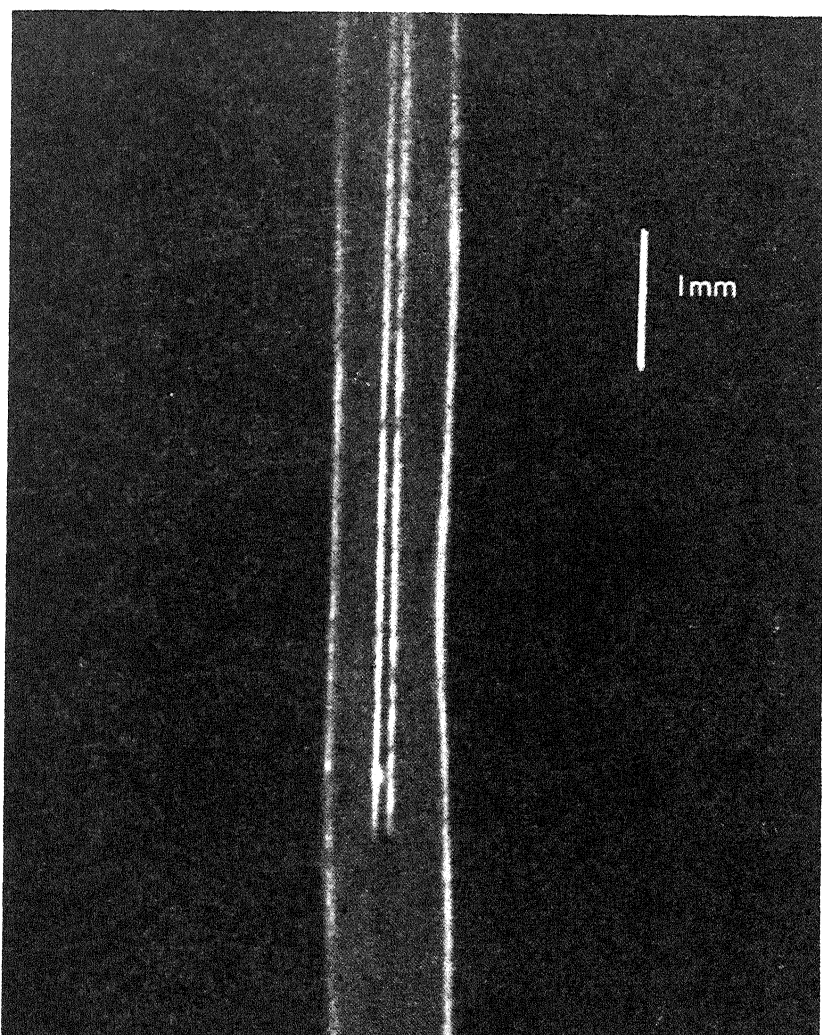


FIGURE 3.4. A segment of an isolated squid giant axon. [From Hodgkin and Keynes (1956), by permission of *Journal of Physiology*.]

potential, which, of course, is the unit message of signal transmission in nerve and muscle.

Before and during the period that the ionic theory was presented, several significant technical advances made possible the accurate recording of both the resting and action potentials of living cells. With these techniques, quantitative theories could be tested in a way that had not been possible before.

One of the new techniques involved the isolated giant axons of the squid (*Loligo*) and cuttlefish (Young, 1938). Figure 3.4, taken from Hodgkin and Keynes (1956),

shows a darkfield-illuminated squid axon with a 0.1-mm-wide glass tube inserted longitudinally. This glass tubing permits accurate recording of the electrical potential difference between the inside and the outside of the squid axon.

Another technical advance was the development of the Gerard-Graham-Ling (GGL) type of glass capillary microelectrode (J. Graham and Gerard, 1946; Ling and Gerard, 1949a). Whereas the squid axon provides electrophysiological recording of nerve activities in a way never before possible, the GGL glass capillary microelectrode technique permits accurate recording of the electrical activities of many types of living cells, big and small (Weidemann, 1971; Lassen and Sten-Knudsen, 1968), and even of those of subcellular compartments of living cells *in vitro* (Tupper and Tedeschi, 1969a) and *in vivo* (Giulian and Diacumakos, 1977).

With these two basic techniques, observations confirming the membrane theory in general, and the ionic theory of Hodgkin, Huxley, and Katz in particular, came in rapid succession. The predictions of this theory are embodied in equation (3.11):

1. *The dependence of the resting potential on absolute temperature.* In agreement with J. Bernstein (1902), Ling and Woodbury (1949) demonstrated that the resting potential of frog sartorius muscle cells varies with the absolute temperature (Fig. 3.5).

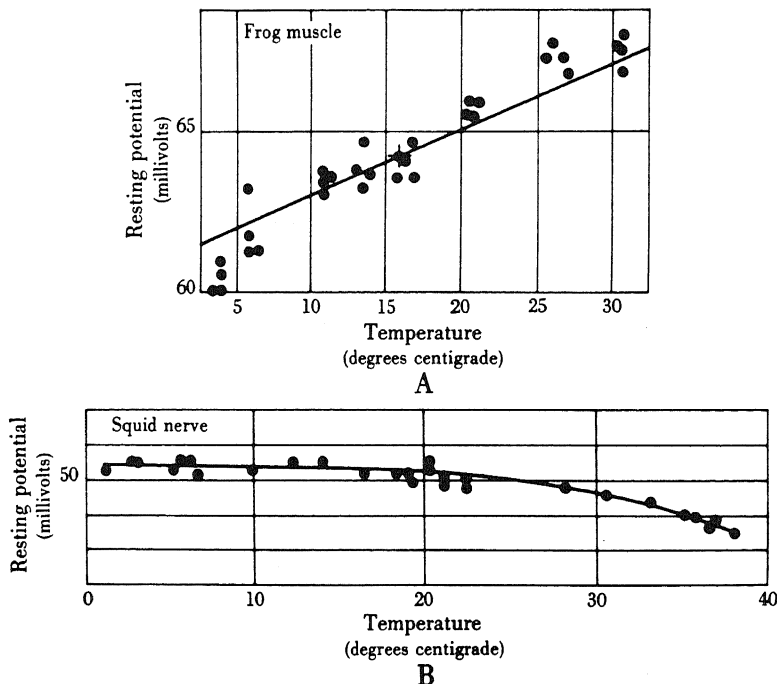


FIGURE 3.5. Effect of temperature on the magnitude of the resting potential. Data from (A) frog voluntary muscle fibers (Ling and Woodbury, 1949) and (B) squid axon (redrawn from Hodgkin and Katz, 1949b) are presented. At temperatures above 35°C, the resting potential of frog muscles declines irreversibly (see Ling and Woodbury, 1949). In (A) the line is theoretical for the potential, proportional to absolute temperatures. [From Ling (1962).]

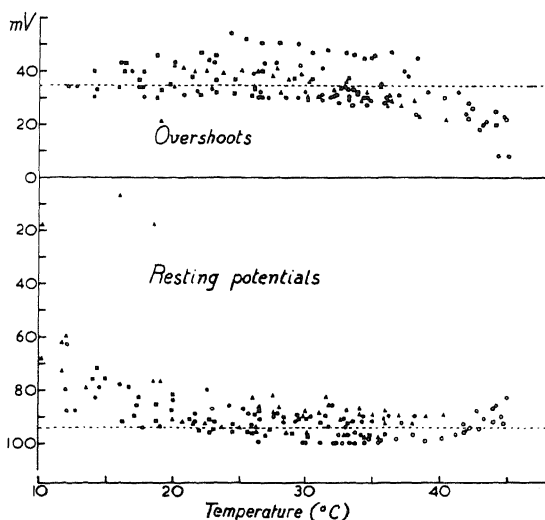


FIGURE 3.6. Effect of temperature on resting potential and overshoot in heart muscle. Different symbols are used for different hearts. Dotted lines indicate average values at 38°C (35 mV, 94 mV). [From Corabœuf and Weidemann (1954), by permission of *Helvetica Physiologica Acta*.]

Essentially the same observation was made by Hodgkin and Katz (1949b) in squid axon (Fig. 3.5) and by Corabœuf and Weidemann (1954) in heart muscle (Fig. 3.6).

2. *The dependence of the resting potential on external K⁺ concentration.* The dependence of ψ on external K⁺ was first reported by MacDonald (1900). Figure 3.7 presents a collection of other earlier findings in a variety of living cells demonstrating that, over a wide range of external K⁺ concentrations, the resting potential is related logarithmically to the external K⁺ concentration. Since the time this figure was constructed, observations have been made in many more types of cells with similar results. To be noted is that the obedience to the logarithm relation shown in equation (2.4) begins to break down at low K⁺ concentration. That is, the potential does not keep on increasing with decreasing external K⁺ concentration but tends to flatten out. This flattening out of ψ at low external K⁺ concentration can be explained by the participation of external Na⁺ in equation (3.11) and will be discussed in Section 14.4.1.

3. *The dependence of the resting potential on intracellular K⁺ concentration.* Grundfest *et al.* (1954) injected 1.3 M potassium aspartate into squid giant axon but could not find a significant change in the resting potential. In contrast, Hodgkin and Keynes (1956) found that injection of 1.0 M NaCl and 1.0 M KCl into squid giant axon did cause the small changes of resting potential theoretically expected. Baker, Hodgkin, and Shaw (1961) demonstrated that, by internally perfusing isolated squid axon with a medium containing varying amounts of KCl (in mixtures of KCl and NaCl) while the axon was bathed externally in an artificial seawater containing 10 mM K⁺, the resting potential could be made to vary with [K⁺]_{in} (Fig. 3.8). Adrian (1956) altered intracellular K⁺ concentration by exposing frog muscle to hypo- and hypertonic solutions; he concluded that ψ varies with the intracellular K⁺ concentration. A similar but more qualified conclusion was reached by Hagiwara *et al.* (1964), who perfused barnacle giant muscle fibers with solutions containing K⁺ concentrations varying up to 200 mM. Beyond 200 mM, however, the observed change in ψ was in the wrong direction.

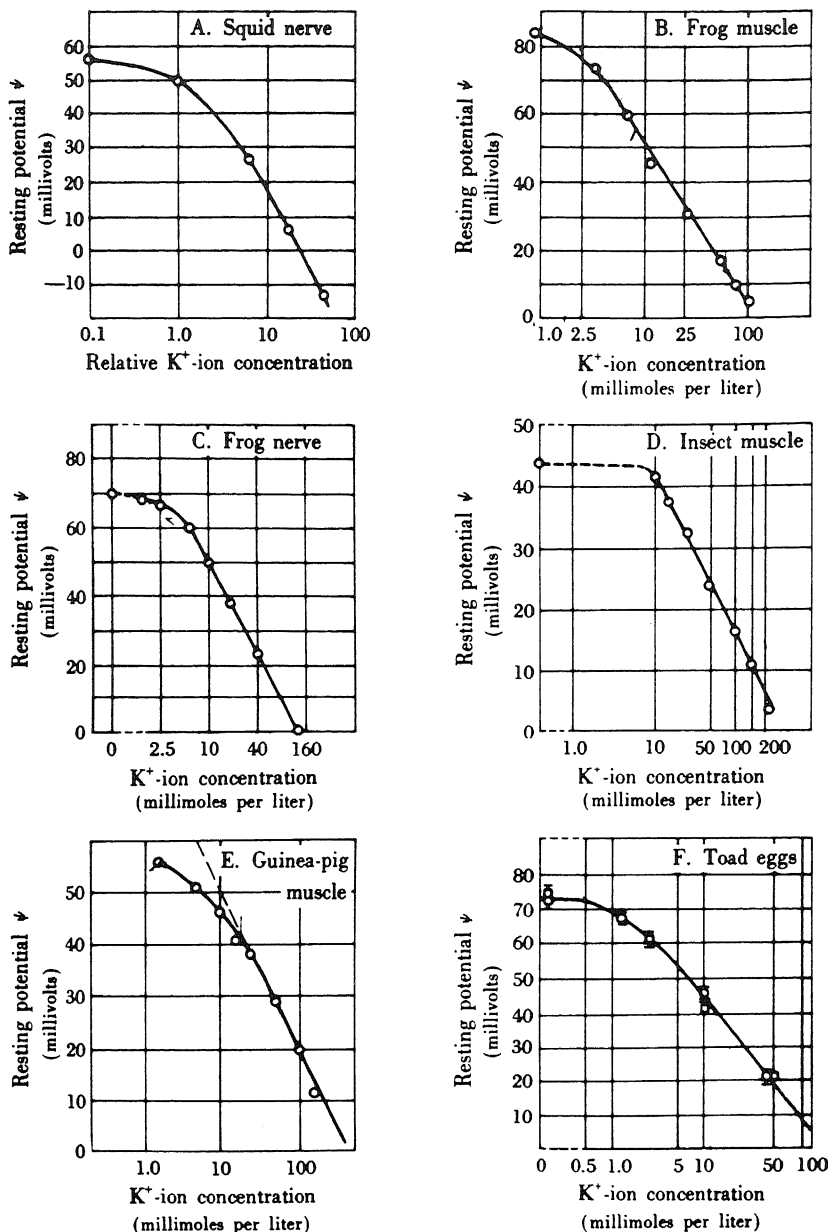


FIGURE 3.7. Relation between the external K⁺ concentration and the resting potential in a variety of cells. In each case the potential in millivolts is plotted on the ordinate and the concentration of external K⁺ is plotted on the abscissa. All external K⁺ concentrations are represented as millimoles per liter of solution except that in (A), which is given as a multiple of the concentration of a standard solution (13 mM). [From Ling (1962).]

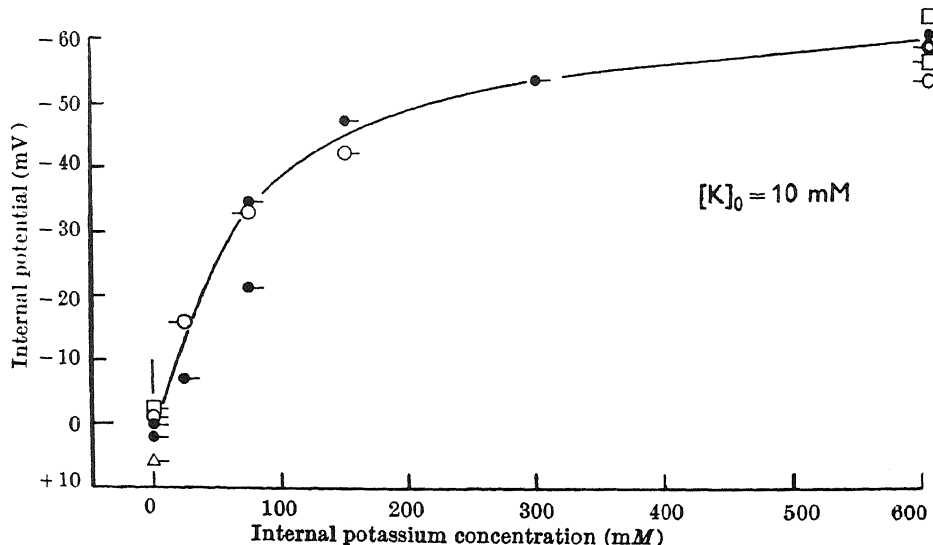
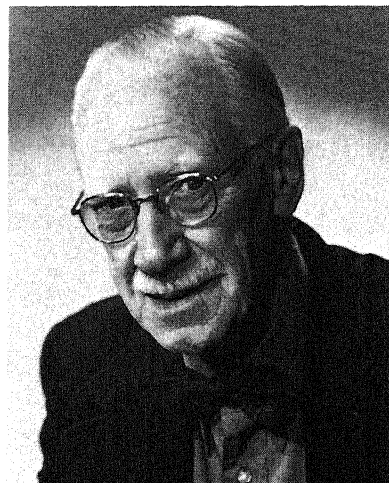


FIGURE 3.8. Effect of internal K^+ concentration on resting potential. External solution, seawater; internal solution, NaCl-KCl solutions isotonic with seawater. [From Baker *et al.* (1961), by permission of *Nature*.]

These studies, showing at least a partial relation between ψ and the intracellular K^+ concentration, constitute only a part of the reported studies on this issue, and evidence contradicting equation (3.11) will be discussed in Chapter 14.

4. *The dependence of the resting and action potentials on external Na^+ concentration.* That external Na^+ is essential for the normal excitability of living cells was rec-



Kenneth S. Cole

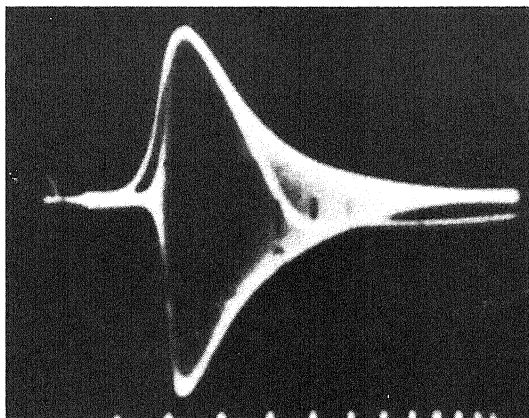


FIGURE 3.9. Transient impedance change of the squid axon during the passage of an action potential. Double exposures of the impedance change at 10 kc with the action potential. [From Cole and Curtis (1938-1939b), by permission of *Journal of General Physiology*.]

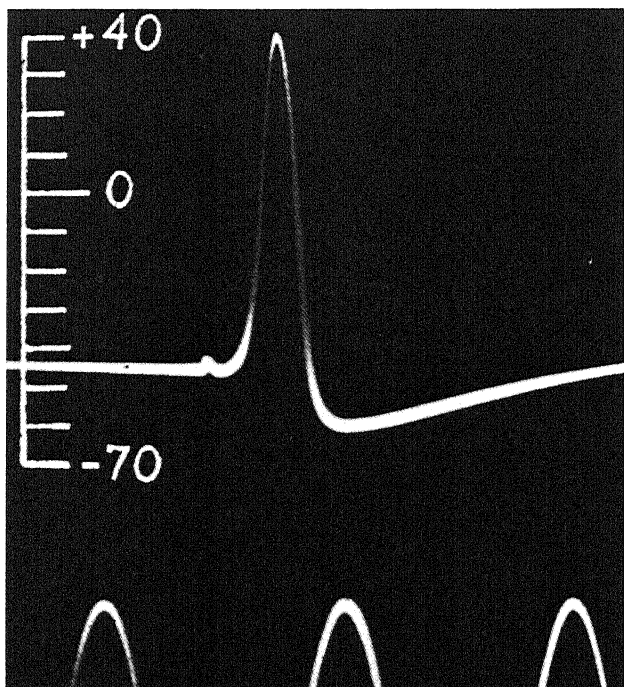


FIGURE 3.10. Action potential recorded between the inside and the outside of a squid giant axon. The ordinate indicates the electrostatic potential difference between the inside of the axon and the external seawater, which is taken as zero potential. The oscillographic recording shows an initial resting potential of -44 mV and an action spike 84 mV in height, at which peak the internal microelectrode becomes positive with respect to the seawater. Time markers: 500 cycles/sec. [From Hodgkin and Huxley (1945), by permission of *Journal of Physiology*.]

ognized by Overton (1902b). His remarkable paper was published in the same volume of *Pflügers Archiv* in which Bernstein's important article (mentioned in Section 2.2.2) appeared. In Bernstein's membrane theory of the cellular potential, the "negative variation" accompanying cell activity, or the action potential, is a transient membrane depolarization occurring as a consequence of an increase in the membrane permeability (J. Bernstein, 1912). Bernstein's theoretical prediction that during the action potential there is a transient increase in membrane permeability was confirmed by the studies of Kenneth S. Cole and Curtis in *Nitella* (1938–1939a) and in the squid giant axon (1938–1939b). Figure 3.9, taken from the latter publication, shows the transient drastic decrease of impedance accompanying the action potential, from $1000 \Omega/\text{cm}^2$ to $20 \Omega/\text{cm}^2$.

In other studies (Hodgkin and Huxley, 1945), it became clearly established that the action potential does not merely represent a cancellation of the potential difference seen in the resting cells, as Bernstein's original membrane theory of the action potential would have predicted. The potential actually overshoots its baseline (Fig. 3.10). However, this was not the first time that such a discrepancy had been observed. As far back as 1891, Burdon-Sanderson and Gotch observed an action potential (100 mV) exceeding the resting potential (80 mV) in muscle cells. In 1939 Hodgkin and Huxley observed an action potential of 90 mV in squid axon with a resting potential of only 50 mV. [For other data, see Table 3.4, taken from Troshin (1966).] Thus, during the action potential,

TABLE 3.4. Value of Resting Potentials (RP) and Action Potentials (AP) of a Variety of Nerves and Muscles Described before 1951^a

Animal	Tissue	RP	AP
<i>Loligo forbesi</i>	Nonmedullated nerve	50	90
<i>Loligo forbesi</i>	Nonmedullated nerve	48	88
<i>Loligo pealii</i>	Nonmedullated nerve	51	104
<i>Sepia officinalis</i>	Nonmedullated nerve	62	120
<i>Sepia officinalis</i>	Nonmedullated nerve	—	124
<i>Homarus vulgaris</i>	Nonmedullated nerve	—	110
<i>Homarus vulgaris</i>	Nonmedullated nerve	62	106
<i>Carcinus maenas</i>	Nonmedullated nerve	—	116
<i>Carcinus maenas</i>	Nonmedullated nerve	71–96	116–153
<i>Rana esculenta</i>	Sciatic nerve	71	116
<i>Rana temporaria</i>	Skeletal muscle	88	119
<i>Rana pipiens</i>	Heart muscle	50–90	65–115
<i>Canis familiaris</i>	Heart, Purkinje's fibers	90	121
<i>Capra hircus</i>	Heart, Purkinje's fibers	94	135

^aFrom Troshin (1966), by permission of Pergamon Press.

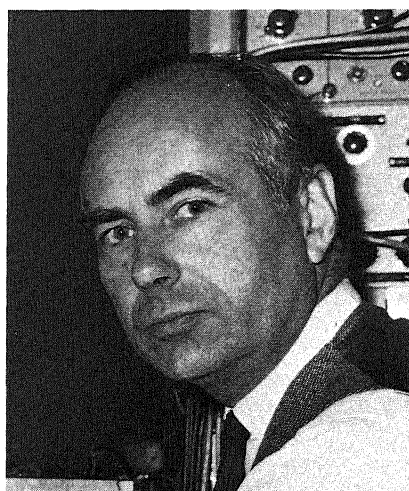
there is actually a reversal of the sign of the electrical potential, making the inside of the cell momentarily positive by some 40–70 mV.

A most important contribution that Hodgkin and Katz (1949b) made was the suggestion that the action potential is created, not merely as a result of a large gain of permeability to all solutes, but as a result of a large increase specifically in the permeability of the cell membrane to Na^+ . At the time that Hodgkin and Katz presented this new theory, they believed that in squid axons the resting potential of some 60 mV, inside negative, could be explained by the assumption that the permeability constants P_K , P_{Na} , and P_{Cl} of equation (3.11) follow the proportion 1:0.04:0.45. During the height of the action potential P_K and P_{Cl} remained unchanged but P_{Na} increased 500-fold, resulting in ratios of $P_K:P_{\text{Na}}:P_{\text{Cl}}$ of 1:20:0.45 and the creation of the overshoot.

The work of Hodgkin and Katz was soon followed by the publication of the Hodgkin–Huxley theory describing the temporal profile of the action potential.

3.4.2. The Hodgkin–Huxley Theory of the Action Potential

In 1952, in a series of five papers, one of which was coauthored with Katz (Hodgkin and Huxley, 1952a–d; Hodgkin *et al.*, 1952), Hodgkin and Andrew F. Huxley presented their studies of the action potential of squid giant axon with the aid of the *voltage clamp* method, a technique introduced by Cole (1949) (see also Marmont, 1949). The voltage clamp allows the investigator to set the electrical potential difference between the inside and the outside of an axon at any desired level and to hold it there with a feedback amplifier. Since the electrical potential is altered uniformly throughout the whole axon at any one time, there is no propagation along the length of the axon and at any one instant the current at one place on the surface is the same as that at any other place. The electric current across the cell surface can be divided into a *capacity current* involving charge distribution within the cell surface and an *ionic current* involv-



Andrew F. Huxley

ing current passing through the membrane. By holding the voltage constant, the capacity current vanishes, and so the voltage clamp method provides a means to study the ionic current uncomplicated by the capacity current.

The ionic current, I_i , is separated into three components: the sodium current (I_{Na}), the potassium current (I_K), and the remainder, called leakage current (I_l). I_{Na} and I_K , but not I_l , vary in the course of an action potential. At the region of excitation, the electrical potential reverses its sign so that the outside of the nerve becomes negative with respect to the inside (Fig. 3.10). The flow of local current within this region causes depolarization at the neighboring region and propagation of the action potential.

With the voltage clamp, a depolarizing voltage of greater than 12–15 mV applied as a short pulse across the resting membrane also produces an action potential. Its absolute value is about 100 mV, i.e., it cancels the resting potential of 60 mV and then “overshoots” by another 40 mV. There is a surge of inward current that reaches a maximum a fraction of a millisecond after the application of the shock; the inward current decreases, and at about 2 msec an outward current occurs that then slowly returns to the resting level. These current flows are shown in the top tracing in Fig. 3.11A. The initial part of the current flow is very similar to that of a normal action potential. The voltage clamp, however, exaggerates the later phase of the action potential, creating a sustained delayed outward current. This delayed outward current will then return to the normal resting level if the voltage clamp is turned off.

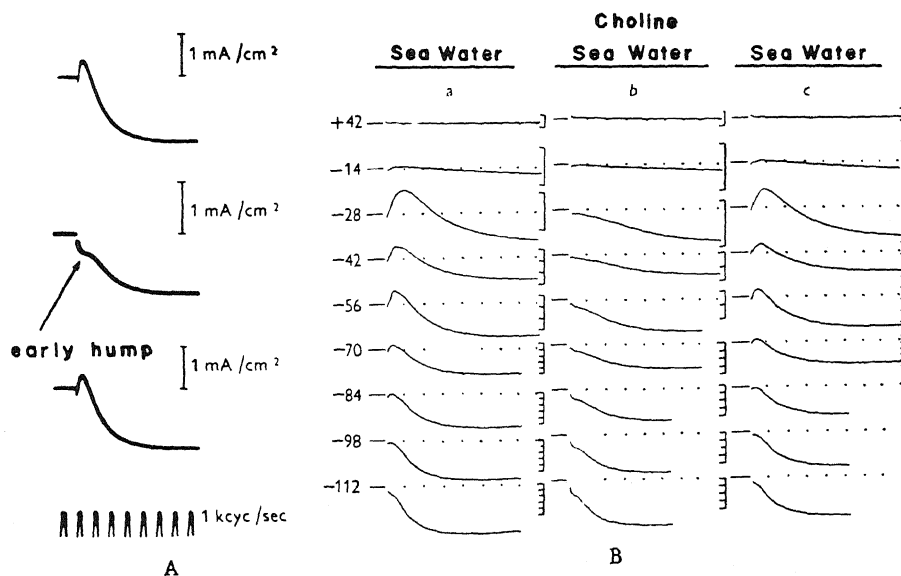


FIGURE 3.11. (A) Records of membrane current during voltage clamps in which membrane potential was lowered by 65 mV. Top record: axon in seawater. Middle record: axon in choline seawater. Bottom record: after replacing seawater. Inward current is shown upwards in this and all other figures. Note the early outward hump in the center record. (B) Records of membrane current during voltage clamps. (a) Axon in seawater; (b) axon in choline seawater; (c) after replacing seawater. Displacement of membrane potential indicated in mV. Vertical scale: 1 division is 0.5 mA/cm². Horizontal scale: interval between dots is 1 msec. [From Hodgkin and Huxley (1952a), by permission of *Journal of Physiology*.]

It was known that the action potential involves a local exchange of K^+ and Na^+ between the cell and its surrounding medium. The next question was: What is the precise contribution of each of these ions to the generation of the action potential? To answer this, the voltage clamp technique offered still another unique advantage. If all the NaCl in seawater is replaced by choline chloride, the nerve becomes inexcitable and the natural action potential does not occur. But the voltage clamp method permits an analysis of the underlying ionic movements under these conditions. Hodgkin and Huxley observed that the early inward current vanishes with the substitution of choline for Na^+ in seawater. However, the delayed outward current remains largely unchanged (middle tracing, Fig. 3.11A). A more careful look at the record shows that, at the time when an axon in normal seawater shows the large inward current, there is now a small hump corresponding to a very small current in the opposite (outward) direction (Fig. 3.11A,B).

Hodgkin and Huxley then argued that the cathodal depolarization opened the cell membrane to the passage of Na^+ and that this *outward* hump in choline seawater as well as the normal initial *inward* current in normal seawater is quantitatively determined by the balance of the applied electrical potential difference and the sodium potential, V_{Na} , where

$$V_{Na} = \frac{RT}{\mathcal{F}} \ln \frac{[Na^+]_{in}}{[Na^+]_{ex}} \quad (3.12)$$

When there is much more Na^+ in the external solution, as is the case in normal seawater, V_{Na} provides the driving force for the inward surge of Na^+ . When there is more Na^+ in the cell water than in the external medium, as is the case in choline seawater, V_{Na} drives Na^+ outward.

All these observations are in harmony with the notion that the early ionic current is carried by Na^+ moving under its joint electrical and concentration gradients. The driving force for the Na^+ movement is the difference between the membrane potential (V) and the Na^+ equilibrium potential and is represented by $(V - V_{Na})$. The Na^+ permeability is then represented as a Na^+ conductance, g_{Na} ,

$$g_{Na} = \frac{I_{Na}}{V - V_{Na}} \quad (3.13)$$

By making certain simplifying assumptions, it is possible to separate the experimentally observed ionic current into its Na^+ and K^+ components and to show that the Na^+ conductance rises rapidly to a maximum and then declines along an exponential curve (Fig. 3.12). The K^+ conductance, on the other hand, rises more slowly along an S-shaped curve and, under the voltage clamp, is maintained at a high level indefinitely. The K^+ conductance, g_K , is

$$g_K = \frac{I_K}{V - V_K} \quad (3.14)$$

where V_K is the K^+ potential, analogous to V_{Na} and similarly defined as in equation (3.12). While the Na^+ potential seems adequately explained by the concentration gra-

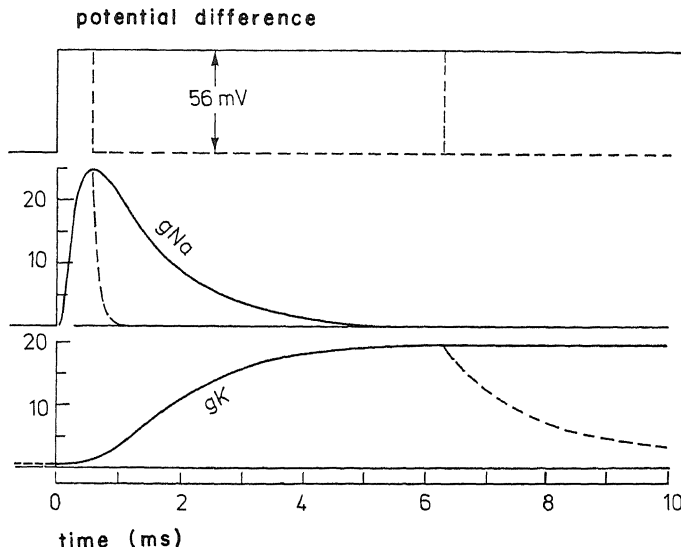


FIGURE 3.12. Time course of Na^+ conductance (g_{Na}) and K^+ conductance (g_{K}) associated with 56-mV depolarization. Vertical scale in mmho/cm^2 . The continuous curves are for a continued depolarization; broken curves show the effect of repolarizing after 0.6 or 6.3 msec. [From Hodgkin (1958), by permission of *Proceedings of the Royal Society of London*.]

dient calculated from the Na^+ concentration in the cell water and that present in the seawater, the effect of changing external K^+ concentration on the K^+ potential, though in the right direction, is far from that predicted quantitatively. Indeed the observed change in V_K as determined from the potential needed to annul I_K is only half of that calculated on the basis of the known intracellular K^+ concentration.

Another phenomenon that accompanies electrical depolarization is *inactivation*, which is a loss of the ability to undergo the usual large increase of Na^+ conductance with further *depolarization*. This is produced by a steady small depolarization. On the other hand, a small *hyperpolarization* (making the outside more positive) has the effect of removing preexisting inactivation. Inactivation is quantitatively related to the magnitude of the membrane potential; it is virtually complete at -30 mV or lower but vanishes at $+30$ mV or higher.

3.4.3. The Hodgkin-Huxley Theory of Permeability Changes during the Action Potential

At least three alternatives for the mechanisms underlying the ionic currents during the action potential were considered: ion carriers, a channel for both K^+ and Na^+ , and separate channels for K^+ and Na^+ . Hodgkin and Huxley chose a separate-channel model, and a brief description of the theory follows.

The advancing front of an action potential causes depolarization of the neighboring quiescent region. This electrical depolarization causes a certain number of charged particles (CP_{Na}) to migrate from one position (A) to another (B). CP_{Na} are not carriers, but

they allow Na^+ to pass through the membrane when they occupy position B and not when they occupy position A. The decline of the Na^+ conductance is attributed either to a chemical change of CP_{Na} after leaving position A or to another charged slowly migrating particle (CP'_{Na}), which blocks Na^+ movement. No mechanism was offered to explain how the chemically changed CP_{Na} blocking the channel is subsequently removed to allow the next impulse to go through.

Hodgkin and Huxley postulated that a K^+ channel is formed when four units of CP_K move from position C to position D. Using n to represent the probability that a single CP_K moves to position D, the K^+ conductance, g_K , is:

$$g_K = \bar{g}_K n^4 \quad (3.15)$$

where g_K , a constant, is the maximum K^+ conductance. For the Na^+ channel,

$$g_{\text{Na}} = \bar{g}_{\text{Na}} m^3 h \quad (3.16)$$

where \bar{g}_{Na} is a constant equal to the maximum Na^+ conductance, m is the probability that a single CP_{Na} occupies position B, and it takes the movement of three units of CP_{Na} from position A to position B to open the Na^+ channel. h is the probability of a single CP'_{Na} moving to the blocking position, and only one CP'_{Na} moving to the right position is adequate to block the Na^+ channel. The rate of change of the probabilities n , m , and h with time is described by

$$\frac{dn}{dt} = \alpha_n(1 - n) - \beta_n n \quad (3.17)$$

$$\frac{dm}{dt} = \alpha_m(1 - m) - \beta_m m \quad (3.18)$$

$$\frac{dh}{dt} = \alpha_h(1 - h) - \beta_h h \quad (3.19)$$

where the α 's and β 's are rate constants. It should be emphasized that these are not true constants but vary with the membrane potential. Depolarization (i.e., making the cell interior more positive) increases α_n and α_m but decreases β_n and β_m . However, depolarization also increases β_h and decreases α_h .

The complete equation for the membrane current density, I , is

$$I = C \frac{dV}{dt} + (V - V_K) \bar{g}_K n^4 + (V - V_{\text{Na}}) \bar{g}_{\text{Na}} m^3 h + (V - V_l) \bar{g}_l \quad (3.20)$$

where C is the membrane capacity. The four terms on the right are the capacity current, the K^+ current, the Na^+ current, and the leakage current, respectively.

3.4.4. Experimental Confirmation of the Membrane Theory of the Resting and Action Potentials

The Hodgkin-Huxley theory provided the basis for a great deal of research on the action potential of a variety of excitable cells. In a general way, the basic concepts intro-

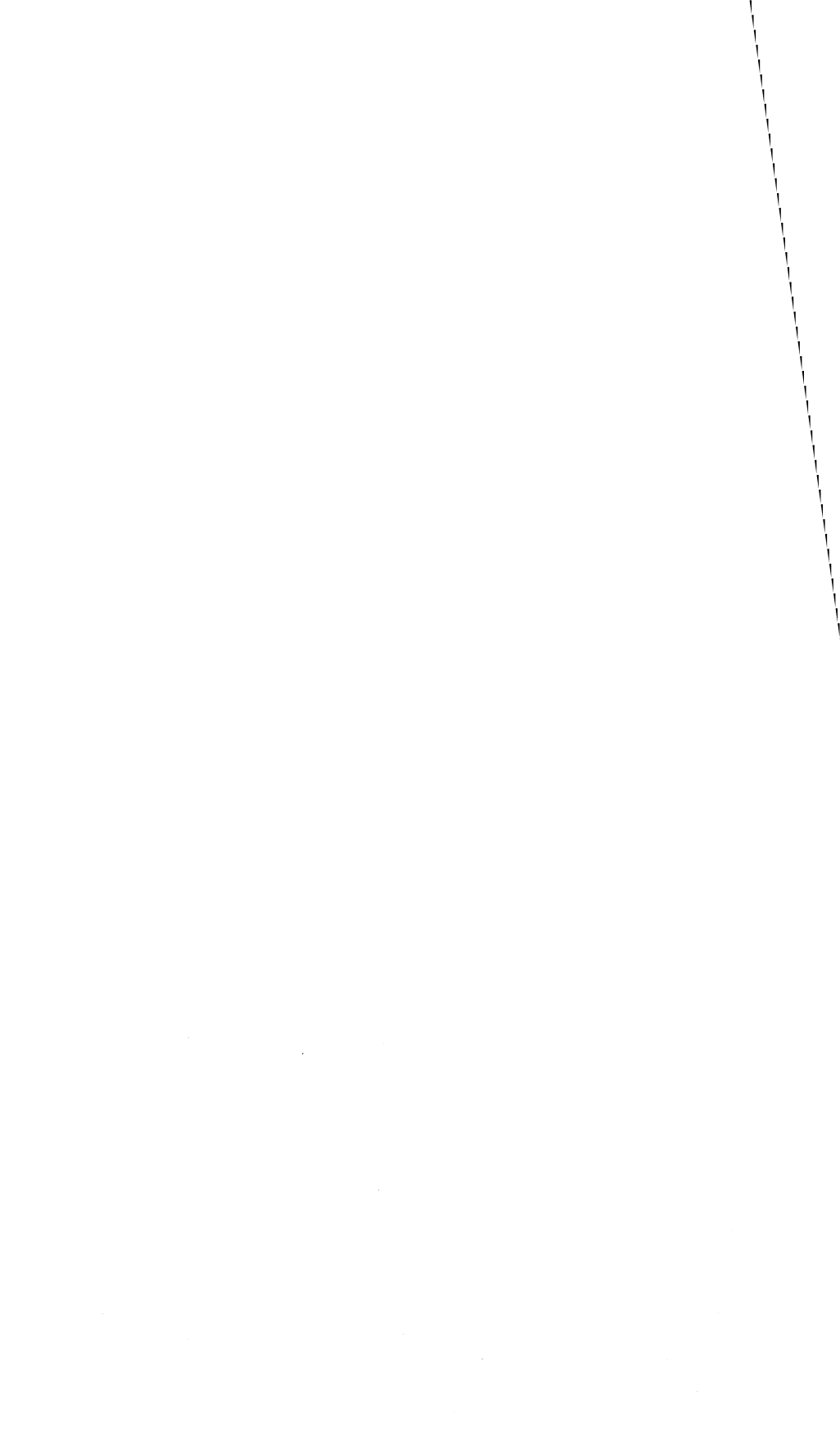
duced were widely confirmed and extended. The discovery of more or less specific blockers of the Na^+ channels (e.g., tetrodotoxin, saxitoxin) and of the K^+ channels (e.g., tetraethylammonium, 4-aminopyridine) is in accord with the two-channel concept. So in a broad sense are Hille's model of a rigid pore of $3 \times 5 \text{ \AA}$ surrounded by eight oxygen atoms for the Na^+ channel (Hille, 1972) and Armstrong's model of the K^+ channel with a narrow mouth facing the outside and a wide mouth facing the cell interior (Armstrong, 1975). Armstrong's idea was supported by the work of Hucho and Schiebler (1977), using a photolabeling technique. Similarly, the recent discovery of the gating current offers support for the Hodgkin-Huxley theory (Lansdowne *et al.*, 1975). However, not all evidence supports the theory and some contradictory findings will be reviewed in Chapter 14; more can be found in the recent monograph by Tasaki (1982).

3.5. Summary

The discovery in 1939 and 1940 that Na^+ , like K^+ , readily penetrates cells and exchanges continuously in and out meant that, within the confines of the membrane theory, the net exclusion of Na^+ from the cell, relative to its much higher concentration in the environment, could occur only if there were an outwardly directed Na^+ pump to counterbalance its tendency to leak inward down its electrochemical gradient. The only alternative would have been to challenge the basic assumption of the membrane theory—that cell water and ions exist in a physical state like that of a dilute aqueous solution. The steady-state Na^+ pump hypothesis was in accord with the concept that hydrolysis of ATP provides the source of energy for biological work performance, and was supported by the dependence of normal ionic distributions on continued metabolic activity of the cell and on temperature.

At the same time, the membrane theory of cellular potentials evolved through the development of the Hodgkin-Huxley theory, which described the roles of changes in permeability of K^+ and Na^+ in generating the currents that underlie the action potential of nerve and muscle. This theory dovetailed with the Na^+ pump hypothesis, for the Na^+ pump is needed to counterbalance the tendency of active nerve and muscle to gain Na^+ and lose K^+ during the passage of action potentials.

These two major developments in cell physiology placed the membrane theory in a position of dominance and stimulated the imagination of most physiologists, who now felt that there could be no doubt about the correctness of its assumptions. There were only a few dissenters, and in the next chapter I outline the reemergence of the bulk phase theories of cell physiology.



The Reemergence of the Bulk Phase Theories

4.1. Kamnev's Study of Sugar Distribution in Frog Muscle

In Chapter 2 the work of Nasonov was mentioned. One of his students, Kamnev, published a paper in 1938 entitled "Permeability of Striated Muscle of Frog to Sugar." In this paper Kamnev described experiments in which he followed the uptake of sucrose and galactose by frog muscle (Fig. 4.1). It took 2–4 hr for the sugars in the muscle tissues to reach equilibrium, and they did so at levels specific for each sugar (42.1% of the external solution concentration for galactose, 32.7% for sucrose). Both of these levels were considerably higher than those found in the extracellular space, which makes up about 9% of the cell volume. Kamnev further showed that in killed muscles the final equilibrium levels of both sugars were equal to those in the external solution. Kamnev concluded that the low equilibrium level of sugars in the living muscle cell could not have been the result of membrane permeability but must reflect a difference in the solubility of these substances in the protoplasm of the cells, and that this solubility must have increased after cell death.

In fact, as far back as 1849, Carl Ludwig had demonstrated that dried pig's bladder imbibes water from concentrated Na_2SO_4 solutions. The concentration of Na_2SO_4 within the imbibed water, however, was from 64% to 70% of that in the surrounding fluids (Table 4.1).

M. H. Fischer, in 1909, suggested that reduced solubility in cell water could account for the level of a solute in a living cell. However, within my knowledge Kamnev was the first to have produced an actual experimental study in living cells that was interpreted on the basis of such a mechanism. Regrettably this paper also appears to be the only one Kamnev published on this topic. However, this important subject was taken up and extensively studied by A. S. Troshin, another outstanding and capable student of Nasonov.



A. S. Troshin

4.2. Troshin's Sorption Theory

In 1956 Troshin published the original Russian version of his book *The Problems of Cell Permeability*. It was published in German in 1958, in Chinese in 1961, and then in a revised form in English in 1966. It is beyond the scope of this chapter to present more than a cursory examination of what I believe to be the most important and representative contributions from this work. The reader is urged to read the original book, now no longer behind a difficult language barrier.

The term *permeability* in the title of Troshin's book was chosen to conform to conventional usage, but one of the intentions of his work was to show that permeability is of secondary importance in the determination of patterns of equilibrium solute distribution between the cell and its environment.

Troshin, like Fischer, Moore, and Lepeschkin, was strongly opposed to the membrane theory. He provided many pieces of experimental evidence against it, using what may appear at first to be simple or even primitive methods. Yet in many ways this very

TABLE 4.1. Na_2SO_4 Distribution in Imbibed Water of Dried Pig's Bladder^{a,b}

Initial weight of external solution (g)	Initial concentration		Final concentration		Gain of bladder weight (g)	Concentration of salt in imbibed water (%)	$\frac{\text{Salt}_{\text{imbibed fluid}}}{\text{Salt}_{\text{external solution}}}$
	of salt in external solution (%)	Final weight of external solution (g)	of salt in external solution (%)				
99.750	4.995	91.319	5.120	8.431	3.617	3.617	0.706
115.0	4.995	107.172	5.120	7.828	3.283	3.283	0.641

^aDried pig's bladder was introduced into a weighed quantity of a Na_2SO_4 solution. The Na_2SO_4 concentration in the water imbibed by the dry bladder was calculated from the weight and the salt concentration change of the external solution.

^bFrom Ludwig (1849).

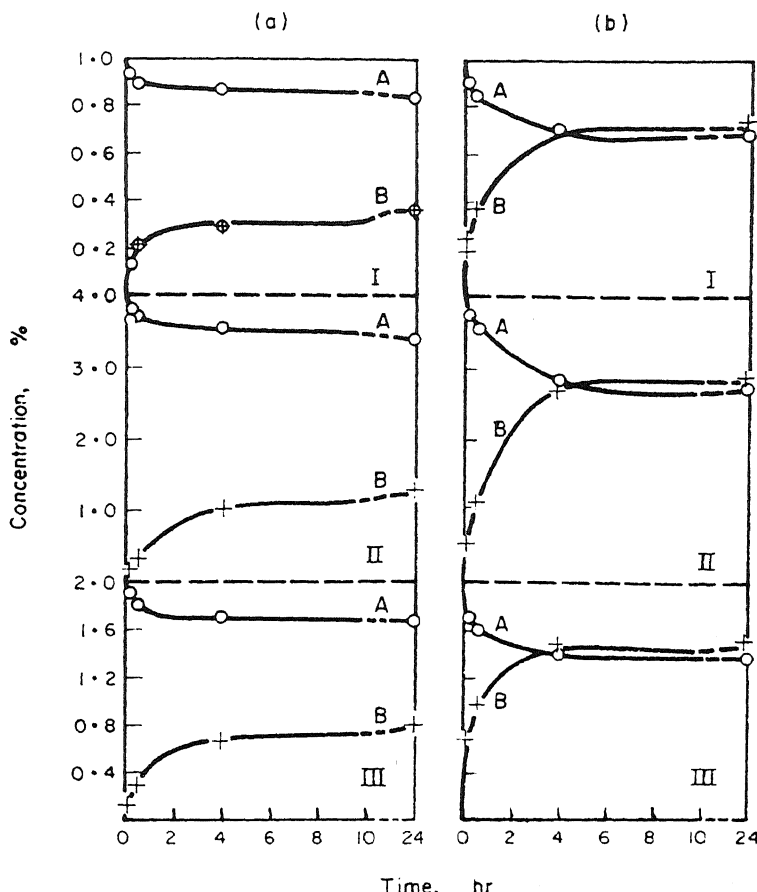


FIGURE 4.1. Passage of sugar into live and dead skeletal muscles of frogs from the surrounding medium with time. (a) Live muscles, (b) dead muscles; (A) diminution of sugar in the medium, (B) adsorption of sugar by the muscles. Initial sugar concentrations in the solution: (I) 1% sucrose solution, (II) 4% sucrose solution, (III) 2% galactose solution. [Data of Kamnev; graph from Troshin (1966), by permission of Pergamon Press.]

simplicity of experimental approach often helps scientists to pursue truly fundamental issues.

4.2.1. Osmotic Behavior of Living Cells

Figure 4.2 presents Troshin's studies of the loss of water from rabbit erythrocytes when they were exposed to a solution containing 2% galactose. A similar study of frog muscles exposed to a solution containing 20% urea was also described. Although the cell water decreases to a new low level, neither galactose nor urea are impermeant. Indeed each of these solutes steadily rises in concentration within the cells, while the total water content is steadily decreasing. These data contradict the membrane theory, according to

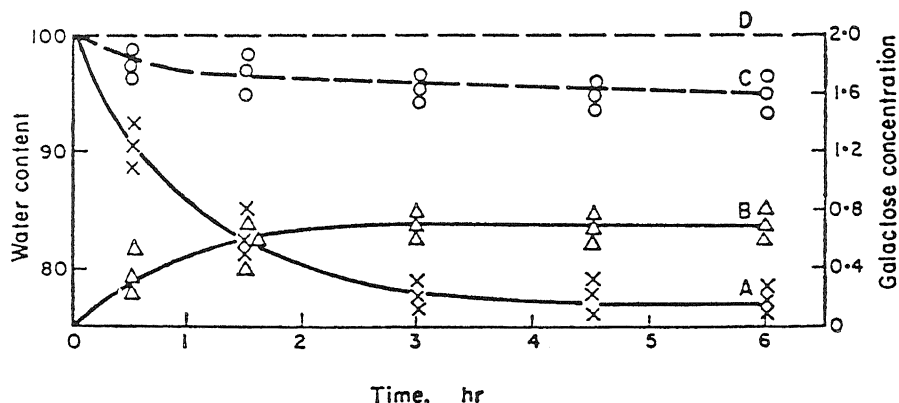


FIGURE 4.2. Change with time in the water content (expressed as percent of control) and galactose content (in percent) in rabbit erythrocytes placed in a 2% solution of galactose made up in Ringer solution. (A) Decrease of the erythrocyte water content; (B) absorption of galactose by the erythrocytes; (C) decrease of galactose in the medium; (D) initial water content of the cells. [From Troshin (1966), by permission of Pergamon Press.]

which only impermeant solutes can cause a sustained cell shrinkage. Troshin concluded: "The increase or decrease in the water content of a cell in solutions of different substances is a colloidal phenomenon connected with the penetration of molecules of the solute into the cell."

4.2.2. Cells as Colloidal Coacervates

As mentioned in Section 2.7.2, colloidal chemistry in the West underwent a serious decline in the 1940s. Yet in the Soviet Union, some biologists continued to describe living phenomena in terms of colloidal concepts. Indeed, Troshin's main theme is built around an analogy between living protoplasm, on the one hand, and *coacervates*, a colloidal state described by Bungenberg de Jong and Kruyt (1929) (Section 2.5.5), on the other.

4.2.3. Solute Exclusion and Accumulation

Troshin's early work was published in 1951 and 1952 in a series of six short papers in the Russian *Byulleten Eksperimental'noi Biologii i Meditsiny* (*Bulletin of Experimental Biology and Medicine*) and in *Biokhimiya* (Troshin, 1951a-e, 1952). He considered that any solute in living cells can exist either dissolved in the cell water or in an adsorbed or chemically bound state. In support, Troshin cited Na_2SO_4 and resorcinol distributions in the simple coacervate of gelatin described by Holleman, Bungenberg de Jong, and Modderman in 1934. Their data, reproduced here as Table 4.2, show that gelatin gel demonstrated "negative" adsorption (or exclusion) of Na_2SO_4 . This is shown in the table by the negative quantities of X , which is grams of Na_2SO_4 adsorbed per gram of gelatin. At the time of these studies, adsorption phenomena were seen largely as interfacial phenomena. Substances which reduce interfacial tension cause "positive"

TABLE 4.2. Na_2SO_4 Distribution between a Gelatin Coacervate and the External Solution^{a,b}

Expt. No.	Temp. (°C)	External solution			Coacervate			X	$\frac{[\text{Na}_2\text{SO}_4]_{\text{c.w.}}}{[\text{Na}_2\text{SO}_4]_{\text{ex}}}$
		Gelatin (%)	Water (%)	Na_2SO_4 (%)	Gelatin (%)	Water (%)	Na_2SO_4 (%)		
1	50.04	2.8	87.8	9.4	10.4	82.1	7.5	-0.007	0.85
2	50.04	0.7	87.1	12.2	24.1	69.7	6.2	-0.147	0.64
3	50.04	0.2	85.0	14.8	27.2	66.6	7.2	-0.155	0.62
4	50.04	0.2	82.4	17.4	36.7	57.0	6.3	-0.155	0.53
5	60.02	0.8	87.0	12.2	26.1	67.6	6.3		0.66

^a X expresses the "negative adsorption" of Na_2SO_4 in the coacervate. The last column shows the ratio of Na_2SO_4 in coacervate water (c.w.) to that in the external solution (ex).

^b Data from Holleman *et al.* (1934).

"adsorption" on the gelatin surface; substances which increase the gelatin-water interfacial tension cause "negative adsorption." It was assumed by these authors that the bulk phase water in the gelatin gel or coacervate has the same solubility for Na_2SO_4 and other solutes (see Bungenberg de Jong, 1949, p. 252).

However, the last column of Table 4.2, newly added, was calculated on the basis of a different viewpoint. By assuming an even distribution of Na_2SO_4 in all the coacervate water, one calculates the equilibrium concentration of Na_2SO_4 in the coacervate water and expresses it as a ratio of the concentration in the medium. The degree of exclusion shown by this ratio increased with increasing concentration of gelatin, and decreased as the concentration of external Na_2SO_4 increased. Troshin attributed this decline to saturation of adsorption sites, a concept he expressed more precisely in the following equation:

$$C_c = C + A \quad (4.1)$$

where C_c is the concentration of a solute in the coacervate, C is the concentration of the solute dissolved in the water of the coacervate, and A is the amount of adsorbed solute. The distribution of the solute between coacervate water and external solution follows the relation

$$C = KC_s \quad (4.2)$$

where C_s is the concentration of solute in the solution and K is the "coefficient of proportionality characteristic of the aqueous phase of the coacervate as a solvent." The adsorbed fraction was assumed to follow a Langmuir adsorption isotherm:

$$A = \frac{A_\infty C_s K}{C_s K + a} \quad (4.3)$$

where A_∞ is the limit of adsorption and a is a constant. Substituting equations (4.2) and (4.3) into equation (4.1), one obtains the Troshin equation:

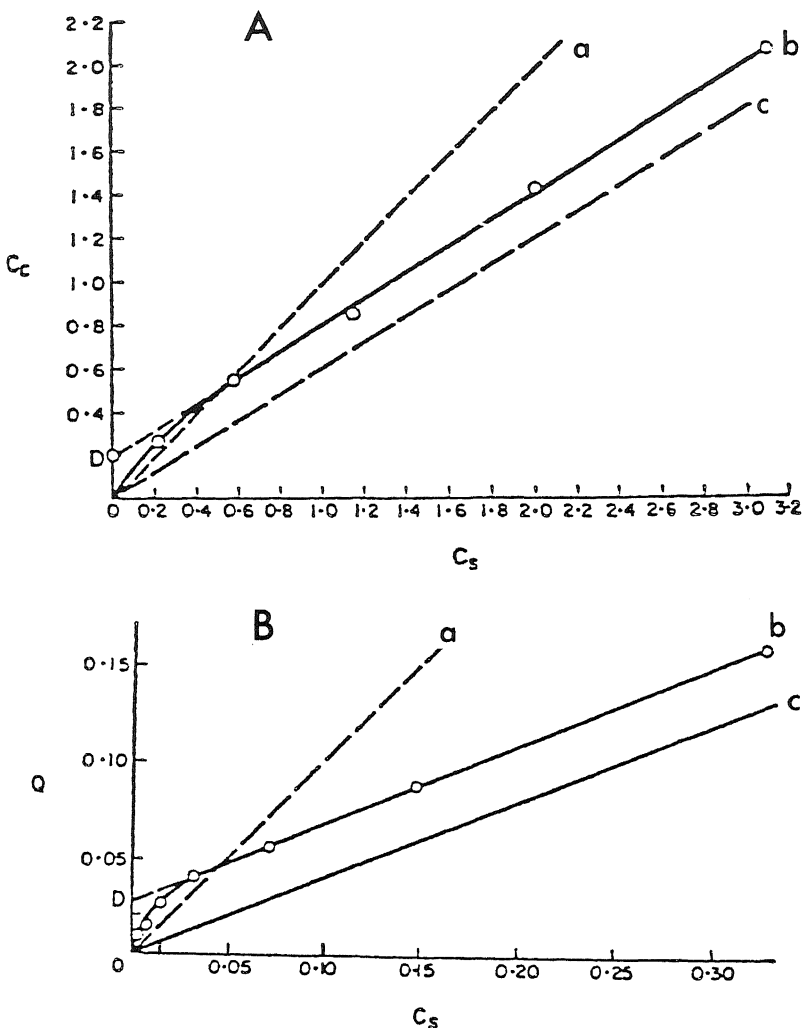


FIGURE 4.3. Dependence of sugar concentration (ordinate) on its concentration in the medium (C_s , in percent). (A) Sucrose in a coacervate. (B) Galactose in rabbit erythrocytes. (C) Lactose in yeast. a, Curve of equal concentration in water in the cell and in the medium; c, slope of the nonsaturable fraction of sugar. [From Troshin (1966), by permission of Pergamon Press.]

$$C_c = C_s K \left(1 + \frac{A_\infty}{C_s K + a} \right) \quad (4.4)$$

Troshin showed that this equation accurately described the distribution of sugars and a variety of other solutes in coacervates as well as living cells, as illustrated in Fig. 4.3. Furthermore, in nonliving model coacervates, as well as in living cells, K is as a rule below unity. Killing the living cell destroys this property of solute exclusion, and K then becomes unity, as Kamnev had shown.

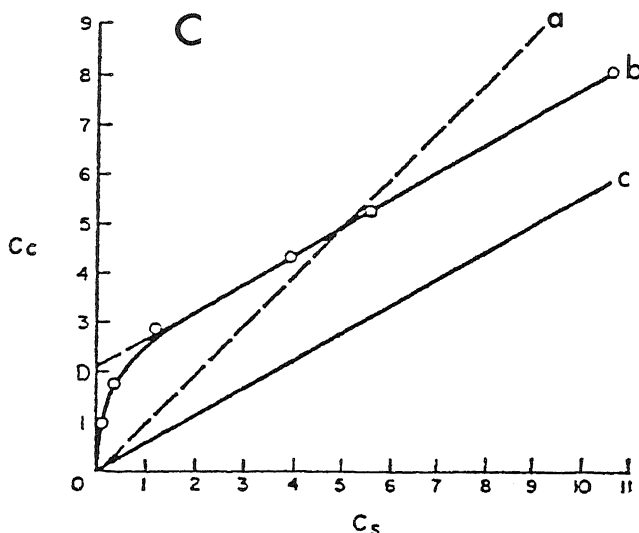


Figure 4.3. (Continued)

In the 1958 German edition of his monograph, Troshin applied his equation to the distribution of "mineral substances" in living cells, and he plotted the experimental data of Fenn, Cobb, and Marsh (1934) for Na^+ and Cl^- distribution in frog muscle cells, shown here in Fig. 4.4.

Troshin explained the role of metabolism in the maintenance of solute distribution (which Kamnev had already demonstrated) in these words:

To maintain certain physicochemical properties of the cell colloids which can ensure some particular form of physiological activity of the protoplasm, including the permeability of cells on a determinate level, it is essential that there should be an uninterrupted flow of energy metabolism. [Troshin, 1966, p. 371]

The rate of penetration of substances into a cell and their distribution between cell and medium are determined by the rate of enzymatic process directly or thanks to the fact that metabolism maintains the sorptional activity of live matter on a definite level. . . . [p. 374]

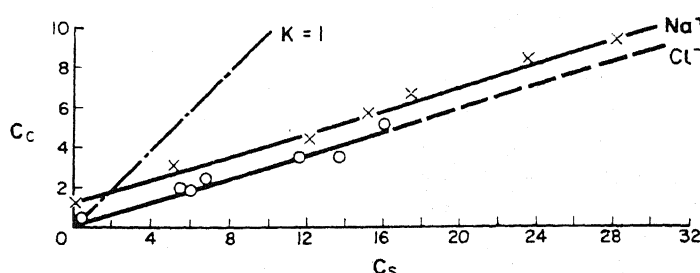


FIGURE 4.4. Dependence of the concentration of Na^+ and Cl^- in muscle fibers (C_c , in milliequivalent percent in the water of the muscle fibers) on their concentration in the medium (C_s , in milliequivalent percent). [Data from Fenn *et al.* (1934). Figure from Troshin (1966), by permission of Pergamon Press.]

4.3. Rekindled Doubts about the Revised Membrane Pump Theory

The rapid succession of events following the publication of the Boyle-Conway theory—the disproof of one of its major concepts (one first introduced by Mond and Netter), the remedial postulation of the Na^+ pump, and the brilliant exploitation of the new model by Hodgkin, Huxley, and Katz—left little time for a judicious evaluation of the validity of other aspects of the Boyle and Conway theory, e.g., the cell as a Donnan system of membrane equilibration. Nevertheless it was not difficult to see serious fundamental problems now facing this revised version of the membrane theory, more properly termed the *membrane pump theory*.

4.3.1. Discovery of the Non-Donnan Distribution of Many Permeant Substances

Donnan's membrane theory as applied to living cells demands the presence of a large concentration of an impermeant anion in the cells. Yet the most obvious candidates, the intracellular proteins, do not carry a large number of net negative charges under physiological conditions. Boyle and Conway offered the attractive hypothesis that the impermeant anions exist, nevertheless, in the form of impermeant organic phosphates; the permeant K^+ then would still accumulate to high concentrations in cells according to Donnan's theory. In the case of frog muscles it is known that such organic phosphates include creatine phosphate at a concentration of 21.8 mmoles/kg and ATP at 5.0 mmoles/kg of fresh tissue. At the pH of the living cell, these two phosphates alone amount to 98.4 mEq of anionic charge per liter of intracellular water. The idea that permeant glucose and inorganic phosphate enter cells and therein combine to form the impermeant organic phosphate had much appeal. However, large concentrations of creatine phosphate and ATP are not ubiquitous features of living cells.

In mammalian red blood cells, which selectively accumulate K^+ to levels similar to those in muscle, the predominant anion is not organic phosphate but simply Cl^- . Thus, from R. E. Bernstein's review in 1954, one obtains from nine mammalian sources the surprisingly uniform intracellular Cl^- concentration of 81.9 ± 1.17 mmoles/liter of cell water. However, Cl^- is definitely not impermeant. Indeed, the high permeability of the red cell membrane to Cl^- has long been known (Bonninger, 1909; Dirkin and Mook, 1931; Tosteson, 1959), even though the red cell membrane was once also widely and erroneously believed to be impermeable to Cl^- (Hedin, 1897; Hamburger, 1904).

In brain and retina, Terner, Eggleton, and Krebs (1950) found that the major anion that accumulates in the cells with K^+ is glutamate, and that glutamate is not impermeant but travels in and out of cells with no difficulty.

In *Escherichia coli*, K^+ accumulates in cells accompanied by hexosephosphates (R. B. Roberts *et al.*, 1949). This finding by itself could agree with Boyle and Conway's theory. However, Roberts and Wolffe showed two years later (1951) that the intracellular hexosephosphate was in rapid exchange with labeled hexosephosphate in the outside medium and is therefore not an impermeant anion.

Equally important was the finding of M. Eggleton and Eggleton (1933) that carnosine—a dipeptide which carries no net charge in cell water and which therefore cannot, according to the Donnan theory, accumulate in the cell as K^+ and other cations

TABLE 4.3. Ionic Distribution in Frog Muscle and External Medium^{a,b}

	Intracellular concentration (mEq/liter cell water)	Extracellular concentration (mEq/liter extracellular water)	Observed "Donnan ratio"
K ⁺	128.0	2.53	50.6
Na ⁺	16.9	105	0.16
Ca ²⁺	11.3	4.04	1.67
Mg ²⁺	31.6	2.46	3.61
Cl ⁻	1.04	76.8	73.8
HCO ₃ ⁻	9.2	26.4	2.86
Lactate	3.5	3.42	0.98
P _i	16.2	3.21	0.20

^aThe observed "Donnan ratio" is calculated according to equation (2.10) and the data given in the first two columns.

^bData from Ling (1962).

do—nevertheless is found almost exclusively in muscle cells and not in the medium. Yet the Eggletons found that carnosine can enter the muscle cell readily.

Taken as a whole, these findings added further doubts that absolute membrane impermeability plays a significant role in the steady-maintenance of the levels of many solutes in living cells.

Other evidence showed that the postulation of a Na⁺ pump solved only some of the difficulties which the findings of Brooks, Cohn and Cohn, Hahn, Heppel, and Steinbach had posed for the membrane theory (Section 3.1.1). They showed the disobedience of one permeant solute, Na⁺, of the prediction of Donnan's theory of membrane equilibrium, according to which *all permeant ions should distribute themselves according to the same Donnan ratio* described in equation (2.10). The postulation of one pump, the Na⁺ pump, may give the impression that other solutes found in living cells do obey Donnan's theory. In fact this is not the case at all. Cl⁻ in red blood cells, glutamate in brain and retina, and hexosephosphate in *E. coli* are accumulated within the cells in ways other than that predicted by a Donnan equilibrium. What is more, as shown in Table 4.3, *even in frog muscle, no two permeant solutes distribute with the same Donnan ratio*. The postulation of a Na⁺ pump does not provide a general solution to the problem, and many more pumps are required. Moreover, energy sources must be found for these pumps as well.

4.3.2. Reinvestigation of the Question of Whether or Not Cells Have Enough Energy to Operate the Postulated Na⁺ Pump

The Na⁺ pump concept was based on the idea that in a normal resting cell metabolically energized pumping activity keeps the intracellular Na⁺ concentration at a low level in spite of a constant inward diffusion of this ion into the cell. Diffusion as a rule has a low temperature coefficient. Pumping activity, on the other hand, is expected to have a higher temperature coefficient. Thus cooling will have less effect on inward Na⁺ flux than on outward pumping; as a result, an increase in the level of Na⁺ and a decrease in the level of K⁺ in the cells may be expected. Indeed, as mentioned earlier

TABLE 4.4. K^+ and Na^+ Contents of Frog Muscle after Prolonged Exposure to Nitrogen and Iodoacetate at $0^\circ C$ ^a

	K^+ (μ moles/g fresh tissue)	Na^+ (μ moles/g fresh tissue)
Control	74.9 ± 1.31	28.4 ± 1.21
Pairs after 7.74 hr ($0^\circ C$) in 5 mM IAA and pure nitrogen	76.3 ± 1.64	29.2 ± 1.72
<i>P</i>	> 0.5	> 0.7

^aData from Ling (1962).

(Section 3.3.1), there are experimental observations that cooling has just that effect in a variety of living tissues. This reaction does not involve a permanent injury to the cells, which fully regain their lost K^+ upon warming (Reisin and Gulati, 1973; Negendank and Shaller, 1979b).

It therefore seemed strange that frog muscles behave so differently: Cooling to $0^\circ C$ has no effect on the level of K^+ and Na^+ in these tissues (Ling 1951, 1952). This indifference to temperature lowering suggests that the inward and outward movements of Na^+ have exactly the same temperature coefficient. What is even more surprising is that not only can these cells withstand low temperature, they can also maintain their high K^+ and low Na^+ contents for many hours at $0^\circ C$ even after both respiratory and glycolytic activity have been brought to a halt (Table 4.4). In contrast, at $25^\circ C$, the combined action of iodoacetate and pure nitrogen leads rapidly to the loss of K^+ and the gain of Na^+ (Fig. 4.5). Thus cooling, which of itself should slow down the pump and bring about K^+ loss and Na^+ gain, does just the opposite: It protects the cells against

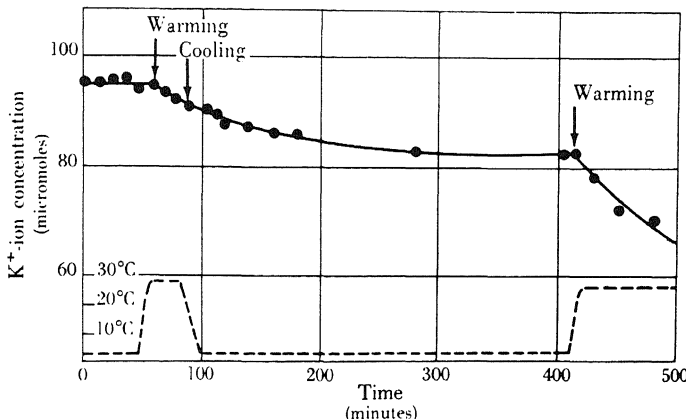


FIGURE 4.5. Effect of temperature upon the K^+ content of poisoned frog muscle. Ordinate: upper, K^+ content of muscle in μ moles per 1.15 g muscle; lower, temperature in degrees centigrade. Abscissa: time in minutes. Muscles were kept in Ringer solution containing 5 mM IAA and 1 mM NaCN. Warming caused a rapid loss of K^+ ; cooling stopped the loss after a delay. [From Ling (1952), by permission of the Johns Hopkins University Press.]

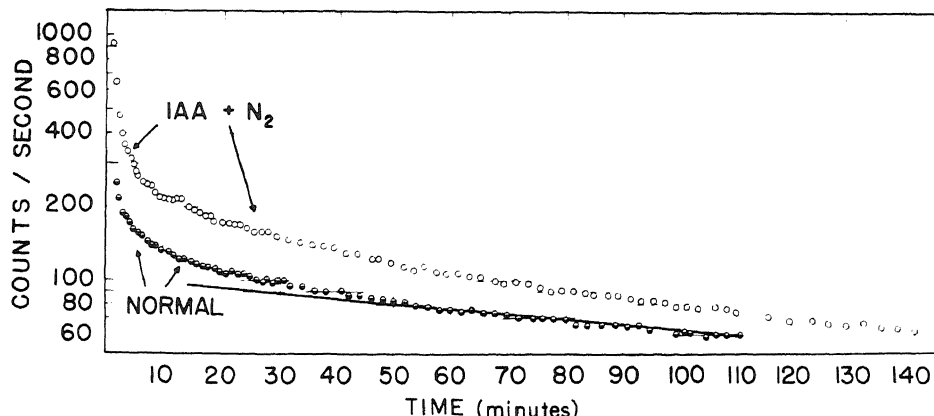


FIGURE 4.6. $^{22}\text{Na}^+$ efflux from frog toe muscle. Data indicate no significant change of Na^+ efflux rate after exposure to nitrogen and iodoacetate. Experiment was carried out at 0°C . [From Ling (1962).]

metabolic poisons. All in all, these data did not fit into the general framework of the Na^+ pump hypothesis.

In 1952 Ling briefly reported his study of Na^+ efflux at 0°C from normal frog muscle and muscle poisoned with iodoacetate plus pure nitrogen. As shown in Fig. 4.6, taken from a later publication (Ling, 1962), poisoning produced no detectable change in the Na^+ efflux rate.

The essence of this finding was confirmed by Keynes and Maisel (1954), who state, "neither 0.2 mM of 2,4-dinitrophenol (DNP), nor a combination of 0.5 mM iodoacetate with 3 mM cyanide (at pH 7.6), applied to the muscles for over 3.5 h, caused any really obvious reduction in the sodium efflux." Their figure is reproduced as Fig. 4.7. In 1961 Conway and co-workers made still another study of the same phenomenon in the same tissues; they too reached the same conclusion. Their study is reproduced in Fig. 4.8. It should be pointed out that, whereas the experiments of Ling were carried out at 0°C , those of Keynes and Maisel and of Conway *et al.* were conducted at room temperature. This point will be discussed again in Section 5.2.1. Suffice it to say that these sorts of observations led me to doubt seriously the Na^+ pump hypothesis and to seek different mechanisms for the selective accumulation of K^+ and exclusion of Na^+ by cells.

4.4. Ling's Fixed-Charge Hypothesis

In the evolution of theories of the living cell, an increasingly important role was being played by the isolated frog sartorius muscle. This became evident not long after W. F. Pfeffer's propounding of the membrane theory in 1877, and marked a significant shift from a primarily botanical to a zoological approach. The arguments of Overton, Bernstein, Mond and Netter, and Boyle and Conway, and then the cataclysmic discoveries of Steinbach leading to the postulation of the Na^+ pump, all rested primarily on experimental studies of this single tissue. This is not surprising, for frog muscle has

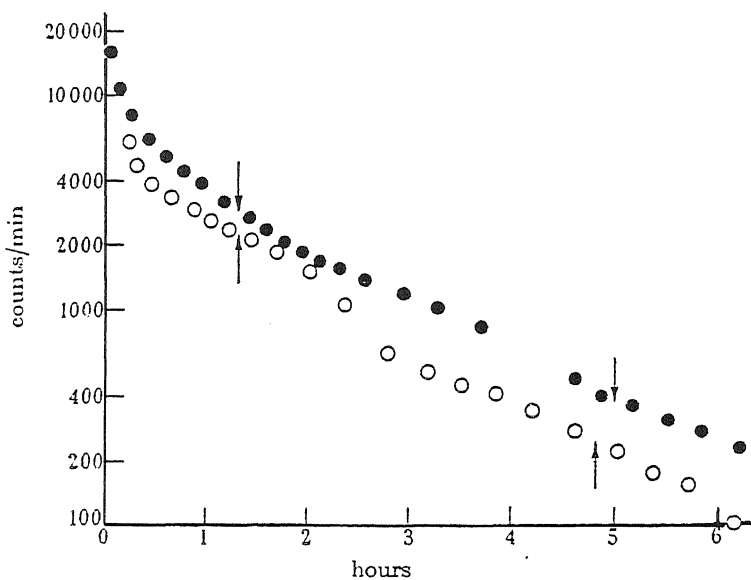


FIGURE 4.7. Disappearance of $^{24}\text{Na}^+$ from sartorius muscles poisoned with metabolic inhibitors. ●, Treated with 0.2 mM dinitrophenol for the period between the arrows, temperature 17°C. ○, Treated with 0.5 mM iodoacetate and 3 mM cyanide for the period between the arrows, temperature 21°C. [From Keynes and Maisel (1954), by permission of *Proceedings of the Royal Society of London*.]

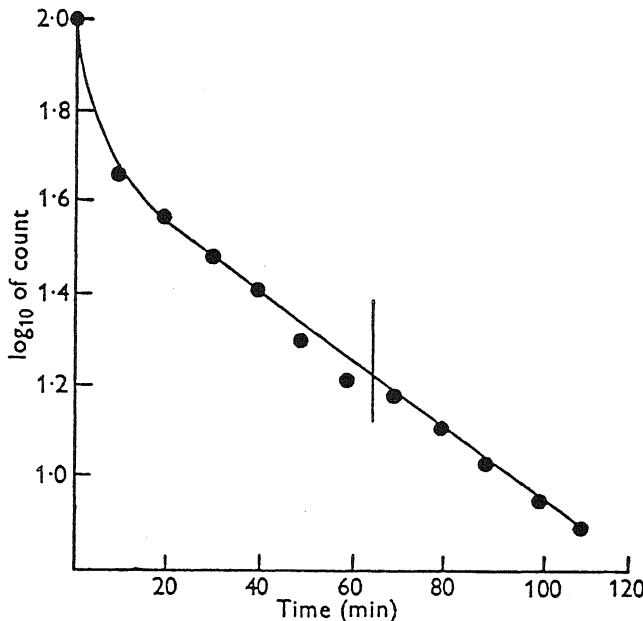


FIGURE 4.8. Effect of iodoacetate on loss of $^{24}\text{Na}^+$ from Na^+ -rich muscle. Inhibitor added at time indicated by vertical bar. [From Conway *et al.* (1961), by permission of *Journal of Physiology*.]

many merits. Readily available in large quantities and sturdy in incubation, it provides an easily isolated, uniform population of large intact cells whose osmotic, ionic, and electrical behavior lends itself readily to quantitative study.

4.4.1. A New Molecular Mechanism for the Selective Accumulation of K^+ over Na^+ in Living Cells

As far back as 1906 Benjamin Moore had likened the accumulation of K^+ in cells to the accumulation of oxygen in red blood cells, both due to some sort of binding. Others, like Neuschloss, Ernst, and Meigs and Ryan, had expounded different versions of a bound K^+ concept (Section 2.6.2). None of these ideas was broadly accepted. The evidence against K^+ binding reviewed by Lillie in his monograph *Protoplasmic Action and Nervous Action* (1923) was as follows:

According to Bugarszky and Liebermann (1898) the addition of even large quantities of proteins to salt solution affects the ionic concentration only slightly. Michaelis and Rona (1908) have shown by "compensation dialysis" that the salts in serum (containing 10% protein) are fully dialyzable. Pauli and Samec (1909) have also shown that alkali salts are not more soluble in serum than in water. These and other experimental studies simply did not bear up the contention that proteins can adsorb K^+ in large enough quantity to account for the phenomenon of selective accumulation of K^+ in living cells. . . .

As the first point of departure from earlier views, Ling (1952) pointed out that not all proteins were expected to adsorb K^+ over Na^+ selectively. Even a protein that possesses an inherent propensity for K^+ adsorption would do so only when it exists in a specific conformation, and, to assume this conformation, proteins may require at the same time interaction with, for example, a key metabolic product like ATP.

It was then considered that the interaction of certain suitable intracellular proteins with ATP and other essential agents would prevent the internal neutralization of fixed anionic sites (in the form of β - and γ -carboxyl groups) by fixed cationic sites (in the form of ϵ -amino groups and guanidyl groups) on the same and other proteins (Ling, 1952). The free β - and γ -carboxyl groups can then serve as the seats of selective K^+ adsorption. This basic theory provides a simple explanation for past failures, cited above, to demonstrate K^+ adsorption in isolated proteins.

In Section 2.3 it was mentioned that Bayliss, as well as Mitchell, Wilson, and Stanton, had suggested that the familiar physiological activity of K^+ that is lacking in the highly similar cation, Na^+ , may be related to the differences in the mobilities, and eventually to the different hydrated diameters, of these ions. Michaelis related the greater depolarizing effect of K^+ than Na^+ on the electrical potential of collodion membranes to the smaller hydrated diameter of K^+ . This concept was then applied to the living cell membrane, first by Mond and Netter and then by Boyle and Conway. This promising lead in its original context was not further pursued when Na^+ , with its large hydrated diameter, was proven to be quite permeant to the cell membrane.

In 1951 and 1952, Ling briefly outlined a new theory of selective K^+ accumulation, once more utilizing the differences in the hydrated diameters of K^+ and Na^+ , but in a totally different context that involved in essence nothing less than the abandonment of the membrane theory in favor of the bulk phase view. To distinguish it from other

theories bearing the name *fixed-charge hypothesis*, this early version of the association-induction hypothesis will be referred to as *Ling's fixed-charge hypothesis* (LFCH).

It was argued that, if one considers a muscle cell, one major protein, myosin, alone contains enough free β - and γ -carboxyl groups (156 mmoles per liter of fresh muscle) to provide fixed anionic adsorption sites for all of the cell K^+ (126 mmoles per liter of fresh muscle). Now 156 mmoles of anionic sites is equivalent to $0.156 \times 6.06 \times 10^{23} = 9.45 \times 10^{22}$ sites per liter of fresh muscle. With this enormous number of sites, the

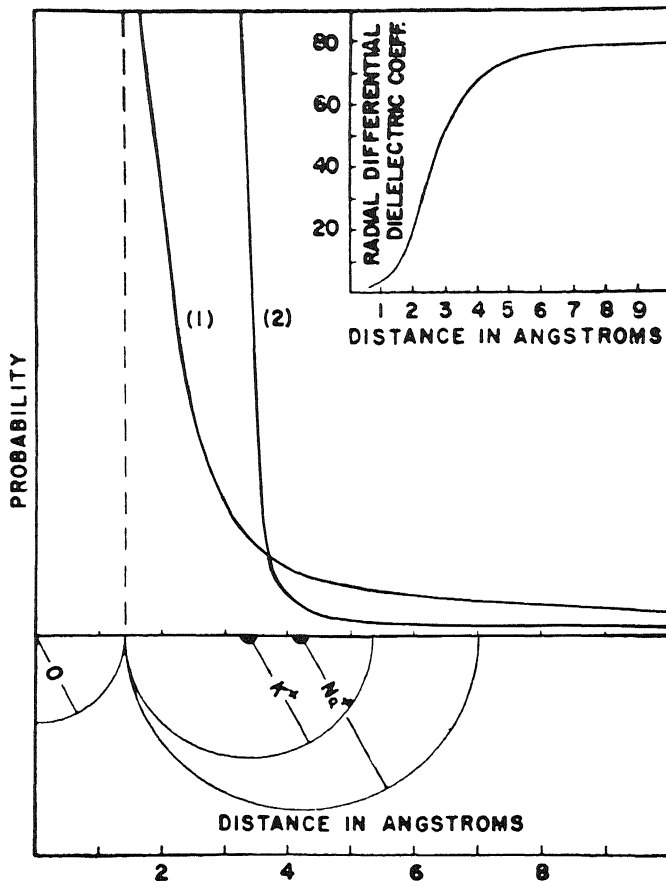


FIGURE 4.9. Probability of finding a positive charge at distances from the center of a fixed negative oxygen atom. Curve (1): probability of finding any positive ion at a given distance from the center of a fixed oxygen atom in a solution of uniform dielectric constant. Curve (2): probability of same in a solution whose dielectric properties follow the course shown in the inset. In this curve the probability rises so steeply at 4 Å (a distance within which K^+ , but not Na^+ , can approach) that in a mixture of Na^+ and K^+ the great majority of cations associated with fixed negative charges would be K^+ . The half circles at the bottom of the figure represent the diameters of hydrated K^+ , Na^+ , and a naked oxygen atom without hydration atmosphere (since organic anions are only weakly hydrated). [From Ling (1952), by permission of Johns Hopkins University Press.]

problem could only be treated in a statistical manner, or, more precisely, in a statistical mechanical way.

The basic concept was that, owing to the intense electrical field near an anionic site, the probability of finding a counterion in its immediate vicinity rises sharply as the distance between the fixed anions and the free cations decreases. This sharp increase in the probability of finding a cation in close proximity to a fixed anion occurs not only because of the exponential increase in the electrical forces as the distance of separation decreases but also because of the phenomenon of *dielectric saturation* in the immediate neighborhood of the ions, as was first pointed out by Hückel (1925). This steep rise in probability is illustrated in the inset of Fig. 4.9, taken from Ling (1952). It shows the variation of the dielectric constant in the immediate neighborhood of a fixed anion that is represented by a negatively charged oxygen atom. In this theory K^+ is accumulated over Na^+ in living cells because its smaller size permits K^+ to enter into the spherical shell where the highest probability of finding a counterion is located. As a result, most of the fixed anionic sites are associated with K^+ .

This theory could explain the selective accumulation of K^+ over Na^+ in living cells as well as the similar accumulation of K^+ over Na^+ in a variety of inanimate systems (e.g., permutit, soils) which, though widely different in chemical composition, share the common feature of a fixed matrix bearing anionic sites. Among these inanimate systems are the man-made ion exchange resins, which, as water-containing matrixes of fixed, anion-bearing, cross-linked linear polymers, bear the greatest resemblance to living cells from the viewpoint just outlined.

4.4.2. Some Distinctive Features of Ling's Fixed-Charge Hypothesis

4.4.2.1. A High Degree of Ionic Association as the Basis of Ionic Selectivity

As outlined earlier (Sections 2.1.3 and 2.2.5), Bethe and Toropoff and Michaelis and co-workers long ago recognized the presence of fixed charges on the pore walls of model membranes. Fixed charges in membranes were important in Meyer and Sievers's theory of ion permeability, in Teorell's treatment of membrane electrical phenomena (Teorell, 1953), and in the studies of permselective membranes by Michaelis's pupil Sollner (Sollner *et al.*, 1941a,b; Sollner, 1949). Fixed charges also played a central role in the Procter-Wilson theory of swelling phenomena (Section 2.2.6.1). However, the concept of fixed charges in Ling's theory is different for three reasons: (1) Ling's theory proposed the presence of fixed charges throughout the cell and not only on the cell membrane; (2) Ling's theory proposed extensive association of one counterion with one fixed ion; and (3) Ling's theory proposed selective K^+ adsorption as the result of favorable electrostatic adsorption energy for K^+ over Na^+ associated with the fixed negatively charged sites. Without close association, the basic differences between hydrated K^+ and hydrated Na^+ cannot be perceived, since these differences are differences in *short-range* attributes. The *long-range* attributes (e.g., Coulombic forces) of the monovalent cations are not distinguishable.

An excellent model for LFCH is the ion exchange resin. Indeed, four years after Ling's publication, F. E. Harris and Rice (1956), apparently unaware of the earlier work, published a similar electrostatic theory for selective uptake of K^+ over Na^+ in ion

exchange resins. Ling's theory was not widely accepted by workers in the ion exchange resin field (see, however, Reichenberg, 1966). Indeed the more popular view was that proposed by Gregor (1948, 1951), who considered direct counterion-fixed ion contact as trivial and assumed complete dissociation of countercations from fixed anions within the resin phase. Therefore, he explained selectivity of K^+ over Na^+ on the basis of the larger size of hydrated Na^+ compared to hydrated K^+ . These counterions in the resin water are then subject to the swelling pressure that retains the smaller K^+ but squeezes out the larger hydrated Na^+ . However, Gregor's theory cannot, for example, explain the much higher degree of selectivity for Ag^+ and Tl^+ over Cs^+ , for they are of the same size (Helfferich, 1962, p. 162). Neither LFCN nor Gregor's theory can explain the selective preference of Na^+ over K^+ in phosphonic and carboxylic resins. This subject will be brought into focus in Chapter 6, where it will be seen how a resolution of the problem led to the development of the full version of the association-induction (AI) hypothesis.

4.4.2.2. Living Cells as Labile Amphoteric Fixed-Charge Systems

One basic difference between living cells and ion exchange resins lies in the fact that living cells are labile systems capable of shuttling between alternative physiological states, while man-made ion exchange resins are fixed in one state. One reason for the lability of the cellular fixed-charge system is that the living cell is neither an anionic

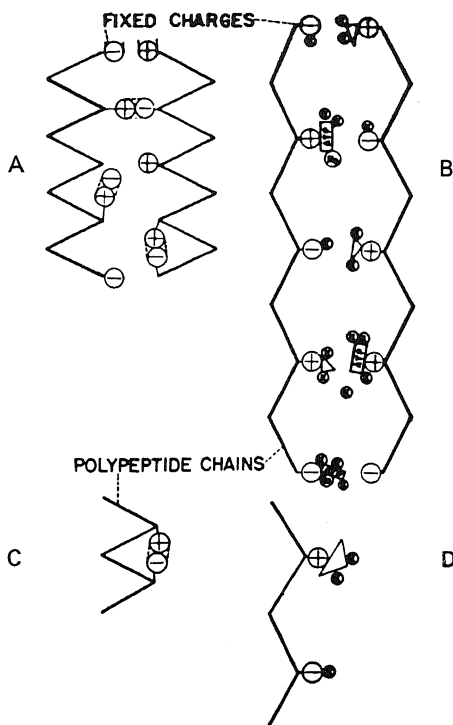


FIGURE 4.10. Diagrammatic representation of the hypothetical unfolding of protein chains as a result of adsorption of anions. (C) and (D) indicate that the adsorption of a trivalent anion onto a fixed cation would produce three fixed negative charges. For simplicity, almost all ATP molecules are represented as directly adsorbed onto fixed positive charges on the protein chains. [From Ling (1952), by permission of Johns Hopkins University Press.]

fixed-charge system like the sulfonate type of cation exchange resin nor a cationic fixed-charge system like the amino type of anion exchange resin. *Rather the living cell is an amphoteric fixed-charge system carrying both fixed anions and fixed cations.* These fixed cations and fixed anions tend to form electrostatic bonds or salt linkages (Speakman and Hirst, 1931, 1933; Perutz, 1978). It is only when salt linkages are prevented from forming or are dissociated that fixed anions are available for selective K^+ adsorption. This relationship is illustrated in Fig. 4.10. This concept will be developed later in a variety of contexts. One example is the involvement of the formation of salt linkages and the displacement and liberation of adsorbed K^+ from muscle cells during contraction.

4.4.2.3. A Nonhydrolytic Mechanism for the Function of ATP

Metabolism ultimately is essential for the continued maintenance of selective K^+ accumulation (Section 3.3.1) and in many cells ATP is the metabolic product that plays the key role. In the LFCH, this dependence of selective K^+ accumulation on metabolism is not due to the hydrolysis of ATP, but to its presence *per se*. The amphoteric nature of the living cell fixed-charge system endows it with a natural ability to assume either one of two alternate states, one in which the fixed negative charges are neutralized by fixed positive charges in the formation of salt linkages and another in which the fixed negative charges selectively adsorb K^+ or Na^+ and the fixed positive charges selectively adsorb anions. The adsorbed anions may include glutamate in brain and retina, hexosephosphate in *E. coli*, Cl^- in mammalian red cells, and creatine phosphate in frog muscle cells (Section 4.3.1).

In particular, ATP plays a special role in keeping the proteins from forming salt linkages and assuming a contracted conformation. In this role ATP acts by adsorbing onto the proteins at key sites, thereby causing them to assume an expanded conformation because of long-range electrostatic repulsion. In addition, ATP causes a selective preference for K^+ over Na^+ . Although this specific mechanism of ATP action was revised in the later and complete version of the AI hypothesis, in both hypotheses, in order to maintain selective K^+ accumulation, ATP functions as an *intact* adsorbed molecular ion and not through its hydrolytic cleavage to liberate energy stored in postulated "high-energy" phosphate bonds. Nonhydrolytic roles of ATP in maintaining the relaxed conformation of muscles had been suggested earlier by Riseman and Kirkwood (1948) and by Botts and Morales (1951).

4.5. Molecular Mechanisms of Selective Ionic Permeability

In 1904 and succeeding years, Devaux published a series of notes in which he showed that plant cells of diverse types can rapidly and reversibly exchange their ionic contents with ions of different types in the environment (Devaux, 1904–1916). Indeed, he was able to demonstrate that such ion exchanges follow a mass action law. These striking quantitative findings elicited surprisingly few responses from more influential scientists of his time. Some 30 years later, his pupil Genevois summarized Devaux's important work (Genevois, 1930), and pointed out that it was virtually completely ignored. In the meantime, the term *ion exchange* had become a highly popular notion

among plant physiologists (for review see Epstein, 1956). Yet there were profound differences in the meaning of the term *ion exchange* as used by Devaux and by later investigators. Devaux's exchange referred to the ions throughout the entire cell and he therefore was dealing with ion distribution in the context of a bulk phase theory. Later plant physiologists used the term to describe an aspect of the kinetic phenomena of ion permeation and interpreted it in terms of the membrane theory.

In reference to ion exchange in cell membrane permeability, one may raise the question: How can a homogeneous, isotropic lipid membrane, or indeed a mosaic membrane with pores, provide the basis for ion exchange, when ion exchange demands, whether in its equilibrium or its kinetic manifestation, a limited number of molecular sites for binding? The answer lay in the additional postulation of membrane "carriers."

4.5.1. The Membrane Carrier Model

The concept of *carriers*, ferry-boat-like devices in the lipid membrane shuttling back and forth between the outer and inner boundaries, transporting ionic passengers, was first discussed by Osterhout (1936), and later by Brooks (1937), Lundegårdh (1940), Brooks and Brooks (1941), and Wohl and James (1942). The first four papers dealt with plants, the last, with the subject in general terms.

In 1952, Epstein and Hagen showed that the rate of entry of radioactively labeled Rb^+ into barley roots is competitively inhibited by nonlabeled K^+ , Rb^+ , and Cs^+ in the bathing medium. These authors theorized that

At the outer surface of a membrane which is impermeable to the free ion, the ion combines with metabolically produced binding compounds or carriers. They traverse the membrane in this form. Upon reaching the inner surface, the binding compound or carrier is chemically altered by metabolic processes so that the ions are set free.

These ideas were set forth as follows:



where R and R' represent different chemical states of the metabolically produced carrier; M_{inside} and $\text{M}_{\text{outside}}$ are the alkali-metal ions inside and outside the cell membrane respectively; MR is the unstable carrier-ion complex, and k_1 , k_2 , k_3 , and k_4 are constants for the reactions indicated. Epstein and Hagen drew attention to the basic analogy between the formulation given above and that describing the kinetics of an enzyme reaction:



where E is the free enzyme, S is the substrate, ES is the enzyme–substrate complex, and P is the product of the reaction. They adapted Michaelis's theory of enzyme kinetics (Michaelis and Menten, 1913), relating the observed rate of ionic permeation to the concentrations of the ion–carrier complex:

$$v = \frac{V_{\max}[S]}{K_s + [S]} \quad (4.9)$$

where v is the rate of ionic permeation, $[S]$ is the external ionic concentration, V_{\max} is the maximum value of v at infinite $[S]$, and K_s is the Michaelis constant for the ion–carrier complex. Writing equation (4.9) in the reciprocal form according to Lineweaver and Burk (1934) for enzyme kinetic studies, Epstein and Hagen showed that

$$\frac{1}{v} = \frac{K_s}{V_{\max}[S]} + \frac{1}{V_{\max}} \quad (4.10)$$

predicting a linear relation between $1/v$ and $1/[S]$. The intercept at the ordinate ($1/[S] = 0$) yields V_{\max} ; the slope multiplied by V_{\max} yields K_s .

In the presence of a second external ion competing for the same carrier,

$$\frac{1}{v} = \frac{1}{V_{\max}} \left(K_s + \frac{K_s[I]}{K_i} \right) \frac{1}{[S]} + \frac{1}{V_{\max}} \quad (4.11)$$

where $[I]$ is the concentration of the competing ion I and K_i is its binding constant to the carrier. In studying the rate of entry of an external ion S at varying concentrations, in the absence and presence of varying concentrations of a competing ion I, one plots the reciprocals of v against the reciprocals of $[S]$. Equation (4.11) predicts a family of straight lines converging on the same locus on the ordinate, each with a different slope. Epstein and Hagen showed that K^+ and Rb^+ compete for the same carrier, and their figure is reproduced as Fig. 4.11. From the slopes and intercepts, the parameters of the carrier–ion complex of the entrant ion and those of the competing ion were obtained.

4.5.2. Ling's Fixed-Charge Hypothesis

In the following year, Ling (1953) confirmed Epstein and Hagen's finding by demonstrating an entirely similar competition between K^+ and Rb^+ entering isolated frog muscles. However, Ling offered a different interpretation of the data by extending the theory that he had proposed for the bulk phase accumulation of K^+ . The basic assumption is simple. The cell surface is endowed with fixed anionic sites with properties similar to those envisaged inside the cells. Then the cell surface can, in essence, be seen as a two-dimensional replica of the three-dimensional cell. As such, a momentary snapshot of the cell surface would show most of the surface anionic sites to be occupied by K^+ (or Rb^+), which is preferred over Na^+ by the same mechanism described in Section 4.4.1 for the selective accumulation of K^+ over Na^+ . Here it is the concentration or density of the surface anionic sites that are associated with labeled external ions that

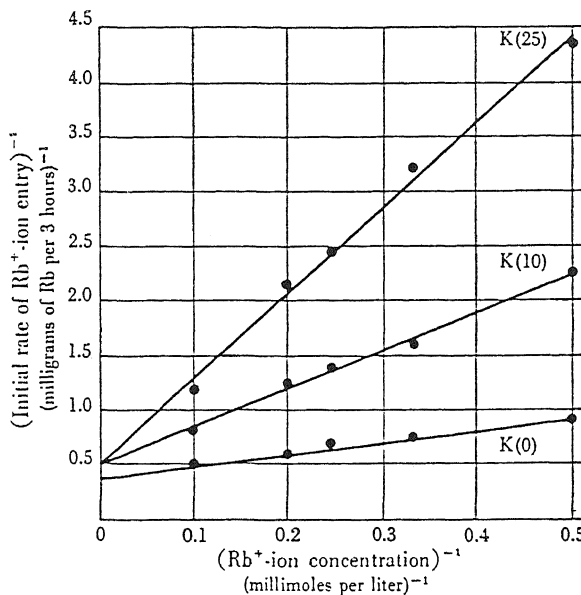


FIGURE 4.11. Inhibition by K^+ of the initial rate of radioactive Rb^+ entry into barley roots (24°C). [From Epstein and Hagen (1952), by permission of *Plant Physiology*.]

corresponds to the enzyme-substrate complex ES of equation (4.7). The subsequent step, corresponding to equation (4.8) in the enzyme analogy, does not involve a chemical alteration as in enzyme kinetics, nor does it involve a transmembrane migration of the ion-carrier complex as proposed in the carrier model. Instead, it involves merely a dissociation of the labeled ion in the right direction, i.e., toward the cell interior in influx studies. It should also be pointed out that the key postulation of Michaelis's theory of enzyme kinetics is that the substrate adsorbs onto an enzyme site in such a manner as to follow a Langmuir adsorption isotherm. Thus, the hypothesis of cell permeation proposed in the LFCH is merely that the monovalent cations K^+ and Rb^+ adsorb onto surface anionic sites following a similar Langmuir adsorption isotherm. It is the basic property of such an adsorption isotherm that it shows *competition*, since different entrant ions compete for the same sites, and *saturability*, since ions of the same species compete for the same sites.

Thus both the carrier model and the LFCH can predict the kind of ion permeability data shown in Fig. 4.11. Both theories lead to the same mathematical equation describing the permeation. The differences between the two theories are, however, profound. The LFCH of selective K^+ permeation is in fact merely another aspect of the LFCH of selective K^+ accumulation by the cell. No additional assumption need be made, while in the carrier model additional assumptions are required.

Epstein and Hagen (1952) suggested that the postulated carriers are continuously metabolically synthesized, so that, even though they are constantly being destroyed on reaching the inner surface of the cell membrane, an accurately controlled synthesis permits the maintenance of just the right carrier concentration in the membrane. Since transport rate obviously varies with the nature and concentration of external ion, many further postulations would have to be made to outline a servomechanism to keep a steady concentration of carriers in the membrane. If carriers have to be continually synthesized,

more energy would be needed than is required only to pump Na^+ out. This additional energy consumption had not been taken into account in the calculations of the energy need of Na^+ pumps discussed in Section 3.3.2.

In contrast, the requirements of the LFCH model are simple: the presence of fixed anionic sites on the cell surface. Since virtually all proteins contain anionic side chains in the form of β - and γ -carboxyl groups and since the presence of hydrophilic charged groups at the cell surface is also indicated by its low surface tension (Section 2.1.4), it is hard not to assume that the surfaces of living cells are as a rule endowed with fixed ionic groups.

The concept that a cell surface with regularly and properly spaced fixed anionic sites would cause cations to enter the cell in accordance with equation (4.11) may be illustrated with the aid of two familiar analogies:

1. Flamed cotton wads were at one time used to isolate sterile flasks from bacterial contamination. Yet the interstices among the cotton fibers are much larger than bacteria and bacterial spores. The effectiveness of cotton wads lies in the electrical charges on the cotton fibers, which attract and capture bacteria and spores and prevent them from entering the flasks.
2. In a vacuum tube, electrons emitted from the heated cathode filament can be prevented from reaching the positively charged plate by applying a bias voltage on the grid placed between the filament and the plate, even though the meshes of the grid are vastly larger than the size of electrons.

The LFCH of ionic permeation is based on the electrostatic field of the surface-fixed ions and their counterions (Figs. 4.12, 4.13). This implies that ionic entry follows-

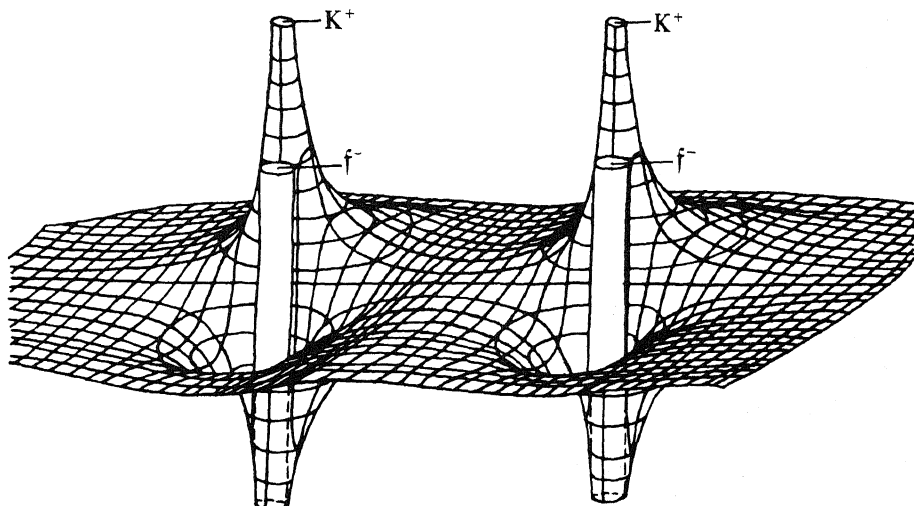


FIGURE 4.12. Electrostatic field near a pair of fixed anions and their counterions. The height or depth of the isopotential line at any locus qualitatively represents the sum of the repulsive and attractive forces acting on a cation. f^- and K^+ indicate location of fixed anion f^- and of countercation K^+ . [From Ling (1962).]

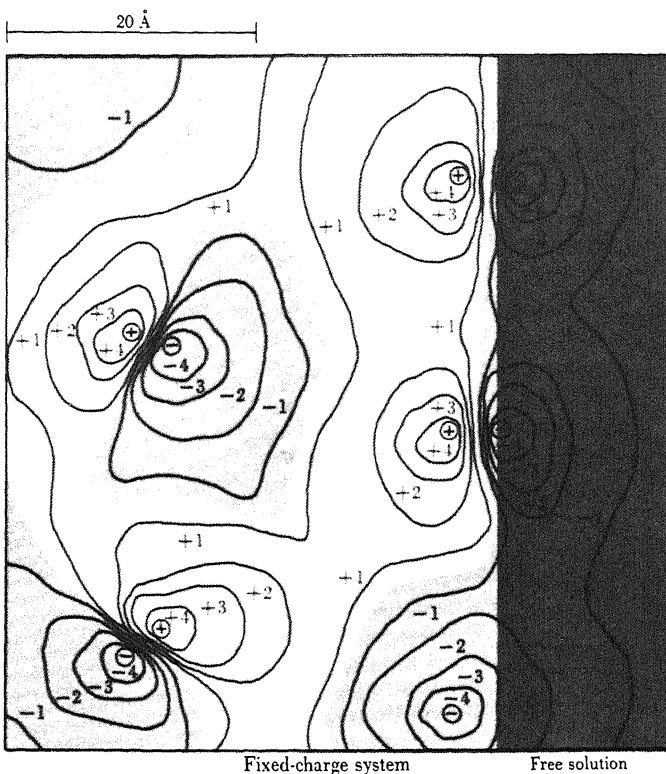


FIGURE 4.13. Diagrammatic illustration of the electrical potential fields near the surface of a fixed-charge system. Each line represents a more or less permanent isopotential line. The diagram demonstrates the continuous energy barriers toward the entry of cations and anions through the "meshes." [From Ling (1962).]

ing equation (4.11) is not unique to living cells but also may apply to other types of water-containing systems that possess fixed anionic sites. Two examples may be cited: (1) a man-made cation exchange resin which possesses fixed anionic sites in the form of sulfonate groups on a three-dimensional polyvinylstyrene framework, and (2) sheep's wool, a natural matrix of polypeptide chains containing about 15% of its amino acid residues in the form of glutamic and aspartic side chains with their β - and γ -carboxyl groups, respectively. It is true that a substantial portion of these must be locked in salt linkages, but some may be expected to be in the "free" state at the surface of the wool fibers.

Experiments to test these theoretical expectations were carried out in the late 1950s (Ling, 1960). The results are presented in reciprocal plots, according to equation (4.11), for $^{134}\text{Cs}^+$ entering a sulfonate ion exchange resin sheet (Fig. 4.14), and for labeled K^+ permeation into living frog muscles (Fig. 4.15).

The strict obedience of all these systems to equation (4.11) clearly shows that competition and saturability are not synonymous with the presence of membrane carriers or

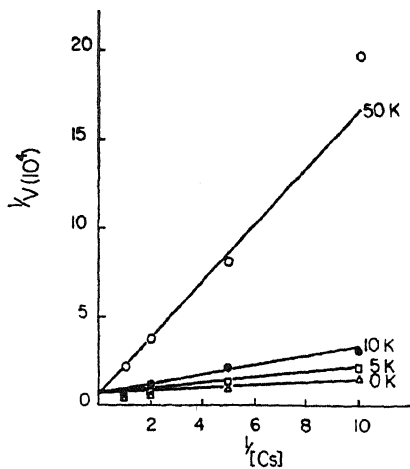


FIGURE 4.14. Effect of varying the external K^+ ion concentration on the rate of entry of $^{134}\text{Cs}^+$ (the values for KCl concentrations are to be multiplied by 4 mmoles/liter) into sheets of the sulfonate exchange resin Nalfilm-1. [From Ling (1960), by permission of *Journal of General Physiology*.]

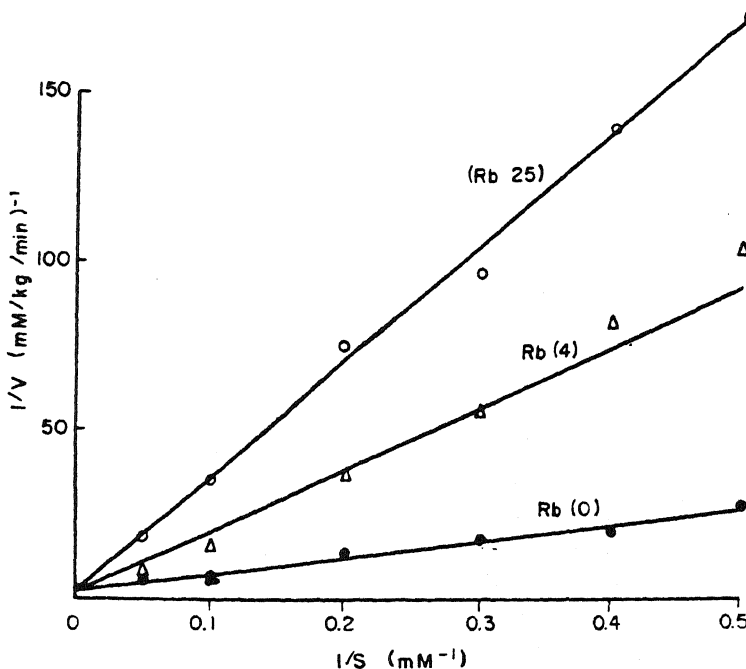


FIGURE 4.15. Effect of varying the external Rb^+ ion concentration (0, 4, and 25 mmoles/liter) on the initial rate of entry of K^+ into frog muscle (sartorius, semitendinosus, tibialis anticus, and ileofibularis). $^{42}\text{K}^+$ was used as a tracer. The experiment was performed at 0°C (pH 7.4). [From Ling (1960), by permission of *Journal of General Physiology*.]

pumps. In addition, the obedience to equation (4.11) shows that in this two-dimensional replica of the three-dimensional fixed-charge system there is a high degree of association of K^+ and Rb^+ with fixed anions regardless of whether the fixed anionic groups are sulfonate or β - and γ -carboxyl groups. These findings confirm a very basic and important tenet of the theory: *The degree of ionic association increases sharply if one species of the ion is fixed in space.* Were it otherwise most ions would have entered into the system much as they would have entered from one dilute aqueous solution into another dilute solution and there would be neither competition nor saturability. This important subject will be taken up again in Chapter 6.

4.6. The Surface Adsorption Theory of the Cellular Resting Potential

4.6.1. Three Historical Models: Glass, Oil, and Collodion

The membrane theory of cellular electrical potentials assumes that intracellular K^+ is in a free state much as it is in a dilute KCl solution. The concept in the LFCH that intracellular K^+ exists in an adsorbed state made it difficult at first glance to understand how there can be a K^+ -dependent resting potential. The resolution of this conflict began in the early 1950s with a reevaluation of studies of the electrical potentials of simpler model systems, studies which had molded the thinking of cell physiologists in earlier days.

4.6.1.1. Glass

Traube's copper ferrocyanide gel membrane inspired Ostwald to propose a membrane potential mechanism for cellular electrical potentials (Section 2.2.2). Later studies of the collodion electrode reaffirmed Michaelis's belief that the cellular resting potential is a membrane potential deriving its ionic specificity from the differences in specific ionic permeability of the membrane.

However, Baur (1913) suggested surface adsorption as the mechanism of the cell potential, using the oil chain as a model. Horovitz (1923) observed the behavior of glass electrodes, which led him to suggest that the sensitivity of the potential to a specific ion may not depend on its permeability through the glass, but on its adsorption onto the surface of the glass.

In studies of glass electrodes prepared from various hard Thüringer glasses, Horovitz observed the steep rise of the potential following neutralization of the acidic solution bathing the glass electrode; however, further addition of NaOH did not lead to the expected slow rise to the highest potential observed when soft glass electrodes were used, as was shown in Fig. 2.3. Instead, the potential steadily went down again (Fig. 4.16, bottom curve). This downward trend was due to the added Na^+ , since NH_4OH did not produce the same effect (Fig. 4.16, top curve). In support, he found that if the hard glass bulbs were first immersed in distilled water, and NaCl added step-by-step, a rectilinear relation was observed between the potential and the logarithm of the external Na^+ concentration (Fig. 4.17), indicating that this glass behaves as a Na^+ electrode. Similarly, electrodes prepared from glasses containing Zn^{2+} and K^+ were shown to function as

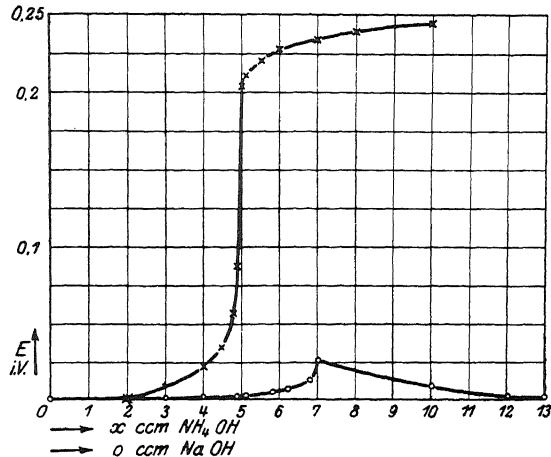


FIGURE 4.16. Electrical potential of Thüringer hard glass electrodes. Increasing amounts of NH_4OH (top curve) or NaOH (bottom curve) were added to the electrode. [From Horovitz (1923), by permission of *Zeitschrift für Physik*.]

Zn^{2+} and K^+ electrodes, respectively. Even more interesting, Horovitz was able to endow glass electrodes with a sensitivity to Ag^+ , which was not an ingredient in any of the glasses he studied, merely by soaking them in a 0.2 N AgNO_3 solution for 24 hr.

In interpreting his data, Horovitz (alias Lark-Horovitz, 1931) suggested that the cations Na^+ , K^+ , Zn^{2+} , and even Ag^+ entered into the solid glass phase and that only cations can migrate in the solid. The electrical potential at the glass surface was given as

$$\psi = \frac{RT}{\mathcal{F}} \ln \frac{(K_1/u_1)u_2 a}{C_1 + (K_1 u_2 / K_2 u_1) C_2} \quad (4.12)$$

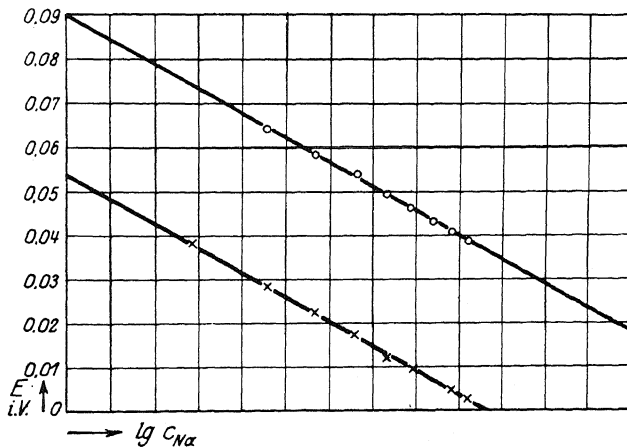


FIGURE 4.17. Effect of the logarithm of external Na^+ concentration on the electrical potential of glass electrodes of two different types of glass (397¹¹¹, top curve; 59¹¹¹, bottom curve). [From Horovitz (1923), by permission of *Zeitschrift für Physik*.]

where u_1 and u_2 are the mobilities of the two species of ion in the solid phase, K_1 and K_2 are the "integration constants in the expression for the thermodynamic potential of the ions present in the solid phase-solution tension," C_1 and C_2 are the concentrations of the two ions present in the solution, and a is the number of "places" available in the solid phase and is a constant. This equation can be simplified into the following form:

$$\psi = \text{Constant} - \frac{RT}{\mathcal{F}} \ln (C_1 + AC_2) \quad (4.13)$$

where A is a constant equal to $\mu_2 K_1 / \mu_1 K_2$.

Later Nicolsky (1937) derived a formally similar equation:

$$\psi = \psi^\circ + \frac{RT}{\mathcal{F}} \ln (a_1 + Ka_2) \quad (4.14)$$

in which the activities a_1 and a_2 , rather than concentrations of the two species of ions,

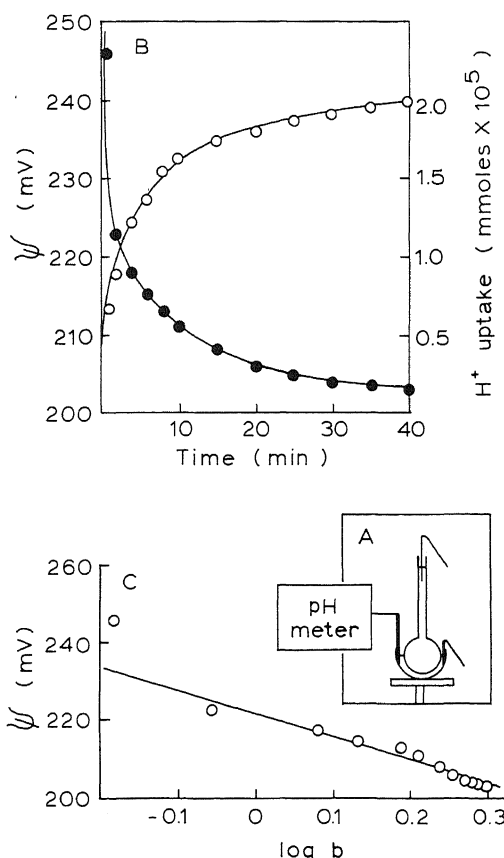


FIGURE 4.18. Dependence of the glass electrode potential upon the H^+ adsorbed at the glass surface from the external medium in exchange for Na^+ . A freshly blown glass bulb sits in a dish anchored to a rotating platform (A). The electrical potential (●) and H^+ concentration (○) are monitored over 40 min and plotted in (B). In (C), the logarithm of the amount of H^+ taken up per unit surface area (b) is plotted against the electrical potential recorded at any one time. The slope of the solid line is 59, quite close to the theoretical value (59.1 at $25^\circ C$). The data indicate not only that H^+ adsorbed at the glass surface determines the potential, but also that, at any one time in the course of the 40-min observation period, the potential represents a state of equilibrium. [From Haugaard (1941), by permission of *Journal of Physical Chemistry*.]

are used. However, K here is the equilibrium constant for the exchange of ion 1 for ion 2 adsorbed on the glass surface.

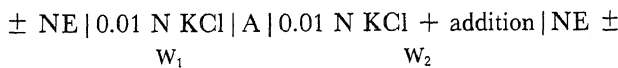
In years following, important experimental findings brought strong support to the concept that the surface of the glass is the seat of the potential. Only two will be cited (see also Lengyel and Blum, 1934):

1. As the glass pH electrode came into broad use, the National Bureau of Standards of the United States set up a standard technique to measure electrode behavior (Thompson, 1932). In this technique, the inside of the glass bulb was not filled with dilute HCl as was conventionally the case. Instead the inside of the bulb was plated with copper, to which an electric lead was soldered. In such a system the glass membrane does not separate two aqueous phases. The electrode behavior cannot be that of a membrane potential; it can only be a surface potential.
2. Haugaard (1941) showed that a freshly blown glass bulb which is not sensitive to H^+ becomes sensitive to H^+ as the glass exchanges its Na^+ for H^+ in the solution. Indeed, the electrical potential was shown (Fig. 4.18) to depend on the quantity of H^+ taken up by the glass surface, such that

$$\psi = \frac{RT}{\mathcal{F}} \ln \frac{[H^+]_{\text{glass surface}}}{[H^+]_{\text{ex}}} \quad (4.15)$$

4.6.1.2. Oil

Baur (1913) suggested a model of the electric organ of the fish in the form of an oil (or nonwater) phase which takes up ions from the surrounding aqueous phases, generating an "ion adsorption potential" (Section 2.2.4). In the experiments of Baur and Kronmann (1917), an "oil" phase of amyl alcohol (A) faces two aqueous solutions, W_1 and W_2 , both of which contain 0.01 N KCl; into each a calomel electrode is placed. The Volta chain is:



If the positively charged alkaloid strychnine is added to W_2 , it enters the oil phase and creates a potential which is more positive on the left-hand side. When NaCl is added instead of strychnine sulfate very little potential difference is observed. When negatively charged picrate is added to W_2 , the left electrode becomes negative. The uptake of positively charged strychnine or negatively charged picrate by the oil gives rise to the potential differences, which were shown to be quantitatively dependent on the concentration of potassium picrate or strychnine sulfate in the aqueous phase W_2 .

The oil potential was again investigated by Ehrensvard and Sillen (1938), who also concluded that it is due to an ion adsorption equilibrium between the two aqueous phases and the interfacial layers. They pointed out that "the ion adsorption equilibrium P.D.'s may play a part in physiology, for example, in the mechanism of the olfactory and gustatory system."

4.6.1.3. Collodion

Nitration of cotton produces pyroxylin, which is mostly nitrocellulose. When pyroxylin is dissolved in a mixture of ether and ethanol, it is called collodion. When glass tubes are dipped into collodion and the collodion allowed to dry partially, collodion thimbles or “electrodes” are made. Collodion electrodes were another important model of the cell membrane and were intensively studied by Michaelis and his co-workers (Section 2.2.5).

It is most significant that Michaelis and Perlzweig had actually considered Horowitz's concept that surface adsorption rather than membrane permeability underlies the creation of the potential. However, they dismissed the idea thus:

The theory of mixed electrodes [Horovitz] need not be considered because the chemical nature of collodion (and of some lipid membranes such as the wax in apple skin) excludes this possibility. The substance of this membrane is not an electrolyte-like material nor does it consist of a cation and anion-like glass. . . . [Michaelis and Perizweig, 1927, p. 577]

The Second World War cut off the German supply of the Schering brand of collodion that Michaelis's laboratory had been using most successfully, which permitted the preparation of collodion electrodes exhibiting high concentration potential. Suspension of the supply forced Sollner, Abrams, and Carr (1941a) to find alternative sources. Eventually they gave a most interesting account of their discovery that it was not pure collodion that gave rise to the electrical potential; rather it was an acidic impurity. This confirmed an earlier conclusion of Meyer and Sievers (1936b). Pure collodion also could be made to generate an electrical potential by the deliberate introduction of carboxyl groups by oxidizing the collodion with, for example, HBr or NaOH.

Sollner attributed the origin of the electrical potential across oxidized collodion membranes to the relative rates of permeation of the ions involved, “the more readily permeable critical ions impressing a potential on the other solution which is identical in sign with that of their own charges” (Sollner, 1949). However, in the same article, Sollner also pointed out that “competitive exchange adsorption of ions” may be involved. Figure 4.19, taken from Sollner, illustrates the mechanism involved. In Sollner's words:

of the nine anionic groups of the pore shown in [Fig. 4.19] only one is compensated electrically by the less adsorbable Cl^- ions, the other eight being compensated for by the (eight times) more strongly adsorbable Br^- as counterions. According to the premises Cl^- and Br^- are dissociated off completely and since they are of identical size, the diffusion velocities are identical. The ratio of the assumed transference number in the membrane of the two critical ions is therefore the same as the ratio of the adsorbabilities, 8:1 in favor of Br^- ion.” [Sollner, 1949, p. 1223]

Few of the counterions in Fig. 4.19 appear associated with the fixed charges. In Fig. 4.20, taken from a more recent review (Ives and Janz, 1961), the lack of association between counterion and fixed ion in the permselective membrane pores is more clearly illustrated.

Sollner's diagram (Fig. 4.19) shows that the fixed ionic sites are uniformly distributed throughout the pore. He had, therefore, departed somewhat from an earlier, highly significant statement made by Sollner, Abrams, and Carr (1941b, p. 9): “the activity of a membrane is obviously determined only by the degree of oxidation at the surfaces. . . .” This statement implies that only fixed carboxyl groups at the surface of the collodion

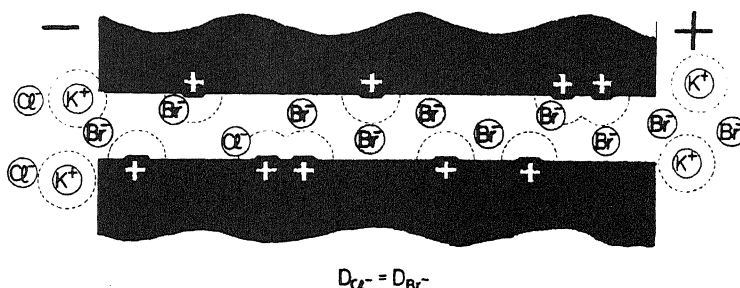


FIGURE 4.19. Diagrammatic illustration of charged pores of collodion membranes and their (dissociated) counteranions Cl^- and Br^- . [From Sollner (1949), by permission of *Journal of Physical Chemistry*.]

membrane play a significant role in determining the electrical properties of the membrane. However, for some unstated reason, this point was apparently abandoned by Sollner.

4.6.2. The Surface Adsorption Theory of Cellular Electrical Potentials

Ling (1955, 1959) postulated that the surfaces of muscle and nerve cells are endowed with fixed anionic sites in the form of β - and γ -carboxyl groups carried on aspartic and glutamic acid residues of cell-surface proteins, and that the resting potential of living cells originates from these groups. The equation for the cellular electrical potential, in a somewhat simplified form, is

$$\psi = \text{Constant} - \frac{RT}{\mathcal{Z}} \ln (K_K[K^+]_{ex} + K_{Na}[Na^+]_{ex}) \quad (4.16)$$

where K_K and K_{Na} are the adsorption constants of K^+ and Na^+ on the surface β - and

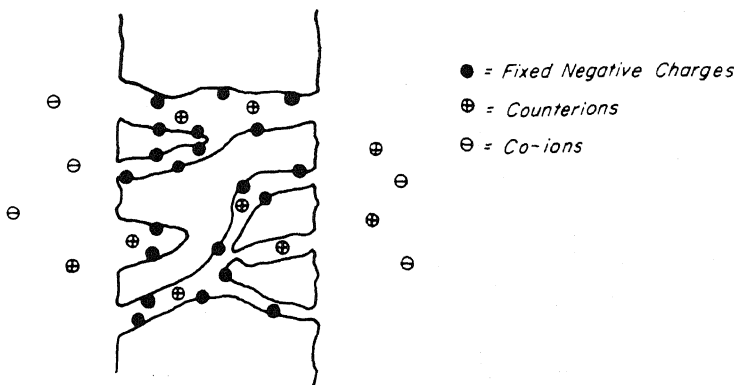


FIGURE 4.20. Diagrammatic illustration of a permselective membrane. [From Ives and Janz (1961), by permission of Academic Press.]

γ -carboxyl groups, and $[K^+]_{ex}$ and $[Na^+]_{ex}$ are the extracellular K^+ and Na^+ concentrations, respectively. A more complete presentation of this theory was given in 1960 and 1962, and will be outlined in Chapter 14.

The major concept is that, in resting cells, $K_K[K^+]_{ex} \gg K_{Na}[Na^+]_{ex}$; hence the cell surface functions as a K^+ electrode. During activity, the relative value of K_{Na} increases; as a result part of the cell transiently becomes a Na^+ -sensitive electrode. How such a change in relative values of K_{Na} and K_K occurs will be discussed in Chapters 6, 7, and 14.

The LFCH of cellular electrical potentials expressed in equation (4.16) explicitly predicts only three sets of quantitative relationships: that between ψ and T , that between ψ and $\ln [K^+]_{ex}$, and that between the action potential and $\ln [Na^+]_{ex}$. All three sets of relationships have been experimentally verified, as outlined in Section 3.4.1. A fourth variable is the density of cell-surface anionic sites. It is included in the constant of equation (4.16).

Apparently the surface charged sites in a variety of resting cells are primarily anionic, as evidenced by a number of observations: (1) High-molecular-weight substances like poly-L-lysine or other polycationic amino acids are adsorbed into *E. coli*, poly-anionic amino acids are not (Katchalski *et al.*, 1953). (2) Poly-L-aspartic acid has no effect on the resting potential of frog sartorius muscle, but poly-L-lysine has a depolarizing effect at a concentration as low as 2 $\mu\text{g}/\text{ml}$ (Neville, 1962). (3) Cationic poly-amino acids, but not neutral or anionic ones, cause agglutination and hemolysis of red blood cells (Katchalsky *et al.*, 1959). The anionic nature of cell-surface sites leads to equation (4.16), which of course predicts no sensitivity of ψ to external Cl^- concentration, a prediction which has been confirmed (Chapter 14).

The surface adsorption theory predicts no relation between the intracellular K^+ , Na^+ or Cl^- concentrations and ψ , while the Hodgkin-Katz theory does. The long list of evidence (to be discussed in Chapter 14) that shows the lack of such relationships will be seen to be compatible with the surface adsorption theory.

4.7. Summary

A number of observations made during the 1940s and 1950s raised doubts about the validity of the membrane pump theory, especially since not only Na^+ , but also many solutes, were found to be permeable and to reach distributions between the cell and the external medium that were not due to a Donnan equilibrium (for ions) or a simple equilibrium (for nonelectrolytes). These observations contributed to doubts that cells have enough energy to operate the multiple pumps that would be required. In this setting, two major bulk phase theories developed: Troshin's sorption theory and Ling's fixed-charge hypothesis (LFCH). In these concepts, the net accumulation of a solute (e.g., K^+) by the cell is due to its specific adsorption onto fixed sites on macromolecules within the cell, while the net exclusion of a solute (e.g., Na^+) is due to its diminished solubility within ordered cell water.

The LFCH, developed in 1952, accepted the concept of fixed charges that had been recognized many years before by Bethe and Toropoff (1914), Michaelis (1925), Teorell (1953), Meyer and Sievers (1936b), Sollner *et al.* (1941a,b), and others. The new con-

cepts in the LFCH were that of the presence of fixed ionic sites throughout the entire cell and that of virtually complete association of counterions with fixed anions or cations, which then makes possible the selective adsorption of, say, K^+ over Na^+ . This high degree of association of fixed charges and their counterions underlies the selective accumulation of K^+ , which is due to fixed charges within the bulk interior of the cell, as well as the selective K^+ permeability and the resting potential, which are due to similar fixed charges at the cell surface.

It soon became evident that the molecular mechanism that explained selective adsorption of the smaller hydrated K^+ ion over the larger hydrated Na^+ ion was not adequate to explain experimental observations in which Na^+ is preferred over K^+ . The resolution of this problem required that attention be directed toward the nature of the fixed charges and changes in their charge densities. This led to the development of the association-induction hypothesis, published in 1962, which will be described in Chapters 6 and 7. Before that, however, it is worthwhile to recall the events described in Chapter 3, and the dominance and popularity of the membrane pump theory at that time. In the next chapter, I discuss in some detail the major evidence developed over the past thirty years that supports and contradicts the membrane theory.

Experimental Tests of the Alternative Theories

5.1. Evidence Supporting the Membrane Pump Theory

Since the postulation of the Na^+ pump theory in the 1940s, the number of publications implicitly and explicitly based on this view has been enormous. The most important evidence in support of the membrane pump theory was collected largely in the 1950s and early 1960s and is reviewed here.

5.1.1. Full Ionic Dissociation of K^+ Salts in Water at Ionic Strengths Similar to Those in Living Cells

Arrhenius (1887) established that most K^+ and Na^+ salts when dissolved in water in the concentration range seen in most living cells (up to about 200 mM) exist in the free dissociated state. It is true that the activity coefficients of the ions in this range of concentration are not unity but often significantly lower (e.g., 0.77 for 0.1 M KCl). However, the theory of Debye and Hückel (1923) for very dilute salt solutions adequately explains this lowering of activity coefficients on the basis of an ion cloud effect, without the need to postulate a significant degree of anion–cation association. Therefore, a belief in total ionic dissociation has prevailed and has led many to shun the concept of bound K^+ , even in very concentrated electrolyte solutions. In the ion exchange resin theory of Gregor (1948, 1951), for example, no significant degree of counterion association with fixed anions was assumed, even though the concentration of fixed ions and their counterions may reach more than 1 or 2 molar. In cells, the arguments put forward by Hill and others (Section 2.7) also supported the concept that virtually all intracellular K^+ and Na^+ exist in an undissociated state.

5.1.2. High Mobility of K^+ in Living Cells

Hodgkin and Keynes (1953) studied the mobility of K^+ in the giant axon of the cuttlefish, *Sepia officinalis*. They first exposed a short segment of an isolated axon to

seawater containing 10–50 mM K⁺ labeled with ⁴²K⁺ for 1–3 hr. They then washed away the free ⁴²K⁺ outside the axon and immersed the axon in oil. The movement of labeled K⁺ along the axon under a voltage gradient (varying from +0.415 through 0 to –0.63 V/cm) was followed by moving the axon over a Geiger counter with a narrow window. The K⁺ mobility (μ) was measured from the rate of movement of the radioactive patch under the influence of an applied electric field, and the diffusion coefficient (D) was determined from the rate of broadening of the patch.

It is worth mentioning that mobility (μ), which is the absolute velocity of any ion within a potential gradient of 1 V/cm, is obtained in cm/sec. μ is related to ionic conductance, λ , given in ohm⁻¹ cm² by the relations

$$\mu_+ = \lambda_+ / \mathcal{F} \quad (5.1)$$

$$\mu_- = \lambda_- / \mathcal{F} \quad (5.2)$$

where μ_+ and μ_- are the mobilities of the cation and anion, respectively, and λ_+ and λ_- are the corresponding conductances. \mathcal{F} is the Faraday constant, equal to 96,500 coulombs. Mobility in turn is related to the diffusion coefficient D by the equation (Glasstone *et al.*, 1941):

$$D = \left(\frac{RT}{Z_i \mathcal{F}} \right) \mu_i \quad (5.3)$$

where Z_i is the valence of the ion. It must be pointed out that this relation holds only in a dilute solution.

To test the state of health of the axons, they were periodically examined for electrical excitability. A total of eleven studies were reported. In two of these no electric field gradients were applied; in the remaining nine, voltage gradients of from +0.412 to –0.432 V/cm were applied. Three of these axons lost electrical excitability before the end of the experiment. The authors noted, however, that "There is, in any case, no evidence to suggest that loss of excitability caused any large change in mobility."

The K⁺ mobility measured was 4.87×10^{-4} cm²/sec·V. The diffusion coefficient was either 1.30×10^{-5} or 1.73×10^{-5} cm/sec, depending on which of two different methods of data computation was used. Hodgkin and Keynes calculated from literature values a mobility for K⁺ equal to 5.2×10^{-4} cm²/·V in 0.5 M KCl at 18°C, and a diffusion coefficient of 1.5×10^{-5} cm²/sec. Pointing out the essential equality of these figures with those measured in *Sepia* axons, the authors concluded that the "K⁺ which enters an axon exists in the axoplasm in much the same state as in an 0.5 M KCl solution." Hodgkin and Keynes's comparison was based on the assumption that the self-diffusion coefficient of K⁺ is the same as that of KCl. However, measurements of the self-diffusion coefficient of K⁺ (D_{K+}) in aqueous solutions became available (Mills and Kennedy, 1953) as Hodgkin and Keynes's paper appeared in print. The experimentally measured D_{K+} is $(2.030 \pm 0.030) \times 10^{-5}$ cm²/sec in a 0.5 M solution of KCl and is thus 33% higher than the value Hodgkin and Keynes assumed.

Sixteen years after the appearance of Hodgkin and Keynes's paper, Kushmerick and Podolsky (1969) published a study of the diffusion of K⁺ and other ions in frog muscle cytoplasm. They cut 3- to 6-mm-long frog muscle fiber segments and placed

them in mineral oil. They then removed the "surface membrane" (presumably the sarcolemma). Two micropipettes were inserted near the center of the segment, one filled with a radioactive solute, the other with 140 mM KCl. Radioactive tracers were introduced into the fiber segment by applying a short voltage pulse across the micropipettes. After 1–45 min of diffusion, the fiber segment was dehydrated in acetone, imbedded in parafilm, and cut into 20- μm -thick sections. Radioactivity measurements of the sections provided the data for the estimate of the diffusion coefficients.

From these studies, the authors reported that the diffusion coefficients of six of seven labeled materials in muscle cytoplasm were uniformly reduced by a factor of two, when compared to their diffusion coefficients in a dilute salt solution. These materials were K^+ , Na^+ , SO_4^{2-} , sorbital, sucrose, and ATP^{3-} . The lone exception was Ca^{2+} . The authors concluded that all six solutes must exist in the free state in muscle cells and that the uniform reduction of the diffusion coefficient is the result of the presence of mechanical barriers to diffusion in the cell. Ca^{2+} alone was bound, hence its much slower diffusion.

These studies in squid axon and frog muscle provided what at that time was considered strong evidence that K^+ in cells is freely dissolved in normal water. Contradictory studies will be outlined in Section 5.2.6 and Chapter 8.

5.1.3. High K^+ Activity in Living Cells

Caldwell (1954) was the first to prepare and use an intracellular H^+ -sensitive microelectrode to measure the pH of giant muscle and nerve fibers (Caldwell, 1968). That electrodes made from glass of different compositions can function in a similar manner to assay activities of Na^+ , Zn^{2+} , and Ag^+ had been recognized by Horovitz in 1923 (Section 4.6.1). In years following other investigators continued these studies (Hughes, 1928; Urban and Steiner, 1931; D. Hubbard, 1946). After Na^+ - and K^+ -sensitive glass became widely available—to a large extent through the efforts of Eisenman (Eisenman *et al.*, 1957; Eisenman, 1967)—Hinke (1959), 1961), Lev and Buzhinsky (1961), and Lev (1964) prepared ion-specific microelectrodes to study the activity of K^+ and Na^+ in living cells. Hinke measured an average K^+ activity of 0.233 moles/liter of water in the squid axon and a total concentration of 0.370 moles/kg of cell water, thus yielding an activity coefficient of 0.602. From the data in the literature the activity coefficient of a 460 mM KCl solution is about 0.690. Hinke considered that "... the present value of potassium being 100% free ... remains a reasonable provisional estimate." However, Hinke concluded from Na^+ activity measurements in these axons that only 76% of Na^+ in the axoplasm gel is free. It is significant to note that the activities of K^+ and Na^+ similarly measured in axoplasm that had been removed from the squid axons were close to those measured *in situ*. This subject will be discussed again in Section 8.4.2.

Many additional studies of ion activity in cells have been performed, and the results vary widely. These will be outlined in more detail in Chapter 8.

5.1.4. Genetic Control of Permeases or Sugar Pumps

Wild *Escherichia coli* does not accumulate or metabolize lactose ($\text{D}\text{-glucose-}\beta\text{-galactoside}$) and other β -galactosides. However, if these bacteria are exposed to a medium containing lactose, the bacteria will develop both the capacity to accumulate lactose and



Jaques Monod (1910–1976)

other galactosides in the cell to levels higher than those in the surrounding medium and the capacity to break down lactose into glucose and galactose.

The work of Jaques Monod and his co-workers (Cohen and Monod, 1957; Jacob and Monod, 1961a,b) showed that the sequence of galactoside accumulation and metabolism depends on the operation of three different enzymes: β -galactosidase and β -galactoside acetylase, involved presumably in the metabolism of the galactose, and another enzyme, galactose permease, which was considered to be a galactoside pump located in the cell membrane. Although lactose is not present in any significant amount in wild *E. coli*, exposure of these bacteria to the sugar *induces* the formation of galactoside permease as well as the other two enzymes.

The synthesis of each of these enzymes is determined by a specific gene: the Y gene specifies permease, the Z gene, β -galactosidase, and the AC gene, acetylase. These three genes are located next to each other in the sequence Z-Y-AC and together they constitute what is known as the lac operon (Fig. 5.1). Before exposure to galactosides, these genes

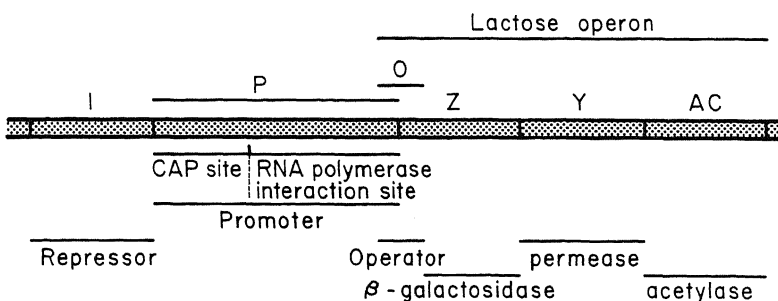


FIGURE 5.1. Diagram of the stretch of the *E. coli* gene containing the lactose operon.

are not active, owing to the binding to a key position on the DNA molecule of a protein called *repressor*. The binding of the *inducer*, galactoside, to the repressor protein causes it to detach from the DNA molecule, thereby activating the lac operon.

The region of the DNA molecule that combines with the repressor protein is called the *operator* (repressor binding site); it is located very close to the region where the messenger RNA transcription for the lac operon commences. Once the repressor is inactivated by combining with the inducer, galactoside, copies of mRNA of the lac operon will be made, setting in motion the synthesis of all these proteins, including the permease (Watson, 1977).

Cohen and Monod (1957) argued that the protein permease acts like a pump catalyzing the inward movement of galactoside. They compared the *pump or catalytic model* with what they called a *stoichiometric or adsorption model*. Both models predict a hyperbolic relation between the concentration of lactose accumulated in the bacterial cell and the external lactose concentration:

$$[\text{galactoside}]_{\text{in}} = Y \frac{[\text{galactoside}]_{\text{ex}}}{[\text{galactoside}]_{\text{ex}} + K} \quad (5.4)$$

where $[\text{galactoside}]_{\text{in}}$ and $[\text{galactoside}]_{\text{ex}}$ are the intra- and extracellular galactoside concentrations, respectively. In the stoichiometric model, the accumulated galactoside is simply adsorbed onto a number of binding sites equal to Y . K is the dissociation constant of the bacterium-galactoside complex. In the catalytic model, the rate of galactoside uptake by the cells is described by the equation

$$\frac{d [\text{galactoside}]_{\text{in}}}{dt} = y \frac{[\text{galactoside}]_{\text{ex}}}{[\text{galactoside}]_{\text{ex}} + K} - c [\text{galactoside}]_{\text{in}} \quad (5.5)$$

where y represents permease activity and c is the galactose exit rate constant. In the steady-state condition, the left-hand side of equation (5.5) equals zero. Equation (5.5) then assumes the same shape as equation (5.4). In this case Y is equal to y/c , and K is the dissociation constant of the galactoside-permease complex.

Cohen and Monod offered three reasons for their preferring and accepting the catalytic model:

1. The maximum amount of galactoside accumulated in the bacterial cell may sometimes reach 5% of the total dry weight (i.e., about 30 mmoles/kg fresh cells). This would, in their opinion, demand an unreasonably large concentration of binding sites.
2. The initial rate of entry of galactoside into *E. coli* is not faster than its rate of exchange into cells already saturated with the galactoside. Moreover, at saturating concentrations, the initial rate of entry is independent of galactoside concentration. These observations were considered to contradict the stoichiometric model, which Cohen and Monod thought to predict a direct dependence of rate of entry on the number of vacant sites and therefore a concentration-dependent rate of entry.
3. In the stoichiometric model Cohen and Monod thought that the total number of adsorption sites [Y of equation (5.4)] should be the same for all galactosides.

(Actually they vary widely for different galactosides.) They considered that both γ and c should vary with the molecular structure, so that the variation of Y would support the catalytic model.

The studies of Cohen and Monod, and the conclusions drawn from them, provide an example of a large number of similar studies in a wide variety of cells. In Chapter 11, it will be seen that the data are in fact consistent with an adsorption model.

5.1.5. Na^+, K^+ -Activated ATPase as the Na^+ Pump

J. C. Skou (1957) reasoned that, if ATP provides the energy for the Na^+ pump, the energy stored in the high-energy phosphate bonds of ATP could be made available only by a specific enzyme, i.e., an ATPase, that for maximal activity depends on the very same ions that are pumped, i.e., Na^+ and K^+ . Skou suggested that the ATPase, which he had isolated from the particulate fraction of crab nerves, and which is enhanced in its activity by the presence of Na^+ and K^+ , may be a part or the entirety of the postulated Na^+ pump. One set of evidence Skou cited for this idea was that both the ATPase activity (Skou, 1960) and the ability of red blood cells to recover lost K^+ , are inhibited by cardiac glycosides such as ouabain (Schatzmann, 1953).

The correlation between ATPase activity and ion transport was the subject of extensive investigation by Dunham and Glynn (1961) and by Post and co-workers (1960). These investigations came to the conclusion that the properties of the enzyme system and the transport systems are qualitatively and quantitatively the same:

1. Both systems are present in the cell membrane.
2. Both systems utilize ATP but not inosine triphosphate.
3. Both systems require the presence of Na^+ and K^+ .
4. Both systems require the same concentration of cations for half-maximal activity.
5. Both systems are inhibited by cardiac glycosides.



J. C. Skou

TABLE 5.1. Comparison of Cation Fluxes and Na^+,K^+ -ATPase Activities in Six Tissues^a

Tissue	Temp. (°C)	Cation flux (10^{-14} mole/cm ² . sec)	Na^+,K^+ -ATPase activity ^b (10^{-14} mole/cm ² . sec)	Ratio
Human erythrocytes	37	3.87	1.38 (\pm 0.36; 4)	2.80
Frog toe muscle	17	985	530 (\pm 94; 4)	1.86
Squid giant axon	19	1200	400 (\pm 79; 5)	3.00
Frog skin	20	19,700	6640 (\pm 1100; 4)	2.97
Toad bladder	27	43,700	17,600 (\pm 1640; 15)	2.48
Electric eel, noninnervated membrane (Sachs organ)	23	86,100	38,800 (\pm 4160; 3)	2.22
				2.56
		$r = +0.866$	$P = 0.017$	(\pm 0.19)

^aFrom Bonting (1970), by permission of Wiley-Interscience.^bIn parentheses standard error of the mean and number of determinations.

Bonting and Caravaggio (1963) further supported this conclusion by showing a significant correlation, over a 25,000-fold range, between ATPase activity and the active cation flux in six tissues: human erythrocytes, frog toe muscle, squid giant axon, frog skin, toad bladder, and the Sachs organ of electric eels. The ratio of cation transported per cm² per second to the number of moles of ATP hydrolyzed per cm² per second averages 2.6 ± 0.19 (Table 5.1) (Bonting, 1970).

However, this good correlation between enzyme activity and ion flux rate may not reflect a postulated pumping activity of this enzyme. It may merely reflect the fact that this large protein molecule in the cell surface may offer the seat of water polarization (Section 12.3) and that it is the total area of the cell surface occupied by this water that determines the rate of ion fluxes.

5.1.6. "High Energy" Contained in the Phosphate Bonds of ATP Provides the Immediate Source of Energy for Na^+ Pumping

It was shown earlier (Section 4.3.2) that inhibition of oxidative and glycolytic metabolism of frog muscle did not bring about a noticeable change in the Na^+ efflux rate. However, since muscle (and nerve) tissues are rich in creatine phosphate (CrP) (or arginine phosphate) and ATP, both of which were considered to contain high-energy phosphate bonds, it was suggested that this extra energy store is utilized to provide the energy for the Na^+ pumping (Ling, 1952; Keynes and Maisel, 1954). Indeed, this interpretation received strong support from the work of Hodgkin, Keynes, Caldwell, and others in their investigations into the linkage between metabolism and ionic movements in the giant axon of the cuttlefish.

Hodgkin and Keynes (1955a) showed that, in sharp contrast to muscle (Section 4.3.2), squid axon is quite sensitive to 2,4-dinitrophenol (DNP). $^{24}\text{Na}^+$ was introduced into the axons during a burst of electrical stimulation while the nerve was immersed in seawater containing $^{24}\text{Na}^+$. The application of 0.2 mM DNP slowed down the Na^+ efflux from the axon. Rinsing off the DNP restored the Na^+ efflux rate to its normal value. It would thus seem that the Na^+ pump in the cuttlefish giant axon depends intimately on energy from oxidative metabolism. Figure 5.2, taken from Caldwell *et al.*

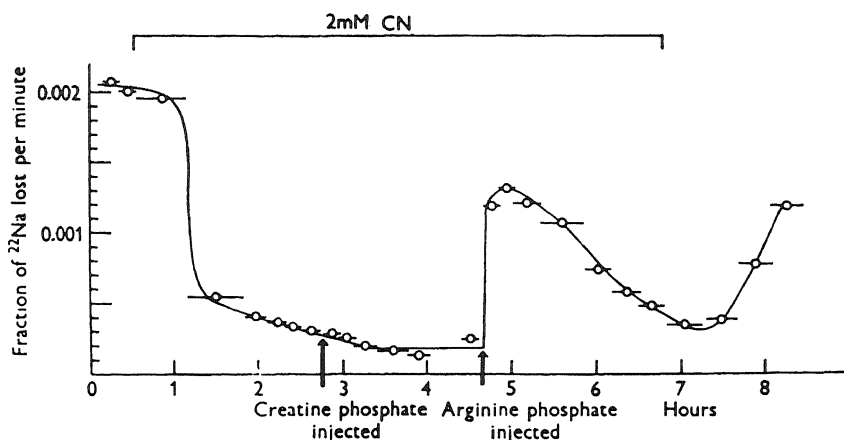


FIGURE 5.2. Effect of CN on the outflow of Na^+ from squid axon and its partial reversal by arginine phosphate. The mean concentrations in the axon immediately after the injections were 15.3 mM CrP and 15.8 mM arginine phosphate. [From Caldwell *et al.* (1960), by permission of *Journal of Physiology*.]

(1960), demonstrates beautifully a link between the rate of outward flux of labeled Na^+ from cyanide-poisoned *Sepia* nerves and the presence in the perfusing fluid of arginine phosphate (but not of CrP). This is exactly as expected because cuttlefish nerves contain arginine phosphokinase but not creatine phosphokinase, and therefore arginine phosphate can transfer its energy in the "high-energy phosphate bond" to ADP to synthesize ATP, while CrP cannot. These findings are in excellent agreement with the membrane pump theory and offer in addition a possible explanation of why Na^+ efflux from muscle failed to respond to respiratory and glycolytic poisons: The large store of ATP and CrP normally present in muscle cells could continue to provide energy for the pumping of Na^+ , as was indicated by Ling in 1952 and by Keynes and Maisel in 1954.

Hodgkin and Keynes (1955a) also noted that a reduction of the external K^+ concentration slows Na^+ efflux from giant axons and that cardiac glycosides and metabolic poisons which alter the rate of Na^+ efflux have little or no effect on the action potentials (Caldwell and Keynes, 1959; Hodgkin, 1971). On the basis of these findings, Hodgkin and Keynes suggested that there is a coupling of outward Na^+ efflux with an inward K^+ pumping. This coupled Na^+-K^+ pump derives its energy from metabolism and is sensitive to cardiac glycosides, while a separate system of downhill Na^+ and K^+ movements is not sensitive to metabolic poisons or to cardiac glycosides. It was suggested that the pump is energized by the ionic gradients normally existing across the cell surface. Hodgkin and Keynes's diagram, shown as Fig. 5.3, indicates two types of Na^+ efflux coupled to the pump: One is slowed by removing external K^+ , the other (represented by the broken line) is not. This additional postulation was based on Caldwell's finding that in cyanide-poisoned *Sepia* axons the rate of Na^+ efflux was sensitive to the presence of external K^+ only if a high concentration of arginine phosphate (33 mM) or phosphopyruvate was included in the perfusion fluid (Fig. 5.4A). ATP (at least 4.8 mM) was ineffective (Fig. 5.4B). This was, I believe, a highly significant discovery, suggesting that arginine phosphate (and phosphopyruvate) act independently and not via ATP.

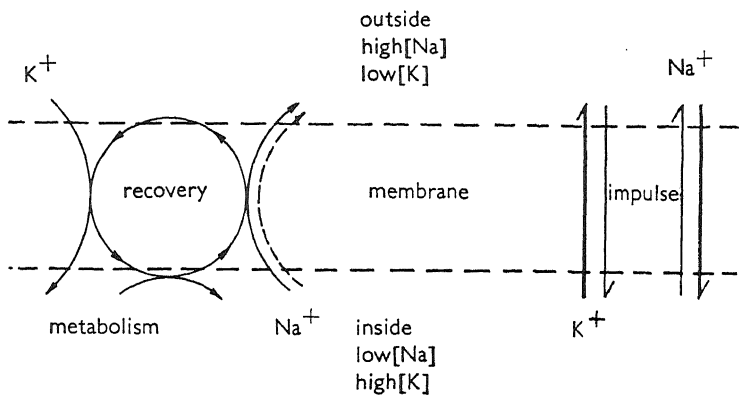


FIGURE 5.3. Diagram illustrating movements of ions through the nerve membrane. The downhill movements which occur during the impulse are shown on the right; uphill movements during recovery are shown on the left. The broken line represents the component of the Na^+ efflux which is not abolished by removing external K^+ . [From Hodgkin and Keynes (1955a), by permission of *Journal of Physiology*.]

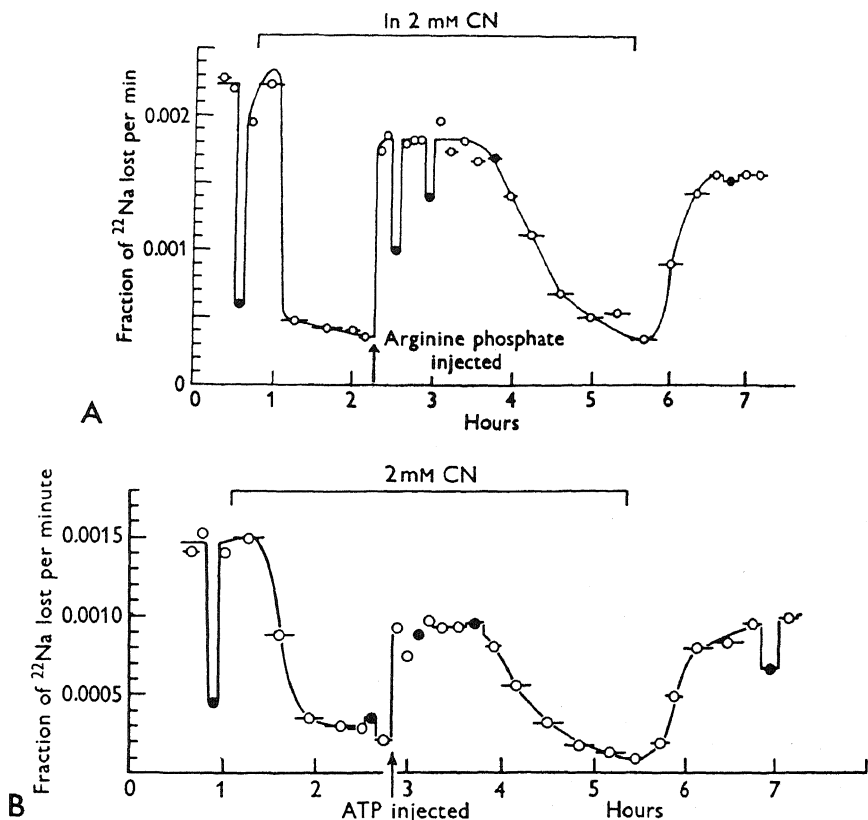


FIGURE 5.4. (A) Effect of injecting arginine phosphate in restoring a K^+ -sensitive Na^+ efflux to an axon poisoned with cyanide. ●, K^+ -free external solution; ○, external solution containing 10 mM K^+ . The injection raised the concentration of arginine phosphate in the axon by 33 mM. (B) Failure of ATP to restore a K^+ -sensitive Na^+ efflux. The injection raised the concentration of ATP in the axon by 4.8 mM. [From Caldwell *et al.* (1960), by permission of *Journal of Physiology*.]

Based on these impressive findings, one would have anticipated easy success in demonstrating net Na^+ and K^+ transport against concentration gradients in sacs of axoplasm-free squid axon sheaths. However, this was not to be the case, as Section 5.2.3 will show. What is more, ATP does not even contain a package of energy that can be tapped for work performance in the way once widely believed (Section 10.3). Nor can it be established that what is measured as Na^+ efflux rate determines the level of Na^+ in the cell; in fact quite the opposite is the case: Na^+ efflux rate and the level of Na^+ are not causally related to each other (Section 12.4.2.3) (Ling and Ochsenfeld, 1976; Ling *et al.*, 1981).

5.2. Evidence against the Pump Hypothesis

5.2.1. There Is Not Enough Energy to Operate the Na^+ Pump

Living cells as a rule maintain within themselves ions and nonelectrolytes at concentrations different from those in the surrounding medium. As mentioned in Section 3.1, a sustained difference in the concentrations of solutes in contiguous spaces can only be achieved in one of three ways: by the presence of an insurmountable energy barrier that separates the spaces, by the continual operation of pumps, or by a difference in the physicochemical environments in the two spaces. A variant of the second mechanism, applicable to ions, is the presence of a Donnan electrochemical equilibrium. Of these, only the pump demands a continual supply of energy to maintain the steady state of ion distribution.

All of these mechanisms have been proposed as causes for the asymmetrical pattern of solute distribution between living cells and their environment, as discussed in Chapter 3. Absolute membrane permeability to K^+ and Na^+ was at one time widely believed to be the case. Selective (absolute) impermeability to Na^+ and other solutes with a Donnan equilibrium of K^+ was the central theme of Boyle and Conway's sieve theory. With the advent of radioactive tracers, the concept of *absolute* membrane impermeability toward ions and many other solutes was disproven, and with further studies of ion distribution patterns it was found that most do not follow a Donnan equilibrium.

Since one of the most immutable laws of physics is the law of conservation of energy, a crucial test of the two remaining theories—the steady-state pump and the equilibrium bulk phase—can be found in the energy requirements of the pumps and a comparison of them with the energy available.

It was mentioned in Section 3.3.2 that early calculations of the energy requirement of Na^+ efflux convinced some scientists that there was enough energy to operate the hypothetical pump. What about all the other pumps? For an auditor to pronounce a balanced budget, it is not valid to single out one specific expenditure from among a total of an unknown number of expenditures and declare it to be within budget. To make a valid statement of the energy balance, one must assess the total number of needed pumps and the energy need of all the pumps together, and then compare the total energy need with the total energy available, after subtracting from it the energy needs of other, non-pumping cellular processes.

Of all the solutes known to be present in frog muscle, no two share the same Donnan ratio (e.g., Table 4.3). The difficulty of assessing the energy needs of all the plasma membrane pumps is dwarfed by the difficulty of assessing the energy needs of the subcellular particle membrane pumps, because these subcellular particles (e.g., mitochondria) have different solute concentrations than the cytoplasm and thus are also in need of pumps (for theories of ionic pumps already proposed for mitochondria, see Chapter 15). Yet the fact is that, some thirty years after the postulation of the Na^+ pump, none of the proponents of the pump concept has made even a rough estimate of the *total* energy need of all the pumps put together. Nevertheless, one can test the pump hypothesis by focusing on one pump alone, for if in this kind of experiment there is *not* enough energy for the one pump, then the entire pump theory is disproven.

It was with this in mind that I undertook the experiments described earlier (Section 4.3.2). I showed that chilling to 0°C combined with inhibition of both respiration and glycolysis failed to produce a change in the rate of Na^+ efflux from frog muscle, and hence, in the pump theory, the rate of Na^+ pumping (Fig. 4.6). These findings were confirmed by Keynes and Maisel (1954) and by Conway and co-workers (1961) (Figs. 4.7, 4.8). Since their experiments were conducted at $17^\circ\text{--}21^\circ\text{C}$, rather than at 0°C , it seemed reasonable to Keynes and Maisel, as well as to myself at first, that frog muscles contain a large store of CrP and ATP and that the energy stored in the high-energy phosphate bonds of these compounds sustained normal activity of the Na^+ pump for some time even though the cells were unable to replenish ATP and CrP. To test this hypothesis, and to reevaluate the question of energy sources, the following experiments were done.

Both respiration and glycolysis were inhibited in the frog muscle by exposure to pure nitrogen and IAA at 0°C . After this was achieved, some muscles were taken out (at time $t = 0$) and analyzed for CrP, ATP, and ADP, while paired muscles were analyzed for CrP, ATP, and ADP after 4–10 hr of continued exposure to the IAA–nitrogen solution maintained at 0°C . The differences in CrP, ATP, and ADP contents, plus the very small amount of lactate that had accumulated, provided the basis for calculating the maximal amount of energy available, using for these calculations the highest reported values for the energy in the high-energy phosphate bonds of these compounds.

Under precisely the same experimental conditions, muscles or small muscle fiber bundles isolated from the same frogs were used to measure at various times t the total intracellular Na^+ concentration, the Na^+ efflux rate, and the resting potential in the course of the 4- to 10-hr period. The minimal energy need, ΔE , was then calculated by an equation similar to that used earlier by Levi and Ussing (1948), E. J. Harris and Burn (1949), and Keynes and Maisel (1954):

$$\Delta E = \int_{t_0}^t [\mathcal{F}\psi(t) - E_{\text{Na}}(t)] j_{\text{Na}}^{\text{in-ex}}(t) dt \quad (5.6)$$

where $\psi(t)$ is the resting potential at time t . \mathcal{F} is the Faraday constant. $j_{\text{Na}}^{\text{in-ex}}(t)$ is the rate of pumping at time t , in moles of Na^+ exchanged per kilogram of fresh muscle per hour. $E_{\text{Na}}(t)$ is defined as

$$E_{\text{Na}}(t) = RT \ln \left(\frac{[\text{Na}^+]_{\text{ex}}}{[\text{Na}^+]_{\text{in}}} \right)_t \quad (5.7)$$

where $([\text{Na}^+]_{\text{ex}}/[\text{Na}^+]_{\text{in}})_t$ is the Na^+ concentration gradient at time t .

Details of the experiments are presented in the following sections.

5.2.1.1. Inhibition of Respiration and Glycosis

To inhibit respiration, the Ringer solution bathing the muscles was equilibrated with 99.99% pure nitrogen, further purified by passage first through a quartz tube containing heated copper turnings and then through a heated activated copper tower. In addition, 1 mM NaCN was included in the solution. To inhibit glycosis the muscles were first incubated in 1 mM IAA for 1 hr (0°C), at which time glycolysis was shown to be stopped. However, as further insurance, lactate in the muscles and in the surrounding fluids was measured at the beginning and end of an incubation. A very small gain of lactate was observed and taken into consideration in calculating the maximum energy available.

5.2.1.2. Estimation of the Na^+ Efflux Rate

Na^+ efflux from frog muscle cells does not follow simple first-order kinetics. Instead, at least two fractions can be easily recognized (e.g., Figs. 3.3 and 4.6). In the conventional view, the fast fraction of Na^+ efflux is assumed to be entirely from the extracellular space, and the slow fraction is assumed to come from within the inside of the cells. There were, however, serious doubts that this is correct (Section 12.4.2.3) and a compromise measure was taken in my estimations of the Na^+ efflux rate. Small isolated muscle fiber bundles containing a few tens of single fibers were dipped briefly into a Ringer solution containing $^{22}\text{Na}^+$ (0°C). The bundles were then washed in a large body of Ringer solution, also kept at 0°C . The time course of decline of radioactivity in

TABLE 5.2. Energy Balance Sheet for the Na^+ Pump in Frog Sartorius Muscles (0°C)^{a,b}

Date	Duration (hr)	Rate of Na^+ exchange integrated average (moles/kg per hr)	$\psi + E_{\text{Na}}/\mathcal{F}$ integrated average (mV)	Minimum rate of energy required for Na^+ pump (cal/kg per hr)	Maximum rate of energy delivery (cal/kg per hr)	Minimum required energy	
						Maximum available energy	
9-12-56	10	0.138	111	353	11.57 (highest value, 22.19)		3060%
9-20-56	4	0.121	123	343	22.25 (highest value, 33.71)		1542%
9-26-56	4.5	0.131	122	368	20.47 (highest value, 26.10)		1800%

^aThe minimum rate of energy delivery required to operate a Na^+ pump according to the membrane pump theory was calculated from integrated values of the measured rates of Na^+ exchange and the energy needed to pump each mole of Na^+ ion out against the measured electrical and concentration gradients. The maximum energy delivery rate was calculated from the measured hydrolysis of CrP, ATP, and ADP, the only effective energy sources available to the muscles, which had been poisoned with IAA and nitrogen.

^bFrom Ling (1962).

the muscle cells was plotted semilogarithmically against time. From these plots, after correction had been made for contributions from, for example, connective tissue elements, the slow exponential fraction was peeled off and its intercept used to determine what in the conventional view represents intracellular labeled Na^+ that has entered during the short exposure. This allows a determination of the rate of influx of the $^{22}\text{Na}^+$. Since the Na^+ concentration hardly changed during the entire experiment, this influx rate is equal to the Na^+ efflux rate.

The results of these experiments are shown in Table 5.2. The minimum energy need of the postulated Na^+ pump is from 1500% to 3000% of the maximum energy available. Before accepting these findings, the possibility of other energy sources must be examined.

5.2.1.3. The Question of Additional, Unknown Energy Sources

Although it is the general consensus of biochemists that the total energy available is provided by respiration, glycolysis, and the compounds CrP, ATP, and ADP, we checked this by comparing the *total* heat output of frog muscles poisoned with IAA and nitrogen, as measured by A. V. Hill and Parkinson (1931) (367 cal/g) and by Hukuda (1931) (420 cal/g), with the expected heat output from CrP, the hydrolysis of ATP, and the residual lactate production from muscles treated under the same conditions employed by Hill and Parkinson and Hukuda. The result (Table 5.3) was a value of 486 cal/g, which is in reasonable agreement with the heat data. This indicates that there is no unknown energy source. It must also be mentioned that the total heat output measured by Hill and Parkinson and by Hukuda was independent of the environmental temperature or the frequency of electrical stimulation. Had there been some additional unknown energy source, the heat most likely would have varied.

TABLE 5.3. Creatine Phosphate, ATP, and Lactate Contents of IAA/ N_2 -Poisoned Frog Sartorius Muscles^{a,b}

		Expt. No.	Mean \pm SE ($\mu\text{moles/g}$)	ΔH (cal/g)
Creatine phosphate	Control	5	26.0 \pm 0.79	
	Experimental	5	23.68 \pm 1.83	0.249
ATP	Control	5	3.86 \pm 0.69	
	Experimental	5	2.99 \pm 0.68	0.102
Residual lactate production	Control	6	3.86 \pm 0.46	
	Experimental	6	12.38 \pm 2.17	0.135
				0.486

^aOne muscle from each frog was analyzed for its CrP and ATP following isolation (controls). The paired muscles were treated to the higher concentration of sodium iodoacetate (1/12,500) for 45 min with oxygen bubbling and then analyzed for CrP and ATP. The data so obtained are labeled "experimental." The conditions of the experiments were made to conform as closely as possible to those used by A. V. Hill and Parkinson (1931). Lactate contents of muscles treated in a similar manner are referred to as "control." Lactate contents after these IAA-poisoned muscles had been stimulated in nitrogen until complete exhaustion are called "experimental."

^bFrom Ling *et al.* (1973), by permission of *Annals of the New York Academy of Sciences*.

5.2.1.4. *The Question of the Contribution of Nonpumping Mechanisms to the Measured $^{22}\text{Na}^+$ Efflux*

When in 1948 Levi and Ussing noted that the rate of Na^+ efflux from frog muscle seemed to require a large fraction of the total energy available (Section 3.3.2), they did not conclude that there was insufficient metabolic energy to operate the pump. Rather, they concluded that a large fraction of the measured $^{24}\text{Na}^+$ efflux did not occur via the outwardly directed Na^+ pump, and that some other membrane process was responsible for carrying much of the $^{24}\text{Na}^+$ out. Since under these conditions the concentration of cell Na^+ was maintained, Ussing postulated a $\text{Na}^+ \text{-Na}^+$ exchange diffusion carrier that simply shuttles Na^+ back and forth across the membrane.

One feature of an exchange diffusion carrier postulated to reduce the energy need of Na^+ efflux is that in the absence of Na^+ on one side of the membrane the Na^+ efflux would be expected to come to a halt. By this criterion, Keynes and Swan (1959) concluded that about half of Na^+ efflux from frog muscle is due to exchange diffusion. They noted, however, that the effect of a Na^+ -free medium does not occur below 10°C , and this would suggest that $\text{Na}^+ \text{-Na}^+$ exchange diffusion does not contribute to our results described here, which were obtained at 0°C . Moreover, Ling and Ferguson (1970) studied frog muscle at 0 and 25°C and failed to find evidence for $\text{Na}^+ \text{-Na}^+$ exchange diffusion, just as others have described in studies in squid giant axon (Hodgkin and Keynes, 1955a), human red blood cells (Hoffman and Kregenow, 1966), and guinea pig smooth muscle (Buck and Goodford, 1966).

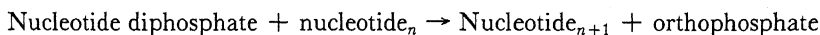
I concluded that the Na^+ pump alone could consume far more energy than the cell has at its command. There is, therefore, logically no need to consider the many other postulated plasma membrane pumps and subcellular particle membrane pumps.

5.2.2. Reassessment of the High Energy of the “High-Energy Phosphate Bond”

Podolsky and Kitzinger (1955) and Podolsky and Morales (1956) in very carefully conducted calorimetric experiments showed that the enthalpy of hydrolysis of ATP is not -12 kcal/mole as was once believed, but is only -4.75 kcal/mole. This finding removed the experimental basis for the high-energy phosphate bond theory.

A second way to determine the free energy, ΔF , of hydrolysis is by combining a series of appropriately chosen reactions and obtaining ΔF by energy summation. It was pointed out that with simplifying assumptions $\neg P$ could be assessed (Lipmann, 1941). However, further efforts of this kind, using a more judicious choice of reactions, led to the downgrading of ΔF to about -7 to -7.5 kcal/mole (Levintow and Meister, 1954; Robbins and Boyer, 1957; Slater, 1971).

From investigation of the synthesis of ribopolynucleotides Ochoa (see George and Rutman, 1960, p. 8) studied the reaction



If a $\neg P$ in the diphosphate is broken and a ribose-3',5'-diester phosphate with a "low-energy phosphate bond" is formed, a ΔF change of -3 to -5 kcal/mole is expected. Actually a ΔF of zero was obtained. For further analysis of this and other general problems, see George and Rutman (1960) and Banks and Vernon (1970).

These different approaches all led to a serious doubt that one can really separate classes of phosphate bonds as being "high-energy" or "low-energy" in character. The key role of ATP in biological work performance is not the capture and storage of energy within a certain bond and its subsequent release to drive pumps or contractile machines or other types of biological work. Rather, ATP must function in a different manner. In fact, a nonhydrolytic role of ATP had already been suggested by Riseman and Kirkwood and Botts and Morales, and in connection with Ling's fixed-charge hypothesis (Section 4.4), and this role will be further developed as part of the association-induction hypothesis in Chapter 10.

5.2.3. Failure to Demonstrate Selective K^+ Accumulation and Na^+ Exclusion by a Cytoplasm-Free Squid Axon Membrane Sac

In 1961 Baker, Hodgkin, and Shaw in England, and Oikawa, Spyropoulos, Tasaki, and Teorell in the United States independently reported success in preparing a squid axon membrane sheath free from cytoplasm. By perfusing these membrane sheaths with proper solutions, it was possible to maintain their normal electrical activity for many hours. I wish to emphasize two consequences of the observation made in this preparation.

1. The maintenance of the normal potential with this preparation shows the functional dissociation of electrical activity from the physiological state of the axoplasm, so that normal electrical activity cannot be considered as implying the normal state of the axoplasm. Hence, the high K^+ mobility measured by Hodgkin and Keynes (Section 5.1.2) does not necessarily mirror properties of axoplasm in a physiological state. This subject will again be discussed in Section 8.4.
2. If the squid axon membrane sheath is electrically active in a normal manner as observed, then the plasma membrane and its Na^+ pump also should be in a sound and functional state. Therefore, for the first time in history, an unusual opportunity presented itself to test the Na^+ pump hypothesis. That is, if both ends of a segment of the cytoplasm-free axon membrane sheath were tied after filling the sac with seawater containing suitable concentrations of ATP and arginine phosphate, the membrane pump should act to extrude Na^+ and accumulate K^+ . Keynes mentioned early in 1963 in a seminar given at the Johnson Research Foundation of the University of Pennsylvania that such attempts had been made but that they had failed (see Ling, 1965b). Moreover, studies that are often quoted as having proven Na^+ pumping in perfused or dialyzed squid axon (Baker *et al.*, 1971; Brinley and Mullins, 1968; Mullins and Brinley, 1969), did show an ATP-induced increase in Na^+ efflux, but *did not in fact show ATP-induced net Na^+ extrusion* (see Ling and Negendank, 1980).

5.2.4. Failure to Prove Selective Ion Pumping in Membrane Vesicles

The knowledge that experiments using axoplasm-free squid axon membrane sacs failed to demonstrate net K^+ and Na^+ pumping was to the best of my knowledge never published. It is of course much more difficult to be certain about the meaning of a negative experiment than a positive one. Nevertheless, this issue has been brought to public attention on several occasions (Ling, 1965b, p. 95; Ling *et al.*, 1973, p. 31; Ling, 1977a, p. 160), and a careful literature survey over the past twenty years reveals no statement contrary to the one made by Keynes. I reasoned that if "nature's own" squid axon membrane cannot pump ions against concentration gradients, it would be fruitless indeed to expect man-made vesicles to succeed in the same task. However, a considerable amount of effort has been spent trying to demonstrate ion pumping in various artificial and natural membrane vesicles.

One kind of "natural" vesicle was prepared by exposing *E. coli* and other cells to hypotonic shock. These vesicles were found to retain many of the solute distribution patterns of the intact cells. This type of preparation was not able to prove the existence of membrane pumps because, with few if any exceptions, *the vesicles contain as much or more solids than the original intact cells and therefore cannot possibly be pure membrane vesicles*. Thus, whereas normal living cells usually contain from 15% to 25% solids, the vesicles of Kaback (1976) contain 37%; those of Hirata, Altendorf, and Harold (1974), more than 50%; those of McDonald and Lanyi (1975), 33%; and those of McKinley and Meissner (1977), 25% solids. Pure membrane vesicles of their size should contain no more than 2% to 5% solids.

Another type of vesicle was artificially prepared from pure phospholipids into which were incorporated what are believed to be the ionic pumps, e.g., K^+ - and Na^+ -activated ATPases (Goldin and Tong, 1974; Hilden *et al.*, 1974). These preparations showed an apparent uptake of Na^+ induced by ATP. However, the interpretation of the results of these studies is complicated by a number of problems. For example, determination of the water content of the vesicle, and hence the concentration of Na^+ within it, depends on the distribution of a probe such as inulin, glucose, or Na^+ itself in the absence of ATP. Yet different probes gave different volumes. From a detailed analysis of these studies, Ling and Negendank (1980) concluded that ATP did not actually cause a net gain of Na^+ by these vesicles.

5.2.5. Studies of the Red Cell Ghost

Finally I would like to examine in some detail the story of another "natural" membrane, the red blood cell ghost. In the nineteenth century, it was noted that exposure of red blood cells to a hypotonic solution causes hemolysis (i.e., loss of hemoglobin) (Section 1.6). The remains of the hemolyzed red cells are called *ghost* or *stroma*. The definition of the word *stroma* on the other hand is given by *Webster's New Collegiate Dictionary* (1977) as "the spongy protoplasmic framework of some cells (as a red blood cell)." Other descriptions of the red cell suggest that indeed it does have a stroma, or "protoplasmic framework":

It is probable that . . . hemoglobin is bound in some way to the cell structure. One reason for this belief is that purely mechanical agencies will not liberate the pigment. The cell may be

torn into the finest shreds, yet each minute particle still retains its hold upon the hemoglobin.”
 [Best and Taylor, 1945, p. 48]

Evidence that contradicts the notion that the red cell ghost is a hollow membrane vesicle came from Eric Ponder, who in 1948 published his authoritative monograph *Hemolysis and Related Phenomena*. Three years later Ponder (1951) published an article specifically addressed to the problem described in its title, “Is the Red Cell Ghost Solid or Hollow?” His test consisted of measuring the volume of the red cell ghosts before and after their fragmentation. If the ghosts are hollow, he reasoned, the fragments will occupy less volume; if they are solid the fragments will retain the same volume. His results showed no change in volume, leading Ponder to the conclusion that red cell ghosts are solid.

With these past findings in the background, how, may one ask, did the red cell ghost become in recent years almost synonymous with pure red cell membrane? As one among many examples, I point out that in Volume 31 of *Methods in Enzymology* the section title reads “The Preparation of Red Cell Ghosts (Membranes).” This parenthetical equation is echoed in another statement, “In the preparative method described here, the membranes (ghosts) are observed through the use of osmotic lysis” (Hanahan and Ekholm, 1974). Clearly the authors, like many others of the time, expressed without equivocation the belief that membranes and ghosts are identical. But then how can the ghost be at once solid and hollow?

Along with the widely held belief that red cell ghosts are hollow membrane vesicles, there is also a widely held belief that, when ATP is supplied as an energy source, these pure membrane vesicles can pump Na^+ out and K^+ in. In retrospect, it would seem that this opinion could claim some legitimate support from two short papers of Hashimoto and Yoshikawa (1963a,b), who showed ATP-induced ^{86}Rb uptake and whose results are reproduced here in Fig. 5.5. Bodemann and Hoffman (1976), in their Table I, suggested a slight “net” accumulation of K^+ and exclusion of Na^+ . However, Freedman (1976) showed clearly that red cell ghosts prepared by the Bodemann-Passow technique (1972) and supplied with ATP could indeed extrude Na^+ and accumulate K^+ (Fig. 5.6). This Na^+ and K^+ contents of the ghosts were, however, given in units of fresh weight of the ghosts and not in units of ghost water. Freedman defended his usage on the ground that “Since the water content was constant at 95%, the conclusions do not depend on whether the ion contents are expressed on a wet weight or water basis” (Freedman, 1976, p. 991). However, no data measuring the water contents of the ghosts

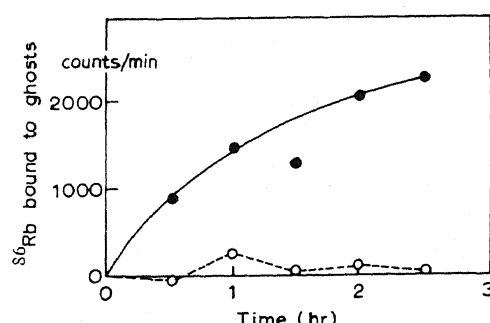


FIGURE 5.5. Binding of ^{86}Rb by ghost cells of erythrocytes at 37°C in the presence (●—●) or absence (○---○) of 1 μmole of ATP. Binding of ^{86}Rb was assayed by measuring the decrease in radioactivity of the supernatant after removal of the ghosts by centrifugation. [From Hashimoto and Yoshikawa (1963a), by permission of *Biochimica et Biophysica Acta*.]

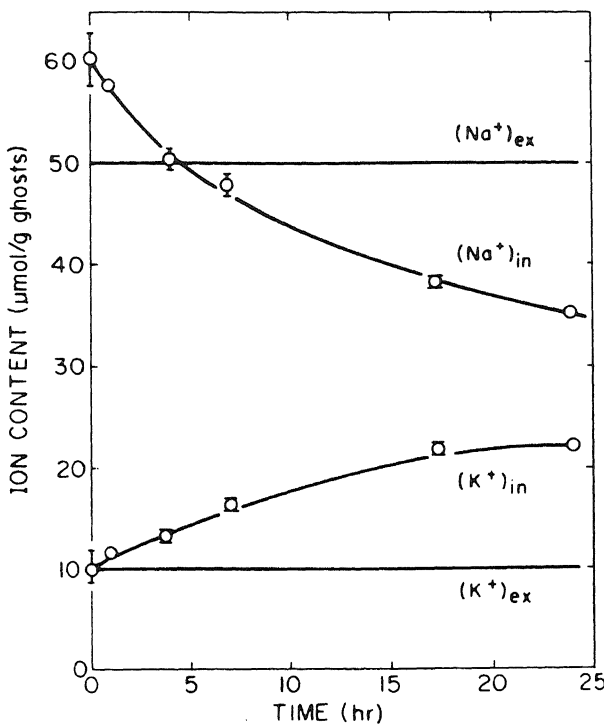


FIGURE 5.6. Net accumulation of K^+ and extrusion of Na^+ against concentration gradients by human erythrocyte ghosts. [From Freedman (1976), by permission of *Biochimica et Biophysica Acta*.]

appeared in either the article of 1976 just cited or a much lengthier dissertation (Freedman, 1973). Are these ghosts hollow or solid?

In the summer of 1974, a young man named Michael Balter drove all the way from the West Coast to Philadelphia in order to answer the question, "Does the method used by Freedman to prepare red cell ghosts that 'pump' ions actually produce cytoplasm-free ghosts?" Three months later we had the answer: The ghosts are not cytoplasm-free (Ling and Balter, 1975). Ling and Balter's conclusion was confirmed and extended by Hazlewood, Singer, and Beall (1979), whose findings are reproduced in Fig. 5.7. They showed quite unequivocally that, in contrast to ghosts prepared by Dodge *et al.* (1963) and Marchesi and Palade (1967), the ghosts prepared by methods such as those used by Freedman do not consist of hollow membranes. These results also resolve the apparent conflict mentioned above regarding the hollowness or solidity of the red cell ghosts. Clearly Ponder (1951) prepared red cell ghosts by a method closer to that of Bodemann and Passow (1972) and of Freedman (1976) than to those of Dodge *et al.* (1963) and of Marchesi and Palade (1967).

Ling and Tucker (1983) then studied the K^+ uptake and Na^+ extrusion by these two types of ghost preparations. Their results are shown in Figs. 5.8 and 5.9: Ghosts prepared by the method of Marchesi and Palade (and by the method of Dodge *et al.*, not shown) are white; they do not accumulate K^+ or extrude Na^+ . On the other hand,

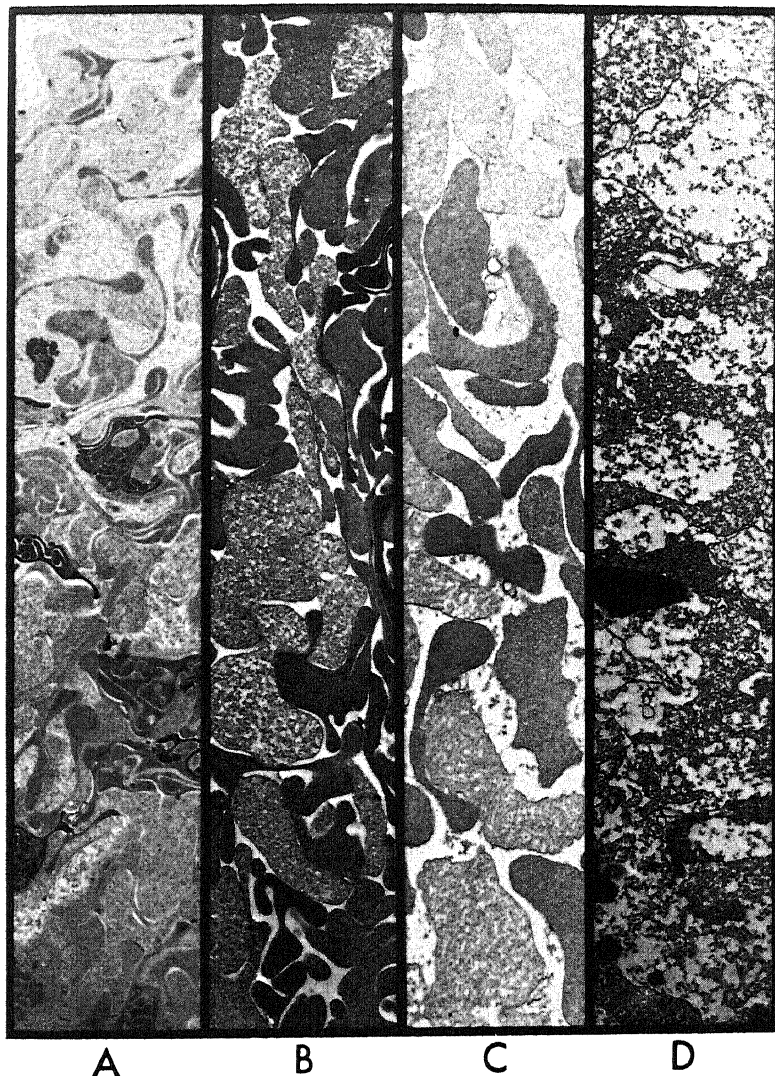


FIGURE 5.7. Electron micrographs of red cell ghosts (6000 \times). Prepared by the methods of (A) Garrahan and Glynn (1967), (B) Freedman (1976), (C) Freedman "resealed" in clean buffer, and (D) Bodemann and Passow (1972). Micrographs enlarged 30% for reproduction. [From Hazlewood *et al.* (1979), by permission of *Physiological Chemistry and Physics*.]

ghosts prepared by the method of Freedman are red; they do transport K⁺ and Na⁺ against concentration gradients. However, *this confirmation of Freedman's finding was only partial*. We could not confirm his claim of a uniform 95% water content. Quite the contrary, only the white ghosts prepared by the Marchesi-Palade method contained as a rule 95% water. Red ghosts prepared by the Freedman method had lower and more variable water contents. Moreover, this variability in the relative solid and water con-

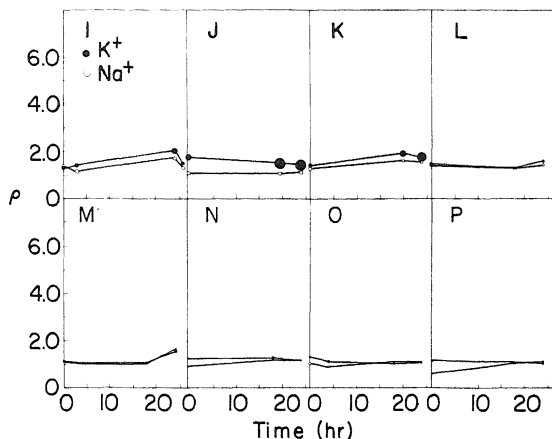


FIGURE 5.8. White ghosts prepared by the method of Marchesi and Palade (1967) do not transport K^+ or Na^+ . The value ρ is defined as mmoles/liter ghost water divided by mmoles/liter external medium. [From Ling and Tucker (1983), by permission of *Physiological Chemistry and Physics*.]

tents seemed to be related to the degree of K^+ uptake and Na^+ extrusion. This impression was substantiated by later data of Ling and Zodda (1983), shown in Fig. 5.10. Here Freedman's (1976) procedure was used in all samples of red cells collected from a large number of different donors. The net uptake of K^+ and net loss of Na^+ after 18 hr of incubation were plotted against the solid contents (minus salt contents). A correlation coefficient of +0.77 exists between net K^+ uptake and salt-free dry solid content and one of +0.71 between net Na^+ extrusion and solid content. Since the salt-free dry solid is virtually all protein, these data clearly show that it is the cytoplasmic proteins that determine both the selective K^+ uptake and the Na^+ exclusion. Red cell ghosts prepared and treated by the Freedman procedure can neither accumulate K^+ nor exclude Na^+ when their water content rises above 92%. In no instance have we observed K^+ uptake in and Na^+ extrusion from ghosts with a 95% water content.

In summary, red cell ghosts do not produce evidence proving the membrane pump theory, contrary to widely held belief. In fact, the data actually provide strong evidence

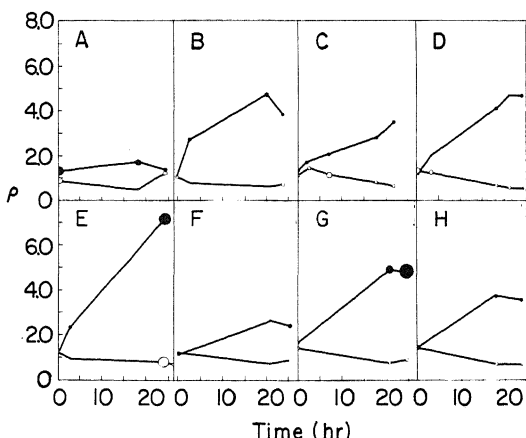


FIGURE 5.9. Red ghosts prepared by the method of Freedman (1976) do transport K^+ (\bullet) and Na^+ (\circ), but to varying degrees. ρ is defined as in Fig. 5.8. [From Ling and Tucker (1983), by permission of *Physiological Chemistry and Physics*.]

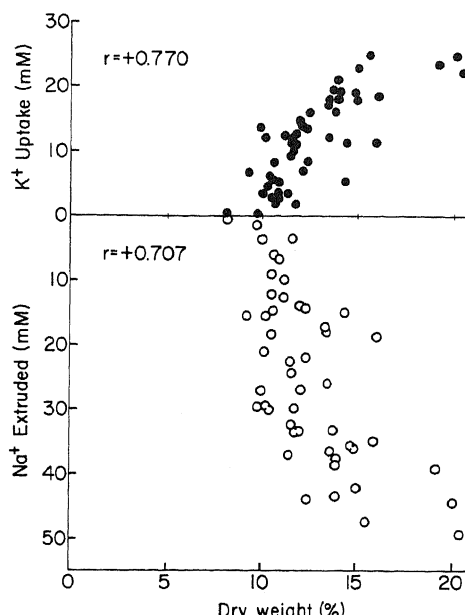


FIGURE 5.10. Dependence of K^+ reuptake and Na^+ extrusion on the protein content of ghosts, expressed as salt-free dry weight. [From Ling and Zodda (1983), by permission of *Physiological Chemistry and Physics*.]

in favor of the concept that ion accumulation and exclusion are bulk phase properties of the intracellular protein-water system.

5.2.6. Ouabain-Sensitive Selective Accumulation of K^+ over Na^+ in an Effectively Membrane (Pump)-less Open-Ended Muscle Cell (EMOC) Preparation

A basic requirement of a membrane pump is that it must have both a *sink* and a *source*. Thus, to pump K^+ inward there must be an external source of K^+ ; to pump Na^+ outward there must be an external sink into which the Na^+ pumped out is taken up. Without the source and sink, the pump cannot function. This requirement provides the basis for another discriminatory experiment to test the membrane pump theory versus the bulk phase hypothesis. The basic principle of the experimental set-up is shown in Fig. 5.11. The amputated end of the cell is directly exposed to a Ringer solution containing its normal K^+ and Na^+ concentrations, labeled with a radioactive isotope, e.g., ^{42}K or ^{22}Na . The intact part of the cell membrane is isolated from the Ringer solution by a tight-fitting gasket and is exposed to moistened air (or Vaseline), which is neither a source of K^+ nor a sink for Na^+ .

A detailed plan of the experiment, in which a frog sartorius muscle is used, is shown in Fig. 5.12. By careful dissection of single muscle fibers from an isolated sartorius muscle, one can readily show that all the fibers run from one end of the muscle to the other end (Ling, 1973a). Therefore, by cutting off the end of the muscle, it is possible to cut open all the cells at their ends. The whole-muscle preparation in Fig. 5.12 does not entirely conform to the simple model in Fig. 5.11, since each muscle cell or fiber is surrounded by extracellular fluid. To reduce diffusion of Na^+ and K^+ between the extracellular fluid and the solution bathing the cut end of the muscle, the

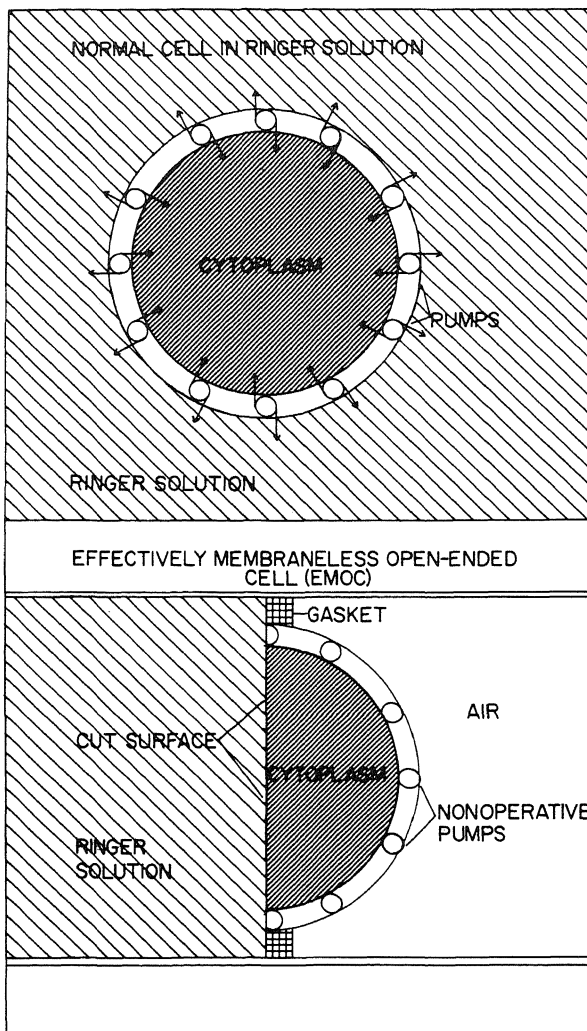


FIGURE 5.11. Diagrammatic illustration of the effectively membraneless open-ended cell preparation. Amputation of part of the cell membrane and exposure of the remaining intact membrane to air incapacitates the plasma membrane pumps. [From Ling (1978a), by permission of *Journal of Physiology*.]

cut end was compressed in a silicone rubber gasket. As shown in Fig. 5.13, the effect of this compression is to reduce the area available for diffusion into and out of the extracellular space. By then using [^{14}C]inulin and $^{35}\text{SO}_4^{2-}$ equilibration for up to 72 hr, it was possible to show that the area of extracellular space is less than 1% of the total area exposed to the bathing solution. Then, by direct analysis of the extracellular fluid of the muscles at the end of the experiments, it was found that the cells had not "pumped" any $^{22}\text{Na}^+$ into the extracellular space (Ling, 1978a).

The next question to answer is "Does the cut end regenerate a new membrane?"

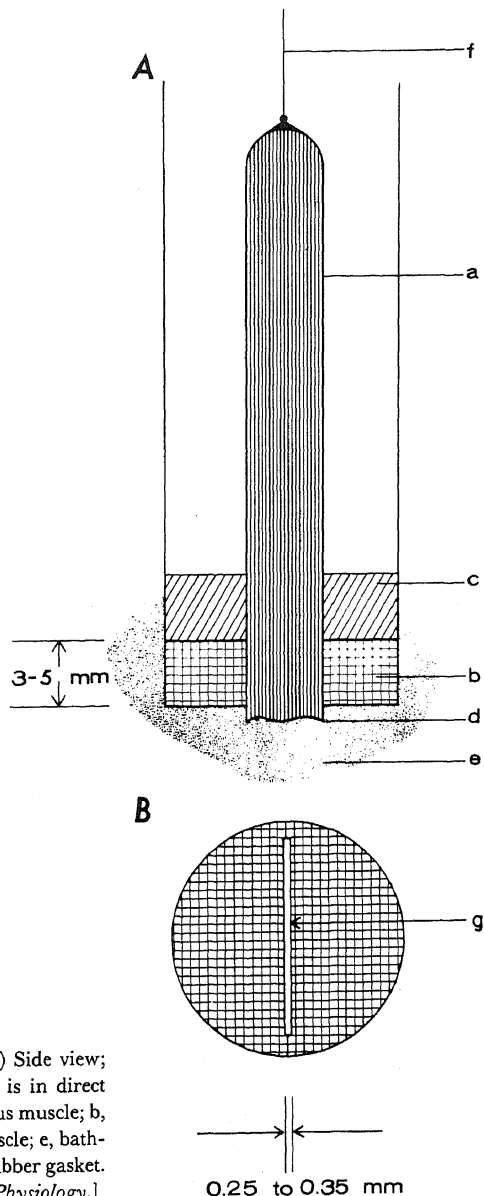


FIGURE 5.12. Diagram of the EMOC tube. (A) Side view; (B) bottom view. Only the cut end of the muscle is in direct contact with the labeled Ringer solution. a, Sartorius muscle; b, silicone rubber gasket; c, Vaseline; d, cut end of muscle; e, bathing solution; f, anchoring string; g, slit in silicone rubber gasket. [From Ling (1978a), by permission of *Journal of Physiology*.]

Indeed, it was once widely believed that an amputated muscle soon regenerates another membrane. Table 5.4 shows that no membrane was regenerated for as long as 28 hr at 25°C. [For additional evidence, see Ling, (1973a).]

After exposure of the cut end of the muscle to the radioactively labeled solution the sartorius muscles were frozen in liquid nitrogen, and, while frozen, cut into 1- and 2-mm-long segments. The radioactivity of each segment as well as that of the bathing

TABLE 5.4. Uptake of Labeled Solutes through Cut End of Muscle^{a,b}

	Uptake of labeled sucrose through cut end in 2 hr (25°C) (μmoles/g)	Uptake of labeled Na ⁺ through cut ends in 28 hr (25°C) (μmoles/g)	Uptake of labeled D- arabinose through cut ends in 27 hr (25°C) (μmoles/g)
Immediately after cut	0.174 ± 0.031 (4)	22.3 ± 5.1 (4)	3.53 ± 0.20 (5)
After incubation	0.169 ± 0.016 (4) (24 hr; 25°C)	22.7 ± 2.5 (4) (51 hr; 25°C)	3.28 ± 0.20 (5) (43 hr; 25°C)

^aTime in last row refers to duration of incubation after ends of muscles were amputated and before exposure to labeled solutions.

^bData from Ling (1973a).

solution before and after exposure was assayed. From the data and the weights of the segments, one can plot the intracellular/extracellular concentration ratio of the labeled solute at the center of each segment x mm from the cut end. Figure 5.14 shows that paired muscles from the same frog after similar exposure produced profiles of labeled Na⁺ distribution indistinguishable from each other.

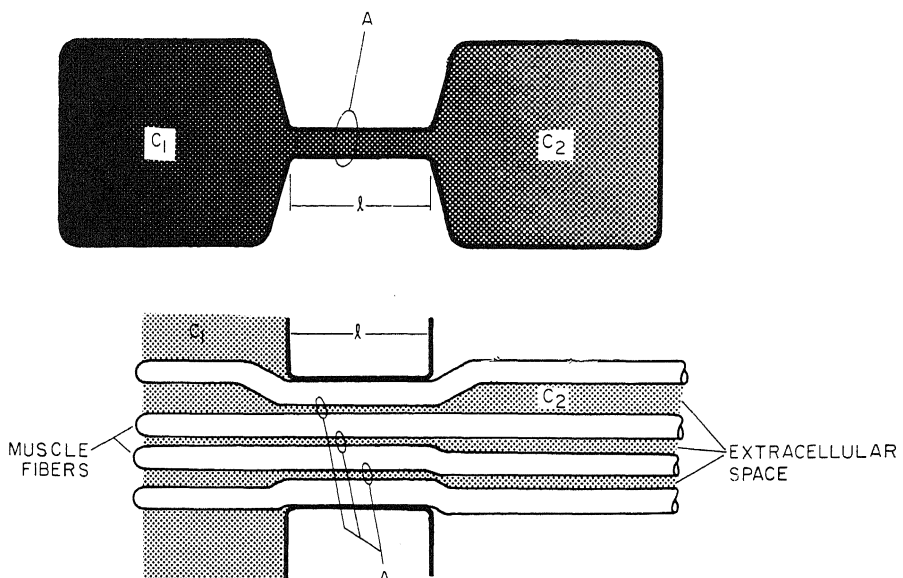


FIGURE 5.13. Diagrammatic illustration of the functions of the snug-fitting silicone rubber gasket in reducing solute and solvent movement into the intact end of the muscle. The top part shows the classic setup for measuring diffusion coefficients. The narrow capillary bridge linking the two compartments 1 and 2 is of cross-sectional area A and length l and determines the rate of diffusion from compartment 1 containing the solute at concentration C_1 to compartment 2 containing the solute at concentration C_2 . In the bottom part the compressed region of the extracellular spaces serves the same purpose as the narrow capillary; it determines the rate of diffusion of solute from the source solution (C_1) bathing the left end of the muscle to the sink in the form of the uncompressed extracellular space of the right portion of the muscle (C_2). [From Ling (1978a), by permission of *Journal of Physiology*.]

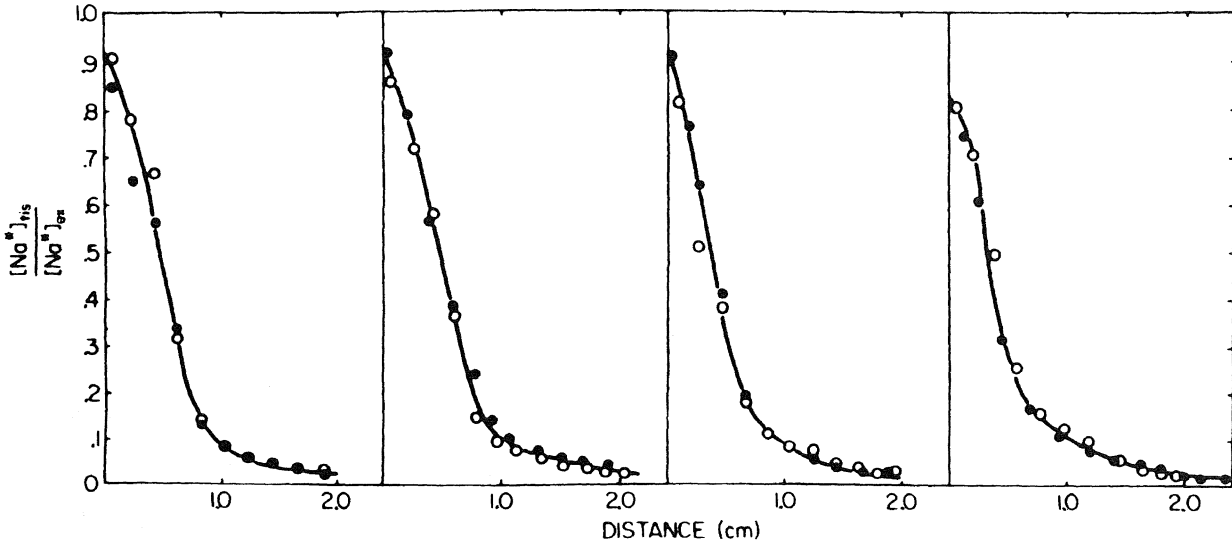


FIGURE 5.14. Concentration distribution of labeled Na^+ in paired sartorius muscles. Exposure was 20 hr at 25°C . Data show agreement in uptake between paired muscles. Abscissa represents distance from cut end; ordinate, labeled Na^+ in cell water as a fraction of final equilibrium concentration of labeled Na^+ in the source solution (ca. 100 mM). [From Ling (1973a), by permission of *Physiological Chemistry and Physics*.]

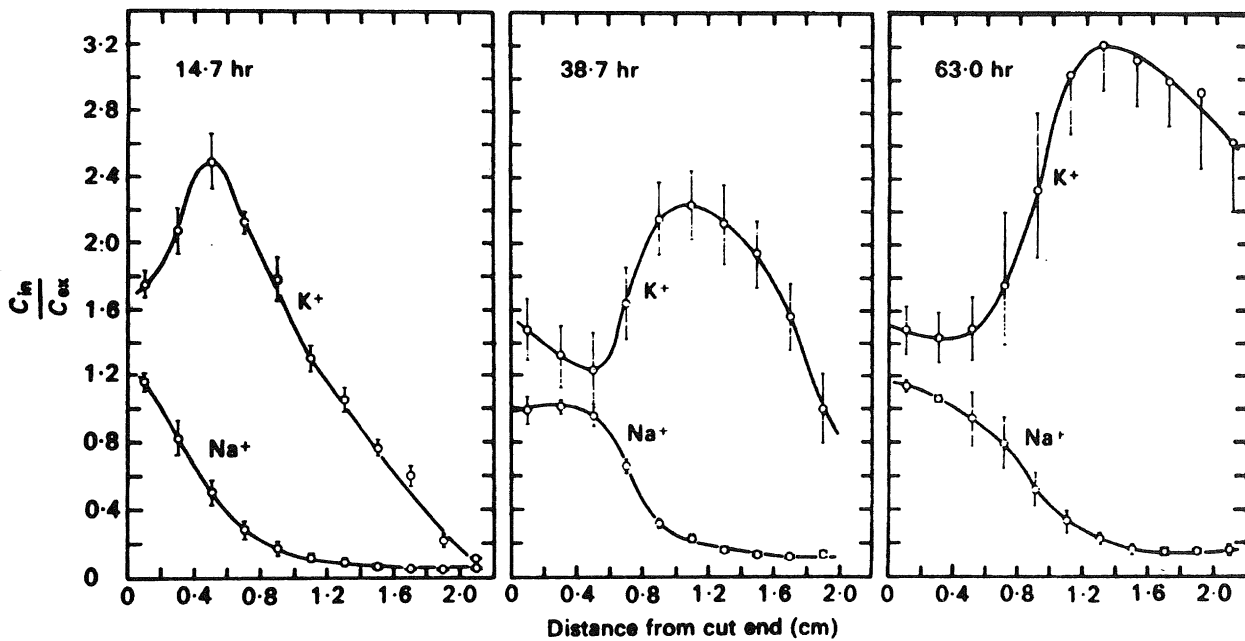


FIGURE 5.15. Simultaneous influx of labeled K^+ and labeled Na^+ into sartorius muscles through their cut ends. The three groups of frog sartorius EMOC preparations were exposed to normal Ringer solutions labeled with both ^{42}K and ^{22}Na for 14.7, 38.7, and 63.0 hr, respectively. The abscissa represents the distance of the midpoint of each cut segment from the cut surface of the muscle fibers. The ordinate represents the ratio of the labeled ion concentration in the water of each muscle segment (C_{in}) to the concentration of the same labeled ion in the solution bathing the cut end of the muscle at the conclusion of the experiment (C_{ex}). [From Ling (1978a), by permission of *Journal of Physiology*.]

Figure 5.15 shows a set of three simultaneous labeled K^+ and Na^+ uptake studies in muscles after 14.7, 38.7, and 63.0 hr of exposure at 25°C. The patterns of distribution of these two ions are greatly different.

Part of this difference could arise from the different mobilities of the two ions. To assess this, both K^+ mobility (Ling and Ochsenfeld, 1973a) and Na^+ mobility in healthy muscle cytoplasm (Ling, 1978a) were determined. These values were 2.63×10^{-6} and $2.03 \times 10^{-6} \text{ cm}^2/\text{sec}$, respectively. In diffusion, the basic variable is Dt , the product of the diffusion coefficient and the duration of diffusion. For this reason, if, as according to the membrane pump theory, the cytoplasm is similar to a dilute solution, the K^+ and Na^+ diffusion through the cut end into the cells should be similar to diffusion into an open capillary filled with an aqueous solution. The differences between the diffusion coefficients of K^+ (D_K) and of Na^+ (D_{Na}) can then be exactly compensated by different durations (t_K , t_{Na}) of the experiment, such that

$$t_K/t_{Na} = D_{Na}/D_K = \frac{2.63 \times 10^{-6}}{2.07 \times 10^{-6}} = 1.27$$

Thus if we compare the Na^+ diffusion profile after 63.0 hr of exposure with the K^+ profile after either 38.7 or 14.7 hr of exposure, the differences in t 's would have more than compensated for the faster diffusion of K^+ . The data shown in Fig. 5.15 leave little doubt that, contrary to the expectation on the basis of the membrane pump theory, vast differences between K^+ and Na^+ remain after the Dt normalization.

Other analyses led to the conclusion that the disparity could not be due to sequestration of K^+ in subcellular particles, nor to inward K^+ pumping. Finally it can be shown that the difference could not be due to outward Na^+ pumping. Under these circumstances the only result of outward Na^+ pumping would be to transport more Na^+ from the intracellular to the extracellular compartment against both an osmotic and a Na^+ concentration gradient. The projected accumulation of Na^+ in the extracellular space would make the extracellular space fluid hypertonic and cause movement of water from within the cells into the extracellular space. This osmotic compensation would prevent the building up of a diffusion head of Na^+ in the extracellular space to cause the return of Na^+ to the only sink remotely available—the solution bathing the cut end of the muscle. Analysis of the extracellular space fluid (esf) of muscles in the EMOC preparation showed a normal volume of esf as well as a normal concentration of Na^+ , indicating quite clearly that not only was there no return of Na^+ to the source, but there was no indication that the cells had even made an attempt to do so.

These data readily agree with the more up-to-date association-induction (AI) hypothesis, to be presented in the following chapter, according to which K^+ and Na^+ distributions reflect primarily the properties of the muscle cytoplasm. Thus the uptake of K^+ to levels higher than those in the surrounding medium and the extrusion of Na^+ to levels below those in the surrounding medium in this membrane-pump-less preparation are not fundamentally different from the actions of intact muscles that had been exposed to a labeled Ringer solution. The only major difference is the slow but spreading decline of the selectively accumulated K^+ and rise of Na^+ near the cut end, an observation that is attributed to damage there and to a decline of ATP. The rather abrupt drop of total K^+ and the rising Na^+ at the cut end are shown in Fig. 5.16.

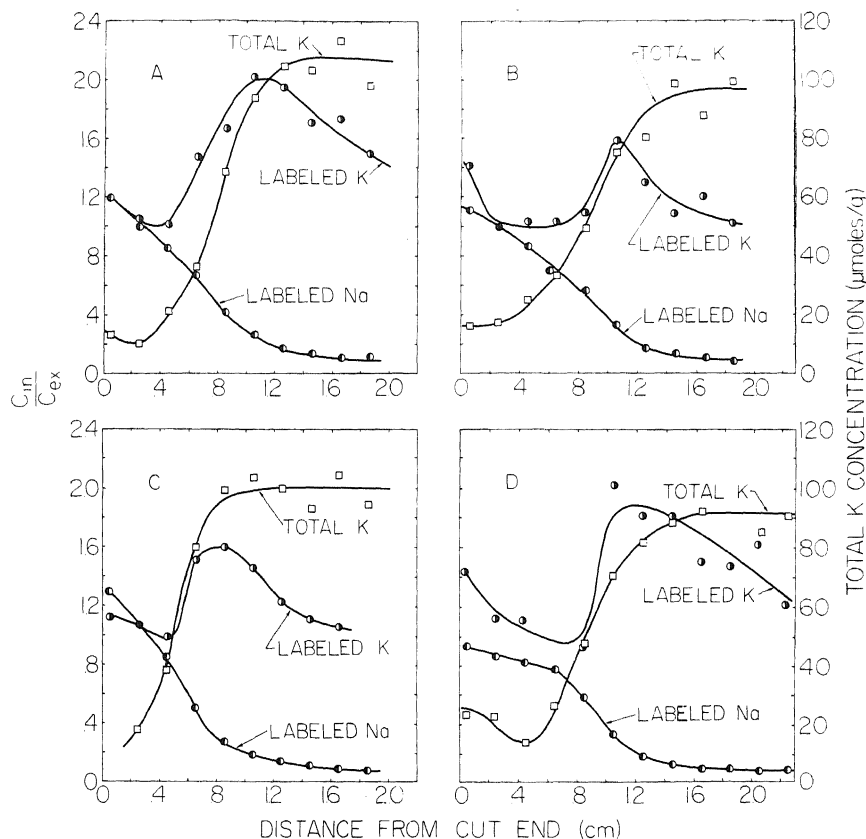


FIGURE 5.16. Distribution of total K^+ , labeled K^+ , and labeled Na^+ in cut frog sartorius muscles. The duration of the experiment was 40 hr at 25°C. Total K^+ of muscle segments was analyzed after a second counting of the HNO_2 extract. Otherwise similar to data given in Fig. 5.15. [From Ling (1978a), by permission of *Journal of Physiology*.]

Thus, failure of the perfused squid axon and the red cell ghost to show Na^+ pumping is complemented by the EMOC preparation, which shows that removal of the hypothetical membrane pump function did not prevent the cell from accumulating K^+ and excluding Na^+ . Moreover, the results in Fig. 5.17 show that the action of ouabain, which causes less K^+ accumulation and less Na^+ extrusion, widely regarded as offering a key support for the membrane pump theory, occurs just as well even though there is no functional Na^+ pump to begin with. The interpretation of the effect of ouabain in terms of the AI hypothesis will be described in following chapters.

5.3. Summary

This chapter has reviewed results of experiments performed in the past thirty years that have provided perhaps the strongest arguments in favor of the membrane pump

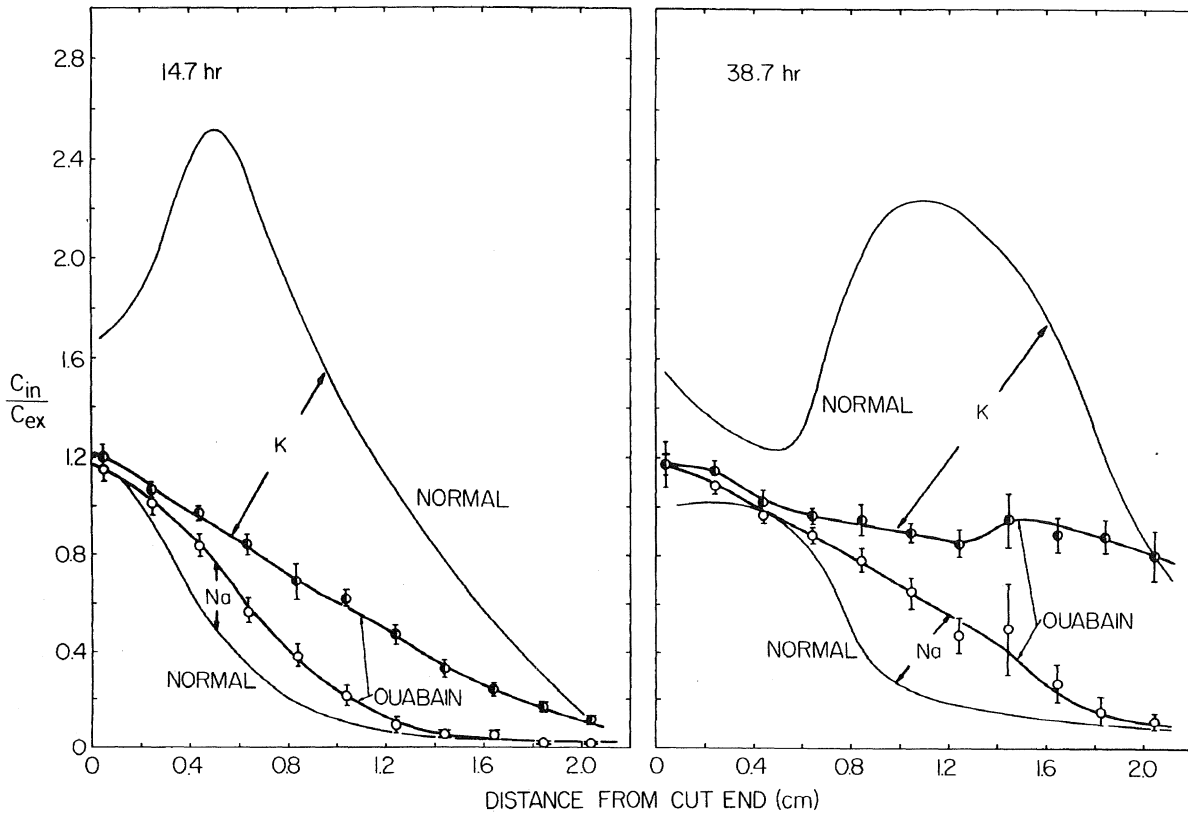


FIGURE 5.17. Effect of ouabain on the accumulation of labeled K^+ and Na^+ by sartorius muscles through their cut ends. Experimental procedures used were the same as those described in the caption of Fig. 5.15 except that the Ringer solution bathing the cut end of the muscles contained initially $10^{-4} M$ ouabain. Continuous lines without experimental points were reproduced from the data of Fig. 5.15 to provide a basis for visualizing the effect of ouabain. [From Ling (1978a), by permission of *Journal of Physiology*.]

theory. These are illustrated by the evidence for full ionic dissociation of K^+ salts in cell water, the high mobility of K^+ in squid axon and frog muscle, the high K^+ activity in squid axon measured with ion-sensitive microelectrodes, the concept of the sugar permease in *E. coli*, the extensive circumstantial evidence that the Na^+,K^+ -ATPase is the Na^+ pump, and the evidence that ATP provides the immediate source of energy for Na^+ pumping. Additional studies quoted as proof of the existence of the Na^+ pump include those of ATP-induced Na^+ efflux in perfused or dialyzed squid axon and in red blood cell ghosts and ATP-induced Na^+ uptake by vesicles containing Na^+,K^+ -ATPase. In Chapter 8, further investigations of these subjects will be described. The results of these new studies no longer support the membrane pump theory.

A number of other studies described in this chapter have suggested that the apparent Na^+ "pumping" can work well in frog muscle in the absence of any source of metabolic energy. The energy requirement of the Na^+ pump alone is insufficiently met, making it impossible to support the assumption of the large number of additional pumps that, to be logically consistent, must be found in order to explain the intra- to extracellular distributions of a large number of solutes. Moreover, the concept that energy is derived from the hydrolysis of a "high-energy phosphate bond" of ATP is suspect.

In addition to the failure of the cytoplasm-free squid axon membrane to show a net ion accumulation or exclusion, studies with a number of different red blood cell ghost preparations show that only solid ghosts containing at least 8% protein are able to accumulate K^+ and extrude Na^+ , negating the assumption that these preparations are simply membranes.

Finally, the effectively membrane-pump-less open-ended muscle cell preparation shows selective K^+ accumulation over Na^+ that clearly is determined by cytoplasmic, not membrane, processes.

These arguments provide some, but not all, of the reasons why I feel that there is no alternative to the rejection of the membrane pump paradigm and the development of a theory that is based on entirely different assumptions about the physical state of the intracellular protein-ion-water system. In the next section of this book, I outline such a theory—the association-induction hypothesis.

II

The Association–Induction Hypothesis

The Association–Induction Hypothesis I

Association of Ions and Water with Macromolecules

6.1. The Living State

The term *living state* has a specific meaning in the association–induction (AI) hypothesis, as suggested in the title of the monograph published twenty-two years ago: *A Physical Theory of the Living State* (Ling, 1962). In this concept the living state does not mean merely the presence of an assortment of the right ingredients in the right stoichiometric proportions, even though this requirement is vital; rather, the living state denotes two additional criteria: that the right ingredients are in a correct physical relation to one another in space–time coordinates, and that together in the resting cell they exist in a high-energy, low-entropy state.

6.1.1. The General Concept of a High-Energy Resting State

Consider the seashore. When the sun and the moon align themselves in a particular way, the tide is high; water reaches a much higher level. This system is then in a high-energy state. When the sun and moon move away from their optimal alignment, the water will flow back to its usual low tide mark. It is then in a low-energy state. Indeed, if a barrier could be set up and a water turbine installed, water trapped in the high tide could be made to perform work.

Consider next a string of soft iron nails joined together loosely end to end with bits of thin thread (Fig. 6.1A). Left alone, the chain of nails would assume a random configuration, and so would the iron filings strewn around the chain of loosely tethered nails. If a strong magnet is brought close to the end of one of the terminal nails, the nail will become magnetically polarized. As a result it will magnetize the second nail, and this can go on a number of steps until the entire chain assumes a more rigid and less random configuration. Along with this propagated magnetization, the nails also will orient the iron filings around them, forcing them also into a more defined and less ran-

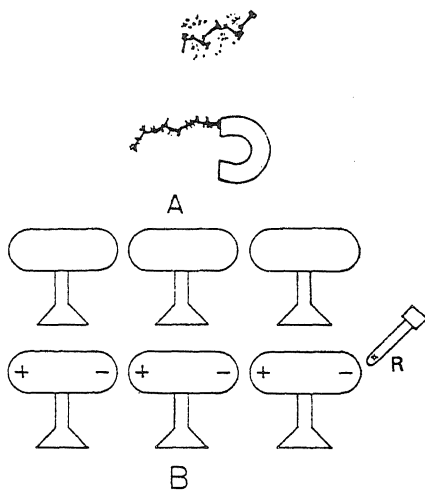


FIGURE 6.1. Two simple models demonstrating information and energy transfer over distances due to propagated short-range interactions. (A) A chain of soft iron nails joined end to end with pieces of string is randomly arrayed and does not interact with the surrounding iron filings. The approach of a magnet causes propagated alignment of the nails and interaction with the iron filings. (B) Electrons in a series of insulators are uniformly distributed before the approach of the electrified rod, R. Approach of the rod displaces the electrons by induction such that the insulator becomes polarized, with regions of low electron density and regions of high electron density. [From Ling (1969a), by permission of *International Review of Cytology*.]

dom configuration. This magnetized state is a high-energy, low-entropy state. Removal of the magnet leads to randomization and a return to a low-energy, high-entropy state.

Consider yet a third model (Fig. 6.1B): a chain of insulators aligned end to end. As a charged electrifying rod is brought close to one of the terminal insulators, a propagated polarization, this time electric rather than magnetic, will proceed down the line. If lightweight electrically charged styrofoam balls were in the vicinity, they too would congregate and orient themselves on the polarized insulators much as iron filings do near magnetized nails. The system of insulator chain, charged styrofoam balls, and electrifying rod would then be in a high-energy, low-entropy state. Removal of the electrifying rod causes the return of the whole assembly to a low-energy, high-entropy state.

From these models several deductions can be made:

1. *The high-energy state and association of components.* The high-energy state is more organized in the sense that all the components of the assembly are more closely associated, so that they lose much of their normal configurational randomness. Conversely, in the low-energy state, the components lose their coherence, are dissociated, and assume a more random relation to one another.
2. *The high-energy state versus the equilibrium state.* Another point which the models may help to clarify is the nature of the high-energy state. Note that one state is high-energy because it is higher in potential energy than is the state which the components tend to assume if left alone. Thus in the electrified insulators maintained in the high-energy state one end is made more electron-rich while the other is made electron-poor. One would be mistaken to say that either the electron-rich end or the electron-poor end is "high-energy."
3. *Coherence or cooperativity of the assembly depends on interaction of neighboring elements.* The chains of soft nails and of insulators behave together in unison. If one element is polarized, the other elements also are polarized. If one element becomes depolarized, the other elements also become depolarized. In each case,

the coherence of the assembly is not due to a long-range effect reaching out from the magnet or from the electrifying rod, directly through space to all the elements of the assembly. Rather, the long-range effect is due to the operation of a dominolike, propagated, short-range magnetic or electrical *inductive effect* between the nearest-neighboring elements. In other words, near-neighbor interaction provides the basis for coherence. In the language of statistical mechanics, which deals with large numbers of microscopic atoms, ions, or molecules, the coherence bespeaks of *cooperative behavior*.

The concept of the living state of the cell in the AI hypothesis includes these three deductions. First, it is a temporary reprieve from the trend toward ever-greater randomness and entropy. Second, only the assembly of associated cellular components (macromolecules, solutes, ions, water) can be designated as being in either a high-energy or a low-energy state. Third, its coherence mirrors cooperative behavior mediated by short-range, induced near-neighbor interactions between sites on macromolecules that associate with ions or water.

6.1.2. The Major Components of Living Systems

In mass, the largest component of all living cells is water and the second largest is protein. In number, the most abundant again is water, the second most abundant is K^+ . Living cells function normally in their natural environments. Thus, to understand living phenomena, the external environment cannot be ignored. By and large, it is a salt solution containing water as its largest component and NaCl as its next largest component. *Thus, living cells are primarily water, proteins, and K^+ in an environment of water and Na^+ .*

6.1.3. Protoplasm and the Living State

Protoplasm, a concept at one time so eloquently described and so fondly believed in (Sections 1.3 and 2.5) lost out in the decline of colloidal chemistry and the ascendance of the membrane theory (Section 2.7). The basic tenets of this theory—free water and free K^+ —regard the inside of the cell as nothing more unusual than a buffered solution containing a mixture of native proteins and salts. In contrast, in the AI hypothesis, protoplasm in the living state is considered a unique substance, with its major components intricately associated in a most specific and coherent manner, that is maintained in a high-energy state.

French impressionists discovered long ago that the essence of a forest, for example, is more accurately seen when the observer squints his eyes so that confusing details are deliberately placed out of focus. I believe that the same principle applies to science. Thus, in order to perceive the features common to all living matter, one must sometimes forget all the beautiful electron microscopic plates of fixed cell sections and look at a living cell directly under a light microscope. A single voluntary muscle cell, a structure of such elaborate morphology on electron microscopy (see Fig. 8.3A), now appears in life as a simple homogeneous transparent cylinder. Indeed, if prints are placed below it, they can be easily read right through the muscle cell. It is then that we can get a feeling

for the "sameness" of all parts of the living cell. With this picture in mind, one can recapture some of the great enthusiasm once felt by biologists about protoplasm and one can perhaps grasp what it is that the AI hypothesis intends to say: Protoplasm maintained in the living state makes up all components of the cell—cytoplasm, nucleus, membranes, ribosomes; the differences between them are the details which a squinting biologist may want momentarily to ignore.

According to the AI hypothesis, the major components of living protoplasm—water, proteins, and K^+ —exist in a closely associated, high-energy state. More specifically, the association falls into three categories: (1) association of proteins with ions, in particular with K^+ and Na^+ , (2) association of proteins with water, and (3) association of proteins with other proteins and macromolecules. The first two types of association are outlined in this chapter and in Chapters 8 and 9 and the third is discussed within specific contexts (e.g., Chapters 13, 16, 18, and 19).

6.2. Association of Ions

6.2.1. Enhanced Counterion Association in a Fixed-Charge System

The theory of the selective accumulation of K^+ over Na^+ , described in 1952 and illustrated in Fig. 4.9, was intended to apply to both living cells and inanimate systems such as the ion exchange resin. A basic postulate of this model is that counterions in a fixed-charge system are nearly completely in an associated or adsorbed state in which one counterion is adsorbed to one site. In contrast, Gregor (1951) offered his theory of

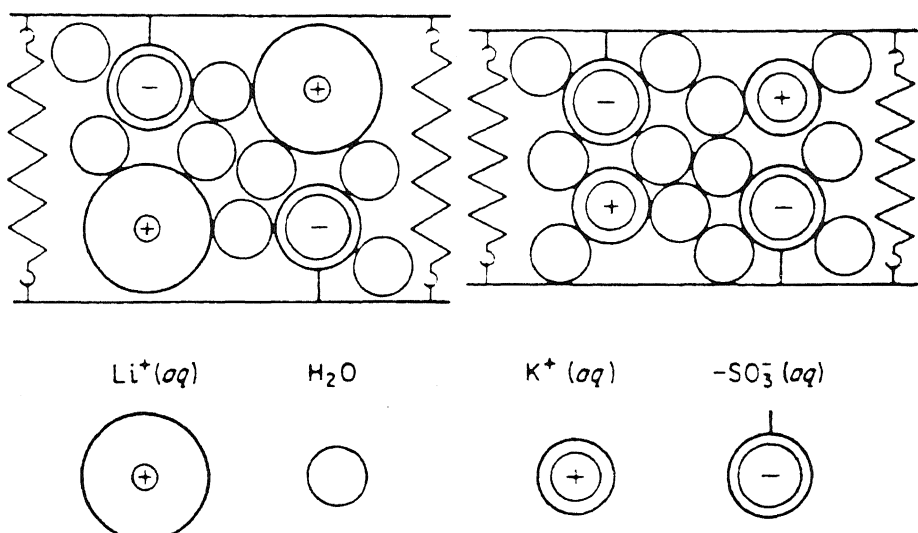


FIGURE 6.2. Schematic diagram of the inside of a cation exchange resin, demonstrating the swelling pressure mechanism of selectivity between different, but fully dissociated, counterions (the Gregor model). [From Buser *et al.* (1955), by permission of *Chimia*.]

selective accumulation of K^+ over Na^+ in sulfonate ion exchange resin on the basis of the opposite assumption that all the counterions are completely dissociated (Fig. 6.2, Section 4.4.2.1). The theoretical and experimental bases for the postulation of a high degree of counterion association are discussed next.

6.2.1.1. Theoretical Basis

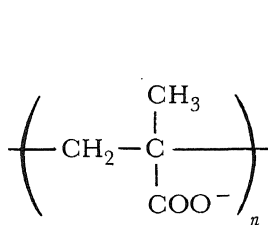
Complete ionic dissociation, as demonstrated by Arrhenius (1887) and described in the theory of Debye and Hückel (1923), is restricted to simple dilute solutions and was not intended to explain ionic association in a fixed-charge system.

Consider a dicarboxylic succinic acid. Its two acid dissociation constants are not equal but are, respectively, 4.16 and 5.61. The difference in their pK_a values can be described by the equation (Bjerrum, 1923)

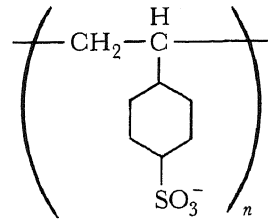
$$\Delta pK_a = (pK_a^2 - pK_a^1) - \log 4 \quad (6.1)$$

where $\log 4$ (equal to 0.60) mirrors the entropic factor, i.e., the probability is twice as high for the first dissociation as for the second association. The difference in the pK_a s of the two carboxyl groups of succinic acid exceeds 0.60 by 0.85, which corresponds to 0.50 kcal/mole and is primarily due to the electrostatic attraction of the dissociated carboxyl group for the proton dissociating from the second carboxyl group.

Now let us consider a linear polymer carrying many anionic groups, such as polymethacrylate or polystyrene sulfonate. In this case the dissociation of the first few pro-



Polymethacrylate



Polystyrene sulfonate

tons will have a cumulative effect, just as does the dissociation of one proton from succinic acid. As a result the effective pK_a values of the remaining anionic sites become greatly enhanced. Furthermore, the cumulative effect of the total negative charges would tend to restrict the dissociated protons to within a tighter ion cloud. In other words, the average dissociated proton no longer can enjoy a free distribution, limited only by the size of the vessel, as would be the case for monovalent-monovalent salts containing the same total number of charged groups.

The increased ionic association occurring as a result of the reduced free volume available to the dissociated counterions is illustrated by the sublimation of ice. In subzero weather, frozen laundry can dry if kept outdoors in the open air; it cannot dry at the same temperature in a small enclosed container.

In fact, this restrictive effect reaches a still higher level when these linear chains of polymethacrylate and polystyrene sulfonate are joined together into a three-dimensional matrix, as they are in an ion exchange resin bead. Under this condition, very few free protons can diffuse out of the matrix when the fixed-charge system is soaked in distilled water. Thus, counterion dissociation becomes a matter of dissociation *within* the fixed-charge system.

It has long been known that electrostatic interaction is so strong that dissociation of salts occurs only in highly polar solvents like water. On the one hand hydration of the dissociated ion reduces the enthalpy gain on dissociation, and on the other hand hydration greatly increases the rotational entropy of the dissociated ion (see Ling, 1962, p. 24; Fowler and Guggenheim, 1939). There is strong evidence that water in both ion exchange resins and normal resting cells is not normal (Chapter 9). In this case, there is a further reduction of the entropy of dissociation due to restriction of rotational freedom of the dissociated counterion, thereby providing another reason for a higher degree of counterion association in the fixed-charge system than in a dilute salt solution. The subject of rotational entropy changes in the water of ion exchange resins and of living cells will be taken up in Section 6.3.

6.2.1.2. Experimental Models

6.2.1.2a. Ion Exchange Resins. There is evidence that counterions are in fact associated in commercial exchange resins; for example, Helfferich (1962) pointed out that Ag^+ and Tl^+ are quite similar to Cs^+ in size and therefore, according to Gregor's theory, should be accumulated to the same degree. Actually Ag^+ and Tl^+ are 4–5 times preferred over Cs^+ in Dowex 50 [16% divinylbenzene (DVB)] (Helfferich, 1962, p. 169). This difference between Ag^+ (or Tl^+) and Cs^+ indicates a specific recognition by the fixed anionic sites of attributes that are short-range (e.g., size, Born repulsion constant, polarizability). Discrimination on the basis of short-range forces can only be the result of close contact between counterions and fixed anionic sites. Long-range attributes (i.e., valency) that determine the behavior of a free and fully dissociated counterion are identical for these monovalent cations and would not be able to provide the basis for the high degree of selectivity among them.

Another set of evidence which argues against the notion of free counterions in resins is the fact that whereas the sulfonate ion exchange resin selectively accumulates K^+ over Na^+ and Li^+ , the carboxylic and phosphonic resins actually prefer Na^+ and Li^+ over

TABLE 6.1. Selectivities for Alkali Cations in Various Types of Cation Exchange Resins^a

Cation	Sulfonic	Carboxylic	Phosphonic
K^+	1.0	1.0	1.00
Na^+	0.80	1.14	1.51
Li^+	0.40	1.59	2.33

^aData from Bregman (1953), but expressed in terms of K_{X^+}/K_+ , where X^+ refers to any one of the different cations studied.

K^+ (Table 6.1). If size of the counterions alone determines selectivity, there should be only one order of preference. However, this criticism of Gregor's theory can equally be directed at Ling's fixed-charge hypothesis (LFCH), described in Chapter 4. Indeed this contradiction of the LFCH stimulated the development of the more complete AI hypothesis, which is capable of explaining the different ion selectivity orders observed in cells and resins.

Kern (1938, 1939) demonstrated long ago by cryoscopic, osmotic, and electrical conductance measurements that in aqueous solutions polyacrylic acid produces a strong "electrostatic inactivation" of the counterions. Table 6.2, taken from Kern's 1948 paper, illustrates the marked lowering of the activity coefficient of Na^+ present in polyacrylate when compared to that in the isobutyrate salt. Clearly, the most straightforward explanation of this inactivation of the counterion is its adsorption onto the anionic carboxyl groups of the polyacrylate.

Kern's findings are relevant here because the carboxylic type of ion exchange resin, such as Rohm and Haas IRC-50, is simply a cross-linked concentrated polyacrylic acid. Since the degree of ionic association as a rule increases with concentration, Kern's findings have already provided additional strong evidence that in IRC-50 Na^+ is adsorbed and not free. Kern's data as such do not prove that counterions in the strongly acidic sulfonate type of exchange resin, such as Dowex 50, are similarly adsorbed. Since Gregor's theory was primarily directed toward the sulfonate type of ion exchange resin, Ling and Zhang (1983a) carried out a series of studies on both polymethacrylate and poly-

TABLE 6.2. Electrometric Measurements of
 Na^+ Activity of Aqueous Solutes of Na^+
 Isobutyrate and Na^+ Polyacrylate^a

Concentration of Na^+ (M)	Activity of Na^+ (M)	Activity coefficient
Isobutyric acid, $CH_3CHCOOHCH_3$		
0.2	0.186	0.93
0.1	0.090	0.90
0.05	0.049	0.98
0.025	0.025	1.00
0.0125	0.0122	0.98
Polyacrylic acid, $(-CH_2CHCOOHCH_2)_n$		
0.2	0.060	0.30
0.1	0.0315	0.315
0.05	0.0146	0.292
0.025	0.0058	0.232
0.0125	0.0021	0.168

^aData from Kern (1948), by permission of *Makromolekulare Chemie*.

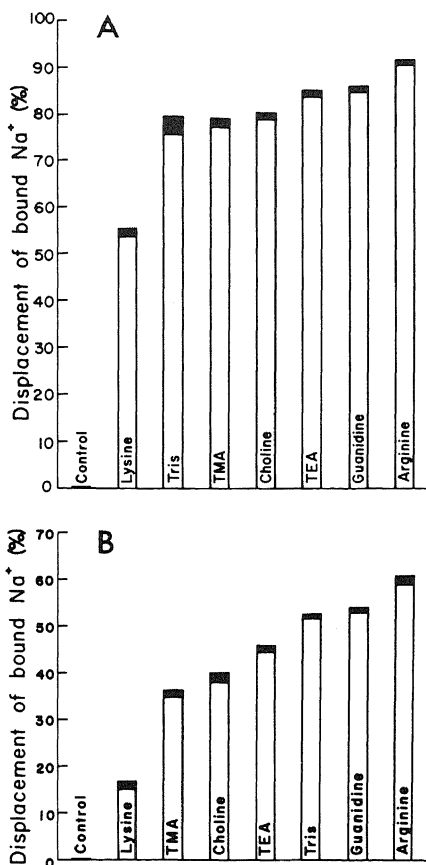


FIGURE 6.3. Displacement of bound Na^+ by organic cations (75 mM) in a solution of Na^+ polystyrene sulfonate (A) and in a solution of Na^+ polymethacrylate (B). [From Ling and Brady (see Ling and Zhang, 1983a), by permission of *Physiological Chemistry and Physics*.]

vinylbenzene sulfonate.* In these studies Ling and Brady dialyzed solutions of the (un-cross-linked) linear polymers whose counterions are exclusively Na^+ . They then measured the Na^+ activity with a Na^+ -selective electrode in both the absence and the presence of 75 mM competing organic cation to which the Na^+ electrode is not sensitive. The results, shown in Fig. 6.3, provide evidence that the Na^+ "inactivation" observed by Kern is due to direct-contact association, or adsorption. Thus part of the Na^+ not observed by the Na^+ electrode becomes "observable" to a varying degree when lysine, tetramethylammonium (TMA), choline, tetraethylammonium (TEA), Tris, guanidine, or arginine is added. Since the differences between these organic ions are only in their short-range attributes, these findings proved conclusively that even in a polystyrene sulfonate solution as dilute as this (1–5%), there is a high degree of specific one-on-one adsorption of counterion to the fixed anionic sites.

The data of Fig. 6.3 also demonstrate that the effectiveness in displacing Na^+ from adsorption sites follows essentially the same order (arginine > guanidine > TEA >

*Cross-linked polyvinylbenzene sulfonate is known commercially as Dowex 50 or Amberlite IRC-120, and by other familiar trade names.

choline > TMA > lysine) in both sulfonate and carboxylate polymers. The position of Tris varied, however, probably owing to greater sensitivity of this cation to minor pH differences in these series of studies. This similarity in the order of binding strengths of the organic cations is in sharp contrast to the degree of displacement of Na^+ in the two polymers, a fact which suggests that Na^+ is much more tightly adsorbed in the carboxyl polymer than in the sulfonate polymer.

Teunissen and Bungenberg de Jong (1939) studied three types of colloids—carboxylate, phosphate, and sulfate—and showed a reversal in their directions of migration in an electrophoretic field after the ion concentrations in the surrounding medium reached a certain level. On the assumption that this charge reversal denotes the combination of a certain number of cations with the anionic colloid, they and Bungenberg de Jong (1949) showed that the concentration at which charge reversal occurs is both ion- and colloid-specific. In the case of phosphate colloids, binding preference occurs in the order $\text{Li}^+ > \text{Na}^+ > \text{K}^+$, while in the sulfate colloids the order is $\text{K}^+ > \text{Na}^+ > \text{Li}^+$, in agreement with similar rank orders given in Table 6.1. They interpreted their data on the basis of the assumption that there is a difference in the polarizabilities of the phosphate, carboxylate, and sulfate groups in comparison to that of H_2O , such that polarizabilities decreased in the order phosphate > carboxyl > $\text{H}_2\text{O} >$ sulfate. The net effect of the fixed anion on the cation is a balance between polarization on the one hand and "field strength" on the other (see Bungenberg de Jong, 1949, p. 287). They argued that the high polarizability of the phosphate anion makes it energetically most favorable for the smallest cation, Li^+ , to give up its water of hydration and interact with the fixed phosphate anion, next Na^+ , and last the largest, K^+ . Hence the order is $\text{Li}^+ > \text{Na}^+ > \text{K}^+$. Assuming that the sulfate ion has lower polarizability than H_2O , each ion will retain its full share of hydration, and the electrostatic energy is then in the order $\text{K}^+ > \text{Na}^+ > \text{Li}^+$.

It is worth mentioning that Bregman (1953) cited Teunissen and Bungenberg de Jong's ideas to explain the similar reversal of order in the selectivity of ion exchange resins for these ions.

6.2.1.2b. Glass Electrodes. In 1957, Eisenman, Rudin, and Casby suggested that, with an increase in the field strength of the fixed anion of the glass, the most hydrated ion loses its shell of hydration first, and the least hydrated ion loses its shell last. By taking into account variable field strengths of the fixed anions of different kinds of glass, and by considering only the coulometric charge-charge energy between nonpolarizable point charges, Eisenman (1962) analyzed the relative hydration energies of the series of monovalent cations and their differences in relation to differences in the anionic field strengths. He produced eleven sequential orders of cationic selectivity. These ranged from $\text{Cs}^+ > \text{Rb}^+ > \text{Na}^+ > \text{Li}^+$ at the lowest field strength to $\text{Li}^+ > \text{Na}^+ > \text{K}^+ > \text{Cs}^+$ at the highest. These orders of selectivity are shown in Fig. 6.4.

It is not certain that the different selectivity patterns really reflect a continuous change of the "field strength" of the glass anions. One could perhaps also make a case that the various glasses manufactured actually contain two or more different kinds of negatively charged oxygen atoms, one of very high field strength and the other of the lowest field strength, and that a varying mixture of these different sites then contributes to the intermediate orders.

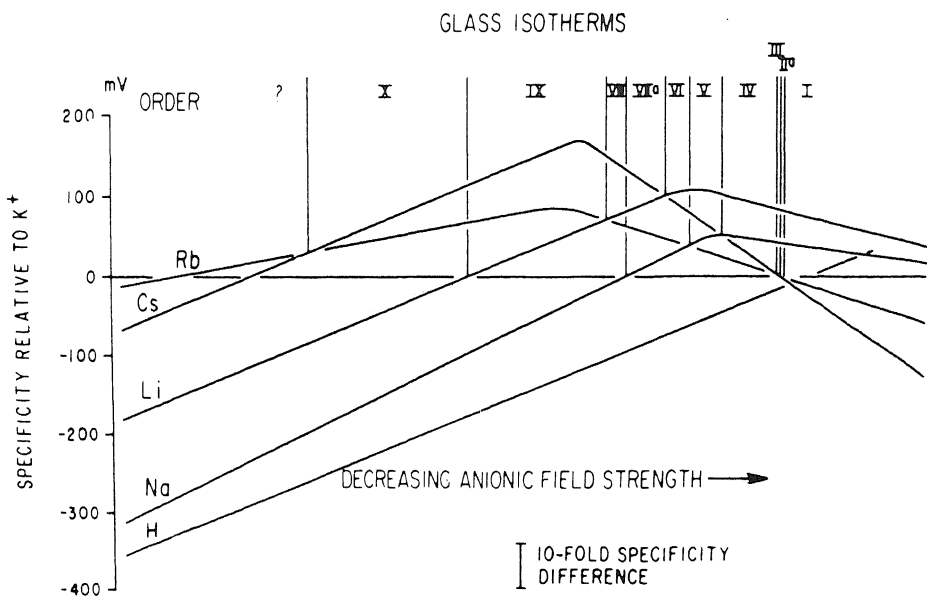


FIGURE 6.4. Combined selectivity isotherms of glass electrodes. [From Eisenman (1967), by permission of Marcel Dekker.]

6.2.2. The Theory of Selective Ionic Adsorption and Its Variation with the Electron Density or *c*-Value of the Fixed Anionic Sites

The development of the sulfonate type of ion exchange resin offered evidence in favor of the simple theoretical model for selective accumulation of K^+ over Na^+ presented some 31 years ago (Ling, 1952). The discovery that carboxylic and phosphonic types of ion exchange resins actually prefer Na^+ over K^+ (Table 6.1) stimulated development of a new theoretical model in order to account for both types of selective accumulation. Other important factors contributing to the development of the new model included Teunissen and Bungenberg de Jong's (1939) concept that the reversal of ion selectivity reflects differences in the balance of electric field strength and the polarizability of the fixed anions in colloids, and Eisenman, Rudin, and Casby's (1957) studies of glass electrodes, which led them to the finding that variations of the field strength of the fixed anions, coupled with the varied hydration energies of the countercations, would create eleven different orders of selectivity among the five alkali metal ions, Cs^+ , Rb^+ , K^+ , Na^+ , and Li^+ (see Ling, 1957).

The differences of selectivity between K^+ and Na^+ in sulfonic, carboxylic, and phosphonic resins were remarkable because all three of their acidic groups are oxyacids. In each a singly charged oxygen atom is in direct contact with the associated alkali metal ion. In the original LFCH it was assumed that the critical parameter in the selective adsorption of K^+ over Na^+ was the difference in hydrated ionic diameters, which were assumed to be unchanging. This assumption of a fixed hydrated ionic diameter was incorrect and is abandoned in the new model.

6.2.2.1. *The Definition of the c-Value*

It is well known that a weak carboxylic acid such as acetic acid, CH_3COOH ($\text{p}K_a = 4.65$), can be converted into a strong carboxylic acid, trichloracetic acid ($\text{p}K_a < 1$), by substituting three chlorine atoms for the three hydrogen atoms on the methyl group of the acetic acid, creating CCl_3COOH . This difference in $\text{p}K_a$ value is the classic example of the inductive effect: The more electronegative chlorine atom, with its greater attraction for electrons than the H it replaces, reduces the electron density of the singly charged oxygen atom of the carboxyl group. Since the attractive force of the carboxyl group for H^+ is primarily electrostatic (Kossiakoff and Harker, 1938), the result is a decrease of affinity for H^+ , i.e., a decrease of $\text{p}K_a$. Such a change in $\text{p}K_a$ value may, however, be but one manifestation of the altered electron density at the oxyacid group. This alteration of the electron density may, for example, have an effect on the preference of the site for K^+ or Na^+ . The question was then asked whether one could theoretically predict such an effect.

To aid in the development of such a theoretical calculation, I introduced a parameter called the *c-value* (in Å). Beginning with a singly charged oxygen atom with the unit charge located at the center of the atom, the total inductive effect of whatever complex molecule on which this oxygen is borne can be simulated by a displacement of the unit negative charge either toward or away from the interacting cation, which may be a proton, a K^+ , or a Na^+ . Thus, a high *c*-value signifies a higher electron density and would correspond to a high $\text{p}K_a$, such as in the case of acetic acid. A low *c*-value signifies a lower electron density and corresponds to a low $\text{p}K_a$, such as in the case of trichloracetic acid. A more rigorous and complete definition of the *c*-value was given in 1962 (see Ling, 1962, p. 58), and is shown schematically in Fig. 6.5.

6.2.2.2. *The Linear Model*

The next step in the development of the new theory involved setting up a linear model (Ling, 1962). This was chosen in preference to a three-dimensional model because the much greater computational effort involved in the three-dimensional model would not have been justified, partly because of inadequate existing knowledge of some of the basic parameters, e.g., the structure of liquid water itself, and partly because of the lack of suitably powerful computers at that time. The linear model clearly could only give us a rough idea about parameters like relative affinities, but this rough estimate is probably the best that one can hope for at this stage of development.

As shown in Fig. 6.6, the linear model was constructed in a cylindrical cavity in a dielectric (aqueous) medium. At one end of the cylindrical cavity is placed the singly charged oxygen atom and next to it none, one, two, or three water molecules, to be followed by a cation and two or more water molecules. These are referred to as the 0, I, II, and III conformations.

Using physical constants from the literature, I then calculated the total energy of each of the four conformations for each of the seven ions— Li^+ , Na^+ , K^+ , Rb^+ , Cs^+ , H^+ , and NH_4^+ —for varying *c*-values and for three values of the polarizability of the oxyacid group. In these calculations eight types of energies were taken into account, among them charge-charge, charge-dipole (both permanent and induced), dipole-

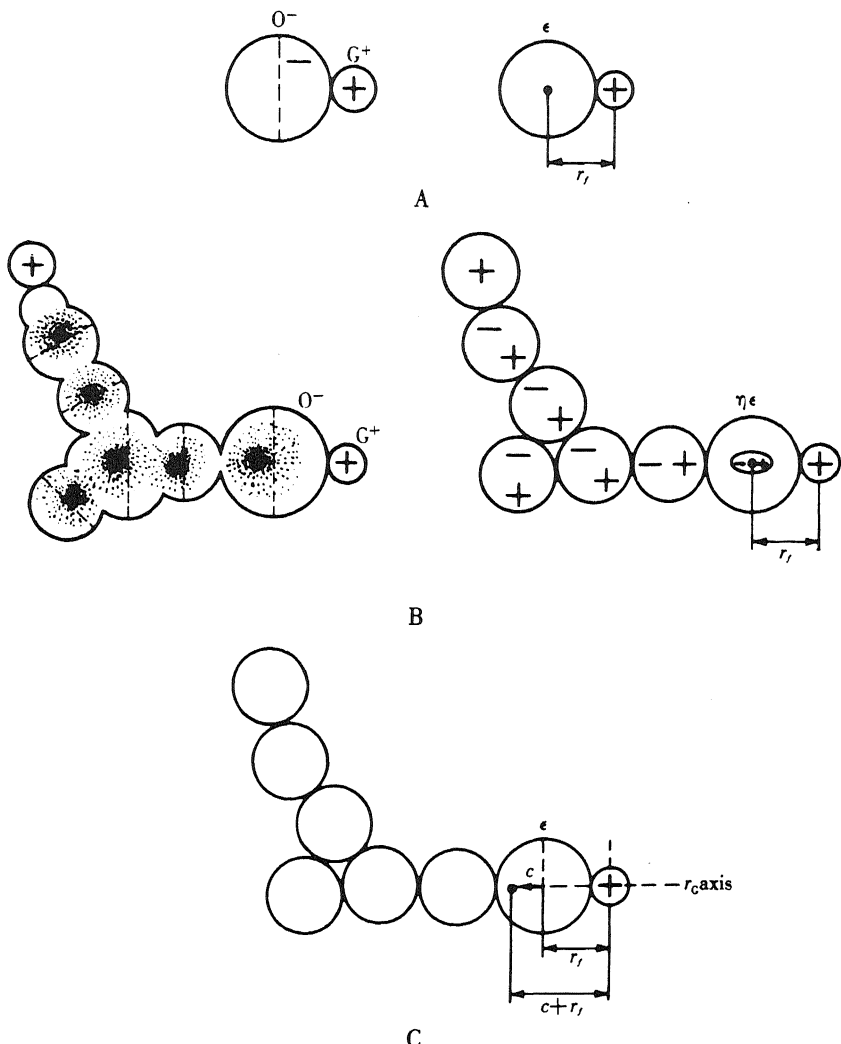


FIGURE 6.5. Definition of the c -value. The c -value is the displacement in Å of the unit negative charge carried by the oxygen atom from the center of the atom either away (negative c -value) or toward (positive c -value) the interacting cation (C) so that the net interaction with the cation matches the cumulative action of the inductive effects exerted by the rest of the molecule (B). [From Ling (1962).]

dipole, London dispersion energy, and Born repulsion energy. The computed data permitted the calculation of the statistical weights of each conformation at a particular c -value.

In general, for each ion, the high conformation (III) (Fig. 6.6) is preferred at low c -value. As the c -value increases, the lower conformation becomes more and more favored energetically until at the highest c -value the 0 conformation is preferred above all others. At any c -value, as a rule, a mixture of conformations exists for each ion,

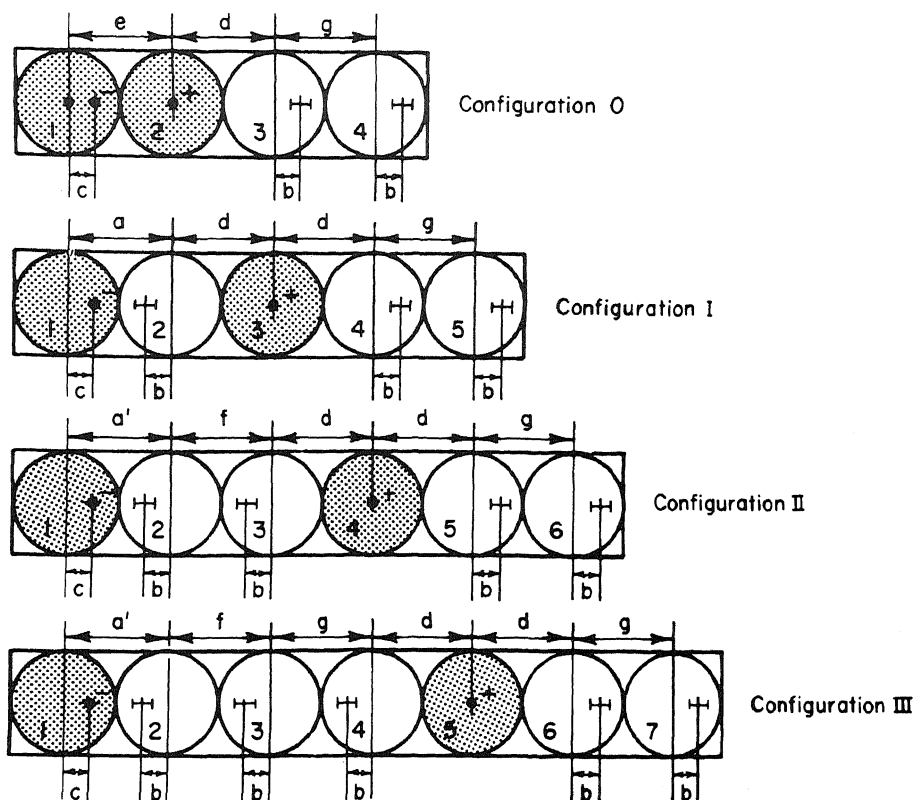


FIGURE 6.6. The linear model. The interaction energies were calculated for each of the monovalent cations in each of the four configurations of fixed anions and water. The shaded circle on the left is the anionic oxyacid on a protein. The shaded circle to the right is a monovalent cation. The open circles are water molecules. See text for further description. [From Ling (1962).]

although in some cases one conformation far outweighs others in statistical weight. Knowing the statistical weights of each of the conformations, I then calculated the dissociation energy.

The ideal way to calculate the dissociation energy is to obtain the difference between the energy of the fixed anion–water–countercation assembly and the sums of the energies of the hydrated fixed anion and the hydrated cation, separated from each other by an infinite distance. The limit imposed by the linear model made such a calculation impossible and a less desirable way, the Born charging method, was chosen.

The final calculated dissociation energies vary with the polarizability of the oxyacid oxygen. Our calculations included three values for oxyacid polarizability: $\alpha = 0.876 \times 10^{-24}$, 1.25×10^{-24} , and $2.0 \times 10^{-24} \text{ cm}^3$, clustering around the polarizability of H_2O , $1.444 \times 10^{-24} \text{ cm}^3$. Changes in α have definite effects on the details of the order of ion selectivity, but this effect is by no means as important as the c -value. (Our c -value would correspond to Teunissen and Bungenberg de Jong's "field strength," mentioned in Section 6.2.1.2a.)

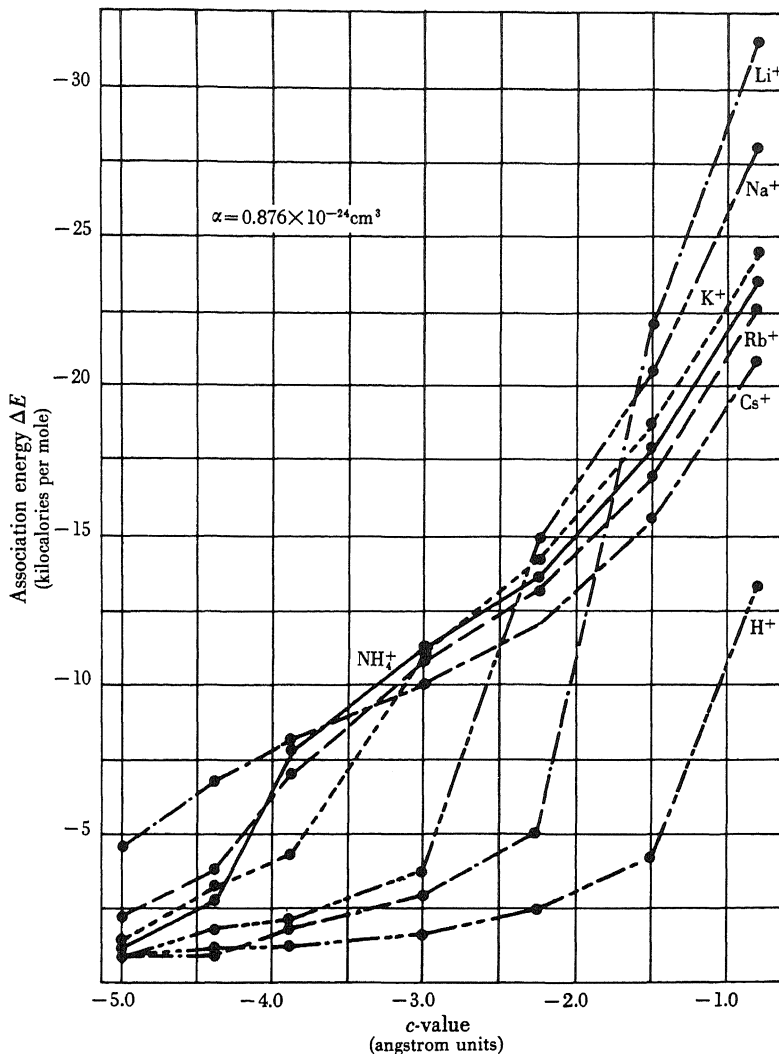


FIGURE 6.7. Relation between calculated association energy ΔE of various cations and c -value of the anionic group. Polarizability of anionic site, α , is $0.876 \times 10^{-24} \text{ cm}^3$. [From Ling (1960), by permission of *Journal of General Physiology*.]

One of the sets of data calculated is taken from Ling (1960) and shown in Fig. 6.7, in which the anionic oxygen polarizability is $0.876 \times 10^{-24} \text{ cm}^3$. In Fig. 6.8 the theoretical data are presented in terms of selectivity coefficients expressed relative to K^+ ; in this case the anionic oxygen polarizability is $1.25 \times 10^{-24} \text{ cm}^3$.

The main conclusions to be drawn from these computations are as follows: First, these computations confirm the original idea that a relatively small change in the electron density of the oxyacid oxygen atom can indeed alter the order of ion selectivity.

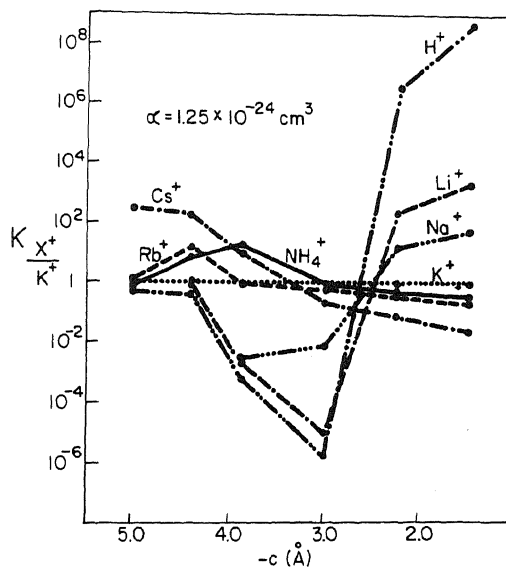


FIGURE 6.8. Relation between selectivity ratios of various cations and *c*-value. The K^+ ion is taken as unity and selectivity ratios are calculated from association energies. [From Ling (1962).]

Second, and more specifically, these theoretically calculated curves show that, in terms of the variation of adsorption energy with change in *c*-value, the different ions appear to fall into two separate categories: K^+ , NH_4^+ , Rb^+ , and Cs^+ show a steady increase of the adsorption energy with an increase in *c*-value; Na^+ , Li^+ , and H^+ show a more or less unchanging adsorption energy with an increase in *c*-value at low *c*-values, followed by an abrupt increase in adsorption energy when the *c*-value has gone beyond a certain point.

6.2.3. Reversal of Ionic Selectivity Ratios: Comparison of Theory with Experiment in Ion Exchange Resins

As mentioned above (Section 6.2.1.2a) Bregman's demonstration of different orders of alkali metal selectivity played a major conceptual role in the evolution of the AI hypothesis. Both Eisenman's and my model were extensively discussed by Reichenberg (1966).

For an exchange of A and B:



where the overbar indicates ions in the resin phase. The equilibrium constant is

$$K_{B/A} = (\overline{X}_B / \overline{X}_A) / (X_A / X_B) \quad (6.5)$$

where \overline{X}_A , \overline{X}_B are the equivalent fractions of A and B in the resin phase and X_A , X_B are those in the external solution phase. If the resin phase is homogeneous, $K_{B/A}$ will

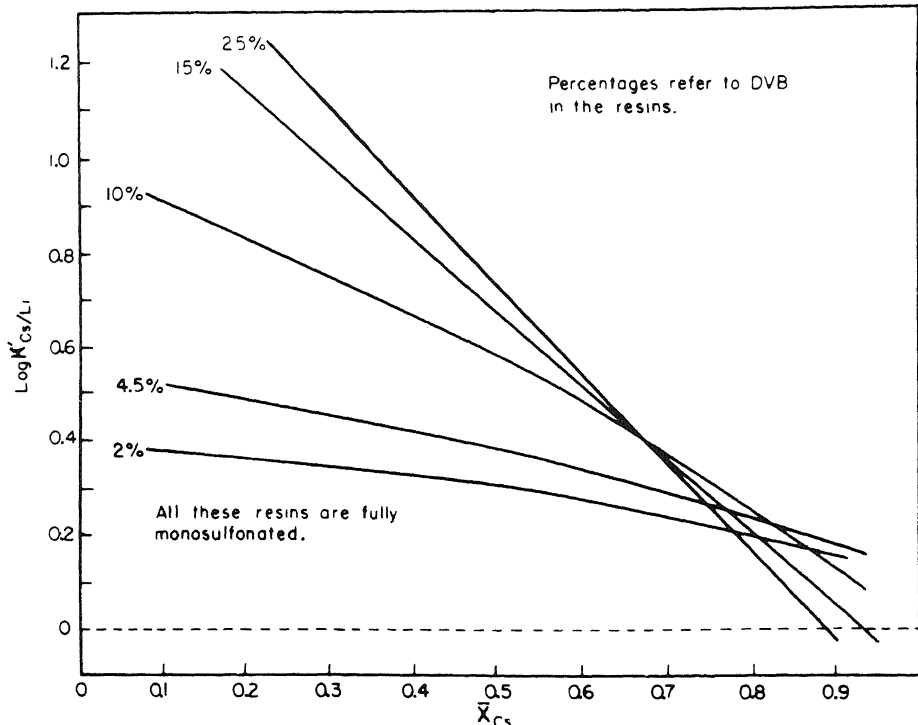


FIGURE 6.9. Cs^+/Li^+ selectivity on monosulfonated cross-linked polystyrene resins showing affinity reversals. [From Reichenberg (1966), by permission of Marcel Dekker.]

remain constant regardless of the value of \bar{X}_B/\bar{X}_A . In 1943 Walton showed that, if the sites are not uniform but fall into at least two categories, each characterized by a different $K_{B/A}$, then the apparent $K_{B/A}$ of the whole assembly will change with gradual increases of \bar{X}_B and decrease of \bar{X}_A .

Figures 6.9 and 6.10 are reproductions of the work of Reichenberg (1966) on a monosubstituted polystyrene sulfonate type of ion exchange resin and that of Gregor *et al.* (1956) on the polymethacrylate ion exchange resin. The resins are cross-linked with DVB. In each case, at low cross-linking, loading with one or the other ion produces little change in $K_{A/B}$. But, as the percentage of the cross-linking agent (DVB) increases, the (negative) slope of $K_{A/B}$ versus \bar{X}_B increases steadily, reaching its maximum at the highest percentage of cross-linking. Thus it would seem that the introduction of DVB brings about an increasing degree of selectivity. To the best of my knowledge, no explanation has been offered for this widely observed phenomenon (see Helfferich, 1962, p. 159).

Gregor *et al.* (1955) presented data which revealed that in the series of methacrylic acid–divinylbenzene copolymers the pK_a values corresponding to the pH titrated at half saturation in the absence of added salt increased progressively with the percentage of DVB. A rough estimate from their published data shows that the pK_a of the carboxyl group was 8.3 at 0.5% DVB, 9.3 at 2% DVB, 9.2 at 6% DVB, and 9.6 at 15% DVB.

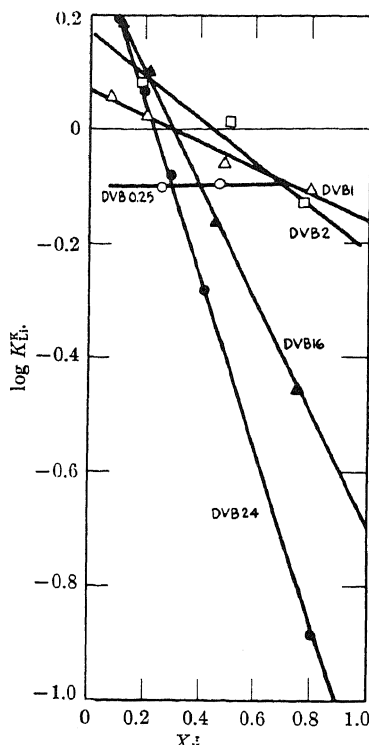


FIGURE 6.10. Selectivity coefficients for K^+-Li^+ exchange from base solutions as a function of the fraction of resin exchange sites occupied by K^+ . Resins are (DVB in percent): \circ , DVB 0.25; Δ , DVB 1; \square , DVB 2; \blacktriangle , DVB 10; \bullet , DVB 24. [From Gregor *et al.* (1956), by permission of *Journal of Physical Chemistry*.]

This interesting and at that time unexplained phenomenon may be interpreted as an increase in the *c*-value of neighboring carboxyl groups with introduction of DVB through the inductive effect (see Section 7.1). Since a pK_a of 8.3 indicates an initially high *c*-value, a further increase of *c*-value may well enhance $K_{\text{Cs}/\text{Li}}$, as observed (Fig. 6.9). Similar inductively mediated *c*-value increases of sulfonate groups may also explain the decrease of $K_{\text{K}/\text{Li}}$ (or increase of $K_{\text{Li}/\text{K}}$) shown in Fig. 6.10 (compare with Figs. 6.8, 6.9).

If the hypothesis that DVB increases the *c*-value of nearby anionic sites is correct, one would expect that with increasing percentage of DVB in the exchange resin one would see sequential changes in the preferences of monovalent cations like those theoretically calculated. In fact this was what Gregor and Bregman (1951) observed. Their data, reproduced in Fig. 6.11, clearly show that, as the percentage of DVB increases, the relative preference of the five ions does indeed follow the general trends theoretically calculated from our linear model where $K_{M/K}$ is plotted against the *c*-value (Fig. 6.8).

The general similarity between the theoretical curves and Bregman's graph needs no emphasis. Both exhibit the striking features of first a declining preference for Na^+ , Li^+ , and H^+ in comparison with K^+ in the low-*c*-value range, and then the abrupt reversal of this trend in the high-*c*-value range. The only significant differences between the theoretical curves and Bregman's data lie in the relative *c*-value at which the Li^+ and H^+ swing over. However, the position of the H^+ curve depends strongly on the

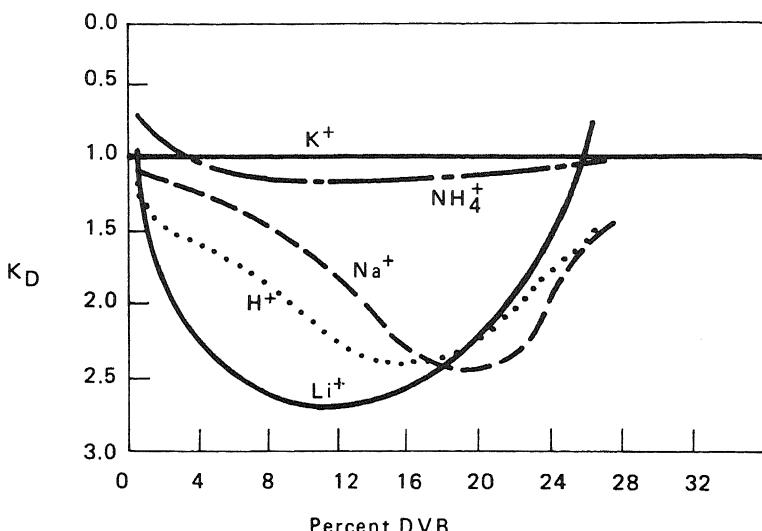


FIGURE 6.11. Relative selectivity coefficients of H^+ , NH_4^+ , and alkali metal ions compared to K^+ in sulfonate ion exchange resin with varying percentage of DVB. [Redrawn from Bregman (1953).]

polarizability of the fixed anion. At a higher polarizability, Li^+ and H^+ curves swing over at a lower c -value, as shown in theoretical data with $\alpha = 2.0 \times 10^{-24} \text{ cm}^3$ (Ling, 1962, p. 77).

6.2.4. Generalized Relations between c -Value and Adsorption Constants

So far we have concentrated on the theoretical calculations and experimental data regarding H^+ , NH_4^+ , and alkali metal ion selectivity in their adsorption on monovalent anionic sites. The major point of interest is that, as the c -value changes, counterions with different polarizability or Born repulsion constants interact with the fixed anion and water in such a way as to produce a sequential order of selectivity. Qualitatively there is no reason to believe that the basic properties discerned should be limited to cases where fixed sites carry net electronic charges but may be extended to sites that are electron- or proton-donating groups. Thus, to generalize, I have also introduced the c' -value to serve as an equivalent for measuring the cationic positive charge density, as well as the c -value analogue and c' -value analogue to describe the charge density of electronegative and electropositive sites that do not bear net electric charges, as in the case of carbonyl and imino groups.

We shall then postulate that as the c' -value, c -value analogue, or c' -value analogue vary, a pair of free counteranions, or proton-donating solutes, or proton-accepting solutes also may demonstrate changes in their relative preferences just as in the case of cation adsorption on fixed anions of varying c -values.

The most important conclusion to be drawn here is that the relative preferences in ionic adsorption can be changed by small changes of the electron density of the anionic group. In Chapter 7, I shall present the theory of how such electron density changes can provide the molecular basis for physiological activities of the most diverse kinds.

6.2.5. Salt Linkages, *c*-Value, and the *in Vitro* Demonstration of Selective Na⁺ and K⁺ Adsorption on Isolated Proteins

Isolated proteins usually exhibit little capacity for specific adsorption of K⁺, Na⁺, and other alkali metal ions *in vitro*. In Section 4.4.1 it was pointed out how earlier failure to demonstrate significant adsorption of K⁺, Na⁺, and other alkali metal ions had played a major role in the acceptance of the membrane pump theory. However, in 1952 I pointed out that this failure to adsorb K⁺ (or Na⁺) may not be an immutable property of proteins but may reflect a specific conformation that the isolated proteins assume under *in vitro* conditions. More specifically it was argued that the main reason for this failure is the formation of salt linkages between the essential anionic sites (e.g., β - and γ -carboxyl groups) and fixed cations (Section 4.4.1). Thus combined, the anionic sites are no longer available for K⁺ and Na⁺ adsorption. This theory, therefore, predicts that if the salt linkages are broken, say by a rise of the pH of the medium which removes the positive charge of the fixed cations (e.g., ϵ -amino groups of lysine residues), the anionic sites would be liberated. The liberated anionic sites would then be expected to adsorb K⁺ (or Na⁺) specifically according to their *c*-values. Very recently, this prediction has been confirmed (Ling and Zhang, 1983b).

6.3. Association of Water

6.3.1. Historical Background

In 1929 de Boer and Zwikker presented their polarized multilayer theory of gaseous adsorption to explain the increased uptake of argon gas at the crystal surface at higher pressure. The electric charges of the surface ions induce an electric dipole in one layer of argon atoms. The induced dipole in turn induces another layer of dipoles, and this goes on a number of steps.

An equation was derived on the basis of this model:

$$\ln \frac{p}{K_3 p_0} = K_2 K_1^a \quad (6.6)$$

where p is the pressure of the gas, p_0 is the pressure of a saturated gas under similar conditions, and a is the number of the adsorbed gas molecules. K_1 , K_2 , and K_3 are constants; K_3 is usually close to unity. De Boer and Zwikker pointed out that a crystal surface with a checkerboard of positively and negatively charged sites may enhance multilayer polarization.

In 1938, Brunauer, Emmett, and Teller criticized de Boer and Zwikker's theory of the adsorption of nonpolar molecules on ionic lattice surfaces, on the ground that the electrical polarization is too weak to proceed beyond one layer of gas molecules. They then proposed what was to become known as the *BET theory*, in which the ionic lattice surface polarizes only one layer of gaseous molecules, followed by a simple condensation of additional layers as in normal liquids. The BET isotherm is as follows:

$$\frac{p}{v(p_0 - p)} = \frac{1}{v_m c} + \frac{(c - 1)}{v_m c} \frac{p}{p_0} \quad (6.7)$$

where v is the total volume of gas adsorbed at vapor pressure p , v_m is the volume adsorbed in a unimolecular layer, and c is a constant. In a plot of $p/v(p_0 - p)$ against p/p_0 , a straight line results, from which v_m and c may be obtained.

Although Brunauer, Emmett, and Teller severely criticized de Boer and Zwikker's theory for argon adsorption, they also made the following statement: "On the other hand, if the adsorbed gas has a large dipole moment it is possible that many layers may be successively polarized by the mechanism of de Boer and Zwikker. This case has been treated by Bradley (1936)" (Brunauer *et al.*, 1938, p. 310). Water, for example, has such a large dipole moment.

6.3.1.1. Bradley's Theory

Bradley dealt with the adsorption on polar surfaces of gaseous molecules that have a permanent dipole moment. His isotherm resembles that of de Boer and Zwikker:

$$\ln \frac{p_0}{p} = K_2 K_1^a + K_4 \quad (6.8)$$

where p , p_0 , and a have the same meanings as in equation (6.6). K_2 and K_1 are functions of the field of the sorptive polar groups and the dipole moment and polarizability of the polar gas. Under specified conditions, K_1 , K_2 , and K_4 are constant.

6.3.1.2. Hoover and Mellon's Application of "Polarization Theory" to Adsorption of Water Vapor by Polymers

Studies of water adsorption on proteins and polypeptides led Mellon, Korn, and Hoover (1948; Hoover and Mellon, 1950) to the belief that water adsorbs in multilayers and that the active adsorption sites include free amino and peptide groups. In addition they observed that uptake of water at high relative humidity depends on the prior adsorption of water on these active sites. They found that water adsorption on a wide variety of high-molecular-weight polymers can often be fitted by Bradley's adsorption

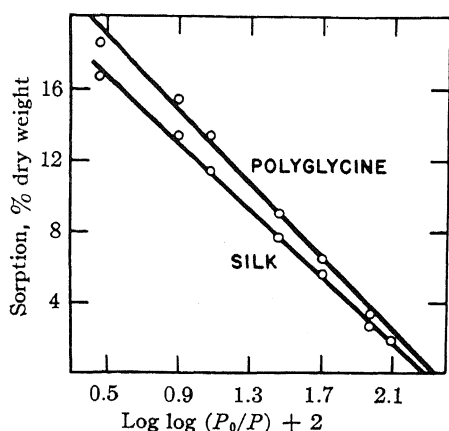


FIGURE 6.12. Water adsorption on silk and on polyglycine plotted according to the Bradley isotherm. [From Hoover and Mellon (1950), by permission of *Journal of the American Chemical Society*.]

isotherm [equation (6.8)]. Figure 6.12, from Hoover and Mellon (1950), demonstrates water adsorption on silk and on polyglycine in agreement with theory. The amount of water adsorbed by amorphous polyglycine ester far exceeded that provided for by the end amino and ester groups and must be due to adsorption on the peptide keto and imino groups.

6.3.1.3. *Jordan-Lloyd's Theory of the Sites of Protein Hydration*

Jordan-Lloyd and co-workers (Jordan-Lloyd and Phillips, 1933; Jordan-Lloyd and Shore, 1938) suggested that water interacting with proteins is not uniformly distributed over the protein surfaces but is localized to special groups (that are carried by both polar side chains and the backbone). This broad view, now almost universally accepted, was clearly established by Benson, Ellis, and Zwanzig (1950; Benson and Ellis, 1948, 1950) when they showed that the uptake of N_2 and O_2 on solid proteins depended only on the state of division of the solids and was indifferent to the nature of the protein, while uptake of H_2O depended only on the nature of the proteins and not on the state of division of the protein solids.

6.3.1.4. *Pauling's Polar Side Chain Theory of Protein Hydration*

In 1944 Bull published his careful work on water adsorption on a variety of pure proteins including nylon, using essentially the same technique employed in the meticulous work of J. R. Katz (1919). Bull's work was often cited to test one or another protein hydration theory. Pauling (1945) plotted Bull's data according to the BET isotherm [equation (6.7)], deriving v_m values which he compared with the number of polar side chains in each protein. The data agree with his theory that at low vapor pressure each polar side chain adsorbs one water molecule. Pauling rejected the backbone amide groups as seats of hydration because nylon, which resembles a polypeptide chain but has no polar side chains, takes up very little water.

Bull and Breese (1968a,b) made a similar estimate of the number of polar side chains but compared their theoretical values with the total water uptake at 92% relative humidity. Their theory differed from Pauling's in assuming that each polar side chain coordinates six water molecules and that the amide groups of asparagine and glutamic residues, by forming H bonds with nearby polar groups, reduce hydration. While their theory gave excellent agreement with the experimental data (Table 6.3), some notable exceptions were observed. In particular, collagen adsorbed much more water than predicted. In addition, Bull and Breese did not consider the data on gelatin. The work of Fisher on hydration of proteins in solution (1965) also considered polar side chains as the seats of hydration, providing further support to Pauling's original concept that protein hydration is due to polar side chains, with little or no involvement from the peptide imino and carbonyl groups.

6.3.1.5. *Sponsler, Bath, and Ellis's Theory of Hydration Involving Backbone Sites*

Sponsler, Bath, and Ellis (1940) noted that certain cells in dormancy contain only some 30–35% water instead of the 80% found in active cells. From X-ray diffraction

TABLE 6.3. Moles of Water Bound per Gram of Protein at a Relative Humidity of 0.92 and 25°C^a

Protein	Moles of H ₂ O × 10 ³ /g protein	
	Observed	Calculated ^b
Lysozyme	13.8	14.1
Bovine serum albumin	17.7	(22.3) ^c
Bovine hemoglobin	20.4	21.2
Bovine ribonuclease	19.7	19.4
Horse heart cytochrome <i>c</i>	21.6	22.0
Egg albumin	16.4	16.1
β-Lactoglobulin	17.8	16.8
Sperm whale myoglobin	23.4	23.1
Bovine insulin	13.1	14.6
α-Chymotrypsinogen A	16.1	15.2

^aFrom Bull and Breese (1968b), by permission of *Archives of Biochemistry and Biophysics*.

^bCalculated by assuming each polar side chain coordinates six water molecules.

^cBovine serum albumin not included in the theoretical formulation.

and infrared adsorption data they showed that polar side chains of proteins as well as the backbone amide groups bind water. In gelatin gel containing 33% water, they found that about 58% of the water molecules adsorbed are on the backbone and 42% of the water molecules are on the side chains. Their conclusions supported Jordan-Lloyd's theory. Indeed, as years went by, the concept that the backbone is a significant seat of protein hydration gained additional powerful support from the fact that synthetic esterified polypeptides with no polar side chains and few polar end groups adsorb a considerable amount of water. These include polyglycine, polyglycine-D, L-alanine, and synthetic polyamides that adsorb water only if they exist in an amorphous form. Similar polymers in a crystalline form, as in the case of nylon, adsorb little water (Mellon *et al.*, 1948; McLaren and Katchman in McLaren and Rowen, 1951; Dole and Faller, 1950). Dole and Faller showed that polyvinylpyrrolidone (PVP), which has neither terminal polar groups nor H-donating groups on its N atoms, nevertheless has extensive water uptake. The only H-bonding groups in this case are the backbone carbonyl groups. The water-PVP interaction will be discussed again in Section 6.3.4.3b.

6.3.1.6. Resolution of a Paradox

Readers of the preceding section may be puzzled by the apparent contradiction of evidence in support of two diametrically opposed theories. In 1972 it occurred to me that workers in these two groups came from different kinds of laboratories. Those supporting the absence of participation of the backbone came largely from chemistry and biochemistry laboratories; those supporting the backbone participation theory came largely from

industrial laboratories. The former, preferring purity and better-defined characteristics, studied largely native globular proteins, while the latter dealt primarily with fibrous proteins and fibrous polymers. The paradox is thus resolved. In the native globular form, in which the backbone amide groups are mostly locked in α -helical and other H bonds, proteins hydrate only on polar side chains, which are directed outward. In fibrous proteins, on the other hand, a substantial portion of the backbone NHCO groups may be directly exposed to the external environment and are thus able to adsorb water (Ling, 1972a,b).

6.3.2. The Polarized Multilayer Theory of Cell Water

Although the concept that all or part of the cell water exists in a bound form had been around for many years (see Section 2.5.1.2), Kamnev (1938) and Troshin (1951a,b) first clearly considered cell water to be physically different from normal liquid water and believed this to be the cause of the relatively low concentrations of sugars maintained in many normal resting cells. The AI hypothesis also considered a difference in the free energy of solute distribution between water in living cells and in the surrounding aqueous medium to be the cause of solute exclusions (Ling, 1962, Chapter 12). None of these earlier theories, however, offered a molecular mechanism for either the altered state of water or its reduced solubility for solutes.

In 1965, the AI hypothesis was extended to offer such a molecular mechanism for these phenomena in terms of the polarized multilayer theory of cell water.

Brunauer *et al.* (1938) pointed out that, in the case of molecules with a large permanent dipole moment, many layers can be built up by a propagated polarization from the charged crystal surface lattice. We want to examine more closely the polarization of layers of water molecules, which possess a sizable permanent dipole moment (1.834×10^{18} esu).

6.3.2.1. Water Polarization and Orientation over a Uniformly Charged Surface

Consider a uniformly and positively charged spherical ion. Water molecules surrounding this cation will be oriented in a more or less uniform way with their oxygen end facing the cation and the hydrogen atoms away from it. If we represent each water molecule as a simple dipole, the probable configuration would be like that shown in Fig. 6.13A. One may then consider that each of the water dipoles will in turn polarize another water dipole and that this process may repeat itself a number of steps beyond the second layer.

The force holding each of the water molecules emanates radially from the charged cation through the intervening water molecules. However, the water-to-water interaction is not limited to radial interaction but also includes lateral interaction with other water molecules. Most important are the water molecules belonging to the same layer. Since these water molecules are oriented in the same direction, these lateral dipole-dipole interactions are not cohesive but repulsive. It can be easily shown that this lateral repulsion just about cancels the radial cohesion for water molecules beyond one or at most two layers. Therefore, as is known, the hydration of ions like Na^+ or K^+ does not involve deep layers of water molecules.

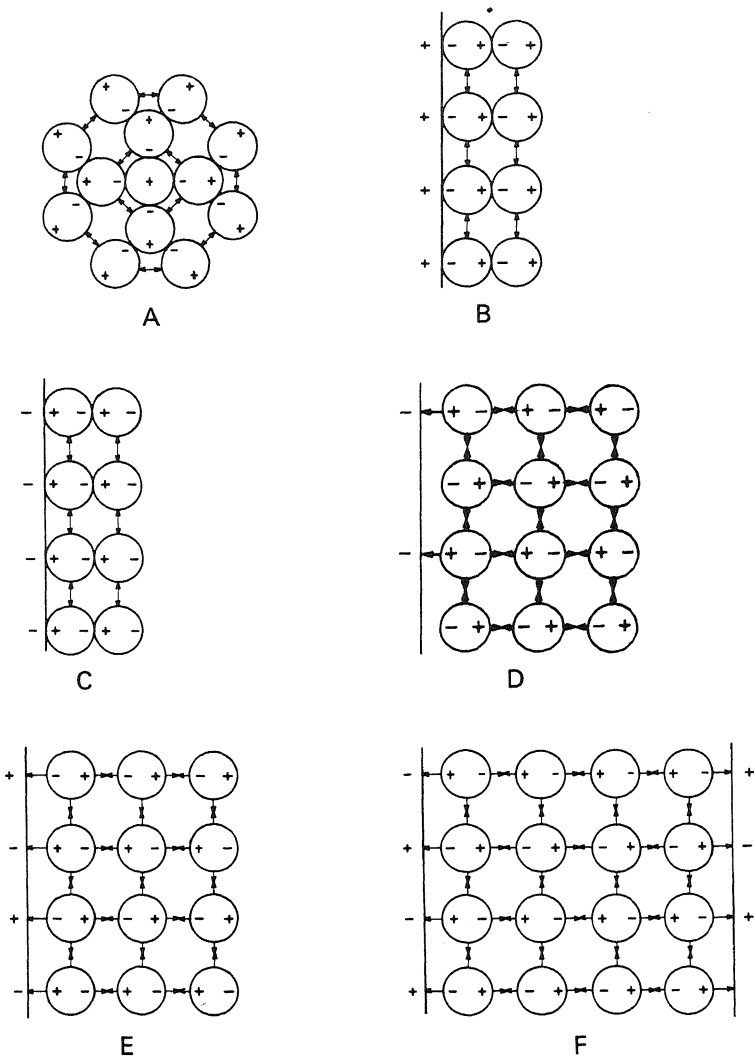


FIGURE 6.13. Effect of charged site distribution on the stability of polarized multilayers of water molecules: \leftrightarrow , repulsion; $\rightarrow\leftarrow$, attraction. Unstable multilayers are produced in surfaces because of lateral repulsion between molecules in the same layer: (A) P-type site, charged positive ion; (B) P-type site, uniformly positive; (C) N-type site, uniformly negative; (D) unipolar surface with charges separated by the distance of two water molecules; (E) NP-type surface with alternating positive and negative sites; (F) two NP-type surfaces placed face to face (greatest stability). [From Ling (1972a), by permission of Wiley-Interscience.]

6.3.2.2. Unipolar Surfaces with Localized Charged Sites and the Critical Importance of the Distance between Them

If the electrical charges of the surface are not uniformly distributed but are localized and separated by distances of the right magnitude, deep layers of water may become

polarized. Consider the cases shown in Figs. 6.13B–D. Here once again there is only one type of charge but each of the electric charges is immobilized and fixed at a specific site. Each site is therefore able to polarize radially a row of water molecules. Whether multiple polarized layers can be built up will depend on how great the distances are between the individual neighboring charged sites of the same polarity. If the similarly charged sites are separated by distances roughly equal to the diameter of one water molecule, then the rows of water molecules polarized by the four neighboring sites would be oriented in the same direction and, as a result, there would be strong lateral repulsion. Polarized multilayers cannot in this case be built up.

On the other hand, if the neighboring charged sites of the same electric polarity are separated by a distance roughly equal to twice the diameter of one water molecule, as in Fig. 6.13D, then the two rows of similarly oriented water molecules would be easily cemented together by another row of oppositely oriented water molecules between them. In this case the lateral interaction will not be disruptive but will enhance the radial cohesiveness. The result would be a mutually reinforcing or cooperative interaction among all the water molecules to create deep layers of polarized water.

6.3.2.3. *Dipole Surface with Localized Sites of Alternating Positive and Negative Signs*

In the case of a unipolar surface of localized sites, the site-to-site distance must be equal to twice the diameter of one water molecule, or a multiple of twice the diameter, in order to polarize water in multilayers. However, if instead of a monopolar surface, where each site bears the same kind of electric charge, one has a checkerboardlike distribution of both negative and positive fixed sites separated by distances equal to the diameter of one water molecule (Fig. 6.13E), then a more stable multilayer polarization of water can occur, since now the cementing rows of water molecules are themselves polarized in a radial direction, further enhancing the stability of the three-dimensional network. Even greater stability can be achieved if such a checkerboard of fixed polar sites is juxtaposed with another similar properly placed surface at a reasonably close distance (Fig. 6.13F).

6.3.2.4. *Matrix of Chains of Localized Charged Sites*

So far we have used surface models for our discussion. It is obvious that arrays of linear chains bearing localized sites would be able to simulate plane surfaces. This is of importance because the basic building blocks of living matter are linear chains.

6.3.2.5. *Nomenclature*

Let us designate by N a negative site; P, a positive site; and O, a neutral or vacant site. We can then designate a surface checkerboard of positive and negative sites with distances between the nearest neighboring sites equal to the diameter of one water molecule as an N-P system. An NP-NP system then stands for a system of two such N-P surfaces standing in juxtaposition. A matrix of chains bearing N-P sites is called an NP-NP-NP system. The meanings of NO, PO, NO-NO, PO-PO, NO-NO-NO, and PO-PO-PO systems are then self-explanatory.

6.3.3. Theory of Solute Exclusion from Water Existing in the State of Polarized Multilayers

6.3.3.1. The q - and ρ -Values

According to Henry's Law:

$$\frac{\text{Concentration of gas in liquid phase}}{\text{Concentration of gas in gaseous phase}} = \text{Constant} \quad (6.9)$$

This relationship is a special case of a more general law called the *distribution law* (or *partition law*), which states that, if a third substance is added to a system of two *immiscible* liquids and if the third substance is soluble in both layers at concentrations C_I and C_{II} , then its distribution in the two phases follows the relation

$$\frac{C_I}{C_{II}} = \text{Constant} \quad (6.10)$$

This law was discussed by Berthelot in 1872 (Berthelot and Jungfleisch, 1872) and later by Nernst (1891). The relationship is readily derived from the equations representing the chemical potential μ_I and μ_{II} of the third substance in the two phases, I and II, where

$$\mu_I = \mu_I^0 + RT \ln a_I \quad (6.11)$$

$$\mu_{II} = \mu_{II}^0 + RT \ln a_{II} \quad (6.12)$$

where μ_I^0 and μ_{II}^0 are the standard chemical potentials of the third substance in the two liquid phases and a_I and a_{II} are their activities. At equilibrium $\mu_I = \mu_{II}$, and

$$\ln \frac{a_I}{a_{II}} = \frac{\mu_{II}^0 - \mu_I^0}{RT} \quad (6.13)$$

$$\frac{a_I}{a_{II}} = \exp \left(\frac{\mu_{II}^0 - \mu_I^0}{RT} \right) \quad (6.14)$$

When the concentration of the third substance is not too high, the activities are approximately equal to the concentrations; hence,

$$\frac{C_I}{C_{II}} = \frac{a_I}{a_{II}} = \exp \left(\frac{\mu_{II}^0 - \mu_I^0}{RT} \right) = \text{Constant} \quad (6.15)$$

If phase II refers to normal liquid water while phase I refers to water existing, for example, in the state of polarized multilayers, then we shall refer to the distribution or partition constant as the *q -value* or *equilibrium distribution coefficient* of the i th substance:

$$q_i = \frac{a_i^i}{a_{II}^i} = \frac{C_i^i}{C_{II}^i} = \exp\left(\frac{\mu_{i(II)}^0 - \mu_{i(I)}^0}{RT}\right) \quad (6.16)$$

where a_i^i , C_i^i , and $\mu_{i(I)}^0$ refer to the activity, concentration, and standard chemical potential of the i th solute in phase I. Under certain conditions, it is not possible to establish clearly that all of the i th substance is dissolved in the liquid phase. Some may be adsorbed or otherwise complexed on a known or unknown component present in either one or both phases. We then employ *an apparent equilibrium distribution coefficient*, or *q -value*. It is clear that $\rho_i \geq q_i$.

6.3.3.2. What Determines the q -Value?

If the two liquid phases are identical in nature, the q -value of any substance between them could only be equal to 1. However, the q -value between water in the state of polarized multilayers and normal liquid, in theory, depends on properties of both the polarized water and the probe molecule. In the present theory, there is no “nonsolvent” water in the sense that such water does not dissolve any solute. Instead, for one probe molecule the q -value may approach zero while for another probe molecule it may be equal to unity (or may even exceed unity). However, as expressed in equation (6.14), what determines the q -value is the difference in the Gibbs standard chemical potential, μ^0 , or partial molar standard free energy. μ^0 in turn consists of two terms, an enthalpy term and an entropy term, one or both of which could be the cause of a q -value below or above unity.

6.3.3.2a. The Enthalpy Mechanism. To move a solute molecule from normal liquid water into polarized water involves (schematically) the following steps:

1. The solute is removed from the normal water, leaving a “hole” (hole 1).
2. A “hole” (hole 2) is then excavated in the polarized water; the water so extracted from hole 2 is inserted into hole 1.
3. The solute is then inserted into hole 2.

The electrical polarization of water molecules in the state of polarized multilayers is more intense than that in normal liquid water. Therefore, more energy must be spent to excavate hole 1 than is recovered in filling hole 2. This extra energy includes that needed to loosen up the molecule-to-molecule polarization among water molecules outside the hole. This enthalpic mechanism generates a lower q -value for larger molecules. However, under certain conditions the probe molecule may fit into the hole in the polarized water with a gain of free energy that may exceed the enthalpy loss described above and the q -value for that probe molecule may approach or exceed unity.

6.3.3.2b. The Entropy Mechanism. Entropy measures the motional freedom. Water molecules in ice are tightly held by neighboring immobilized water molecules but can, nevertheless, sublime at subzero temperature *in vacuo* because the motional freedom gained on vaporization more than compensates for the enthalpy that tends to hold molecules within the ice. Now consider a sugar molecule or a hydrated Na^+ dissolved

in a dilute aqueous solution. They both enjoy a fairly high entropy. Among the different kinds of motions contributing to the entropy (translational, vibrational, and rotational), the rotational entropy is predominant because each of these substances has a large number of rotational axes of symmetry and therefore a total of many rotational motions.

In polarized water the water matrix is less free to accommodate rotation. As a result, a sugar molecule or hydrated Na^+ would have less motional freedom, in particular rotational motional freedom, in this water than in normal liquid water. In other words, to transfer such a solute molecule from normal water to the polarized water would decrease its entropy. This decrease is proportionally greater, the greater the molecular size or complexity of the solute.

6.3.3.2c. Molecular Size of the Probe Molecule and Its q-Value. As shown in equation (6.16), the q -value is determined by the difference in standard chemical potential, or ΔF^0 , where

$$\Delta F^0 = \mu_{\text{II}}^0 - \mu_{\text{I}}^0 = RT \ln q \quad (6.17)$$

Now

$$\Delta F^0 = \Delta H^0 - T\Delta S^0 \quad (6.18)$$

where ΔH^0 and ΔS^0 are the differences in standard enthalpy and entropy, respectively. Both ΔH^0 and $-\Delta S^0$ tend to increase with increase of the size and complexity of the probe molecule, to result in a lower q . On the other hand, for small spherically symmetrical molecules, there is a lesser ΔH^0 and $-\Delta S^0$, and their q -values tend to be close to or equal to unity.

6.3.4. *In Vitro* Experimental Testing of the Polarized Multilayer Theory of Cell Water in Model Systems

6.3.4.1. Theory

In several previous publications, I have cited a number of nonliving systems, such as polished glass or quartz surfaces, that have profound influence upon a variety of physical properties of thin layers of water held between them (Ling, 1970b, 1972a; see also Fig. 9.7), and these are examples of what we call N-P and NP-NP systems or their variants. I shall concentrate here on materials that are present in living cells and that theoretically can exercise a long-range effect on cell water.

If many of the basic properties of living cells can be traced to a different state of water, as suggested in the AI hypothesis, then the water-polarizing component must be present in all living cells, including cells like the human red blood cell which contain no DNA or RNA. And, since the q -value of solutes like Na^+ can be as low as 0.1, nearly all the water in a living cell must be in the altered physical state. With these points in mind, one soon realizes that the polarized multilayer theory of cell water must include

the specific postulation that it is one or more intracellular proteins that bring about the long-range polarization of virtually all the cell water.

In the preceding section I discussed the evidence that proteins existing in a "native" globular form polarize water only on their polar side chains. The studies of Bull and Breese (1968a), for example, have shown that hydration on polar side chains does not have long-range effect on water. Yet the maintenance of these native conformations clearly is essential for a variety of enzyme and other physiological functions. Therefore, only a portion of the intracellular proteins can exist in a form suitable for polarizing virtually all the cell water. This portion of proteins, from the foregoing discussion, must be able to provide a *regular array* of positive or negative sites, or both, at proper distances apart. Now each protein is distinguished from other proteins by a unique sequence of side chains. Therefore it is unlikely that the side chains provide a regular array of negative and positive sites at definite intervals. However, all proteins possess a polypeptide chain, and this chain contains a regular sequence of negatively charged carbonyl groups and positively charged imino groups. They can function to polarize deep layers of water, according to theory, only if the chain exists more or less in an extended conformation, and if the NH and CO groups are directly exposed to the bulk phase water.

6.3.4.2. Criteria for the Existence of Water Polarized in Multilayers

In the past a variety of criteria have been chosen to establish "bound" water. Some of these criteria were discussed earlier in Section 2.6; others will be discussed in more detail in Chapter 9. In our investigations to be discussed here I shall rely primarily on the solvent properties of water. Thus, according to theory, water polarized in multilayers has a reduced solubility for those solutes that are normally present in low concentrations in living cells. Notable among these are Na^+ , sugars, and free amino acids. Solute exclusion as a criterion for "bound" water is by no means a new concept (see Section 2.6), and it is the method of choice here because interpretation of the data is not model-dependent.

The basic method used to detect and measure reduced solvency is that of equilibrium dialysis. A dialysis bag containing a solution of proteins or other polymers was placed into a solution containing the probe solute. Following incubation, over times longer than needed for equilibrium to be established, the probe solute concentrations in the water inside and outside the dialysis bag were determined by chemical, radioisotopic, or other methods and expressed as p -values. To swamp out an electric charge effect, ionic probes were employed at very high concentration (e.g., 1.5 M). To test for polarized water under more physiological ionic strengths, neutral (e.g., sucrose) or effectively neutral (e.g., glycine) molecules were used in the presence of physiological salt concentrations (ca. 0.1 M).

6.3.4.3. Model Systems and Proteins That Reduce the Solubility of Water for Solutes Normally Excluded from Living Cells

6.3.4.3a. *Native Globular Proteins.* Thirteen pure native proteins were dissolved in water at an initial 20% concentration, injected into quarter-inch dialysis tubing, and incubated in 1.5 M Na_2SO_4 solution tagged with radioactive $^{22}\text{Na}^+$. Table 6.4A shows

TABLE 6.4. ρ -Values of Na^+ in Water Containing Native Globular Proteins, Gelatin, Polyvinylpyrrolidone, Polyethylene Oxide, and Methylcellulose^{a,b}

Group	Polymer	Concentration of medium (M)	Number of assays	Water content (%) (mean \pm SE)	ρ -Value (mean \pm SE)
A	Albumin				
	Bovine serum	1.5 a	4	81.9 \pm 0.063	0.973 \pm 0.005
	Egg	1.5 a	4	82.1 \pm 0.058	1.000 \pm 0.016
	Chondroitin sulfate	1.5 a	4	84.2 \pm 0.061	1.009 \pm 0.003
	α -Chymotrypsinogen	1.5 a	4	82.7 \pm 0.089	1.004 \pm 0.009
	Fibrinogen	1.5 a	4	82.8 \pm 0.12	1.004 \pm 0.002
	γ -Globulin				
	Bovine	1.5 a	4	82.0 \pm 0.16	1.004 \pm 0.004
	Human	1.5 a	4	83.5 \pm 0.16	1.016 \pm 0.005
	Hemoglobin	1.5 a	4	73.7 \pm 0.073	0.923 \pm 0.006
	β -Lactoglobulin	1.5 a	4	82.6 \pm 0.029	0.991 \pm 0.005
	Lysozyme	1.5 a	4	82.0 \pm 0.085	1.009 \pm 0.005
	Pepsin	1.5 a	4	83.4 \pm 0.11	1.031 \pm 0.006
	Protamine	1.5 a	4	83.9 \pm 0.10	0.990 \pm 0.020
	Ribonuclease	1.5 a	4	79.9 \pm 0.19	0.984 \pm 0.006
B	Gelatin	0.1 b	4	84.0 \pm 0.78 ^c	0.89 \pm 0.002
		1.5 a	37	57.0 \pm 1.1	0.537 \pm 0.013
C	Polyvinylpyrrolidone (PVP)	1.5 a	8	61.0 \pm 0.30	0.239 \pm 0.005
D	Polyethylene oxide (PEO)	0.75 a	5	81.1 \pm 0.34	0.475 \pm 0.009
		0.5 a	5	89.2 \pm 0.06	0.623 \pm 0.011
		0.1 a	5	91.1 \pm 0.162	0.754 \pm 0.015
E	Methylcellulose (MC)	0.1 b	4	89.3 \pm 0.36	0.588 \pm 0.006
F	PVP	0.2 b	4	89.9 \pm 0.06	0.955 \pm 0.004
	S*	0.2 b	4	87.2 \pm 0.05	0.865 \pm 0.004
	Q	0.5 b	3	83.3 \pm 0.09	0.768 \pm 0.012
	S	0.5 b	3	81.8 \pm 0.07	0.685 \pm 0.007
	Q	1.0 b	3	67.0 \pm 0.26	0.448 \pm 0.012
	S	1.0 b	3	66.6 \pm 0.006	0.294 \pm 0.008
	Q	1.5 b	3	56.3 \pm 0.87	0.313 \pm 0.025
	S	1.5 b	3	55.0 \pm 1.00	0.220 \pm 0.021

^aTemperature was $25 \pm 1^\circ\text{C}$ and test tubes were agitated, except in the experiments of (F), which were carried out at $0 \pm 1^\circ\text{C}$ and in which some test tubes, marked Q, were quiescent and unstirred. S represents sacs shaken in test tubes at 30 excursions/min (each excursion spans 1 in.), except the first set (S*), for which agitation was achieved by to and fro movement of silicone-rubber-coated lead shot within the sacs. The symbols a and b indicate that the media contained initially 1.5 M Na_2SO_4 and 0.5 M sodium citrate, respectively. In (D), PEO (molecular weight 600,000) was dissolved as a 10% (w/w) solution, and the viscous solution was vigorously stirred before being introduced into dialysis tubing. In (F), the quiescent samples contained more water. This higher water content accounts for only a minor part of the difference, as shown by comparison of the sixth and seventh sets of data; even with a larger water content, the ρ -value is lower in the stirred samples (sixth). Na^+ was labeled with $^{22}\text{Na}^+$ and assayed with a gamma counter.

^bFrom Ling *et al.* (1980a) and Ling and Ochsenfeld (1983a), by permission of *Physiological Chemistry and Physics*.

^cTemperature was 37°C .

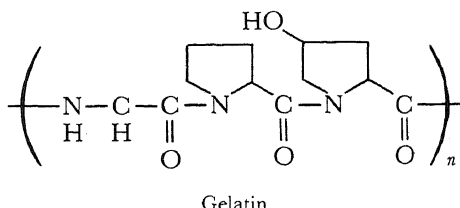
that the ρ -value of labeled Na^+ was close to unity and, with one minor departure in the case of hemoglobin, there was no evidence of exclusion of Na_2SO_4 from the water in the protein solution.

This finding confirms the theoretical prediction that proteins in their native globular conformation, with peptide carbonyl and imino groups locked in α -helical or other peptide-to-peptide H bonds, are unable to influence water solubility to any substantial degree.

6.3.4.3b. Gelatin and Other Polymers; Tribute to Thomas Graham. Gelatin played an important role in what one may call the protoplasmic approach to cell physiology. It was the properties of gelatin that Thomas Graham (1861) saw as representative of a unique state, and he named this state gelatinlike or colloidal. In years since, gelatin has continued to serve as an illuminating model of colloidal chemistry. From J. R. Katz (1919), to Moran (1926), Jordan-Lloyd and Moran (1934), Holleman, Bungenberg de Jong, and Modderman (1934), and Troshin (1951a), gelatin has continued to remind biologists of what Thomas Huxley (1853) once defined as the physical basis of life, protoplasm. Yet for some time now the expectation that colloids represent something unusual has been all but lost, as many have come to believe that colloids are different from crystalloids only because of the large size of the colloidal molecules (i.e., they are macromolecules) and nothing much beyond that (see Ferry, 1948). I now believe that there is indeed something different in gelatin which sets it apart from other macromolecules like the 13 native proteins discussed above. This difference is very much in harmony with the original concepts of protoplasm.

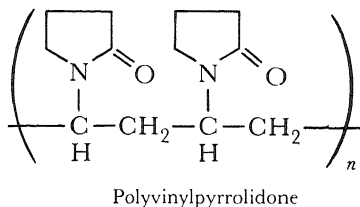
Section B of Table 6.4 shows that gelatin causes a marked reduction of the solubility of Na_2SO_4 (see also Table 4.2).

I suggest that this pronounced difference between gelatin and the 13 native proteins in Table 6.4A is related to the fact that gelatin, which is denatured collagen, has an unusual amino acid composition with the repeating sequence of glycine–proline–hydroxyproline. The bulky side chains, the lack of H at the N atoms of proline and



hydroxyproline, as well as the strong helix breaker, glycine (Chou and Fasman, 1974) make it difficult if not impossible to form α -helical folds (Ramachandran, 1967; Veis, 1964). The chain-to-chain H bonds between the backbone amide groups in native collagen are broken in the process of gelatin preparation. The result is that a considerable portion of the backbone amide groups are directly exposed to the solvent water. It is this direct exposure of the backbone NP-NP-NP system that accounts for the polarization of bulk phase water and the reduced ρ -value observed.

To test this interpretation further we studied the Na_2SO_4 exclusion properties of another polymer, polyvinylpyrrolidone (PVP). Dole and Faller had already found a



Polyvinylpyrrolidone

high water adsorption on this polymer (Section 6.3.1.5). Like proline and hydroxyproline, the pyrrolidone monomer has the same pyrrole ring and no H on the ring N atom. Thus, as far as direct exposure of the backbone to bulk phase water is concerned, PVP should be even more effective than gelatin because all of the PVP monomer cannot form H bonds while only part of the monomer of gelatin cannot form H bonds. On the other hand, PVP exists as a viscous solution and not a gel.

The data shown in Table 6.4C quite clearly establish that PVP is even more effective than gelatin in reducing water solvency for Na_2SO_4 . It is the failure to form intra- and interchain H bonds, and the consequent direct exposure of the backbone NH-CO groups to bulk phase water, that creates a reduction of the solvency of the water in these systems.

The powerful effect of PVP solution in reducing the solvency of water shows first that neither a gel state, as I suggested in 1972 (Ling, 1972a), nor the coacervate state, as suggested by Troshin (Troshin, 1966), is essential for reducing water solvency. In addition, the effectiveness of PVP shows quite clearly that an NP-NP-NP system is not mandatory. PVP is an NO-NO-NO system: There is no positively charged proton group at the position of N, while in normal proteins and peptides the NH groups provide a positively charged site. The data also strongly suggest that the carbonyl oxygens must be of greater importance than the imino groups in water polarization. This idea agrees well with a similar conclusion of Wolfenden (1978) from his vapor phase analysis of amide-water systems.

Table 6.4 presents results of similar studies of two other polymers (Ling *et al.*, 1980a,b): methylcellulose (MC) and polyethylene oxide (PEO). Both are quite effective in reducing the solvency of water for Na_2SO_4 and sodium citrate as well as MgSO_4 , sucrose, and glycine (Ling *et al.*, 1980b).

Several significant conclusions can be drawn from these data:

1. While both gelatin and PVP possess sequences of carbonyl oxygens, MC, polyvinylmethyl ether (PVME), and PEO all contain ether oxygens. Thus both forms of oxygen are able to act on bulk phase water.
2. PEO is outstanding because of its extreme simplicity, being nothing else than a chain of oxygen atoms separated by $-\text{CH}_2-\text{CH}_2-$ groups. It is an NO-NO-NO system that demonstrates the basic requirements for water solvency reduction: the presence of fixed oxygen atoms a suitable distance apart. This is dra-

matically pointed out by the fact that neither polymers with one less CH_2 group between the oxygen atoms (polyformaldehyde) nor polymers with one more CH_2 group (polypropylene oxide) reduce water solvency. In fact neither is water-soluble, and the copolymer of either one with PEO has a solubility proportional to the percentage of PEO (Stone and Stratta, 1967).

3. PVME resembles PEO in having a relatively simple structure and no positively charged proton-donating groups, and is therefore of the NO-NO-NO type. MC is more complex, but presumably it is the ether oxygen in the hexose ring that is the major center of water polarization. However, whether one or more of the hydroxyl groups function as P sites is not clear.

6.3.4.3c. Denatured Globular Proteins. Thus far we have shown that the 13 native globular proteins studied exhibit no effect on the solvency of bulk phase water for Na_2SO_4 . This ineffectiveness agrees with the theory because the polypeptide N and P sites, though present, are unable to act on bulk phase water because of their engagement with other protein peptide groups in α -helical and other macromolecular H bonds. Gelatin, PVP, PEO, PVME, and MC all have significant effects on water solvency. This is attributed to their structural characteristics, which do not allow these molecules to form a significant number of intra- or intermolecular H bonds. What if the native globular proteins are made to lose their α -helical and other chain-to-chain H bonds by chemical denaturation? Denaturation is known to unravel these intramolecular amide-to-amide bonds, referred to as the secondary structure of proteins.

To answer the question, we needed a somewhat different method than those mentioned above: Instead of studying the distribution of Na_2SO_4 and sodium citrate as probe molecules at very high concentrations (in order to swamp out electric charge effect), we employed neutral molecules (e.g., sucrose) or effectively neutral molecules (e.g., glycine at near-neutral pH) in a medium containing only physiological concentrations of salt ions (Ling *et al.*, 1980a).

It is well known that urea at high concentrations unravels the secondary structure of native proteins. Solutions of from 11 to 15 native proteins all showed only a small degree of sucrose exclusion (Fig. 6.14). Inclusion of 10 M urea in the bathing solution decreased the ρ -values for sucrose in these solutions of denatured proteins (Fig. 6.14A,C). Since we found that urea itself has a ρ -value of unity (0.991 ± 0.0085 , $n = 15$) (Ling *et al.*, 1980a), the below-unity ρ -value of solutes in urea-denatured proteins would be the same whether one refers to water alone in the urea-water mixture or to urea-water together as a solvent. Guanidine HCl (7 M) has an entirely similar effect in reducing the ρ -value for sucrose, again confirming theoretical predictions (Ling *et al.*, 1980a).

In recent years, it has become known that, whereas denaturants like urea and guanidine HCl unravel secondary structure, other denaturants may act quite differently. Thus, sodium dodecyl sulfate (SDS) and long-chain aliphatic alcohols like *n*-propanol denature proteins by unravelling their tertiary and quaternary structures, leaving intact or even enhancing their α -helical contents (Herskovitz *et al.*, 1970; Jirgensons, 1972). With this knowledge at hand, the polarized multilayer theory would predict that denaturation by SDS or *n*-propanol would have little or no effect on the ρ -value of sucrose in the bulk phase water containing these denatured proteins. Figure 6.14A,B shows that

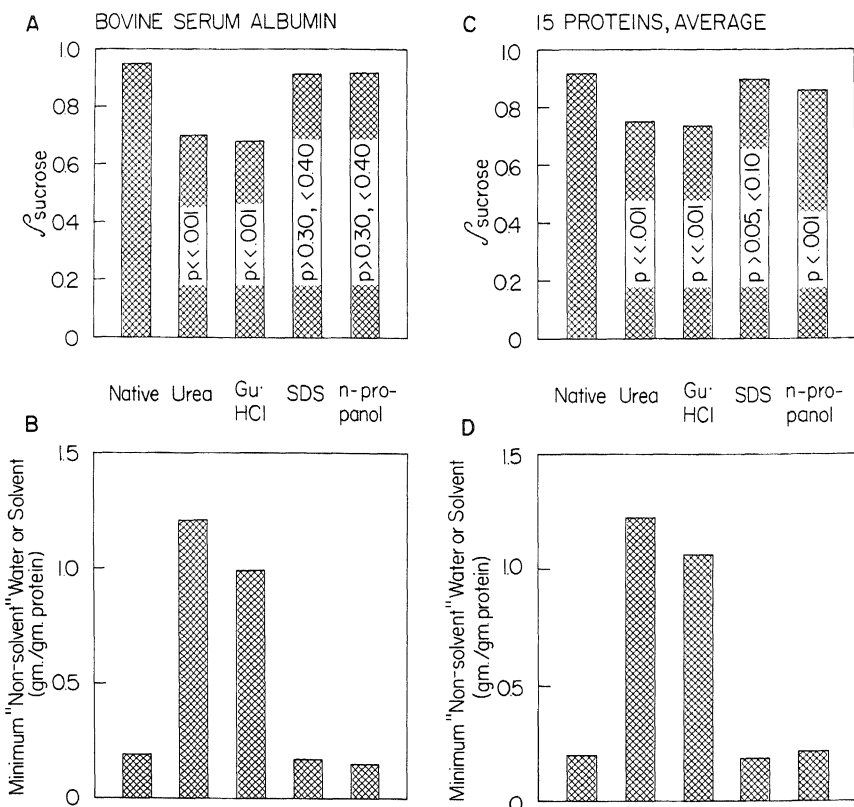


FIGURE 6.14. ρ -Values of sucrose (A and C) and apparent minimum "nonsolvent" water (B and D) of native and denatured proteins. (C) and (D) represent the averages of 15 proteins studied: actin, albumin (bovine), albumin (egg), chondroitin sulfate, α -chymotrypsinogen, edestin, fibrinogen, γ -globulin, hemoglobin, histone, β -lactoglobulin, lysozyme, myosin, trypsin, and trypsin inhibitor. Values for the native and urea-denatured states were determined from all 15 proteins; guanidine HCl values, from proteins 2–11, 13, and 14; and sodium dodecyl sulfate (SDS) and *n*-propanol values, from proteins 2–11. No significant p -value difference was observed in the native protein value whether it was determined from 15, 12, or 10 proteins. Incubating solutions contained Na_2SO_4 (100 mM), glycine (10 mM), sucrose (10 mM), and MgCl_2 (10 mM). In addition, urea (9 M) and guanidine HCl (6 M), SDS (0.1 M), and *n*-propanol (2 M) were present as indicated. Incubation at $25 \pm 1^\circ\text{C}$ lasted from 28 to 96 hr, a sufficient time to establish equilibrium. The test tubes were shaken (30 excursions/min, each excursion measuring % in.). Water contents were assayed by three different methods (see text); sucrose was labeled with ^{14}C or ^3H ; extracts were assayed with a beta scintillation counter. [From Ling *et al.* (1980a), by permission of *Physiological Chemistry and Physics*.]

this prediction was also confirmed. The sucrose exclusion properties remained entirely unchanged when compared to those of the native proteins. In these and other parallel experiments glycine was used as the probe, with essentially similar conclusions.

6.3.4.3d. Comparison of the Degree of Water Polarization by Denatured Proteins and Polymers with That Required to Explain Solute Exclusion by Living Cells. I intro-

duce a convenient parameter, the *apparent minimal nonsolvent water* (AMINOW) (Ling *et al.*, 1980a). Though I emphasize that there is no such thing as "nonsolvent water," nevertheless, for a given probe molecule, this arbitrary device is of help in assessing the quantitative aspect of the problem.

Let us consider a 20% PVP solute with a ρ -value for Na_2SO_4 equal to 0.4; the AMINOW is then $(1 - 0.2) \times (1 - 0.4)/0.2 = 0.8 \times 0.6/0.2 = 2.4$ g/g dry polymer.

From the ρ -value of a solute in the PEO-water system one can calculate the maximum number of water molecules that are under the influence of each oxygen atom. For example, with a ρ -value for Na_2SO_4 equal to 0.4 in a 20% PVP solution, there are at least 12 H_2O molecules per oxygen atom that are apparently "nonsolvent." Using a space-filling model, one can readily show that there is only room for six water molecules in a first layer covering the oxygen atom. Consequently more than one layer of water molecules must be involved. Since it is highly unlikely that the water so influenced has completely lost its solvency for sucrose, the actual number of water molecules affected by the oxygen atom could be considerably higher than 12. Multilayers must therefore be involved.

Is this kind of effect quantitatively sufficient to account for the postulated properties of cell water? Solute exclusion varies considerably from one type of cell to another. For safety we shall choose skeletal muscle as an example since many of its solutes tend to have a low q -value. In frog skeletal muscle cells, the q -value for sucrose is 0.18 (Ling and Kromash, 1967) and for glycine, 0.30 (Neville, 1973); its total protein content is about 20%. If all the intracellular proteins participate, the AMINOW needed would be 2.5 and 3.0 g/g dry protein which are 2-3 times higher than shown for urea-denatured proteins (Fig. 6.14B,D). In fact not all intracellular protein could be in the extended state. The required AMINOW may well be still higher.

There are, however, several reasons why our model systems are not expected to be able to duplicate the situation in a living cell in an exact and quantitative way.

First, proteins in a solution are largely in a random orientation. In theory, the maximum effect on water polarization is achieved when the protein chains are arranged in perfect parallel arrays. It is known that to-and-fro stirring motion in a solution containing linear protein chains tends to line them up in a parallel manner, as witnessed by the phenomenon of flow birefringence. Thus, theoretically, one may expect such to-and-fro stirring to produce a better alignment of the polymer chain. This better alignment in turn will increase the efficiency of water molecule polarization, which will lead to a lower ρ -value for probe molecules.

Table 6.4E shows that experimental studies of the effect of stirring do indeed confirm this expectation. Stirring does decrease the ρ -value for sodium citrate in PVP solutions [for more detailed studies, see Ling *et al.* (1980b)]. It is most interesting that Woessner and Snowden (1973) had earlier showed an entirely parallel effect: Stirring of the bacterial polysaccharide Kelzan® enhances the long-range ordering effect of water in the immediate surroundings of these macromolecules.

Besides the absence of polymer chain alignment, there is another factor that tends to reduce the water-polarizing effect of the denatured proteins. This relates to the total number of NHCO groups in the system. Thus it is well known that in gelatin a considerable number of the peptide bonds reform H bonds with other chains, in what is called *collagen folds* (Veis, 1964). Since we know that urea at the highest concentration

permitted by its solubility cannot denature poly-L-alanine (Doty and Gratzer, 1962), pepsin (Lineweaver and Schwimmer, 1941), CO-hemoglobin (Kawahara *et al.*, 1965), lysozyme (Leonis, 1956), and immunoglobulins (Buckley *et al.*, 1963), one may expect that not all NHCO groups in gelatin are severed from their intra- and interchain H-bonding partners. A third factor is the tendency of denatured proteins to aggregate and clump together, by forming, for example, chain-to-chain hydrophobic bonds and salt linkages, rather than distributing themselves uniformly in the solution.

All three factors can be expected to be substantially less pronounced in the case of a solution of PEO because (1) it possesses no side chains of any kind and therefore cannot undergo chain-to-chain interaction; (2) it possesses no H-donating groups and therefore cannot form strong inter- or intrachain H bonds; and (3) it readily aligns itself in parallel arrays, as witnessed by the remarkable property of a drop of PEO in water to be pulled into an ever-lengthening, ever-thinning thread in a quiescent atmosphere.

As expected, the data shown in Table 6.4D for PEO in an 0.5 M sodium citrate solution yield an AMINOW value of 4.0 g/g dry polymer, a value approaching that envisaged in living cells.

However, in spite of those factors favoring PEO interaction with water, it is inferior to an extended protein chain because PEO represents a NO-NO-NO system, which is theoretically less effective than a protein, an NP-NP-NP system. One can thus expect that properly oriented protein chains at a relatively low concentration may exercise a more powerful effect than PEO. In Chapter 9 I examine in detail the origins of water polarization in cells.

6.4. Summary

In the association-induction hypothesis, the resting state of the living cell is one of high potential energy, poised in a metastable state that can be triggered to perform work. The degree of association between its components gives protoplasm its coherence and its unique properties, and only the assembly of associated cellular components, which include macromolecules, water, ions and other solutes, can be thought of as being in either a high- or a low-energy state. The associated state is not limited to cellular ions, but it is mirrored by properties of ion accumulation and exclusion.

In this regard, the association-induction hypothesis includes three major concepts. The first is that cations may be adsorbed onto fixed carboxyl groups of proteins. In the resting state, these usually have an electron density, or *c*-value, that permits them to prefer K⁺ over Na⁺, and this is the mechanism of the normal net accumulation of K⁺ by most cells. The second concept is that cell water exists in a state of multilayers, polarized by interaction with the alternating electropositive, electronegative regions of extended polypeptide chains of certain proteins. In this state, water tends to exclude solutes, and different solutes are excluded to different degrees depending on entropic and enthalpic factors. As a rule, the degree of exclusion increases with molecular size and complexity of the solute involved. This is the mechanism of the normal exclusion of Na⁺ by most cells. The third major concept is that the transmission of electron-density changes from site to site within proteins permits propagated changes, for example, in their properties of ion adsorption. This is the mechanism that underlies the coherent,

cooperative nature of ion-site interaction and the all-or-none nature of changes in affinities of sites for different counterions. It will be described in detail in the following chapter.

This chapter has elaborated the description of the fixed-charge system begun in Chapter 4, in which counterions are not free in solution but associate closely with the macromolecular fixed ionic sites. Variations in patterns of selectivity of different fixed anionic sites for a series of cations were explained by variations in electron density of the anionic sites and described by their c -values. This was seen to underly variations in the orders of ion selectivity in model systems like ion exchange resins and glass electrodes.

This chapter also elaborated the concept of multilayer polarization of water, and described its establishment in model systems. These, which include polyethylene oxide and polyvinylpyrrolidone, were seen to resemble extended polypeptide chains in their properly spaced electronegative sites, and in their ability to cause exclusion of solutes by water associated with them.

The Association-Induction Hypothesis II

The Inductive Effect and the Control of Physiological Activities

7.1. The Inductive Effect

Thus far in this book the picture of the living cell has been a static one. The key characteristic described has been that of *association* among the three major components of the resting cell: water, protein, and ions. I now examine the second major principle of the association-induction (AI) hypothesis: *induction*. The inductive effect underlies the individuality of living cells and provides the mechanisms that they use for the coordinated, reversible changes which set the living apart from the nonliving.

7.1.1. Early Theories of the Molecular Inductive Effect

At the beginning of the preceding chapter, I described the effects of magnetic and electrical induction in the examples of chains of soft nails and insulators (Fig. 6.1). These are inductive effects occurring in macroscopic systems. In the microscopic world of ions and molecules, the inductive effect plays a most important role. In 1911 Derick calculated the acid dissociation constants of fatty acids on the basis that a substituent group produces a change in the dissociation constant and that the magnitude of this change is specific to each substituent and decreases proportionally with an increasing number of atoms intervening between the acidic functional group and the substituent group. This inductive effect was the core of G. N. Lewis's *induction theory* (Lewis, 1916, 1923). Lewis specifically cited the large difference between the acid dissociation constants of acetic acid, CH_3COOH ($\text{p}K_a = 4.76$) and trichloroacetic acid, Cl_3COOH ($\text{p}K_a < 1$) that occurs as a result of the substitution of three hydrogens by the more electronegative chlorine atoms. This greater electronegativity originates from the possession of a charge of +7 by a chlorine atom stripped of its valence electron while a hydrogen atom has a charge of only +1. Such a substitution of Cl for H causes an

asymmetry in the distribution of electrons in the Cl—C bond, which in turn causes the electrons of the neighboring C—C bond to shift in the direction of the chlorine atom. This inductive effect eventually reaches the oxygen atom, causing a reduction of the electrostatic component of the force holding the dissociable proton. In consequence, the pK_a decreases and acidity increases.

An inductive effect transmitted through the intervening atom is called the *I-effect*. Another type of intramolecular interaction is an electrostatic effect mediated through space. This is called a direct electrostatic effect, or *D-effect*. Because of the difficulty in separating them in practice, the term *inductive effect* is widely used to include both (N. B. Chapman and Shorter, 1972, p. xii). Together, the I- and D-effects are called the *F-effect*, which is the term used to describe the inductive effect in the AI hypothesis (Ling, 1962).

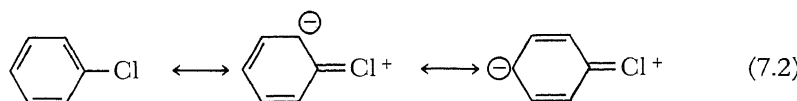
7.1.1.1. Hammett's Equation

Hammett's (1970) description of an inductive effect is given in the following equation:

$$\log k_{ij} - \log k_{oj} = \rho_j \sigma_i \quad (7.1)$$

where k_{ij} is the rate or equilibrium constant of a reaction, j , when the substituent i is present, and k_{oj} is the equilibrium constant for the reaction j in the absence of any substituent i . ρ_j is called the reaction constant. σ_i is an empirical constant specific for the substituent i . Since there are a great deal of experimental data on the ionization of benzoic acid derivatives, Hammett's constant, σ , was based on benzoic acid as the standard, and is limited to meta- and para-substituted aromatic compounds.

Hammett's group constants, σ , are complex in mechanism and include a major inductive (*I*) component and a resonance (*R*) or mesomeric (*M*) component. The inductive component *I* includes the direct electrostatic effect (*D*) and inductive effects on the σ and π bonds (I_σ and I_π , respectively). When a substituent is electron-withdrawing, σ is positive; when it is electron-donating, σ is negative. The resonance effect, *R*, is illustrated by chlorobenzene, which exists as the following resonance hybrids:



The unshared pair of electrons on the chlorine atom is partially delocalized to the ortho and para positions of the ring. This delocalization increases the availability of electrons at the ortho and para positions. Thus the resonance effect is opposite in direction to the inductive effect but also is weaker than the inductive effect.

Another factor that influences the rates and equilibrium constants of reactions is the steric effect. The presence of bulky substituents at the ortho positions near the reaction center impedes its reaction rate. This steric effect may also include other factors, such as the state of hydration in the immediate vicinity of the reaction center.

7.1.1.2. Taft's Equation

While Hammett based his constants on the properties of benzoic acid derivatives, Taft (1953, 1956; Taft and Lewis, 1958) chose the aliphatic acid acetic acid as the standard. Taft proposed that, regardless of any resonance or steric effect, the inductive (I) effect may be represented as

$$I = \rho_I \sigma_I \quad (7.3)$$

where ρ_I depends only on the reaction, and the group constant is

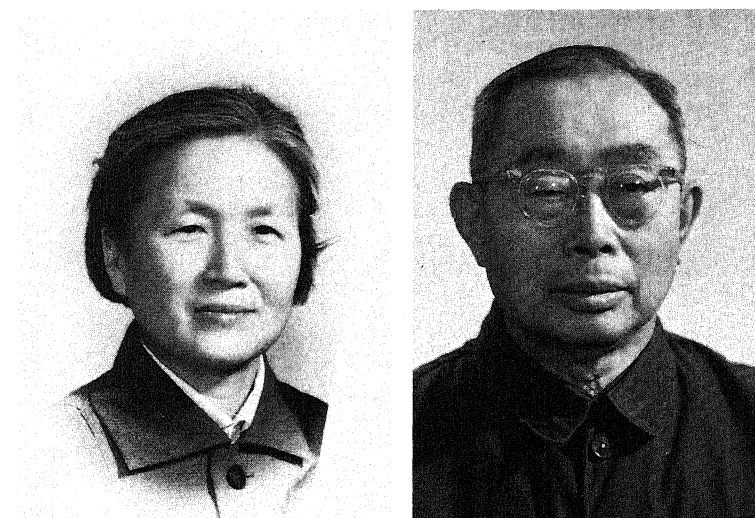
$$\sigma_I = 0.262 \log K/K_0 \quad (7.4)$$

where K_0 is the acid dissociation constant of acetic acid in aqueous solution at 25°C and K is the corresponding constant for the acid XCH_2COOH .

7.1.2. Chiang and Tai's Theory: A Quantitative Relation between Molecular Structures and Chemical Reactivity

In 1963 Ming Chian Chiang and Tsui Chen Tai published a new and much more generalized treatment of the inductive effect. Their publications are virtually unknown in the Western literature and therefore their approach, which is a remarkably powerful one, will be presented here in some detail.

The equations used by Chiang and Tai to calculate equilibrium or rate constants are similar to those used by Hammett [equation (7.1)] and Taft [equation (7.4)]. The main difference lies in the derivation of the group constants. The group constants of Hammett and Taft are empirical ones. The σ value of each substituent is defined and



Ming Chian Chiang and Tsui Chen Tai

determined by known experimental data. One could not, therefore, without new experimental data, obtain σ constants for other substituents. Chiang and Tai approached the inductive effect in a more fundamental manner: *They offered not only a new set of constants called the inductive index but also formulas and methods for calculating the inductive index of any chemical groups from parameters already known, including electronegativity of individual atoms and covalent bond lengths.*

Chiang and Tai's approach differs from those of Hammett and Taft in yet another way. To illustrate we shall use acetic acid and trichloroacetic acid as examples. Instead of calculating the pK_a of trichloroacetic acid on the basis of the σ_I of chlorine atoms, Chiang and Tai actually calculated the inductive index of the CH_3COO^- and CCl_3COO^- groups. Before presenting their equations for calculating the inductive index I shall introduce some of their terms.

We recall that the inductive effect was produced on the target COOH group by manipulating the electrons that constitute the O—H bond. The weaker attraction between the dissociating proton and the oxygen atom to which it is attached is the result of the propagated bond polarization. Thus a basic issue here is that of the polarity of a chemical bond.

Chiang and Tai showed that the polarity of a chemical bond A—B is not merely dependent on the difference in the electronegativities of the two atoms, X_A and X_B , but also depends inversely on their total electronegativity. Thus they defined the *polarity index*, δ , of a chemical bond as

$$\delta_{BA} = \frac{X_B - X_A}{X_A + X_B} \quad (7.5)$$

$$\delta_{AB} = \frac{X_A - X_B}{X_A + X_B} \quad (7.6)$$

The polarity of a bond, reduced to a unit bond length (i.e., δ/r , where r is the bond length), is called the *intensity index*. The loss of alteration of an inductive effect as it propagates along a chain of σ bonds is called the *transmissivity factor*. $1/\alpha$ or ϵ represents the loss of the inductive effect in the transmission through one atom. The ϵ value is usually given as about 0.333.

7.1.2.1. The Inductive Index

The Chiang and Tai treatment of the inductive effect offers the means of calculating the property of any nonconjugating organic compound. To outline their approach I begin with the diagrams shown in Fig. 7.1. A, B, C, D, and E are atoms within a complex molecule. The chemical bond in question is the one between A and B (bond AB). One wishes to describe the effects of the remainder of the molecule on bond AB, and there are three of them: (1) the effect of atom B itself on bond AB, (2) the cumulative inductive effects of all the atoms attached to atom B, and (3) the effects of formal (electric) charges on the bond AB.

The effect of atom B itself on bond AB is represented by i_0 :

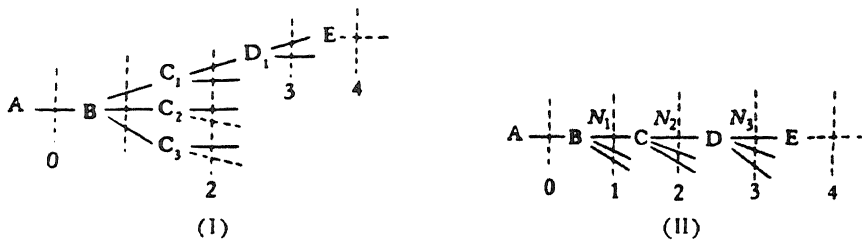


FIGURE 7.1. Diagram of complex molecules used in Chiang and Tai's inductive index calculations. A–E refer to atoms, and N s refer to charges on charged atoms. The numbers refer to bonds, and the chemical bond in question is designated 0. [From Chiang and Tai (1963), by permission of *Scientia Sinica*.]

$$i_0 = \frac{\delta_{BA}}{r_{BA}} \quad (7.7)$$

where δ_{BA} and r_{BA} are the polarity index and bond length of the bond BA.

The total cumulative effects of all atoms (i.e., C, D, E) attached to atom B are represented by i :

$$i = \frac{1}{\alpha} \sum \left(\frac{\delta}{r} \right)_1 + \frac{1}{\alpha^2} \sum \left(\frac{\delta}{r} \right)_2 + \frac{1}{\alpha^3} \sum \left(\frac{\delta}{r} \right)_3 + \dots \quad (7.8)$$

where $1/\alpha = 0.3$, and the ratios δ/r are the intensity indices defined above.

The effects of charges, $\pm N$, on the atoms, applicable to the example on the right side of Fig. 7.1, are represented by i_{\pm} :

$$i_{\pm} = \frac{1}{\alpha} \left(\frac{\pm N_1}{r'_1} \right) + \frac{1}{\alpha^2} \sum \left(\frac{\pm N_2}{r'_2} \right) + \frac{1}{\alpha^3} \sum \left(\frac{\pm N_3}{r'_3} \right) + \dots \quad (7.9)$$

where r'_1, r'_2, \dots are the covalent radii of the charged atoms.

These three effects, i_0 , i , and i_{\pm} , are combined to define the *inductive index*,

$$I = i_0 + i + i_{\pm} \quad (7.10)$$

In Table 7.1, taken from Chiang and Tai (1963), their induction indices, I , are compared with Taft's polar substituent constants, σ^* (Taft, 1956), Hammett's para-substituent constant, σ_p (Jaffé, 1953), and the atomic charges on the hydrogen atom calculated by Del Re (1958). Their correlation is shown in Fig. 7.2. This unusually high degree of accuracy in the predicted values of the chemical properties of a large series of compounds based on the inductive indices led Chiang and Tai to conclude: "The results indicate that by the application of the inductive index for the appropriate groups, some kinds of simple and well-defined quantitative relationships between molecular structure and chemical reactivity can be obtained for any type of non-conjugated compound. . . ."

TABLE 7.1. Comparison of Inductive Index I with Substituent Constants σ^* and σ_p , and Atomic Charges on Hydrogen Atoms in Saturated Compounds^a

Group	$10 \times I$	σ^*	σ_p	Group	$10 \times I$	Atomic charge on hydrogen atom
H	0.0	+0.490	0.0	CCl_3	1.39	+0.131
Me	-0.090	0.000	-0.170	CHCl_2	0.894	+0.105
Et	-0.124	-0.100	-0.151	CH_2F	0.817	+0.060
Pr	-0.136	-0.115	-0.126	CH_2CCl_3	0.423	+0.051
Bu	-0.141	-0.130	-0.161	CH_2Cl	0.402	+0.075
<i>i</i> -Am	-0.145	(-0.13)	-0.225	CH_2OCH_3	0.359	+0.053
<i>i</i> -Bu	-0.149	-0.125	-0.115	CH_2OH	0.285	+0.055
<i>t</i> -BuCH ₂ CH ₂	-0.150	(-0.13)		$\text{CH}_2\text{CCl}_2\text{CH}_3$	0.228	+0.046
<i>s</i> -Pr	-0.157	-0.190	-0.151	$\text{CH}_2\text{CH}_2\text{Cl}$	0.059	+0.043
<i>t</i> -BuCH ₂	-0.161	-0.165		$\text{CH}_2\text{CHClCH}_3$	0.046	+0.043
<i>s</i> -Bu	-0.170	-0.210	-0.123	$\text{CH}_2\text{CH}_2\text{OC}_2\text{H}_5$	0.041	+0.040
Et_2CH	-0.182	-0.225		$\text{CH}_2\text{CCl}(\text{CH}_3)_2$	0.034	+0.042
<i>t</i> -Bu	-0.191	-0.300	-0.191	$\text{CH}_2\text{N}(\text{CH}_3)_2$	0.022	+0.041
(<i>t</i> -Bu)MeCH	-0.194	-0.28		$\text{CH}_2\text{CH}_2\text{OH}$	0.015	+0.041
Me ₂ EtC	-0.203		-0.190	$\text{CH}_2\text{C}(\text{CH}_3)_2\text{OH}$	-0.009	+0.040
ICH ₂	+0.174	+0.85		CH_2NHCH_3	-0.011	+0.047
ClCH ₂ CH ₂	+0.059	+0.385		CH_2NH_2	-0.044	+0.049
C ₆ H ₃ CH ₂ CH ₂ ^b	-0.060	+0.08		$\text{CH}_2\text{CH}_2\text{NH}_2$	-0.107	+0.040
CF ₃ CH ₂ CH ₂ CH ₂	-0.002	+0.12				
C ₆ H ₃ CH ₂ CH ₂ CH ₂	-0.113	+0.02				

^aFrom Chiang and Tai (1963), by permission of *Scientia Sinica*.

^bFor cyclic structures such as the benzene ring, inductive effect is assumed to be transmitted through both sides of the ring. See Branch and Calvin (1941).

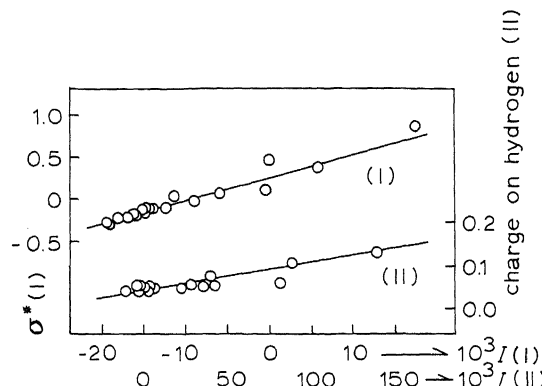
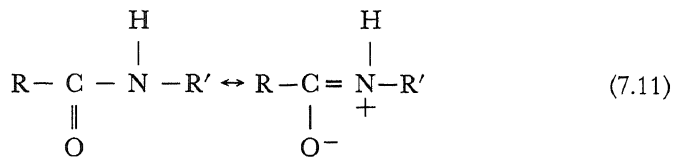


FIGURE 7.2. Relationships between the inductive index I and polar substituent constant σ^* and charge on hydrogen atoms, respectively. Plot of data of Table 7.1. [From Chiang and Tai (1963), by permission of *Scientia Sinica*.]

7.1.2.2. The Transmissivity Factor

Chiang and Tai assumed a transmissivity factor of 0.333. Other calculations yielded somewhat higher values, e.g., 0.48 (Ling, 1964a; Taft, 1953). Estimations also have been made of the transmissivity factor through a unit peptide chain (NHCHCO). The peptide linkages resonate according to the following formula:



The delocalized π electrons of the resonating polypeptide backbones give rise to a high polarizability, so that transmission of an inductive effect can occur over a larger distance in a polypeptide than it can in a saturated hydrocarbon chain of equal length. Edsall and Blanchard (1933) and Zief and Edsall (1937) have shown that the acid dissociation constant pK_a of unionized glycylglycine ($\text{NH}_2\text{CH}_2\text{CONHCH}_2\text{COOH}$) is 3.45, while the pK_a of ionized glycylglycine ($\text{NH}_3^+ \text{CH}_2\text{CONHCH}_2\text{COOH}$) is 3.14. This example suggests that the effect of adding or removing a proton to or from the amino group can be transmitted through three carbons and a peptide linkage to alter significantly the affinity of the carboxyl oxygen for its proton. A similar conclusion can be drawn from the data of Stiasny and Scotti (1930), and those of Ling (1962), shown in Table 7.2, where the pK values of the terminal ionizing groups of glycine, diglycine, and triglycine vary progressively as the number of glycine residues increases. Indeed the pK_a s of the carboxyl group of diglycine and triglycine are significantly different and the pK_b s of the amino group of triglycine and tetraglycine are significantly different. This difference is understandable since there are two atoms (C, O) between the lengthening glycine residues and the dissociating proton in the carboxyl group and only one atom (N) between the lengthening glycine residues, and the dissociating proton in the amino group.

One may raise the question of how much of the observed effect is mediated through the intervening atoms (I-effect) and how much through space (D-effect). The titration

TABLE 7.2. Dissociation Constants of the Carboxyl and Amino Groups of Glycine Peptides^a

	Amino group		Carboxyl group		Water	1 M NaCl
	Water	1 M NaCl	Water	1 M NaCl		
$\text{NH}_2\text{CH}_2\text{COOH}$	9.70	9.60*	9.49	2.42	2.34*	3.02
$\text{NH}_2\text{CH}_2\text{CONHCH}_2\text{COOH}$	8.20	8.13	8.07	3.13	3.06	3.33
$\text{NH}_2(\text{CH}_2\text{CONH})_2\text{CH}_2\text{COOH}$	8.00	7.91	7.83	3.00	3.26	3.39
$\text{NH}_2(\text{CH}_2\text{CONH})_3\text{CH}_2\text{COOH}$	7.75	7.75	7.93	3.05	3.05	3.50
$\text{NH}_2(\text{CH}_2\text{CONH})_4\text{CH}_2\text{COOH}$	7.70	7.70		3.05	3.05	
$\text{NH}_2(\text{CH}_2\text{CONH})_5\text{CH}_2\text{COOH}$	7.60	7.60		3.05	3.05	

^aThe results of titration in water and in 1 M NaCl in aqueous solution are given. The data in water are from Stiasny and Scotti (1930), who give two sets of values. Those values indicated by an asterisk (*) are from Czarnetszky and Schmidt (1931). The results of titration in 1 M NaCl are from Ling (1962).

data of Ling, compiled in 1 M NaCl (Table 7.2), strongly suggest that the observed effect is primarily mediated through the intervening atoms, for otherwise the high salt concentration would have a profound screening effect and remove the differences in the pK values.

The titration data for glycine, diglycine, triglycine, tetraglycine, . . . , shown in Table 7.2, also permitted the calculation of the transmissivity factor through the unit polypeptide chain —NH—CH—CO group, yielding values of 0.15, 0.37, 0.49, and 0.51 in one series and 0.73, 0.72, and 0.67 in another. The overall average is 0.51. This value indicates the degree to which the partial resonance of the polypeptide chain endows it with a propensity to transmit an inductive effect. According to the AI hypothesis, this is one major attribute of the polypeptide chain that serves as the basis for physiological coherence at the molecular level.

7.1.3. Functional Groups Affected by the Inductive Effect

The most remarkable aspect of Chiang and Tai's study of the inductive effect is the universality of its application to reaction rates or to equilibrium states of functional groups. Moreover, Chiang and Tai's equations have opened the door to future studies in biology never before possible. Since Sanger's (1952) elucidation of the primary structure of insulin, the molecular structure of many proteins has been determined. A unique amino acid sequence does not, however, merely provide a scaffold on which special side chain functional groups can be brought together in a sterically favorable manner for, say, enzymatic activity. Rather, through the operation of the inductive or F-effects, the primary structure creates a unique ensemble having a specific electronic distribution. Thus, in an active site of an enzyme, several functional groups carried on certain side chains are bent or twisted into a spatial relationship that forms a reaction center, but, in addition, the appropriate groups are endowed with the electronic characteristics needed to serve their catalytic function.

This concept was presented (Ling, 1962) at a time when there was no way actually to compute such an electronic profile of a unique amino acid sequence. The work of Chiang and Tai may now make this possible. Theoretically, at least, the properties of the functional groups of a protein can be determined from a computed induction index for the rest of the protein molecule. In practice one needs only to calculate the inductive index of a much smaller segment of the protein molecule in the near vicinity of the functional group. The implication of this concept is that the nature of the near-neighbor amino acid residues controls the properties of a particular side chain functional group. Three kinds of functional groups are discussed here—polypeptide hydrogen bonds, oxidation-reduction of thiols, and acid dissociation sites.

7.1.3.1. Strengths of Hydrogen Bonds

The hydrogen bond concept was proposed by Latimer and Rodebush in 1920. Extensive quantitative studies of H-bonding strength by Tsuboi (1951, 1952) and Mizushima (1954) led to the general conclusion that

the proton donating power of the X—H group is determined by the tendency of the X atom to attract the electron of hydrogen to make the proton bare, and the proton accepting power of the Y atom is determined by the tendency of the atom to attract electrons from the adjacent atoms or groups to increase its effective negative charge. [Mizushima, 1954, p. 32]

In other words, the proton-donating and proton-accepting powers of H-bonding groups are influenced by an inductive effect. Two specific examples of experimental data illustrate this point:

1. Gordy and Stanford (1941) observed that the substitution of a strongly electronegative chlorine atom for a less-electronegative hydrogen atom in diethyl ether reduces the electron-donating power of the oxygen atom. Such an effect parallels that of a substitution of chlorine for hydrogen in acetic acid, mentioned in Section 7.1.1.
2. Reiser (1959) studied the effects of substitution on the dimerization of acetophenone oximes (see inset of Fig. 7.3). Since each acetophenone oxime molecule contains both a proton-accepting group and a proton-donating group, substitution by X at the para position will have opposite effects on these groups. Reiser's study led him to the conclusion that it is primarily the proton-accepting power of the nitrogen atom that determines the affinity between a pair of acetophenone oxime molecules. The stronger the electron-donating power of the X substituent, the stronger are the H bonds formed between the pair. Qualitatively, the data of Reiser, recalculated, show a linear relation between Hammett's σ constant and the free energy of dimer association (Fig. 7.3) (Ling, 1964a).

The findings of Gordy and Stanford (1941) and of Tsuboi (1951, 1952) clearly showed that, as in all other types of functional groups, the inductive effect has a profound influence on the strength of H bonds. According to the AI hypothesis, this inductive effect plays a major role in determining the conformation of a protein. Why then does one protein prefer to have a proponderantly α -helical structure, while another prefers a random-coil conformation?

In the conventional view, the H-bonding strengths of all the polypeptide-to-polypeptide H bonds are essentially the same. The α -helical content of the protein is then determined largely by a balance between factors which prevent the formation of α -helices (such as the presence of proline and hydroxyproline or microscopic electrostatic

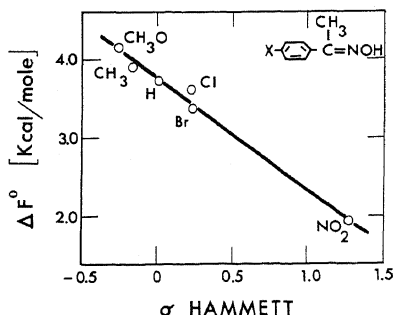


FIGURE 7.3. Linear relation between the calculated standard free energy of dimerization of *p*-substituted acetophenone oximes and Hammett's σ constants. Data recalculated from Reiser (1959), assuming that no higher polymer exists in significant amount except dimers. [From Ling (1964a), by permission of *Biopolymers*.]

repulsion between closely neighboring ionic side chains) and factors which stabilize the H bonds (such as salt linkages, hydrophobic bonds, S—S bonds, and H bonds between side chains). In addition to these factors, I suggest that the differences in H-bonding strengths of the peptide-to-peptide H bonds also are due to differences in the inductive indices of the nearby side chains (Ling 1964a, 1969a). Two sets of experimental data support this view. First, in spite of the many possible α -helix-stabilizing tertiary bonds, oxidized ribonuclease, at its isoelectric point, remains completely in the random coil conformation (Harrington and Schellman, 1956). Second, poly-L-alanine, solubilized by being sandwiched between equivalent segments of D- and L-glutamic acid, exists in water entirely in the α -helical form. Indeed so strong are its α -helical H bonds that it does not denature in 10 M urea or 4 M guanidine HCl. Yet, poly-L-alanine possesses such short side chains that they cannot form any helix-stabilizing tertiary bonds (Doty and Gratzer, 1962). Ling (1964a, 1969a) suggested that the unusual helical stability of poly-L-alanine is due to the strong electron-donating power of the alanine side chains, which are simply CH₃ groups. However, like acetophenone oximes, each peptide chain contains a proton-donating group (NH) and a proton-accepting group (CO)



Since the side chain is centrally placed between each pair of these groups, the electron-donating or -accepting effect of the side chain will have the opposite effect on each. In a homopolar polyamino acid like poly-L-alanine, one may argue that these effects will annul each other, leaving the H bond strength indifferent to the inductive index of the side chain. Since this is not the case, these groups must have different properties, so that they are affected differently by the inductive effect exerted by the same side chain. Indeed there is evidence pointing in this direction. First, poly-L-alanine, which forms very strong helical bonds, differs from, say, the non-helix-forming oxidized ribonuclease only in the nature of its side chains. The side chains of poly-L-alanine are the strongly electron-donating methyl groups. These data suggest that the peptide CO group must be more susceptible to the electron-donating effect, and that the enhancement of its proton-accepting strength is greater than the weakening of the electron-donating strength of the NH group. Expressed in terms of Hammett's or Taft's equations, the CO has a higher ρ_j of one sign and the NH group has lower ρ_j of the opposite sign.

A second example of this differentiated effect is seen in Cannon's (1955) investigation of the interactions of CONH groups with H-bonding substances. He studied the infrared spectrum of *N*-ethylacetamide in a non-hydrogen-bonding solvent CCl₄, to which various other substances were added. He found that whereas the C=O bond is very polar the NH bond is not. Mizushima *et al.* (1958) did parallel infrared studies and reached a similar conclusion: The amide C=O group is a strong proton acceptor whereas the NH group is a relatively weak proton donor. Wolfenden's (1978) results, as well as our own findings, described in Section 6.3.4.3, add further evidence for the

view that in the C=O, NH pair it is the C=O group that plays the decisive role. The enhancement of helical strength by strongly electron-donating CH₃ groups in poly-L-alanine can then be explained. However, the unusually strong α -helical H bonds in poly-L-alanine have additional significance.

Most native proteins contain significant portions of their polypeptide in the α -helical conformation when in an aqueous solution containing some 55 M H₂O, but they become denatured when in the presence of 10 M urea or 4 M guanidine HCl. This suggests that the urea-polypeptide amide bonds are stronger than either the polypeptide-H₂O or polypeptide-polypeptide amide bonds. The fact that 10 M urea fails to disrupt the α -helical structure of poly-L-alanine suggests that the strongly electron-donating effect of the side chain methyl group enhances primarily the proton-accepting power of the CO groups; as a result the polypeptide CO group shifts its affinity from one preferring urea (or water) to one preferring a polypeptide amide group.

7.1.3.2. Oxidation-Reduction Potentials and Chemical Reactivities

Proteins are assortments of the same fundamental amino acids. However, the chemical reactivities of the side chain functional groups of individual amino acids vary greatly. This is illustrated by the SH (thiol) group of cysteinyl residues (Hellerman *et al.*, 1943; Guzman-Barron, 1951). Some thiols in a protein molecule readily react with a certain oxidizing reagent, while others do not. Yet after denaturation with urea, all SH groups seem to become reactive to the same oxidizing agent, and a similar effect occurs in the oxidation of tyrosine and tryptophane groups (Anson, 1941-1942). The prevailing interpretation of this type of phenomenon is that unreactive groups are sterically blocked, so that the reagent cannot reach the reactive groups. In some cases this mechanism is not the only factor involved; for example, urea not only can activate functional groups in proteins, it can activate simple (monomeric) amino acids like tryptophane (Anson, 1941-1942) and cysteine (Benesch *et al.*, 1954; Ling *et al.*, 1964). In these cases, the thiol groups could not have been buried or masked.

A similar steric interpretation of the nonreactivity of functional groups is often used to explain the unusual reactivity of the four heme groups of hemoglobin with oxygen. The stronger reactivity of the second heme than of the first is attributed to the burial of the former group in a sterically inaccessible "crevice" of the hemoglobin molecule; reaction of the more superficially placed first heme group with oxygen opens up the crevice. This interpretation was disproved when Perutz and his group (Muirhead *et al.*, 1967; Perutz *et al.*, 1968) elucidated the steric structure of native hemoglobin crystals, in which it is obvious that the four heme groups are all on the surface of the molecule. These kinds of observations support the nonsteric interpretations of the different reactivities of the SH and other functional groups of proteins (Ling, 1962).

Chemical reactions are electronic transactions. Thus Ingold (1953) classified all reagents as electrophilic or nucleophilic. Not every nucleophilic reagent will react with every electrophilic reagent, and the determining factors in the occurrence of a reaction are the electron-donating and the electron-accepting tendencies of the participating functional groups. These are measured by the oxidation-reduction potential, ϵ^0 . Experimentally it is well known that electron-donating groups reduce the potential and electron-withdrawing groups increase it (Branch and Calvin, 1941; Ling, 1962, p. 135).

TABLE 7.3. Oxidation-Reduction Potentials (ϵ^0) of Various Substituted Compounds^{a,b}

Substituted group	Quinones, 25°C	Indophenols, 30°C
Nitro		
Chloro	712 (Chloroquinone)	663 (<i>o</i> -Chloro phenol indophenol)
Bromo	715 (Bromoquinone)	659 (<i>o</i> -Bromo phenol indophenol)
Hydrogen	699 (Benzooquinone)	649 (Phenol indophenol)
Methyl	645 (Toluquinone)	616 (<i>o</i> -Cresol indophenol)
Ethyl		
Isopropyl		
<i>t</i> -Butyl		
Isopro-methyl	588 (Thymoquinone)	592 (Thymol indophenol)
Substituted group	Aldehydes and ketones, 25°C	
Nitro		152 (<i>m</i> -Nitroacetophenone)
Chloro	277 (Trichloroacetaldehyde)	
Bromo		129 (<i>p</i> -Bromoacetophenone)
Hydrogen	257, 270 (Formaldehyde)	118 (Acetophenone)
Methyl	226 (Acetaldehyde)	115 (<i>p</i> -Methylacetophenone)
Ethyl		110 (Diethyl ketone)
Isopropyl	220 (Isobutylaldehyde)	100 (Diisopropyl ketone)
<i>t</i> -Butyl	211 (Trimethylacetaldehyde)	
Isopro-methyl		

^aThe table illustrates the consistent effect of various substituent groups in modifying oxidation-reduction potentials. There is a difference in the sign of ϵ^0 used by European physical chemists and biologists in America. We follow the biological convention, giving a more positive value to a better oxidant and a more negative value to a better reductant. All values in millivolts.

^bFrom Ling (1962).

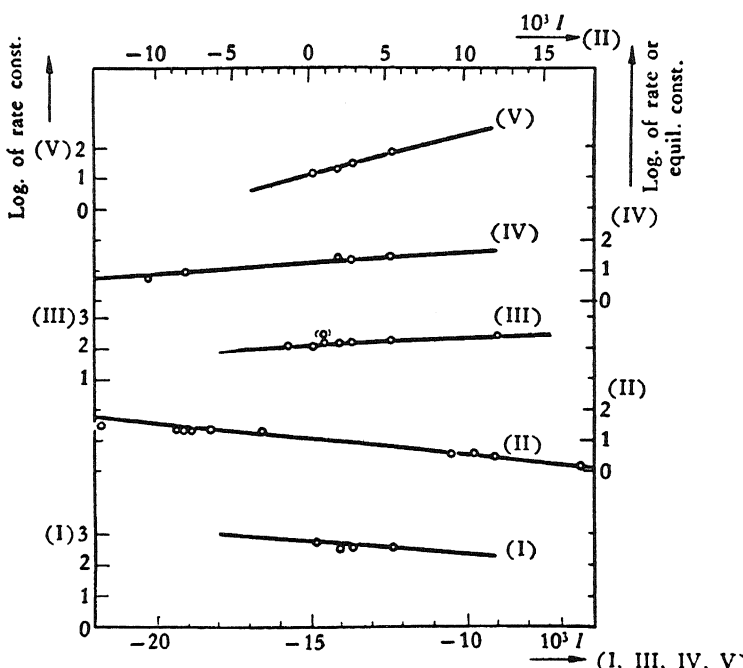


FIGURE 7.4. Chemical reactivities of acetals and ethers and of thiols and sulfides. [From Chiang and Tai (1963), by permission of *Scientia Sinica*.]

Table 7.3 shows specific examples of the effect of substituted groups on the ϵ^0 of quinones, indophenols, aliphatic aldehydes, and ketones. Figure 7.4, taken from Chiang and Tai (1963), shows a plot of the chemical reactivities of acetals, ethers, thiols, and sulfides as a function of their inductive indices, I .

7.1.3.3. Acid Dissociation Constants

The systematic variation of acid dissociation constants of organic acids set the stage for the development of the inductive theory (Derick, 1911; Lewis, 1923). Figure 7.5 shows how the pK_a s of substituted *n*-propionic acid (XCH_2CH_2COOH) and substi-

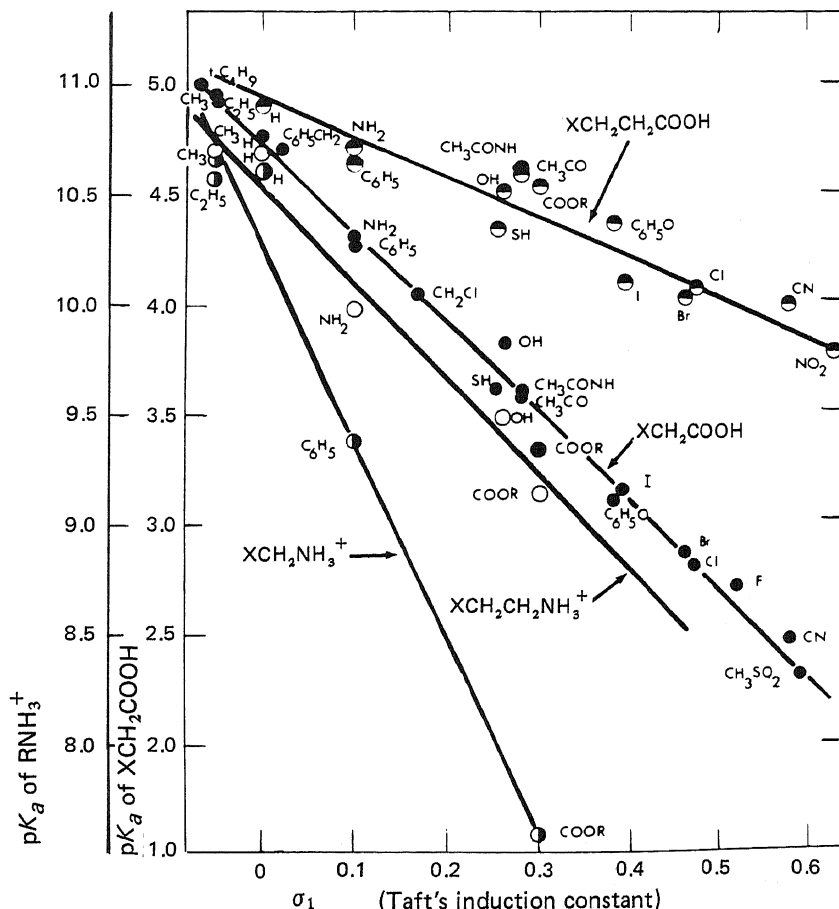


FIGURE 7.5. Relation between Taft's induction constant σ_1 and the acid dissociation constants pK_a of α -substituted acetic acid (XCH_2COOH), β -substituted propionic acid (XCH_2CH_2COOH), α -substituted methyl ammonium ion ($XCH_2NH_3^+$), and β -substituted ethylammonium ion ($XCH_2CH_2NH_3^+$). In these formulas, X represents the substituent, which varies. The abscissa represents the σ_1 of each substituent indicated in the graph. The ordinate gives the acid dissociation constant of that particular substituted compound as it is indicated on the graph. [From Ling (1964b), by permission of *Texas Reports on Biology and Medicine*.]

TABLE 7.4. Theoretically Calculated Inductive Indices and Experimentally Determined Acid Dissociation Constants of Organic and Inorganic Acids^a

Compound H-OX	$10^3 I$ for -OX	pKa 25°	Compound H-OX	$10^3 I$ for -OX	pKa 25°	Compound H-OX	$10^3 I$ for -OX	pKa 25°	
H-OCIO ₃	455.4	~ -8(2)	Phosphorus group	H-OPO(OH)-OPO(OH) ₂	305.7	1.0 (18°)	H-OCOCOOH	269.8	1.2
H-OCIO ₂	389.9	~ -3(2)		H-OPO(OH)-OPO ₂ ⁻ (OH)	298.4	1.5 (18°)	H-OCOOH	257.6	3.9; ~3.7(2)
H-OCIO	319.5	2.3; 2.0 (23°)		H-OPO(OH)-OPO ₂ ⁻ -OPO ₂ ⁻ (OH)	297.5	2.3	H-OCHO	245.7	3.8
H-OIO ₂	311.2	0.8		H-OPO(OH) ₂	288.1	2.1	H-OCOCOO-	245.3	4.3
H-OIO(OH) ₄	257.6	1.6		H-OPO(OH)	280.0	2.0	H-OCOCH ₂ CH ₂ SiMe ₃	242.9	4.9
H-OCl	243.2	7.4 (27°); 7.0(2)		H-OAsO(OH) ₂	275.6	2.2	H-OCOMe	242.5	4.7
H-OBr	237.6	8.5; 8.7(2)		H-OPO(Me)(OH)	275.6	2.3(3)	H-OCOCH ₂ SiMe ₃	242.0	5.2
H-OI	225.7	9.7; 11.0(2)		H-OPOH ₂ (O)	270.9	1.0; 2.0(2)	H-OSi(OH) ₃	228.3	9.7 (30°); 10(2)
H-OIO ₂ ⁻ (OH) ₃	192.6	8.3		H-OPO(Me) ₂	263.2	3.1(3)	H-OGe(OH) ₃	228.3	8.5(2)
H-OIO ₃ ⁻² (OH) ₂	127.7	12.4		H-ONO	257.8	3.2 (20°); 3.2 (30°)	H-OOCO-	191.3	10.3
H-OIO ₄ ⁻³ (OH)	62.7	>15	Sulfur group	H-OAsO(Me) ₂	252.4	6.1	H-OSiO-(OH) ₂	162.8	11.7 (30°)
H-OIO ₅ ⁻⁴	-2.3	>15		H-OPO ₂ ⁻ -OPO ₂ ⁻ -OPO ₂ ⁻ (OH)	232.0	6.3			
				H-OPO ₂ ⁻ -OPO ₂ ⁻ (OH)	230.9	6.6			
				H-OPO ₂ ⁻ -OPO ₂ ⁻ -OPO ₃ ⁻²	230.8	8.9			
				H-OPO ₂ ⁻ (OH)	222.6	7.2			
H-OSO ₃ H	367.8	~ -3(2)		H-OPO ₂ ⁻ -OPO ₃ ⁻²	221.7	9.6; 8.4 (18°, 3)	H-OB(OH)	251.9	9.1
H-OSeO ₃ H	332.8	~ -0.5		H-OAs(OH) ₂	220.0	9.4	H-OB(OH) ₂	217.0	9.2
H-OS ₂ O ₂ ⁻	317.9	1.6-1.7		H-OPO ₂ ⁻ (H)	214.5	6.6	H-OAl(OH) ₂	214.0	11.2
H-OSO ₃ ⁻	302.2	1.9; 2.0		H-OAsO ₂ ⁻ (OH)	210.4	7.0	H-OB(OH)-C ₆ H ₃	210.7	9.9
H-OSO(OH)	297.4	1.9; 1.9(2)		H-OAsO ₂ ⁻ (Me)	210.2	7.1(3)			
H-OSeO(OH)	280.3	2.5 (18°)	Boron group	H-ONH ₂	191.1	8.0	H-OB(OH)-CH ₂ C ₆ H ₅	205.2	9.1
H-OSeO ₃ ⁻	267.5	2.0 (30°)		H-OPO ₃ ⁻²	157.1	12.0(2)	H-OB(OH)-CH ₂ CH ₂ C ₆ H ₅	203.2	10.0
H-OTeO(OH)	260.8	2.5		H-OAsO ⁻ (OH)	154.9	13.5	H-OB(OH)-Bu-n	202.0	10.7
H-OTe(OH) ₅	233.1	7.8		H-OAsO ₃ ⁻²	145.2	11.5 (18°)	H-OBO ⁻ (OH)	151.0	12.7 (~20°)
H-OSO ₂ ⁻	228.8	7.0 (18°)		H-OAsO ₂ ⁻	89.8	>15 (32°)	H-OGaO ⁻ (OH)	150.5	10.3 (18°)
H-OSeO ₂ ⁻	231.9	8.0 (18°)					H-OBO ₂ ⁻²	85.1	13.8 (~20°)
H-OTeO ₂ ⁻	195.9	7.8					H-OGaO ₂ ⁻²	83.0	11.7 (18°)
H-OTeO ⁻ (OH) ₄	168.3	10.3							

^aFrom Chiang and Tai (1963), by permission of *Scientia Sinica*.

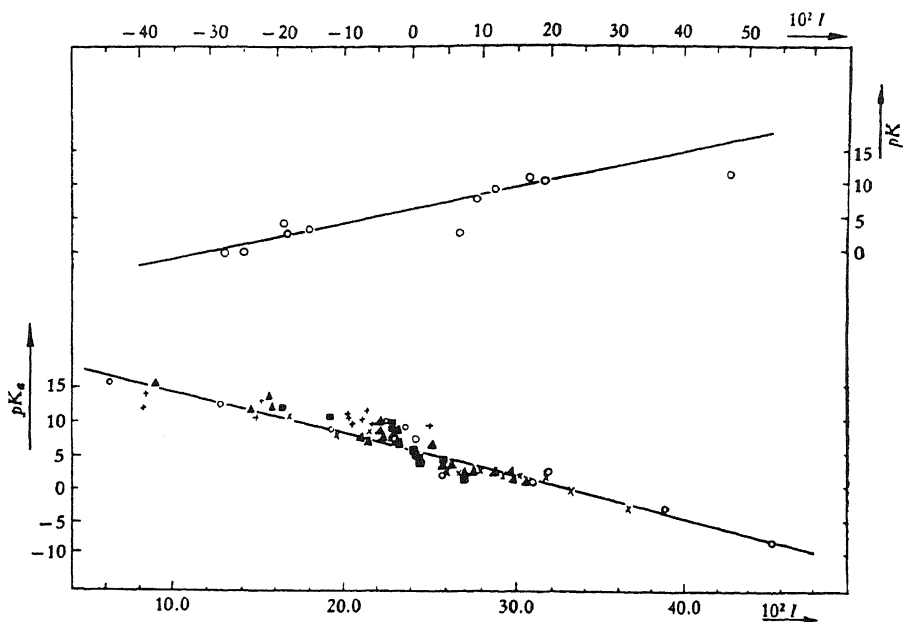


FIGURE 7.6. Relations between inductive index I and dissociation constants pK_a of oxygen acids and metallic hydroxides. Acid dissociation constants were collected by Chiang and Tai from the literature, and are the same as those in Table 7.4. [From Chiang and Tai (1963), by permission of *Scientia Sinica*.]

tuted ethyl ammonium ion ($\text{XCH}_2\text{CH}_2\text{NH}_3^+$) vary with Taft's induction constant,* σ_I . The substituted group X is separated from the H^+ -dissociating group by as many as three saturated carbon atoms. While the inductive effect in these fatty acid derivatives has been well-recognized, Chiang and Tai's data on a much wider variety of acids, reproduced in Table 7.4 and Fig. 7.6, show once again the extraordinary ability of their inductive indices to predict chemical reactivity.

These simple model systems leave no doubt that the pK_a of an acid is determined by the inductive indices of the remainder of the molecule. The pK_a values of the carboxyl groups of aspartic and glutamic acid residues are not the same in different proteins. This is shown in Fig. 7.7, which illustrates the diversity of apparent heats of ionization of H^+ in different proteins at different pHs. The apparent heat of ionization, $\Delta H'$, is defined as

$$\Delta H' = -2.303 RT^2 \left(\frac{\partial \text{pH}}{\partial T} \right)_{\bar{X}} \quad (7.13)$$

where R and T have the usual meanings. $\Delta H'$ is a measurement of the change of the pH of a protein solution with changing temperature where the amount of base or acid added (\bar{X}) remains constant. These data suggest that the sequential order of the amino acids, rather than the fractional amino acid composition of the protein, determines the

* σ_I is related to but not equal to σ^* (Table 7.1) (see Taft and Lewis, 1958).

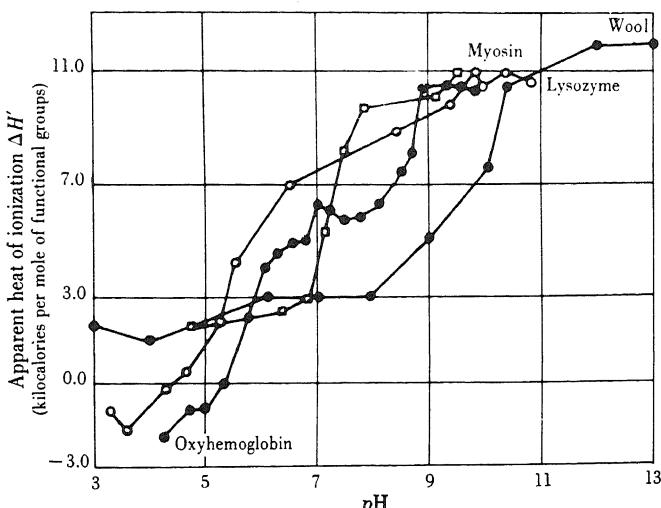


FIGURE 7.7. The apparent heat of ionization $\Delta H'$ of ionizing groups of various proteins plotted against pH. Note the great diversity of the $\Delta H'$ values in functionally different proteins. Data from Mihalyi (1950): myosin (25°–38°C); from Wyman (1939): oxyhemoglobin (25°–37.7°C); from Tanford and Wagner (1954): lysozyme (4°–25°C); from J. Steinhardt *et al.* (1941): wool (0°–25°C). [From Ling (1962).]

pK_a s of all the ionic groups. This in turn contributes to the unique biological characteristics of each protein.

The diversity of pK_a values may originate from a variety of factors: (1) The ionic groups may form salt linkages or H bonds to other parts of the molecule, producing an apparent decrease in the association and hence in pK_a . (2) Inductive effects of near-neighbor side chains may be transmitted through the intervening polypeptide backbone to the acid group. (3) Inductive effects may be exerted by H-bonding molecules that react with the nearby peptide CONH groups as well as other ions and molecules that react with some side chains (e.g., β - and γ -carboxyl groups).

7.2. The Direct F-Effect and the Molecular Mechanisms of Physiological Control

In the preceding chapter, the concept was introduced that the varying electron density of a reactive site on a protein plays a major role in determining its specificity for reactants. In the case of the anionic oxyacid (COO^-) groups, the varying electron density was measured by the c -value. In the case of a cationic group, it was measured by the c' -value. For groups that are not charged, but that vary in their degrees of electronegativity or electropositivity (e.g., H bond sites), the c - and c' -analogues were suggested. In this chapter I demonstrate how the changes of the c -value and c' -value, and their respective analogues, may underlie physiological activities through the operation of the inductive effect (F-effect).

So far, discussion of the inductive effect has been limited to the effects of substitu-

tion of chemical groups held together by covalent bonds. Yet the basic electrostatic nature of the fundamental mechanism suggests that a similar inductive effect may occur as a result of changes of groups that are held together by ionic or H bonds.

7.2.1. Association of Protons and Adsorption of Cations

The dissociation of a proton from a carboxyl group some distance away has a pronounced effect on the pK_a (and hence the *c*-value) of the second carboxyl group of a dicarboxylic acid. This is shown by comparing the pK_{as} of the carboxyl groups of the following two sets of dicarboxylic acids (Branch and Calvin, 1941):

1. $\text{COO}^- \text{CH}_2 \text{CH}_2 \text{COOH}$, 5.5; $\text{COOH} \text{CH}_2 \text{CH}_2 \text{COOH}$, 4.2.
2. $\text{COO}^- \text{CH}(\text{CH}_3) \text{CH}(\text{CH}_3) \text{COOH}$, 5.9; $\text{COOH} \text{CH}(\text{CH}_3) \text{CH}(\text{CH}_3) \text{COOH}$, 3.9.

Since the primary force holding the proton of the acidic group is electrostatic (Kossiakoff and Harker, 1938), another ion, say K^+ , may be expected to have a similar effect on the pK_a of the second acidic group when it adsorbs onto or desorbs from the first carboxyl group. Moreover, a cation in a higher conformation (conformation II or III) (Section 6.2.2.2 and Fig. 6.6) will have a different effect on the pK_a (and hence *c*-value) of the target carboxyl group than one in a low conformation (conformation 0) for the simple reason that the positive charge in a low configuration is further removed from the “receptor” carboxyl group.

7.2.2. Changes in H-Bonding

7.2.2.1. Effect of H Bond Formation on the Electronic Spectra of Phenolic Substances

Burawoy (1959) pointed out that H bonds are essentially electrostatic in character and that formation of a H bond will produce electronic polarization that may influence the whole molecular system by an inductive effect. Burawoy found that *substitution of a H atom by the more electron-repelling CH₃ group induces electronic shifts, resulting in shifts in the positions of the K, B, and R bonds. The formation of a H-bond with ethanol has a similar but even greater effect.*

7.2.2.2. Effect of the Formation of Peptide-Urea H Bonds upon Reactivity of Thiol Groups

It is generally agreed that, in denaturation by urea, urea forms H bonds with the amide groups of the polypeptide chains (Lauffer, 1943; R. B. Simpson and Kauzmann, 1953; Bresler, 1949; O. D. Bonner, 1978). Since 10 M urea can denature most proteins, but 55 M H₂O cannot, urea must be a stronger H-bonding agent than H₂O. It is also known that, in general, amides (e.g., urea) are much stronger proton acceptors than proton donors (Bamford *et al.*, 1956; Cannon, 1955; Mizushima *et al.*, 1958). Thus it is likely that the replacement of peptide-peptide bonds or peptide-H₂O H bonds by peptide-urea H bonds will lead to a net electron gain of the protein molecule. If this assessment is correct, one could expect that simple peptides containing thiol groups on

TABLE 7.5. Effect of 7 M Urea on the Reactivity of Sulfhydryl Groups with Nitroprusside Reagents^{a,b}

	No. of peptide linkages	$\epsilon_{\text{urea}}/\epsilon_{\text{H}_2\text{O}}$	
		Benesch <i>et al.</i>	Ling <i>et al.</i>
Methanethiol	0		1.16
Ethanethiol	0	1.0	
Thioglycolic acid	0	1.0	
Homocysteine	0	1.14	1.35
Cysteine	0	1.43	1.73
L-Cysteinyl-D-valine	1	1.71	
L-Glutamyl-L-cysteine	1	1.78	
L-Cysteinyl-L-valine	1	1.71	
Glutathione	2	2.34	2.83
Phenacylcysteinyl-D-valine	2	2.51	

^aData of Benesch *et al.* (1954) and Ling *et al.* (1964). $\epsilon_{\text{H}_2\text{O}}$ and ϵ_{urea} are, respectively, the molecular extinction coefficients of the thiols when the reaction occurs in water and in 7 M aqueous solutions of urea. A close-to-unity value for the quotient $\epsilon_{\text{urea}}/\epsilon_{\text{H}_2\text{O}}$ for methanethiol and ethanethiol indicates that urea does not directly interfere with the nitroprusside reactions (by, for example, forming H bonds with the sulfhydryl group). The quotient rises above unity for simple compounds with H-bonding groups. It then rather sharply increases with the number of peptide bonds in the molecule.

^bFrom Ling (1964a), by permission of *Biopolymers*.

short side chains would be "unmasked" or made more reactive to thiol reagents such as nitroprusside. In fact, Benesch *et al.* (1954) demonstrated that this is indeed the case (although they interpreted their data differently; see Ling 1964a, p. 109). Table 7.5 reproduces their findings, as well as the data of Ling, Kalis, and Gale (1964). Urea (7 M) has no effect on the reactivity of simple thiols that contain no peptide groups, but there is an increase in reactivity with increase in the number of peptide linkages.

Since the reactivity of SH groups is a measure of the oxidation-reduction potential, these findings show that exchange of weaker electron-donating adsorbents for stronger electron-donating ones on the polypeptide chain produces a decrease of oxidation-reduction potential and that this inductive effect is additive. As mentioned earlier, Anson (1941-1942) found that urea also increases the reactivity of free tyrosine and free tryptophane.

7.3. Modulation and Control of Physiological Activities

The interaction of living systems with molecules and ions leads to characteristic variations in physiological responses; these are known by terms such as *activation* and *inhibition*, *synergism* and *antagonism*. Enzymologists have generally accepted the theory of Michaelis and Menten (1913), who considered the rate of enzyme activity to depend on an enzyme (E)-substrate (S) complex, shown as ES in equation (4.8). Clark's theory of drug action (1926, 1933) is derived from the same principle. Clark related the effect of a drug or pharmacon (A) to the concentration of the drug-receptor (R) complex (RA). In the terminology of Ariëns *et al.* (1954, 1957; Ariëns, 1964), the effect, F_a , of a pharmacon is described by the equations



$$K_a = \frac{k_2}{k_1} \quad (7.15)$$

$$\begin{aligned} F_a &= \alpha [RA] \\ &= \frac{\alpha [R]_0}{(K_a/[A]) + 1} \end{aligned} \quad (7.16)$$

Here $[R]_0$ is the total receptor-site concentration and α is a proportionality constant. Ariëns and co-workers introduced the terms *affinity* for $1/K_a$ and *intrinsic activity* for α .

The theories of Michaelis and Menten for enzyme action and of Clark for drug action describe direct competitive types of interactions but do not describe noncompetitive types of interactions (see Woolley, 1946, and Gaddum, 1957). By assuming changes of K_s [equation (4.9)] and K_a [equation (7.15)], however, investigators in the field of pharmacology gained important insights into basic mechanisms (Clark, 1933; Raventos, 1937; Ariëns *et al.*, 1954, 1957; Ariëns, 1964).

To describe both competitive and noncompetitive types of interactions, we assume that a physiological process may be quantitatively represented by the mole fraction of a particular set of fixed sites occupied by a particular adsorbent. Thus the physiological effect Φ is:

$$\Phi = k X_{\mathfrak{X}}^{f_0} \quad (7.17)$$

Here k is a constant and $X_{\mathfrak{X}}^{f_0}$ is the mole fraction of fixed sites, f_0 , occupied by the specific adsorbent \mathfrak{X} . I emphasize that not all physiological activity may be directly represented by such a simple equation.

Certain physiological processes are related to the concentration rather than the mole fraction of sites adsorbing \mathfrak{X} ; equation (7.17) may then be reformulated as

$$\Phi = k' X_{\mathfrak{X}}^{f_0} [f_0] \quad (7.18)$$

where $[f_0]$ is the total concentration of sites f_0 . In the case of enzymes, Φ represents the rate of enzyme activity and $X_{\mathfrak{X}}^{f_0} [f_0]$ represents the concentration of the enzymatically active sites adsorbing the substrate which forms the activated complex.

In the following sections I present a few typical examples to illustrate the modulation and control of physiological activities by changes in the concentrations of molecules in the environment.

7.3.1. The One-Receptor-Site System as a Model for Competitive Interaction

Let us consider two sites that are inductively linked to each other. One of these sites is a physiologically active site (0) and has a certain c -value, and the other site (I) has a higher c -value. Exchange of adsorbent at site I produces a significant c -value shift at site 0, but not vice versa. Let us also assume that two species of ions, G and J, can react

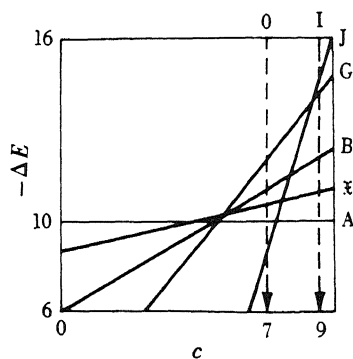
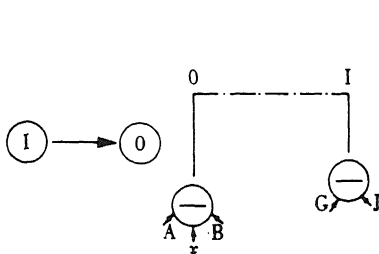
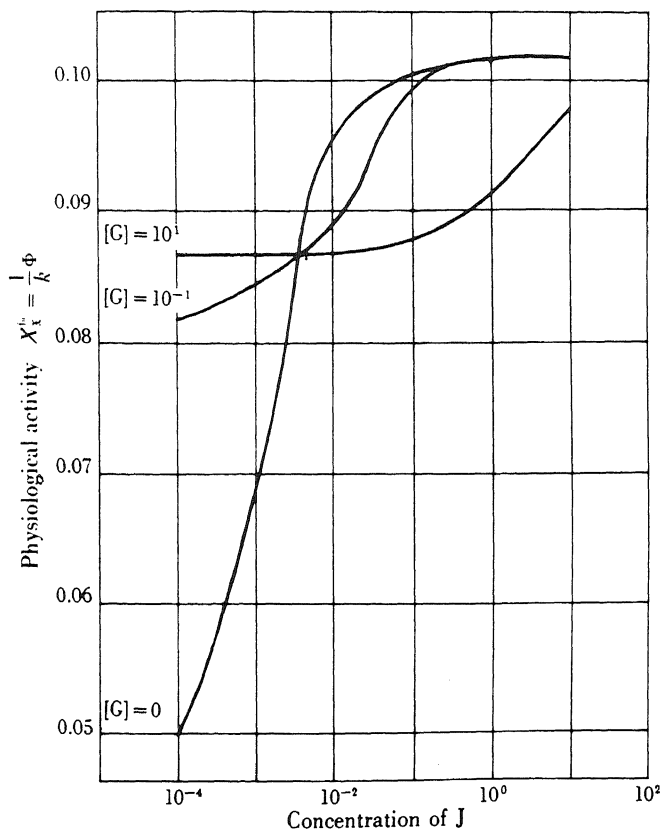


FIGURE 7.8. Variation of physiological activity Φ with variations in the concentrations of cardinal adsorbents J and G in a one-receptor-site system. The physiological activity in question is assumed to be proportional to the mole fraction of sites 0 adsorbing χ . The concentration of A is 0.03 M; that of B, 0.10 M; and that of χ , 0.01 M. [From Ling (1962).]

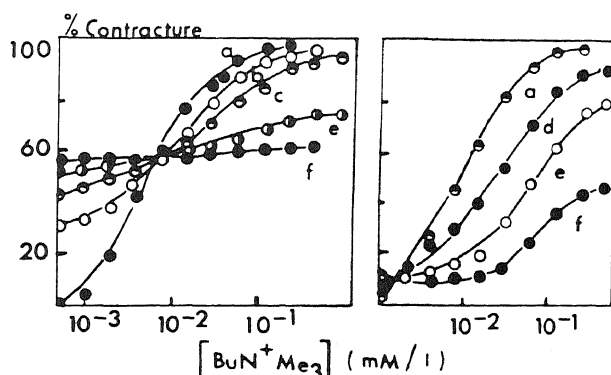


FIGURE 7.9. Dose-activity relation experimentally observed is chosen to demonstrate the resemblance in the pattern of interaction of a physiological manifestation to the theoretical curve in Fig. 7.8. The ordinate represents the percentage of shortening of frog rectus muscle in response to variations of butyltrimethylammonium ion concentration (shown at the abscissa) and of decapyrrolinium (left) or decapiperidinium (right) ion concentration (labels a-f represent increasing concentrations). From van Rossum and Ariëns (1958). [From Ling (1964b), by permission of *Texas Reports on Biology and Medicine*.]

with site I, their relative preference depending on their adsorption energies, ΔE , at a specified c -value. This condition is depicted in the lower right inset of Fig. 7.8. Similarly, site 0, the physiologically active site, may react with the substrate or critical adsorbent \mathfrak{X} , or with A or B. Adsorption of \mathfrak{X} but not of A or B produces the physiological activity. The effects of different concentrations of J and G are the result of their competitive adsorption on site I and their different effects on the charge or c -value at site 0. The inductively altered c -value of site 0 in turn permits \mathfrak{X} to be more or less effective in competition with adsorbents A and B. The physiological activity determined by the presence of \mathfrak{X} at site 0, at different concentrations of J and G, is shown in Fig. 7.8. The details of the computations were given in Ling (1962). Figure 7.9 shows examples from van Rossum and Ariëns (1958) of the shortening of frog rectus muscle in response to variation of butyltrimethylammonium ion in the presence of increasing concentrations of decapyrrolinium or decapiperidinium.

7.3.2. The Two-Receptor-Site System as a Model for Noncompetitive Facilitation and Inhibition

Figure 7.10 shows a two-receptor-site (I and II) system where adsorption of a molecule at one site can influence adsorption at the other receptor site and at the physiologically active site (0). Given the ΔE versus c -value plot for the cationic adsorbent \mathfrak{X} and for the agents A, B, and G, and the ΔE versus c' -value plot for the components J' and A', one can compute the results shown in the main graph in Fig. 7.10 (Ling, 1962). Figure 7.11 shows four examples of enzyme activities as they are influenced by two reagents (Ling, 1964b); the similarity between these and the model in Fig. 7.10 is evident.

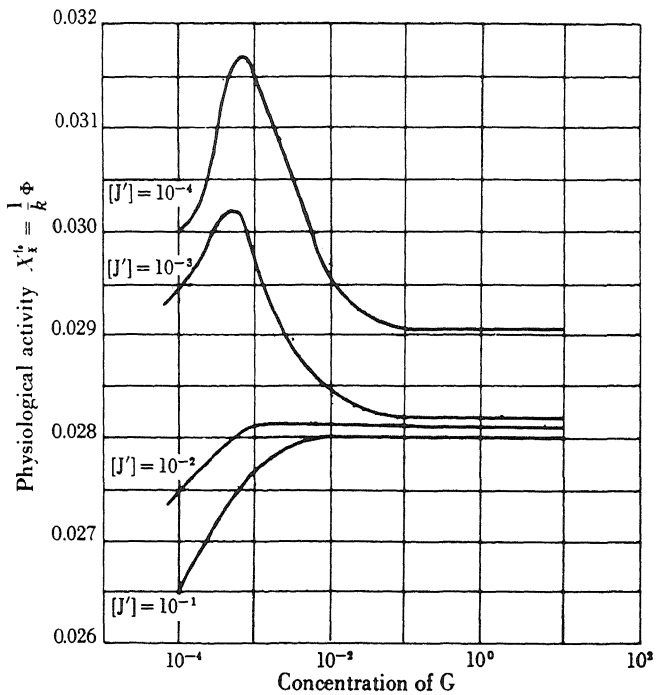


FIGURE 7.10. Variations of physiological activity Φ with variation in the concentration of two cardinal adsorbents J' and G in a two-receptor-site system. Interaction between the two receptor sites is present. The physiological activity is directly proportional to the mole fraction of sites 0 adsorbing \mathfrak{X} (0.01 M). The concentration of A is 0.30 M; that of \mathfrak{X} , 0.01 M; that of B, 0.10 M; and that of A' , 1.00 M. [From Ling (1962).]

7.4. Cooperativity: Molecular Basis for Controlled and Coordinated Physiological Activities

Living beings are distinguished by their internal coherence. Physiologists are well aware of two systems that serve to maintain coherence on a macroscopic level: the nervous system and the endocrine system. Another kind of coherence exists at the micro-

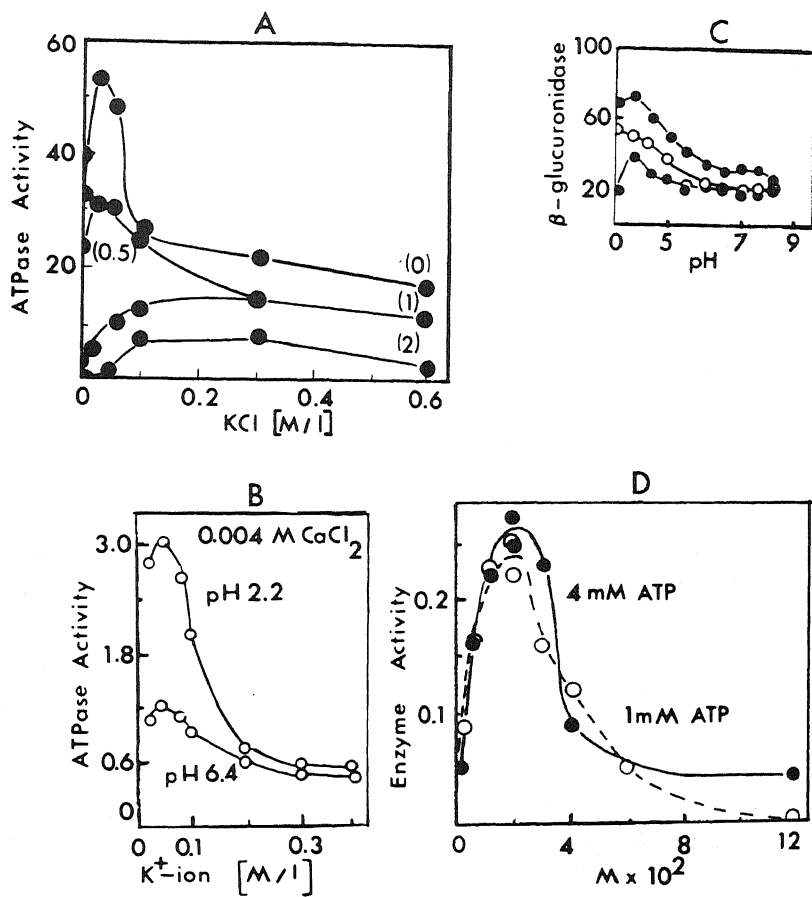


FIGURE 7.11. Dose-activity relations experimentally observed are chosen to demonstrate the resemblance in the pattern of physiological response to the theoretical curves shown in Fig. 7.10. For details of data see source article. [From Ling (1964b), by permission of *Texas Reports on Biology and Medicine*.]

scopic, molecular level. A dramatic example is the detergent-extracted paramecium. This protozoan, although not alive in the usual sense, moves about in water containing Mg²⁺ and ATP, propelling itself in a coordinated motion much like an intact living cell (Naitoh and Kaneko, 1972) (Fig. 7.12).

In Section 7.3 it was suggested that the inductive effect provides the means to modulate and control physiological activities. Two types of experimental data illustrate patterns of interaction very much like those theoretically calculated, one occurring in the modulation of enzymatic activity (Fig. 7.11), the other in the modulation of muscle contraction (Fig. 7.9). In this section I discuss the concept that in instances like that of muscle contraction, not one site but a whole chain of sites is involved. Moreover, sites in the chain, called a *gang*, are linked together by the inductive effect. A general description of the behavior of such a gang of sites is given here, and specific examples are

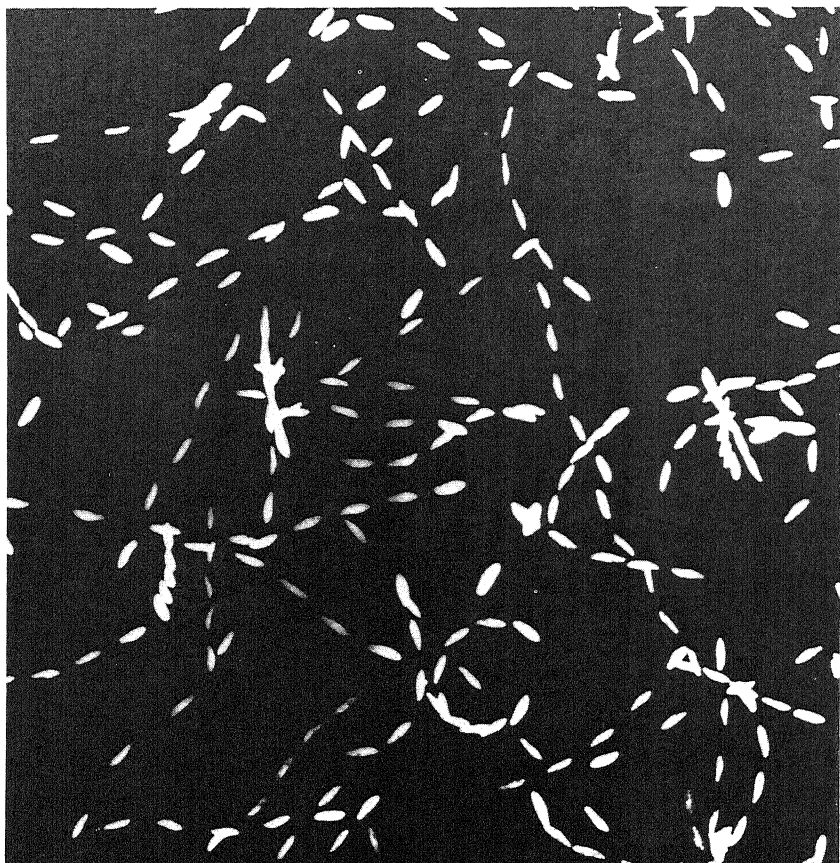


FIGURE 7.12. Photographs of swimming Triton-extracted (dead) paramecium in the presence of Mg^{2+} and ATP (repeated exposures). [From Naitoh and Kaneko (1972), by permission of *Science*.]

described later, as for example in generation of action potentials in Chapter 14, and in muscle contraction in Chapter 16.

7.4.1. The Indirect F-Effect: The Propagated Inductive Effect

A model of a small segment of a protein chain containing a controlling site (cardinal site) is shown in Fig. 7.13.

The backbone peptide groups have two choices of hydrogen-bonding partners, either peptide on an adjacent protein segment (a^+ , a^-) or free hydrogen-bonding molecules such as water (b^+ , b^-) (Here I use + or - to mean electropositive or electronegative, not as valences.) In the absence of an adsorbent at the cardinal site, the c -value analogues of the peptide CO groups, as well as the c' -value analogues of the peptide NH groups, have the low value of, say, 1 (see inset). In this state, the backbone groups prefer to interact with the fixed groups a^+ and a^- (upper diagram). If a cardinal adsorb-

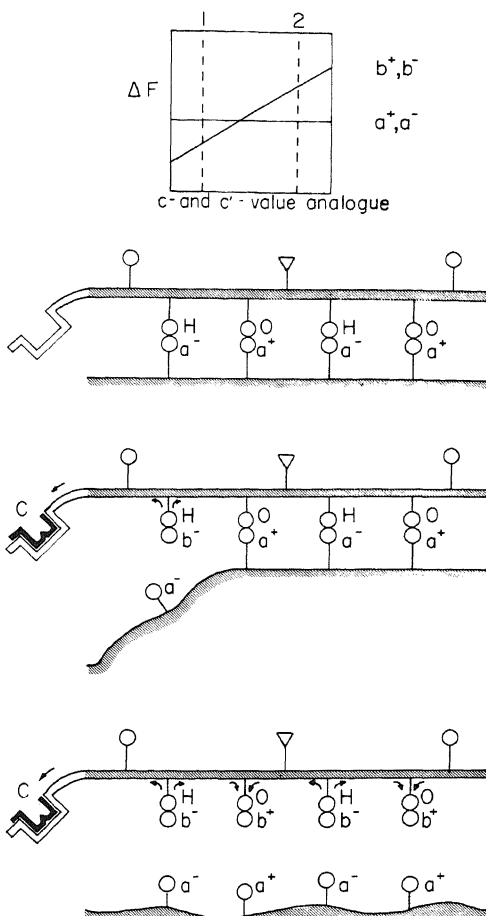


FIGURE 7.13. Model of a small segment of a protein chain with backbone peptide groups (H and O) and a cardinal site (C). See text for description. [From Ling (1969a), by permission of *International Review of Cytology*.]

bent W (see Section 7.4.3) reacts with the cardinal site C, the inductive effect withdraws electrons, which then raises the c' -value analogue of the nearest-neighboring NH group from 1 to 2. At this c' -analogue value, b^- is preferred over a^- . Exchange of b^- for a^- takes place. Because b^- is more polarizing than a^- , the replacement of a^- by b^- tends to reinforce the electron-withdrawing effect at the cardinal site C and to withdraw electrons from the next-neighboring CO group. The c -value analogue of this group then rises from 1 to 2, leading to an analogous exchange of b^+ for a^+ at this site. This process continues until all the a^+ and a^- are replaced by b^+ and b^- . As an example, the effect of the adsorption of the cardinal adsorbent W at the cardinal site C may be to create, in an all-or-none manner, a series of water adsorption sites and to cause an all-or-none dissociation of the protein from the adjacent protein. Hence, a new discrete conformation may ensue (lower diagram in Fig. 7.13).

If the numerous hydrogen-bonding, ionic, and other sites on a protein molecule were all independent of one another, then each site would have a large variety of choices in its partner. Such a protein could exist in a variety of conformations not sharply distinguishable from one another. In the present model, there is site-to-site interaction between nearest-neighboring sites so that the occupation of neighboring sites by the same adsorbent is favored. This interaction, called *autooperative interaction*, leads to the existence of discrete molecular states (conformations) of the protein molecules.

7.4.2. The Yang-Ling Cooperative Adsorption Isotherm

7.4.2.1. The Isotherm

The first statistical mechanical treatment of a cooperative transition was made by Bragg and Williams (Bragg and Williams, 1934) for the order-disorder transition of β -brass with increasing temperature. More recently, it has been recognized that the denaturations of proteins and DNA are also cooperative phenomena (Schellman, 1955; Zimm and Bragg, 1958; Gibbs and DiMarzio, 1958). In all these cases, the nearest-neighbor interaction energy was considered to be primarily entropic in nature, resulting from the increase in motional freedom as the native helical structure is broken. Our treatment of cooperative phenomena in living cells uses similar statistical mechanical methods; it differs primarily in that the transition is not considered to be one between an ordered state and a disordered state but between two alternative states of adsorption, either of which can be ordered or disordered. Furthermore, the nearest-neighbor interaction has an enthalpic as well as an entropic component. The basic method used by Yang and Ling (Ling, 1964a) was derived from the one-dimensional Ising model (Ising, 1925). The isotherm can be written in the form

$$[p_i]_{\text{ad}} = \frac{[f]}{2} \left[1 + \frac{\xi - 1}{\sqrt{(\xi - 1)^2 + 4\xi \exp(-\gamma/RT)}} \right] \quad (7.19)$$

where $[p_i]_{\text{ad}}$ is the concentration of the i th solute adsorbed; $[f]$ is the concentration of adsorption sites; R and T are the gas constant and absolute temperature, respectively; $-\gamma/2$ is the free energy of the nearest-neighbor interaction; and ξ is defined as follows:

$$\xi = \frac{[p_i]_{\text{ex}}}{[p_j]_{\text{ex}}} K_{j \rightarrow i}^{00} \quad (7.20)$$

where $[p_i]_{\text{ex}}$ and $[p_j]_{\text{ex}}$ are the concentrations of the i th and j th solutes in the free solutions with which the macromolecules are in equilibrium, and $K_{j \rightarrow i}^{00}$ is the intrinsic equilibrium constant. It is related to $\Delta F_{j \rightarrow i}^{00}$, the intrinsic free energy of the j th \rightarrow i th solute exchange on the adsorption site, by the relation

$$\Delta F_{j \rightarrow i}^{00} = -RT \ln K_{j \rightarrow i}^{00} \quad (7.21)$$

Here $\Delta F_{j \rightarrow i}^{00}$ refers to the free energy change in an exchange of adsorption of an i th solute

for a j th solute that occurs without altering the total number of $i-j$ pairs adsorbed on adjacent sites. Thus, in a triad of sites occupied sequentially by jji , when the middle j is replaced by an i th solute, there will be no increase or decrease of the numbers of nearest-neighboring ij pairs. In this case, the total free energy change is equal to $\Delta F_{j \rightarrow i}^{00}$. On the other hand, in a triad of jjj , the exchange of the j th solute adsorbed on the middle site by an i th solute involves the creation of two new ij pairs, and the total free energy change is then $\Delta F_{j \rightarrow i}^{00} + 2(-\gamma/2) = \Delta F_{j \rightarrow i}^{00} - \gamma$.

The value of the nearest-neighbor interaction energy, $-\gamma/2$, holds the key to the nature of the adsorption of solutes (Fig. 7.14). When $-\gamma/2$ is greater than zero, the adsorption isotherm is autocooperative, i.e., the system prefers to adsorb either all j th solutes or all i th solutes. This type of cooperative adsorption is most important physiologically. In autocooperative adsorption, a plot of $[p_i]_{ad}$ against $[p_i]_{ex}$ yields a sigmoid-shaped curve. If $-\gamma/2 = 0$, equation (7.19) reduces to a Langmuir adsorption isotherm; in a plot of $[p_i]_{ad}$ against $[p_i]_{ex}/[p_j]_{ex}$, a hyperbolic curve is obtained. If $-\gamma/2$ is less than zero, the adsorption is heterocooperative, that is, the system prefers to have i th and j th solutes occupying adjacent sites.

The adsorption isotherm expressed in equation (7.19) can also be written in the following form:

$$\frac{[p_i]_{ad}}{[p_j]_{ad}} = \frac{\sqrt{(\xi - 1)^2 + 4\xi \exp(\gamma/RT)} + \xi - 1}{\sqrt{(\xi - 1)^2 + 4\xi \exp(\gamma/RT)} - \xi + 1} \quad (7.22)$$

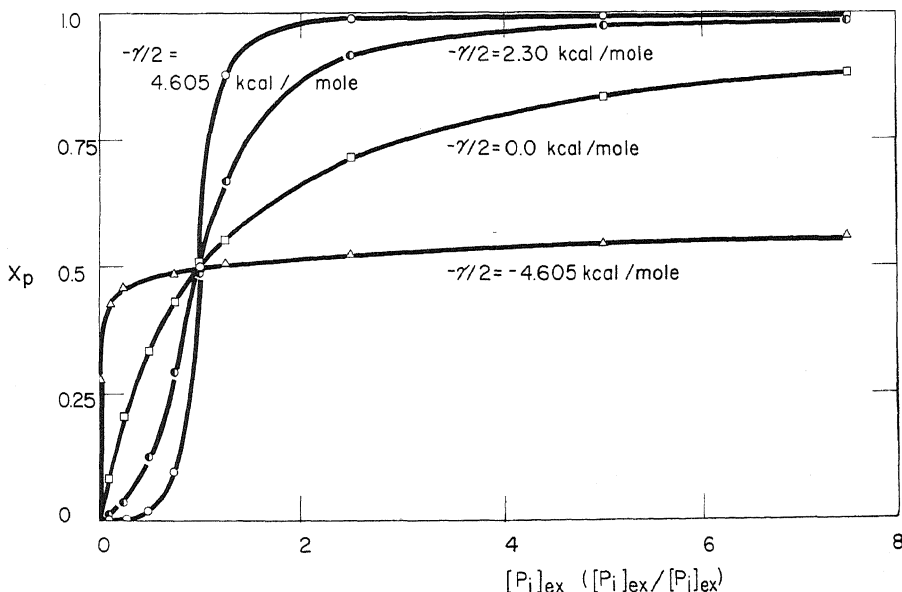


FIGURE 7.14. Theoretical plots of autocooperative ($-\gamma/2 > 0$), Langmuir ($-\gamma/2 = 0$), and heterocooperative ($-\gamma/2 < 0$) adsorption isotherms.

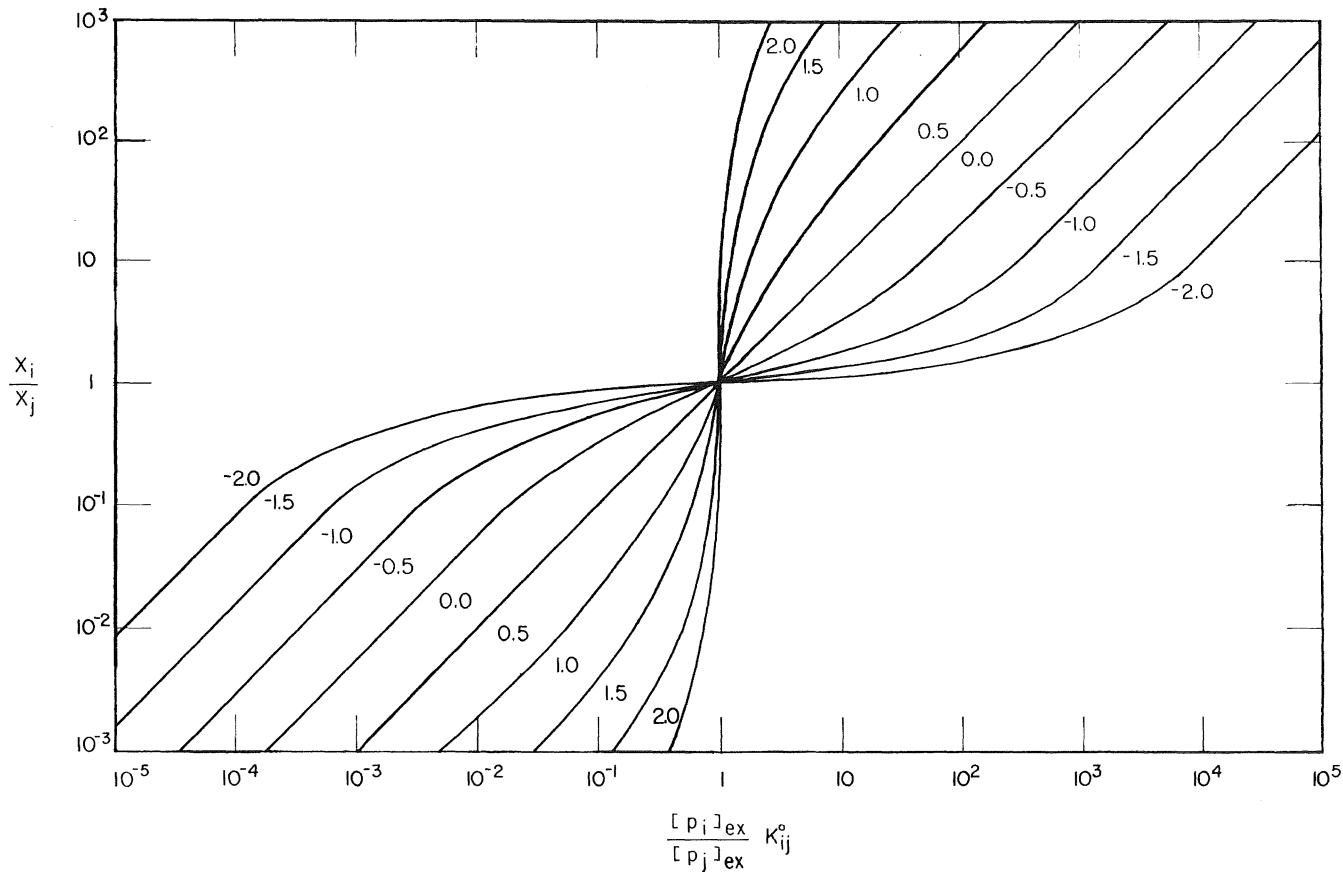


FIGURE 7.15. Theoretical plot of the cooperative adsorption of two solutes. Theoretical curves are calculated according to a generalized version of equation (7.22). The numbers near each curve refer to the free energy of nearest-neighbor interaction ($-\gamma/2$) and are in kcal/mole, calculated for a temperature of 25°C. The abscissa represents values of $([p_i]_{\text{ex}} / [p_j]_{\text{ex}})$ normalized by multiplying them with $K_{j \rightarrow i}^{00}$. X_i and X_j are respectively the mole fractions of sites adsorbing i th and j th solutes. [From Ling and Bohr (1970), by permission of *Biophysical Journal*.]

A plot of $\log ([p_i]_{\text{ad}}/[p_j]_{\text{ad}})$ against $\log ([p_i]_{\text{ex}}/[p_j]_{\text{ex}})$ with varying values of $-\gamma/2$ is shown in Fig. 7.15. This plot resembles the well-known Hill plot.

7.4.2.2. The Relation between the Hill Equation and the Yang-Ling Isotherm

In 1910 A. V. Hill introduced an empirical equation to describe the binding of oxygen on hemoglobin. This equation has since then been widely used and is referred to as the Hill equation:

$$\log \frac{y}{1-y} = n \log P_{O_2} + n \log K \quad (7.23)$$

where P_{O_2} is the partial pressure of oxygen in the gas phase, y is the mole fraction of oxygen bound to hemoglobin, $1 - y$ is the mole fraction of sites not binding oxygen, and n is an empirical constant called the Hill coefficient, which often has been recognized to be an index of the "sigmoidity" of the oxygen binding curve: The larger the value of n , the greater the steepness of the S-shaped oxygen uptake curve.

The tangent of the isotherm depicted by equation (7.22) at the locus where $[p_i]_{\text{ad}}$ equals $[p_j]_{\text{ad}}$ is described by the following equation (Ling, 1964a):

$$\log \frac{[p_i]_{\text{ad}}}{[p_j]_{\text{ad}}} = n \log \frac{[p_i]_{\text{ex}}}{[p_j]_{\text{ex}}} + n \log K_{j \rightarrow i}^{00} \quad (7.24)$$

Equations (7.23) and (7.24) are analogous. The j th adsorbent is explicitly represented in equation (7.24) but not in the Hill equation. The constant K of the Hill equation is in fact $K_{j \rightarrow i}^{00}$. n of equation (7.24) and, by analogy, n of equation (7.23) are an explicit function of the free energy of nearest-neighbor interaction:

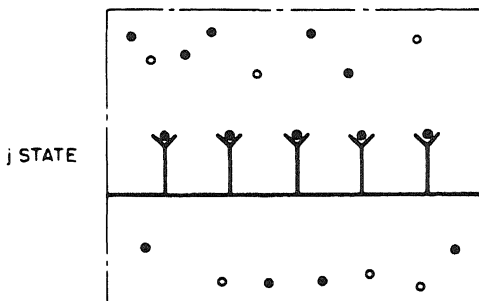
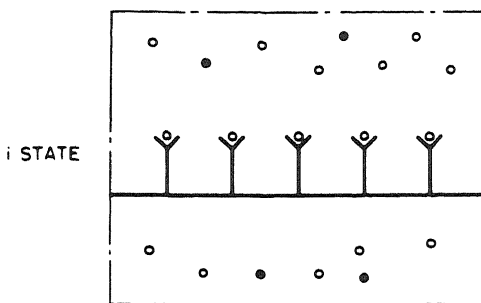
$$n = \exp (\gamma/2RT) \quad (7.25)$$

From this relation, $n > 1$ for autocooperative adsorption, $n < 1$ for heterocooperative adsorption, and $n = 1$ for noncooperative Langmuir adsorption.

7.4.2.3. Cooperative Adsorption on Proteins According to the AI Hypothesis

7.4.2.3a. The Primarily Inductive Nature of the Nearest-Neighbor Interaction Energy. Section 7.3 stressed the concept that the physiological manifestation (e.g., enzyme activity) of an exchange of one adsorbed ion for another occurs as a result of the different effect these adsorbed ions exercise on the c -value at the active (e.g., enzymatic) site (site 0). In the simple case, a single receptor site or a few receptor sites surround the active site. In cooperative adsorption, however, one is dealing with a whole chain of similar sites. Nevertheless, the same type of nearest-neighbor interaction, here referred to as $-\gamma/2$, is involved. $-\gamma/2$ also is dependent on the different effects induced by the alternative adsorbed species. If the exchange is between a pair of ions or other solutes very similar in their inductive effects, then neighboring sites are unaffected and $-\gamma/2$ is zero; the isotherm would behave as if all the sites were noninteracting (lower middle

A



B

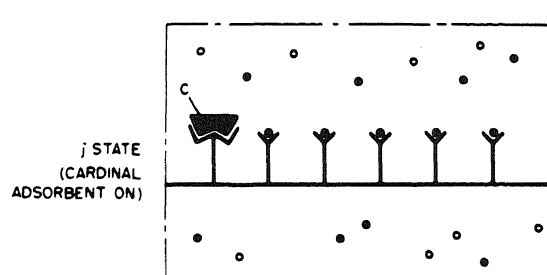
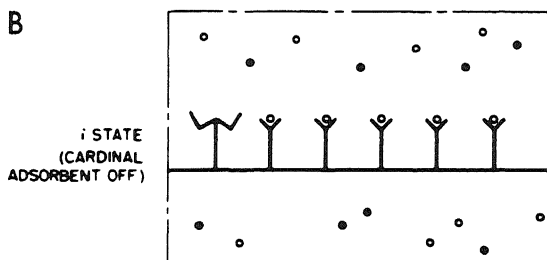


FIGURE 7.16. (A) Cooperative shifts between i and j states owing to a change in the relative concentration of the i and j solutes in the environment. Theory corresponds to equation (7.19). (B) Cooperative shift between i and j states owing to adsorption/desorption of cardinal adsorbent in an environment with unchanging i and j concentrations. Theory corresponds to equation (7.28). [From Ling and Ochsenfeld (1973b), by permission of *Annals of the New York Academy of Sciences*.]

curve in Fig. 7.14). Only when alternative adsorbents have significantly different inductive effects is $-\gamma/2$ large enough to generate autocooperative behavior.

7.4.2.3b. Threshold and All-or-None Responses. In physiological processes, the most significant kind of adsorption is autocooperative. When $-\gamma/2$ is positive and sufficiently large, a stepwise transition from the all-*i*th state to the all-*j*th state occurs when the steadily increasing ratio of $[p_j]_{\text{ex}}/[p_i]_{\text{ex}}$ reaches a threshold value (Fig. 7.16A). The system appears to behave in an "all-or-none" manner, tending to exist in either one or the other discrete state. The basic molecular mechanism provides a theoretical explanation for the shifts between discrete states of protein conformations. At the same time, the "zipperlike" behavior of autocooperative interactions between nearest-neighboring sites suppresses the endless array of alternative conformations in which a large molecule such as protein, with its many binding sites, might become entangled.

7.4.2.3c. What Constitutes a Site in the Cooperative Protein-Water-Ion System? Those sites on one or more protein chains that are cooperatively linked are referred to as a "gang" of sites (Ling, 1962, p. 97). The theory, therefore, demands that in these "all-or-none" transitions the entire assembly of sites, including all the NHCO groups belonging to the gang, take part in the transition. Since NHCO groups are responsible for the secondary structure of the protein, extensive changes in the conformation of the protein involved in the cooperative shift of state may occur.

If there is involvement of all the sites in a gang in a cooperative transition, then what constitutes an individual site or "regular site" may vary with the focal point from which the observer views the phenomenon in question. A site may correspond to a single NHCO group. It may include several amino acid residues if adsorption on anionic side chains is under study. Such variability in the "site" is illustrated in Fig. 7.17.

Specific sites, such as a heme site or an enzyme site, may be part of the gang involved. In this case, with the cooperative shifts of states, these specific sites will change their properties, as by alteration in the binding strength for oxygen by heme or by the activation or deactivation of enzymatic function.

7.4.2.4. Some Diagnostic Criteria for the Cooperative Properties of Adsorption

A list of diagnostic criteria for distinguishing autocooperative, noncooperative (Langmuir), and heterocooperative adsorption on a homogeneous population of sites is

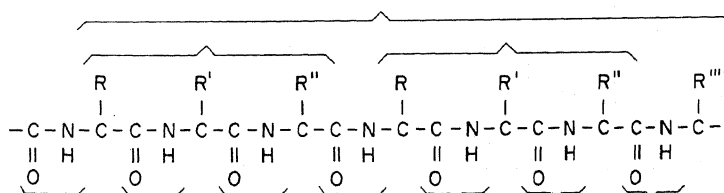


FIGURE 7.17. Diagram of a "gang" of sites and the different definition of a "regular site" according to the nature of observation. Brackets delineate different individual regular sites in the same gang of sites. [From Ling (1980a), by permission of Pergamon Press.]

TABLE 7.6. Diagnostic Criteria of the Autocooperative, Noncooperative, and Heterocooperative Adsorption Isotherms of a Homogenous Population of Sites^a

		Autocooperative	Noncooperative (Langmuir)	Heterocooperative
Linear plot (e.g., Fig. 7.14)	$[p_i]_{ad}$ vs. $[p_i]_{ex}/[p_j]_{ex}$	S-shaped	Hyperbola	Quasi-hyperbola
	$[p_j]_{ad}$ vs. $[p_i]_{ex}/[p_j]_{ex}$	Inverted S-shaped	Inverted hyperbola	Inverted quasi-hyperbola
Log-log plot (e.g., Fig. 7.15)	Slope at $[p_i]_{ad} = [p_j]_{ad}$	> 1	$= 1$	< 1
Reciprocal plot (e.g., Fig. 7.18)	$1/[p_i]_{ad}$ vs. $[p_j]_{ex}/[p_i]_{ex}$	S-shaped	Straight line	Lying down S-shaped
Scatchard plot	$[p_i]_{ad}/[p_i]_{ex}$ vs. $[p_i]_{ex}$	Concave downward	Straight line	Concave upward

^aFrom Ling (1980a), by permission of Pergamon Press.

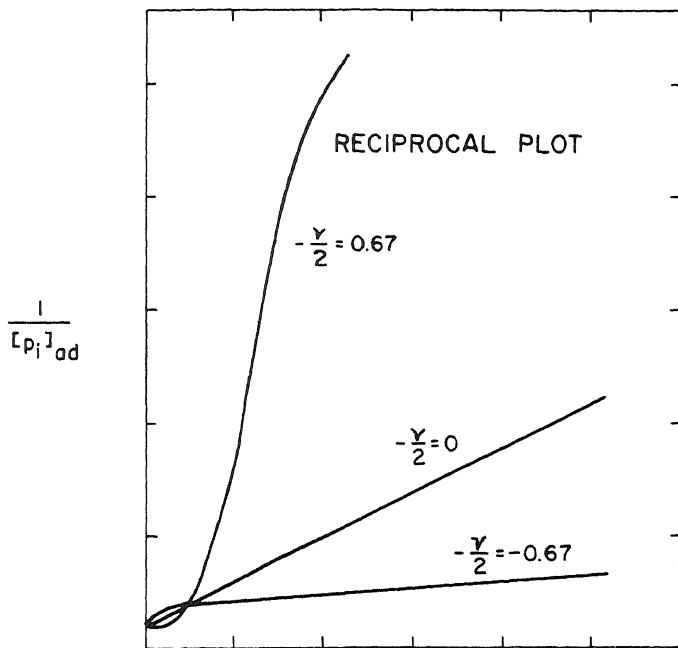
assembled in Table 7.6. The reciprocal plot and the Scatchard plot are illustrated in Fig. 7.18. A heterogeneous population of heterocooperative or noncooperative sites usually shows characteristics similar to heterocooperative adsorption. For a heterogeneous population of sites containing autocooperative adsorption sites, a more complex pattern is the case. This case will be discussed in Section 7.4.2.5b.

7.4.2.5. Comparison of the Theory of Cooperative Adsorption with Experimental Data in Vitro

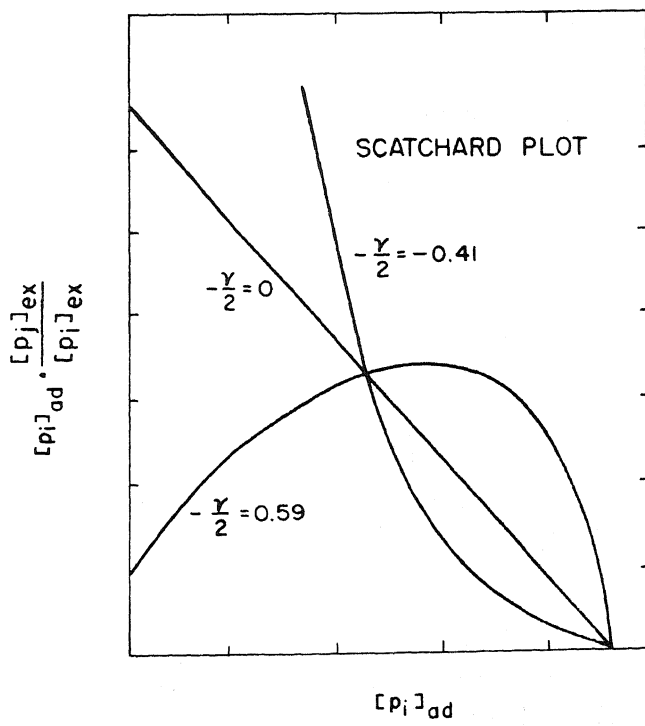
7.4.2.5a. Homogeneous Population of Gangs. Figure 7.19 demonstrates that equation (7.19) can quantitatively describe the data for binding of oxygen by human hemoglobin where the interacting binding sites are the heme groups on the four subunits (data points are from Lyster, cited by Rossi-Fanelli *et al.*, 1964). Figure 7.20 demonstrates that equation (7.19) also describes the binding of dodecyltrimethylammonium bromide by bovine serum albumin, where the adsorption sites are the β - and γ -carboxyl groups (data points are from Few *et al.*, 1955). Figure 7.21 demonstrates that equation (7.19) also describes phenol binding by collagen, where the interacting binding sites are the backbone NHCO groups (data of Kuntzel and Schwank, 1940). In all these cases, the adsorption is autocooperative, and binding sites in each case appear to have very similar

FIGURE 7.18. Reciprocal and Scatchard plots. In the reciprocal plot, the reciprocal of adsorbed solute (ordinate) is plotted against $[p_j]_{ex}/[p_i]_{ex}$ (abscissa). The autocooperative adsorption curve is sigmoid, the heterocooperative adsorption curve is quasihyperbolic, and the noncooperative (Langmuir) adsorption curve is a straight line.

In the Scatchard plot, $[p_i]_{ad}/([p_j]_{ex}/[p_i]_{ex})$ is plotted against $[p_i]_{ad}$. The autocooperative adsorption curve concaves downward, the heterocooperative adsorption curve concaves upward, and the noncooperative (Langmuir) adsorption curve is a straight line. [From Ling (1980a), by permission of Pergamon Press.]



$$\frac{[p_i]_{ex}}{[p_i]_{ad}}$$



$$[p_i]_{ad}$$

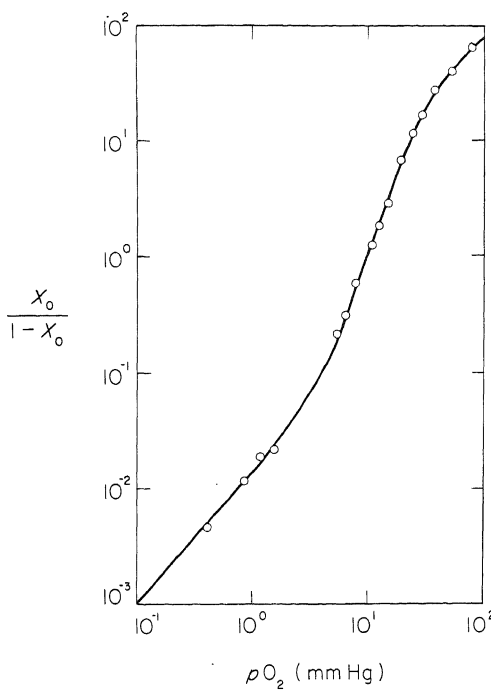


FIGURE 7.19. A log-log plot of the data of Lyster on oxygen uptake by human hemoglobin at pH 7.0 at 19°C. Data of Lyster as presented in the review by Rossi-Fanelli *et al.* (1964). Points are experimental; the line is theoretical according to equation (7.19) with $K = 5.88 \times 10^{-6}$ M and $-\gamma/2 = 0.67$ kcal/mole. [From Ling (1969a), by permission of *International Review of Cytology*.]

intrinsic equilibrium constants. The values of n are 3.1, 9.3, and 3.51, respectively, and the nearest-neighbor interaction energies are +0.67, +1.31, and +0.74 kcal/mole.

Figure 7.22 is a Scatchard plot of the binding of K^+ on the Na^+, K^+ -activated ATPase purified from canine kidney outer medulla (Matsui *et al.*, 1977). The plot is, of course, typical of autocooperative binding as illustrated in Fig. 7.18.

Autocooperative adsorption occurs not only with proteins, but also in the interaction of DNA with histone (Rubin and Moudrianakis, 1972), with actinomycin (Sobell, 1974), and with K^+ (Hughes, 1970).

7.4.2.5b. Heterogeneous Population of Gangs. If more than one type of gang is present, the binding is then described by the composite of several isotherms with different K_{j-i}^{00} and $-\gamma/2$ values. Figure 7.23 shows a theoretical curve with two gangs of sites. In one gang, $-\gamma/2$ is negative (heterocooperative); in the other, $-\gamma/2$ is positive (autocooperative) (Ling, 1966a). At approximately the concentration where adsorption on the autocooperative gang begins, the composite curve shows an abrupt change in the slope of the straight line segments. Usually, unfolding of protein chains or disassembly of subunits can be expected with autocooperative adsorption, as the adsorbed molecules displace intra- or intermolecular bonds between protein chains that maintain the original native conformation.

Figure 7.24 shows the data of J. Steinhardt and Zaiser (1951) on the acid titration of carbonylhemoglobin; Fig. 7.25 shows the data of Pallansch and Briggs (1954) on the binding of dodecyl sulfate by bovine serum albumin. In each case, the point at which

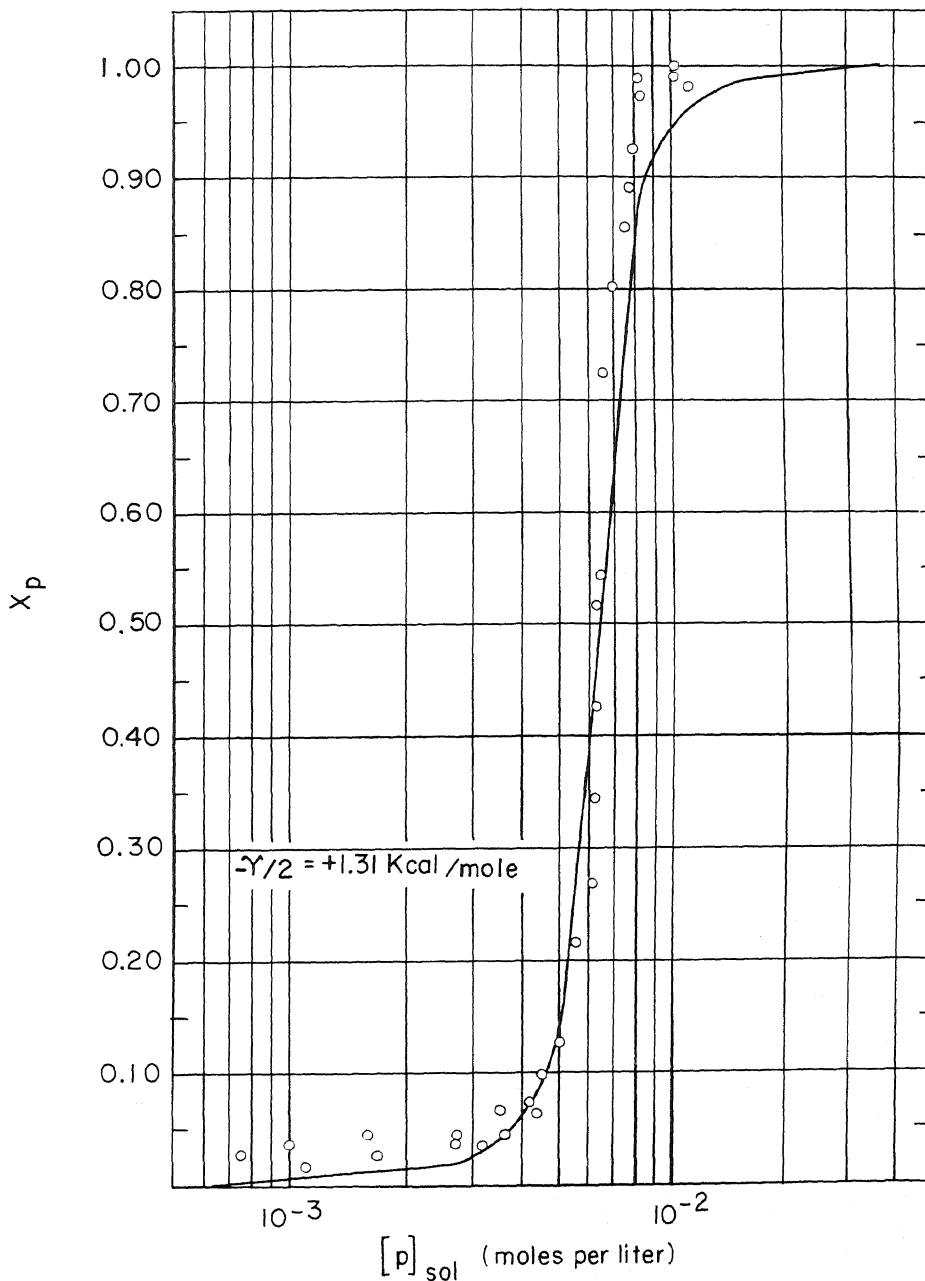


FIGURE 7.20. Adsorption isotherm of dodecyltrimethylammonium bromide on bovine serum albumin. Data of Few *et al.* (1955) (20°C). Theoretical curve was constructed from equation (7.19) with $K_{f^0}^{00} = 158 \text{ M}^{-1}$ and $-\gamma/2 = 1.31 \text{ kcal/mole}$. Ordinate represents the mole fraction of sites occupied by dodecyltrimethylammonium bromide. Total number of sites is the maximum number of binding sites found, e.g., 100 per mole of protein. [From Ling (1964a), by permission of *Biopolymers*.]

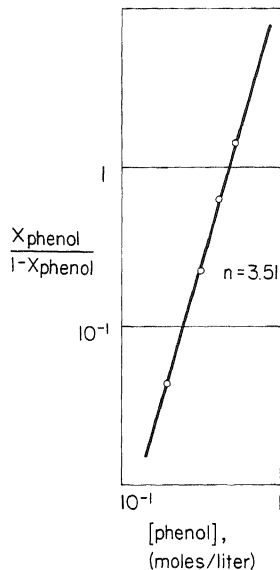


FIGURE 7.21. Phenol adsorption on collagen. Ordinate represents on a logarithmic scale the mole fraction of collagen sites adsorbing phenol divided by the mole fraction of sites not adsorbing phenol. Total number of binding sites in this calculation is the total number of backbone NHCO groups in 1 kg of collagen. Slope of 3.51 corresponds to an apparent nearest-neighbor interaction energy of 0.74 kcal/mole. The collagen used was in the form of skin powder. Data of Kuntzel and Schwank (1940). [From Ling (1966a), by permission of *Federation Proceedings*.]

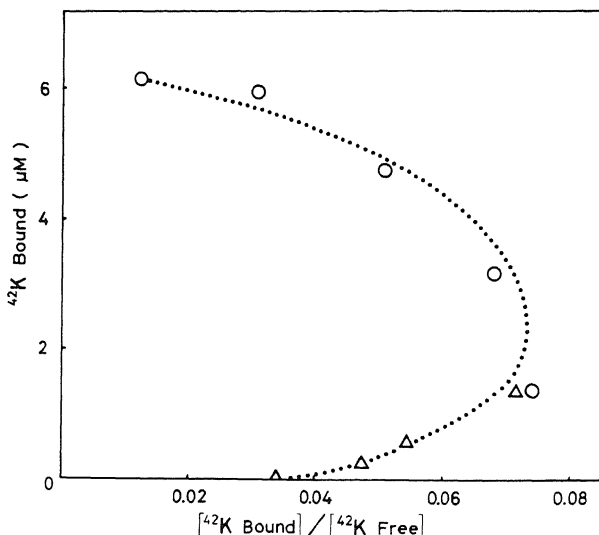


FIGURE 7.22. Scatchard plot of ouabain-sensitive binding of ^{42}K to Na^+,K^+ -ATPase from outer medulla of canine kidney. [From Matsui *et al.* (1977), by permission of *Biochemical and Biophysical Research Communications*.]

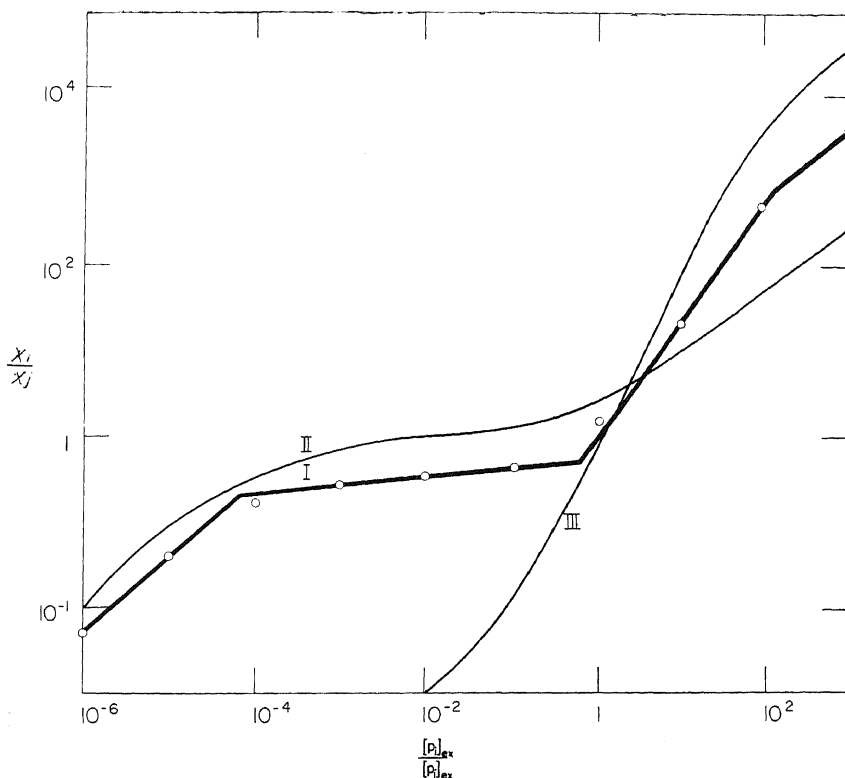


FIGURE 7.23. Complex cooperative adsorption isotherms. Adsorption isotherms for two linear polymers, one autocooperative and the other heterocooperative, are shown, respectively, in curves III and II. Circles represent a complex adsorption isotherm for a mixture containing equal amounts of the above linear polymers and treated as though it contained only a single polymer. Curve I has been drawn as a series of straight lines showing the significant parts of the more exact curve which would join all the circles. Note that the two outermost straight lines have slopes of unity; the slopes of the two middle lines indicate the hetero- or autocooperative nature of the component systems. [From Ling (1966a), by permission of *Federation Proceedings*.]

the straight line segment changes slope is also the point at which changes in molecular conformation were observed.

7.4.3. The Control of Shifts between Discrete Cooperative States by the Adsorption and Desorption of Cardinal Adsorbents

One of the most outstanding features of the living state and its physiological perturbations is their control by such agents as drugs, transmitters, Ca^{2+} , and ATP, which are collectively called *cardinal adsorbents* in the AI hypothesis.

Like the magnet in the model of tethered nails (Fig. 6.1A) or the electrified rod in the model of the insulator chain (Fig. 6.1B), cardinal adsorbents affect the protein-water-ion system by a strong interaction with the proteins to produce a particular state

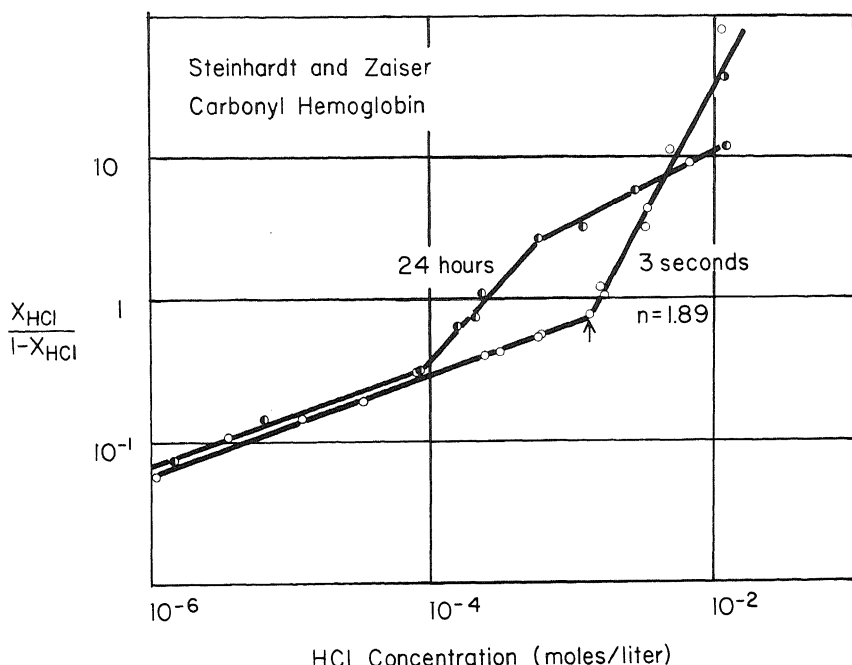


FIGURE 7.24. Acid binding by carbonyl hemoglobin at 25°C. Ordinate represents, on a logarithmic scale, the ratio of the mole fraction of HCl bound to the mole fraction of sites not binding HCl. Abscissa represents, also on a logarithmic scale, the HCl concentration. Total number of acid binding sites is that given by the authors (i.e., 1.6 moles/kg of protein). The curve labeled "3 seconds" was measured 3 sec after mixing the protein and acid; the curve labeled "24 hours" was measured 24 hr after mixing. Arrow indicates the acid concentration at which the protein becomes denatured. Data from J. Steinhardt and Zaiser (1951). [From Ling (1966a), by permission of *Federation Proceedings*.]

of electronic polarization. Cardinal adsorbents hold protoplasm in one or another state by a propagated polarization along the length of polypeptide chains. Adsorption or desorption of the cardinal adsorbents may alter the cooperative state of the protein-water-ion system in an "all-or-none" manner (Fig. 7.16B). These states may correspond to resting and active ones, or to living and dead ones.

In terms of the cooperative adsorption isotherm, the effect of adsorption or desorption of cardinal adsorbents on cardinal sites (often equivalent to receptor sites), is to shift $K_{j\rightarrow}^{00}$ and/or $-\gamma/2$ to new values.

In the simplest case, each gang of sites has a single cardinal site and a number of regular sites in a gang. If the total concentration of gangs, and hence cardinal adsorbents, is $[F]$, and the concentration of cardinal adsorbents in the medium is $[C]_{ex}$, the general equation for the concentration of adsorbed cardinal adsorbent is entirely analogous to equation (7.19):

$$[C]_{ad} = \frac{[F]}{2} \left[1 + \frac{\Xi - 1}{\sqrt{(\Xi - 1)^2 + 4\Xi \exp(\Gamma/RT)}} \right] \quad (7.26)$$

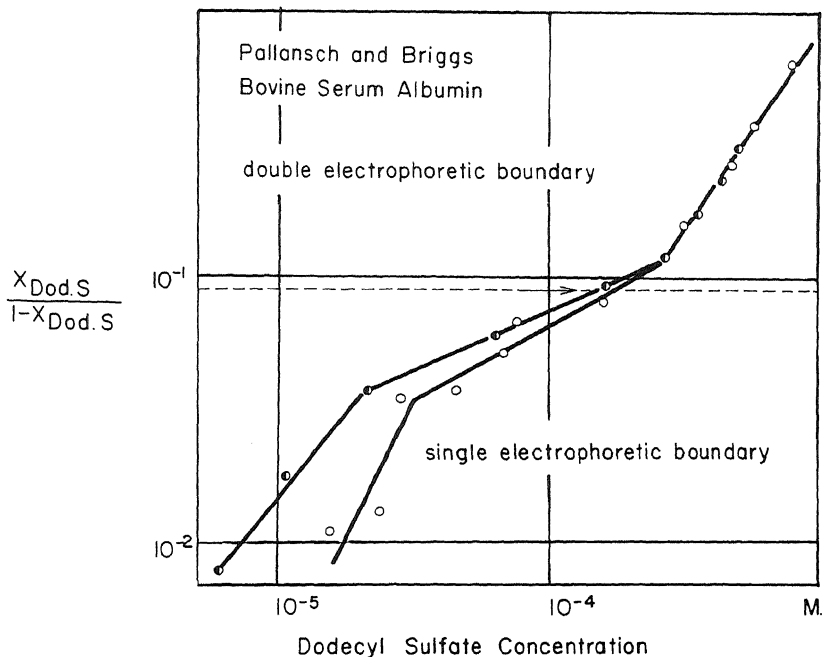


FIGURE 7.25. Adsorption of dodecyl sulfate on bovine serum albumin. Ordinate represents, on a logarithmic scale, the mole fraction of sites binding the anionic detergent, dodecyl sulfate, divided by the mole fraction of sites not binding the detergent. Abscissa represents, also on a logarithmic scale, the dodecyl sulfate concentration. Total number of binding sites, 102, is the sum of the number of arginine, lysine, and histidine residues per protein molecule. Note that the change from a single to a double electrophoretic boundary (dotted line) occurs at a concentration of dodecyl sulfate corresponding to the abrupt shift of slope from heterocooperative to autocoperative adsorption of detergent. Empty and half-filled circles represent two different series of experiments. Data from Pallansch and Briggs (1954). [From Ling (1966a), by permission of *Federation Proceedings*.]

Ξ is defined, again by analogy with equation (7.20), as

$$\Xi = [C]_{\text{ex}} \cdot \mathfrak{R}_c^{00} \quad (7.27)$$

Here the alternative adsorbent on the cardinal site is unspecified, but is a constant and thus included in the apparent association constant \mathfrak{R}_c^{00} .

The adsorption of a cardinal adsorbent potentially can change both ξ and $-\gamma/2$. Thus, the total concentration of the i th adsorbed solute is described by the following equation:

$$[p_i]_{\text{ad}} = \frac{g[C]_{\text{ad}}}{2} \left[1 + \frac{\xi_c - 1}{\sqrt{(\xi_c - 1)^2 + 4\xi_c \exp(\gamma_c/RT)}} \right] + \frac{g[F] - [C]_{\text{ad}}}{2} \left[1 + \frac{\xi_0 - 1}{\sqrt{(\xi_0 - 1)^2 + 4\xi_0 \exp(\gamma_0/RT)}} \right] \quad (7.28)$$

where ξ_c and ξ_0 are defined as follows:

$$\xi_c = \frac{[p_i]_{\text{ex}}}{[p_j]_{\text{ex}}} \cdot K_{(j \rightarrow i)C}^{00} \quad (7.29)$$

and

$$\xi_0 = \frac{[p_i]_{\text{ex}}}{[p_j]_{\text{ex}}} \cdot K_{(j \rightarrow i)0}^{00} \quad (7.30)$$

$K_{(j \rightarrow i)C}^{00}$ is the intrinsic equilibrium constant of the j th-to- i th exchange in a gang with its cardinal site occupied by the cardinal adsorbent C; $K_{(j \rightarrow i)0}^{00}$ is the constant in a gang in which the cardinal site is not so occupied. Similarly, $-(\gamma_c/2)$ and $-(\gamma_0/2)$ refer, respectively, to the nearest-neighbor interaction energies for the gang controlled by the cardinal adsorbent and for the one not controlled by the cardinal adsorbent. $[C]_{\text{ad}}$ is described by equation (7.26). In the case where there is no interaction among the cardinal sites themselves, $-(\Gamma/2)$ is zero; in the case where there is cooperative interaction among the cardinal sites, $(\Gamma/2)$ is greater or smaller than zero (autocooperative or heterocooperative, respectively).

It is to be noted that, in theory at least, the cooperative shift between the i and j states by the alteration of $[p_i]_{\text{ex}}/[p_j]_{\text{ex}}$, as illustrated in Fig. 7.16A, is nondirectional, since there is no fixed site whose $j \rightarrow i$ exchange precedes those of others. On the other hand, transitions initiated by cardinal adsorbents always begin with the regular site next to the cardinal site and proceed away from the cardinal site (Fig. 7.16B).

Figure 7.19 shows that the binding of oxygen by hemoglobin follows the cooperative adsorption isotherm in equation (7.19). In 1964 Chanutin and Curnish (1964, 1967)* made the discovery that 2,3-diphosphoglycerate (2,3-DPG) and ATP react with hemoglobin to cause a decrease in the affinity of hemoglobin for oxygen. The effects of 2,3-DPG and of inositol hexaphosphate on the oxygen equilibrium were carefully studied by Benesch and Benesch (1969). Their quantitative data were shown to be described with a reasonable degree of accuracy by equation (7.28), as presented in Fig. 7.26.

7.4.4. An Analysis of the Theoretical Model of Controlled Cooperative Interaction

7.4.4.1. Basic Traits

Trait I. The key component is a protein which reacts with the cardinal adsorbent.

Trait II. The cardinal adsorbent, usually found at very low concentrations in the environment, strongly interacts with specific sites on receptor proteins. The cardinal adsorbents exert their prime physiological or pharmacological effects by their adsorption

*Chanutin and Curnish (1964, 1967) interpreted their data on the basis of the assumption that deoxygenated and oxygenated hemoglobins have different affinities for ATP. While correct, this assumption of course begs the question: Why do the ATP binding sites, which are not heme sites, exist in only two discrete states and not in an array of many states? For this question, the AI hypothesis provides an answer.

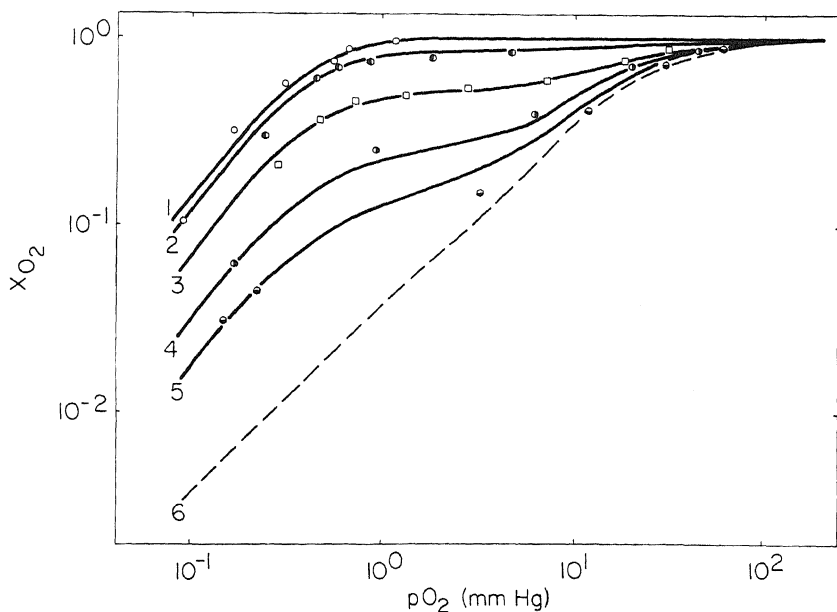


FIGURE 7.26. Oxygen uptake by hemoglobin (stripped) in the presence and absence of inositol hexaphosphate (IHP). Hemoglobin solution was 0.3%, pH = 7.0, 10°C. (1) No IHP; (2) 1.2×10^{-5} M IHP; (3) 2.4×10^{-5} M IHP; (4) 3.6×10^{-5} M IHP; (5) 4.8×10^{-5} M IHP, (6) ∞ IHP. Points are experimental data of Benesch and Benesch (1969). Lines are theoretical, calculated according to equation (7.28). [From Ling (1970a), by permission of *Proceedings of the National Academy of Sciences*.]

(or desorption) without necessarily undergoing a chemical change, although under certain conditions a chemical change of the cardinal adsorbent may occur as a means of reversing the physiological effect and returning the protoplasm to its original resting state.

Trait III. As a stochastic process involving sequential reactions, the cardinal-adsorbent-induced changes are temperature-dependent, achieving the end result at a higher temperature much more rapidly than at a lower temperature.

Trait IV. For the same reason, the cardinal-adsorbent-induced changes can be expected to be time-dependent—that is, there tends to be an initial delay before the full effect is achieved.

7.4.4.2. Potential Capabilities

Capability I. Long-range information and energy transfer. Since the nearest-neighbor interaction contains a major inductive component propagated along the resonating polypeptide chain, the cooperative system has the fundamental traits of a one-dimensional assembly. The effect produced by a cardinal adsorbent is propagated along the length of the protein chain to reach all sites within the segment or gang of cooperatively linked sites and, through intermolecular bonds, to extend to other protein molecules.

Capability II. Maintenance and control of all-or-none changes in the tertiary or

quaternary structure of cell proteins. Figure 7.13 illustrates how the cooperative shifts between partners in one gang could result either in a conformational change (e.g., α -helix—"random coil" transition, if all the b^+ and b^- refer to the proton-donating and proton-accepting ends of water molecules) or in subunit dissociation (or association with protein or other macromolecules such as DNA, if b^+ and b^- are H-bonding sites of the same or other proteins or of other macromolecules).

Capability III. All-or-none binding, release, or exchange of solutes brought about by the adsorption of cardinal adsorbents on a distant site. These solutes may be ions (K^+ , Na^+ , anions), sugars, amino acids, or other molecules. In this capacity the cooperative protein system can serve the role of a storage reservoir for a prompt release of an adsorbent on command.

Capability IV. All-or-none binding and release of water. This is significant in secretory functions and in the maintenance of cellular volume.

Capability V. Allosteric change in enzyme activity on specific enzymes. Sites within the gang of cooperative sites change in response to the adsorption onto a distant site of a cardinal adsorbent.

These traits and capabilities of controlled cooperative interactions between sites on a protein will be illustrated by a number of physiological phenomena to be described in detail throughout the remainder of this book.

7.5. Summary

The concept of the cell in the association-induction hypothesis includes the idea that the coherence of the assembly of associated cellular components mirrors its cooperative behavior. This is mediated by near-neighbor interactions between sites on macromolecules that associate with ions, other solutes, water, and other macromolecules. The unique properties of proteins that permit this interaction to occur include the high polarizability and partial resonance of the polypeptide backbone, making it particularly well suited for the induction of electron density changes between side chain functional groups. This inductive effect is essentially the same as that which is well known in organic chemistry and is illustrated by the Taft and Hammett constants and the Chiang-Tai inductive index.

Examples were cited in this chapter that illustrated the role of the inductive effect in determining the strengths of hydrogen bonds between and within proteins, the oxidation-reduction potentials of thiol groups, and the acid dissociation constants of carboxyl groups. A formulation of the modulation and control of physiological activities was given, taking into account the inductive influence of factors that affect the active site. This led to a description of models of competitive interaction between sites and of noncompetitive facilitation and inhibition in a two-receptor site system.

The concept of a propagated, autocooperative interaction between near-neighbor sites was developed, leading to a general statistical-mechanical equation (the Yang-Ling isotherm) for the description of solute adsorption onto these sites. The cooperative adsorption isotherm was shown to be analogous to the empirical Hill equation developed to describe the oxyhemoglobin dissociation curve. Finally, the inductive modulation of a

set or "gang" of cooperatively linked sites by a single cardinal adsorbent was described and illustrated by the well known effects of 2,3-DPG and other substances on the oxyhemoglobin dissociation curve.

The cooperatively linked system provides the molecular basis for long-range transfer of information and energy within a cell and for physiological processes that have an all-or-none characteristic. In Sections III and IV of this book, specific manifestations of this mechanism will be presented.

The Physical State of K^+ and Na^+ in Living Cells

The experimental studies of A. V. Hill and Kupalov (1930; Hill, 1930) on frog muscle led them to the conclusion that virtually all water and K^+ exist in the free state in living cells. The persuasiveness of their arguments played a major role in the abandonment of the colloidal approach to cell physiology and led to the dominance of the membrane theory (Section 2.7). This trend was greatly enhanced by measurements of the high mobility and thermodynamic activity coefficient of K^+ in living cells as well as by other evidence described in Section 5.1. In this chapter I present the results of the most recent studies on the subject, usually carried out with the aid of sophisticated techniques not available in the past. These results lead to conclusions that are dramatically different from what was once widely believed. Indeed, there now remains little doubt that virtually all the K^+ in resting living cells exists in an adsorbed state. Before presenting the details of these new findings, and following up in depth on old ones, I want to remind the reader of the recent successful demonstration of ion binding on isolated proteins briefly mentioned in Section 6.2.5: When salt linkages are prevented from forming, all proteins studied adsorb K^+ , Na^+ , or other alkali metal ions in a selective manner and at a high enough level to match those seen in living cells (Section 11.2.2.2). Failure in the past to demonstrate the same played a major role in the acceptance of the pump theory (see Section 4.4.1).

8.1. A Reassessment of the Critical Experiments of Hill and Kupalov

A. V. Hill and Kupalov found the total osmotic activity of K^+ and other solutes in the cell to equal that of an isotonic NaCl solution. Since Na^+ (and Cl^-) in an isotonic solution is free, the K^+ in the cell water also must be free. However, Hill and Kupalov's argument for free cell K^+ rests entirely on the evidence that all muscle cell water also is free. The evidence for free water given by Hill (1930) was twofold:

1. The equilibrium concentration of urea in muscle cell water is the same as that in the external bathing solution, hence no bound or "nonsolvent" water exists. However, according to the association-induction (AI) hypothesis, water existing

in the state of polarized multilayers *should* have a q -value close to unity for small molecules like urea that can readily fit into the water structure. Thus, urea exhibits a ρ -value of 0.99 in denatured protein solutions which clearly exclude sucrose and glycine (Section 6.3).

2. Equilibration of frog muscle in an equal volume of double-strength Ringer solution changes the vapor pressure of the external solution to that of 1.5 Ringer solution. This finding led Hill to conclude that all muscle water is free. The validity of this experiment rests on the assumption that in a double-strength Ringer solution, in essence 0.2 M NaCl, frog muscles remain healthy. In fact, they do not. In this solution, muscle loses virtually all its K^+ and its ability to exclude Na^+ and D-arabinose (Ling and Peterson, 1977).

Since Hill's arguments for free cell water are no longer tenable, the conclusion that cell K^+ must all be free also becomes untenable.

8.2. Experimental Proof That the Bulk of Muscle K^+ Is in an Adsorbed State

The physical state of K^+ and water in living cells remains the critical issue that will decide which model, the membrane model or the bulk phase model, more correctly represents the living cell. In this section I shall present a series of new experimental findings, diverse in approach, that yield a unanimous conclusion that virtually all K^+ in muscle cells exists in an adsorbed state.

In 1952 I suggested that selective K^+ accumulation in living cells originates from selective adsorption on the β - and γ -carboxyl groups of intracellular proteins and that in muscle cells myosin alone provides enough β - and γ -carboxyl groups to adsorb all the intracellular K^+ (Section 4.4). Long before that it had been discovered that in voluntary muscle myosin is found primarily in the A bands (Engelmann, 1873). In recent years interest in this subject was reawakened by the demonstration by Hasselbach and Schneider (1951) and Hanson and Huxley (1953) that in voluntary muscles myosin comprises the thick filaments, which in turn are localized exclusively in the A bands. One can deduce therefore that the bulk of K^+ in voluntary muscle cells must be localized in the A bands.

Moreover, from studies of collagen by Hodge and Schmidt (1960) in which they showed that the cationic electron microscopic stain, the uranyl ion, binds to the β - and γ -carboxyl groups, one may predict that K^+ in normal resting striated muscle fibers is localized in the same loci that in conventional EM pictures are stained dark with uranium.

8.2.1. Early Work on Localization of K^+

There have been several reports in the past that K^+ in voluntary muscle cells is indeed localized in the A bands. In 1905 Macallum (1905, 1911) published his microchemical studies of a variety of living cells. He found that, when the K^+ -precipitating reagent sodium coboltinitrite is added to wing muscles of beetles and claw muscles of crayfish, the characteristic crystalline precipitate of potassium coboltinitrite formed

mostly in the "dim" or A bands. McCallum's work was confirmed and extended by his pupil Menten (1908).

Another early technique suggesting K⁺ localization was microincineration, either in an oven or under the electrom beam of an electron microscope (Draper and Hodge, 1949). Insect wing muscles provide muscle fibers from which individual myofibrils can be isolated easily with dissecting needles. Tigyi-Sebes (1962), from Ernst's Institute of Biophysics at Pecs, Hungary, incinerated these isolated myofibrils at 400°C with or without prior treatment with sodium coboltinitrite. Washing with distilled water removed the ashes of untreated myofibrils while the myofibrils treated with the K⁺ reagent retained banded ashes, a difference attributed to the insolubility of the potassium salt of coboltinitrite. In another paper from the same laboratory, Nesterov and Tigyi-Sebes (1965) exposed isolated myofibrils to another K⁺ reagent, tetraphenylborate, followed by washing and incinerating. Using an interferometer, they recorded the dry matter distribution in the ashed myofibrils. From these findings the authors concluded that K⁺ is localized primarily (60%) in the A bands, but also in the Z line. Giese and Rekowski (1970) demonstrated a banded distribution of ¹³⁴Cs in voluntary muscles but could not tell whether the ¹³⁴Cs was in the A bands or the I bands.

Unfortunately, some of the earlier techniques used were fraught with pitfalls. Thus, the early microincineration work was severely criticized by Gersh (1938), who considered all cell K⁺ to be evenly distributed and pointed out the great inherent propensity of this type of experiment to produce artifacts. In preliminary trials to confirm the work of Macallum and Menten, I had no trouble visualizing patterns of dark crystals in insect muscle fibers but could not convince myself that the crystals were indeed potassium coboltinitrite because K⁺-depleted muscle appeared to yield similar patterns. In trying my hand at microincineration experiments, I found it difficult to convince myself that the banded ashes were due to K⁺, the major cation, and not due to incompletely incinerated protein residues. At a more elevated temperature, where all protein residues were burnt away, what would be taken as K⁺ ash also vanished.



Ludwig Edelmann

The unreliability of the microincineration method led to the development by the young German scientist Ludwig Edelmann of new techniques to study K^+ localization, which will be described here in some detail.

8.2.2. Electron Microscopic Demonstration of Localization of K^+

For light microscopic work one stains biological preparations with dyes that absorb visible light of one or more specific wavelengths. The color distribution informs us about the dye-binding properties of different parts of the living cell. In electron microscopy (EM), instead of visible light, electron beams are utilized. Again the pattern one sees is the pattern of varying affinity of the cytological structures for the heavy atoms, such as uranium or phosphotungstate, that are used to "stain" the preparation. Ling and Ochsenfeld (1966) presented evidence that Cs^+ and Tl^+ can stoichiometrically compete for the same sites which normally adsorb K^+ in living frog muscle (Figs. 8.1 and 8.2). These ions, in contrast to K^+ (whose atomic weight is 39.1), are electrondense, with atomic weights of 132.9 and 204.4, respectively.

Edelmann (1977a) developed a new and simplified freeze-drying technique that allowed direct visualization on EM of Cs^+ and Tl^+ that had replaced K^+ in normal living cells (Edelmann, 1977b). These cells were not killed by chemical fixation, but were frozen very rapidly by abrupt contact with a polished metal surface cooled to liquid nitrogen temperature. They were not stained, and the electron-dense regions visualized mirror simply the positions of the Cs^+ and Tl^+ . Figures 8.3B,C show that Cs^+ and Tl^+ duplicate the pattern seen in a muscle preparation fixed in glutaraldehyde and stained with uranium (shown in Fig. 8.3A). On exposing the Tl^+ -loaded muscle section to air, part of the Tl^+ accumulated in the A band precipitates out as crystals (Fig. 8.3D).

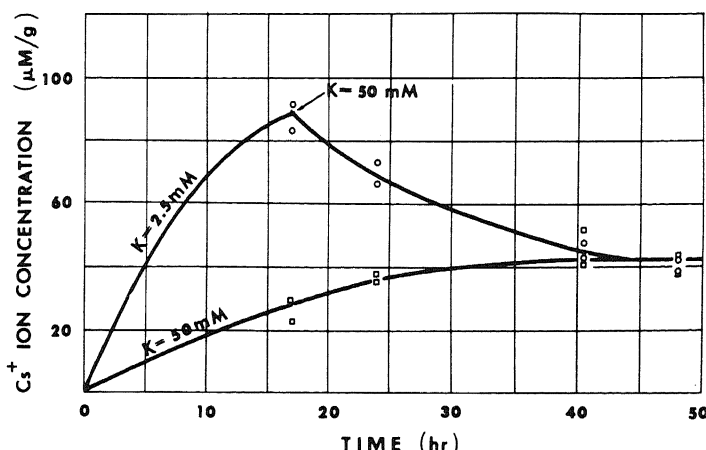


FIGURE 8.1. Effect of K^+ ion on level of labeled Cs^+ accumulation. Frog sartorius muscles were incubated in Ringer solution containing 25 mM labeled Cs^+ and 2.5 mM K^+ (24°C); their paired muscles were incubated in Ringer solution containing the same amount of labeled Cs^+ and 50 mM of K^+ (\square). After 17 hr the muscles in the solution containing 2.5 mM K^+ were transferred to another Ringer solution containing 50 mM K^+ (\circ). [From Ling and Ochsenfeld (1966), by permission of *Journal of General Physiology*.]

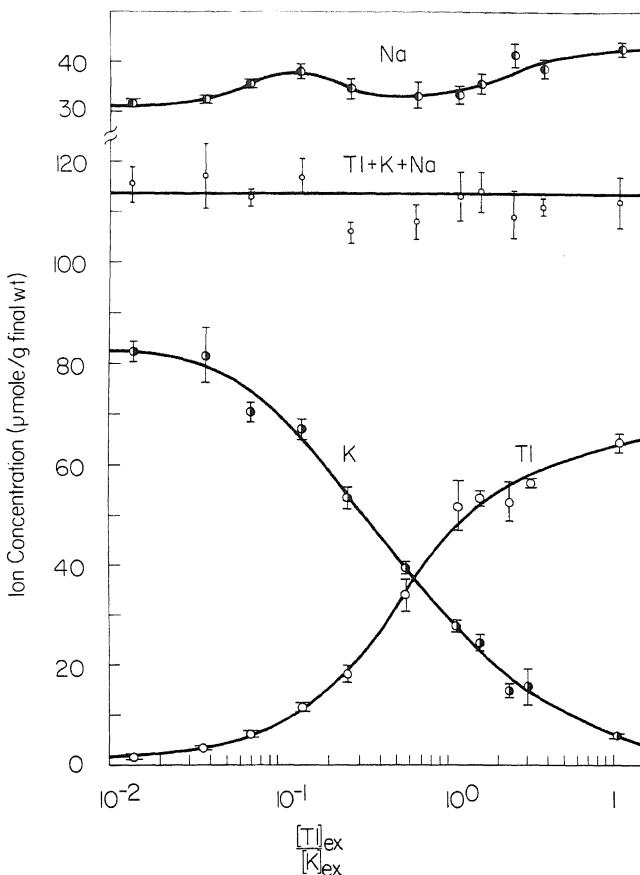


FIGURE 8.2. Equilibrium distribution of Tl^+ , K^+ , and Na^+ in frog muscles. To produce the wide range of $[Tl^+]_{ex}/[K^+]_{ex}$ represented on the abscissa, $[K^+]_{ex}$ was kept constant at 2.5 mM below a $[Tl^+]_{ex}/[K^+]_{ex}$ value of unity. Above that, $[Tl^+]_{ex}$ was kept constant at 4 mM. [From Ling (1977b), by permission of *Physiological Chemistry and Physics*.]

Leaching the sections with distilled water removes the dark-staining materials (Fig. 8.3E), and muscles containing only their normal K^+ , which is not electron-dense, show only vague contours (Fig. 8.3F). Figure 8.4 (Edelmann, 1980a) shows that Rb^+ (atomic weight 85.5) (Fig. 8.4C) and even K^+ itself (Fig. 8.4D) can be visualized when compared with controls that had been leached in water during sectioning. Since we know that Cs^+ and Tl^+ have stoichiometrically replaced K^+ in functionally intact cells, these EM studies show that much of the K^+ is localized in the A bands, and that loci stained with uranium in conventional preparations are the K^+ -binding sites.

8.2.3. Autoradiographic Demonstration of Localization of K^+

Autoradiography offers another possible way to test the prediction that β - and γ -carboxyl groups are the seat of K^+ adsorption. Unfortunately, radioactive K^+ isotopes

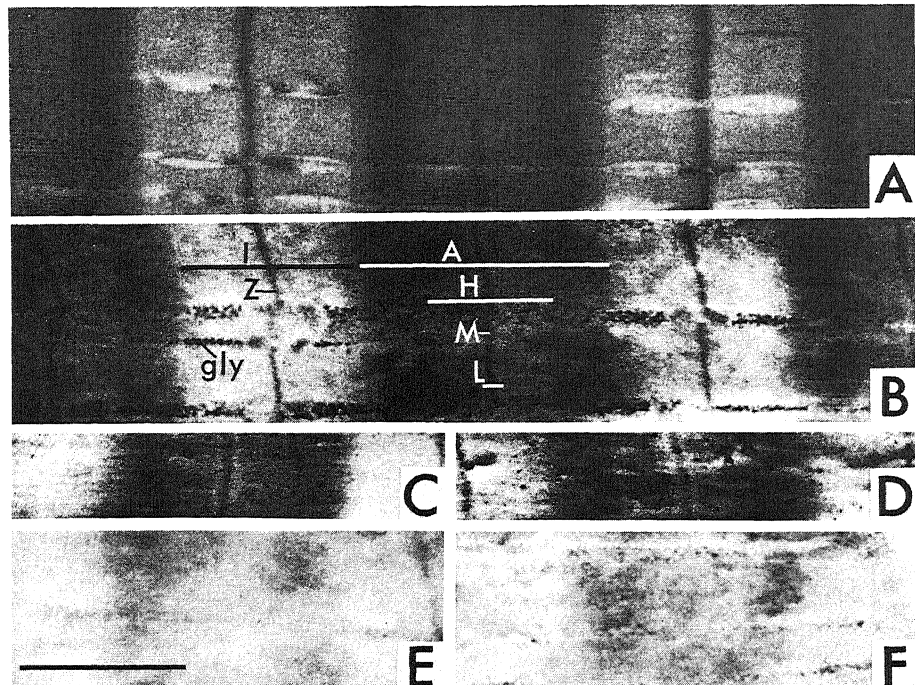


FIGURE 8.3. Electron micrographs of frog sartorius muscle. (A) Muscle fixed in glutaraldehyde only and stained only with uranium by conventional procedure. (B) EM of section of freeze-dried Cs^+ -loaded muscle, without chemical fixation or staining. (C) Tl^+ -loaded muscle without chemical fixation or staining. (D) Same as (C) after exposure of section to moist air, which causes the hitherto even distribution of thallium to form granular deposits in the A band and Z line. (E) Section of central portion of (B) after leaching in distilled water. (F) Normal " K^+ -loaded" muscle. Scale bar: 1 μm [(A) From Edelmann, unpublished. (B-F) From Edelmann (1977b), by permission of *Physiological Chemistry and Physics*.]

are either too short-lived ($^{42}\text{K}^+$) or too expensive ($^{40}\text{K}^+$). Again Cs^+ and Tl^+ are excellent substitutes for K^+ , in the form of their long-lived isotopes $^{134}\text{Cs}^+$ and $^{204}\text{Tl}^+$. As pointed out earlier (Ling and Ochsenfeld, 1966; Ling, 1977b) both ions can stoichiometrically and reversibly replace K^+ in living frog muscles, and muscles with all or a major share of their K^+ replaced by either one of these isotopes remain alive and functional.

8.2.3.1. Air-Drying Technique

Autoradiography of diffusible material in living cells is difficult because the steps involved in preparing thin sections lead to profound alterations in solute distribution. To overcome this difficulty, I chose a simple expedient—to rapidly air-dry $^{134}\text{Cs}^+$ - or $^{204}\text{Tl}^+$ -loaded single muscle fibers (Ling, 1977d).

Figure 8.5A is a picture of a section of a single muscle fiber that has undergone all this treatment, except that no photoemulsion was applied. The picture demonstrates that the dark (A) and light (I) bands are well preserved, showing the orderliness of the myofibrillar structure.

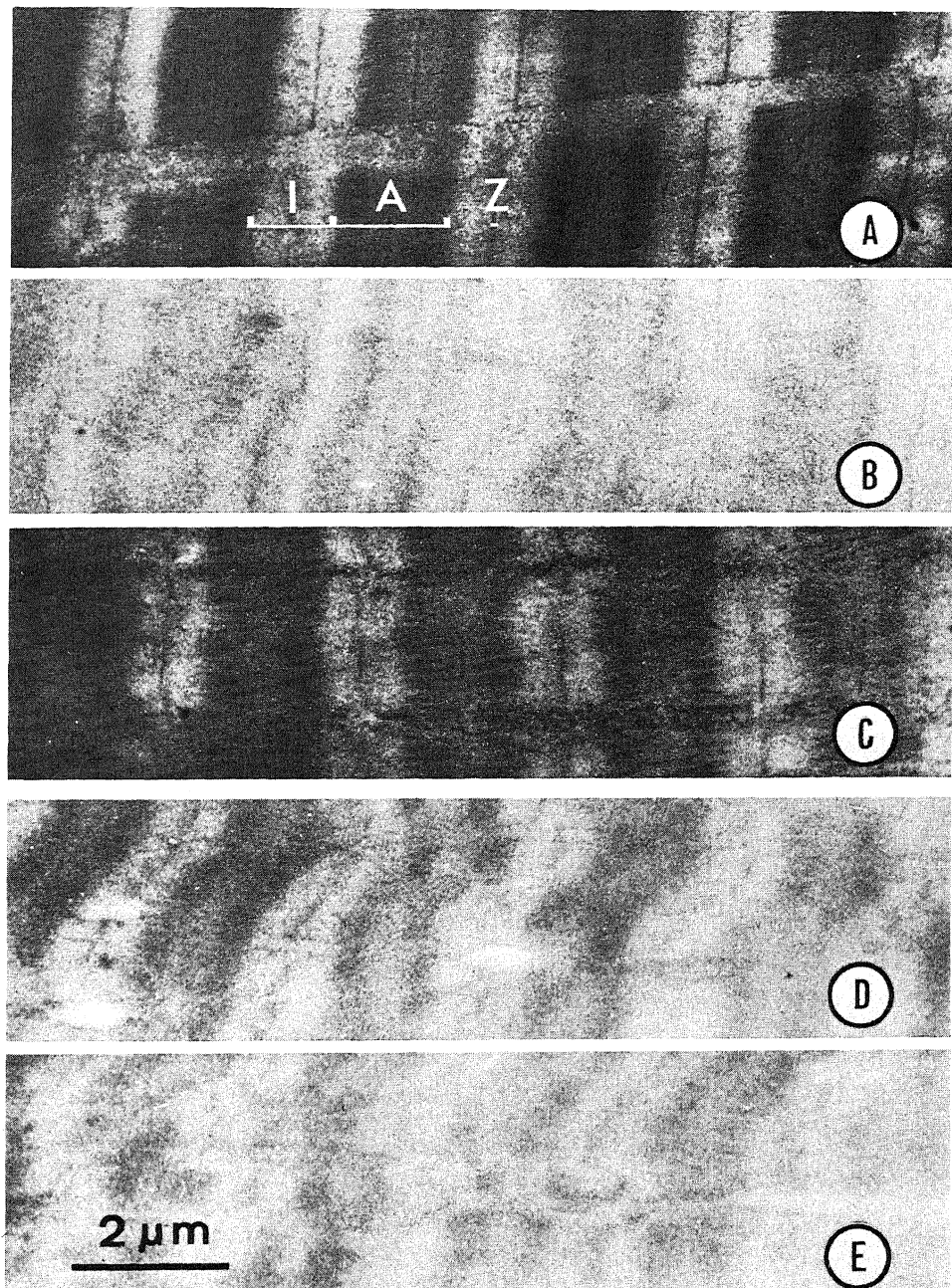


FIGURE 8.4. Transmission electron micrographs of 0.3-μm-thick sections of freeze-dried frog sartorius muscle. (A) Dry-cut section of Cs⁺-loaded muscle. (B) Wet-cut section of Cs⁺-loaded muscle. (C) Dry-cut section of Rb⁺-loaded muscle. (D) Dry-cut section of normal K⁺-containing muscle. (E) Wet-cut section of normal K⁺-containing muscle. A, A band; I, I band; Z, Z line. [From Edelmann (1980a), by permission of *Histochemistry*.]

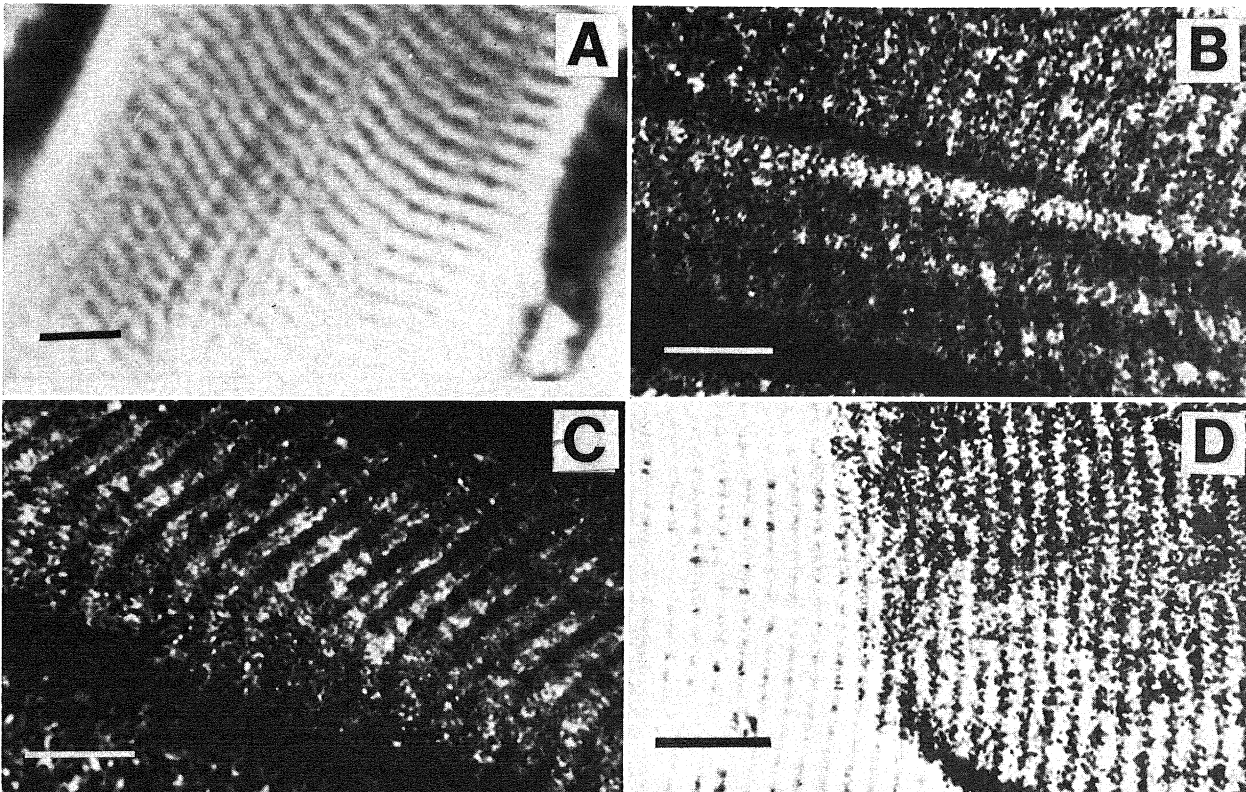


FIGURE 8.5. Autoradiographs of air-dried frog muscle fibers. (A) Single fiber processed as those in the accompanying autoradiographs but not loaded with radioisotopes. (B) Single $^{204}\text{Tl}^+$ -loaded fibers. (C) Single $^{134}\text{Cs}^+$ -loaded fibers that had been stretched before drying. (D) Single $^{134}\text{Cs}^+$ -loaded fiber that was partially covered with photographic emulsion. Scale bars: 10 μm . [From Ling (1977d), by permission of *Physiological Chemistry and Physics*.]

brillar arrangement. Figures 8.5B,C are autoradiographs of ²⁰⁴Tl⁺- and ¹³⁴Cs⁺-loaded muscles. The silver grains are not evenly distributed but are largely arranged in transverse bands. This is in agreement with the finding of Giese and Rekowski (1970), who observed a striated distribution of silver granules in ¹³⁴Cs⁺-loaded rat muscle sections. They could not tell whether the radioactive isotopes were located in the dark A bands or the light I bands. However, Fig. 8.5D, in which the coverage of photoemulsion was only partial, demonstrates that ¹³⁴Cs⁺ is localized in the A band, confirming the conclusions drawn from the EM studies.

Figure 8.5C shows an autoradiograph of a ²³⁴Cs⁺-loaded muscle fiber that had been stretched before drying. The sarcomere length is about 3.5 mm. With this extension, finer structures are revealed: The silver granules are not evenly distributed in the A band but are localized at the two edges of the bands, and there is ¹³⁴Cs⁺ at the Z line. Comparing these autoradiographs with standard uranium-stained sections (Fig. 8.3A), one sees further confirmation of the prediction that ¹³⁴Cs⁺, and hence K⁺, is distributed at loci which in regular EM plates are stained dark.

8.2.3.2. Frozen-Cell Technique

Since the dried muscle cells were retained below the photoemulsion films in the radioautographs shown in Fig. 8.5, one could argue that the banded distribution was due to some sort of visual artifact. To prove unequivocally that this is not the case, Edelmann developed another new technique in which single muscle fibers loaded with ¹³⁴Cs⁺ (as well as other radioactive alkali metal ions) were very rapidly frozen by swift contact with a chilled 3-μm layer of Ilford K5 emulsion deposited on a Formvar-coated glass slide at liquid nitrogen temperature. The application of photoemulsion and exposure were both carried out at the same low temperature. After exposure was completed, the emulsion was first stripped off the glass slide and the muscle cells, and then developed (Edelmann, 1980a). An example of Edelmann's autoradiographs is reproduced here as Fig. 8.6. It is not different from that obtained from the air-dried muscle fibers.

8.2.4. Energy-Dispersive X-Ray Microanalysis

Edelmann (1978) produced yet a third method to investigate the localization of K⁺ in voluntary muscle cells. He directed a focused 0.5 × 0.4-μm beam of electrons in a scanning or transmission electron microscope at different loci in sections of frog muscles, either in their natural K⁺ state or loaded with Cs⁺ or Tl⁺, and analyzed the X-ray spectrum observed. In collaboration with G. Hubert (Siemens, Karlsruhe), he found that (1) the concentrations of Cs⁺, Tl⁺, and K⁺ in the A band are three times higher than those in the I band, (2) the cation concentration is much higher in the Z line than in the surrounding I band, and (3) the concentrations of alkali metal ions accumulated in the two edges of the A band are higher than those in the middle of the A band (Edelmann, 1978). Thus, the X-ray microprobe technique also provides direct evidence for K⁺ (and Cs⁺ or Tl⁺) localization in the A bands.

Trombitas and Tigyi-Sebes (1979; see also Tigyi *et al.*, 1981) soon confirmed the energy-dispersive X-ray microanalysis results of Edelmann, using a similar technique applied to isolated single myofibrils of honeybees. Their data are reproduced in Fig. 8.7.

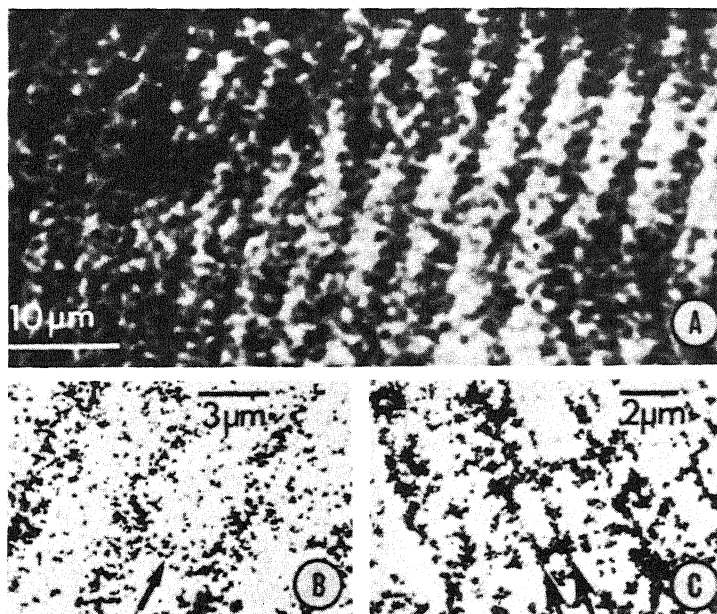


FIGURE 8.6. Autoradiographs of frozen, fully hydrated frog muscle fibers. (A) Light microscopic autoradiograph of a stretched $^{134}\text{Cs}^+$ -loaded fiber. (B) Electron microscopic autoradiograph of a stretched $^{134}\text{Cs}^+$ -loaded fiber. The sarcomere length is about 4.4 μm . Between two dark bands (A bands) a line of silver grains indicates the Z line (arrow). (C) Electron microscopic autoradiograph of a stretched Rb^+ -loaded fiber. The sarcomere length is about 3.3 μm . Arrows indicate dark lines at the outer edges of an A band. [From Edelmann (1980a), by permission of *Histochemistry*.]

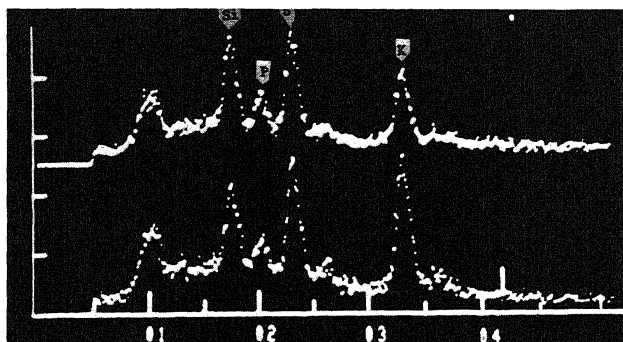


FIGURE 8.7. X-ray microanalytic curves. A bands (lower curve) and I bands (upper curve) of single isolated myofibril from honeybee thorax muscle. [From Tigyi *et al.* (1981), by permission of Springer-Verlag.]

However, the X-ray microprobe analyses of Somlyo *et al.* (1981) led them to the opposite conclusion, i.e., more K^+ in the I band than in the A band. Using new refined techniques not previously available, Edelmann, in conjunction with K. Zierold (in work soon to be published), was able to reproduce Somlyo's data when the K^+ concentration at the *center* of the A band was compared to the K^+ content at the *center* of the I band, including the Z line. On the other hand, a much higher concentration of K^+ is found in the A band than in the I band if K^+ measurement of the I band does not include the Z line (Edelmann, 1983).

8.2.5. Laser Microprobe Mass Spectrometric Analysis

Edelmann's (1980b) fourth method to examine the question of K^+ localization is the new technology called laser microprobe mass spectrometric analysis (LAMMA). Thin sections of freeze-dried normal frog muscle were dipped in a solution containing 50 mM K^+ , 50 mM Na^+ , and 10 mM Cs^+ and then freed of adhering fluid. A hole was vaporized in the A band by a focused laser beam and the atoms collected and analyzed quantitatively in a mass spectrometer. Peak heights in Fig. 8.8B, when compared to a control gelatin film containing known quantities of 50 mM K^+ , 50 mM Na^+ , and 10 mM Cs^+ (Fig. 8.8A), revealed a preferential uptake of K^+ over Na^+ . This preference becomes more prominently displayed in Fig. 8.8D, where the sections were exposed to a solution containing only 100 mM Na^+ and 10 mM K^+ . Even more remarkable is the finding that the inclusion of Li^+ (50 mM) causes not only accumulation of Li^+ but also an enhanced uptake of Cs^+ (Fig. 8.8C). Indeed, if a freeze-dried dry-cut section was exposed for 5 min to a solution containing 100 mM LiCl and 10 mM CsCl, a picture

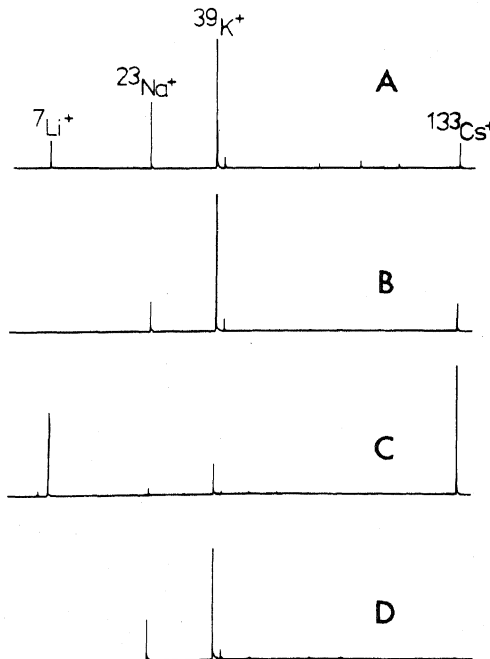


FIGURE 8.8. LAMMA spectra. (A) Gelatin standard containing 50 mM LiCl, 50 mM NaCl, 50 mM KCl, and 10 mM CsCl. (B-D) A-band regions of muscle sections exposed to a solution containing (B) 50 mM NaCl, 50 mM KCl, and 10 mM CsCl; (C) 50 mM NaCl, 50 mM KCl, and 10 mM CsCl in addition to 50 mM LiCl; and (D) only 100 mM NaCl and 10 mM KCl. [From Edelmann (1980b), by permission of *Physiological Chemistry and Physics*.]

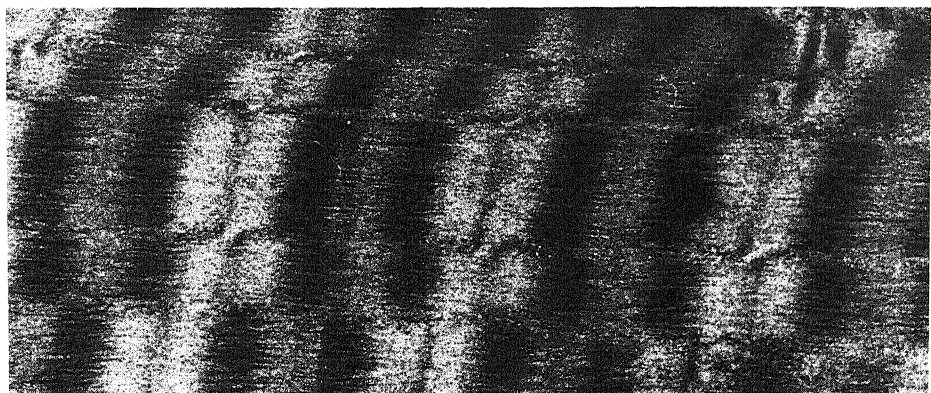


FIGURE 8.9. 0.2- μm -thick section of chemically unfixed frog sartorius muscle, freeze-dried and embedded. The section was exposed for 5 min to an aqueous solution containing 100 mM LiCl and 10 mM CsCl. [From Edelmann (1980b), by permission of *Physiological Chemistry and Physics*.]

in every way duplicating the conventionally fixed and uranium-lead-stained EM plate was produced (Fig. 8.9).

More detailed studies are shown in Figs. 8.10 and 8.11 (Edelmann, 1981). The upper left corner of Fig. 8.11 represents a standard gelatin strip containing the same concentrations of the five alkali metal ions that are in the solution to which the freeze-dried, plastic embedded, 0.2- μm -thick sections of sartorius muscle were exposed (50 mM Li⁺, 50 mM Na⁺, 10 mM K⁺, 10 mM Rb⁺, and 10 mM Cs⁺). The numbers of the observed spectra in Fig. 8.11 correspond to holes similarly labeled in Fig. 8.10. Hole 7 was in the embedding medium; the corresponding spectrum in Fig. 8.11 showed only trace amounts of the alkali metal ions. Holes 6 and 9 were in areas where another hole had already been burnt; these spectra show relatively low levels of ions, in particular Li⁺. The remaining spectra from holes in fresh areas indicate a consistent pattern, where the selectivity follows the order of either Li⁺ > Cs⁺ > Rb⁺ > K⁺ > Na⁺ or Cs⁺ > Li⁺ > Rb⁺ > K⁺ > Na⁺. In all cases a high degree of selectivity of K⁺, Rb⁺, Cs⁺, and Li⁺ over Na⁺ was observed. Thus, by comparing peak heights with those of the standard gelatin, the data of Figs. 8.10 and 8.11 indicate a higher selectivity coefficient of Cs⁺ over Na⁺, as seen in living frog muscle cells (Ling and Bohr, 1971a,b).

8.2.6. Implications of the Adsorbed State of K⁺ in Muscle Cells

The application of these four different methods in three different laboratories provides strong, mutually supportive evidence that K⁺ in striated muscle cells is localized in the A bands and Z lines. Moreover, the K⁺—and ions like Cs⁺, Rb⁺, or Li⁺ that can replace it—are not simply hovering in the vicinity of fixed charges, as visualized in Gregor's theory of ion exchange resins (Section 4.4.2.1), but are adsorbed specifically onto fixed anions within the A bands and Z lines. The LAMMA spectra of sections of muscle (Figs. 8.8–8.11), which are obtained in thin slices of muscle $\frac{1}{500}$ th the diameter of the cell, prove conclusively that the selectivity observed among the cations is not deter-

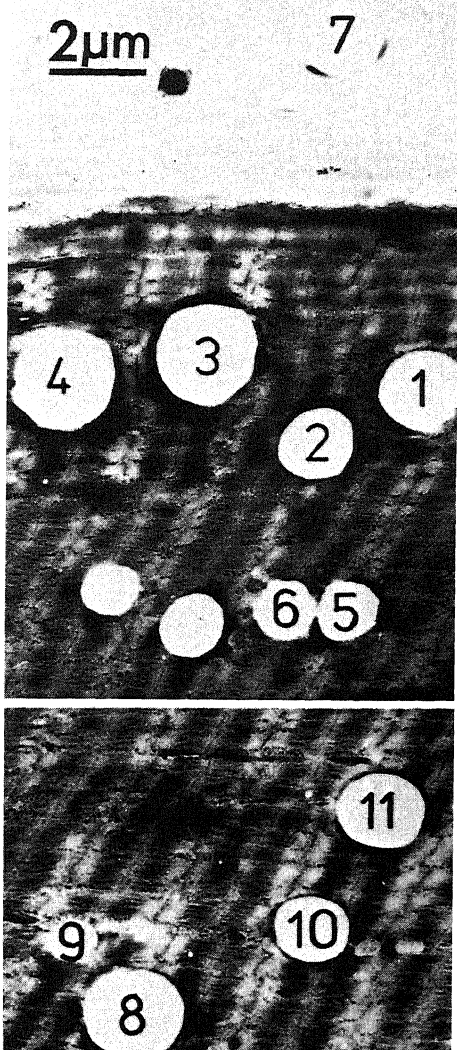


FIGURE 8.10. Sections of frog sartorius muscle perforated by the laser beam. [From Edelmann (1981), by permission of *Fresenius' Zeitschrift für Analytische Chemie*.]

mined by surface membrane processes. Moreover, the ability of the A^{\prime} band to choose selectively between cations of the same valence means that the short-range forces between cation and fixed anion are the critical ones. Short-range attributes such as dipole moment, polarizability, or Born repulsion constant can make one univalent cation preferred over another only if the cation is in constant contact with the fixed anion.

Experiments to be fully described in Section 11.2.1.1a show that in frog muscle two alkali metal ions (K^+ and Cs^+), both permeant to the cell membrane, can have different quantitative effects in displacing $^{42}\text{K}^+$ -labeled K^+ originally in the cell. Again, the short-range attributes of the competing ions are playing a decisive role in deciding the relative preference of one ion over another. Yet another technique proves that the specificity in

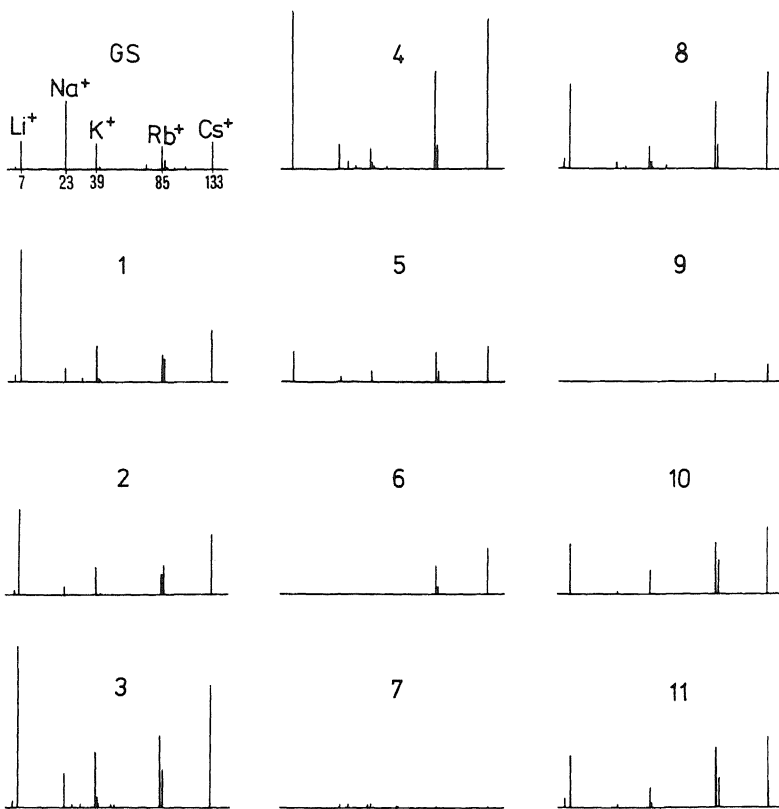


FIGURE 8.11. LAMMA spectra recorded from a muscle specimen. The numbers correspond to the respective probing areas shown in Fig. 8.10. The spectrum labeled "GS" stems from a gelatin standard containing 50 mM Li^+ , 50 mM Na^+ , 10 mM K^+ , 10 mM Rb^+ , and 10 mM Cs^+ . The spectra are described in the text. [From Edelmann (1981), by permission of *Fresenius' Zeitschrift für Analytische Chemie*.]

this ion preference cannot be at the cell membrane. Figure 8.12 shows that the same specificity in monovalent cation accumulation seen in intact cells is present in an effectively membraneless open-ended muscle cell preparation after the cell membrane has been partly amputated and the remaining membrane (and postulated pumps) made effectively nonfunctional, as outlined in Section 5.2.6.

Proof that K^+ is adsorbed specifically within the A bands and Z lines has additional, profound implications for the membrane theory of the cellular resting potential and of cellular volume control. It means not only that intracellular K^+ is not free in solution, but also that intracellular water cannot exist in a normal state. Indeed, mere localization of K^+ as a free ion in the A band and Z line would create just as insurmountable a difficulty for the membrane theory: A large osmotic pressure difference between the K^+ -rich A band and the K^+ -poor I band would develop since K^+ is the only major solute in the muscle cells. The result would be extensive swelling of the A band and shrinkage of the I band, neither of which, of course, occurs.

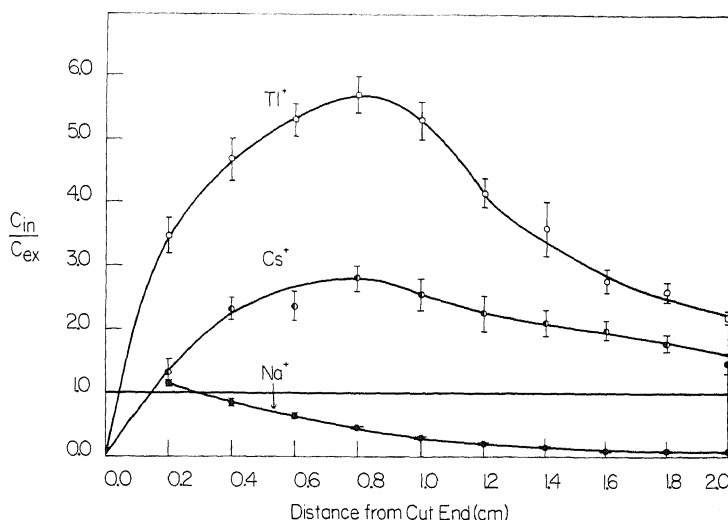


FIGURE 8.12. Accumulation of labeled Tl⁺, Cs⁺, and Na⁺ in frog sartorius EMOC preparation. Source solution contained 1 mM ²⁰⁴Tl-labeled Tl⁺, 1 mM ¹³⁴Cs-labeled Cs⁺, and 100 mM ²⁴Na⁺-labeled Na⁺. Ordinate represents ionic concentration in cell water divided by the final concentration of the same ion in the source solution bathing the cut end at the conclusion of the experiment. Incubation was for 3 days at 25°C. [From Ling (1977b), by permission of *Physiological Chemistry and Physics*.]

Although this evidence for K⁺ adsorption now seems irrefutable, I will present in Section 8.4 a reevaluation of the results of other studies, many of which have been previously cited as proof for "free" K⁺ in living cells (Chapter 5).

8.3. X-Ray Absorption Edge Fine Structure of K⁺ in Frog Erythrocytes

When a monochromatic X-ray beam passes through a thin sample of an aqueous solution, part of the beam is absorbed to a degree depending on the photon energy of the incident beam. By expressing the intensity of the incident beam (I_0) as a ratio of the transmitted beam at different photon energies, an edge spectrum is obtained. This spectrum offers a direct measurement of the atomic state of the atoms. Huang *et al.* (1979) showed that the absorption edge fine structure of various K⁺ salts and complexes is quite specific. The absorption edge fine structure of K⁺ in frog erythrocytes is quite different from that of a salt solution that contains K⁺ in a similar concentration. This finding led Huang *et al.* to conclude that "the differences represented [in Fig 8-13] are the characteristic of the complex binding of K⁺ in these frog blood cells and that for potassium, the cell cannot be regarded as an aqueous solution" (Huang *et al.*, 1979, p. 193).

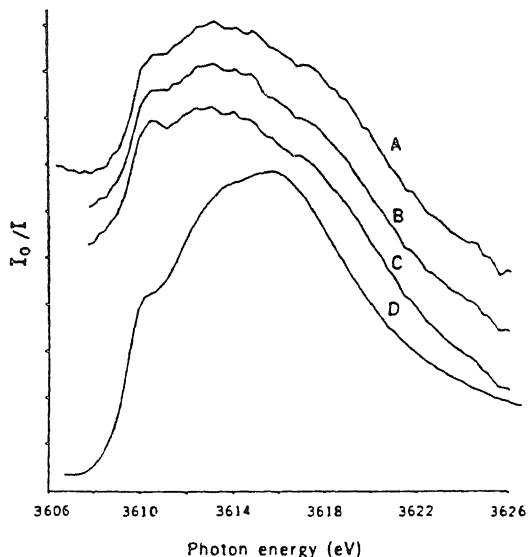


FIGURE 8.13. Peak regions of the absorption edge fine structures. (A) Peak region of spectrum of frog blood cells where the measuring time per data point was 10 sec. (B and C) Same spectrum with better statistics, 30 and 50 sec per data point, respectively. (D) Peak region of spectrum of dilute aqueous solution. [From Huang *et al.* (1979) by permission of *Science*.]

8.4. Secondary Evidence for K^+ Adsorption in Living Cells

8.4.1. K^+ Mobility in Living Cells

The demonstration by Hodgkin and Keynes (1953) (Section 5.1.2) that K^+ in squid axons has a mobility virtually the same as that in seawater has been widely cited as evidence against selective K^+ adsorption.

Thus B. Katz in his book *Nerve, Muscle, and Synapse* (1966) wrote

Moreover these latter authors [Ernst, Troshin, and Ling] take the view that the potassium ions do not merely form counterions to the negatively charged colloidal structure but possess selective affinity and are chemically bound to the proteinates.

It seems, however, very difficult to support this view in the face of the following pertinent observation by Hodgkin and Keynes (1953). These results are discussed in detail because they are of crucial importance in the still persistent argument about the validity of the membrane concept. . . . It was clear therefore that the labeled $[K^+]$ ions that had entered the axoplasm continued, inside cells, to behave as free ions with approximately normal mobility.

8.4.1.1. New Findings in Squid Axons

Isolated squid or cuttlefish axons are separated from their cell nuclei and are deficient in the sense that they cannot survive over long periods of time, as can, for example, intact frog muscle cells. Hodgkin and Keynes took great pains to monitor the health of their axons by testing their electrical excitability from time to time. However, subsequent development of the perfused axon preparation showed a total functional isolation of electrical activity from properties of the axoplasm (Section 5.2.3). Indeed the axo-

plasm could be removed altogether without affecting the normal electrical activity of the surface membrane sheath.

8.4.1.2. Ionic Association Does Not Necessarily Lead to a Drastic Reduction in Mobility

B. Katz (1966), in criticizing my theory of selective K^+ adsorption in 1966, did not mention what was clearly stated in my monograph (Ling, 1962), that ions adsorbed on a chain or surface of fixed ionic sites do not necessarily have reduced mobility. The mobility of these ions may be equal to or even higher than that in free solution (Ling, 1962, p. 338). Thus K^+ adsorbed on a glass surface diffuses faster than in free solution (McBain and Peaker, 1930; Mysels and McBain, 1948; Nielsen *et al.*, 1952). Similarly, the longitudinal conductance of a polyelectrolyte is higher than its lateral conductance in long tubes containing a flowing solution of linear polyanions (e.g., polyphosphate, DNA), again indicating the greater mobility of counterions along the length of a parallel array of oriented polyanions than across it (Schwindewolf, 1953; Heckmann, 1953; Eigen and Schwarz, 1957).

These findings support the idea that ionic association does not *necessarily* lead to drastic reduction of ionic mobility. When closely placed anionic sites are oriented along the direction of measurement of mobility or conductivity, the counter cation may move rapidly. On the other hand, if the sites are far apart or are not oriented in the direction of the measurement, the mobility may then be much lower (Fig. 8.14).

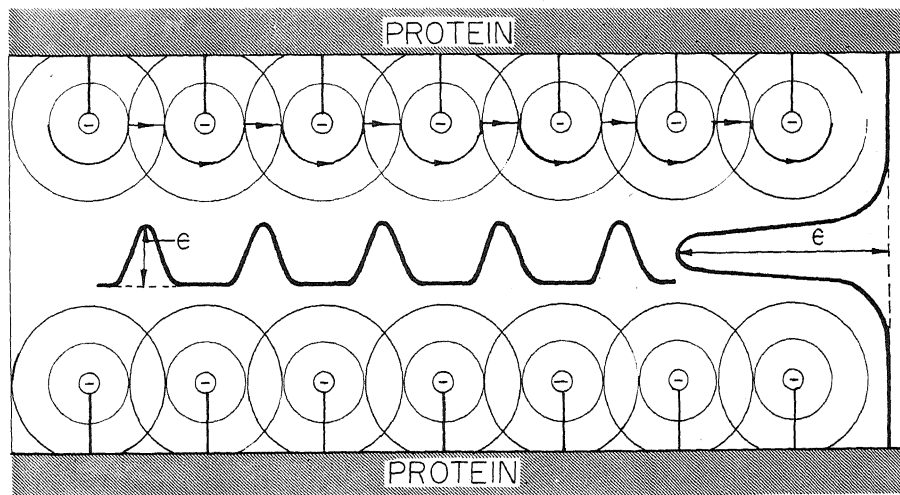


FIGURE 8.14. Diagrammatic illustration of an effective conduction band for adsorbed ions along a longitudinal array of anionic sites. Transversely, the anionic sites are too far apart to produce a conduction band, and low conductance results. The concentric circles represent equipotential lines, with lower potentials closer to the anions. The line with the arrows indicates a probable path for an adsorbed ion moving along the conduction band; it has to overcome relatively low activation energies because of the overlapping of the electric fields. Much larger activation energy has to be overcome for transverse migration. [From Ling (1969a), by permission of *International Review of Cytology*.]

8.4.1.3. Measurement of Ionic Mobility and Conductivity in Frog Muscle, Human Erythrocytes, and Other Tissues Using High-Frequency Alternating-Current Impedance Bridges

Hodgkin and Keynes measured the mobility of K^+ in isolated squid axon under a steady, direct-current (DC) electric field of +0.43 to -0.63 V/cm. Since the axon was cut at both ends and the electrodes were placed just outside the amputated ends, the interference resulting from the high resistance of the plasma membrane was avoided. This method obviously is limited to very large cells.

Another way to achieve the same end is to measure the conductance with alternating currents (AC) of high frequency, in which case the membrane resistance is short-circuited. Indeed this approach was taken by Höber (1912, 1913) to measure the conductance of frog muscle (Table 8.1). His conclusion was that the cytoplasmic conductance of intact frog muscles is equivalent to that of 0.1–0.2% NaCl instead of that of an isotonic 0.7% NaCl solution. Thomson (1928), using an improved technique and a frequency of 10 megacycles per second (MHz) confirmed Höber's finding and showed that muscle cytoplasm has a conductivity equal to that of a 0.2% NaCl solution (Table 8.1). Later Fricke and Morse (1926) and Fricke and Curtis (1934) measured conductivity of the cytoplasm of sheep and bovine erythrocytes, again obtaining values considerably lower than those to be expected if the intracellular ions were in the free state.

In years following, techniques were developed that permitted measurement at a much higher frequency, thereby completely eliminating the contribution of membrane resistance. Thus Pauly and Schwan (1966) showed that the membrane resistance of human erythrocytes was completely cancelled at frequencies of 50–100 MHz. Measurements were therefore made at these frequencies.

To analyze their data, Pauly and Schwan calculated an *ideal internal conductivity* on the basis of the ionic composition of human erythrocytes and on the assumption that all ions are free to diffuse as if the entire erythrocyte were filled with an aqueous salt solution. The ideal specific internal conductivity was 14.5 mmho/cm. Since a large part of the cell interior is occupied by hemoglobin, the actual volume in which the ions, supposedly free, are distributed is smaller and therefore the ionic conductivity higher.

TABLE 8.1. Electrical Conductance of Frog Muscle Compared to That of an 0.1 M KCl Solution

Reference	Solution/preparation	Frequency (Hz)	mmho/cm
Hodgman <i>et al.</i> (1961)	0.1 M KCl (25°C)		12.9
Höber (1913)	Sartorius	0.9×10^7	1.7–3.6
Philipsson (1920)	Sartorius	90	5.5
Hartree and Hill (1921)	Sartorius		6.8
Thomson (1928)	Gastrocnemius	10^7	3.5
B. Katz (1966)	Gastrocnemius	10^7	4.5
G. N. Ling (unpublished)	Sartorius	DC	3.6 ^a
G. N. Ling and C. Miller (unpublished)	Mixed small muscles	2.5×10^9	6.2

^aLongitudinal conductance, ends of muscles amputated, extracellular space fluid removed by prior centrifugation.

Pauly and Schwan showed that the conductivity should be about 23.0 mmho/cm. The measured internal specific conductivity in red blood cells at 25°C, however, is only 4.4–5.9 mmho/cm. Pauly and Schwan made various corrections in an attempt to bring the experimentally observed conductivity and the ideal conductivity into agreement, but reached the conclusion that a discrepancy of a factor of 2 still remained. They further pointed out that the same conclusion could be drawn from data from prior studies on liver cells (Rajewsky, 1938), eye lens (Pauly and Schwan, 1964), and muscle tissues (Table 8.1).

Table 8.1 also shows the recent measurements of conductivity of frog muscle from this laboratory. Note that the long-duration longitudinal DC conductivity of frog sartorius muscle cytoplasm is equal to about two thirds of the high-frequency (250 MHz) conductance of randomly oriented intact frog muscles. This subject will be taken up again in the next section.

8.4.1.4. K⁺ Mobility in Frog Muscle Cells

Ling and Ochsenfeld's (1973a) study of K⁺ mobility in frog muscle cytoplasm contradicted both that of Hodgkin and Keynes (1953) and that of Kushmerick and Podolsky (1969) (Section 5.1.2).

In both of these earlier works a small amount of ⁴²K⁺ was introduced into the excised axon or muscle cell fragment. In each case the nerve or muscle cell segment had both ends open, a condition favoring deterioration. In our experiments, we took advantage of the fact that isolated intact frog muscle could be maintained for a whole week at room temperature without serious deterioration (Ling and Bohr, 1969). Thus it became possible to replace all or most of the cell K⁺ by ⁴²K-labeled K⁺. Clearly, in this case we could measure the mobility of all or nearly all the K⁺ in the cell, and not just a small fraction of it which might not be representative of the total K⁺.

Frog sartorius muscle charged with ⁴²K⁺ was mounted in a glass tube essentially the same as that shown in Fig. 5.12 [see also panel (A) of Fig. 8.15]. The tibial end was then cut at a point sufficiently far removed from the tapering tip to avoid the inclusion of any fibers with intact ends. As was pointed out in Section 5.2.6, all fibers in a sartorius muscle run from one end of the muscle to the other.

Altogether 72 sets of experiments were carried out on normal muscles. Representative data are shown in Fig. 8.15B–H. Of the 72 sets, 22 experiments showed a diffusion profile of ⁴²K⁺ that can be fitted by a single diffusion coefficient. This type is illustrated in F–H. The self-diffusion coefficient D_K for ⁴²K⁺ in the cytoplasm is $(2.7 \pm 0.13) \times 10^{-6}$ cm²/sec. The majority of experiments show data points that cannot be fitted with a single D_K. Rather, these disjointed profiles can be fitted with two distinctly different values of D_K, as illustrated in B–E. The part of the data from the area toward the intact end of the muscle yielded, in all 50 experiments, a D_K of $(2.61 \pm 0.11) \times 10^{-6}$ cm²/sec, in reasonable agreement with the 22 sets of experimental data showing nondisjointed profiles. However, the points near the cut end of the 50 disjointed profiles gave a much higher D_K of $(7.60 \pm 0.37) \times 10^{-6}$ cm²/sec. This higher diffusion coefficient obviously corresponds to the part of the muscle fiber that is deteriorated, as confirmed in Fig. 5.16, which shows the rather abrupt drop of total K⁺ concentration at the cut edge.

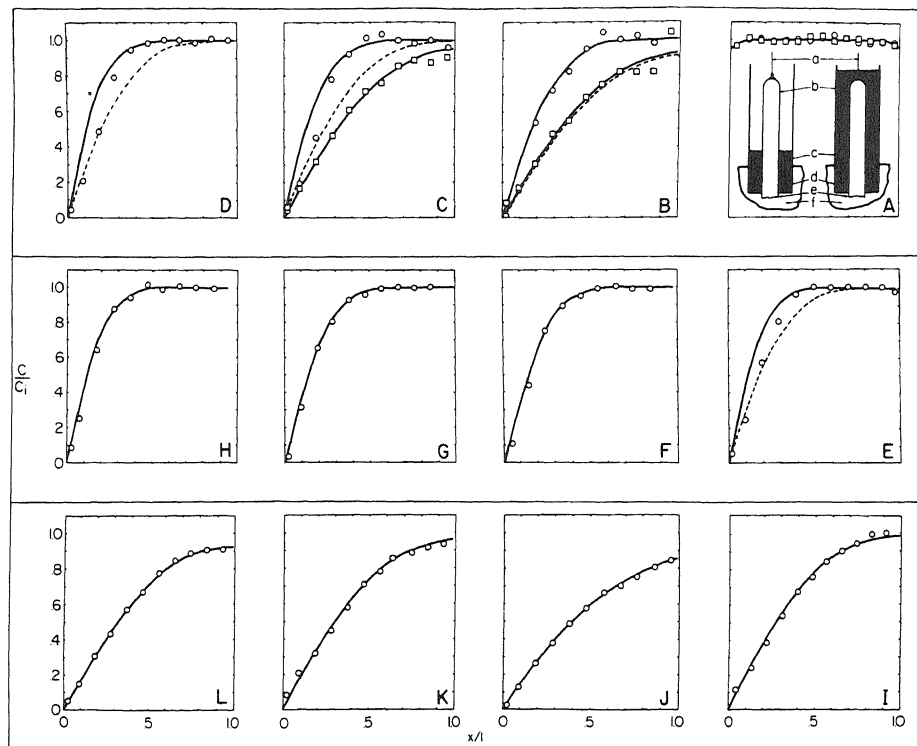


FIGURE 8.15. Diffusion profiles of labeled K^+ from living (A–H) and dead (I–L) frog sartorius muscles. The ordinate represents the concentration (C) of labeled K^+ as a fraction of the initial concentration (C_i) in the muscle. The abscissa is x/l , where x is the distance from the cut end and l is the total length of the muscle. O, $^{42}K^+$; □, tritiated water. (A) The curve at the top shows the initial distribution of ^{42}K throughout the length of the muscle. The figures at the bottom illustrate two types of EMOC setups with varying levels of Vaseline: a, anchoring string; b, sartorius muscle; c, Vaseline; d, silicone rubber gasket with close-fitting slit; e, cut end of muscle; f, bathing solution. (B–E) The solid lines going through most of the open circles are based on one D_{Kt}/l^2 value, and the dotted lines going through the open circles near the cut edge are based on another value. (F–L) The solid lines are theoretical diffusion profiles that fit all the experimental points on the basis of a single value of D_{Kt}/l^2 . The incubating solution for normal muscles contained 2.5 mM labeled K^+ ; that for muscles killed with IAA contained 5 mM labeled K^+ (to provide enough counts). [From Ling and Ochsenfeld (1973a), by permission of *Science*.]

Any doubts that cell deterioration led to the increase of the K^+ diffusion coefficient are dispelled by the data of Fig. 8.15I–L, showing the $^{42}K^+$ diffusion profiles of dead muscles. These muscles in full rigor at resting length were killed while still *in situ* by injection of iodoacetate (IAA) into the live frogs. The diffusion profile of 19 sets of data yielded a D_K equal to $(1.47 \pm 0.10) \times 10^{-5}$ cm 2 /sec. Comparing all these data with the self-diffusion coefficient of $^{42}K^+$ in a 0.1 N KI solution, 2.005×10^{-5} cm 2 /sec (Mills and Kennedy, 1953), we reached the following conclusions:

1. D_K in normal healthy cytoplasm is one eighth of that in free solution.

2. D_K in injured cytoplasm is about one third of that in free solution.
3. D_K in IAA-killed cytoplasm is about three quarters of that in free solution.

We also addressed the question raised by Kushmerick and Podolsky: Is the slowdown due to the presence of mechanical barriers that offer the same impediment to diffusion of all solutes? The data of Figs. 8.15B,C show that this is not the case. Simultaneous runs of ⁴²K-labeled K⁺ and tritiated water showed that, while in these muscles D_K was one seventh of that in free solution, the diffusion coefficient of tritiated water in the same muscles measured over the same period often is only one half of that of tritiated water in dilute salt solution.

Six years after the publication of this work, Kushmerick (1979) suggested that the greatly reduced D_K that we had observed might be due to the restraining effect of a residual electrical potential between the cytoplasm and the cut end. He argued that the cell interior is electrically negative and would thus tend to hold the K⁺ inside, reducing D_K . However, we have on three separate occasions presented evidence that such an electrical potential difference does not determine the rate of ionic movement (Ling, 1979c):

1. In the paper (Ling and Ochsenfeld, 1973a, p. 81) that Kushmerick criticized, we pointed out that, if there were any force restraining ⁴²K⁺ diffusion at the cut surface, the diffusion profile could not possibly be one described by diffusion equations derived without such restraint.
2. The diffusion coefficient of labeled Na⁺ in frog muscle cytoplasm is, within an experimental error of 18%, the same whether one measures the movement of labeled Na⁺ into the cells from the external solution bathing the tibial end or the movement of labeled Na⁺ outward from loaded muscles (Ling, 1978a). This is so in spite of the fact that the tibial ends of the muscles in these experiments remained intact and must have had a full resting potential.
3. In frog sartorius muscles with their cut ends dipped into the bathing solution containing ³⁵SO₄, one would expect the resting potential to retard the inward flux of SO₄²⁻, and that depolarization of the resting potential by prior soaking in a 0.1 N K₂SO₄ solution would cause an increased penetration of labeled SO₄²⁻. Data reproduced in Fig. 8.16 show clearly that the potential has no effect on the entry of labeled sulfate.

Edzes and Berendsen (1975) suggested that the low diffusion coefficient of K⁺ found by Ling and Ochsenfeld (1973a) might be due to intracellular membrane barriers impeding K⁺ diffusion. However, Edzes and Berendsen ignored the fact, just mentioned, that simultaneously measured tritiated water mobility is reduced to only half of that in free aqueous solution. This rules out simple mechanical barriers. The coexistence of a low K⁺ mobility and high water mobility requires the presence of selective membrane barriers *across* the interior of the individual muscle fibers.

The data presented in Table 8.1 also rule out such an interpretation. If K⁺ is all free and its mobility reduced because of transcellular membranes, the longitudinal conductivity when measured with DC must be greatly reduced compared to that measured with high-frequency AC. Yet the longitudinal DC conductance is only slightly less than the AC conductance at 250 MHz, and this difference is about the same as that found

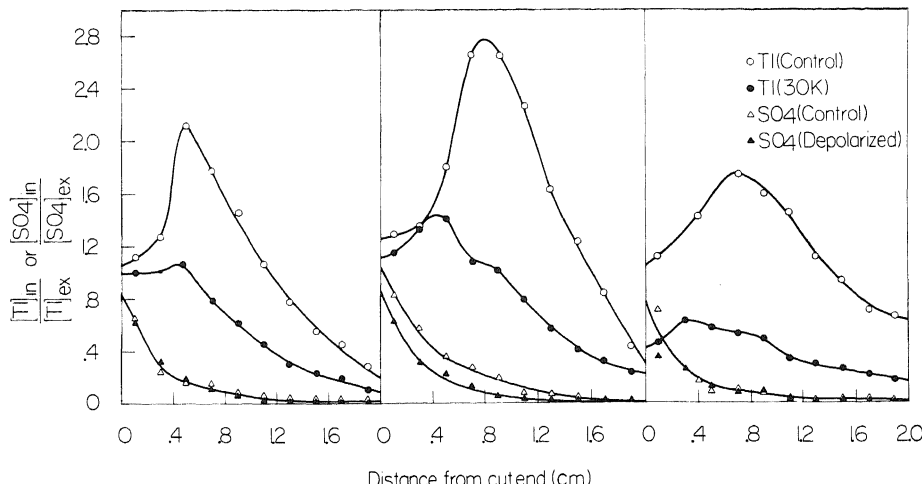


FIGURE 8.16. Influence of K^+ and electrical depolarization upon the accumulation of cationic-labeled Tl^+ and anionic-labeled sulfate. Source solution contained either 0.5 mM KCl (control) or 30 mM KCl (experimental). Experimental muscles (but not the controls) were exposed with gentle shaking to K_2SO_4 Ringer containing 100 mM K^+ for 1 hr before being mounted in EMOC tubes to depolarize the muscle. Incubation was at 25°C for 24 hr. [From Ling (1977b), by permission of *Physiological Chemistry and Physics*.]

in red cell suspensions measured at 250 and 10 MHz (5.8 versus 4.7 mmho/cm) (Pauly and Schwan, 1966).

With the knowledge that K^+ is adsorbed (Section 8.2), the interesting question arises: Why should the ohmic longitudinal DC conductance be reduced from that of a 0.1 N KCl solution by a factor of only 3, while K^+ mobility is reduced by a factor of 8? First, one must remember that conductance of KCl is partly due to K^+ and partly due to Cl^- . Thus the low mobility of K^+ may be compatible with a much higher conductivity if one assumes that all the anions in the cell are free and conducting. However, this is not likely because the major intracellular anions in muscle are creatine phosphate (CrP) and ATP, and their higher molecular weights imply lower diffusion coefficients and conductivities. D for ATP is about 0.3×10^{-5} cm 2 /sec (Kushmerick and Podolsky, 1969) and thus only one fifth of that of Cl^- (1.60×10^{-5} cm 2 /sec) (Mills, 1961). Evidence exists that neither CrP nor ATP is free in living cells. For example, they have been shown to be localized in distribution in muscle much as K^+ is (D. K. Hill, 1960, 1962), and the binding constant of ATP on myosin (10^{10} - 10^{11} M $^{-1}$) (Goody *et al.*, 1977; Cardon and Boyer, 1978) is enormous. From these considerations, it would appear that the longitudinal conductance must be largely due to K^+ .

A possible solution to the disparity between diffusion coefficient and conductance is, however, given in Fig. 8.14, which shows a sort of K^+ -conducting band along linear arrays of fixed anions. This system permits a row of adsorbed K^+ ions to work like a chain of billiard balls (Fig. 8.17), as in the well known von Grotthuss phenomenon, in which the conductance of H^+ at 24°C (in mho/cm 2) is nearly five times higher than that of ions of approximately similar size such as K^+ , NH_4^+ , and Na^+ (Glasstone, 1946,

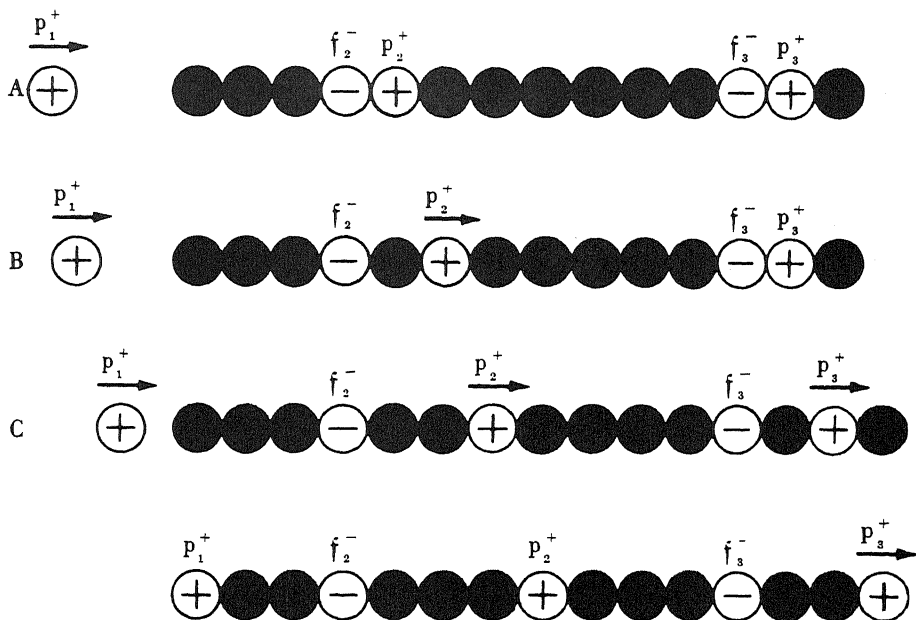


FIGURE 8.17. The migration of cations through a fixed-charge system by triplet formation. This diagram represents the events that occur as an interstitial cation (p_1^+) approaches a fixed anion–countercation pair ($f_2^- p_2^+$). (A) As the cation p_1^+ approaches the fixed anion f_2^- , p_1^+ effectively decreases the c -value of this fixed anion. (B and C) Consequently p_2^+ tends to assume a high conformation, with more water molecules interspersed between f_2^- and p_2^+ (water molecules are represented as solid circles). At this greater distance of separation from f_2^- , p_2^+ has to overcome a much lower activation energy to migrate from f_2^- toward an adjoining fixed anion–countercation pair, $f_3^- p_3^+$. (D) In this process, it acts on $f_3^- p_3^+$ as p_1^+ acted on $f_2^- p_2^+$, thereby initiating a chainlike migration. This type of migration—which is very effective when p_2^+ and p_3^+ are like the K⁺ ion, which readily shifts its conformation number with a c -value change—becomes less effective when p_2^+ and p_3^+ are like the Cs⁺ ion, which tends to remain at a fixed low conformation in spite of c -value changes. [From Ling (1962).]

p. 895). In the von Grotthuss chain type of electric conductance one H⁺ can cause displacement of another H⁺ of a neighboring H₂O molecule through a chain of displacement and dissociation without actual long-range migration. In the following section I shall discuss other findings that can be explained by the K⁺-conducting band concept.

8.4.1.5. Intracellular Conductivity in *Aplysia* Neurons and Squid Axons

Carpenter *et al.* (1973) measured the electric conductivity of the cytoplasm of the giant neuron bodies (ca. 800 μm in diameter) of the visceral, pleural, and pedal ganglia of the sea slug, *Aplysia californica*. They used two techniques. The primary technique utilized a single platinum electrode insulated with glass except for the tip, which was coated in platinum black. The finer electrodes used had a tip diameter of 1 μm . A second technique, adapted from Li, Bak, and Parker (1968), used a linear array of four equally spaced glass-coated platinum electrodes, the total distance between the outermost electrodes being 500 μm . A constant current pulse (1 to 10 μamp , 1-msec duration) was

passed between the two outermost electrodes and the voltage drop between the middle pair was measured.

With the first technique these authors measured equivalent capacity, C_x , which, when the frequency of the current is high enough and when other conditions are met, is linearly related to $1/p$, where p is the specific resistance (in ohm·cm):

$$C_x = \frac{1}{p} \cdot \frac{4\pi a}{\omega} \quad (7.1)$$

where $4\pi a/\omega$ is a calibration factor. From single and multiple electrode measurements they showed that the average equivalent conductance in the cell bodies is markedly reduced and is equivalent to that of only a 5.7% seawater solution!

With the same technique, these authors measured the conductivity of giant squid axons and of *Myxicola infundibulum*. Although these axon studies were much less extensive and were carried out with poorer electrodes, the results suggest that the conductance in squid axons is not far from that of full-strength seawater, and that the conductance in *Myxicola* is close to that of 50% seawater.

In a later paper, Foster, Bidinger, and Carpenter (1976) used a larger electrode and a higher frequency and measured a higher cytoplasmic conductance in *Aplysia* neuron bodies, although one still much lower than that of seawater. They suggested that the low values could be due to blocking of the electrode surface by intracellular membranes. However, they also expressed surprise that giant squid axons, also rich in membrane-bound organelles, produced no parallel effect.

In my view, the profound differences in conductance between axons and neuron bodies can be reconciled by assuming that in axons but not in cell bodies protein filaments that are oriented longitudinally (R. Chambers and Kao, 1952; Tasaki, 1982, p. 162) provide evenly placed anionic sites that serve as a K^+ -conducting band.

8.4.2. K^+ Activity in Living Cells Measured with an Ion-Specific Microelectrode

8.4.2.1. "Normal" K^+ Activity in Squid Axon, Skeletal Muscle Cells, and Frog Eggs

Following the development of the ion-specific microelectrode, a great deal of effort was made to measure K^+ activity in a variety of living cells. Most of the early work was done on giant squid axons (Hinke, 1961), giant crab (Hinke, 1959), and barnacle muscle fibers (Hinke and Gayton, 1971, Lev, 1964), using glass electrodes. In general, the intracellular K^+ activity agreed with the intracellular K^+ concentration multiplied by an activity coefficient, 0.76, equal to that of K^+ in an aqueous solution of ionic strength similar to that expected in the living cells (see Walker and Brown, 1977, for review).

These results led a number of scientists to assume that the activity of K^+ measured in these cells reflects a similar activity of K^+ in normal, unimpaled cells, and that the high activity observed confirms the basic tenet of the membrane pump theory, that virtually all cell K^+ is free in solution. It was also thought that these ion-specific electrodes would not have done more damage to the cells than would the Gerard-Graham-Ling (GGL) type of microelectrode commonly used to measure cell potentials.

However, these two types of intracellular microelectrodes have fundamentally different mechanisms. In the GGL type of microelectrode the tip of the microelectrode inside the cell serves only as an indifferent nonpolarizable electric lead. On the other hand, the tip of the ion-specific electrode is the sensing element. The physiological state of cytoplasm in immediate contact with the electrode tip of the GGL microelectrode is of no particular significance, since most of the potential measured is created at the cell surface a distance away from the tip location. An ion-specific electrode is like any ordinary pH electrode and can monitor only the ionic activity in a microscopically thin layer of fluid in immediate contact with the microelectrode tip. Thus, even though the bulk of the cytoplasm of a cell may be in a perfectly good state of health and its K⁺ in a normal physiological state, the inserted ion-specific microelectrode cannot "see" that K⁺. It can only sense the activity of K⁺ in the microscopic portion of the cytoplasm that must have been forcibly torn apart to make room for the impaling ion-sensing electrode. The recorded activity is therefore that of disturbed cytoplasm and not that of normal cytoplasm. This argument, presented in *Nature* (Ling, 1969b) in response to Spanswick's (1968) claim of a free state of K⁺ in living cells, was later challenged by Dick and McLaughlin (1969), who employed K⁺-specific microelectrodes to measure the K⁺ activity in frog ovarian eggs. In defending the use of an ion-selective microelectrode for intracellular monitoring of ion activity, they pointed out that trauma could indeed liberate K⁺, but that such liberated K⁺ would soon diffuse away, while in actual measurements the K⁺ activity remained more or less the same for as long as 30 min.

In response to this, Ling *et al.* (1973) pointed out that Dick and McLaughlin's argument is not valid, for two reasons:

1. *Slowness of diffusional loss.* If the impaling electrode liberates K⁺ from an adsorbed state in the vicinity of the microelectrode tip, and its concentration is at zero time equal to, say, 100 mM, how long would it take this level of liberated K⁺ to diffuse away so that the local K⁺ concentration would reach a 10 mM level? A consultation of any treatise on diffusion will show that this could take a very long time, much longer than half an hour. This is illustrated in Fig. 8.18, taken from the work of Hodgkin and Keynes (1953). They introduced a small amount of labeled K⁺ into a small segment of an isolated squid axon. The initial distribution is indicated by the taller bell-shaped curve. The other bell-shaped curve was obtained after the introduced ⁴²K⁺ had been allowed to diffuse for more than 7 hr (445 min). Even after such a long period of time, the peak has fallen to only two thirds of its initial value.

Now the self-diffusion coefficient for ⁴²K⁺ which Hodgkin and Keynes determined in these axons was about two thirds to three quarters of that of the D_K in an 0.5 M salt solution. This is just about the highest value that has ever been measured in what the authors believed to be normal cytoplasm. While we have serious doubts about this, it is clear that D_K measured in what is certainly more normal cytoplasm is as low as one eighth of that in a free solution (Ling and Ochsenfeld, 1973a) (Section 8.4.1.4). In that case, the time for the liberated K⁺ to fall to even two thirds of its initial value would be far longer than 445 min. A half hour of diffusion probably would not cause any easily detectable fall at all.

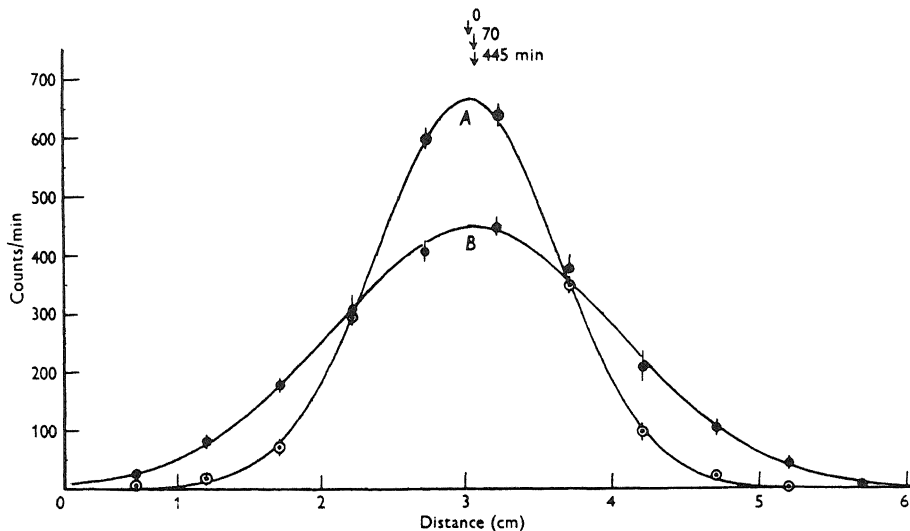


FIGURE 8.18. Distribution of $^{42}\text{K}^+$ injected into a spot in an isolated squid axon. Control experiment with no voltage gradient. Curve A shows the initial distribution of radioactivity and curve B the final distribution 445 min later. The arrows show the position of the maximum at various times. Vertical lines give $\pm \text{SD}$. [From Hodgkin and Keynes (1953), by permission of *Journal of Physiology*.]

2. *Spreading cytoplasmic deterioration and continued liberation of K^+ .* In the studies depicted in Fig. 5.15 we showed not only that mechanical injury at the cut end of a muscle, which by and large must resemble similar trauma induced by an impaling electrode, causes liberation of K^+ in the immediate neighborhood of the cut area, but also that this deterioration spreads progressively to healthier regions along with additional liberation of K^+ (Section 5.2.5). This spreading liberation of K^+ from a focus of injury could further delay the diffusional decay of the level of free K^+ .

Finally, one may ask: What if the measurement of intracellular K^+ activity with an ion-specific microelectrode were carried out while the cells were bathed in a Ringer solution? Couldn't the liberated K^+ rapidly diffuse out of the cell? The answer is that, in the case of squid axon, muscle cell, and frog egg, the surface permeation of K^+ is as a rule very slow. Thus the half-time of exchange of K^+ across the frog muscle cell surface is more than 10 hr at 24°C (Ling, 1962, p. 292). In these tissues, therefore, the cell surface barrier will not allow rapid outward leakage of liberated K^+ .

8.4.2.2. Variable K^+ Activity Coefficients in Epithelial Cells

The finding of the “right” answer (i.e., apparent activity coefficients of K^+ , γ_{K^+} of around 0.76) in the studies cited in the last section seems to have given most investigators in this field confidence that microelectrodes give accurate readings of the physiological K^+ activity of normal resting cells. Consequently, when “wrong” values of γ_{K^+} are

obtained, the *ad hoc* assumptions are often made that a large fraction of the K⁺ is sequestered (by compartments or "binding") in the case of a low γ_{K^+} or is excluded (from a compartment or from "nonsolvent water") in the case of a high γ_{K^+} .

All living cells studied are derived from a single egg cell which shares with its descendants the ability to accumulate K⁺ and exclude Na⁺. It is therefore unlikely that only some cells are equipped with compartments and K⁺-"binding" sites (to reduce the a_{K^+} in the cytosol), while other cells are equipped only with "nonsolvent" water (to increase the a_{K^+} in the cytosol). If cells containing K⁺-binding sites and/or K⁺-sequestering compartments also contain "nonsolvent" water, the "too high" and "too low" explanations will annul each other. Living cells are in osmotic equilibrium with plasma and tissue fluids that have virtually constant osmotic activities equal to those of 0.118 and 0.154 M NaCl for amphibian and mammalian plasma, respectively. K⁺ is the major cation in the cells. True physiological changes of K⁺ activity would be compensated for and corrected by the passage of water from the cell to the plasma or vice versa. *Therefore the "too high" apparent K⁺ activities, $a_{K^+}^{app}$, cannot reflect a permanent condition in resting cells. Rather, they can only be a transient situation, created locally in the cytoplasm as a result of the trauma induced by the intruding ion-selective microelectrode.*

In the preceding section I discussed how a spuriously high γ_{K^+} could be recorded for K⁺ in a living cell, measured with an intracellular K⁺-specific microelectrode, owing to liberation of adsorbed K⁺. According to the AI hypothesis, trauma may bring about another change in the protoplasm in the vicinity of the microelectrode, namely a local depolarization of the cell water with a concomitant local increase of the *q*-value for K⁺ (and other solutes normally excluded). Under suitable conditions this also may increase $a_{K^+}^{app}$.

There is a third possible reason for the intracellular K⁺-selective microelectrode to record an apparently high γ_{K^+} : electrodes with preference for K⁺ may also respond to NH₄⁺, ε-NH₃⁺, α-NH₃⁺, or guanidyl groups carried on proteins. This possible source of error has, to the best of my knowledge, not been ruled out in published studies (see Durst, 1974, p. 15).

In summary, there are three possible causes of artifacts in the intracellular microelectrode recording of intracellular γ_{K^+} : (1) liberation of adsorbed K⁺, (2) localized depolarization of water with rise in its *q*-value for K⁺, and (3) interference by charged amino groups on proteins. Since all three of these sources of artifacts favor the recording of a spuriously high γ_{K^+} , it is remarkable that one finds so many reports of a low γ_{K^+} . A likely cause for this is a greater stability of the cytoplasm of these epithelial cells when compared to that of, for example, nerve and muscle (see Fig. 8.19B). If γ_{K^+} is so much lower than in the plasma, what prevents water from moving out? The measured value is likely to be a localized one, not fully in equilibrium, and water is in fact slowly moving out during the measurement. However, osmotic balance is maintained in the undamaged parts of the cell because of the effect of water polarization on the osmotic activity, a subject that will be fully discussed in Chapter 13.

Next let us turn our attention to the extremely high γ_{K^+} values that have been reported. A K⁺ activity coefficient of 1.15 was obtained in giant barnacle muscle fibers in which γ_{K^+} and C_{K^+} were determined in the same cell (McLaughlin and Hinke, 1968)

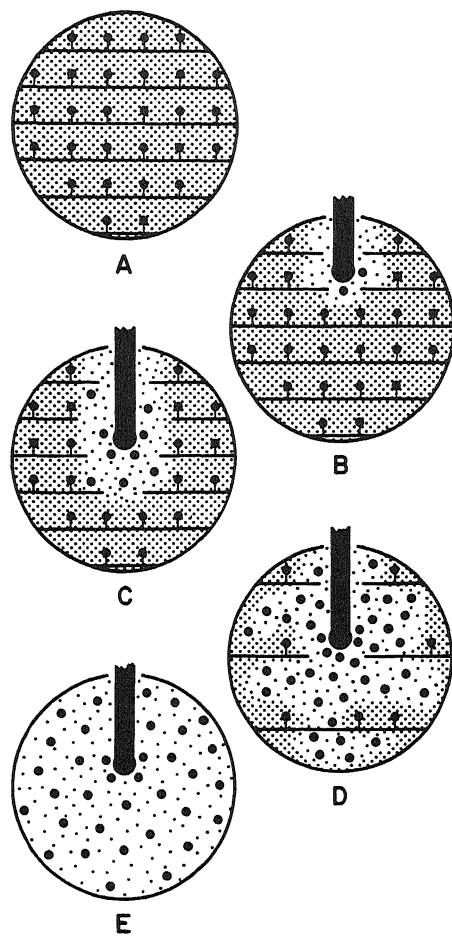


FIGURE 8.19. Diagrammatic illustration of the consequences of the insertion of an intracellular K^+ -specific microelectrode on the apparent K^+ activity recorded with the microelectrode. (A) Normal cell: K^+ adsorbed, water polarized. (B) Stable cell after electrode impalement: Modest K^+ liberation and water depolarization. γ_{K^+} slightly higher than in normal cells but lower than if all cell K^+ were free ($a_{K^+}^{app} < C_{K^+}$). (C) Labile cell: Extensive local K^+ liberation and water depolarization ($a_{K^+}^{app} = C_{K^+}$). (D) Labile cell: Extensive local K^+ liberation and water depolarization; K^+ liberation accompanied by lesser water depolarization in areas farther away. Electrode records γ_{K^+} higher than average K^+ concentration in cell ($a_{K^+}^{app} > C_{K^+}$). (E) Final state of trauma: All K^+ liberated, all water depolarized ($a_{K^+}^{app} = C_{K^+}$).

using glass microelectrodes. C. O. Lee and Armstrong (1972) also used glass electrodes and measured a γ_{K^+} of 1.0–1.2 in bullfrog intestine. In later studies, a_{K^+} measured in epithelial cells was lower (Table 8.2); one might suppose that glass electrodes, which are much less selective for K^+ over Na^+ than are the liquid ion exchange (LIE) electrodes, gave an artifactually high value. However, glass and LIE electrodes give the same a_{K^+} in frog muscle (see Walker and Brown, 1977), and in mature frog oocytes the apparent activity coefficient, a_{K^+}/C_{K^+} , obtained with LIE electrodes is 1.29 (Palmer *et al.*, 1978). Thus, the nature of the microelectrodes cannot be the whole explanation for the variations in the data in Table 8.2.

Since the γ_{K^+} of a KCl solution isotonic with seawater is 0.65 and the γ_{K^+} of a KCl solution isotonic with frog plasma is 0.76, the much higher γ_{K^+} measured in frog intestinal epithelia by Lee and Armstrong (see Table 8.2), in barnacle giant muscle cell by McLaughlin and Hinke (1968), and in mature frog oocytes by Palmer *et al.* (1978) all must represent a *transient* condition created by the impaling electrodes. There is no

TABLE 8.2. Membrane Potential ($\Delta\Psi$), K⁺ Activity (a_{K^+}), K⁺ Concentration (Chemical) (C_{K+}), and Activity Coefficient (γ_{K^+}) in Epithelial Cells^a

Reference		$\Delta\Psi$ (mV)	ΔE_{K^+} electrode	a_{K^+} (mM)	C _{K+} (mM)	a_{K^+}/C_{K^+} (γ_{K^+})
Low-resistance epithelia						
Intestine						
Bullfrog	C. O. Lee and Armstrong (1972)	-45	Glass	85/65	86/54	1.0/1.2
Rabbit	Zeuthen and Monge (1974)	-20	LIE	38		
<i>Amphioxus</i>	White (1976)	-30	DB	LIE	38.5	
<i>Necturus</i>	Garcia-Diaz <i>et al.</i> (1978)			LIE	146	0.27
					108	
Renal proximal tubule						
<i>Necturus</i>	Khuri <i>et al.</i> (1972a)	-56	DB	LIE	59	103
Rat	Khuri <i>et al.</i> (1974)	-68	DB	LIE	54.4	136
Gallbladder						
<i>Necturus</i>	Zeuthen (1978)	Mucosal	-20	DB	LIE	49
		Serosal	-50	DB	LIE	131
	Garcia-Diaz and Armstrong (1980)		-52		LIE	96
High-resistance epithelia						
Renal distal tubule						
Rat	Khuri <i>et al.</i> (1972b)		DB	LIE	46.5	136
Urinary bladder						
Bullfrog	Kimura and Fujimoto (1977)	-12		LIE	39.3	115
Toad	Kimura <i>et al.</i> (1977)	Mucosal	-18	LIE	42	129
		Serosal	+16	LIE	40	129
	DeLong and Civan (1978)		-50	LIE	43	129
	DeLong and Civan (1979)			DB	LIE	0.33
	DeLong and Civan (1980)				LIE	81
						140/155 ^b
						0.58/0.52
						70
						140/155 ^b
						0.50/0.45
Skin						
Frog	Nagel <i>et al.</i> (1981)	-68		LIE	132	155
						0.85

^aAbbreviations: DB, double-barrel electrode for simultaneous measurement of $\Delta\Psi$ and ΔE_{K^+} ; LIE, liquid ion exchange electrode.^bDetermined by electron microprobe analysis.

way for K^+ activity to be permanently kept at levels this high and not draw water from the external medium to equalize γ_{K^+} in and out of the cells. These high γ_{K^+} cannot reflect the true γ_{K^+} of normal resting cells.

8.4.2.3. Concluding Remarks Regarding Ion-Specific Microelectrodes

In the AI hypothesis, the bulk of K^+ in the living cell is in an adsorbed state and the bulk of water has low solubility, and hence a low q -value, for K^+ , Na^+ , and other large molecules and ions. Trauma brought about by the intrusion of the intracellular electrode liberates K^+ and depolarizes water locally. If these two events are entirely limited to the same area, the K^+ specific electrode may read an $a_{K^+}^{app}$ that is lower than (Fig. 8.19B), or equal to, that of the average K^+ concentration of the cell, as was noted in the case of barnacle muscle and squid axon (Section 8.4.2.1) (Fig. 8.19C). However, if this trauma spreads to areas of the cell beyond the region immediately surrounding the electrode, the amount of liberated K^+ may exceed the capacity of the local water to accommodate it and K^+ may then diffuse into and accumulate in the region of the electrode, with its more extensively depolarized water and higher q -value. In this case the $a_{K^+}^{app}$ measured with the electrode may well exceed that of the average K^+ concentration of the cell. This background permits a reevaluation of the various explanations postulated to explain high or low values of γ_{K^+} .

1. "*Compartmentation*" to explain low γ_{K^+} . If we assume an average intracellular K^+ concentration of 140 mM, then, in the cells with a_{K^+} around 40 mM, the K^+ in the region surrounding the microelectrode is 40/0.77 or 50 mM, and the remaining K^+ is in some subcellular compartment. If this compartment occupied about half the intracellular space then it would contain 230 mM K^+ ! It is difficult to imagine how such a large difference in osmotic pressure could be sustained without movement of water into the compartment. Other ions like Ca^{2+} and Mg^{2+} cannot be used to balance this large osmotic difference because they are mostly adsorbed. Na^+ exists in too low a concentration to make up the difference. This difficulty can be resolved by assuming that the K^+ is adsorbed and hence osmotically inactive in the first place, and that is of course exactly what the AI hypothesis has long contended.
2. "*Nonsolvent*" water to explain high γ_{K^+} . As mentioned in Section 8.1, the concept of "nonsolvent" water, though of historical interest (Section 2.6.1) is untenable. There is no known example of such water. Polarized water in polyvinylpyrrolidone, polyethylene oxide, and denatured protein solutions freely dissolve some solutes like urea even though they exclude Na^+ , sugars, and free amino acids like living cells do (Section 6.3.4). However, if by "nonsolvent" water is meant water that has a relatively low solubility for molecules that are larger and more complex, and a higher solubility for molecules that can fit into the polarized multilayer water structure owing to their small size or special structure, then the conflict is removed. But then this also is what has long been suggested by the AI hypothesis (Section 6.3.3).

In conclusion, the use of K^+ -specific intracellular microelectrodes to measure γ_{K^+} has yielded widely different values. This great divergence of measured γ_{K^+} is not consistent with the membrane pump theory, according to which all cell K^+ is free and thus



Freeman W. Cope (1930–1982)

should have γ_{K^+} uniformly equal to that of an isotonic solution. Two certain, and one possible, sources of artifact spuriously increase γ_{K^+} measured in living cells. Trauma created by the intruding microelectrode causes local liberation of adsorbed K⁺ and local depolarization of cell water to variable degrees in different cells, explaining the apparent conflicts in reported studies.

8.4.3. NMR Relaxation Times of $^{23}\text{Na}^+$ and $^{39}\text{K}^+$ in Living Cells*

8.4.3.1. Early Studies in Cells and Ion Exchange Resins

Jardetzky and Wertz (1960) studied the steady-state NMR spectrum of $^{23}\text{Na}^+$ in wet Dowex 50 ion exchange resin (cross-linked polystyrene sulfonate) which contained only Na⁺ as its counterion. They observed that the size of the NMR Na⁺ signal corresponds to only a fraction of the size of the Na⁺ signal expected if all the Na⁺ were present in free solution. Jardetzky and Wertz suggested that there are two fractions of Na⁺ in the resin: one “free” and one “bound.” The free Na⁺ exhibits an NMR signal (the NMR-“visible” fraction) with a peak height linearly related to Na⁺ concentration (Jardetzky and Wertz, 1956), while the Na⁺ adsorbed on charged anionic sites produces a signal so broadened that it is no longer visible on the spectrum (the NMR-“invisible” fraction).

Using Jardetzky and Wertz’s method, Cope investigated the steady-state NMR spectrum of Na⁺ in isolated actomyosin and various rabbit tissues, including muscle, nerve, kidney, and brain (Cope, 1967, 1970a,b). He found that a substantial fraction of the Na⁺ is NMR-invisible. Based on Jardetzky and Wertz’s two-fraction theory, Cope concluded that the NMR-invisible Na⁺ indicated complexing of this ion in living tissues

*For an elementary discussion of NMR concepts and terminology, see Appendix A.

TABLE 8.3. NMR-Visible and Invisible Na⁺ in Actomyosin and Living Tissues

Tissue or protein	Animal	No. of samples	Total Na ⁺ (μmoles/g)	NMR-visible Na ⁺ (μmoles/g)	NMR-invisible Na ⁺		Reference
					μmoles/g	Percent of total	
Actomyosin	Rabbit	6	94 ± 1.9	49 ± 2.3	45 ± 3.6		Cope (1967)
Voluntary muscle	Frog	6	28.4 ± 1.16	8.0 ± 1.15	20.4 ± 1.15	71.8%	Cope (1967)
	Frog	3	25.0 ± 1.7	10.3 ± 0.88	14.3 ± 0.88	47.2%	Ling and Cope (1969)
	Frog	4	22.9 ± 1.2	14.5 ± 1.4	8.4 ± 1.0	36.7%	Martinez <i>et al.</i> (1969)
	Frog		40	15	25	62.5%	Czeisler <i>et al.</i> (1970)
Nerve	Rabbit	5	71 ± 1.3	33 ± 1.2	37 ± 2.0	52.2%	Cope (1970b)
Testicle	Rat		60.0 ± 3.4	45.4 ± 0.6	14.6 ± 2.8	24.4%	Reisin <i>et al.</i> (1970)
Liver	Frog	3	27.2 ± 1.2	9.3 ± 1.2	18.0 ± 0.94	66.2%	Martinez <i>et al.</i> (1969)
Kidney	Rabbit				60–65%		Cope (1967)
Brain	Rabbit				57–63%		Cope (1967)
Skin	Frog	1	76.2	32.4	43.8	57.5%	Yeh <i>et al.</i> (1973)
	Frog	1	81.4	29.1	52.3	64.3%	Yeh <i>et al.</i> (1973)
Erythrocytes	Human	29	15.6 ± 0.88	14.7 ± 1.03	0.9	5.8%	Yeh <i>et al.</i> (1973)

and in actomyosin. Cope's observations were confirmed by others in a variety of living tissues (Table 8.3). Most of these authors concluded that a substantial fraction of cell Na⁺ is in an adsorbed state. This conclusion was in harmony with results obtained from intracellular Na⁺-sensitive microelectrode studies (Hinke, 1959, 1961; Lev, 1964; McLaughlin and Hinke, 1966; Dick and McLaughlin, 1969).

In 1969 Ling and Cope extended this technique to determine the physical state of K⁺ in frog muscle by an indirect method. It was pointed out that, if the bulk of cell K⁺ exists in an adsorbed state in normal cells, its displacement by Na⁺ when cells are exposed to a low-K⁺/high-Na⁺ environment should lead to a stoichiometric displacement of adsorbed K⁺ by Na⁺. The additional Na⁺ taken up should be largely "invisible" on the NMR spectrum. Table 8.4 shows that, within the limited accuracy achievable, this expectation was borne out. However, there was also an increase of NMR-visible Na⁺ (Table 8.4), which was not expected and was unexplained.

A year later Freeman W. Cope (1970a) published a spin-echo NMR study of Na⁺ in muscle, brain, and kidney. He found that the spin-spin relaxation time (T_2) is composed of two fractions. He attributed the fast fraction to complexed Na⁺ and the slow fraction to free Na⁺ dissolved in tissue water. The two-fraction theory demands that the spin-lattice relaxation time (T_1) should also be separable into similar fractions. However, subsequent studies in a variety of cells—summarized in Table 8.5, taken from Edzes and Berendsen (1975)—showed only a single T_1 .

It was not possible at that time to study K⁺ NMR directly, even though the major isotope of K⁺, ³⁹K⁺, which makes up 93.3% of natural K⁺, has a greater than zero nuclear spin and should yield an NMR spectrum. The ³⁹K⁺ spectrum was too weak to be observed even at very high concentration and using the most powerful conventional electromagnets (ca. 17,000 G) available. Cope and Damadian (1970), using a superconducting magnet, were able to generate a magnetic field of 50,300 G and to record properties of ³⁹K⁺ in the microbe *Halobacterium halobium*, which lives in a highly saline environment and contains K⁺ at a very high concentration of 4–5 M. The spin-spin relaxation time, T_2 , in the bacterium was shorter than that in an aqueous 1.0 M KCl solution. The authors pointed out that the true T_2 could be even shorter because of instrumental limitations. The data did not reveal whether there was an NMR-invisible fraction. However, in the case of the sulfonate ion exchange resin Dowex 50, loaded with K⁺, only 41% of the NMR signal was visible; the remaining 59% was not (Table 8.5).

TABLE 8.4. Concentration of Na⁺ and K⁺ in Frog Sartorius Muscle Preserved in a Medium with a Low K⁺ Concentration (0.2–0.5 mM) and Na⁺ 118 mM^{a,b}

Duration of <i>in vitro</i> incubation (days)	Total K ⁺ (μmole/g)	Total Na ⁺ (μmole/g)	NMR-visible Na ⁺ (μmole/g)	NMR-invisible Na ⁺ (μmole/g)	Sum of NMR-invisible Na ⁺ and total K ⁺ (μmole/g)
0	89.9	23.3	9	14	104
2–5	34.5	81.3	28	54	89

^aTotal K⁺ and Na⁺ contents determined from hot HCl extracts by flame photometry. NMR-visible Na⁺ determined with a wide-line spectrometer. NMR-invisible Na⁺ determined as the difference between total Na⁺ and NMR-visible Na⁺ concentrations. Means of nine muscles incubated 2–5 days.

^bFrom Ling and Cope (1969), by permission of *Science*.

TABLE 8.5. NMR Relaxation Times of $^{23}\text{Na}^+$, $^{39}\text{K}^+$, $^7\text{Li}^+$, $^{87}\text{Rb}^+$, and $^{133}\text{Cs}^+$ in Aqueous Solutions, Sulfonate Exchange Resins, and Living Cells

Ion	Medium	T_1 (msec)	T_{2s} (msec)	T_{2f} (msec)	Reference
$^{23}\text{Na}^+$	Aqueous solution	56		56	Abragam (1961), Eisenstadt and Friedman (1966)
	Sulfonate ion exchange resin	6.3 \pm 0.2	7.7 \pm 1.8	3.5 \pm 0.4	Berendsen and Edzes (1973)
	Frog muscle	22	13.5	2.9	Shporer and Civan (1974)
	Rat muscle	12 \pm 0.5	14 \pm 3.4 (38%)	0.91 \pm 0.07	Cope (1970a)
	Rat brain	16 \pm 3.2	10 \pm 0.4 (33%)	0.75 \pm 0.08	Cope (1970a)
	Rat kidney		9 \pm 0.7 (33%)	0.76 \pm 0.1	Cope (1970a)
	Rabbit nerve	18 \pm 1.3	14 \pm 1.1 (41%)	1.1 \pm 0.2	Cope (1970b)
$^{39}\text{K}^+$	<i>Halobacterium</i>		12.3 (38%)	4.6	Edzes et al. (1977)
	Aqueous solution	57		59	Damadian and Cope (1973)
		45		45	Civan et al. (1976)
	Sulfonate ion exchange resin	0.43		0.32	Damadian and Cope (1973)
	Rat muscle	6.6, 7.2		0.55 (41%)	Cope and Damadian (1970)
	Rat brain	12.4		0.35, 0.32	Damadian and Cope (1973)
	<i>Escherichia coli</i>	1.9, 1.3		0.18, 0.06	Damadian and Cope (1973)
$^7\text{Li}^+$	<i>Halobacterium</i>			0.35	Damadian and Cope (1973)
	Frog muscle	12.7		4.37	Cope and Damadian (1970)
	(21–22°C)				Civan et al. (1976)
$^{87}\text{Rb}^+$	Aqueous solution	10,000			Bystrov et al. (1972)
	Frog muscle	2,000			Bystrov et al. (1972)
$^{133}\text{Cs}^+$	Aqueous solution			2.5	Edzes et al. (1977)
	<i>Halobacterium</i>		0.12	0.05	Edzes et al. (1977)
$^{133}\text{Cs}^+$	Aqueous solution			4760	Edzes et al. (1977)
	<i>Halobacterium</i>	28.6		<0.05	Edzes et al. (1977)

Three years later Damadian and Cope (1973; see also Cope and Damadian, 1974), used a better instrument and measured both T_1 and T_2 of living tissues with lower K^+ contents than in *Halobacteria*. In rat muscle, they found that T_1 and T_2 of $^{39}\text{K}^+$ were reduced 8-fold and 200-fold respectively, compared to those of a KCl solution of similar concentration. In rat brain T_1 and T_2 were reduced 6-fold and 200-fold, respectively. An even greater reduction of T_1 and T_2 was observed in *Escherichia coli* and in K^+ -loaded Dowex 50 ion exchange resin (Table 8.5). The authors thought that these data agreed with the theory that the bulk of K^+ in living cells is associated with fixed anionic sites of cellular macromolecules.

In 1972, a symposium on the physicochemical state of ions and water in living cells and model systems was held in New York (Hazlewood, 1973). Discussion of the results of studies of the NMR of Na^+ in cells, and especially that initiated by a paper presented by Berendsen and Edzes on $^{23}\text{Na}^+$ NMR of muscle tissue, led to the realization that the interpretation of the NMR data in terms of "visible" and "invisible" Na^+ was oversimplified.

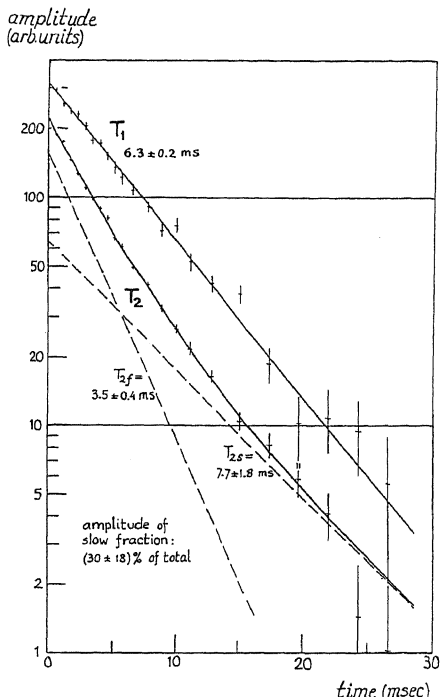


FIGURE 8.20. Pulsed NMR measurements of T_1 and T_2 of Dowex 50 ion exchange resin. [From Berendsen and Edzes (1973), by permission of *Annals of the New York Academy of Sciences*.]

8.4.3.2. The Quadrupolar Effect

Berendsen and Edze's paper (1973) challenged the concept originally introduced by Jardetzky and Wertz, and later adopted by Cope and others, that a part of the cell Na^+ is free and NMR-“visible” and another part is bound and NMR-“invisible.” Rather, they postulated that the separation of the signal into a “visible” and an “invisible” part originates from the presence of an electric field gradient, which produces a uniform effect on a single population of free Na^+ , splitting the NMR signal into a major “visible” peak, consisting of about 40% of the Na^+ signal, and two weaker satellite peaks, which may be “invisible” because of high noise levels. They concluded their article with these words: “These observations prove that sodium in tissue behaves nearly as it does in the normal liquid state; this is in complete disagreement with the conclusion drawn from the same NMR observations before.”

Berendsen and Edzes also showed that, by making certain quantitative assumptions, it was possible to use P. S. Hubbard's theory (1970) of relaxation phenomena of nuclei with a quadrupolar moment to account for the observation that $^{23}Na^+$ in an ion exchange resin, as well as in deteriorated rat muscle, has only one T_1 but two T_{2s} (Figs. 8.20 and 8.21).

8.4.3.3. Interpretation of the Quadrupolar Effect

Certain nuclei, like 2H , ^{23}Na , and ^{35}Cl , which do not have a perfectly spherical charge distribution and have a spin quantum number ≥ 1 , possess an electric quadru-

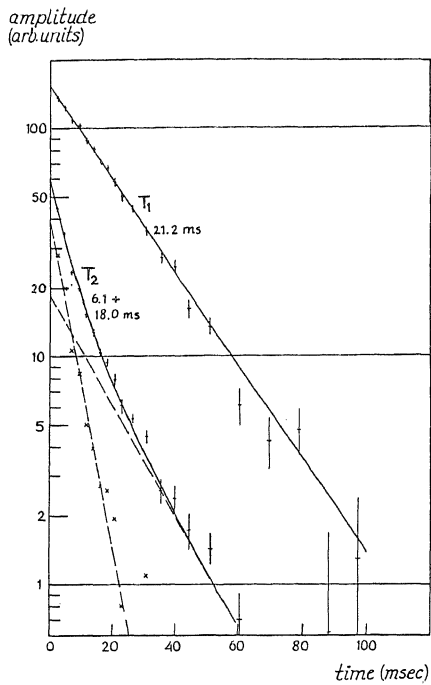


FIGURE 8.21. Pulsed NMR measurements of spin-lattice (T_1) and transverse (T_2) relaxation times of wet, deteriorated rat muscle that was allowed to stand for 14 days in Ringer solution and then in a closed tube at 4°C for another 14 days. [From Berendsen and Edzes (1973), by permission of *Annals of the New York Academy of Sciences*.]

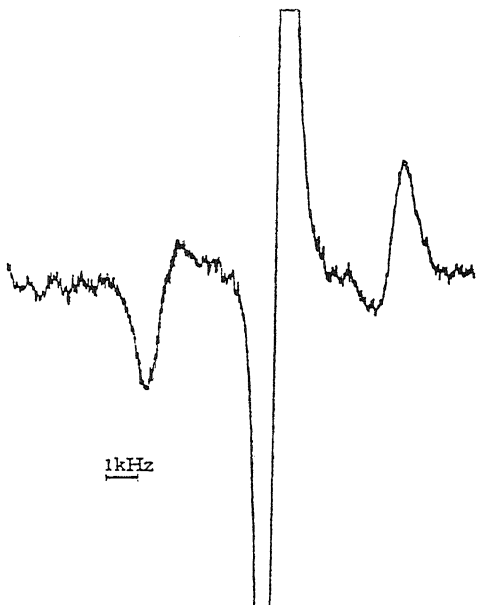


FIGURE 8.22. $^{22}\text{Na}^+$ NMR spectrum of a lamellar liquid crystalline sample with the composition (by weight) 64% lecithin, 16% sodium cholate, and 20% water. The spectrum was obtained at $25 \pm 2^\circ\text{C}$ and at a resonance frequency of 15.82 MHz. (The intense central peak cannot be displayed in full at the amplification employed.) [From Lindblom (1971), by permission of *Acta Chimica Scandinavica*.]

pole moment from the charge distribution like — + —. If these nuclei are placed near a single electric charge, then the inhomogeneous electric field causes the splitting of energy levels mentioned above (Brand and Speakman, 1960).

The first transition owing to quadrupolar splitting of the resonance signal was reported by Dehmelt and Krüger in 1950, and was that of ³⁵Cl and ³⁷Cl nuclei in solid 1:2-dichloroethane. Some theories and experimental studies dealt with other nuclei, like the ²³Na signal in a lamellar liquid crystalline sample of 64% lecithin, 16% sodium cholate, and 20% water, shown in the derivative mode in Fig. 8.22. The two satellite peaks were readily visible. Lindblom (1971) observed a single T_1 (60 msec) one order of magnitude less than that of an aqueous NaCl solution. Throughout this paper, Lindblom regarded the quadrupolar signal splitting as due to Na⁺ binding and indeed concluded his report with a statement referring to an ongoing project "to investigate certain aspects of ion binding to membrane models by this method" (p. 2768, italics supplied).

A year later Shporer and Civan (1972) reported a very similar study in liquid crystals of sodium linoleate. They too observed the signal splitting, but only when the signal was presented in the more sensitive derivative mode. Signal integration showed that the central peak comprised 34–39% of the signal, in agreement with the theoretical 40–60 split. They pointed out that the presence of satellite peaks could not be reconciled with the concept that this portion of the signal is due to simple line-broadening. However, concerning the mechanism of the signal splitting, Shporer and Civan said, "The physical basis for the quadrupolar effect observed is less clear, possibly an immobilization of all the ²³Na nuclei, or an ordering effect induced by the liquid crystalline structure" (p. 119). A likely mechanism for immobilization is, of course, adsorption.

Berendsen and Edzes (1973) attributed the quadrupolar splitting to a "medium-range" diffuse electric field gradient. As they put it, "The only requirements necessary to produce a broad and a narrow component are the presence of (negative) charged groups and structural heterogeneity extending over at least 100 Å" (p. 479).

Anticipating data to be mentioned later, I point out that the simplest interpretation for the signal splitting, one already offered by Lindblom, is that Na⁺ is electrostatically adsorbed. *The theory of quadrupolar splitting requires only the presence of a quadrupolar moment and an electric field gradient. The simplest electric field gradient is that experienced by a cation like Na⁺ adsorbed on a singly charged anion* (Brand and Speakman, 1960, p. 115).

8.4.3.4. Experimental Findings Favoring Adsorption of Na⁺ and K⁺ on Individual Anionic Sites on Cellular Macromolecules

8.4.3.4a. Na⁺ and K⁺ in Dowex 50 Ion Exchange Resin. In 1952 I used the ion exchange resin as a specific model of selective K⁺ accumulation in the living cell (Ling, 1952) and considered virtually all the counterions to exist in an adsorbed state. Jarretzky, Wertz, Cope, and Damadian utilized the similarity between the NMR behavior of ²³Na⁺ and ³⁹K⁺ in the ion exchange resin Dowex 50 and in living cells as the foundation for their conclusion that a substantial portion of intracellular Na⁺ (and K⁺) exists

in the adsorbed state (Table 8.3). Berendsen and Edzes, on the other hand, also noted the close similarity in the behavior of $^{23}\text{Na}^+$ in Dowex 50 and living cells (Figs. 8.20 and 8.21), but concluded that K^+ and Na^+ must be free in living cells. They perhaps started out with the assumption that counterions are free in ion exchange resins because this was the conventional view, espoused by Gregor (1948, 1951) and widely cited in standard textbooks on ion exchange resin theory and technology (Helfferich, 1962).

In Section 6.2.1, the rather strong arguments against Gregor's theory were presented, including the studies of Ling and Zhang (1983) which provide direct evidence that Na^+ in sulfonate resins exists in close association with the fixed anions. In describing the theory of ionic permeability, I also presented evidence that the rate of ion entry into an ion exchange resin follows Michaelis-Menten kinetics (Section 4.5.2). That is, at the resin surface, at any moment, the number of ions associated with the fixed anionic sites is overwhelmingly larger than that of ions in the interstices between the fixed anionic sites. Since the resin sheets or beads are not covered with anything significantly different from what is inside the system (e.g., a membrane), the high degree of ionic association at the surface itself provides another kind of evidence against the assumption of ionic dissociation within the resin.

In summary, Na^+ and K^+ in ion exchange resins are neither all free, nor half-free and half-adsorbed, but virtually all adsorbed in a one site-one ion manner. The electric field gradient that brought about the quadrupolar $^{23}\text{Na}^+$ NMR signal splitting is not a weak gradient extending over large areas some 100 Å in dimension, as suggested by Berendsen and Edzes, but is a more intense gradient in the immediate vicinity of the individual fixed anionic sites. The similarity in NMR behavior of Na^+ and K^+ in living cells and in Dowex 50, therefore, is consistent with preponderant ion adsorption as suggested in the AI hypothesis. Since some 40% of the NMR signal of adsorbed Na^+ is visible, we now can understand why the NMR-visible Na^+ signal also increases on substituting Na^+ for K^+ in muscle cells (Section 8.4.3.1 and Table 8.4).

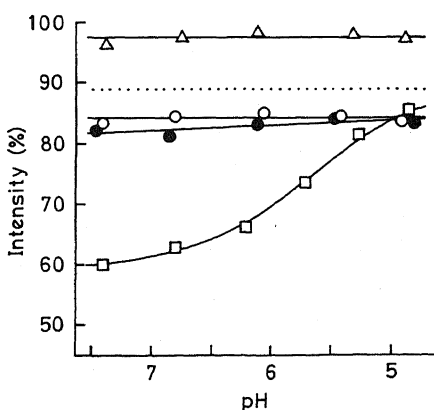
8.4.3.4b. Further Evidence for Na^+ Adsorption in Muscle Cells from the Work of Chang and Woessner. P. S. Hubbard (1970) analyzed theoretically the quadrupolar relaxation of $^{23}\text{Na}^+$ nuclei. Based on his theoretical calculation, Berendsen and Edzes suggested that the single T_1 and double T_2 in living and dead muscles, as well as in ion exchange resin, indicate that in all these systems Na^+ exists in one physical state—free—but wanders in and out of electrically heterogeneous environments. Chang and Woessner (1978) confirmed the single T_1 and double T_2 of Na^+ in frog muscle. They pointed out that a single T_1 equal in magnitude to the slow component of T_2 , as shown in Figs. 8.20 and 8.21, indicates the existence of at least two different correlation times, τ_c (see Appendix A). From the measured T_1 and T_2 , they were able to give a range of values for each of the two τ_c 's. The faster, τ_{c1} (ca. 10^{11} sec), was shown to correspond well to that of Na^+ in a free solution and was attributed to the electric field gradient owing to the water of hydration surrounding the Na^+ . The slow time, τ_{c2} , must be between 10^{-8} and 10^{-5} sec. From this range of τ_c values and the T_2 values, it was possible to calculate the average electric field gradient. This was far steeper than that

predicted in the diffuse field gradient postulated by Berendsen and Edzes, but was compatible with that experienced by Na⁺ adsorbed onto an anionic site. Indeed the region corresponding to the field gradient is as small as 4.5 Å, entirely in harmony with adsorption on an anionic site of a Na⁺ in conformation I (Fig. 6.6).

8.4.3.4c. Selectivity in Modulation of the NMR Signal of Na⁺. Monoi (1976) studied the ²³Na⁺ NMR spectrum of liver homogenate, confirming the earlier observations that only about 40% of the liver Na⁺ is NMR-visible (Table 8.3). He then measured the amount of NMR-visible ²³Na⁺ when competing alkali metal ions and H⁺ were added to the homogenate. The addition of H⁺ of high enough concentration converts NMR-invisible ²³Na⁺ to NMR-visible ²³Na⁺. The addition of 100 mM Cs⁺, K⁺ or Rb⁺ unmasks the invisible Na⁺, but to different degrees (Fig. 8.23). These data cannot be readily explained by the Berendsen-Edzes theory. If the NMR-“invisible” fraction is due to the effect of a weak electric field gradient extending over large regions in which the ²³Na⁺ is in a free state, it is reasonable to expect that externally added H⁺ or K⁺ can displace the ²³Na⁺ from these areas so that it would become “visible,” but, as explained fully in the preceding section, such an effect should be only valence-specific. The data show great *ionic specificity*. Thus, while Cs⁺ unmasks virtually all the Na⁺, choline has no effect at all (Fig. 8.24). This high degree of specificity among univalent ions further suggests that the quadrupolar splitting of ²³Na⁺ is not created by a diffuse electric field gradient but is due to specific one site-one ion adsorption.

8.4.3.4d. Free Na⁺ in Living Tissues. In the foregoing studies, the NMR-visible Na⁺ was obtained by calibrating the peak height of experimental material with that of a NaCl solution standard. It was by this method that many of the data of Table 8.3 were obtained. That the invisible Na⁺ tended to be near 60% was generally taken as

FIGURE 8.23. Effect of pH on the resonance intensity of ²³Na⁺ in rat liver homogenate in the presence or absence of Cs⁺. pH was adjusted by adding HCl or by replacing some part of NaCl with equimolar NaOH. ● and ○, 62.5% homogenate containing Cs⁺ (300 and 600 mmole/kg sample, respectively) □, 50% homogenate containing no additional cations; Δ, 62.5% homogenate containing guanidine-HCl (600 mmole/kg sample). The dotted line represents the resonance intensity for 50% homogenate containing Cs⁺ (600 mmole/kg sample). Each point is the mean of three or four samples. [From Monoi (1976), by permission of *Biophysical Journal*.]



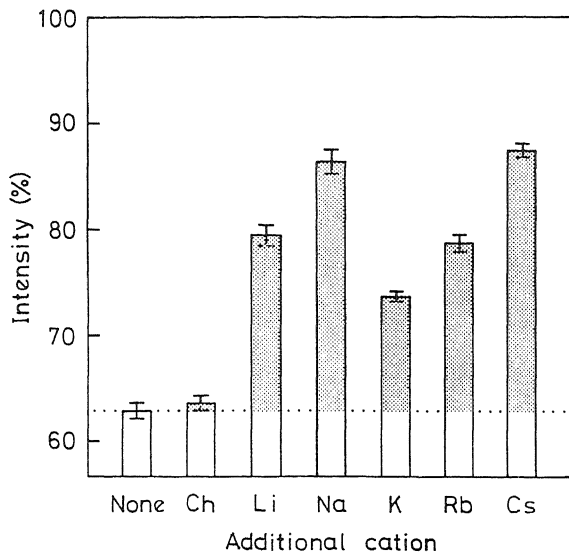


FIGURE 8.24. Relative effects of alkali cations on the resonance intensity of $^{23}\text{Na}^+$ in rat liver homogenate. The concentration of additional cations is 300 mmole/kg sample. The concentration of homogenized tissue is 50% as wet weight. Vertical bars denote SEM (of six samples). Ch, choline ion. [From Monoi (1976), by permission of *Biophysical Journal*.]

confirming the 40–60 splitting of the $^{23}\text{Na}^+$ signal under an electric field gradient. We have now come full cycle back to the concept of adsorbed $^{23}\text{Na}^+$, only instead of 60% of Na^+ being adsorbed, now the data appear to indicate that nearly all of the tissue Na^+ is adsorbed. This is, however, not entirely true, because of the 25–30 $\mu\text{moles/g}$ in muscle, at least 8–10 $\mu\text{moles/g}$ is extracellular Na^+ which can only be in a free state. Moreover, part of the intracellular Na^+ (ca. 5–10 $\mu\text{moles/g}$) also must be free (Sections 6.3.3, 11.2, and 12.4). To solve this conflict, a logical answer is that we have underestimated the total free Na^+ revealed by the height of the visible peak. I would like to suggest that this occurs not merely because adsorbed Na^+ undergoes a 40–60 split, but because the central peak is broadened. This broadening, clearly demonstrated in Fig. 8.25, implies that the peak height of the signal of adsorbed Na^+ cannot be calibrated against a free NaCl solution standard. In cases in which this was done, the free Na^+ would be underestimated. Line broadening would also offer an explanation of why the gain of NMR-visible Na^+ on substituting Na^+ for cell K^+ , which should be 40/60 or 66.7% of the NMR-invisible Na^+ gained, was only 45.7% (see Table 8.4).

That the visible $^{23}\text{Na}^+$ peak is broadened was pointed out by Czeisler and his co-workers in studies of tissue Na^+ (Czeisler *et al.*, 1970; Czeisler and Swift, 1973), by Jardetzky and Wertz (1956) in studies of concentrated Na^+ salt solutions, and more extensively and definitively by the use of Na^+ linewidth to measure bound Na^+ (Manning, 1978; Gustavsson *et al.*, 1978). This is illustrated in Fig. 8.25, taken from Bleam *et al.* (1980), where specific displacement of Na^+ in DNA by various alkali metal ions reveals itself as a line-narrowing rather than a peak-height increase, in contrast to Monoi's studies (Figs. 8.23 and 8.24). Both studies, however, prove specific Na^+ adsorption on individual sites.

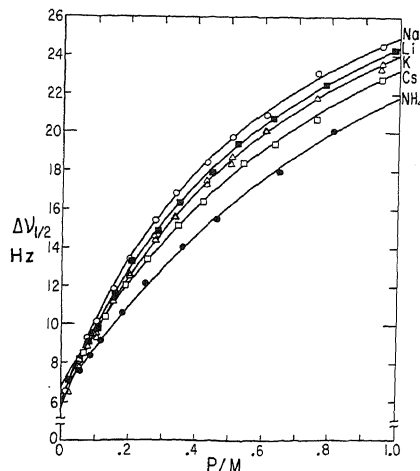


FIGURE 8.25. Effect of alkali metal ions on the line-width of the NMR signal of Na⁺ in NaDNA. Line-width measurements as a function of the ratio of DNA phosphate to added salt, P/M , for 0.015 M calf thymus NaDNA. The curves represent nonlinear least-squares fits of the data. [From Bleam *et al.* (1980), by permission of *Proceedings of the National Academy of Sciences*.]

In the preoccupation with NMR-visible and -invisible fractions and the 40–60 split, one tends to forget the data presented by Yeh *et al.* (1973) on ²³Na⁺ in human erythrocytes. Note here that only 5.8%, rather than 60%, of the cell ²³Na⁺ is invisible. K⁺ is selectively accumulated over Na⁺ in erythrocytes in a manner similar to that in muscle tissues. This sharp contrast with most other tissues studied suggests that in erythrocytes very little Na⁺ is adsorbed and that virtually all intracellular Na⁺ is in the free state, corresponding to a q -value for Na⁺ in erythrocytes equal to 0.15.

8.4.3.4e. NMR Relaxation Times of ⁷Li⁺, ³⁹K⁺, ⁸⁷Rb⁺, and ¹³³Cs⁺ in Living Cells. Since Cope and Damadian's pioneer study of ³⁹K⁺, further studies have been reported of ³⁹K⁺, as well as of ⁷Li⁺, ⁸⁷Rb⁺, and ¹³³Cs⁺. The report of ³⁹K⁺ relaxation times by Civan *et al.* (1976) is significant in that they found two T_2 s for the ³⁹K⁺ signal in frog muscle at 4–7°C, but a single T_1 . From these and other findings they reached the conclusion that ³⁹K⁺, like ²³Na⁺, exhibits a quadrupolar splitting. In view of the evidence just discussed, pointing to specific ionic adsorption rather than free diffusion in a "medium-range" electric field gradient as the cause of the signal splitting, this similarity between ³⁹K⁺ and ²³Na⁺ suggests ³⁹K⁺ adsorption in cells.

In studies of ⁸⁷Rb⁺ and ¹³³Cs⁺ in *Halobacterium*, which contains a very high concentration of K⁺, Edzes *et al.* (1977) supported Cope and Damadian's (1970) earlier conclusion in these words: "The NMR results therefore substantiate that the intracellular ions K⁺, Rb⁺, and Cs⁺ are somehow bound to *Halobacterium*." The NMR data that led them to this view are cited in Table 8.5. But why are frog muscle and *Halobacterium* so fundamentally dissimilar? The muscle accumulates K⁺ selectively only to a level of 0.15 M, while *Halobacterium* may accumulate K⁺ to a level 30 times higher. Moreover, "K⁺ accumulation in *Halobacterium* is retained in the absence of metabolism while the cell membrane is quite permeable" (Edzes and Berendsen, 1975, p. 283). However, the first cannot be considered a valid reason to segregate so completely the

TABLE 8.6. K⁺ Contents of Several Microbes^a

<i>Vibrio costiculus</i>	221 ± 54
<i>Salmonella oranienburg</i>	239 ± 14
<i>Micrococcus halodenitrificans</i>	474 ± 38
<i>Staphylococcus aureus</i>	680 ± 52
<i>Sarcina morrhual</i>	2020 ± 359
<i>Halobacterium solinarium</i>	4750 ± 120

^aData (in millimoles per kg cell water) are taken from Christian and Waltho (1962).

selective K⁺ accumulation in these two organisms; indeed living cells do not accumulate K⁺ to two different discrete levels (e.g., 0.15 M or 4.0 M). Rather, organisms with K⁺ contents covering a wide range are known, as shown for bacteria in Table 8.6. The second reason cannot be used to set muscle tissue and *Halobacterium* apart either; indeed, precisely the same reasons (i.e., retention of permeant K⁺ in the absence of metabolism) led me in 1952 to the theory of selective K⁺ adsorption as the basis for its accumulation in frog muscle and other cells (Table 4.4).

It is ironic that the earlier conclusions of Cope, Jardetzky and Wertz, and others that the NMR-“invisible” fraction of K⁺ and Na⁺ is due to ion binding turn out to be correct, although reached for the wrong reasons.

8.5. Summary

The use of a rapid freezing technique as well as studies using electron microscopy of unfixed, unstained samples; autoradiography; electron probe microanalysis; and laser microprobe mass spectrometric analysis of striated muscle all provide strong evidence that K⁺—and ions like Cs⁺, Rb⁺, and Li⁺ that can replace it—is localized to COO⁻-rich regions of the A band and Z line. These data show that K⁺ in frog muscle cannot be free in solution but is adsorbed, and the results are supported by the study of the X-ray adsorption edge fine structure of K⁺ in frog red cells. This information forced a reevaluation of the results of studies that are often cited as evidence against K⁺ adsorption. For example, ionic conductivity in various cells, and K⁺ mobility in frog muscle cells, are clearly reduced much more than expected were K⁺ to be free in solution. A brief review of studies using K⁺-sensitive intracellular microelectrodes showed a marked variability in the derived activity coefficients, in contradiction to the free-K⁺ concept of the membrane pump theory, and a need for any number of *ad hoc* postulations in order to reconcile the data with the assumption of free cellular K⁺. Finally, the dominant feature of the NMR signals of cellular K⁺ and Na⁺, a quadrupolar interaction with an electric field, is exactly what is expected in the case of ions associated with fixed charges, as perceived in the association-induction hypothesis.

The establishment of the adsorbed state of K⁺ in living cells adds yet another piece of evidence, which is in full agreement with the association-induction hypothesis but cannot be explained by the membrane pump theory, to those already presented, includ-

ing (1) the excessive energy need of the pump (Section 5.2.1); (2) the failure to demonstrate net transport of K⁺ and Na⁺ against concentration gradients in squid axon membrane sheath freed of cytoplasm (Section 5.2.3) and in true membrane vesicles free of cytoplasm; and (3) the success in demonstrating selective K⁺ accumulation and Na⁺ exclusion in cells effectively without a functional cell membrane and postulated pumps (Section 5.2.6). Still other decisive experiments in favor of the association-induction hypothesis but against the membrane pump theory will be presented in following chapters (e.g., Sections 10.3, 12.1, and 13.1).

The establishment of an adsorbed state of the bulk of intracellular K⁺ also leads us back to the question that Hill at one time asked: How is the cell to maintain its equilibrium with an isotonic salt solution if the major cation, K⁺, is not free to exert an equal osmotic pressure? The next chapter provides the answer in the form of the polarized multilayer theory of cell water.



The Physical State of Water in Living Cells

9.1. Introduction

The end of Chapter 2 documented the strong influence of A. V. Hill in the rejection of the earlier theories of "bound K⁺" and "bound water" in cells. Hill's argument was essentially that the evidence supports the concept of free water in cells, and that if the water is free, K⁺ also must be free. In the first half of the preceding chapter, I documented the recent evidence that proves the localization of K⁺ in muscle and its adsorption on fixed carboxyl groups. I now reverse Hill's argument: If all K⁺ is not free, water cannot be free either. That is to say, if K⁺ is not available to reduce the thermodynamic activity of cell water to equal that of the environment, then the cell volume can be maintained only if the water is associated with intracellular macromolecules.

In Chapter 2, I also indicated that one of the reasons for the failure of earlier "bound water" concepts was the lack of a physical theory describing such water. In Chapter 6, however, the theory of the multilayer polarization of water was outlined, and simple model systems were described. In these systems, the cardinal feature of cell water—solute exclusion—is demonstrated. In this chapter I extend the descriptions of properties of water in model systems, and compare them with the behavior of cell water, with the following question in mind: What are the cardinal characteristics of water in the state of polarized multilayers, and in what manner is it distinguished from normal liquid water in regard to not only its solvent properties but also the nature of its response to low temperature and freezing, its vapor sorption isotherm, its NMR relaxation characteristics, and its dielectric relaxation and neutron diffraction patterns? I will recall a number of the earlier observations that, when made, were unexplained, and I will suggest that a reevaluation of the prior studies of cell water using NMR and dielectric relaxation techniques is indicated.

9.2. Solvent Properties

In the polarized multilayer theory, water has different solubility for different solutes. Molecules that because of their small size and specific structure can fit into the water lattice may have near-normal solubility and hence a distribution coefficient between the polarized water and the normal water in the environment (q -value) of close to or in excess of 1. Molecules that cannot easily fit into the water lattice are excluded to varying degrees in direct proportion to their size and complexity.

9.2.1. Inanimate Models

Three sets of inanimate model systems are considered here: sulfonate ion exchange resin, a solution of polyvinylmethyl ether (PVME), and silica gel.

Figure 9.1 shows that the equilibrium levels of alcohols and sugars in the sulfonate ion exchange resin are such that the q -value decreases with increasing size of the molecules. This observation could be explained by heterogeneity of the size of rigid pores in the resin beads; while all pores are accessible to small molecules, only big pores would

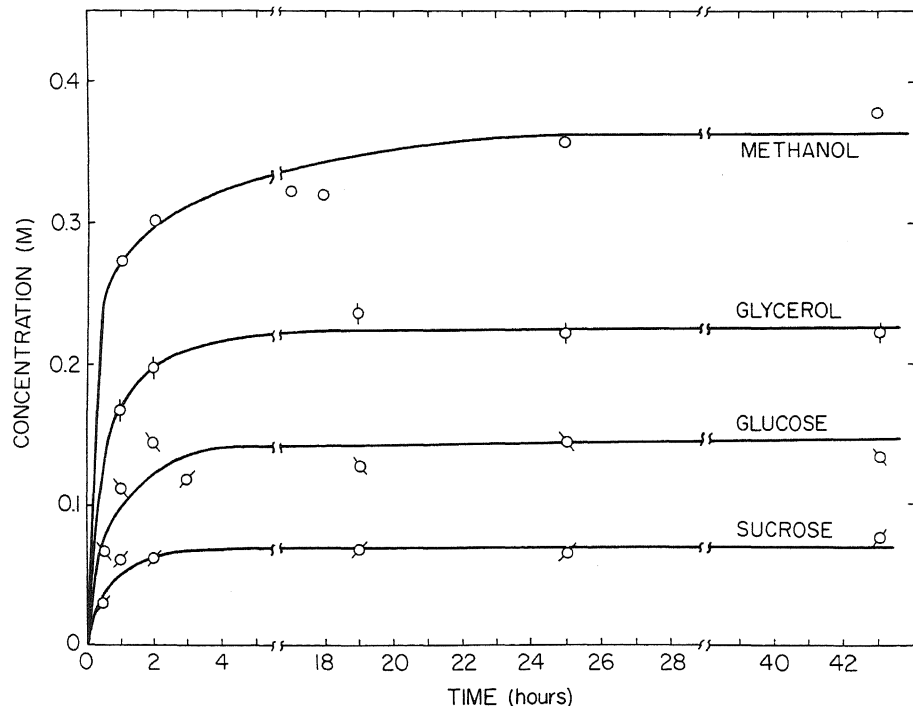


FIGURE 9.1. Time course of uptake of methanol, glycerol, glucose, and sucrose by sulfonate ion exchange resin, Rexyn RG50 (H form) at 0°C. Final external concentrations were 0.38 M for methanol, 0.382 M for glycerol, 0.485 M for glucose, and 0.458 M for sucrose. The equilibrium distribution coefficients (q -values) were 0.97 for methanol, 0.464 for glycerol, 0.309 for glucose, and 0.153 for sucrose. [From Ling *et al.* (1973), by permission of *Annals of the New York Academy of Sciences*.]

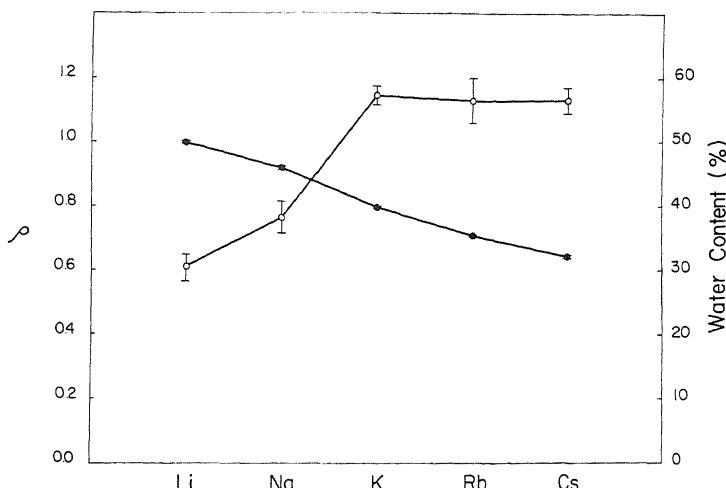


FIGURE 9.2. Water contents (○) and apparent equilibrium distribution coefficients (ρ -values) (●) of D-arabinose in sulfonate ion exchange resin (X-8) with different alkali metal counterions. [From Ling and Sobel (1975), by permission of *Physiological Chemistry and Physics*.]

be accessible to large molecules. This interpretation is ruled out by the experimental results described in Fig. 9.2, which show that increase of the water content, and hence increase of average pore size, did not cause an increase of the ρ -value of the probe molecule, D-arabinose. Indeed, quite the opposite is the case. The exclusion of D-arabinose is greatest when the resin is most swollen with Li^+ as counterion, and it is least excluded in the least swollen resin with Cs^+ as counterion. Ling and Sobel (1975) concluded that it is polarized water rather than rigid pore size that determines solute exclusion.

Figure 9.3 further supports this view. Here the system contained no rigid pores at all; the polymer PVME is made of linear chains fully soluble and dispersed in water. It was enclosed in dialysis bags with membrane pores allowing passage of molecules of about 16,000 daltons, and the sac filled with PVME was fully permeable to all solutes investigated, including polyethylene glycol (molecular weight 4000). The data indicate that the ρ -value varies roughly with the molecular size and complexity of the solute studied, in agreement with the theory that polarized water determines solubility (Ling *et al.*, 1980b).

On theoretical grounds one expects hydrated ions like K^+ , Na^+ , Mg^{2+} , Ca^+ , sugars, and sugar alcohols to be partially excluded from water existing in the state of polarized multilayers. These exclusions have been experimentally established in a variety of model systems (Table 6.4; Fig. 6.14). Similarly the exclusion of free amino acids has been demonstrated both in polymer-water systems and in urea- and guanidine-denatured proteins (Ling *et al.*, 1980b; Ling and Ochsenfeld, unpublished).

Table 9.1, taken from Dalton *et al.* (1962), demonstrates that the exclusion of nitrate salts from the water in silica gel varies with the nature of the cation. Thus the ρ -value of CsNO_3 is close to unity while that of KNO_3 is lower than unity but higher than that of NaNO_3 .

TABLE 9.1. Apparent Equilibrium Distribution Coefficient (ρ -Value) of Various Salts in Silica Gel Water^a

Salt	ρ -Value
$\text{Al}(\text{NO}_3)_2$	0.240
$\text{Mg}(\text{NO}_3)_2$	0.435
$\text{Ba}(\text{NO}_3)_2$	0.478
HNO_3	0.493
NaNO_3	0.519
$\text{Ca}(\text{NO}_3)_2$	0.522
LiNO_3	0.534
$\text{Sr}(\text{NO}_3)_2$	0.538
NH_4NO_3	0.577
KNO_3	0.698
RbNO_3	0.784
CsNO_3	1.00

^aData from Dalton *et al.* (1962), by permission of *Journal of Colloid Science*.

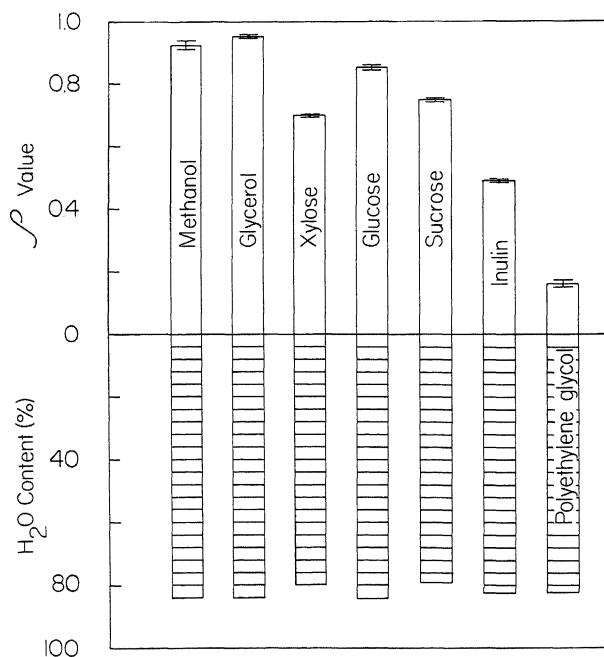


FIGURE 9.3. Water contents and ρ -values of alcohols, sugars, and other compounds in polyvinylmethyl ether solutions (25°C). Initial concentration of the polymer was 50%. All incubation solutions contained 100 mM NaSO₄ plus 10 mM of each of the compounds presented, except inulin and polyethylene glycol, in which cases only trace amounts of labeled materials were added. Incubation lasted 4 days. [From Ling *et al.* (1980b), by permission of *Physiological Chemistry and Physics*.]

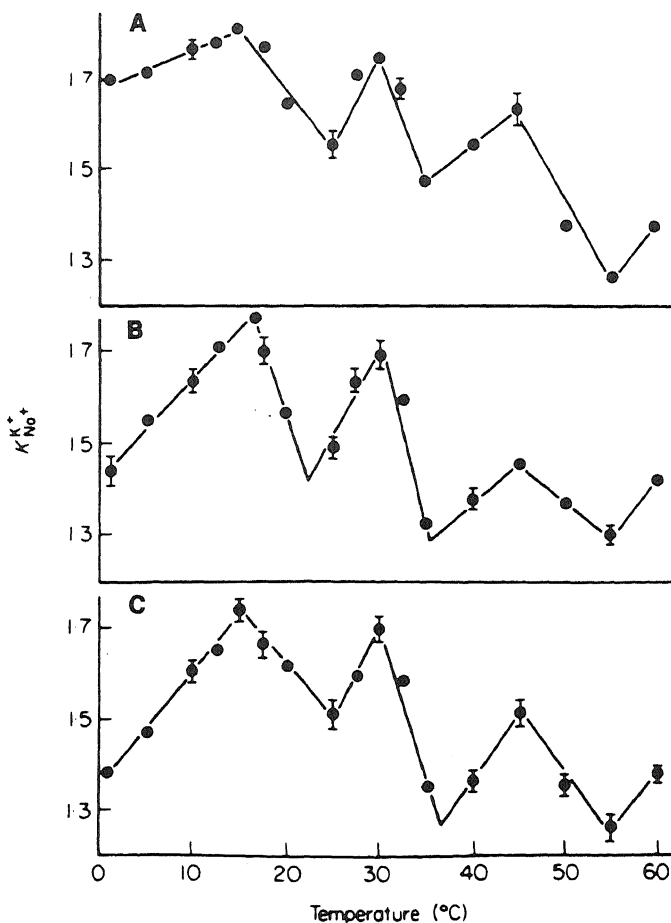


FIGURE 9.4. Variations of the selectivity coefficient, $K_{\text{Na}^+}^{\text{K}^+}$ (defined as $K_{\text{Na}^+}^{\text{K}^+} = [\text{K}^+]_i / [\text{Na}^+]_e$), with temperature in Davison silica gel code 950. The accompanying anions are (A) SO_4^{2-} , (B) I^- , and (C) Cl^- . Each point is the mean of selectivity coefficients calculated from six or eight equilibrations. Vertical lines indicate SDs. [From Wiggins (1975), by permission of *Clinical and Experimental Pharmacology and Physiology*.]

Figure 9.4, taken from Wiggins (1975), shows the variation of the selectivity of K^+ over Na^+ in the water in silica gel. Distinct peaks at 15° , 30° , and 45°C were observed. Water between fused silica plates, an NP-NP system, shows similar peaks in disjoining pressure (Peschel and Belouschek, 1979). For a more extensive collection of this type of temperature transition, see Drost-Hansen (1979).

9.2.2. Biopolymers and Viruses

Table 9.2, taken from Gary-Bobo and Lindenberg (1969), shows ρ -values of non-electrolytes in gelatin that are similar to those in living muscle cells as well as in other

TABLE 9.2. Apparent Equilibrium Distribution Coefficient (ρ -Value) of Various Alcohols and Sugars in Gelatin Gel Water (0.5°C)^{a,b}

Alcohol/sugar	ρ -Value
Methanol	0.94
Ethanol	0.91
n-Propanol	0.91
sec-Propanol	0.89
n-Butanol	0.91
tert-Butanol	0.87
Ethylene glycol	0.93
Propylene-2,3-glycol	0.91
Butylene-2,3-glycol	0.89
Pinaol	0.86
Glycerol	0.90
Glucose	0.94
Fructose	0.95
Sucrose	0.77
Raffinose	0.62
Inulin	0.30
Hemoglobin	0.30

^aTotal water content of the gels is 4.65 g/g dry gelatin.

^bFrom Gary-Bobo and Lindenberg (1969), by permission of *Journal of Colloid and Interface Science*.

TABLE 9.3. Volume of Sucrose- and Egg-Albumin-Inaccessible Water Associated with Vaccinia Virus Particles^{a,b}

Solute added to viral suspension	Concentration of solute in supernatant (g/100 ml)		Volume of H ₂ O per volume of dry viral particles (ml/ml)
	Expected	Observed	
Sucrose	0.62	0.74	5.80
	0.56	0.80	6.55
Albumin	1.13	1.52	5.68
	0.45	0.64	7.56

^aA known volume of virus particles was suspended in a known volume (0.4–0.6 ml) of solution; 0.2 ml of solutions of sucrose or albumin of known concentration was added to the suspension. If the sucrose or albumin were diluted by and dissolved in the entire volume of solution, its concentration in the supernatant should have been that labeled "Expected." Since the observed concentration was higher, part of the water in the viral suspension must have excluded the solutes. If one assumes complete exclusion from such water, then one may calculate a minimum volume of water associated with the viral particles, and this is shown in the last column.

^bFrom McFarlane *et al.* (1939), by permission of *British Journal of Experimental Pathology*.

models (Figs. 9.1 and 9.3). Table 9.3 reproduces data of A. S. McFarlane *et al.* (1939) which show that the sucrose- and egg-albumin-inaccessible water associated with Vaccinia virus particles is from five to seven times the volume of the virus itself.

In 1961, Hearst and Vinograd used an ultracentrifugation method to study the buoyant density of T-4 bacteriophage DNA in a solution containing mixtures of different Li^+ and Cs^+ salts. The hydration water of DNA excludes Cs^+ salts. Since a more concentrated solution of Cs^+ salt is heavier than the hydrated DNA, the buoyant density permits an exact calculation of the minimum amount of water associated with the DNA. Hearst and Vinograd's data are presented in Section 9.4 (Fig. 9.14). A direct quotation from them seems most illuminating:

In this case of complete exclusion, the thickness of the water shell about the DNA molecule in the lithium silicotungstate solution is 11 to 12 Å. This corresponds to approximately 4 layers of water molecules. . . . If the salt is not totally excluded from the hydration water, the extent of the salt-poor hydration will be larger. . . . [Hearst and Vinograd, 1961, p. 1010]

Hearst and Vinograd's data clearly established the *multilayer nature of the water oriented by DNA and the fact that this multilayered water excludes salts*.

The data of McFarlane *et al.* (Table 9.3) established that a large amount of water associated with intact viral particles has a low q -value for sucrose and egg albumin. A more precise measurement of the hydration of another virus, tobacco mosaic virus, was given by Bernal and Frankuchen (1941). Their data was discussed in Chapter 16 (Fig. 16.19), and show that the interparticle distances are up to 300 Å and vary with the normality of the salt solutions. This dependence of the interparticle distance on salt concentration makes it highly unlikely that the forces holding the particles in order are long-range electrostatic forces, because such forces would be ineffective owing to the shielding effect of ions present in the highly concentrated salt solution used (see S. Levine, 1939; Hamaker, 1946; Ferry, 1948, p. 7). Indeed the shrinkage with increase of salt concentration suggests that deep layers of water, far deeper than that suggested by the association-induction (AI) hypothesis for cell hydration, may also exclude salt ions just like T-4 bacteriophage DNA in Hearst and Vinograd's data.

9.2.3. Living Cells

Figure 9.5 shows the equilibrium distribution of different alcohols and sugars in frog muscles at 0°C (Ling *et al.*, 1973). At this temperature, even D-glucose is not being consumed (Ling *et al.*, 1969b). Thus the steady levels of each solute reflect true ρ -values. As in the model systems in Table 9.1 and Fig. 9.1, the ρ -value varies inversely with the size and complexity of the solute molecules.

Horowitz and his co-workers (S. B. Horowitz, 1972; Horowitz and Moore, 1974) demonstrated that the q -value for sucrose in amphibian oocyte cytoplasm is at most 0.64 while that for inulin is 0.24. They too noted the inverse relation between solute size and q -value, theoretically predicted by the polarized multilayer theory of cell water.

As mentioned in Chapter 2, the near-unity ρ -value of urea in the water of frog muscle cited by A. V. Hill (1930; see also Troshin, 1966, p. 128) and the similar ρ -value of ethylene glycol in the water in erythrocytes cited by MacLeod and Ponder (1936) played key roles in rejecting the "nonsolvent" water concept. Neither of these

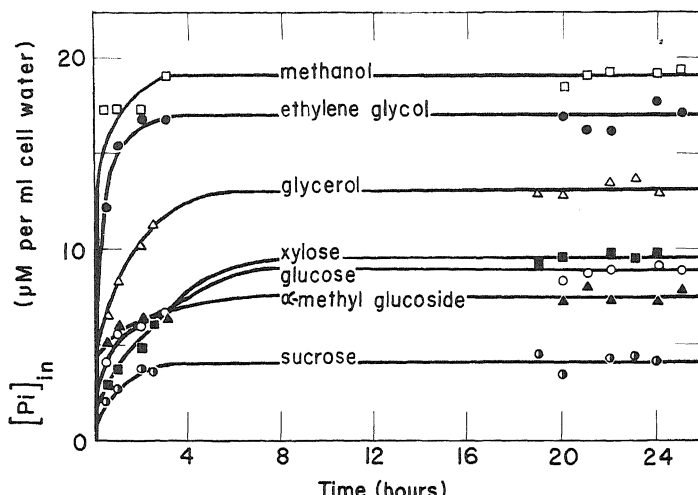


FIGURE 9.5. Time course of uptake of methanol, ethylene glycol, glycerol, xylose, glucose, α -methyl glucoside, and sucrose by frog muscles at 10°C. The initial concentration of all solutes was 25 mM. The final external concentrations were: methanol, 17.0 mM; ethylene glycol, 17.1 mM; glycerol, 18.5 mM; xylose, 19.7 mM; glucose, 21.4 mM; α -methyl glucoside, 20.8 mM; and sucrose, 22.04 mM. The q -values are 1.1 for methanol, 0.99 for ethylene glycol, 0.71 for glycerol, 0.48 for xylose, 0.44 for glucose, 0.36 for α -methyl glucoside, and 0.18 for sucrose. [From Ling *et al.* (1973), by permission of *Annals of the New York Academy of Sciences*.]

findings conflict with the polarized multilayer theory of cell water; on the contrary, urea and ethylene glycol can fit into the polarized multilayer lattice. Thus, as shown in Section 6.3.4, urea distributes equally in polarized water and in normal liquid water. We have also shown that glycerol and ethylene glycol exhibit q -values of unity or even higher than unity in certain model systems as well as in living cells (Ling, unpublished). Why a solute has a lower-than-unity q -value in frog muscle but a unity q -value in other cells poses an interesting question that will be brought up again in Chapter 20.

9.3. Freezing Points

9.3.1. Theoretical Expectations

Jacobson (1955) proposed an ice (I) structure surrounding proteins. Similar views were expressed by Klotz (1958) and A. Szent-Györgyi (1957). In contrast, in the AI hypothesis, water in the state of polarized multilayers is energetically and conformationally *farther removed* from an ice-I structure than is normal liquid water. The reason for this is that water in the state of polarized multilayers does not assume a static ice structure but a dynamic structure dictated by the polarizing NP-NP surfaces of NP-NP-NP chains. Thus the polarized multilayer theory will predict that water between NP-NP surfaces or among NP-NP-NP chain matrices will tend to supercool or even not freeze at all. Jacobson's model will predict the opposite.

The dynamic structure of water in the state of polarized multilayers can be imagined to be revealed after taking photographs repeatedly over a long period of time. This is true, however, only when the NP-NP-NP chains themselves are fixed in space. On the other hand, for a solution of polymer chains which themselves undergo constant random motion, little water structure is revealed, even after many repeated photographic exposures; in that case a wrong impression is created—that there is no water structure at all.

9.3.2. Behavior of Models

9.3.2.1. Water Held between Polished Glass Surfaces and AgCl Plates

It has long been known that water held between glass and quartz surfaces assumes unusual properties (Henniker and McBain, 1948; Peschel and Belouschek, 1979), among which is a lowered freezing point. Figure 9.6, taken from Hori (1956), shows the freezing point of water held between polished glass surfaces as the thickness of the water film changes. At a thickness of 0.01 mm ($10\ \mu\text{m}$) or higher, the freezing point varied within the limits 0 and -30°C . However, at a thickness below $10\ \mu\text{m}$, the freezing point was lower than -80°C .

In order to study the infrared (IR) spectrum (see Section 9.5) of water and ice, only very thin films can be used. Giguère and Harvey (1956) found, to their surprise, that "essentially the same spectrum was obtained for all temperatures studied even down to that of liquid air, confirming that no crystallization had occurred" (p. 801) as illustrated in their figure reproduced here as Fig. 9.7. (For the differences in the IR spectrum of liquid water and ice, see Fig. 9.18.) I suggest that this water is in the form of polarized multilayers and that the AgCl surface represents an NP-NP system. The nonfreezing behavior of thin water films offers another important message: Nonfreezing is not due

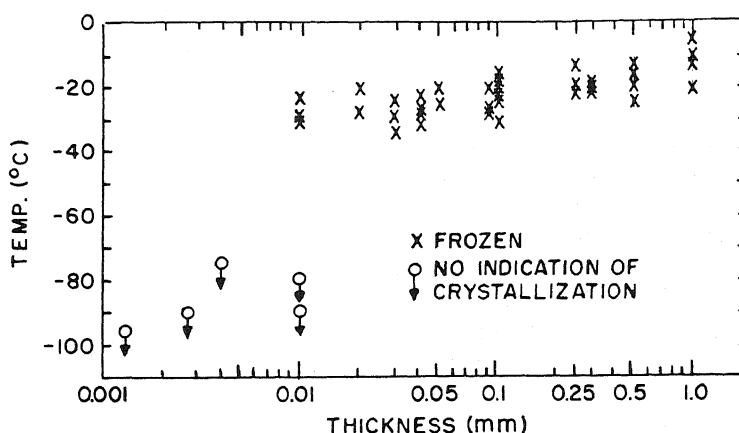


FIGURE 9.6. Freezing properties of thin films of water held between polished glass plates. When the distances fell below $10\ \mu\text{m}$, water did not freeze at the lowest temperature studied. [After Hori (1956), by permission of Wiley-Interscience.]

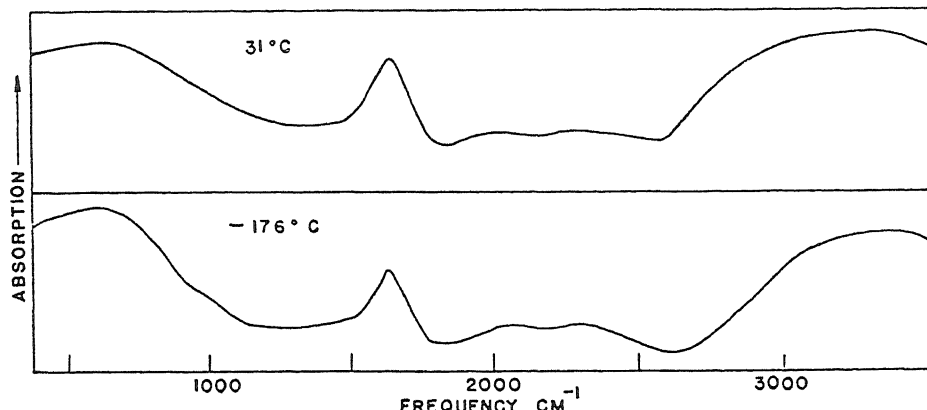


FIGURE 9.7. Infrared absorption spectra of thin films of water between AgCl plates at 31° and -176°C. [From Gigue   and Harvey (1956), by permission of *Canadian Journal of Chemistry*.]

to supercooling as a result of the steric blockage of ice crystal propagation, since in the present case there are no intermingled polymers, only layers of water.

9.3.2.2. Gelatin and PVP

Moran (1926) long ago showed that a supercooled thin gelatin disc forms ice on its outer surface and that the ice will grow thicker at the expense of water from within the gelatin disc without ice crystals penetrating into the gelatin. In a 60% gelatin gel no ice will form at all even in liquid nitrogen (-190°C). Figure 9.8, taken from Luyet, Tanner, and Rapatz (1962) (see also Meryman, 1958), shows that if 50% gelatin is plunged into a -150°C bath none of the X-ray diffraction peaks corresponding to the seven reflecting planes of hexagonal ice is visible. However, if the gelatin is frozen less rapidly, the peaks begin to appear, but not all at the same time. When the freezing is slow (-10°C), all seven peaks can be detected, though in detail they are still not quite similar to normal Ice-I.

Jellinek and Fok (1967) demonstrated the decreasing tendency of water to freeze at low temperature with increasing concentration of polyvinylpyrrolidone (PVP). At a PVP concentration of 60.55%, no ice formed at -40°C.

In Section 6.3.4 it was shown that water under the influence of gelatin and PVP has reduced solubilities for ions and other solutes normally excluded from living cells. The question is: Is the nonfreezing behavior described previously observed with the other NP-NP-NP or NO-NO-NO polymers and proteins? In fact, these systems have now all been studied using differential scanning calorimetry, and new and interesting findings have been made (Ling and Zhang, 1983c).

9.3.2.3. Antifreeze Proteins from Fish Blood

The remarkable ability of antarctic fishes to survive in subzero ocean water was investigated by Scholander and co-workers (Scholander *et al.*, 1957). Serum from their

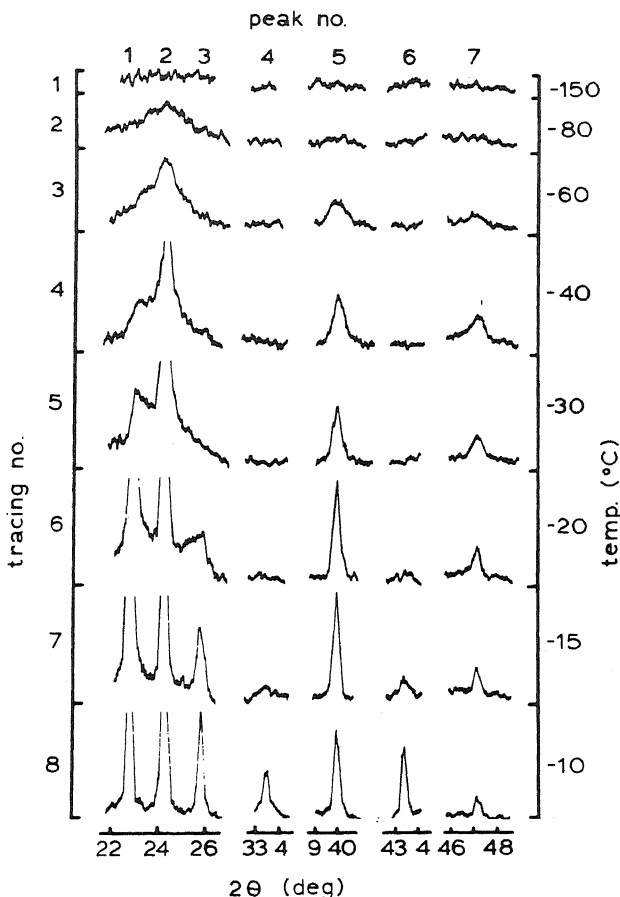
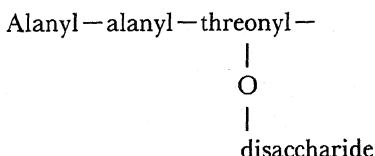


FIGURE 9.8. Stationary stages in the rise of the seven main X-ray diffraction peaks of ice when 50% gelatin preparations were frozen at various rates by immersion in baths at various temperatures (as indicated on each tracing). The order numbers of the angles or peaks are given in the top line, the order numbers of the tracings in the column at left, the freezing temperatures in the column at right, and the scale of 2θ angles underneath the tracings. [From Luyet *et al.* (1962), by permission of *Biodynamica*.]

blood does not freeze at the freezing temperature of a NaCl solution of similar ionic strength owing to the presence of certain glycoproteins (A. L. de Vries and Wohlschlag, 1969) (Fig. 9.9). These proteins contain only alanine, threonine, *N*-acetyl galactosamine and galactose, organized into repeating units with the sequence



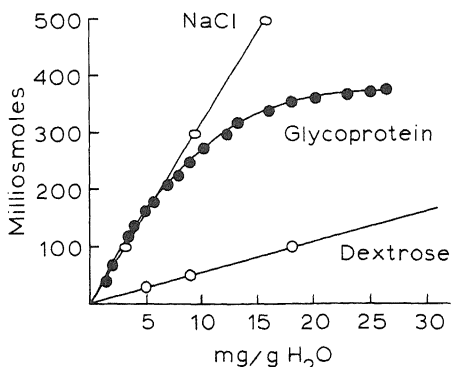


FIGURE 9.9. Freezing points as a function of concentration for aqueous solutions of the freezing point depressant glycoprotein, sodium chloride, and dextrose. The freezing point of a 100 mOsM solution is -0.186°C . [From A. L. de Vries and Wohlschlag (1969), by permission of *Science*.]

The serum of some northern fishes, including the sculpin and northern flounders, also contains antifreeze proteins, but they are not glycoproteins. However, these proteins also contain large percentages of alanine (and aspartic acid).

In terms of the AI hypothesis, these proteins may owe their antifreeze properties to traits similar to those of gelatin (and PVP): an extended polypeptide chain and the consequent long-range polarization of water. Considerable evidence that the antifreeze glycoproteins exist in an extended state has already been collected (see Feeney and Yeh, 1978, p. 216). The antifreeze proteins from sculpin and northern flounders appear to have high α -helical contents; however, the high helical content may not be the state these proteins assume in their natural functional state. A synthetic random polymer of alanine and aspartic acid in a molar ratio of 2:1 has weak but definite antifreeze properties (Ananthanarayanan and Hew, 1977). Such a copolymer at near-neutral pH can only exist in an extended conformation because of mutual electrostatic repulsion among the large number of negative charges carried by the aspartic acid residues.

The role of alanine residues in the antifreeze protein is also very interesting. As indicated earlier, poly-L-alanine exists in a highly stable α -helical form (Section 7.1.3.1). Indeed alanine is a well known helix-former (Chou and Fasman, 1974). In terms of the AI-hypothesis, this is the consequence of the strong electron-donating property of the aliphatic side chain, CH₃. Perhaps these alanine residues, prevented from forming helices by the disaccharide groups, or by negative charges on the aspartic side chains, are capable of influencing an unusually deep layer of water molecules. DeVries called attention to the fact that "large volumes of water are affected [by the antifreeze proteins]" (A. L. de Vries *et al.*, 1970, p. 2907).

9.3.3. Freezing Pattern of Living Cells

Like gelatin gel, when muscle cells were frozen very rapidly no ice crystals could be detected (Menz and Luyet, 1961). Indeed this is the basis of a freeze-drying technique used so successfully in recent years. Ice crystals of increasing size are formed when the freezing is slow. However, at very high subzero temperatures (e.g. -3°C), the pattern of ice formation tells us that the cell water cannot be that of a simple aqueous solution.

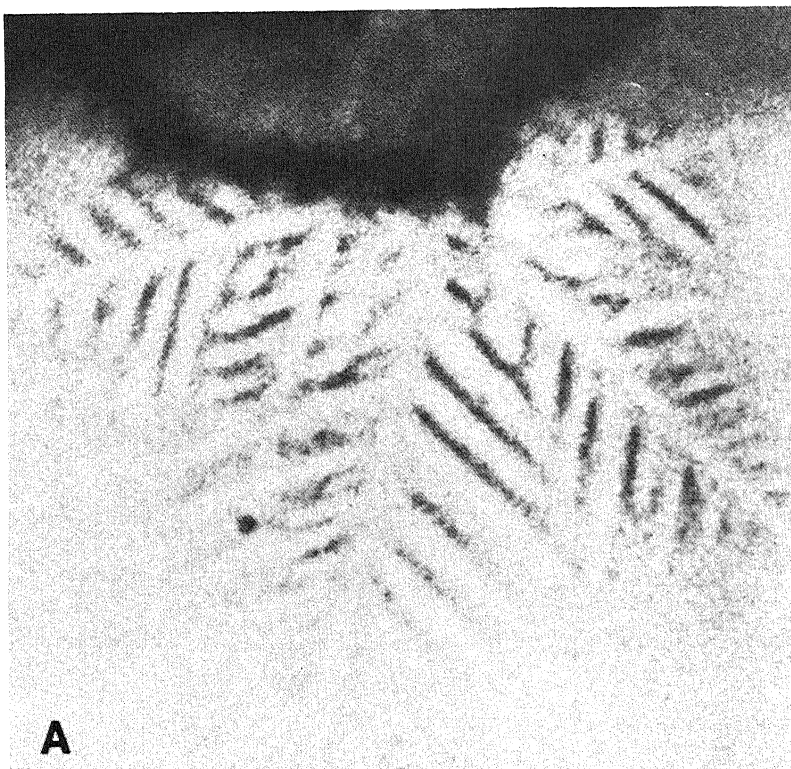
In 1932 R. Chambers and Hale observed different patterns of ice crystal formation

in various types of supercooled cells. The most remarkable was the pattern of ice formation in frog muscle cells. Figure 9.10A shows how a normal ice crystal forms in pure water: It is featherlike with regular branches (Hallet, 1965). Figure 9.10B shows single ice crystal formation in an 11% actomyosin gel (Rapatz and Luyet, 1959). Here clearly the sharp points of the featherlike crystals have been blunted, but the overall snowflake-like shape is retained. A much greater degree of distortion was observed by Chambers and Hale when supercooled muscle cells were touched through a cut end with ice crystals. Many of Chambers and Hale's findings were repeated and confirmed by Miller and Ling (1970), whose observations are reproduced here as Fig. 9.11. One or more rapidly propagating simple spikes without branches are formed (Fig. 9.11A). In normal relaxed muscles these spikes are largely straight. However, these spikes become twisted if the muscle fiber is twisted (Fig. 9.11B). Two other highly significant findings were (1) that ice spikes in continually supercooled muscle fibers will grow in width as well as in length, and (2) that ice spikes will reform at the same loci after the spike has melted by warming. Of particular interest was the finding that a drastic change in intracellular ice formation occurs when an advancing ice spike in a supercooled muscle hits a region of the muscle fiber that is in contraction following local exposure to caffeine. Here the rapid growth of the ice spike abruptly stops, and a bulbous structure slowly grows larger (Fig. 9.11C-E). These results of Chambers and Hale and Miller and Ling offer insight into the physical state of water in living cells. If the cell water is essentially that of a dilute solution, there is no reason why ice crystals can grow only in a predetermined direction, or why ice crystals once begun should not branch as they do outside the living cell. Ice crystal formation following the twisting of the muscle fiber clearly shows that spike propagation is dictated by the orientation of cell proteins. The fact that a thawed spike leaves a track to be faithfully followed by another new spike formed later on further cooling suggests that both the first and the second spike are artifacts arising from splitting of adjacent protein filaments and the consequent distortion of water polarized in multilayers between these filaments. It is in the region where water structure has broken down that ice forms.

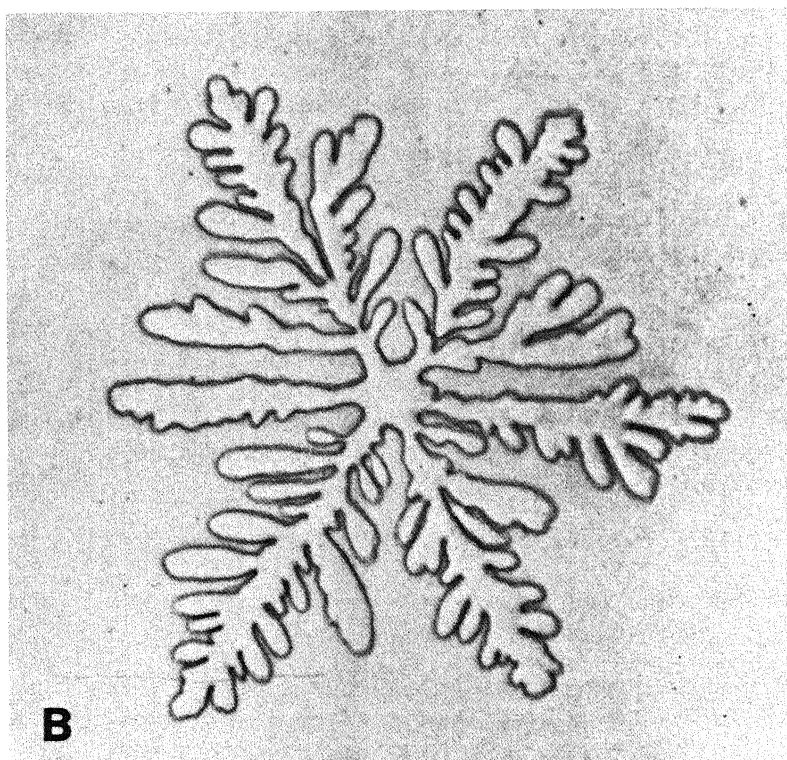
Of equal importance in understanding the pattern of ice formation in muscle cells was the finding of Menz and Luyet (1961) that the diameters of ice crystals found in muscle cells decreased with an increase in the speed of freezing. At the fastest speed, no discernible ice crystals could be found. These findings not only are of great technical use in preparing freeze-dried preparations for electron microscopy, but also provide support for the notion that water in normal resting cells exists in a different physical state. Its structure resists freezing in a manner different from that of supercooled liquid water, because no matter how rapidly liquid water is cooled, it has not been possible to freeze it without crystal formation (Kamb, 1972, p. 11).

9.4. Vapor Sorption Isotherms

One way to study protein hydration is by exposing proteins at constant temperature to an air phase in which the partial vapor pressure is controlled by aqueous solutions of NaCl or H₂SO₄ of different strengths. Nearly 60 years ago Walter (1923) compared the vapor sorption isotherm of plant protoplasm with those of gelatin, nucleic acids, and



A



B

FIGURE 9.10. (A) Normal ice crystal. [From Hallet (1965), by permission of *Federation Proceedings*.] (B) Ice crystal formation in an 11% actomyosin solution. [From Rapatz and Luyet (1959).]

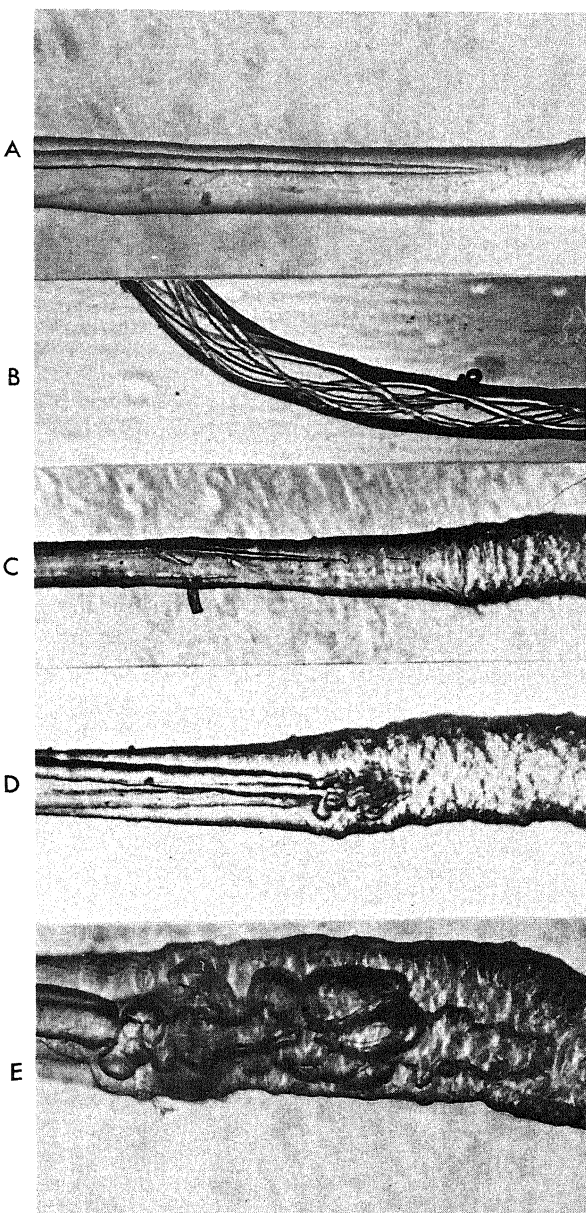


FIGURE 9.11. Freezing pattern of water in a single frog muscle fiber. (A) Single spike rapidly propagating in a normal muscle fiber. (B) Several spikes grow simultaneously in a twisted muscle fiber. (C-E) Three stages in the ice formation at the junction between a normal relaxed portion (left) and a contracted portion induced by local exposure to 5 mM caffeine. [From Miller and Ling (1970), by permission of *Physiological Chemistry and Physics*.]

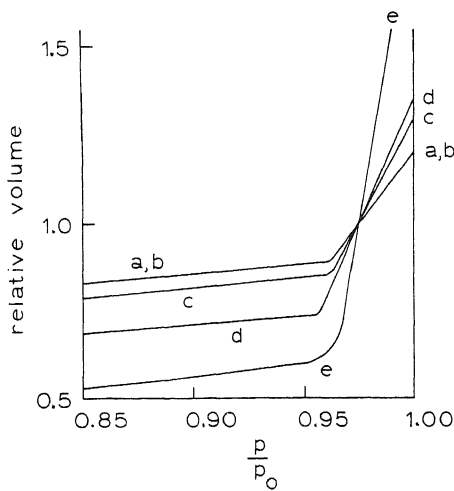


FIGURE 9.12. Comparison of the water uptakes of gelatin, nucleic acid, casein, and starch with that of living protoplasm. (a) Starch, (b) nucleic acid, (c) casein, (d) protoplasm, (e) gelatin. Ordinate: Volume relative to that in 1.0 M glucose solution. Abscissa: Relative vapor pressure. [Redrawn from Walters (1923), by permission of *Jahrbücher für Wissenschaftliche Botanik*.]

starch (Fig. 9.12), and J. R. Katz (1919) studied water sorption in albumin and gelatin (Fig. 9.13A,B). In 1944, Bull studied albumin as well as oxyhemoglobin, and his data are compared with Katz's in Fig. 9.13.

As pointed out in Section 6.3.1.4, Bull and Breese (1968a, b) provided data in support of Pauling's concept that only polar side chains hydrate; they chose water sorption at 92% vapor saturation and showed that with few exceptions the hydration could be accounted for by counting the number of polar side chains and assuming that each adsorbed six water molecules. The choice of 92% humidity is, of course, arbitrary; at higher humidity each protein continues to take up more water, as shown by Katz's

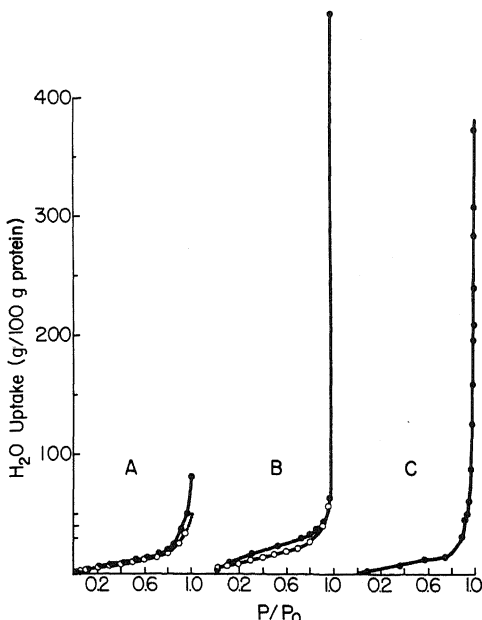


FIGURE 9.13. (A) Water sorption on bovine serum albumin, from J. R. Katz (1919) (●) and Bull (1944) (○). (B) Water sorption on gelatin, from J. R. Katz (1919) (●), and on oxyhemoglobin, from Bull (1944) (○). (C) Water sorption on frog muscle, from Ling and Negendank (1970).

studies, in which he took meticulous care to devise ways to study sorption at 100% humidity. At full saturation, the maximum number of water molecules taken by each polar side chain would have to be much more than six, if one accepts Bull and Breese's way of counting.

In Fig. 9.13B I have plotted Katz's data on water sorption on gelatin. For sorption at relative humidity below 95%, the curve is not much different from that of oxyhemoglobin. However, at relative humidity above 95%, a drastically different picture emerges. Thus in oxyhemoglobin, a globular protein, water sorption doubled on increasing humidity from 95% to 100%; in gelatin, an extended protein, it rose nearly ten times!

According to the AI hypothesis the extensive uptake of water when the humidity increases from 95% to 100% bespeaks of the buildup of polarized multilayers of water and reflects water adsorbed on the exposed NHCO groups. In gelatin, the presence of glycine-proline-hydroxyproline triads prevents the formation of α -helices, allowing NHCO groups to remain exposed (Section 6.3.4).

In Fig. 9.14 the data of Hearst and Vinograd (1961) are reproduced; the amount of water that excludes Cs^+ on T-4 bacteriophage DNA is shown as a function of water

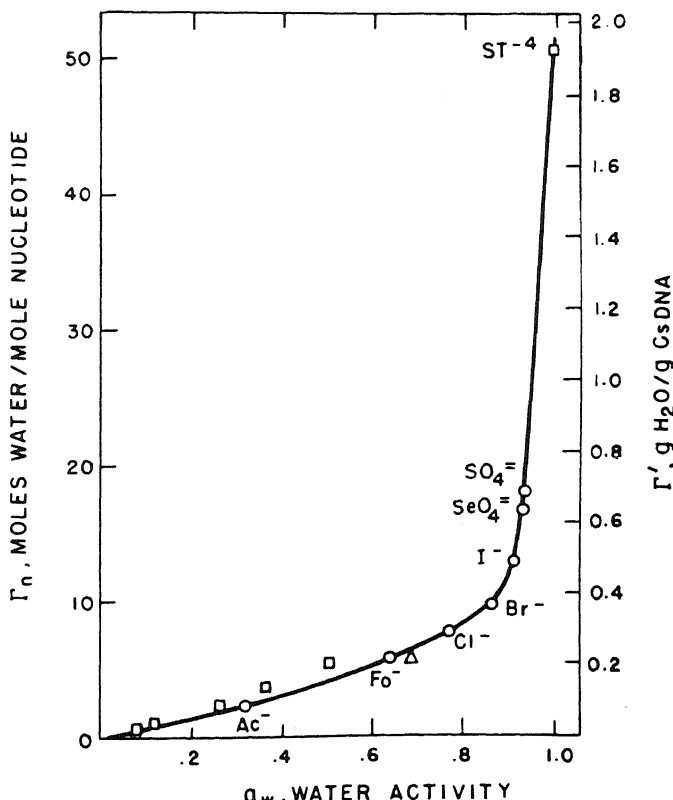


FIGURE 9.14. The net hydration of T-4 bacteriophage DNA. \circ , CsDNA; \square , LiDNA. [From Hearst and Vinograd (1961), by permission of *Proceedings of the National Academy of Sciences*.]

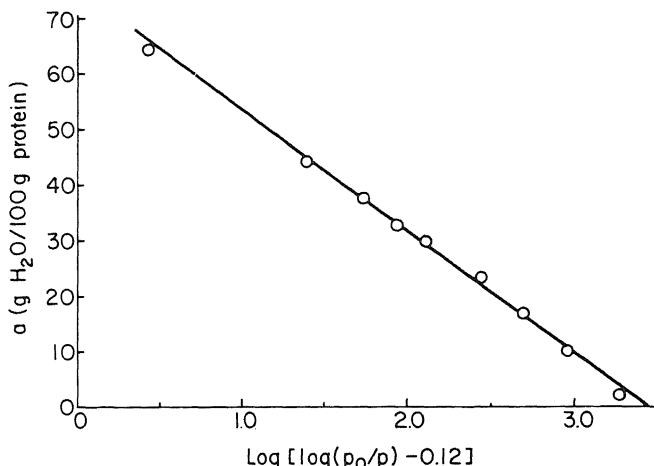


FIGURE 9.15. Water sorption on gelatin. Data taken from J. R. Katz (1919). Straight line through most data points indicates obedience to predictions of Bradley's polarized multilayer adsorption isotherm.

activity. It shows a pattern at high humidity like that of gelatin in Fig. 9.13. This is of course the same water that has another attribute of water in living cells: solute exclusion (Section 9.2.2).

The curve shown in Fig. 9.13C is the water sorption of frog sartorius muscle cells. Like gelatin, PVP, and T-4 bacteriophage, muscle cells show a large and abrupt increase of water uptake after the relative humidity reaches 95%. Ling and Negendank (1970) have shown also that the water contents of frog muscle cells equilibrated in a vapor phase of relative humidity above 0.986 are indistinguishable from those determined in cells immersed in modified Ringer solutions of similar vapor pressures.

If the water taken up by these systems is primarily in the form of polarized multilayers, then the water adsorbed at different relative humidities or vapor pressures should follow the theory of multilayer adsorption derived by Bradley (1936) and given in equation (6.8). In other words, in a plot of $\log [\log (p_0/p) - K_4]$ against a , grams

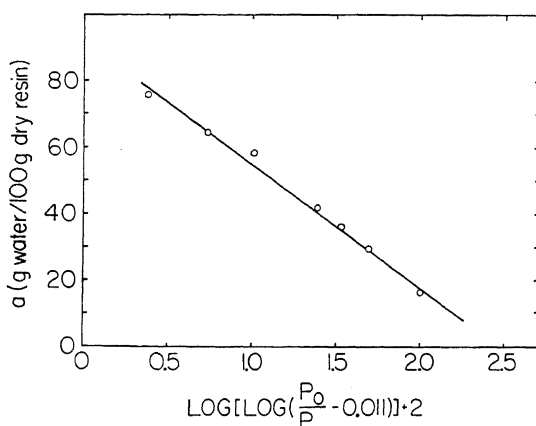


FIGURE 9.16. Equilibrium water of sulfonate ion exchange resin (H form) containing 10% cross-linking agent, DVB. Data from Glueckauf (1952). Straight line through most data points indicates obedience to predictions of Bradley's polarized multilayer adsorption isotherm. [From Ling (1970b), by permission of *International Journal of Neuroscience*.]

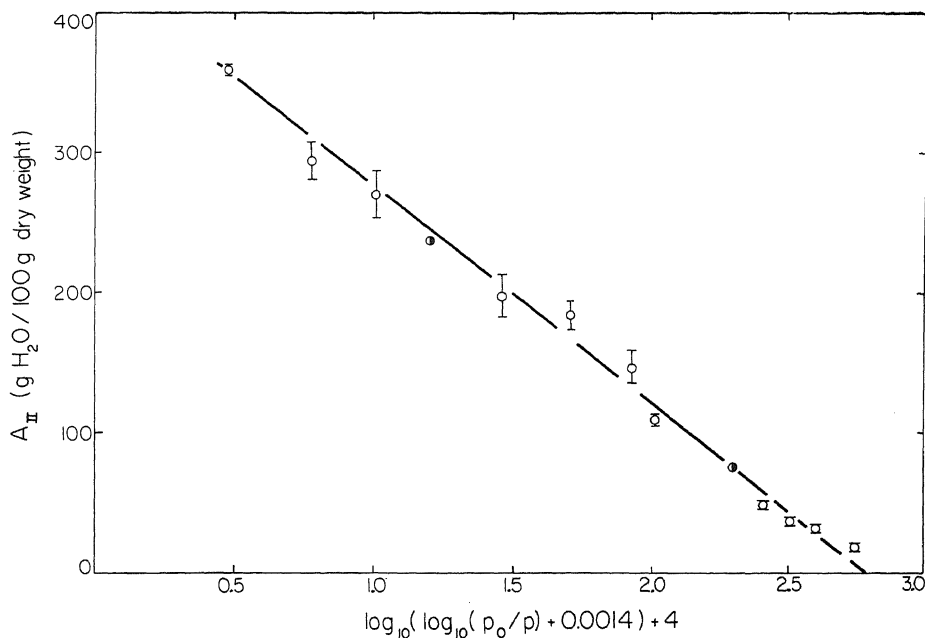


FIGURE 9.17. Water sorption isotherm of isolated frog muscle fibers. Data refer to 95% of the total muscle water. The remaining 5% behaves according to a Langmuir monolayer isotherm and has been subtracted. Straight line through most data points indicates obedience to predictions of Bradley's polarized multilayer adsorption isotherm. Half-filled circles are data from time-course studies. [From Ling and Negendank (1970), by permission of *Physiological Chemistry and Physics*.]

of water sorbed per 100 g dry protein, the data should fall on a straight line. Figure 9.15 shows that this is indeed the case for Katz's data (Fig. 9.13B) on gelatin. Figure 9.16 shows a similar behavior of water in sulfonate ion exchange resin, which we have just discussed in relation to its solute exclusion properties (Section 9.2.1). Figure 9.17 is the vapor sorption isotherm of 95% of the water of frog sartorius muscle (Ling and Negendank, 1970). The remaining 5% appeared to be primarily adsorbed in monolayers, presumably on polar side chains, following a Langmuir type of isotherm.

In summary, the shape of the vapor sorption isotherm offers strong evidence that in gelatin and in muscle cells extended proteins with their polypeptide chains directly exposed to water bring about its multilayer polarization.

9.5. Infrared and Raman Spectra*

Both infrared (IR) and Raman spectra have been extensively used in chemistry, as in the difficult task of understanding the structure of liquid water. Changes in the shapes

*For an elementary discussion of infrared and Raman spectroscopy concepts and terminology, see Appendix B.

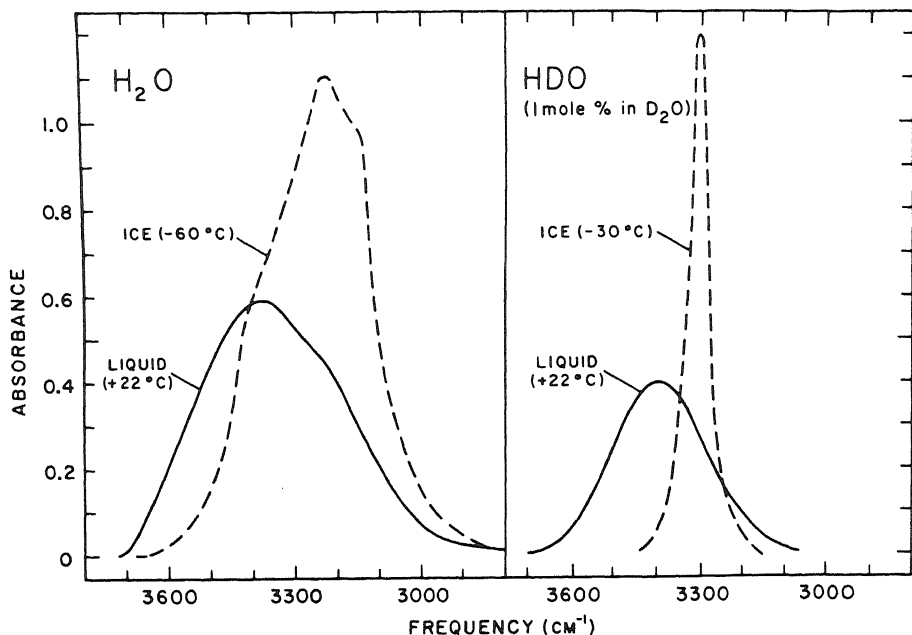


FIGURE 9.18. Comparison of the absorbance profiles of H_2O and of isotopically dilute HDO in the OH stretching region. [From M. Falk *et al.* (1970), by permission of *Canadian Journal of Chemistry*.]

of IR and Raman bands with temperature and pressure have given insight into the existence of different species of water in chemical equilibrium (Buij and Choppin, 1963; Walrafen, 1968).

In Section 9.2.2, we demonstrated extensive water uptake by DNA at high humidity and the ability of the water taken up to exclude solutes like salt ions. Figure 9.18, taken from M. Falk *et al.* (1970), shows the absorption profiles of pure H_2O and of isotopically dilute HDO in the OH stretching region. Note the markedly different spectra between liquid water and ice. Figure 9.19, taken from the same authors, shows that isotopically dilute HDO adsorbed on DNA has the same band profile as that of HDO in liquid water. This indifference of the spectrum to adsorption on DNA is not surprising as we are dealing with very high energy changes, out of the range of weak electrical polarization in multilayer formation.

In other experiments Falk *et al.* showed that an inner shell of water of about nine molecules per nucleotide cannot be frozen into ice, although excess water beyond this limit readily freezes.

I have cited the work of Falk *et al.* in some detail because it shows quite clearly that water under the influence of DNA and that exists in the state of polarized multilayers with reduced solubility for salt ions does not show significant IR spectrum changes. Since, according to the AI hypothesis, water in living cells is in a similar state, one may reasonably not expect significantly different IR spectra in the near IR range. However, other IR studies of water associated with gelatin (Sponsler *et al.*, 1940) and with PVP (de Phillips, 1965), and Raman spectra studies of lysozyme solution (Cavatorta *et al.*, 1976), did demonstrate some changes.

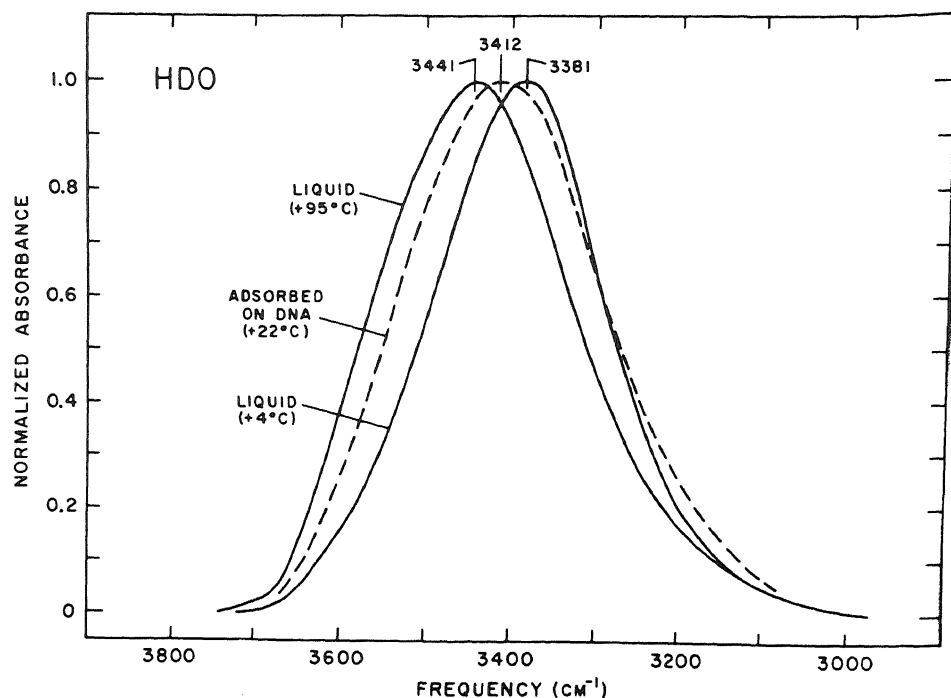


FIGURE 9.19. Comparison of the OH stretching profiles of 1 mole % of HDO in D₂O for liquid water at 4° and 95°C and adsorbed water on DNA at room temperature (difference profile corresponding to DHO desorbed between 4% and 3% relative humidity). [From M. Falk *et al.* (1970), by permission of Canadian Journal of Chemistry.]

Pezolet *et al.* (1978), in a study of the Raman spectrum of intact single barnacle muscle fiber in the 2700- to 3800-cm⁻¹ region (2.6–3.7 μm), reported no difference between water in the muscle and normal liquid water. From what has already been discussed this is not surprising.

9.6. Dielectric Dispersion

In a vacuum, electric charges on a parallel plate condenser give rise to a potential difference, *V*. The introduction of water into the space between the plates causes a reduction of *V* by a factor of 81; this is the *static dielectric constant* (ϵ_s) of water. Water molecules have an asymmetric charge distribution and are polarized by the electric field of the charged condenser in such a way as to almost completely annul the electric field produced by the charges originally present on the parallel plate condenser.

If the electric field is not static but fluctuates with time, then the electrical polarization of the dielectric medium, water, will not follow instantly but will exhibit inertia. The field strength of the periodically fluctuating field is

$$E = E_0 \cos \omega t \quad (9.1)$$

where E_0 is time-independent and $\omega/2\pi$ is the frequency in cycles per second (Hz). The dielectric displacement D , is equal to ϵ_s , hence,

$$D = D_0 \cos (\omega t - \Phi) \quad (9.2)$$

where Φ is the *phase shift* resulting from the lag owing to the inertia of the polarization of the water molecules. From equation (9.2) and elementary trigonometry,

$$D = D_0 \cos (\omega t - \Phi) = D_0 (\cos \omega t \cos \Phi + \sin \omega t \sin \Phi) \quad (9.3)$$

The dielectric displacement, D , may then be perceived as having two parts:

$$D = D_1 \cos \omega t + D_2 \sin \omega t \quad (9.4)$$

where

$$D_1 = D_0 \cos \Phi, \quad D_2 = D_0 \sin \Phi \quad (9.5)$$

Introducing two different dielectric constants, ϵ_1 and ϵ_2 , both of which are frequency-dependent,

$$D_1 = \epsilon_1 E_0, \quad D_2 = \epsilon_2 E_0 \quad (9.6)$$

From equation (9.5),

$$\frac{D_2}{D_1} = \frac{\sin \Phi}{\cos \Phi} = \tan \Phi \quad (9.7)$$

and from equation (9.6),

$$\frac{D_2}{D_1} = \frac{\epsilon_2}{\epsilon_1} \quad (9.8)$$

Therefore,

$$\tan \Phi = \frac{\epsilon_2}{\epsilon_1} \quad (9.9)$$

ϵ_2 is proportional to the energy loss in the dielectric. Φ , the phase shift, is usually described as the *loss angle* (Fröhlich, 1958).

As one increases the frequency of the electric field, the polarization of water can follow, until the frequency reaches a level so high that the polarization can no longer keep up. At this point the dielectric constant begins to decrease with further increase of frequency to reach another steady low level designated as ϵ_∞ . The decrease of dielectric constant with increase of frequency is called *dielectric dispersion*.

FIGURE 9.20. Frequency dependence of the dielectric constants of ice and bound and normal (free) water. All three curves have comparable limit values. The curve for bound water is less steep than the others. [After Schwan (1965).]

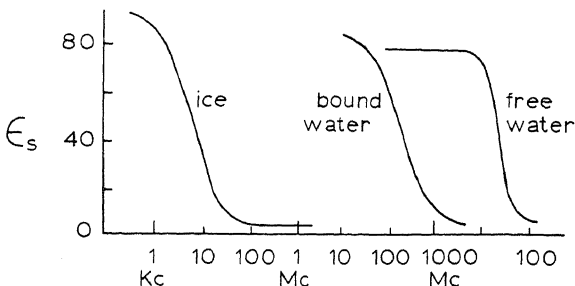


Figure 9.20, after Schwan (1965), shows that normal liquid water has a dispersion at 20 GHz (20×10^9 cycles/sec), while ice has a dispersion at less than 10 KHz (10×10^3 cycles/sec). The difference is due to the much higher energy (enthalpy) barrier for the rotation of water molecules in the ice crystals (D. Eisenberg and Kauzmann, 1969). In addition, Fig. 9.20 shows the dispersion of "bound water" associated with native globular proteins at about 100 MHz (100×10^6 cycles/sec) (Pennock and Schwan, 1969); this bound water is that discussed in Chapter 7, which corresponds to water "bound" to polar side chains.

A set of exact equations (the Debye equations) for the complex dielectric dispersion phenomenon of a solution containing molecules with permanent dipole moments was presented by Debye (1929):

$$\epsilon_1(\omega) = \epsilon_\infty + \frac{\epsilon_s - \epsilon_\infty}{1 + \omega^2 \tau_d^2} \quad (9.10)$$

$$\epsilon_2(\omega) = \frac{(\epsilon_s - \epsilon_\infty)\omega\tau_d}{1 + \omega^2 \tau_d^2} \quad (9.11)$$

As mentioned earlier, ϵ_1 is the dielectric constant, ϵ_2 is the dielectric loss, and Φ is the loss angle:

$$\tan \Phi = \frac{\epsilon_2}{\epsilon_1} = \frac{(\epsilon_s - \epsilon_\infty)\omega\tau_d}{\epsilon_s + \epsilon_\infty \omega^2 \tau_d^2} \quad (9.12)$$

In these equations ω is 2π times the frequency of the periodically oscillating field in cycles per second and τ_d is the (Debye) dielectric *relaxation time*, or the rate constant for the decay of the macroscopic polarization when the applied field is removed. For pure liquid water, the dielectric dispersion can be described by the Debye equations. In this case, the assumption that there is only one relaxation time, τ_d , seems adequate. This is, however, not so with other more complex systems, and a modification of the Debye equation was given by Cole and Cole (1941):

$$\epsilon^*(\omega) = \epsilon_\infty + \frac{\epsilon_s - \epsilon_\infty}{1 + (i\omega\tau_d)^{1-\alpha}} \quad (9.13)$$

where the complex dielectric constant ϵ^* is equal to $\epsilon_1(\omega) - i\epsilon_2(\omega)$. In this treatment it is no longer assumed that the dielectric has a single relaxation time as in the Debye equations. Rather there is a variety of τ_d 's whose values follow a bell-shaped distribution curve. α measures the width of this distribution curve. In cases like pure liquid water, where a single τ_d adequately describes the data, $\alpha = 0$. Cole and Cole also introduced a graphic representation of their equation which gives the arc of a semicircle in the complex plane plotting ϵ_2 against ϵ_1 , with the diameter of the semicircle making an angle $\alpha\pi/2$ with the real (ϵ_1) axis (see Fig. 9.23).

9.6.1. Model Systems*

9.6.1.1. Protein Solutions

Oncley (1953) measured the dielectric properties of aqueous solutions of proteins up to a frequency of 20 MHz. A dispersion at 2 MHz was attributed to rotation of the protein molecules themselves. Haggis *et al.* (1951) and Buchanan *et al.* (1952) discovered another dispersion between 20 MHz and 3 GHz, which they attributed to a shell of water of hydration. Later Pennock and Schwan (1969) measured the complex dielectric constant of horse hemoglobin solution up to 26.6 g/100 ml at frequencies between 1 MHz and 1.2 GHz. From these studies they concluded that there are altogether three distinct dispersions: One below 10 MHz is due to rotation of whole protein molecules; another one between 10 and 100 MHz is due to rotation of polar side chains; and a third one near 500 MHz is due to a shell of bound water. E. H. Grant (1966) attributed the dispersion of an albumin solution above 100 MHz to hydration water only.

Technically it is very difficult to study dielectric properties at very high frequencies, especially in protein solutions, where the behavior of hydration water may be difficult to observe because of the limited solubilities of the proteins and the overwhelmingly large population of free water in the system.

Using a technique introduced by Masszi and Örkényi (1967), Masszi (1972) measured the dielectric constant of 5–50% gelatin solutions at the frequency range of 2.6 to 4.0 GHz. From these studies Masszi drew the conclusion that gelatin causes the reduction of the entropy of rotation of water in support of the polarized multilayer concept introduced by Ling.

9.6.1.2. Water Sorption on Protein Powders

One way to overcome the limitation in the study of protein hydration in protein solutions is to study water sorbed on protein powders and crystals. A very important study of this kind on chicken egg white lysozyme was reported by S. C. Harvey and Hoekstra (1972) using frequencies from 10 MHz to 25 GHz. They found that with increasing hydration both the dielectric constant ϵ' or (ϵ_1) and the dielectric loss ϵ'' or (ϵ_2) at 25 GHz exhibit a sharp break at 0.3 g H₂O/g protein (Fig. 9.21). For this break, Harvey and Hoekstra considered two possible interpretations: (auto)cooperativity in the uptake of water or two kinds of sites for hydration. They then chose to study two hydration levels: 0.34 and 0.54 g H₂O/g protein, each representing the regions below and beyond the break.

*For important additional data, see the footnote on p. 298.

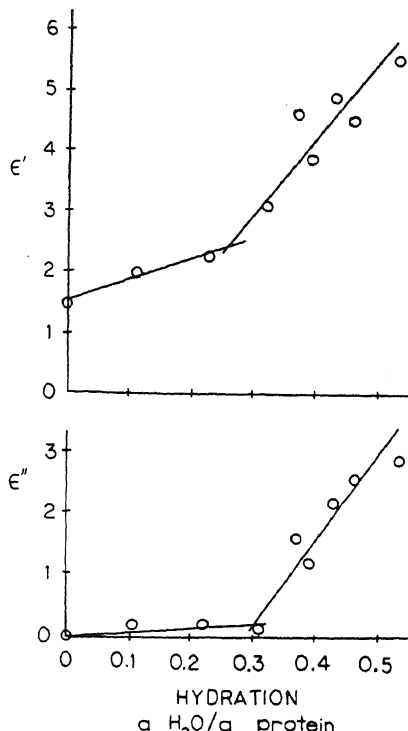


FIGURE 9.21. Dielectric constant (ϵ') and loss (ϵ'') of packed lysozyme powder as a function of water content; $f = 25$ GHz, $T = 25^\circ$. [From Harvey and Hoekstra (1972), by permission of *Journal of Physical Chemistry*.]

Figure 9.22 shows the dielectric constant (ϵ_1) and loss (ϵ_2) at varying frequencies at the two different levels of hydration. At 0.3 g H₂O/g protein it appears that a single monolayer of adsorbed water is formed; two layers are found at the higher level of hydration. At the lower level of hydration there is a well-defined dispersion at 250 MHz, but very little dispersion at higher frequencies. However, as the second layer of water is taken up, the dispersion at 250 MHz remains the same, but another dispersion occurs over a range of frequencies indicated by $\alpha = 0.3$, which corresponds to the second layer, as indicated by the Cole-Cole plots (Fig. 9.23). The dielectric loss around 10 GHz is primarily due to the secondary layer.

Harvey and Hoekstra's finding that water in the second hydration layer is, like that in the first layer, rotationally hindered has been confirmed in other protein crystals (Kent, 1970, 1972; Bone *et al.*, 1977). The data clearly show that water may be taken up by proteins not only as a monolayer on polar side chains but also as additional layers of water which also suffer rotational restriction—in general agreement with the polarized multilayer theory of cell water.

9.6.2. Living Cells

Measurements of dielectric properties of living cells at the appropriate frequencies provide in principle an excellent means of testing the alternative theories that the bulk phase cell water is free or in polarized multilayers. Unfortunately the task is hampered

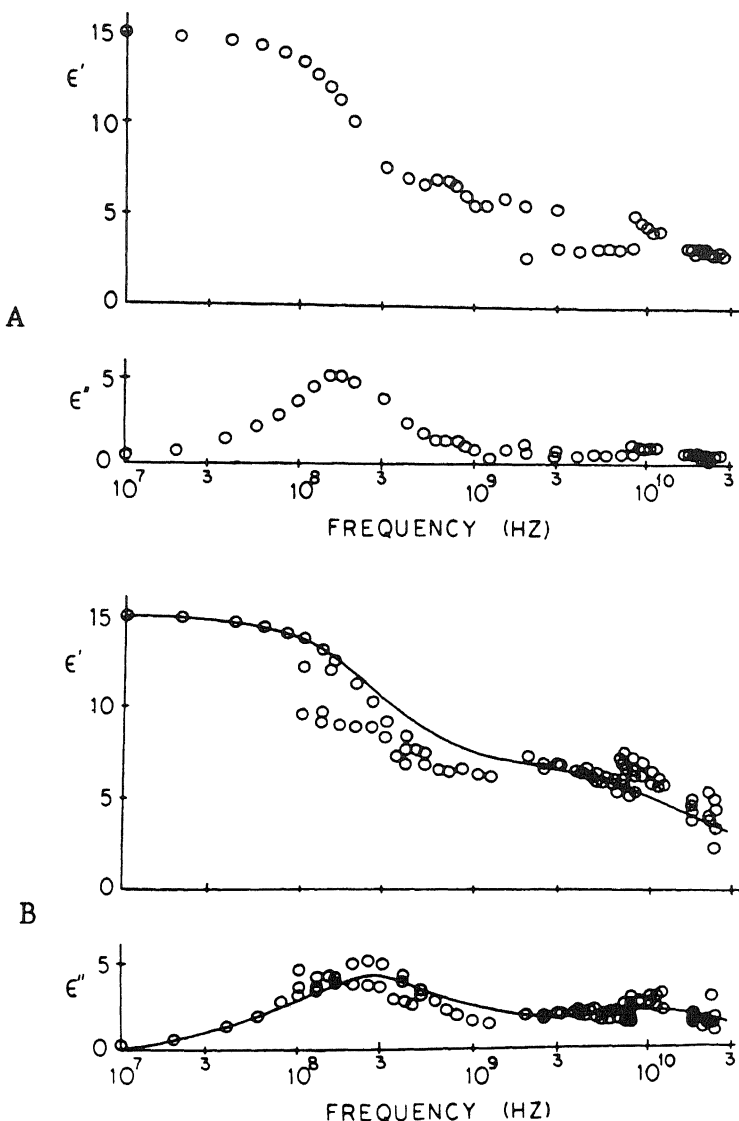


FIGURE 9.22. Dielectric constant (ϵ') and loss (ϵ'') as a function of frequency for packed lysozyme samples containing (A) slightly more than one monolayer of water ($h = 0.34 \pm 0.03$ g of H_2O/g of protein; $T = 25^\circ C$) and (B) nearly two monolayers of water ($h = 0.54 \pm 0.04$ g H_2O/g of protein; $T = 25^\circ C$). The curves correspond to the values given by the Debye equation for two dispersions. [From Harvey and Hoekstra (1972), by permission of *Journal of Physical Chemistry*.]

by three major difficulties. One is purely technical, and arises from the need to measure dielectric properties at very high frequencies near the frequency of normal liquid water dispersion (i.e., 10–70 GHz). Another is the lack of knowledge about the dielectric properties of water models known to exist in the state of polarized multilayers. A third source of difficulty is the deterioration of tissue during the measurement.

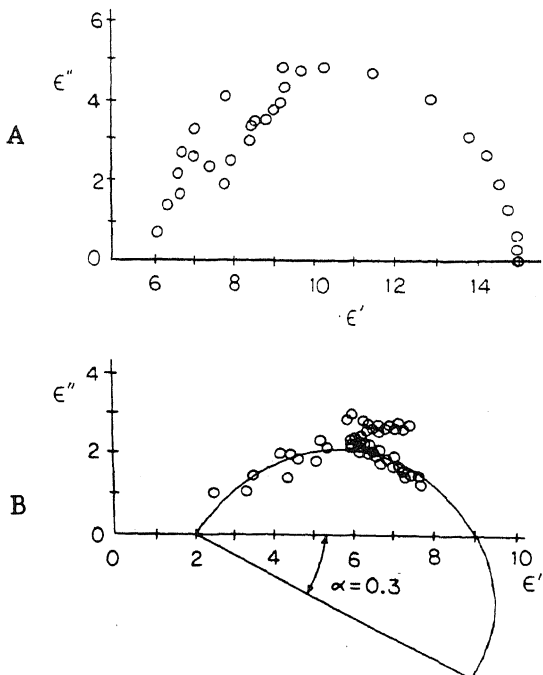


FIGURE 9.23. (A) Cole-Cole plot of the low-frequency ($f < 1.5$ GHz) observed in Fig. 9.22. From this figure $f_0 = 0.25$ GHz, $a = 0$. (B) Cole-Cole plot of the high-frequency dispersion observed in Fig. 9.22. The contributions made to ϵ'' by the low-frequency dispersion were calculated using the Debye equation, with $f_0 = 0.25$ GHz, $a = 0$. These contributions were then subtracted point by point from the data of Fig. 9.22, and the resulting values of ϵ' and ϵ'' are plotted here. [From Harvey and Hoekstra (1972), by permission of *Journal of Physical Chemistry*.]

Some of these difficulties are seen in the papers of Schwan, Foster, and their co-workers (Schwan and Foster, 1977; Foster *et al.*, 1979; Jenin and Schwan, 1980), in which they reported their studies of dielectric properties of living tissues. From these studies they concluded that 90% or more of the cell water is simply normal liquid water and that its properties can be described by the simple Debye equation. However, in most of their studies, their instruments were not able to study frequencies higher than 10 GHz, while the *characteristic relaxation frequency* (f_r) for normal liquid water at 37°C is around 25 GHz. Thus extensive data extrapolation had to be carried out, making it uncertain whether their data truly support their conclusions. However, this criticism does not extend to a more recent paper (Foster *et al.*, 1980) in which, although still using frequencies to a maximum of only 17 GHz, they took advantage of the reduction of f_r at 1°C (to 9 GHz) and studied the dielectric properties of isolated giant barnacle muscle fibers. From these they concluded that 95% of the muscle water is normal liquid water.

Even though these authors used excitability and contractility to establish the normalcy of the muscle cells after the measurements had been made, these properties might reflect only partial survival, and therefore these muscles could not be regarded as truly normal. Indeed, there are good reasons to suspect this from my own experience with these muscles. The barnacle muscle cells are always firmly attached to the shells. In order to isolate them, one end has to be cut. Unlike Vermont frog muscles, in our hands at least, these cut barnacle muscle fibers deteriorate rapidly. For this reason, most of the studies of Reisin and Ling (1973) on barnacle muscle fibers were conducted on intact cells with the shell attached. Foster *et al.* (1980) did not use muscle fibers with shells attached. It would seem that an easy way to overcome these difficulties would be to use

frog muscles, which are easily isolated in intact form and can well stand 0°C temperature (see below).

Recently Clegg *et al.* (1982) reported a study of the dielectric properties of brine shrimp (*Artemia*), a primitive crustacean which enters dormancy by dehydration (Bagsaw and Warner, 1979) and is thus able to survive extensive dehydration and oxygen deprivation. These qualities and the organisms' availability in large quantity make them a much better choice than giant barnacle muscle fibers for the study of dielectric properties.

Clegg and Grant used an instrument which permitted the measurement of dielectric properties up to 70 GHz, thereby permitting adequate coverage of frequencies high enough to require no extensive extrapolation. After correcting for the contribution of, for example, the shell, Clegg *et al.* arrived at the conclusion that the dielectric constant or permittivity of intracellular water is just under 16, compared to 23 ± 1 for the permittivity of pure water at 34 GHz and 25°C (van Loon and Finsy, 1975). They also found the spread factor, α , to be larger than that of pure water by 50%.

Clegg and Grant assumed the difference in permittivity between *Artemia* cell water and pure water to be due to the presence of two fractions of water, one with a permittivity equal to that of normal liquid water ($\epsilon_1 = 78$). With this assumption, they concluded that less than half (43%) of the cell water could be normal water.

However, I believe that the same data may be interpreted quite differently as indicating a reduction of ϵ_r of most of the water by a factor, say, of 10. The wider spread factor, α , may then reveal itself as an apparent fractional reduction at 34 GHz (25°C), as observed. Such a picture would be in agreement with the polarized multilayer theory of cell water, for this water is expected to have properties that differ from those of normal water to a degree less than that of "bound" water in the case of water attached closely to polar side chains of proteins. This expectation will be shown to be confirmed in studies of NMR and dielectric relaxation* of model systems.

It may be mentioned that Masszi *et al.* (1976) did measure the dielectric constant and conductivity of the much sturdier frog muscle at 25°C in the frequency range of 2–4 GHz. They concluded that "the relaxation wave length belonging to the dipole rotation of muscle water is greater than that of pure water . . . , thus, the rotation of water dipoles is more hindered in muscle than in water."

9.7. NMR Relaxation Times of Water Protons and Other Nuclei

The great advantage of NMR lies in its nondestructiveness. The static magnetic field and weak radio frequency signals applied to the specimen do not harm it. The potential capabilities of the method have not yet been fully developed, and many of the fundamental theories and experimental techniques are still undergoing change. Therefore, at this stage of the game, NMR is not capable of providing decisive information on the physical state of water in living cells. Nevertheless, the discussion here will provide the background for future studies.

*I thank Prof. Herman Schwan for bringing to my attention a very important paper of Kaatze *et al.* (1978) on the dielectric relaxation of aqueous solutions of PEO, PVP, PVME, and polyvinylalcohol. Their data showed that as the polymer concentration increases τ_d decreases and α increases. Furthermore τ_d of the aqueous polymer solution is longer than that of pure water by a factor of 2 and increases to higher values at higher polymer concentrations.

Appendix A describes basic NMR concepts and terms. I shall introduce here some additional basic theories relevant to the study of the physical state of water in cells.

9.7.1. NMR Theories

9.7.1.1. *The Bloembergen-Purcell-Pound, Kubo-Tomita Theory*

In 1948 Bloembergen, Purcell, and Pound presented their theory of NMR relaxation times. This theory was put into a more rigorous framework by Kubo and Tomita (1954):

$$\frac{1}{T_1} = 2A \left(\frac{\tau_c}{1 + \omega_0^2 \tau_c^2} + \frac{4\tau_c}{1 + 4\omega_0^2 \tau_c^2} \right) \quad (9.14)$$

and

$$\frac{1}{T_2} = A \left(3\tau_c + \frac{5\tau_c}{1 + \omega_0^2 \tau_c^2} + \frac{2\tau_c}{1 + 4\omega_0^2 \tau_c^2} \right) \quad (9.15)$$

where T_1 is the longitudinal spin-lattice relaxation time and T_2 is the transverse or spin-spin relaxation time. τ_c is the correlation time, which is the average time interval between rotations of the nuclei, or the time for the nucleus to diffuse into a neighboring position. ω_0 is the Larmor angular frequency, which varies with the nature of the nucleus and the strength of the applied steady magnetic field. ω_0 is in units of radians per second; it is equal to $2\pi\nu_0$, where ν_0 is the Larmor precession frequency in units of hertz. For the water proton in liquid water, A , a constant, may be taken as 0.83×10^{10} sec⁻². Figure 9.24 shows a plot of T_1 and T_2 against τ_c according to this theory. Note that T_1 has a minimum, corresponding to a τ_c value equal to $(2\tau\omega_0)^{-1}$. At τ_c below this minimum, T_1 and T_2 are equal; beyond the minimum, T_1 and T_2 diverge. Then, as τ_c becomes very long, T_1 becomes longer and longer while T_2 reaches a limiting value equal to that of the T_2 of solids. For the water proton in a dilute aqueous solution, τ_c is 3×10^{-12} sec.

Equations (9.14) and (9.15) provide the means of estimating τ_c , given both T_1 and T_2 . However, this is so only when one has a homogeneous system; it is not possible if the system is heterogeneous and contains water in more than one environment.

The relaxation times, T_1 and T_2 , for the water proton in Ringer solution at around 25°C are about 2600 and 2000 msec, respectively. Any degree of ordering of water is expected to shorten these times.

9.7.1.2. *The Zimmerman-Brittin Theory of Heterogeneous Systems with More Than One Kind of Environment for Water*

Zimmerman and Brittin (1957) considered NMR relaxation phenomena in a heterogeneous system where water, for example, may exist in different phases or compartments. In these different phases water may have different relaxation times. They pointed out that if there is slow exchange of water molecules, and hence their protons, between the water in different phases, then in a plot of the logarithm of magnetization against

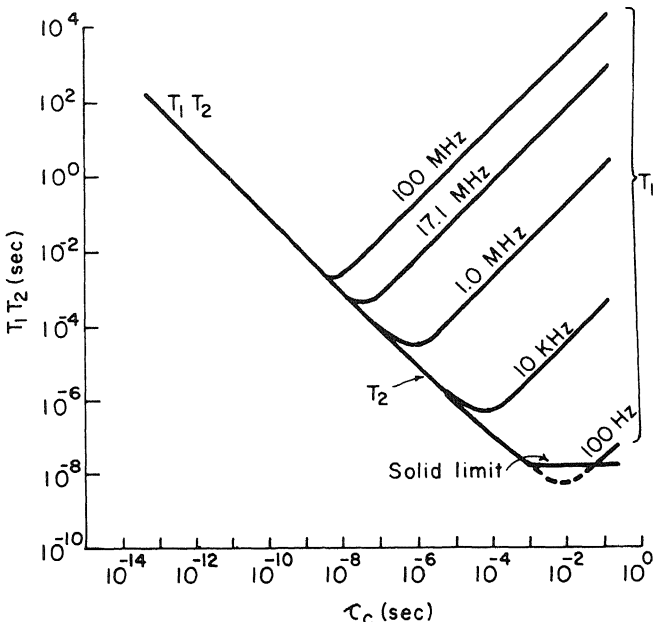


FIGURE 9.24. Theoretical curves of T_1 and T_2 plotted against the correlation time τ_c at various field frequencies calculated according to equations (9.14) and (9.15).

time, two or more separate components would be seen. On the other hand, if the proton (or water) exchange is rapid in comparison with the correlation times, then only a single relaxation time would be seen. The observed relaxation time, T_{obs} , is given by the following equation:

$$T_{\text{obs}}^{-1} = \sum_i P_i T_i^{-1} \quad (9.16)$$

T_i is the relaxation time of the i th phase, and P_i is the probability that the nuclei under discussion are found in that phase. As an approximation, P_i may be assumed to be equal to the population density. That is, if 20% of water is found in one environment and 80% in another, then the probability, P , of water in the first environment is 0.20, that in the second, 0.80.

9.7.1.3. Cross-Correlation and Spin Diffusion

Under certain conditions, when the molecules are closely associated, the flipping of one magnetic nucleus may be coupled to that of a nucleus in another molecule. The result is a transfer of magnetism (Abragam, 1961; Noack, 1971; Kalk and Berendsen, 1976; Edzes and Samulski, 1977). Cross-correlation of spin diffusion affects T_1 but not T_2 (Edzes and Samulski, 1977).

9.7.2. NMR Studies of Water in Solutions of Native Globular Proteins

Daszkiewicz *et al.* (1963) first observed the decrease of T_1 of the solvent water proton in an aqueous solution of diamagnetic proteins. These authors explained their data by the presence of a small fraction of irrotationally bound water in rapid exchange with bulk phase water. The dependence of $1/T_1$ in protein solutions on the magnetic field, and hence the Larmor frequency, ω_0 , was first demonstrated by Koenig and Schillinger (1969) and shortly after by Kimmich and Noack (1970; see also Blicharska *et al.*, 1970). These and other studies led Koenig and co-workers to the conclusion that a cross-relaxation effect is present, as suggested by the work of Kimmich and Noack (1970) and of Edzes and Samulski (1977).

In 1974 R. Cooke and Kuntz offered a three-fraction model of protein solutions. One fraction (Type I) consists of bulk phase normal liquid water making up 90% of the total water, with a τ_c of 3×10^{-12} sec. A second fraction (Type II) of (protein) hydration water makes up 10% of the total water, with a τ_c of 10^{-9} sec. A third fraction (Type III) of hydration water makes up 0.1% of total water, with a τ_c of 10^{-6} sec. With these assumptions and data provided by equations (9.14)–(9.16) they were able to account for T_1 and T_2 at 100 MHz and 1 MHz. Indeed, Cooke and Kuntz were convinced that the same three-fraction model could explain the water relaxation properties of living muscle cells. Cooke and Kuntz's model did not include spin diffusion mechanisms for water proton relaxation, as discussed previously in relation to the more recent work of Koenig, Noack, Edzes, and others.

9.7.3. NMR Studies of Water in Living Cells

9.7.3.1. Early Studies

Odeblad *et al.* (1956) were the first to report NMR studies of the water proton in living cells. From the large difference between the T_1 and T_2 values observed, Odeblad (1957) suggested that in living cells there may be an "admixture of solid and liquid states of water."

Bratton, Hopkin, and Weinberg (1965) subjected isolated muscle tissues to tetanic stimulation while recording the T_1 and T_2 of the water protons in the muscle. They found that T_1 (0.25–0.4 sec) did not change with contraction but that T_2 changed from 0.04 sec at rest to 0.06 sec during contraction. Since T_1 and T_2 of normal water are each about 3.0 sec, and thus many times longer, Bratten *et al.* suggested a two-phase model in which exchange of water protons between a minor phase of bound water and the bulk phase of *normal* water was fast enough to yield a single T_1 . This model was basically similar to that formulated by Zimmerman and Brittin (1957).

9.7.3.2. Early NMR Studies of Water Interpreted in Terms of Extensive Ordering of Cell Water

The polarized multilayer theory of cell water (Ling, 1965c) postulated that virtually all cell water exists in the state of polarized multilayers occurring as a consequence of the presence of a matrix of proteins which exist in the extended conformation

with a sequence of alternatingly positive (NH) and negative (CO) sites. The average number of water molecules layered between neighboring protein chains was estimated to be below ten. The water structure is not static or crystalline but dynamic in nature. Each water molecule in this cooperative assembly is distinguished from similar water molecules in normal liquid water in that it maintains a certain directionality owing to a three-dimensional dipolar orientation. In other words, we expect the water molecule to undergo motional restriction in general and rotational restriction in particular. In NMR terms, we expect the bulk phase water to have a slower rotational correlation time, i.e., τ_c should be longer than that of normal liquid water whose τ_c is 3.6×10^{-12} (Chiarotti and Giulotto, 1954).

In 1967 G. Chapman and McLaughlan observed in the rabbit sciatic nerve an orientation-dependent water proton signal splitting which led them to conclude that the bulk of the water in this tissue is not randomly distributed but is "in a partially oriented state." In 1967 Fritz and Swift noted in frog sciatic nerves that the NMR signal was broader than in normal water and broadened further, to 3.3 Hz, when the nerve was electrically stimulated. Since linewidth ($\nu_{1/2}$) is related to T_2 according to the equation

$$T_2 = \frac{1}{\pi\nu_{1/2}} \quad (9.17)$$

line broadening indicates a decrease of T_2 . Fritz and Swift pointed out that linewidth broadening with electrical stimulation indicates a marked change in the state of water. Cope (1969) studied the NMR of D₂O introduced into rat muscle and brain. The deuteron T_1 and T_2 in muscle are 0.092 and 0.009 sec, respectively, in comparison with values of 0.47 and 0.45 sec for the deuteron in normal liquid D₂O. After arguing that the reduction of T_1 and T_2 is not due to other causes, such as the presence of paramagnetic impurities or magnetic inhomogeneity, Cope concluded that "the continuous distribution of structures is the more likely hypothesis." Cope also noted that there is a smaller fraction of cell water with an even higher degree of structure, and therefore such a short T_2 and broad linewidth that it was NMR—"invisible." Hazlewood, Nichols, and Chamberlain (1969) studied the NMR of the water proton in rat muscle and reached a finding similar to Cope's, including the conclusion that there is a small NMR—"invisible" fraction of tightly bound water.

Thus far, the evidence for the coexistence of more than one fraction of water with different relaxation times was based primarily on these authors' observation that the NMR signal of the water proton accounted for only a fraction of the total water assayed by drying. However, Czeisler *et al.* (1970) and Swift and Barr (1973) could not find an NMR-invisible fraction of cell water. Additional evidence for NMR-invisible water was reported by Shporer and Civan (1972) and by Belton *et al.* (1972), although they cited technical difficulties which made it difficult to assess the real magnitude as well as the significance of this "invisible" fraction.

9.7.3.3. Arguments against the Concept of Ordered Bulk Phase Water

As mentioned earlier, Odeblad considered the coexistence in cells of "solid" and liquid water. Bratton, Hopkin, and Weinberg (1965) suggested the two-fraction rapid exchange model to explain the low T_1 and T_2 . They assumed that the bulk of cell water

is simply normal liquid water. In 1967 Abetsedarskaya and her co-workers reached the same conclusion from their studies of muscle. These were followed by the papers of Walter and Hope (1971), R. Cooke and Wien (1971), Outhred and George (1973), Finch and Homer (1974), and Fung and McGaughy (1974)—all agreeing on the basic model of a small fraction of hydration water with a relatively long correlation time in rapid exchange with the bulk phase water, which is simply normal liquid water.

As an example of the more specific arguments offered in favor of this view, that of Cooke and Wien may be cited. These authors showed that, in frog muscle with varying water contents, both T_1 and T_2 of the water proton were linearly related to the reciprocal of the protein concentration of the samples, in accordance with the theoretical expectation based on the Zimmerman-Brittin equation [equation (9.16)].

The orientation-dependent signal splitting of the water proton signal in rabbit nerve and Chapman and McLaughlan's conclusion that the bulk phase water was partially oriented were challenged two years later by M. P. Klein and Phelps (1969), who could not confirm in D_2O -charged nerves the earlier finding, which they attributed to experimental artifact. Interestingly enough, in 1975 Fung reported a similar orientation-dependent water proton signal splitting in frog muscle, but attributed this to orientation of a small fraction of water in rapid exchange with randomly distributed bulk phase water. A few years later Fung and his co-workers (1980) also concluded that the signal splitting was an artifact.

Figure 9.25 shows the demonstration by Held *et al.* (1973) of the field dependence

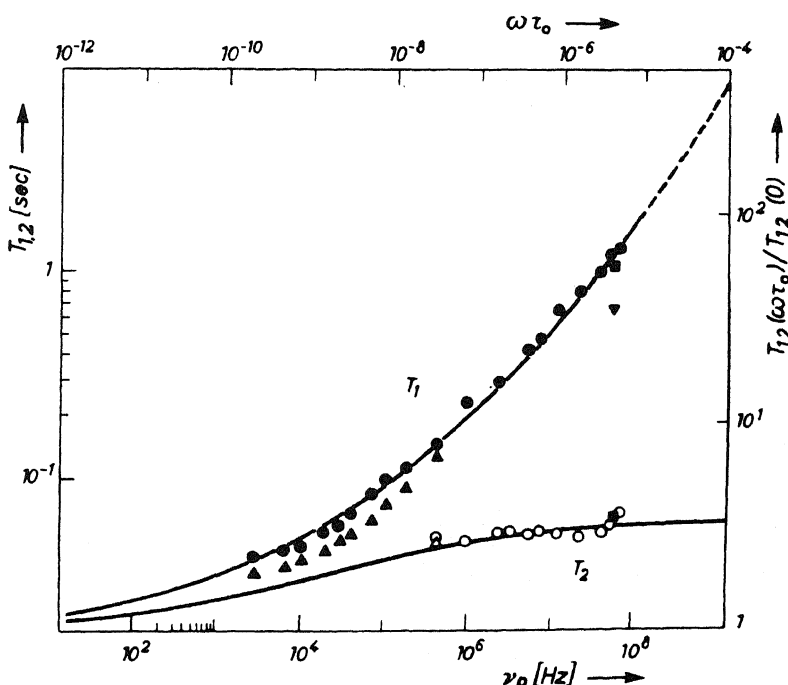


FIGURE 9.25. Dependence of the longitudinal and transverse relaxation times (T_1 , T_2) in frog skeletal muscle on the proton Larmor precession frequency (ν_p) and on the dispersion product ($2\pi\nu_p\tau_0 = \omega\gamma_0$). Lines are theoretical. [From Held *et al.* (1973), by permission of *Zeitschrift für Naturforschung*.]

of T_1 in frog muscle, which resembles a similar observation they and others made in solutions of bovine serum albumin (Kimmich and Noack, 1970), adding further weight to the by then widely accepted notion that living cells behave like simple protein solutions.

Finally, the findings of Neville *et al.* (1974) and of Civan and Shporer (Civan and Shporer, 1974; Shporer *et al.*, 1976) that cell deterioration led to shortening rather than lengthening of T_1 in frog lens, frog muscle, and rat lymphocytes also contradicted the notion that normal cell function is essential for the maintenance of the polarized multilayer state of cell water and that it is this polarized multilayer state that significantly accounts for the reduced T_1 of cell water.

9.7.3.4. *The Demonstration of Multiple Fractions of Water with Different Relaxation Times and Other Evidence Not Readily Reconcilable with the Rapid Exchange Model*

In 1972, in a total of over 70 experiments on more than 30 separate tissue samples, Belton, Jackson, and Packer demonstrated three fractions of water protons with different T_2 's. Two years later Hazlewood, Chang, Nichols, and Woessner (1974) published another series of their careful studies, in which they also observed three components of T_2 . Table 9.4 compares these two sets of data. While some differences exist, by and large the agreement is good if one takes into consideration the differences of tissue origin and experimental details. Both groups were inclined to think that the slow component is from water in the extracellular space and the fast component from hydration water of cell macromolecules and that the intermediate component corresponds to the bulk of cell water. Indeed Belton *et al.* also suggested that the water bound to macromolecules may be the same water that remains unfrozen at low temperature. These data suggest that this hydrated water proton does not exchange rapidly enough with the bulk water to average this fraction with the main fraction; otherwise, there would not be a separation into different fractions. Failure to exchange rapidly enough to average the bulk water and the rapidly exchanging fraction leaves unanswered the question of why the bulk phase water relaxes as rapidly as it does: The T_2 of the bulk phase cell water (40–45 msec) is much lower than that of normal liquid water (2000 msec). Hazlewood *et al.* suggested that this reduction of T_2 could be due to exchange of the cytoplasmic water with "interfacial water."

TABLE 9.4. Demonstration of Three Components of T_2 in Muscle Tissues

Reference	Muscle(s)	Slow component		Intermediate component		Fast component	
		Percent of total	T_2 (msec)	Percent of total	T_2 (msec)	Percent of total	T_2 (msec)
Belton <i>et al.</i> (1972)	Frog sartorius and gastrocnemius muscle	15	250	64	40	20	9
Hazlewood <i>et al.</i> (1974)	Rat gastrocnemius muscle	9.8	155	83	43.7	7.2	<5

Similar reports of multiple relaxation times came from Civan and Shporer (1974), who studied the T_1 of ^{17}O from $^{17}\text{H}_2\text{O}$ introduced into frog muscles. Like Belton, Hazlewood, and co-workers, they found that about half of the ^{17}O has a faster relaxation time than the other half. After cell deterioration, the slow component disappears, leaving only one fraction with a T_1 the same as that of the fast component. Similarly, in a later study of lymphocytes, Shporer *et al.* (1976) observed multiple fractions of T_1 of ^{17}O ; the slow fraction included two-thirds of the total, the fast fraction, one-third. Again with cell death the slow fraction disappeared to leave only a single fast fraction.

Taken together, these reports show clearly that the simple model of a rapid exchange of normal liquid bulk phase water with a 5–10% hydration water on protein polar side chains is inadequate to explain the data. Moreover, there are additional arguments supporting this conclusion:

1. Hydration water of proteins does not have a uniform relaxation time. Thus, Fuller and Brey (1968) showed that at a vapor sorption by bovine serum albumin of 0.3 g $\text{H}_2\text{O}/\text{g}$ dry protein, the linewidth corresponds roughly to a T_2 of 7 msec. At a total water sorption of 0.05 g/g dry protein, T_2 is only 0.2 msec. More recent studies by Kimmich and Noack (1971) showed that in serum albumin solution there are two correlation times, one at 2.4×10^{-9} sec and another at 1.8×10^{-6} sec. Indeed, Kimmich and Noack suggested that there is spin diffusion (cross-correlation) between protein and solvent protons.
2. Since the important finding by Kuntz and co-workers (1969) that the hydration water of proteins in aqueous solution does not freeze at -60°C , nonfreezable water in tissues has often been equated with the rapidly relaxing hydration water in the two-phase rapid exchange model. However, as pointed out in Section 9.3.3, the nonfreezable water does not exist as a single well-defined quantity but strongly depends on the speed of freezing and other variables. Indeed Fung and McGaughy (1974) have shown that nonfreezable water in muscle tissues is greatly increased if dimethyl sulfoxide (DMSO) is introduced into the tissue. Since hydration water of globular proteins is generally agreed to be due to hydration of polar side chains (Bull and Breese, 1968b), the cause of the DMSO effect is obscure and in need of explanation not readily provided by the usual model.

9.7.3.5. *New Experimental Findings and Their Significance in Relation to the Polarized Multilayer Theory of Cell Water*

Thus far, NMR studies cannot provide proof for or against the concept that the bulk of cell water is different from normal water. It is my opinion that part of the indecisiveness in interpretation of NMR studies on the nature of the bulk of cell water lies in a lack of studies of a clearly demonstrable example or model of water in the state of polarized multilayers. Without such a model to give definition to the NMR characteristics of water existing in this state, various words like *icelike*, *quasicrystallinity*, and *structured water* cropped up, and NMR data on cell water not in agreement with characteristics of crystalline ice were held as evidence against the polarized multilayer theory of cell water.

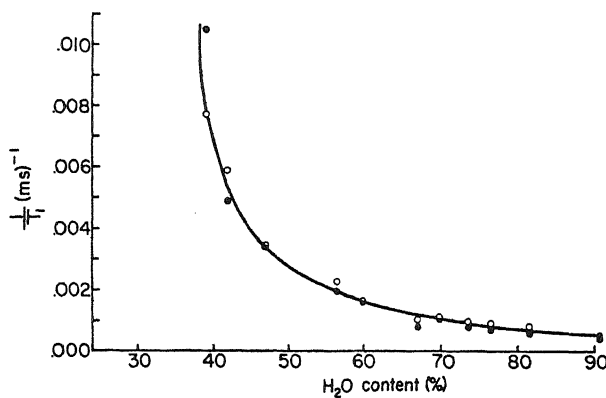


FIGURE 9.26. NMR relaxation times T_1 (●) and T_2 (○) of water in PVP solutions with different water contents. [From Ling and Murphy (1983), by permission of *Physiological Chemistry and Physics*.]

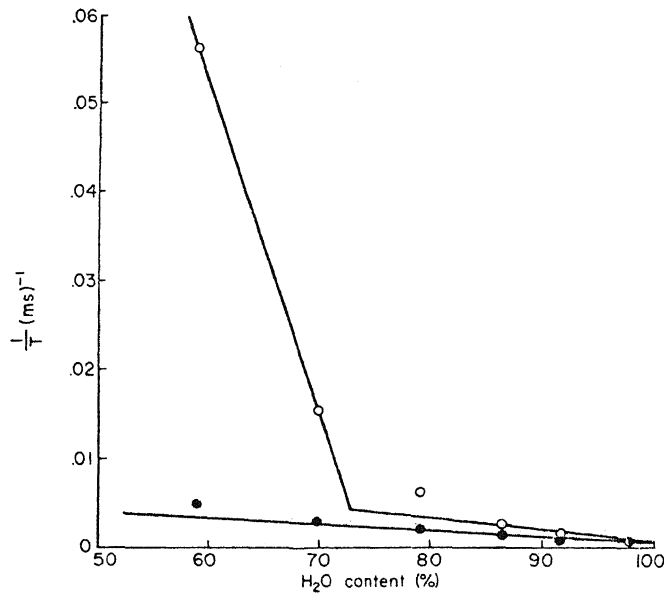


FIGURE 9.27: Longitudinal and transverse relaxation rates ($1/T_1$, $1/T_2$) for solutions of bovine serum albumin of different water contents. (●) $1/T_1$, (○) $1/T_2$. [From Ling and Murphy (1983), by permission of *Physiological Chemistry and Physics*.]

As mentioned in Chapter 6, however, the situation has changed drastically; we now have on hand water existing in the state of polarized multilayers and performing solute exclusion like that seen in cells as exemplified by the polyethylene oxide (PEO)-, polyvinylpyrrolidone (PVP)-, and polyvinylmethyl ether (PVME)-water systems. The most outstanding findings of the NMR studies of the water in these model systems is that in each case T_1 and T_2 are in essence equal in studies performed with a pulse NMR spectrometer operating at 17.1 MHz (Ling and Murphy, 1983). The results are illustrated in Fig. 9.26. Note that, as the water content increases, both T_1 and T_2 increase. At between 40% and 60% water content, the bulk of water in the PEO, PVP, and PVME systems is in the state of polarized multilayers, as judged by the low ρ -value for various probe molecules (Ling *et al.*, 1980a,b). These data should be contrasted with those for albumin (Fig. 9.27), in which T_1 and T_2 are not affected equally.

9.7.4. Concluding Remarks on the Current Status of NMR Studies

The fundamental problem of the physical state of water in living cells has already been resolved indirectly through the demonstration of the adsorbed state of K^+ in muscle cells (Chapter 8). This adsorbed and osmotically inactive state of the major cell cation leaves no alternative but to suppose that the reduction of cell water activity to equal that of the environment must be brought about by its interaction with biopolymers. The establishment *in vitro* that water interacting with extended protein chains, and with polymers having similar attributes, can indeed yield an osmotic activity far beyond that due to the number of polymer molecules, makes it all but certain that this is the basis for the osmotic balance in cells. The fact that water in this state excludes Na^+ , sucrose, and glycine as they are excluded from most living cells also permits a quantitative estimate of the number of water molecules involved—this estimate confirms the multilayer nature of the water adsorbed. With this background information, the measurements of the equally shortened T_1 and T_2 of water oriented by PEO, PVP, and PVME furnish the basis for estimating a τ_c value ($1-3 \times 10^{-11}$ sec) no more than 3–10 times longer than that of pure liquid water (Ling and Murphy, 1983). Let us now see how these data can help us to understand the NMR studies thus far recorded.

First, the large difference between T_1 and T_2 seen in living cells (and in albumin, Fig. 9.27) indicates that some part of the water must have a long τ_c (Fig. 9.24). The corresponding low T_2 value cannot be that of bulk phase water, or else the diffusion coefficient would be reduced by much more than a factor of 2 as measured (Cleveland *et al.*, 1976; Hazlewood, 1979). Therefore the low T_2 must originate from a small fraction of water in rapid exchange with the bulk phase water. Referring to equation (9.16), one realizes that in fact only a minute amount of water with a τ_c of, say, 10^{-6} sec will all but overwhelm the contribution of the bulk phase water regardless of whether it has a τ_c of 3×10^{-11} sec (as in water in the PEO, PVP, and PVME systems) or 3×10^{-12} sec (as in normal water). Therefore, the T_2 value recorded from a complex system like the living cell is virtually completely masked by this minute, rapidly relaxing fraction of water (Ling, 1979b). The same may not, however, apply to T_1 , because $\tau_c = 10^{-6}$ sec. T_1 measured at high field frequency may be as large as T_1 of water with τ_c equal to 3×10^{-11} or 3×10^{-12} sec (Fig. 9.24).

In Cooke and Kuntz's three-fraction model of protein solutions, which was

extended to living cells, they used for the bulk phase water the τ_c of pure liquid water, 3×10^{-12} sec. This would have predicted a T_1 much larger than was actually recorded. To explain the lower T_1 , they assigned 10% of the cell water to hydration water with a longer τ_c . This was necessary because in 1974 they did not have the data published only very recently by Ling and Murphy (1983) on the T_1 and T_2 of water polarized by PEO and other polymers. I would like to suggest that a major share of the spin-lattice relaxation (T_1) is due to bulk phase water in the state of polarized multilayers with a τ_c somewhere near 1×10^{-11} sec.

If this is the case, T_1 of the water proton should reflect the multilayer state of normal cell water and it would be expected to increase with cell death and deterioration. Yet the data of Neville, Civan, Shporer, and others mentioned previously showed the opposite: T_1 decreased with cell deterioration and death. Future research is needed to answer this question fully, but the following suggestions can be made. Our investigations suggest that water associated with proteins, or perhaps protein-paramagnetic ion complexes, in living cells may undergo changes in T_1 in such a way as to counter the effect of a lengthening of T_1 owing to depolarization of bulk phase water as a result of deterioration. In support of this, we found that fresh sartorius muscle yields a T_1 of 620 msec, but that, after heating for 10 min at 60°C, T_1 lengthened to 700 msec. Paired muscle, which was exposed to a Ringer solution containing 5×10^{-4} M Mn²⁺, had a T_1 of only 260 msec. After similar heating, T_1 of the Mn²⁺-treated muscle did not lengthen, instead it went down to 100 msec.

Normal frog gravid oviduct showed a T_1 of 98 msec; heating for 10 min at 60°C caused a shortening to 34 msec. Another normal oviduct gave a T_1 of 100 msec. After exposure to a Ringer solution containing 5 mM iodoacetate (IAA) and 1 mM NaCN for 30 min T_1 increased to 140 msec. Three hours later it rose still higher, to 165 msec, but then it began to decline, reaching 108 msec after 18 hr and 31 msec after 2 days.

It is well known that heating frog tissues at 60°C causes the loss of their ability to exclude sucrose (Section 11.2.3.2), which according to the AI hypothesis denotes depolarization of cell water. A consequent lengthening of T_1 would be expected. Heating of frog sartorius muscle does indeed produce a T_1 lengthening but nowhere nearly as much as anticipated. Heating frog gravid oviduct, however, brought about shortening of T_1 . Since inclusion of Mn²⁺ converts a heat-induced T_1 lengthening to a T_1 shortening in frog muscle, one may suppose the weak T_1 lengthening in muscle and the T_1 shortening in oviduct to be consequences of an enhancement of the T_1 shortening effect of the Mn²⁺-protein complex as a result of heat denaturation.

That IAA and NaCN also brought about a T_1 lengthening of frog oviduct suggests that IAA-NaCN topples the living state by lowering the cell ATP content. The resulting depolarization of water produces T_1 lengthening. This is then gradually overpowered by the secondary T_1 shortening effect of the changing protein-paramagnetic ion complex of the cells. In support of this view I found that trichloroacetic acid extracts of various tissues added to a solution of bovine serum albumin reduce its T_1 .

9.8. Quasielastic Neutron Scattering

Nuclear reactors provide a source of slow neutrons which travel at a speed ($\sim 10^5$ cm/sec) 100,000 times slower than X rays (3×10^{10} cm/sec). When slow neutrons

impinge on liquids like water, they are scattered, largely by the H atoms of water and on a time scale comparable to the time that the water molecules take to jump from one position to another. As a result, the observed scattering of neutrons contains information about the diffusive motions of the water molecules involved (Springer, 1972; D. I. Page, 1972). Since the major prediction of the theory of cell water of the AI hypothesis is that these water molecules suffer reduction of both rotational and translational motional freedom (Ling, 1965c, 1967a, 1969a, 1979a; Ling *et al.*, 1967), the scattering of slow neutrons offers a powerful tool to test this theory.

Depending on whether or not the scattering process involves a change in the energy of the neutrons scattered, scattering is called *elastic* (without energy change) or *inelastic* (with energy change). For most liquids, the energy spectrum of scattered neutrons in the elastic portion of the scattered beam exhibits some broadening, and is called *quasielastic*. This broadening is caused by the diffusive motions (translation, rotation) of the scattering molecules and is therefore of great interest here.

The quasielastic neutron scattering (QNS) spectra are usually interpreted on the basis of the theory of van Hove (1954), who showed that the scattering probability is related to certain space-time correlation functions of the scattering particles. These correlation functions can be calculated for the various theoretical models of diffusion motions. The shapes of the predicted QNS spectra can then be compared with those actually observed and from the best fitting theoretical model one can obtain such data as the residue time and rotational diffusional coefficients of the scattering molecules involved.

It was with the aid of QNS study and analyses that the diffusion of water in its normal liquid state was found to be best described by the "jump-wait model." That is, each water molecule oscillates about a position of transient equilibrium for some time before making a second diffusional jump (Singwi and Sjölander, 1960; Larsson, 1965).

In a highly significant QNS study of water in the cells of the cysts of brine shrimp (*Artemia*), Trantham, Rorschach, Clegg, Hazlewood, Nicklow, and Wakabayashi (1983) came to the conclusion that *the bulk of cell water has strongly reduced translational and rotational diffusion coefficients that are not due to obstruction, compartments, or exchange with a minor phase*. Their important findings have therefore confirmed the predictions of reduced rotational and translational mobility of the bulk of cell water based on the polarized multilayer theory of cell water. Equally significant were their findings that water in 36% PEO exhibits QNS behavior patterns highly similar to those observed for *Artemia* cysts (Rorschach, 1984), adding further evidence that PEO can influence properties of water in such a way as to make this water behave like water in living cells (see Section 6.3.4.3).

9.9. Summary

The documentation of an adsorbed state of K⁺ in cells in Chapter 8 demands that a mechanism other than the osmotic pressure of ions be responsible for the lowering of the activity of cell water to equal that of the environment. Water in the state of polarized multilayers provides this mechanism. Model systems containing water in this state were outlined in Chapter 6 and shown to exclude solutes dissolved within this water to a degree similar to that postulated for cell water in the AI hypothesis. Additional prop-

erties of these models and of other inanimate systems were described in this chapter and were compared to properties of cell water. These properties include solute exclusion, resistance to freezing, sorption of water in multilayers following the Bradley isotherm, NMR relaxation times, dielectric relaxations, and quasielastic neutron scattering. The analysis of these properties includes a reevaluation of the results of studies, especially those of NMR relaxation times, and a reinterpretation of their significance. In the case of NMR, it is clear from studies of model systems that water in the state of polarized multilayers has a correlation time that is only longer than that of normal liquid water by a small factor. Consequently, its effect on the relaxation times may be overshadowed by factors that include very small fractions of tightly "bound" water and paramagnetic ions associated with proteins. The concept of water polarized in multilayers is now well established theoretically and experimentally, and it provides a specific model that must replace vague concepts or *ad hoc* notions like "bound," "immobilized," "icelike," and "nonsolvent" water in the interpretation of the results of the physical and physical-chemical techniques applied to study cell water.

ATP and the Source of Energy for Biological Work Performance

10.1. The General Question of the Energization of Biological Work

A living cell moves, conducts electric impulses, transports solutes against concentration gradients, and synthesizes chemicals. In these and other activities, the cell behaves like a reversible cyclic machine and performs work. Energy is transformed from one form to another in the process.

The ultimate source of energy for most living cells is solar radiant energy, which is utilized by green plants to produce organic chemical compounds such as glucose. If glucose is burned, a large amount of heat is given off. This is the heat of combustion. The basic question is: How can this chemical energy be tapped to perform biological work?

10.2. The Heat Engine Theory

At the turn of the century, Engelmann (1906) introduced a heat engine theory in which the heat produced by the combustion of food material drives the biological engine in a way similar to the combustion of coal or firewood in manmade heat engines. This theory, however, did not survive long, because the high temperature required would denature and kill the cells.

10.3. The High-Energy Phosphate Bond Concept

As outlined in Section 3.1.4, the discovery of the pivotal roles of ATP and creatine phosphate (CrP) in biological work performance and early calorimetric work led to the hypothesis that certain phosphate bonds contain an unusually large amount of energy and that by hydrolysis of these bonds this energy is tapped for biological work perfor-

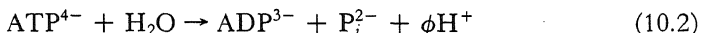
mance (Lipmann, 1941). This special chemical bond, called the "high-energy phosphate bond," is represented as $\neg P$ to distinguish it from the ordinary phosphate bond, $-P$. We discussed in Section 5.2.2 how later more precise calorimetric and other studies (Podolsky and Kitzinger, 1955; Podolsky and Morales, 1956) generated serious doubts that there is indeed a distinction between high- and low-energy phosphate bonds. A clarification of this fundamental problem was given by George and Rutman (1960) in a paper entitled "The High-Energy Phosphate Bond Concept." The essence of this review can be summarized as follows.

The ΔH of a chemical equilibrium is the result of a complex interplay of a number of factors, of which the bond energies of the participating molecules are but one. The heats of fusion, evaporation, solution, and ionization all contribute to ΔH . Not only does the ionization contribute to ΔH , it affects ΔF in two ways. First the degree of ionization determines the participation of H^+ at the low H^+ concentration prevailing in the physiological environment. This can have a very significant effect. Second, increasing ionization produces substantially more negative partial molal entropy.

Thus, the observed free energy change for various phosphate hydrolyses may be written as

$$\Delta F_{\text{obs}} = \Delta H - T\Delta S + \phi RT \ln H^+ \quad (10.1)$$

where ϕ , a factor which can vary from -1 to $+2$, indicates the number of H^+ ions that are taken into account. In the reaction



ϕ increases from 0 to about 1 as the pH increases from 5 to 9. The major contribution of the H^+ ion concentration can be put in another way. The truly correct *standard* free energy of the reaction demands that all the participants of the reaction exist at unit activity. For H^+ , this means a concentration of 1 M! In reality the reaction must occur near neutrality, i.e., at a H^+ concentration 10 million times lower. By the principle of Le Chatelier, the low H^+ concentration of the medium provides a major driving force for the reaction to proceed to the right, thereby giving rise to a ΔF_{obs} having a negative value. This trend increases with increasing pH of the medium and, with it, increasing ionization of the acidic group. However, the matter is further complicated by a change of the $-T\Delta S$ term, which is characterized by a progressively more negative partial molal entropy, owing to the increasing immobilization of water around the dissociated ions.

Table 10.1, taken from George and Rutman (1960), shows the different contributions of these various terms to the observed free energy change. Compare in particular reaction (a), hydrolysis of ATP into AMP and pyrophosphate, and the second part of reaction (h), in which pyrophosphate hydrolyzes into two orthophosphates. The ATP hydrolysis, with a ΔF_{obs} of -14.0 kcal/mole, contains a ΔH term of only -3.0 kcal/mole, while the pyrophosphate hydrolysis, with a ΔF_{obs} of only -2.1 kcal/mole, has a much higher ΔH of -6.5 kcal/mole. It is the $\phi RT \ln H^+$ and $-T\Delta S$ terms, not the ΔH term, that make the ATP reaction a "high-energy" one.

TABLE 10.1. Thermodynamic Data (in Kcal/mole) for Various Hydrolyses at pH 7.5^{a,b}

Reaction	ΔF_{obs}	$\Delta F'$	ΔH	$-T\Delta S$	$\phi RT \ln H^+$
a. $\text{ATP} + \text{H}_2\text{O} \rightarrow \text{AMP} + \text{pyrophosphate}$	~ -14.0	~ -4.2	-3.0	~ -1.2	-9.8
c. Phosphoenol Pyruvate + $\text{H}_2\text{O} \rightarrow \text{pyruvate} + \text{orthophosphate}$	-13.7	-16.6	-8.5	-8.1	+2.9
d. Creatine phosphate + $\text{H}_2\text{O} \rightarrow \text{creatine} + \text{orthophosphate}$	-10.6	-14.1	-4.8	-9.3	+3.5
e. $\text{ATP} + \text{H}_2\text{O} \rightarrow \text{ADP} + \text{orthophosphate}$	-8.3	-1.3	-4.8	+3.5	-7.0
h. Glycerol phosphate + $\text{H}_2\text{O} \rightarrow \text{glycerol} + \text{orthophosphate}$	~ -2.4	~ -4.6	-1.3	~ -3.3	+2.2
Pyrophosphate + $\text{H}_2\text{O} \rightarrow 2 \text{ orthophosphate}$	-2.1(-1.7)	+2.5	-6.5	+9.0	-4.2

^a $\Delta F_{\text{obs}} = \Delta F' + \phi RT \ln H^+ = \Delta H - T\Delta S + \phi RT \ln H^+$.

^bFrom George and Rutman (1960), by permission of *Progress in Biophysics and Biophysical Chemistry*.

The importance of the $\phi RT \ln H^+$ term is not determined by the thermodynamic properties of the reactants and products but only indirectly, through the dissociation constants. Similarly, as George and his co-workers (Phillips *et al.*, 1966; George *et al.*, 1970), as well as Shikama (1971), demonstrated in later years, different affinities in complexing with Mg^{2+} and Ca^{2+} and with H_2O provide other driving forces that make the free energy observed more negative. As in the case of H^+ , this is not determined by the thermodynamic properties of the reactants and products, and certainly is not due to a particular bond in the reactants or products.

Although the high-energy phosphate bond concept is no longer defensible, the role of ATP in biological work performance and as a common intermediate in enzyme-mediated coupled phosphate group transfers is not at all in doubt. The only way chemical energy can be transferred from one reaction to another is through a common intermediate. In such reactions coupled through a common intermediate, the product of the first reaction is the substrate of the second reaction. Virtually all metabolic reactions in the living cell proceed in sequential steps of this kind. Group transfer reaction chains are not limited to phosphate groups. Other groups, like amino groups and acetyl groups, can be similarly handled. However, in most living cells the main metabolic pathway utilizes phosphate groups.

Table 10.2 shows that in these enzyme-catalyzed phosphate group transfer reactions ATP serves a pivotal role because its standard free energy of hydrolysis is poised in the middle of the scale. Thus, ADP can receive phosphate from a compound with a more negative standard free energy of hydrolysis at pH 7 (ΔG°) (or higher phosphate group transfer potential, defined as $-\Delta G^\circ$) and thus conserve the energy in the form of ATP. When ATP reacts with a compound of lower phosphate group transfer potential, it causes the latter compound to acquire a high energy content.

TABLE 10.2. Standard Free Energy of Hydrolysis of Some Phosphorylated Compounds^a

Compound	ΔG°		Phosphate group transfer potential ^b
	kcal/mole	kJ/mole	
Phosphoenolpyruvate	-14.80	-61.9	14.8
3-Phosphoglycerol phosphate	-11.80	-49.3	11.8
Phosphocreatine	-10.30	-43.1	10.3
Acetyl phosphate	-10.10	-42.3	10.1
Phosphoarginine	-7.70	-32.2	7.7
ATP (\rightarrow ADP + P _i)	-7.30	-30.5	7.3
Glucose 1-phosphate	-5.00	-20.9	5.0
Fructose 6-phosphate	-3.80	-15.9	3.8
Glucose 6-phosphate	-3.30	-13.8	3.3
Glycerol 1-phosphate	-2.20	-9.2	2.2

^aFrom Lehninger (1975), by permission of Worth Publishers.

^bDefined as $-\Delta G^{\circ}$ (kcal/mole).

10.4. The Energy Source for Biological Work Performance According to the AI Hypothesis

As outlined early in Chapter 6, the concept of the living state of the cell in the association-induction (AI) hypothesis includes the notions, first, that the living state is a temporary reprieve in the trend toward randomness and increasing entropy; second, that only the entire assembly of associated cellular components can be designated as being in a "high" or a "low" energy state; and third, that the coherence of the cell mirrors cooperative behavior resulting from short-range, nearest-neighbor interactions between macromolecular sites that adsorb ions and water. The resting state of the cell is a metastable, high-energy state. Among the key elements that help maintain this state are cardinal adsorbents that in small quantities control the properties of a large number of macromolecular sites in their interactions with ions, water, and other cellular components. ATP is one of these cardinal adsorbents (see p. 222).

As noted previously, the primary source of energy for living organisms is the radiant energy from the sun, mediated by photosynthesis, although various bacteria and deep sea organisms may directly utilize chemical energy in a process called chemosynthesis. In general, the AI hypothesis views energetic processes in a manner similar to more conventional theories. However, there are profound differences in attitude concerning the more immediate source of energy for work performance.

10.4.1. The Immediate Source of Energy for Biological Work Performance

According to the AI hypothesis the immediate source of energy for biological work performance is the potential energy sustained in the high-energy resting living state. The cooperative interaction among the major components of the cell—including proteins, water, and ions—and cardinal adsorbents like ATP maintains a high state of potential

energy which is transformed into work when a key ingredient, ATP, is removed or otherwise destroyed.

If one considers a single muscle contraction or a single nerve action potential, the immediate energy source is that which represents the net of various adsorption-desorption events that occur as a result of the transient toppling of the high-energy resting state.

10.4.2. The Source of Energy for Cyclic Work Performance

Cyclic work performance—as exemplified by repeated contraction of muscles, trains of action potentials, or steady solute transport across intestinal epithelium—requires restoration of the state of high potential energy. This requires readsoption of ATP, and hence resynthesis of ATP that may have been hydrolyzed. The energy source of cyclic work performance is the energy used in the resynthesis of ATP.

ATP is unique because it has the right phosphate group transfer potential to mediate transfer reactions, and because it is a ubiquitous cardinal adsorbent that can be removed rapidly on command by hydrolysis and reinstalled by synthesis, utilizing the energy derived from glucose and other food matter.

10.5. Summary

The coherence of the living cell mirrors cooperative behavior resulting from short-range, nearest-neighbor interactions between macromolecular sites like those that orient ions and water. Only the entire assembly of associated cellular components can be designated as being in a high- or a low-energy state. The resting state of the cell is a metastable state of high potential energy, maintained in part by interaction with cardinal adsorbents like ATP. Work is done when the cell or one of its parts is triggered to drop to a lower energy state. One way to do this is to remove ATP, and one way to remove ATP is to hydrolyze it. Cyclic work performance requires reestablishment of the high-potential-energy resting state, and this often requires resynthesis of ATP. It is the adsorption of ATP, not its hydrolysis, that characterizes its energetic function. Specific examples of biological work performance—such as conduction of action potentials, muscle contraction, and active transport by epithelial tissues—are described in subsequent chapters.

III

Applications of the Association- Induction Hypothesis to Traditional Problems in Cell Physiology



Selective Distribution of Ions, Sugars, and Free Amino Acids

11.1. The General Theory of Solute Distribution

There are few subjects in cell physiology that have played as large a role in the development of concepts of the cell as the selective accumulation and exclusion of solutes. Certainly, investigation of this subject helped the formulation of Troshin's sorption theory as well as the association-induction (AI) hypothesis. In particular, the unusual distribution patterns of K^+ and Na^+ gave important clues to the molecular mechanisms that underlie the general patterns of solute distribution in, as well as the physicochemical makeup of, living cells.

In contrast to the high concentration of Na^+ and low concentration of K^+ found in the plasma, a very high concentration of K^+ and a low concentration of Na^+ are found in most living cells (Fig. 11.1), even though chemically these two ions are closely similar. The interpretation of this asymmetrical distribution phenomenon in terms of the AI hypothesis is illustrated in Fig. 11.2. The high concentration of K^+ in the resting cell is the consequence of specific adsorption on certain β - and γ -carboxyl groups of cell proteins which are maintained at a c -value such that K^+ is greatly preferred over Na^+ , even though there is a much higher concentration of Na^+ than K^+ in the surrounding medium.

However, not all K^+ (and Na^+) in the resting cell is adsorbed on fixed anionic β - and γ -carboxyl groups. Some Na^+ and K^+ exist as free ions in the cell water. The levels of the free K^+ and Na^+ in the cell water depend on the concentration of these ions in the surrounding medium and on the equilibrium distribution coefficient (q -value) of the ion in the cell water, which exists in the state of polarized multilayers. According to the AI hypothesis, the q -value is not a constant but tends to be lower, the larger and more complex is the molecule or the hydrated ion (Section 6.3.3). The q -values of hydrated cations like K^+ and Na^+ also depend on the nature of the accompanying anions, as was clearly demonstrated in the study of synthetic polymers and proteins (Ling *et al.*, 1980b).

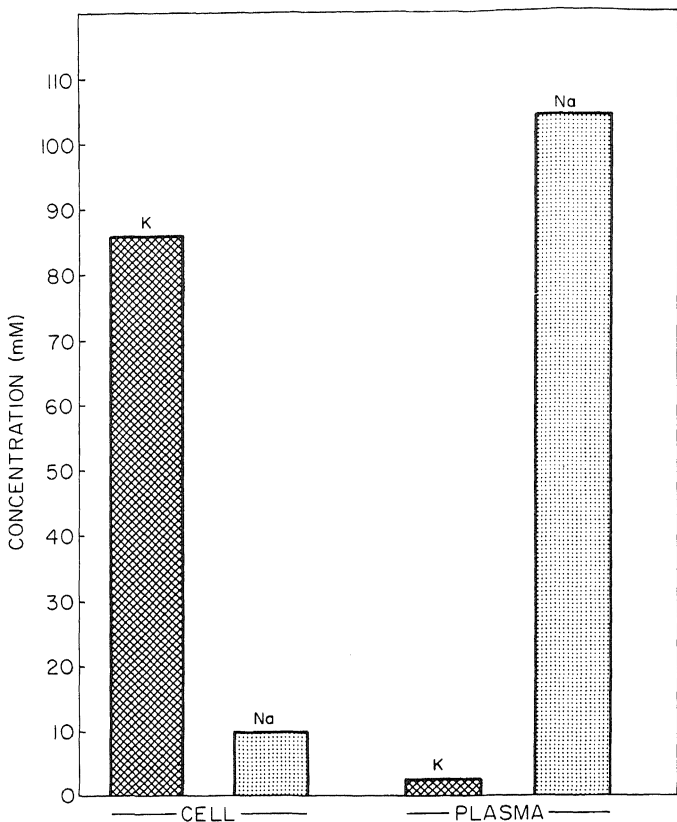


FIGURE 11.1. Equilibrium concentrations of K^+ and Na^+ in frog muscle cells and in frog plasma.

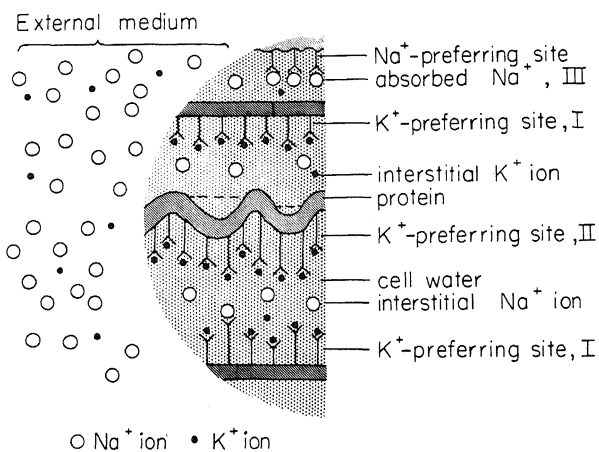


FIGURE 11.2. Schematic illustration of basic mechanisms of selective K^+ accumulation and Na^+ exclusion in living cells. K^+ accumulation results from preferential adsorption on β - and γ -carboxyl groups of cell proteins. Na^+ exclusion results from exclusion from cell water existing in the state of polarized multilayers on a matrix of extended protein chains existing throughout the cell. [From Ling (1969a), by permission of International Review of Cytology.]

11.1.1. Equation Describing Solute Distribution

The concentration of a solute, p_i , dissolved within cell water is described by the equation

$$[p_i]_{cw} = \alpha q_i [p_i]_{ex} \quad (11.1)$$

where $[p_i]_{cw}$ is expressed in mmoles/kilogram fresh cells and $[p_i]_{ex}$ in mmoles/liter of water in the external medium. α is the water content in liters/kilogram fresh cells and q_i is the equilibrium distribution coefficient of the i th solute in cell water. It is understood that cell water may not be uniform in its solvent properties and that the parameters $[p_i]_{cw}$ and q_i are weighted averages.

The solute, p_i , also may be adsorbed onto proteins, and the general equation for the adsorbed solute $[p_i]_{ad}$, in competition with p_j , is:

$$[p_i]_{ad} = \frac{[f]}{2} \left\{ 1 + \frac{\frac{[p_i]_{ex}}{[p_j]_{ex}} \cdot K_{j \rightarrow i}^{00} - 1}{\left[\left(\frac{[p_i]_{ex}}{[p_j]_{ex}} \cdot K_{j \rightarrow i}^{00} \right)^2 + 4 \frac{[p_i]_{ex}}{[p_j]_{ex}} \cdot K_{j \rightarrow i}^{00} \exp(\gamma^{ij}/RT) \right]^{1/2}} \right\} \quad (11.2)$$

where $[p_i]_{ad}$ is expressed in mmoles/kilogram fresh cells and $[f]$ is the concentration of adsorption sites in the same units. $K_{j \rightarrow i}^{00}$ is the equilibrium constant of exchange of j for i , and $-\gamma^{ij}$ is twice the energy of nearest-neighbor interaction between adsorption sites (all as described in Section 7.4).

Equation (11.2) is simplified by using the parameter ξ^{ij} ,

$$\xi^{ij} = \frac{[p_i]_{ex}}{[p_j]_{ex}} \cdot K_{j \rightarrow i}^{00} \quad (11.3)$$

to give

$$[p_i]_{ad} = \frac{[f]}{2} \left\{ 1 + \frac{\xi^{ij} - 1}{[(\xi^{ij} - 1)^2 + 4\xi^{ij} \exp(\gamma^{ij}/RT)]^{1/2}} \right\} \quad (11.4)$$

The general equation for the distribution of solute i in the cell combines $[p_i]_{cw}$ and $[p_i]_{ad}$ [equations (11.1) and (11.4)] and assumes that there may be a total of N types of adsorption sites in the cell, of which the L th is one:

$$[p_i]_{cell} = \alpha q_i [p_i]_{ex} + \sum_{L=1}^N \frac{[f_L]}{2} \left\{ 1 + \frac{\xi_L^{ij} - 1}{[(\xi_L^{ij} - 1)^2 + 4\xi_L^{ij} \exp(\gamma_L^{ij}/RT)]^{1/2}} \right\} \quad (11.5)$$

Theoretically, $K_{j \rightarrow i}^{00}$ for the N types of sites may be widely different, and, if the concentrations of sites in each type are roughly comparable in magnitude and the total

concentration of the i th solutes is comparable to or higher than the free interstitial fraction, we would have a complex curve similar to those shown in Fig. 7.23. On the other hand, if the adsorption sites have uniform values for $K_{j \rightarrow i}^{00}$, then equation (11.5) can be simplified and described by only a single type of adsorption site:

$$[p_i]_{\text{cell}} = \alpha q_i [p_i]_{\text{ex}} + \frac{[\mathfrak{f}]}{2} \left\{ 1 + \frac{\xi^{ij} - 1}{[(\xi^{ij} - 1)^2 + 4\xi^{ij} \exp(\gamma^{ij}/RT)]^{1/2}} \right\} \quad (11.6)$$

An even simpler form of equation (11.5) can be used if $-\gamma^{ij}/2$ is zero, which could occur if all the adsorption sites are isolated from each other, or if the pair of competing solutes i and j are very similar in nature and their substitution for one another involves no change in the energy of the neighboring sites. Under this condition, equation (11.6) can be further simplified into

$$[p_i]_{\text{cell}} = \alpha q_i [p_i]_{\text{ex}} + \frac{[\mathfrak{f}] K_{j \rightarrow i}^{00} [p_i]_{\text{ex}}}{[p_i]_{\text{ex}} K_{j \rightarrow i}^{00} + [p_j]_{\text{ex}}} \quad (11.7)$$

which is in essence the Troshin equation [equation (4.4)].

Equation (11.7) can be written in a more general form to deal with a total of n types of solutes. Representing the adsorption constant of the i th solute as K_i , we have

$$[p_i]_{\text{cell}} = \alpha q_i [p_i]_{\text{ex}} + \frac{[\mathfrak{f}] K_i [p_i]_{\text{ex}}}{1 + \sum_{i=1}^n K_i [p_i]_{\text{ex}}} \quad (11.8)$$

The second term of the right side of equation (11.8) can be written in double reciprocal form, an approach which is, of course, analogous to similar double reciprocal plots that Lineweaver and Burk used in enzyme (and permeability) studies (Section 4.5.1). Only here, instead of rates, equilibrium concentrations are involved. For the case where only two species of solutes, i and j , are studied,

$$\frac{1}{[p_i]_{\text{ad}}} = \frac{K_i}{[\mathfrak{f}]} \left(1 + \frac{[p_j]_{\text{ex}}}{K_j} \right) \frac{1}{[p_i]_{\text{ex}}} + \frac{1}{[\mathfrak{f}]} \quad (11.9)$$

In a plot of $1/[p_i]_{\text{ad}}$ against $1/[p_i]_{\text{ex}}$ in the presence of different concentrations of the j th competing solute, one obtains a family of straight lines converging on the same locus on the ordinate. This locus should be equal to $1/[\mathfrak{f}]$. From the slopes of the lines and the value of $[\mathfrak{f}]$, one can calculate the adsorption constants K_i and K_j . (Note: $K_{j \rightarrow i}^{00} = K_i - K_j$.)

Two aspects of solute distribution bear emphasis:

1. *The relation between $-\gamma^{ij}/2$ and $\Delta F_{j \rightarrow i}^{00}$.* Equation (11.6) differs from the Troshin equation [equation (4.4) or (11.7)] in that equation (11.6) includes adsorption onto sites with nearest-neighbor interaction energies ($-\gamma/2$) other than zero. One may ask, What determines the value of $-\gamma/2$? According to the AI hypothesis, $-\gamma/2$ is equal to zero when the adsorption sites are far apart and not cooperatively linked. How-

ever, even adsorption on cooperatively linked sites may have a zero $-\gamma/2$ under certain conditions. This arises from the fact that $-\gamma^{ij}/2$ is directly related to the free energy of exchange adsorption, $-\Delta F_{j \rightarrow i}^{00}$, because the primary component of $-\gamma^{ij}/2$ is the inductive effect created on a neighboring site when an exchange of j for i occurs. In other words,

$$-\frac{\gamma^{ij}}{2} = \tau(-\Delta F_{j \rightarrow i}^{00}) \quad (11.10)$$

where τ , a transmissivity constant, depends on the number and nature of chemical groups separating the neighboring sites on which i or j is adsorbed (see Section 7.1.2.2).

2. *The independence of ion distribution and resting potential.* Neither the general equation (11.5), nor the more specific Troshin equation (4.4) takes into account the electrical potential in describing ion distributions. Why is the electrical potential difference between the inside and the outside of the cell not taken into account in the equations for ion distribution? Troshin offered no explanation. My reason is that the law of macroscopic electroneutrality demands that, as far as bulk phase ion distribution is concerned, either the same number of cations and anions migrate together or an exchange of extracellular ions for an equivalent amount of intracellular ions of the same electric charge take place, so that there is no net transfer of a significant number of charges. A transfer of a significant amount of Na^+ between the cell and its environment may appear to involve charge transfer; in fact, it is as neutral as the transfer of water. Experimental evidence in support of this view is given in Section 8.4.1.4. It is only at the microscopically thin surface boundaries that the law of macroscopic electroneutrality may not apply. Under that condition alone is ion transfer dependent on the electrical potential, as will be outlined in Chapter 14.

11.1.2. Control of Solute Distribution by Cardinal Adsorbents

In the simplest case, illustrated in Fig. 11.3, the proteins adsorbing a solute also polarize water; in this case the cardinal adsorbent controls at once the distribution of adsorbed solute and the free solute dissolved in the water. In nature, perhaps the more frequently observed case is one in which different proteins are involved in solute adsorption and in water polarization. The theoretical aspects of the control of distribution of adsorbed and free solutes by cardinal adsorbents will be discussed separately.

11.1.2.1. Control of Adsorbed Solutes by Cardinal Adsorbents

11.1.2.1a. *The Effect of Concentration of Cardinal Adsorbent.* In Section 7.4.3 I presented the case where the proteins adsorbing the solute have a single cardinal site. This type of control of adsorption is illustrated in Fig. 7.26. Figure 11.4 presents the theoretical adsorption curves for the i th solute in response to different concentrations of the cardinal adsorbent when two cardinal sites control each gang of regular adsorption sites. Figure 11.5 is a plot of the j th solute distribution in response to increasing concentrations of the cardinal adsorbent.

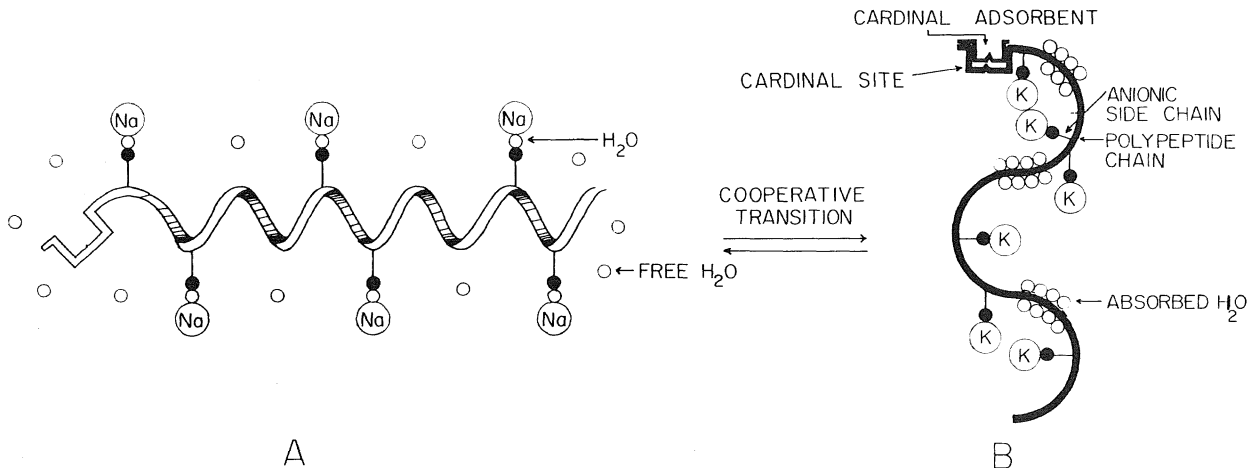


FIGURE 11.3. Schematic representation of a portion of a protein molecule undergoing cooperative transformation in response to the cardinal adsorbent ATP. Adsorbed water molecules are perceived as existing in a state of polarized multilayers but are schematically depicted as one layer. [From Ling and Negendank (1980), by permission of *Perpectives in Biology and Medicine*.]

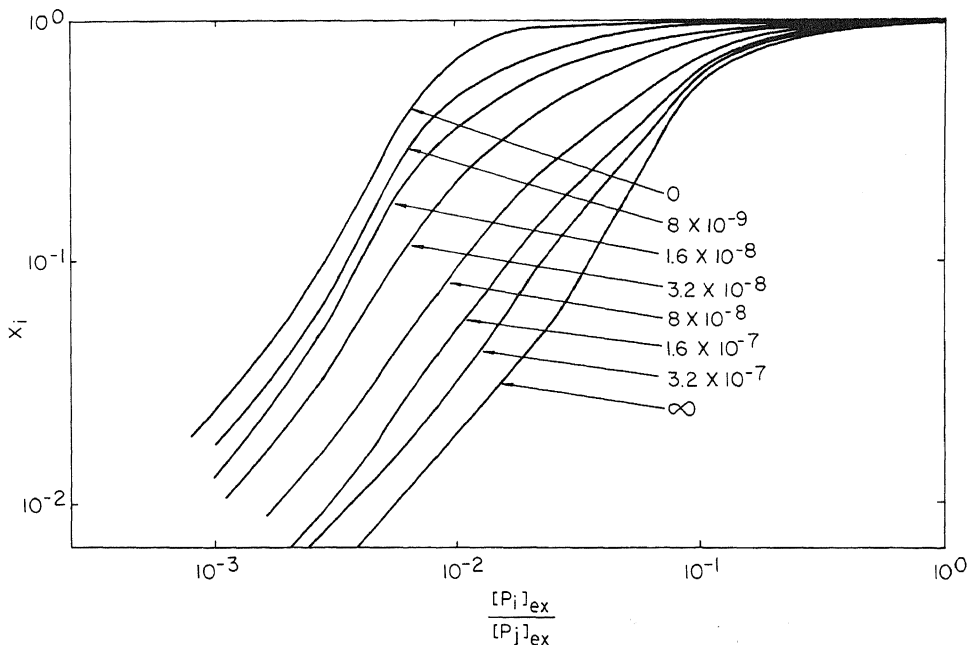


FIGURE 11.4. Theoretical adsorption isotherm of the i th solute expressed as mole fraction, X_i , with varying concentrations (M) of a cardinal adsorbent in an environment containing the i th and j th solutes at different concentration ratios. Each gang of adsorbing sites on the protein is under the control of two cardinal sites. [From Ling and Bohr (1971a), by permission of *Physiological Chemistry and Physics*.]

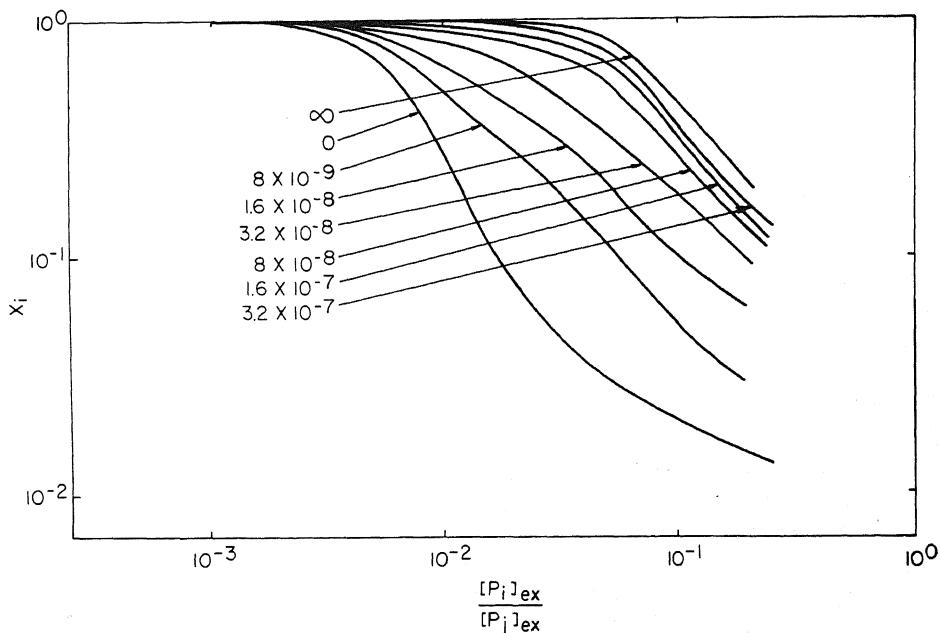


FIGURE 11.5. Theoretical adsorption isotherm of the j th solute for gangs of sites with two controlling cardinal sites. Other conditions similar to those described for Fig. 11.4. [From Ling and Bohr (1971a), by permission of *Physiological Chemistry and Physics*.]

11.1.2.1b. The Relation between Adsorbed Cardinal Adsorbent and Concentration of Adsorbed Solutes. If each gang of sites does not adsorb the i th solute unless a specific cardinal adsorbent C occupies the cardinal site, then a rectilinear relation should exist between the concentration of C and the concentration of the adsorbed i th solute. The slope of a plot of the concentration of the adsorbed i th solute against the concentration of the adsorbed cardinal adsorbent C should yield the number of regular sites in the gang of sites that are controlled by each cardinal site.

11.1.2.2. Control of Freely Dissolved Solutes by Cardinal Adsorbents: The Universality Rule

According to the AI hypothesis, the maintenance of the polarized multilayer state of water requires certain matrix proteins to exist in an extended conformation (Section 6.3). In dead cells, water is no longer polarized in multilayers because the cardinal adsorbent essential for the maintenance of the proper extended conformation of these matrix proteins is depleted. Again one would expect that there is a quantitative relation between the concentration of the adsorbed cardinal adsorbent and the degree of exclusion of the i th solute from cell water.

An important corollary to this concept is the *universality rule*: If, owing to the change in the essential cardinal adsorbent or for other reasons, the q -value of a particular solute changes, then a parallel change should occur in the q -values of all solutes that are normally excluded by the system.

11.1.3. The Effect of Temperature on Solute Distribution

The one-dimensional Ising model, on which the derivation of equation (11.2) was based (Section 7.4) is well known for its inability to predict temperature transitions; however, temperature transitions are a major characteristic feature of cooperative phenomena in three-dimensional systems, which the protein–water complexes in fact are (Huang, 1977). Hence the cooperatively linked ion-adsorbing protein may go from a state where all the sites adsorb the i th solute (i state) to another in which they adsorb only the j th solute (j state) by a small change of temperature around a particular temperature called the *critical temperature*.

11.2. Experimental Testing of the Theory

In Chapter 4, I presented some evidence in support of the early version of the AI hypothesis and Troshin's sorption theory (Figs. 4.3–4.4). Troshin, using what may be called the *limiting slope method*, resolved the free and adsorbed fractions of intracellular solutes. In cases where the adsorption is strong, the method is effective. In cases where the adsorption is moderate or weak, the separation may be more difficult. When the q -value is low, it is also difficult to sort out solutes in the extracellular space and on connective tissue elements. Take as an example the familiar frog sartorius. Even though it is one of the most extensively studied tissues, at the time when we began our investigations, the extracellular space (ecs) for frog sartorius muscle reported in the literature varied from 13% to 35%.

TABLE 11.1. Extracellular Space of Frog Sartorius Muscle

Method	Extracellular space (%)	Reference
Poly-L-glutamate distribution	8.3–9.1	Ling and Kromash (1967)
Br ⁻ efflux analysis	8.2 ± 0.13	Ling (1972c)
Centrifugation	9.3–9.4	Ling and Walton (1975a)

Beginning in 1967, our laboratory evolved three independent methods to estimate the ecs of the frog sartorius muscle. The results are compiled in Table 11.1. The ecs for frog sartorius muscle is 8–9%. Besides the ecs proper, there are such components as connective tissues, small nerves, and blood vessels. They too are taken into account, usually by making parallel studies on loose connective tissues isolated from the same animal from the areas surrounding the sartorius muscle. When corrections are made, attention must be paid to the fact that the loose connective tissue model also contains its own "ecs."

11.2.1. Basic Patterns of Solute Distribution: Free and Adsorbed Fractions

11.2.1.1. K^+ and Other Alkali Metal Ions

11.2.1.1a. *Frog Muscles.* Figure 11.6 shows the equilibrium distribution of labeled K^+ in frog muscle cells after full correction for ecs, in the absence and presence of nonlabeled K^+ ; the data points are experimental, the lines theoretical according to equation (11.7). Figure (11.7) is a double reciprocal plot of the same set of data as in

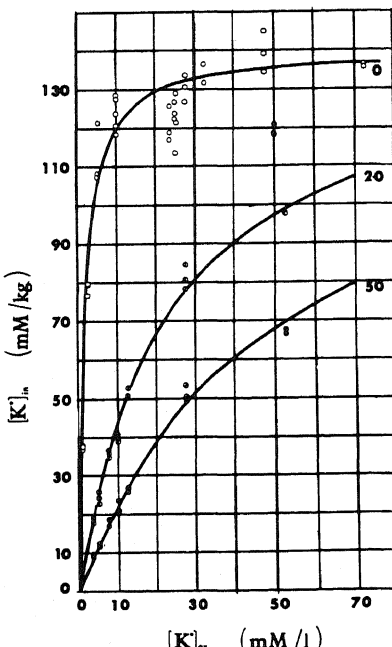


FIGURE 11.6. Equilibrium intracellular labeled K^+ concentration at various external K^+ concentrations ($24^\circ C$). Curves theoretically calculated on the basis of equation (11.7) and the following: (1) $q_1 = 0$, (2) one type of adsorption site at a concentration of 140 mmoles/kg, and (3) an association constant in M^{-1} of 6.65×10^{-2} for K^+ and 0.996 for Na^+ . [From Ling and Ochsenfeld (1966), by permission of *Journal of General Physiology*.]

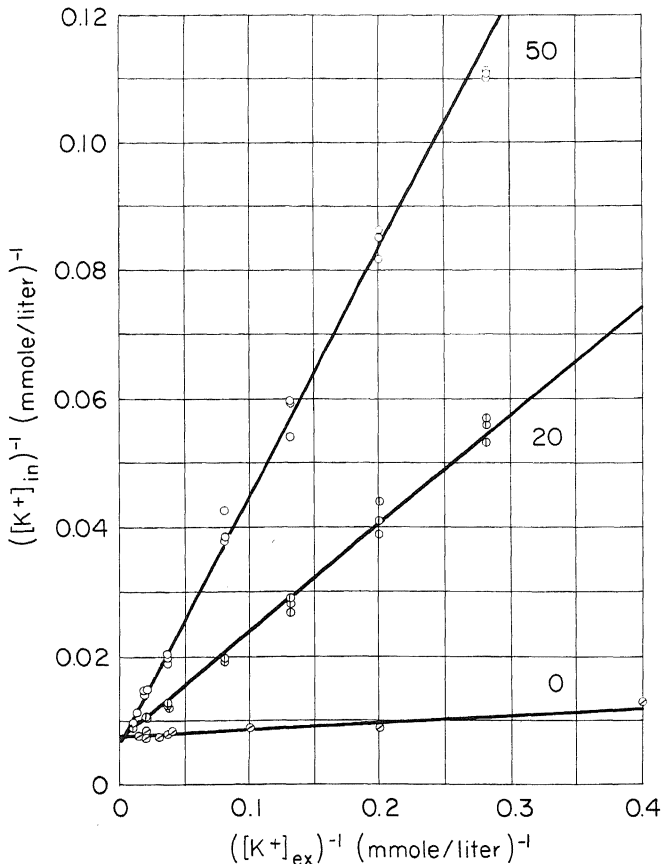


FIGURE 11.7. Intracellular labeled K⁺ concentration plotted reciprocally against the external labeled K⁺ concentration, with which it is in equilibrium, in the presence of 0, 20, and 50 mmoles/liter of nonlabeled potassium acetate. Labeled K⁺ was also in the form of acetate salt. Each point represents the labeled K⁺ concentration in a single frog sartorius muscle; lines obtained by the method of least squares. [From Ling and Ochsenfeld (1966), by permission of *Journal of General Physiology*.]

Fig. 11.6, according to equation (11.9). Similarly Fig. 11.8 is a double reciprocal plot of labeled Cs⁺ distributions in the presence and absence of competing nonlabeled K⁺. Two additional points worth mentioning are:

1. A reciprocal plot like those shown in Figs. 11.7–11.8 does not by itself prove adsorption. The Donnan equilibration theory predicts a quite similar pattern. However, in the Donnan equilibration, ion accumulation is only valency-specific. The vastly different effects of the same concentration of K⁺ and Cs⁺ in depressing labeled Cs⁺ accumulation, shown in Fig. 11.8, disprove the Donnan theory and affirm the adsorption theory (Ling and Ochsenfeld, 1966).
2. The K⁺ data yielded an anionic site concentration of 140 mmoles/kg fresh cells while the Rb⁺ and Cs⁺ data yielded only 108 and 75 mmoles/kg respectively.



R. C. Murphy, Z. Zhang, J. F. Brogan, J. T. Greenplate, M. M. Ochsenfeld, W. Negendank, G. Karreman, C. F. Hazlewood, and G. N. Ling

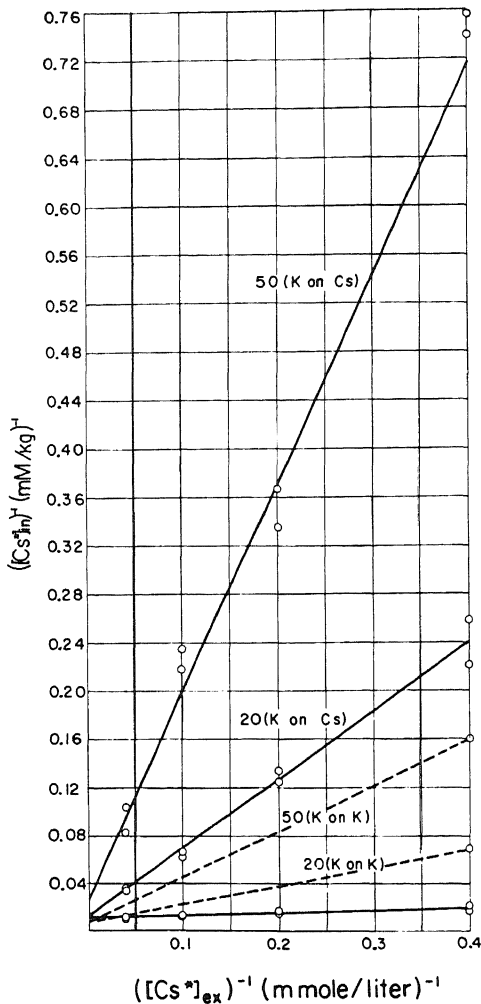


FIGURE 11.8. Equilibrium labeled Cs^+ concentration in muscle cells plotted reciprocally against the external labeled Cs^+ concentration, with which it is in equilibrium. Competing K^+ concentrations are 0, 20, and 50 mmoles/liter, respectively. Both Cs^+ and K^+ were in the form of acetates (24°C). Each point represents a single determination on one frog sartorius muscle; lines obtained by the method of least squares. The effect of K^+ ion on the accumulation of labeled K^+ ion (dashed lines) taken from Fig. 11.7 for comparison. [From Ling and Ochsenfeld (1966), by permission of *Journal of General Physiology*.]

This difference is significant and interesting and will be referred to again (see Section 13.5).

From data like those of Figs. 11.6–11.8 the apparent free energies of adsorption for Cs^+ , Rb^+ , K^+ , and Na^+ are, respectively, -3.66 , -3.92 , -3.85 , and 0 kcal/mole, to give the following rank order of selectivity: $\text{Rb}^+ > \text{K}^+ > \text{Cs}^+ > \text{Na}^+$. The same rank order was obtained from a time course study of muscles incubated in a Ringer solution containing Cs^+ , Rb^+ , K^+ , Na^+ , and Li^+ (Fig. 11.9). By comparing the final steady level of each ion with the level in the surrounding medium a set of selectivity ratios was obtained and these are illustrated in Fig. 11.10 in comparison to the theoretical selectivity ratios derived from the calculated values given in Fig. 6.7 at a c -value of -4.5 Å.

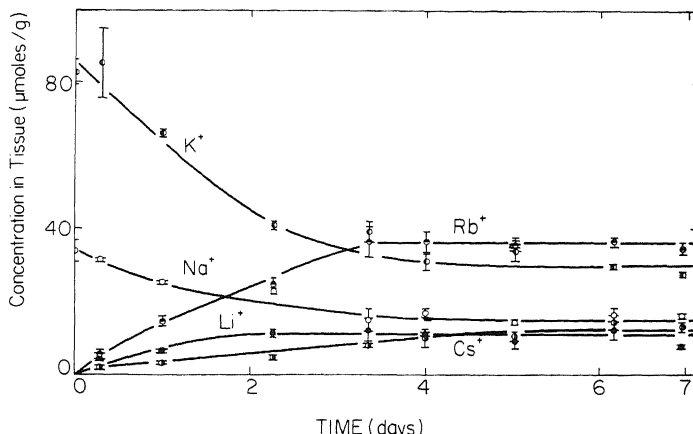


FIGURE 11.9. Time course of uptake of Rb^+ , Cs^+ , and Li^+ and loss of K^+ and Na^+ in normal frog muscle ($25^\circ C$). The final external ion concentrations (mM) were 0.83 (Cs^+), 0.88 (Rb^+), 1.35 (K^+), 8.20 (Li^+), and 99.9 mM (Na^+). The corresponding ρ -values ($[M^+]_{in}/[M^+]_{out}$) are 11.4 (Cs^+), 41.0 (Rb^+), 20.3 (K^+), 1.53 (Li^+), and 0.12 (Na^+). [From Ling and Bohr (1971b), by permission of *Physiological Chemistry and Physics*.]

Because of the much higher concentrations of adsorbed K^+ , Rb^+ , and Cs^+ , the data shown in Figs. 11.6 and 11.7 are not very useful in determining the q -value of these ions in cell water. However, at much higher external K^+ concentration a q_K of 0.5 was estimated (Ling, 1977e). Since adsorbed Na^+ is less, and external Na^+ is high, the q -value of Na^+ in frog muscle water can be determined more easily, as it was by Troshin (see Fig. 4.4) and by us (Fig. 11.11). Here the apparent q_{Na} is 0.18.

11.2.1.1b. Amphibian Eggs. In studies of frog muscle the level of intracellular ion is assessed in reference to the outside Ringer solution. Horowitz and his associates (S. B. Horowitz and Paine, 1979; Horowitz *et al.*, 1979) developed a new approach to the problem in the giant egg cell by producing an intracellular *reference phase* (RP) in the form of a gelled droplet of injected gelatin solution. After freezing, analysis of the ion contents of the cytoplasm, the nucleus, and the RP is performed by microsurgery or cryosectioning. One set of data obtained by this technique is that of Paine *et al.* (1981). Their data, shown in Figs. 11.12 and 11.13, can be nicely described by Troshin's equations. Figure 11.12 shows cytoplasmic ion concentrations versus concentrations in the RP, and Fig. 11.13 shows nuclear ion concentrations versus RP. Cytoplasmic ions have fractions with q -values of 0.45 for Na^+ and 0.36 for K^+ , and fractions that appear to be saturable. Nuclear ions, except for a small adsorbed fraction, have fractions with q -values of unity, suggesting that in the oocyte nucleus the water has normal solvency for both K^+ and Na^+ .*

*This conclusion ($q = 1.0$ for nuclear water) must now be revised. At a recent international workshop held in Houston (June 20–25, 1983) Horowitz showed that a ρ -value well below unity was found for nuclear water when other probe molecules were used.

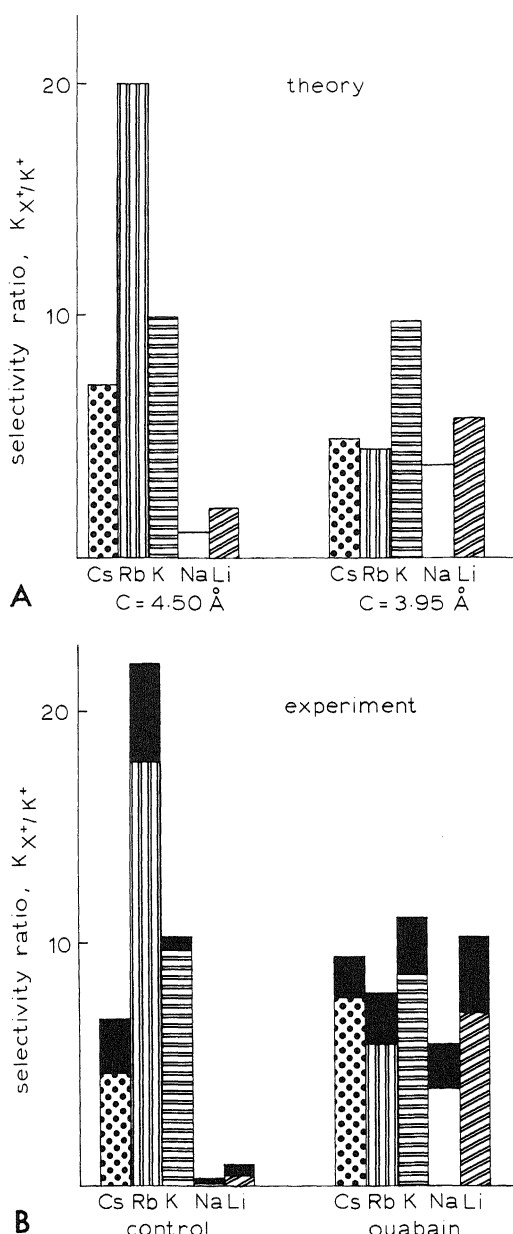


FIGURE 11.10. (A) Theoretical selectivity ratios at c -values of -4.50 Å and -3.95 Å. (B) Experimental selectivity ratios measured in normal frog muscle and in muscle treated with 3.27×10^{-7} M ouabain (Fig. 11.9). [From Ling and Bohr (1971b), by permission of *Physiological Chemistry and Physics*.]

TABLE 11.2. Equilibrium Distribution of K^+ and Mg^{2+} in Frog Muscles Exposed to Normal and High External K^+ Concentrations^{a,b}

		W_f/W_i	$[K^+]_{ex}$ (mM)	$[K^+]_{in}$ (μ moles/g)	$[Mg^{2+}]_{ex}$ (mM)	$[Mg^{2+}]_{in}$ (μ moles/g)	$\frac{[Mg^{2+}]_{in}}{[Mg^{2+}]_{ex}}$	$\frac{[Mg^{2+}]_{in} W_f}{[Mg^{2+}]_{ex} W_i}$
I	Control	0.97 ± 0.03	2.91	90.9 ± 3.4	0.88	9.24 ± 0.53	10.50 ± 0.61	10.20 ± 0.62
	Experiment	1.00 ± 0.03	94.10	186.0 ± 2.7	0.82	8.39 ± 0.60	10.20 ± 0.07	10.20 ± 0.71
II	Control	0.99 ± 0.02	2.71	93.5 ± 2.9	1.08	9.16 ± 0.75	8.50 ± 0.70	9.02 ± 1.12
	Experiment	0.96 ± 0.03	96.70	193.3 ± 5.0	0.84	8.64 ± 0.68	10.30 ± 0.81	10.00 ± 0.73
III	Control	0.99 ± 0.02	2.76	93.1 ± 3.3	1.08	9.81 ± 0.11	9.33 ± 0.16	9.24 ± 0.34
	Experiment	0.78 ± 0.02	113	193.7 ± 8.4	0.98	12.00 ± 0.72	12.00 ± 0.72	9.42 ± 0.33
IV	Control	1.00 ± 0.01	2.71	77.8 ± 6.2	1.00	8.68 ± 0.76	8.67 ± 0.75	8.68 ± 0.66
	Experiment	0.79 ± 0.02	106	168.8 ± 7.8	0.89	9.64 ± 0.66	10.90 ± 0.76	8.96 ± 0.29

^aThe first column gives the ratio of final weights of the muscles over the initial weights. The last column represents the intracellular/extracellular ratio of Mg^{2+} after corrections for weight change. In experiments I and II, KCl was added to a normal Ringer solution; in experiments III and IV, KCl was added to a Ringer solution in which NaCl had been replaced by isosmolar concentrations of sucrose, which led to marked shrinkage. Averages from four determinations \pm SE.

^bFrom Ling *et al.* (1979), by permission of *Journal of Cell Physiology*.

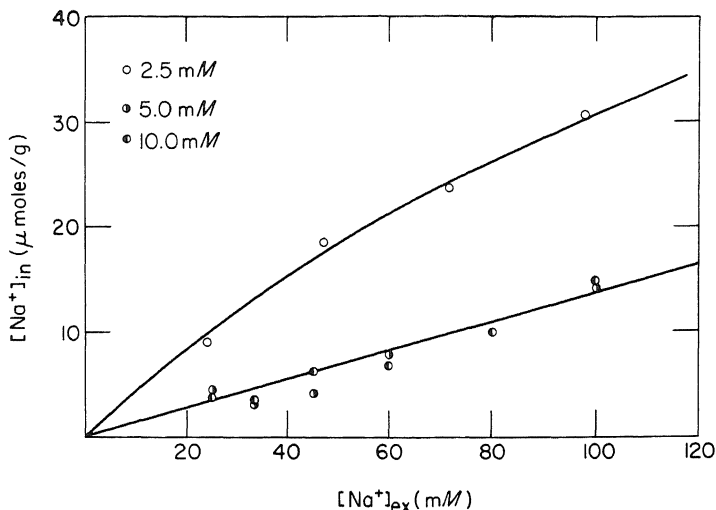


FIGURE 11.11. Equilibrium distribution of Na^+ ion in frog sartorius muscle in the presence of varying external K^+ ion concentrations (2.5 mM, 5.0 mM, and 10.0 mM). The data were calculated on the basis of a 10% extracellular space. The slope of the straight line going through the points at the higher K^+ concentrations is 0.14. The muscle cells contain 78% water. If all Na^+ in the cell at the higher K^+ concentrations is assumed to be in the cell water, the equilibrium distribution coefficient of Na^+ between the cell water and the external medium is 0.18. [From Ling (1969a), by permission of *International Review of Cytology*.]

11.2.1.2. Mg^{2+}

Figure 11.14 shows the equilibrium distribution of Mg^{2+} in frog muscle at 25°C. A very similar set of curves was obtained at 5°C. There is a very tightly bound fraction of Mg^{2+} which reached saturation at the lowest external concentration of Mg^{2+} studied (1 mM). Increase of external Mg^{2+} beyond 1 mM produces a rectilinear gain of Mg^{2+} with a slope of 0.206 (25°C) and 0.220 (5°C). Note how much the lower curve of Fig. 11.14 resembles Fig. 11.12. Note also that, as the cell gains Mg^{2+} , the intracellular K^+ remains unchanged. Conversely, a large increase of intracellular K^+ did not influence the intracellular Mg^{2+} concentration (Table 11.2). These findings clearly show that the Donnan theory of membrane equilibrium cannot be applied in these living cells because the Donnan theory predicts profound mutual interaction of all permeant ions, i.e., a rise of external Mg^{2+} to 73.2 mM should lead to virtually complete replacement of intracellular K^+ ; an increase of external K^+ from 2.5 to 100 mM should reduce intracellular Mg^{2+} concentration to near zero. None of these results was observed. On the other hand, the data are readily explained by equations (11.6)–(11.8). The independence of the concentrations of Mg^{2+} and K^+ in the cell is also explained by a difference in the specificity of their adsorption sites (e.g., isolated β - and γ -carboxyl groups for K^+ and pairs or groups of chelating anionic sites for Mg^{2+}). In the broad range of Mg^{2+} studied, the entry of Mg^{2+} is accompanied by an equivalent amount of Cl^- (or SO_4^{2-}), as little or

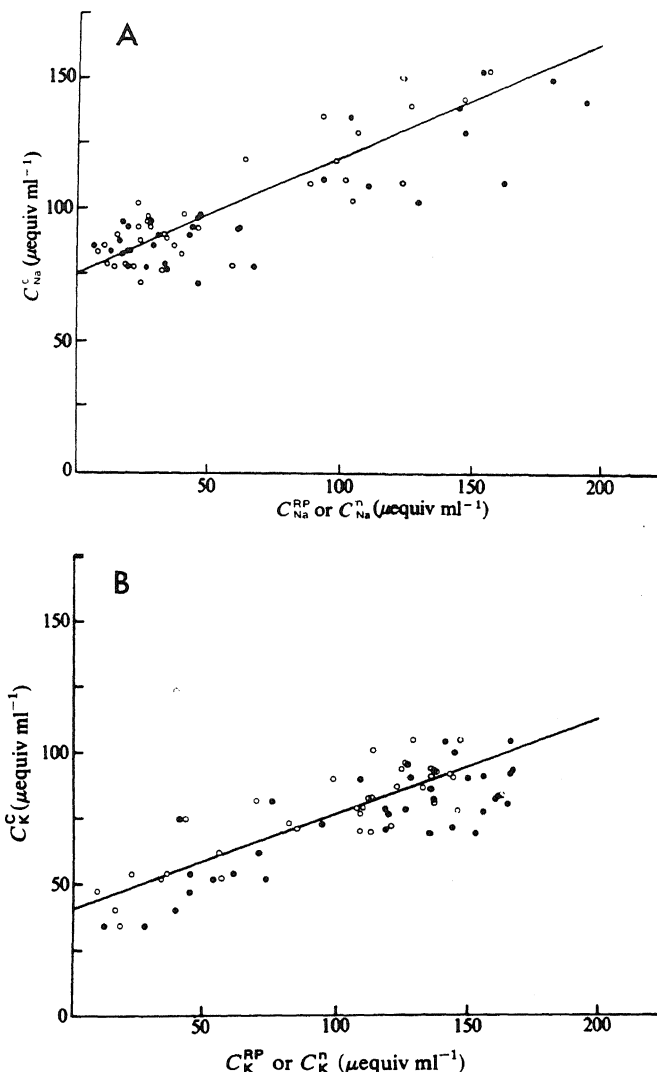


FIGURE 11.12. (A) Na^+ isothermal relations. Cytoplasmic Na^+ concentration, C_{Na}^c , versus reference phase (RP) Na^+ concentration, $C_{\text{Na}}^{\text{RP}}$ (\circ), and nuclear Na^+ concentration, C_{Na}^n (\bullet): The line is the least-squares line for the cytoplasm/RP data, $C_{\text{Na}}^c = 0.45C_{\text{Na}}^{\text{RP}}$. (B) K^+ isothermal relations. Cytoplasmic K^+ concentration, C_{K}^c , versus RP K^+ concentration, C_{K}^{RP} (\circ): The least-squares line is $C_{\text{K}}^c = 0.36C_{\text{K}}^{\text{RP}} + 41 \mu\text{equiv ml}^{-1}$. C_{K}^c compared with nuclear K^+ concentration, C_{K}^n (\bullet): The least-squares line (not shown) is $C_{\text{K}}^c = 0.34C_{\text{K}}^n + 38 \mu\text{equiv ml}^{-1}$. Cytoplasmic Na^+ and K^+ in oocytes injected with a gelled RP. [From Paine *et al.* (1981), by permission of *Nature*.]

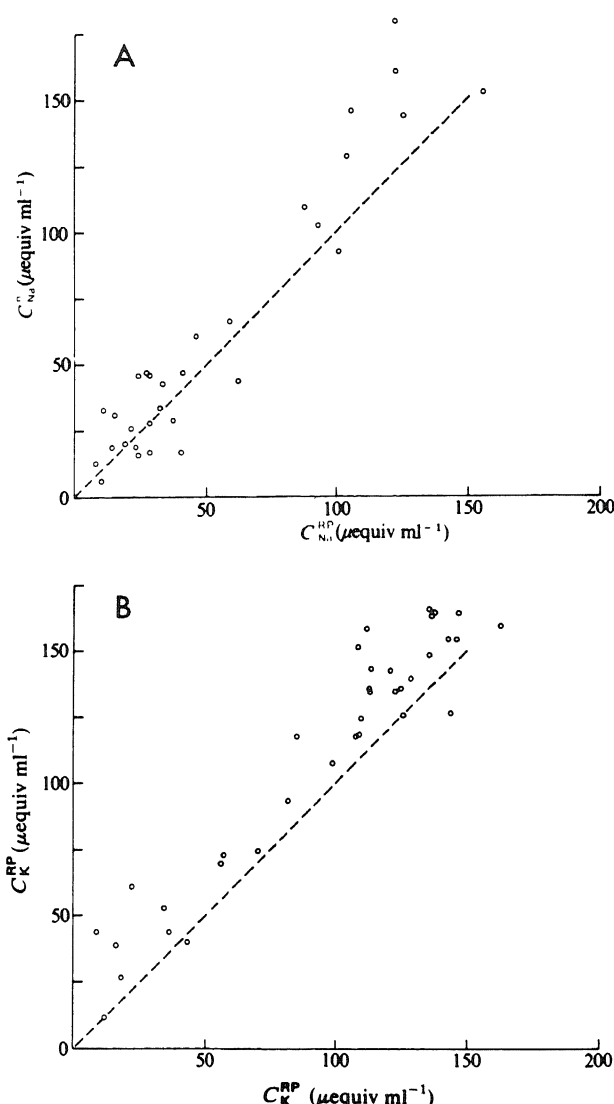


FIGURE 11.13. (A) C_{Na}^n versus $C_{\text{Na}}^{\text{RP}}$. The dashed line is isomolar; the least-squares line (not shown) is $C_{\text{Na}}^n = C_{\text{Na}}^{\text{RP}} + 4 \mu\text{equiv ml}^{-1}$. (B) C_{K}^n versus C_{K}^{RP} . The dashed line is isomolar; the least-squares line (not shown) fitting the data points is $C_{\text{K}}^n = C_{\text{K}}^{\text{RP}} + 19 \mu\text{equiv ml}^{-1}$. Nuclear Na^+ and K^+ in oocytes injected with gelled RP. [From Paine *et al.* (1981), by permission of *Nature*.]

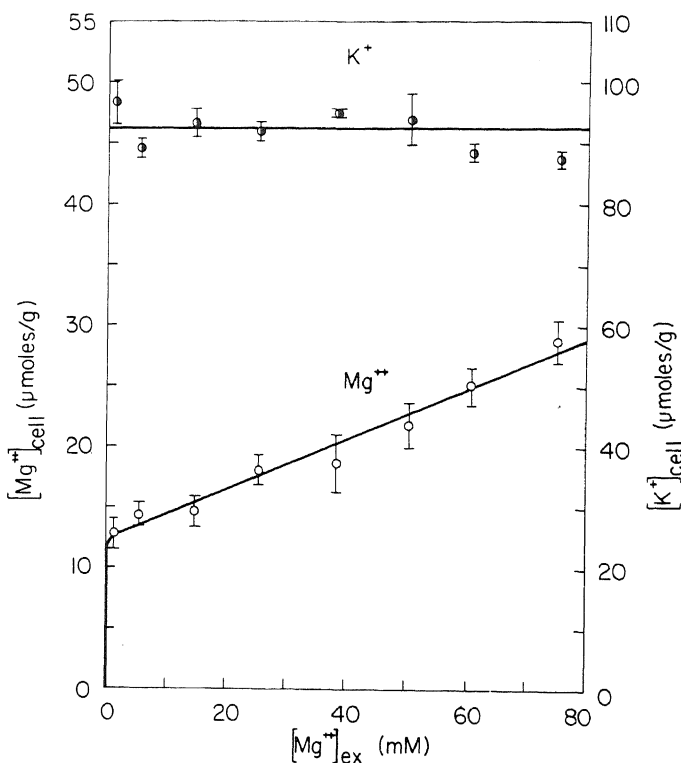


FIGURE 11.14. Equilibrium Mg^{2+} and K^+ distribution in frog voluntary muscles at 25°C. Incubation was in a 25°C shaking water bath for 17.5 hr. Muscles were centrifuged to remove extracellular fluids before extraction of and analysis for Mg^{2+} . Each point is the average of four determinations; the distance between the horizontal bars is twice the SE. The solid line intersecting most of the Mg^{2+} data points is theoretical according to equation (11.8). The numerical values used are $\alpha = 0.78$, $q_{Mg} = 0.280$, $K_{Mg}^\infty = 10^{-4}$ M, $[f] = 12.3 \mu\text{moles/g}$ fresh muscle cells [From Ling *et al.* (1979), by permission of *Journal of Cell Physiology*.]

none enters in exchange for other ions; thus the Cl^- distribution curve has the same slope as that of Mg^{2+} (Fig. 11.15).

The unambiguous rectilinear plot of intracellular Mg^{2+} concentration against external Mg^{2+} concentration higher than 1 mM allows the calculation of the enthalpy and entropy of distribution of Mg^{2+} between cell water and the external medium. The data show that there is a small favorable enthalpy ($\Delta H = 0.516$ kcal/mole) for Mg^{2+} in the cell water, which is more than compensated by an unfavorable entropy ($\Delta S = 4.37$ cal/deg per mole). In this case, the primary mechanism for Mg^{2+} exclusion from cell water is entropic.

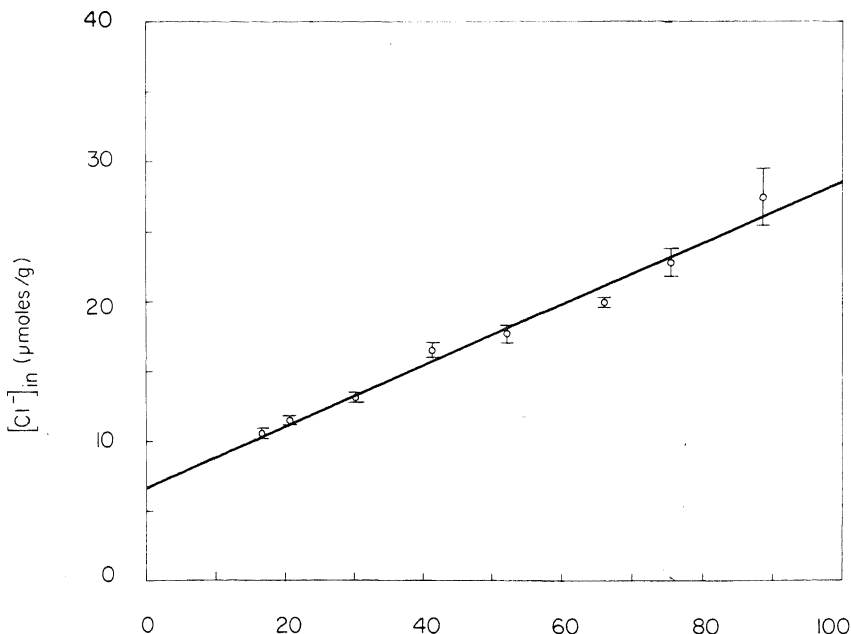


FIGURE 11.15. Equilibrium distribution of Cl^- in frog voluntary muscles at 5°C plotted against external Cl^- concentration. Each point represents means of four determinations \pm SE. By the method of least squares, the slope of the curve is 0.220. [From Ling *et al.* (1979), by permission of *Journal of Cell Physiology*.]

11.2.1.3. Ca^{2+}

Following introduction of the Ca^{2+} -sensitive luminescent protein, aequorin, into giant salivary gland cells of *Chironomus*, Rose and Lowenstein (1975) injected pulses of Ca^{2+} into these cells through a micropipet. With the aid of an image intensifier and a TV camera they studied the free Ca^{2+} distribution in the cell by recording light emitted in different parts of the cell (see Fig. 11.41). An outstanding phenomenon observed was the confinement of the luminescent glow to the vicinity of the tip of the injecting micropipet. Thus, these authors estimated that the Ca^{2+} concentration was less than 10^{-4} M within a radius of $16 \pm 2\text{ }\mu\text{m}$ surrounding the micropipet tip but that it fell precipitously to less than 10^{-6} M in areas only $1\text{--}2\text{ }\mu\text{m}$ beyond. Rose and Loewenstein interpreted the rapid quenching of luminescence following each injection and the restricted luminescence distribution as being due to an efficient pumping of the injected Ca^{2+} into mitochondria. They apparently assumed that aequorin could not penetrate into the mitochondria, a condition which their explanation requires.

There is little question that some of the injected Ca^{2+} might well have found its way into the surrounding mitochondria (see Ling, 1981a). However—even though under *in vitro* conditions (where, for example, high concentrations of phosphate or oxa-

late were present) profuse Ca^{2+} accumulation in mitochondria had been demonstrated [for a new explanation of the mechanism of this type of Ca^{2+} concentration, see Ling (1981a), p. 88]—the concept that mitochondria therefore can act as bottomless “sinks” for Ca^{2+} under different conditions is less easy to defend. More likely, the injected Ca^{2+} might partly diffuse out of cells and partly become adsorbed on cytoplasmic proteins which depend on ATP as a cardinal adsorbent for Ca^{2+} adsorbing function.

However, what seems far more important in Rose and Loewenstein's finding is the restricted free Ca^{2+} distribution following its injection. I believe that, as pointed out in Section 8.4.2.1, there must be local damage of the protoplasm by the penetrating tip of the micropipet. This damage, which tends to spread, could have altered the physical state of water from its normal polarized multilayered state to one closer to normal liquid water. As a result a local rise of the q -value for Ca^+ could have occurred. In contrast, in areas away from the impaling pipet, the normal polarized state of water with a much lower q -value for Ca^{2+} would be preserved. Therefore, high free Ca^{2+} concentration would be restricted to the punctured area. Indeed the observed $<10^{-4}$ M Ca^{2+} in the micropipet tip region, when compared to the $<10^{-6}$ M Ca^{2+} in the surrounding unpermeated region, suggests a q -value for Ca^{2+} of normal *Chironomus* salivary gland cells near 10^{-2} .

A similar assumption could also provide simple explanations for three other sets of reported findings which parallel those of Rose and Loewenstein: (1) Much higher free Na^+ and K^+ concentrations were found in the gelatin reference phase injected into amphibian eggs than in the normal cytoplasmic water away from the injected gelatin (see Section 11.2.1.1b). (2) With ion-selective microelectrodes an activity coefficient for K^+ higher than 1.0 was repeatedly observed (Section 8.4.2.2), indicating congregation of K^+ in the near vicinity of the impaling microelectrode. (3) A region immediately adjacent to the cut end of a muscle cell was sharply separated from the remaining normal cytoplasm even though no new membrane was formed. The damaged region contained much higher concentrations of Na^+ and D-arabinose than the adjacent healthy region (Section 5.2.6). In this damaged area K^+ also diffused much more rapidly than in the normal cytoplasm away from the cut (Section 8.4.1.4).

11.2.1.4. Sugars and Sugar Alcohols

In Chapter 9, it was shown that the uptake by frog muscle (without insulin) of methanol, ethylene glycol, glycerol, xylose, glucose, and sucrose agrees with theory, i.e., the q -value decreased with increasing size and complexity of the molecules (Fig. 9.5). This conclusion rests upon the assumption that all of these solutes exist as free solutes in the cell water, and relatively little is adsorbed. To establish the free state, we have used two kinds of tests:

1. *Competition test.* This is illustrated in Fig. 11.16. The addition of nonlabeled D-glucose did not materially change the slope of the labeled D-glucose uptake in frog muscle freed of insulin and equilibrated at 0°C .

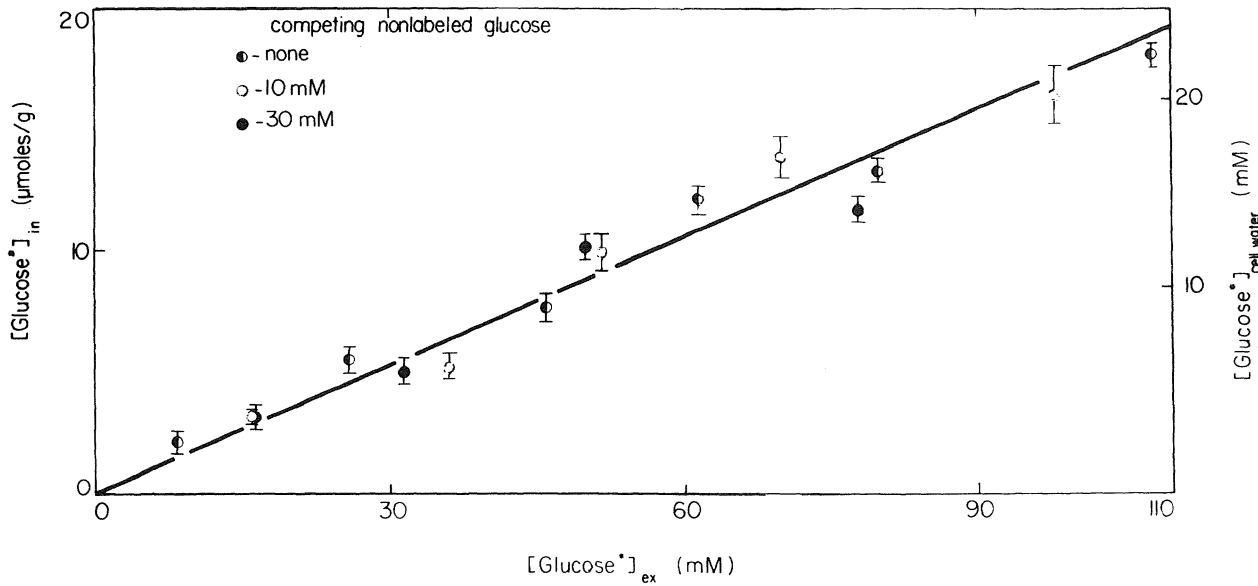


FIGURE 11.16. Effect of competing nonlabeled D-glucose on the uptake of labeled glucose by washed frog muscles. Mixed muscles were washed for 6 hr in Ringer solution containing no glucose and no insulin at 25°C followed by incubation at 0°C with varying concentrations of glucose and labeled glucose. [From Ling and Will (1969), by permission of *Physiological Chemistry and Physics*.]

TABLE 11.3. Equilibrium Distribution of Pentoses in Mouse Diaphragm Muscles^a

Sugar	External concentration (mM)	N	$q \pm SE$
D-Xylose	0.2-80	38	0.358 ± 0.009
L-Xylose	20	8	0.39 ± 0.08
D-Arabinose	20	7	0.35 ± 0.02
L-Arabinose	0.2-45	19	0.36 ± 0.02

^aFrom Miller (1974), by permission of *Biochimica et Biophysica Acta*.

2. *Isotope test.* According to the AI hypothesis, size and complexity of molecules and ions (often hydrated) determine the q -value. In contrast to adsorption, steric configuration, unless it changes the molecular size and form, will not alter the q -value. For this reason, the use of a battery of pentoses, each with a different steric configuration, offers a convenient method to demonstrate the dissolved nature of the solute involved. Experimental data obtained with this method are illustrated in Fig. 11.17, in which the equilibrium distributions of four pentoses, D- and L-xylose and D- and L-arabinose, in four frog tissues are shown. In all cases the plots are rectilinear and the relative relationships among the four tissues are maintained. However, D-arabinose yields a somewhat lower q -value in all four tissues than does L-arabinose. We suggest that the conformation may not be the same and hence that the entropy and enthalpy of distribution are somewhat different. Similar pentose distributions were reported in mouse diaphragm (Table 11.3) (Miller, 1974).

11.2.1.5. Free Amino Acids

Figure 11.18 reproduces Troshin's early work on alanine distribution in frog muscle and Fig. 11.19, later work of Neville on glycine distribution in the same type of tissue. Both sets of data agree with equations (11.7) and (4.4) (Troshin equation), in which an adsorbed fraction is superimposed on a free fraction, with a q -value considerably less than unity. Using low-temperature microdissection and autoradiographic techniques in oocytes, Frank and Horowitz (1975) showed that the nonmetabolizable amino acid α -amino isobutyric acid (AIB) is maintained in the nuclear water at a higher level than in the cytoplasmic water. They suggested a difference in the q -value for AIB as the cause of the observed asymmetry, in agreement with a similar asymmetry of sucrose and inulin distribution across the nuclear envelope reported earlier (S. B. Horowitz, 1972; Horowitz and Moore, 1974).

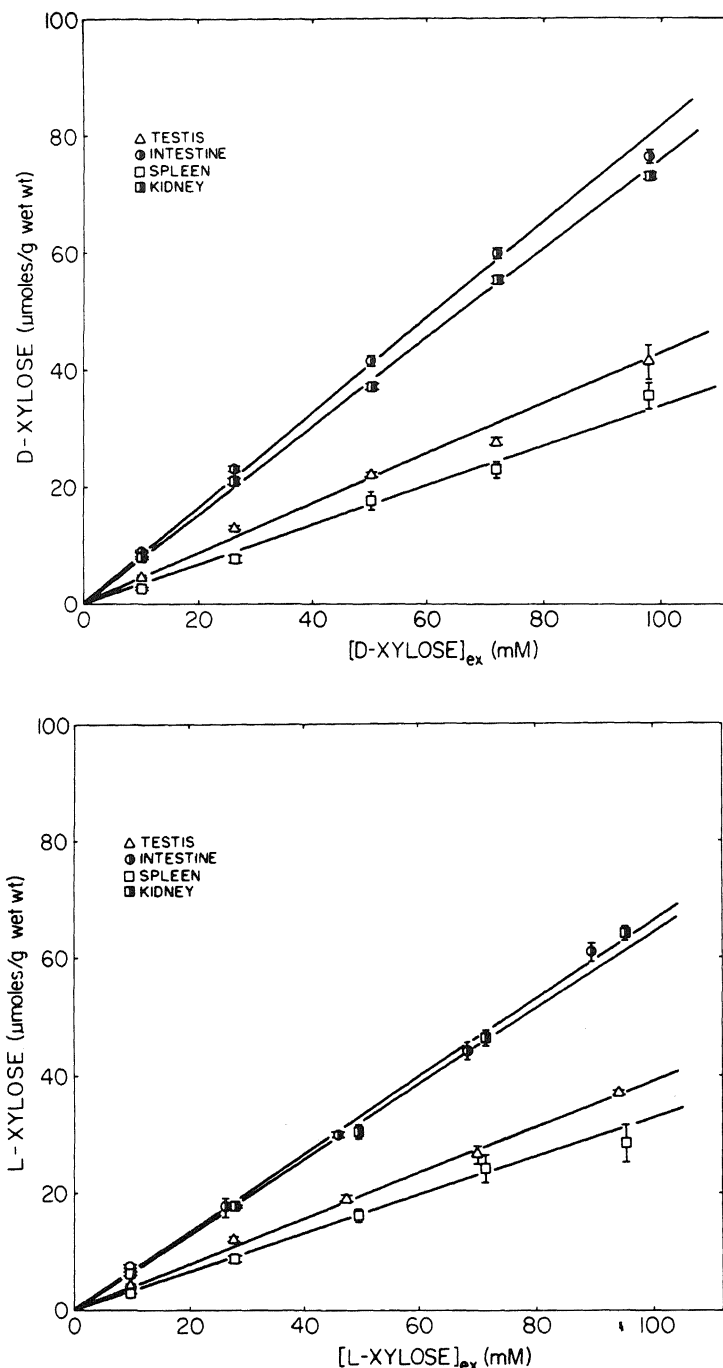


FIGURE 11.17. Equilibrium distribution of four pentoses between frog tissues and their external environments (5°C). [From Ling and Ochsenfeld (1983b), by permission of *Physiological Chemistry and Physics*.]

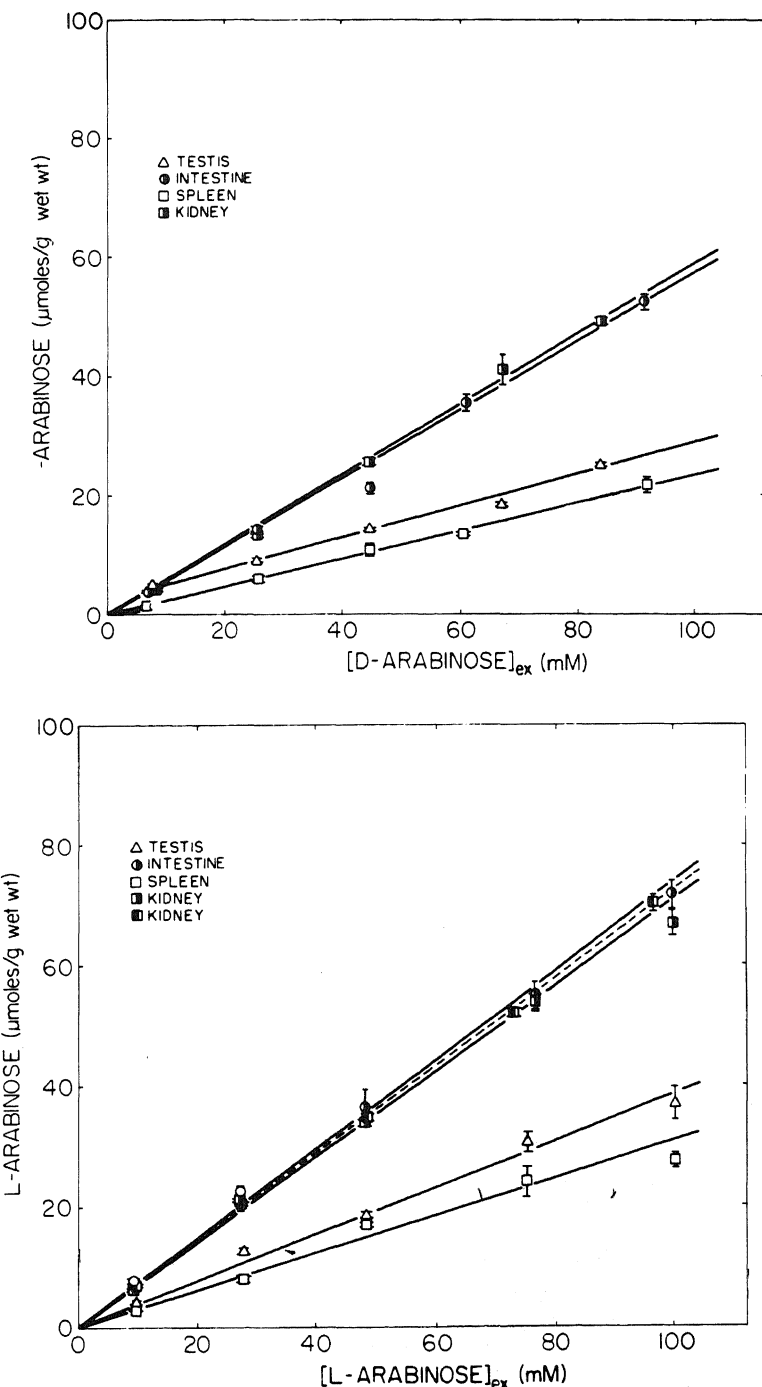


FIGURE 11.17 (Continued)

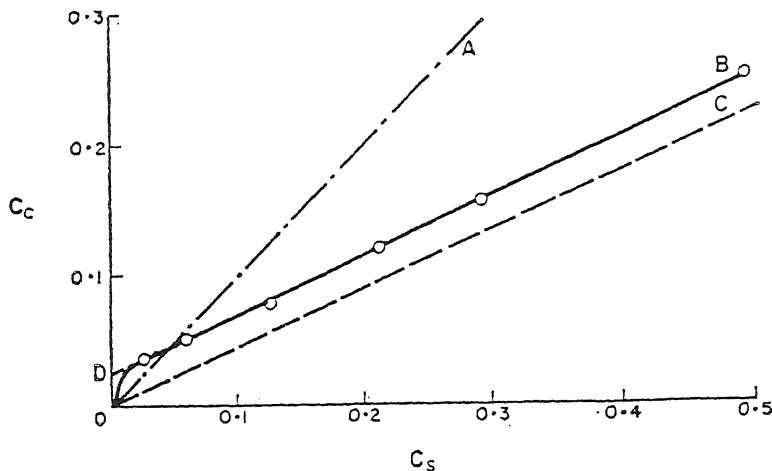


FIGURE 11.18. Dependence of the alanine concentration in muscle fibers (C_C) on alanine concentration in the equilibrated medium (C_S). [From Troshin (1966), by permission of Pergamon Press.]

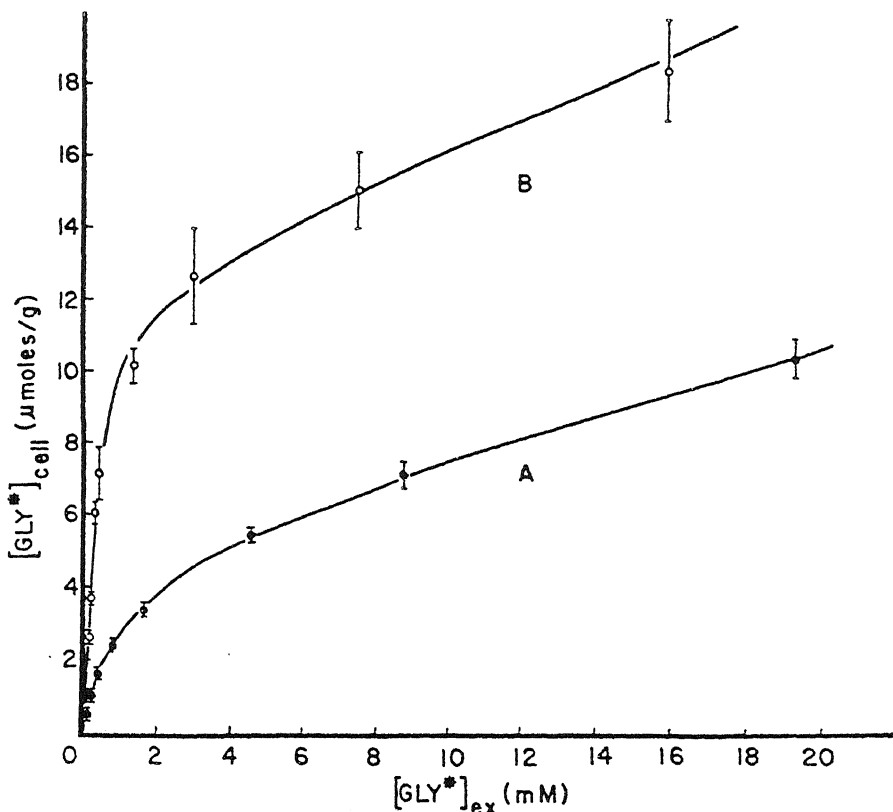


FIGURE 11.19. Steady level glycine accumulation in washed (A) and insulin-treated (B) frog muscle at 0°C. Muscles washed 6 hr in RP at 25°C in the absence and presence of 0.1 U/ml insulin prior to incubation at 0°C for 6 days with varying concentrations of glycine and [^{14}C]glycine. [From Neville (1973), by permission of *Annals of the New York Academy of Sciences*.]

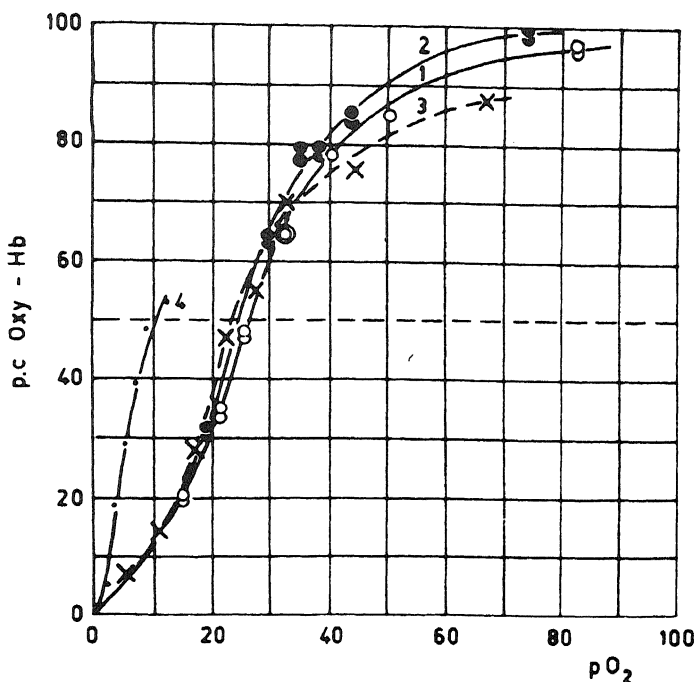


FIGURE 11.20. Oxygen dissociation curves of human hemoglobin in blood: (1) A concentrated erythrocyte suspension; Van Iersel and Wolvekamp. (2) A dilute suspension. (3) A dilute hemoglobin solution; Hill and Wolvekamp. [From Wolvekamp (1961), by permission of Academic Press.]

11.2.2. Cooperativity in Solute Adsorption

11.2.2.1. Oxygen Accumulation in Erythrocytes

The oxygen concentration in blood is about 5 mM, that in erythrocytes, 30 times higher (ca. 150 mM) (Best and Taylor, 1945, Chapter 30). This selective uptake of oxygen (over nitrogen, for example) has long been recognized to be due to oxygen binding onto the intracellular protein hemoglobin. Indeed the oxygen binding curve of hemoglobin solution (Curve 3) and that of an erythrocyte suspension (Curves 1 and 2) are very similar (Fig. 11.20).

As discussed in Section 7.4, the Hill coefficient, n , for oxygen dissociation is in the range of 3–3.5, which is equivalent to a nearest-neighbor interaction energy of 0.6–0.7 kcal/mole [see equation (7.25)]. The evidence that led me to believe that this interaction is not purely mechanical, as suggested by Perutz (1979), but is primarily due to an inductive effect, will be discussed in Section 15.4.2.

11.2.2.2. Competitive Uptake of K⁺ and Na⁺ in Living Cells

In 1908, Moore and Roaf seriously questioned the then already prevalent belief that K⁺ accumulation in cells is due to its entrapment by an impermeant cell membrane.

He pointed out the parallel between selective oxygen uptake and selective K^+ accumulation in living cells and suggested that K^+ accumulation may be due to binding of this ion onto intracellular proteins. The subsequent history of the development and reaffirmation of this basic idea has been amply discussed in Chapter 4. In 1966, I expressed the view that oxygen uptake in erythrocytes and K^+ accumulation in frog muscle are similar not only as adsorption phenomena, but also in their autocoopérativité, with similar values of the nearest-neighbor interaction energy (Fig. 11.21) (Ling, 1966a).

However, this similarity does not prove that the cell K^+ is adsorbed as oxygen is known to be. It is possible to construct a pump model that would incorporate a similar sigmoid accumulation pattern, i.e., by assuming that the Na^+ pumping is slowed down at low external K^+ concentration. Indeed the Na^+, K^+ -activated ATPase which is strongly believed to be the Na^+, K^+ pump also shows autocoopérativité K^+ and Na^+ concentration dependences in its enzyme activity (Bonting, 1970). However, the recent advances described in Chapter 8 leave no doubt that virtually all the K^+ in frog muscle cells is adsorbed in the A bands and Z lines, and that the selective uptake of K^+ , Rb^+ , Cs^+ , and Tl^+ is preserved in effective membrane (pump)-less open-ended cell preparations and in thin slices of muscle cells. Therefore, the autocoopérativité in K^+ uptake reflects properties of the intracellular adsorption of K^+ .

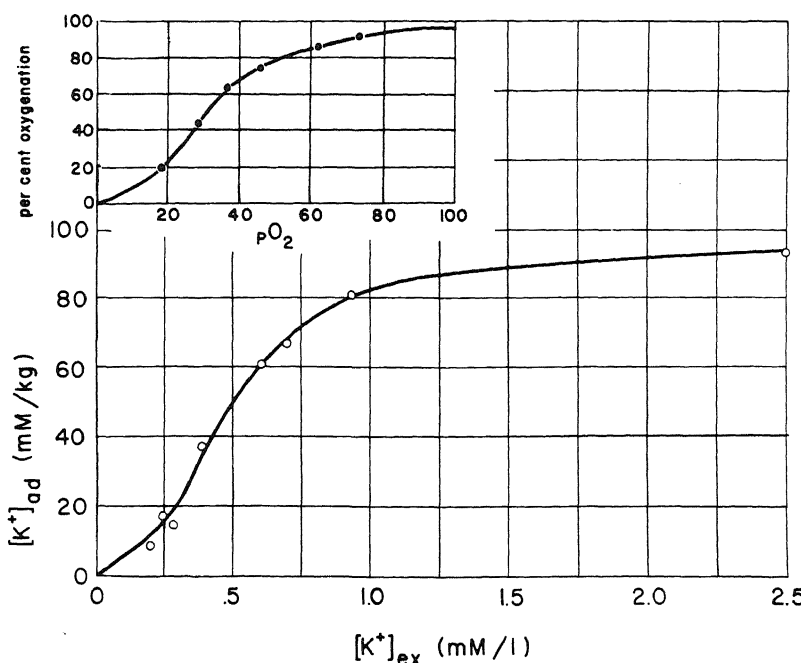


FIGURE 11.21. Equilibrium K^+ concentration in frog sartorius muscle in solutions with low K^+ concentrations but a high Na^+ concentration. Sterilely isolated sartorius muscles were shaken for 72 hr at 25°C in Ringer solutions containing a fixed concentration (100 mM) of Na^+ and varying low K^+ concentrations. Inset shows oxygen uptake by human erythrocytes. [From Ling (1966a), by permission of *Federation Proceedings*.]

TABLE 11.4. Quantitative Data on the Adsorption of K^+ in Several Living Tissues

	Temperature	[f]	$K_{Na \rightarrow K}^{00}$	$-\Delta F_{Na \rightarrow K}^{00}$ (kcal/mole)	$-\gamma/2$ (kcal/mole)	n	Reference
Frog sartorius muscle	25°C	109 ± 4.8 μ moles/kg fresh cells	135	2.84	0.54	2.33	Ling (1966a), Ling and Bohr (1970)
Dog carotid artery	37°C	119 mEq/kg d.s. ^a	93	2.8	0.61	2.7	A. W. Jones and Karreman (1969)
Rabbit myometrium							
Estrogen-dominated	37°C	366 mEq/kg d.s.	142	3.04	0.51	2.2	A. W. Jones (1970)
Progesterone-dominated	37°C	366 mEq/kg d.s.	170	3.18	0.47	2.0	A. W. Jones (1970)
Guinea pig taenia coli	37°C	490 mEq/kg d.s.	96.4	2.82	0.75	3.4	A. W. Jones (1973)
Human lymphocytes	37°C	129 μ moles/kg fresh cells	374	3.64	0.66	3.0	Negendank and Shaller (1979a)

^ad.s., Dry substance.

Since the first demonstration of autocooperativity in the accumulation of K^+ in frog skeletal muscle (Ling, 1966a), similar observations have been reported in three varieties of mammalian smooth muscles: canine carotid artery (A. W. Jones, 1973); rabbit myometrium (Jones, 1970); and guinea pig taenia coli (Karreman, 1973; Gulati, 1973)—as well as in human lymphocytes (Negendank and Shaller, 1979a) and in Ehrlich ascites cells (Reisin *et al.*, 1971). All these data could be quantitatively described by equation (11.6), as illustrated in the linear plots of Figs. 11.22A–D, in the log-log plots of Figs. 11.23A,B, and finally in the Scatchard plot of Figs. 11.24A,B. In all cases, these data satisfy the criteria of autocooperativity as described in Table 7.6. Quantitative parameters from these studies are assembled in Table 11.4.

Several important conclusions can be drawn from these studies.

11.2.2.2a. A Striking Uniformity. A striking feature of the K^+ and Na^+ distributions in living cells thus far studied is the uniformity in autocooperative behavior. Thus over the whole range of K^+ and Na^+ concentrations, for each cell type the distribution patterns can be described by equation (11.6), in which the adsorbed fraction is represented by a single isotherm rather than by a complex curve comprising different kinds of K^+ and Na^+ adsorption sites. The intrinsic free energies of $Na \rightarrow K$ exchange fall within the relatively narrow range of -2.8 to -3.6 kcal/mole, and the nearest-neighbor interaction energies are between 0.47 and 0.75 kcal/mole (Table 11.4).

11.2.2.2b. The Nature of Nearest-Neighbor Interaction Energy. Like the oxygen uptake of hemoglobin, the K^+ versus Na^+ uptake curve demonstrates a sigmoid shape

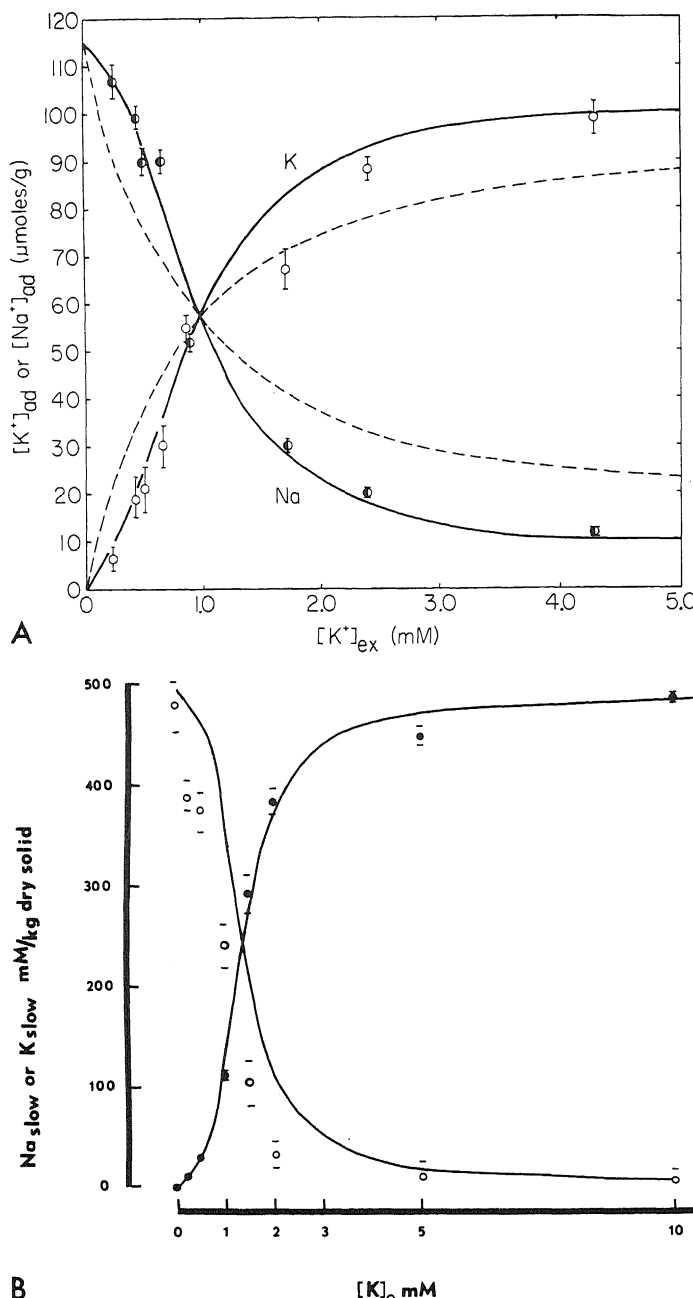


FIGURE 11.22. K^+ and Na^+ contents of various cells in equilibrium with external ions. (A) Frog muscle. [From Ling and Bohr (1970), by permission of *Biophysical Journal*.] (B) Guinea pig taenia coli. [After A. W. Jones (1973), by permission of *Annals of the New York Academy of Sciences*.] (C) Canine carotid artery. [From A. W. Jones and Karreman (1969), by permission of *Biophysical Journal*.] (D) Human lymphocytes. [From Negendank and Shaller (1979a), by permission of *Journal of Cell Physiology*.]

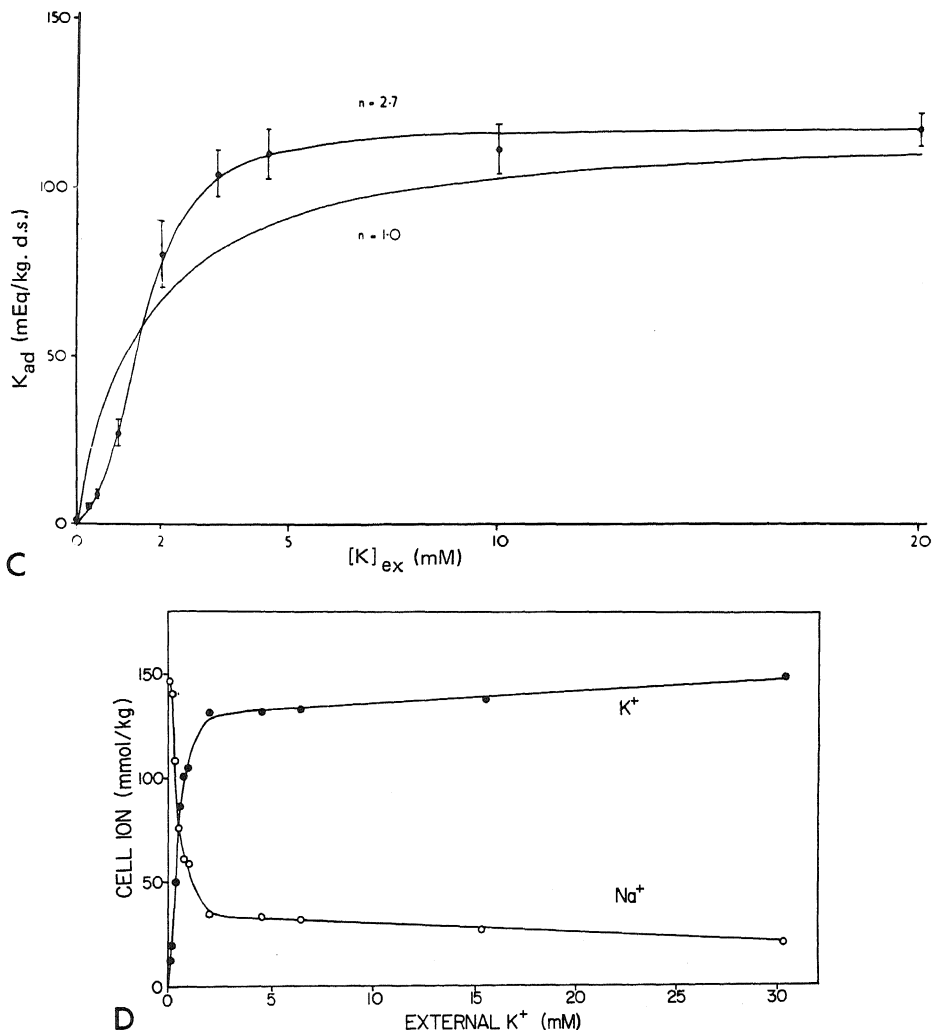


FIGURE 11.22 (Continued)

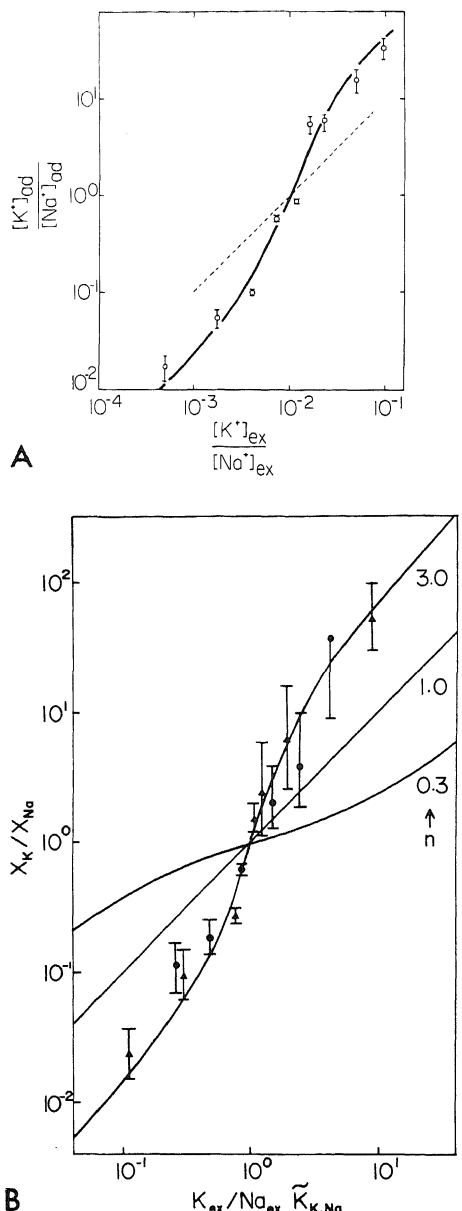
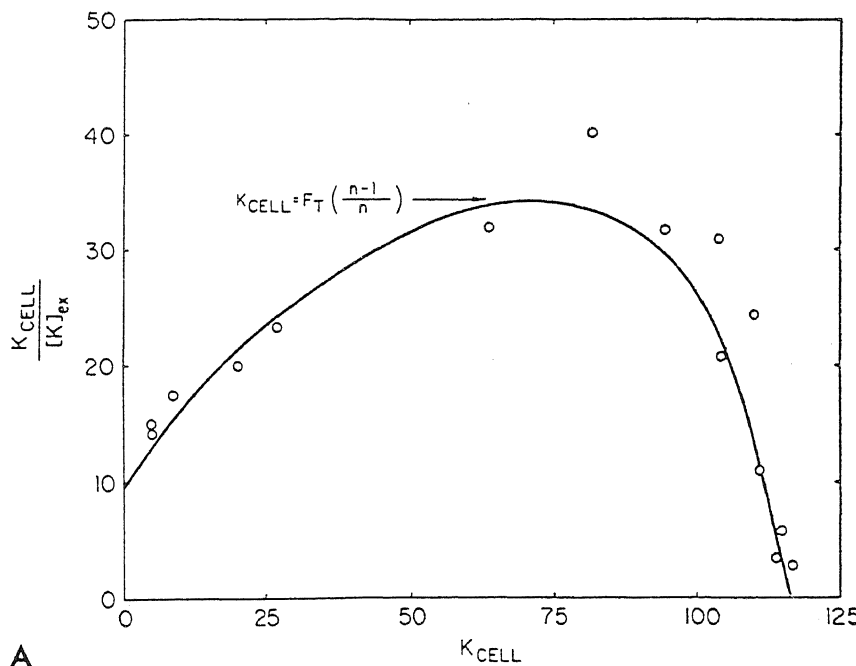


FIGURE 11.23. Log-log plots of the ratio of adsorbed K^+ and Na^+ against the ratio of external K^+ and Na^+ . The solid lines are theoretically calculated according to equation (11.2), with $n = 2.3$ in A and 0.3, 1.0, or 3.0 in B. (A) Frog muscle. [From Ling and Bohr (1970), by permission of *Biophysical Journal*.] (B) Human lymphocytes. [From Negendank and Shaller (1979a), by permission of *Journal of Cell Physiology*.]

and a Hill's coefficient, n , larger than unity. The purely empirical parameter n has been shown to have an exact physical meaning in the AI hypothesis and is equal to $\exp(-\gamma/2RT)$ [equation (7.25)]. In both cases I believe that the nearest-neighbor interaction energy ($-\gamma/2$) depends on the difference in the inductive effect exerted by the pair of ions competing for the sites [equation (11.10)]. The sizable $-\gamma/2$, illustrated in Table



A

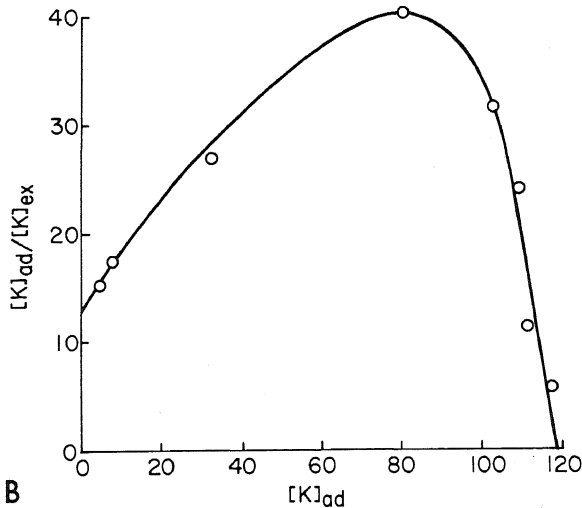


FIGURE 11.24. Scatchard plots of adsorbed K^+ . (A) Guinea pig taenia coli. [From Gulati (1973), by permission of *Annals of the New York Academy of Sciences*.] (B) Human lymphocyte. [Data from Negendank and Shaller (1979a).]

11.4, shows that adsorbed K^+ and Na^+ in all these cells must have significantly different inductive effects on the neighboring sites.

Roughly speaking; the inductive effect of K^+ or Na^+ depends on the adsorption energy of each of these ions. Thus, as a first approximation, $-\gamma/2$ should be related to the intrinsic free energy of exchange adsorption, $-\Delta F_{Na-K}^{00}$, which, of course, is in the

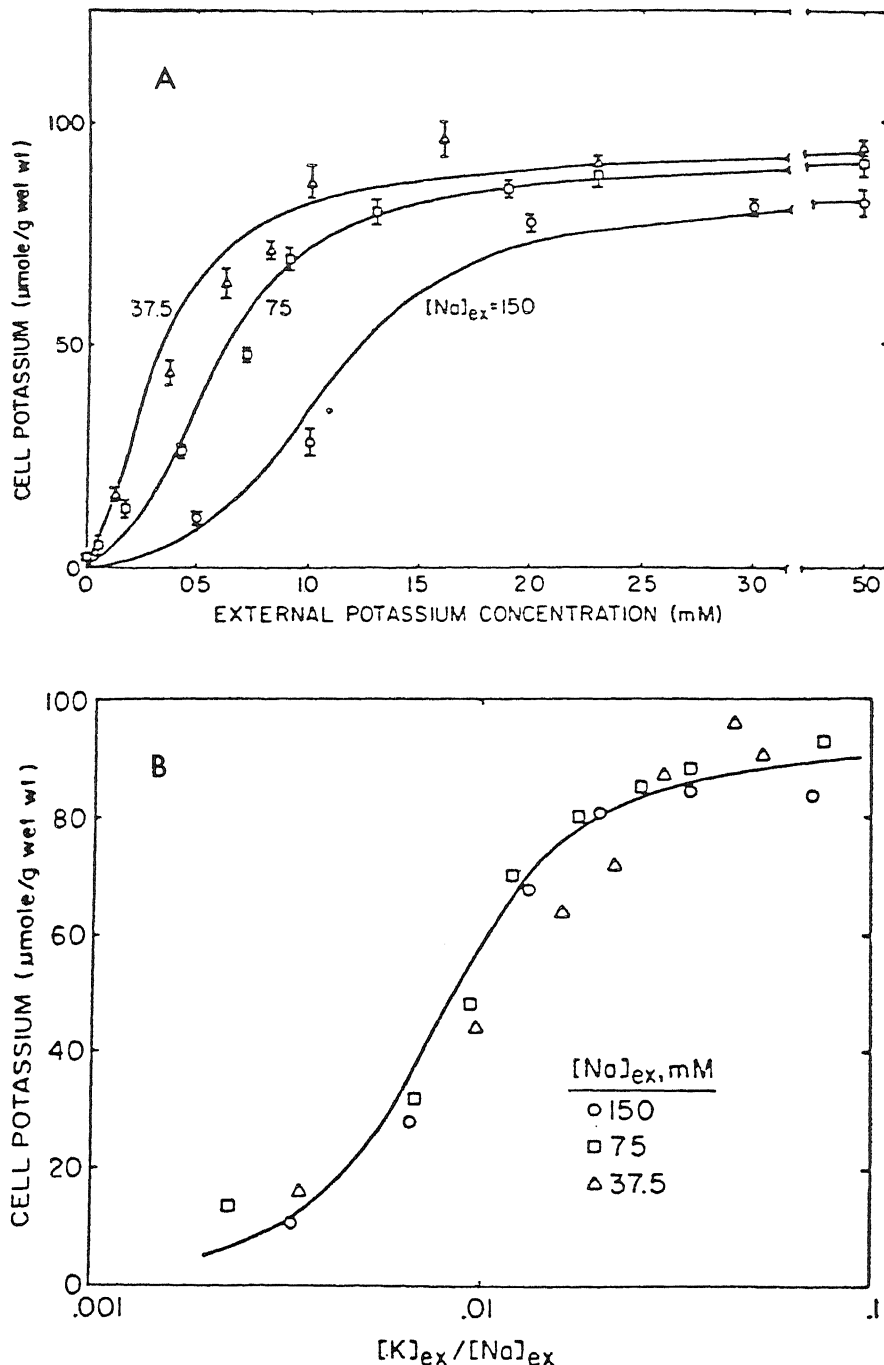


FIGURE 11.25. (A) Effect of replacing Na^+ with sucrose on the steady-state accumulation of K^+ in the guinea pig taenia coli. (B) Same data but plotted with a different abscissa. The solid line is a theoretical plot of equation (11.2) with parameter values averaged from the different curves in A: $n = 2.5$, $K_{\text{Na} \rightarrow \text{K}}^{90} = 125$, and $f = 91 \mu\text{moles/g wet weight}$. [From Gulati (1973), by permission of *Annals of the New York Academy of Sciences*.]

range of 2.8–3.6 kcal/mole. That is, K^+ is more strongly adsorbed than Na^+ . A site, in exchanging a Na^+ for a K^+ , will create an inductive effect similar to that which occurs in acetic acid when a H atom is replaced by the more electronegative Cl, lowering the electron density of the nearest-neighboring sites. The resulting alteration of the adsorption at the nearest-neighboring sites creates the observed value of $-\gamma/2$ of around 0.5 kcal/mole. The theory also suggests that, if the pair of competing ions is adsorbed with equal intensity, then $-\gamma/2$ may approach zero. In that case the ion adsorption and hence accumulation in the cell may be described by the simpler equation (11.7) [or (11.8)].

11.2.2.2c. The Significance of ξ . As shown in equation (11.3), ξ^y is equal to $([p_i]_{ex}/[p_j]_{ex}) K_{j-i}^{00}$. Thus, given the concentration of adsorption sites $[f]$, the same concentration of adsorbed i th solute can be achieved at different values of $[p_i]_{ex}/[p_j]_{ex}$, or different values of K_{j-i}^{00} , as long as ξ remains constant. Gulati tested this basic theory by studying K^+ accumulation in guinea pig taenia coli at varying external K^+ concentration, $[K^+]_{ex}$, in the presence of different constant concentrations of Na^+ ($[Na^+]_{ex} = 37.5$, 75, or 150 mM) (Gulati, 1973). His results showed three distinct sigmoidal isotherms (Fig. 11.25A). However, when the same data are plotted against $[K^+]_{ex}/[Na^+]_{ex}$, the three curves now merge into one, as expected (Fig. 11.25B). Clearly in this case K_{Na-K}^{00} had remained constant.

11.2.2.2d. The Simultaneous Accumulation of K^+ , Rb^+ , and Na^+ . Karreman (1973) extended the Yang-Ling cooperative adsorption isotherm to deal with the case of three ions competing for the same sites. This theory was able to describe accurately the simultaneous accumulation of K^+ , Rb^+ , and Na^+ in guinea pig taenia coli studied by Jones (Fig. 11.26). The theoretical curves were calculated on the assumption that $n_{K,Na} = n_{Rb,Na} = 3.8$; $n_{K,Rb} = 1.0$; $K_{K-Na}^{00} = 130$; and $K_{K-Rb}^{00} = 0.84$. In Fig. 11.26A the external Rb^+ concentration was low (0.25 mM), while in Fig. 11.26B it was raised to 5 mM. In (A) the sigmoidal K^+ and Na^+ curves were evident as the main event was exchange of Na^+ for K^+ . In (B), in the presence of high Rb^+ concentration, the main exchange was between K^+ and Rb^+ ; since $n_{K,Rb} = 1$ and K_{K-Rb}^{00} is very small, the curves were not sigmoidal but of the Langmuir type. Again the data agree with the theory, which relates $-\gamma/2$ to the differences in the free energy of adsorption of the adsorbed ions [equation (11.10)].

11.2.3. Effect of Temperature on Solute Distribution

11.2.3.1. Temperature Transition of K^+ and Na^+ Distributions

In the theoretical section I pointed out that the protein-ion-water system is a three-dimensional cooperative assembly and as such can undergo a sharp transition between two alternative states with a relatively minor temperature change. Such an expectation was experimentally verified in the K^+ versus Na^+ distribution in Ehrlich ascites cells by Reisen *et al.* (1971), in guinea pig taenia coli by Gulati and Reisin (1972), and in human lymphocytes by Negendank and Shaller (1980a); the critical temperatures were, respectively, 7°, 14°, and 3°C. The taenia coli and lymphocyte data are reproduced in

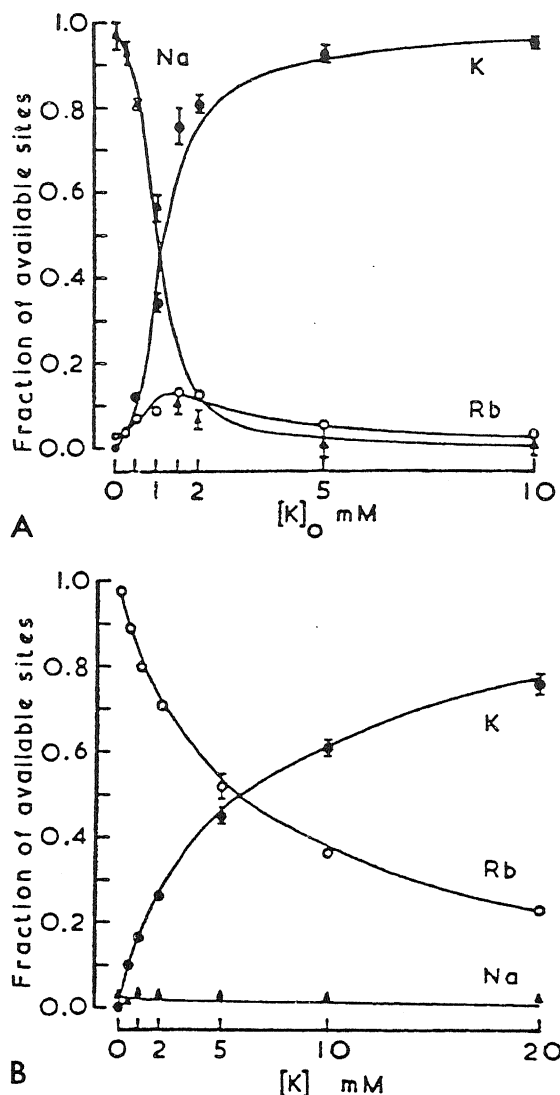
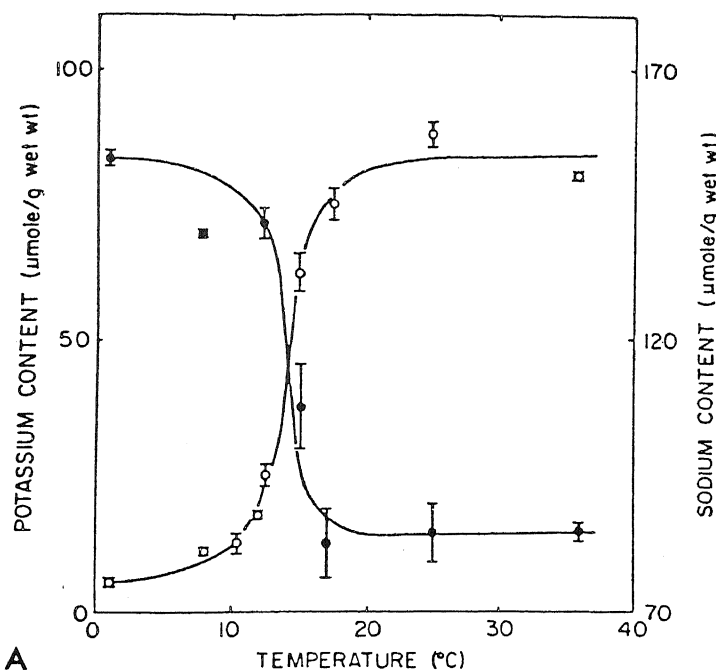


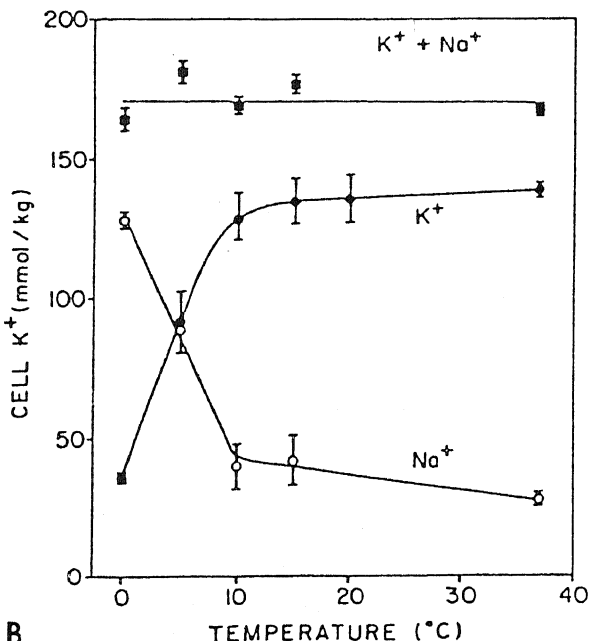
FIGURE 11.26. Fractions of total *taenia coli* smooth muscle cell contents (six guinea pigs were used) contributed by Na^+ (Δ), K^+ (\bullet), and Rb^+ (\circ) at the exterior concentrations $[\text{Na}^+]_{\text{ex}} = 136 \text{ mM}$ and $[\text{Rb}^+]_{\text{ex}} = 0.2 \text{ mM}$ (A) or 5.0 mM (B). The total tissue contents were corrected for extracellular K^+ , Rb^+ , and fast-exchanging Na^+ . The vertical bars indicate the SEM, except where these are smaller than the symbols' size. [From Karreman (1973), by permission of *Annals of the New York Academy of Sciences*.]

Fig. 11.27. Negendank and Shaller plotted their isotherms at 37° and 5°C in a log-log plot (Fig. 11.28). The data indicate that n remains the same, 3.0, which corresponds to $-\gamma/2$ of 0.65 kcal/mole. The sums of the intracellular K^+ and Na^+ are also constant, which shows that there was no change in the total concentration of anionic adsorption sites [f]. The only parameter that is markedly affected by the lowering of temperature is $K_{\text{Na}-\text{K}}^{00}$, which drops from a value of 374 at 37°C to 187 at 5°C . Reisin and Gulati further demonstrated that the isotherm data provide the means of calculating the enthalpy of $\text{Na} \rightarrow \text{K}$ exchange. Based on the value obtained and on unchanging $-\gamma/2$ and [f], they were able to predict the K^+ distribution curve at a lower temperature (Fig. 11.29).



A

FIGURE 11.27. (A) Effect of temperature on K^+ (○) and Na^+ (●) in steady-state contents of *Taenia coli*. The points are means of 6–16 determinations \pm SEM in three different experiments. The high Na^+ content above 17°C is due mainly to the large extracellular space in smooth muscles. The solid lines are arbitrarily drawn to connect the experimental points. [From Reisin and Gulati (1973), by permission of *Annals of the New York Academy of Sciences*.] (B) Cell K^+ and Na^+ contents in human lymphocytes at various temperatures. Cells were incubated 24–48 hr at 5–6 mM external K^+ . Mean \pm SEM, $N = 3–6$, except at 37°C, where $N = 31$. [From Negendank and Shaller (1980a), by permission of *Journal of Cell Physiology*.]



B

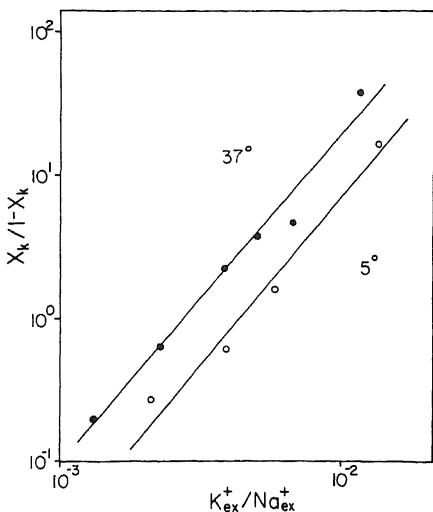


FIGURE 11.28. Log-log plot of equilibrium K^+ content in human lymphocytes. The slopes n are both near 3.0. The positions on the abscissa at half saturation reflect K_{Na-K}^{eq} values of 374 at $37^\circ C$ (●) and of 187 at $5^\circ C$ (○). [From Negendank and Shaller (1980a), by permission of *Journal of Cell Physiology*.]

It may be mentioned that Huang (1977) had provided a more extensive treatment of the cooperative adsorption process based on Landau's theory of phase transitions. Huang's treatment predicts that temperature shifts the position of the adsorption curve along the axis of adsorbent concentration but does not change its shape, as indeed the data of Negendank and Shaller demonstrated.

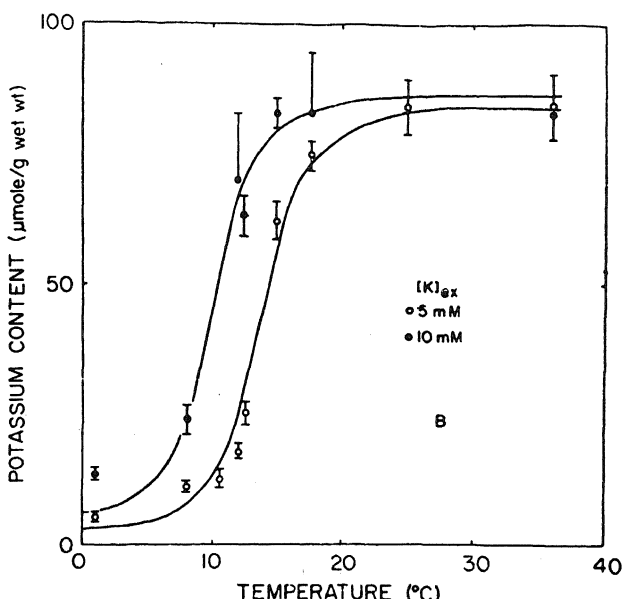


FIGURE 11.29. Effect of external K^+ concentration on the thermal transition in guinea pig taenia coli [From Reisin and Gulati (1973), by permission of *Annals of the New York Academy of Sciences*.]

11.2.3.2. Temperature Transition of Solvent Properties of Cell Water

I showed earlier (Section 6.3.4) how water polarized by polymers like polyvinylmethyl ether (PVME), polyethylene oxide (PEO), and polyvinylpyrrolidone (PVP) has a reduced solubility for large solute molecules or hydrated ions. Figure 11.30 shows that this solute exclusion property of PVME-polarized water remains unchanged from 0°C to much higher temperature. However, at 35°C the polymer-water system undergoes an abrupt change. As a result the bulk of the water becomes totally normal; indeed it separates from the polymer-water that now exists as a separate coacervate phase. Methylcellulose behaves in a similar manner, but the critical temperature is several degrees higher. The critical temperatures for PVP and PEO are at higher temperatures not too far away from the boiling point of normal liquid water.

A similar all-or-none change of the properties of water occurs in the equilibrium distribution of sucrose in frog sartorius muscles at temperatures between 0° and 60°C (Fig. 11.31). The ordinate represents sucrose concentration in $\mu\text{moles/g}$ tissue water. The equilibrium external sucrose concentration was 8.4 to 9.5 mM (Ling, 1967a). Note the abrupt increase of sucrose concentration in the muscle at temperatures above 37°C. Indeed at 40°C the sucrose concentration equals that of the external medium.

Before accepting the parallel behavior of PVME-polarized water and the muscle cell as due to a similar change in the solvency of the bulk phase water, let us first make certain that the uptake of sucrose is not a membrane permeability problem. Indeed there is a large collection of data indicating that normal muscle cells are quite permeable to sucrose just as they are permeable to Na^+ :

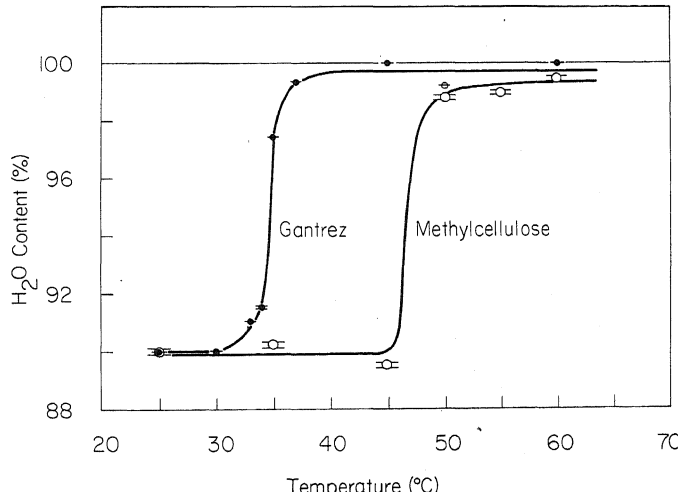


FIGURE 11.30. Temperature transition in the state of water in polyvinylmethyl ether (Gantrez) and in methylcellulose. Ordinate indicates the percentage of water in the major phase of the polymer-water system. Below the critical temperature there is only one single homogeneous phase with about 90% water. At the critical temperature, the bulk phase separates out from a small, dense coacervate phase. It is the water content of the water-polymer phase that is indicated at this and higher temperatures.

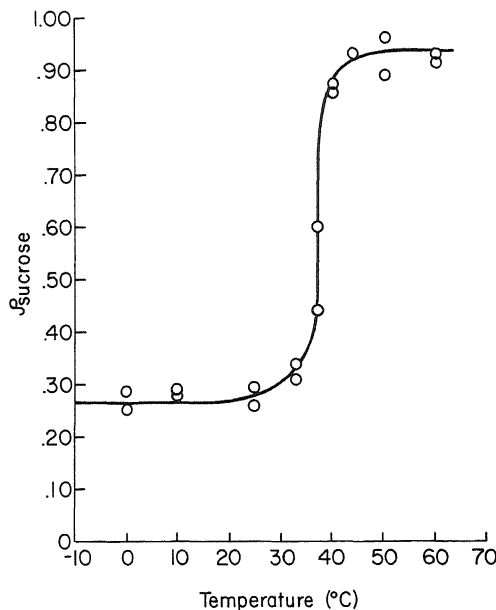


FIGURE 11.31. Sucrose distribution of frog sartorius muscle exposed to different temperatures. The equilibrium external sucrose concentration was 8.4 mM. [From Ling (1967a), by permission of Academic Press.]

1. The sucrose space is much larger than the inulin space of the same tissue (Ling and Kromash, 1967) (see also Fig. 4.1).
2. Sucrose space in normal muscle, shown in Fig. 11.31 at temperatures between 0° and 25°C, is much larger than the true extracellular space (Table 11.1).
3. Substantial amounts of sucrose enter isolated intact single frog muscle fibers that have been rinsed free of extracellular space (Ling *et al.*, 1969b).

In conclusion, the low concentration of sucrose in normal cells is due to the solute exclusion property of polarized water; this property is altered at high temperature in an all-or-none manner, much as PVME-polarized water becomes normal liquid water in a similar abrupt manner.

11.2.4. Control of Solute Distribution by Cardinal Adsorbents

11.2.4.1. Ouabain and Other Cardiac Glycosides

That cardiac glycosides can affect K^+ and Na^+ distribution in living cells, including muscle, has been known for a long time (Calhoun and Harrison, 1931; Wood and Moe, 1938). The establishment that K^+ in frog muscle cells exists in an adsorbed state demands that the effect of agents like ouabain that profoundly alter the level of K^+ and Na^+ must occur by manipulating one of the three variables in equation (11.4): $[f]$, ξ , or $-\gamma/2$.

Figure 11.32 shows the profound effect of ouabain on the equilibrium distribution of K^+ and Na^+ in frog muscle cells. The data clearly show that ouabain has little effect on $[f]$ or on $-\gamma/2$. Instead, its effect is primarily on ξ , or more specifically on $K_{Na \rightarrow K}^{00}$,

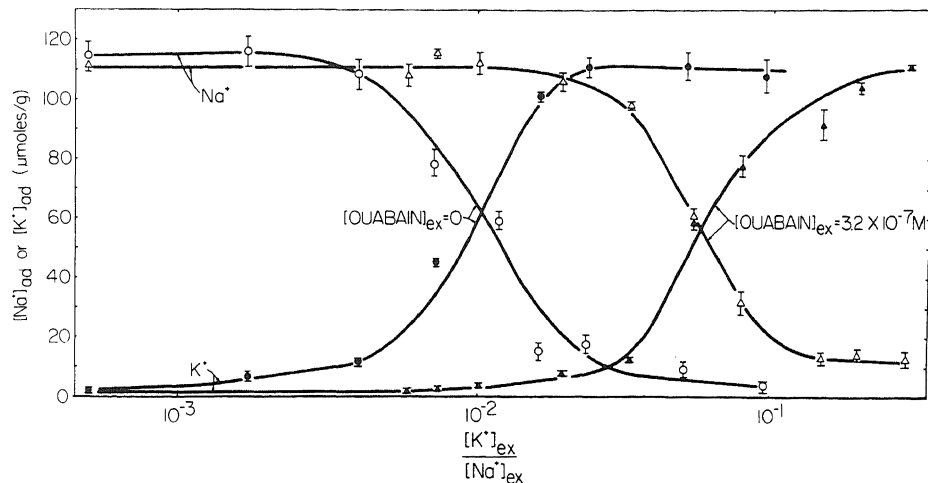


FIGURE 11.32. Effect of ouabain on the equilibrium distribution of K^+ and Na^+ ion in frog muscle. Curves with open (Na^+) and filled (K^+) circles were equilibrium distribution data from muscles not treated with ouabain. The point of intersection gives a K_{Na-K}^{eq} of 100. In muscles treated with ouabain (3.2×10^{-7} M), K_{Na-K}^{eq} has shifted to 21.7. [From Ling and Bohr (1971a), by permission of *Physiological Chemistry and Physics*.]

which is reduced from 200 to about 20. Figure 11.33 shows a similar ouabain-induced change of intracellular K^+ concentration in canine carotid arteries (Gulati and Jones 1971), and the same occurs in human lymphocytes (Negendank and Collier, 1976).

Figures 11.34 and 11.35 present a more extensive study of the effect of different concentrations of ouabain on the equilibrium levels of K^+ and Na^+ in muscle cells. The

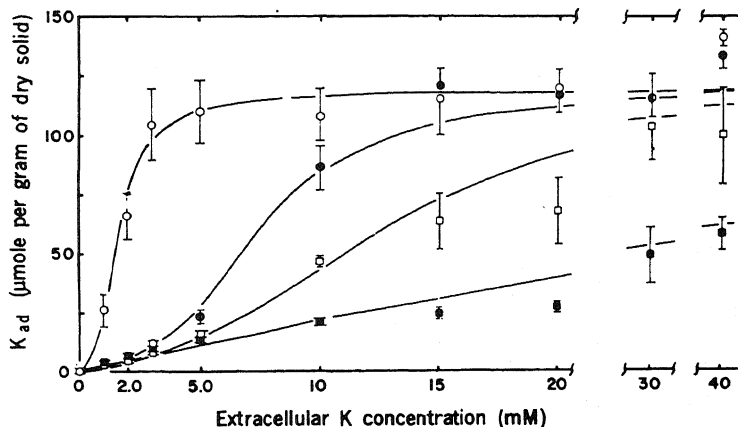


FIGURE 11.33. Accumulation of K^+ by canine carotid artery cells at varying $[K^+]_{ex}$ (and $[K^+]_{ex} + [Na^+]_{ex} = 150$ mM) and at different concentrations of ouabain. Each point is the mean of three to six determinations. The following doses were employed: control (\circ), 5×10^{-8} M (\bullet), 10^{-7} M (\square), 10^{-6} M (\blacksquare). [From Gulati and Jones (1971), by permission of *Science*.]

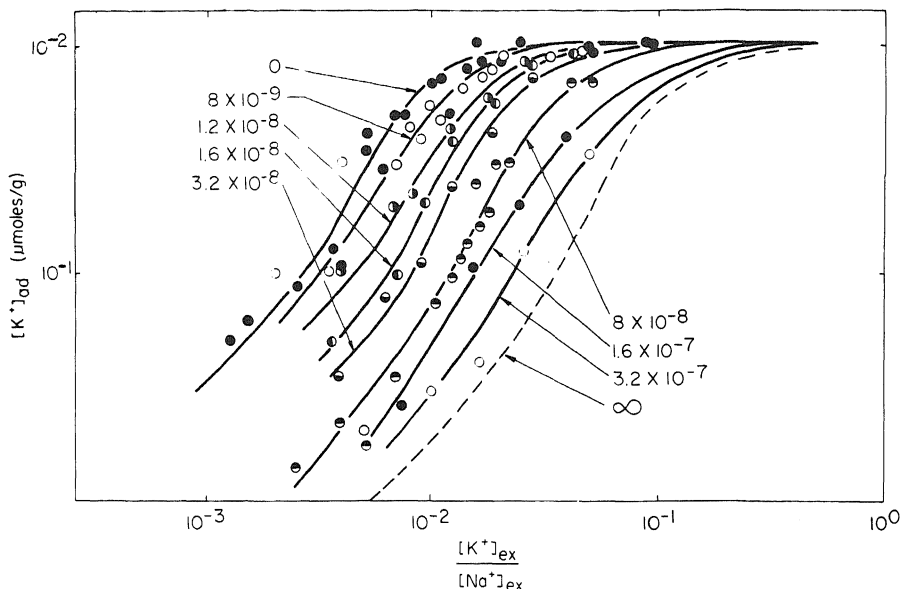


FIGURE 11.34. Effect of different concentrations of ouabain on the equilibrium distributions of K^+ in frog muscle. Each point is the average of four determinations. SEMs not shown to avoid confusion. Numbers in this and the following figure refer to equilibrium molar concentrations of ouabain in the external media. [From Ling and Bohr (1971a), by permission of *Physiological Chemistry and Physics*.]

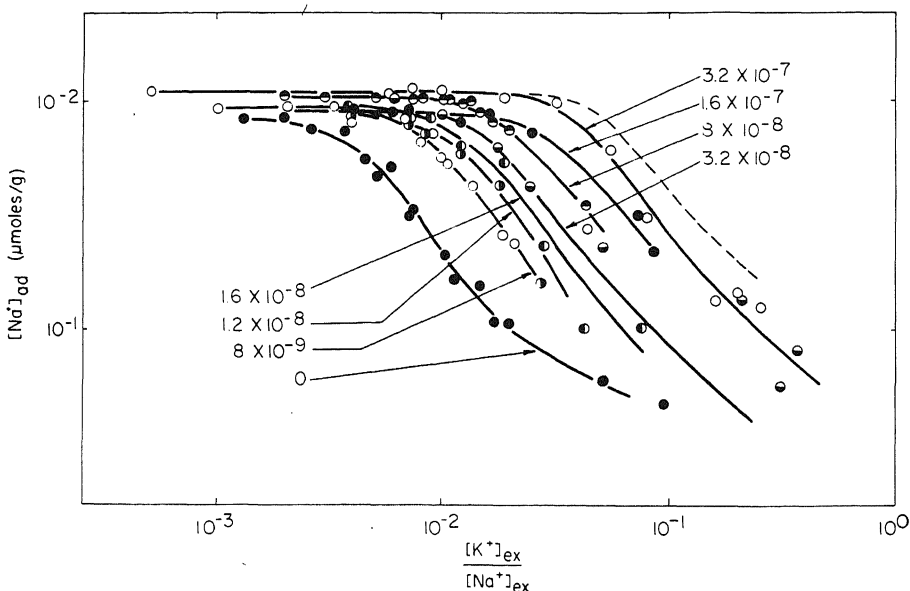


FIGURE 11.35. The effect of different concentrations of ouabain on the equilibrium distribution of Na^+ in frog muscles. Experiments are the same as in Fig. 11.34. [From Ling and Bohr (1971a), by permission of *Physiological Chemistry and Physics*.]

K^+ and Na^+ distribution curves bear a general resemblance to oxygen binding curves in the presence of 2,3-diphosphoglycerate or inositol hexaphosphate (for comparison, see Fig. 7.26). However, a more careful investigation shows that the curves are more accurately described if each gang of K^+ or Na^+ binding sites has two ouabain-binding cardinal sites (compare with theoretical curves in Figs. 11.4 and 11.5).

That the primary effect of a cardinal adsorbent, ouabain, is to change $K_{Na \rightarrow K}^{00}$ shows that like low temperature, ouabain switches the cells from a normal K^+ state to a Na^+ state by lowering $K_{Na \rightarrow K}^{00}$.

Table 11.5 shows that the Na^+ gained by frog muscles exposed to ouabain ($3.8 \times 10^{-7} M$) is largely NMR-invisible. As mentioned in Section 8.4 (Table 8.4), a similar effect occurs when Na^+ is gained by cells in a medium with low $[K^+]_{ex}$. At the time this work was published, we believed that the entire NMR-invisible fraction corresponded to adsorbed Na^+ and that the entire NMR-visible fraction corresponded to free Na^+ . We were then puzzled why in response to K^+ depletion and ouabain there was also a gain of visible Na^+ (Tables 8.4 and 11.5). In Section 8.4.4.4 I pointed out that our early interpretation of NMR-visible and -invisible Na^+ was not completely correct. The NMR signal of $^{23}Na^+$ does not become entirely invisible as a result of its adsorption. The quadrupolar effect of the anionic adsorption sites splits the signal of the adsorbed Na^+ into one central peak, making up 40% of the signal, and two satellite peaks, which together make up 60% of the signal. Therefore, the "invisible" fractions represent only 60% of the signal from adsorbed Na^+ .

With this new insight, the increase of both NMR-visible and NMR-invisible fractions becomes more understandable, although the NMR-visible fraction in all the data then collected appears somewhat lower than 40/60 or two thirds of the invisible fraction. Thus the gains of the NMR-invisible fraction in response to K^+ depletion and ouabain are, respectively, 38 and 41 $\mu\text{moles/g}$. Two thirds of these values are 25 and 27 $\mu\text{moles/g}$, respectively; the actually observed gains of the visible fractions were only 16 and 15 $\mu\text{moles/g}$. As suggested earlier (Section 8.4.4), however, this could be due to line broadening of the visible peak, leading to an underestimate of its amount.

Figure 11.36 shows a plot of the equilibrium K^+ , Na^+ , and ATP concentrations in muscles treated with varying concentrations of ouabain. Note that up to a concentra-

TABLE 11.5. NMR Analysis of Free and Adsorbed Na^+ in Normal, K^+ -Depleted, and Ouabain-Treated Frog Muscles^{a,b}

	Total K^+ ($\mu\text{moles/kg}$)	Total Na^+ ($\mu\text{moles/kg}$)	NMR-visible Na^+ ($\mu\text{moles/kg}$)	NMR-invisible Na^+ ($\mu\text{moles/kg}$)	Sum of NMR-invisible Na^+ and total K^+ ($\mu\text{moles/kg}$)
Control	78.4	25.0	10	14	93
Depleted	41.0	77.4	25.7	51.7	93
Ouabain	43.6	80.3	25.0	55.3	99

^aMeans of three experiments with four types of small frog voluntary muscles (sartorius, semitendinosus, tibialis anticus longus, and iliofibularis). Approximately 2 g of muscles were used for each sample. Total K^+ and Na^+ ion contents were analyzed using flame photometry. NMR-invisible Na^+ was obtained by difference between total Na^+ and NMR-visible Na^+ .

^bFrom Ling and Bohr (1971a), by permission of *Physiological Chemistry and Physics*.

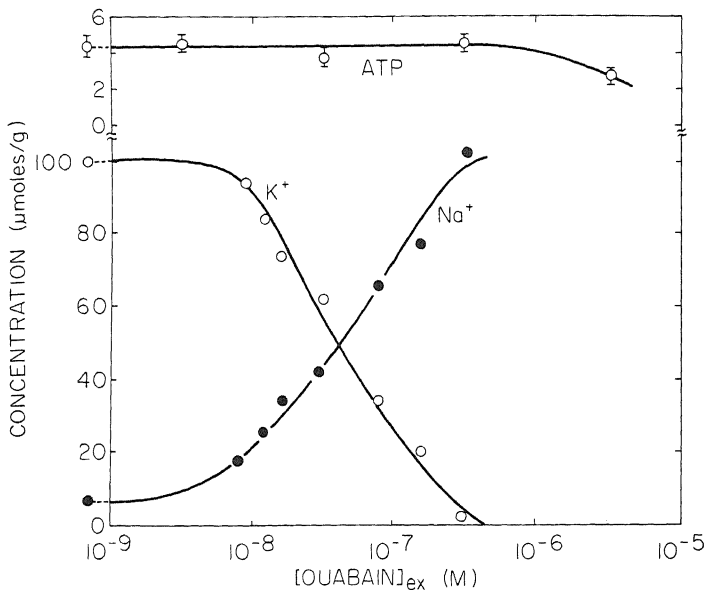


FIGURE 11.36. Effect of different concentrations of ouabain on the K^+ , Na^+ , and ATP contents of frog sartorius muscles. Muscles were exposed to different concentrations of ouabain in a Ringer-GIB medium (100 mM Na^+ , 2.5 mM K^+) for 3 days. [From Ling and Bohr (1971a), by permission of *Physiological Chemistry and Physics*.]

tion of 5×10^{-7} M ouabain has no detectable effect on ATP concentration. This finding is important because changes of ATP concentration have profound effects on K^+ and Na^+ levels in living cells—the subject of Section 11.2.4.3.

11.2.4.2. Ca^{2+}

Unlike cardiac glycosides, which are drugs, Ca^{2+} is a natural cardinal adsorbent of broad significance in the function of living cells. In the AI hypothesis, specific functions of Ca^{2+} often are expressions of the general properties of cardinal adsorbents.

It has long been known that K^+ loss by isolated tissues can be prevented by raising the concentration of external K^+ (Fenn and Cobb, 1934; Boyle and Conway, 1941) or Ca^{2+} (Aebi, 1952; Geyer *et al.*, 1955; Gardos, 1960; Kleinzeller *et al.*, 1968). Jones studied the distribution of K^+ in guinea pig taenia coli in the presence of varying external Ca^{2+} concentrations. His data are reproduced in Fig. 11.37, in which the points are experimental and the solid lines going through most of the points were theoretically calculated on the basis of equation (11.6) with the assumption that the K_{Na-K}^{00} varies as a hyperbolic function of external Ca^{2+} concentration. This assumption is supported by the rectilinear relationship between the reciprocals of the differences in K_{Na-K}^{00} at specified levels of $[Ca^{2+}]_{ex}$ (A. W. Jones, 1973).

Figure 11.38, taken from I. G. F. Gilbert (1972), shows the effect of Ca^{2+} on the K^+ level in liver slices. The effect of Ca^{2+} , which shifts the K^+ adsorption isotherm

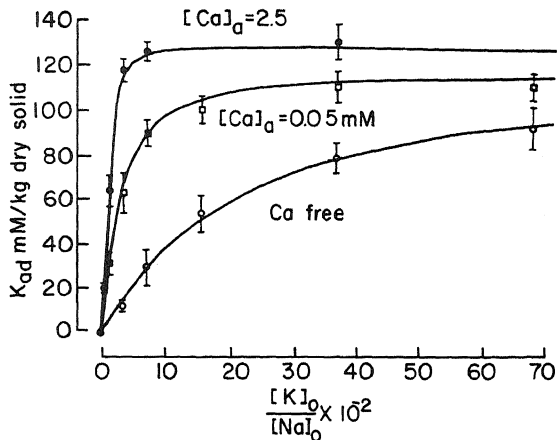


FIGURE 11.37. Slowly exchanging K^+ in the steady state, with various ratios of $[K^+]_{ex}/[Na^+]_{ex}$ at $37^\circ C$ in carotid artery. Three levels of $[Ca^{2+}]_{ex}$ were employed: 2.5 mM (●), 0.05 mM (□), and Ca^{2+} -free (○). The vertical bars indicate $\pm SEM$. Ten, nine, and eight dogs were used, respectively. [After A. W. Jones (1973).]

leftward, is opposite to that of ouabain. Within the range of concentrations investigated, Ca^{2+} increases K_{Na-K}^{00} while ouabain decreases it. In guinea pig brain cortex slices, the reduction of cell K^+ by low external Ca^{2+} was partly prevented by an increase of external Ca^{2+} to 5mM (Gardos, 1960). In *taenia coli* (A. W. Jones, 1973) and rat liver (Geyer *et al.*, 1955), Ba^{2+} and Ca^{2+} have quantitatively similar effects, while Sr^{2+} is much weaker, and in rat liver I. G. F. Gilbert (1972) showed that the relative effectiveness of alkaline earth ions in conserving cell K^+ follows the order $Ca^{2+} > Sr^{2+} > Co(NH_3)_5 Cl^{2+} > Mg^{2+} > 0$.

11.2.4.3. ATP

ATP, like Ca^{2+} , acts to conserve the K^+ -adsorbing resting living state. ATP too acts by adsorbing onto cardinal sites. Since each cardinal site controls a number of reg-

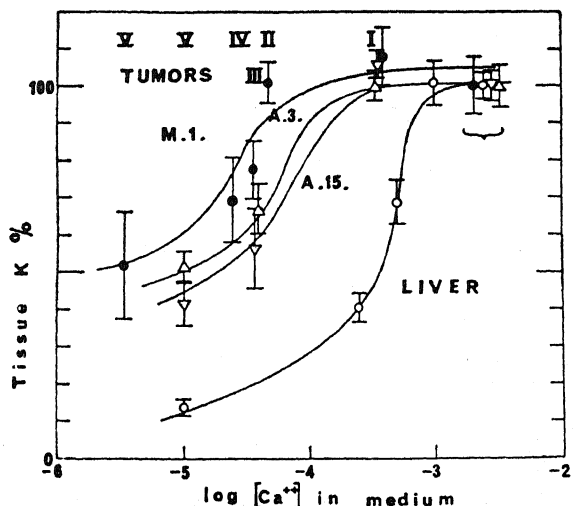


FIGURE 11.38. Steady-state K^+ concentration (percent of controls in normal extracellular Ca^{2+}) in three transplanted tumors and in normal liver, plotted against the free Ca^{2+} concentrations of the incubation media. [From I. G. F. Gilbert (1972), by permission of *European Journal of Cancer*.]

ular sites adsorbing K^+ (or Na^+), there should be a rectilinear relation between the concentration of adsorbed ATP and the concentration of adsorbed K^+ in the cell. It is well established that virtually all K^+ is adsorbed in muscle cells (Chapter 8). The extremely high binding constant of ATP on myosin (10^{10} – $10^{11} M^{-1}$; Goody *et al.*, 1977; Cardon and Boyer, 1978) also leaves no room for existence of a substantial concentration of free ATP in cells; virtually all ATP must also be adsorbed. With this in mind, the AI hypothesis predicts that under equilibrium conditions the total cell K^+ when plotted against the total ATP content should yield a straight line if all the ATP- K^+ -adsorbing proteins are of a similar nature.

Figure 11.39 shows a plot of K^+ in isolated frog sartorius muscles against ATP concentration after exposure to 0.1 mM iodoacetate at 0°C for varying lengths of time. The data can be described by a composite of two rectilinear curves. In the range of ATP concentrations from 1 to 5 μ moles/g, the slope is approximately 10. In other words, in this range, each ATP-binding cardinal site controls 10 regular K^+ binding sites. In the range of ATP concentrations from 0 to 1 mM, the slope is much higher, in the range of 50.

The Na^+ distribution is the mirror image of the K^+ distribution. This may be interpreted as representing a similar $Na^+ \rightarrow K^+$ exchange, as seen in the case of ouabain-treated muscles. However, the sucrose distribution curves suggest a different story. This almost exact parallel behavior of the Na^+ and sucrose distributions suggests that as ATP declines there is also a progressive depolarization of water and a progressive rise of the q -value for both Na^+ and sucrose.

Rangachari *et al.* (1972) studied the relation between ATP and K^+ in rat uterine myometrium that has been exposed to a variety of poisons and other treatments. From their results they concluded that "the linear correlation between ATP and K^+ contents

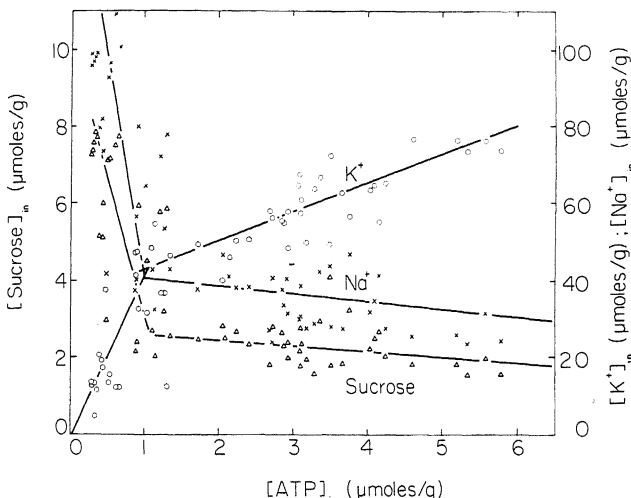


FIGURE 11.39. Equilibrium distribution of K^+ , Na^+ , and labeled sucrose in frog muscles with different concentrations of ATP, having been exposed to 0.1 mM iodoacetate for up to 9 days (0°C). [From Ling and Ochsenfeld (1983b), by permission of *Physiological Chemistry and Physics*.]

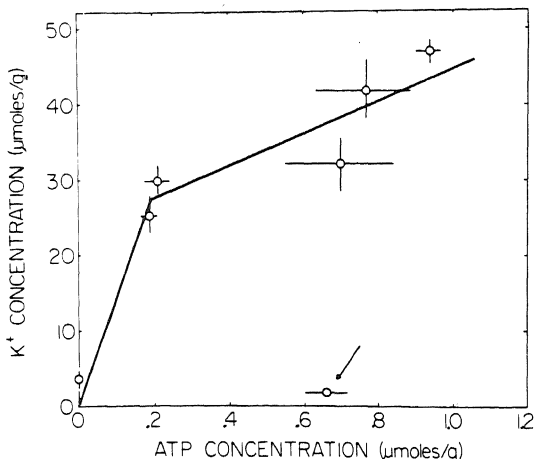


FIGURE 11.40. Plot of ATP versus K⁺ concentration in rat myometrium. Variations of ATP concentration were brought about by various metabolic poisons and by cooling (marked with arrow). Data from Rangachari *et al.* (1972). [From Ling (1974), by permission of *Physiological Chemistry and Physics*.]

predicted by the association-induction model did not always hold." However, a comparison of their data, reproduced in Fig. 11.40, shows that it agrees quite well with ours, illustrated in Fig. 11.39 (see also Ling, 1964b), with the exception of one point (marked by an arrow). This point resulted from an experiment in which the rat myometrium was cooled to 0°C, which sharply reduced the K⁺ content but not the level of ATP. However, data presented in Figs. 11.27–11.29 demonstrated that mammalian smooth muscles undergo a temperature transition at low temperature.

I now return to the Ca²⁺ distribution study of Rose and Loewenstein discussed in Section 11.2.1.3. Their figure is reproduced here as Fig. 11.41. As pointed out earlier, the luminescence rise following Ca²⁺ injection into the cell was confined to a small spherical region near the micropipet tip. The luminescence returned to the same steady low level afterwards. However, after exposure to 1 mM cyanide, the luminescence no longer returned to the same low level. Instead, with each pulse of Ca²⁺ injected, the luminescence steadily rose to higher levels, side by side with an expansion of the area of enhanced luminescence. My interpretation of these findings is that cyanide blocked the regeneration of ATP. With ATP concentration falling, cell water depolarized and the *q*-value for Ca²⁺ increased over the whole cell. No longer being confined by the low *q*-value of the polarized water, the Ca²⁺ injected spread rapidly and the free Ca²⁺ level rose and was sustained at high levels in the areas reached.

Rose and Loewenstein also found that when the cyanide-treated cells were washed in Ringer solution without the poison the original localized Ca²⁺ distribution pattern returned. This finding could be explained as being due to the reestablishment of the polarized, low-*q*-value state of the cell water once the cyanide block was removed and ATP regenerated. The regenerated ATP then interacted with the matrix protein, bringing about once more the normal polarized state of the cell water.

However, the postulated ATP control of Ca²⁺ distribution may not be limited to free Ca²⁺ distribution. Thus Rose and Loewenstein showed that, if cyanide concentration was raised to 5 mM from 1 mM, as used in the experiment described in Fig. 11.41, liberation of normally sequestered Ca²⁺ appeared as spontaneous centers of luminescence at loci away from the micropipets. Thus, taken as a whole, the level of cyanide

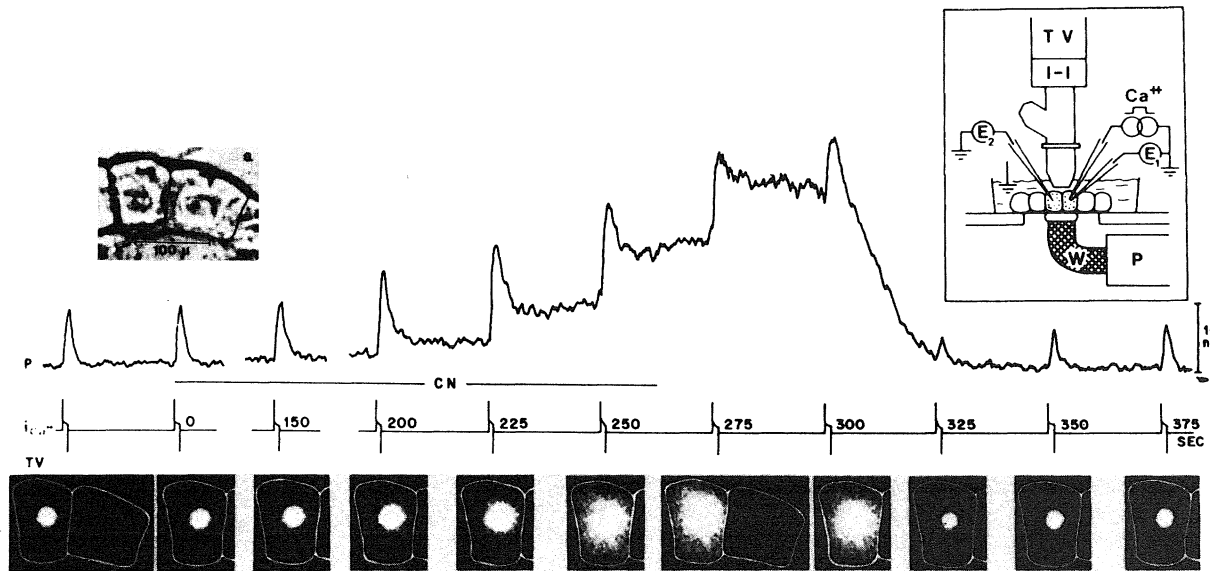


FIGURE 11.41. Energy-dependent Ca^{2+} diffusion restriction in the cytosol. (Inset) Experimental setup. Dotted cells contain aequorin, whose luminescence displays spatial distribution of cytoplasmic Ca^{2+} . The cells' luminescence is scanned by an image intensifier-TV system (I-I and TV) and integrated separately by photomultiplier P (W, waveguide). The Ca^{2+} is pulsed out of microelectrode Ca^{2+} ; microelectrodes E_1 and E_2 measure membrane potentials. (Main figure) Aequorin luminescences produced by standard Ca^{2+} test pulses (2.4 per min): TV, dark-field TV pictures giving the spatial distribution of luminescence at the time of maximum spread of each luminescence pulse; P, chart record of photomultiplier current giving time course of pulses; $i_{\text{Ca}^{2+}}$ injection current ($1.5 \times 10^{-8} \text{ A}$, 1 sec). The bar (CN) signals superfusion with 2 mM cyanide; the numbers are the times (sec) after start of superfusion (time for half-maximal concentration change ≈ 0.5 min). Cells are in Ca^{2+} -free medium. (a) Bright-field TV picture of cells. [From Rose and Lowenstein (1975), by permission of *Science*.]

needed to deplete the postulated cardinal adsorbent (ATP) that controls water polarization seems lower than that needed to deplete the postulated cardinal adsorbent (ATP) controlling Ca^{2+} adsorption or sequestration. This order is the reverse of what we observed for water depolarization and K^+ adsorption in frog tissues.

11.2.4.4. *Insulin*

ATP and Ca^{2+} are natural cardinal adsorbents, essential for the maintenance of the resting living state. Insulin, a hormone, is another natural cardinal adsorbent. In multicellular organisms, the production of hormones often occurs in different, highly specialized cells separate from the target cells in which the hormonal cardinal adsorbents work. Cardinal sites that adsorb and interact with drugs and hormones are obviously identical with what have long been called *receptor sites* by pharmacologists. Yet in terms of the AI hypothesis, cardinal sites reacting with ATP, Ca^{2+} , drugs, and hormones are basically alike. In this section we shall concentrate on the function of insulin in promoting the uptake of D-glucose from its aqueous environment. It hardly needs emphasis that, in the case of insulin deprivation, the classical signs of hyperglycemia and glycosuria follow as a consequence of the inability of the muscle and other cells to take up D-glucose (R. Levine and Goldstein, 1955; Park *et al.*, 1955; Narahara *et al.*, 1960).

At the outset, I want to point out that the experimental studies of levels of D-glucose accumulation in the cell are entirely analogous to those of K^+ and Na^+ and are not "membrane phenomena." Part of the glucose is dissolved in cell water (which under normal conditions remains relatively constant), and part is adsorbed onto protein sites (which are under the control of cardinal sites interacting specifically with insulin) (Ling *et al.*, 1969a,b; Ling and Will, 1969).

At 0°C frog muscle cells remain healthy and can readily accumulate D-glucose but do not metabolize it (Ling *et al.*, 1969a). All the D-glucose accumulated in the cells over a period of many hours can be quantitatively recovered as D-glucose.

If isolated frog muscles are washed in repeated changes of Ringer solution at room temperature and then exposed to D-glucose at 0°C , D-glucose will enter the cells and reach an equilibrium level in a few hours. The concentration of D-glucose accumulated plotted against the external concentration yields a simple straight line after the results have been corrected for the extracellular space contribution (Fig. 11.16). This pattern of distribution agrees with the concept that in frog muscles without any insulin the D-glucose is taken up only in the cell water. The slope of the curve yields a *q*-value for D-glucose in frog muscle of 0.25 ± 0.01 (Ling *et al.*, 1969a). Furthermore, the presence of competing nonlabeled D-glucose has no effect on the concentration of labeled glucose in the cell (Fig. 11.16). This is in accord with the theoretical interpretation that under these conditions all the D-glucose is in the cell water and none or very little is adsorbed. Similar rectilinear curves are seen for methanol and D-ribose distribution, with *q*-values of 0.91 and 0.26, respectively (Ling and Will, 1969; see also Fig. 9.5).

If isolated frog muscles are first incubated in a Ringer solution containing 10^{-3} – 10^{-1} U insulin/ml, the subsequent equilibrium D-glucose uptake in a 0°C bath follows a quite different pattern. The distribution curve then yields the sum of a hyperbola and a rectilinear fraction; the first is "saturable" and, as indicated in Fig. 11.42, follows the Troshin equation. Indeed, if from the concentration of labeled D-glucose in the cell is

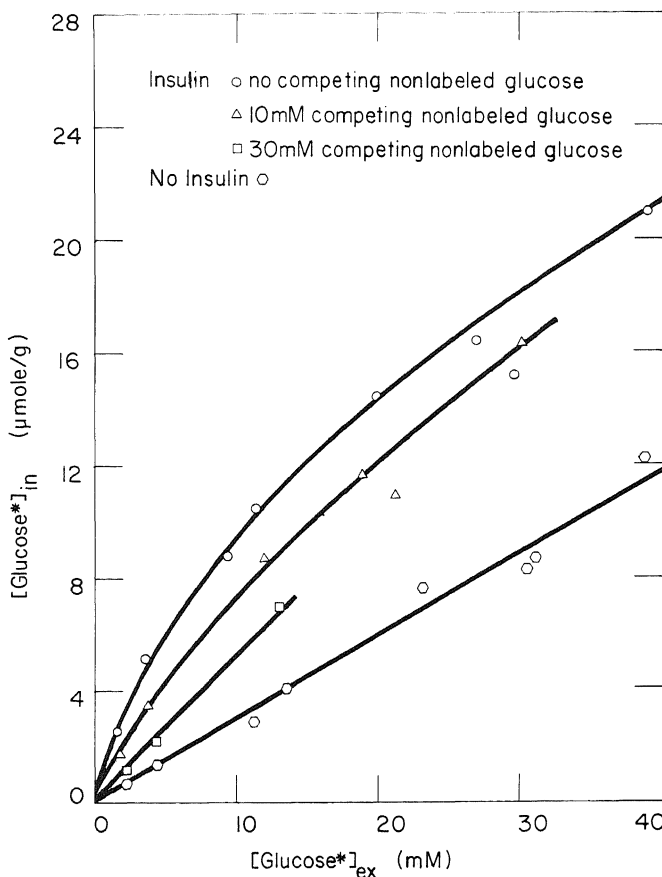


FIGURE 11.42. Steady level of glucose uptake at 0°C in insulin-treated (upper curves) and washed (lower curves) muscles. Mixed frog muscles were preincubated in Ringer solution containing no glucose and no insulin (lower curve) or 24 mM glucose and 0.1 U insulin/ml for 6 hr at 25°C. They were then incubated overnight at 0°C in Ringer solution containing varying concentrations of glucose and labeled glucose. [From Ling and Will (1969), by permission of *Physiological Chemistry and Physics*.]

subtracted the linear, nonsaturable fraction given in Fig. 11.16, and the data are plotted in a double reciprocal plot, one obtains a family of straight lines (Fig. 11.43) in agreement with equation (11.9). The slope of this curve, but not the intercept on the ordinate, is changed by the presence of competing nonlabeled glucose. The concentration of D-glucose adsorption sites in muscle treated with 0.1 U insulin/ml was 10.3 ± 0.23 mmoles/kg fresh cells and the adsorption constant was $(8.26 \pm 0.48) \times 10^{-3}$ M. In contrast, ribose distribution is unaffected by insulin (Fig. 11.44).

It was found that to produce the pronounced subsequent uptake of labeled D-glucose, the preincubation medium must contain not just insulin but also D-glucose or sugars closely related to D-glucose (e.g., 3-O-methyl glucose). Figure 11.45 shows the subsequent level of labeled D-glucose uptake at 0°C when plotted against the concentration of D-glucose in the preincubation medium at 25°C. The curve is sigmoidal, suggesting autocoopérativity (Ling *et al.*, 1969c).

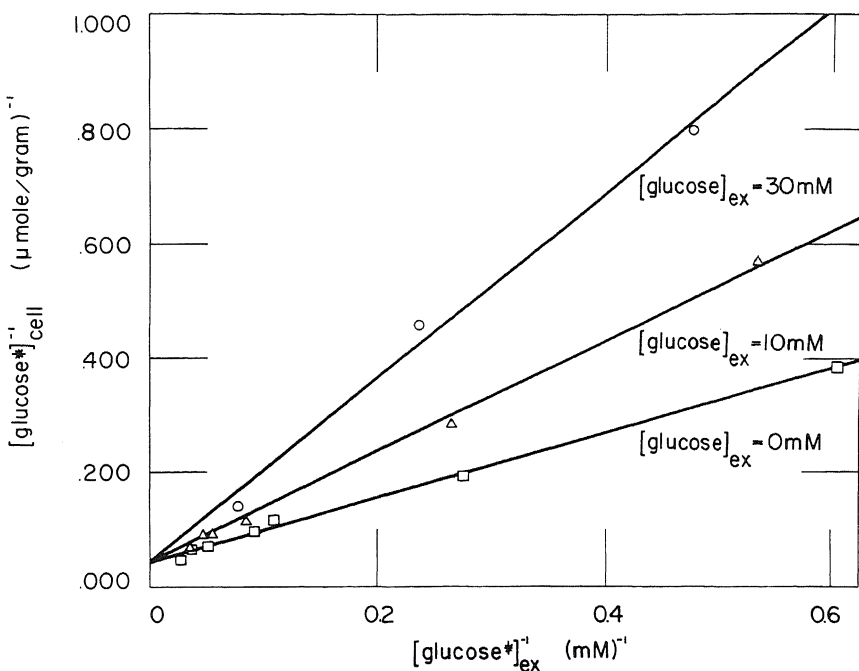


FIGURE 11.43. Reciprocal plot of data in Fig. 11.42. The amount of glucose taken up by washed muscles (lowermost curve, Fig. 11.42) was subtracted from the glucose taken up by insulin-treated muscles (upper curves, Fig. 11.42). The reciprocal of the difference is plotted against the reciprocal of the external glucose concentration. The data conform to equation (11.9). [From Ling and Will (1969), by permission of *Physiological Chemistry and Physics*.]

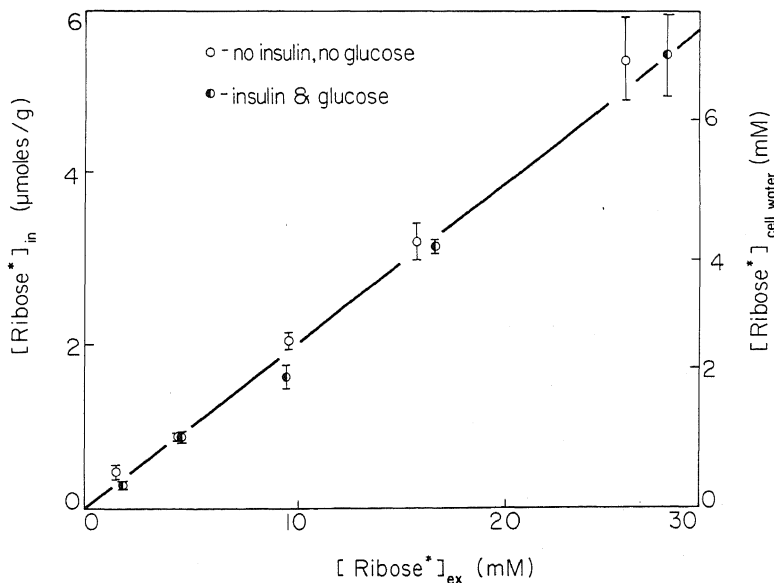


FIGURE 11.44. Steady level of D-ribose uptake in washed muscles and muscles preincubated with glucose and insulin. Six hours of preincubation at 25°C with no insulin and no glucose or 24 mM glucose and 0.1 U insulin/ml were followed by overnight incubation at 0°C with varying concentrations of D-ribose and labeled D-ribose. [From Ling and Will (1969), by permission of *Physiological Chemistry and Physics*.]

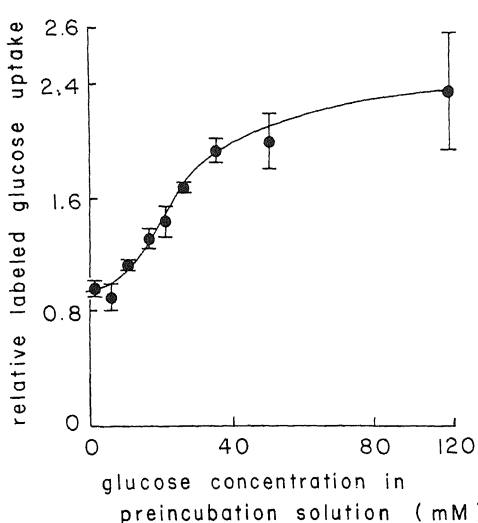


FIGURE 11.45. Effect of glucose concentration in the preincubation medium at 25°C on the steady level of labeled glucose subsequently accumulated in muscle cells at 0°C. Each set of muscles was preincubated for 6 hr 45 min at 25°C in Ringer solution containing glucose (0–100 mM). Incubation at 0°C lasted 18 hr. The ordinate of the graph represents a ratio of the value of glucose uptake in these muscles to that in muscles preincubated in the absence of glucose. Since the "carryover" from the preincubation solution changes the final glucose concentration in each vial to a different degree, the uptake for each set is normalized to correspond to the same final external glucose concentration. The abscissa represents the concentration of glucose in the preincubation solution. Each point is the average of four determinations \pm SE. [From Ling *et al.* (1969c), by permission of *Physiological Chemistry and Physics*.]

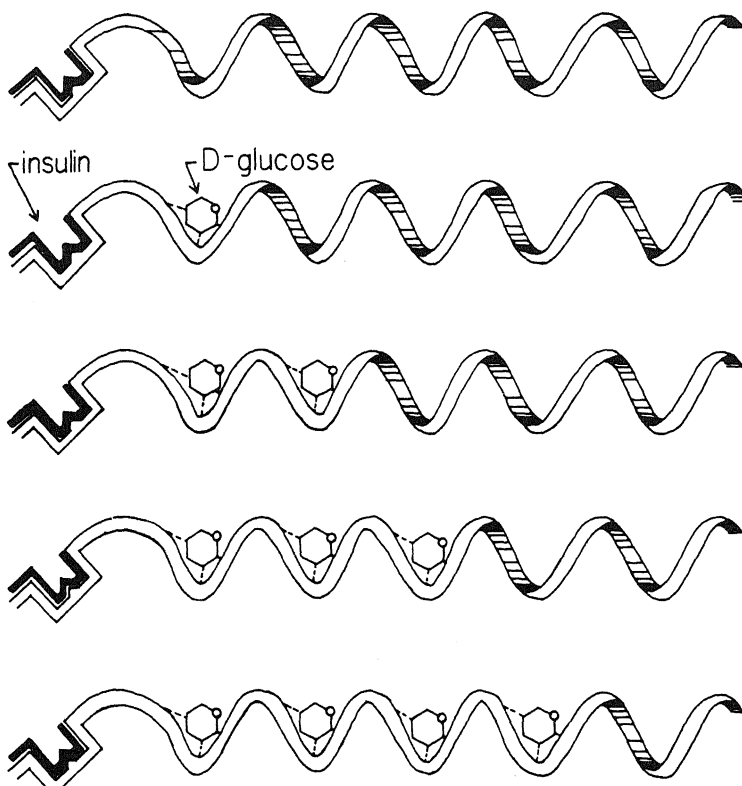


FIGURE 11.46. Diagrammatic illustration of the theoretical role of D-glucose in the preincubation medium containing insulin in "exposing" the D-glucose absorption sites.

For these observations the AI hypothesis offers the following interpretation (Fig. 11.46). Through the indirect F-effect insulin brings about a change in the conformation of certain intracellular proteins. As a result these proteins will adsorb D-glucose in a cooperative manner. This cooperative reaction occurs very slowly at 0°C but more readily at 25°C. The stepwise nature of the indirect F-effect can only progress if each opened site is occupied by the preferred adsorbent D-glucose. Thus the insulin-initiated cooperative adsorption can only reach completion at 25°C and in the presence of either D-glucose or another compound with similar attributes. Such compounds (2-deoxyglucose, 3-O-methyl glucose, D-arabinose, D-xylose) are called *primers*. The subsequent incubation at 0°C in the presence of labeled D-glucose involves primarily an exchange with already-adsorbed D-glucose or an analogue. An extensive study of the steric requirements of an effective primer suggests that virtually all the H-bonding groups of D-glucose are involved, but to different degrees (Fig. 11.47) (Ling and Will, 1976). However, the most important are a free OH and a free H on C-1, and "upward" orientation of OH and "downward" orientation of H on C-3. Primers are not *inducers* (see Section 5.1.4), since no *de novo* synthesis of new proteins is involved (Ling *et al.*, 1969c).

Insulin controls not only the accumulation of D-glucose in frog muscle but also the accumulation of the free amino acid glycine. As in the case of D-glucose accumulation, glycine must be present in the preincubation medium to induce a full labeled-glycine uptake in a subsequent incubation at 0°C (Neville, 1973). The relation between D-glucose and glycine accumulation, to the best of my knowledge, has not yet been investigated.

11.2.4.5. Permeases

The wild-type *Escherichia coli* does not metabolize lactose. However, on exposure to lactose it soon acquires this ability. The process by which exposure to lactose produces in these microbes the ability to assimilate the same sugar is called *induction* (which is not to be confused with the inductive effect of the AI hypothesis) (Fig. 5.1).

In 1957 Cohen and Monod discussed the reasons that led them to believe that the lactose (and other β -galactosides) which accumulates in *E. coli* is all in a free state, and that the protein whose synthesis the glycoside induces is a permease, i.e., a protein that can specifically shuttle lactose into the cell and maintain it at a higher level therein (Section 5.1.4). The permease does not merely facilitate the attainment of an equal distribution of lactose between the cell water and its environment; it actually promotes its selective accumulation to levels 100 times higher than in the external medium. Thus the permease must be a lactose pump. In view of the excessive energy requirements of other pumps (Section 5.2), this model is no longer tenable.

If the protein specified by the *Y* gene is not a sugar pump, how can one interpret its facilitation of lactose accumulation? To answer, let us return to the preceding section, in which I discussed how the accumulation of another sugar, D-glucose, in frog muscle cells requires exposure of the cells to D-glucose or an analogue at a high enough level, and a low-molecular-weight protein, insulin. By analogy, I suggest that the protein specified by the *Y* gene is in fact a protein molecule having a function similar to that of insulin (Ling, 1966a; Ling *et al.*, 1969a,c). This protein is synthesized within the *same* cell in which it works, but also in response to demand. (Only later in evolution did this

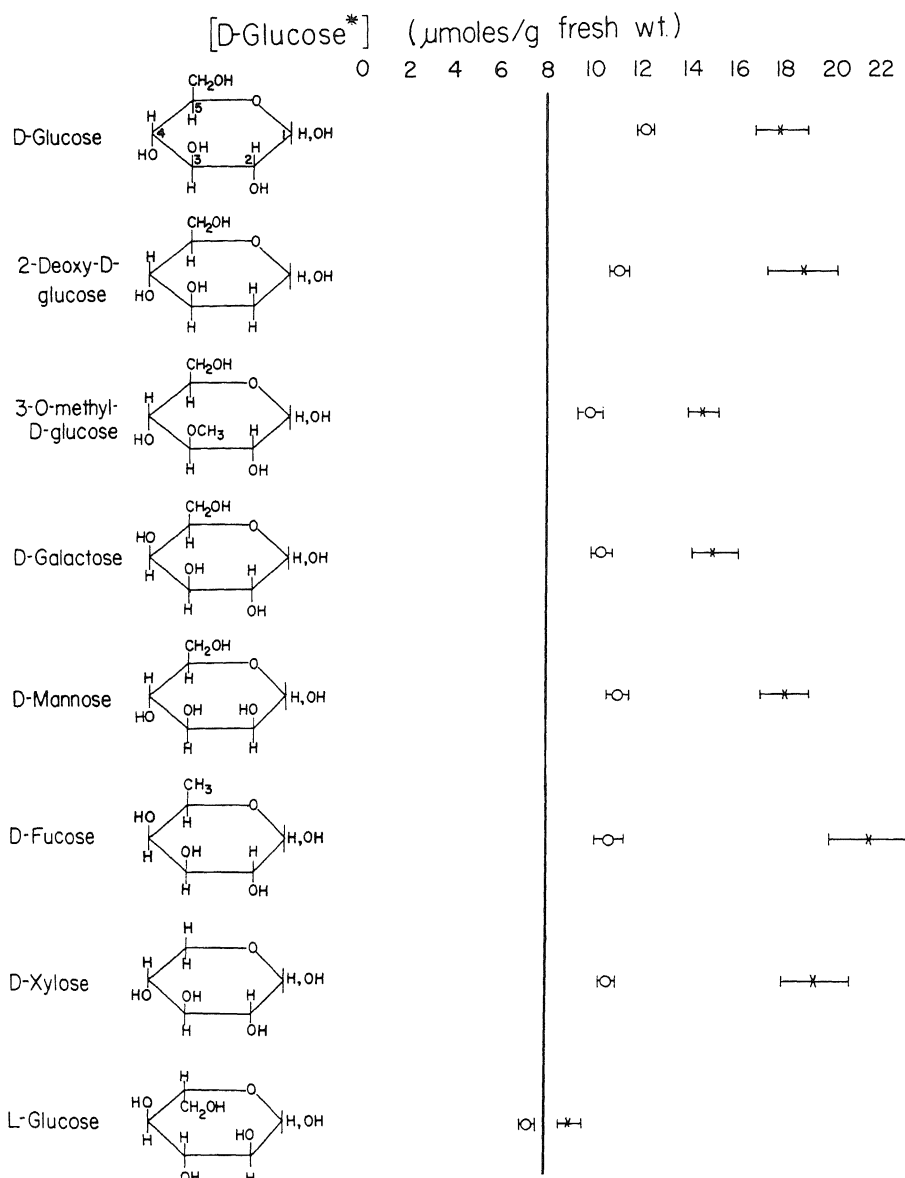
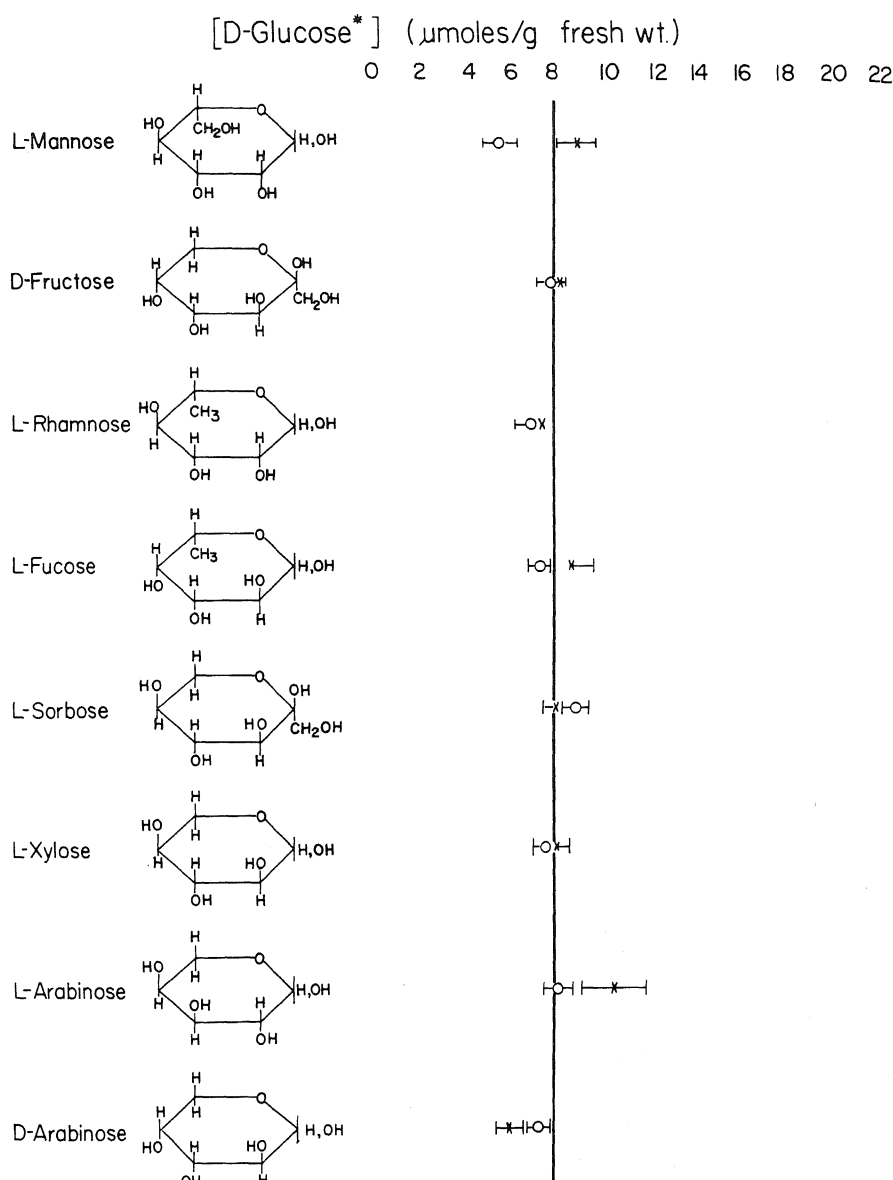


FIGURE 11.47. Effects of sugars and related compounds in the preincubation media upon the subsequent steady levels of labeled D-glucose accumulated in frog muscles at 0°C. The preincubation media (kept at 25°C) contained 0.1 U insulin/ml and either 24 mM (○) or 100 mM (X) of the primer indicated on the left. The incubation medium, kept at 0°C, contained 24 mM labeled D-glucose but no insulin. The vertical



line represents the level of labeled D-glucose accumulated in the tissue following preincubation in a medium containing only 0.1 U insulin/ml but no D-glucose or other primers. [From Ling and Will (1976), by permission of *Physiological and Chemical Physics*.]

portion of the gene function become relegated to the special beta cells of the pancreatic islets of Langerhans.) The following are two sets of evidence in favor of this hypothesis:

1. In 1966, Kolber and Stein reported their successful isolation of the protein specified by the *Y* gene. They labeled proteins synthesized in induced permease-positive *E. coli* (*F Lac⁺*, 200 PS) with ^{14}C and proteins synthesized in non-induced culture with ^3H . DEAE-cellulose chromatographs of the extracts were then superimposed; the extra proteins synthesized in the induced culture of *E. coli* are indicated in Fig. 11.48 as the three darkened areas. Enzyme assays established the second and third peaks as transacetylase and β -galactosidase, respectively, leaving the first peak as the permease protein. It was a well conceived and executed experiment, but its results were not entirely what Kolber and Stein had expected. They expressed their surprise in these words: "While we recognize the anomaly that material present in our permease is presumably cytoplasmic, thorough extraction of the membrane fraction by vigorous methods

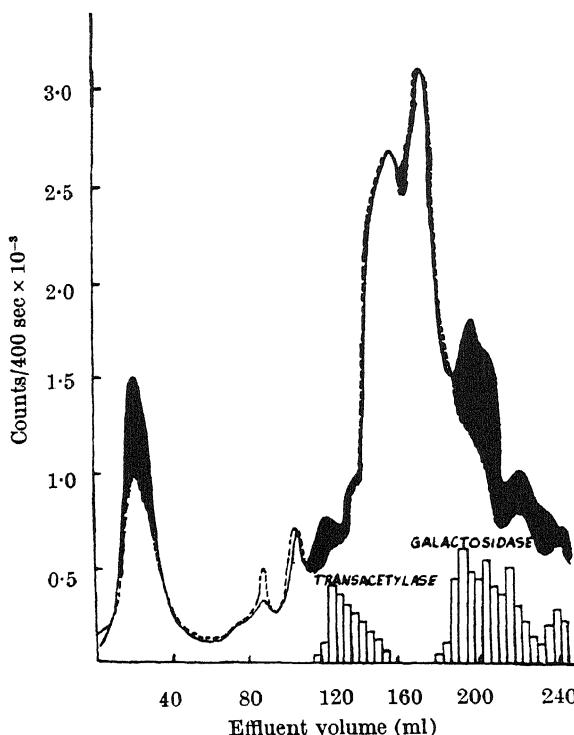


FIGURE 11.48. Isolation and identification of lactose permease from cell extracts of permease-positive *E. coli*. Induced permease-positive *E. coli* (*F Lac⁺*, 200 PS) was labeled with ^{14}C and noninduced culture, with ^3H . DEAE-cellulose chromatographs of each were matched. Extra radioactivity of ^{14}C over ^3H is indicated by the three darkened areas obtained by subtraction. Two later peaks were clearly identified by enzyme activities as transacetylase and galactosidase, and these are shown as block diagrams. The remaining early peak is identified as the permease. [From Kolber and Stein (1966), by permission of *Nature*.]

has failed to yield any enrichment" (Kolber and Stein, 1966, p. 694). From its early appearance in the effluent one may guess that this permease has a rather low molecular weight, similar to that of insulin.

2. Araku (1968) was able to isolate a protein from a permease-positive strain of *E. coli* by exposure to a hypotonic solution. This extracted protein (presumably the same isolated by Kolber and Stein), added to a culture of a permease-negative strain of *E. coli*, confers on it an ability to accumulate β -galactoside. In this case the permease-positive strain stands in the same relation to the permease-negative strain as the beta cells in the islets of Langerhans do to muscle cells in the higher organism.

11.3. Summary

The association-induction hypothesis, outlined in Chapter 6 and 7, is built on three basic concepts:

1. The bulk of cell water exists in a state of polarized multilayers; in this state it tends to exclude solutes and does so to variable degrees, depending on the size and complexity of the solute. This provides the mechanism for the normal exclusion of Na^+ from most cells.
2. Solutes are accumulated by the cell if they are adsorbed onto macromolecules within the cell; for example, cations are adsorbed onto fixed carboxyl groups and sugars onto hydrogen-bonding groups of proteins. This provides the mechanism for the normal accumulation of K^+ by most cells.
3. The polypeptide chain is especially well suited for the induction of electron distribution changes from one side chain to another. This underlies the interaction between sites that adsorb solutes, permitting them to function in a cooperative manner, and it underlies the ability of cardinal adsorbents to affect a large number of sites in an allosteric manner.

These concepts predict four fundamental properties of equilibrium solute distribution between cells and their environments:

1. Nonsaturable fractions of solutes dissolved in cell water in a ratio to external solute concentration (q -value) often less than 1.0.
2. Saturable fractions of solutes adsorbed onto intracellular macromolecules.
3. Cooperative interactions that are manifested by steep, sigmoidal solute adsorption isotherms.
4. The shifting of the adsorption isotherms rightward or leftward under the influence of cardinal adsorbents.

The last three properties are well known to biologists in the case of the oxyhemoglobin dissociation curve and the effects of 2,3-diphosphoglycerate and other agents on it.

This chapter has documented the equilibrium distributions of a variety of solutes in a variety of cells, all of which are described by the properties outlined. Examples included K^+ and other alkali metal ions in a variety of muscles, in oocytes, and in lymphocytes; Mg^{2+} in muscle; sugars in muscle and a number of other tissues; and amino

acids in muscle and oocytes. The cooperative nature of the K^+ and Na^+ adsorption isotherms was found to be strikingly uniform in a variety of cells, and consistent with this uniformity are the critical temperature transitions of ion distribution that are also observed in the same cells.

Finally, examples of the control of large numbers of solute-adsorbing sites by cardinal adsorbents that are present in low concentrations include the effects of ATP, Ca^{2+} , and ouabain on K^+ and Na^+ distributions; the effect of insulin on glucose uptake by muscle; and the effect of permeases on sugar accumulation by *E. coli*.

This chapter dealt with the equilibrium (or steady-state) distribution of solutes. The next chapter uses the same basic concepts to describe the kinetic properties of solute (and solvent) movements into and out of cells (i.e., their permeabilities).

Permeability

Permeability is the *sine qua non* of the membrane theory. On the basis of permeability or impermeability, higher or lower permeability, passive or active permeability, explanations of many facets of cell physiology have been sought. The membrane theory was founded on the studies of Traube's copper ferrocyanide gel membrane, a membrane once widely believed to be virtually impermeable to anything but small water molecules. Traube's atomic sieve theory for the copper ferrocyanide membrane appeared reasonable at the time (Traube, 1867). As pointed out in Chapter 1, however, later X-ray and electron diffraction studies revealed the large size of pores in this membrane—much larger than the diameters of molecules, like sucrose, to which the membrane is impermeable (Section 1.5). The failure of the atomic sieve theory left the behavior of the copper ferrocyanide gel membrane unexplained. Unfortunately these X-ray and electron diffraction studies that had disproved the sieve or rigid pore idea were apparently not widely known among cell physiologists. Thus, in years following, the rigid pore or "channel" idea has been reintroduced over and over again to explain selective permeability of living cell membranes.

The lipoidal theory of Overton (Section 2.1.1) was at one time more popular among plant physiologists and physiologists studying red blood cells than among those concerned with permeability of muscle and nerve, for example. The plant physiologists Collander and Bärlund (1933) demonstrated the correlation of the permeability of many nonelectrolytes into *Nitella* cells and their oil/water distribution coefficients (Fig. 2.1). *A serious flaw of this lipoid membrane model is that such a membrane is not truly semipermeable.* Thus, the oil/water distribution coefficient of ethanol is higher than that of water. In consequence, a lipoid membrane should be, according to Overton's theory, less permeable to water than to ethanol. Yet, in the first known recorded observation of osmosis by the Abbé Nollet (1748), dried pig bladder was shown to be permeable to water but not to ethanol. Perhaps it was with this fault in mind that Nathansohn (1904) and others introduced the mosaic concept (Section 2.1.2), a variant of the atomic sieve or rigid pore theory, to get around this basic discrepancy. It is true that, unlike olive oil or any simple lipid membrane, a phospholipid membrane is semipermeable (see Jain, 1972, p. 123). Here the grafting of phosphate groups onto lipid molecules adds an alto-

TABLE 12.1. Resistance of Cell Membranes

Tissue	Membrane resistance (Ω/cm^2)	Reference
Phospholipid bilayers	100,000,000	Tosteson <i>et al.</i> (1968)
<i>Nitella</i> protoplasmic droplet	50–4000	Miyake <i>et al.</i> (1973)
Myelin sheath	100,000	Tasaki (1982)
<i>Nitella</i>	100,000	L. R. Blinks (1930)
Squid nerve axon	700–1000	Cole and Hodgkin (1938–1939), B. Katz (1966)
Cuttlefish nerve axon	9200	Weidmann (1951)
Crab nerve axon		
<i>Portunas</i>	120	Fatt and Katz (1953)
<i>Carcinus</i>	3360	B. Katz (1948)
Puffer nerve axon	500–1000	Hagiwara (1960)
Roach nerve axon	800	Narashashi (1960)
Nodal membrane	8–40	Tasaki (1982)
Cat motor neuron	400	Coombs <i>et al.</i> (1955)
Toad motor neurons	270	Araki and Otani (1955)
Glial cells		
Cat and rat cerebella	3–10	Hild and Tasaki (1962)
Neocortical	200–500	Trachenberg and Pollen (1970)
<i>Aplysia</i> ganglion cells	2200	Fessard and Tauc (1957)
<i>Onchidium</i> ganglion cells	2500–4500	Hagiwara and Saito (1959)
Electric eel electroplaque cells		Keynes and Martins-Ferreira (1953)
Nervous face	10	
Nonnervous face	0.23	
Frog muscle	4000	Shanes (1958)
Calf and sheep cardiac Purkinje cells	480–2400	Coraboeuf and Weidemann (1954)
Human erythrocytes	7 (maximum)	Lassen and Sten-Knudsen (1968)
	10.6	S. L. Johnson and Woodbury (1964)
Mouse Ehrlich ascites cells	70	Lassen <i>et al.</i> (1971)
<i>Drosophila</i> giant mitochondria	2.2	Tupper and Tedeschi (1969a)
Mouse mitochondria (cuprizone-fed)	1–6	Maloff <i>et al.</i> (1978)

gether different set of attributes owing to the negative fixed charges, not intended by Overton in his lipoidal theory. I shall discuss this subject again in Section 12.3.

In 1938, Langmuir and Waugh introduced a technique to build thin lipoprotein films across holes in plates separating two aqueous solutions. Twenty-four years later Müller, Rudin, Tien, and Wescott (1962, see also Müller *et al.*, 1963) improved this basic method to prepare bimolecular lamellar membranes [black lipid membranes (BLM)] from various lipids, thereby inaugurating an intensive burst of efforts to reproduce models of the cell membrane (see Jain, 1972).

Such artificial phospholipid bilayers have extremely high electrical resistance, i.e., $100,000,000 \Omega/\text{cm}^2$ (see Table 12.1). In contrast, the resistance of living cell membranes varies from $100,000 \Omega/\text{cm}^2$ for the *Nitella* membrane to as low as $0.23 \Omega/\text{cm}^2$ for the nonnervous side of the electroplaque cells of electric eels. Thus the phospholipid bilayer is virtually impermeable to ions while living cell membranes are quite permeable.

Beside the divergence in membrane conductance from one cell membrane to another, there is also a great divergence in the conductance of one ion when compared to that of another through the same membrane. An example is the human red blood cell. The half time of exchange ($t_{1/2}$) of labeled K^+ is longer than 2.5 hr or about 10,000 sec (Solomon, 1952); the $t_{1/2}$ for Cl^- exchange is only 0.2 sec (Dirkin and Mook, 1931; see also Luckner, 1939, and Tosteson, 1959). One interpretation for these variabilities relies on the postulation of the absence or presence of specific ionic carriers which can shuttle certain ions across the phospholipid membrane while barring others (Section 4.5.1). Another interpretation relies on the revival of the rigid pore idea.

12.1. Evidence against the Conventional Lipoidal Membrane Theory

12.1.1. K^+ -Specific Ionophores Do Not Increase the Permeability of Living Cell Membranes to K^+

In recent years a number of naturally occurring compounds have been isolated as toxic byproducts in the search for therapeutic antibiotics. Compounds like valinomycin, monactin, and nonactin were found to exhibit a powerful *ionophore* effect in synthetic phospholipid membranes. Figure 12.1 shows studies in a bilayer membrane prepared from lipids extracted from sheep red cells that is by itself extremely impermeable to K^+ and other ions (Andreoli *et al.*, 1967; Tosteson *et al.*, 1968). Addition of 10^{-7} M of

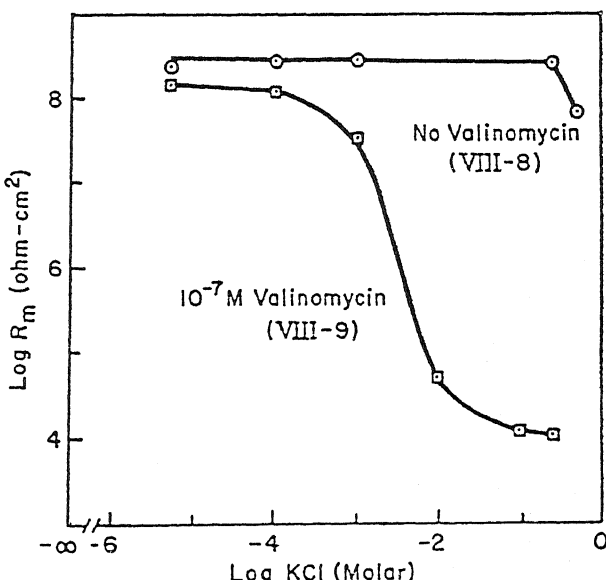


FIGURE 12.1. Effect of KCl concentration in solutions bathing the membrane on membrane electrical resistance (R_m) in the absence (○) and presence (□) of 10^{-7} M valinomycin. [From Andreoli *et al.* (1967), by permission of *Journal of General Physiology*.]

valinomycin, monactin, or dinactin causes a prompt and drastic increase of K^+ permeability of the phospholipid membrane, while it has virtually no effect on the permeability to Na^+ . These findings at one time raised hopes among many scientists that these compounds might be the prototypes of the long-postulated ion carriers (Section 4.5.1), and much effort was devoted to attempting to incorporate into lipid membranes other materials thought to be natural ionophores.

In 1970 the first set of what then were unexpected reports came from Stillman, Gilbert, and Robbins (1970). They used a variety of techniques to test the sensitivity of the K^+ permeability of squid axon membrane to monactin but found none, as indicated in the title of their article, "Monactin Does Not Influence Potassium Permeability in the Squid Axon Membrane." Eight years later, Maloff *et al.* (1978) looked for the expected effect of valinomycin on the K^+ conductance of mouse liver mitochondrial inner membrane and found none. In addition, the data demonstrated a very high electrical conductivity of the mitochondrial inner membrane, in contradiction to the then popular view of a low ionic permeability of this membrane (Ling, 1981a).

Ling and Ochsenfeld (1983c) then undertook studies of the effect of three K^+ -specific ionophores—nonactin, monactin, and valinomycin—on frog ovarian eggs, frog muscles, and human erythrocytes at varying external K^+ concentrations. A consistent twofold increase of K^+ permeability was observed for all three ionophores in human erythrocytes. No observable effects could be detected in frog muscle or frog ovarian eggs. Similar results were described in human lymphocytes (Negendank and Shaller, 1982a).

The failure to demonstrate any observable effect of 10^{-7} M valinomycin (and the other two ionophores) on the K^+ permeability of frog sartorius muscle is significant. Figure 12.1 shows that, in the presence of 30 mM KCl, 10^{-7} M valinomycin reduces the resistance of phospholipid bilayers from $10^8 \Omega/cm^2$ to about $2 \times 10^4 \Omega/cm^2$. Frog muscle membrane resistance is $4000 \Omega/cm^2$ (Table 12.1). More than half of the frog muscle membrane conductance is due to Cl^- (Hutter and Padsha, 1959). Thus, if a large area of the muscle cell surface is covered with a phospholipid bilayer, the exposure of frog muscle to 10^{-7} M valinomycin in the presence of 30 mM external K^+ should produce a marked increase of K^+ permeability. In fact, as just mentioned, none was observed. This failure to demonstrate a valinomycin-induced increase of K^+ permeability indicates that a relatively very small percentage of the muscle cell surface is covered with a phospholipid bilayer. This conclusion is corroborated by the twofold increase of K^+ permeability in response to 10^{-7} M valinomycin and other ionophores of the red blood cell, which has the highest lipid content in its membrane (Table 12-1).

Following the development of the BLM technique and the discovery of the ionophore properties of such substances as valinomycin, much effort was spent to search for "natural ionophores." These attempts were not successful. Müller, who together with Rudin and other co-workers introduced the BLM technique, remarked in 1975: "A lot of us have spent a wasted ten years or so trying to get these various materials into bilayers . . ." (Müller, 1975).

12.1.2. There Is Not Enough Lipid in Many Membranes to Provide a Continuous Bilayer

Typical samples of the lipid contents of a variety of plasma membranes, as well as of membranes of subcellular particles, are collected in Table 12.2, taken from Jain's

TABLE 12.2. Composition of Some Typical Plasma Membranes^{a,b}

Type of cell	Protein (%)	Lipid (%)
Ox brain myelin	18-23	73-78
Human erythrocyte	53	47
<i>Saccharomyces cerevisiae</i> NCYC 366	49	45
<i>Pseudomonas aeruginosa</i>	60	35
<i>Saccharomyces cerevisiae</i> ETH 1022	37 ^c	35
<i>Bacillus megatorium</i>	70	25
Rat muscle	65	15
Rat liver	85	10
Avian erythrocyte	89	4
Rod outer segment	40-50	20-40
Chlorophylls	35-55	18-37
Mitochondria		
Total membrane	70	30
Inner membrane	75	25
Sarcina lutea	57	23
<i>Mycoplasma laidlawii</i>	47-60	35-37
<i>Bacillus</i> spp.	58-75	20-28
<i>Micrococcus lysodeikticus</i>	65-68	23-26
<i>Staphylococcus aureus</i>	69-73	25-30

^aData are percent dry weight.^bFrom Jain (1972), by permission of Van Nostrand-Reinhold.^cUp to 27% mannan was found in the preparation.

monograph on lipid membranes (1972). The percentages of lipids and proteins are as a rule those expressed by the original authors in terms of dry weight and not the total (wet) weight of the membrane. Thus the actual percentage of lipids found in the fresh living membrane must be considerably lower. Table 12.2 also shows that in this list of membranes, in contrast to the variable and often very low lipid content, *it is the proteins that constitute the more constant and abundant component. The missing water content also gives the false impression that lipids and protein are the only components of the isolated membranes.* How far we have strayed in this direction will be made clear from some new experimental findings on water diffusion to be described in Section 12.2.

A set of experimental evidence cited extensively in support of the lipoid membrane concept was that of Gorter and Grendel (1925), who showed that the lipids extracted from human (and other mammalian) erythrocytes are just enough to provide a continuous bilayer covering of the cell. Table 12.2 shows that, of the list of cell membranes cited, those of human erythrocytes have the highest lipid content. Clearly, if these findings of Gorter and Grendel are correct, then the other membranes listed in Table 12.2 do not have enough lipids to form a similar continuous bilayer covering. This conclusion agrees with the similar one drawn from ionophore studies cited in the preceding section.

The outer membrane of a mitochondrion is highly permeable and is widely regarded as not serving as a permeability barrier. The inner membrane, on the other hand, is regarded as far less permeable (Section 15.3.3). Yet lipid analysis showed that it is the outer membrane that is rich in lipid (50% of dry weight), while the inner membrane is poor in lipid (20% of dry weight) (Ernster and Kuylenstierna, 1970; Lehninger, 1975, p. 512)! With this in mind, it is not surprising that Sjöstrand and Bernhard

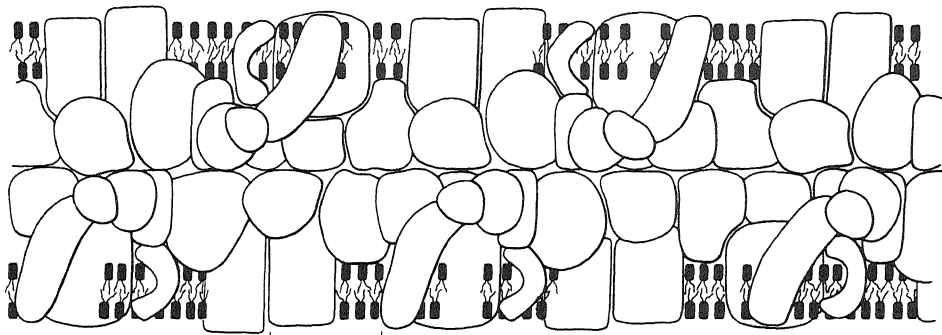


FIGURE 12.2. Schematic presentation of a model proposed for the inner mitochondrial membrane. The location of lipid molecules at the matrix surface is shown. The drawing illustrates the structure of the cristae, with two closely apposed inner membranes and no intercristal space. The diagram should be conceived of as representing the structure in a plane cut through the membranes perpendicular to their surfaces. Scale bar: 100 Å. [From Sjöstrand (1978), by permission of *Journal of Ultrastructural Research*.]

(1976), by cross-linking the protein components of the membrane before chemical fixation for EM, came to the conclusions that “there is no continuous, uninterrupted lipid bilayer forming a backbone structure in these membranes” (Sjöstrand and Bernhard, 1976, p. 243) and that lipids occur only as “islands” or patches in the membrane. Figure 12.2 is Sjöstrand’s schematic diagram of the makeup of the mitochondrial inner membrane (Sjöstrand, 1978).

12.1.3. Removal of Membrane Lipids from the Liver Mitochondrion Inner Membrane Does Not Alter the Trilayer Structure

Robertson’s demonstration of the trilaminar structure of what he regarded as a *unit membrane* was broadly hailed as having positively proved the Davson–Danielli or paucimolecular lipid membrane model (Section 2.1.4) (Robertson, 1960).

However, contradictory evidence soon began to appear. Fleischer *et al.* (1967) extracted with organic solvents 95% or more of the lipids of mitochondrial membranes before fixing and staining them for electron microscopic examination. The unit membrane structure in lipid-free membranes is clearly visible (Fig. 12.3). Using a densitometer they measured the density distribution of the electron microscopic (EM) plates of defatted membrane and compared it with that of a control membrane with its normal content of lipids. If the trilayered unit membrane structure truly contains a continuous central lipid layer, as in the Davson–Danielli paucimolecular membrane model, and if the darkly stained laminar structures represent proteinaceous materials on both sides of the lipid layer (Fig. 2.2), after near-total removal of lipids, the dark lines should come very close together and perhaps even coalesce. Yet, as shown in Fig. 12.4, quite the opposite was observed: The distance between the dark lines actually broadened slightly. On the other hand, if the trilayered structures are primarily a lipid bilayer and the darkly stained laminar structures are the phosphate polar groups of the phospholipids, as in the fluid mosaic model of the cell membrane proposed by S. J. Singer and Nicolson



FIGURE 12.3. Electron micrograph of a portion of a "lipid-free" mitochondrion. The unit membrane structure of the cristae membranes is clearly visible. Magnification 192,000 \times , reproduced at 65%. [From Fleischer *et al.* (1967), by permission of *Journal of Cell Biology*.]

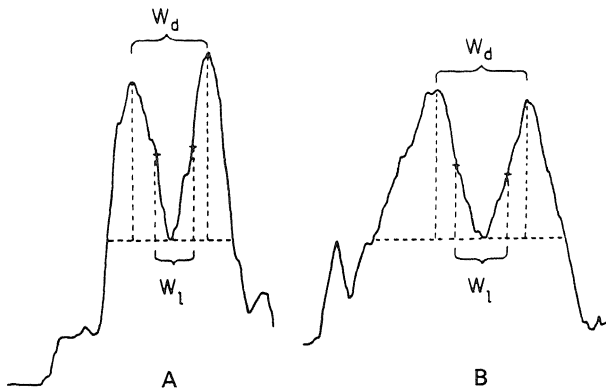


FIGURE 12.4. Typical microdensitometer tracings of mitochondrial membranes (A) of untreated control mitochondria and (B) of "lipid-free" mitochondria. [From Fleischer *et al.* (1967), by permission of *Journal of Cell Biology*.]

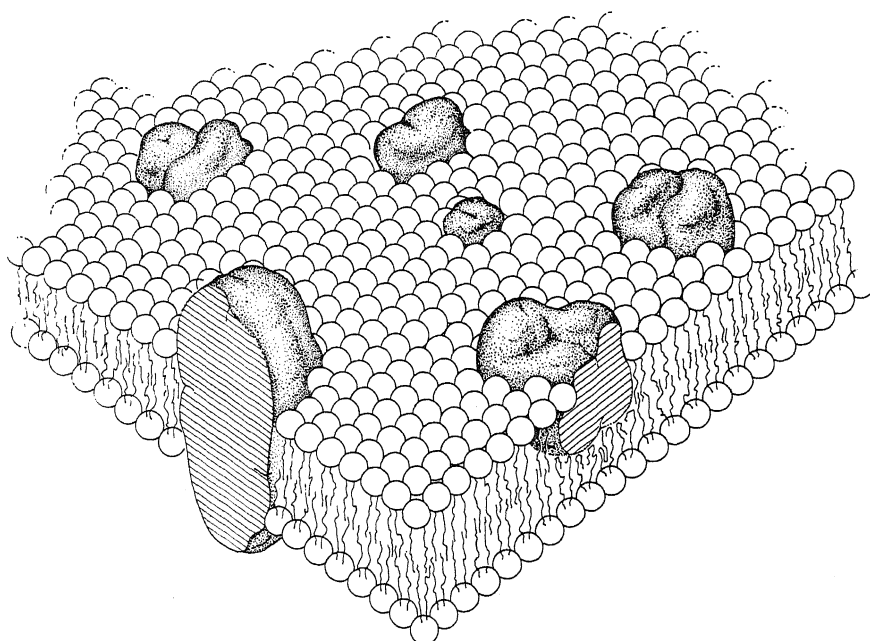


FIGURE 12.5. Lipid-globular protein mosaic model (fluid mosaic model): schematic three-dimensional view. The solid bodies with stippled surfaces represent the globular integral proteins, which at long range are randomly distributed in the plane of the membrane. At short range, some may form specific aggregates. [From Singer and Nicolson (1972), by permission of *Science*.]

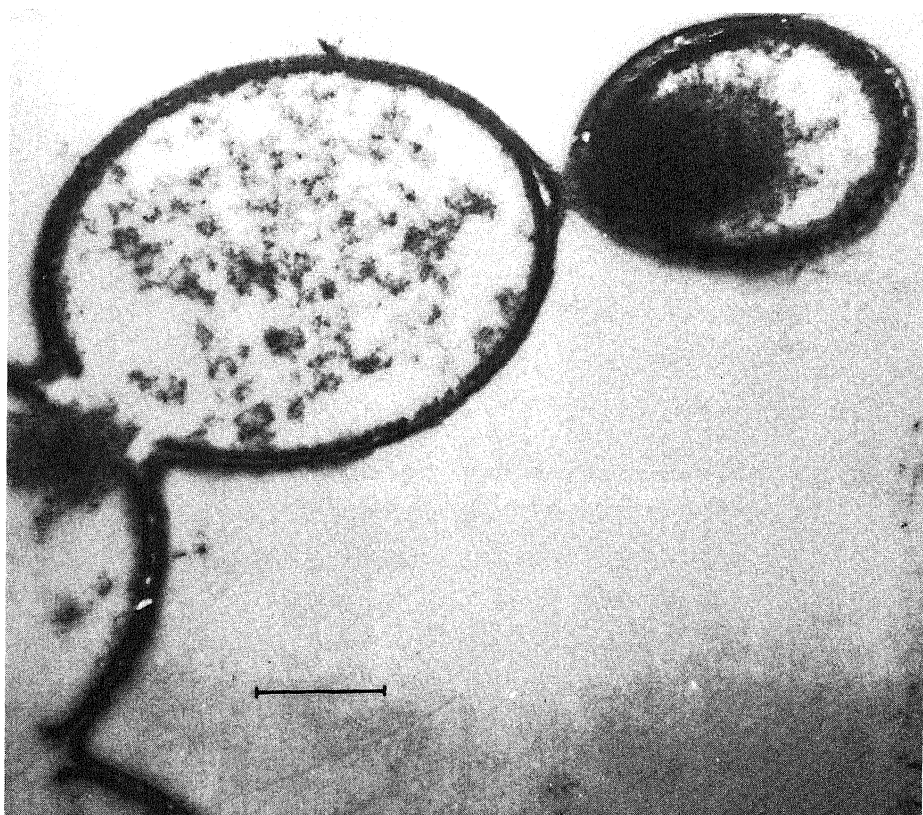


FIGURE 12.6. Electron micrograph of proteinoid microspheres, subjected to elevated pH (6). Scale bar: 1 μm . [From Fox (1973), by permission of *Naturwissenschaften*.]

(1972) (Fig. 12.5), then the near-total removal of the membrane lipids should cause the disappearance of the trilaminar structure altogether. Figure 12.3 clearly shows that this was also not the case (see also Ling, 1977c).

Fleischer *et al.* (1967) were not the only investigators who studied the effect of lipid removal on membrane structure. Napolitano *et al.* (1967) and Morowitz and Terry (1969) found a similar indifference of membrane trilaminar structure to lipid removal in studies of the plasma membrane of mammalian eukaryotic and microbial prokaryotic cells. Since after the removal of the lipids the thickness of the whole membrane does not change, one can only conclude that lipids exist in pockets or islands and that it is the total area of the membrane that undergoes shrinkage; this might not be easily discernible under usual high EM magnifications. The question arises, What then gives rise to the trilaminar structure? There is evidence that it may be simply the proteins, which, as shown in Table 12.2, are the most constant component of all cell membranes and hence a more reasonable candidate for the widely observed trilaminar structure.

Figure 12.6 reproduces an electron micrograph of microspheres prepared by Fox (1965, 1973) from proteinoid materials, synthesized artificially from heated mixtures of

pure amino acids. The trilaminar structure resembles the unit membrane; yet, no lipids were present.

12.2. What Is the Rate-Limiting Step for the Entry of Water into Living Cells?

In the earliest days of biology it was recognized by de Vries, von Nägeli, and others that the content of a living cell, or protoplasm, can sometimes be isolated from the cell and suspended in an aqueous medium without dissolving away. Figure 2.5 shows how the protoplasm poured out from cut *Nitella* cells collects on the bottom of the vessel without mixing with the surrounding aqueous medium (in which small air bubbles can be seen). Indeed, when microelectrodes are inserted into these protoplasm droplets, electrical potentials like those observed in living cells can be observed. What is more, the droplet can even be excited to create action potentials (Miyake *et al.*, 1973; Inoue *et al.*, 1973a; Koppenhofer, 1974). This subject will be taken up again in Chapter 14.

It is unlikely that the droplets could instantaneously regenerate new cell membranes (see also Section 2.4). In fact we have already shown that direct exposure of muscle protoplasm to an external aqueous medium does not lead to the regeneration of

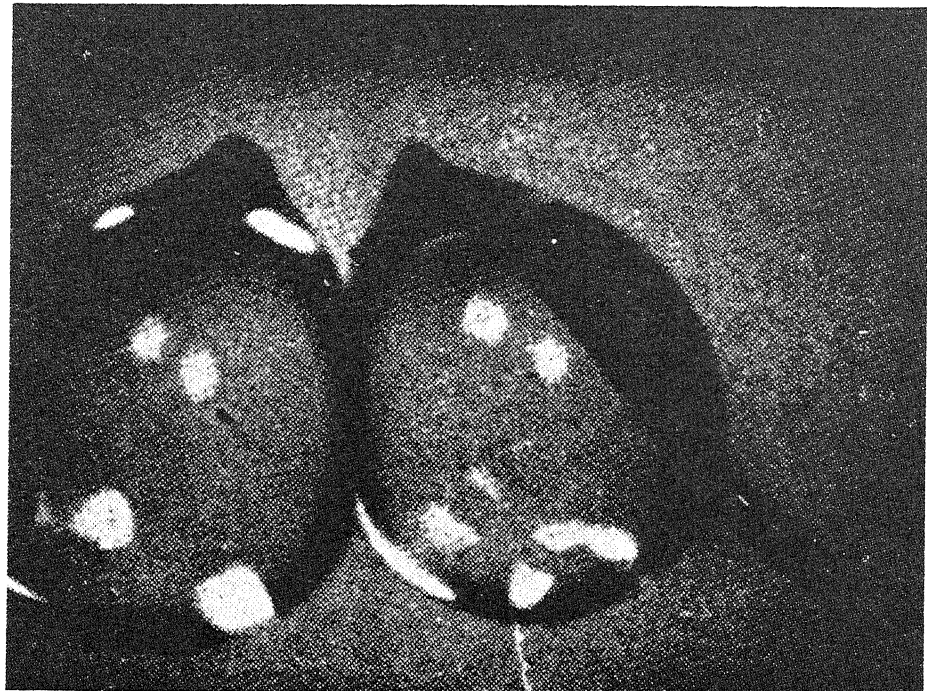


FIGURE 12.7. Flattening of drops and appearance of lens in coalescence: demonstration of the resistance of the water droplet to coalescing instantly on contact. [From Owe-Berg (1965), by permission of *Annals of the New York Academy of Sciences*.]

a new membrane at all (Table 5.4) but that it is the inherent property of the protoplasm itself that keeps them from mixing with the aqueous medium. Thus it seems that in some cells, like frog muscle, exposed protoplasm remains unchanged; in other cells, like *Nitella*, exposure to the external medium causes modifications of the properties of the protoplasm to take place. In support, as Fig. 12.7 shows, even the surface of a pure water droplet develops properties quite different from those of normal bulk phase water: Two droplets can bounce against each other without coalescing immediately. Clearly the imbalance of attractive forces at the surface has created this behavior. So molecules at the surface of the protoplasm may also redistribute and reorganize themselves in such a way as to yield qualities that are usually considered surface or membrane properties. But the cell surface in essence is nonetheless of the same chemical composition as the bulk phase protoplasm: It is primarily a protein-ion-water system containing varying amounts of phospholipids. There is therefore no good reason for the traffic of all materials to be always rate-limited by passage through the cell surface. It is conceivable that in some cases the rate of diffusion of molecules through the cell surface and within the cell interior may take place at similar rates. In that case, one would have what is called *bulk-phase-limited diffusion* in contrast to *surface-limited diffusion*. Fortunately the mathematics of diffusion in each of these cases is well established. Theoretical criteria can be set up to distinguish between these types of diffusion and provide the basis for quantitative studies.

Basically there are two sets of criteria by which one can determine the rate-limiting step of a diffusion process:

1. *The influx profile.* If one plots the amount of a substance that has diffused into a system at time t , M_t , as a fraction of the final amount reached at time infinity, M_∞ , against the square root of t , totally different theoretical profiles are obtained in bulk-phase- and surface-limited diffusion. This is shown in Fig. 12.8. The simple surface-limited influx is sigmoid-shaped (A). The bulk-phase-limited diffusion curve has a straight initial part before leveling off (B). The curves show a break if a substantial portion of the diffusing substance becomes adsorbed or enters a subcellular compartment (C).
2. *The efflux profile.* One can also plot M_t/M_0 in an efflux study, where M_t is the amount remaining after washing the system in a solution free of the substance in question for a duration t . In the case of surface-limited diffusion $\log(M_t/M_0)$ plotted against t is a straight line; in the case of a bulk-phase-limited diffusion, it becomes a straight line only after some time. In the latter, extrapolation of the straight line portion of the curve to 0 time yields a value less than 1.0 which varies with the shape of the system under study. For a spherical system the intercept is 0.665; for a long cylindrical system, it is 0.692 (Dünwald and Wagner, 1934; Jost, 1960).

Figure 12.9A shows the efflux of $^3\text{H}\text{HO}$ from a small cylindrical collodion bag (microsac) 2.5 cm long and 0.11–0.15 cm in outer diameter. The experimental points follow the theoretical surface-limited diffusion profile. Figure 12.9B, on the other hand, shows the efflux of $^3\text{H}\text{HO}$ from a cylindrical filament of agar gel. The intercept of the straight line portion of the curve is 0.727. Figure 12.10A shows the influx of $^3\text{H}\text{HO}$ into a collodion microsac, and Figure 12.10B, that into an agar filament. These data

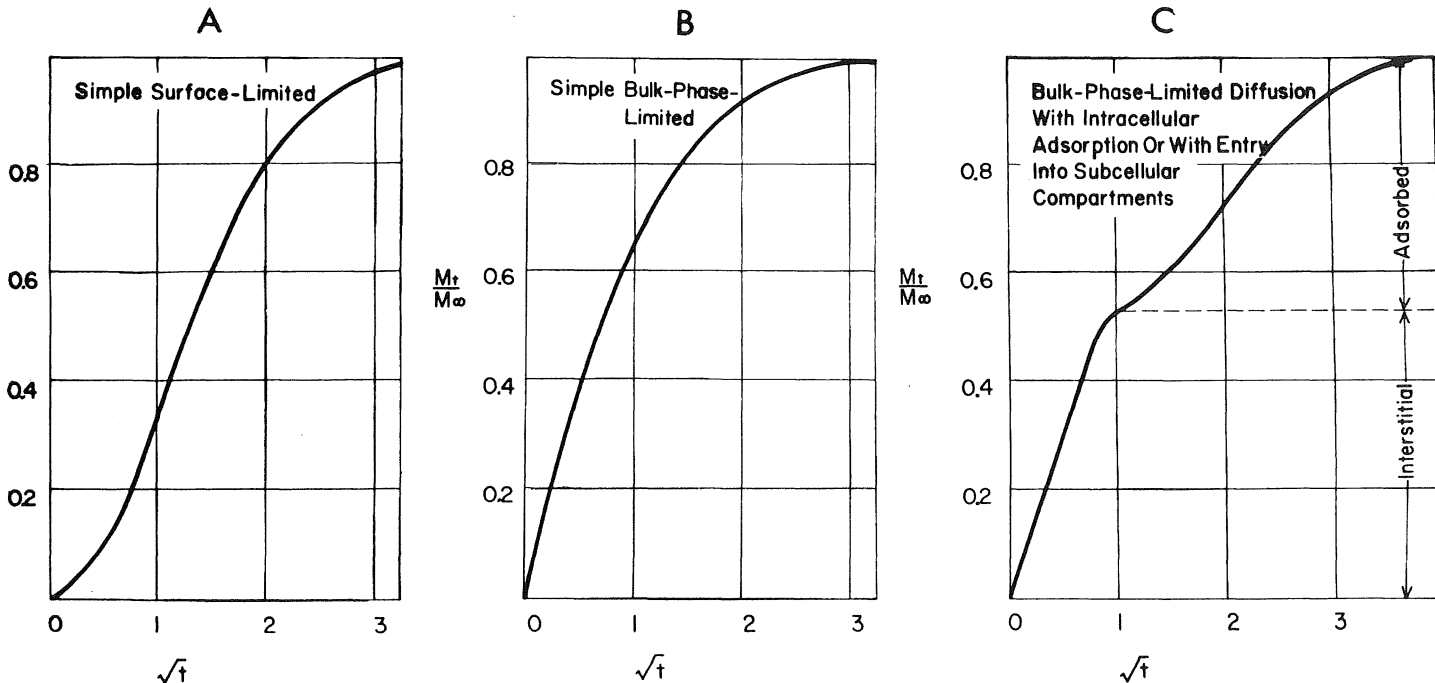


FIGURE 12.8. Time course of influx of a labeled substance into model systems with rate-limiting steps as indicated in each panel. The influx profiles are theoretically calculated. The ordinate represents the uptake, M_t , of the labeled material at time t as a fraction of the final amount of the material in the system (M_∞). The abscissa represents the square root of t . [From Ling (1966b), by permission of *Annals of the New York Academy of Sciences*.]

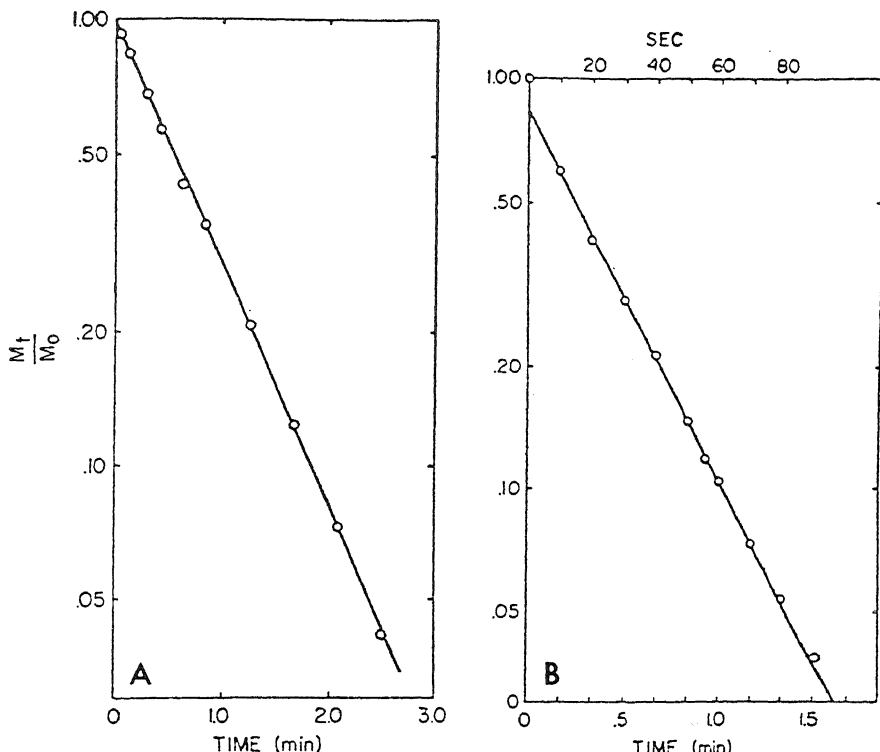


FIGURE 12.9. Efflux of labeled water from a collodion microsac (A) and from a cylindrical filament of agar gel (B). (A) Semilogarithmic plot of the amount of $^3\text{H}\text{HO}$ remaining in the sac at time t (M_t) as a fraction of the initial amount (M_0) as a function of time t . The extrapolation of the straight line is 0.98 and the rate constant is 1.045 min^{-1} . (B) The filament of agar gel, 4% (w/v), is 0.0520 cm in radius. The final straight line obtained by regression has an intercept of $\ln 0.727$. [From Reisin and Ling (1973), by permission of *Physiological Chemistry and Physics*.]

clearly confirm the expectations based on the theory of diffusion. Let us next see what is the rate-limiting step in the exchange of $^3\text{H}\text{HO}$ of living cells.

Figure 12.11 shows the efflux of $^3\text{H}\text{HO}$ from isolated single giant barnacle muscle fibers. The zero time intercepts are 0.700 and 0.705, which are close to the theoretical intercept for bulk-phase-limited diffusion (0.692). Influx profiles of $^3\text{H}\text{HO}$ into frog ovarian eggs (Ling *et al.*, 1967) are illustrated in Fig. 12.12. The solid curve in (A) and dashed curves in (B-F) are simple bulk-phase-limited influx diffusion profiles. All other lines are theoretical curves for bulk-phase-limited diffusion with intracellular adsorption.

From these data the somewhat startling conclusion was reached that the rate of exchange of water between frog ovarian egg cells (or giant barnacle muscle cells) and the environment is not limited by a water-impermeable cell membrane. Rather the diffusion rate of water through the cell surface is very similar to that within the cytoplasm

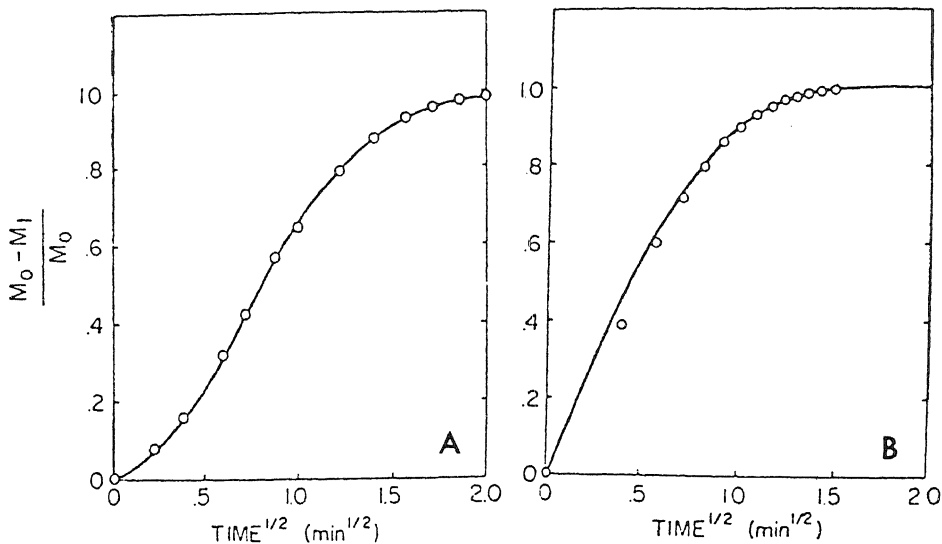


FIGURE 12.10. Influx of labeled water into a collodion microsac (A) and into a cylindrical filament of agar gel (B). Data obtained from efflux studied by the inversion method (Ling *et al.*, 1967). Points are experimental, solid lines are theoretical for surface-limited (A) and bulk-phase-limited (B) diffusion. [From Reisin and Ling (1973), by permission of *Physiological Chemistry and Physics*.]

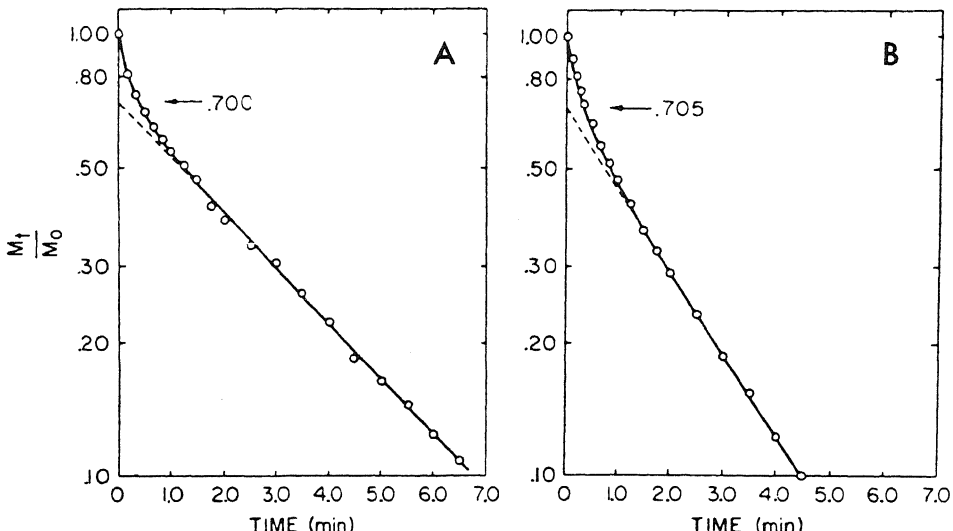


FIGURE 12.11. Efflux of $^3\text{H}-\text{HO}$ from intact isolated muscle fibers. The fibers were previously equilibrated for at least 1 hr in barnacle Ringer solution containing 10 $\mu\text{Ci}/\text{ml}$ of $^3\text{H}-\text{HO}$. The graphs are semi-logarithmic plots of the fraction of initial $^3\text{H}-\text{HO}$ activity as a function of time. The experimental points do not follow a simple straight line. The intercepts of the final straight lines are 0.700 and 0.705, respectively. [From Reisin and Ling (1973), by permission of *Physiological Chemistry and Physics*.]

TABLE 12.3. Diffusion Coefficients of Water in Ovarian Egg and Muscle Cells

	Organism	Method of study	(D^*) at 25°C ($\times 10^5$ cm 2 /sec)	Reference
Egg	Frog	Radial diffusion	0.72–1.47	Ling <i>et al.</i> (1967)
		NMR	0.68	Hansson-Mild <i>et al.</i> (1972)
Muscle	Barnacle	Longitudinal diffusion	2.42	Bunch and Kallsen (1969)
		Radial diffusion	1.35	Reisin and Ling (1973)
		Longitudinal diffusion	1.34	Caillé and Hinke (1974)
	Frog	NMR	1.56	Abetsedarskaya <i>et al.</i> (1968)
	Toad	NMR	1.20	Finch <i>et al.</i> (1971)
Rat	NMR		1.35	Walter and Hope (1971)
			1.43	Chang <i>et al.</i> (1972, 1973)
Pure water			2.40	Mills (1973)
			2.44 ($^3\text{H}_2\text{O}$)	Wang <i>et al.</i> (1953)
			2.43 ($^2\text{H}_2\text{O}$)	Wang <i>et al.</i> (1953)

and, in both, the diffusion rate is slower than diffusion in normal liquid water by a factor not larger than 2. By comparing the experimental points with the theoretical curves, the exact diffusion coefficient of $^3\text{H}_2\text{O}$ in the cell water is also readily obtained, and it is shown in Table 12.3. Corroboration of this conclusion is also given in Table 12.3, in which diffusion coefficients of $^3\text{H}_2\text{O}$ obtained from our two sets of studies are compared with data obtained by others using totally different methods (e.g., NMR). With the exception of one set of data,* there is good accord.

Taken as a whole, these findings suggest that the cell surface protoplasm and the cytoplasmic protoplasm are quite similar in their role as diffusion media. The diffusion medium in the cells is unquestionably water. This means that in these cells water diffuses just as rapidly through water in the cell surface (membrane) as in the cytoplasm. Furthermore, the cross-sectional area occupied by water in the cell surface membrane is roughly equal to that at any imaginary concentric spherical (egg) or cylindrical (muscle fiber) surface throughout the cell interior. This is indeed a far cry from the conventional picture of the cell surface, in which lipids and proteins are the only components of the membrane.

12.3. Polarized Water as the Semipermeable, Selective Permeability Barrier

According to the AI hypothesis, it is water polarized in multilayers by cell-surface proteins that serves as a continuous semipermeable barrier, at once separating the living cell from its environment and maintaining a continuity essential for its functional activities.

To test this hypothesis, I chose a “water membrane” in the form of cellulose acetate sheets. As shown in Chapter 9, cellulose, when prevented from assuming a crystalline

*The exceptionally high value of Bunch and Kallsen (1969) might be due to the use of short muscle fiber segments, which deteriorate rapidly (see Sections 5.2.6 and 8.4.1.4).

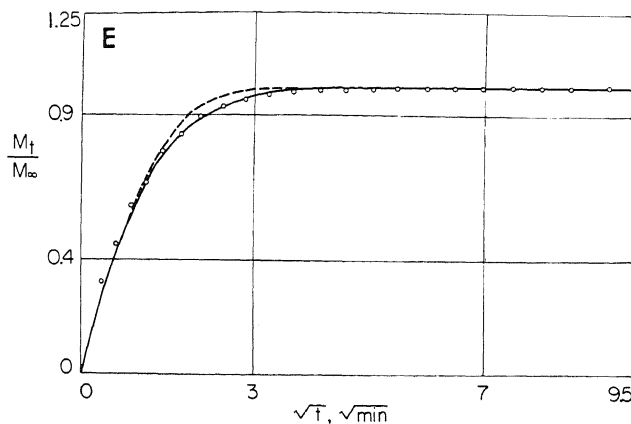
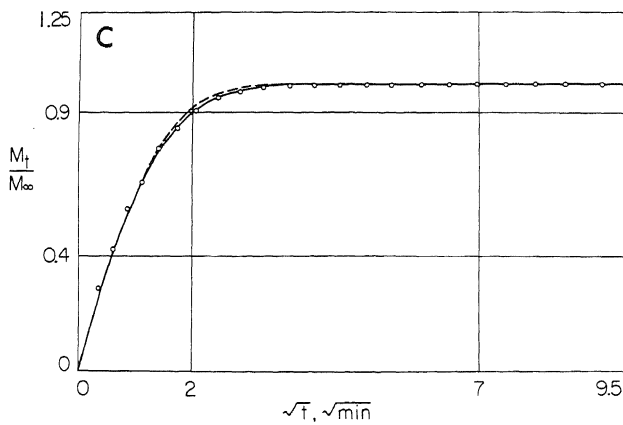
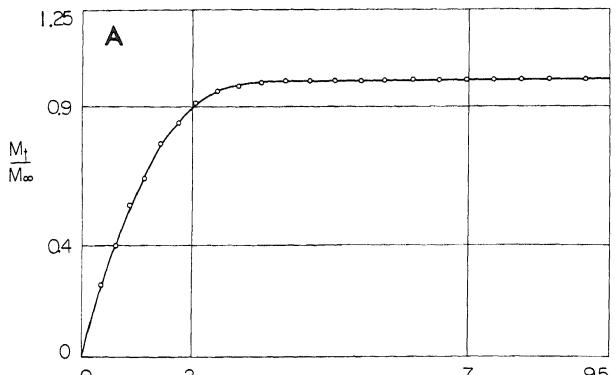
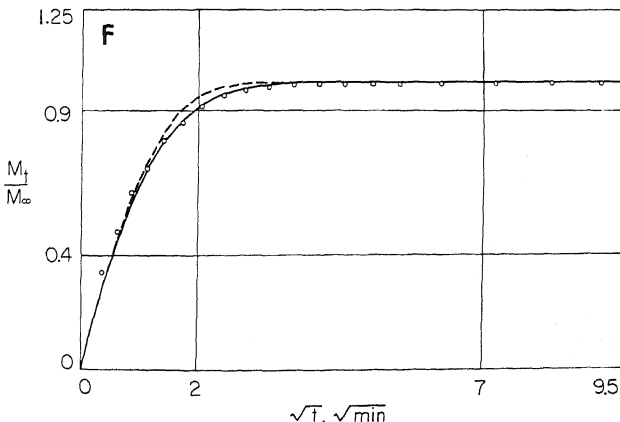
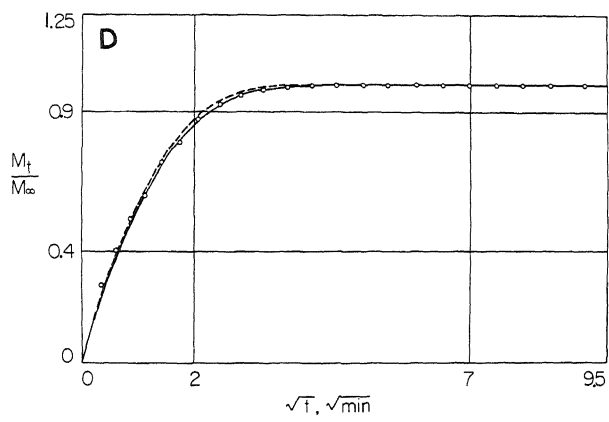
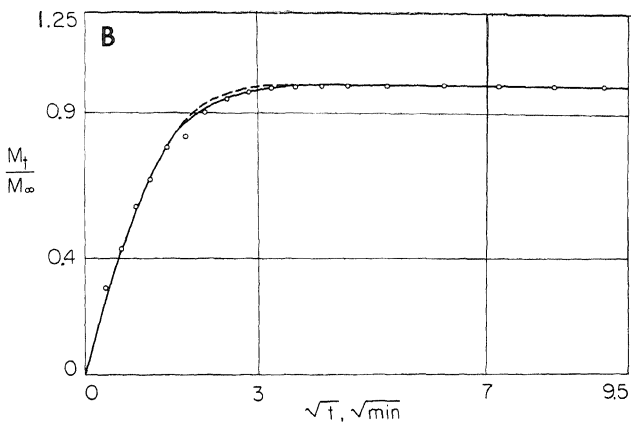


FIGURE 12.12. $^3\text{H}\text{HO}$ influx into frog ovarian eggs. Influx profiles showing simple bulk-phase-limited diffusion and bulk-phase-limited diffusion with intracellular adsorption. Influx time course obtained by the inversion method. The solid curve in (A) and the dashed curves in (B-F) show a theoretical plot for simple



bulk-phase-limited diffusion. All other lines are theoretical curves for bulk-phase-limited diffusion with intracellular adsorption. [From Ling *et al.* (1967), by permission of *Journal of General Physiology*.]

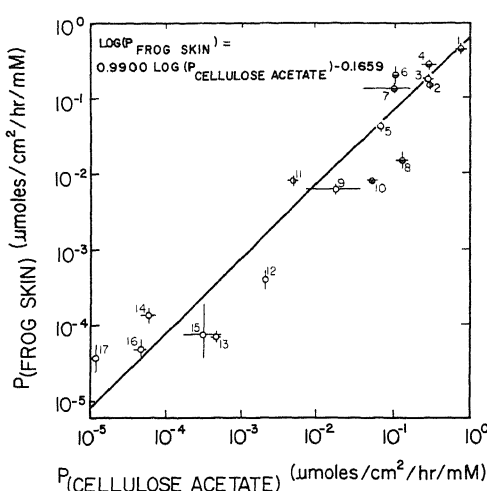


FIGURE 12.13. Plot of the permeability of reversed living frog skin against the permeability of heat-treated cellulose acetate membrane. Horizontal and vertical lines indicate SE, except in the few cases when only two determinations were made. Straight line described by equation shown in graph was obtained by the method of least squares. Numbers in graph refer to different compounds: 1, THO, 25°C; 2, THO, 4°C; 3, THO, 0°C; 4, methanol, 25°C; 5, methanol, 0°C; 6, ethanol, 25°C; 7, n-propanol, 25°C; 8, ethylene glycol, 25°C; 9, ethylene glycol, 0°C; 10, glycerol, 25°C; 11, glycerol, 4°C; 12, glycerol, 0°C; 13, erythritol, 0°C; 14, xylitol, 0°C; 15, sorbitol, 0°C; 16 L-glucose, 0°C; 17, sucrose, 0°C. The empty circle (○) represents experiments at 0°C; circle with the right half filled (◐) 4°C; circle with the bottom half filled (◑) 25°C. [From Ling (1973b), by permission of *Biophysical Journal*.]

form by the introduction of bulky groups (e.g., CH₃, as in methylcellulose), polarizes water in multilayers just as proteins in the extended conformation do (Ling *et al.*, 1980a,b). It would be expected that cellulose acetate, which does not exist in the crystalline form, would polarize multilayers of water also. Figure 12.13 plots the permeability of water and nine other hydroxylic compounds at three different temperatures (0°, 4°, and 25°C) through (inverted) frog skin against permeability through a sheet of cellulose acetate. The correlation coefficient is +0.96. In fact, the ordinate and abscissa are in the same units; the slope of the curve determined by the method of least squares is 0.9900. Thus there is good correspondence in the two sets of data, not merely a good correlation.

The rate-limiting step in the passage of water and solutes through the cellulose acetate sheets occurs at the thin surface "active" layer. With an electron microscope, R. D. Schultz and Asunmaa (1969) measured the diameters of the pores in the active layer. The average pore size was 44 Å. Since each water molecule is 2.7 Å in diameter, the pores are filled with no less than 15 layers of water. Yet this membrane is virtually impermeable to sucrose, which has a diameter of only 9.4 Å. This great discrepancy between the much larger pore size and the size of a molecule that cannot go through the pore repeats the story of the copper ferrocyanide gel, which also has interstices many times bigger than the size of the sucrose molecule (Section 1.5). Once more our data show that the molecular mechanism of semipermeability is not that of an atomic sieve.

The data of Fig. 12.13 are readily explained by the polarized multilayer theory of water in the cell surface as well as in the "active" surface of cellulose acetate sheets. The steady-state permeability P of a substance through a thin membrane is determined by the product of two parameters, the equilibrium distribution coefficient or q -value and the diffusion coefficient (D) of the substance in question in the membrane (see Crank, 1956):

$$P = qD \quad (12.1)$$

Let us now compare the permeability of water with that of sucrose. The q -value of sucrose can be assumed to be about 0.1 of that of water, which has a q -value of unity. Yet the permeability of sucrose at 0°C is 10,000 times slower than that of water. Thus D for sucrose must be at least 1000 times slower than that of water. Yet the diffusion coefficient of sucrose in normal liquid water at the same temperature is only 5.57 times slower than water (see Hodgman *et al.*, 1961). This suggests that, for diffusion to proceed, the energy needed to excavate a “hole” into which to move a sucrose molecule is much larger than that needed to excavate a similar hole in free solution. In terms of the AI hypothesis, this extra energy is required to overcome the stronger H₂O–H₂O interaction occurring as a result of the (multilayer) polarization.

In the course of history many other models of semipermeable membranes have been proposed, including dead animal bladder, parchment, gelatin, copper ferrocyanide, Prussian blue, various tannates and silicates (T. Graham, 1861; Traube, 1867; Findlay, 1919), porous glass (Kraus *et al.*, 1966), and the cellulose acetate sheet described here. With the possible exception of animal bladder from a fat animal, none of these semipermeable membranes contains lipids. They all contain water and a matrix of charged sites on crystalline or amorphous lattices. In terms of the AI hypothesis, all of these models satisfy the criterion of an NP-NP-NP system or its variant, and theoretically can be expected to polarize multilayers of water (Section 6.3.2). This knowledge, accumulated over two centuries, blends naturally with the present interpretation of cell surface semipermeability. In this context, it should be pointed out that, since pure lipid membrane is not semipermeable (p. 377) the semipermeability of phospholipid membrane can only result from the presence of charged phosphate groups. This idea is supported by the finding of Y. Katz and Diamond (1974) that water in small “solid” water-containing phospholipid bodies, called liposomes, excludes sucrose very much like gelatin and urea-denatured proteins (Section 6.3.4.3).

The experimental findings of Collander (1937), as represented in Fig. 2.1, have been cited in many textbooks in support of Overton’s lipoidal membrane theory. The living cell studied was *Nitella*. The data presented in Fig. 12.13 were intended to support the association-induction (AI) hypothesis. The living cell studied was (inverted) frog skin.

Table 12.1 shows how widely divergent are the electrical conductances (which measure ionic permeability) of the living cell membranes. Both Fig. 2.1 and Fig. 12.13 deal with water and nonelectrolyte permeability. There are reasons to believe that neither *Nitella* nor frog skin can be considered as typical. Rather they seem to represent cell membranes of a highly impermeable kind: a special adaptation to their respective unique natures and functions. Thus neither type of cell depends on a continual influx of D-glucose from the external pond water for its survival. Such is not the case for most other cells of multicellular organisms and some unicellular organisms as well: Brain, nerves, heart, muscle, liver, and eggs, as well as *E. coli*, require D-glucose from their surrounding media.

Nitella is so impermeable that erythritol is the least permeable nonelectrolyte that Collander quantitatively studied. With the availability of radioactively labeled sugar, I was able to study erythritol permeability as well as the permeability of L-glucose and sucrose. L-Glucose rather than D-glucose was chosen to avoid complications owing to its metabolic degradation. All three have permeabilities 10,000 times lower than that of labeled water. The data of Fig. 11.12 show that it takes only 1 min for half of the egg

cell water to exchange with external labeled water. If the egg cell membrane is like *Nitella* or inverted frog skin, then it would take 10,000 min for it to acquire half of the concentration of glucose in the external medium. This is about 7 days! The cells would not be able to survive. Indeed it was with this kind of difficulty in mind that the carrier or pump idea was introduced. However, without a continuous lipid layer, it is difficult to imagine how such a mechanism can operate. On the other hand, there is clear evidence, as will be shown in Section 12.5, that the resting cells can obtain glucose and other nutrients very rapidly from the external environment and that that is how they can survive and grow.

I will demonstrate next that the polarized multilayer theory of cell surface (and bulk phase) water can readily explain the great diversity of water and solute permeabilities through variations in two mutually dependent parameters: the total area of polarized water at the cell surface and the degree of polarization of this water. Indeed we need go no further to search for a model demonstration of these expected changes than the cellulose acetate membrane. When freshly prepared cellulose acetate membrane contains about 50% water, it is highly permeable to various solutes and only moderately selective—as is the case for many living cell surfaces like those of muscle (Fig. 9.5) or egg. To produce the type of highly selective permeability seen in *Nitella* and frog skin, cellulose acetate membrane has to be “activated” by exposure to a higher temperature (60°C) for a few minutes. What happens as a result is that the surface of the membrane shrinks and the total area of polarized water is greatly reduced. With this area reduction, and the closer opposition of the polarizing sites, the water becomes more intensely polarized and the diffusion coefficient for glucose and other larger solutes is greatly reduced. Yet, as pointed out above, the pores of the *active* membrane are much larger than the virtually impermeable sucrose molecules. It is only polarized water in these pores that can function as a selective barrier in this manner.

Thus far we have dealt with the permeation of water and neutral solutes, often called nonelectrolytes, that apparently enter and leave cells via polarized water. Here, molecular size and complexity, which determine the q -value of dissolved solutes, are the primary determining factors for permeability. A higher degree of specificity is seen, however, in the rate of permeation of ions into living cells. This, and other examples of highly selective solute permeation, will be the subjects of the remainder of this chapter.

12.4. Permeability of Cells to Ions

Much of the early information on the permeability of cells to ions and other solutes was based on a partially incorrect assumption of the membrane theory: that permeant solutes in the external medium cause cell shrinkage. Since exposure to 0.1 M KCl causes cell swelling while exposure to equiosmolar solutions of NaCl and glucose does not, it was believed that the cell membrane is permeable to K^{+} but not to Na^{+} and glucose, and the rate of swelling was used to measure K^{+} permeability. As pointed out in Sections 3.1. and 11.2.4.4, the advent of radioactive tracers and other new techniques permitted more direct measurements of permeability, and experimental studies using radioisotopes soon showed that Na^{+} and glucose are permeant.

12.4.1. Influx of Ions

The more or less equal rate of diffusion of water through the cell surface layer and the cytoplasm of ovarian eggs and barnacle muscle cells suggests a basic similarity of properties of the cell surface and the cell interior. Each is a proteinaceous fixed-charge system containing water in the state of polarized multilayers. As pointed out in Section 4.5.2, the cell surface is a two-dimensional version of the three-dimensional structure of the cell interior. As such, it has fixed anionic sites that adsorb K^+ preferentially over Na^+ , and few K^+ ions find themselves in the polarized water between the fixed anionic sites. Indeed this concept was put into the form of an elementary scheme for ionic permeation through the surface of living cells and models (Ling, 1953), and it is shown here in Fig. 12.14.

Like equilibrium distribution, ionic permeation can be sorted out into a nonsaturable fraction and a saturable fraction. Solute permeation through the interstices (saltatory route, Route 1 in Fig. 12.14) is nonsaturable and shows specificity determined only by the molecular size and complexity of the solute. This pattern is illustrated in Fig. 12.13. Solute entry via the adsorption-desorption route (Route 2) is saturable and highly specific. The entering ion adsorbs onto a fixed anion, librates around it, desorbs and then enters the cell interior.

Based on this model, the rate of entry of the i th ion, V_i , is given as the sum of the ions entering through the water (Route 1) and those entering via the anion sites:

$$V_i = A [p_i]_{ex} + \frac{V_i^{\max} K_i [p_i]_{ex}}{1 + K_i [p_i]_{ex} + K_j [p_j]_{ex}} \quad (12.2)$$

where A is constant; K_i and K_j are the adsorption constants of the i th and j th solutes, whose concentrations in the external solution are expressed as $[p_i]_{ex}$ and $[p_j]_{ex}$, respectively; and V_i^{\max} is the maximum rate of entry of the i th solute. If one plots V_i against $[p_i]_{ex}$, one obtains a composite curve: a straight line representing the saltatory route ($A[p_i]_{ex}$), and a saturable hyperbola representing the adsorption-desorption route. If the saltatory fraction is small, i.e., $V_i^{\max} K \gg A$, or if A can be assessed and the term $A[p_i]_{ex}$ subtracted from the right-hand side of equation (12.2), then

$$V_i = \frac{V_i^{\max} K_i [p_i]_{ex}}{1 + K_i [p_i]_{ex} + K_j [p_j]_{ex}} \quad (12.3)$$

Equation (12.3) can be written in the reciprocal form,

$$\frac{1}{V_i} = \frac{1}{V_i^{\max}} \left(1 + \frac{[p_i]_{ex}}{K_j} \right) \frac{1}{[p_i]_{ex}} + \frac{1}{V_i^{\max}} \quad (12.4)$$

Though based on an entirely different theory, a double reciprocal plot of the rate of solute entry versus the solute concentration is formally identical to one introduced in 1952 by Epstein and Hagen for the entry of Rb^+ into barley roots and based on a membrane carrier model [equation (4.11)]. While experimental data conforming to equations of a form similar to equation (4.11) have been used to describe carrier-

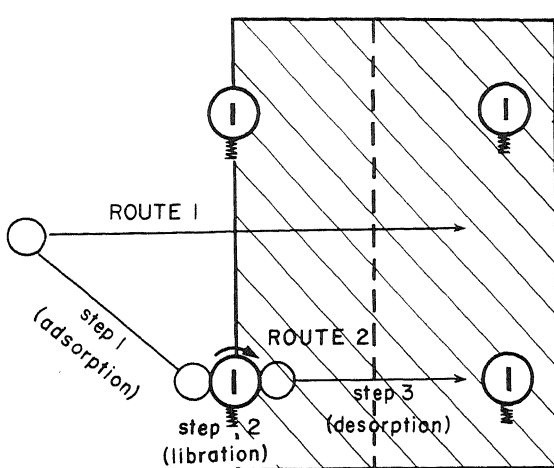


FIGURE 12.14. Diagrammatic illustration of the two routes of ion entry into a fixed-charge system. Shaded area represents a microscopic portion of the surface of a fixed-charge system in which four fixed anions are represented. Route 1 is the saltatory route. Route 2, the adsorption-desorption route, involves a sequence of three steps: adsorption, libration around the fixed anion, and desorption. This adsorption-desorption route corresponds to the doublet type, since two ions are involved (the free cation and the fixed anion). [From Ling and Ochsenfeld (1965), by permission of *Biophysical Journal*.]

mediated transport, these equations by themselves do not differentiate between the carrier model and the AI hypothesis, nor do they differentiate between what conventionally is referred to as "facilitated" diffusion and active transport or pumping. Equation (12.4) describes the entry of a variety of solutes into barley roots (Fig. 4.11), frog muscle (Fig. 4.15), mouse Ehrlich ascites cells (Ling, 1962, p. 314), guinea pig heart muscle (Fig. 12.15), and yeast (Fig. 12.16). Moreover, it describes solute entry into all sorts of inanimate systems that are known to possess fixed anionic charges, including cation exchange resin sheets (Fig. 4.14), oxidized collodion (Ling, 1960), sheep's wool (Fig. 12.17), and

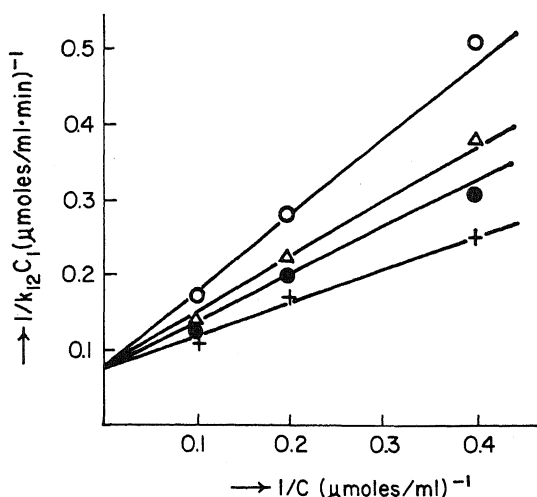


FIGURE 12.15. Double reciprocal plots of the effects of 5 mM (○) or 2.5 mM (△) external Rb^+ and 5 mM external Cs^+ (●) on the initial rate of entry of labeled K^+ into guinea pig heart muscle, at concentrations (C) indicated on the abscissa. Bottom line (+), without competing ion. [From Edelmann *et al.* (1971), by permission of *Biophysik*.]

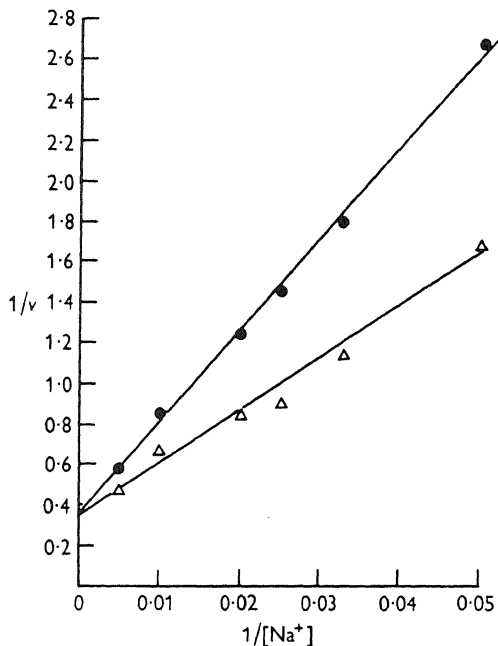


FIGURE 12.16. Demonstration of competitive inhibition of uptake of Na^+ by K^+ during fermentation of yeast. Δ , Sodium acetate alone; ●, sodium acetate with 5 mM potassium acetate. The abscissa is the reciprocal of the concentration (mM) and the ordinate, the reciprocal of the rate of uptake expressed as milliequivalents of Na^+ /kilogram of yeast per minute. While the slope was changed by the presence of K^+ , the intercept of $1/v$ on the ordinate remained the same, indicating competition for the same active site. [From Conway and Duggan (1958), by permission of *Biochemical Journal*.]

even a layer of actomyosin gel (Fig. 12.18). The data of Fig. 12.18 show in fact that the fixed anionic sites do not have to be neatly arranged on the cell surface but can be those distributed at and under the cell surface in the bulk phase system. Therefore, demonstration of competition and saturability in the entry of a cation does not necessarily prove the existence of fixed anions on the cell surface; it only proves the existence of a fixed-charge system. In most cases, it is likely that the surface layer of fixed ion sites determines the initial rate of entry. With prolonged exposure, competition and saturability are retained, but then equation (12.4) begins to merge with equation (11.9), with rate constants blending with equilibrium constants, reflecting properties of bulk phase fixed sites.

For cells and resins whose permeability for ions is rather high, as in the case of K^+ , Rb^+ , and Cs^+ entry into heart muscle (Fig. 12.15) or into ion exchange resin sheets (Fig. 4.14), adsorption and desorption seem adequate to describe the kinetics. In other cases, such as alkali metal ion permeation into frog muscles (Fig. 4.15), somewhat more complicated mechanisms must be involved. This is illustrated by the fact that, while Rb^+ clearly inhibits K^+ entry into frog muscle cells (Fig. 4.15), K^+ does not inhibit Rb^+ entry, as one would expect on the basis of the simple model [equation (12.3)]. Instead, K^+ facilitates Rb^+ entry (Fig. 12.19). A similar facilitory effect of Na^+ on Rb^+ entry was also observed (Ling, 1962, p. 215).

The facilitation of Rb^+ entry by external K^+ or Na^+ is explained by a mechanism introduced originally to explain rapid diffusion of ions along chains of fixed anionic sites (Ling, 1962, p. 336), called the *triplet mechanism* (Fig. 12.20).

In cases where the adsorption energy of the cation on the surface anionic site is

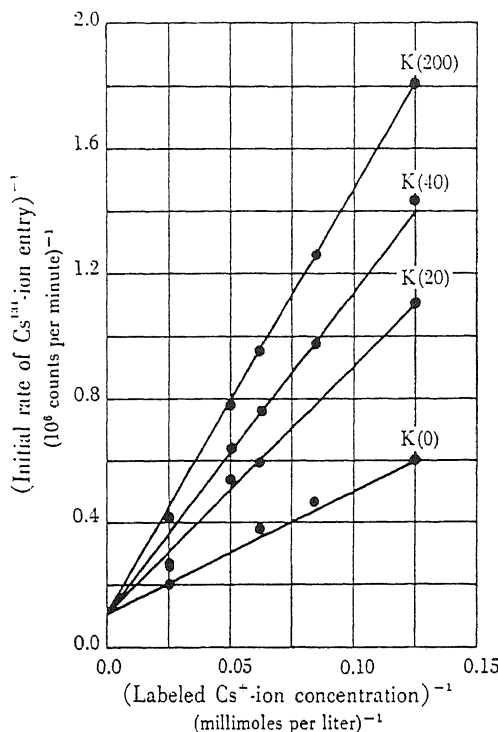


FIGURE 12.17. Effect of varying the external K^+ concentration on the rate of $^{134}\text{Cs}^+$ entry into wool. The experiment was performed on 0.03 g of virgin, scoured, defatted sheep's wool. The values for the K^+ and Cs^+ concentrations are in millimoles per liter (25°C , pH 7.0–7.1). [From Ling (1962).]

strong, the probability of the ion entering the cell by the simple adsorption–desorption route, as depicted in Fig. 12.14, may be statistically unfavorable. Under this condition, desorption can be greatly facilitated by the participation of a second free cation. If the second cation (the lightly shaded K^+ in Fig. 12.20) comes from the same side of the cell surface as the entering ion, it is referred to as the *billiard-type* triplet adsorption–desorption route (Ling and Ochsenfeld, 1965). If the second free ion comes from the phase that the first ion is entering, it involves a libration motion and is called the *pinwheel-type* triplet adsorption–desorption route. The facilitation of Rb^+ entry into frog muscle cells by external K^+ (or Na^+) is of the billiard type. Unfortunately, when triplet routes are involved the adsorption constants can no longer be accurately estimated by double reciprocal plots [equation (12.4)].

12.4.1.1. The Separation of Ions Entering via the Saltatory Route from Those Entering via the Adsorption–Desorption Route

So far the discussion has largely dealt with permeation of strongly adsorbed ions, e.g., K^+ , Rb^+ , and Cs^+ . In the discussion of selective ion accumulation in Chapter 11, it was pointed out that in resting cells most K^+ is adsorbed, but only a fraction of cell Na^+ is in the same state. Because of the much higher concentration of Na^+ in the external medium, half or more of the normal cell Na^+ is found in the cell water. Extending this to the cell surface of muscle cells, one can anticipate that Na^+ entry also must not

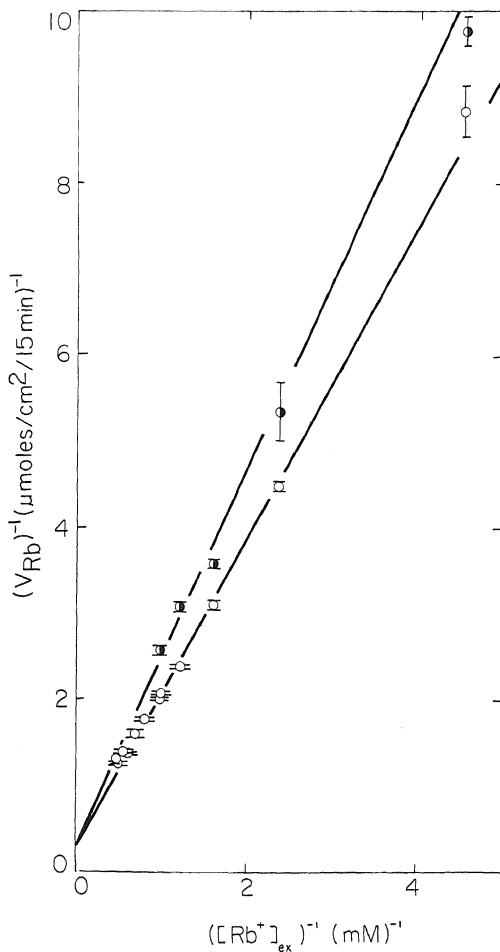


FIGURE 12.18. Effect of nonlabeled Rb^+ on the rate of entry of labeled Rb^+ into actomyosin gel. Lower curve (○) represents the rate of Rb^+ entry with no added competing ion, upper curve (●) the entry with 1.0 mM nonlabeled Rb^+ present. Gel incubated for 15 min at 26°C, followed by 10 sec of washing at 0°C. The pH of the final experimental solution and the washing solution was 6.8. The protein concentration of the gel was 4.28%. Each point represents the average value \pm SE of four individual determinations. [From Ling and Ochsenfeld (1970), by permission of *Physiological Chemistry and Physics*.]

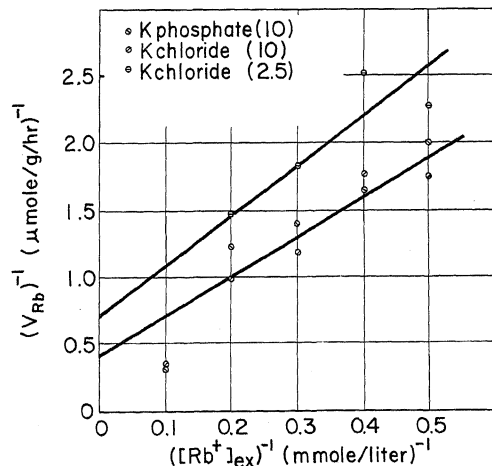


FIGURE 12.19. Facilitatory effect of K^+ ion on the rate of entry of labeled Rb^+ ion into frog sartorius muscles. K^+ (as chloride) concentrations were 2.5 and 10 mmoles/liter. Each point represents a determination on a single muscle. Muscles soaked 30 min at 0°C followed by 10 min of washing at 0°C. [From Ling and Ochsenfeld (1965), by permission of *Biophysical Journal*.]

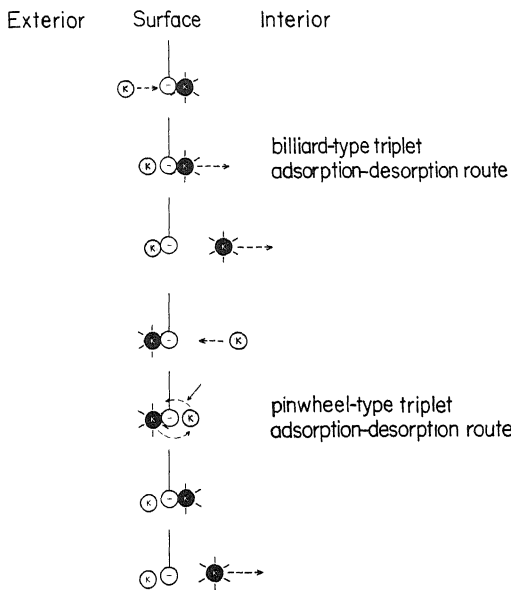


FIGURE 12.20 Diagrammatic illustration of two types of triplet adsorption–desorption modes of entry of labeled ion (●). In one (the billiard type) the third ion (●) comes from the external solute; in the other (the pinwheel type) it comes from the interior of the cell.

be limited to the adsorption–desorption route but must include a substantial fraction entering via the saltatory route (Route 1 in Fig. 12.14). Figure 12.21 presents evidence that supports this anticipation. Increasing external K^+ concentration decreases the rate of entry of labeled Na^+ , but this inhibiting effect reaches a limit beyond which further increase of the external K^+ concentration produces no further inhibition of Na^+ entry. In fact the data suggest that half of the Na^+ enters by the β - and γ -carboxyl groups via the adsorption–desorption route; the other half enters via the saltatory route. This distribution of course is limited to normal frog muscle in a normal environment.

12.4.1.2. *The Nature of the Surface Anionic Sites of Frog Muscle*

The major fixed anions on proteins are the β - and γ -carboxyl groups belonging, respectively, to aspartic and glutamic acid residues. These anionic groups have a pK_a of 4.5. Other anionic groups that can be expected at cell surfaces include sulfonic or sulfate groups, which have a pK_a of 2.0 or lower, and phosphate or polyphosphate groups, which as a rule have a pK_a between 6.1 and 6.5.

Figure 12.22 shows that increasing H^+ concentration in the medium from a pH of 10.5 to pH 6.0 had no discernible effect on the rate of entry of labeled K^+ into frog muscle cells (V_K). When the pH reaches 5.5, V_K begins to decline until at pH 2.5 V_K apparently levels off. The midpoint of the acid titration curve is roughly at a pH of 4.5, confirming the anticipation that it is indeed β - and γ -carboxyl groups that determine the rate of K^+ entry. Evidence to be discussed in Chapter 14 led to the conclusion that

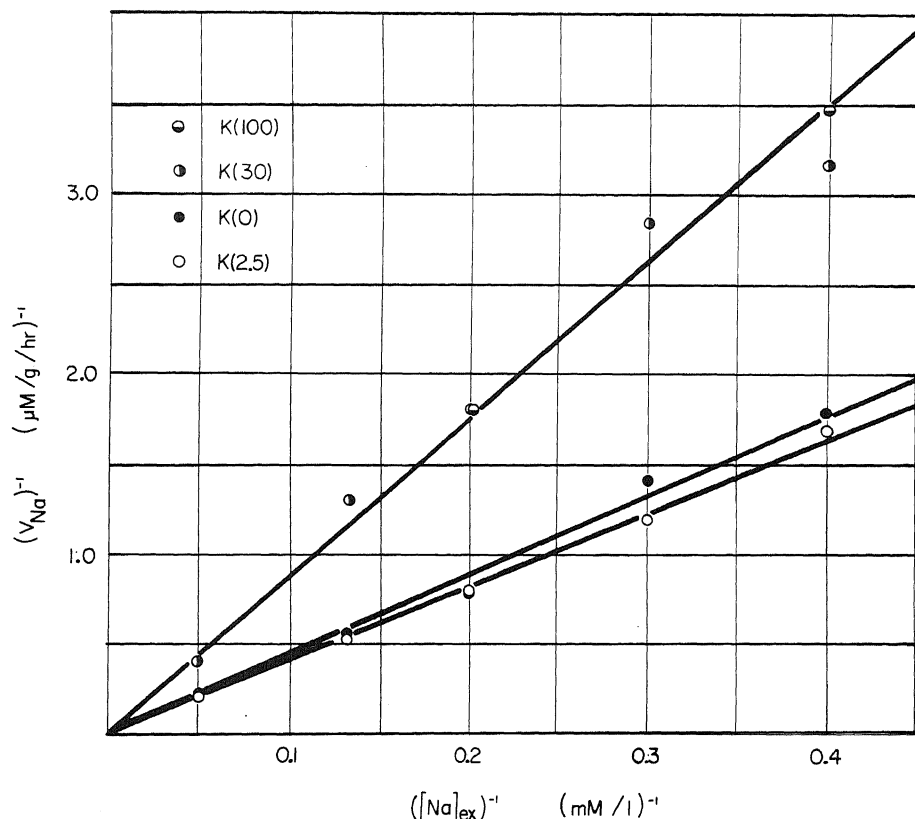


FIGURE 12.21. Effect of various concentrations of K^+ on the initial rate of entry of Na^+ into frog sartorius muscles. Increasing K^+ concentration from 30 to 100 mmoles/liter causes no apparent effect on the rate of Na^+ entry, while reduction from 30 to 2.5 mmoles/liter causes an increased rate of Na^+ entry. Fifteen minutes of soaking at 25°C were followed by washing for 20 min at 0°C. Each point represents the average of three individual determinations. [From Ling and Ochsenfeld (1965), by permission of *Biophysical Journal*.]

on these surfaces β - and γ -carboxyl groups occur as isolated sites and not in pairs or clusters.

12.4.1.3. The Nature of Surface Cationic Sites of Erythrocytes

By extension of the basic principle outlined above for the entry of monovalent cations, one would expect an entirely analogous behavior in anion entry in suitable cells. The most reasonable candidates for the fixed cationic sites would be those provided by the ϵ -amino groups of lysine residues and the guanidyl groups of arginine residues of cell surface proteins. Indeed Passow (1969) has presented evidence that the entry of anions into erythrocytes depends on fixed cationic sites carried by lysine residues.

Among the pieces of evidence that ϵ -amino groups serve a key role in anion permeation into red cells is the demonstration of inhibition by high pH (Passow 1969), by

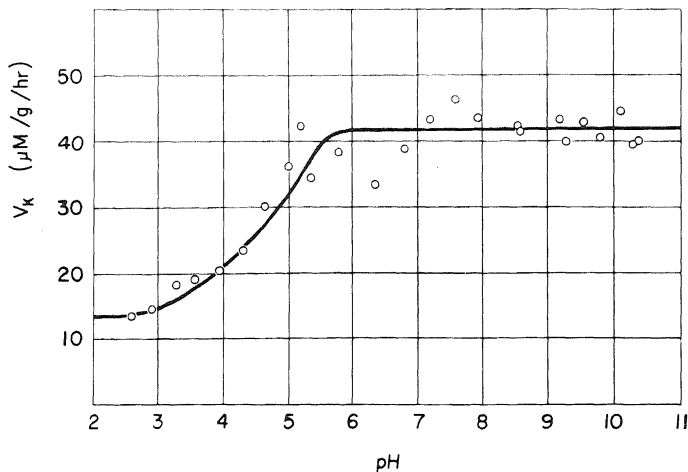


FIGURE 12.22. Effect of pH on the initial rate of entry of labeled K^+ into frog sartorius muscles. Labeled K^+ concentration was 20 mmoles/liter; of phosphate buffer, 10.8 mmoles/liter; of the glycine, succinate, and veronal buffers, 5.4 mmoles/liter. Fifteen minutes of soaking at 25°C were followed by 10 min of washing at 0°C. pHs of experimental solutions were measured after the experiment. Each point represents the average of three individual determinations. [From Ling and Ochsenfeld (1965), by permission of *Bio-physical Journal*.]

amino-group-specific reagents (Rothstein *et al.*, 1976), and by pyridoxal phosphate (Cabantchik *et al.*, 1975).

12.4.2. Efflux of Ions

12.4.2.1. An Apparent Paradox

The initial influx of an ion can be easily obtained simply by exposing the cell or tissue to a solution containing the isotopically labelled ion, p_i , for a brief time. After suitable corrections for extracellular space and other contaminants, the inward flux rate, F_{inw} , can be described by the simple relation

$$F_{\text{inw}} = \frac{d[p_i]_{\text{ex}}}{dt} = k_{\text{inw}}[p_i]_{\text{ex}} \quad (12.5)$$

where F_{inw} , the rate of influx, is in units of moles per liter of cells per second. $[p_i]_{\text{ex}}$ is the concentration (M) of the i th ion under study in the external solution. k_{inw} is the rate constant or exchange constant and is in units of seconds^{-1} ; it is equal to the reciprocal of the time constant, τ , in seconds. The permeability constant κ_{inw} , in centimeters per second, is related to k_{inw} by the equation

$$k_{\text{inw}} = \frac{A}{V} \kappa_{\text{inw}} \quad (12.6)$$

where A and V are the surface area and volume of the cells in question.

TABLE 12.4. Comparison of Data for the Inward Permeation Rate Constant k_2 and the Inward Permeability Constant κ_{inw} in Frog Muscle^a

Ion	Reference	k_2 (hr ⁻¹)	Average	κ_{inw} (cm/sec)	Relative permeability
K^+	Mullins (1959)	1.92	2.97	9.69×10^{-7}	1
	Ling (1962) (25°C)	3.06		15.4×10^{-7}	
	Ling and Ochsenfeld (1965) (24°C)	3.10		15.6×10^{-7}	
	Katz (1966)	3.80		21.1×10^{-7}	
Rb^+	Mullins (1959)	1.04	1.16	5.25×10^{-7}	0.39
	Ling (1962) (25°C)	1.27		6.51×10^{-7}	
Cs^+	Mullins (1959)	0.11	0.24	0.556×10^{-7}	0.081
	Ling (1962) (25°C)	0.36		1.81×10^{-7}	
Na^+	Mullins (1959)	0.085	0.13	0.429×10^{-7}	0.044
	Ling (1962) (20°C)	0.15		0.758×10^{-7}	
	Harris (1950) (18°C)	0.22		1.22×10^{-7}	
	Katz (1966)	0.063		0.35×10^{-7}	
Na^+	Ling (1980b)	1.28		6.47×10^{-7}	0.43

^aFrom Ling (1980b), by permission of *Physiological Chemistry and Physics*.

Using the basic technique, one finds that κ_K for frog muscle is $10-20 \times 10^{-7}$ cm/sec, whereas κ_{Na} is quoted as being some 20 times lower ($0.4-1.2 \times 10^{-7}$ cm/sec) (Table 12.4).

Radioisotopes also are a powerful tool for studying ion efflux. In the conventional membrane pump model of the living cell, in which the membrane is the rate-limiting step in both influx and efflux, exactly analogous conditions govern efflux and influx. Thus, initial ion efflux, F_{outw} , is

$$F_{\text{outw}} = \frac{d[p_i]_{\text{in}}}{dt} = -k_{\text{outw}} [p_i]_{\text{in}} \quad (12.7)$$

and

$$k_{\text{outw}} = \frac{A}{V} \kappa_{\text{outw}} \quad (12.8)$$

where all the symbols have the same meanings as in equations (12.5) and (12.6), except that they refer to efflux. Equation (12.7) can be integrated to yield

$$\ln [p_i]_{\text{in}}^t = \ln [p_i]_{\text{in}}^{t=0} - kt \quad (12.9)$$

where $[p_i]_{\text{in}}^{t=0}$ is the initial i th ion concentration in the cell.

A standard technique for studying ion efflux from frog muscle is to wash the radioactive-isotope-loaded muscle in a stream or successive portions of a nonlabeled Ringer solution. The radioactivity of the cells is continually monitored, or the declining radioactivity in the cell is reconstructed from the radioactivity appearing in the washing solution and that remaining in the cell at the conclusion of the experiment. The result is

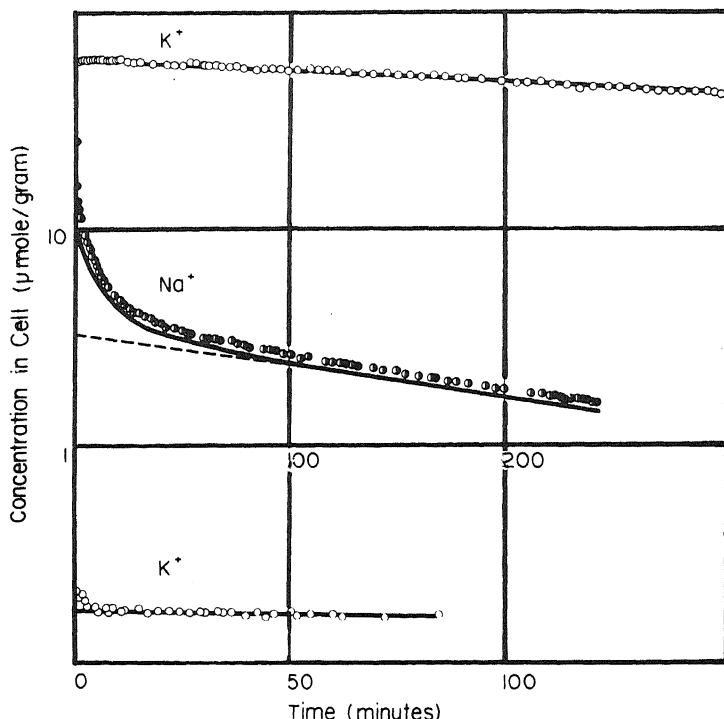


FIGURE 12.23. Time course of efflux of labeled K^+ and Na^+ from frog sartorius muscles. The ordinate represents labeled ion concentration on a logarithmic scale, the abscissa, the time of washing in a nonlabeled Ringer solution. The top curve represents the efflux ($25^\circ C$) of ^{42}K -labeled K^+ from a sartorius muscle previously incubated for 40 hr ($4^\circ C$) in normal Ringer solution containing ^{42}K . The experiment from which the data were taken was prolonged to 600 min with no discernible change of slope throughout the entire period. The amount of $^{42}\text{K}^+$ trapped in the extracellular space and taken up by connective tissue elements is too trivial in comparison with the total cellular content to alter the curve. The middle curve represents the efflux of ^{22}Na -labeled Na^+ from a frog sartorius muscle, previously incubated at $2^\circ C$ in a $^{22}\text{Na}^+$ -labeled Ringer solution for 24 hr. The efflux study was carried out at $0^\circ C$ (essentially the same kind of efflux time course is obtained at $25^\circ C$). The line was drawn according to the experimental points after corrections had been made for isotope trapped in the extracellular space and taken up by connective tissue elements. The bottom curve is the efflux of ^{42}K -labeled K^+ after incubation at $0^\circ C$ in labeled Ringer solution for 7.9 min. Efflux was studied at $0^\circ C$. The line was drawn according to the experimental points after correction had been made. [From Ling (1966b), by permission of *Annals of the New York Academy of Sciences*.]

plotted semilogarithmically according to equation (12.9); typical experiments are shown in Fig. 12.23.

From equation (12.9), one also derives the relation

$$k_{\text{outw}} = \frac{\ln 2}{t_{1/2}} = \frac{0.692}{t_{1/2}} \quad (12.10)$$

where $t_{1/2}$ is the half-time of exchange, i.e., the time it takes for the labeled ion concentration in the cells to fall to one half of its initial value.

Permeation of ions, according to Hodgkin and Katz, is asymmetrically affected by the electrical potential, ψ ; to obtain the true permeability constants, P_K and P_{Na} , the

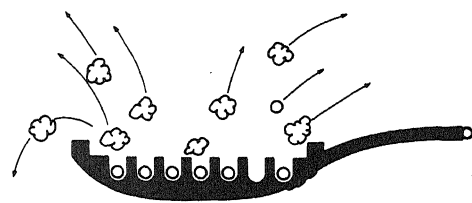


FIGURE 12.24. Popcorn model. Large pieces of popped corn, which cannot fall into a low-energy position at the bottoms of small holes in the heated pan, pop out more frequently than smaller pieces that fall into the holes.

corresponding κ_{inv} or κ_{out} is multiplied by a factor $(\psi F/RT)/[1 - \exp(-\psi F/RT)]$ (Katz, 1966). This factor is 3.5 for a monovalent cation moving outward from muscle cells and 0.108 for one moving inward. Since K^+ and Na^+ are both monovalent cations, the same factor is needed to convert κ_{inv}^K to P_K and ψ_{inv}^{Na} to P_{Na} . Thus $P_K/P_{Na} = \kappa_{\text{inv}}^K/\kappa_{\text{inv}}^{Na}$ and $P_K/P_{Na} = \kappa_{\text{outw}}^K/\kappa_{\text{outw}}^{Na}$. Since $\kappa_{\text{inv}}^K/\kappa_{\text{inv}}^{Na} = 20$, P_K/P_{Na} calculated on the basis of influx data is 20.

One can find $\kappa_{\text{outw}}^K/\kappa_{\text{outw}}^{Na}$ from the K^+ and Na^+ efflux studies. Since $\kappa_{\text{outw}} = 0.692/t_{1/2} \cdot V/A$, $\kappa_{\text{outw}}^K/\kappa_{\text{outw}}^{Na} = t_{1/2}^{Na}/t_{1/2}^K$. For frog muscle according to the conventional view, $t_{1/2}^{Na}$ is 30 min; $t_{1/2}^K$ is 600 min, and $P_K/P_{Na} = 1/20$. Thus P_K/P_{Na} is 20 to 1 in favor of K^+ when calculated from influx data but 1 to 20 in favor of Na^+ when calculated from the efflux data!* A paradox appears on hand.

While a complete quantitative solution of this paradox lies in the future, qualitatively the AI hypothesis offers some general ideas to deal with it. It should also be mentioned that part of the inconsistency comes from faulty interpretation of experimental data. These and other fine points will be discussed in the next section.

From Chapter 8, we know that the bulk of cell K^+ is preferentially adsorbed. Half of cell Na^+ is also adsorbed but less tightly than K^+ ; the remainder is free and dissolved in cell water (Table 8.6). Therefore cell Na^+ , free and adsorbed, exists in a higher-energy state than cell K^+ . The popcorn analogy shown in Figure 12.24 illustrates this point: small pieces of popped corn (like K^+) find themselves at the bottom of the lower-energy wells and do not bounce out of the pan as fast as the larger ones (like Na^+). This explains why K^+ efflux is much slower than Na^+ efflux. On the other hand, if we regard an empty pan as a model of the cell surface and scoop up from a pan containing equal numbers of large and small pieces of popped corn, we would have collected more small pieces than large ones, because the spaces represented by the narrow pits (anionic adsorption sites) are available to small ones (K^+) but not to large ones (Na^+). This explains why K^+ is more “permeable” than Na^+ from influx measurements.

12.4.2.2. K^+ Efflux and Its Dependence on External K^+ Concentration

A cation exchange resin bead or sheet charged with radioactive-isotope-labeled cations and washed in distilled water at a pH above neutral loses little radioactivity (Fig. 12.25). This phenomenon follows from the law of the conservation of macroscopic electroneutrality. To demonstrate this, Guggenheim (1950) cited the case of a charged

*Proponents of the membrane pump theory often ascribe this inconsistency to differences in mechanisms: Na^+ is actively pumped out while exchange of K^+ and influx of Na^+ are all passive. This explanation presumes that the rate of inward passive leakage of Na^+ is determined by the rate of its outward pumping. If this were correct, inward leakage of Na^+ would stop when the pump stops, hardly a reasonable conjecture.

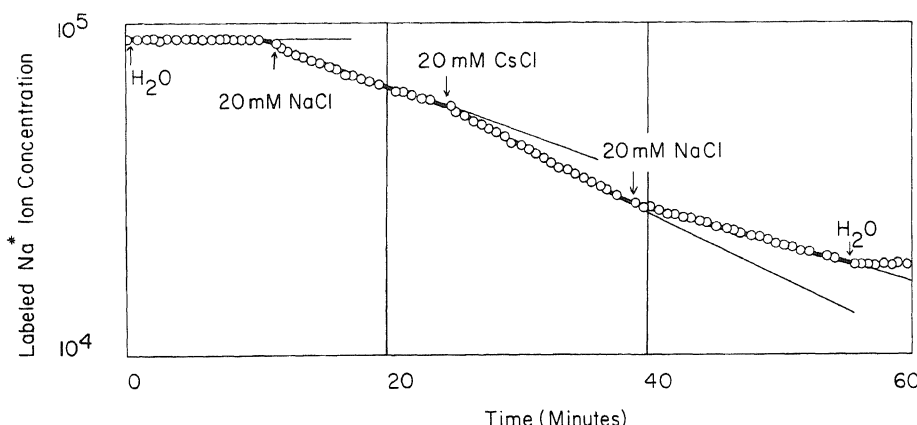


FIGURE 12.25. $^{22}\text{Na}^+$ concentration in a loaded sulfonate ion exchange resin sheet washed first in distilled water and then in 20 mM NaCl or 20 mM CsCl. [From Ling (unpublished).]

sphere 1 cm in diameter suspended in a vacuum that is given an excess charge of 10^{-10} g ions of valency +1. Though this amount of charged ion is so minute that it cannot be detected by chemical means, it would create an electrical potential of approximately 10 million volts. The law of macroscopic electroneutrality forbids any chemically measurable amount of counterion to leave the system unless (1) it is accompanied by an equal number of anions—which is not feasible since all the available anions are attached to the resin matrix, or (2) by exchange with an equivalent number of free cations. Distilled water at a high pH contains virtually no free cations to exchange. Therefore the labeled counterion remains in the resin system. However, if a salt is dissolved in the external medium, then an exchange process will proceed until ultimately all the original labeled ion leaves the system (Fig. 12.25).

Figure 12.25 shows that the rate of efflux of labeled Na^+ depends not merely on the external ion concentration but also on the nature of the cation in the washing medium. In sulfonate ion exchange resin Cs^+ is more strongly preferred over Na^+ (Helferich, 1962, p. 169). Therefore Cs^+ accelerates labeled Na^+ efflux more than does Na^+ . This observation is of considerable importance, because it indicates that ionic adsorption-desorption is dependent on specific ion-for-ion exchange, subject to differences in short-range forces, and is not just an exchange of one charge for another.

When frog muscles loaded with $^{42}\text{K}^+$ were washed in Ringer solutions containing increasing concentrations of K^+ (at the expense of equivalent amounts of Na^+) and the data plotted semilogarithmically, the slope of the efflux increased with each increment of external K^+ concentration (Fig. 12.26). If the exchange constants are plotted against the external K^+ concentration, one finds curves like those shown in Fig. 12.27. There appears to be both a saturable and a nonsaturable fraction. Figure 12.28 shows similar data in the inanimate sulfonate cation exchange resin sheets. The exchange constants of labeled Cs^+ plotted against the concentration of external Na^+ yield a curve (Fig. 12.29) very similar to that shown in Fig. 12.27. It is my belief that the basic mechanisms in these effluxes are similar. Referring to Fig. 12.20, one sees that the activating effect of

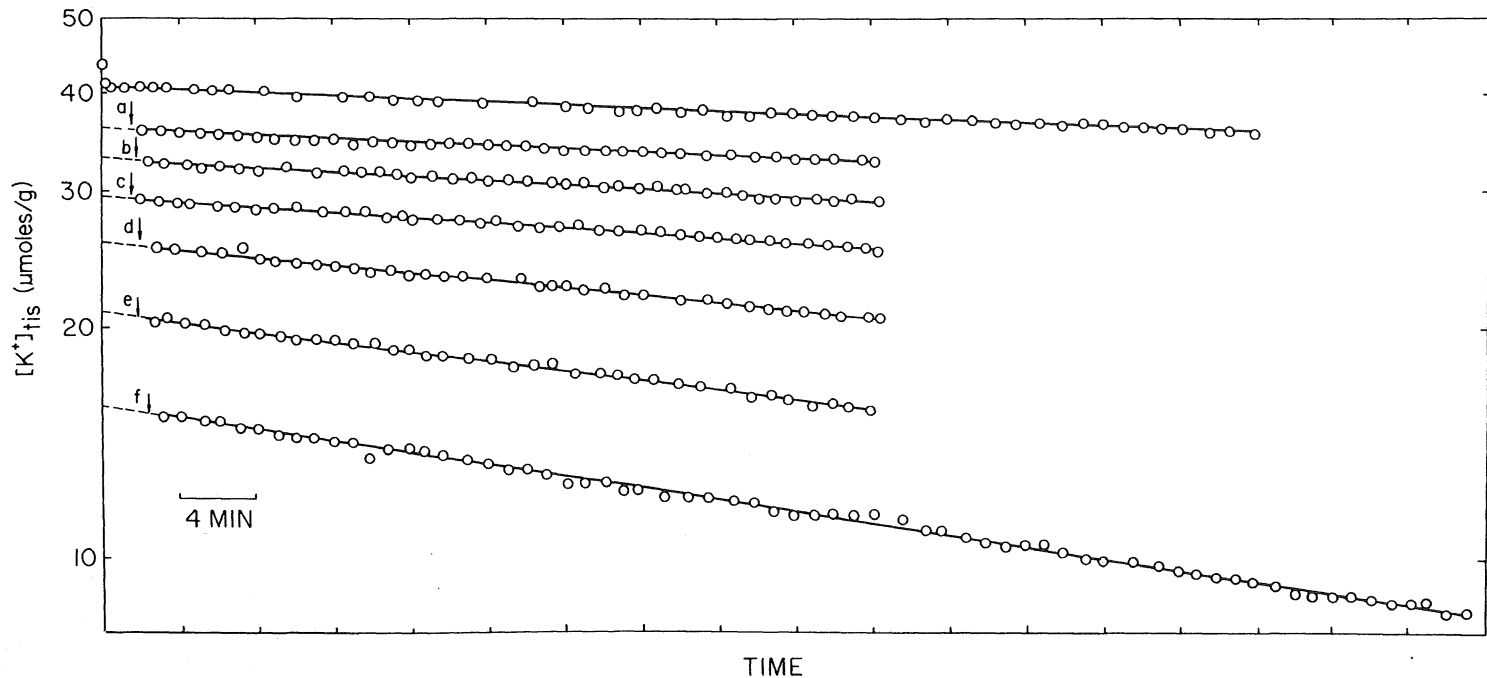


FIGURE 12.26. Time course of loss of radioactivity in $^{42}\text{K}^+$ -loaded frog sartorius muscle when washed (25°C) with a normal Ringer solution containing 2.5 mM K^+ and then with Ringer solutions containing increasing concentrations of K^+ (a, 3.33 mM; b, 5.0 mM; c, 10.0 mM; d, 20.0 mM; e, 40 mM; f, 100 mM). Ordinate represents $^{42}\text{K}^+$ remaining in the muscle. [From Ling (unpublished).]

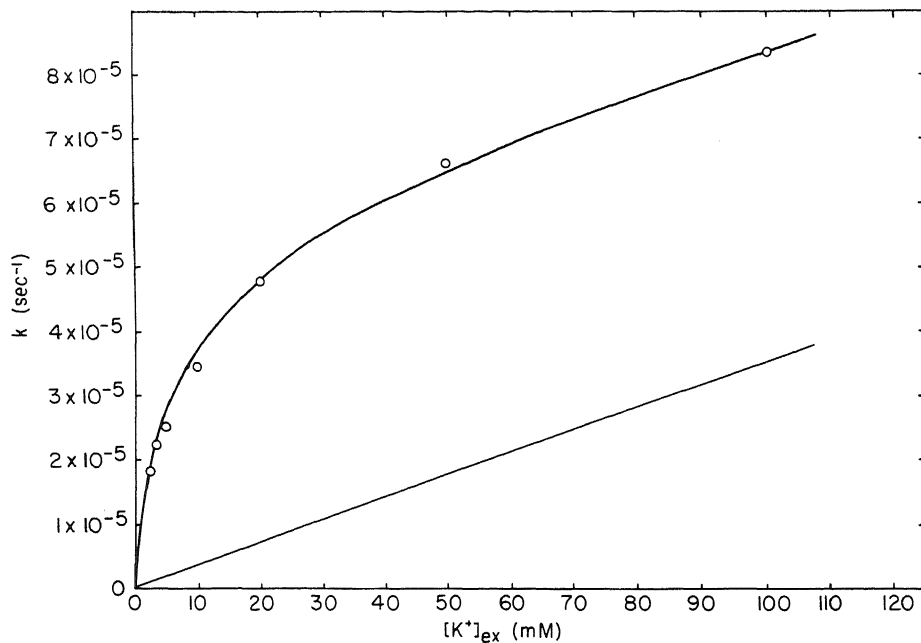


FIGURE 12.27. Plot of the rate constants k (sec^{-1}) from data given in Fig. 12.26 against K^+ concentration in the washing solution. Data can be plotted with a hyperbola superimposed on a straight line. [From Ling (unpublished).]

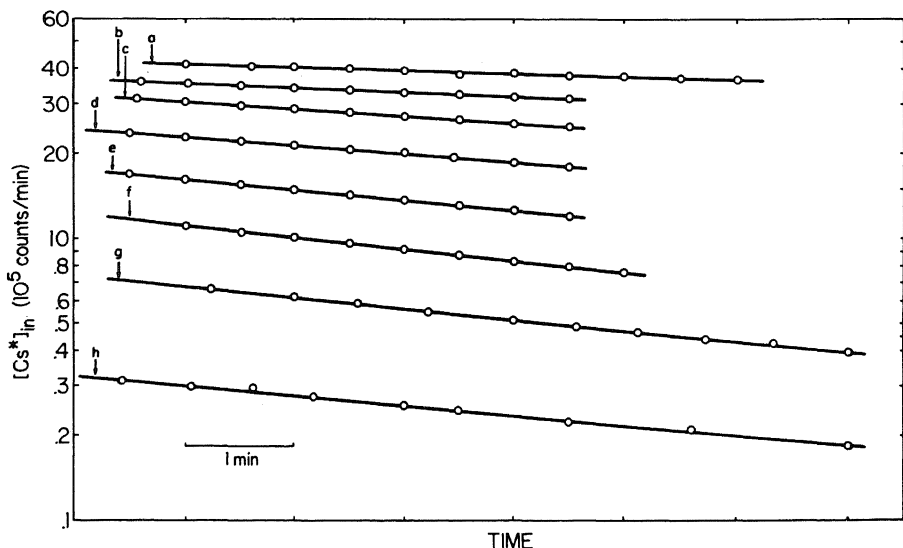


FIGURE 12.28. Time course of loss of radioactivity in $^{134}\text{Cs}^+$ -loaded sulfonate ion exchange sheet when washed in a solution containing increasing concentrations of NaCl (a, 1.66 mM; b, 2.5 mM; c, 3.33 mM; d, 10 mM; e, 20 mM; f, 40 mM; g, 100 mM; h, 200 mM). [From Ling (unpublished).]

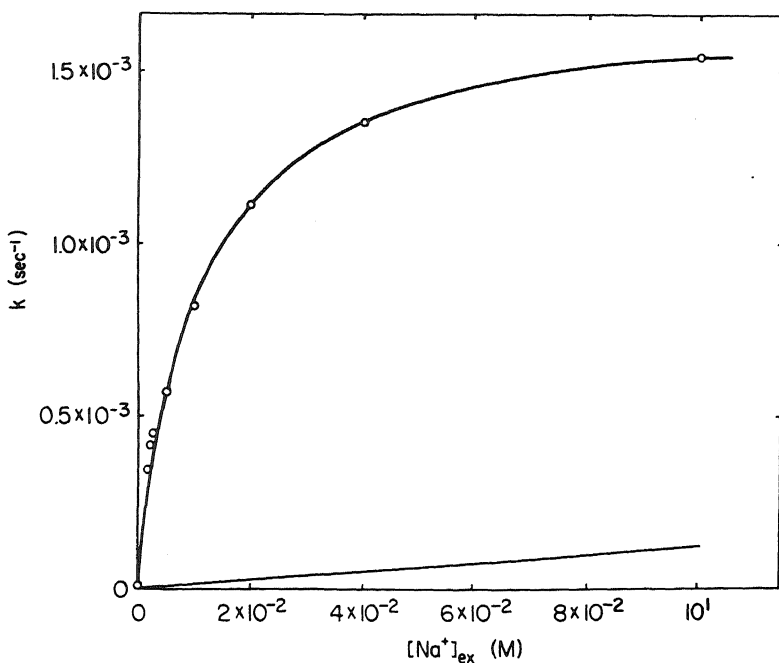


FIGURE 12.29. Plot of the rate constants k (sec^{-1}) of labeled Cs^+ efflux from data given in Fig. 12.28 against Na^+ concentration in the washing solution. Data can be fitted with a hyperbola superimposed on a straight line. [From Ling (unpublished).]

external ion involves primarily the pinwheel type of triplet mechanism. This type of activity is saturable since the number of labeled K^+ ions adsorbed onto surface fixed anions is limited. The nonsaturable fraction can be due to a combination of cation exchange via the saltatory route (Fig. 12.14) and exit as pairs with free anions that have entered through the interstices.

In recent years, the question has been raised of whether the slow fraction of Na^+ exchange is far too slow to be compatible with the expected rate of desorption from fixed anions, as for example of K^+ from valinomycin (Shporer and Civan, 1978; Edzes and Berendsen, 1975). To answer, let us turn to Fig. 12.25, which shows desorption from fixed anionic sites in the ion exchange resin sheet surface. Clearly, the rate is not in milliseconds but very much slower, with $t_{1/2}$ in the range of many minutes or hours. Furthermore, this rate intimately depends on both the concentration and the nature of similar ions in the free solution bathing the fixed sites. In living cells, owing to the low q -value, the free ion concentration in the cell water is much lower and therefore the rate of desorption of adsorbed ion would be much slower than if these sites were exposed directly to a Ringer solution.

12.4.2.3. The Nature of the Rate-Limiting Steps of the Fast and Slow Fractions of Na^+ Efflux from Frog Muscle

When Levi and Ussing (1948) first reported their study of the efflux of labeled Na^+ from frog sartorius muscle, they noted that the efflux curve was not a simple

straight line on a semilogarithmic plot, as for example it is in the case of labeled K⁺ efflux (see Fig. 12.23). Instead, the curve can be easily resolved into two fractions: a fast fraction with a $t_{1/2}$ of a few minutes and a slow fraction with a $t_{1/2}$ of about 30 min (Fig. 3.3). These authors concluded that the fast fraction corresponds to Na⁺ trapped in the extracellular space; the slow fraction then comes from the cells. Although the original assignment of the source of the fast fraction as being entirely extracellular in origin has been questioned, most workers adhered to the view that the 30-min (slow) fraction is rate-limited by the permeation of Na⁺ through the cell membrane.

In the last twenty years or so, my laboratory has become deeply involved in the question of the origin of the fast and slow fractions. Our conclusions are as follows: (1) The fast fraction is only partly due to Na⁺ trapped in the extracellular space. (2) A second fast fraction with a $t_{1/2}$ of 3 min represents free Na⁺ in the cell, its efflux rate limited by passage through the cell surface. (3) The slow fraction with $t_{1/2}$ of about 25 min represents adsorbed Na⁺, its rate determined by the rate of desorption. For complete discussion of all the reasoning leading to these conclusions, the reader should consult the original publications cited in the following paragraphs. Several of the more important arguments are presented here.

1. Na⁺ efflux from single muscle fibers (freed of tendons) that have no extracellular space shows the typical two fractions seen in whole muscles (Ling *et al.*, 1973).
2. Removal of labeled Na⁺ by a centrifugation technique (Ling and Walton, 1975a) and correction for contribution from connective tissue elements does not remove the fast fraction, even though parallel corrections in the case of simultaneously recorded K⁺ efflux from the same muscle produced a single straight line in the semilogarithmic plot (Ling and Walton, 1975b) (Fig. 12.30).
3. Very brief exposure (3–5 min) of isolated muscle fiber bundles containing from 14 to 60 single cells to labeled Na⁺, followed by centrifugation to remove extracellular space fluid, revealed two typical fractions in efflux curves. The cells remained in exactly the same chemical environment throughout the whole incubation and washout process. Under these conditions the Na⁺ permeability can be assessed from two quantities: (a) the amount of labeled Na⁺ that had entered the cells from the zero time intercept of the efflux curve, divided by the time of exposure to the labeled Na⁺ and (b) the $t_{1/2}$ of the same efflux curve. Only the fraction of the efflux curve which truly represents the surface-limited process yields the same value for the inward permeability rate as obtained by the two methods. Experimental results (Table 12.5) show that it is the fast fraction with a $t_{1/2}$ of 3 min and not the slow fraction ($t_{1/2} = 25$ min) that represents surface permeation of Na⁺.
4. In muscles slowly dying from exposure to low concentrations of iodoacetate, the slow fraction either does not change or undergoes changes of no fixed direction. It is the fast fraction that steadily increases in size until its concentration approaches the concentration of Na⁺ found in the incubation solution. This suggests that the fast fraction represents Na⁺ in the cell water, and as the cells die, the q -value for Na⁺, and hence the free Na⁺ level in the cells, steadily increases until it reaches the same concentration as in the bathing medium (Fig. 12.31).

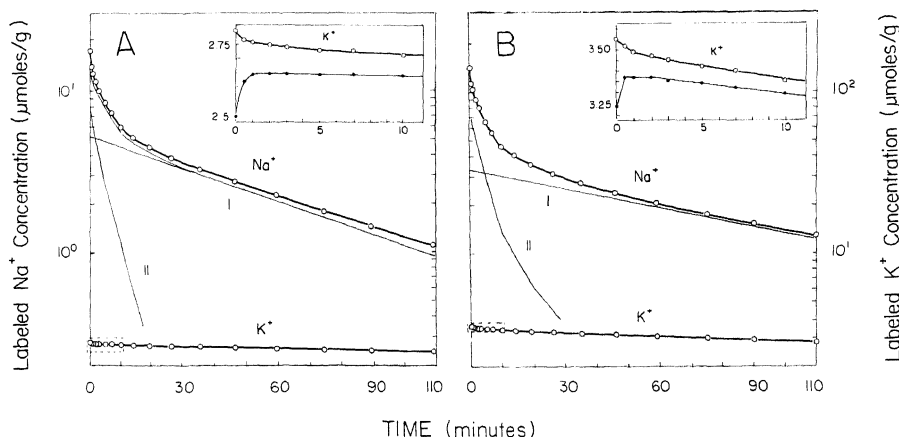


FIGURE 12.30. Time course of simultaneous Na^+ and K^+ efflux from centrifuged frog sartorius muscles. The muscles were incubated overnight at 25°C with labeled Na^+ . Labeled K^+ was added to the solution for the final 43 min of incubation. The muscles were centrifuged at 1000g for 4 min before washing in successive tubes of Ringer-phosphate solution at 25°C. Correction for connective tissue was made on the basis of a composite curve of $^{22}\text{Na}^+$ efflux from similarly incubated connective tissues. The ordinate is in $\mu\text{moles per gram}$ of fresh muscle tissue. Line I was obtained after a 7% connective tissue correction. An enlargement of the first 10 min of K^+ efflux for each muscle is illustrated with the connective tissue correction to show that the overcorrection for the connective tissue contribution revealed in the K^+ efflux does not significantly alter the two-component efflux of Na^+ . [From Ling and Walton (1975b), by permission of *Physiological Chemistry and Physics*.]

Neither the fast nor the slow fraction shows any consistent reduction of its rate of efflux from the beginning in a normal muscle till its eventual death.

From these and other findings it is clear that the Na^+ permeabilities of frog muscle that have been cited are no longer correct. As shown in the last line of Table 12.4, the revised inward permeability constant is 6.4×10^{-7} cm/sec, and therefore only 2–3 times smaller than that for K^+ . It is not difficult to understand how underestimates were

TABLE 12.5. $^{22}\text{Na}^+$ Efflux from Frog Muscle^{a,b}

$^{22}\text{Na}^+$ efflux				Influx rate (mmoles/liter \times min)					
Slow fraction		Fast fraction		Slow fraction			Fast fraction		
Intercept (mM)	$t_{1/2}$ (min)	Intercept (mM)	$t_{1/2}$ (mM)	From slope (A)	From intercept (B)	B/A (%)	From slope (A)	From intercept (B)	B/A (%)
4.07 \pm 0.36	25.1 \pm 1.86	5.76 \pm 0.48	3.17 \pm 0.17	0.22 \pm 0.02	0.96 \pm 0.063	481 \pm 395	2.25 \pm 0.14	2.41 \pm 0.19	107 \pm 3.6

^aTwenty-two muscle fiber bundles were studied. The number of fibers ranged from 14 to 60. Cells were briefly exposed to $^{22}\text{Na}^+$ (3.0–5.0 min, plus the first 1–5 min of the centrifugation process to remove the extracellular labeled $^{22}\text{Na}^+$). $^{22}\text{Na}^+$ efflux was then determined, and an analysis of the data which resembled those plotted in Fig. 12.23, is given on the left under “ $^{22}\text{Na}^+$ efflux.” $^{22}\text{Na}^+$ influx was then calculated in two ways (from slope or from intercept) for both the slow and the fast fractions. The ratio B/A of near 1.0 (107%) for the fast fraction shows that it must be the surface-limited one.

^bFrom Ling (1980b), by permission of *Physiological Chemistry and Physics*.

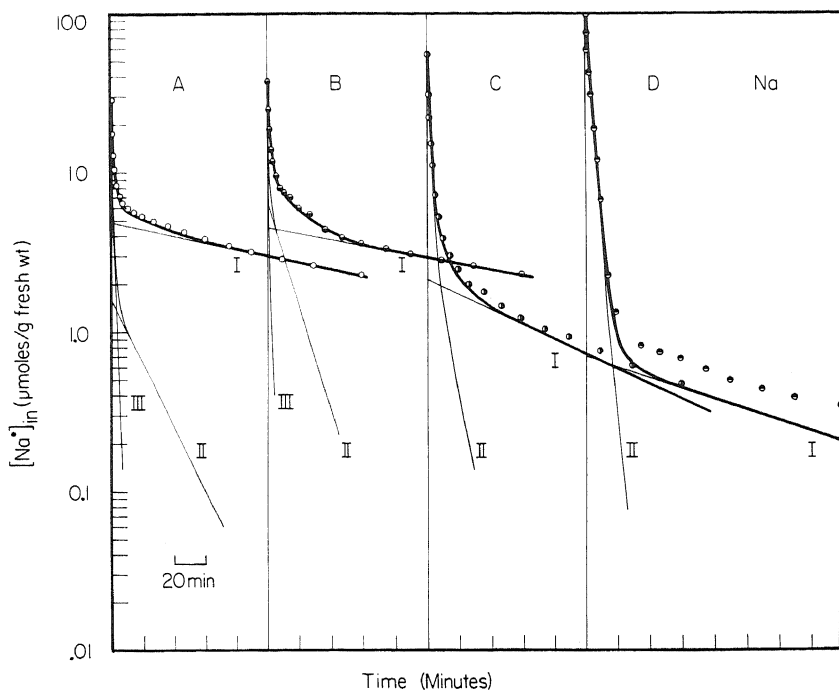


FIGURE 12.31. Successive efflux curves of labeled Na^+ in a dying frog sartorius muscle repeatedly loaded with labeled Na^+ and washed in Ringer solution containing 10 mM KCl and 0.05 mM sodium iodoacetate. Curve A was the first washing curve, curve B the next, and so on. Heavy solid lines are the best-fitting curve to the experimental points after subtracting the contribution of the connective tissue. These corrected curves were then resolved into a slow fraction (I) and a fast fraction (II) or fractions (II, III). [From Ling *et al.* (1981), by permission of *Journal of Cell Physiology*.]

made in the older published data. Most of the data cited were obtained from efflux data with the assumption that the slow fraction is rate-limited by passage through the cell surface. In the cases where the data were obtained by influx studies (Ling, 1962, p. 312), 5–10 min of washing at 0°C, intended to remove only extracellular space fluid, also removed most of the fast fraction.

12.4.2.4. The Correspondence of the Nonsaturable and Saturable Fractions of Equilibrium Ion Levels and the Rapidly and Slowly Exchanging Fractions of Ions in Human Lymphocytes

Negendank and Shaller (1979a, 1980b) reviewed the literature and showed widespread observation of fast and slow fractions in the flux of cations in a variety of living cells. Working with human lymphocytes they found that both K^+ and Na^+ efflux have fast and slow fractions. They then offered evidence that the fast fractions represent free Na^+ or K^+ in the cell water and the slow fractions represent adsorbed Na^+ or K^+ . According to the AI hypothesis, the fast fraction represents free K^+ or Na^+ and should correspond to the nonsaturable fraction described by the first term on the right-hand

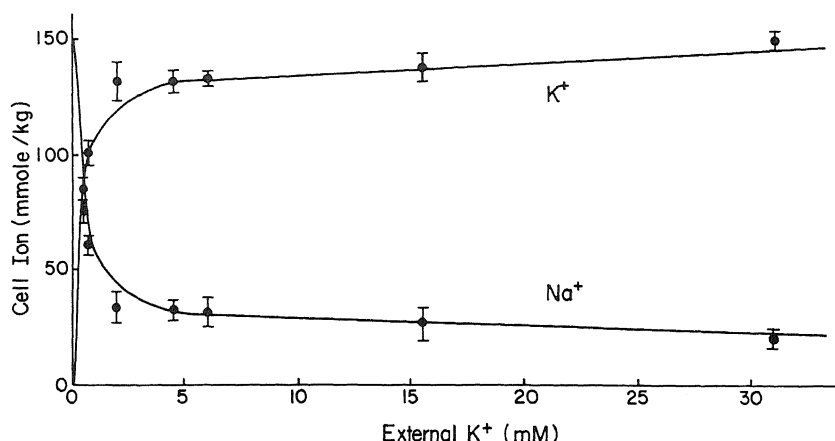


FIGURE 12.32. Cell K⁺ and Na⁺ contents of human lymphocytes (means \pm SEM). [From Negendank and Shaller (1979b), by permission of *Journal of Cell Physiology*.]

side of equation (11.5); the slow fraction, on the other hand, represents adsorbed K⁺ or Na⁺ and should correspond to the saturable fraction described by the second term on the right-hand side of equation (11.5). From the equilibrium distribution data shown in Fig. 12.32, Negendank and Shaller obtained the magnitude of the nonsaturable K⁺ and plotted it against the fast fraction of K⁺ from efflux studies under identical conditions (Fig. 12.33). A correlation was established with $r = +0.82$. Since the sum of the fast and slow fractions is equal to the sum of the saturable and nonsaturable fractions, this correlation implies a similar positive correlation between the slow fraction and the nonsaturable adsorbed fraction.

12.4.2.5. Amphibian Ovarian Eggs: Further Insight into the Nature of the Fast and Slow Fractions

When frog ovarian eggs were exposed for increasing lengths of time to a labeled Ringer solution containing radioactive $^{22}\text{Na}^+$ and the efflux of labeled Na⁺ was then

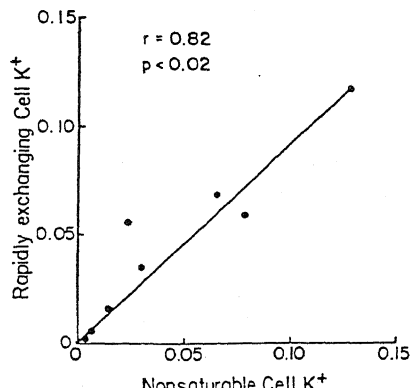


FIGURE 12.33. Correlation between rapidly exchanging cell K⁺ and nonsaturable cell K⁺ in human lymphocytes. Significance was determined from the correlation coefficient, r , by the t -test. [From Negendank and Shaller (1979b), by permission of *Journal of Cell Physiology*.]

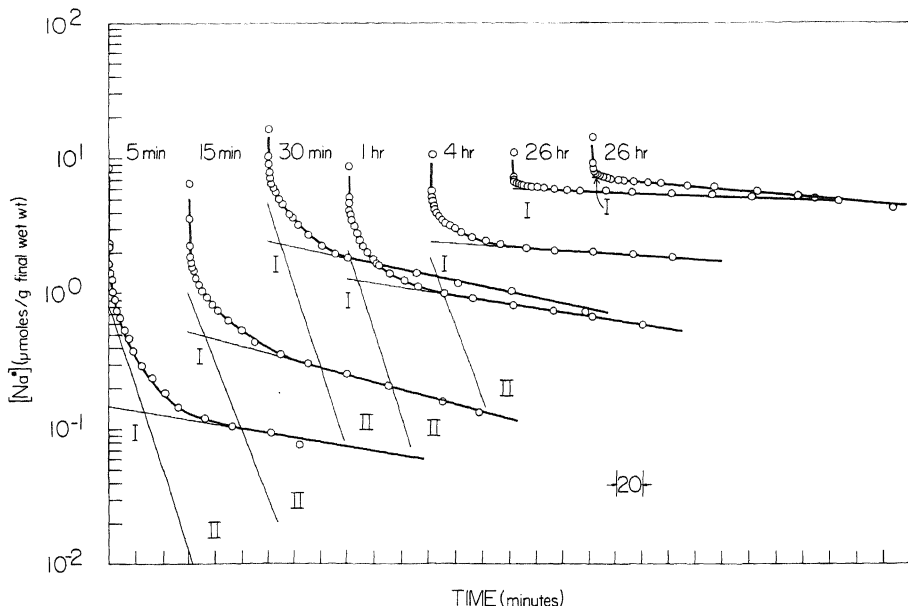


FIGURE 12.34. Labeled Na^+ efflux of single frog ovarian eggs after exposure to labeled Ringer solution for different lengths of time. Exposure times ranged from 5 min to 26 hr, as indicated in graph. Distance between ends of arrows represents 20 min time interval. Lines representing the fast fraction (fraction II) are not given for eggs with 26 hr of exposure to labeled Na^+ . [From Ling and Ochsenfeld (1977a), by permission of *Physiological Chemistry and Physics*.]

studied, the family of efflux curves shown in Fig. 12.34 was obtained. Each curve can be resolved into a slow and a fast fraction. A plot of the magnitude of the fast fraction against the time of exposure shows that this fraction reaches a steady level after 30–40 min of exposure and remains constant from then on (Fig. 12.35A) while the slow fraction continues to increase long after 4 hr of exposure (Fig. 12.35B) (Ling and Ochsenfeld, 1977b).

In trying to explain the fast fraction of Na^+ in muscle, various investigators have suggested that it exists in separate regions of the cell, such as the sarcolemma (Carey and Conway, 1954) or the sarcoplasmic reticulum (SR) (Rogus and Zierler, 1970; Zierler, 1972). I have already pointed out that dispersive X-ray microprobe analyses (Somlyo *et al.*, 1977) showed Na^+ distribution to be even throughout normal frog muscle cells and not in agreement with the suggestion that Na^+ is localized in the sarcolemma or the SR. It is in the study of frog ovarian eggs, which have no SR, that one gets very clear evidence that the fast fraction, which reaches equilibrium after 44 min of exposure, in fact has reached all areas of the cell, even though this $^{22}\text{Na}^+$ has exchanged with the adsorbed fraction to a limited extent.

Figure 12.36 reproduces the radioautograph of Abelson and Duryee (1949). $^{22}\text{Na}^+$ has permeated and reached a high concentration in the entire nucleus after 30 min, even though there is no direct pathway between the external solution and the nucleus except the cytoplasm, which contains a lower level of $^{22}\text{Na}^+$. After a much longer period of exposure, the cytoplasm becomes progressively darker and darker. A similar demonstra-

tion of rapid equilibration of $^{22}\text{Na}^+$ with a globule of gelatin injected into salamander eggs tells the same story (S. B. Horowitz *et al.*, 1979; Horowitz and Paine, 1979), but the most recent work of Paine *et al.* (1981), discussed in Chapter 11 (Figs. 11.12 and 11.13), demonstrates that the initial preferential darkening of the nucleus (Fig. 12.36) is due to a high q -value for Na^+ in the nucleus and a low q -value in the cytoplasm.*

In the course of our study of Na^+ efflux from frog ovarian eggs, we found that, while the great majority of eggs exhibit two-fraction efflux curves, occasionally eggs are observed to have only a single component (Ling and Ochsenfeld, 1977a). Similarly, among the large number of Na^+ efflux studies of frog sartorius muscle we carried out, on three occasions we obtained a single surface-limited efflux of Na^+ . Apparently, the Na^+ permeability of the cell surface can switch from the usual high- Na^+ -permeability state to a low- Na^+ permeability state, and this effect will be considered again in Section 12.4.2.7.

12.4.2.6. Coupling of K^+ Influx and Na^+ Efflux

An important argument for the hypothesis of a coupled K^+ - Na^+ pump was based on the observation, in cuttlefish axon, erythrocytes, and other cells, of a slowdown in the rate of Na^+ efflux when the external K^+ concentration was reduced below normal (E. S. Harris and Maisels, 1951; Keynes, 1954; Glynn, 1954; T. I. Shaw, 1954; Hodgkin and Keynes, 1955b). In cells that have a single surface-limited Na^+ efflux, removal of external K^+ could be expected to slow Na^+ efflux on the basis of the model shown in Fig. 12.20. A reduction of external K^+ concentration, however, produces hardly any change in the Na^+ efflux from frog muscle (Fig. 12.37). That is not to say that lowering of external K^+ has no effect. *Rather, to reduce the apparent efflux rate of labeled Na^+ , the low- K^+ environment must be applied while the muscle cells are being loaded with radioactive $^{22}\text{Na}^+$.* Figure 12.38 shows the effect of increasing the duration of exposure of frog muscles to a "K⁺-free" Ringer solution containing 100 mM ^{22}Na -labeled Na^+ . As time goes on, less $^{22}\text{Na}^+$ is in the fast fraction and more is in the slow fraction. This is the same effect noted in oocytes (Fig. 12.34), but is a consequence of the autocooperative shift of the adsorption sites from a normal K^+ state to a Na^+ state, discussed at length in the preceding chapter. With this in mind, it is readily understandable why removal of K^+ from the washing solution has an effect on Na^+ efflux only when the muscle was previously in the presence of K⁺-free $^{22}\text{Na}^+$, because this procedure affects only the adsorbed Na^+ .

Earlier, I presented the equilibrium cooperative adsorption isotherm [equation (7.19)] based on the one-dimensional Ising model. Some time ago Glauber (1963) suggested a time-dependent Ising model, but it unfortunately has severe theoretical limitations. Two later developments of this basic model were given by Karreman (1971) and Huang (1979). Figure 12.39 presents theoretical curves of Huang and Seitz (1980) for the kinetics of adsorption of a solute with varying values of the nearest neighbor interaction from $-\gamma/2 = 0$ to $-\gamma/2 = 2.0$. The kinetic uptake curve becomes more and more sigmoidal as $-\gamma/2$ increases. Figure 12.40 plots the magnitude of the slow frac-

*This interpretation is not entirely correct (see footnote on p. 331). The nucleus may also contain Na^+ -adsorbing sites.

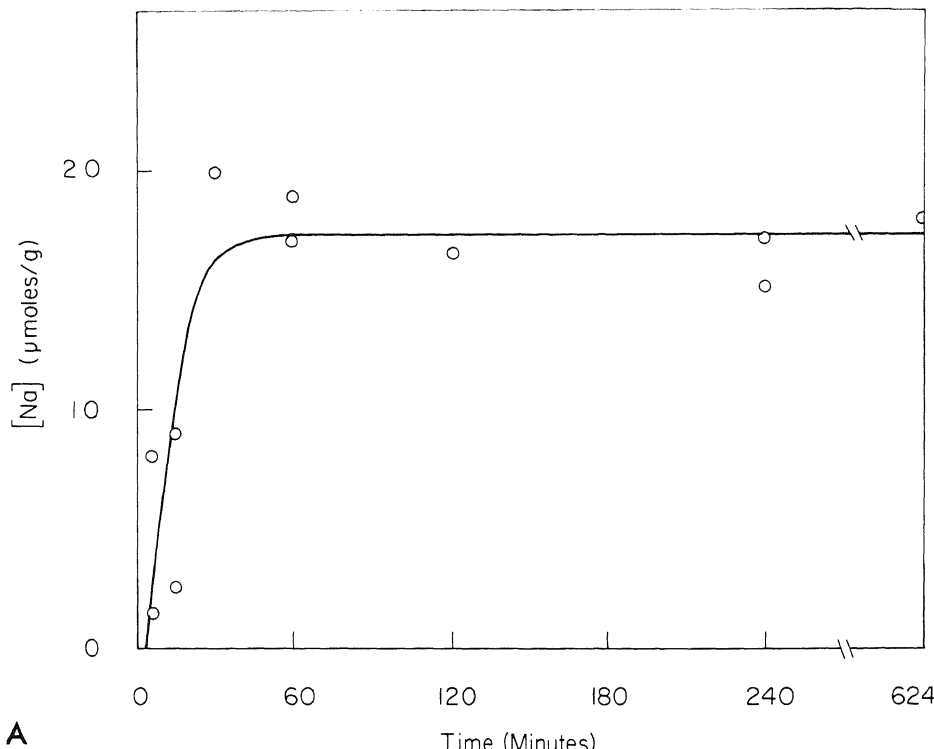
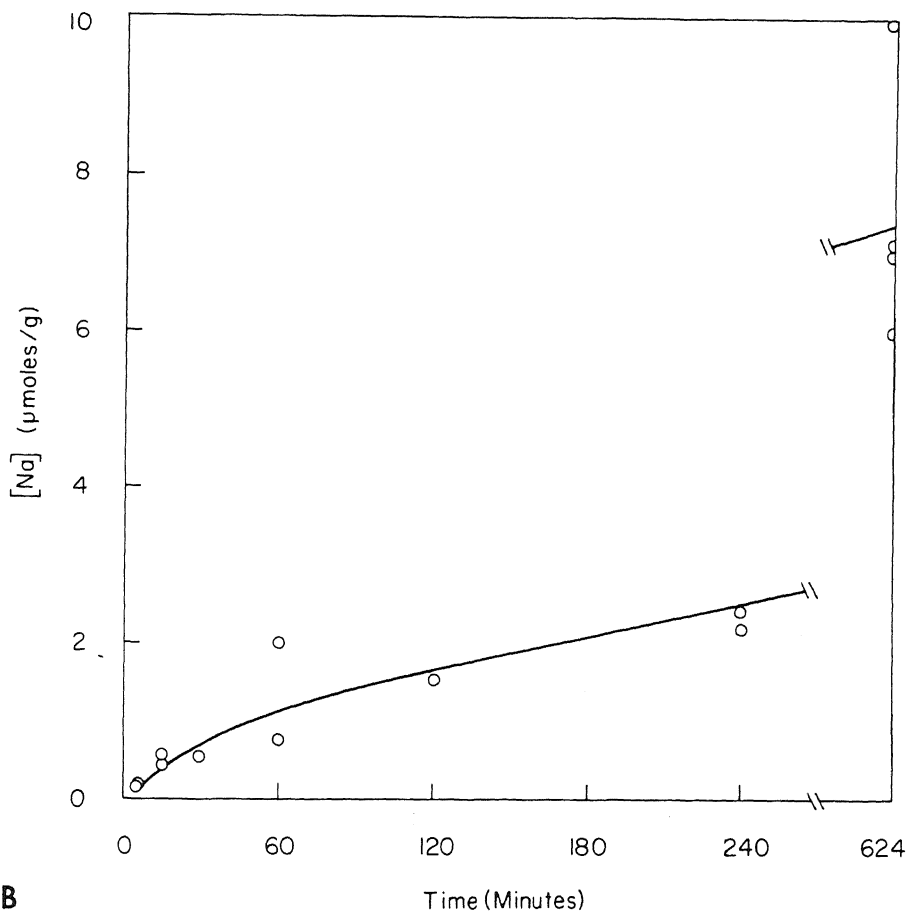


FIGURE 12.35. (A) Time course of the increase in magnitude of the fast fraction of labeled Na^+ with increasing duration of exposure to labeled Na^+ in the data of Fig. 12.34. Data indicate rapid increase, with attainment of equilibrium in about 30 min. (B) Time course of the increase in magnitude of the slow fraction

tion of labeled Na^+ in frog muscle against the time of exposure to K^+ -free labeled Na^+ . In general, the curve resembles the theoretical curves in Fig. 12.39 with a relatively large value of $-\gamma/2$. Negendank and Shaller carried out the converse experiment in human lymphocytes in that they studied the time course of reuptake of K^+ in K^+ -depleted, Na^+ -loaded cells. The sigmoidal uptake curve of their data is shown in Fig. 12.41 (Negendank and Karreman, 1979). The solid line is a theoretical curve calculated from Karreman's equation (Karreman, 1971). Figure 12.42 shows their average data points and a theoretical curve calculated on the basis of Huang's equations, with only a single adjustable parameter α determined by the slope of the curve at $t = 0$ (Huang and Negendank, 1980). The other two parameters, corresponding to $K_{\text{Na}-\text{K}}^{00}$ and $-\gamma/2$, were those derived previously from equilibrium studies (Fig. 11.22D).

12.4.2.7. Effect of Cardiac Glycosides on the Na^+ Fluxes: Another Apparent Paradox

In Na^+ efflux studies of frog muscle, exposure to the cardiac glycoside ouabain (10^{-7} M) caused little change in the efflux rate for the next 4 hr (Fig. 12.43, curve C). However, when the same concentration of ouabain was added to the $^{22}\text{Na}^+$ -containing preloading solution, a marked slowdown of the Na^+ efflux occurred, as indicated by an



of labeled Na^+ with increasing duration of exposure to labeled Na^+ in the data of Fig. 12.34. Data indicate slow gain and failure to attain equilibrium even after exposure of 26 hr. [From Ling and Ochsenfeld (1977a), by permission of *Physiological Chemistry and Physics*.]

eightfold increase of $t_{1/2}$ (Fig. 12.43, curve A). Thus the effect of ouabain is similar to the effect of K^+ depletion: To produce a discernible effect on $^{22}\text{Na}^+$ efflux, both ouabain and K^+ depletion have to be applied while the cells are exposed to the radioactive labeled Na^+ . Both involve a time-dependent switch from K^+ occupancy of the adsorption sites to Na^+ occupancy.

As is clearly indicated in Fig. 12.43, simultaneous exposure to 10^{-7} M ouabain and $^{22}\text{Na}^+$ also changed the two-fraction Na^+ exchange to a single surface-limited fraction. In contrast to normal frog muscle and normal frog egg in which labeled Na^+ leaves the cell with a $t_{1/2}$ of only a few minutes, now $t_{1/2}$ has slowed down to 290 min. If the cell membrane alone is the rate-limiting step in Na^+ exchange, one could expect a great slowdown of the Na^+ influx as a result of ouabain treatment. Yet, P. Horowitz and Gerber (1965) clearly showed that this is not the case. Even at a concentration of 10^{-5}

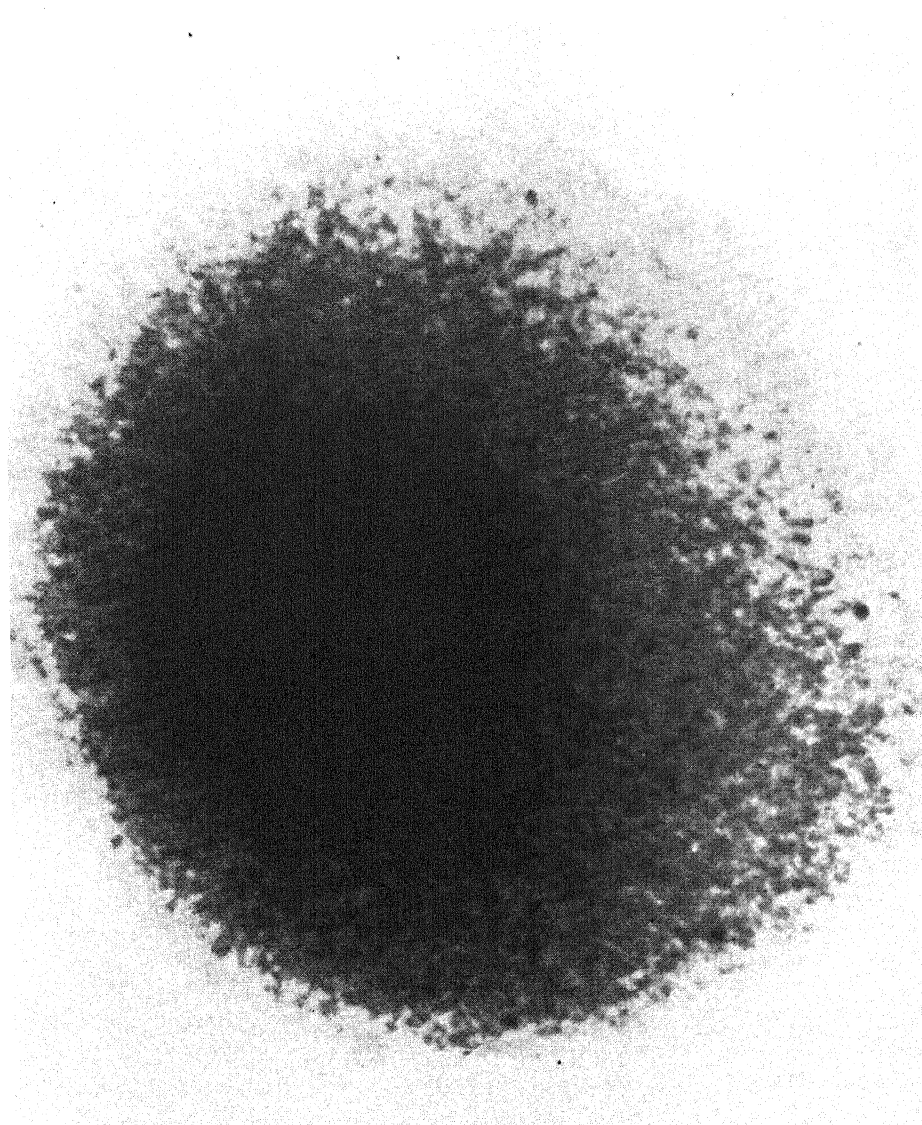


FIGURE 12.36. Radioautograph of a frog egg exposed to $^{24}\text{Na}^+$ for 30 min. After soaking in Ringer solution containing $^{24}\text{Na}^+$, the egg was frozen in liquid air and sectioned meridionally. The dark circle on the left side corresponds to the size and position of the nucleus, which appears vividly white in the frozen section, in contrast to the darker cytoplasm surrounding it. [From Abelson and Duryee (1949), by permission of *Biological Bulletin*.]

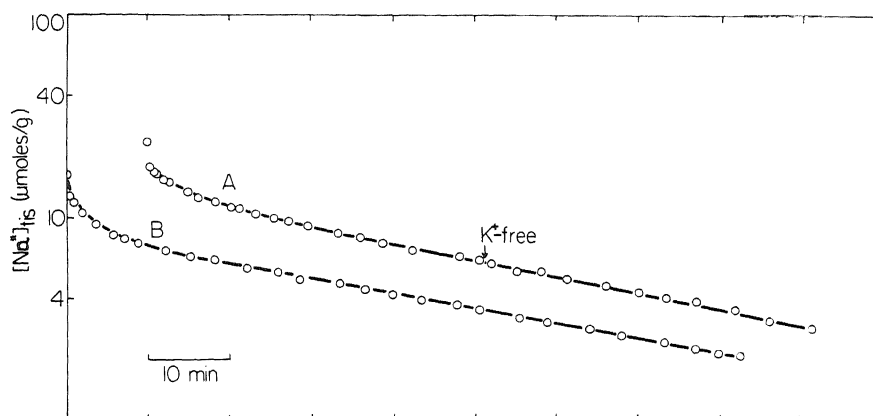


FIGURE 12.37. Lack of effect of lowering external K^+ concentration on the rate of Na^+ efflux after the loaded muscle had been washed in normal Ringer solution for 40 min. Control and experimental muscles were pairs from the same frog incubated in the same ^{22}Na -tagged Ringer GIB medium and otherwise treated in the same way. Washout solution was normal Ringer solution ($K^+ = 2.5$ mM) for both experimental (A) and control (B) muscle until the 40th minute, after which the experimental muscle alone was switched to K^+ -free washing solution. [From Ling (1978b), by permission of *Physiological Chemistry and Physics*.]

M, strophanthidin had no effect on Na^+ influx into frog muscles. Since there may be some quantitative differences between the two cardiac glycosides ouabain and strophanthidin, Ling and Ochsenfeld also conducted a series of studies using ouabain. Their results, shown in Table 12.6, confirmed and extended Horowitz and Gerber's finding. In fact ouabain at 10^{-7} M actually accelerates Na^+ influx. Again an apparent paradox seems to have developed. Again an explanation can be found on the basis of the AI hypothesis: The effect of ouabain is to change the system in such a way that cell-surface Na^+ takes on the characteristics of surface K^+ in normal cells. The surface anionic sites shown in Fig. 12.14 now prefer Na^+ over K^+ , and Na^+ entry and exit both become surface-limited (as described for K^+ in Section 12.4.2.2).

TABLE 12.6. $^{22}Na^+$ Permeability into Ouabain-Treated Frog Sartorius Muscle^{a,b}

	[Ouabain] (M)	κ_{Na} (cm/sec)	[K] _{in} (μmoles/g)	[Na] _{in} (μmoles/g)
A	0	4.25 ± 0.43	103.7 ± 2.11	16.5 ± 1.34
B	3.27×10^{-7}	5.22 ± 0.54	10.8 ± 2.21	105.9 ± 4.16
C	3.27×10^{-7}	5.48 ± 1.15	23.1 ± 2.72	96.6 ± 2.99

^aSartorius muscles isolated from *Rana pipiens pipiens* were incubated in a Ringer solution for 72 hr at 25°C. B and C solutions contained 3.27×10^{-7} M ouabain; however, for the last 4 hr of incubation, C was transferred to a solution containing no ouabain. All samples were then treated for 5 min in ^{22}Na -tagged Ringer solution, A and C containing no ouabain, B with 3.27×10^{-7} M ouabain. Extracellular space was removed by the centrifugation method (Ling and Walton, 1975a) and a correction for the contribution of connective tissue elements was made.

^bFrom Ling and Ochsenfeld (unpublished).

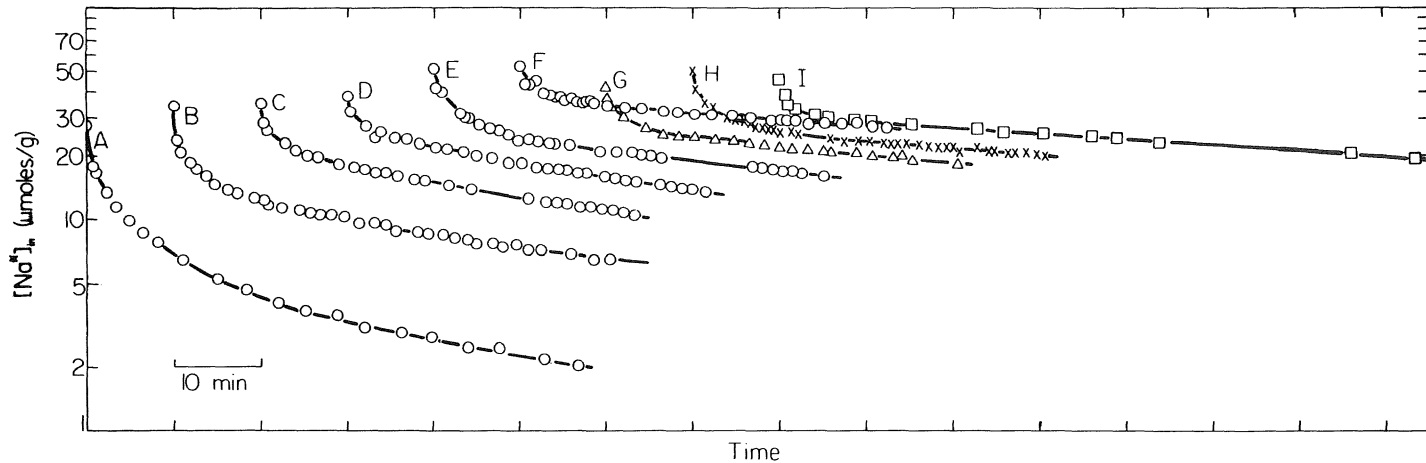


FIGURE 12.38. Effect of the duration of exposure to $^{22}\text{Na}^+$ -containing K^+ -free solution on the $^{22}\text{Na}^+$ efflux rate. From left to right, the duration of incubation increases thus: A, 40 min; B, 2.5 hr; C, 3.5 hr; D, 4.5 hr; E, 6 hr 23 min; F, 8 hr; G, 8 hr 37 min; H, 12 hr 42 min; and I, 18 hr 40 min. [From Ling (1978b), by permission of *Physiological Chemistry and Physics*.]

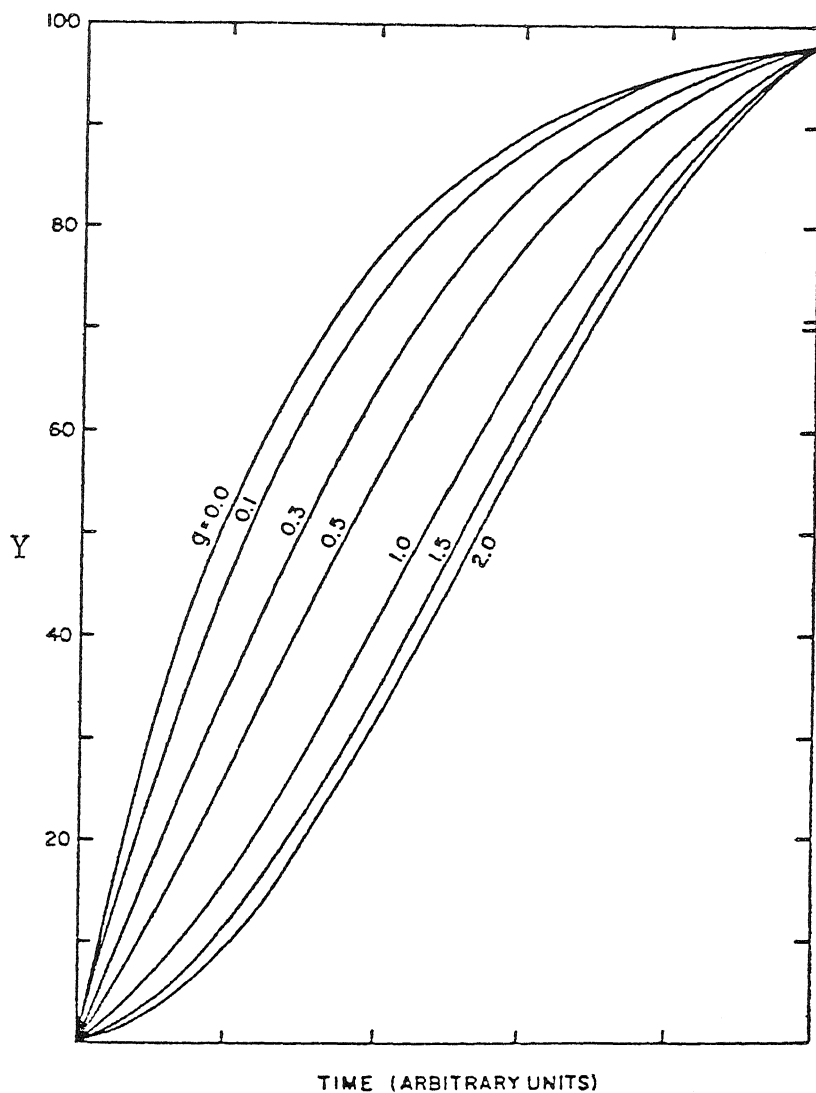


FIGURE 12.39. Kinetics of the Ising model for various choices of interaction parameter g . The choice $g = 0$ is the result for classical noninteracting systems. Qualitative deviations from this single exponential occur with increasing subunit interaction. The ordinate Y is the fraction of total adsorption sites that are occupied. g is equal to $-\gamma/2$ in equation (7.19). [From Huang and Seitz (1980), by permission of Pergamon Press.]

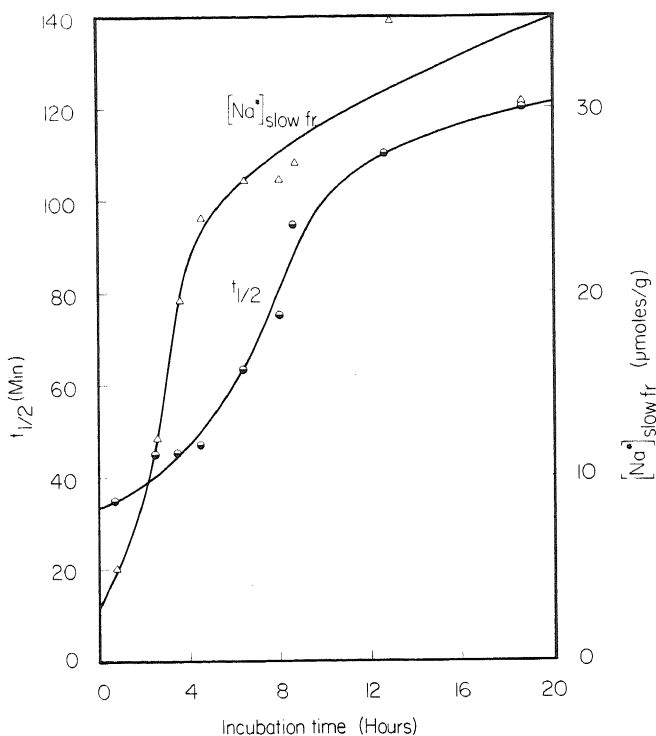


FIGURE 12.40. Relation of duration of incubation in a $^{22}\text{Na}^+$ -containing K^+ -free solution to magnitude of slow fraction, $[\text{Na}^+]_{\text{slow fr.}}$, and apparent $t_{1/2}$ of efflux curve, in frog muscle. [From Ling (1978b), by permission of *Physiological Chemistry and Physics*.]

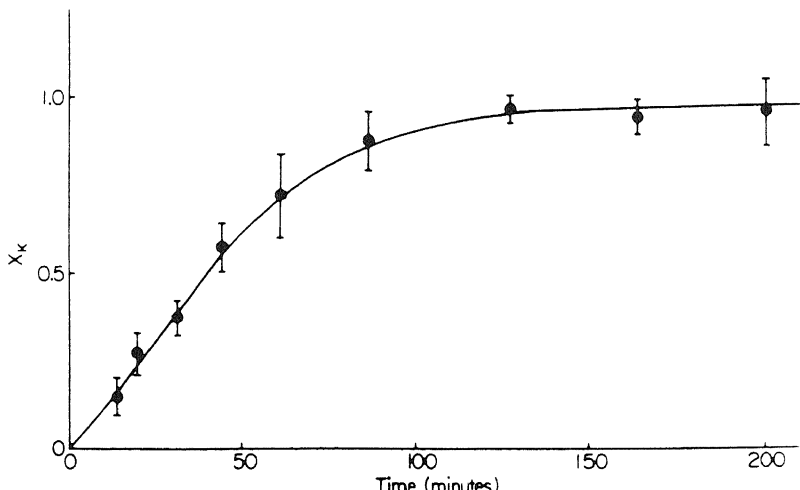


FIGURE 12.41. Time course of K^+ - Na^+ exchange in human lymphocytes. Cells depleted of K^+ were exposed to $[\text{K}^+]_{\text{ex}}$ equal to 5.4 mM containing 100 μCi of ^{42}K at 0 time. Points are means \pm SD of data accumulated in seven experiments. The curve is theoretical, normalized to a time of half-saturation of 40 min. X_{K^+} is the fraction of K^+ taken up, with $X_{\text{K}^+} = 1$ at the saturation level. [From Negendank and Karreman (1979), by permission of *Journal of Cell Physiology*.]

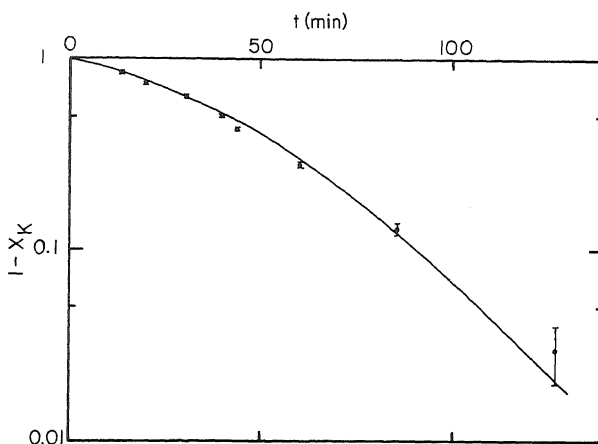


FIGURE 12.42. K^+ uptake in K^+ -depleted Na^+ -loaded cells as a function of time. The data are from Fig. 12.41. [From Huang and Negendank (1980), by permission of *Journal of Chemical Physics*.]

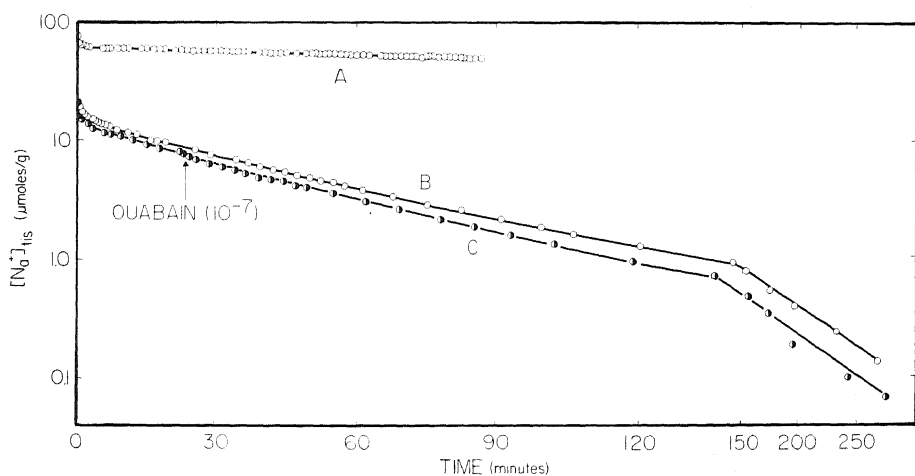


FIGURE 12.43. Effect of ouabain on the Na^+ efflux of frog sartorius muscle. B and C were the Na^+ effluxes of a pair of sartorius muscles from the same animal incubated in $^{22}Na^+$ -labeled normal Ringer phosphate (NRP) for the same length of time (18 hr at 25°C). Whereas both B and C were washed in NRP during the first 23 min, only C was switched to a Ringer solution containing 10^{-7} M ouabain. Note change of scale of abscissa after 150 min. A was incubated in a similar $^{22}Na^+$ -containing NRP for the same length of time at the same temperature, except this preincubation solution contained 10^{-7} M ouabain. The washing solution for A was NRP containing no ouabain. [From Ling and Palmer (1972), by permission of *Physiological Chemistry and Physics*.]

12.5. Sugar Permeation and Its Control by Insulin

In Section 11.2.4.4, evidence was presented that insulin increases D-glucose adsorption in frog muscle. Without insulin, glucose distribution follows a linear relation to external concentration and is nonsaturable. Exposure to insulin adds a saturable fraction to this nonsaturable one (Fig. 11.42).

Studies of the efflux of labeled D-glucose from muscles whose endogenous insulin had been removed (Fig. 12.44) and from muscles which had been loaded with insulin (Fig. 12.45) substantiate this concept. These efflux curves, after correcting for labeled glucose trapped in the extracellular space, can be resolved into a fast and a slow fraction. The concentration of the slowly exchanging fraction is plotted against the external glucose concentration from insulin-free muscles in Fig. 12.46C and from muscles treated with different concentrations of insulin in Fig. 12.46A,B,D. The fast fractions from all these sets of data are plotted together in Fig. 12.47. It is clear that the fast fraction of glucose is rectilinear and thus nonsaturable in all cases, the slope yielding a single q -value of about 0.1. Insulin treatment had no significant effect on this fraction. In contrast, insulin affects primarily the slowly exchanging fraction. The insulin-induced fraction exhibits saturability and competition, much as we have obtained in equilibrium studies (Chapter 11). These analyses demonstrate once more the correspondence of the nonsaturable fraction of solute accumulation with the rapidly exchanging fraction and that of the saturable fraction with the slowly exchanging fraction, as Negendank and

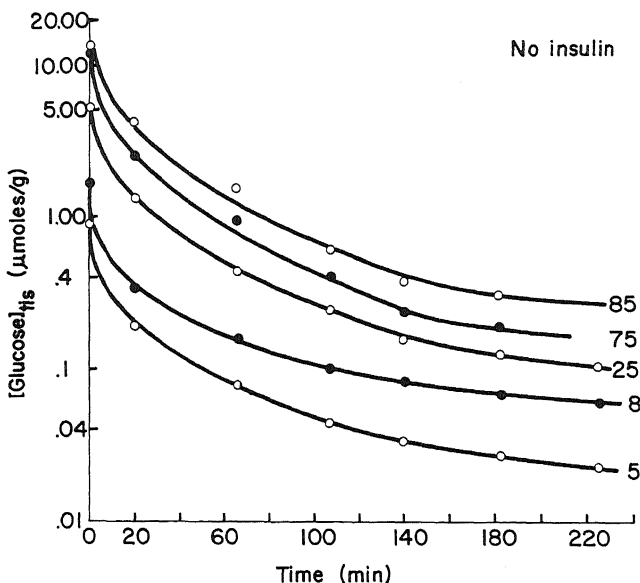


FIGURE 12.44. Labeled D-glucose efflux curves of frog sartorius muscles exhaustively washed in insulin-free Ringer solution to remove endogenous insulin before incubation at 0°C in labeled D-glucose of various concentrations (given in millimolarity at the end of each curve). Ordinate refers to labeled D-glucose remaining in the tissue and is in units of $\mu\text{moles per gram of fresh muscle}$. [From Ling (1983a), by permission of *Physiological Chemistry and Physics*.]

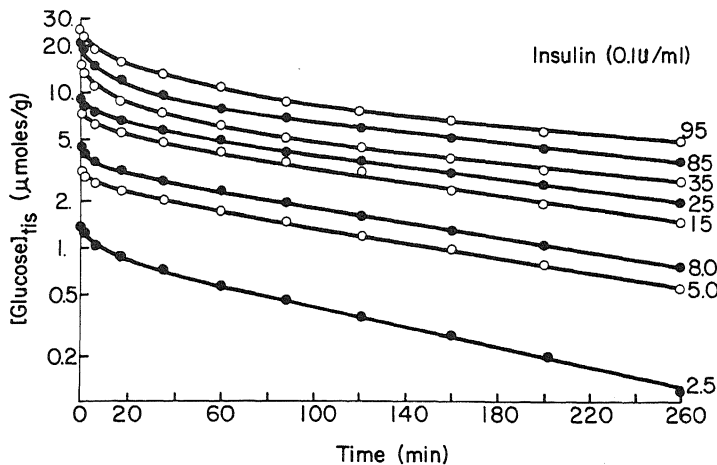


FIGURE 12.45. Labeled D-glucose efflux curves of frog sartorius muscles preincubated in insulin (0.1 U/ml) and incubated at 0°C in various concentrations of labeled D-glucose (given in millimolarity at the end of each curve). Ordinate refers to labeled D-glucose remaining in the tissue and is in units of $\mu\text{moles per gram of fresh muscle}$. [From Ling (1983a), by permission of *Physiological Chemistry and Physics*.]

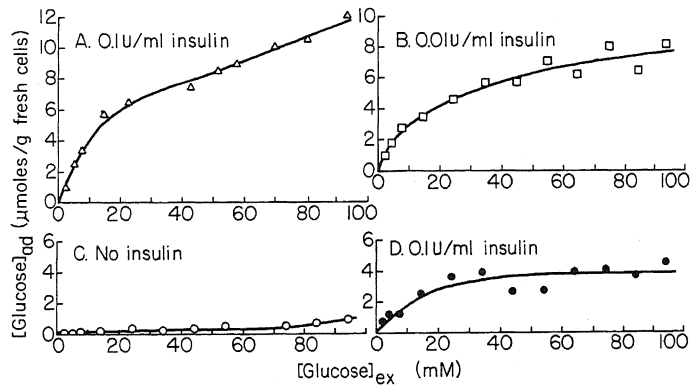


FIGURE 12.46. Concentration of slowly exchanging labeled D-glucose from sartorius muscles treated with no (C) or varying (A, B, D) concentrations of insulin, obtained from data like those shown in Figs. 12.44 and 12.45 by "exponential peeling." [From Ling (1983a), by permission of *Physiological Chemistry and Physics*.]

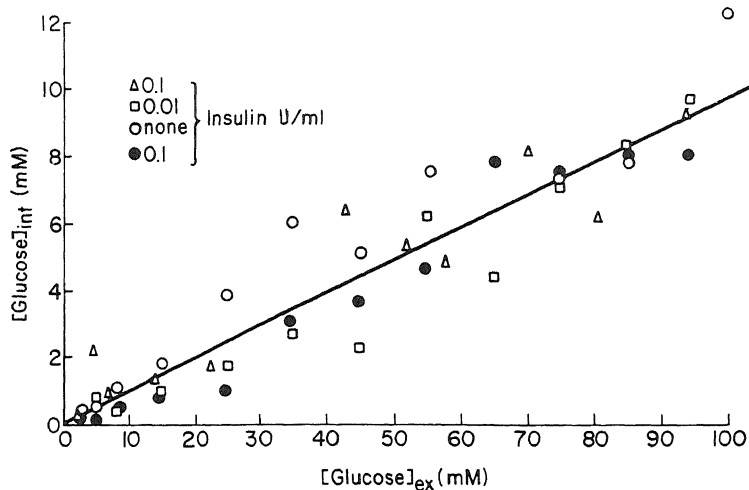


FIGURE 12.47. Fast fraction of labeled D-glucose in muscles untreated or treated with insulin of different concentrations, obtained from data like those shown in Fig. 12.44 by “exponential peeling.” [From Ling (1983a), by permission of *Physiological Chemistry and Physics*.]

Shaller had demonstrated in human lymphocytes for K^+ and Na^+ (Section 12.4.2.4). In addition, these comparisons strengthen earlier conclusions that insulin, acting as a cardinal adsorbent, increases an adsorbed fraction of glucose (Section 11.2.4.4).

12.6. Amino Acid Permeation and Its Dependence on External Na^+

12.6.1 The Saturable and Nonsaturable Fractions in the Uptake and Exodus of Amino Acids

In the same year that the AI hypothesis was presented, and both theory and evidence for the separation of permeation of solutes into a nonsaturable “saltatory route” and a saturable “adsorption–desorption route” were developed (Ling, 1962), Akedo and Christensen showed that the entry of α -amino-isobutyric acid (AIB), a nonmetabolizable amino acid, into rat diaphragm muscles also shows a saturable and a nonsaturable fraction. The general existence of a nonsaturable fraction in the permeation of amino acids has been repeatedly confirmed, including the permeation of glycine, choline, and alanine into pigeon erythrocytes (Vidaver, 1964; Eavenson and Christensen, 1967) (Fig. 12.48) and of neutral amino acids into Ehrlich ascites cells (Oxender and Christensen, 1963). Christensen and his co-workers regarded the nonsaturable fraction as representing simple diffusion through the cell membrane. This interpretation was not easily reconcilable with the conventional membrane theory for the following reason: Free amino acids are electrically charged; their permeability through a phospholipid membrane, like that of Na^+ , can be expected to be very slow. Thus the permeability constant of Na^+ through a phosphatidylcholine BLM is 10^{-12} cm/sec (see Jain, 1972, p. 143; also Fig. 12.1), and this membrane is 100,000 times less permeable to Na^+ than is frog sartorius muscle

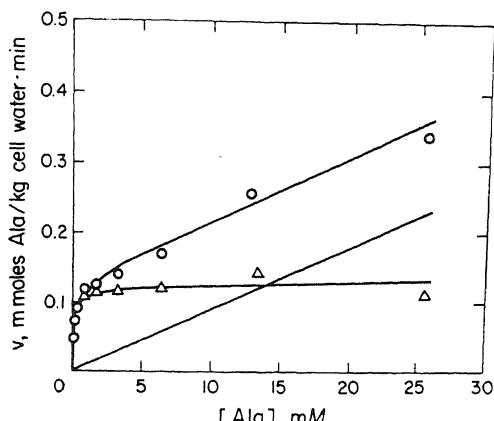


FIGURE 12.48. Concentration dependence of the uptake of alanine by pigeon erythrocytes. Upper curve, total uptake; straight line, nonsaturable uptake; lower curve, saturable uptake. [From Eavenson and Christensen (1967), by permission of *Journal of Biological Chemistry*.]

(10^{-7} cm/sec; Table 12.4). The permeability of living cells toward amino acids (which reach new equilibrium levels in less than 30 min at 37°C) is as fast as Na^+ permeability into frog muscles (see Oxender and Christensen, 1963). Thus rapid free diffusion of the nonsaturable fraction cannot be through a lipid layer, in agreement with other evidence cited earlier against lipid layers as the diffusion barrier of cell surfaces (Section 12.1). On the other hand, the AI hypothesis, by proposing polarized water in lieu of a phospholipid layer as the seat of "nonsaturable" saltatory permeation, resolves this conflict, because permeability via the saltatory route can vary according to the degree of polarization of the water involved.

In analyzing the data of AIB entry into rat diaphragm muscle, Akedo and Christensen came to another conclusion: Exposure to insulin had no effect on the nonsaturable fraction of amino acid permeation—a conclusion in harmony with conclusions I have drawn from the studies of the effect of insulin on glucose efflux mentioned above (Fig. 12.47). It is also interesting that the minimal insulin concentration needed to bring about a full effect on glucose accumulation in frog muscle is roughly the same as that needed to bring about a full effect on L-proline accumulation in rat diaphragm muscle (i.e., 10^{-3} U/ml; Fig. 12.49).

In a later paper, Christensen and co-workers (Christensen and Liang, 1966) revised the earlier view that the nonsaturable fraction represents simple diffusion, citing as the reason a difference in the diffusion rate constants via this route between α - and β -alanine. I believe that their original view should not be abandoned without more study. It is conceivable that α - and β -alanine have different rotational entropies and hence q -values. If so, a different rate of saltatory entry may be expected.

12.6.2. Permeation of Glycine and Other Neutral Amino Acids into Ehrlich Ascites Cells

By careful analysis of the influx of neutral amino acids into Ehrlich ascites cells, Oxender and Christensen (1963) made the important discovery that, by and large, the affinity for some cell surface moiety falls into clusters around two groups, which they called leucine-preferring or L mediation and alanine-preferring or A mediation. They found that almost every neutral amino acid has affinity for both mediating systems;

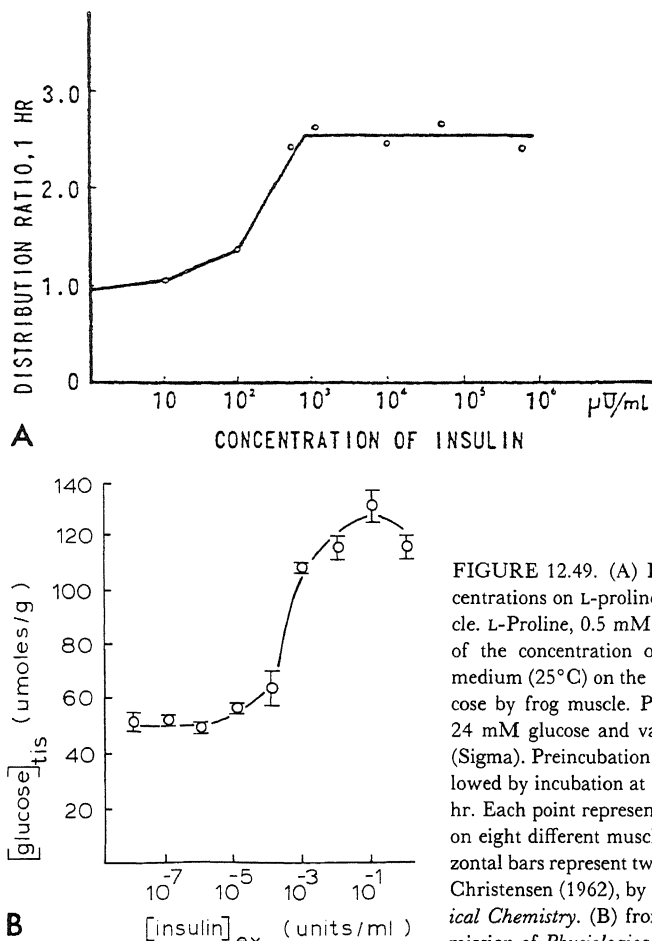


FIGURE 12.49. (A) Effect of insulin at various concentrations on L-proline uptake in rat diaphragm muscle. L-Proline, 0.5 mM; incubation for 1 hr. (B) Effect of the concentration of insulin in the preincubation medium (25°C) on the subsequent uptake (0°C) of glucose by frog muscle. Preincubation solution contained 24 mM glucose and varying concentrations of insulin (Sigma). Preincubation lasted 6 hr at 24°C and was followed by incubation at 0°C with 24 mM glucose for 18 hr. Each point represents the average of determinations on eight different muscles. Distances between the horizontal bars represent twice the SE. [(A) from Akedo and Christensen (1962), by permission of *Journal of Biological Chemistry*. (B) from Ling *et al.* (1969a), by permission of *Physiological Chemistry and Physics*.]

methionine, in particular, has strong affinities for both systems. Each mediating system has distinctive features. The question is: What are these mediating systems?

The great majority of scientists believed that the mediating systems are "carriers" which shuttle back and forward in the lipid phase of the cell membrane. As mentioned earlier there is strong new experimental evidence against this view: Since 1953 I have suggested that such a complicated carrier model is not necessary to account for saturation and competitive characteristics (Sections 4.5 and 12.4.1). All that is needed are specific adsorption sites on the cell surface proteins.

12.6.3. The Saturable Fraction

12.6.3.1. Dependence of Efflux Rate on External Amino Acid Concentration

Oxender and Christensen (1963) presented data showing that the rate of efflux of labeled leucine from pig erythrocytes is related to intracellular leucine concentration in

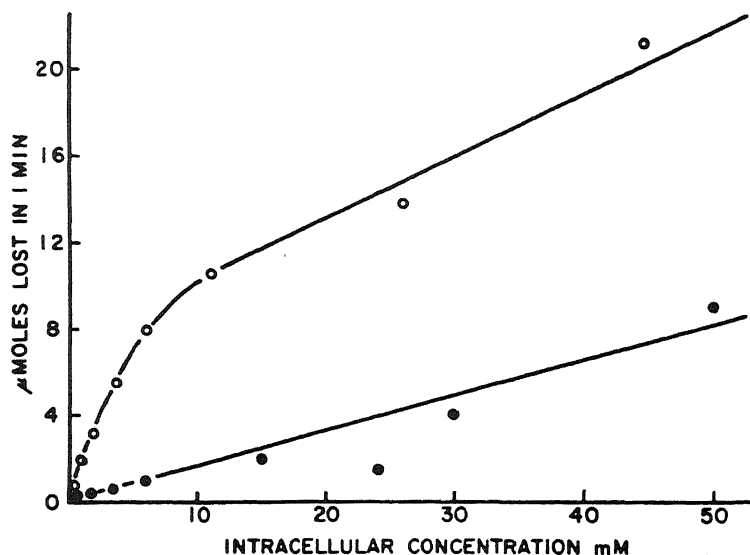


FIGURE 12.50. Exodus of labeled leucine from previously loaded cells into solutions of unlabeled leucine at various concentrations (upper curve). One-minute intervals at 37°C. The top curve represents exodus into an external solution containing unlabeled leucine, while the bottom curve represents exodus into an external solution containing no leucine. [From Oxender and Christensen (1963), by permission of *Journal of Biological Chemistry*.]

a manner quite similar to that of amino acid influx, and also is separable into a saturable and a nonsaturable fraction. Again the nonsaturable fraction seemed to be independent of the presence of external leucine, while the rate of the saturable fraction of leucine efflux was highly dependent on *external* leucine concentration (Fig. 12.50). This dependence of labeled leucine efflux on the concentration of external leucine is, of course, analogous to the dependence of labeled K⁺ efflux on external K⁺ as shown in Figs. 12.26 and 12.27, and the triplet interpretation can also be invoked to explain it, with the difference that the gradual lowering of the activation energy for the departure of an adsorbed leucine involves a stepwise displacement of more than one site of contact between the leucine molecules and the proteinaceous adsorption sites on the cell surface. Figure 12.51 is a diagrammatic rendition of this concept.

12.6.3.2. The Roles of Extracellular Na⁺ and Intracellular K⁺ in the Entry and Accumulation of Glycine and Alanine

The rate of entry of glycine into Ehrlich ascites cells exemplifies the dependence of amino acid uptake on extracellular Na⁺ concentration and intracellular K⁺ concentration seen in a variety of living cells (Christensen *et al.*, 1952; T. R. Riggs *et al.*, 1958; Kromphardt *et al.*, 1963; Johnstone and Scholefield, 1965; Eddy *et al.*, 1967). I shall discuss two examples of the exciting developments in this field, which up to now have been interpreted only within the context of the membrane theory, and offer a new theoretical interpretation of this general phenomenon in terms of the AI hypothesis.

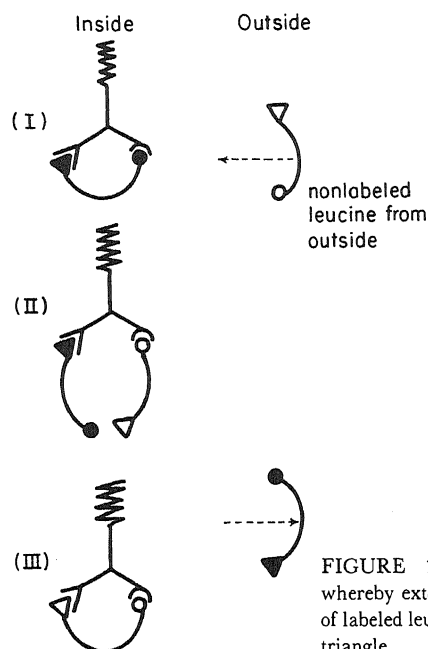


FIGURE 12.51. Diagrammatic illustration of the mechanism whereby external nonlabeled leucine can accelerate the rate of efflux of labeled leucine. Labeled leucine represented by joint filled circle and triangle.

12.6.3.2a. Effect of External K^+ and Na^+ Concentration on Rate of Glycine Entry. Eddy *et al.* (1967) suggested that a carrier molecule E in the cell membrane has two binding sites, one for glycine (Gly) and the other an anionic site which binds either K^+ or Na^+ . By assuming that only the formation of a complex (ENaGly) can lead to entry, he wrote out a list of seven equilibrium dissociation constants, k_1, k_2, \dots, k_7 corresponding respectively to the seven reactions listed in Table 12.7.

Utilizing the technique of Florini and Vestling (1957) for analyzing the kinetics of an enzyme reaction with two substrates, they were able to devise experimental studies

TABLE 12.7. Equilibrium "Carrier" Adsorption Constants of Amino Acid, K^+ , and Na^+ Singly and in Sequenced Pairs^a

Ligand bound	Equilibrium adsorption constant (M^{-1})
1. Na^+	26.7
2. K^+	13.2
3. Amino acid	156
4. Na^+ , then amino acid	286
5. Amino acid, then Na^+	47.6
6. K^+ , then amino acid	10.9
7. Amino acid, then K^+	1.0

^aFrom Eddy *et al.* (1967), by permission of *Biochemical Journal*.

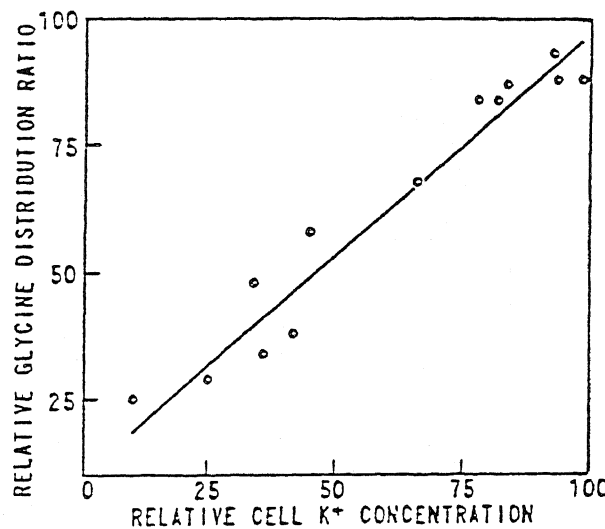
to estimate each one of the seven dissociation constants. The results of these studies are also shown in Table 12.7. In these lists however, the adsorption constants are given rather than their reciprocals, the dissociation constants, which were given in the original article. Note that prior binding of Na^+ augments the strength of adsorption of the amino acid by a factor of 2; prior binding of K^+ , on the other hand, reduces the strength of adsorption of the amino acid by a factor of 14.3!

12.6.3.2b. Effect of Intracellular K^+ Concentration on Glycine Accumulation. In 1958, T. R. Riggs, Walker, and Christensen demonstrated that the level of glycine accumulated in Ehrlich cells is correlated ($r = +0.91$) with the level of K^+ in the cells that had been pretreated with 2,4-dinitrophenol. The loss of K^+ from the cells was made up by increasing external K^+ in the bathing solution (Fig. 12.52). Eddy *et al.* (1967) extended these findings by showing that the rate of glycine entry into Ehrlich cells is negatively correlated ($r = -0.50, P < 0.001$) with the level of Na^+ in the cell. Normal respiration and glycolysis, as well as the level of ATP, do not seem important in glycine entry rate as long as the cell has a high level of K^+ and a low level of Na^+ .

These findings are in harmony with Christensen's concept that the accumulation of glycine derives its energy not from ATP or other metabolic processes but from the ionic gradient of K^+ and Na^+ ; as long as these gradients persist, glycine accumulates (Riggs *et al.*, 1958). This idea was the first statement of what was later called the Na^+ gradient hypothesis, a hypothesis more explicitly expressed in 1960 by Crane in regard to Na^+ -dependent intestinal sugar transport (Crane, 1960, 1962) (see Section 17.2.4).

The Na^+ gradient hypothesis forms part of a large body of publications in which the idea was advanced that the various ionic gradients across the surface of cells or subcellular particles can be tapped for work performance or for the synthesis of ATP. The best known of these hypotheses is Mitchell's chemiosmotic hypothesis. The fundamental theoretical weakness of this theory and its contradictions by experiments have

FIGURE 12.52. Association between cell K^+ levels and uptake of glycine by tumor cells pretreated with 2,4-dinitrophenol. Cells were depleted of K^+ by 30-min preincubation with 0.15–0.5 mM dinitrophenol, after which glycine and varying amounts of K^+ were added in fresh buffer medium. The correlation coefficient for the association is 0.91 ($P \ll 0.01$). [From T. R. Riggs *et al.* (1958), by permission of *Journal of Biological Chemistry*.]



been recently reviewed (Ling, 1981a) and are discussed in Chapter 15. The simplest and most unequivocal evidence against the idea of an ionic gradient as an energy source is the extensive evidence given in Chapter 8 showing that the bulk of cell K⁺ is not free but adsorbed. *The low Na⁺ and high K⁺ concentrations are not due to a nonequilibrium state which can be tapped for energy but in fact represent different facets of an equilibrium state.* In the following section, I shall attempt to reinterpret all these findings in the simple framework of the AI hypothesis.

12.7. Surface Protein Adsorption Sites as the Seat of the Selective Adsorption-Desorption Route for Entry of Amino Acids

The evidence against the lipoidal membrane theory discussed in Section 12.1 provides one kind of fundamental reason for rejecting the “carrier” concept for “mediated transport” of ions and other solutes. Other convincing arguments against the carrier concept were provided long ago by Hodgkin and Huxley (1952d) and more recently by Armstrong (1971) in regard to the specific instance of nerve excitation.

In terms of the AI hypothesis, mediated transport simply represents adsorption of the (labeled) amino acid on surface protein sites followed by its desorption and entry (adsorption-desorption route). With no lipid layer to transverse, the same sites, fixed in space, are all that is required for mediated transport. One recalls that entry of labeled ions into inanimate fixed-charge systems like a piece of sulfonate ion exchange resin shows similar saturability and competition (Figs. 4.15 and 12.17), phenomena that have often been regarded as evidence for carriers or pumps. Such carriers or pumps are obviously absent in the resin. The idea of a ternary complex can be transferred to the AI hypothesis model of the cell surface and considered as a part of the protein-polarized water complex capable of inductive electronic interaction between neighboring sites, as described in Chapter 7. One of these sites is a β - or γ -carboxyl group, the essential role of which in both ionic permeability (see Section 12.4) and the generation of the electrical potential (see Section 4.6) has been long a part of the AI hypothesis. The following is a stepwise description of this model:

1. *Adsorption.* To enter the cell by the adsorption-desorption route the amino acid must first combine with the surface adsorption sites (see Fig. 12.51). The higher preference of these sites for Na⁺ over K⁺ (Table 12.7) and the preponderance of Na⁺ in the external medium ensure that in normal Ehrlich ascites cells the surface anionic sites are primarily adsorbing Na⁺, in contrast to frog muscle cells, whose surface anionic sites are primarily occupied by K⁺. This extensive Na⁺ adsorption on Ehrlich ascites cell surfaces favors the adsorption of labeled glycine from the external medium (Table 12.7). Note that if external Na⁺ concentration is lowered or the concentration of competing K⁺ is increased, clearly less glycine will adsorb onto the surface site and a decrease in the glycine rate will follow, as often observed.

2. *Desorption.* The adsorption constant for the amino acid flanked by an adsorbed K⁺ is 26 times weaker than that for one flanked by an adsorbed Na⁺ (Table 12.7). Thus the displacement of a surface-adsorbed Na⁺ by a K⁺ greatly enhances the chance

of desorption of the neighboring adsorbed labeled glycine. If the desorbed labeled glycine should by chance return to the external solution, it will constitute a nonobservable event. On the other hand, if the desorbed labeled glycine should enter the cell, it would be registered as Na^+ -induced glycine permeation.

3. *Accumulation.* In the AI hypothesis, the accumulation of a solute in a cell to a much higher level than that in the external medium is as a rule due to adsorption. We therefore stipulate that the intracellular glycine adsorption sites are favored by the protein existing in the K^+ state—a situation quite opposite to that of the surface glycine adsorption sites. The Riggs, Walker, and Christensen experiment shown in Fig. 12.52 can be interpreted on the same principle as the conservation of ξ of equation (11.4). The decline of ATP lowers $K_{\text{Na}-\text{K}}^{00}$, and would have led to a shift of K^+ adsorption in the intracellular adsorption sites to Na^+ adsorption, but was compensated for by the increase of $[\text{K}^+]_{\text{ex}}/[\text{Na}^+]_{\text{ex}}$ by the increase of $[\text{K}^+]_{\text{ex}}$. In other words, the basic logic is the same as that of restoring K^+ to muscle cells in the presence of ouabain by raising the level of K^+ in the external medium (Figs. 11.32 and 11.34).

12.8. Summary

Semipermeability, or a greater permeability to water than to other substances, is an almost universal property of cells and tissues. Among nonliving models that display semipermeability is the copper ferrocyanide gel membrane, discovered by Traube in 1867 (Chapter 1). He thought that the membrane contained pores small enough that only water molecules could pass readily. Based on membrane models like this, W. R. Pfeffer founded the membrane theory of cell physiology in 1877, and in 1899 Overton put forth the concept that the cell membrane is essentially a continuous lipid barrier. Subsequent elaboration of the membrane theory included postulation of more complex, charged and uncharged pores, as outlined in Chapter 2, and postulation of carriers within the membrane that can shuttle ions, sugars, amino acids, and other substances across it, as outlined in Section 4.5.1 and in this chapter.

The copper ferrocyanide gel membrane, however, was found in the 1930s not to be a molecular sieve but to contain interstices of a size of the order of hundreds of angstroms (Section 1.5). This membrane can at once be a barrier to the movement of relatively small molecules like sucrose and very permeable to water only if the interstices are filled with what in the association-induction hypothesis is referred to as water polarized in multilayers (Chapter 6). Moreover, there is not enough lipid in most cell membranes to provide a continuous barrier. These two sets of facts prompt a reevaluation of concepts of permeability of cell membranes, of cells, and of tissues. It is now clear that the permeability barrier to the movement of water is water itself, i.e., water polarized in multilayers within rather large “pores.” Indeed, a model like the cellulose acetate membrane, which also contains large interstices and which adsorbs water in multilayers (Chapter 6), has permeability properties to water and a variety of solutes that are identical to those of a living tissue, the frog skin.

The treatment of permeability of cells to ions, sugars, and amino acids by the association-induction hypothesis is based on three major concepts. First, the surface, or sur-

face membrane, is in general a two-dimensional replica of the fixed-charge system that is the entire cell; as such, it contains interstices filled with water polarized in multilayers, and it contains proteins with potential adsorption sites for ions, sugars, amino acids, and other substances. Second, the passage of a solute into and out of the cell may in some cases be limited by its adsorption onto and desorption from macromolecules at the cell surface, and in other cases may be limited simply by diffusion through the water that is polarized in multilayers within the interstices. Third, the nonsaturable and saturable fractions of the equilibrium distribution of a solute between the cell and the environment, described in Chapter 11, often will have their counterparts in the movements of ions into and out of the cell.

These concepts explain the well known phenomena of nonsaturable and saturable fractions in the permeation of solutes into cells, and of saturability and competition for solute entry. In addition, they explain paradoxical phenomena like the facilitation of ion entry by a different ion, or the difference between initial $^{22}\text{Na}^+$ influx (which is slow) and initial $^{22}\text{Na}^+$ efflux (which is fast) in frog muscle.

Finally, the control of permeability is analogous to the control of solute distribution outlined in Chapter 11. For example, insulin facilitates glucose entry into muscle inductively by creating adsorption sites, and Na^+ facilitates amino acid uptake by the inductive modulation of adsorption sites at or near the cell surface.

Clearly, "permeability" often is a manifestation of events occurring at the cell surface and the surface does indeed have unique properties, even if not those of a membrane in the classical sense. Another surface phenomenon, the cell potential, will be described in Chapter 14, and will be seen to be not a membrane potential but a surface adsorption potential.

Swelling, Shrinkage, and Volume Control of Living Cells

13.1. The Refutation of the Membrane Theory of Cell Volume Regulation

An aqueous phase gains or loses water when separated by a copper ferrocyanide gel membrane from a contiguous aqueous phase containing a different level of solutes. The similarity of these phenomena to the osmotic behavior of living cells led W. F. Pfeffer (1877, 1921) to found the *membrane theory*, in which he postulated that surrounding all living cells is a plasma membrane having attributes (e.g., semipermeability) similar to those of the copper ferrocyanide gel membrane (Section 1.6). According to this theory, living cells are in essence sacs full of an aqueous solution of proteins, (free) K^+ , and a complex mixture of (free) anions. Cellular proteins and other macromolecules contribute little to the intracellular osmotic activity, owing to their large molecular weights and trivial molar concentration, and cell volume is maintained primarily by the osmotic activity of K^+ salts. The proof that the bulk of intracellular K^+ in frog muscle cells is in an adsorbed state (Chapter 8) removed the basis for the membrane theory of cell volume. Still other findings, to be described next, show that the maintenance of *cell volume in a normal or a swollen state does not even require an intact cell membrane*.

An intact membrane is essential in the membrane theory for the maintenance of cell volume and shape in the same way that an intact membrane is essential for the maintenance of the volume and shape of an inflated balloon. Intactness of a balloon membrane can be easily destroyed by cutting with a sharp razor blade. The intactness of the cell membrane of frog sartorius muscle cells can also be easily destroyed by the repeated application of a razor blade. Three independent sets of evidence have already been presented showing that frog muscle cells, once amputated with a razor blade, do not regenerate a new membrane (Section 5.2.6).

Centrifugation of frog sartorius muscles for 4 min at 1000g removes only fluids from the extracellular space (Ling and Walton 1976). Cutting the muscles with a razor blade into 2- and 4-mm-long segments does not significantly affect the centrifugation-extractable fluid of frog sartorius muscles or rat diaphragm muscles (Fig. 13.1a-c). Nor

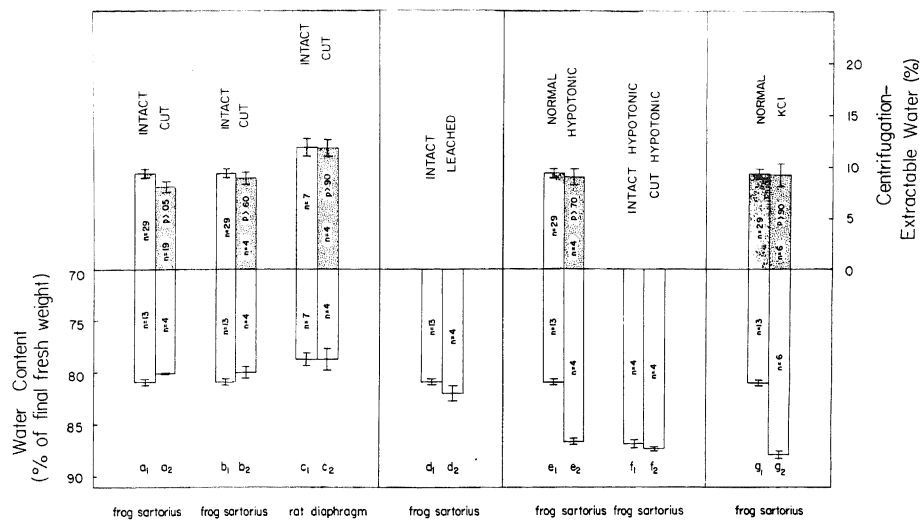


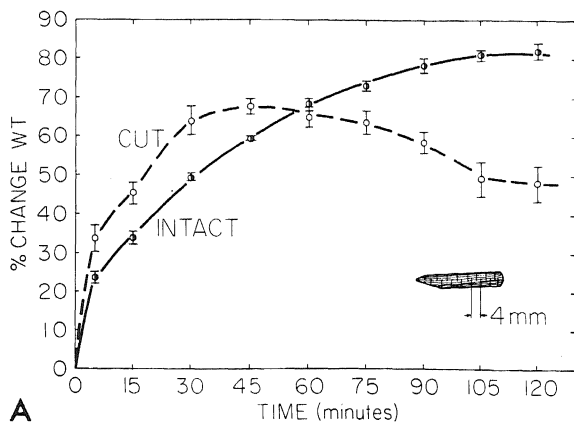
FIGURE 13.1. Water content and centrifugation-extractable fluid of intact muscles and muscles cut into 2- and 4-mm-long segments. (a-c) Untreated muscles. Muscles of b₂ were incubated in a Ca²⁺-free Ringer solution containing 1 mM ethylenediaminetetraacetic acid for 30 min at 4°C before cutting. (d) Removal of intracellular solutes produced no significant change in the amount of water retained in muscles after centrifugation at 1000g for 4 min. Swelling was brought about by exposure to (e) hypotonic solution (osmolarity 20% that of normal Ringer solution) for 4 hr at 0°C. (f) Similar water contents of intact and cut muscles after exposure to hypotonic solution (osmolarity 40% that of normal Ringer solution) for 5 hr at 0°C, but in this case the muscles were blotted but not centrifuged. (g) A high KCl concentration (93 mM, 72 hr at 4°C). [From Ling and Walton (1976), by permission of *Science*.]

does cutting of frog muscles into 2- and 4-mm-long segments hamper their swelling when they are placed in a hypotonic Ringer solution (Figs. 13.1e,f and 13.2A). Clearly, the maintenance of normal cell volume and swelling and shrinkage do not depend on the possession of an intact surface membrane.

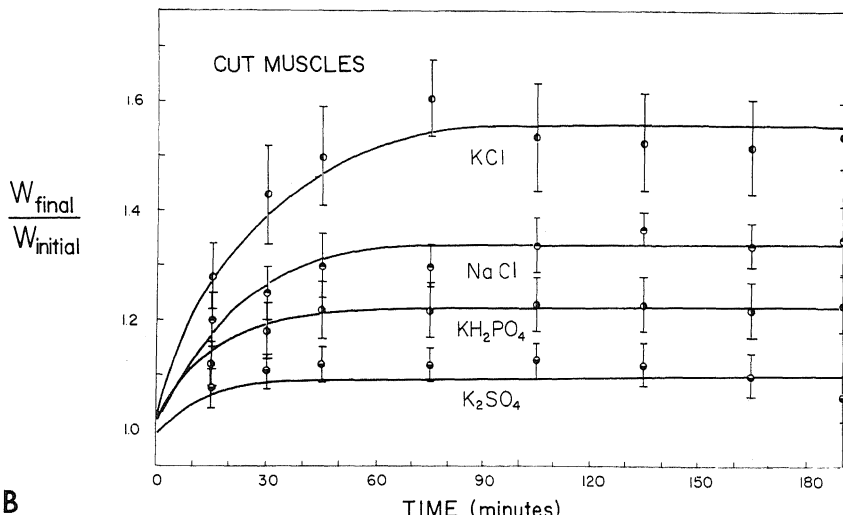
13.2. Polarized Water in Lieu of Free Intracellular K⁺ in the Maintenance of Osmotic Pressure of Living Cells

Living cells maintain their normal volume, swell in hypotonic solution, and shrink in hypertonic solution; yet these phenomena do not depend on the presence of an intact membrane. What then are the molecular mechanisms involved? Before answering, let us clarify the concept of osmotic activity.

Living cell surfaces are, with no known exception, permeable to water. Net movement of water from the cell interior to the outside indicates a difference in the *activity* of water in the two phases. For example, introduction of normal cells into a hypertonic external solution, which has a lower activity of water, leads to loss of water from the cell. On the other hand, the maintenance of a steady level of water in a normal cell bathed in an isotonic Ringer solution must mean that water in the cell has an activity



A



B

FIGURE 13.2. Swelling of frog sartorius muscle without an intact membrane. (A) In a mixture of 80% water and 20% normal Ringer solution, muscles cut into 2- and 4-mm segments (see inset) swell faster than intact muscle, followed by deterioration and gradual loss of weight gained. (B) Swelling of cut muscle in isotonic solutions of KCl, NaCl, KH_2PO_4 , and K_2SO_4 [(A) From Ling (unpublished). (B) From T. H. Ling and G. N. Ling (unpublished).]

exactly equal to that of an isotonic salt solution. For a long time, this osmotic balance between living cells and environments was attributed to free K^+ salt in the cell—a belief that has been made untenable by the evidence in Chapter 8 that the bulk of cell K^+ is not free but specifically adsorbed.

According to the association-induction (AI) hypothesis, the lowering of water activity in the living cell is to a large extent due to the multilayer polarization of this water by the matrix proteins. One recalls that water existing in the state of polarized multilayers can be brought about by proteins existing in the extended form or by other polymers also containing oxygen atoms at distances equal to twice the diameter of a water

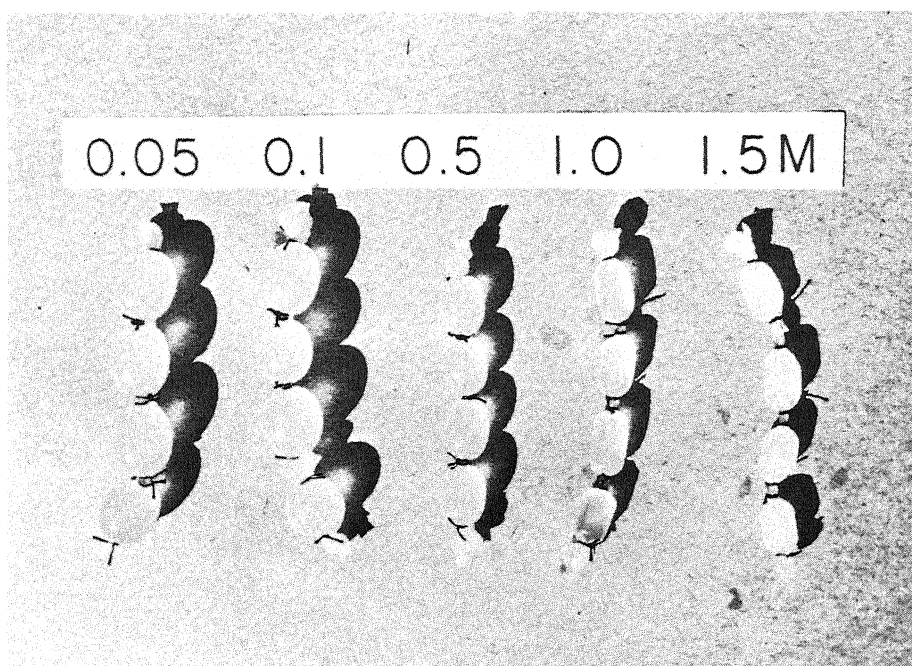


FIGURE 13.3. Swelling and shrinkage of dialysis bags filled with (initially) a 30% solution of polyethylene oxide and equilibrated in solutions of sodium citrate at the strengths indicated. [From Ling and Ochsenfeld (1983d), by permission of *Physiological Chemistry and Physics*.]

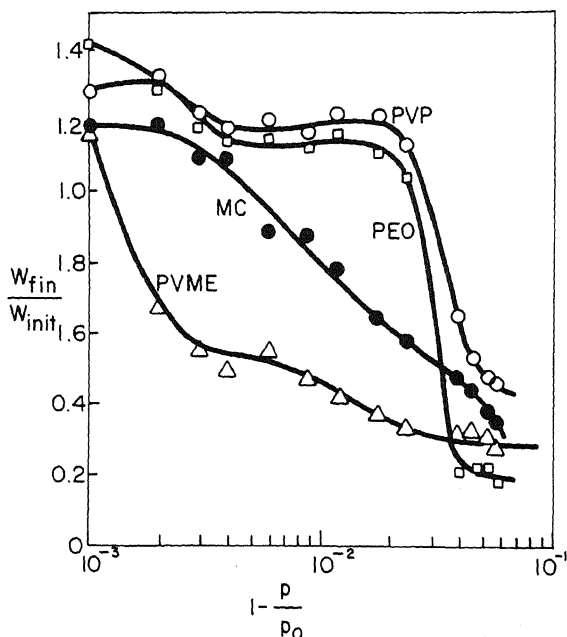


FIGURE 13.4. Volumes of dialysis bags filled with polyvinylpyrrolidone (PVP) polyethylene oxide (PEO), methylcellulose (MC), and polyvinylmethylether (PVME) in solutions containing different concentrations of sodium citrate. p/p_0 is the relative vapor pressure of the sodium citrate solution used. Sodium citrate concentration increases from left to right. W_{fin} and W_{init} are the final and initial weights of the dialysis bags minus the weight of the dialysis tubing used. [From Ling and Ochsenfeld (1983d), by permission of *Physiological Chemistry and Physics*.]

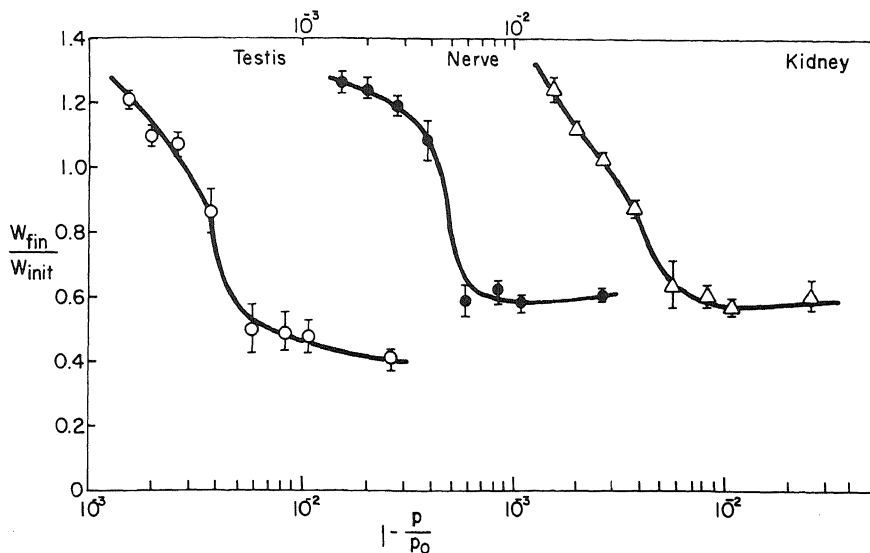


FIGURE 13.5. Volumes of frog testis, sciatic nerve, and kidney expressed as a ratio of final (W_{fin}) to initial (W_{init}) weight after equilibrating at 0°C in Ringer solution containing all its normal constituents (isotonic) but with less NaCl (hypotonic) or with sucrose added (hypertonic). p/p_0 is the vapor pressure of the Ringer solution used. From left to right, the abscissa indicates increasing osmolarity. [From Ling and Ochsenfeld (1983d), by permission of *Physiological Chemistry and Physics*.]

molecule (Table 6.4, Fig. 6.13). The simplest polymer satisfying this criterion is polyethylene oxide (PEO), an *electrically neutral* polymer. A 30% solution of PEO with an average molecular weight of 600,000 is only 0.5 mM. Yet when placed within a $\frac{1}{4}$ -in. dialysis tube it will swell, shrink, or remain unchanged in volume and thereafter maintain these volumes according to the concentration of sodium citrate in the external solution, even though the *dialysis bag membrane is fully permeable to sodium citrate* (Fig. 13.3). Quantitative data from this and other water-polarizing polymers are shown in Fig. 13.4. p/p_0 of the abscissa represents the partial vapor pressures of the different concentrations of sodium citrate in the external bathing solutions. $1 - (p/p_0)$ is a rough measurement of their osmotic pressures. Thus from left to right, the sodium citrate concentration increases. The ordinate represents the ratio of the final weight and initial weight of the polymer solution in the sacs.

The characteristics of these curves are basically similar to those of living cells as illustrated in Fig. 13.5. Having demonstrated in living cells (Figs. 13.1 and 13.2) and in model systems that an intact membrane impermeable to salt ions is not necessary for the swelling and shrinkage phenomena observed, one raises the question, How is this concentration-dependent volume regulation achieved? The explanation according to the AI hypothesis is as follows.

If a dialysis bag containing 30% PEO is placed in distilled water, the activity of water owing to its multilayer polarization by the polymer is lower than that in the surrounding distilled water. This imbalance of water activity will draw water into the bag until the tension of the dialysis bag can no longer permit further increase of volume. If sodium citrate is added to a concentration of, say, 1.0 M in the outside water, the

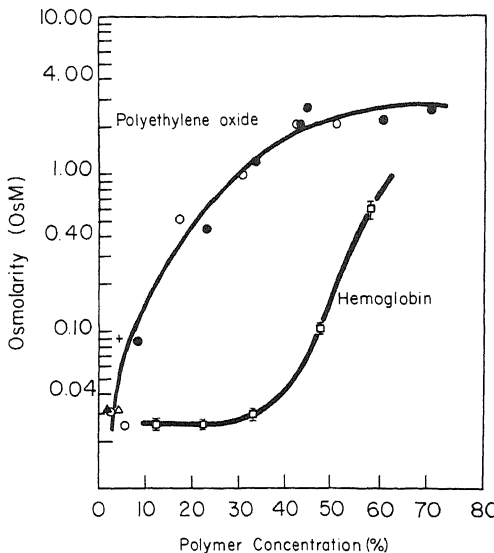


FIGURE 13.6. Vapor pressure of polyethylene oxide and hemoglobin at different concentrations. Vapor pressure is expressed as osmolarity calibrated against NaCl solution standards. [From Ling (1983c), by permission of *Physiological Chemistry and Physics*.]

swollen bag will begin to lose water. However, since the dialysis bag membrane is permeable to sodium citrate, there is also a countermovement of sodium citrate into the bag. As has been made clear in Chapter 9, water in the PEO solution inside the bag has a reduced solubility for sodium citrate. Thus when the swollen bag is exposed to 1.0 M sodium citrate, the inward movement of sodium citrate does not reach a concentration equal to that in the outside medium. Rather it comes to a stop when sodium citrate reaches a concentration a fraction (say, 40%; $q = 0.4$) of that in the external medium. Under this condition, the total osmotic activity produced by the 0.4 M sodium citrate in the bag, when added to the reduction of water activity owing to the PEO, equals the osmotic activity of the external 1.0 M sodium citrate. Net water movement comes to a halt and a new equilibrium condition is established. According to the AI hypothesis, solutes like NaCl and sucrose—long considered as impermeant to the cell membrane since their addition to the Ringer solution causes cell shrinkage, but shown later to be quite permeant—affect cell volume by a similar mechanism.

Support for this interpretation is also provided by measurement of the vapor pressure of polymer–water systems. *Figure 13.6* shows that a 30% PEO solution exhibits a partial vapor pressure which matches that of a 1 M solution of sucrose! In contrast, a 30% solution of native hemoglobin exhibits very little osmotic activity. Since partial vapor pressure is in fact a direct expression of water activity, these data leave no doubt that PEO drastically reduces the water activity, as suggested in the polarized multilayer theory of cell water.

13.3. What Does the Vapor Sorption Isotherm Tell Us about the Osmotic Behavior of Living Cells?

According to the membrane theory, the water content of living cells should follow the van't Hoff equation,

$$\pi V = nRT \quad (13.1)$$

where π is the osmotic pressure, V is the volume of water associated with n moles of solute in the cell, R is the gas content, and T is the absolute temperature. In past studies of cell volume, changes were as a rule produced by adding an increasing concentration of an "impermeant" solute to the external solution. A favorite solute was sucrose, since it is highly water soluble and less damaging to the cell than, for example, high concentrations of NaCl (Section 8.1). However this type of study has serious limitations because the cells are damaged by a still higher concentration of sucrose and because even a saturated solution of sucrose has a quite low π .

A different approach to this problem was that adopted by Ling and Negendank (1970). In their vapor equilibrium studies of frog muscles, referred to earlier in Section 9.4, the air phase separating the cells from the solution of varying partial vapor pressure acts as a perfect semipermeable barrier, allowing the traffic of water but nothing else. Since the solute added to lower the water activity (which is equal to the partial vapor pressure, p/p_0) was not in direct contact with the cells, one could use highly effective agents like sulfuric acid. Water activity approaching zero could thus be studied.

Figure 13.7, taken from Ling and Negendank (1970), shows that, in the range of water activity usually investigated by conventional direct-contact methods, corresponding to a low limit of $1/\pi$ of 0.0495 (i.e., the partial vapor pressure of a 0.8 molal solution of sucrose), a straight line relation between V and $1/\pi$ indeed occurs, as equation (13.1) demands. Extrapolation from this portion of the curve to $1/\pi = 0$ would yield an apparent "osmotically inactive" water equal to 30% of the total cell water, as had been claimed in past studies.

Figure 13.7, however, shows quite clearly that the linearity observed here and in more conventional studies of cell volume is fortuitous. As $1/\pi$ approaches zero, the cell does not retain 30% of its water; rather it loses all its water. Indeed if there were truly such a thing as "osmotically inactive" water in living muscle and other cells, how could one ever dry them? Modern as well as ancient cultures drying plant and animal materials for storage and preservation have found that living tissue can be freed of just about all its water.

13.4. Swelling of Living Cells in Isotonic KCl and Other Salt Solutions

Frog muscles remained unchanged in weight in an isotonic physiological NaCl solution indefinitely (J. Loeb, 1897; E. Cooke, 1898), yet exposure to a KCl solution of equal concentration produced extensive swelling (von Korósy, 1914; Gellhorn, 1931). Both NaCl and KCl are now known to be permeant; the old explanation of the difference in the effect of NaCl and KCl as being due to the impermeability of one and the permeability of the other has long been disproven. Figures 13.1g and 13.2B show that cutting a sartorius muscle into 2- and 4-mm-long segments does not materially alter the ability of an isotonic KCl solution to cause swelling, again demonstrating that an intact cell membrane is not essential for this phenomenon.

According to the AI hypothesis, the resting frog muscle cell would have picked up more water, thereby building up deeper layers of water in its matrix of extended protein chains, if it were not for the presence of salt linkages (as well as H-bonding linkages)

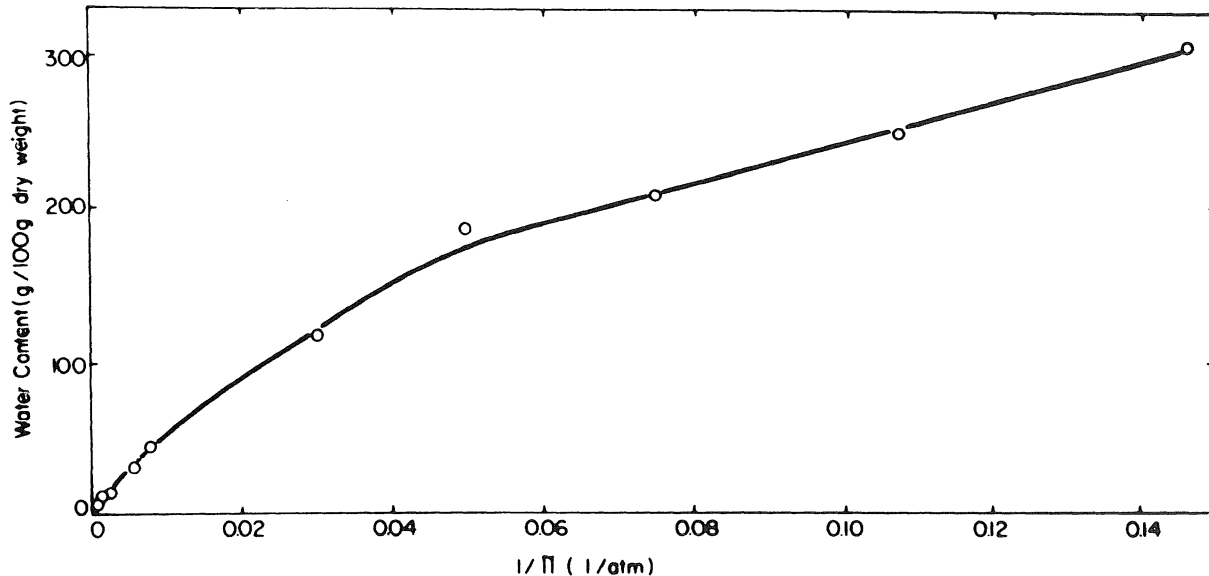


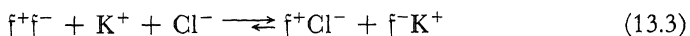
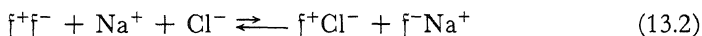
FIGURE 13.7. Equilibrium water content of frog sartorius muscles as a function of $1/\pi$. π is the osmotic pressure of the H_2SO_4 solutions with which the muscles are in equilibrium. At $1/\pi = 0.0495$, $p/p_0 = 0.985$, indicating the pronounced condensation of a wide range of water activities between 0 and 0.05 on the $1/\pi$ axis. [From Ling and Negendank (1970), by permission of *Physiological Chemistry and Physics*.]

between protein chains, which restrain the cell from gaining additional water (Ling and Peterson, 1977; see also Ling, 1962, p. 246). These salt linkages are formed primarily between cationic and anionic side chains.

Cationic groups include ϵ -amino groups belonging to lysine residues and guanidyl groups belonging to arginine residues; anionic groups include β - and γ -carboxyl groups belonging, respectively, to aspartic and glutamic acid residues. Salt linkages also may involve terminal α -amino and α -carboxyl groups and histidyl groups. Thus, in general, the fixed anionic sites, the β - and γ -carboxyl groups, that provide the sites for selective K^+ adsorption also comprise the anionic members of the salt linkages. Furthermore, experimental data suggest that a significant portion of these anionic groups have similar c -values.

Figures 6.7 and 6.8 show that the anionic groups at a c -value highly favoring K^+ adsorption (over Na^+) also prefer NH_4^+ over Na^+ . Since NH_4^+ can be regarded as a prototype of ϵ -amino and guanidyl groups, $NH_3^+ - C(NH_2)_2$, the salt linkage is expected to resist competitive dissolution by the prevailing cation in the environment, Na^+ . K^+ , which would be more effective in dissociating the salt linkage, is found at too low a concentration (2.5 mM) in the normal environment of the living cell to cause excessive dissociation of salt linkages and consequent swelling. This is not to say that under normal conditions all fixed anions and cations capable of forming salt linkages are locked in these linkages. Experimental data to be discussed later indicate that quite often the opposite is the case.

When normal cells are brought into contact with a high concentration of KCl , many salt linkages are dissociated, the previously restrained tendency to sorb more water exerts itself, and as a result swelling occurs. If one represents fixed cations and anions as f^+ and f^- and a salt linkage as f^+f^- , these changes can be represented as



where the lengths of the arrows roughly indicate the greater effectiveness of KCl than $NaCl$ in dissociating salt linkages. Also to be noted here is the fact that relative cation preference by the fixed anion is only half of the story; the other half is a competition between the fixed anion, f^- , and the free anion, Cl^- , for the fixed cation f^+ . Other K^+ salts like the sulfate may be less effective in causing swelling owing to the weaker binding of SO_4^{2-} to the fixed cations (Fig. 13.2B; see also Fig. 13.19). The relative binding affinities of Cl^- , SO_4^{2-} , and other anions on an amino-type exchange resin and some proteins are shown in Fig. 13.8.

The complex but reproducible patterns of swelling after long exposure to high concentrations of KCl are illustrated in Fig. 13.9, in which very similar patterns are exhibited among four different types of frog voluntary muscles. One observes similar patterns of swelling in frog kidney and spleen in response to increasing concentrations of KCl . As a rule, increasing concentration of KCl does not bring about a progressively greater increase of swelling. Detailed theoretical interpretations of these patterns were given by Ling and Peterson (1977). The KCl -induced salt linkage dissociation is, like K^+ uptake in Na^+ -loaded cells (Figs. 11.22–11.24), autocooperative; abrupt, stepwise swelling occurs with minor increments of KCl concentration. After one set of linkages are broken

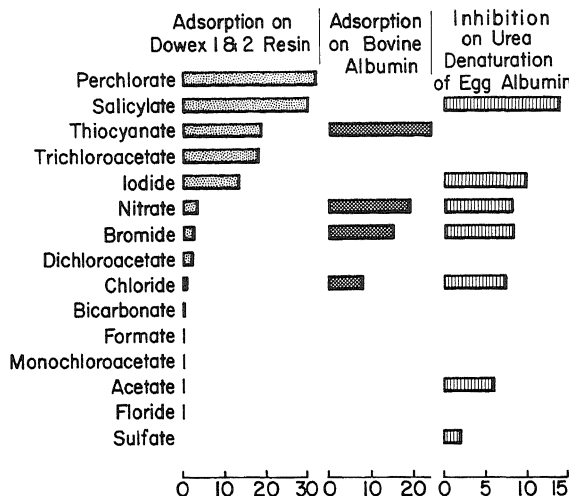


FIGURE 13.8. Relative affinity of various anions for the fixed amino groups of the model ion exchange resin Dowex 1 and 2 and two proteins. Units of affinity given in the abscissa are arbitrary. For a more detailed description, see Ling (1962), Table 7.5.

with swelling, further increase of KCl as a rule causes shrinkage for the same reason that the addition of any substance with a low q -value causes shrinkage, i.e., owing to decreased external water activity. With still further increase of KCl concentration, another group of stronger salt linkages may be autocooperatively dissociated, producing another swelling step, followed by another shrinkage step.

The present interpretation of KCl-induced swelling in living cells involves the assumption of the dissociation of salt linkages and apparent creation of new adsorption sites for both K^+ and Cl^- . For frog muscles, one of these new sites appears at an external K^+ concentration approaching 100 mM; the second group appears at about 300 mM (see Fig. 13.9). With these assumptions, it was possible to explain quantitatively both

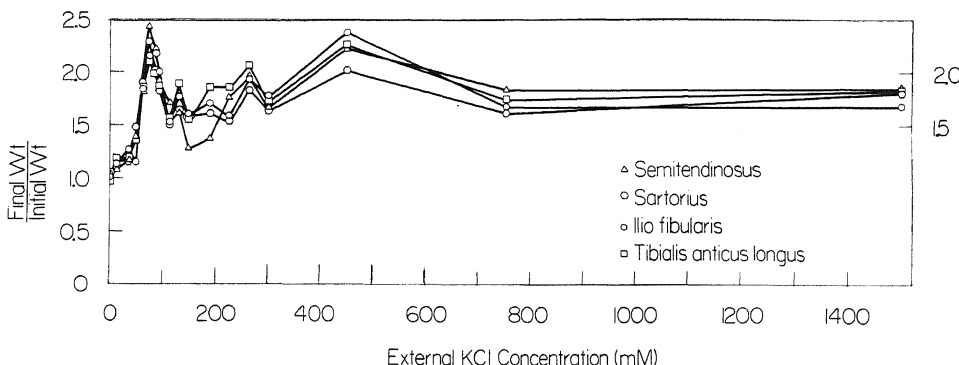


FIGURE 13.9. Equilibrium swelling of frog voluntary muscles in varying concentrations of KCl. Each point is a single determination. [From Ling and Peterson (1977), by permission of *Bulletin of Mathematical Biology*.]

the selective uptake of K^+ and Cl^- and the swelling phenomena observed (Ling, 1977e). Figure 13.10 demonstrates the good fit of theoretical curves to the equilibrium K^+ and Na^+ distribution data as well as to the data of Palmer and Gulati (1976). However, the argument would be more persuasive if we could find some additional independent experimental method to test this theory.

In Chapter 12, I went into some detail discussing the rate-limiting steps in the efflux of labeled solutes. A variety of examples (Figs. 12.23, 12.34–12.35, and 12.44) were cited to show that, in cases where the rate of surface permeation is fast, the efflux rate of a solute may be resolvable into multiple fractions and that the slower fraction or fractions may be rate-limited by desorption.

Now the theoretical basis for KCl-induced swelling, as described in equation (13.3) and the experimental observations shown in Figs. 13.9–13.10, dictates that, with increase of external KCl concentration, there are not only additional K^+ adsorption sites as a result of the splitting of salt linkages but also Cl^- adsorption sites. For frog muscle [Figs. 13.9 and 13.10A(B)] one class should be generated at an external KCl concentration of about 35 mM, reaching a peak at 100 mM; a second class at 140 mM, reaching a peak at 300 mM; and a third class at 300 mM, reaching a peak at 500 mM. One would predict that, after exposing frog sartorius muscle to increasing concentrations of radioactive ^{36}Cl -labeled KCl-Ringer, complex ^{36}Cl efflux curves would be obtained. When they are resolved into logarithmic fractions they should correspond to the newly created classes of bound Cl^- mentioned previously. Moreover, one would expect a slower rate of exchange with increasing $t_{1/2}$, as a result of the stronger linkage between Cl^- and the site, and hence stronger Cl^- binding constants. With these expectations in mind, an extensive series of studies was carried out by Ling and Graham (1983). The results were remarkably close to the theoretical expectations.

Figure 13.11 shows the normal Cl^- efflux of a frog sartorius muscle in a normal Ringer solution containing 2.5 mM KCl. The curves resemble the Na^+ efflux curves (Fig. 12.30) except that, after correcting for Cl^- in the connective tissue elements, only a very minute fraction of slowly exchanging Cl^- remains, amounting to some 0.1 μ moles/g of fresh cells. The main Cl^- efflux curve is that emerging from the cell with a $t_{1/2}$ of about 3 min (fraction b), which is not resolved from Cl^- from the extracellular space (fraction a) in this and the following sets of data. This is in agreement with the assumption that the bulk of cell Cl^- in normal sartorius muscle cells is virtually all free in cell water. Exposure to Ringer solution containing 30 mM KCl generates a new fraction (fraction c) with a $t_{1/2}$ of about 8 min (Fig. 13.12). The magnitude, but not the $t_{1/2}$ of about 15 min, begins to emerge in some preparations (Fig. 13.13C). Figure 13.14 compiles results obtained over the range of the $[KCl]_{ex}$ up to 450 mM. One can then compare these with theoretically postulated fractions, shown in the inset, taken from Fig. 13.10A, described several years before the Cl^- experiments were performed. Remembering that equimolar concentrations of K^+ and Cl^- are involved in all steps, one finds correspondence between fractions a and b of Fig. 13.14 and fraction C of Fig. 13.10; fraction c of Fig. 13.14 and fraction E of Fig. 13.10, and fraction d + e of Fig. 13.14 and fraction F of Fig. 13.10. Also note how closely the composite total Cl^- binding curve shown in Fig. 13.14 parallels the observed swelling curve shown in Fig. 13.10A(B).

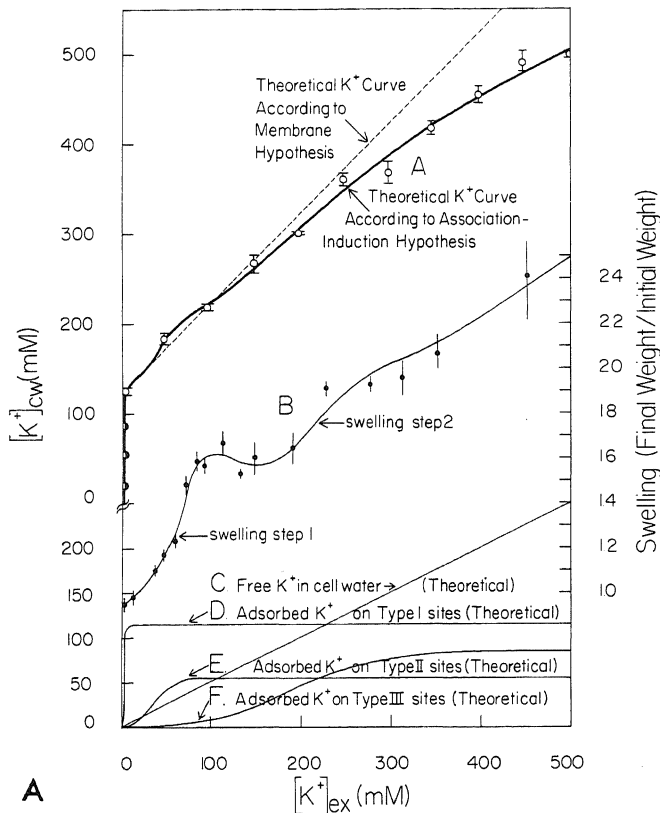
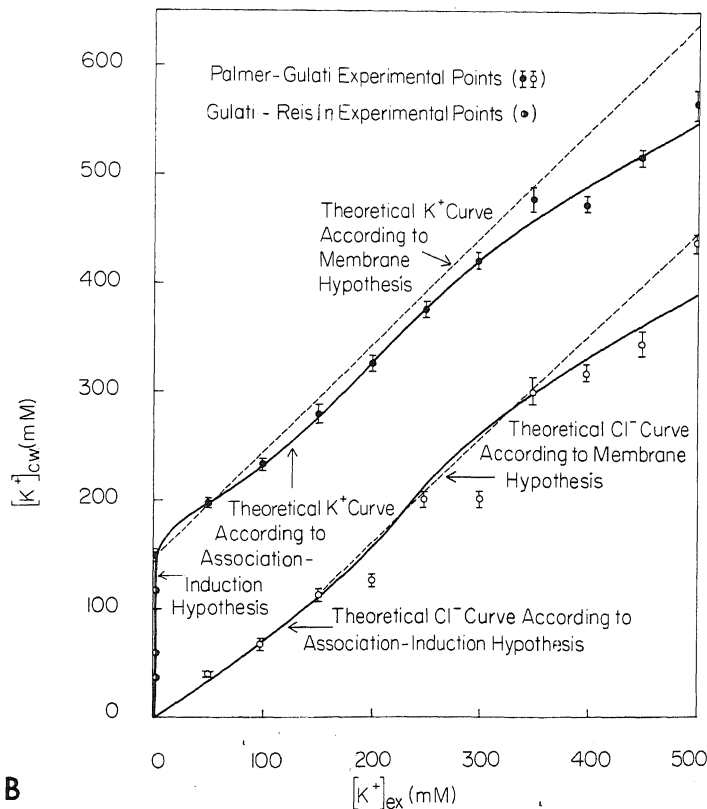


FIGURE 13.10. (A) K^+ concentration in frog muscle cells in the presence of 91 mM external NaCl. \circ , New data on K^+ accumulation; \bullet , new data on muscle swelling; \ominus , old data of Ling and Bohr (1970) on K^+ accumulation. Curve A is a theoretical curve which is resolvable into components shown as curve C [$\text{free } K^+(Cl^-)$], curve D (type I adsorption), curve E (type II adsorption), and curve F (type III adsorption). The contribution of type I sites was determined from the results of previous studies; those of type II and type III sites were estimated from curve B, which records the two-step swelling of frog muscles under conditions similar to those of curve A, except that a low external NaCl concentration of 30 mM was used. The q -value used to obtain curve C was 0.5. Other numerical values used to obtain curves D, E, and F, respectively, were $[f]_L = 122, 55$, and 85 mM; $K_L = 1.35, 35$, and 185 mM; and $-\gamma/2 = 0.54, 1.36$, and 0.91



kcal/mole. For all data points the lengths of the error bars represent twice the SE based on four or more determinations. The dashed straight line, predicted on the basis of the membrane theory as given by Palmer and Gulati (1976), intercepts the ordinate at about 130 mM. (B) K^+ and Cl^- in frog muscle cells. The experimental points are from Palmer and Gulati (1976) and Gulati and Reisin (1972), as indicated. Solid curves are theoretical as in (A). Dashed lines were derived on the basis of the membrane theory (i.e., a Donnan equilibrium). The numerical values used to obtain the theoretical curves for K^+ were $q = 0.5$ for curve C and, for curves D, E, and F, respectively, $[f]_L = 150, 12, \text{ and } 120 \text{ mM}$; $K_L = 1.0, 28, \text{ and } 210 \text{ mM}$; and $-\gamma/2 = 0.60, 1.36, \text{ and } 0.91 \text{ kcal/mole}$. The theoretical curve of Cl^- accumulation is equal to that for K^+ accumulation minus type I adsorption. [From Ling (1977e), by permission of *Science*.]

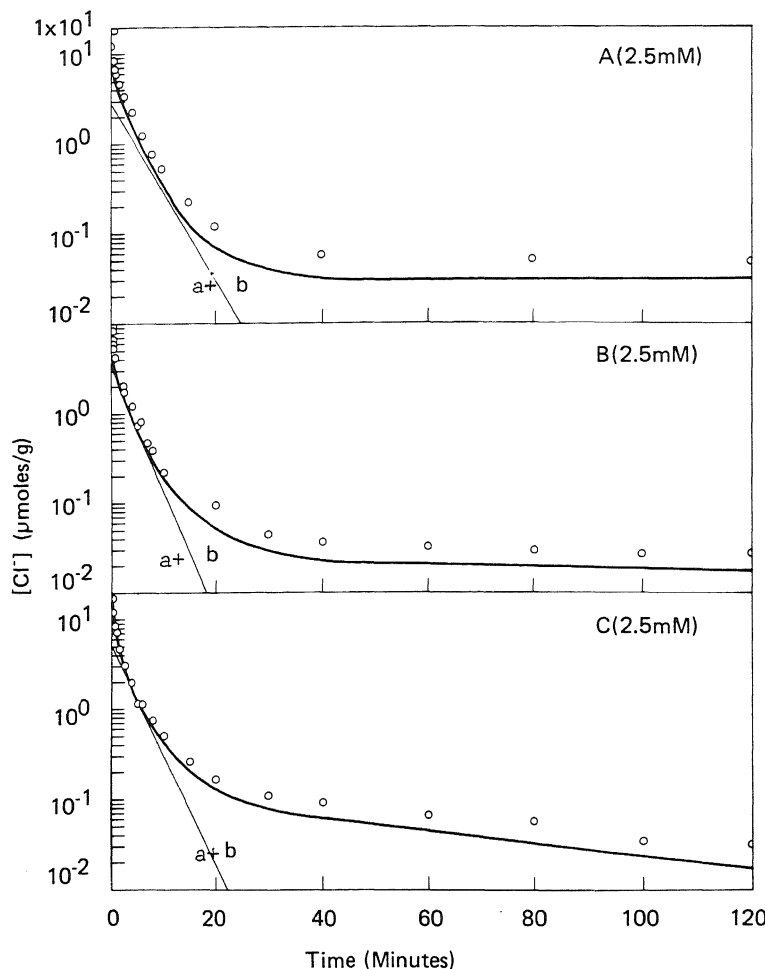


FIGURE 13.11. Cl^- efflux curves of frog muscle exposed to a Ringer solution containing 2.5 mM K^+ . Size of the major fraction ($a + b$) was determined by extrapolating to zero time. [From Ling and Graham (1983), by permission of *Physiological Chemistry and Physics*.]

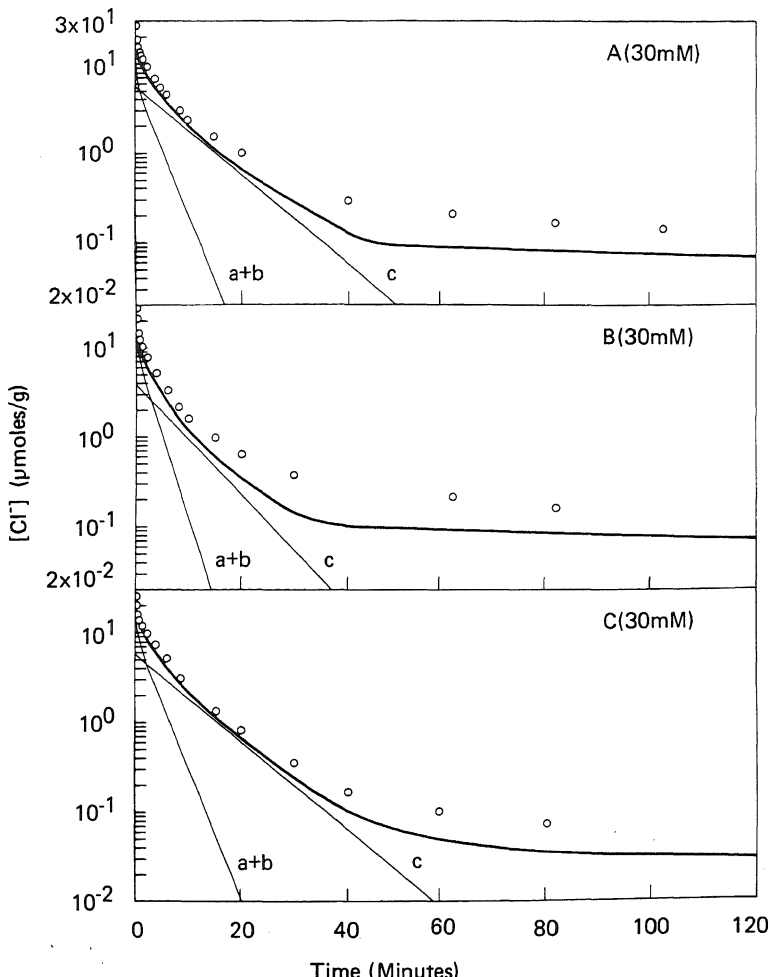


FIGURE 13.12. Cl^- efflux curves of frog sartorius muscle exposed to a Ringer solution containing 30 mM K^+ . Sizes of the fractions (a + b, c) were obtained by extrapolating to zero time. [From Ling and Graham (1983), by permission of *Physiological Chemistry and Physics*.]

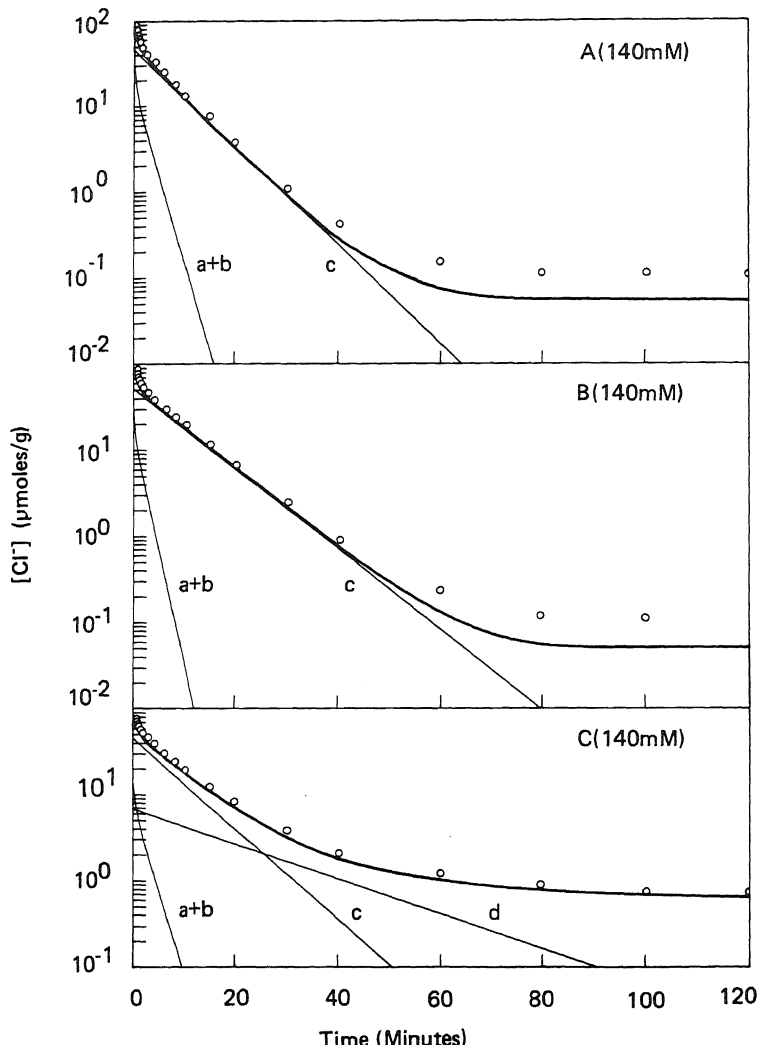


FIGURE 13.13. Cl^- efflux curves of frog sartorius muscle exposed to a Ringer solution containing 140 mM K^+ . Sizes of the fractions (a + b, c, d) were obtained by extrapolating to zero time. [From Ling and Graham (1983), by permission of *Physiological Chemistry and Physics*.]

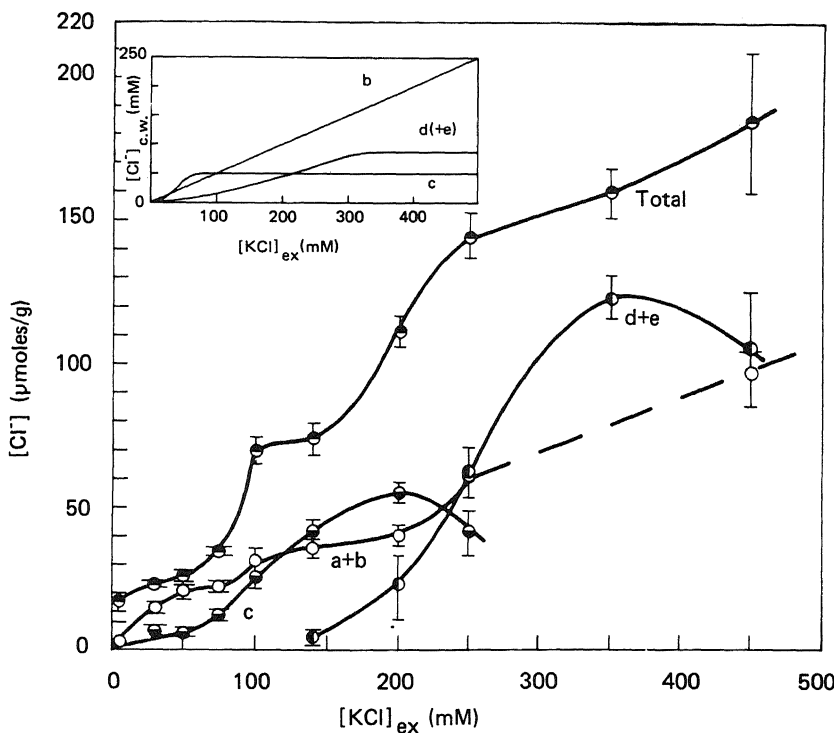


FIGURE 13.14. Concentration of Cl^- in muscle exposed to different KCl concentrations (indicated on the abscissa) as determined by studies of efflux with different rate constants (a + b, c, d, and e) and obtained from data illustrated in Figs. 13.10–13.12 by extrapolating the efflux fractions to zero time. These experimentally determined fractions should be compared with the three fractions theoretically derived from swelling curves (inset, also Fig. 13.10A). Compare the composite curve labeled “Total” with the swelling curve (B) in Fig. 13.10A. [From Ling and Graham (1983), by permission of *Physiological Chemistry and Physics*.]

13.5. The Variable Number of K^+ , Rb^+ , and Cs^+ Adsorption Sites: The Role of Salt Linkages

In Section 11.2 I mentioned how from reciprocal plots of the equilibrium concentrations of K^+ , Rb^+ , and Cs^+ accumulated in the cell one could obtain the maximum number of adsorption sites. On first thought one would expect that the concentration of sites, $[f]$, should be the same whether one studies K^+ , Rb^+ , or Cs^+ accumulation in the same tissue. In reality, the data obtained varied a great deal: 140 (K^+), 108 (Rb^+), and 75 mmoles/kg (Cs^+). The data presented in Fig. 13.15 offer at least a partial solution to this mystery.

Figure 13.15 shows the swelling curve of frog muscle in KCl as well as other salts: $RbCl$, $CsCl$, $LiCl$, $NaCl$, and choline chloride. Note that only KCl and $RbCl$ caused extensive swelling, while other permeant Cl^- salts of Cs^+ , Li^+ , Na^+ , and choline caused no swelling until their concentration went beyond 150 mM. We have presented evidence that swelling involves additional cation and anion binding, shown in equations (13.2) and (13.3). One would expect that, as one increased the concentration of K^+ or Rb^+ salts, as in Figs. 11.6 and 11.7, more salt linkages would be dissociated, thus giving rise to more K^+ (or Rb^+) binding sites than in the case of Fig. 11.8, where Cs^+ uptake was studied. In this concentration range, Cs^+ does not cause swelling (Fig. 13.15), hence does not cause salt linkage dissociation and the creation of more Cs^+ binding sites. While this interpretation must be held as tentative until the possible effect of the difference in the anion used is evaluated (acetate in Figs. 11.6 and 11.7, chloride in Fig. 13.15), it seems quite obvious that in living cells there are few unoccupied K^+ adsorption sites. The additional sites revealed by high concentrations of K^+ or Rb^+ were originally engaged in salt linkages, a part of the volume-maintaining system.

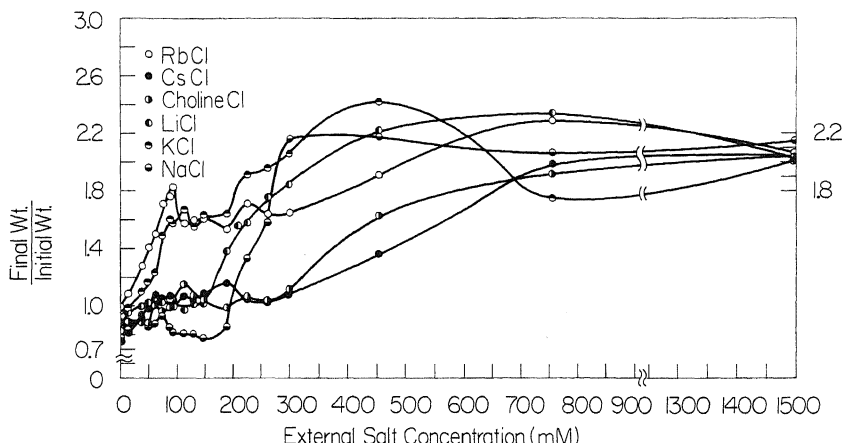


FIGURE 13.15. Swelling of frog voluntary muscles in varying concentrations of $LiCl$, $NaCl$, KCl , $RbCl$, $CsCl$, and choline chloride, demonstrating segregation into roughly three types of curves. Each point represents the average of four determinations from one of each of the four different types of muscles. To avoid confusion the SEM are not shown here. [From Ling and Peterson (1977), by permission of *Bulletin of Mathematical Biology*.]

13.6. The Mechanism of Cell Swelling Caused by the Depletion of ATP and the Role of NaCl in the Medium

Swelling and shrinkage in concentrated KCl solutions have been shown to conform to the concept that salt linkages between protein chains play a role in the maintenance of the normal cell shape and that the salt linkage depends on the proper *c*-value of the anionic sites, so that tight salt linkages are maintained in competition with other cations. Since the normal *c*-value of these sites, according to the AI hypothesis, is under the control of the cardinal adsorbent ATP, one can expect that the volume (size) and shape of living cells will be dependent on ATP.

Experimental findings that can be explained by this theory have been in existence for a long time. Thus Bendall (1951) showed that rabbit psoas muscle fiber bundles abruptly shortened in an "all-or-none" manner when their ATP content fell below 50% of its normal value. Nakao and his co-workers (1961) showed that dependence of the shape and size of human erythrocytes on their ATP content when the cells were suspended in physiological saline to which was added glycolytic poison, NaF. ATP contents were manipulated by adding to or removing from the medium NaF, adenosine, inosine, and glucose. When ATP was between 100 and 50 μ moles/100 ml of cells, the cells assumed normal biconcave disc shapes. When ATP fell below 50 μ moles/100 ml they assumed the crenated shape, and when it reached 10 μ moles/100 ml of cells, the cells assumed the smooth spherical shape (Figs. 13.16 and 13.17).

The assumption of the spherical shape involves swelling. Indeed, that injured and dying cells swell has been known since the time of J. Loeb (1905, 1913), who was credited to have first reported muscle cell swelling in death (Lucke and McCutcheon, 1932).

The AI hypothesis offers the following explanation for the swelling of injured and dying cells induced by ATP depletion. ATP adsorption at the cardinal sites maintains the anionic side chains of the involved proteins at such a *c*-value that K^+ , Rb^+ , NH_4^+ and the fixed cations (α -amino, ϵ -amino, and guanidyl groups) are preferred over Na^+ , Li^+ , or Cs^+ . Therefore, in normal resting cells with a normal amount of ATP, 100 mM KCl and RbCl cause cell swelling but 100 mM NaCl or 100 mM LiCl does not (Fig. 13.15). *Loss of ATP causes an increase of the c-value of the anionic sites. Consequently the relative affinity for Na^+ increases and that for fixed cations decreases (see Figs. 6.7 and 6.8)*, so that 100 mM NaCl can now achieve in these ATP-depleted cells what 100 mM KCl achieves in normal cells with normal ATP contents.

Three corollaries can be derived from this theory:

Corollary 1. Dying cells will swell only in the presence of a high concentration of Na^+ , as, for example, is found in blood plasma or Ringer solution. Swelling would be absent or reduced if Na^+ salt were replaced by an equimolar concentration of neutral molecules of similar osmotic strength (i.e., sucrose with an approximately similar *q*-value in cell water as NaCl).

Corollary 2. Swelling of dying cells would also depend on the binding energy of the major anion of the surrounding medium. More strongly adsorbed anions would cause a greater degree of swelling.

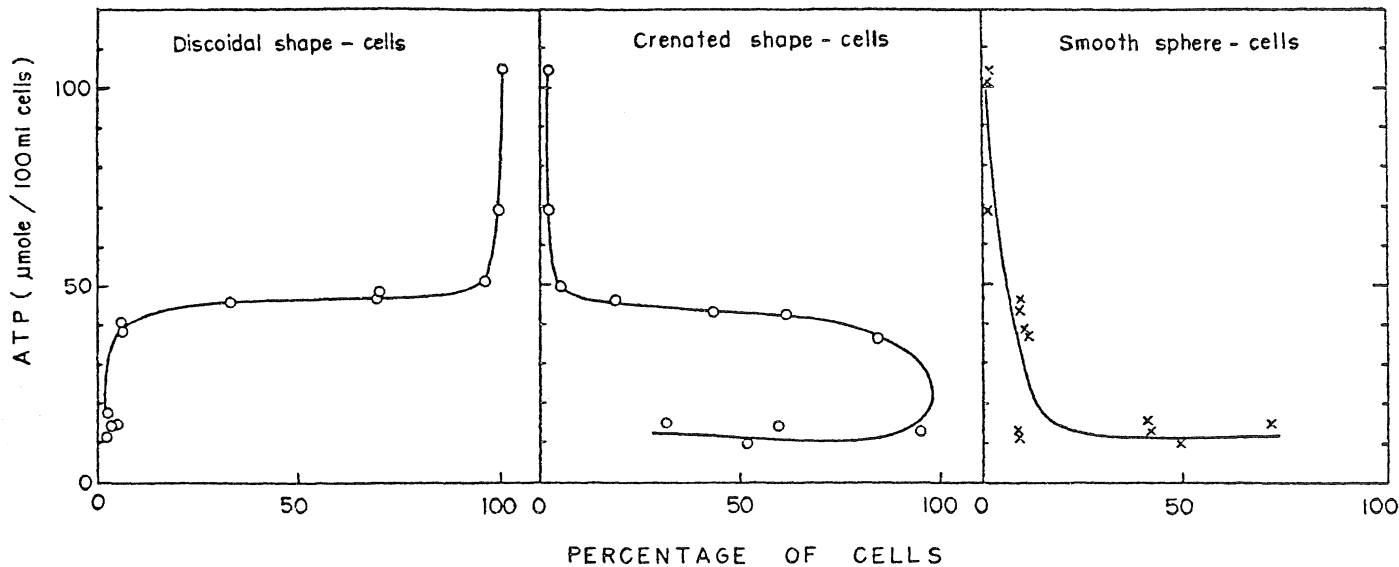


FIGURE 13.16. Adenosine triphosphate level in erythrocytes and their shape. Abscissa: Percentage of the cells with various shapes. Ordinate: Content of ATP in erythrocytes. [From Nakao *et al.* (1961), by permission of *Journal of Biochemistry (Tokyo)*.]

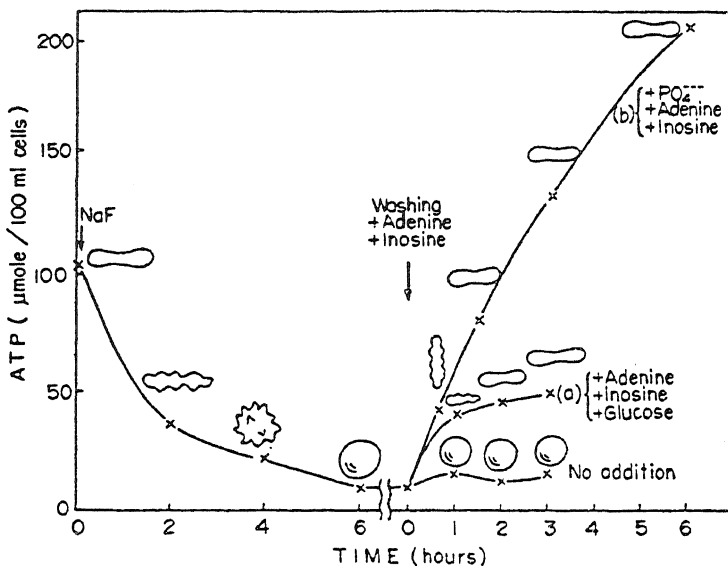


FIGURE 13.17. Washed erythrocytes were incubated with NaF at 37°C for 6 hr and, after washing out fluoride, reincubation was carried out with addition of inosine, adenine, and glucose (a), and with addition of adenine, inosine, and inorganic phosphate (b). [From Nakao *et al.* (1961), by permission of *Journal of Biochemistry (Tokyo)*.]

TIME	TISSUE ^{22}Na cpm/mg dry wt		MORPHOLOGY	
	CONTROL	aB+Na-R	SODIUM RINGER (Na-R)	SUCROSE RINGER (CHO-R)
0	—	—		
2 MIN	—	600±90		
8 MIN	—	765±117		
2 HRS	455±36	2147±506		
8 HRS	684±46	1299±71		

FIGURE 13.18. Sequential changes in morphology of toad bladder cells after addition of amphotericin B (aB) to mucosal sodium Ringer solution (Na-R) or sucrose Ringer solution (CHO-R). Changes in tissue-exchangeable Na^+ content are also shown. Each value is reported as the mean \pm SD of four separate experiments. [From Saladino *et al.* (1969), by permission of *American Journal of Pathology*.]

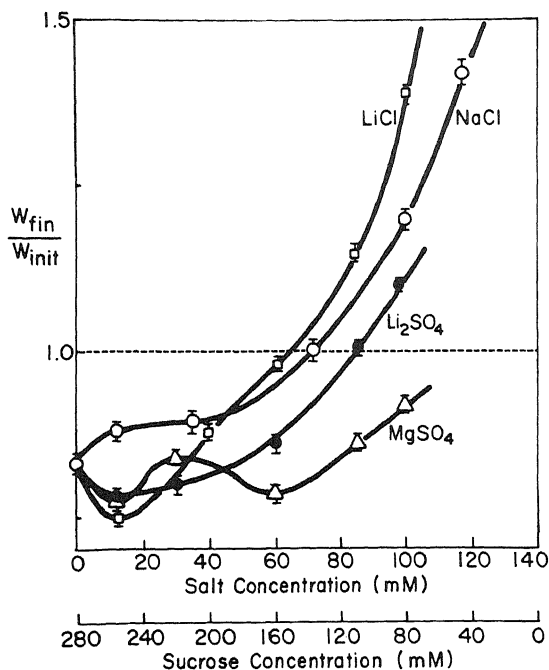


FIGURE 13.19. Swelling and shrinkage of mouse kidney in various isosmolar mixtures of sucrose and Na^+ or Li^+ salts. Ringer solution used contained, besides Ca^{2+} , Mg^{2+} , and other ingredients, NaCl (or Na_2SO_4) and sucrose in isosmolar mixtures. Ordinate represents ratio of final wet weight (W_{fin}) to initial weight (W_{init}). [From Ling and Kwon (1983), by permission of *Physiological Chemistry and Physics*.]

Corollary 3. Li^+ can substitute for Na^+ because at high *c*-value both Na^+ and Li^+ are preferred (see Figs. 6.7 and 6.8).

Figure 13.18 presents the findings of Saladino, Bentley, and Trump (1969) on the swelling of toad bladder epithelium when exposed to the poison amphotericin B in normal Na^+ Ringer and in sucrose Ringer. Extensive swelling occurred only in Na^+ Ringer solutions but not in sucrose Ringer solution, in agreement with Corollary 1.

Figure 13.19 shows that the extent of swelling of mouse kidney that was exposed to cold increases progressively with a higher proportion of NaCl over sucrose in the Ringer solution. Note also that (1) LiCl and NaCl brought about the maximum swelling at each concentration. (2) Li_2SO_4 has much less swelling effect than LiCl . (3) MgSO_4 had very little swelling effect. These data confirm all three corollaries mentioned above. Cl^- is more strongly adsorbed on cationic amino groups than is SO_4^{2-} (Fig. 13.8).

It might also be noted that an isosmolar concentration of sucrose substituting for all the NaCl in the mammalian Ringer solution actually causes considerable shrinkage (see also Ling *et al.*, 1979). This shrinkage in sucrose Ringer suggests that there are, preexisting in normal cells, potential salt linkages that are kept apart by NaCl in the Ringer solution. These salt linkages are joined when NaCl is replaced by sucrose with consequent shrinkage of the cells. A similar effect was noted in lymphocytes (Negendank and Shaller, 1982a,b).

Figure 13.20 shows how, in mouse brain dying from exposure to low temperature (4°C) in a NaCl -Ringer solution, the increase of water content (and hence weight) is quantitatively related to the decrease of the level of ATP in the cell. The increase of

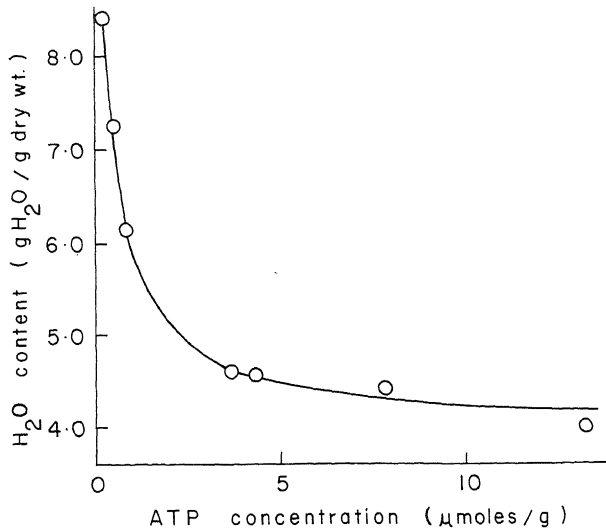


FIGURE 13.20. Relation between decreasing ATP and swelling of mouse brain in normal mammalian Ringer solution. [From Ling (1983a), by permission of *Physiological Chemistry and Physics*.]

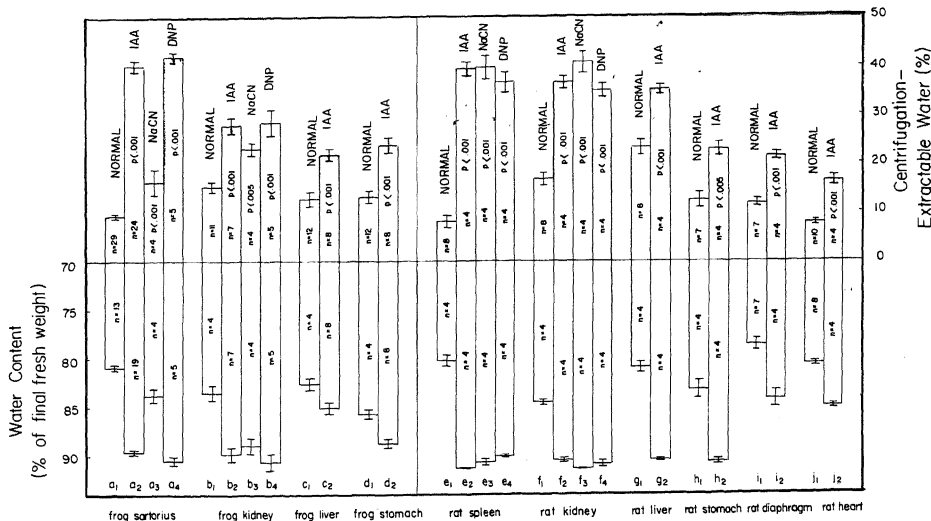


FIGURE 13.21. Effects of metabolic poisons on the water that is extractable by centrifugation and total water contents of frog and rat tissues. Before centrifugation poisoned tissues were exposed for 7 days at 4°C to a Ringer solution containing 1 mM IAA, 1 mM NaCN, or 1 mM DNP. [From Ling and Walton (1976), by permission of *Science*.]

water content was relatively modest during the initial fall of ATP content and then rapidly accelerated with disappearance of the last μ moles of ATP per gram of fresh tissue.

In Fig. 13.1, I demonstrated that the retention of water in normal muscle cells does not depend on the presence of an intact cell membrane. Muscles were cut into 2- and 4-mm segments with both ends open. The retention of water by the "naked" protoplasm was demonstrated by its resistance to centrifugation at 1000g for 4 min, a process that is quite effective in removing water trapped in the extracellular space. This retention of cell water, according to the AI hypothesis, is primarily due to its multilayer polarization on the matrix of extended protein chains maintained at the correct electronic configuration by the adsorption of ATP. The question may now be raised, What happens to the water in swollen cells in which the ATP has dropped to zero? The answer is provided by the data shown in Fig. 13.21. Centrifugation for 4 min at 1000g, which is unable to remove cellular water of normal cells with or without an intact membrane, removes much of the water of swollen cells in response to treatment with metabolic poisons (Ling and Walton, 1976). These findings show quite clearly that there is a fundamental difference in the cohesiveness and retention of water between cells that are normal, swollen in response to a hypotonic solution, or swollen in isotonic KCl (Fig. 13.1) and cells swollen from ATP depletion brought on by poisons or cold temperatures (for certain mammalian tissues). The mechanism for KCl-induced swelling, i.e., the tendency to build up deeper layers of polarized water, cannot be fully operative in these dying cells and a somewhat different mechanism must be involved.

To introduce this mechanism, we return to Section 13.2. One recalls that the reason polarized water can maintain a finite volume, illustrated in the case of the PEO-water system (Fig. 13.3), is the below-unity q -value for the external sodium citrate in the polarized water. If depolarized water has an increased q -value for sodium citrate, sodium citrate will continue to move into the bag with continued swelling toward the maximum volume permitted by the bag. This swelling, which has been referred to as *depolarization swelling*, is at least in part responsible for the swelling of dying cells. Another contributing factor to the swelling of dying cells is the osmotic effect exerted by the K^+ liberated from its normal adsorption sites in consequence of ATP depletion. Thus, the inward movement of NaCl with the c -value increase and the liberation of K^+ from adsorption sites more than compensates for the fall of osmotic activity of polarized water. The influx of water will then go *pari passu* with the dissociation of salt linkages by Na^+ and Cl^- entering the cells, leading to the accumulation of loosely held normal water, readily extracted by centrifugation at 1000g.

13.7. Classification of Cell and Tissue Swelling

In the foregoing sections various mechanisms have been suggested for cell swelling. For convenience I shall classify them into three major types:

Type I. Simple osmotic swelling (and shrinkage). When living cells or model sys-

tems are transferred from a more concentrated solution of an excluded solute to a more dilute one, the difference of water activity leads to movement of water.

Type II. Dissociative swelling (and associative shrinkage). Swelling of muscle cells in isotonic KCl belongs to this class. The effectiveness of different salts in causing *Type IIA swelling*, through the dissociation of volume-holding salt linkages, depends on the relative adsorption energies of both the cation and the anion of the salt and their concentrations. Swelling produced by isotonic NaCl in ATP-depleted cells involves depolarization of cell water and is referred to as *Type IIB swelling*.

Type III. Desorptive swelling. In dying cells, before exhaustion of ATP, there may be a stage at which cell K^+ has desorbed before water is depolarized. The decrease of water activity owing to the introduction of free K^+ then induces a swelling called Type III.

13.8. Summary

In the association-induction hypothesis, the normal lowering of the activity of cell water, so that it remains in equilibrium with that of water in the external medium, is a result of the polarization of water in multilayers by a matrix of extended cell proteins. The activity of cell water adjusts rapidly to balance any change in the activity of external water (i.e., exposure to a hypotonic or hypertonic solution), and this adjustment, at equilibrium, follows the Bradley adsorption isotherm outlined in Chapter 9. This accounts for the apparent behavior of cells as osmometers even though the actual concentration of ions and other solutes dissolved within cell water is much smaller than usually assumed (Chapter 8).

There are two major factors that determine cell volume: (1) the degree of polarization or depolarization of cell water and (2) the formation or release of inter- and intramacromolecular salt linkages. In this chapter I have reviewed a large amount of data in frog muscle that documents the formation and breakage of salt linkages and their effect on equilibrium cell water and volume. This is manifested especially in the phenomenon of swelling of cells in moderately concentrated salt solutions that is accompanied by selective uptake of a cation (e.g., K^+) and an anion (e.g., Cl^-). One of the major functions of ATP is to maintain cell volume, and it does this via three mechanisms: (1) It potentiates polarization of water in multilayers, (2) it potentiates adsorption of a cation (usually K^+) onto fixed anionic sites that could potentially form salt linkages with fixed cationic sites, and (3) it tends to maintain preexisting salt linkages that are otherwise susceptible to breakage by the usual high concentration of Na^+ in the external medium. The effects of ATP depletion are therefore (1) a decrease in the number of adsorbed cations (i.e., a decreased K^+ that is not replaced by Na^+), (2) an increase in the q -value of solutes (including Na^+) that are dissolved within cell water, and (3) a tendency of NaCl to break open preexisting salt linkages. Cells depleted of ATP tend to swell. However, the net resultant of these factors may differ during the course of depletion of ATP, under different conditions, or in different cells.

The modulation of salt linkages between macromolecules may have a role not only in cell volume regulation but also in a variety of phenomena, and it will be discussed in various contexts in subsequent chapters.

Electrical Potentials

14.1. Evidence against the Membrane Theory of Cellular Electrical Potentials

The ionic theory of Hodgkin and Katz (1949a) and the Hodgkin–Huxley theory of the action potential (Hodgkin *et al.*, 1952; Hodgkin and Huxley, 1952a–d) described in some detail in Section 3.4, are major landmarks in the evolution of cell physiology and provided the foundation for a great deal of skillful research in basic electrophysiology. Considering the confusion regarding the nature of cellular electric potentials before these theories developed, their importance is evident. It is now clear, however, that these theories rest on a fundamentally unsound basic theory of the living cell—the membrane pump theory. I shall first examine evidence against the membrane pump theory of the cellular electrical potential and then show how much of the accumulated findings can be grafted onto an altogether different theory of the living cell, the association–induction (AI) hypothesis.

14.1.1. The Indifference of Resting Potential in Frog Muscle to External Cl^- Concentration

In 1956 Adrian showed that the resting potential of frog muscle remained unchanged if the Cl^- in the Ringer solution was substituted by SO_4^{2-} (Fig. 14.1). This experimental observation was confirmed by Hodgkin and Horowicz (1960). Caldwell (1968) explained this indifference to external Cl^- concentration as being due to a relatively low Cl^- permeability. However, this explanation is not correct. Hutter and Padsha (1959) showed that the frog muscle membrane resistance increased to more than twice its normal value when Cl^- in the Ringer solution was replaced by ions like I^- and NO_3^- . They concluded that the contribution of Cl^- to membrane conductance is more than twice that of K^+ . More recently, Lorkovic and Tomanek (1977) measured the K^+ conductance (g_{K}) and Cl^- conductance (g_{Cl}) of mammalian muscles. g_{Cl} s were 845 and $1025 \mu\text{mho}/\text{cm}^2$ for the gastrocnemius and soleus muscles, respectively, while the corresponding g_{K} s were only 99 and $161 \mu\text{mho}/\text{cm}^2$. Thus in these mammalian muscles the Cl^- conductance is from six to eight times larger than the K^+ conductance.

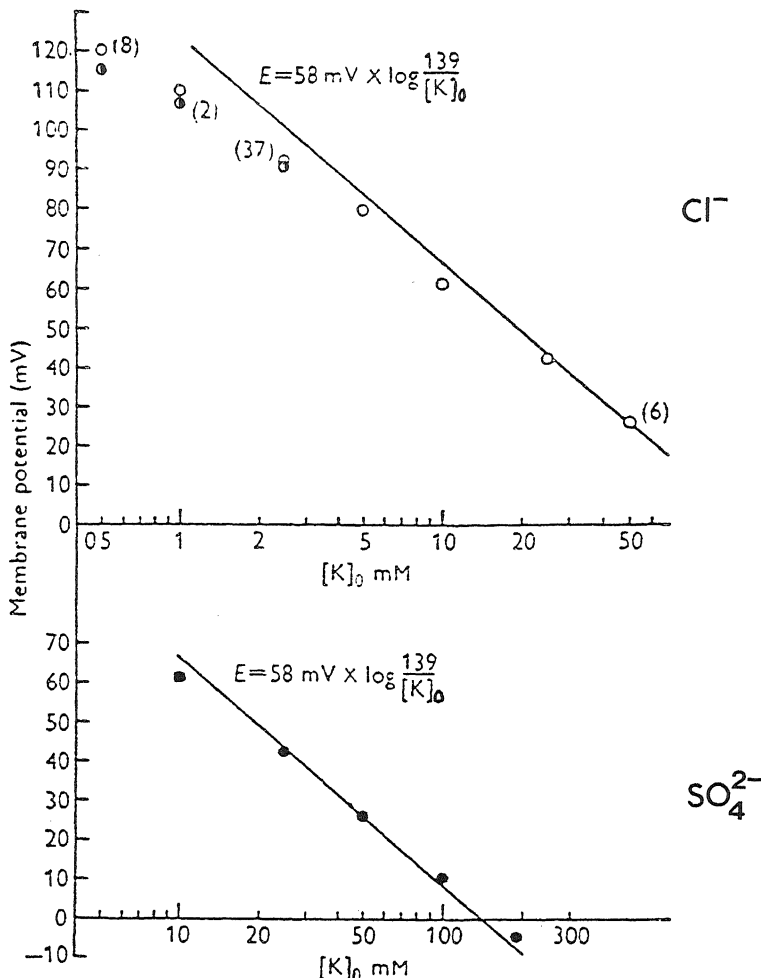


FIGURE 14.1. Effect of external K⁺ concentration on the membrane potential of the sartorius muscle. Abscissa: K⁺ concentration in mM. O, Membrane potential in Cl⁻ solutions; ●, membrane potential in SO₄²⁻ solutions; ○, membrane potential in Cl⁻ solutions with half the normal concentration of NaCl. Where the number of muscles is not indicated by a figure in parentheses, the point is the average value of four muscles. The lines are drawn according to equation (2.4). [From Adrian (1956), by permission of *Journal of Physiology*.]

A Cl⁻ permeability higher than K⁺ permeability is also suggested by the much shorter *t*_{1/2} of labeled Cl⁻ efflux (ca. 3 min, Fig. 13.11), than of K⁺ efflux (ca. 10 hr, Figs. 12.23, 12.26, and 12.30).

Hodgkin and Katz (Hodgkin, 1958; B. Katz, 1966) then modified the Hodgkin-Katz equation by eliminating the Cl⁻ term from the original Hodgkin-Katz-Goldman equation [equation (3.11)] and obtained

$$\psi = \frac{RT}{\mathcal{F}} \ln \frac{P_K [K^+]_{in} + P_{Na} [Na^+]_{in}}{P_K [K^+]_{ex} + P_{Na} [Na^+]_{ex}} \quad (14.1)$$

or

$$\psi = \frac{RT}{\mathcal{F}} \ln \frac{[K^+]_{in} + b[Na^+]_{in}}{[K^+]_{ex} + b[Na^+]_{ex}} \quad (14.2)$$

where $b = P_{Na}/P_K$.

The omission of the Cl^- term from the original equation [equation (3.11)] was justified on the grounds that Cl^- distribution is already "at equilibrium" (B. Katz, 1966, p. 62). This explanation cannot be correct either. Most electrical potential differences observed at interfaces of one sort or another, including that proposed by Bernstein for the cell resting potential, are *equilibrium* potentials. That is to say, in the equilibrium state, the number of K^+ ions leaving the muscle cell is exactly equal to that returning. This state of equilibrium is in fact an integral part of the electrical potential difference observed. In other words, attainment of ionic equilibrium, at a temperature other than absolute zero, does not eliminate the potential differences. Otherwise, there could not be a Donnan potential in a Donnan equilibrium (see Section 2.2.6).

Another self-contradiction arose from this kind of interpretation of the indifference of the muscle resting potential to external Cl^- . The resting potential of human erythrocytes is only a few millivolts (-8.0 mV, Jay and Burton, 1969; -5.0 mV, Lassen and Sten-Knudsen, 1968) and thus not compatible with the high K^+ content and high K^+ concentration gradient observed (i.e., $[K^+]_{in}/[K^+]_{ex} = 27.4$, R. E. Bernstein, 1954), which would have predicted a ψ of 83 mV. The explanation often offered here is that in the erythrocytes the much higher membrane permeability to Cl^- makes the red cell membrane a Cl^- electrode. Thus the finding of a higher permeability to Cl^- than to K^+ in two different types of cells would seem to have produced exactly opposite effects: ψ of frog muscle is independent of external Cl^- concentration and dependent only on external K^+ , while ψ of human erythrocytes is dependent only on Cl^- and independent of external K^+ . Explanations offered to explain the low ψ measured in a variety of other cells that also are rich in K^+ are similarly flawed (Lassen *et al.*, 1971; T. C. Smith and Adams, 1977).

The indifference of ψ to Cl^- , and indeed to anions in general, in some cells, and the sensitivity to Cl^- in other cells (see Section 14.4.4), show quite clearly that the potential-generating systems among different types of cells, or even the same cell at different times, are quite selective. In some cases, they are selective for cations, and in other cases, for anions. A homogeneous isotropic membrane of the kind envisaged in the derivation of the Hodgkin-Katz-Goldman equation is too simple to provide a mechanism whereby one kind of ion can exert an effect on ψ while the oppositely charged ion does not.

14.1.2. Do the Resting and Action Potentials Depend on the Intracellular Concentrations of K^+ and Na^+ ?

Among the evidence supporting the Hodgkin-Katz model of the cellular potential was the results of Baker, Hodgkin, and Shaw (1961), of Adrian (1956), and of Hagiwara *et al.* (1964), showing a dependence of the resting potential on internal K^+ concentration (Section 3.4.1). However, as briefly indicated in that section and elsewhere (Ling, 1960, 1962, 1978c), these studies were in apparent contradiction to other results reported on this same subject. Thus, between 1950 and 1965 at least six other labora-



Ichiji Tasaki

tories, besides that of Grundfest *et al.* (1954) (Section 3.4.1), reported results of a different kind:

1. Tobias (1950) reported that virtually complete removal of intracellular K^+ from frog muscles after soaking in distilled water did not cause the predicted disappearance of the resting potential.
2. Falk and Gerard (1954) reported a similar failure to observe the expected changes of the resting potential following the injection of 3 M KCl or 3 M NaCl into frog muscle fibers.
3. In spite of the presence of normal K^+ and Na^+ concentration gradients across the cell surface of *Fundulus* eggs, Kao (1956) could not detect the presence of a measurable resting potential, even though with a similar technique he and co-workers readily measured a resting potential in starfish eggs.
4. F. H. Shaw and co-workers (Shaw and Simon, 1955; Shaw *et al.*, 1956) found that variation of intracellular K^+ and Na^+ contents did not produce changes of the resting potential of frog muscles according to equation (3.11).
5. Koketsu and Kimura (1960) reported a normal resting potential in frog muscle leached free of most of its K^+ content by prior exposure to a simple half-isotonic sucrose solution. This finding was confirmed by Neville (see Ling, 1962, p. 265).
6. Ichiji Tasaki and his co-workers (Tasaki and Takenaka, 1963, 1964; Tasaki *et al.*, 1965) showed that large variations in the Na^+ / K^+ ratio of the internal perfusion fluid do not significantly affect the resting potential of squid axons (Fig. 14.2). Furthermore Tasaki, Luxoro, and Ruarte (1965) found that an overshoot persists in the action potentials of Chilean squid axon, even though the intracellular perfusion fluid and the extracellular bathing fluid have the same con-

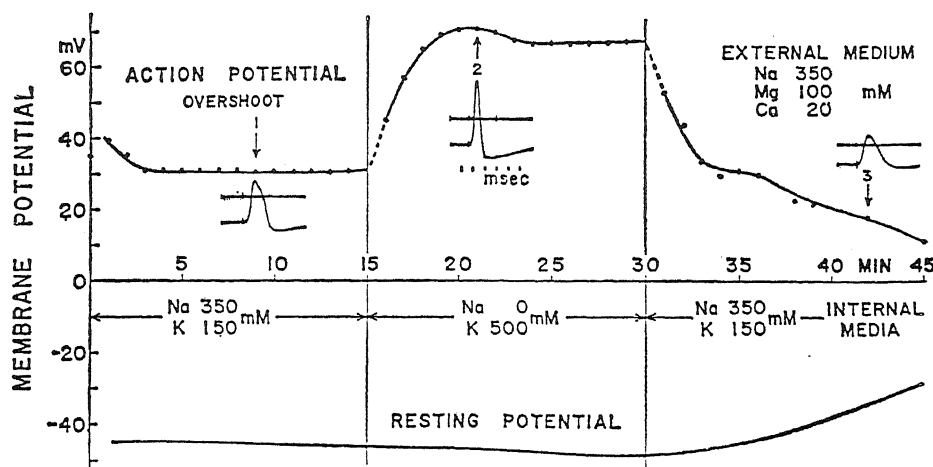


FIGURE 14.2. Resting and action potentials of an axon, intracellularly perfused first with a solution high in Na^+ , then with a solution high in K^+ , and finally with a Na^+ -rich medium. A calomel electrode ($0.6\ \text{M}\Omega$ resistance) was used for recording. [From Tasaki *et al.* (1965), by permission of *Science*.]

centrations of Na^+ (Fig. 14.2). This also contradicts the predictions of the Hodgkin-Katz-Goldman equation.

To the best of my knowledge, so far no adequate explanation has been provided for these contradictory findings.

14.1.3. The Electrogenic Na^+ Pump Hypothesis

In the preceding section, evidence demonstrating inconsistency with the Hodgkin-Katz theory of the relation between the measured resting and action potentials and the intracellular concentration of K^+ and Na^+ was presented. A similar inconsistency between internal ionic concentration and measured potential has been noted often to accompany physiological or pharmacological changes. Thus Burnstock (1958) expressed doubts that the electrical hyperpolarization of smooth muscle (i.e., inside becoming more negative) following inhibition of spike activity by adrenaline could have arisen from a change in the ratio of K^+ concentration inside to that outside the fiber. Draper *et al.* (1963) also noted that changes of the resting potential of frog sartorius muscle after treatment with cocaine or with G-strophanthin were not accompanied by the changes in the intracellular K^+ concentration expected according to the Hodgkin-Katz theory. Draper *et al.* suggested that the effect was on the ionic permeability. More extensive studies on similar subjects showed that this also was not the correct answer. Thus Kernan (1962) found that, as loaded muscle regained K^+ on return to a normal- K^+ Ringer solution, the resting potential was higher than that predicted on the basis of the measured intra- and extracellular K^+ concentrations and the equation

$$\psi_K = \frac{RT}{F} \ln \frac{[K^+]_{in}}{[K^+]_{ex}} \quad (14.3)$$

This familiar equation [equation (2.4)] can be regarded as a modified Hodgkin-Katz equation [equation (14.2)], with the assumption that $b = 0$. This assumption implies that the cell membrane is infinitely more permeable to K^+ than to Na^+ ; clearly no further decrease of b is possible beyond the theoretical value calculated by Kernan on the basis of equation (14.3). Kernan's findings were repeatedly confirmed and extended (for references see Thomas, 1972).

A large number of other experimental findings demonstrate a similar inconsistency between the electrical potential measured and that determined on the basis of equation (14.3): "In all these cases electrical potentials shifted more rapidly than would be expected from gross changes of ion concentration" (Koketsu, 1971, p. 85; see also Fru-mento, 1965; Slayman, 1965). These results led to the suggestion of the *electrogenic Na^+ pump*, which Kernan in his review described in the following words: "The electrogenic pumping of ions may be recognized by a change of the membrane potential which cannot be accounted for in terms of the passive ion movement and which has some characteristics of metabolic processes . . ." (Kernan, 1970, p. 399).

The diagnostic criteria for the electrogenic Na^+ pump according to its proponents included inhibition of the hyperpolarization by (1) lowering of the temperature, (2) exposure to 2,4-dinitrophenol, (3) exposure to ouabain, or (4) exposure to a low- K^+ medium. Still another accepted criterion for the electrogenic pump is its stimulation by intracellular injection of Na^+ salts (Coombs *et al.*, 1955; Kerkut and Thomas, 1965). Accepting the omission of the Cl^- terms in the Hodgkin-Katz-Goldman equation (Section 14.1.1), Mullins and Noda (1963) further modified the modified Hodgkin-Katz equation [equation (14.2)] by introducing a coupling factor, r , i.e., the number of Na^+ ions pumped out for each K^+ ion pumped in:

$$\psi = \frac{RT}{\mathcal{F}} \ln \frac{r[K^+]_{in} + b[Na^+]_{in}}{r[K^+]_{ex} + b[Na^+]_{ex}} \quad (14.4)$$

It was pointed out that, when $r = 1$, equation (14.4) reduces to equation (14.2). When only K^+ is transported, $r = \infty$. Equation (14.4) then reduces to equation (14.3).

The postulation of an electrogenic pump, as described by Kernan and others, is an *ad hoc* one, and not much more than a restatement of the observation; as such, it presents no testable predictions. As a variant of the membrane theory, it is not tenable in the face of the proven adsorbed state of cell K^+ . Moreover, it is in fact a special form of Maxwell's famous demon, which, by opening and closing a frictionless shutter, allows the sorting out of pure nitrogen and oxygen gases from air, thus creating free energy *de novo*. In reality, in this world, no such demon can exist. Here the electrogenic pumps sort out Na^+ and K^+ to hold up a potential difference larger than and different from what the laws of physics would have dictated.

14.1.4. All-or-None Opening and Closing of Na^+ and K^+ Gates

The concept of opening and closing of Na^+ and K^+ gates in the cell membrane is at least awkward when viewed with the fact that the resting cell membrane is at all times quite permeable to both K^+ and Na^+ . Since the radioactive tracer technique became available, the old concept that the cell membrane is impermeable to K^+ , Na^+ ,

and Cl^- which would harmonize with gate-opening and closing ideas—has long been disproven. For example the half-time of exchange of labeled Na^+ has been shown to be on the order of seconds in *Spirogyra* (Section 3.1) and (a few) minutes in frog muscle cells (Section 12.4.2). With such rapid traffic of Na^+ at all times, it is hard to visualize a specific all-or-none type of opening (and closing) of Na^+ (and K^+) gates during an action potential.

14.1.5. The Independence Principle

A fundamental assumption underlying the Hodgkin-Katz theory of cellular potentials and the Hodgkin-Huxley theory of action potentials is what has been referred to by Hodgkin and Huxley as the *independence principle*, i.e., that the cell membrane represents a homogeneous and isotropic medium and that diffusion of one ion in this medium is independent of that of other ions of the same or different species that are present. This principle was implicitly assumed in the development of the Hodgkin-Katz-Goldman equation. Earlier testing by Hodgkin and Huxley led to the conclusion that the principle was obeyed in their examination of the relation between Na^+ concentration and Na^+ current during excitation (Hodgkin and Huxley, 1952a).

Since 1952, a number of authors have expressed doubts about the validity of the independence principle. One of the most outstanding examples is Hodgkin and Huxley's (1952d) own discovery that, during the passage of an impulse, the influx of labeled K^+ observed was only about one sixth of that calculated on the basis of the independence principle. This discovery led to the postulation of the *long-pore model* by Hodgkin and Keynes (1955b). Similarly Tasaki and Takenaka (1964) and Chandler and Meves (1965) showed that in perfused squid axons alkali metal ions in the internal perfusing solution reduce delayed current with decreasing effectiveness: $\text{Cs}^+ > \text{Rb}^+ > \text{Na}^+$. These findings were further confirmed by Adelman and Senft (1966) and by Bezanilla and Armstrong (1972). Mozhayeva (1969) found P_K to depend on $[\text{K}^+]_{\text{ex}}$. Similarly, Hagiwara *et al.* (1974) found that in the giant barnacle muscle fibers the inward Ca^{2+} current, which is equivalent to the Na current in squid axons, saturates at high Ca^{2+} concentration. Both K^+ conductance and Na^+ conductance have been shown to be reversibly depressed by low pH (Hille, 1968, 1975; Drouin and The, 1969; Stillman *et al.*, 1971; Woodhull, 1973; Schauf and Davis, 1976). Although some investigators thought that the H^+ effect is indirect via the gating process (Fishman *et al.*, 1971) others regarded the H^+ effect as a direct blocking of Na^+ migration, and thus in contradiction to the independence principle.

14.1.6. The Significance of the Demonstration of the Localization of the Bulk of Intracellular K^+ in Frog Muscle

From the very beginning, a basic tenet of the membrane theory was that of free cell K^+ . The concepts of Bernstein, Hodgkin, Katz, and Huxley rest squarely on the postulation of the existence of intracellular K^+ in the free state, evenly distributed throughout the cell.

Purely as a thought exercise, let us assume that the K^+ in frog muscle is free but localized in the A band, as shown in Figs. 8.1–8.12. This would mean that the intra-

cellular K^+ activity would be many times higher in the K^+ -rich A bands than in the K^+ -poor I bands. A good microelectrode tip of the Gerard-Graham-Ling (GGL) type is from 0.2 to 0.5 μm in diameter. The A and I bands in a slightly stretched frog sartorius muscle are about 1.5 and 1.0 μm in width, respectively; in highly stretched muscle, the bands are even wider (see Fig. 8.5). Thus, random impalement of frog muscle fibers with a good microelectrode would then certainly pick up two populations of potentials in the same muscle fiber.

However, in the more than 30 years of resting potential measurements of normal or highly stretched frog sartorius muscle since 1949 (Ling and Gerard, 1949b), no fluctuation of this sort has ever been observed. Therefore the localized K^+ cannot exist in a freely diffusible state.

The unequivocal establishment of the adsorbed state of cell K^+ discussed in detail in Chapter 8 has disproved the membrane theory of cellular electric potentials. However, this does not by any means invalidate many of the important data acquired in past decades. To explain the large volume of findings in a new and different way is what I shall attempt to do next. I shall first examine additional evidence that specifically supports the AI hypothesis of the cellular potentials.

14.2. Evidence for the Surface Adsorption Theory of Cellular Resting Potentials

Since the publication of the surface adsorption theory of the cellular resting potential in 1955 (Ling, 1955, 1960, 1962), supportive evidence has been collected and will be briefly described in the following sections. The first two pieces of evidence are from model studies; the third is from studies of living cells.

14.2.1. Collodion-Coated Glass Electrode

To check the earlier conclusion drawn from studies of the glass membrane, the oil layer, and collodion membranes that it is the surface fixed ions that determine the potential (Section 4.6.1), Ling and Kushnir (Ling, 1960; 1967b) coated soft glass electrodes (Corning 015 glass) with a thin layer of oxidized collodion. Earlier, Sollner *et al.* (1941a,b) had established that oxidized collodion contains potential-generating carboxyl groups. Michaelis and his co-workers showed that a collodion membrane electrode exhibits a sensitivity toward K^+ (Section 2.2.5). Corning 015 glass electrodes, on the other hand, exhibit no K^+ sensitivity. Thus if it is indeed the ionic group on the electrode surface that determines the potential, the Corning 015 glass electrode coated with a thin layer of collodion should behave like a collodion membrane electrode and exhibit K^+ sensitivity.

The results of these studies show that indeed the collodion-coated glass (CG) electrode behaves like a collodion electrode, showing sensitivity to K^+ . Furthermore there is a 10-to-1 preference for K^+ over Na^+ (Fig. 14.3). These electrodes demonstrate no sensitivity to divalent ions (Fig. 14.4).

Figure 14.5 shows the behavior of a variant of the CG electrode, one that had been further exposed to polylysine and then dried. This polylysine-treated collodion-coated

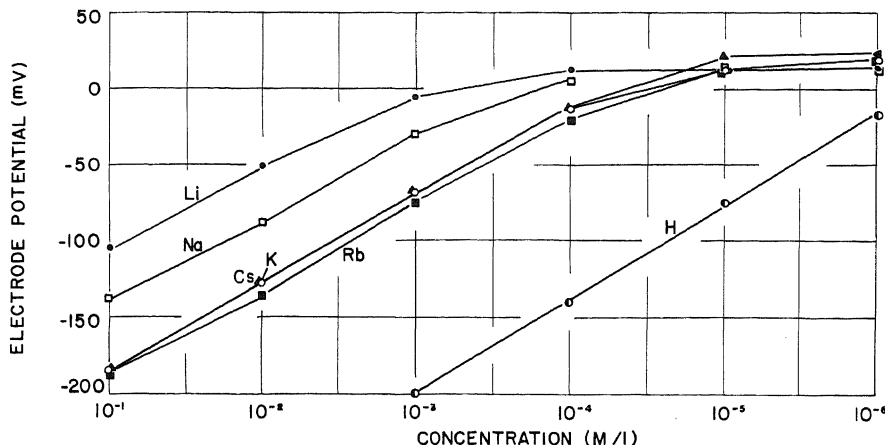


FIGURE 14.3. Monovalent cation sensitivity of a collodion-coated glass electrode. The potential is considered positive if the outside solution is positive with respect to the collodion-glass phase. [From Ling (1967b), by permission of Marcel Dekker.]

glass electrode (PCG) behaves quite differently from the simple CG electrode. Thus, at pH 5, the CG electrode acts as a K^+ electrode; at the same pH the PCG electrode acts as a Cl^- electrode with a nearly ideal slope (58) at KCl concentrations between 10^{-3} and 10^{-2} M. However, at pH 7, the PCG electrode shows a much reduced slope of a little over 10 between 10^{-3} and 10^{-2} M KCl. These behaviors indicate that at pH 7 both fixed anionic carboxyl groups of the collodion and cationic ϵ -amino groups on the adsorbed polylysine are functional. Thus the positive slope owing to fixed anions canceled much of the negative slope owing to the fixed cations at the electrode surface. In

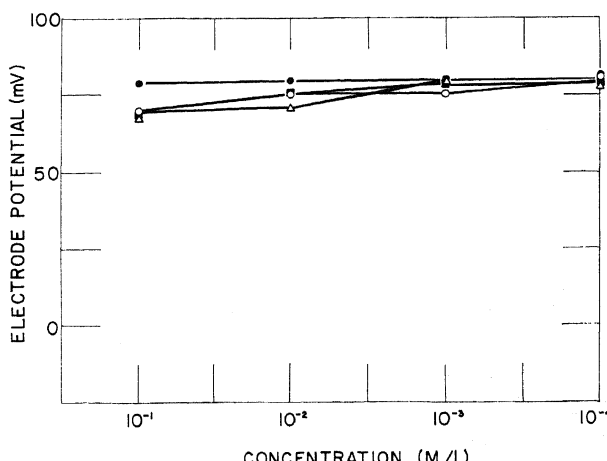


FIGURE 14.4. Divalent cation sensitivity of a collodion-coated glass electrode, oxidized for 10 min. The abscissa gives the concentration of the chloride salt of the ion indicated. ●, Mg^{2+} ; ○, Ba^{2+} ; △, Ca^{2+} ; ■, Sr^{2+} . [From Ling (1967b), by permission of Marcel Dekker.]

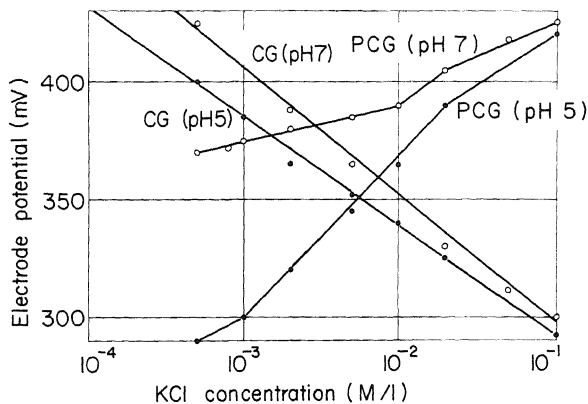


FIGURE 14.5. Anion and cation sensitivity of a collodion-coated glass electrode (CG) and of a polylysine-treated collodion-coated glass electrode (PCG) at pH 5 and 7. [From Ling (1967b), by permission of Marcel Dekker.]

both the CG and the PCG electrodes it is the nature and polarity of the fixed ionic sites that determine the ionic sensitivity of these models.

14.2.2. Colacicco's Experiment on Oil Membranes

Colacicco in 1965 presented further evidence of the primary importance of fixed surface ionic sites for the creation of electric potentials at interfaces. Colacicco's theoretical illustration, reproduced as Fig. 14.6, shows how negative head charges at the upper interface (B) of an oily layer, or positive head charges at the lower interface (A), should produce a negative potential ($-b$, $-c$). These expectations were verified by injecting an anionic detergent, sodium dodecyl sulfate (SDS), or a cationic detergent, cetyltrimethylammonium bromide (CTAB), which produce the expected effects. Figure 14.7, drawn from Colacicco's data, shows the effect of introducing SDS or CTAB at the interface on the potential difference measured across the oil phase in the presence of varying concentration of KCl in the aqueous phase. With their different head charges, SDS and CTAB endow the oil layer with sensitivity to K^+ or to Cl^- , respectively. The author

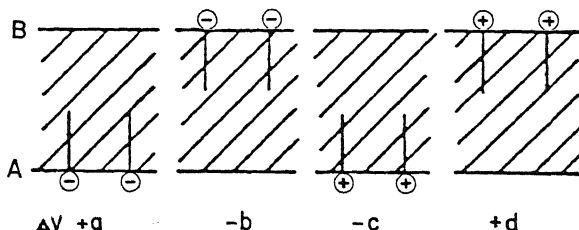


FIGURE 14.6. Relation of sign of ΔV to sign of head charge of surfactant. [From Calacicco (1965), by permission of *Nature*.]

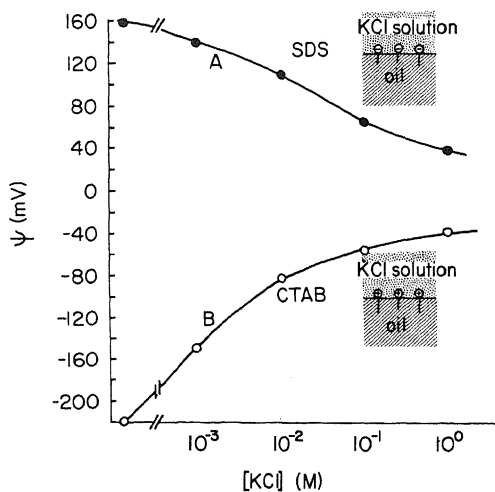


FIGURE 14.7. Electrical potential measured across an oil layer after introduction of sodium dodecyl sulfate (SDS) or cetyltrimethylammonium bromide (CTAB). Oil layer separates KCl solutions of different concentrations indicated on the abscissa. [Data from Colacicco (1965), by permission of *Nature*.]

also pointed out that the highest potential of 370 mV was observed when SDS was injected into the oil at interface A and CTAB at interface B. If only SDS is injected at interface B, a potential difference of one half that magnitude would be observed. In other words, each interface with its fixed anionic or cationic sites is an independent potential-difference-generating system. In this case each interface may be likened to a charged parallel plate condenser. A potential difference is produced owing to the excess charges on the fixed-charge surface of one sign and excess charges in the less defined outer (Helmholtz-Gouy-Chapman) layer of counterions of the opposite sign. The normal muscle or nerve resting potential, according to the AI hypothesis, therefore, very much resembles the potential at one of the oil-water interfaces at which negatively charged SDS was introduced.

14.2.3. Edelmann's Experiment on Guinea Pig Heart Trabecular Muscle

The Ling fixed-charge hypothesis (LFCH) of cellular resting potentials, described in Section 4.6.2, can be written in a more general form (Ling, 1962, 1967b,c):

$$\psi = \text{Constant} - \frac{RT}{\mathcal{F}} \ln \left(\sum_{i=1}^n K_i [p_i]_{\text{ex}} \right) \quad (14.5)$$

where K_i is the adsorption constant of the i th cation on the surface anionic sites and $[p_i]_{\text{ex}}$ is the concentration of the i th monovalent cation in the external solution. Since the title *Ling fixed-charge hypothesis* was abandoned with the introduction of the AI hypothesis in 1962, the LFCH of the cellular resting potential will be referred to henceforth as the *surface adsorption model* (SAM) of the cellular resting potential.

For a short-duration experiment in which the intracellular concentrations of K^+ and Na^+ may not change significantly, the modified Hodgkin-Katz equation [equation (14.1)] also can be written in a similar form:

$$\psi = \text{Constant} - \frac{RT}{\mathcal{F}} \ln \left(\sum_{i=1}^n P_i [p_i]_{\text{ex}} \right) \quad (14.6)$$

where P_i is the permeability constant of the i th monovalent cation in the external medium. A comparison of equations (14.5) and (14.6) shows that their only difference lies in the physical significance of the coefficients: adsorption constants in one case, permeability constants in the other.

Edelmann and Baldauf (1971) saw an opportunity to put the two theories to a test. First they determined with the aid of radioactive tracers both the adsorption constants and the permeability constants of three alkali metal ions, Rb^+ , K^+ and Cs^+ , on the surface of guinea pig cardiac papillary muscles. By studying the effect of external Rb^+ , K^+ , and Cs^+ on the entry of labeled K^+ into the heart muscle fibers (Fig. 12.15), they obtained the following sets of surface adsorption constants (K_i) and permeability constants, given as V_{max} in microequivalents per milliliter per minute:

K_{K}	K_{Rb}	K_{Cs}	$V_{\text{K}_{\text{max}}}$	$V_{\text{Rb}_{\text{max}}}$	$V_{\text{Cs}_{\text{max}}}$
0.19	0.28	0.10	12.5	5.0	0.40

The surface adsorption constant is much higher for Rb^+ than for K^+ ; the permeability constant, on the other hand, is just the opposite, being more than twice as high for K^+ as for Rb^+ . Armed with these data, Edelmann and co-workers (Edelmann and Baldauf, 1971; Edelmann, 1973) then went on to compare the resting potential mea-

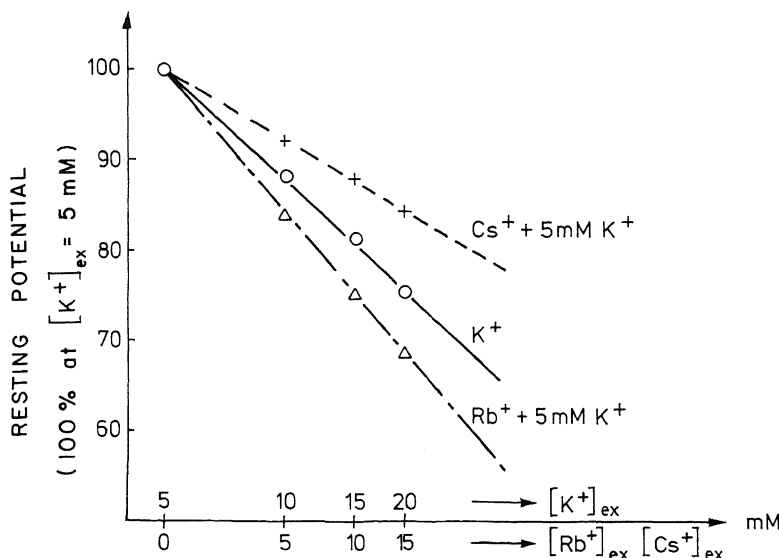


FIGURE 14.8. Effect of external Cs^+ , K^+ , and Rb^+ on the resting potential of guinea pig heart muscle. Points are experimental; dashed lines are theoretical based on the adsorption constants and equation (14.5). [After Edelmann (1973).]

sured in the presence of varying concentrations of K^+ . From the K^+ -versus- ψ curve obtained they were *not* able to predict the experimentally observed Rb^+ -versus- ψ as well as Cs^+ -versus- ψ data if they used the relative permeability coefficients $V_{K_{max}}$, $V_{Rb_{max}}$, and $V_{Cs_{max}}$ listed above. On the other hand, if they used the adsorption constants K_K , K_{Rb} , and K_{Cs} , then the theoretical curves fit perfectly with the experimental data (Fig. 14.8).

14.3 Experimental Observations Not Explicable by the Membrane Theory but in Harmony with the Surface Adsorption Theory

From the discussion above, one sees that, of the various relationships described in the Hodgkin-Katz-Goldman equation, only a part has been confirmed experimentally, and this part is enclosed in dashed lines below:

$$\boxed{\psi = \frac{RT}{\mathcal{F}} \ln \frac{P_K [K^+]_{in} + P_{Na} [Na^+]_{in} + P_{Cl} [Cl^-]_{ex}}{P_K [K^+]_{ex} + P_{Na} [Na^+]_{ex} + P_{Cl} [Cl^-]_{in}}} \quad (14.7)$$

In form, the experimentally verified portion of the Hodgkin-Katz-Goldman equation is therefore identical to the equation for the cellular potential according to the SAM of the AI hypothesis shown as equation (4.15). This analysis shows that all the observations supporting the Hodgkin-Katz-Goldman model also support the SAM. The observations contradicting the Hodgkin-Katz-Goldman equation also are in harmony with the SAM, as the following discussions will show.

14.3.1. The Adsorbed State of Cell K^+

In contrast to the membrane theory, the SAM does not require that intracellular K^+ exist in a free state. Indeed, in the SAM the intracellular K^+ as well as other intracellular ions does not play an immediate role in the operation of the potential.

14.3.2. The Lack of a Relation between External Cl^- and ψ

The failure to demonstrate the expected relation between external Cl^- concentration and ψ (Section 14.1.1) offers a major piece of evidence against the Hodgkin-Katz theory. In contrast, it is in full harmony with the SAM, according to which the surface sites on resting frog voluntary muscle cells are primarily anionic and therefore, like the CG electrode (Fig. 14.5), exhibit no Cl^- sensitivity. On the other hand, if in some other cells the surface contains only fixed cations, or both fixed anionic and cationic sites like the PCG electrode in Fig. 14.5, different patterns of ion sensitivity emerge (see Section 14.4.4).

14.3.3. The Contradictory Reports on the Relation between ψ and Intracellular K^+

Since the early 1950s many investigators have attempted to verify an anticipated relation between ψ and the internal K^+ concentration in living cells. The results have

been conflicting: Three papers reported finding such a relationship (Section 3.4.1); at least seven others reported just the opposite (Section 14.1.2). Before attempting to resolve this confusing situation, I shall sort out the findings on the basis of whether or not a new potential-generating protoplasm-aqueous solution interface was created in the cell preparation studied. Since K^+ and Cl^- have closely similar self-diffusion coefficients ($D_K = 1.87 \times 10^{-5}$, $D_{Cl} = 1.91 \times 10^{-5} \text{ cm}^2/\text{sec}$ in a 0.1 M KCl solution, Friedman and Kennedy, 1955), a 3 M KCl-filled GGL microelectrode has long been used to provide an intracellular lead without creating a new liquid-junction potential; whatever potential may exist at the microelectrode tip is swamped out by the high concentration of K^+ and Cl^- . Thus in the reports of Tobias, Shaw *et al.*, Koketsu, and Kimura described in Section 14.1.2, impaling intact cells with a GGL electrode would be expected to produce no new protoplasmic interface potential within the cells. In these cases the electrode serves as a neutral lead as intended, and in each case no dependence of ψ on intracellular K^+ concentration was observed, in agreement with the SAM.

In another class of studies, typified by the microinjection experiment in frog muscle and the squid axon perfusion experiments, the axoplasm was to a varying extent removed or forcibly pushed apart. In these cases, the tip of the electrode inside the cell is far from the newly created protoplasmic surface, which is bathed in a solution often different from 3 M KCl. As a result a new surface potential may be created at the artificially created interface. In agreement one recalls that electrical potential differences were consistently reported at the surface of naked *Nitella* protoplasm (see p. 498). The key question here is what kind of solution bridges the gap between the new protoplasmic surface and the tip of the intracellular electrode. In the experiments of Grundfest *et al.* (Section 3.4.1) and of Falk and Gerard, highly concentrated KCl and NaCl solutions were used. In these cases the new interface potential will be swamped out or minimized. It is not surprising that both groups reported no dependence of ψ on intracellular K^+ concentration.

Kao's *Fundulus* eggs showed no measurable ψ (Section 14.1.2). This observation can be explained by the SAM on the assumption that the normal surface of this egg is amphoteric. The fixed anions and fixed cations have little or no affinity for the external ions whose concentrations were varied in the study (e.g., surface anionic sites exist in closely placed pairs with strong affinities for divalent cations, whose concentrations were not varied).

Of the three reports demonstrating a relation between ψ and intracellular K^+ , that of Adrian can also be explained in terms of the SAM in a straightforward manner. Adrian changed the intracellular K^+ concentration in muscle by changing the cell volume in response to exposure of the muscles to hyper- or hypotonic solutions. His data can be explained since, with cell swelling and shrinkage, there is a corresponding change in the density of surface anionic sites [f^-], which, though not explicitly given is represented as $\ln [f^-]$ and included in the constant of equation (4.16).

The two remaining sets of data which confirmed the expected relation between ψ and $\ln [K^+]_{in}$ involved the creation of a new protoplasmic interface inside the cells and the exposure of the new interface to experimentally introduced relatively dilute KCl solutions. One may, on the basis of the SAM, expect a potential difference sensitive to K^+ concentration at this new artificial interface, and it is this internal surface that gave rise to the sensitivity of ψ to $[K^+]_{in}$ observed by Baker *et al.* and Hagiwara *et al.*

Our next task is to provide an explanation for the much lower slope of the ψ -versus- $\ln [K^+]_{in}$ plots observed, than of plots of ψ versus $\ln [K^+]_{ex}$ (only 30 in the data of Hagiwara *et al.*, and below 20 in the data of Baker *et al.*). From model studies described earlier (Fig. 14.5), we know that at pH 7 both the carboxyl groups on the collodion and the ϵ -amino groups on the polylysine of the PCG electrode are ionized. The electrode is therefore at once a K^+ electrode and a Cl^- electrode. As a result the ψ -versus- $\ln [K^+]_{in}$ plot becomes flat. A CG electrode without the polylysine, in contrast, has a near-ideal slope. Clearly it is the simultaneous presence of fixed anions and fixed cations that produces in this case the low slope.

Although in the SAM it is hypothesized that the cell surface of frog sartorius muscle is covered with isolated fixed anionic β - and γ -carboxyl groups (see Figs. 12.14 and 12.20), the interior of the cell, whether a squid axon or a giant barnacle muscle fiber, must be amphoteric and possess both anionic β - and γ -carboxyl groups and cationic ϵ -amino and guanidyl groups. Thus, the variation of ψ with variation of K^+ or Na^+ salt concentration in the internal perfusing fluid may reveal more or less fixed anionic as well as fixed cationic sites at the artificially created surface lining the cavities inside the cell, whether these cavities were brought about by axoplasm extrusion or by solution injection.

14.4. The Molecular Mechanism of the Resting and Action Potentials

In the years following the introduction of the SAM (Ling, 1955, 1959, 1960), the concept was further developed that, during excitation, in response to the removal of the cardinal adsorbent Ca^{2+} (Ling, 1957, 1962), there is an electronic conformational change of the cell surface proteins: the c -value of these surface anionic sites shifts transiently in an all-or-none manner from one state, in which K^+ is preferred over Na^+ (low c -value), to another, in which the relative Na^+ preference is greatly increased (high c -value) (Ling, 1955, 1960, 1962, 1982, 1983b). Concomitantly a transient depolarization of cell surface water occurs, creating an increase of nonspecific membrane conductance (Ling, 1971, 1973b). The molecular event during the propagation of an action potential was described in terms of the indirect F -effect, and the transition from the resting to the active state is autocooperative in nature (Ling, 1962), with the inductive effect providing the major component of the nearest-neighbor interaction energy.

14.4.1. The New Equation for the Cellular Resting Potential

The original, simple equation of the cellular resting potential [equation (4.16)] was based on the assumption that the surface anionic sites do not interact and that ionic adsorption on these β - and γ -carboxyl groups follows a Langmuir adsorption isotherm. The equation did not take into account cooperative interaction, which is an essential feature of physiological manifestations of all sorts according to the AI hypothesis (Sections 7.4 and 11.1). If an autocooperative transition in cell surface protein does occur by the adsorption or desorption of a cardinal adsorbent, it would be important to show that the system is indeed capable of autocooperative transition. With this in mind I introduced an improved equation for the cellular resting potential (Ling, 1979a):

$$\psi = \text{Constant} - \frac{RT}{\mathcal{F}} \ln \frac{1}{[K^+]_{\text{ex}}} \left(1 + \frac{\xi - 1}{\sqrt{(\xi - 1) + 4\xi \exp(\gamma/RT)}} \right) \quad (14.8)$$

ξ and γ have the same meanings as in equation (7.19), from which equation (14.8) was derived. One recalls that $\xi = ([p_i]_{\text{ex}}/[p_j]_{\text{ex}}) K_{j \rightarrow i}^{00}$, where $K_{j \rightarrow i}^{00}$ is the intrinsic equilibrium constant for the j th-to- i th solute adsorption exchange and γ is related to the free energy of nearest-neighbor interaction, $-\gamma/2$. In Fig. 14.9, theoretical curves according to equation (14.8) are plotted with different values of $-\gamma/2$, in which $-\gamma/2$ is expressed as Θ and $\Theta = \exp(\gamma/RT)$. When there is no near-neighbor interaction ($-\gamma/2 = 0$, $\Theta = 1$), the theoretical curve is identical to that predicted by either equation (4.16) or equation (14.5). That is, in an external environment of constant or nearly constant Na^+ concentration, an increase of external K^+ concentration causes ψ to fall with an ideal or

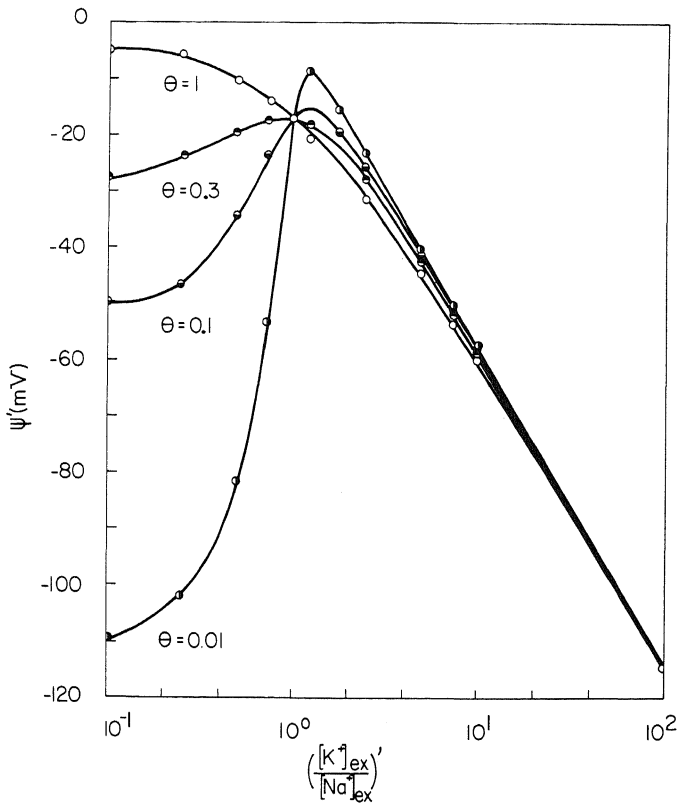


FIGURE 14.9. Plot of the resting potential against external K^+ and Na^+ concentration ratio according to equation (14.8). Ordinate represents ψ' which is equal to $\psi - \text{constant}$; abscissa represents $([K^+]_{\text{ex}}/[Na^+]_{\text{ex}})'$, which is $([K^+]_{\text{ex}}/[Na^+]_{\text{ex}} \cdot K_{Na-K}^{00})$. For experiments carried out in the presence of a constant concentration of Na^+ (e.g., 100 mM), the abscissa is then $[K^+]_{\text{ex}} \cdot (K_{Na-K}^{00}/0.1)$. Θ is related to $-\gamma/2$ by $\Theta = \exp(\gamma/RT)$. For $\Theta = 1$, $-\gamma/2 = 0$ kcal/mole; for $\Theta = 0.3$, $-\gamma/2 = 0.356$; for $\Theta = 0.1$, $-\gamma/2 = 0.682$; and for $\Theta = 0.01$, $-\gamma/2 = 1.363$. [From Ling (1979a), by permission of *Physiological Chemistry and Physics*.]

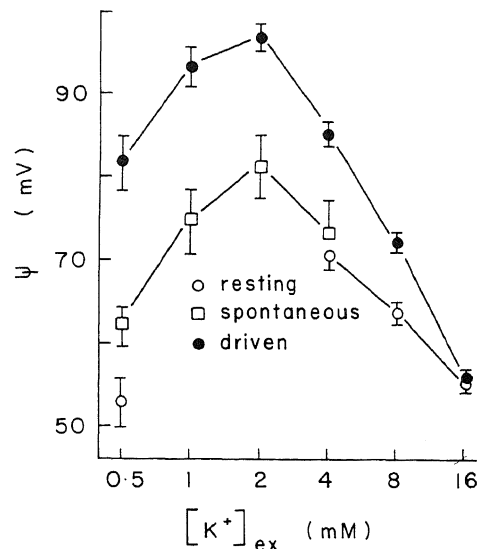


FIGURE 14.10. Cellular resting and diastolic potentials of canine cardiac Purkinje cells (mean values \pm SEM) measured in various extracellular concentrations of K^+ . "Driven" means the state of hyperpolarized diastolic potential in response to repeated propagated activities at the rate of 3.5 Hz. [From Ruzyllo and Vick (1974), by permission of *Journal of Molecular and Cellular Cardiology*.]

near-ideal slope (58). A decrease of external K^+ concentration below its normal level in a Ringer solution, on the other hand, does not cause a continual increase of ψ . Rather, ψ then becomes constant at low $[K^+]_{ex}$, as was indeed widely observed in squid axon, frog sartorius muscle, frog myelinated nerve, insect muscle, guinea pig smooth muscle, and toad eggs (Fig. 3.7).

However, in a number of other cell types studied, a different pattern was observed (Figs. 14.10 and 14.11). In the presence of a near-constant and high $[Na^+]_{ex}$, decreasing $[K^+]_{ex}$ caused a fall of ψ of the cardiac Purkinje cells (Ruzyllo and Vick, 1974) like that shown in the theoretical curve in Fig. 14.9 with $-\gamma/2 > 0$. It should be pointed out that this type of behavior is not predicted by the Hodgkin-Katz-Goldman equation or the early equation [equation (4.16)] of the SAM.

Observations similar to those of Ruzyllo and Vick were made in other cells, including HeLa cells (shown in Fig. 14.11) (Okada *et al.*, 1973) and pancreatic islet cells (P.

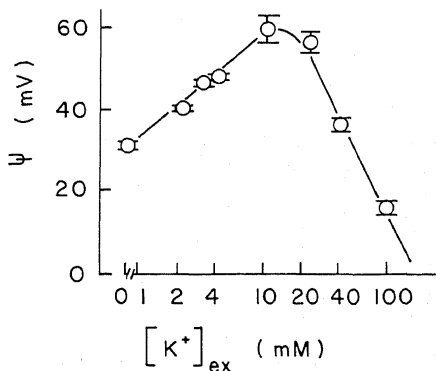


FIGURE 14.11. Relation between membrane potential and $\log [K^+]_{ex}$ in HeLa cells. Vertical bars represent SEMs on either side of averages. [From Okada *et al.* (1973), by permission of *Biochimica et Biophysica Acta*.]

M. Dean and Matthews, 1970), as well as in other cells and subcellular particles to be mentioned later (Sections 14.4.4 and 15.3.3.2). The question must be asked, Why does autocooperative interaction appear to occur only among surface sites of some cells (like those of Figs. 14.10 and 14.11) but not others (Fig. 3.7)? It seems to contradict the thesis that cooperative adsorption is basic to all cellular excitation phenomena (Ling, 1957, 1960, 1962). To answer, one needs to review the SAM in more detail. In this theory, when K^+ is preferentially adsorbed on most of the cell surface anionic sites, the depolarizing effect of the 100 mM of external Na^+ is minimal owing to the large value of K_{Na-K}^{eq} , which more than sufficiently compensates for the much higher Na^+ concentration in the external medium [see equations (14.8) and (7.20)]. Reduction of external K^+ would tip the balance in favor of Na^+ adsorption; depolarization would then follow. However, external K^+ is not the only source of K^+ for the surface anionic sites. The large amount of intracellular, adsorbed K^+ is another source of K^+ . For this reason one would expect that the depolarization in a cell in a low- K^+ medium would not reach its final equilibrium value until the intracellular source of K^+ had fallen to a comparably low level. Ling and Bohr (1971a) have shown that it takes frog muscle cells about 72 hr to reach a new K^+ equilibrium at room temperature. Since most of the data collected in Fig. 3.7 were obtained after only a brief exposure (e.g., 10 min) of the cells to both high and low external K^+ concentrations, only those experimental points at normal or higher than normal external K^+ concentration are valid equilibrium values, as Ling has demonstrated (Ling, 1960, 1962); for external K^+ concentrations lower than normal, the measured ψ 's are *not* equilibrium values.

Cardiac Purkinje muscle fibers, on the other hand, are quite different from frog voluntary muscles in that they have a very high rate of exchange of cell K^+ ; thus it took only 40 min at room temperature for a new K^+ equilibrium to be reached (Ruzylo and Vick, 1974; E. Page and Storm, 1965) instead of 72 hr, as in frog muscle. This suggests that ψ measured in cells like Purkinje cells, as well as HeLa cells and pancreatic islet cells, at low as well as at high external concentration had already reached equilibrium.

Figure 14.12 shows the time course of the change of the resting potential following the introduction of the muscle into a large volume of a Ringer solution virtually free of K^+ . Note that after an initial rise, ψ steadily declines until it approaches a new low steady level after a total duration of 70 hr. The inset in Fig. 14.12, taken from an earlier publication of Ling and Bohr (1971a), shows that it also took about 70 hr for the total cell K^+ and Na^+ concentrations to reach new steady levels following exactly the same treatment. This close parallel of the time courses of ψ and of total K^+ content confirms the suggestion that the new equilibrium potential is reached only when the internal K^+ concentration reaches a level in equilibrium with the low K^+ level in the external medium. Moreover, Fig. 14.12 presents another piece of evidence in support of the SAM. The inset of Fig. 14.12 shows that it took just as long for the muscle to regain its lost K^+ as it took the muscle to lose it, i.e., 70 hr at 25°C. In sharp contrast, ψ regains its normal value on returning the muscle to a normal Ringer solution containing 2.5 mM K^+ in a much shorter time (e.g., from 4 to 6 hr). After 4–6 hr, the total K^+ of the muscle has made only a very modest gain. This large discrepancy confirms the concept that ψ is determined only by surface K^+ adsorption.

It is suggested that essentially the same phenomenon—the more rapid repolarization of the cell surface of K^+ -depleted muscle beyond that calculated on the basis of *total*

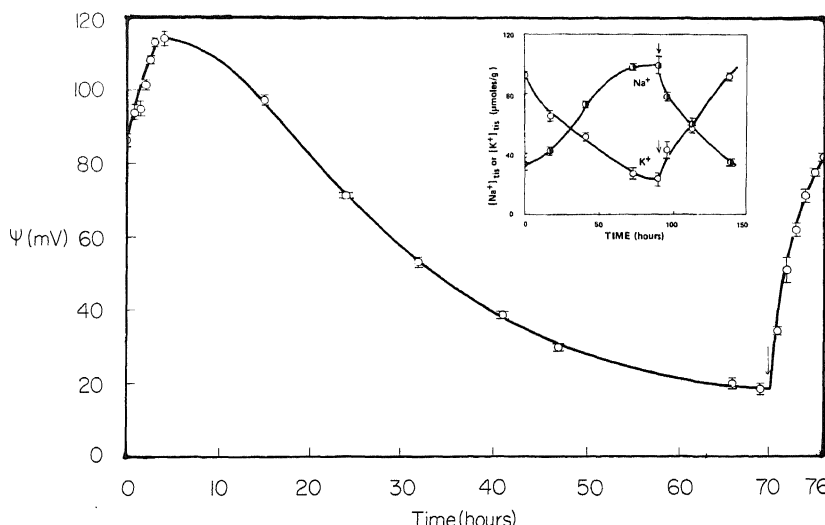


FIGURE 14.12. Time course of changes of the resting potential of frog muscle after exposure to a large volume of “ K^+ -free” Ringer solution. At the 70th hour, the muscle was transferred to a normal Ringer solution containing 2.5 mM K^+ ($25^\circ C$). Inset, from Ling and Bohr (1970), shows the time course of total K^+ and Na^+ contents after exposure to “ K^+ -free” Ringer solution and subsequent return to a normal Ringer solution containing 2.5 mM K^+ ($25^\circ C$). [From Ling and Fisher (1983), by permission of *Physiological Chemistry and Physics*.]

cell K^+ —compelled Kernan (1962) and others to suggest the electrogenic Na^+ pump. The shortcomings of such a theory and the experimental evidence contradicting it have already been presented.

The experiment of Fig. 14.12 provided a way of measuring accurately the equilibrium ψ in low external K^+ and high external Na^+ concentration: 72 hr of incubation in a “ K^+ -free” Ringer solution followed by incubation in a Ringer solution containing the desired K^+ and Na^+ concentration for a period of 6 hr or longer. It was with this technique that the data shown in Fig. 14.16 were collected: These data (curve B) show quite clearly that the behavior of frog muscle, and presumably other tissues (Fig. 3.7), is not basically different from that of cardiac Purkinje cells. Both show autocooperative interaction between surface anionic sites.

14.4.2. The Control of the Resting Potential by Cardinal Adsorbents According to the AI Hypothesis

The cell surface and the cell interior share many basic properties. Yet only the cell surface is directly exposed to the external medium. Being exposed to the external medium, the surface gives rise to electrical potentials. The underlying electronic and molecular events at rest, and in response to changes, are seen as not fundamentally different from those in other proteins held within the cells and described in Chapter 7.

In Chapter 11 it was shown that low concentrations of the cardiac glycoside ouabain control the level of K^+ and Na^+ in frog muscle cells by reducing the value of

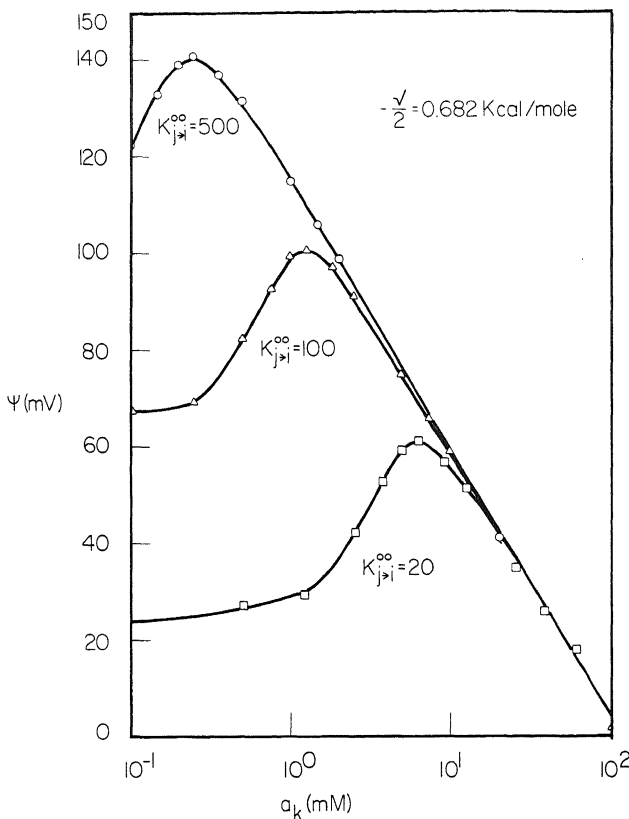


FIGURE 14.13. Cellular potential as a function of external K^+ . Theoretical curves calculated from equation (14.8) with the same $-\gamma/2$ (0.682 kcal/mole) but different $K_{j>i}^{00}$, as indicated. [From Ling (1982), by permission of *Physiological Chemistry and Physics*.]

$K_{Na \rightarrow K}^{00}$ of the K^+, Na^+ -adsorbing sites, quantitatively in agreement with equation (7.28) (Section 11.2). If a similar effect of a cardinal adsorbent like ouabain occurs at the cell surface, equation (14.8) would predict the potential to vary with changes of $K_{Na \rightarrow K}^{00}$, as shown in Fig. 14.13.

As in the case of K^+ depletion by removing K^+ from the external medium, Ling and Bohr (1971b) found that on exposure to ouabain ($3.26 \times 10^{-7} M$) it also took some 60–70 hr for frog muscles to reach a new equilibrium. By analyzing the changes in ψ in low $[K^+]_{ex}$ one expects that the effect of externally applied ouabain on ψ would take a similar length of time to reach a new equilibrium value. That this is indeed true is shown in Fig. 14.14. Figure 14.14 also shows that, on switching to a Ringer solution containing the same concentration of ouabain but 20 mM K^+ instead of 2.5 mM, a new equilibrium potential is reached rapidly. Figure 14.15 shows that, if the muscle is switched to a solution containing 20 mM K^+ but no ouabain, the potential first dips to the same level as in Fig. 14.14, but then rises to a higher and constant level. This occurs in about 4 hr, even though for the bulk phase K^+ to return to a normal level after

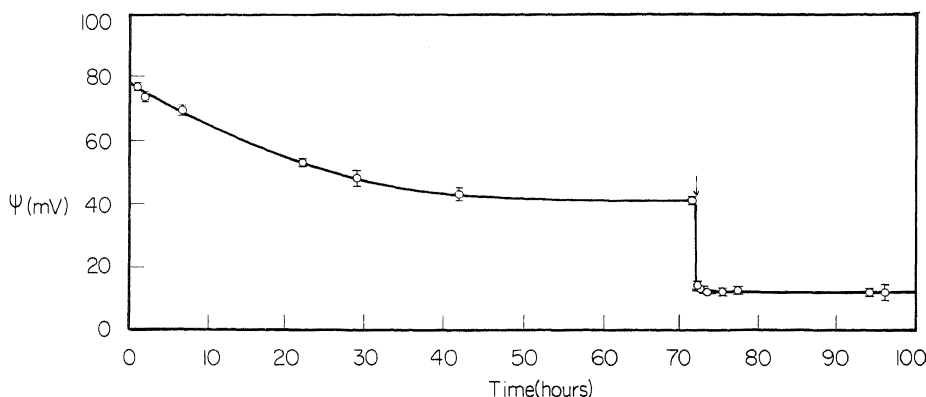


FIGURE 14.14. Time course of change of the resting potential of a frog sartorius muscle in $2.5 \text{ mM } [\text{K}^+]$ _{ex} after exposure to $3.2 \times 10^{-7} \text{ M}$ ouabain. At the arrow, the muscle was transferred to a Ringer solution containing the same concentration of ouabain and 20 mM K^+ . [From Ling *et al.* (1983), by permission of *Physiological Chemistry and Physics*.]

switching to a ouabain-free Ringer solution took 60 hr (inset of Fig. 14.15). These data once more demonstrate the separation of the ouabain-controlled system at the cell surface (which controls the resting potential and takes only 4 hr for reversal), from the control by ouabain of cytoplasmic sites at the A bands and Z line (which control the cell ion levels and require 60 hr or more for reversal).

These data provide a technique for studying the effect of ouabain and similar car-

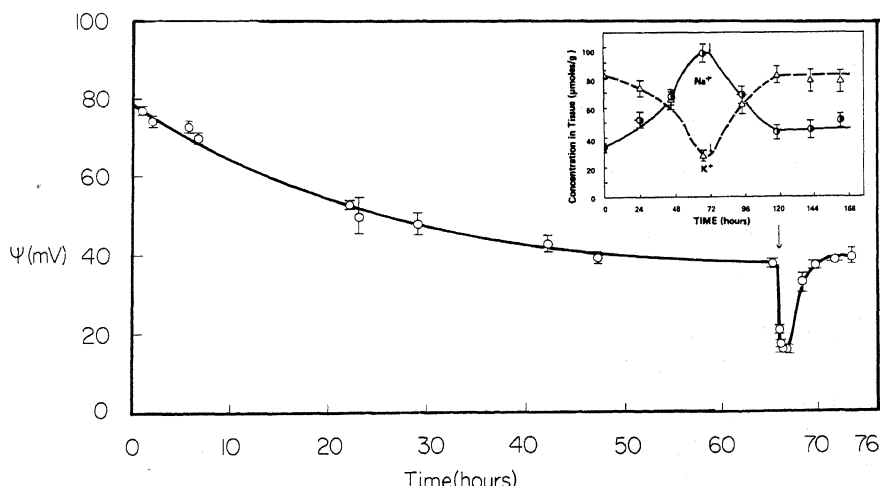


FIGURE 14.15. Time course of change of the resting potential of a frog sartorius muscle after a transfer to a normal Ringer solution containing 2.5 mM K^+ and $3.2 \times 10^{-7} \text{ M}$ ouabain. At the arrow the muscle was transferred to a Ringer solution containing 20 mM K^+ but no ouabain. [From Ling *et al.* (1983), by permission of *Physiological Chemistry and Physics*.]

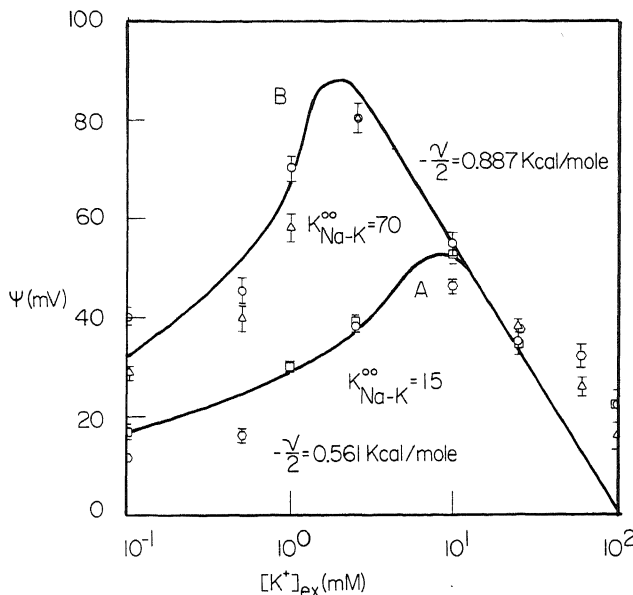


FIGURE 14.16. Equilibrium resting potential (ψ) of normal frog sartorius muscle (B) and following exposure to $3.2 \times 10^{-7} \text{ M}$ ouabain (A). Muscle A was first treated with $3.2 \times 10^{-7} \text{ M}$ ouabain in a Ringer solution containing no K^+ and then returned to solutions containing the same concentration of ouabain and different concentrations of K^+ . External Na^+ concentration was constant in all solutions at 100 mM. Solid curves were calculated from equation (14.8) with the following values: $-\gamma/2$ for B, 0.887 and for A, 0.561 kcal/mole; K_{Na-K}^{00} for B, 70 and for A, 15. [From Ling *et al.* (1983), by permission of *Physiological Chemistry and Physics*.]

dinal adsorbents on the resting potential. Muscle was exposed at 25°C to ouabain for 3 days and then to different higher K^+ concentrations for 4 hr or longer. Results of such a study are given in Fig. 14.16 and show that ouabain ($3.26 \times 10^{-7} \text{ M}$) reduces the K_{Na-K}^{00} of the surface adsorption sites from 70 to 15 and $-\gamma/2$ from +0.887 kcal/mole to +0.561 kcal/mole. Similarly, Fig. 14.17 shows the effect of adrenaline, which raises ψ by increasing K_{Na-K}^{00} . Figure 14.18 shows the effect of sodium azide (1 mM), which lowers ψ by lowering K_{Na-K}^{00} . A close comparison of these data with the theoretical curves shown in Fig. 14.13 suggests that the agreement is incomplete. Some other factors, such as changes in the number of fixed anionic sites, may play a subordinate role. But all in all, the theory has provided a new interpretation of those phenomena which puzzled Draper, Burnstock, Kernan (Section 14.1.3), and me (Ling and Gerard, 1949b; Ling, 1952) for many years.

14.4.3. Changes of the Resting Potential of Toad Oocytes during the Maturation Process

Figure 14.19 shows the dependence of the resting potential of toad oocytes on external K^+ concentration (Maeno, 1959). During the maturation process the resting potential increased steadily, and the data in Fig. 14.19 show that there is an increase of the

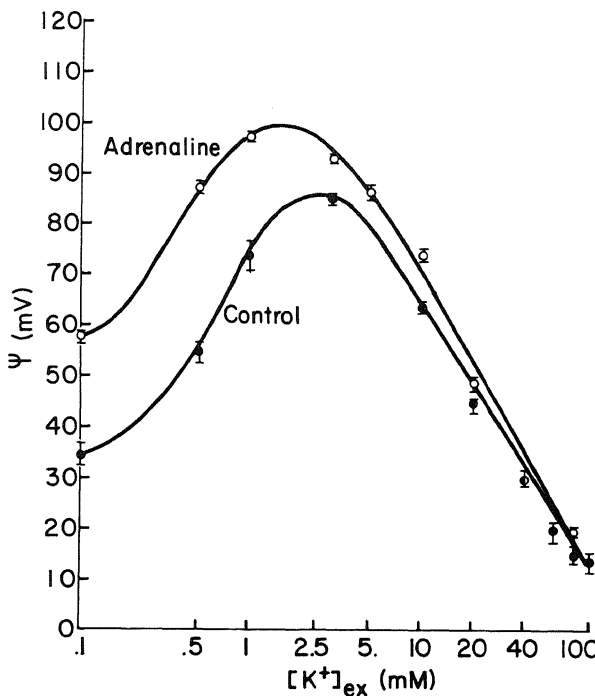


FIGURE 14.17. Effect of 3.82×10^{-5} M adrenaline upon the equilibrium resting potential (ψ) of frog sartorius muscles. Procedures used were essentially the same as in Fig. 14.16. [From Ling *et al.* (1983), by permission of *Physiological Chemistry and Physics*.]

intrinsic equilibrium constant in favor of K^+ (over Na^+). Maeno also showed that the magnitude of ψ at a fixed level of K^+ depends on external Ca^{2+} . A higher concentration of Ca^{2+} appears to increase preference for K^+ at the surface anionic sites, much as was demonstrated to be the case for bulk phase K^+ concentrations in smooth muscle (Fig. 11.37) and liver cells (Fig. 11.38). Similar effects of external Ca^{2+} in raising the resting potential have been known for frog muscle (Jenerick and Gerard, 1953), cardiac Purkinje fibers (Weidmann, 1955), and myelinated nerves (Frankenhaeuser, 1957).

Figure 14.20, taken from Tupper and Maloff (1973), shows that removal of Ca^{2+} causes depolarization of frog oocytes, an effect fully reversible by restoration of Ca^{2+} to the external medium or by introducing a higher concentration of Mg^{2+} . Following the conventional theory of electrical potentials, these authors explained this depolarization as being due to an increase of Na^+ permeability, which in fact they successfully demonstrated (Fig. 14.21). They also referred to a number of other studies in which Ca^{2+} removal induced depolarization, including those in squid axon (Tasaki *et al.*, 1968) and amoeba (Prusch and Dunham, 1972). Tupper and Maloff concluded this discussion by pointing out that "the mechanism by which Ca regulates Na permeability is not clear" (p. 141). However, I believe that a mechanism can be deduced from the AI hypothesis.

The much higher influx rate constant for K^+ over Na^+ in frog muscle, for example, is due to the greater preference of the surface anionic sites for K^+ over Na^+ (Section

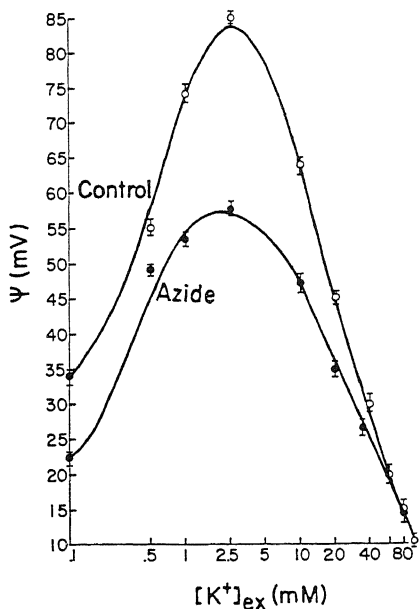


FIGURE 14.18. Effect of 1 mM sodium azide on the equilibrium resting potential (ψ) of frog sartorius muscle. Procedures used were essentially the same as in Fig. 14.16. [From Ling *et al.* (1983), by permission of *Physiological Chemistry and Physics*.]

12.4). Thus K^+ can enter via the adsorption-desorption route as well as the saltatory route, while Na^+ enters largely by the saltatory route (Fig. 12.14). Depletion of Ca^{2+} lowers K_{Na-K}^{00} for the surface anionic sites and enhances the probability for Na^+ to enter the cell via the adsorption-desorption route, hence the increase of Na^+ influx rate demonstrated in Fig. 14.21. However, since the same surface anionic sites also determine

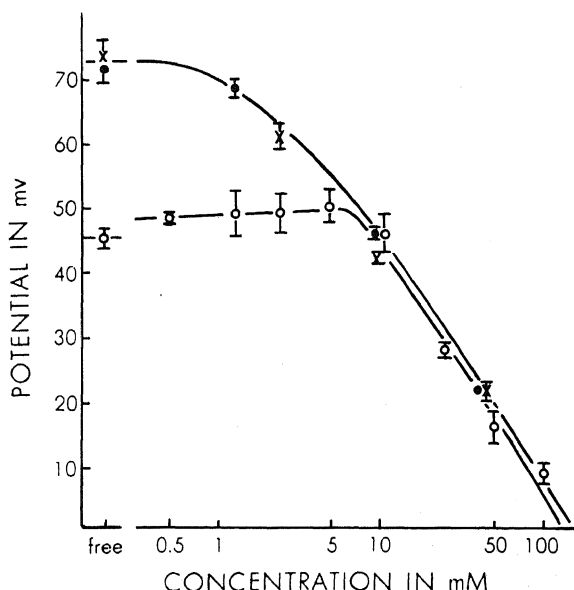


FIGURE 14.19. Effect of external K^+ concentration on the resting potential of oocytes. ●, -70-mV stage; ○, -50-mV stage. The resting potential was used by Maeno to represent stage of egg maturation. [From Maeno (1959), by permission of *Journal of General Physiology*.]

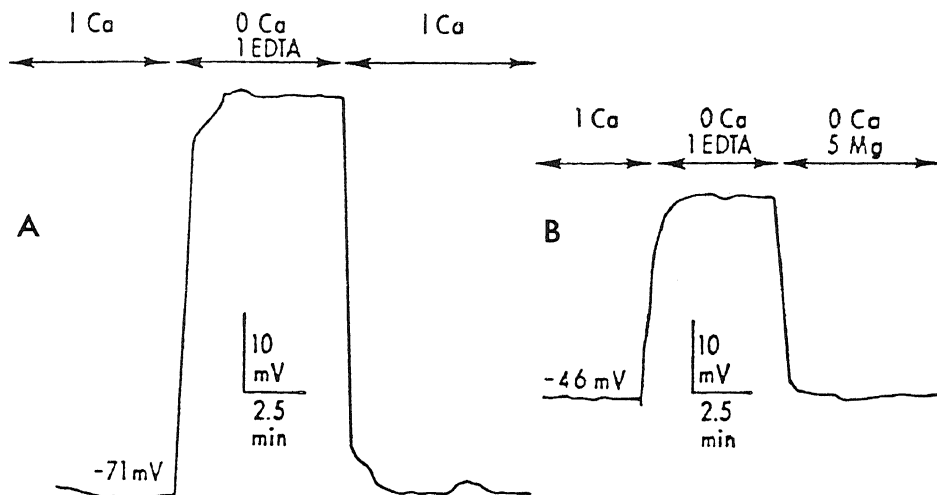


FIGURE 14.20. Oocyte membrane depolarization as a result of the removal of external Ca^{2+} and its reversal upon return of Ca^{2+} (A) or the presence of Mg^{2+} (B). [From Tupper and Maloff (1973), by permission of *Journal of Experimental Zoology*.]

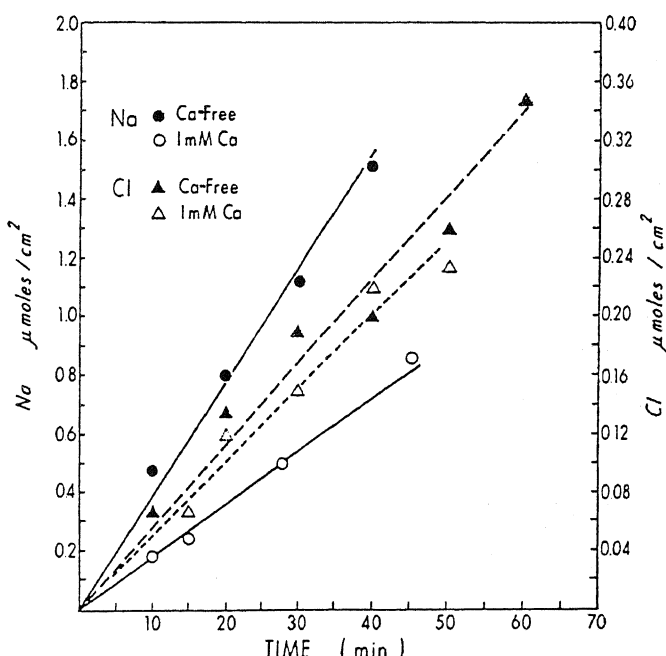


FIGURE 14.21. Unidirectional influx of Na^+ and Cl^- into the oocyte in the presence or absence of external Ca^{2+} . Each point represents the mean of three or more measurements on different groups of oocytes. [From Tupper and Maloff (1973), by permission of *Journal of Experimental Zoology*.]

the magnitude of the resting potential (a theoretical relation already verified by Edelmann, Fig. 14.8), the fall of $K_{\text{Na} \rightarrow \text{K}}^{00}$ as a result of Ca^{2+} depletion will concomitantly cause a depolarization, since the external medium contains a much higher concentration of Na^+ (e.g., 100 mM) than K^+ (e.g., 2.4 mM). This occurs in a manner similar to the depolarization which occurs on the addition of ouabain or sodium azide, as shown in Figs. 14.16 and 14.18.

In summary, the AI hypothesis can explain why Ca^{2+} depletion induces depolarization and increases inward Na^+ permeability. These represent parallel phenomena, both originating from the change in $K_{\text{Na} \rightarrow \text{K}}^{00}$ of the cell surface anionic sites. There is no direct causal relationship between permeability and ψ , as in the conventional membrane theory.

14.4.4. Effect of Mechanical Puncturing of the Cell Surface on Oocyte Activation

Maeno (1959) showed that mechanical puncturing of oocytes with a microelectrode usually produces an *activation potential*, which appears as a slow reversible hyperpolarization in normal Ringer solution but may reverse its sign with reduction of external ionic concentration (Fig. 14.22). Figure 14.23 shows that the peak heights do not depend on external cation (K^+ or Na^+) concentration but only on external Cl^- concentration. Thus the inside of the cell becomes more negative as external Cl^- increases. These findings suggest that the activation process leads to a disappearance or decline of the concentration of fixed anionic sites at the height of the activation potential, and a transient appearance of fixed cationic sites spreading over the cell surface. The effect reminds one of the emergence of an anionic sensitivity in the collodion electrode on exposure to polylysine and with a decrease of pH from 7 to 5 (Fig. 14.5).

An electrical potential change initiated by puncturing with a microelectrode was also reported by Lassen *et al.* (1974) in the large red blood cells of the conger eel. As Fig. 14.24 shows, ψ , initially indifferent to external K^+ concentrations, suddenly becomes K^+ -sensitive, much like the "awakening" of the K^+ sensitivity of the mito-

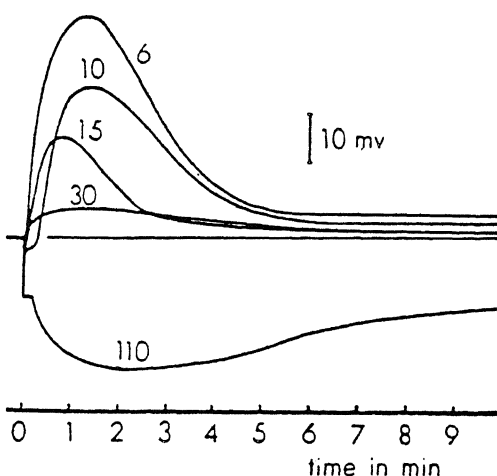
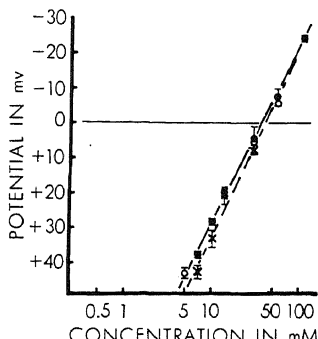


FIGURE 14.22. Time course of the activation potential of *Bufo* eggs. Numerals by each curve denote millimolar concentrations of external Cl^- [From Maeno (1959), by permission of *Journal of General Physiology*.]

FIGURE 14.23. Effect of external Cl^- on the crest level of the activation potential of *Bufo* eggs. ●, in Na^+ -Ringer; ○, in K^+ solution; ×, in Cl^- -Ringer series. Broken line is obtained by correcting the potential difference across the chorion in Na^+ -Ringer and K^+ solution series. It agrees well with the results obtained in Cl^- -Ringer series. [From Maeno (1959), by permission of *Journal of General Physiology*.]

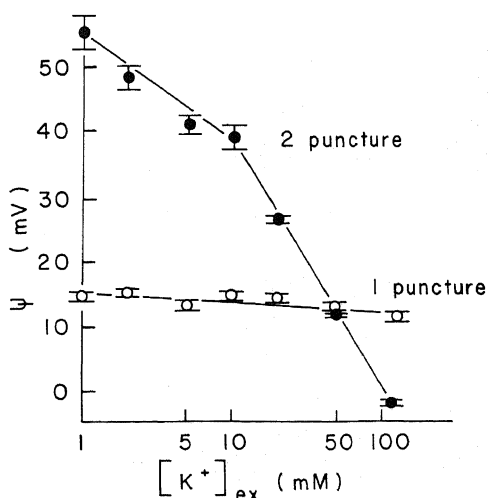


chondrial potential by exposure to 10^{-7} M valinomycin observed by Maloff *et al.* (1978) (to be described in Section 15.3.3.2). Figure 14.25 shows that this hyperpolarizing effect is Ca^{2+} dependent. Lassen *et al.* believed that the mechanical puncture allows Ca^{2+} to reach inside the cell. This may indicate the presence of a Ca^{2+} -binding cardinal site on the inside of the cell surface. Ca^{2+} binding then initiates the cooperative transition in the *c*-value to one favoring K^+ binding over Na^+ binding by increasing $K_{\text{Na} \rightarrow \text{K}}^{00}$ of equation (14.8).

14.5. Molecular Events Underlying Excitation

Bernstein suggested that nerve and muscle excitation involves a transient increase in membrane permeability. Squid giant axons and *Nitella* cells provided the means for the confirmation of this theory by Cole and Curtis (1938, 1939). In these axons, the resting resistance attributed to the cell membrane fell from $1000 \Omega/\text{cm}^2$ to $20 \Omega/\text{cm}^2$

FIGURE 14.24. Membrane potential as a function of the logarithm of the external K^+ concentration in *Amphiuma* red cells. The curve marked "1 puncture" represents the membrane potentials of cells which had not previously been subjected to micropuncture. The potentials recorded on the second puncture, 30 sec after the first, show a hyperpolarization. In these experiments changes in K^+ concentration were compensated by an equal and opposite variation in the Na^+ concentration of the medium. Abscissa: external K^+ concentration (log scale); ordinate: membrane potential in millivolts. The measured potential values are indicated $\pm \text{SEM}$, pH 7.2, 17°C . [From Lassen *et al.* (1974), by permission of *Journal of Membrane Biology*.]



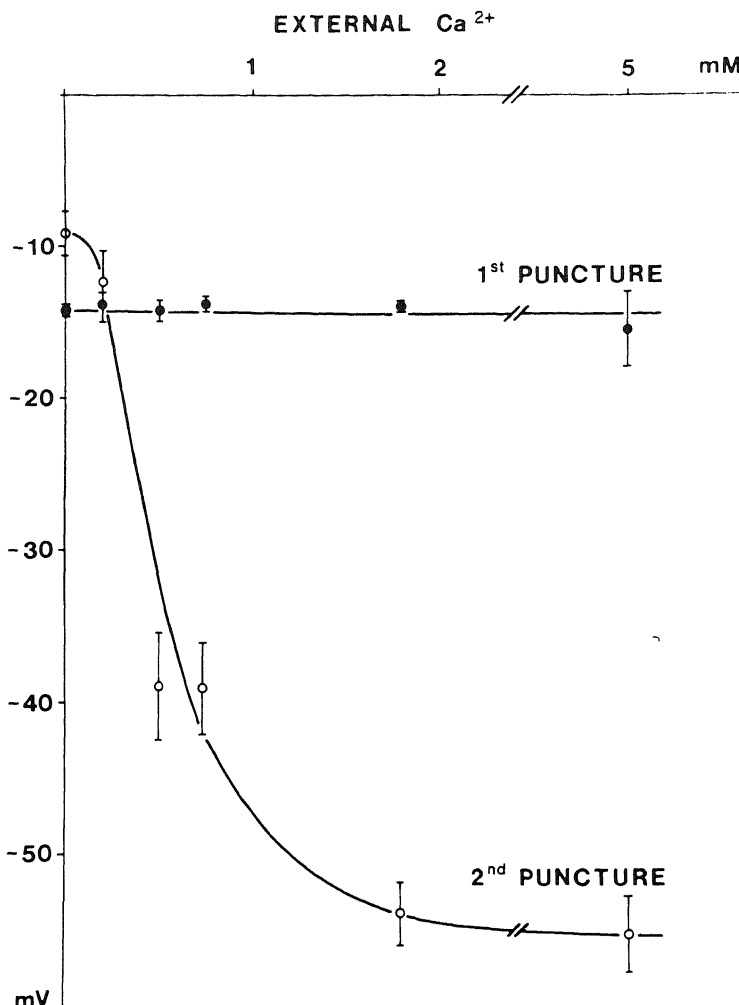


FIGURE 14.25. Effect of external Ca^{2+} concentration on initial membrane potentials and potentials recorded 30 sec after the initial micropuncture of *Amphiuma* red cells. Abscissa: Ca^{2+} concentration of medium (millimolar); ordinate: membrane potential in millivolts. Mean potential values are indicated ± 1 SEM, pH 7.2, 17°C. [From Lassen *et al.* (1974), by permission of *Journal of Membrane Biology*.]

(Cole and Curtis, 1938–1939a,b). As outlined in Section 3.4, this transient permeability increase offered the basis for the theory of excitation and the action potential of Hodgkin, Huxley, and Katz, which includes concepts of opening and closing of specific Na^+ and K^+ gates. Indeed some workers in this field have considered that the closing of the Na^+ gate and the K^+ gate occurs because Ca^{2+} physically blocks Na^+ and K^+ from their respective “pores”; the gates open when this blocking Ca^{2+} is removed. There is reason to doubt this simple pore-blocking hypothesis. One recalls that Moritz Traube (1867) first offered the rigid-pore-size or atomic sieve model as the basis for the solute imperme-

ability of semipermeable membranes. The sieve idea thus has already been disproven, as outlined in Chapters 1 and 12. The pore-clogging model is yet another variant of the same concept and as such not likely to be productive.

14.5.1. Basic Molecular Structure and Properties of the Cell Surface of Muscle and Nerve According to the AI Hypothesis

As illustrated in Fig. 14.26, the functional cell surface is a two-dimensional matrix of proteins carrying fixed anionic sites in the form of an array of β - and γ -carboxyl

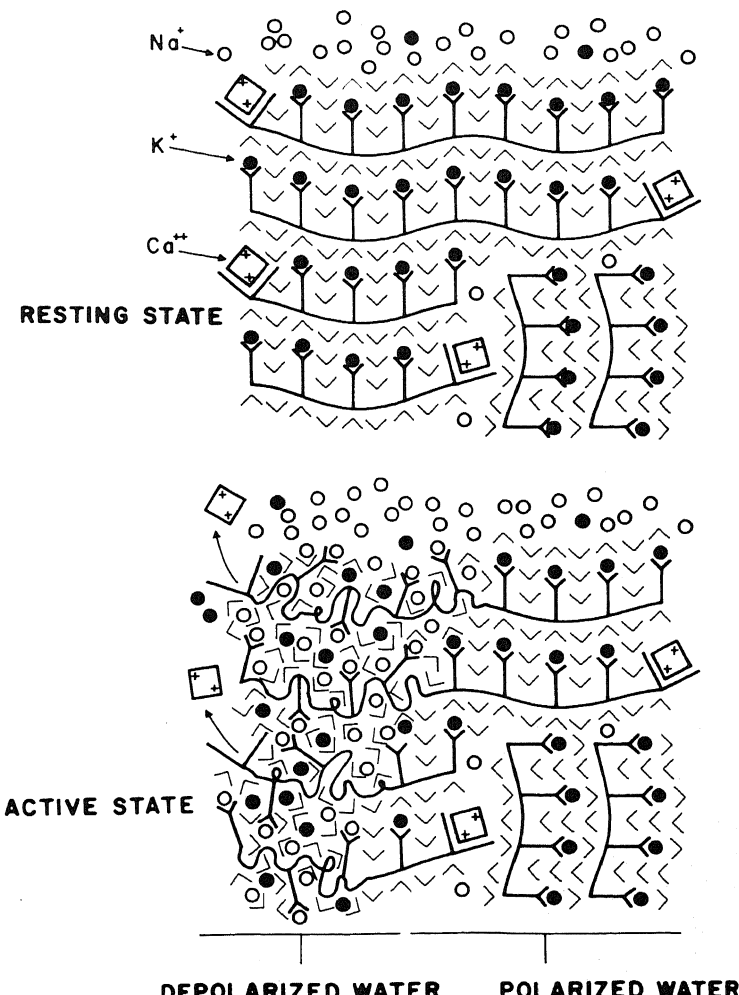


FIGURE 14.26. Diagrammatic illustration of the excitable cell surface at rest (top) and during activation. \wedge represents water molecules. Desorption of cardinal adsorbent, Ca^{2+} , causes switching of surface anionic site occupancy from K^+ to Na^+ and depolarization of water. Note the two types of protein chain orientation illustrated: parallel and perpendicular to the cell surface. External medium at top of figure. (From Ling (1982), by permission of *Physiological Chemistry and Physics*.)

groups, each set being under the influence of a cardinal site. In a resting cell, the cardinal site is occupied by a Ca^{2+} ion, which allosterically controls the c -value of the β - and γ -carboxyl groups, maintaining it at a relatively low value at which K^+ is preferred over Na^+ (see Figs. 11.37 and 11.38). As a result, K^+ is the predominant countercation at the cell surface.

The same or other protein chains offering the β - and γ -carboxyl groups for K^+ adsorption may in fact exist in an extended conformation, thereby lending their exposed backbone NHCO groups to polarize deep layers of water in between the proteins at the cell surface.

Under the cell surface the protein chains may be arrayed in parallel to the cell surface or perpendicular to it (Fig. 14.26, top).

We can now summarize the physiological properties of such a cell surface model:

1. The cell surface is semipermeable, meaning that it is most permeable to water but progressively less permeable to larger and more complex molecules.
2. The cell surface behaves more or less like a K^+ electrode because at the prevailing low c -value of a resting muscle or nerve cell surface, K^+ is preferentially adsorbed over Na^+ .
3. The cell surface potential shows no sensitivity to Cl^- because the resting surface sites are primarily anionic.
4. The cell surface potential shows no sensitivity to external Mg^{2+} concentration (Ling *et al.*, 1979) because β - and γ -carboxyl groups are isolated and not in pairs or clustered.
5. K^+ entry shows competition and saturability because most K^+ traffic is via the adsorption-desorption route (Fig. 12.14) on β - and γ -carboxyl groups, with a pK_a of 4.6 (Fig. 12.22).
6. Na^+ entry is partly by the same adsorption-desorption route as for K^+ , and thus shows partial though much less favorable competition with K^+ , and partly by the saltatory route by jumping through the interstices (Fig. 12.14). The saltatory route offers relatively high resistance to the passage of Na^+ and other cations because of the electric fields of the fixed β - and γ -carboxyl groups and a relatively low permeability to large hydrated ions through the polarized water.
7. In muscle cells, the K^+ -adsorbing sites directly below the cell surface are hypothesized to be arrayed in rows parallel to the cell surface (Fig. 14.26, lower left corner of top). A high activation energy for K^+ migration between chains reduces outward K^+ conductance (Fig. 8.14). This then may account for the anomalous rectification phenomenon first observed by Katz, i.e., a greater resistance to outward K^+ conductance than inward K^+ conductance when muscles were in an external solution containing K^+ at a concentration equal to that inside the cells (B. Katz, 1949; see also Adrian, 1969). In other cases, these protein chains may be random or perpendicular to the cell surface (lower right corner of top of Fig. 14.26); in those cases, K^+ may jump from one site to another, offering a high conductivity (for detail see Fig. 8.14) and hence normal rectification, as in many types of nerves. The same mechanism can also account for the much higher radial cytoplasmic resistance and membrane capacitance of muscle cells in comparison with nerve cells (see B. Katz, 1966).

14.5.2. The Molecular Basis of the Sudden, Transient Permeability Increase during Excitation

14.5.2.1. Theory

The front end of an action potential causes a local depolarization. When this depolarization reaches a certain level, the cardinal adsorbent Ca^{2+} is detached (Frankenhaeuser and Hodgkin, 1957; Fishman *et al.*, 1971). As a result, the proteins which are controlled by the cardinal adsorbent Ca^{2+} undergo a propagated cooperative change (the indirect F -process) (see also Fishman *et al.*, 1971; Chimadzhev *et al.*, 1972). The change contains at least two major components (Fig. 14.26, bottom):

1. *An ion-specific permeability increase.* The c -value of the β - and γ -carboxyl groups on the microscopically thin surface layer of the cell shifts to a higher value, as a result of which the preference for K^+ over Na^+ is lost and the surface anionic sites locally begin to adsorb Na^+ in an autocooperative manner. This is envisaged as a local, transient version of the gross ion shift seen in whole muscle initiated by the loss of Ca^{2+} (Figs. 11.37 and 11.38). The effect on the surface potential is described by equation (14.8), with a Ca^{2+} -dependent change of $K_{\text{Na}-\text{K}}^{00}$.

2. *A nonspecific permeability increase.* Along with the propagated shift in adsorption of Na^+ on the β - and γ -carboxyl groups, there is a step-by-step propagated change of the backbone from its extended water-polarizing conformation to a folded (e.g., α -helix) or other peptide-to-peptide, H-bonded, non-water-polarizing conformation. With this depolarization, cell surface water abruptly loses its property of excluding hydrated Na^+ (and K^+) and a sudden increase of permeability and cation conductance occurs; a transient inward diffusion of Na^+ occurs, creating the inward Na^+ current. This inward diffusion of Na^+ is partly ion-specific because the entering ion has to compete successfully for the surface anionic sites, now at a high c -value, favoring Na^+ . However, additional driving force is provided by the sudden depolarization and normalization of water near the cell surface and the nonspecific permeability increases that ensue. Thus, the final metastable equilibrium state potential has an additional component equal to

$$\psi = \frac{RT}{\mathcal{F}} \ln \frac{[\text{Na}^+]_{\text{in}}^{\text{free}}}{[\text{Na}^+]_{\text{ex}}} \quad (14.9)$$

This is identical to Hodgkin and Huxley's Na^+ potential (Hodgkin and Huxley, 1952a) except that only free intracellular Na^+ rather than total Na^+ concentration is involved.

3. *The general equation.* The general equation for the action potential as well as the resting potential is

$$\begin{aligned} \psi &= \text{Constant} - \frac{RT}{\mathcal{F}} \ln \frac{1}{[\text{K}^+]_{\text{ex}}} \left[1 + \frac{\xi - 1}{\sqrt{(\xi - 1)^2 + 4\xi \exp(\gamma/RT)}} \right] \\ &\quad - \frac{RT}{\mathcal{F}} \ln \frac{\gamma_{\text{in}}^{\text{Na}} [\text{Na}^+]_{\text{in}}^{\text{free}} + \gamma_{\text{in}}^{\text{K}} [\text{K}^+]_{\text{in}}^{\text{free}}}{\gamma_{\text{ex}}^{\text{Na}} [\text{Na}^+]_{\text{ex}} + \gamma_{\text{ex}}^{\text{K}} [\text{K}^+]_{\text{ex}}} \end{aligned} \quad (14.10)$$

where γ_{in}^{Na} , γ_{in}^K , γ_{ex}^{Na} , and γ_{ex}^K are the activity coefficients of Na^+ and K^+ in the cell surface layer water and the external solution, respectively. The second term on the right-hand side of equation (14.10), a diffusion potential term, vanishes when the cell is at rest because under this condition $\gamma_{in}^{Na}/\gamma_{ex}^{Na} = [Na^+]_{ex}/[Na^+]_{in}^{free}$ and $\gamma_{in}^K/\gamma_{ex}^K = [K^+]_{ex}/[K^+]_{in}^{free}$. Now

$$q_{Na} = \frac{\gamma_{ex}^{Na}}{\gamma_{in}^{Na}} \quad q_K = \frac{\gamma_{ex}^K}{\gamma_{in}^K} \quad (14.11)$$

where q_{Na} and q_K are the equilibrium distribution coefficients of Na^+ and K^+ in the cell surface water. Substituting equation (14.11) into (14.10) and taking into account the facts that $\gamma_{ex}^{Na} [Na^+]_{ex} + \gamma_{ex}^K [K^+]_{ex}$ is a constant and that $\gamma_{ex}^{Na} = \gamma_{ex}^K$, equation (14.10) can be simplified as follows:

$$\begin{aligned} \psi = \text{Constant} - \frac{RT}{\mathcal{F}} \ln \frac{1}{[K^+]_{ex}} & \left\{ 1 + \frac{\xi - 1}{\sqrt{(\xi - 1)^2 + 4\xi \exp(\gamma/RT)}} \right\} \\ & - \frac{RT}{\mathcal{F}} \ln \left\{ \frac{[Na^+]_{in}^{free}}{q_{Na}} + \frac{[K^+]_{in}^{free}}{q_K} \right\} \end{aligned} \quad (14.12)$$

During excitation K_{Na-K}^{00} falls, owing to the increase in the c -value of the surface anionic sites, while q_{Na} (and q_K) concomitantly increase. The inrush of Na^+ brings about not only a cancellation of the resting potential but also an overshoot. The adsorption of Na^+ displaces K^+ from adsorption sites at and near the cell surface, causing an increase of free K^+ (i.e., $[K^+]_{in}^{free}$), and hence the delayed outward K^+ current.

It should be pointed out that, because of autocoooperativity, both K_{Na-K}^{00} and γ_{in}^{Na} (and γ_{in}^K) shift between discrete states (Ling, 1957, 1960, 1962; Tasaki, 1963, 1968, 1982). The value of ψ at the active state should be approximated by the value of the peak height of the action potential. The time course of transition between the two autocoooperative states is S-shaped with a steep slope and is analogous to the kinetics of the one-dimensional Ising model, as successfully treated by Huang (1979), Negendank and Karreman (1979), and Huang and Negendank (1980) (Figs. 12.39, 12.41, and 12.42).

In the Hodgkin-Huxley theory, the late outward K^+ current of an action potential was attributed to the opening of a second, different K^+ gate. In the AI hypothesis, no such second K gate is required. Indeed, the outward K current is due partly to the K^+ displaced by the in-moving Na^+ , but it is primarily a shift of intracellular K^+ from its normal resting adsorbed state to a free state that increases momentarily the outward K^+ flux. The loss of the excess positive charge accumulated during inward Na^+ movement is reversed. Ca^{2+} once more returns to its cardinal sites and a reversal of the changes of K_{Na-K}^{00} and γ_{in}^{Na} leads to reestablishment of the resting polarized condition.

14.5.2.2. Comparison of Theory with Experimental Observations

14.5.2.2a. Inward Na^+ Current. By suggesting that the inward Na^+ current is driven by a suddenly activated Na^+ potential described by equation (14.9) and the third term of equation (14.10), the present theory partially agrees with the Hodgkin-Huxley model. However, since Na^+ adsorption, described by the second term of equation

(14.10), is on sites that are available to K^+ , the movements of Na^+ and K^+ are as a rule not independent of each other; the surface adsorption model is therefore in accord with data cited earlier that contradict the Hodgkin-Huxley theory (Section 14.1.5).

The basic concept that the cell surface anionic β - and γ -carboxyl groups undergo a brief, transient increase of c -value, lasting throughout the duration of the inward Na^+ current, is in harmony with the following observations:

1. These surface anionic sites before excitation have a relatively low pK_a value (4.6) (see Fig. 12.22), hence a low c -value. The order of selectivity of the resting surface sites is $Rb^+ > Cs^+ > K^+ > Na^+$ (see Fig. 14.8), roughly corresponding to a c -value of -4.5 \AA according to the theoretical data of Figs. 6.7 and 6.8.

2. The anionic sites essential for the inward Na^+ current have a higher pK_a value. Thus the pK_a value for the anionic site mediating Na^+ entry for squid axons was given as 5.2 by Hille (1972) and 6.5 by Stillman *et al.* (1971). The pK_a value of the node of Ranvier of frog nerve was given by Drouin and The as 5.15 and that of *Myxicola* axon as 4.8 (Drouin and The, 1969). The higher pK_a value agrees with a higher c -value for the activated surface anionic sites than for the resting sites. The order of ion selectivity of the anionic site essential for the Na^+ current is $Li^+ = Na^+ > K^+ > Rb^+ > Cs^+$ (Hille, 1975), which roughly corresponds to a c -value of -1.5 \AA from the theoretical curve of Fig. 6.7, or -2.5 \AA from Fig. 6.8. A large body of evidence has indicated that the Na^+ channel is primarily proteinaceous (for review, see Hucho and Schiebler, 1977). Proteins contain anionic groups, mostly in the form of β - and γ -carboxyl groups. Thus the anionic sites with high pK_a can reasonably be expected to be the same β - and γ -carboxyl groups when the proteins exist in the activated conformation.

14.5.2.2b. Nonspecific Increase of Permeability. The theoretical model of a propagated depolarization of cell surface water is compared with the findings of Villegas *et al.* (1965), whose data are reproduced in Table 14.1. Sugars and sugar alcohols, normally excluded from cells and virtually impermeant through a polarized water model (Fig. 12.13), suddenly become permeant, but only in the presence of Na^+ , in accord with the present model. For other evidence of the increase of nonspecific permeability during activation, see Luxoro *et al.* (1965).

TABLE 14.1. Penetration of [^{14}C]Erythritol, -Mannitol, and -Sucrose into Resting and Stimulated Squid Axons^a

Molecule	Permeability in 10^{-2} cm/sec^b			
	Resting axon (axon a)	Stimulated at 25/sec (axon b)	Net increase 25 stimulations/sec (paired data) (b - a)	Calculated permeability during activity ^c
Erythritol	3.6 ± 0.4	6.1 ± 1.0	2.5 ± 0.8	110
Mannitol	2.3 ± 0.4	4.0 ± 0.5	1.7 ± 0.3	75
Sucrose	0.9 ± 0.1	1.8 ± 0.3	0.9 ± 0.3	40

^aFrom Villegas *et al.* (1965), by permission of *Journal of General Physiology*.

^bThe values are mean \pm SE of ten nerve fiber pairs.

^cCalculated permeability during activity obtained by considering that the permeability change per impulse lasts 1 msec.

Can the present model quantitatively match the 50-fold decrease of membrane resistance during the action potential (from $1000 \Omega/\text{cm}^2$ to $20 \Omega/\text{cm}^2$) and the estimated increase of sucrose permeability of more than 40-fold (Table 14.1)? To answer, let us return to Fig. 12.13. Here the sucrose permeability is more than 10,000 times lower than permeability to water. Since permeability through a thin membrane is equal to $D_i q_i$, where D_i is the diffusion coefficient and q_i is the equilibrium distribution of the i th solute between the membrane phase and the external solution (Crank, 1956), the ratio of sucrose permeability to water permeability through a thin layer of normal water (in which $q_{\text{sucrose}} = q_{\text{water}} = 1$) should be approximately

$$\frac{D_{\text{sucrose}} q_{\text{sucrose}}}{D_{\text{water}} q_{\text{water}}} = \frac{D_{\text{sucrose}}}{D_{\text{water}}} = \frac{5.23 \times 10^{-6}}{2.35 \times 10^{-5}} = 22.2$$

where 5.23×10^{-6} and $2.35 \times 10^{-5} \text{ cm}^2/\text{sec}$ are the diffusion coefficients of sucrose and water in water, respectively (Hodgman *et al.*, 1961; Wang *et al.*, 1953). Thus, if the cell surface is entirely covered with water, as found in the activated layer of cellulose acetate membranes (Ling, 1973b), and during excitation all of it turns into normal water, there would be a $10,000/23.2$ - or 430-fold increase in sucrose permeability. I have chosen water permeability as a reference because the normal resting cell membrane is extremely permeable to water, as is also the cellulose acetate polarized water (Fig. 12.13). However, the permeability of the resting nerve and muscle cell membrane to sucrose is considerably higher than that of frog skin or the activated cellulose acetate layer. With this in mind, one would expect that a very large area of the excited cell membrane water must have become totally depolarized.

One important distinctive feature of this model is that water depolarization not only reduces the resistance of Na^+ permeation but also increases the effective total surface area for Na^+ permeation. This new facet makes it much more reasonable to visualize an all-or-none surge of Na^+ current through a membrane already quite permeable to Na^+ .

14.5.2.2c. Evidence for c-Value Change of Surface β - and γ -Carboxyl Groups. The present model does not prescribe the existence of a second K^+ channel which opens and closes specifically for K^+ during the passage of an action potential. Instead, the reason for outward K^+ movement, according to the AI hypothesis, is its desorption from cell surface β - and γ -carboxyl groups.

The presence of fixed carboxyl groups throughout the cytoplasm with relatively low c -values, at which K^+ is normally preferred, is substantiated by the fact that the acidic groups at the muscle cell surface have a pK_a value of 4.6 (Ling and Ochsenfeld, 1965), very similar to the value obtained from *in vitro* measurements of isolated proteins (Tanford, 1962). The great similarity in the characteristics of the intracellular and surface anionic sites that selectively adsorb K^+ over Na^+ includes sensitivity to ouabain and to Ca^{2+} . That intracellular anionic sites within living cells also have pK_a values similar to those Ling and Ochsenfeld studied on the surface of the frog muscle cell is supported by the following findings.

Drouin and The (1969) observed in frog Ranvier node acidic groups with pK_a values of 4.63 ± 0.05 . Stillman *et al.* (1971) observed acidic groups for K^+ channels in

squid axon to have a pK_a value lower than 5.0. Schauf and Davis (1976) discovered in *Myxicola* giant axon acidic groups with pK_a values of 4.4. These data clearly show that the inside of the cell has the same type of β - and γ -groups as on the cell surface which, like them, function at once as channels and barriers to ionic movement. Just as Rb^+ and Cs^+ slow down K^+ inward permeation (Figs. 4.11, 4.15, and 12.15), the same ions block delayed K^+ current, as Chandler and Meves showed in 1965. Similarly, the reduction of the delayed current by Na^+ (see Armstrong, 1975) can be compared with the blocking of Na^+ entry by K^+ (see Fig. 12.21).

14.5.2.2d. Channel Inactivation. The delayed current normally observed under the voltage clamp condition, described in Section 3.4.2 and Fig. 3.11, shows no inactivation. Yet tetraethylammonium introduced into the squid axon blocks the delayed K^+ current. Similarly, Cs^+ and H^+ inactivate the delayed K^+ current. To explain, the data shown in Fig. 4.15 are useful. Here the entry of K^+ is competitively inhibited by the presence of Rb^+ and yet Rb^+ entry is facilitated by the presence of K^+ (Fig. 12.19). Clearly this shows that ionic migration is not simply by sorption onto a vacant site, followed by desorption leaving behind another vacant site. Rather, there is the transient formation of a triplet with the participation of a second countercation, as illustrated in Fig. 12.20.

It is likely that the optimal condition for maximal ionic conductance occurs among a population of the same kind that assumes a higher configuration (see Fig. 6.6) at equilibrium. If, instead of Rb^+ , a tetraethylammonium ion or its C-9 derivative occupies the fixed anion, \mathcal{F}^- , then the oncoming K^+ has no chance of weakening the C-9 \mathcal{F}^- bond sufficiently to allow it to replace C-9, and ion immigration or conductance must then be arrested. These concepts, introduced in 1962, bear some resemblance to the model of Armstrong (1975).

With this consideration in mind, it seems reasonable to assume that Na^+ channel inactivation is due to the occupancy of the sites with a high c -value by K^+ , and that K^+ channel inactivation is due to the occupancy of the sites by ions, like tetraethylammonium, Cs^+ , and H^+ , that can displace K^+ .

14.5.2.2e. Local Transient Swelling during the Passage of an Action Potential. Iwasa, Tasaki, and Gibbons (1980) have elegantly demonstrated that in squid axon there is a transient local swelling during the passage of an action potential. They offered no specific explanation for the mechanism. In Chapter 13 I showed that isotonic KCl causes cell swelling by dissociating restraining salt linkages between protein chains [equation (13.3)]. I would like to suggest that during the conformation change in the course of the action potential some salt linkages are dissociated transiently and reversibly, thereby creating the transient swelling. In support, I shall mention another paper of Tasaki and his associates (Pant *et al.*, 1978), which showed that perfused squid axons release proteins into the perfusate in response both to high concentrations of K^+ salt and also to repetitive electrical stimulation. It is obvious that if the salt linkages holding a protein molecule in place are all broken the protein will be released; if only part of the salt linkages are broken, swelling will follow as a consequence.

Further support for the present interpretation came from the finding that large protein loss occurred when K^+ salts of Cl^- , Br^- , I^- , or SCN^- were used for perfusion

but that no or little loss occurred when a solution of KF was used (Inoue *et al.*, 1976; Pant *et al.*, 1978; Yoshioka *et al.*, 1978). Figure 13.8 shows that F^- is one of the most weakly adsorbed anions on protein cationic sites; equation (13.3) then predicts the least protein dissociation and loss in a KF solution, as was observed.

Furthermore the effectiveness in releasing proteins by the different anions follows the rank order of $SCN^- \gg Br^- > Cl^- > F^-$ (Inoue *et al.*, 1976). This rank order is exactly the same as that for the strength of anion adsorption (as shown in Fig. 13.8) onto proteins and the model of proteins, the amino type of anion exchange resin.

14.5.2.2f. Electrical Potentials of Protoplasmic Droplets and of Lipid-Free Synthetic Microspheres. Inoue, Ueda, and Kobatake (1973b) isolated droplets of protoplasm from the internodal cells of *Nitella*. One recalls that it was droplets of this type and their behavior, resembling that of intact cells, that had led early physiologists to the protoplasmic approach to the study of living cells (see Section 2.5). Inoue *et al.*, however, went a step further. Using intracellular microelectrodes, they observed steady resting potentials of -50 to -90 mV when Ca^{2+} , Mg^{2+} , Na^+ , and K^+ were present in the surrounding solution. Abrupt autocooperative depolarization was also observed following critical concentration changes of external ions (Ueda *et al.*, 1974).

Inoue *et al.* believed that at the surface of the isolated protoplasmic droplets a membrane of phospholipids was formed first, followed by invasion by and reaction with proteins. The importance of the proteins was indicated by the sensitivity of the potential to SH reagents (e.g., *p*-chloromercuribenzoate), which suppressed the excitability of the droplets—a reaction which could be completely reversed by the addition of dithiothreitol (Inoue *et al.*, 1974). The significance of these studies became further enhanced and their understanding refined in consequence of the recent work of Fox and his associates. One recalls that it was Fox and his group who first produced microspheres with bilayered “membrane” structure from purely proteinoid materials (see Fig. 12.6).

In 1981, Ishima, Przybylski, and Fox inserted capillary GGL microelectrodes into microspheres prepared from heat-treated mixtures of pure amino acids (thermal proteins), glycerol, and vegetable lecithin. They observed steady resting potentials, action potentials, and oscillatory potential changes. These findings *per se* could again be interpreted as Inoue, Ueda, and Kobatake (1973b) did in regard to protoplasmic droplets, emphasizing a primary role of phospholipids. However, this interpretation has been invalidated by the later work of Przybylski, Stratten, Syren, and Fox (1982), who concluded their later work with the following summary: “We report further that the same kinds of electrical behavior are observed when the lecithin and glycerol are omitted entirely. . . .” (p. 561). There is now no doubt that the primary seats of the generation of the potentials are proteins, not phospholipids.

Reassuring in regard to the model represented by the AI hypothesis is the nature of the essential free amino acids from which the electrically active microspheres were prepared. They are glutamic and aspartic acids.

As shown in Fig. 14.27A, microspheres prepared from copolymers of aspartic and glutamic acid gave rise to a potential 2 mV above background; microspheres of copoly(asp, glu) complexed with copoly(asp, glu, arg, his) gave rise to a potential 20 mV above background (Fig. 14.27B). In Fig. 14.27C, a potential of 60–70 mV above background was observed in microspheres made of proteinoid JGII-58 (a 2:2:1 protein-

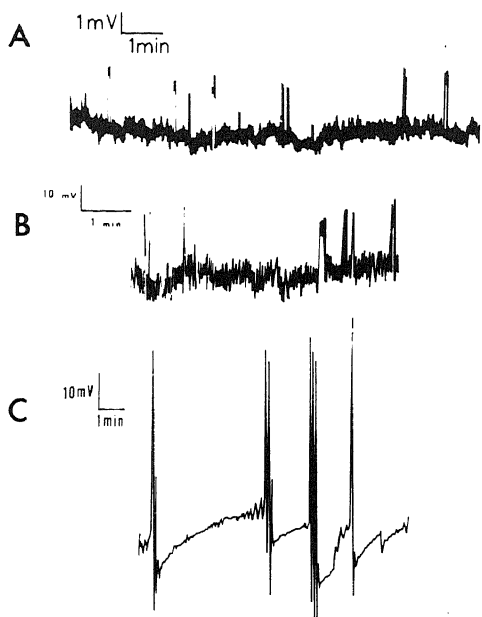


FIGURE 14.27. Tracings of spiking in microspheres assembled from (A) copoly(asp, glu), (B) copoly(asp, glu) complexed with copoly(asp, glu, arg, his), and (C) JGII-58 proteinoid and vegetable lecithin. For each observation, controls in the solution without impalement yielded a horizontal pattern. Proteinoid JGII-58 is a 2:2:1 proteinoid (Fox and Dose, 1977) which contains 66% aspartic acid and 16% glutamic acid but no histidine. [From Przybylski *et al.* (1982), by permission of *Naturwissenschaften*.]

noid containing 66% aspartic acid, 16% glutamic acid, and other amino acids but lacking histidine) containing lecithin. Together their findings suggested that electrical potentials arise from proteins, with their glutamic and aspartic acid residues playing a central role. However, other amino acid residues as well as phospholipids also serve major functions by perhaps stabilizing the conformation of the proteins (Ling, 1977d) where β - and γ -carboxyl groups are stable and free to interact with free ions to generate the type of potential that can exist cooperatively in more than one metastable state.

14.6. Summary

The surface adsorption model of the cell potential was outlined in Chapter 4 within the context of the Ling fixed-charge hypothesis. In this model, the potential depends on four major variables: temperature, the selective affinity of surface fixed charges for counterions, the concentration in the external medium of counterions for which the sites have a high affinity, and the density of the fixed-charge sites. In this chapter the surface adsorption model was extended to include an explicit description of the cooperative interaction between surface sites that adsorb ions.

In this model, the cell potential may be sensitive to any cation or anion, depending on the nature and sign of the surface fixed charges. This explains the variability from cell type to cell type, or within the same cell under different conditions, in the nature of the external ion to which the potential is sensitive. Thus, although the resting potential of most nerve and muscle cells is sensitive primarily to K^+ , the resting potential of other cells may be sensitive to other cations or even to anions.

The molecular events that underly excitation and the action potential include two major sets of phenomena: (1) a specific increase in permeability to cations owing to an autocooperative change in the affinity of surface anionic sites for cations from one that favors K^+ to one that favors Na^+ and (2) a nonspecific increase in permeability owing to depolarization of water within "channels" at the cell surface. These phenomena give rise to the early inward Na^+ current during the action potential and the dependence of the height of the action potential on Na^+ rather than on K^+ . The autocooperative nature of the change in the surface sites gives rise to the all-or-none characteristic of the action potential. The role of Ca^{2+} in this process is one of a cardinal adsorbent, just as it is in determining the adsorption isotherms of K^+ and Na^+ in muscle cells (Chapter 11).

One of the major problems in physiology has been the failure of the resting potential to vary with altered intracellular concentrations of K^+ , or the action potential to vary with altered intracellular concentrations of Na^+ , in the manner expected by the classical membrane theory. This, and a number of additional problems, are resolved by the surface adsorption model, and various phenomena that accompany the action potential, such as the increased permeability to sugars and the transient local swelling, are readily explained.

In the next chapter, the surface adsorption theory of the cell potential will be shown to apply equally well to the potential recorded in an organelle, the mitochondrion.

IV

A Reevaluation of Current Concepts in Physiology and Biochemistry

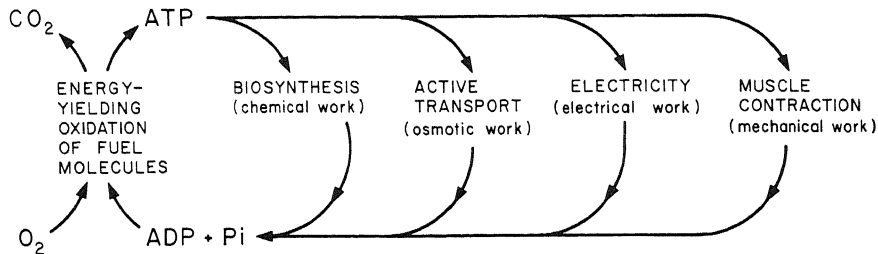
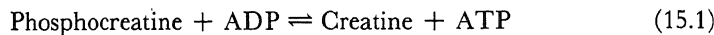


FIGURE 15.1. ATP as the key agent in biological work performance. [After Lipmann (1941).]

and a variety of other living cells where prompt energy supply upon a signal is required. In the case of CrP, the enzyme creatine kinase catalyzes the Lohmann reaction:



The standard free energy change (ΔG°) for this reaction is -3.0 kcal/mole (Lehninger, 1975, p. 406). This negative free energy forces the reaction to the right. Hence, a steady level of ATP can be maintained as long as there is phosphocreatine. The Sanger reagent, 2,4-dinitrofluorobenzene (DNFB), used by Sanger (1952) in his history-making analysis of protein composition, specifically inhibited creatine kinase (Infante *et al.*, 1964), thereby permitting the experimental study of ATP reactions isolated from their immediate source of replenishment, CrP.

15.2.2. Glycolysis or Fermentation

Under anaerobic conditions, glucose may be degraded into lactic acid (glycolysis) or ethanol (alcoholic fermentation). In these processes two molecules of ATP are synthesized from each glucose molecule degraded. In degrading glucose to lactic acid, only some 7% of the total free energy of the glucose is liberated. A much larger amount, however, is released by the total oxidation of glucose through respiration.

15.2.3. Respiratory Chain

Respiration, the major source of ATP, consists of two parts, the *tricarboxylic acid cycle* and the *electron transport-oxidative phosphorylation system* (Fig. 15.2). The tricarboxylic acid cycle, with its enzyme systems located inside the mitochondrion, accepts the acetyl group of acetyl-coenzyme A as a fuel and degrades it eventually to yield CO₂ and hydrogen atoms. The hydrogen atoms are then processed through a sequence of electron-transferring proteins to the ultimate electron acceptor, oxygen, which is reduced to form water.

The electron-transferring reactions begin with the various dehydrogenases, which catalyze the removal of hydrogen from substrates in the tricarboxylic cycle. Some of these dehydrogenases (α -ketoglutarate dehydrogenase, pyruvate dehydrogenase, glutamic acid dehydrogenase) are NAD-linked. In this case, NADH collects the electrons (or H

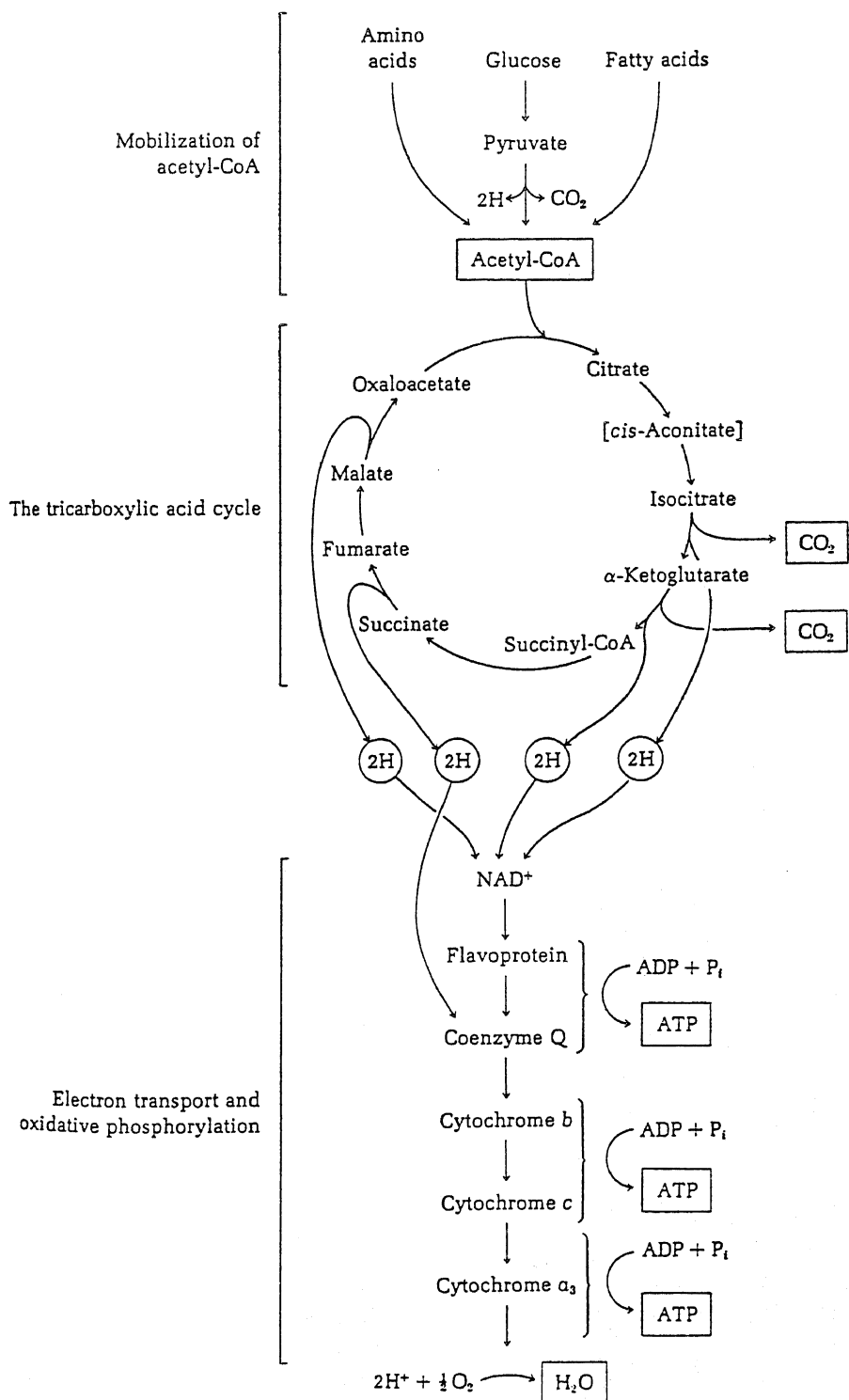


FIGURE 15.2. Flow sheet of respiration. [From Lehninger (1975), by permission of Worth Publishers.]

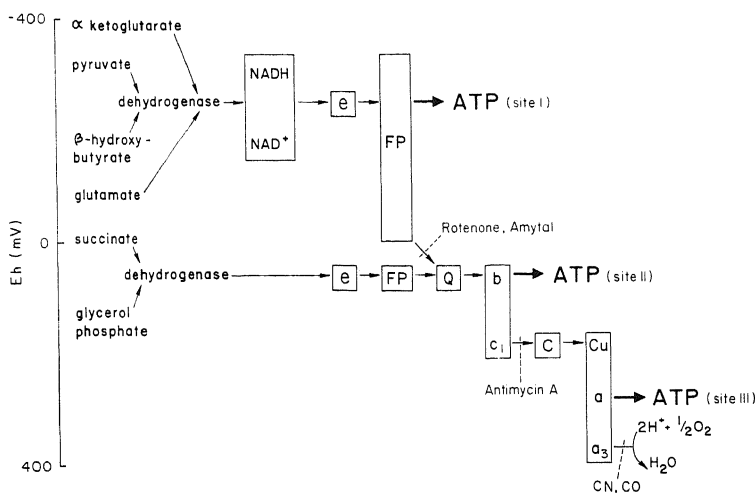


FIGURE 15.3. Diagram of electron transport chain with the three ATP-generating sites (I, II, III). E_h is the standard oxidation-reduction potential. e represents an electron or reducing equivalent; FP, flavoprotein; Q, coenzyme Q or ubiquinone; b, c_1 , cytochromes b and c_1 ; C, cytochrome c ; a, a_3 ; cytochromes a and a_3 .

equivalents) and funnels them into the respiratory chain via the flavoprotein NADH dehydrogenase. Other dehydrogenases like succinate dehydrogenase are flavin-linked, and electrons are funnelled into the chain via coenzyme Q (or ubiquinone). The sequence of electron transport from NAD to oxygen is illustrated in Fig. 15.3. Electrons from the NADH-NAD⁺ system are at a high (negative) oxidation-reduction potential (E_h). Before its final reaction with oxygen, the electron pair gives off energy as it flows down the respiratory chain to yield three ATP molecules, one ATP at each of three different sites. Electrons from succinate, on the other hand, yield only two ATP molecules since they enter the chain at site II, further downstream.

Some of the evidence for the scheme illustrated in Fig. 15.3 came from Chance and Williams (1956). Using a highly precise double-beam spectrophotometer, they were able to obtain the difference spectra of turbid mitochondrial suspensions and to measure quantitatively the oxidation-reduction states of the various electron carriers when the mitochondria were oxidizing intermediates of tricarboxylic acid. When a steady state is reached, a higher percentage of the electron carriers nearest the reducing end of the electron chain (NAD) exist in the reduced state. With each step further down toward the oxidizing end (NAD → FP → cytochrome bc_1 → cytochrome c → cytochrome aa_3), the percentage of electron carriers in the reduced state decreases until cytochrome aa_3 , which exists mostly in the oxidized state, is reached. Under anaerobic conditions, all the carriers exist in the fully reduced state. When oxygen is readmitted, the reduced cytochrome aa_3 becomes oxidized first, followed by cytochrome c and cytochrome bc_1 and finally NADH. The poison antimycin A blocks electron transport between cytochrome bc_1 and c . Introduction of antimycin A changes all the carriers on the reducing end (NAD, FP, and cytochrome bc_1) into a fully reduced state, and carriers on the oxidizing end, cytochromes c and aa_3 , into a fully oxidized state.

When mitochondria are undergoing respiration, and oxygen and substrates are

abundant, the rate of ATP production is controlled primarily by the level of ADP in the cytoplasm (or, more accurately, the ratio of ADP to ATP). This critical dependence of the rate of respiration on ADP is called *respiratory control*. When mitochondria are studied in the presence of adequate substrate and O₂, they have a relatively low rate of O₂ consumption in the absence of ADP and are said to be in *State 4* (resting respiration); when ADP is added, O₂ consumption increases and they are said to be in *State 3* (active respiration) (Chance and Williams, 1956).

15.3. Theories of the Mechanism of Oxidative Phosphorylation and Their Critiques

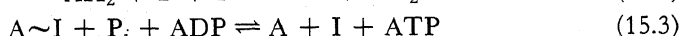
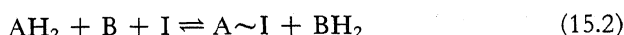
Oxidative phosphorylation, the main source of ATP in all aerobic organisms, occurs inside mitochondria, which may be filamentous, spherical, or of other shapes when *in situ* within living cells. In such vigorously metabolizing cells as the heart muscle, mitochondria may make up 50% of the cell volume; in rat liver they account for about 20%. As a rule mitochondria tend to aggregate near cytological structures which demand a supply of ATP. As an example, Fig. 15.4 shows a scanning electron micrograph of an isolated myofibril and its satellite mitochondria from the wing muscle of a honeybee (Trombitas and Tigyi-Sebes, 1979).

Each mitochondrion is enclosed by two membranes, an outer membrane freely permeable to solutes and an inner membrane which not only presents a selective barrier to solute movement but also contains most of the elements of the respiratory chain. Indeed the respiratory chain components are as a rule difficult to isolate from the inner membrane, suggesting close linkage among its components. Extending into the mitochondria are invaginations of the inner membrane. These infolding double membrane structures, called *cristae*, vary considerably in shape in different types of cells. A gelatinous substance filling the inside of the inner membrane is called the *matrix*. Some 50% of its weight is proteins, including most of the enzymes of the tricarboxylic acid cycle.

Major progress in our understanding of oxidative phosphorylation and other aspects of the physiology of mitochondria followed the establishment of a successful method for isolating mitochondria from rat liver (Hogeboom *et al.*, 1948). To preserve the morphology of the mitochondria's natural state, a highly concentrated sucrose solution had to be used (0.88 M), although subsequent researchers preferred 0.25 M sucrose. The mitochondria thus isolated, although spherical and therefore different in shape than *in situ*, are fully capable of oxidative phosphorylation. The following is a brief review of some current concepts of oxidative phosphorylation.

15.3.1. The Chemical Coupling Hypothesis

In the chemical coupling hypothesis, the energy-yielding electron transfer reaction is coupled to the energy-demanding ATP synthesis through a common high-energy intermediate. An early scheme proposed by Slater (1953) is as follows:



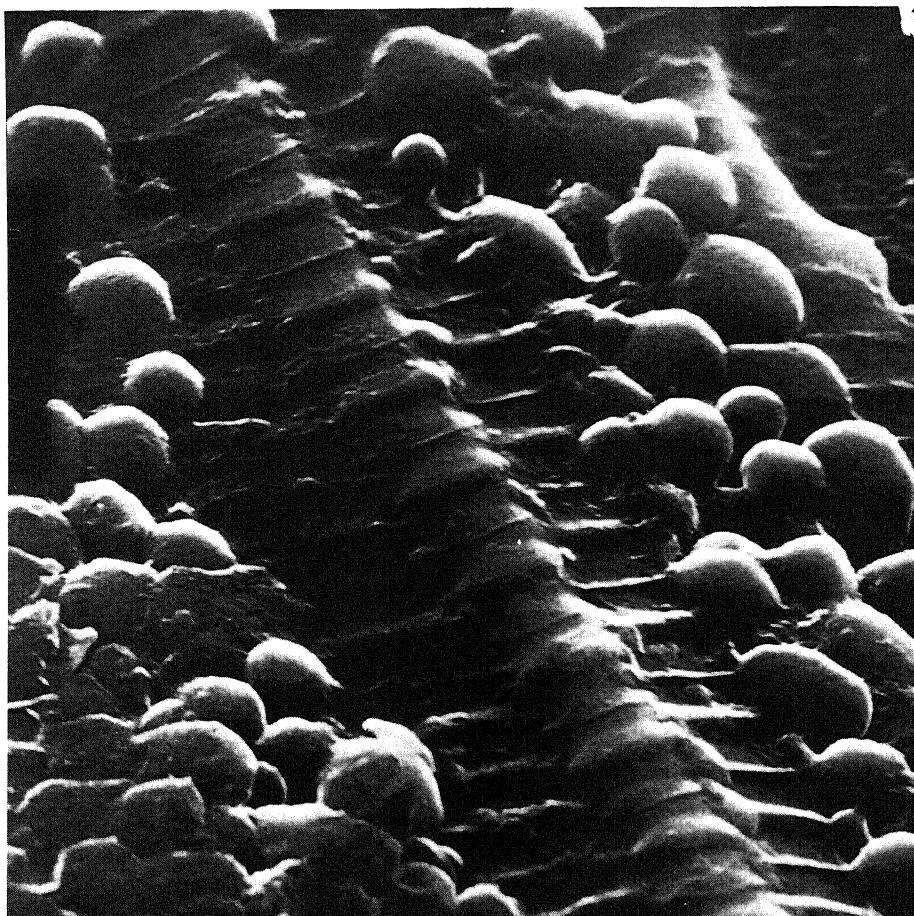
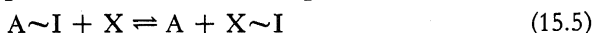


FIGURE 15.4. Scanning electron micrograph of isolated myofibril and adjacent mitochondria from the wing muscle of a honeybee. Magnification 10,000 \times . [From Trombitas and Tigyi-Sebes (1979), by permission of *Acta Physiologica Academiae Scientiarum Hungaricae*.]

Here the intermediate $A \sim I$ is postulated to have a strongly negative standard oxidation-reduction potential of hydrolysis and is generated by the transfer of electrons from one electron carrier of the chain to the next in line. Later, as a result of new knowledge (see Ernster *et al.*, 1967), the scheme was made more elaborate, as represented below:



Here A and B again are adjacent respiratory carriers at a given coupling site. X and I are energy transfer carriers common to all three coupling sites. A main criticism of the

chemical coupling hypothesis is that, in spite of an extensive search for the postulated intermediate for well over 20 years, no such intermediate has ever been discovered. Another criticism is that this hypothesis does not readily answer the question of why oxidative phosphorylation requires an intact mitochondrial inner membrane (Skulachev, 1971).

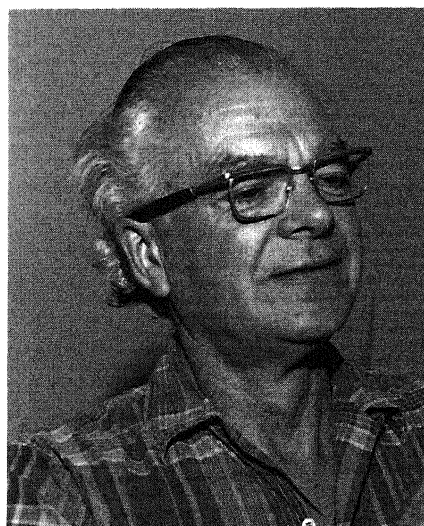
15.3.2. The Conformation Coupling Hypothesis

Boyer (1965) postulated that oxidative phosphorylation is coupled to ATP production by conformational changes of the enzymes involved. Energy from the oxidation is utilized to create a strained conformation of the enzyme. Subsequent relaxation and release from this strain are accompanied by the synthesis of a high-energy intermediate compound. The energy accumulated in this compound is then used to synthesize ATP.

Some evidence in favor of this hypothesis was provided by Green and his group (R. A. Harris *et al.*, 1968): Energization of mitochondria leads to profound morphological changes in the cristae of the mitochondria, as revealed by electron microscopy (Hackenbrock, 1968). In his critique of the conformation coupling hypothesis, Skulachev wrote, “The reference to conformation changes of respiratory carriers during electron transfer [also] seems unconvincing. Such changes accompany the function of many enzymes, and therefore cannot be qualified as specific properties of electron carriers” (Skulachev, 1971, p. 133).

15.3.3. The Chemiosmotic Hypothesis

First proposed by Peter Mitchell in 1961, the chemiosmotic hypothesis postulates that the immediate source of energy comes from an ionic gradient across the inner mem-



Peter Mitchell

brane of the mitochondrion. Since I have written a more extensive critique of this hypothesis (Ling, 1981a), the present discussion will be brief.

According to the chemiosmotic hypothesis, the inner membrane of a mitochondrion is impermeable to H^+ as well as to other ions. The respiratory chain is arranged in three loops corresponding to the three coupling sites. By a special vectorial arrangement of the electron-carrying molecules, an H^+ -absorbing reaction occurs on the inside surface of the inner mitochondrial membrane and an H^+ -releasing reaction occurs on the outside surface of this membrane. As a result, an H^+ gradient develops, with the higher concentration of H^+ on the outside surface of the inner membrane. A reversible ATPase complex on the mitochondrial inner membrane is located in a region impermeable to water but accessible to H^+ from the other side. ATP hydrolysis would be reversibly coupled to the translocation of OH^- ions across the system, with a stoichiometry of one OH^- translocated per ATP hydrolyzed. The proton gradient provides the energy for the synthesis of ATP.

Mitchell noted that the H^+ chemical gradient alone was not sufficient to supply energy for ATP synthesis. The mechanism was further elaborated by postulating the creation of an electrical potential across the inner membrane as a result of asymmetrical electron transport. Mitchell argued that "the sum of the electrical potential difference and the osmotic pressure difference" provides a protomotive force (PMF) for ATP synthesis and other energy-consuming processes (Mitchell, 1966).

The major share of this PMF is attributed to the postulated membrane potential of 210–270 mV, with the inside phase negative, and a small contribution to the PMF is attributed to the postulated pH difference (Mitchell, 1966).

The most appealing evidence in favor of this hypothesis is the interpretation offered for the role of valinomycin and other ionophores in uncoupling oxidative phosphorylation: Valinomycin, by making the membrane permeable to K^+ , discharges the postulated ionic gradient.

Mitchell's hypothesis aroused wide interest and attention and earned Mitchell a Nobel Prize. There is little question that the chemiosmotic hypothesis was based on a great deal of careful research and that the idea is highly original. However, there is now overwhelming evidence against this hypothesis (see Ling, 1981a). Some of that evidence will be mentioned here.

15.3.3.1. Evidence against the Chemiosmotic Hypothesis

The PMF, according to Mitchell's hypothesis, is partly due to a postulated pH gradient maintained across the inner membrane. Actual measurements revealed a minimal pH gradient—and even its existence is not certain (Addanki *et al.*, 1968; Rottenberg, 1970). Thus the bulk of the required PMF must come from the electrical potential difference. Yet extensive measurements with the most reliable method, a Gerard-Graham-Ling microelectrode, reveal an electrical potential not of the 200–300 mV required, but of only 10–20 mV, and then of the wrong polarity (Tupper and Tedeschi, 1969a–c; Maloff *et al.*, 1978; Tedeschi, 1980). The findings of Tedeschi's group are fully confirmed and extended by the mitochondrial electrical potential measured by Giulian and Diacumakos (1977), who showed that within an intact HeLa cell the electrical potential measured across the mitochondrial surface is only 10–20 mV (Fig. 15.5).

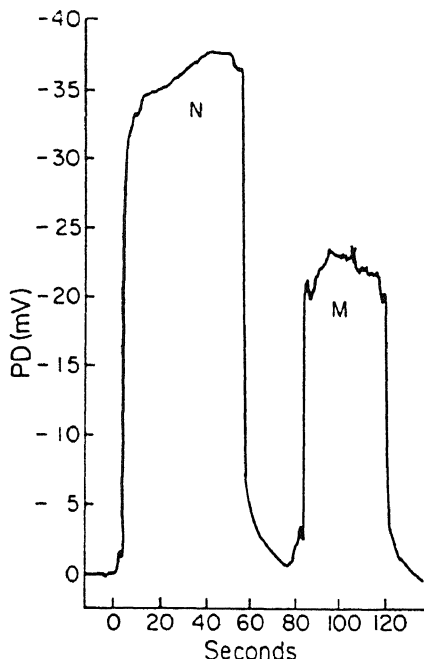


FIGURE 15.5. Trace of electrical potential difference recorded from the nucleus (N) and mitochondrion (M) by two different penetrations of the plasma membrane of an individual HeLa cell. In each case the microelectrode enters the cell, then passes into the nucleus (or mitochondrion), and finally exits from the nucleus (or mitochondrion). Cytoplasmic potential was recorded as 0. The inside of the nucleus and mitochondrion is more negative than the cytoplasm. [From Julian and Diacumakos (1977), by permission of *Journal of Cell Biology*.]

Clearly, without the required PMF of sufficient size, ATP cannot be generated by the ion gradient.

15.3.3.2. Critique of Evidence Supporting the Chemiosmotic Hypothesis

15.3.3.2a. “Membrane Potential” Determined by K^+ Gradient in Presence of Valinomycin. The “membrane potential” of the mitochondria was also estimated by Mitchell using a conventionally accepted method: by computing with the aid of the equation $\psi = (RT/F) \ln ([K^+]_{in}/[K^+]_{ex})$ [equation (2.4)] and the chemically measured K^+ concentration in the mitochondrial matrix, $[K^+]_{in}$, and the external K^+ , $[K^+]_{ex}$, after treatment with valinomycin. I have shown in Chapter 14 that this and other equations based on the membrane theory are no longer valid. In fact, the data of Maloff *et al.* (1978), to be described next, provided exquisite insight into both the basic physiological properties of the mitochondria and the cause of the conflicting conclusions regarding the size of the “membrane potential.”

Figure 15.6 reproduces an original figure of Maloff *et al.* showing the electrical potential recorded across the surface of the giant mitochondrion from the liver of mice fed cuprazone. Before application of valinomycin, there is little or no sensitivity of the potential toward external K^+ concentration. Exposure to $10^{-7} M$ valinomycin brings about a marked increase of the potential difference and K^+ sensitivity. Yet Table 15.1, also from Maloff *et al.* (1978), shows that the K^+ permeability of the mitochondria, measured as membrane resistance in increasing concentrations of external K^+ , remains completely unchanged by the application of valinomycin.

TABLE 15.1. Resistances and Membrane Potentials^{a,b}

$[K^+]_o$ (mM)	Without Valinomycin		With valinomycin	
	R (MΩ)	E (mV)	R (MΩ)	E (mV)
1	2.1 ± 0.1	16.8 ± 1.0	2.0 ± 0.1	-14.0 ± 3.0
5	2.0 ± 0.1	16.0 ± 1.0	2.0 ± 0.2	-15.0 ± 1.0
10	2.1 ± 0.0	17.0 ± 1.0	2.2 ± 0.1	-11.7 ± 1.0
20	2.3 ± 0.1	15.7 ± 0.5	2.2 ± 0.1	-5.2 ± 1.5
28	2.2 ± 0.5	16.2 ± 0.5	2.1 ± 0.0	-3.2 ± 0.5
36	2.1 ± 0.1	15.7 ± 1.0	2.0 ± 0.1	4.2 ± 2.8
50	2.1 ± 0.1	15.7 ± 0.5	2.0 ± 0.0	9.0 ± 0.8
80	2.1 ± 0.1	16.0 ± 0.8	2.0 ± 0.1	13.2 ± 1.0
100	2.0 ± 0.1	16.5 ± 0.6	2.0 ± 0.0	15.5 ± 0.8
160	2.0 ± 0.1	17.3 ± 0.5	2.0 ± 0.1	16.8 ± 0.5

^aThe mitochondria were suspended in 1–160 mM KCl, as indicated. 1 mM MES, pH 7.4. The osmotic pressure was maintained at 0.30 osmole/liter by the appropriate additions of sucrose. Four or more impalements were carried out in the absence of valinomycin. Valinomycin was added after the impalement. The values recorded correspond to potentials or resistances at the steady state (means ± SD).

^bFrom Maloff *et al.* (1978), by permission of *Journal of Cell Biology*.

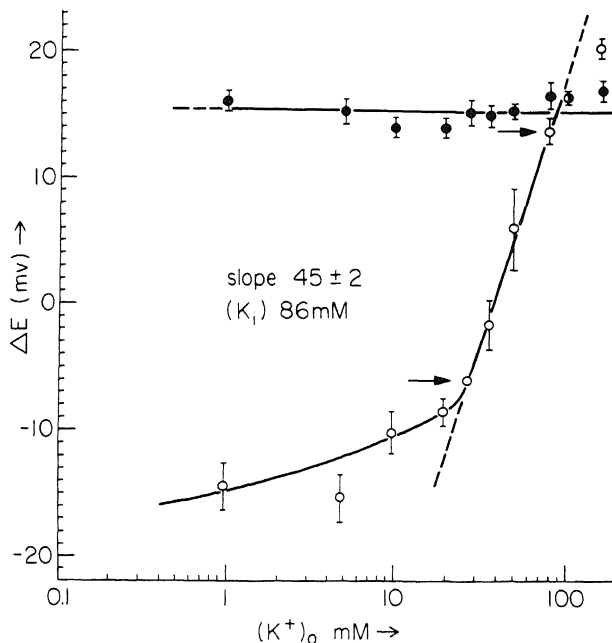


FIGURE 15.6. Dependence of potentials on the external K^+ concentration. The mitochondria were impaled in solutions containing varying concentrations of potassium methanesulfonate (1 mM MES, pH 7.4). The osmotic pressure was maintained at 0.30 osmole/liter by adding the appropriate amounts of sucrose. Each point represents the mean of at least four determinations ± SD. ●, Potentials in the absence of valinomycin; ○, potentials in the presence of valinomycin. The valinomycin was added after impalement, so that each impalement represented by an open circle corresponds to a previously obtained record represented by a closed circle. [From Maloff *et al.* (1978), by permission of *Journal of Cell Biology*.]

FIGURE 15.7. Resting electrical potential of isolated giant mitochondria from cuprazone-fed mice in the presence and absence of valinomycin. Solid lines are theoretically calculated [equation (14.8)]. The intrinsic equilibrium constant for exchange of an unidentified cation (possibly H^+) and K^+ increased by a factor of 3.3 in response to valinomycin treatment. The nearest-neighbor interaction energy, $-\gamma/2$, remained at 0.201 kcal/mole. The polarity of ψ is that used by Maloff *et al.* [Data points from Maloff *et al.* (1978); figure from Ling (1981), by permission of *Physiological Chemistry and Physics*.]

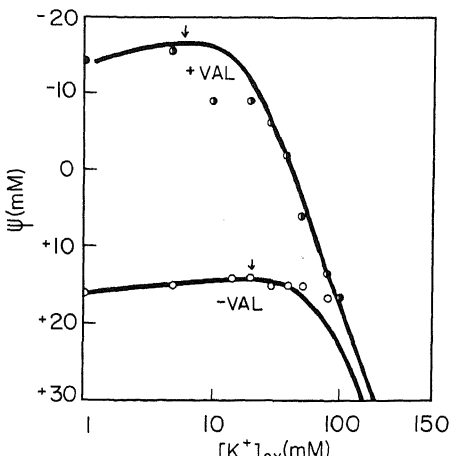


Figure 15.6 and Table 15.1 taken together quite clearly prove that the effect of valinomycin on the electrical potential is not due to its effect on K^+ permeability. Rather, the potential difference is determined by the surface fixed ionic sites [as according to the surface adsorption model of the association-induction (AI) hypothesis], and valinomycin acts as a cardinal adsorbent, pushing the *c*-value in such a direction as to enhance the preference of the surface anionic sites for K^+ over an unidentified cation X^+ . In support of this interpretation, we replot in Fig. 15.7 the data from Fig. 15.6. Here the experimental points are those of Maloff *et al.* and the solid lines are calculated according to equation (14.8). The effect of valinomycin is to increase K_{X-K}^{90} by a factor of 3.3; this qualitatively resembles the effect of adrenaline on the resting potential of frog sartorius muscle (Fig. 14.17) and that of microelectrode puncturing on the electric potential of Conger eel red cells (Fig. 14.24).

Since much higher mitochondrial potentials have been calculated from the K^+ concentration in the mitochondria than Tedeschi and others have actually measured, the apparent conflict offers still another set of data showing that the action of valinomycin in increasing K^+ inside mitochondria runs parallel to its effect on the mitochondrial surface, much as we have shown in the case of the action of ouabain on the resting potential of frog muscles, discussed in Section 14.4.2.

That valinomycin acts as a cardinal adsorbent and thus controls bulk phase intra-mitochondrial K^+ was further supported by the findings of Massari, Balboni, and Azzone (1972), which will be discussed in Section 15.5.3.1.

15.3.3.2b. ATP Synthesis by Ion Gradients. Perhaps the most convincing support for Mitchell's hypothesis was provided by evidence that H^+ and other ionic gradients across membranes can provide energy for the synthesis of the high-energy phosphate bonds of ATP. It began accumulating in 1966 with a report by Jangendorf and Uribe, who observed that isolated spinach chloroplasts could be made to synthesize ATP from ADP and P_i , without illumination or metabolism, by the simple procedure of exposing the chloroplasts first to an acid medium and then to an alkali medium. It seemed that



Tohru Kanazawa

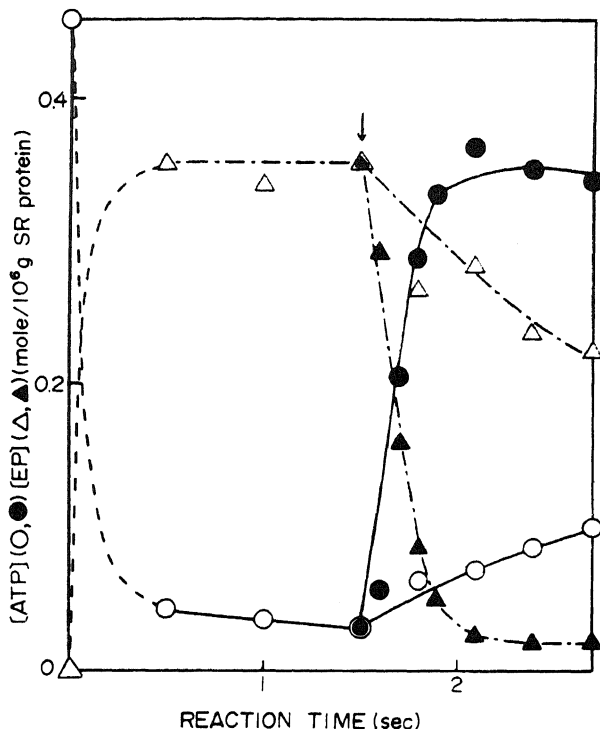
the consequent proton gradient forced an H⁺-ATPase to work backward to synthesize ATP.

Jangendorf and Uribe's work was soon followed by that of Reid *et al.* (1966) and Cockrell *et al.* (1967), who demonstrated ATP synthesis associated with ionic gradients in liver mitochondria. Similar observations were made in red blood cells (Lant *et al.*, 1970; Glynn and Lewis, 1970). Rabbit muscle sarcoplasmic reticulum (SR) vesicles pre-loaded with Ca²⁺ and incubated in the presence of ethylene glycol-bis- β -aminoethyl ether)-N,N,N',N'-tetraacetic acid showed a rapid release of Ca²⁺ accompanied by ATP synthesis (Makinose and Hasselbach, 1971; Panet and Selinger, 1972; S. Yamada and Tonomura, 1973). These findings also appeared to demonstrate that ATP was formed using energy derived from the dissipation of the ionic gradient across the membrane.

However, against this background, Tohru Kanazawa *et al.* in 1970 showed that fragments of SR could be phosphorylated with ATP and could later transfer their phosphate group to ADP to synthesize ATP (Fig. 15.8). Boyer *et al.* showed that a small amount of the phosphorylated enzyme could be formed when the SR was *not* loaded with Ca²⁺ (Boyer *et al.*, 1972; Kanazawa and Boyer, 1973). Kanazawa (1972) and Masuda and de Meis (1973) then showed that SR vesicles were phosphorylated in the absence of a Ca²⁺ concentration gradient. Kanazawa and his co-workers clearly demonstrated the formation of ATP from ADP and P_i in the absence of ion gradients, both in the step generating the phosphoenzyme and in the subsequent step generating ATP from the phosphoenzyme. Knowles and Racker (1975) confirmed Kanazawa's finding by demonstrating the synthesis of ATP from ADP and P_i in purified Ca²⁺-ATPase from the SR without a Ca²⁺ gradient. They proposed that "the energy for ATP formation is derived from the interaction of Ca²⁺ with the protein."

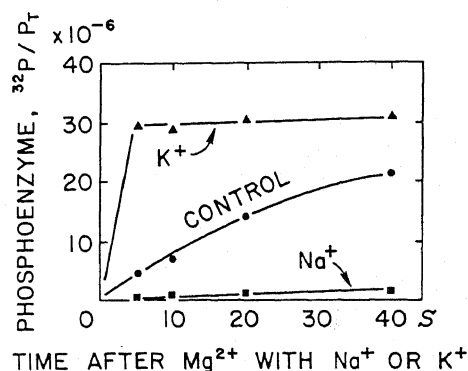
A parallel observation was made almost simultaneously by Taniguchi and Post

FIGURE 15.8. ATP (\circ , \bullet) formation from phosphorylated enzyme (EP) (\triangle , \blacktriangle) and ADP by sarcoplasmic reticulum (SR). Enzyme was phosphorylated with [32 P]-ATP in medium containing 1.1 mM MgCl₂, 55 μ M CaCl₂, 165 mM KCl, and 110 mM tris HCl at pH 8.8 and 13°C. After 1.5 sec, the phosphorylation reaction was stopped by addition (\downarrow) of solution containing EGTA and ADP at pH 8.8 (\bullet , \blacktriangle) or of EGTA alone at pH 8.8 (\circ , \triangle). At intervals after the start of the phosphorylation, SR was denatured with perchloric acid, and the concentrations of [32 P]-ATP (\bullet , \circ) and EQ (\triangle , \blacktriangle) were measured. [From Kanazawa *et al.* (1970), by permission of *Journal of Biochemistry (Tokyo)*.]



(1975, see also Post *et al.*, 1975) using purified Na⁺,K⁺-activated ATPase from guinea pig kidney (Fig. 15.9). They too demonstrated the synthesis of ATP without an ionic gradient and concluded that "binding of sodium ion to a low-affinity site on phosphoenzyme formed from inorganic phosphate is sufficient to induce a conformational change in the active center which permits transfer of the phosphate group to adenosine diphosphate." To prepare for a later discussion, it should be noted that phosphorylation by P_i of both Ca²⁺- and K⁺,Na⁺-activated ATPase requires Mg²⁺ and K⁺ (Knowles and

FIGURE 15.9. Phosphorylation from P_i of unwashed membranes from guinea pig kidney. The membranes were incubated with 1 mM 32 P_i for 10 sec before zero time. [Mg²⁺] = 2 mM. [Na⁺] = [K⁺] = 16 mM. In the control Na⁺ and K⁺ were omitted. "P_T" refers to total phosphorus as an estimate of the amount of membrane in the mixture. Maximal phosphorylation was not estimated but was about 100–200 pmoles 32 P/ μ mole P_T, as judged from other experiments. The level of phosphoenzyme in the presence of K⁺ was not much affected by washing the membranes. [From Post *et al.* (1975), by permission of *Journal of Supramolecular Structure*.]





Efraim Racker

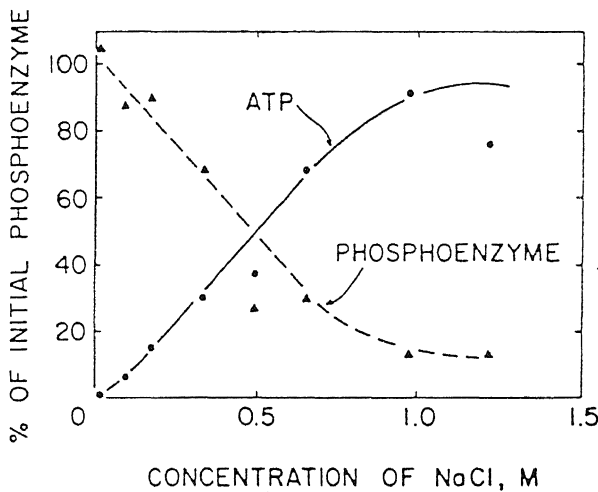


FIGURE 15.10. Synthesis of ATP from K^+ -sensitive phosphoenzyme. In a volume of 0.25 ml, 3.9 mg of washed membrane protein was incubated with 5 μ moles of imidazole glycylglycine, 10 nmoles of $(Tris)_3CDTA$, and 0.5 μ mole of $^{32}P_i$ at pH 7.5 and 0°C. To start phosphorylation 0.25 μ moles of $MgCl_2$ and 8 μ moles of NaCl were added in 0.05 ml. To start ATP synthesis 4 sec later, 10 μ moles of $(Tris)_3CDTA$ and 0.5 μ mole of ADP with various quantities of NaCl were added in 0.2 ml to produce the final concentrations indicated on the horizontal axes. The reaction was stopped with acid 2 sec later to obtain the data shown. Control points were also taken 80 sec later at concentrations of Na^+ at or above 176 mM. At this time no phosphoenzyme remained and the amount of $[^{32}P]$ -ATP was between 51% and 95% on the initial amount of phosphoenzyme, which was 212 pmoles. The yield of ATP increased progressively with the concentration of Na^+ . [From Post *et al.* (1975), by permission of *Journal of Supramolecular Structure*.]

Racker, 1975; Post *et al.*, 1975). On the other hand, ATP synthesis from ADP and both phosphorylated enzymes is inhibited by Mg^{2+} but is stimulated by Ca^{2+} in the Ca^{2+} -activated ATPase and by Na^+ in the Na^+, K^+ -activated ATPase (Fig. 15.10).

These findings cast a new and revolutionary light on the subject of ATP synthesis. *The emphasis has shifted from ionic or "osmotic" gradients, a subject central to the membrane theory, to ion adsorption on proteins, a subject central to the AI hypothesis.* Indeed, they lead to a new and basic question regarding mitochondrial oxidative phosphorylation: How does a mitochondrion, without the aid of a biochemist, carry out a succession of two-step manipulations equivalent to first exposing the ATPase to Mg^{2+} (or K^+) and P_i , thus producing the phosphoenzyme, and next removing the Mg^{2+} (or K^+) already present and replacing it with a different cation, Ca^{2+} (or Na^+)? Finally, we must ask: How does the adsorption of Ca^{2+} or Na^+ create the phosphate transfer from the ATPase to ADP to synthesize ATP?

15.4. A Tentative Model of the Inductive–Associative Coupling Mechanism for Electron Transport and Oxidative Phosphorylation

15.4.1. The Coupling Mechanism

From the work described in the last section, ATP formation from P_i and ADP is shown in model systems to involve two steps: (1) phosphorylation of the ATPase by P_i is achieved by interaction with Mg^{2+} and/or K^+ and (2) phosphorylation of ADP by the phosphoenzyme is achieved by interaction with Ca^{2+} and/or Na^+ . To initiate ATP production, the first step consists of equilibrating the enzyme and P_i in a Mg^{2+} - and/or K^+ -containing medium, followed by dialyzing or otherwise removing the Mg^{2+} and/or K^+ and transferring the phosphoenzyme to the second ionic environment containing Ca^{2+} and/or Na^+ . In short, production of ATP involves a two-step process, which *in vitro* consists of a sequential exposure to two different ionic environments. The simplest explanation of the underlying mechanism is that in the first environment the ATPase adsorbs Mg^{2+} and/or K^+ , and in the second environment the enzyme shifts to adsorb Ca^{2+} and/or Na^+ . Since there are no living beings in the cells to manipulate the ionic environment of the mitochondria, and since mitochondria do not migrate from one ionic environment to another, clearly a different mechanism must exist to bring about the change from adsorption of Mg^{2+} and/or K^+ to adsorption of Ca^{2+} and/or Na^+ , in order to bring about the phosphorylation of ADP and the production of ATP.

Postulate 1. The generation of ATP involves two discrete steps: Phosphorylation of ATPase by P_i (to form EP) is promoted by adsorption of Mg^{2+} and/or K^+ on the enzyme and phosphorylation of ADP is promoted by the phosphoenzyme (EP) when the enzyme adsorbs Ca^{2+} and/or Na^+ .

Postulate 2. Since free Mg^{2+} , Ca^{2+} , K^+ , and Na^+ are available and their concentrations more or less constant in the natural environment of the mitochondria, a shift in adsorption from Mg^{2+} and/or K^+ to Ca^{2+} and/or Na^+ is brought about by an auto-cooperative shift of the *c*-value ensemble and a consequent change of the relative pref-

erence of the adsorption sites for Mg^{2+} over Ca^{2+} or for K^+ over Na^+ . With reference to equation (7.19), such a change in relative preference is achieved by a change in ξ , and the change in ξ is not brought about by altering the ratio of the concentrations of the two alternative ionic species (K^+ versus Na^+ , Ca^{2+} versus Mg^{2+}) but by altering $K_{j \rightarrow i}^{00}$, the intrinsic equilibrium constant for the exchange of the j th (Mg^{2+} or K^+) for the i th (Ca^{2+} or Na^+) ion.

Postulate 3. The respiratory chain units, which are tightly linked in structure, are also cooperatively linked in function by the operation of the indirect *F*-effect (an inductive effect) through the ATPase at each coupling site. As discussed earlier, autocooperative linkage can occur among sites on the same protein chain or among closely associated sites on different protein chains (e.g., cooperative interaction among the four subunits of a hemoglobin molecule). This postulate offers the propagated inductive effect as the mechanism of coupling between the respiratory chain centers and the ATPase.

Postulate 4. The autocooperative linkage between the respiratory chain center and the ATPase allows the *c*-value ensemble of the ATPase to be controlled by the electronic state of the respiratory chain center. When the respiratory chain center is in a reduced state, the *c*-value ensemble of the ATPase has a discretely different set of values than when the respiratory chain center is in an oxidized state. At one set of *c*-values, Mg^{2+} and/or K^+ would be preferentially adsorbed; at the other set, Ca^{2+} and/or Na^+ would be adsorbed. The associated pyridine nucleotide, the coenzyme or ubiquinone, or the iron in the iron-sulfur proteins and in the cytochromes acts as cardinal adsorbents on the cooperatively linked ATPase, much as oxygenation and deoxygenation of the heme iron in a hemoglobin molecule can allosterically affect the pK_a value of distant anionic groups. Each cycle of oxidation and reduction of the respiratory chain center leads to a cyclic change in the *c*-values of the appropriate sites on the ATPase, triggering the generation of one ATP molecule.

In summary, our basic theme is that the coupling between electron transport and phosphorylation is through cooperative shifts mediated by the inductive effect between two different states of the ATPase system, permitting sequential formation of EP and then of ATP from ADP and EP. Selective ionic adsorption plays a key role in this mechanism. This thesis is based on (1) the universality of the inductive effect in chemistry, (2) the fact that cellular cations exist primarily in an adsorbed state, and (3) the fact that selective cation adsorption on proteins in living cells is controlled by cardinal adsorbents. Additional support can be found in the behavior of several other model systems (see Section 15.4.2).

This model represents a special aspect of the more basic concept of the living cell in the AI hypothesis. As such, it has little in common with the chemiosmotic coupling mechanisms that are based entirely on the lipid-membrane pump theory. However, the present model—at least in formal terms—bears some resemblance to Slater's chemical intermediate hypothesis (Slater, 1953) and to the conformation hypothesis of Boyer (1965) and of Green (Blondin and Green, 1967). Kell's review (1979) demonstrates an open-mindedness regarding new and different ideas and holds promise of more unity and coherence in this aspect of cell physiology in time to come.

15.4.2. Comparison with Model Systems

The usefulness of the present model will be decided by future experimental studies. However, present knowledge allows us at least to determine whether oxidation and reduction of prosthetic groups can influence selective ionic adsorption, since it has already been established that such adsorption leads to ATP synthesis (Figs. 15.8–15.10). This mechanism applies especially to the two heme proteins, hemoglobin and cytochrome *c*. Unlike in cytochrome *c*, the oxygenation–deoxygenation cycle of hemoglobin does not involve a transition between Fe^{3+} and Fe^{2+} . However, the oxidation–reduction equilibria of hemoglobin (Fe^{2+}) and methemoglobin (Fe^{3+}) bear a close parallel to oxygenation–deoxygenation equilibria (Rossi–Fanelli *et al.*, 1964, p. 188).

15.4.2.1. Heme–Heme Interaction and the Bohr Effect

In his review on hemoglobin in 1979, Perutz, while reiterating his mechanical interpretation of heme–heme interaction, nevertheless stated that the regulation of the oxygen affinity of heme by the structure of globin could in principle be accomplished by inductive effects (Perutz, 1979, p. 383). Much of Perutz's argument in favor of the mechanical model was based on studies of hemoglobin crystals and evidence that structures similar to those seen in the crystalline state also are maintained in solution. In contrast, in the model presented here, the relative significance of the data is reversed: The long-range effect is modulated primarily through an inductive mechanism, with mechanical steric factors playing an auxiliary role. The following observations support this view:

1. In solution, hemoglobin does not maintain the kind of structural rigidity needed for a purely mechanical interpretation of heme–heme and other interactions. The ease of oxygen uptake and release by hemoglobin in solution and in the erythrocyte is well known. In sharp contrast, the behavior of hemoglobin crystals is entirely different. When deoxyhemoglobin crystals combine with oxygen, the protein crystals break up (Haurowitz, 1938), and crystals of oxyhemoglobin firmly retain oxygen even when they are in a low-oxygen environment (Wyman, 1964, p. 280).
2. The mechanical feature of a rigid (T) structure in the deoxygenated state and a relaxed (R) structure in the oxygenated state is not compatible with the lower entropy associated with the oxygenated state compared to the deoxygenated state (Manwell, 1958).
3. A rigid, impervious deoxygenated state of hemoglobin does not readily fit the observed binding of as many as ten molecules of bromthymol blue to each chain of the deoxygenated, but not the oxygenated, state (Antonini *et al.*, 1963).
4. The reactivity of sulphydryl groups is strongly influenced by the oxygenated or deoxygenated state of hemoglobin: They are much more reactive in the oxygenated state. A simple mechanical steric hindrance cannot readily explain why only oxygenated hemoglobin reacts with mercuric benzoate while neither oxygenated nor deoxygenated hemoglobin reacts with iodoacetate (Benesch and Benesch, 1962). A combination of steric hindrance and differences in the oxi-

dation-reduction potentials of these reagents seems to provide a more complete explanation.

15.4.2.2. Autocooperative Ion Adsorption Shifts Controlled by Oxidation-Reduction

It would seem that cooperative transitions between the oxygenated and deoxygenated states of hemoglobin mediated primarily by the inductive effect are capable of reconciling findings that cannot be readily explained by mechanical steric interpretation alone. Oxygenation and deoxygenation, like oxidation and reduction, can indeed control the transition between the two cooperative states, and in each state many if not all of the functional groups have different properties. Next we must ask: Do these transitions also involve shifts in the states of ion binding? In this case, we can cite observations in both cytochrome *c* and hemoglobin.

15.4.2.2a. *Cytochrome c*. Margoliash *et al.* (1970) and Margolit and Schejter (1974) demonstrated that ferrocyanochrome binds only cations, including Mg^{2+} , while ferricyanochrome binds only anions, including Cl^- , P_i , and ADP. Clearly, oxidation-reduction changes can alter ion binding on these proteins in an all-or-none manner.

15.4.2.2b. *Hemoglobin*. Although hemoglobin is not a part of the electron transport system, a similar behavior makes it a useful model of the cytochromes. It has long been known that KCl and NaCl have different effects on the *in vitro* oxygen dissociation constant of hemoglobin (R. Hill and Wolvekamp, 1936; Rossi-Fanelli *et al.*, 1959). Tosteson and co-workers (Tosteson *et al.*, 1952; Tosteson, 1955) found that, in the red cells of patients with sickle-cell anemia, deoxygenation produces not only sickling but also a profound change in the intracellular levels of K^+ and Na^+ . Since sickle-cell anemia results from a defect of only one gene and one faulty amino acid residue in the β -chain of hemoglobin, these findings suggest that hemoglobin carries sites which, under physiological conditions, adsorb K^+ selectively and that this faulty amino acid in the β -chain permits deoxygenation of the heme group to alter the *c*-value of these sites so that they assume a different value at which the preference of K^+ over Na^+ is reduced.

Oxygenation, like oxidation-reduction, involves a strong electrostatic effect and is likely to produce similar short- and long-range inductive effects. With this parallel in mind, the familiar Bohr effect (dependency of oxygen affinity of hemoglobin on pH) and reverse Bohr effect are outstanding examples that reactions of prosthetic groups and the pK_a value (and hence the *c*-value) of acidic groups are mutually dependent, though spatially separate. In the case of lamprey hemoglobin (Antonini *et al.*, 1964), the large and steep Bohr effect is compatible with autocooperative interaction, even among the anionic groups, most likely β - and γ -carboxyl, in a manner analogous to that noted previously in the interaction of dodecyltrimethylammonium bromide with bovine serum albumin (Fig. 7.20).

15.4.2.2c. *Oxidation-Reduction State of Pyridine Nucleotides in Mitochondria*. Lehninger *et al.* (1978) provided the most direct evidence that the oxidation-reduction state of the mitochondrial electron transport system can determine cooperative

adsorption of cations essential for ATP synthesis in mitochondria of rat liver and heart as well as of Ehrlich ascites cells. They showed that mitochondria take up Ca^{2+} and retain it as long as the pyridine nucleotide is in the reduced state; when the nucleotide is oxidized, Ca^{2+} is promptly released.

15.5. New Interpretations of Observations in Mitochondrial Physiology

15.5.1. Swelling and Shrinkage

15.5.1.1. Role of ATP Concentration

To preserve the normal elongated shape of isolated mitochondria, they must be suspended in a sucrose solution of osmotic strength that is more than three times isotonic (i.e., 0.88 M) (Hogeboom *et al.*, 1948). The standard medium for isolating mitochondria, 0.25 M sucrose, was chosen as a compromise between convenience and preservation. Brenner-Holzach and Raaflaub (1954) noted that spontaneous swelling of mitochondria occurs when their ATP content falls below a certain level. Their findings are in harmony with the findings of Nakao *et al.* (1961) on the dependence of red cell shape on ATP, discussed in Section 13.6. In both isolated mitochondria and erythrocytes it is the presence of a certain level of ATP *per se* that determines normal mitochondrial or cellular shape and size. That ATP maintains the shape and structure of cells and their organelles by its adsorption on cell proteins was first suggested by Ling in 1952.

Pollak (1975) equilibrated mitochondria from the livers of fetal and adult rats in sucrose ranging from 50 to 400 mM and measured their size by recording optical extinction at a wavelength of 546 nm. Mitochondria from 5-day prenatal rats showed no change in volume throughout the entire range of sucrose concentrations. Mitochondria from adult rats showed pronounced shrinkage (Fig. 15.11). The insensitivity of the 5-day prenatal mitochondria to a tenfold increase in external sucrose concentration suggests that they are permeable to sucrose and that they do not exclude sucrose. Otherwise, they would have shrunken.

Nakazawa *et al.* (1973) found that the ATP and ADP contents of rat liver mitochondria were very low during gestation but steadily increased during growth (Fig. 15.12). Addition of ATP to the mitochondrial suspension of fetal rat liver greatly improved its respiratory control, and the addition of ATP and Mg^{2+} enabled respiring fetal mitochondria to release H^+ in response to the addition of Ca^{2+} . Thus fetal mitochondria could be induced to behave like adult mitochondria.

Pollak (1977) later found that both the shrinkage of fetal liver mitochondria and the enhancement of respiratory control by ATP depend on the presence of ATP and its interaction with the mitochondrial inner membrane but do not require hydrolysis of ATP. Similarly Stoner and Sirak (1973) found that contraction of bovine heart mitochondria in the presence of ATP, ADP, or pyrophosphate does not require their hydrolysis, since they are at least as active in the presence of oligomycin or oligomycin and cyanide. Stoner and Sirak also concluded that contraction of the inner membrane is a result of the binding of adenine nucleotide to it. These independent findings support the concept that ATP functions as a cardinal adsorbent (Chapter 10).

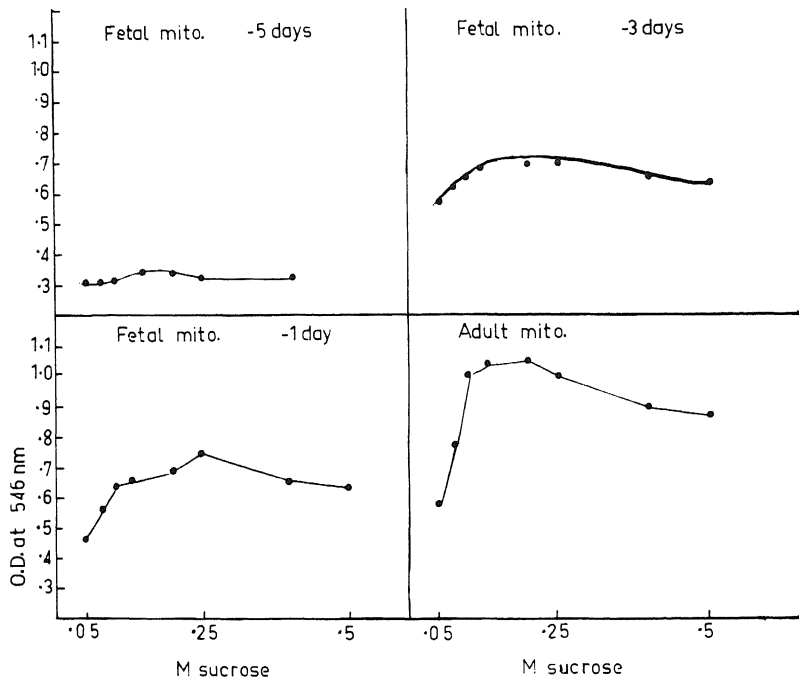


FIGURE 15.11. Comparison of the osmotic properties of fetal and adult rat liver mitochondria in a series of sucrose solutions. Increase in optical extinction, E_{546} , means shrinkage of mitochondria. The sucrose solutions varied between 0.05 and 0.5 M. To 2.9 ml of the sucrose solutions at 30°C, 0.1 ml of mitochondria was added. Mitochondria for adult, 1-day prenatal, and 3-day prenatal rats were added at a concentration of 1 mg of protein/0.1 ml; the mitochondria from 5-day prenatal rats were at a concentration of 0.5 mg/0.1 ml. Changes in extinction were observed at 546 nm at 30°C with a recording spectrophotometer until constant readings were obtained. [From Pollak (1975), by permission of *Biochemical Journal*.]

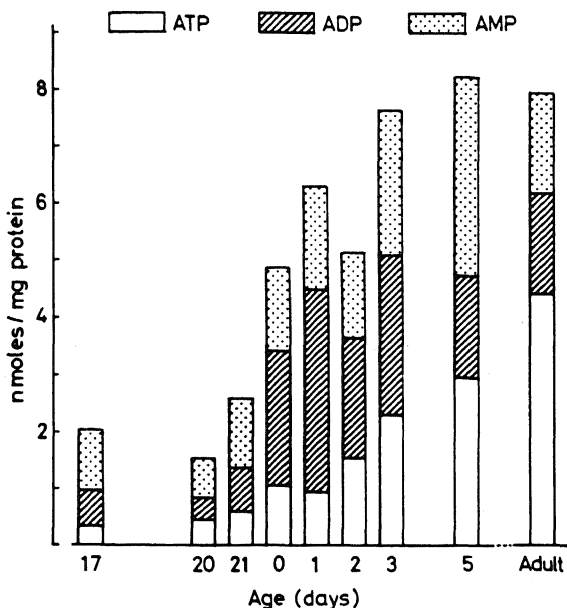


FIGURE 15.12. Adenine nucleoside contents in rat liver mitochondria during development. Each value was the average of three to six experiments. [From Nakazawa *et al.* (1973), by permission of *Journal of Biochemistry (Tokyo)*.]

In adult resting cells, ATP maintains certain matrix, as well as membrane, proteins in an extended, water-polarizing conformation. Loss of ATP from the cell causes swelling; gain of ATP reverses it (Chapter 13). I suggest that this effect of ATP occurs in the mitochondrion as well.

15.5.1.2. Role of Mg^{2+} and Ca^{2+}

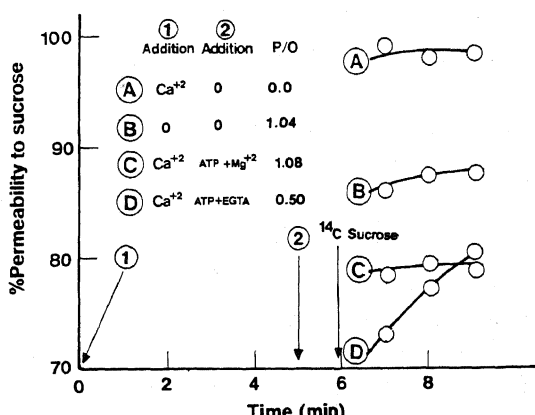
ATP may not be the only cardinal adsorbent controlling the polarization of water. For example Mg^{2+} also may be a cardinal adsorbent, working synergistically with ATP. If Mg^{2+} is competitively displaced from its site by Ca^{2+} , the effect of Mg^{2+} plus ATP on the structure of water may be reversed. Indeed, D. R. Hunter *et al.* (1976) found that the swelling of mitochondria exposed to hypotonic solutions does not cause uncoupling of oxidative respiration. From this they concluded that "our results on hypotonically swollen mitochondria dismiss the long-held view that swollen mitochondria must be damaged and uncoupled...." This swelling is simple osmotic swelling (Type I in Section 13.7).

F. E. Hunter and Ford (1955) had previously noted that simple osmotic swelling did not interrupt normal oxidative phosphorylation. In the context of the AI hypothesis, this would suggest that no cooperative changes of the *c*-value ensemble or of the state of water occurred. Hunter and Ford found that Ca^{2+} caused an increase of the space available to sucrose from about 85% to nearly 100% (Fig. 15.13). This increase occurred for choline and glucose as well, and this effect is promptly reversed by the addition of ATP and Mg^{2+} . This suggests that the addition of Ca^{2+} , like the depletion of ATP, causes swelling because water is depolarized (Type IIB in Section 13.7); ATP and Mg^{2+} induce long-range polarization of water to restore low *q*-values for sucrose and for other normally excluded solutes, and hence cause shrinkage to restore "normal" volume.

15.5.1.3. Passive Osmotic Swelling

Brierly *et al.* (1970) found that isolated heart mitochondria will swell in the presence of both a permeant anion and a permeant cation even if substrate or ATP is absent.

FIGURE 15.13. Restoration of coupling and membrane impermeability. After a 5-min incubation in the presence of 150 nmoles of calcium/mg of protein the additions listed were made. After a further 1-min incubation the [^{14}C]sucrose was added. Aliquots were also removed at 10 min for measurement of P/O ratios in a medium lacking added Mg^{2+} using durohydroquinone as substrate. Final concentrations of additions were: ATP, 6 mM; $MgCl_2$, 6 mM; EGTA, 3 mM. [From D. R. Hunter *et al.* (1976), by permission of *Journal of Biological Chemistry*.]



In the AI hypothesis, the requirement for uptake of both cation and anion indicates that they are forcing open salt linkages between macromolecules, and this induces swelling of the type labeled IIA in Section 13.7 [see equation (13.3)].

That mitochondria swell in KNO_3 or NaNO_3 , but not in KCl or NaCl , suggests that NO_3^- is more strongly adsorbed than Cl^- (see Fig. 13.8). Mitochondria swell in 100 mM KNO_3 or NaNO_3 at pH 8, but not at neutral pH (Brierly and Jurkowitz, 1976); this also agrees with the present interpretation. Salt linkages are formed between β - and γ -carboxyl groups on the one hand and α -amino, histidine, ϵ -amino and guanidyl groups on the other. An increase in pH enhances the ability of OH^- to disrupt the salt linkages.

15.5.2. "Transport" of ATP

In the AI hypothesis there are two modes of entry of a solute into the cell: via water polarized by proteins and via fixed ionic and other binding sites. The latter provide greater specificity in permeability to ions and other solutes. To illustrate the usefulness of this model, I shall briefly discuss a number of fascinating findings of Sandor and Pollak.

Sandor and Pollak (1976) showed that the initial rate of entry and the level of ^{14}C -labeled ATP in adult liver mitochondria are inhibited by atractyloside. In contrast, the initial entry rate of ATP in fetal mitochondria is faster and is indifferent to atractyloside. The uptake of ^{14}C -labeled ATP reached a peak at about 1 min and then began to decline so that it fell to nearly half of its peak level at the end of 5 min. While the accumulated level of [^{14}C]-ATP was declining it developed a responsiveness to atractyloside (Fig. 15.14).

Sandor and Pollak suggested that rapid entry of ATP into the highly permeable fetal mitochondrion was followed by its interaction with the inner mitochondrial membrane "to transform its configuration and permeability characteristics, . . . resulting in a diminished matrix space so that labeled ATP may be regarded as literally squeezed out together with water as the matrix becomes very condensed. . . ." This suggestion agrees in essence with the interpretation of these data by the AI hypothesis. The fetal mitochondrion, with its water relatively depolarized, readily takes up ATP (and sucrose, Figure 15.11). Sandor and Pollak's interesting experiment also clearly showed that the ability of atractyloside to reduce the level of ^{14}C -labeled ATP 2 min after exposure to nonlabeled ATP is dependent on prior interaction of the fetal mitochondrion with ATP, suggesting that the maintenance of the polarized water surface barrier, as well as the presence of specific ATP binding sites, requires that certain cardinal sites be occupied by ATP.

In this context, it is worthwhile to recall some earlier observations. Lehninger *et al.* (1957) found that ATP-induced contraction of mitochondria swollen by thyroxine is most effective in the presence of KCl . M. G. McFarlane and Spencer (1953) and Gamble (1957) found that both ATP and K^+ are essential for the prevention of swelling. These findings agree with the simple theoretical model shown in Fig. 11.3 and first presented 15 years ago (Ling, 1969a), in which adsorption of K^+ on β - and γ -carboxyl groups parallels the long-range polarization of water by the extended protein backbone.

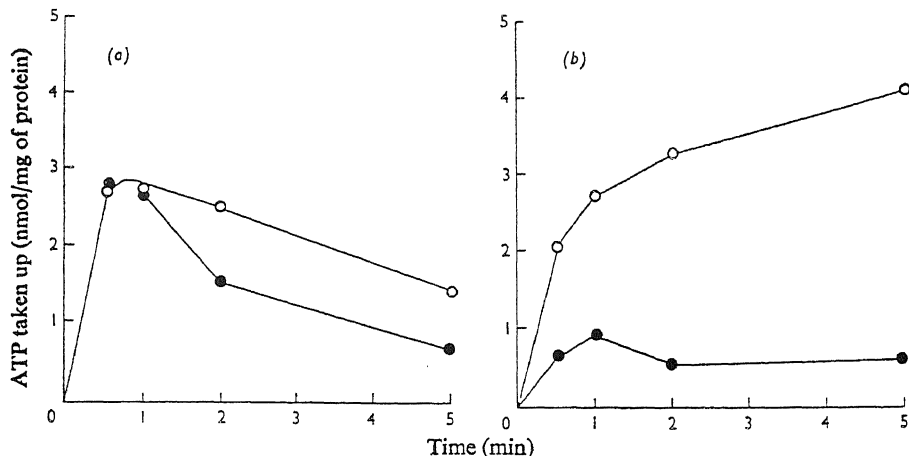


FIGURE 15.14. Uptake of [¹⁴C]-ATP by (a) fetal rat liver mitochondria and (b) adult rat liver mitochondria. O, Control; ●, potassium atracyloside (50 nM) present. Total incubation volume was 1.0 ml, containing 90 mM KCl, 15 mM sodium phosphate buffer, pH 7.5, 2 mM MgCl₂, and 0.33 μCi of [¹⁴C]-ATP/μmole. Reaction was started by adding 0.8 mg of mitochondrial protein. The temperature was 1°C. Reaction was stopped by a rapid filtration method on a 0.8-μm Millipore filter. [From Sandor and Pollak (1976), by permission of *Biochemical Society Transactions*.]

In fact, in a study of intact frog muscle cells, Ling and Ochsenfeld (1973b) showed a correlation between selective K⁺ adsorption and the degree of exclusion of sucrose and Na⁺ from cell water (Fig. 11.39).

15.5.3. Uncouplers, Ionophores, Ca²⁺, Mg²⁺, ATP, and Other Cardinal Adsorbents

Many different chemical agents react with different components of the mitochondrion to produce essentially the same physiological effect. This was noted first by Hunter and Ford in 1955, and 20 years later Siliprandi *et al.* (1975a) noted that inorganic phosphate, the sulfhydryl-oxidizing agent diamide, and the divalent ion "ionophore" A23187 exert almost identical effects. On the other hand, certain agents may produce different effects at different concentrations or under different conditions. For example, oligomycin, usually an inhibitor of oxidative phosphorylation, can at certain concentrations actually stimulate oxidative phosphorylation (C. P. Lee and Ernster, 1968). Valinomycin, a "K⁺ ionophore" that uncouples oxidative phosphorylation in the presence of K⁺, also may stimulate oxidative phosphorylation (Höfer and Pressman, 1966). In the total absence of K⁺ or any other ion, valinomycin inhibits electron transport in isolated chloroplasts (Voegeli *et al.*, 1977; Sokolove and Marsho, 1979). Valinomycin, which does not act as a Ca²⁺ ionophore in experimental phospholipid membranes, does promote the accumulation of Ca²⁺ in mitochondria, in competition with K⁺ (C. S. Rossi *et al.*, 1967) (Fig. 15.15). Although a K⁺ ionophore in the presence of K⁺, valinomycin does not increase K⁺ conductance in isolated liver mitochondria (Maloff *et al.*, 1978) (Table 15.1).

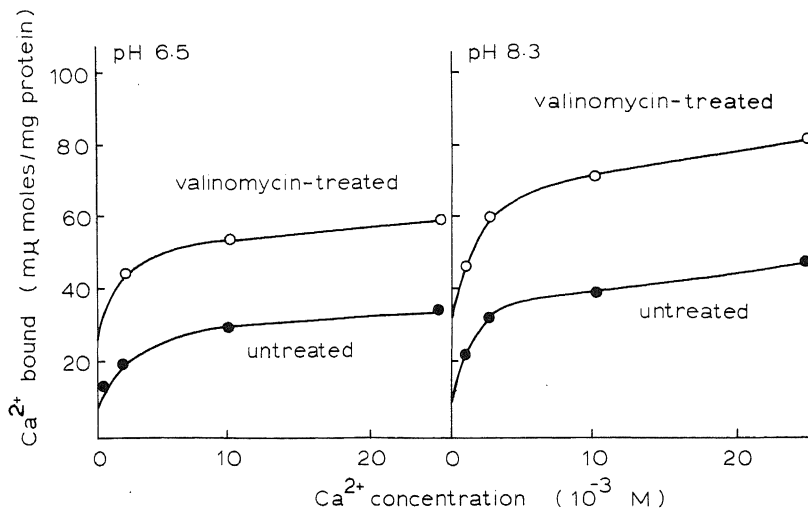


FIGURE 15.15. Binding of Ca^{2+} in valinomycin-treated mitochondria in sucrose media. Mitochondrial protein (4.5 mg) treated with valinomycin and antimycin was incubated for 30 min at 0° in a medium containing 25 M Tris-HCl, 0.25 M sucrose, and various CaCl_2 concentrations, as indicated in the figure. Untreated mitochondria were incubated for 1 min in the same medium in the presence of 2 μg of antimycin. For treatment with valinomycin the mitochondria were incubated at pH 6.5 in 0.25 M sucrose in the presence of valinomycin and antimycin. The mitochondrial suspension was diluted with 0.25 M sucrose, centrifuged, and resuspended in 0.25 M sucrose [From C. S. Rossi *et al.* (1967), by permission of *Journal of Biological Chemistry*.]

The prevailing view in the field of mitochondrial physiology has so far been based on Overton's lipoidal theory of the cell membrane, and the inner membrane is thought to be primarily a continuous sheet of phospholipid serving as a selective, physiological permeability barrier. Let us, however, review these data using the totally different basic assumptions of the AI hypothesis.

15.5.3.1. The Effect of Valinomycin on Mitochondrial K^+ Accumulation

In the AI hypothesis, as described fully in Chapter 11, solutes in the cell tend to fall into two fractions. One is dissolved in cell water in the free state, and its equilibrium level is, as a rule, less than or equal to the concentration of the solute in the external medium, according to the ratio q . The other exists in one (or more) adsorbed states, its level described primarily by the parameter $\xi = ([p_i]_{\text{ex}}/[p_j]_{\text{ex}}) \cdot K_{j \rightarrow i}^{00}$, so that the level of adsorbed i th solute, $[p_i]_{\text{ad}}$, depends on (1) the ratio of its concentration to that of the major competing ion, p_j , in the external medium, and (2) $K_{j \rightarrow i}^{00}$, the intrinsic equilibrium constant for the i -to- j exchange adsorption.

Extending these concepts, I suggest that virtually all K^+ in isolated mitochondria is adsorbed on the β - and γ -carboxyl groups of mitochondrial proteins. Other cations may compete for these sites, and these include H^+ , Rb^+ , Cs^+ , Li^+ , Ca^{2+} , and Mg^{2+} , as well as fixed cations that form salt linkages. Whether the sites adsorb K^+ or some other

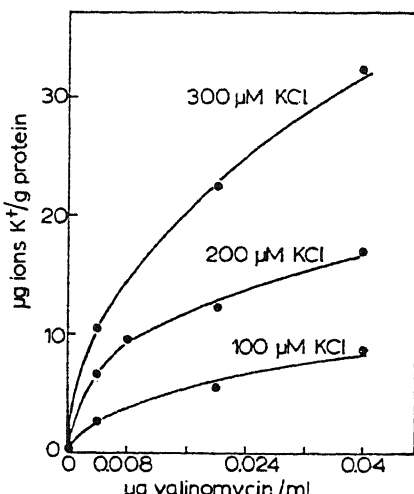


FIGURE 15.16. K^+ uptake at various valinomycin concentrations. [From Massari *et al.* (1972), by permission of *Biochimica et Biophysica Acta*.]

ion depends on their *c*-value and on the proximity of these sites to one another (Ling *et al.*, 1979). The “ionophore” valinomycin, which causes mitochondria to take up K^+ (C. Moore and Pressman, 1964), may function as a cardinal adsorbent and affect the *c*-value of cation-adsorbing sites.

The concept that adsorption is the basis of selective K^+ accumulation was considered by Lardy (1951), Berger (1957), Gamble (1957), Judah *et al.* (1965), C. S. Rossi *et al.* (1967), and Cereijo-Santalo (1970). It would seem, however, that the majority of investigators continue to believe that K^+ , once inside the mitochondrial inner membrane, must be in the free state or else the mitochondrion would suffer osmotic imbalance and shrink. In the AI hypothesis, the loss of osmotic activity owing to adsorption of K^+ is compensated by the long-range polarization of water in multilayers (Section 13.2).

In the chemiosmotic hypothesis, valinomycin acts as an ionophore within the membrane; hence, valinomycin can manipulate the rate of K^+ entry but not the final steady-state level of K^+ , since the inner membrane by itself is considered in this hypothesis to be K^+ -impermeable. In the AI model, the inner membrane is permeable to K^+ at all times, and valinomycin modulates the equilibrium level of mitochondrial K^+ in a quantitative manner in much the same way that Ca^{2+} controls the level of K^+ in intact muscle and liver cells (Figs. 11.37 and 11.38). In 1972, Massari *et al.* showed that steady levels of K^+ varied with changes in the concentration of valinomycin (Fig. 15.16). Clearly, valinomycin does not simply open a “closed door” to K^+ , but affects the degree of accumulation of K^+ as well as of Ca^{2+} (Fig. 15.15).

A third alternative interpretation is that valinomycin affects the steady-state level of K^+ by affecting the operation of a K^+ pump. However, I have pointed out in Sections 4.3 and 5.2 that, of all the pumps postulated for cells, the Na^+-K^+ pump alone in muscle cells, under controlled conditions, would consume at least 15–30 times more energy than the total energy available to the whole cell (Table 5.2). To “install” still more pumps to control ion flux across the mitochondrial membranes—whose total surface area in some cells is 20 times greater than that of the plasma membrane (Lehninger, 1964, p. 30)—would only further confound the energy problem.

An interesting finding by Griffith (1976) suggests that valinomycin interacts with mitochondria by combining with cardinal sites. He found that the mitochondria of certain mutant yeasts are resistant to the effect of valinomycin on K^+ uptake. Such a mutation usually is the result of an error in DNA replication, and since DNA specifies protein sequence, a part of the mitochondrial protein must be faulty. This faulty or missing part may contain the cardinal site that reacts with valinomycin. When C. Moore and Pressman (1964) first reported the effect of valinomycin on mitochondria, they concluded that "the triggering of K^+ transport by valinomycin implies the existence of a mitochondrial receptor site...." In the AI hypothesis, such a receptor site would be called a cardinal site, and it would control K^+ distribution, not via a K^+ pump but by altering the affinity of the protein *regular sites* for adsorption of K^+ . The evidence in favor of this argument was discussed in Chapter 8.

15.5.3.2. *The Effect of Ionophores, Uncouplers, and Other Cardinal Adsorbents on Mitochondrial Ion Distribution*

In the AI hypothesis, the endless variety of biologically active agents resembles that found in Paul Ehrlich's lock and key analogy regarding the action of drugs. However, though greatly varied in shape, the keys can do only one of two things: open a door or close a door. Cardinal adsorbents also can do only one of two things (if one ignores those without any effect): donate electrons or withdraw electrons. Hence, these agents are divided into electron-donating cardinal adsorbents (EDC) or electron-withdrawing cardinal adsorbents (EWC). Steric factors and the multiplicity of attachment sites further influence the specificity of cardinal adsorbents. Another variable, of course, is the intensity of the effect of the EDC or EWC. Thus, although the basic effect is very simple, the observed manifestation of it may be extremely complex. A strong EDC in a cooperatively linked site tends to increase electron density (i.e., increase the c -values of all the negatively charged sites) and positive charge density (or the c' -values of all the positively charged sites). Thus, as a first simple assumption, strong EDCs increase, while EWCs decrease, the c - and c' -values of many of the sites in the proteins of the mitochondria. However, there are pitfalls in the application of this simple concept. Several examples are cited:

1. An EDC displacing a stronger EDC may create an electron-withdrawing effect; conversely, an EWC displacing a stronger EWC may create an electron-donating effect.
2. A strong EDC reacting with a cardinal site adjacent to an anionic site that is the first member of an anionic-cationic sequence may increase the c -value of all the anionic sites and the c' -value of all the cationic sites. On the other hand, if the cardinal site is flanked by a cationic site which in turn is followed by a sequence of anionic and cationic sites, the result will be just the opposite: a decrease of the c -value of the anionic sites and of the c' -value of the cationic sites. Conversely, a strong EWC in the latter system will increase the c - and c' -values, as illustrated in Fig. 7.13.
3. Interaction between two cardinal sites may produce complex effects, including maxima and minima, as illustrated in the theoretical curves in Figs. 7.8–7.11.

4. Changes in the c -value of adsorption sites can only be assessed by changes occurring in the steady levels of ions accumulated in the mitochondria, and not necessarily in the rates of ion exchange. Unfortunately, measurements of steady levels are relatively rare, and often these values must be approximated. Because of this ambiguity, changes occurring in bulk phase sites may be confused with properties of the surface sites.

In spite of these difficulties, it is possible to make a preliminary assessment of the properties of EDCs and EWCs. The behavior of mitochondria in particular, and of living cells in general, exhibits a high degree of internal coherence. An excellent example of this is the oscillatory response of isolated mitochondria, to be discussed in Section 15.5.4. For the moment, in order to assess whether an agent is electron-withdrawing (EWC) or electron-donating (EDC), we shall rely on (1) the theoretical data shown in Figs. 6.7 and 6.8 describing the changes of relative preferences of sites for adsorbed cations in response to various agents and (2) the reasonable assumption that oxidation, or respiration, generally involves a loss of electrons from the system, and hence a decrease in c -value, and that reduction, or anaerobiosis, generally involves a gain of electrons, hence an increase in c -value.

15.5.3.2a. Respiration and Anaerobiosis. A cation exchange resin can replace all its counterions but it cannot lose them, and as long as there are n moles of fixed anionic sites in the resin, n moles of countercation must be present. A living cell resembles a simple ion exchange resin in many ways, but in death—brought about by heat or by metabolic inhibition—the cell's accumulated ions may be lost. In the AI hypothesis this occurs because living cells are a mixed amphoteric ion exchange system (Section 4.4.2.2). In cell death, adsorbed counterions are displaced by the formation of salt linkages between the fixed anions and the fixed cations. Cells tend to assume a final salt linkage formation for two reasons: First, the loss of entropy when a salt linkage is formed is less than when two free ions are adsorbed; second, in the dying state, electrons flow from fixed cationic sites and other sources to fixed anionic sites to raise their c -value, and the high c -value of anion sites allows them to combine with high- c' -value fixed cationic sites to form tight salt linkages. A similar high electron density of the carbonyl oxygen of the backbone promotes the formation of strong H bonds with peptide NH groups of high electropositivity (Ling, 1969a). The internally neutralized amphoteric system also occurs in "dead" proteins, such as sheep's wool and hair (Ling, 1962).

Mitochondria are not dead in any of the six metabolic states defined by Chance and Williams (1956) and Chance (1964). However, it is likely that in State 4 (the resting, slowly respiring state in the absence of ADP) the c -value ensemble is fairly high, in agreement with the highly reduced state of DPNH (Chance and Williams, 1956). Referring to Figs. 6.7 and 6.8, one predicts substantial retention of H^+ in State 4 even in a medium of very low H^+ concentration (i.e., pH 7.4). In State 1, in which there is no substrate, the respiratory carriers are in a somewhat more oxidized state (Chance and Williams, 1956), but the relative effectiveness of alkali metal ions in displacing K^+ and H^+ follows the rank order $Li^+ > Na^+ > K^+ > Rb^+$ (Gear and Lehninger, 1968). This corresponds to adsorption on anionic sites having a relatively high c -value.

The mitochondrion should have the highest *c*-value ensemble when the entire respiratory chain is in the reduced state (high substrate concentration but no oxygen). The high *c*-value accompanied by a high *c'*-value of the fixed cationic sites leads to extensive salt linkage formation, "squeezing" out both adsorbed cations (e.g., K^+) from anionic sites and anions (e.g., phosphates) from cationic sites. This is consistent with the data of Gamble and Hess (1966). The shrinkage concomitant with salt linkage formation (Type IIA shrinkage) is mirrored by the strong increase in light scattering by the mitochondrial suspension. Respiration, which shifts the chain to a more oxidized state, should lower the *c*-value. A low *c*-value should permit K^+ to be preferred over H^+ . Indeed respiration favors K^+ retention in isolated mitochondria (Spector, 1953; Berger, 1957; Gamble, 1957).

15.5.3.2b. "Ionophores." Valinomycin causes additional uptake of K^+ and release of H^+ in respiring rat liver mitochondria (C. Moore and Pressman, 1964). As just discussed, respiration tends to maintain the electron chain in an oxidized state, which leads to a low-*c*-value state of anionic fixed charges. Valinomycin reduces the *c*-value further to a level at which K^+ is preferred over H^+ , and a K^+ -for- H^+ exchange then follows. Therefore, valinomycin is an EWC. Since A23187 also causes K^+ -for- H^+ exchange (D. R. Pfeiffer and Lardy, 1976), it also may be an EWC. The sequence of events in gramicidin-treated mitochondria, as oxygen is becoming exhausted, is: (1) loss of K^+ , (2) loss of Na^+ , (3) uptake of H^+ , and then (4) loss of H^+ with mitochondrial contraction (Fig. 15.17). Figures 6.7 and 6.8 show that the earlier part of this sequence is explained by a steady increase in the *c*-value of the anionic sites as anaerobiosis progresses. The subsequent release of H^+ and the increase in light scattering are due to the further increase in *c*-value that allows salt linkage formation, and its concomitant Type IIA shrinkage, to occur (Stanbury and Mudge, 1953; Christie *et al.*, 1965; Berger, 1957; Gamble, 1957).

15.5.3.2c. Uncouplers. Uncouplers are agents that "uncouple" oxidation from phosphorylation and at the same time activate ATPase activity and stimulate oxygen consumption. One of the oldest known uncouplers, 2,4-dinitrophenol (DNP) causes a loss of K^+ and a gain of H^+ (Judah *et al.*, 1965) in respiring mitochondria (Stanbury and Mudge, 1953; Christie *et al.*, 1965; Berger, 1957; Gamble, 1957). In addition, (1) DNP inhibits liberation of H^+ in response to the addition of external K^+ (Christie *et al.*, 1965); (2) DNP-induced uptake of H^+ is prevented by K^+ and other alkali metal ions in the order of effectiveness $K^+ > NH_4^+ > Na^+$ (Judah *et al.*, 1965); and (3) while valinomycin causes K^+ gain and H^+ loss, DNP and valinomycin together cause K^+ release, which can be prevented by raising the external K^+ concentration (Gamble and Hess, 1966). From these findings it would seem that DNP is primarily an EDC while respiration and valinomycin are EWCs. In this context, one can understand why DNP prevents KCl-induced (Type IIA) swelling (Chance, 1964).

The next question to be asked is: How does DNP increase oxygen consumption, uncouple oxidative phosphorylation, and activate ATPase activity? Some tentative answers can be suggested. It seems clear that K^+ is necessary for the respiratory activity of mitochondria. This was first reported by Pressman and Lardy (1952) and later disputed (Opit and Charnock, 1965). However, studies including those of Krall *et al.*

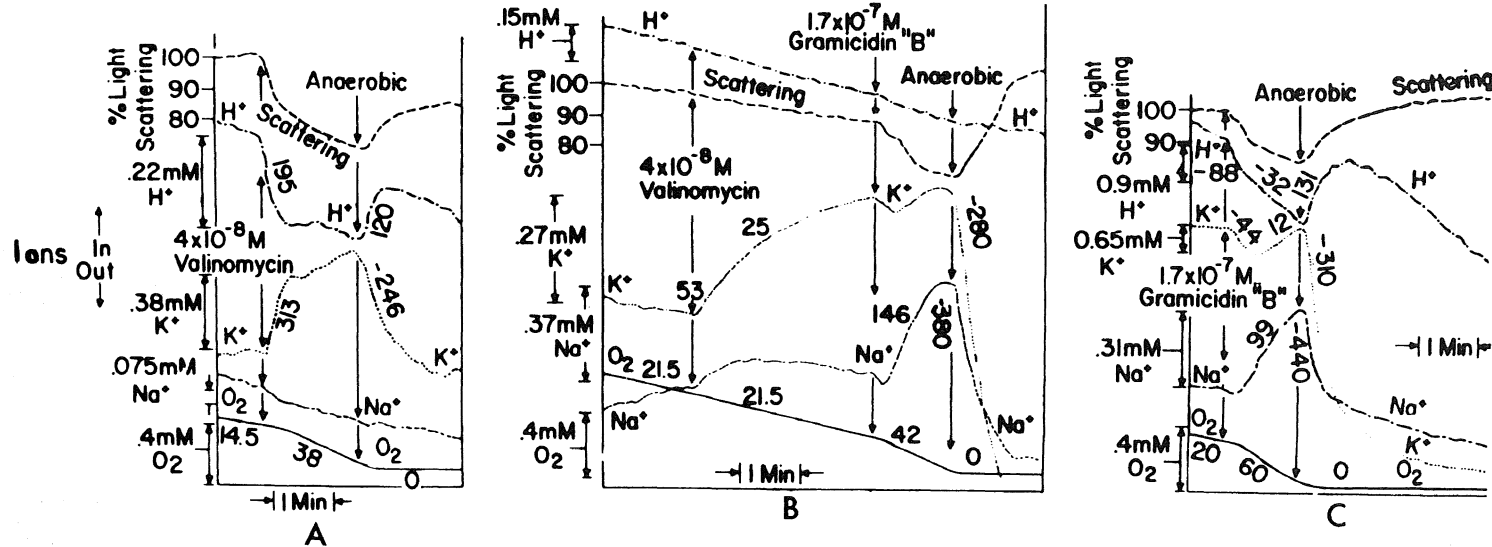


FIGURE 15.17. (A) Valinomycin-induced uptake of K^+ . The medium was equilibrated against 100% O_2 before the addition of mitochondria. Two minutes before addition of 4×10^{-8} M valinomycin, 20 mg oligomycin were added. Figures on tracings represent slopes, expressed in μ moles per gram protein per minute. (B) Valinomycin-induced uptake of "leaked" K^+ and subsequent gramicidin-induced uptake of Na^+ . System contained Tris glutamate, 3 mM; Tris malate, 3 mM; Tris chloride, pH 7.4, 20 mM; NaCl, 1.9 mM; choline chloride, 13 mM; Tris phosphate, pH 7.4, 1.25 M; and sucrose, 240 mM. Oligomycin (20 mg) was added 2 min before valinomycin. (C) Gramicidin-induced uptake. System the same as in (B) except for omission of phosphate and valinomycin. [From Pressman (1965), by permission of *Proceedings of the National Academy of Sciences*.]

(1964), Kimmich and Rasmussen (1967), and Gomez-Puyou *et al.* (1969, 1970) confirm Pressman and Lardy's original finding. The AI hypothesis suggests that a rapidly oscillating cooperative adsorption and desorption of K^+ accompany the propagated oxidation-reduction cycles along the respiratory chain. Such a cooperative adsorption-desorption cycle requires a delicate balance between the *c*-value of the fixed anions and the appropriate ratio of competing counterions. DNP, acting as an EDC, perturbs this state of balance, and the oxidation rate is increased. The delicate balance between the two sets of factors is manifested by a complex response curve in which DNP stimulates respiration at low concentrations and depresses respiration at higher concentrations (Chappell, 1964; Chance *et al.*, 1963). Similarly, K^+ , which is required in a low concentration for increased DNP-induced oxygen consumption, inhibits respiration in a high concentration. These complex behavior patterns are theoretically shown in Figs. 7.8-7.10.

The concept that continued respiratory activity depends on a delicately poised state of the respiratory chain proteins that adsorb K^+ is in harmony with the following findings: (1) K^+ depletion causes inhibition of respiration (Kimmich and Rasmussen, 1967; Aithal and Toback, 1978), and nigericin, which causes K^+ loss, inhibits respiration (Graven *et al.*, 1966; Reed and Fain, 1968). (2) Valinomycin and gramicidin, which tend to increase K^+ in isolated mitochondria, increase respiration (C. Moore and Pressman, 1964; Höfer and Pressman, 1966; Chappell and Crofts, 1965; E. J. Harris, 1966). (3) Increase in the respiratory control index by ADP (i.e., increased O_2 consumption) depends on K^+ (Gomez-Puyou *et al.*, 1969), and loss of respiratory control parallels loss of K^+ content (Gomez-Puyou *et al.*, 1970). (4) The combination of DNP and valinomycin causes loss of K^+ , after which respiration stops. Addition of KCl restores respiration (Kimmich and Rasmussen, 1967).

In normal mitochondria, the delicately balanced adsorption and desorption of K^+ depend on both Mg^{2+} and ATP, which act as cardinal adsorbents: (1) ATP, Mg^{2+} , and diphosphopyridine nucleotide restore mitochondrial respiration and oxidative phosphorylation (F. E. Hunter and Ford, 1955). (2) Mg^{2+} is required for DNP-activated ATPase activity and oxidative phosphorylation (Siliprandi *et al.*, 1975b). (3) Respiration of fetal rat liver mitochondria, which contain very little ATP, is not stimulated by ADP; the respiratory control index is increased by exposure to ATP or to an ATP analogue that cannot be hydrolyzed (Nakazawa *et al.*, 1973).

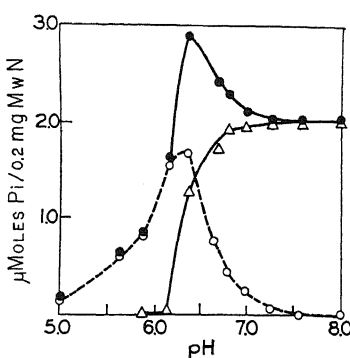


FIGURE 15.18. Effect of pH on K^+ -dependent ATPase from mitochondria stimulated by nigericin. ○, Spontaneous ATPase induced by the pH change in K^+ media and hypotonic conditions; ●, activity of ATPase induced by nigericin at different pH values; Δ, corrected curve of the ATPase activity stimulated by nigericin, obtained after subtracting the spontaneous ATPase from the ATPase in the presence of nigericin. [From Estrada-O *et al.* (1967), by permission of *Journal of Biological Chemistry*.]

The ATPase undergoes a delicate shift from a Mg^{2+} and/or K^+ state, which favors phosphorylation of the ATPase, to a Ca^{2+} and/or Na^+ state, in which ATP is synthesized. Any agent that disturbs the *c*-value would undermine this balance and the oscillation between the Mg^{2+} (and/or K^+) state and the Ca^{2+} (and/or Na^+) state, and thus hinder or arrest oxidative phosphorylation. The key role of the electronic or *c*-value balance of anionic sites on the ATPase is illustrated in Fig. 15.18 (Estrada-O *et al.*, 1967), which shows the effect of pH and nigericin on intramitochondrial ATPase activity. The complex pattern of interaction resembles the theoretical curves calculated on the basis of the AI hypothesis for a pair of interacting agents (Fig. 7.10).

15.5.3.2d. Thiol Reagents. In anoxic rat heart mitochondria, Ca^{2+} is lost and Mg^{2+} is retained during succinate oxidation (Crompton *et al.*, 1976). If oxidation causes a decrease of *c*-value and inhibition of respiration causes an increase in *c*-value, as argued in the preceding sections, then Mg^{2+} would be preferred over Ca^{2+} at a higher *c*-value. That respiration favors Ca^{2+} accumulation has been known for a long time (for review, see Lehninger, 1967). It is also known that all three energy-conserving sites contribute equally to the support of Ca^{2+} uptake (C. S. Rossi and Lehninger, 1964) and that inhibitors of respiration like antimycin A and uncoupling agents cause rapid release of Ca^{2+} (Chappell and Crofts, 1965; Drahota *et al.*, 1965). In contrast, E. J. Harris *et al.* (1979) found that inhibition of respiration favors retention of mitochondrial Ca^{2+} . Lehninger *et al.* (1978) found that uptake of Ca^{2+} parallels the reduced state of pyridine nucleotide. Only future experiments will clarify these apparent conflicts, but some generalizations can be made.

Theoretical curves have not been calculated for the alkaline earth ions for variation of *c*-values. However, from experience with the alkali metal ions one finds that as a rule the ions with smaller atomic weight tend to be preferred at higher *c*-values. Thus an assumption that increased *c*-value should select Mg^{2+} over Ca^{2+} is reasonable and is adopted for the present. Evidence that Ca^{2+} is preferred at low *c*-values was reported by Rossi *et al.* (1967), who showed that valinomycin increases Ca^{2+} uptake (Fig. 15.15). Siliprandi *et al.* (1975a,b) showed that diamide causes Mg^{2+} loss and Ca^{2+} uptake by rat liver mitochondria. The effect of diamide and the other thiol-oxidizing agents, tellurite and selenite, in enhancing the deleterious effect of Ca^{2+} on mitochondria is antagonized by a reduction of thiol groups by dithioerythritol, which enhances the protective action of Mg^{2+} as well (Siliprandi *et al.*, 1975b). Since thiol oxidation, like respiration, removes electrons, it also may be reasonably expected to lower the *c*-value; the effect of diamide suggests therefore that Mg^{2+} is preferred at a high *c*-value. A23187, like diamide, causes release of Mg^{2+} (Taniguchi and Post, 1975) and would appear to act as an EWC, as we already suggested and in agreement with Siliprandi's earlier conclusion that diamide and A23187 have similar effects.

Siliprandi *et al.* (1979) found that diamide is antagonized by the uncoupler carbonyl cyanide *p*-trifluoromethoxyphenylhydrazone (FCCP). This suggests that the primary action of this uncoupler on mitochondria is to increase the *c*-value. This agrees with the earlier suggestion that the uncoupler DNP is an EDC, and the facts that both DNP and FCCP (Harris *et al.*, 1967) favor H^+ uptake at the expense of K^+ and that DNP and FCCP inhibit Ca^{2+} uptake (Chappell and Crofts, 1965).

15.5.3.2e. *ATP.* Uptake of Ca^{2+} by rat liver mitochondria is stimulated by ATP (Wehrle and Pedersen, 1979). Hence, ATP reduced the *c*-value and is an EWC, as would be expected from its ability to support K^+ accumulation in muscle (Ling, 1951, 1952; Ling and Ochsenfeld, 1973b). This explains why externally added ATP and respiration often have similar effects. This effect does not require the hydrolysis of ATP, since Nakazawa *et al.* (1973) have shown that fetal liver mitochondria, which have no ATP, do not release H^+ on exposure to pulses of Ca^{2+} . Addition of ATP with Mg^{2+} in the presence of both rotenone and oligomycin brings about a full liberation of H^+ during exposure to Ca^{2+} pulses. This agrees with the ideas that H^+ is preferred at a high *c*-value and Ca^{2+} at a low *c*-value, and that ATP lowers the *c*-value so that Ca^{2+} can more effectively displace H^+ . That ATP, without undergoing hydrolysis, can maintain the selective accumulation of K^+ over Na^+ in whole living cells has been a major concept of the AI hypothesis (Section 4.4 and Chapter 10).

Another function of ATP is to promote polarization of water (Chapters 6 and 10). ATP, in the presence of oligomycin, alters the osmotic response of mitochondria to sucrose. This suggests once again that ATP causes long-range polarization of water and, with it, a decrease in the *q*-value of sucrose (Fig. 15.13). I suggested in 1964 (Ling, 1964a) and 1969 (Ling, 1969a) that the backbone CONH group tends to assume an α -helical, non-water-polarizing conformation when the side chains are strongly electron-donating. Decreasing *c*-value may indeed be expected to mirror conditions for the long-range polarization of water.

15.5.3.2f. *ADP.* Several sets of evidence suggest that ADP may be electron-donating, and thus have effects opposite to those of ATP:

1. Azzone and Azzone (1966) showed that swelling of mitochondria under anaerobic conditions is reversed by either ADP or DNP, and, as noted above, DNP is an EDC.
2. E. Rossi and Azzone (1970) showed that, upon the addition of rotenone, K^+ that has accumulated in mitochondria in the presence of valinomycin (an EWC) is slowly lost. ADP accelerates this loss.
3. Crompton *et al.* (1976) showed that ADP, like anaerobiosis, inhibits Mg^{2+} release.
4. Höser *et al.* (1976) showed that ADP slows down Mg^{2+} release in a way similar to nigericin.

If ATP and ADP indeed have opposite effects on the *c*-value, this would offer an interesting mechanism for the reversible biological work performance controlled by ATP (Chapter 10).

15.5.4. Synchronous Oscillatory Changes in Properties of Mitochondria

Lardy and Graven (1965) and Pressman (1965) simultaneously reported damped oscillatory changes in mitochondrial swelling and ion transport. To produce these changes several factors are needed: (1) an energy source, which could be substrate plus O_2 or ATP, (2) an alkali metal ion, (3) "permeant" anions such as P_i or acetate, (4) an

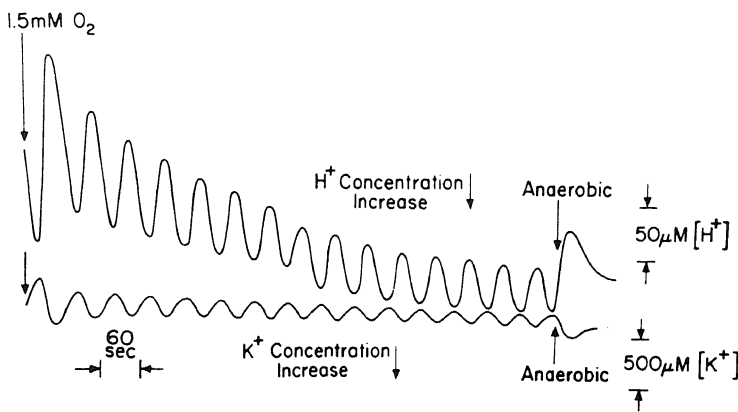


FIGURE 15.19. General characteristics of the H^+ and K^+ oscillations, measured by the glass electrode and K^+ electrode, respectively, in a suspension of pigeon heart mitochondria. The mitochondria were allowed to become anaerobic and then supplemented with 17 μg catalase/ml and 1.5 mM O_2 (as H_2O_2). 83 ng valinomycin/ml and 6.7 mM KCl were present initially in this experiment; initial pH was 0.25. [From Chance and Yoshioka (1966), by permission of *Archives of Biochemistry and Biophysics*.]

"ionophore" or other agent that can increase the permeability of the alkali metal ion, and (5) a suitable pH.

The oscillatory changes have cycles that last one to several minutes under the proper conditions. Examples in pigeon heart mitochondria (Chance and Yoshioka, 1966) are shown in Fig. 15.19; these apparently can go on indefinitely. The following synchronized changes have been described, although not all in phase and not all in the same system:

1. Increase and decrease of volume.
2. Uptake and release of alkali metal ions.
3. Release and reuptake of H^+ .
4. Uptake and release of "permeant" anion.
5. Oxidation and reduction of pyridine nucleotide.
6. Oxidation and reduction of cytochrome *b*.

The most extensively studied systems are rat liver and pigeon heart mitochondria in media containing valinomycin and potassium phosphate. Since it has now been clearly shown that valinomycin does *not* increase K^+ permeability (Maloff *et al.*, 1978) and that both "permeant" and "impermeant" anions are permeant, the phenomenon is given a different interpretation according to the AI hypothesis.

The cooperative adsorption isotherm [equation (7.22)] dictates that an all-or-none type of autocooperative transition occur when the parameter ξ changes, in response either to a change in the ratio of two competing adsorbents or to a change in the intrinsic equilibrium constant $K_{j \rightarrow i}^{00}$, which in turn is under the control of cardinal adsorbents. Ouabain, for example, converts frog muscle from a K^+ -adsorbing state to a Na^+ -adsorbing state if the ratio of medium K^+ to Na^+ is close to $1/K_{j \rightarrow i}^{00}$; (Ling and Bohr, 1971a). If, on the other hand, K^+ is too high or Na^+ is too low, ouabain would be unable to

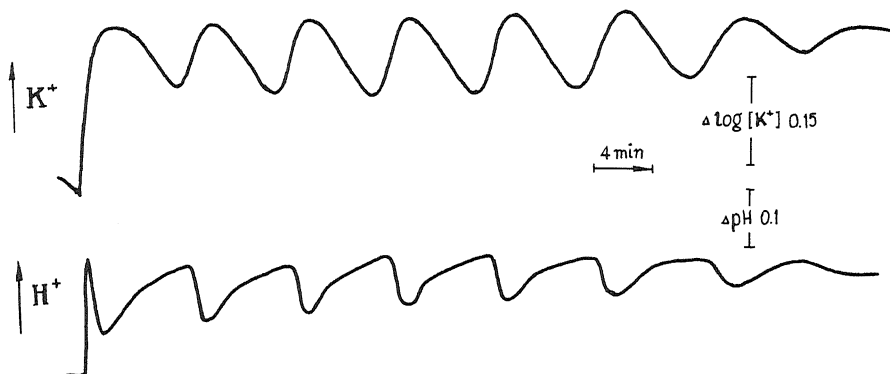
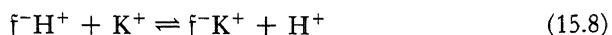


FIGURE 15.20. Sr^{2+} -induced oscillations of K^+ and H^+ fluxes in rat liver mitochondria. Basal medium: sucrose, 20 mM; KCl, 1 mM; Tris, 12 mM. Additions: succinate, 5 mM; valinomycin, 4 ng/mg; rotenone, 4.8 mg/mg mitochondrial protein; mitochondrial protein, 2 mg/ml; 22°C, pH 7.5. [From Gylkhandanyan *et al.* (1976), by permission of *FEBS Letters*.]

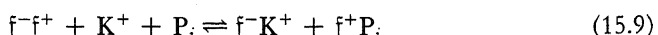
convert the cell from one state to the other. It was suggested previously that the combination of oxidation of the respiratory chain plus valinomycin brings the *c*-value to a value that will bring about a K^+ -for- H^+ exchange. If external K^+ is at a critical level, the K^+/H^+ exchange is in a critical state, i.e., it is capable of changing from one state in which K^+ is adsorbed to another state in which H^+ is adsorbed, correlated with a cyclic change in the oxidation-reduction state of the mitochondria. Salt linkage dissociation in turn allows swelling, which is, of course, the Type IIA swelling described in Chapter 13. The requirements for sustained oscillation (i.e., minimal damping) support this interpretation. In pigeon heart mitochondria in valinomycin- K^+ -containing solutions, sustained oscillations occur only if the external K^+/H^+ concentration ratio is in a narrow range (between 0.9×10^4 and 1.5×10^4). A much higher ratio of alkali metal ion to H^+ of about 3×10^5 is required for rat liver mitochondria in the presence of various nonactin homologues (Graven *et al.*, 1966).

Similarly, the fact that valinomycin (Chance and Yoshioka, 1966; Packer *et al.*, 1966), gramicidin (Graven *et al.*, 1966), EDTA (Falcone and Hadler, 1968), monoazomycin (Estrada-O and Gomez-Lojero, 1971), and Sr^{2+} (Gylkhandanyan *et al.*, 1976) (Fig. 15.20) all promote oscillatory responses agrees with the basic concept that each of these reagents, alone or via intermediates (e.g., Mg^{2+} versus EDTA) acts by shifting the *c*-value of the protein-water-ion system.

The fact that repeated oscillation also requires the presence of “permeant” anions (e.g., P_i) suggests that there is not only a K^+ -for- H^+ exchange, but also salt linkage dissociation:



and



This truly remarkable oscillatory phenomenon demonstrates the splendid coordination that occurs within this complex organelle. Not only is the protein-water-ion system undergoing coordinated changes, but these changes are also synchronized in the time dimension. The AI hypothesis has postulated that similar oscillatory changes underlie transepithelial solute transport, ciliary beating, and other cyclic changes.

Finally I would like to suggest that a similar cyclic event may underlie the accumulation of calcium phosphate in the form of hydroxyapatite in mitochondria when they are "maximally loaded" with Ca^{2+} , i.e., in the presence of ATP (Lehninger 1964, 1967; C. S. Rossi and Lehninger, 1964):

1. Selective adsorption of Ca^{2+} on anionic sites displaces H^+ and, along with P_i , dissociates salt linkages, as shown in equation (15.9). Ca^{2+} and P_i adsorption are favored by the lowered c -value caused by ATP adsorption on cardinal sites.
2. Ca^{2+} adsorption activates ATPase activity, leading to ATP hydrolysis.
3. With the opposing effect of ATP removed, water is depolarized, with an increase of the q -value of solutes within it.
4. As a result, more Ca^{2+} and P_i and ATP enter into mitochondrial water.
5. ATP becomes readsorbed, causing polarization of water and a decrease of the q -value for Ca^{2+} and P_i .
6. The decrease of q -value causes precipitation of calcium phosphate.
7. The decrease in c -value by the readmitted or regenerated ATP causes readsorption of Ca^{2+} and P_i and the cycle repeats itself.

A similar cyclic event may also be responsible for the precipitation of Ca^{2+} as oxalate in microsomal or SR vesicles reported by Hasselbach and Makinose (1961).

15.6. Summary

ATP plays a central role in biological work performance by most cells and tissues, and mitochondria are a major source of ATP synthesis. Mitochondria enable the full degradation of glucose to yield a maximal amount of energy. They couple phosphorylation—ATP synthesis by enzymes that can function reversibly as ATPase—to oxidation—the process by which electrons released during glucose degradation are transferred to the electron acceptor oxygen, so that it is reduced by H^+ to form water.

The mechanism of the coupling between oxidation and phosphorylation has been a major and contentious area of research in biochemistry. Theories include the chemical coupling hypothesis, the conformation-coupling hypothesis, and the currently popular chemiosmotic hypothesis. The chemiosmotic hypothesis, however, suffers from all of the general objections to the membrane osmotic theory outlined throughout this book, and from a number of specific problems outlined in this chapter.

Recent studies of ATP synthesis by ion-activated ATPases show quite clearly that ionic electrochemical gradients across membranes are not required for ATP synthesis, and that specific ion adsorption onto the enzyme is the event that triggers ATP synthesis. Moreover, two steps are required to accomplish this: one is phosphorylation of the enzyme by P_i , which requires K^+ and/or Mg^{2+} ; the second is transfer of P_i to ADP to form ATP, and this requires Na^+ and/or Ca^{2+} . With this in mind, the question was

posed: How does the mitochondrion perform the equivalent of the *in vitro* two-step process? In answering this question, the basic concepts of the association-induction hypothesis, outlined in Chapters 6–10, were invoked, and a mechanism of the coupling between oxidation and phosphorylation was proposed. This mechanism is based on a chemical inductive effect transmitted through parts of the ATPase and conditioned by its interaction with the elements of the electron transport chain. A cyclic change in the *c*-values of the ion-adsorbing sites of the proteins leads to cyclic autocooperative shifts in the affinities of these sites for ions, and this provides the *in vivo* equivalent of the *in vitro* two-step manipulation.

A number of physiological phenomena in mitochondria were reviewed within the context of the association-induction hypothesis. For example, ATP functions in mitochondria as it does in cells generally, and maintains water in a state of polarized multilayers that tends to exclude solutes; in accord with the theory of volume regulation outlined in Chapter 13, ATP is noted to cause shrinkage and sucrose exclusion of mitochondria that initially lack ATP. Like ATP, uncouplers, ionophores, Mg^{2+} , Ca^{2+} , and ADP function as cardinal adsorbents, and may be classified according to whether their inductive effect is primarily electron-withdrawing or electron-donating. Valinomycin, for example, causes a net accumulation of K^+ by an allosteric effect on internal adsorption sites, and by the same mechanism confers a sensitivity of the surface fixed-charge sites to external K^+ concentration, so that its potential becomes K^+ -sensitive. The non-respiring, reduced state of the mitochondrion was seen to be one in which the *c*-value of fixed carboxyl groups is high, and, by reference to the theory outlined in Chapter 7, this readily explains the substantial retention of H^+ in this state. In the actively respiring, oxidized state, the *c*-value is low, and this explains the relative retention of K^+ over H^+ in this state.

Finally, these basic concepts of the association-induction hypothesis were applied to the synchronized, oscillatory changes noted to occur in mitochondrial swelling and shrinkage, K^+ and anion uptake and release, H^+ release and uptake, and oxidation and reduction of pyridine nucleotides and cytochrome *b*. A similar concept of cyclic adsorption-desorption will be applied toward theories of biological work performance in the case of muscle contraction and relaxation in the next chapter and in the case of active transport by epithelial tissues in Chapter 17.

Muscle Contraction and Related Phenomena

Motility is a major living phenomenon, and in higher multicellular organisms specialized muscle cells provide its basic mechanism. Of the different types of muscle, by far the most extensively studied are the skeletal muscles, which are distinguished by the length of the individual cells as well as their cross-striations. Under an ordinary light microscope with proper focusing (A. F. Huxley, 1957), a muscle fiber appears as a series of alternatingly dark (anisotropic) A bands and light (isotropic) I bands (Fig. 16.1). The major protein of muscle cells is myosin, which was first isolated and named by Willy Kühne (1864), a student of Johannes Müller. A. F. Huxley (1974) has reminded us that fully a century ago it was already known that myosin is found in the A bands (T. H. Huxley, 1880). Methods for extracting muscle proteins gradually evolved in the hands of von Muralt, Edsall, Weber, and others (H. H. Weber, 1925; von Muralt and Edsall, 1930; Greenstein and Edsall, 1940). An extracting solution containing 0.5 M KCl at more or less alkaline pH was often referred to as the Weber-Edsall solution.

Hermann (1867), Fletcher and Hopkins (Fletcher, 1902; Fletcher and Hopkins, 1907; Fletcher and Brown, 1914), and O. Meyerhof and Hill (Meyerhof and Hill, 1923) laid the groundwork for an understanding of the basic energetics of muscular contraction. It was believed in those early days that "*something in the resting muscle possesses potential energy of some kind and that on excitation, some change takes place in systems with a loss of this potential energy*" (Bayliss, 1927, p. 441). To restore the higher potential energy of the resting state, some exothermic reaction must take place. It was also recognized that the contraction could take place without oxygen, and that muscle contracting in nitrogen becomes acidic. Finally Fletcher and Brown (1914) established that this acidification was the result of the production of lactic acid.

16.1. Early Theories of Muscle Contraction

The following are brief sketches of a few of the theories of muscle contraction that have been published.

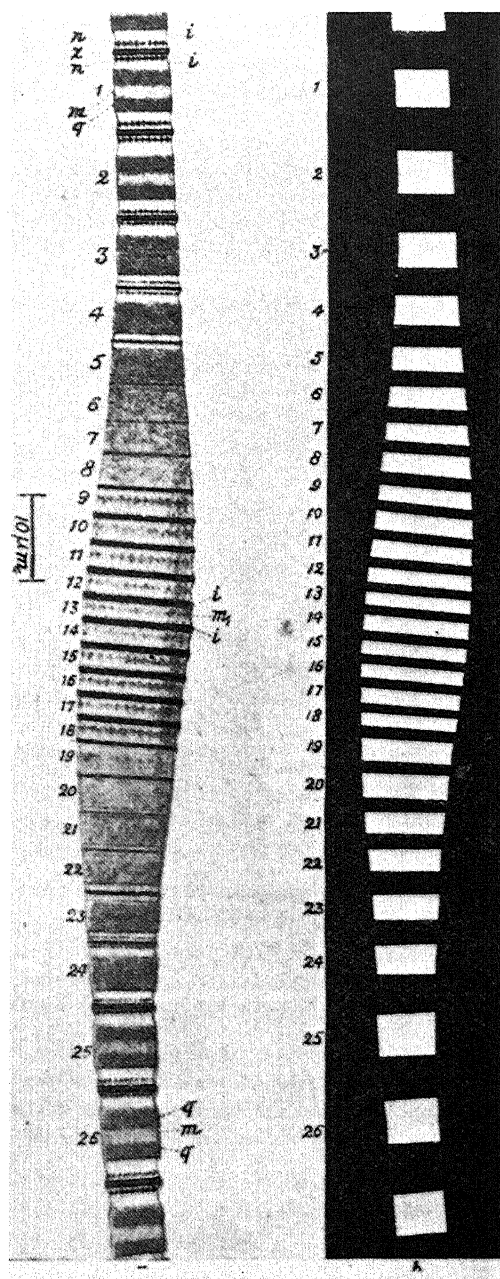


FIGURE 16.1. Muscle fiber from the abdomen of *Telephorus melanurus* with contraction wave. Fixed in 60% alcohol. (Left) In ordinary light; (right) in polarized light, between crossed Nicols. [From Bayliss (1927) after Engelmann, by permission of Longman, Green and Company.]

16.1.1. Engelmann's Heat Engine Theory

Engelmann (1906) argued that the doubly refractile material in the A band possesses the special quality that, when it is heated, its particle undergoes a change in shape. This shape change is accompanied by an increase of association with water. The result

is a lateral expansion of the A band with a concomitant shortening of the I band (Engelmann, 1873, p. 166). Figure 16.1, taken from a drawing by Engelmann (see Bayliss, 1927) shows shortening of both bands at the "contraction band" of an insect muscle. To be noted is the long-recognized fact that shortening does not involve an actual "contraction" or loss in volume. Rather, shortened segments actually widen.

Engelmann made a great contribution to knowledge about muscle, but contraction on the basis of a "heat engine" was not tenable from a thermodynamic standpoint, as was clearly shown by A. Fick (1893), a student of Carl Ludwig. A heat engine adsorbs heat, Q_2 , at the high temperature T_2 , and gives out heat, $-Q_1$, at the lower temperature T_1 . According to the first law of thermodynamics, $Q_2 - (-Q_1)$ is equal to work, W . The efficiency (E) of the engine is

$$E = \frac{Q_2 + Q_1}{Q_2} = \frac{W}{Q_2} = \frac{T_2 - T_1}{T_2}. \quad (16.1)$$

Now T_1 is the ambient temperature and for frog muscle it is equal to 298°K. The efficiency of muscle contraction is usually given as 30%; one calculates from equation (16.1) a T_2 value of 425°K or 152°C. This is above the boiling point of water and cannot possibly be the temperature of a contracting muscle.

16.1.2. The Osmotic Theories of McDougall and MacDonald

McDougall (1897) presented the view that the A bands and other compartments are enclosed in semipermeable membranes and that lactic acid produced increases the osmotic activity in the A bands, drawing water into these sections and causing lateral swelling and shortening of the myofibrils (then called sarcostyles). However, McDougall's osmotic theory was shown to be untenable by J. Bernstein (1905), whose calculations revealed that the osmotic force generated by the estimated amount of lactic acid produced cannot come near to the force generated during contraction.

A different kind of osmotic theory was then offered by J. S. MacDonald (1909), who also considered the contraction of myofibrils to be primarily a result of the movement of water from the I bands to the A bands. However, the osmotic pressure increase at the A band was attributed to a release of inorganic salt associated with the aggregation of colloids during contraction. MacDonald attempted to prove his theory by looking for changes in the K^+ distribution patterns observed by Macallum (1911) with a histochemical technique. These attempts were not very successful. In Chapter 8 I discussed why I believe that—while Macallum's specific technique might not have actually demonstrated K^+ binding—recent work, especially that of Edelmann, has proved the adsorbed state of K^+ at the A bands, as Macallum once argued.

16.1.3. The Lactic Acid Theory

In the several decades following the turn of the century, there was a general belief that muscle contraction involved changes in surface tension at the point of contact between myofibrils and sarcoplasm, brought on either by the lactate ion or the H^+ produced. Evidence in support of this view was given by J. Bernstein (1908) and by Mines

(1913), and later A. V. Hill's name became intimately associated with this theory (Hill, 1926). His dramatic resolution of the controversy concerning the lactic acid theory of muscle contraction was discussed in Section 3.1.3. Lactic acid could not be the cause of muscle contraction because its production comes *after* the contraction and not before it, and because muscle poisoned with iodoacetate (Lundsgaard, 1930) can contract quite normally long after its ability to produce lactic acid has been inhibited.

Lundsgaard showed also that lactic acid production (or glycolysis) was not the immediate exothermic reaction that replenishes the lost potential energy then believed to exist in resting muscle cells. Glycolysis, like oxidation, must also be a late restorative process. Attention was then turned to the newly discovered creatine phosphate (P. Eggleton and Eggleton, 1927; Fiske and Subbarow, 1929) and ATP (Lohmann, 1931). Calorimetric measurements led to the belief that the terminal phosphate bond of ATP is unusual in that its hydrolysis liberates much more heat (enthalpy of hydrolysis: -12 kcal/mole) than do ordinary phosphate bonds. The subsequent history of how this concept was revised was discussed in Chapter 10.

16.1.4. The Engelhardt-Ljubimova Theory

H. H. Weber (1934) was the first to produce an artificial muscle fiber by squirting myosin extracted in 0.5 M KCl into a very dilute salt solution through a hypodermic needle. The technique was adopted by Engelhardt and his wife, Ljubimova (1939, 1942), in a famous experiment. These artificial muscle fibers, mounted on a loaded lever, responded to the addition of 5 mM ATP with a lengthening of the protein thread (Fig. 16.2). Furthermore, this ability to respond to ATP corresponds to the ability of the myosin thread to hydrolyze ATP, and hence, in their view, to liberate and deliver the energy stored in the terminal phosphate bond. The demonstration that the contractile machine, myosin, has the specific ability to unlock the stored energy and utilize it in a mechanical response was widely hailed as a major breakthrough. Engelhardt and Ljubimova's finding was repeatedly confirmed and extended by D. M. Needham's group

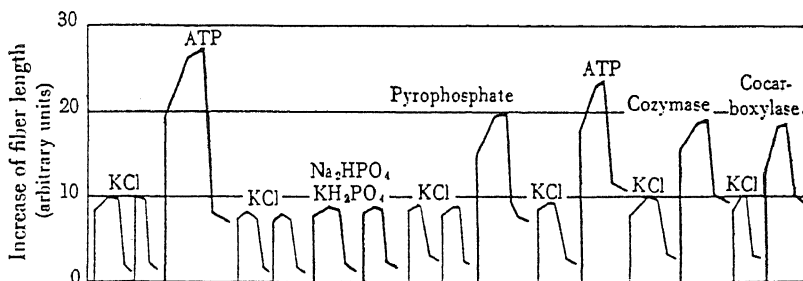


FIGURE 16.2. Dimensional changes of myosin thread caused by ATP and related compounds. By extruding myosin into a solution of low ionic strength, a gel-like thread is formed which, when mounted on a lever, reversibly responds to the addition of a load (usually 200 mg) by lengthening. This extensibility is found to be greatly increased by the presence of ATP at very low concentrations (5 mM). Other related compounds containing the pyrophosphate groups (inorganic pyrophosphate, cozymase, and cocarboxylase) are also effective, but to a smaller degree. [From Ling (1962), after Engelhardt and Ljubimova; see Engelhardt (1946).]

in Cambridge (see Needham, 1971) and many others, who showed in addition that ATP causes a large decrease of birefringence and viscosity of myosin solution, suggesting contraction of the myosin particles. The great enthusiasm generated by the important discovery of Engelhardt and Ljubimova should not obscure the fact that diphosphopyridine nucleotide, inorganic pyrophosphate, and thiamin pyrophosphate also cause myosin relaxation (Fig. 16.2), and these compounds are not split by the ATPase.

16.1.5. The Actin–Myosin Association Theory of Szent-Györgyi

Schramm and Weber (1942), using the ultracentrifuge, first discovered that myosin is not a simple homogeneous protein. They named the fast-moving component, L-myosin (*leicht*) and a slow-moving component, S-myosin (*schwer*). A few months later, Albert Szent-Györgyi and his school at Szeged revealed the results of their brilliant studies, which were to have a profound impact on the development of muscle biochemistry and physiology (A. Szent-Györgyi, 1941–1943). The Szeged school found that myosin is not pure but can be isolated in two different forms, A and B, depending on the length of time of extraction. In due time they evolved a method to produce a pure “crystalline” myosin. A member of the Szeged school, F. B. Straub (1942, 1943), isolated the main “contaminant” of myosin and named it *actin*. Myosin A is contaminated with less actin than Myosin B. Thus myosin (and presumably Schramm and Weber’s L-myosin) is closer to true myosin and myosin B (and probably S-myosin) is a complex of actin and myosin, which was then called *actomyosin*. In all probability, Engelhardt and Ljubimova’s myosin threads were actomyosin threads.

The central set of experimental findings of Szent-Györgyi is illustrated in Fig. 16.3. A mixture of pure actin and pure myosin will be dissolved in solution or will precipitate depending on the concentration of KCl in the medium. Thus in 0.4 M KCl, the protein



Albert Szent-Györgyi

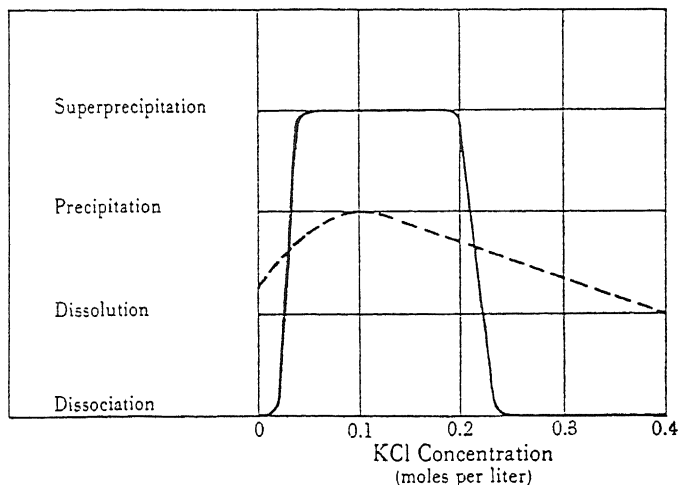
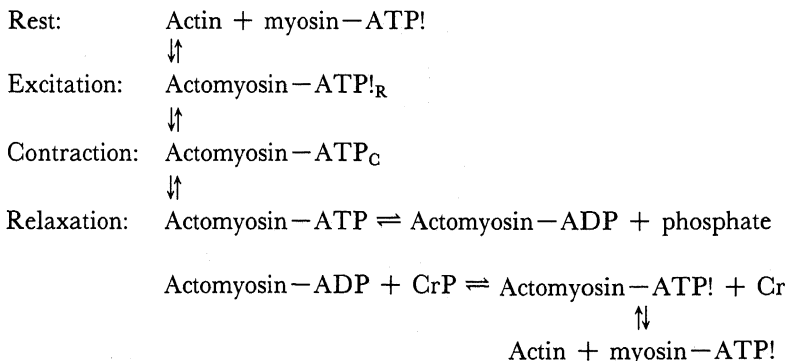


FIGURE 16.3. Superprecipitation of actomyosin by KCl in the presence and absence of ATP. In this diagram the extensive precipitation of actomyosin in the presence of ATP (—) involves a high degree of dehydration and is termed *superprecipitation*, in contrast to ordinary precipitation, in which the proteins are acted on by salts in the absence of ATP (----). [From Ling (1962), after A. Szent-Györgyi (1947, 1951).]

mixture is entirely dissolved; it is also mostly dissolved in pure water without KCl. A peak of precipitation occurs at around 0.1 M KCl. A different picture emerges when ATP is added. ATP enhances both the solubilization effect of low and high KCl concentrations and the precipitation effect of intermediate KCl concentrations; it also causes dissociation of actin and myosin. The abrupt shrinkage brought about by ATP in the presence of moderate concentrations of KCl involves extensive dehydration of the proteins and was called *superprecipitation*. Szent-Györgyi theorized that in resting muscle cells actin and myosin remain dissociated and that it is only after cell activation that they become associated, thereby bringing about a contraction, which corresponds to the superprecipitation of ordered myosin and actin protein chains. Szent-Györgyi pointed out that higher concentrations of ATP as well as of Mg²⁺ intensify superprecipitation and narrow the range of KCl in which actomyosin remains associated.

Szent-Györgyi represented his theory of muscle contraction as follows (1947, 1951, p. 122):



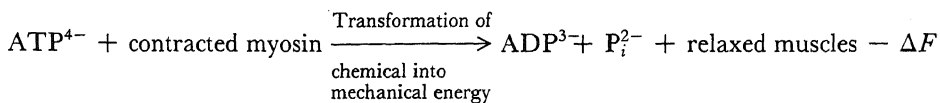
where the exclamation mark was used to denote the high-energy link between ATP and myosin or actomyosin, and R and C refer to the resting and contracted states. It is to be noted, in this model, that ATP hydrolysis is not involved during contraction.

While more sophisticated variants of Weber's actomyosin threads (see Hayashi and Rosenbluth, 1952) continued to be a material of great interest and study, the glycerinated rabbit psoas muscle technique which Szent-Györgyi introduced in 1951 (A. Szent-Györgyi, 1947, 1951) proved to be a substantial improvement over the extruded actomyosin thread, because in the glycerinated muscle fiber model the basic topographical arrangements of myosin and actin, as well as other components, are preserved.

16.1.6. The Active Relaxation Theory

It is well known that muscle poisoned with iodoacetic acid (IAA) and nitrogen can no longer effectively regenerate its ATP. When these poisoned muscles are excited, they can perform normal contraction, but only as long as there remain some ATP and creatine phosphate (CrP), which are interconvertible via the Lohmann reaction [equation (3.1)]. When eventually ATP and CrP are all used up, the muscle ends up in rigor, which is an extreme and irreversible form of contraction.

Based on these observations, D. M. Needham (1937), Lundsgaard (1938), and Kalckar (1942) suggested that the energy liberated from ATP hydrolysis is "utilized in the relaxation of the discharged state" (Kalckar, 1942). Kalckar represented his scheme as follows:



16.1.7. The Electrostatic Extension–Entropic Contraction Theory

Meyer and Mark (1930) and Katchalsky (1949) suggested that the electric charges of ionized carboxyl groups of muscle proteins may repel one another and thus hold the muscle in a relaxed state. Neutralization of these charges would then bring about contraction (see also Bull, 1946; Kuhn, 1949). Other scientists, including Wohlisch (1940) and Pryor (1950), suggested that contraction is entropy-driven. Riseman and Kirkwood (1948) suggested that quadrivalent ATP, adsorbed on the contractile proteins, may provide enough repellent force between them to maintain the muscle proteins in a relaxed, extended state. Hydrolysis of ATP and its desorption may then lead to contraction.

Using myosin threads similar to those of Engelhardt and Ljubimova, Morales and Botts (1952) measured the thread tension at different temperatures and degrees of extension. The results were analyzed to yield separately the entropy and internal energy of the systems. The data so obtained for small extensions (up to 10%) are reproduced in Fig. 16.4. They showed that entropy increases rather sharply with shortening.

These and other similar results led Morales and Botts (1953; Morales *et al.*, 1955) to suggest that the particles of myosin are elastic and that the existing length is determined by a balance between a shortening trend owing to entropy and an extensive force

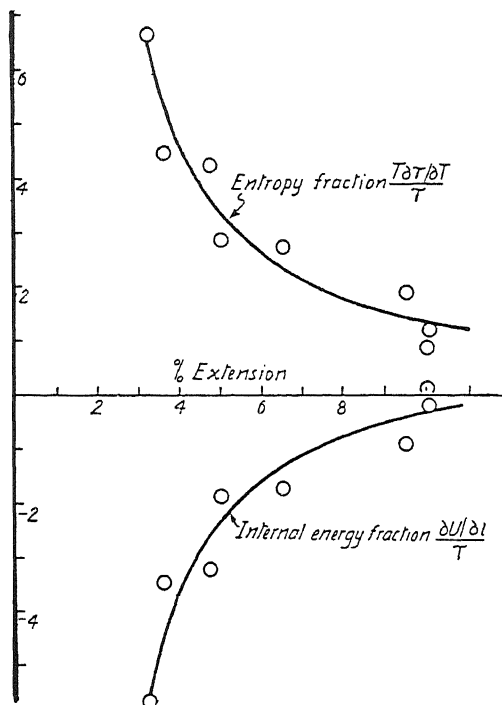


FIGURE 16.4. Resolution of the tension of undried myosin threads. [From Morales and Botts (1952), by permission of *Transactions of the Faraday Society*.]

owing to electrostatic repulsion of like charges, which may be those resulting from protein ionic side chains, adsorbed metallic ions, or adsorbed quadrivalent ATP.

In this model, like that of Szent-Györgyi mentioned previously but in sharp contrast to that of Engelhardt and Ljubimova and several other related models yet to be described, the function of ATP is not linked to the postulated high energy content of the terminal phosphate bonds. Indeed, in Chapter 5 we went into some detail discussing Podolsky and Morales's demonstration that ATP really does not have an unusually high enthalpy of hydrolysis for its terminal phosphate bonds. The Morales-Botts theory was seen by some as being experimentally contradicted (e.g., Yount *et al.*, 1971); it has also received some support (e.g., Bowen and Mandelkern, 1971). Morales and Bott's theory was further extended by Podolsky (1959).

16.1.8. The Earlier Association-Induction Model

The association-induction (AI) model differs from almost all other theories except that of MacDonald in that in this model intracellular K^+ exists in an adsorbed state, and through this, K^+ plays a key role in muscle contraction.

In the Ling fixed-charge hypothesis (Section 4.4) (Ling, 1952), as in the theories

of Riseman and Kirkwood and of Morales and Botts, direct electrostatic repulsion provided the force for the maintenance of the lengthened relaxed state. In contrast to the Riseman-Kirkwood and Morales-Botts theories, the contracted state was seen to involve the formation of inter- and intramacromolecular salt linkages between negatively charged β - and γ -carboxyl groups, which in the resting state are "lubricated" by adsorbed K^+ , and fixed cations. Figure 4.10 illustrates this view. (According to this theory, ATP-induced shortening of glycerinated muscle, which involves a change from a stiff muscle to a relaxed one, is a more suitable model for the relaxation process than the contraction process.) Among evidence cited in favor of this model are the following facts:

1. It is well known that relaxed muscle is elastic while contracted muscle is much more rigid. In the words of Meyer and Pickens (1937), "While in the resting muscle the links of neighboring chains are able to slide freely over each other, like the molecules in a liquid, in the actively contracting muscle, such 'liquid' bonds appear to be replaced by more 'solid linkages.'"
2. In muscle poisoned with IAA, there is a gradual development of stiffness or rigor. The rising tension of the poisoned muscle could be held in check by cooling, which slows down ATP decomposition. When temperature is raised, the faster rate increase of tension resumes (Fig. 16.5). The temperature effect on

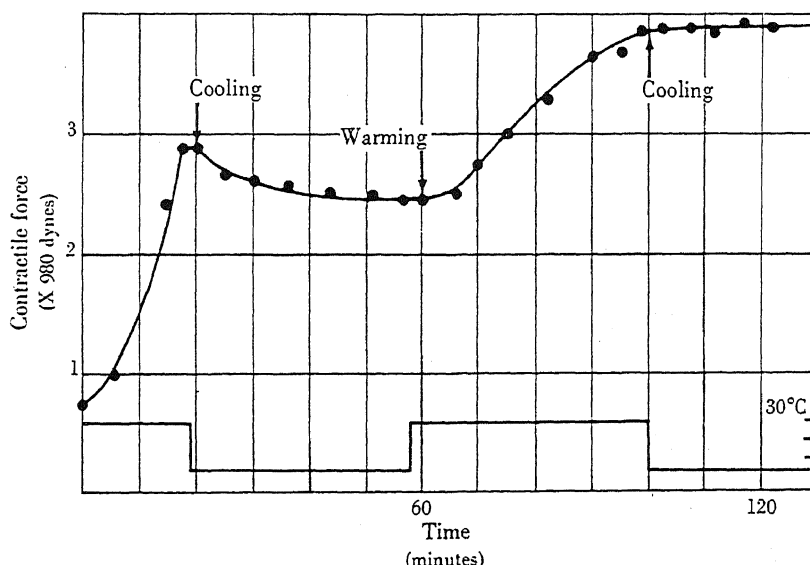


FIGURE 16.5. Effect of temperature on the tension developed by a frog sartorius muscle poisoned with 5 mM IAA. Ordinates: Tension in grams, temperature in degrees centigrade. Abscissa: Time in minutes. The tension was recorded with an isometric lever. The lower curve indicates the variations of temperature, the upper the variations in tension of K^+ . A curve essentially like this is obtained if the isotonic shortening is recorded and plotted against time. [From Ling (1952), by permission of Johns Hopkins University Press.]

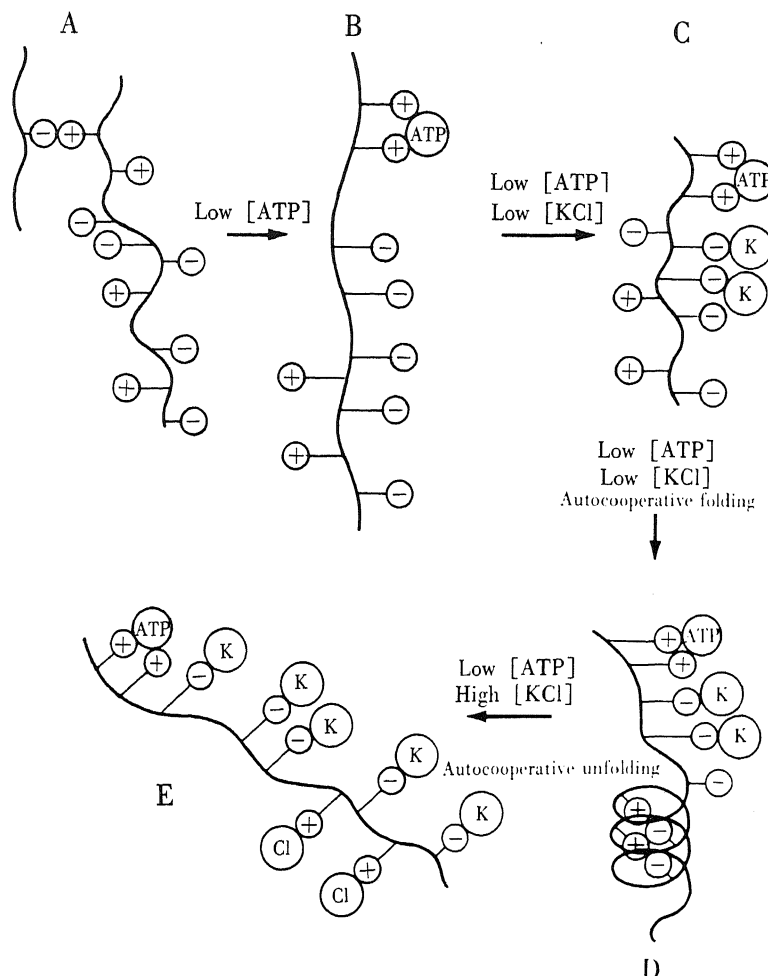


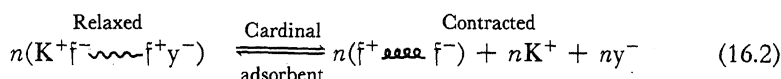
FIGURE 16.6. Interpretation of superprecipitation phenomena in terms of the AI hypothesis. A viscous state of the protein in the absence of ATP (A) indicates the existence of occasional intermolecular ligands. (B) This changes to a state of low viscosity by adsorption of quadrivalent ATP. The protein molecule then exists in more or less extended form and is kept from entangling with other protein molecules by its gross electrostatic charge at the very low ionic strength, where there is little ion-cloud shielding effect. (C) Introduction of a small amount of salt, KCl, leads to adsorption of some K^+ and the effective elimination of the net electrostatic charges that keep the chain in the extended form. (D) This is followed by an autocooperative folding, leading to superprecipitation. (E) Further addition of KCl leads to autocooperative unfolding. [From Ling (1962).]

tension development is paralleled by a loss of K^+ from the muscle. Additional evidence showing that muscle contraction is associated with K^+ release will be presented in Section 16.5.4.2 (see also Hardt and Fleckenstein, 1949).

In 1962, as part of the AI hypothesis, this simple model was revised. Its basic

elements are indicated in Fig. 16.6 in the context of the superprecipitation phenomenon noted in Fig. 16.3.

1. The functional role of ATP in keeping the muscles in a lengthened, relaxed state was changed. Its direct electrostatic repulsive effect mediated through space was replaced by one in which the propagated inductive effect (or indirect *F*-effect) plays the major role. In other words, ATP acts as a cardinal adsorbent.
2. Autocooperativity was offered to interpret the all-or-none nature of superprecipitation (Fig. 16.3) with changes in KCl, as well as the all-or-none nature of normal contraction.
3. Using a coiled–uncoiled model, contraction was represented as being due to the formation of salt linkages between fixed cations (f^+ : ϵ -amino, guanidyl, and histidyl groups) and fixed anions (f^- : mostly β - and γ -carboxyl groups), displacing adsorbed K^+ :



4. The cardinal adsorbent ATP functions by its strong adsorption onto key protein sites and the effect is achieved by electrical polarization. Contraction is initiated by ATPase activity, which dephosphorylates ATP into ADP and P_i , which have much weaker binding energies.

16.2. Current Views of the Mechanism of Muscle Contraction

In the 40 some years since Englehardt and Ljubimova's finding galvanized students of muscle physiology, a great deal of progress has been made. Key discoveries in three different areas made possible the development of a coherent view of muscle contraction.

16.2.1. The Sliding Filament Theories

The first progress was made with the rediscovery that myosin is located in the A bands and with the recognition that actin makes up the bulk of the I band proteins (Hanson and Huxley, 1953; Hasselbach, 1953). Both myosin and actin were shown to exist as filaments running parallel to each other. In relaxed muscle, the thin actin filaments overlap with the thick myosin filaments only at the edges of the A band (Fig. 16.7). In a cross-section of the overlapping region, a regular array of actin and myosin filaments can be seen. Each myosin filament is surrounded by six immediately neighboring actin filaments, and each actin filament is surrounded by three myosin filaments (H. E. Huxley, 1953a) (Fig. 16.8A). During shortening or when the muscle is stretched, the lengths of the myosin filaments and of the actin filaments do not change (H. E. Huxley and Hanson, 1954; A. F. Huxley and Niedergerke, 1954); rather, a sliding motion of these filaments, like that of a telescope, produces the shortening or lengthening of the muscle.

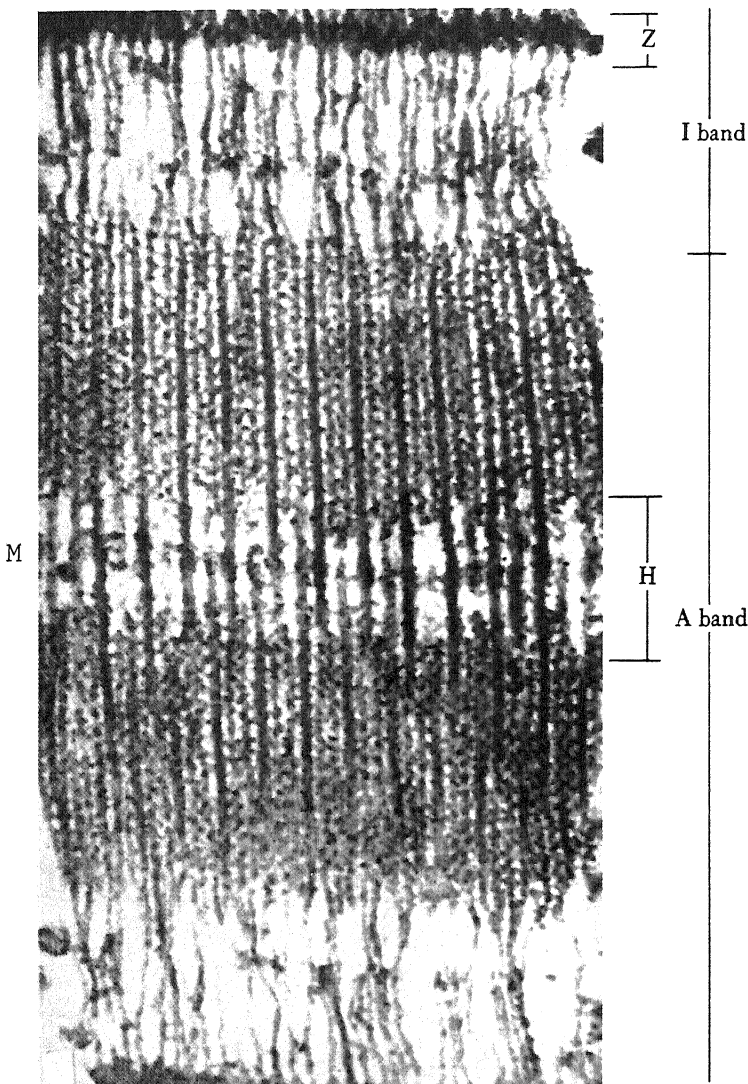


FIGURE 16.7. Electron micrograph of a longitudinal section of rabbit psoas muscle fixed and stained in osmium tetroxide. [H. E. Huxley (1957); reproduced from Ling (1962).]

The story behind this set of conclusions represents one of the most brilliant pages in man's search for the physical basis of life.

Using a specially designed low-angle camera and a fine-focus X-ray tube designed by Ehrenberg and Spear (1951), Hugh E. Huxley (1951, 1953b) investigated the low-angle X-ray equatorial diffraction pattern of living frog sartorius muscle and living rabbit psoas muscle and compared them with these muscles after they had gone into rigor

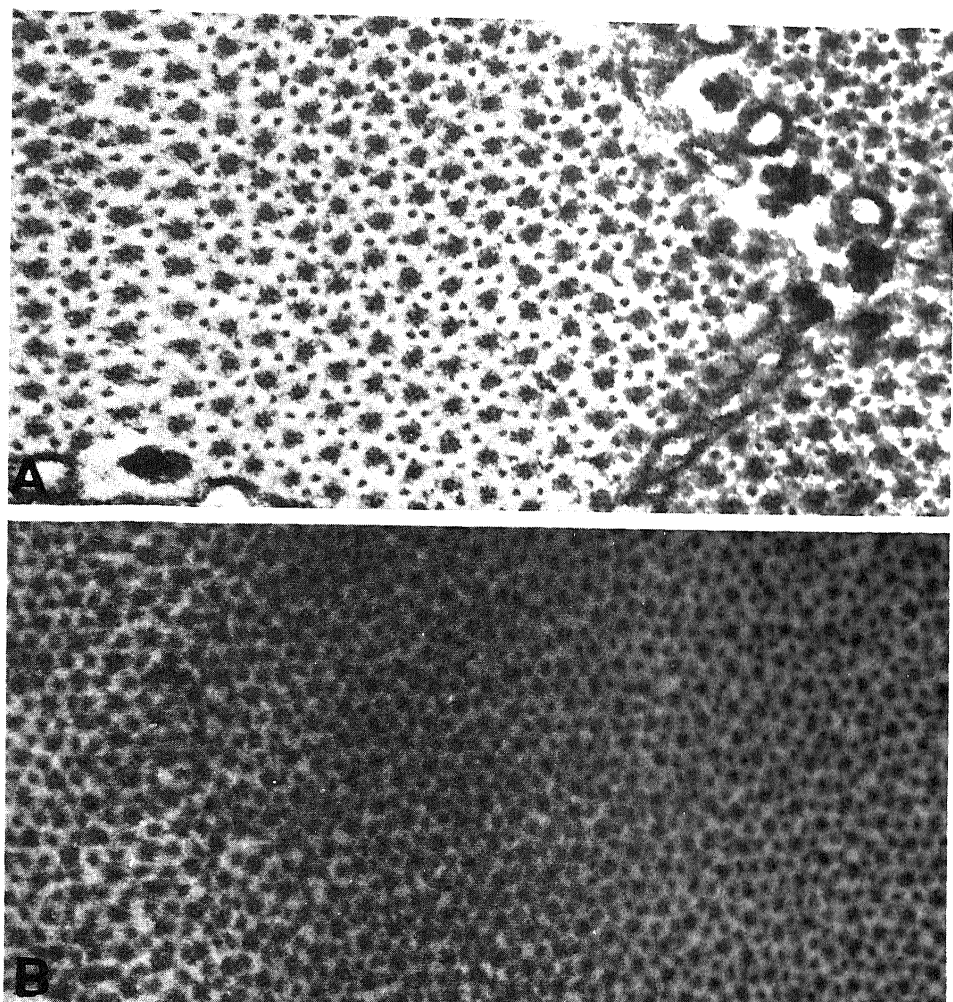


FIGURE 16.8. (A) Electron micrograph of cross-section of live frog sartorius muscle fixed and processed in conventional manner (glutaraldehyde fixation, osmium tetroxide postfixation, Araldite embedding). The thin actin-containing filaments can be seen at the trigonal points of the hexagonal lattice of thick myosin-containing filaments. The myosin filaments have a considerably larger diameter than the actin filaments. Angular penumbra probably represent the projected view of all the cross-bridges in the section. Rabbit psoas muscle, fixed live, has a similar appearance. Magnification 150,000 \times . (B) Electron micrograph of cross-section of glycerinated rabbit psoas muscle, fixed and processed in exactly the same way as the live muscle shown in (A). Thick and thin filaments can be seen in a hexagonal arrangement (not as well ordered as in live muscle), with the thick filaments again at the lattice points and the thin filaments in the trigonal positions. However, the thick filaments now have a considerably smaller diameter than those seen in live muscles (and the thin filaments a larger diameter). Magnification 150,000 \times . [From H. E. Huxley (1968), by permission of *Journal of Molecular Biology*.]

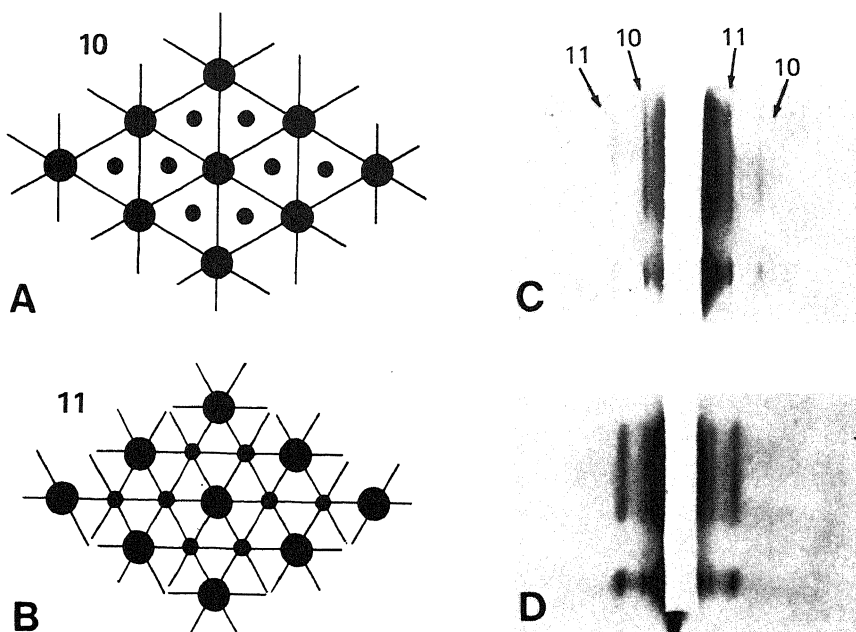
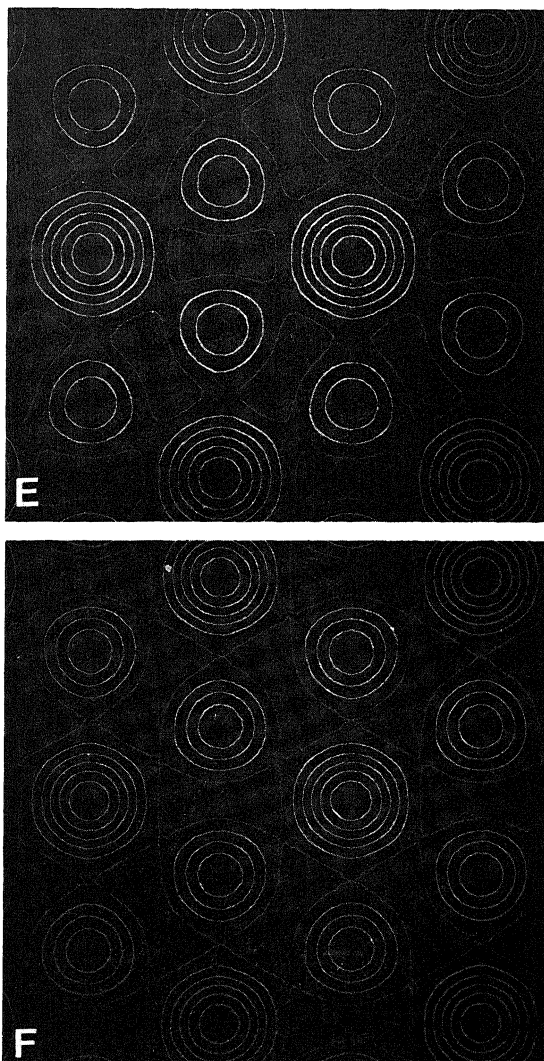
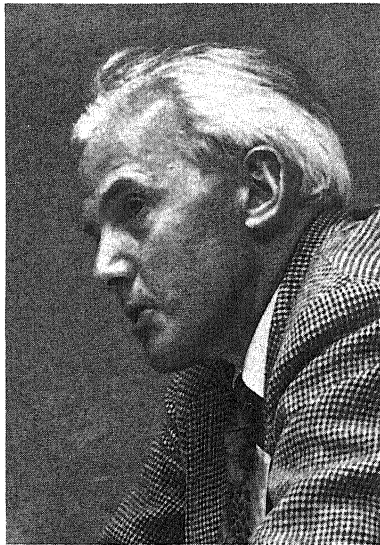


FIGURE 16.9. (A) End-on view of double hexagonal lattice of thick and thin filaments, characteristic of overlap region in A bands of vertebrate striated muscle, showing the three sets of lattice planes in the 10 crystallographic direction. The actin filaments at the trigonal points of the lattice will tend to fill in the space between the dense planes of filaments at the hexagonal lattice points, thereby decreasing the intensity of the 10 X-ray reflections given by the thick filaments on their own. (B) Similar view, showing lattice planes in the 11 crystallographic direction. In this case, both the actin and myosin filaments lie in the same lattice planes and so their contributions to the intensity of the corresponding X-ray reflection are additive. Hence, as the amount of material at the trigonal points is increased, the intensity of the 10 reflections decreases and that of the 11 reflections increases. (C,D) Equatorial X-ray diffraction diagrams from frog sartorius muscle at equilibrium length ($s = 2.0 \pm 0.05 \mu\text{m}$), showing the 10 and 11 reflections from the myofilament lattice. (C) Living muscle (in which the 10 reflection is appreciably stronger than the 11). (D) Rigor muscle (in which the 11 reflection is much stronger than the 10). (E) "End-on" Fourier projection of live sartorius muscle of frog (using 10 and 11 reflections), showing large peaks of electron density at the lattice points, much smaller than at the trigonal positions. (F) Corresponding Fourier projection for frog sartorius muscle in rigor, showing much larger peaks of electron density in the trigonal positions. [A,B, after Huxley (1971), by permission of *Proceedings of the Royal Society of London, Series B*; C-F, from Huxley (1968), by permission of *Journal of Molecular Biology*.]

by treatment with IAA or glycerol, or simply spontaneous deterioration. Figure 16.9A partially reproduces Huxley's diagram showing that, in the double hexagonal lattice of thick and thin filaments, there are three sets of lattice planes in the crystallographic 10 direction. Note that only the thick myosin filaments contribute to the intensity of these X-ray reflections. On the other hand, in the crystallographic 11 direction, the lattice planes are so oriented that both the thick and thin filaments contribute to the reflection intensity. Figure 16.9C shows the observed equatorial X-ray diagram of living frog sar-

FIGURE 16.9 (*Continued*)

torius muscle, showing 10 reflections stronger than the 11 reflections. However, after the muscle has gone into rigor, the X-ray diagram has drastically changed. The 11 reflections have markedly increased their intensity. Figure 16.9E shows an "end-on" Fourier projection of live frog sartorius muscle, using 10 and 11 reflections, demonstrating large peaks of high electron density at lattice points and much smaller density at the trigonal position. Frog muscle in rigor (Fig. 16.9F) shows much larger peaks at the trigonal positions.



Hugh E. Huxley

The increased electron density at the trigonal positions with development of rigor was beautifully corroborated by electron microscopic (EM) studies of a glutaraldehyde-osmium-tetroxide-fixed preparation. In plates prepared from fresh relaxed muscle (Fig. 16.8A) there is little ambiguity between the much larger thick filaments and the much smaller thin filaments. However, after development of rigor, the thick filaments became narrower while the thin filaments became much bigger. Indeed, at a superficial glance, the filaments seem now almost of the same size (Fig. 16.8B). This change in electron density was interpreted as a result of the formation of cross-bridges in which the myosin heads reach out to join the thin filaments, thereby adding electron density to the thin filaments.

More recently, H. E. Huxley and his co-workers (Huxley *et al.*, 1980, 1981) studied the low-angle X-ray diagrams of living frog sartorius muscles with the aid of a new source of high-intensity X rays: synchrotron radiation. This new technique allowed very rapid (time resolution, 1 msec) changes of X-ray reflections to be recorded. Already details of changes during a contraction have been noted.

Besides the frog sartorius, rabbit psoas, and blowfly muscles, a favorite subject of investigation is the dorsal longitudinal muscle of the giant tropical beetle *Lethocerus maximus*. When these muscles are extracted with glycerol and held in simple salt solution containing 50 mM KCl, 5 mM MgCl, 4 mM ethanedioxy-bis(ethylamine) tetraacetic acid (EGTA), and 10 mM Tris (pH 7.15), they are in a state of rigor. The low-angle X-ray diffraction pattern, in conjunction with electron microscopy, led Reedy, Holmes, and Tregear (1965) to suggest the structure shown in Fig. 16.10(left). Note that the cross-bridges between the thick myosin and thin actin filaments were polarized

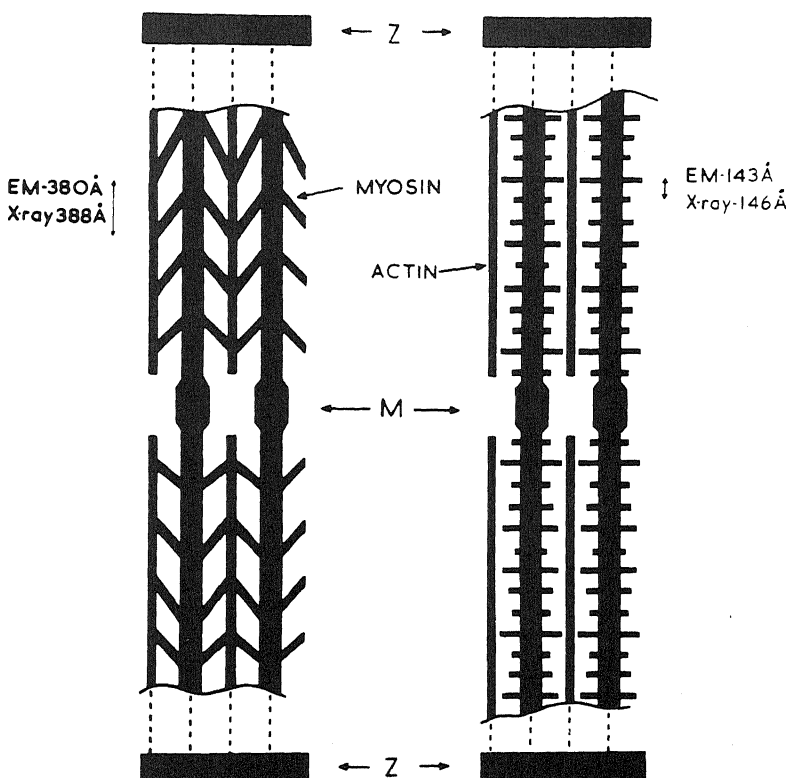


FIGURE 16.10. Diagrams of single layers of actin and myosin filaments, showing cross-bridge positions found to be characteristic of (left) rigor and (right) relaxed states of glycerinated insect flight muscle. Thick filaments represent myosin, from which cross-bridges extend toward actin (thin) filaments. On the right, the variation in length of projections represents varying azimuthal positions of bridge pairs around myosin filaments. The exact azimuthal interval is not known but is apparently near 60°. [From Reedy *et al.* (1965), by permission of *Nature*.]

in a uniform manner, giving rise to an arrowheadlike appearance and pointing in the opposite directions on either side of the M line.

If ATP is now added to the glycerinated muscle in the solution mentioned above, the muscle immediately loses its stiffness and becomes flexible, as is usually seen in normal relaxed muscle (Jewell and Rüegg, 1966). The X-ray diffraction and EM picture now takes on a new pattern, depicted in Fig. 16.10(right). The cross-bridges are no longer slanted but are at right angles to the backbone. The varying lengths of the detached cross-bridges shown are intended to represent their different spatial orientations. For a more explicit illustration of the orientation of the cross-bridges, see H. E. Huxley and Brown (1967).

Important experimental support for this sliding filament theory of muscle contraction came from an old observation by Ramsey and Street (1940) of the relation between tension and the length of an isometrically contracting single isolated muscle fiber. A. F. Huxley's figure presenting Ramsey and Street's data, as well as the confirmatory data

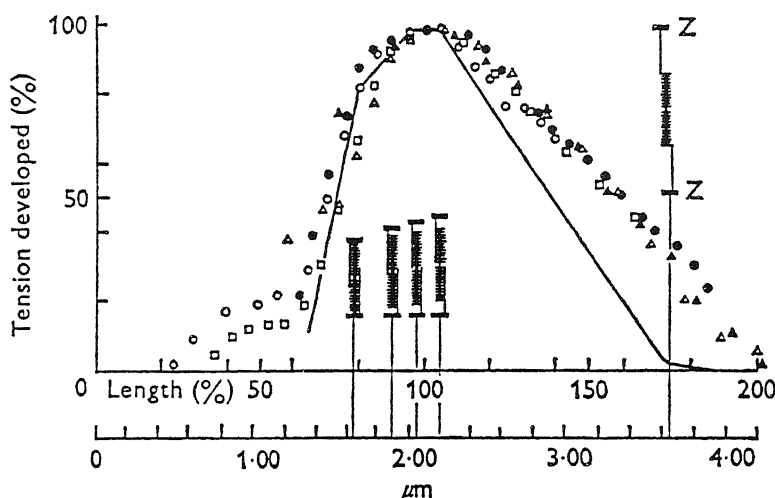


FIGURE 16.11. Length-tension relation in isolated frog muscle fibers. Ordinate: Isometric tetanus tension developed (total tension during tetanus minus resting tension); percent of maximum. Points: From Ramsey and Street (1940). Length expressed as percentage of slack length, which was also the length where developed tension was a maximum. Continuous lines: Length-tension relation found by Gordon *et al.* (1966). Lower abscissa scale gives striation spacing in micrometers. Drawn so that $2.05 \mu\text{m}$ striation spacing, the average slack length, corresponds to 100% on Ramsey and Street's length scale. Diagrams show critical stages in the degree of overlap of the filaments. At all striation spacings above about $2.0 \mu\text{m}$, the developed tension found by Gordon *et al.* is closely proportional to the number of thick filament projections overlapped by thin filaments. [From A. F. Huxley (1974), by permission of *Journal of Physiology*.]

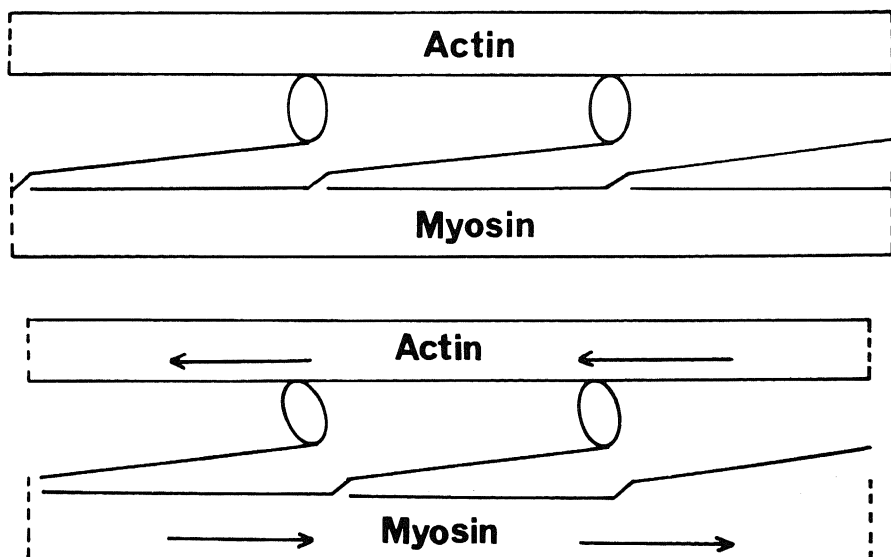


FIGURE 16.12. Possible mechanisms for producing relative sliding movement by tilting of cross-bridges. If separation of filaments is maintained by electrostatic force-balance, tilting must give rise to movement of filaments past each other. [From H. E. Huxley (1969), by permission of *Science*.]

of Gordon, Huxley, and Julian (1966), is reproduced here as Fig. 16.11. These findings agree with the concept that only in the regions of overlap of myosin and actin are the filaments joined together to create tension.

The question of how the overlapping myosin and actin filaments develop tension is still in the investigational stage. Most workers seem to agree that before contraction the myosin and actin filaments are not bound to each other, as already suggested by Szent-Györgyi, but that during contraction cross-bridges are formed between actin filaments and the protruding head portion of the myosin filaments (A. F. Huxley, 1957). The tail segments join with other myosin tails to form the backbone of the heavy filaments and are relatively inflexible. The head, two to a myosin filament, contains not only the actin attachment site but also the ATPase site (see Fig. 16.12).

As mentioned earlier, muscle maintains a constant volume during contraction. This demands that, with shortening, the space between thin and thick filaments must expand (see Fig. 16.1). To accommodate this, it was suggested that the myosin head and neck region have flexible hingelike joints which permit continued contact with actin filaments, with an increased distance between the filaments during contraction. Thus H. E. Huxley presented in 1969 a diagram showing how relative sliding motion could be produced by tilting the head of myosin filaments (Fig. 16.12). A ratchetlike mechanism was given by A. F. Huxley and Simmons in 1971.

16.2.2. The Kinetics of the Unregulated Actin–Myosin–ATP System

At physiological ionic strengths and pH, ATP brings about superprecipitation of actomyosin (Fig. 16.3). It is very difficult to study the insoluble superprecipitated actomyosin. Fortunately, a solution to this difficulty has been developed. It was discovered a long time ago that trypsin can break myosin molecules into two fragments, light meromyosin (LMM) and heavy meromyosin (HMM) (Gergeley, 1950; Mihalyi and A. G. Szent-Györgyi, 1953). As illustrated in Fig. 16.13, LMM comprises the tail region of the myosin molecule while HMM makes up the neck and head (A. G. Szent-Györgyi, 1960). Further enzymatic hydrolysis of HMM with papain yields two subfragments: subfragment 1 (HMM S-1) and subfragment 2 (HMM S-2). HMM S-1, or S-1,

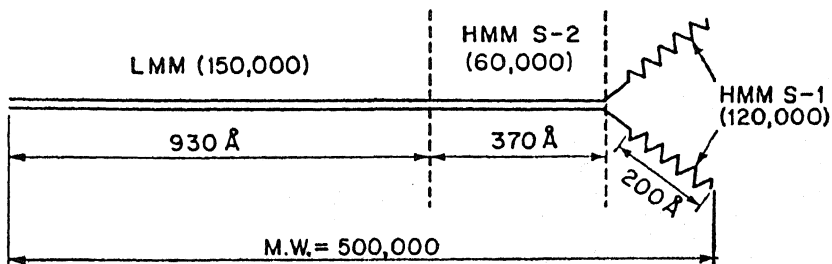


FIGURE 16.13. Diagram of a myosin molecule, as visualized by electron micrographs taken after rotary shadowing of the specimen. LMM, light meromyosin; HMM S-2, heavy meromyosin subfragment 2; HMM S-1, heavy meromyosin subfragment 1. (Note that the long straight portion of the molecule is shown here as two parallel straight rods, which in fact are twisted about one another to give a helical coiled-coil structure.) [From Bendall (1969), by permission of American Elsevier.]

retains all the enzyme- and actin-combining properties of the parent myosin molecule. Since HMM and S-1 fragments are both soluble in dilute salt solutions, they provide convenient models to study quantitatively the pre-steady-state and steady-state kinetics of interactions among myosin, actin, and ATP. Major efforts in this direction came primarily from the laboratories of Bagshaw, Taylor, and Eisenberg (Bagshaw *et al.*, 1974; Taylor, 1979; E. Eisenberg and Greene, 1980; Adelstein and Eisenberg, 1980). The details of this fascinating and extensive field of study cannot be presented, but a very brief sketch will be given.

On mixing pure actin and HMM or S-1, a soluble complex, acto-HMM or acto-S-1, is formed. ATP almost immediately binds to HMM or S-1. The enormous binding constant, 10^{10} - 10^{11} M^{-1} (Goody *et al.*, 1977; Cardon and Boyer, 1978), makes this binding virtually irreversible. Two major findings from these studies are that (1) ATP binding greatly weakens the binding of actin to the myosin head and (2) the binding of actin to the myosin head activates the ATPase activity of the myosin head (E. Eisenberg and Moos, 1968, 1970). Lynn and Taylor (1971) in their classic pre-steady-state kinetic study, revealed that the rate of dissociation of acto-HMM by ATP was much faster than the rate of ATP hydrolysis. It was then thought that ATP hydrolysis occurred only after dissociation of actin. Later, Stein, Schwartz, Boon Chock, and Eisenberg (1979) showed that, at high actin concentration, a substantial fraction of ATP is hydrolyzed while actin and the myosin tail are still associated.

ATP hydrolysis is fast. Yet neither of the products, ADP or P_i , is immediately released (Tonomura *et al.*, 1969). After a short delay, P_i is released, creating the so-called initial P_i burst. Since the P_i burst occurs much faster than the cyclic rate of ATP hydrolysis, Lynn and Taylor suggested that the rate-limiting step in the cycle is the release of bound P_i and ADP. Eisenberg and his co-workers, on the other hand, suggested that, following ATP hydrolysis, the myosin head (whether dissociated from actin or not), goes through a refractory state. Only in a subsequent nonrefractory state are P_i and ADP released in sequence so that actin and the myosin head can recombine. In this model, the bottleneck of the overall cyclic ATPase activity is the refractory state.

16.2.3. The Control Mechanism

16.2.3.1. The Role of Ca^{2+}

In 1957 Porter and Palade described the fine structure of the system of longitudinal and transverse (T) tubules and vesicles that wrap around each myofibril in skeletal muscle cells and together constitute the sarcoplasmic reticulum (SR). Figure 16.14 reproduces a diagrammatic illustration of the SR from Porter and Bonneville (1968), who described the T tubule system as a "grid perforated by large pores through which the myofibrils pass" (see Peachey, 1965, for more details on the SR). The T tubule is a direct invagination of the plasma membrane, its lumen in direct communication with the outside but not with the cavities of the SR or any other space in the cell. The SR and the T system are closely associated with the myofibrils. These anatomical structures took on great significance following two other major discoveries.

An important part of muscle "contraction" is its relaxation. Albert Szent-Györgyi demonstrated ATP-induced shortening of glycerinated muscle fiber. Much effort was

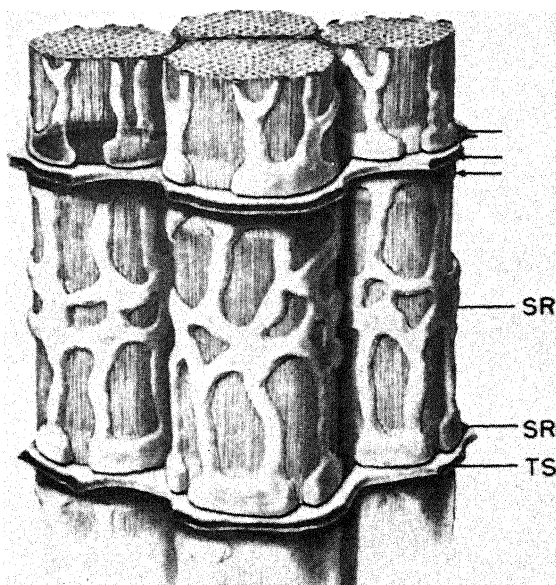


FIGURE 16.14. Three-dimensional drawing designed to clarify the structural relationship between the myofibrils and two smooth membrane systems, the sarcoplasmic reticulum (SR) and the T system (TS), found in skeletal muscle fibers. SR' is the expanded portion of the SR in the region of the I band. [From Porter and Bonneville (1968), by permission of Lea and Febiger.]

devoted to find relaxing factors that reverse the shortening. Among them was the so-called Marsh factor (B. B. Marsh, 1952), discovered by Marsh while he was working in the laboratory of Bailey. This is an aqueous extract of muscle with very interesting properties. While ATP alone causes a muscle homogenate to shrink, ATP plus the Marsh factor causes the muscle homogenate to swell. The active principle in this extract was identified with the granular ATPase isolated earlier by Kielley and Meyerhof (1950) (K. Fujita, 1954; Kumagai *et al.*, 1955).



Setsuro Ebash

In 1959, A. Weber first pointed out that this ATPase activity of myofibrils depends on the presence of a low concentration of Ca^{2+} . In 1960 Setsuro Ebashi demonstrated a perfect correlation between the Ca^{2+} -binding constant of a collection of Ca^{2+} chelators and their effectiveness in relaxing contracted glycerinated fibers. A. Weber and Winicur (1961) demonstrated that Chelex 100 resin beads, as well as EGTA, both of which have strong affinity for Ca^{2+} , inhibit superprecipitation of actomyosin by ATP- Mg^{2+} . They concluded that removal of Ca^{2+} was the factor causing relaxation.

Along with these developments, it was discovered that the isolated relaxing factor, which can accumulate Ca^{2+} in the presence of ATP (Ebashi, 1960; Hasselbach and Makinose, 1960, 1961), contains elements of the SR (Nagai *et al.*, 1960; Ebashi, 1961; Ebashi and Lipmann, 1962). In their review in 1968, Ebashi and Endo presented a schematic diagram (Fig. 16.15) which shows how addition or removal of Ca^{2+} controls the association (i.e., superprecipitation) and dissociation of actin and myosin by shifting Szent-Györgyi's superprecipitation curve (Fig. 16.3) along the abscissa.

In the mid-1950s, A. F. Huxley and R. Taylor (Huxley and Taylor, 1958; Huxley and Straub, 1958) discovered that the T tubule system provides the link between the action potential and the spread of the electrical impulse into the interior of the fiber (Constantin and Taylor, 1971). It was suggested that depolarization of the membrane system of the T tubules triggers the depolarization of the membrane of SR and that a release of stored Ca^{2+} then follows (Ebashi, 1965; Peachey, 1965).

Experimental proof that Ca^{2+} is indeed released during excitation came from experiments using the Ca^{2+} -sensitive dye murexide introduced into toad muscle (Jöbsis and O'Connor, 1966) and from others using the Ca^{2+} -sensitive protein aequorin injected into barnacle muscle (Ridgeway and Ashley, 1967) and single frog muscle fibers (Rüdel

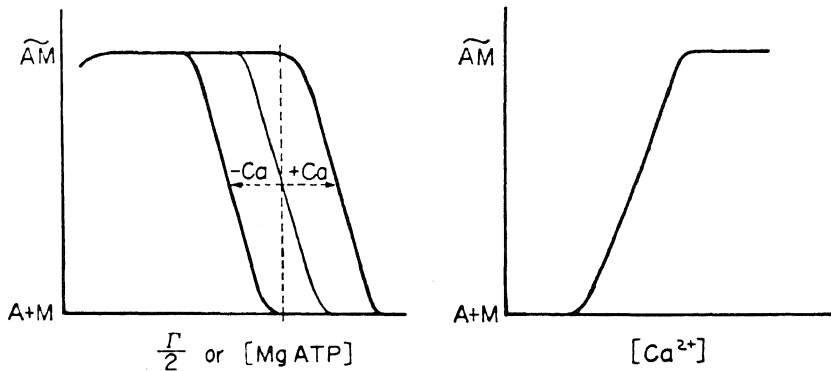


FIGURE 16.15. Schematic presentation of the effect of Ca^{2+} on the response of the actomyosin system to ATP. AM, response of the actomyosin system, which corresponds to contraction; A + M, response which corresponds to relaxation. The figure on the right represents the response of the actomyosin system as a function of Ca^{2+} under the condition indicated by the perpendicular line in the figure on the left. As indicated in the designation A + M, it is usually assumed that in the relaxed state myosin and actin are dissociated, with no interaction existing between the two proteins. This interpretation may apply in the case of organized actomyosin systems, as represented in intact fibers or myofibrils, but may not apply so well in the case of disorganized systems, particularly acto-H-meromyosin. [From Ebashi and Endo (1968), by permission of *Progress in Biophysics and Molecular Biology*.]

and Taylor, 1973). Although in each case, an increase of Ca^{2+} activity in the muscle cell was demonstrated, none of these experiments gave an estimate of the absolute threshold concentration of Ca^{2+} for excitation. The threshold value was obtained by altogether different means, as shall now be described.

Natori (1954, 1955) developed a method for removing the sarcolemma (the surface membrane) of single isolated frog muscle fibers. Using this method Hellam and Podolsky (1969) and Endo and Tanaka (see Ebashi and Endo, 1968) studied the threshold concentration of Ca^{2+} needed to induce contraction. The data of Endo and Tanaka indicated a threshold pCa (i.e., the logarithm of the reciprocal of Ca^{2+} concentration in molarity) of 5.9 and maximum tension at pCa less than 6. These data suggest that the release of Ca^{2+} causes pCa in the cell to rise above a threshold value for contraction and that contraction follows as a result.

Many scientists believe that the subsequent relaxation of a contracting muscle is due to the lowering of myoplasmic Ca^{2+} as a consequence of the return of Ca^{2+} to the SR by the activation of a postulated Ca^{2+} pump in the SR membranes. However, Ebashi and Endo in their review wrote that "some workers [apparently including Ebashi and Endo themselves] insist that Ca^{2+} ion is first bound to some structure in the membrane and mostly retained in this state" (see also Carvalho and Leo, 1967).

16.2.3.2. Tropomyosin and Troponin

Thus far our discussion has included two components of the contraction apparatus, actin and myosin, which together make up about 80% of muscle proteins. In fact, there are several other components, including tropomyosin. Tropomyosin was discovered in 1946 by Bailey. The original method of extraction, with minor modification, remains in use today. As Bailey noted, isolated tropomyosin can be made to polymerize or depolymerize simply by removing or adding salt (Bailey, 1948).

In 1956 Perry and Grey noted in a short communication that "synthetic" actomyosin prepared by mixing purified myosin and purified actin behaved quite differently from "natural" myosin B in the presence of ethylenediamine tetraacetic acid (EDTA). This work, after being neglected for some time, eventually received recognition and repeated confirmation when it was realized that the effect of EDTA was to remove Ca^{2+} (A. Weber and Winicur, 1961). With the aid of this hint, Ebashi and Ebashi (1964) isolated a protein which, when added to synthetic actomyosin, make it behave just like myosin B. This protein resembles tropomyosin but is different. Using Bailey's procedure, a large amount of tropomyosin could be obtained from the actomyosin, so the authors decided to call it *native tropomyosin*. Eventually Ebashi and Kodama (1965, 1966) showed that native tropomyosin consists of two proteins: Bailey's tropomyosin and a new globular protein which they named *troponin*.

Native tropomyosin binds to actin but not to myosin. When troponin and tropomyosin are both added to synthetic actomyosin they confer on it a marked sensitivity to Ca^{2+} , as illustrated in Fig. 16.16. Neither troponin nor tropomyosin alone can do the same. Using a variety of antibody staining methods, it was established that troponin binds to thin filaments. In each sarcomere 24 periods marked by troponin can be counted in the I band on either side of the Z line.

The next question is: Which of the four components—actin, myosin, tropomyosin,

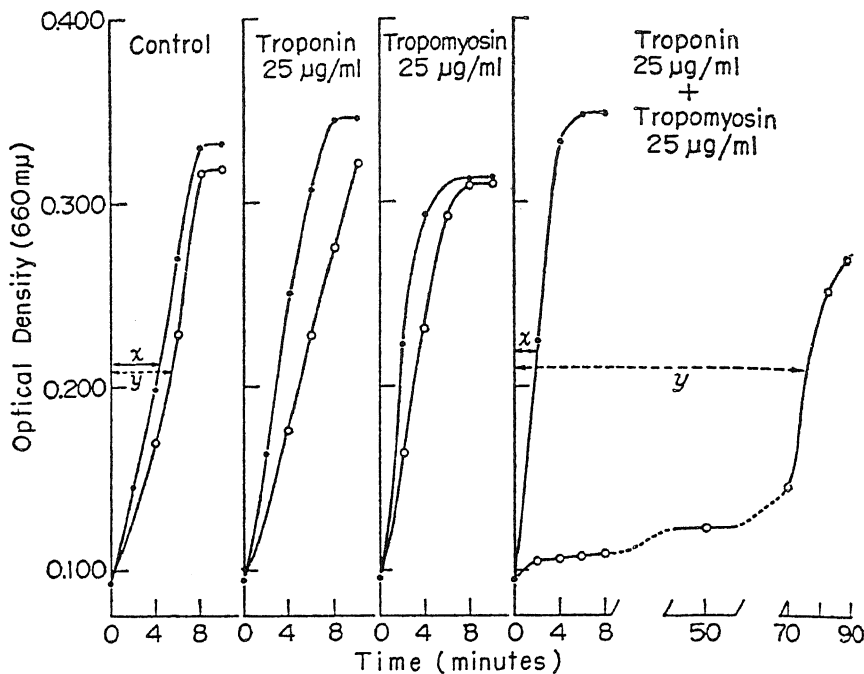


FIGURE 16.16. Reconstitution of native tropomyosin from troponin and tropomyosin. Effect of troponin, tropomyosin, and their complex on the superprecipitation of native tropomyosin-free actomyosin. O, In the presence of 2.5×10^{-4} M of the chelator glycoletherdiamine-tetraacetic acid (GEDTA) (estimated concentration of Ca^{2+} 5×10^{-7} M). ●, In the presence of added 1×10^{-3} M Ca^{2+} (estimated concentration of Ca^{2+} 1.3×10^{-3} M). Final concentrations of ingredients in the reaction mixture were 0.01 M KCl, 4 mM MgCl_2 , 0.02 M Tris-maleate buffer (pH 6.8), 0.5 mM ATP, and 0.75 mg/ml of native tropomyosin-free actomyosin. Reactions were started by adding ATP at zero time. [From Ebashi and Endo (1968), by permission of *Progress in Biophysics and Molecular Biology*.]

or troponin—offers the binding site for Ca^{2+} ? This question was resolved by Ebashi *et al.* (1967) in an ingenious way. It was known that the contractile system of cardiac muscle has five times greater sensitivity to Sr^{2+} than that of skeletal muscle. By isolating each of the four proteins from both cardiac and skeletal muscles, and combining them in various ways, it was recognized that sensitivity to Sr^{2+} is localized entirely in the troponin.

It turns out that troponin also is a complex protein, made up of several components with different functions (Hartshorne and Müller, 1968). Troponin from rabbit muscle has three subunits: calcium-combining subunit (TN-C), inhibitory subunit (TNI), and tropomyosin-binding subunit (TN-T) (Greaser and Gergely, 1971).

16.2.3.3. Regulation Mechanism

X-ray diffraction (Haselgrove, 1973; H. E. Huxley, 1973) and studies of actin paracrystals (Wakabayashi *et al.*, 1975) both suggested that tropomyosin shifts its posi-

tion on the actin filament after Ca^{2+} binds to TN-C. Relaxation occurs when tropomyosin rotates away from the center of the groove of the actin filament, thereby blocking the attachment of the myosin head to actin. This occurs when no Ca^{2+} is present. When Ca^{2+} binds to TN-C, the troponin molecules then allow the tropomyosin to shift to the contracting position. This is the widely accepted steric blocking model of Haselgrove and Huxley. However, more recent experimental findings do not agree very well with this model (see Seymour and O'Brien, 1980; Eaton, 1976; Yang *et al.*, 1977). In its place Adelstein and Eisenberg (1980) favor an allosteric interpretation. The tropomyosin-troponin actin-based regulation system described above applies only to vertebrate skeletal and cardiac muscle. Two other major types of regulation systems have been discovered.

In molluscs, one form of myosin-based regulation is seen in which a specific myosin light chain is inhibitory unless Ca^{2+} binds to the myosin and relieves the inhibition (Kendrick-Jones *et al.*, 1976).

Another type of myosin-based regulatory system is found in contractile proteins from smooth muscle and nonmuscle cells. Here activation of myosin ATPase by actin requires phosphorylation of myosin light chain, and Ca^{2+} is required for the activation of the kinase which activates phosphorylation of myosin (see Adelstein and Eisenberg, 1980).

16.2.4. Other Recent Theories of Muscle Contraction

The sliding filament model for the contraction of striated muscle has become widely accepted. Yet there is no clear consensus on the mechanism of force generation, nor is it clear at all how ATP energizes work performance. Indeed, as Jean Hanson and H. E. Huxley (1955, p. 251) pointed out many years ago, "Appreciable shortening of filament . . . is . . . not a necessary concomitant [*sic*] of the basic process of contraction; in fact, it may merely be the *result* of it."

The sliding filament model was originally suggested to explain a specific kind of motional apparatus—the striated muscle. It has been extended to explain motility of cilia and certain types of flagella (see Satir, 1974). It is not directly applicable to other contractile systems that do not possess such highly ordered filamentary arrangements (Lowy and Hanson, 1962), although attempts have been made (H. E. Huxley, 1973) to thus apply it. Paradoxically, as the sliding filament model has been gaining wide acceptance, a considerable number of alternative theories have also been presented. Some of these concepts are now briefly reviewed.

16.2.4.1. Lateral Expansion Theories

As mentioned earlier, the term *muscle contraction* is a misnomer since there is no change in cell volume during the process (Bayliss, 1927, p. 436; Huxley, 1953b; Elliot *et al.*, 1967). Dragomir (1970) suggested that muscle contraction follows a reduction of the attractive forces between the myofilaments, forces which in resting muscle hold in check a natural tendency toward lateral expansion owing to repulsive long-range forces. Dragomir considered a likely candidate for the attractive force to be that maintaining

normal water structure at the surface of myofilaments in resting muscle. Degradation of this water structure then leads to lateral expansion and shortening of the muscle cells.

Elliott, Rome, and Spencer (1970), in their *electrostatic-hydraulic theory*, contend that during contraction development of electrostatic repulsion forces between the filaments causes shortening. The frictional resistance to water flow created by the hydration of protein filaments sustains tension development.

Later Matsubara and Elliott (1972) found that frog muscle fibers whose sarcolemmas had been removed by the method of Natori (1955) did not behave isovolumetrically. Since these skinned fibers can still reversibly contract, A. F. Huxley believed that the electrostatic-hydraulic theory (and, by implication, other similar lateral expansion theories) was ruled out (A. F. Huxley, 1974). I think that this conclusion might be premature. Each single muscle fiber contains many myofibrils. Contractility and nonvolumetric behavior may not reflect concomitant behaviors of the same sarcomeres. Furthermore, in the standard relaxing solution containing 140 mM KCl that Matsubara and Elliott used, the muscle fibers were swelling steadily (see Figs. 13.9 and 13.10A; also Ling and Peterson, 1977). This inadvertent volume change might confuse the attempt to demonstrate an isovolumetric behavior or the lack of it.

Another version of a lateral expansion theory is due to Ullrick (1967), who suggested that contraction is brought about by a lateral expansion of the Z disk. The tension thus exerted on the sarcolemma causes the telescoping of the filaments and shortening of the muscle.

16.2.4.2. Electrostatic Theories

Yu, Dowben, and Kornacker (1970) suggested that the thick and thin filaments carry opposite electric charges. As a result, a force is generated which strives to maximize the amount of overlap of these filaments. A different type of electrostatic theory was suggested by Iwazumi (1970), who argued that, in the contracting muscle, the thin filaments have a low dielectric constant and high electric conductance when compared to the myoplasmic medium filling in the space between the thick filaments in a resting muscle. As a result a force is generated, pulling the thin filament in.

16.3. Critique of the Sliding Filament Model

For systems as complex as living things, it is obvious that no single concept, no matter how brilliantly conceived and masterfully proven, can explain all aspects of the issue. Meaningful progress must depend on continued improvements. In these efforts, constant vigilance to recognize the weakness of an otherwise attractive theory and to remedy it accordingly is vital. In each of the alternative theories mentioned in the last section, defects of the sliding filament model have been explicitly or implicitly expressed. The following is a selection of other concepts to which the sliding filament model has deliberately or inadvertently been linked which I believe worthy of further discussion.

16.3.1. The Energy Problem

Even though many years have gone by since the establishment that ATP does not contain a special package of energy to be used for work performance of all sorts (see

Chapter 10), some prominent scientists propounding the sliding filament theory of muscle contraction continue to believe that "the energy for muscle contraction, as for most other work in living cells, is provided by the hydrolysis of adenosine triphosphate (ATP). This breakdown reaction splits the high energy ATP into lower energy products: adenosine diphosphate (ADP) and inorganic phosphate. The difference in the energy content of these compounds is available to do useful work. . . ." (Murray and Weber, 1974, p. 64). This is no longer a tenable position.

16.3.2. The Number, Duration, and Synchronization of Cycles of Cross-Bridge Formation and Breakage

The sliding filament model permits the filaments to move during a single cycle of cross-bridge formation and dissociation over a very short distance to account for the shortening during a single muscle twitch. Thus, as pointed out by H. E. Huxley (1969), a 30% shortening of a sarcomere originally 2.5 μm long could entail the filaments sliding past each a distance of 0.375 μm or 3750 Å. For each cross-bridge to move from the perpendicular to the slanted position, no more than 100 Å is covered. Thus 37 jumps have to be made during a single contraction. Now each thick filament contains several hundred myosin molecules; the heads of these myosin molecules are believed to be the substance of the cross-bridges. Is each of these 37 jumps made by hundreds of these cross-bridges all at once in perfect synchrony? At 0°C each single muscle twitch lasts about 200 msec (Bendall, 1969, p. 125). At 25°C, it must be completed in a shorter time. Given a Q_{10} of 2, the time to complete a single twitch would be no longer than 37 msec, which allows only 1 msec for each complete cycle of refractory period cross-bridge attachment, conformation changes, and detachment. Yet in unregulated model systems the rate of ATP-induced conformation change is 10^3 sec^{-1} (K. A. Johnson and Taylor, 1978; Chock *et al.*, 1979); this step alone will consume 1 msec.

It is even more difficult to visualize how *in vivo* Ca^{2+} can orchestrate these synchronous cyclic changes. No matter how fast the postulated Ca^{2+} pump operates to remove the liberated Ca^{2+} during a preceding cycle, the return of Ca^{2+} to the SR must be rate-limited by diffusion, a process that cannot be controlled to give this kind of schedule.

Without perfect synchrony, the nondissociating cross-bridges at any time would act like anchors, preventing filament sliding and hence muscle shortening.

Another option is to allow only one or a few cross-bridges to be formed at a time. This option too has serious difficulties. In the sliding filament theory, the cross-bridges are the seats of tension. One or a few cross-bridges will be too weak to produce the tension observed. Furthermore, dependency of tension on overlap would not be expected. Yet such a dependency has been observed (Fig. 16.11).

16.3.3. What Keeps the Filaments from Tangling Up?

The EM picture of muscle cell cross-sections has become by now so familiar that it seems atavistic to ask the question, What keeps the filaments so neatly arrayed? Indeed these filaments are arranged without tangles not only at rest, but during vigorous repeated contractions as well. H. E. Huxley mentioned the "delicate balance of long-range forces" as the means to keep the filaments in order. There are reasons to doubt

this mechanism (see Section 16.5.3). A. F. Huxley (1957, p. 278) also raised this question and suggested that cross-bridges between the thick filaments might keep them in register. However, if thin filaments are to telescope into the fixed thick filaments, the thin filaments must be free of similar cross-links. Thus the question remains unsettled: How are the thin filaments kept in perfect order without tangling up? Merely being anchored on one end (on the Z membrane) does not solve the problem. The thin filaments are not rigid structures like the teeth of a comb. They obviously have a similar flexibility to that of a relaxed muscle.

16.3.4. Why Should the Bulk of Water in the I Bands Move with the Telescoping Thin Filaments?

Living cells in general contain 80% of their weight in the form of water. In the conventional membrane pump theory, the bulk of the cell water is free. This postulation seems to have been adopted thus far by most investigators championing the sliding filament theory. In terms of the relative mass, when a muscle shortens, it is primarily an event of water movement. But if there are no unusual bonds between the bulk of the (supposedly) free water and the actin thin filaments, what would prevent water from staying where it is and becoming separated from the filaments, much as proteins precipitated from an aqueous solution by trichloroacetic acid become separated from the bulk phase water and collect as precipitates? One possibility is that the thin filaments and Z line together work like a piston. But this requires a confining cylinder. An examination of a low-magnification electron micrograph of a striated muscle cell (Fig. 16.17) shows that the Z membrane does not form a continuous sheet across the entire cell, nor are there lateral barriers that would prevent the squeezed water from escaping the spaces between the myofibrils rather than following the movements of the thin filaments. Physiological evidence that the Z membrane does not extend over all the muscle fibers can be derived from the fascinating observation reported by Cookson and Wiercinski (1949): When isolated frog muscle fibers are exposed to a 0.1 M KCl solution containing hydrogen peroxide, more than one contraction wave may travel along different parts of a single muscle fiber surface, sometimes in opposite directions. Clearly all myofibrils do not always contract together, as would be the case if the Z line went through all fibrils as continuous sheets.

16.4. A Tentative Model of Muscle (and Nonmuscle Cell) Contraction: An Updated Theory According to the AI Hypothesis

The following model is a synthesis of concepts from many theories, including those of MacDonald, Szent-Györgyi, A. F. Huxley, and H. E. Huxley as well as the early models of the AI hypothesis. Although primarily addressed to the contraction of striated muscle, this model can be extended with some modifications to explain the motilities of a variety of nonmuscle cells now being vigorously and brilliantly studied (Allen and Kamiya, 1964; Pollard and Weihing, 1974; Tilney, 1975; Hitchcock, 1977).

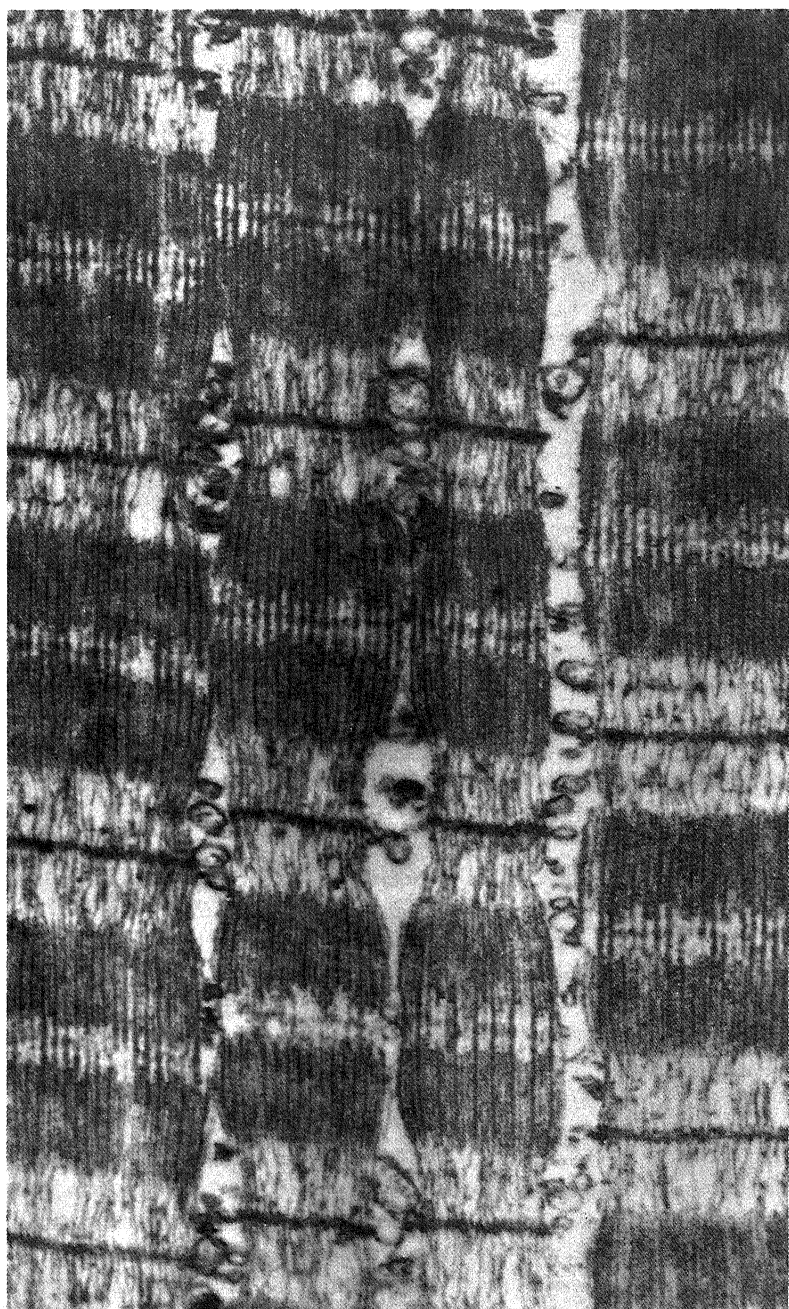


FIGURE 16.17. Very thin longitudinal section of striated muscle. [From H. E. Huxley, reproduced from Murray and Weber (1974), by permission of *Scientific American*.]

16.4.1. The Resting, Relaxed Muscle

16.4.1.1. *The State of Actin*

F. B. Straub (1943) first demonstrated that actin exists in monomeric G-actin form in a solution containing no or little salt. Addition of salts like 0.1 M KCl brings about polymerization into fibrous F-actin.

In conventional thinking, the approximately 0.1 M intracellular K⁺ exists in the free form. Therefore all actin in a muscle cell must exist in the F-actin form, making up the thin filaments as seen in EM preparations (Figs. 16.7 and 16.17).

There is now extensive evidence that the bulk of K⁺ in voluntary muscle cells is absorbed and therefore unavailable to act on actin to sustain its existence in the F-actin form. The low K⁺ and hence low ionic strength inside resting cells thus demands that in resting muscle cells actin not exist in the F- or thin filament form. This is a drastically different view from that usually held. It is, nevertheless, a likely consequence of the establishment of the adsorbed state of cell K⁺ (Chapter 8). It may be mentioned that, since with few exceptions all living cells contain a high concentration of K⁺, the demonstration that actin does exist in monomeric, non-F-actin form in some cells (for review, see Hitchcock, 1977) supports this view.

I am not very certain as to exactly what conformation the non-F-actin assumes, only that it must be a state in which a substantial part of the whole of the backbone NHCO groups of the actin molecule are directly exposed to the bulk phase water. Perhaps the term *profilamentous actins* coined as part of a discussion of formation of the acrosomal process in certain sperm (Tilney, 1976; Tilney *et al.*, 1973), may be appropriate. In any case I shall designate the postulated state as "profilamentous," leaving the door open for future change if Tilney's profilamentous form has different attributes. The identity of this "profilamentous" actin with G*-actin (Oosawa and Kasai, 1971; Rich and Estes, 1976; Rouayre and Travers, 1981) is another possibility awaiting future clarification.

The bulk of the actin is suggested to exist in this form not only in the I band but also between thick filaments in the A band. A very small part of actin is postulated to exist in F-actin form in the middle of the A band at the M line (see Fig. 16.7) and is permanently attached to myosin with a different polarity of orientation on either side of the M line. It is possible that this local complexing with preexisting F-actin may account for the difficulty in extracting myosin from the narrow zone of high electron density in the center of the A band (A. F. Huxley, 1957, p. 262; Hanson and Huxley, 1955).

16.4.1.2. *The State of Myosin*

As of now no change is suggested for the state of aggregation of myosin from that conventionally conceived. It exists in the form of thick filaments and the myosin heads undergo conformation changes and form cross-bridges. ATP as a cardinal adsorbent keeps neighboring anionic sites at a *c*-value favoring K⁺ adsorption.

16.4.1.3. *The State of Water*

In Chapters 7 and 9 we have presented evidence that water in cells in the resting state exists in the state of polarized multilayers, in consequence of interaction with a

matrix of protein chains existing throughout the cells with their backbone NHCO groups directly exposed to the bulk phase cell water. Because of its ubiquitous presence in many types of cells, and for other reasons, actin was suggested as a possible candidate for this role (Ling, 1979a; see also Minkoff *et al.*, 1976). If this stipulation is correct, clearly actin cannot be in the F-form because in F-actin each actin monomer is in the form of "sphere" with all its backbone NHCO locked in the non-water-polarizing α -helical form. There is some evidence that actin can exist in a form that does polarize water.

First, Asakura, Kasai, and Oosawa (1960) showed that actin in the presence of ATP, urea, and $MgCl_2$ remains in a monomeric form at 0°C but transforms into F-actin when the temperature is raised to 25°C. These authors concluded that G→F transformation occurs as a consequence of increasing entropy of the system. Asakura *et al.* did not specifically point this out, but it seems obvious that a condensation of many G-actin monomers with their many degrees of motional freedom into long filaments could by itself only involve the opposite change, i.e., a *decrease* of entropy. Therefore the gains of entropy observed with polymerization of actin in all likelihood involve a liberation of adsorbed water molecules.

J. C. Lee and Timasheff (1977) studied another cytoskeletal protein, brain tubulin, which also undergoes entropy-driven polymerization. From the thermodynamic parameters measured, Lee and Timasheff concluded that water molecules are also released during this polymerization.

These two parallel sets of data indicate that substantially less water interacts with the protein in the polymerized form than in the monomer form.

Our next step is to identify this water associated with the monomers with water existing in the state of polarized multilayers. We look for telltale characteristics of such polarized water: solute exclusion and enhanced osmotic activity. It is fortunate that data of this sort are already available. First, Lee and Timasheff (1977) studied the interaction of glycerol with polymerizing tubulin. From this study, they concluded that the monomer tubulin preferentially interacts with (i.e., binds) water over glycerol. Put differently, the water associated with monomeric tubulin excludes glycerol. Second, Charnasson (1981) measured the osmotic pressure of a solution of brain tubulin when the temperature was increased from 4°C to 25°C. Figure 16.18 reproduces his result. A sharp drop of osmotic pressure accompanies the polymerization of monomeric tubulin. In Section 13.2 I presented evidence that multilayer polarization of water causes a decrease of water activity, appearing as an increase of osmotic activity (see Fig. 13.5).

From this indirect evidence I draw the tentative conclusion that in resting muscle the "profilamentous" state of actin plays a major role in polarizing in multilayers the bulk of cell water and that it is this water polarization that maintains the osmotic equilibrium of a major part of the cell.

16.4.1.4. The State of K^+

The evidence described in Chapter 8 adequately shows that the bulk of muscle K^+ is adsorbed at the two edges of the A band, in areas where most of the myosin heads are located. Less than 1 mM of free K^+ and about 5–10 mM of free Na^+ exist in resting muscle.

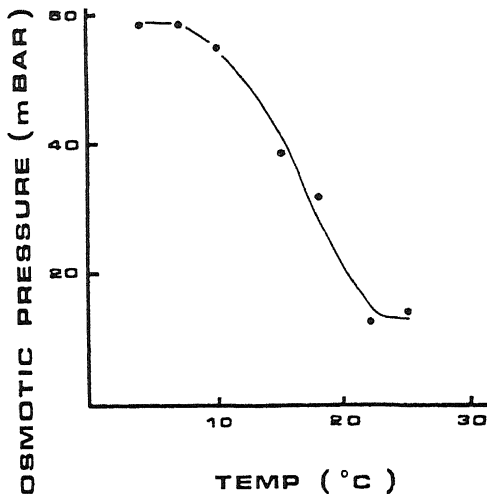


FIGURE 16.18. Effect of polymerization of tubulin upon the osmotic pressure of the tubulin solution. Tubulin concentration was 5.5 mg/ml. 1 mM MES buffer; 1 mM $MgCl_2$, 0.1 mM EDTA, 1 mM GTP. Average of three determinations. [From Charmasson (1981), by permission of *Physiological Chemistry and Physics*.]

16.4.1.5. The State of Energy

The resting muscle cells, like all other resting cells, exist in a high-energy state. It is this potential energy involving all the associated components of the resting protoplasm that provides the energy for contraction. ATP's contribution is that of a cardinal adsorbent (see Chapters 7 and 10).

16.4.2. Contraction

1. The action potential propagating through the T tubules causes the release of bound Ca^{2+} in the SR. This liberated Ca^{2+} then combines with troponin. Acting as a cardinal adsorbent, by the propagated inductive effect, Ca^{2+} allosterically brings about the combination of the prepolymerized F-actin with nearby myosin heads. As a result the myosin ATPase is activated, hydrolyzing the other cardinal adsorbent ATP at the site.

2. The hydrolysis of ATP, followed by the release of ADP and P_i , causes a propagated *c*-value change whereby K^+ is liberated and salt linkage formation between actin and myosin heads occurs, forming the cross-bridges at that locus.

3. The liberation of K^+ has a dual effect: It abruptly *increases* the local osmotic activity and it promotes the transformation locally of actin in the "profilamentous" form, beginning at the nucleation sites of preformed F-actin at the center of the A band. At these nucleation sites the polymerized actin is oriented in opposite directions on either side of the M line. (For known examples of this type of polar orientation of F-actin polymerization in various types of cells, see Woodrum *et al.*, 1975; Tilney *et al.*, 1981.)

4. The polymerization of actin at a position near to but distinct from the center of the A band liberates water from its original state of multilayer polarization. As a result, the osmotic activity at this position becomes decreased.

5. As a result of the enhanced osmotic activity at the position where K^+ is liberated proximal to the center of the A band and the reduced osmotic activity at a more distal

site away from the site of K^+ liberation, water will flow toward the center of the A band, resulting in a lateral expansion and longitudinal shortening, bringing the expanse of "profilamentous" actin closer to the center of the A band.

6. The F-actin formed then combines with more myosin heads distally, activating its ATPase, and the cycle begins again with further growth of filamentous actin. Eventually all "profilamentous" actin polymerizes into thin filaments, which then find themselves in positions between the thick filaments as in a typical diagram of "sliding filaments" in the contracted state.

16.4.3. Relaxation

1. With no additional nerve impulse coming in, the SR returns to its resting, Ca^{2+} -preferring state. Since the SR binds Ca^{2+} very tightly, free Ca^{2+} will be removed, eventually causing its desorption from the cardinal site on troponin.

2. With Ca^{2+} removed, F-actin detaches from myosin heads, whose ATP-binding cardinal site soon takes up ATP resynthesized in the nearby mitochondria (Fig. 15.4).

3. The adsorption of ATP on myosin cardinal sites restores K^+ preference. As a result K^+ is taken up from the vicinity, displacing salt linkages formed between myosin heads and actin. The resultant dissociation of the cross-bridges restores the flexible relaxed condition of the muscle locally. The adsorption of K^+ lowers the local osmotic activity and free K^+ concentration decreases.

4. F-actin now depolymerizes into the "profilamentous" form, polarizing water, and returns to the minimum-free-energy configuration of the resting muscle fiber.

16.5. Agreements and Disagreements with Relevant Existing Knowledge

16.5.1. Electron Microscopic and X-Ray Diffraction Evidence of the Continuing Existence of Thin Filaments

There are beautiful electron micrographs of relaxed muscle in many textbooks and reviews, including this one (Figs. 16.7 and 16.17). All show clearly defined thin filaments. In the face of this evidence, it is indeed difficult to prove that the thin filaments seen are all created as a result of the inevitable activation of the muscle during specimen preparation. Perhaps one may suggest that in the EM techniques there is a natural selective process favoring those procedures that would enhance the sharpness of the images over that of other pictures that are diffuse, as would be the case if actin were to exist in a nonfilamentous form. Muscle in IAA rigor or treated with glycerol but prevented from shortening with the aid of strings clearly has already reached a low energy state and thus is more likely to yield reproducible pictures; this type of preparation may reasonably be assumed to give the impression of what relaxed muscle may look like.

In fact, one may argue that even the major low-angle X-ray data shown in Fig. 16.9, as well as the electron micrographs shown in Fig. 16.8A,B, may also be more simply interpreted as being in favor of the present model, involving the polymerization of "profilamentous" actin to regularly arrayed F-actin filaments at trigonal locations during contraction. Indeed Hanson and Huxley (1955, p. 236) commented on their X-

ray finding in these words:

X-ray diffraction photographs of extensible fibres (. . . of a surviving frog sartorius preparation in Ringer solution) show that the primary hexagonal array of filaments is present but suggest that *the material between them is randomly arranged* [italics mine]. . . . When frog fibres have been exhausted by repetitive stimulation in the presence of iodoacetate (a method of depleting their ATP content), the diffraction pattern they give is now the same as that of glycerol-extracted muscle, i.e., *the material between the primary filaments is now regularly arranged* [italics mine].

16.5.2. A Key Role of Cell Water in Muscle Contraction

I pointed out earlier that the common notion that, if thin filaments move, water always moves with them is incorrect. In the model presented here, the movement of water itself provides the primary driving force. Actin filament polymerization and cross-bridge formation are events that occur side-by-side with water movement and are not the cause of water movement.

It is interesting to note that Overton, who introduced the lipoidal cell membrane theory (Section 2.1.1) also pointed out the critical role of Na^+ for cell excitability (Section 3.4.1), thereby setting the stage for Hodgkin, Katz, and Huxley's new theory of electrical activities. In the same paper, Overton (1902b) also pointed out that muscle becomes unable to contract when it loses a part of its cell water after exposure to hypertonic solution. It was A. L. Hodgkin again who, in collaboration with P. Horowicz (Hodgkin and Horowicz, 1957; also Howarth, 1958), showed that the loss of muscle contractility is not the consequence of loss of electrical excitability. Indeed perfectly normal action potentials persist in muscle no longer contracting in a hypertonic solution. Caputo (1966) then showed that a hypertonic solution actually enhanced caffeine-induced contracture, proving that the Ca^{2+} release mechanism remains intact. By demonstrating a uniform decline of tension independent of the method producing the contraction (i.e., twitch, tetanus, maximum K^+ , or caffeine contracture) Gordon and Godt (1970) concluded that the primary seat of hypertonic solution effect is directly on the contraction mechanism. The conclusion is in harmony with the present model, wherein the contractile force depends on an osmotic gradient, which of course is an expression of water activity. Exposure to a hypertonic solution reduces the amount as well as the thermodynamic activity of water in the cell. How precisely this water activity reduction affects contraction is not known and may prove to be a fruitful area for future research. Nevertheless, in general one may deduce that, since the transformation of "profilamentous" actin into F-actin involves a liberation of water, drastic reduction of water activity may, by the Le Chatelier principle, cause premature actin polymerization. If this truly happens, it would be one possible reason for the widely observed stiffness of muscle treated with hypertonic solutions (e.g., Howarth, 1958).

16.5.3. A Mechanism That Prevents the Filaments from Tangling Up

As mentioned earlier, in the sliding filament model it is difficult to imagine how the filaments are kept in such perfect order at rest and especially during contraction.

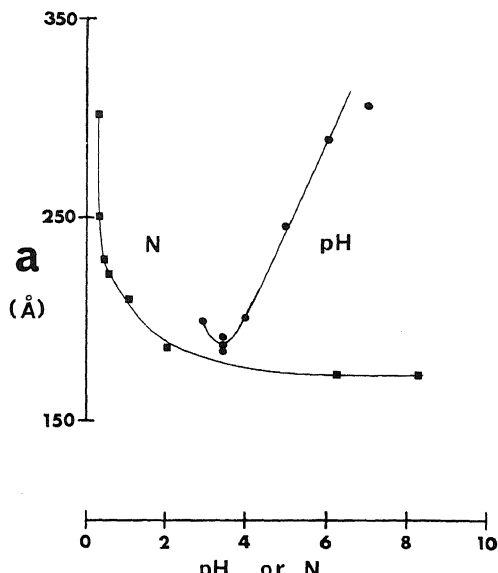


FIGURE 16.19. Interparticle spacing (a) in gels of TMV as a function of the normality (N) and pH of the surrounding buffer solution. [Based on Bernal and Frankuchen; from Elliott (1973), by permission of *Annals of the New York Academy of Sciences*.]

The problem is hardest to understand in the case of thin filaments. This part of the problem does not exist in the present model, since at rest the "profilamentous" actin forms a matrix and does not exist in the form of filaments. When actin does transform into F-actin, it is held in place at least partly by the cross-bridges. The question remains, How are the thick filaments kept in perfect order?

Elliott (1973), in discussing the filament spacing of muscle cells, called attention to the similar highly regular spacing of tobacco mosaic virus (TMV) observed by Bernal and Frankuchen (1941) and referred to in Section 9.2.2. Figure 16.19 partially reproduces Elliott's figure based on Bernal and Frankuchen's data. It indicates that the interparticle spacing (a) of the TMV gel determined from X-ray diffraction studies varied with the concentration of salt solution in which TMV was dissolved. It is often believed that the extremely regular array is due to electrostatic repulsive forces on the viral proteins. However, if this were the only cause, high salt concentrations should destroy the regularity. Obviously this is not the case, as Fig. 16.19 shows. Indeed this indifference of TMV gel structure to high salt concentration was puzzling to Bernal and Frankuchen, to Levin, and to other participants in a discussion at the meeting of the American Chemical Society held September 9–13, 1946 (see Ferry, 1948).

A partial explanation of the regular myosin and actin filament spacing, as well as that of the TMV gel, may be offered in terms of the model of cell volume maintenance given in Chapter 13. Water existing in the state of polarized multilayers is largely responsible for the separation and regularity. The shrinkage of the interparticle spacing with increasing salt concentration is due fundamentally to the low q -value of the salt in the polarized water, as in the swelling and shrinkage of polyethylene-oxide-filled dialysis bags in salt solutions (Section 13.2). If this is correct for TMV, it also may help to explain how muscle fibers and other cell structures can maintain their regular spacings.

16.5.4. A Key Role of K⁺ Adsorption and Desorption in Muscle Contraction

In the model presented, K⁺ adsorbs on sites on myosin heads when ATP is adsorbed on cardinal sites. When ATP desorbs, K⁺ is liberated, as its adsorption sites now combine with actin sites, forming cross-bridges.

16.5.4.1. Evidence That K⁺ Adsorbs on Myosin Heads and Adsorbed K⁺ Prevents Cross-Bridge Formation in Relaxed Muscle

In studies of the ATPase activity of acto-HMM, E. Eisenberg and Moos (1968) introduced the double reciprocal plot of actin concentration and ATPase activity of acto-HMM. The results show that combination with actin greatly enhances HMM ATPase activity, as mentioned earlier. The technique also yields another piece of important information: KCl reduces the binding strength of actin and HMM in a quantitative manner. Figure 16.20 presents the data of Rizzino *et al.* (1970) and of Tawada and Oosawa (1969). Both sets of data show different intercepts on the abscissa of straight-line double reciprocal plots at varying KCl concentrations. The data of Yagi *et al.* (1965) also support Eisenberg and Moos's original conclusion (see, however, Szentkiralyi and Oplatka, 1969, for different finding). These important data confirm that the crucial role of K⁺ in muscle contraction, as outlined previously, is not due to its shielding effect as part of a diffuse ion cloud. Rather K⁺ acts as a competitive inhibitor, as in enzyme kinetics. Such inhibitors must be specifically adsorbed.

Similarly, Thamés, Teichholz, and Podolsky (1974) found that increase of KCl concentration from 0 to 280 mM caused progressive decrease of the calcium-activated contractile force of skinned frog muscle fibers. Increase of K⁺ concentration from 0 to 140 mM increased the contraction velocity and decreased the resting tension (Fig. 16.21). These findings too agree with the model presented earlier.

If cellular K⁺ concentration is free and strictly constant at all times, as according to the membrane theory, then the beautiful findings of Eisenberg and Moos; of Thamés, Teichholz, and Podolsky; and of many others are no more than elegant exercises that have nothing to do with the physiology of normal muscle contraction. This is obviously not true.

16.5.4.2. Evidence That K⁺ is Reversibly Liberated during Muscle Contraction

According to the model presented, K⁺ is liberated from its adsorption sites during muscle contraction. Therefore, one may expect that, as a result of repetitive contractions, there may be (1) an increase of osmotic activity of the muscle cell when it is suspended in moist air and (2) a reversible loss of K⁺ when the contracting muscle is suspended in a Ringer solution. Findings have been reported which can be interpreted as substantiating both expectations.

16.5.4.2a. *Stimulation-Induced Increase of Osmotic Activity.* In 1930 A. V. Hill measured the osmotic activity of frog muscle after exhaustive electrical stimulation and noted a 40% increase in the total osmotic activity of the tissues. He figured that this could be explained in part by the lactic acid produced and in part by the splitting of

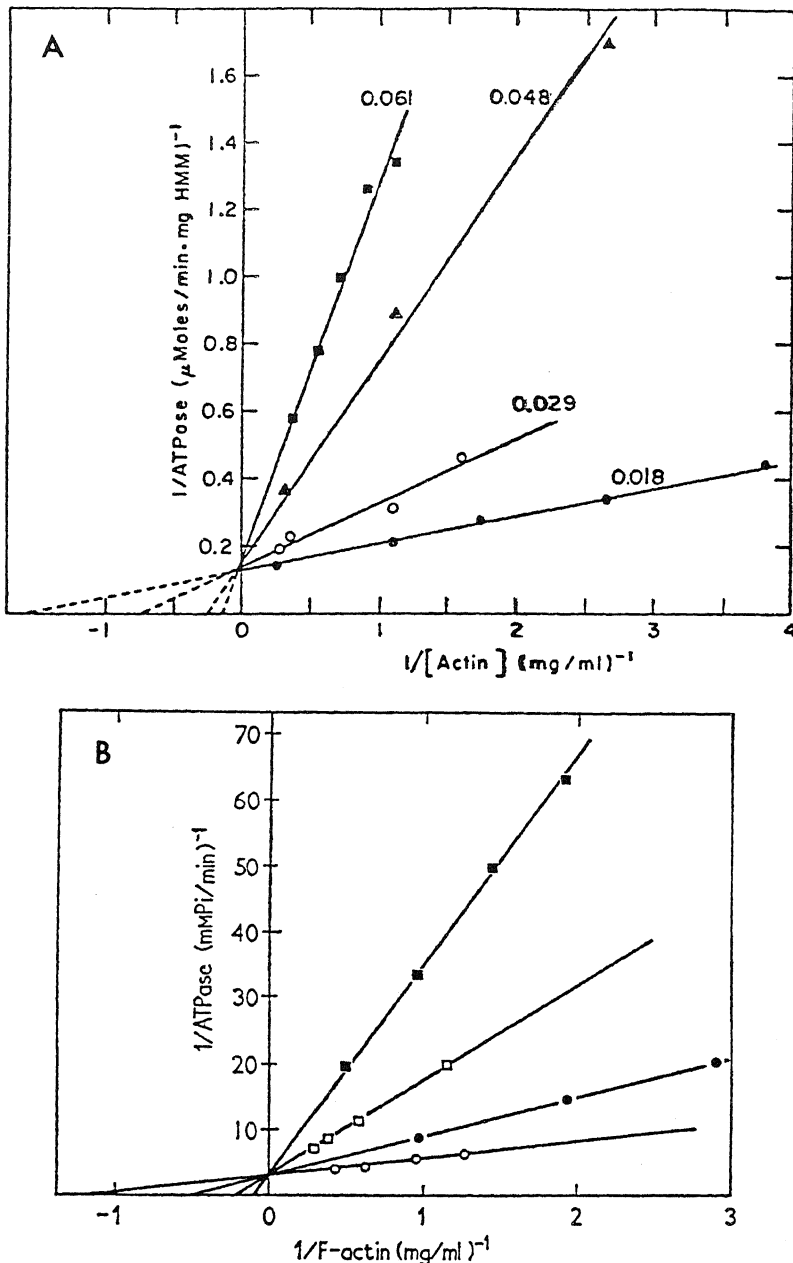


FIGURE 16.20. (A) Effect of ionic strength on acto-HMM ATPase system. The total ionic strength (M) is indicated on each line. Samples contained 2 mM ATP, 1.4 mM (\circ, \bullet, Δ) or 1.0 mM (\blacksquare) $MgCl_2$, 10 mM imidazole-HCl buffer (pH 7), and KCl to make up the balance of the ionic strength. HMM concentration was 0.04 mg/ml for \circ and \bullet , and 0.08 mg/ml for Δ and \blacksquare . Temperature 25°C. [From Rizzino *et al.* (1970), by permission of *Biochemistry*.] (B) Double reciprocal plots of ATPase versus actin concentration. - $\square-\square$, - $\circ-\circ$ -, in the presence of F-actin at 60 and 30 mM KCl, respectively; - $\blacksquare-\blacksquare$, - $\bullet-\bullet$ -, in the presence of CM-F actin at 60 and 30 mM KCl, respectively. Solutions contained 0.1 mg of HMM/ml, 10 mM Tris-maleate buffer (pH 7.0), 1 mM $MgCl_2$, and 2 mM ATP. [From Tawada and Oosawa (1969), by permission of *Journal of Molecular Biology*.]

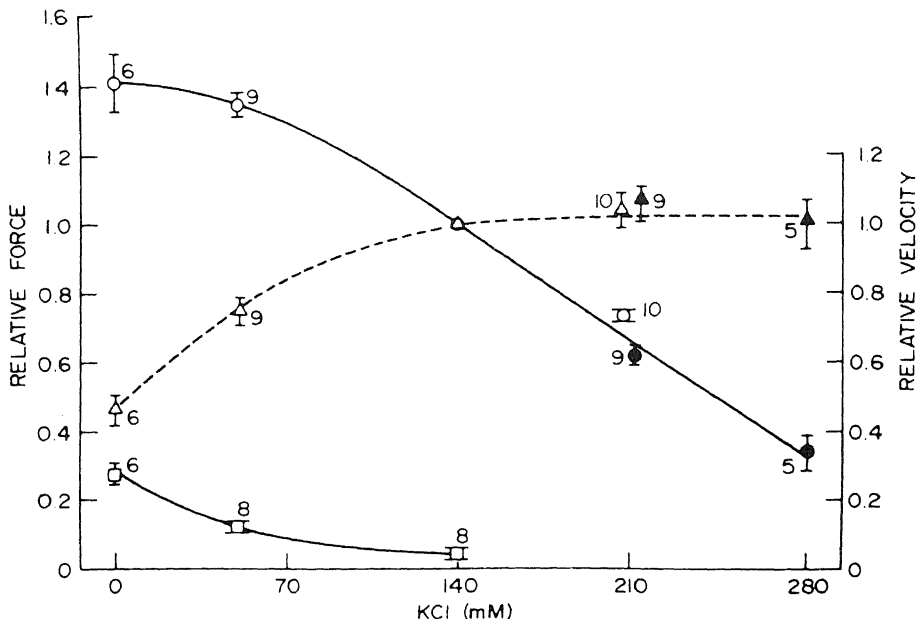


FIGURE 16.21. Summary of force, velocity, and resting tension measurements from skinned muscle fibers activated in high Ca^{2+} at 5–7°C. The open symbols are from *Rana pipiens pipiens* fibers that were activated by high calcium (pCa 5) at the indicated KCl concentrations and then relaxed (pCa 9) in a solution containing 140 mM KCl. The closed symbols are data obtained using *Rana pipiens berlandieri* fibers which were equilibrated for 10 sec in a relaxing solution at the indicated KCl concentration before and after being activated. Each force (○, ●) and velocity (Δ , ▲) point is expressed as a fraction of the force and velocity obtained in the same fiber in 140 mM KCl at the same relative load. The resting tension in 140 mM KCl after contractions at the KCl concentration indicated (□) is expressed as a fraction of the calcium-activated force developed in 140 mM KCl. When the KCl concentration was increased above 140 mM, the calcium-activated force decreased while the speed of shortening was unchanged. As the KCl concentration was reduced below 140 mM, the calcium-activated force increased, the speed of shortening decreased, and the resting tension following contraction increased. Error bars give the SEM. [From Thamés *et al.* (1974), by permission of *Journal of General Physiology*.]

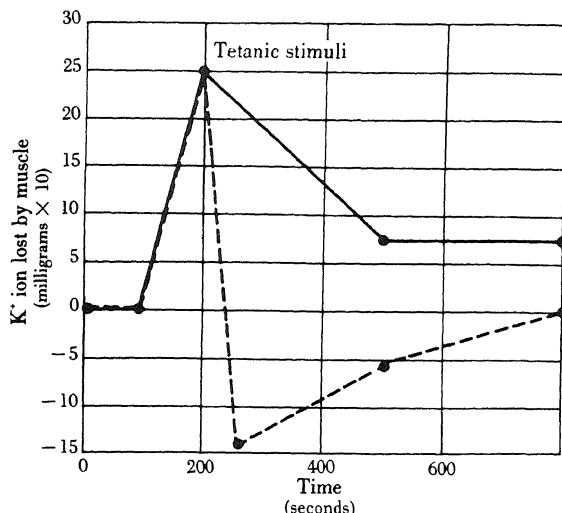
CrP and ATP. However, when all of these activities were carefully tallied, there was still a deficit of osmotic particles not accounted for. To the best of my knowledge, this subject was abandoned.

16.5.4.2b. Stimulation-Induced Reversible Loss of K^+ from Contracting Muscles.

1. Wood, Collins, and Moe (1940) collected blood samples from the vein returning from the gastrocnemius muscle contracting *in situ* in response to electrical stimulation of its normal nerve supply. They showed that with each burst of stimuli there was a prompt increase of K^+ in the blood. After cessation of stimuli, there was an immediate reversal; K^+ then returned from the blood to the muscle. Figure 16.22 shows the level of K^+ in the blood and the rate of K^+ loss before and following stimulation (solid line).

2. Creese *et al.* (1958) loaded rat diaphragm muscle with $^{42}\text{K}^+$. They showed that there was a prompt loss of $^{42}\text{K}^+$, as well as total K^+ content, following electrical stimulation.

FIGURE 16.22. Loss of K^+ ion during stimulation and its gain immediately following stimulation in dog gastrocnemius muscle. The K^+ gain and loss were determined by analyzing the K^+ content of blood circulating through the gastrocnemius muscle in the heart-lung gastrocnemius preparation. Stimulation was indirectly applied through the sciatic nerve. —, K^+ loss by muscle; ---, rate of K^+ loss. [From Ling (1962), after Wood *et al.* (1940).]



3. Unquestionably, one of the most elegant experiments in this realm was that of Wilde and his co-workers (Wilde and O'Brien, 1953; Wilde *et al.*, 1956). As illustrated in Fig. 16.23, a turtle heart previously loaded with $^{42}K^+$ was perfused through its coronary vessel with a nonradioactive Ringer solution. The outflow was collected continuously by being allowed to flow onto a continuously moving strip of absorbing paper. The heart contracts normally at a rate of about once every 20 sec. The top curve of Fig. 16.23 is the electrocardiogram recorded, showing individual beats. The bottom curve of Fig. 16.23 shows the rapid $^{42}K^+$ release with each contraction, completing each cycle within 5 sec. Other data show that these cycles can continue for some time.

16.5.4.2c. Cause of Osmotic Activity Increase and K^+ Release. In terms of the conventional theory, the release of labeled K^+ could be due to a transient increase of K^+ permeability of the cell membrane. Noonan, Fenn, and Haege (1941) tested this hypothesis. To their surprise, exposure of frog muscle for 60 min to electrical stimulation at one stimulus per second produced no significant extra gain of $^{42}K^+$ from the surrounding medium than control unstimulated muscles (Table 16.1). Seventeen years later, Creese and co-workers (1958) repeated this experiment on the isolated rat diaphragm muscle. After 5 or 10 minutes of stimulation at five stimuli per second, stimulated and unstimulated muscles gained equal amounts of ^{42}K -labeled K^+ from the external medium (Table 16.1).

In 1962 Ling attempted to find answers to two questions: Does frog muscle also lose K^+ on stimulation? If so, does the K^+ loss involve an exchange with extracellular Na^+ (as demonstrated by Hodgkin, Huxley, and others in various excitable tissues)? In five sets of experiments where frog muscles were stimulated for 15 min at five stimuli per second, they remained relaxed at the end of stimulation. In these muscles there was a loss of total K^+ amounting to 7–19% of initial K^+ content. There was either no change of the Na^+ content or a small loss of Na^+ . In only one set of muscles (from a single frog) was there a gain of Na^+ , the highest of the entire experiment amounting to about

TABLE 16.1. Lack of Change in the Rate of $^{42}\text{K}^+$ Entry into Stimulated Muscles^{a,b}

Animal	Muscle type	Control and experimental muscles	Duration of stimulation (min)	No. of stimuli per sec	$^{42}\text{K}^+$ uptake (%)	Source
Frog	Sartorius	Control (1)	—	—	9.4	Noonan <i>et al.</i> (1941)
		Experimental (1)	60	1.1	11.3	
	Semitendinosus	Control (1)	—	—	13.2	
		Experimental (1)	60	1.1	12.4	
	Sartorius	Control (1)	—	—	13.5	
		Experimental (1)	90	1.0	14.0	
	Semitendinosus	Control (1)	—	—	12.4	
		Experimental (1)	90	1.0	12.7	
	Peroneus	Control (1)	—	—	7.2	
		Experimental (1)	90	1.0	6.7	
Rat	Diaphragm	Control (6)	—	—	10.7 ± 0.56	Creese <i>et al.</i> (1958)
		Experimental (7)	5	5.0	11.0 ± 0.88	
	Diaphragm	Control (7)	—	—	20.6 ± 2.13	
		Experimental (7)	10	5.0	20.4 ± 1.36	

^aThe $^{42}\text{K}^+$ uptake is expressed as a percent of intracellular K^+ content. Data from Creese *et al.* include the mean values as well as their SEs. The numbers of individual experiments are indicated in parentheses.

^bData from Noonan *et al.* (1941) and Creese *et al.* (1958). From Ling (1962).

half of the total K^+ lost; in this set, the muscles at the end of the experiment were all in a state of contracture, presumably owing to exhaustion of ATP (Ling, 1962, p. 440).

The loss of K^+ from physiologically contracting heart and skeletal muscle, unaccompanied by a demonstrable increase of membrane permeability to K^+ or a gain of intracellular Na^+ in exchange for K^+ loss, provides strong support for the notion that the contraction cycle involves a reversible displacement of the adsorbed K^+ by salt linkage formation, as depicted in equation (16.2).

16.5.5. The Source of Energy and Force in Muscle Contraction

16.5.5.1. ATP as a Cardinal Adsorbent Maintaining the High-Energy Resting Relaxed State

According to Engelhardt and Ljubimova's theory (1939), the energy in the high-energy phosphate bond is used by the contractile protein to increase its length. In Kalckar's theory (1942), this energy released by hydrolysis is used to cause active relaxation. In contrast, the group of theories including those of Albert Szent-Györgyi (1947, 1951), of Morales and Botts (1953; Morales *et al.*, 1955), and of myself (Ling, 1952) regarded the function of ATP to be discharged through its binding onto the contractile protein, to maintain a relaxed state. Removal of ATP brings about contraction.

Some researchers, like Bendall (1969), considered the function of ATP in resting muscle to be achieved by its "plasticizing action," which keeps actin and the myosin heads from binding to each other; a model for this idea is the dissociation of actomyosin by high concentrations of ATP (Bozler, 1953). According to the now widely accepted

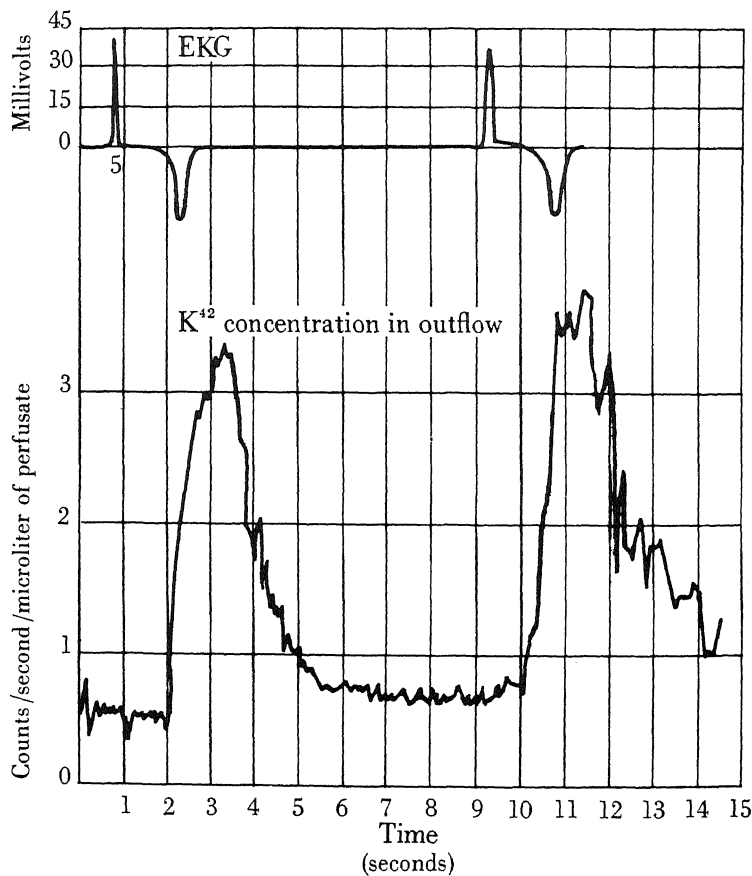


FIGURE 16.23. K^+ efflux during contraction of turtle heart. A heart equilibrated with $^{42}K^+$ was then perfused with nonradioactive Ringer solution through its coronary vessels. The electrocardiogram (EKG) was recorded simultaneously. The first contraction was elicited by an electrical stimulus; the second was spontaneous. [From Ling (1962), after Wilde *et al.* (1956).]

steric blocking theory of Haselgrove (1973) and H. E. Huxley (1973) no such “plasticizing” action is needed: Actin and myosin heads are kept apart by the steric blockage of tropomyosin. However Adelstein and Eisenberg (1980) cited many arguments against this view.

The AI hypothesis agrees in general principle with a “plasticizing” action of ATP and offers a possible molecular mechanism. The cardinal adsorbent ATP acts in an allosteric manner, through the propagated indirect *F*-effect, and maintains the β - and γ -carboxyl groups in myosin in the K^+ -adsorbing state. This is the relaxed state. Desorption or hydrolysis of ATP leads to an autocooperative shift to the contracted state in which K^+ is liberated and the β - and γ -carboxyl groups now form salt linkages with fixed cationic charges, including some on actin (or troponin-tropomyosin), and thus myosin and actin are bound together. The only modification of the model presented in 1962 (Fig. 16.6) is the specification that the salt linkages are not formed intramolecu-

larly, as indicated in Fig. 16.6, but are formed between actin filaments and the myosin heads in the form of cross-bridges.

A very crucial aspect of this model is that ATP must exercise a stronger polarization effect on the contractile protein than does its hydrolytic product, ADP. This requires that ATP bind to myosin much more tightly than ADP. In the last ten years or so, accurate determinations have established that this is true. The binding constant of ATP to myosin is now known to be 10^{10} - 10^{11} M $^{-1}$ (Wolcott and Boyer, 1974; Mannherz *et al.*, 1974; Goody *et al.*, 1977; Cardon and Boyer, 1978). In contrast, the binding constant of ADP is only 10^5 M $^{-1}$ and thus nearly a million times weaker (Lowey and Luck, 1969; D. J. Marsh *et al.*, 1977; Greene and Eisenberg, 1980).

Finally, it may be mentioned that this theory is consistent with the results obtained using nonhydrolyzable ATP analogues, such as AMP-PNP, in which the terminal oxygen bridge of ATP is replaced by an imido group. Since the availability of this interesting compound, it has been demonstrated repeatedly that like ATP, AMP-PNP can cause dissociation of actin and myosin (Yount *et al.*, 1971; Goody *et al.*, 1975; Greene and Eisenberg, 1978; Hofmann and Goody, 1978; Margossian and Lowey, 1978; Marston *et al.*, 1976) without the intervention of tropomyosin.

16.5.5.2. The Missing Energy of Muscle Contraction

When a muscle contracts it may perform work (W) and liberate heat (h). The laws of thermodynamics tell us that the sum of these two items must equal the sum of heat content or enthalpy change of all the involved individual reactions. Thus

$$h + W = \sum_{i=1}^n \xi_i \Delta H_i \quad (16.3)$$

where ΔH_i is the molar enthalpy change in the i th reaction and ξ_i the magnitude of change of the i th reaction. For quite some time it was thought that the heat of hydrolysis of ATP and CrP would account for the heat generated during and immediately following a burst of isometric contraction of a muscle, and that the heat production continuing slowly in the course of the next 40–50 min (the recovery heat) was due to heat produced in the glycolytic and oxidative activities. This expectation was sharpened when after an initial period of uncertainty it was finally proven with the aid of Sanger's reagent, which inhibits the resynthesis of ATP from CrP (Section 15.2.1), that a single muscle twitch is indeed accompanied by ATP hydrolysis (Infante *et al.*, 1964). Moreover, the amount of ATP hydrolysis corresponds to the drop of CrP concentration observed following a single twitch of muscle poisoned with IAA, and also to the P_i liberated in an unpoisoned muscle (Infante *et al.*, 1965; Kuhmerick *et al.*, 1969).

Careful comparison of heat and work produced in contracting muscle with expected enthalpy output from known chemical changes led C. Gilbert, Kretzschmar, Wilkie, and Woledge (1971) and Curtin and Woledge (1975) to the surprising but highly significant conclusion that there remains an unknown source of energy. Figure 16.24 is a partial reproduction of an illustration from the careful compilation of experimental data by Homsher and Kean (1978) from a large number of publications showing the unknown

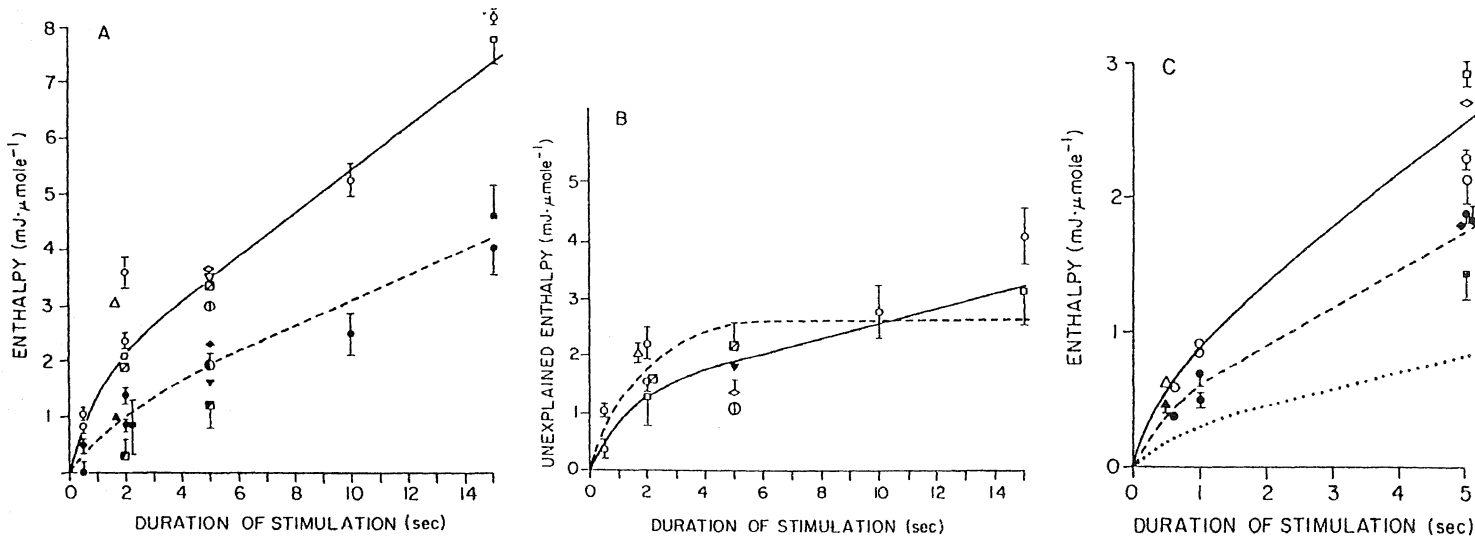


FIGURE 16.24. Results of energy balance studies on isometric tetani of *Rana temporaria* (A and B) and *R. pipiens* (C) sartorius muscles at 0°C. In panels A, B, and C, the observed enthalpy ($h + w$) is given by the open symbols and solid lines; the explained enthalpy ($\xi\Delta H$), by the solid symbols and dashed lines. The symbol size or brackets represent the SEM of the observation. The unexplained enthalpy for the data from *R. temporaria* is plotted in panel B, where the solid and dashed lines represent the possible time courses of the unexplained enthalpy that might fit the data. The approximate time course of the unexplained enthalpy production in *R. pipiens* is given by the dotted line in panel C. Different symbols represent different sources of data collected from published work in the literature. See original article for more details. [From Homsher and Kean (1978), by permission of *Annual Review of Physiology*.]

exothermic reaction in frog muscle following a burst of isometric tetanus. Similar energy deficiencies were observed from studies of tortoise, chicken, and rat muscles (for references see Homsher and Kean, 1978).

I would like to suggest, following naturally from the basic concept of the high-energy resting state in the AI hypothesis, that a major share if not all of the missing energy represents dissipation of the high-energy state of relaxed muscle, which is "stored" in the entire assembly and not in a particular compound or a particular chemical bond.

It is interesting that, owing to the wider acceptance of Ca^{2+} binding and release, readsorption of Ca^{2+} has been considered the source of much of the early heat production. The firm establishment of the adsorbed state of the much larger concentration of K^+ (ca. 0.1 mole/kg fresh muscle) (Chapter 8) adds new dimensions to future investigations in this area.

16.5.5.3. The Source of Muscle Contraction Force

The next question is: How is this potential energy trapped in the resting muscle made to perform mechanical work? Water trapped at high tide on a higher level can be made to perform work only when a suitable mechanism (i.e., a water-driven generator) exists. The mechanism suggested involves an osmotic force with cross-bridges serving a ratchetlike function in preventing premature backward slippage. The key question is: Is the osmotic force large enough to produce a tension amounting to as high as 4–5 kg/cm² (H. H. Weber and Portzehl, 1952)? A rough estimate shows that the theoretically calculated osmotic force may be adequate.

The average K^+ concentration in a frog muscle is such that if it is entirely free and uniformly distributed in the cell it is 128 mM (Table 4.3). Figure 8.3 shows that the bulk of this K^+ in resting muscle is not evenly distributed but is localized in an adsorbed state in the A band, and thus at a 1.5–2.0-times higher concentration locally. If this K^+ is locally liberated, it will provide an extra osmotic activity equivalent to that of from 190 to 256 mmoles of K^+ . This, added to the osmotic activity of the local polarized water, equivalent to 118 mmoles of NaCl, provides at least a total of $118 \times 2 + 190 = 426$ mOsM of osmotic activity.

In the adjacent area, where water-polarizing "profilamentous" actin undergoes polymerization into non-water-polarizing *F*-actin, there is a fall of osmotic activity equal to $118 \times 2 = 236$ mOsM. The total osmotic activity difference is then $426 + 236 = 662$ mOsM.

Now at 25°C 1 mole of a substance dissolved in 1 liter of water yields an osmotic pressure of 24.5 atm (Tombs and Peacocke, 1974, p. 97), which is equivalent to $24.5 \times 1.0332 \text{ kg/cm}^2 = 25.3 \text{ kg/cm}^2$. For 662 mOsM of substance, the osmotic pressure would be $25.3 \times 0.662 = 16.7 \text{ kg/cm}^2$. This is more than three times higher than the maximum tetanic tension of 5 kg/cm². However, the estimate of 16.5 kg/cm² is based on a number of assumptions that may be considered as ideal conditions. In reality, for example, water at the K^+ -liberating position may also be partly depolarized and water at the position further away may not be completely depolarized. Suffice it to recognize that the anticipated osmotic force is quite adequate to meet the maximum need demanded by the force of contracting muscle.

16.6. Summary

Muscle contraction is one of the most extensively studied examples of biological work performance. In skeletal muscle, there are at least nine critical elements involved in the contraction-relaxation cycle: actin, myosin, tropomyosin (which binds to actin), troponin (which binds Ca^{2+}), Ca^{2+} , ATP, binding or sequestration of Ca^{2+} by the sarcoplasmic reticulum, K^+ , and a means of excitation. In the sliding filament model tension develops when the filaments of myosin (which are primarily in the A bands) and of actin (which are primarily in the I bands) overlap and slide past one another. The myosin heads extend laterally at angles from the filament to form apparent cross-bridges between the myosin and actin filaments. During contraction, the cross-bridges appear to extend more perpendicularly and the space between the filaments widens. The major point of contact between actin and myosin appears to be at the actin-binding site on the myosin head, and the myosin head also binds ATP and contains the ATPase activity.

Some major questions about the mechanism of muscle contraction and relaxation include the following: (1) How do actin and myosin interact during “sliding”? (2) Why is there an expanded space between actin and myosin filaments during contraction? (3) Why is K^+ released during contraction? (4) What turns the ATPase activity on and off? (5) How do tropomyosin and troponin, which together impose a sensitivity of actomyosin to Ca^{2+} , work? Is their action simply steric or structural, or does it involve “allosteric” or inductive influences?

A tentative alternative approach to the mechanism of muscle contraction in the context of the association-induction hypothesis does not necessarily conflict with the many suggestions made by others, but begins from a different vantage point provided by the following observations: (1) The majority of muscle K^+ is adsorbed onto the carboxyl groups of myosin and localized within portions of the A band (Chapter 8). (2) Muscle water exists in a state of polarized multilayers oriented by interaction with extended polypeptide backbones (Chapters 9 and 13), especially those of “profilamentous” actin. (3) ATP, as a cardinal adsorbent, conditions inductively the autocooperative K^+ -adsorbing state and the water-polarizing state (Chapters 7–9). (4) The energetic role of ATP in biological work performance is not via its hydrolysis *per se*, but via its adsorption onto key proteins, and the function of the ATPase is to trigger biological work performance by permitting an all-or-none drop of the high-potential-energy resting state of the relaxed muscle to a low-energy state (Chapter 10). (5) The role of Ca^{2+} , as a cardinal adsorbent, includes its conditioning of the autocooperative K^+ -adsorption process (Chapter 11).

The relaxed, resting, lengthened state is one of high potential energy, maintained by the adsorption of ATP onto cardinal sites, where it induces changes that lead to the dissociation of salt linkages and the adsorption of K^+ . Triggering of the ATPase converts ATP, which has an extremely high binding energy to the myosin head, to ADP, which has a much weaker binding energy and a weaker (or opposite) effect as a cardinal adsorbent (as outlined in Chapter 15). The system drops to a lower energy state, doing work in the process. K^+ , along with an anion, is released, and the “liberated” COO^- groups of myosin may form salt linkages with the “liberated” fixed positive groups of actin. “Profilamentous” actin polymerizes to form the thin filaments. These processes also occur in an autocooperative manner, hence the all-or-none nature of contraction of an

individual cell. The interprotein salt linkages account for the more rigid state of the contracted muscle. Finally, it is postulated that localized changes in the osmotic activity of water (concomitant with release of K^+ in one area and depolarization of water in another) provide the major force for muscle contraction.

There remain many unsolved problems in the understanding of muscle contraction and relaxation and of related phenomena in nonmuscle cells. It is anticipated that the approach outlined here will provide further insight into the nature of the interactions among the numerous components that are involved.

Active Transport across Intestinal Epithelia and Other Bifacial Cell Systems

17.1. Unifacial and Bifacial Cells

In Chapter 11 the subject of selective solute accumulation and exclusion in isolated cells was extensively discussed. The weight of evidence supports the view that the asymmetry in the distribution of ions and other solutes across the surface of living cells is not the result of the continuous operation of pumps or active transport, but rather is an expression of a metastable equilibrium in which selective adsorption raises the intracellular solute level and partial exclusion from cell water reduces the intracellular solute level. Together these two mechanisms produce the great variety of solute distribution patterns seen in living cells. Cells like frog muscles, squid axons, and red blood cells are typically “solid bodies” surrounded by a single interface with the cells’ aqueous environment. We refer to these cells as *unifacial cells*.

In many multicellular organisms, there exists another type of asymmetrical solute distribution phenomenon, in which the asymmetry is not between a protoplasmic phase and a normal liquid water phase, but between *two* normal liquid water phases. An example is the frog skin. The continuous functional activity of the skin keeps the concentration of, for example, Na^+ in the tissue fluid different from that in the external pond water. Another example occurs in single-cell plants with large central vacuoles, such as *Valonia macrophysa* (Table 3.3). Living in seawater, which contains nearly 50 times more Na^+ than K^+ , these cells may retain three times more K^+ than Na^+ . The bulk of K^+ and Na^+ in these algal cells is found in the cell sap contained in the central vacuole. Since the cell sap contains little more than water and salt ions and is therefore not significantly different in this respect from seawater, clearly the maintained asymmetry of K^+ and Na^+ distribution between the cell sap and external medium can only be due to active transport. Over fifty years ago, Chambers and Höfler (1931) studied

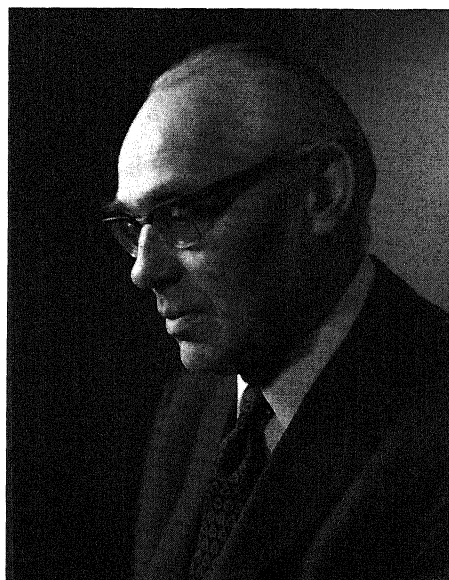
the osmotic behavior of the isolated central vacuole and showed that the tonoplast membrane has quite different properties from the outer plasma membrane. Thus, the epithelial cells of frog skin, intestinal epithelium, or kidney tubules and giant algal cells all possess two different and separate surfaces and will be referred to as *bifacial cells*.

17.2. Concepts of Active Solute Transport Based on the Membrane Pump Theory

The majority of cell physiologists in the past have adhered to the conventional membrane pump theory; consequently, concepts of epithelial transport have been built on the basic tenets of this theory. Hence epithelial solute transport and selective solute accumulation and exclusion in "simpler" cells like muscle and erythrocytes have been considered to be basically the same phenomenon, both due to membrane pumps. This approach has not taken full account of the profound difference between unifacial and bifacial cells.

17.2.1. The "Two-Membrane Theory" of Koefoed-Johnson and Ussing

Frogs pump Na^+ inward through their skin into serosal fluids. From electrical potential studies in isolated frog skin, Koefoed-Johnson and Hans H. Ussing (1958) concluded that the apical surface of the skin facing the outside solution has a high Na^+ permeability and that the basal surface facing the inside of the frog has a high K^+ permeability (Fig. 17.1). In their theory, the inner basal membrane is typical of that of



Hans H. Ussing

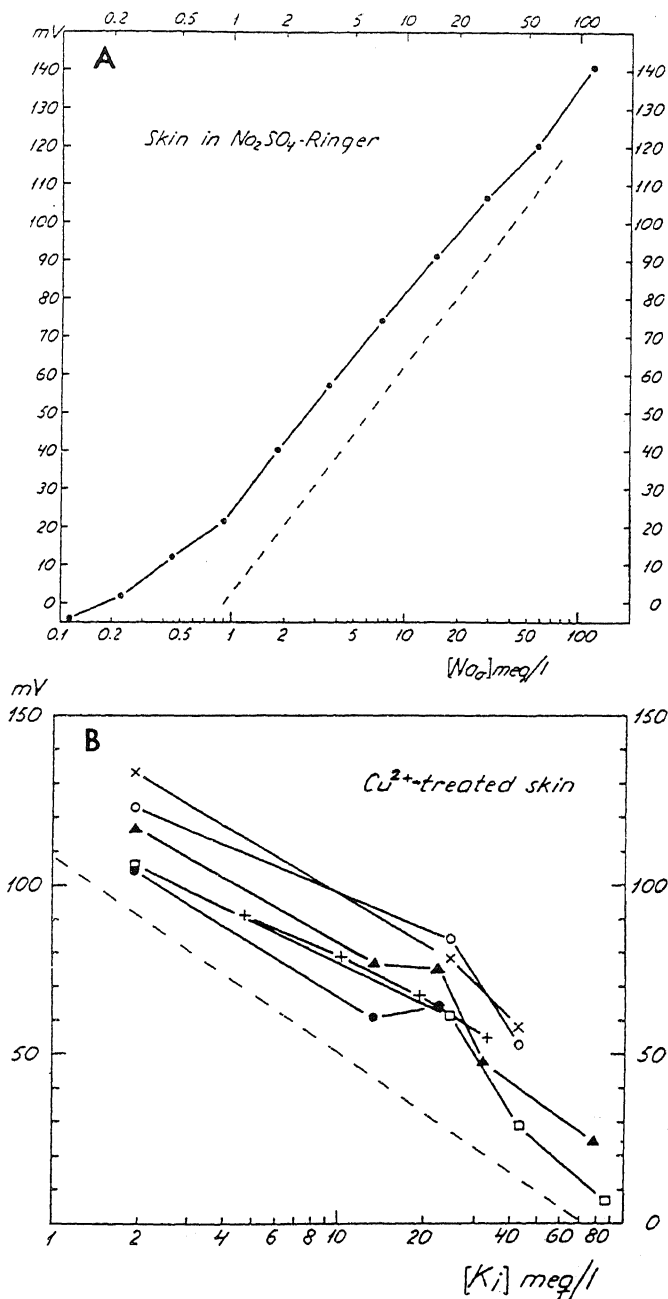


FIGURE 17.1. (A) Frog skin with sodium sulfate on both sides. Ordinate: Skin potential. Abscissa: Na^+ concentration of outside solution. ---, Slope for ideal Na^+ electrode. (B) Frog skin with Ringer solution on both sides. Outside bathing solution made 10^{-5} M with respect to Cu^{2+} in order to reduce chloride shunt. Ordinate: Skin potential. Abscissa: K^+ concentration of inside solution. ---, Slope of ideal K^+ electrode. [From Koefoed-Johnson and Ussing (1958), by permission of *Acta Physiologica Scandinavica*.]

most cells, including the presence of the Na^+,K^+ pump in the form of the Na^+,K^+ -activated ATPase. The membrane facing the outside solution is unusual and functions to regulate transport through the control of its Na^+ permeability.

17.2.2. The Standing Osmotic Gradient Theory of Diamond and Bossert

The gallbladder, intestinal mucosa, and renal proximal tubule transport salt and water as an isotonic solution. Diamond and Bossert (1967) suggested that this secretion is due to the pumping of ions into the spaces between the folds of the basolateral membrane of the epithelial cells. The hypertonic solution thus formed draws water from the cell, becoming more dilute and eventually isotonic as the fluid moves outward toward the serosal "sink."

17.2.3. The Pericellular Pump Theory of Cereijido and Rotunno

Cereijido and Rotunno (1967) postulated that the transport of Na^+ by frog skin involves the migration of Na^+ along an array of fixed negative sites on the outside surface of the epithelial cells.

17.2.4. The Na^+ Gradient Hypothesis of Sugar and Amino Acid Transport

Intestinal transport of D-glucose requires the presence of Na^+ in the mucosal fluid (Riklis and Quastel, 1958; Czaky and Thale, 1960). Crane *et al.* (1961; Crane, 1965) suggested that glucose, Na^+ , and a carrier form a complex that crosses the mucosal membrane and then dissociates and delivers Na^+ and glucose to the other side of the cell membrane. Movement of the Na^+ down its gradient from the mucosal fluid to the cell interior provides the energy for the inward transport of sugar. It was observed earlier that uptake of amino acids by duck erythrocytes and Ehrlich ascites cells and by bifacial kidney cells requires Na^+ (see Christensen, 1970; Segal and Crawhall, 1968). S. G. Schultz and Curran further elaborated the Na^+ gradient hypothesis to include transport of amino acids (Schultz and Curran, 1970). Studies of sugar and amino acid transport into "vesicles" of isolated microvilli (microscopic fingerlike protrusions of the mucosal surface of intestinal epithelial cells) support this hypothesis. These isolated microvilli transiently take up more sugar or amino acids than in the surrounding medium, thereby exhibiting an "overshoot," when the sugar or amino acid is added with a high concentration of Na^+ (Sacktor, 1977).

Since it is clear from preceding chapters that the Na^+ pump theory applied to unifacial cells is incorrect, that part of the bifacial transport theories which relies on the membrane Na^+ pump theory must be revised. The following model is based partly on what I believe to be the correct parts of the preceding theories and partly on the basic concepts of the association-induction (AI) hypothesis.

17.3. Cooperative Adsorption-Desorption Model of Active Transport across Epithelia and Other Bifacial Cell Systems

A hemoglobin solution inside a dialysis bag suspended in an oxygen-containing solution will take up oxygen to an equilibrium level. If ATP is added to the internal

solution, oxygen will move out of the hemoglobin-containing phase into the external solution (Ling and Ochsenfeld, 1973b; Chanutin and Curnish, 1967). ATP interacts with the oxygen-binding protein hemoglobin to exert a long-range allosteric effect. If ATP is removed, oxygen will reenter the bag, apparently against a concentration gradient. This effect of ATP on the concentration of a solute in the hemoglobin-containing system does not require the hydrolysis of ATP, since hemoglobin has no ATPase activity.

One may achieve a cyclic movement of the solute oxygen into and out of the hemoglobin-containing system by introducing or removing ATP. In this case, the laboratory worker provides the mechanism for ensuring the cyclic process. This cyclic transport of oxygen would also occur if the bag contained a specific enzyme, an ATPase, which could destroy and thus remove ATP from the hemoglobin-containing phase; another enzyme system which could regenerate ATP; and a coordinating system that could synchronize ATP destruction and its subsequent resynthesis and readorption. Many biological systems are of course designed to provide just this kind of synchrony and coordination, as shown in the example of ATPase-dependent oscillatory changes of ion and water uptake and release in isolated mitochondrial suspensions (Fig. 15.19).

This simple model demonstrates that it is possible to understand how a cyclic change of ATP adsorption and hydrolysis can bring about a cyclic change of selective accumulation of a solute from the medium and its subsequent release back into the medium. This provides one of the key elements of a theoretical model that can perform true active transport. Another key element needed is a one-way valve.

As discussed in Sections 12.1–12.3, the physiological surface barrier of the living cell is not a continuous lipid layer but much more likely channels of water polarized in multilayers by surface proteins. Synchronized cyclic ion and water release and uptake requires that the cell surface water alternate between a polarized, poorly permeable state and a depolarized, permeable state. If the basolateral or serosal surface has these properties, and the apical or mucosal surface does not undergo cyclic changes but has high-*c*-value anionic sites and hence a selectively high permeability for Na^+ (as Koefoed-Johnson and Ussing demonstrated) (Fig. 17.1), then we will have all the basic elements needed for active transport by bifacial cells.

The model of active transport is outlined in Fig. 17.2. The ion to be transported from the external or mucosal solution, Na^+ , is represented by solid triangles. The mucosal surface is considered to have a higher permeability for Na^+ than does the resting serosal surface because the serosal surface anionic sites have a high *c*-value that promotes selective Na^+ adsorption and permeation via the adsorption–desorption route. Water in the serosal surface, in the cytoplasm, and in the normal cell surface exists in the polarized multilayer state at the beginning of the cycle when the cell is at rest. In this model ATP-binding cardinal sites and ATPases activated by the transported ion play a key role in transport. The ATP-binding cardinal site is likely to be the ATPase site, but in a different cooperative state.

Stage 1. At this stage the higher mucosal surface permeability for Na^+ allows both Na^+ and water to enter the cell primarily from the mucosal side. Once inside, the Na^+ adsorbs onto anionic sites on the cytoplasmic proteins which are under the control of the cardinal adsorbent, ATP. The same or other proteins, also under control by ATP, exist in an extended state with their backbones orienting water in polarized multilayers. This

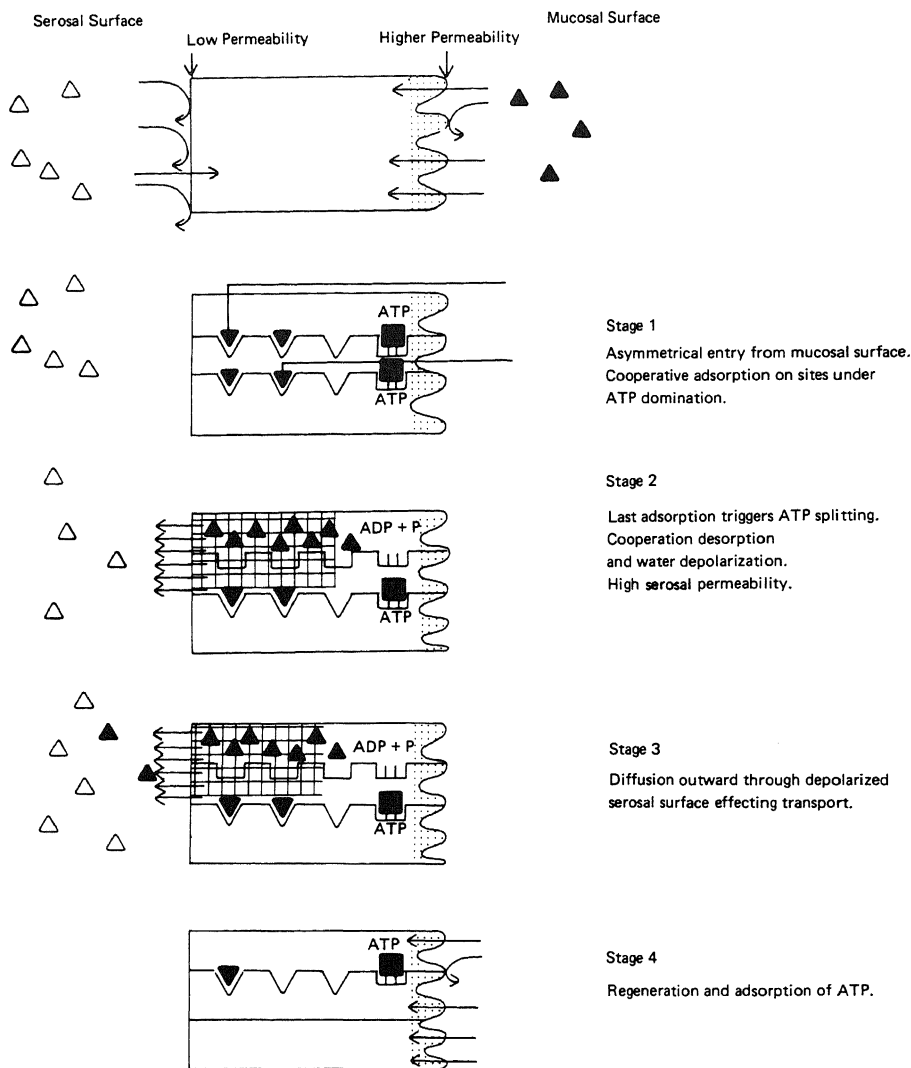


FIGURE 17.2. Diagrammatic illustration of a four-stage active transport model for solutes from the aqueous phase in contact with the mucosal surface to the aqueous phase in contact with the serosal surface of a bifacial cell system. [From Ling (1981b), by permission of *Physiological Chemistry and Physics*.]

process continues until the protein enters into the cooperative Na^+ state with a high concentration of adsorbed Na^+ locally accumulated.

In the specific case under discussion ATP favors Na^+ adsorption (and active transport). In other cases, like insect Malpighian tubules (Maddrell, 1978), ATP is postulated to favor K^+ adsorption (and active transport). This seemingly contradictory role of ATP is theoretically feasible because it is the *c*-value of the regular sites that determines the specificity of K^+ or Na^+ adsorption, and this *c*-value is not determined solely by one cardinal adsorbent (e.g., ATP) but by other factors as well (e.g., auxiliary cardinal adsorbents, nature of proteins).

Stage 2. The autocooperative shift to the Na^+ state involves the site adjacent to the cardinal site, which also adsorbs Na^+ . This Na^+ adsorption then activates the Na^+, K^+ -activated ATPase activity of the cardinal site, causing the hydrolysis of ATP, and thereby triggering Stage 2. The protein now undergoes an autocooperative desorption of Na^+ (possibly of Cl^- as well) with the formation of salt linkages, depolarization and release of water, and the liberation of a high concentration of Na^+ . At the same time or slightly later the serosal surface protein undergoes a change from the extended to a more helical conformation with depolarization of water.

Stage 3. Recalling that only water in the state of polarized multilayers offers selective resistance to ion permeation (Fig. 12.13), one expects that depolarization of the serosal surface water would increase the serosal surface permeability to ions and the osmotic flow of water, permitting the liberated Na^+ and water to exit through the serosal surface.

Stage 4. ATP is regenerated and adsorbed onto the cardinal site, inducing an autocooperative shift back to the Stage 1 condition in which adsorption of Na^+ on anionic side chains and multilayer polarization of water near the serosal membrane are favored. The cycle is now ready to repeat itself.

17.4. Application of the Model to Experimental Findings

17.4.1. Cyclic Changes of Adsorption–Desorption as the Basis for Active Transport

The cyclic changes of adsorption and desorption proposed in this model may not be easy to detect in a multicellular epithelium. However, evidence for cyclic changes exists in single giant algal cells, such as those studied by S. C. Brooks (1939, 1940) (Fig. 17.3). When *Nitella* cells were exposed to salt solutions containing radioactive K^+ , Na^+ , or Rb^+ , these ions first accumulated in the protoplasmic layer surrounding the central vacuole. This accumulation exhibited a distinct periodic increase and decrease, and they reached a concentration in protoplasm many times higher than that in the surrounding medium. Later, the labeled cations reached the cell sap in the central vacuole. Figure 17.3, taken from Brooks (1939), shows the time course of labeled Rb^+ accumulation in the sap. The rising phase of sap Rb^+ coincides with the falling phase of the protoplasmic Rb^+ , while the falling phase of sap Rb^+ coincides with the rising phase of the protoplasmic Rb^+ . Eventually the sap Rb^+ reached concentrations “notably exceeding those present in the immersion fluid,” but the concentrations of ion in the sap were never higher than those in the protoplasm.

17.4.2. Location of the Pumping Mechanism

This model incorporates the two-membrane theory of Koefoed-Johnson and Ussing (1958) to the extent that it recognizes and utilizes the different permeability characteristics of the serosal and mucosal membranes (Fig. 17.1). In other aspects the model is based on the AI hypothesis rather than on conventional membrane pump theory. The

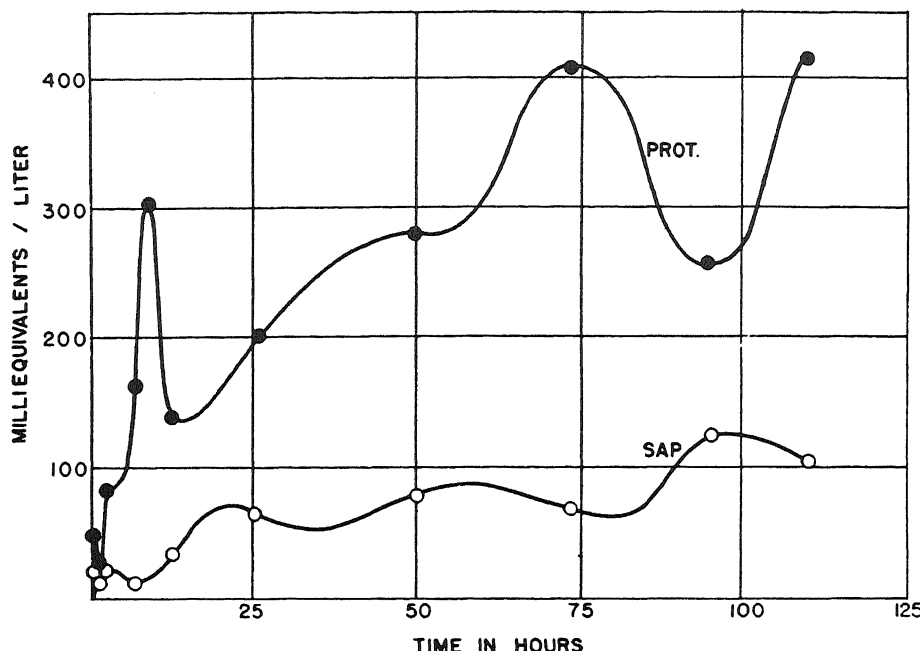


FIGURE 17.3. Concentration of Rb^+ in protoplasm and sap of *Nitella* internodal cells during 120 hr of immersion in 0.005 M RbCl (means of five series). pH 7.3; continuous illumination. [From Brooks (1939), by permission of *Journal of Cellular and Comparative Physiology*.]

part of the protoplasm involved in the adsorption-desorption cycle has been presented as including the entire cytoplasm as well as the serosal surface, because there is experimental evidence suggesting the involvement of the entire cell content (see next paragraph). It is theoretically possible that the protoplasm involved in the cyclic changes may be entirely limited to the serosal surface, in which case it would approximate the location of pumping proposed by Ussing's two-membrane theory.

The evidence that the cyclic adsorption-desorption mechanism is not confined exclusively to the thin serosal cell surface but to a more extensive part of the cytoplasm includes the following:

1. Maddrell (1978) showed that the rate of transport of K^+ and Na^+ by the isolated Malpighian tubule of the blood-sucking insect *Rhodnius* is strongly correlated with the *total* intracellular concentrations of each of these ions.
2. Spring and Giebisch (1977) showed that the rate of net Na^+ transport by perfused *Necturus* kidney cells is linearly related to the *total* intracellular Na^+ concentration.
3. Morel (1961) showed that after injection of radioactive K^+ into rabbits the specific activity of urinary K^+ quickly attains that of the renal tissues but does not follow the time course of specific activity in the arterial plasma.

These results suggest that K^+ that has undergone effective exchange with total cell K^+ plays the major role in urinary K^+ excretion.

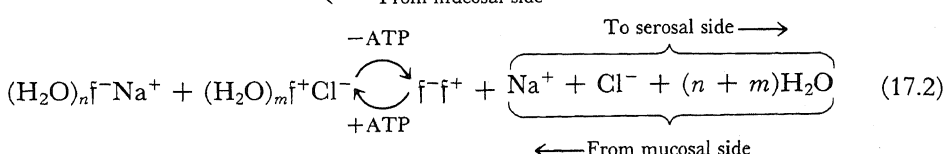
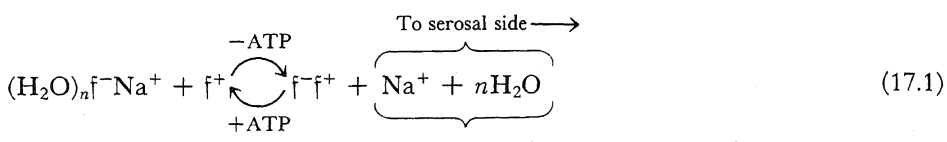
17.4.3. The Source of Energy for Active Transport

In the AI model, the immediate source of energy for active transport is stored in the protein–water–ion assembly existing in the high-potential-energy resting state, and the ultimate source of energy for transport of solutes and water is that used in the synthesis of ATP from ADP and P_i (Chapter 10). If one assumes that this synthesis is relatively efficient, then the energy used for transport would be proportional to the free energy derived from substances used for ATP synthesis. Further, since there are a fixed number of ATP molecules synthesized for each molecule of oxygen utilized or substrate metabolized, the energy for active transport should be quantitatively related to the extra oxygen consumed or to the main substrate available.

Kinne (1979, p. 540) cited work that had led to the general conclusion that there may be a correlation between the Na^+ transport and oxygen consumption of, for example, frog skin. On the other hand, failure to demonstrate such a relation in all tissues may reflect either a predominantly glycolytic source of ATP regeneration or the presence of a high and variable rate of oxygen consumption for cell functions not directly concerned with active transport. Nevertheless, Franke *et al.* (1975) found a close correlation between the amount of Na^+ transported across isolated perfused rat kidney and the amount of pyruvate metabolized (Fig. 17.4).

17.4.4. Coupling of Ion and Water Transport

Gallbladder, proximal kidney tubules, and small intestine are “low-resistance” epithelia and transport water in the form of an isotonic fluid. The standing gradient osmotic flow theory (Diamond and Bossert, 1967)—a refinement of the earlier double-membrane theory of local osmosis to explain the apparent coupling of solute and water flow (Curran and McIntosh, 1962; Patlak *et al.*, 1963)—indicates that a second membrane is not necessary and that any confined space lined by a membrane possessing both active salt transport and semipermeability could function as a local osmotic coupling space. A. E. Hill pointed out that this theory critically depends on the osmotic permeability of the membrane and that the required permeability range of 10^{-1} – $10^1 \text{ cm}^2/\text{sec}$ “lies completely outside that of any living . . . membrane studied to date by at least three orders of magnitude” (Hill, 1975). The present adsorption–desorption model, in the case of coupled NaCl and water transport, is described by two sets of alternative equations:



As shown in Fig. 17.2, the synchronized dephosphorylation of ATP at Stage 2 causes simultaneous liberation of Na^+ from its adsorption sites, f^- , and of water from

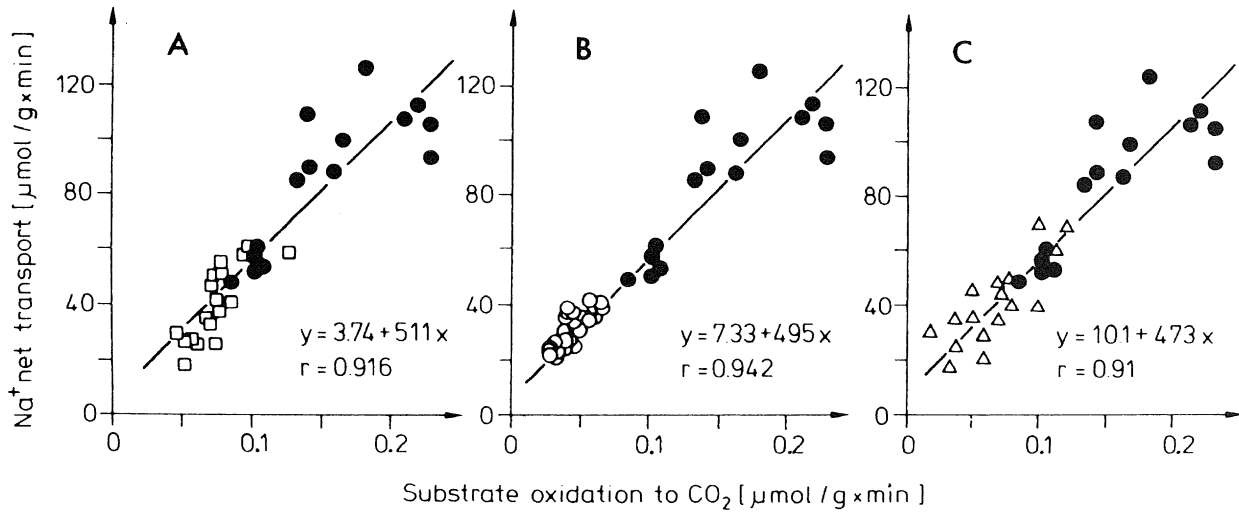


FIGURE 17.4. Correlation between oxidation of pyruvate and Na^+ transport in isolated perfused rat kidney. Data represent results of experiments in which Na^+ transport was reduced (A) by addition of 0.5–1 mg/ml ouabain to the perfusion medium (\square), (B) by reduction of Na^+ concentration in perfusion medium (\circ), or (C) by lowering perfusion pressure (\triangle). Control periods indicated by solid circles. [From Kinne (1979), data of Franke *et al.* (1975), by permission of Springer-Verlag.]

its polarized multilayered adsorption on polypeptide NHCO sites. A "normal" free aqueous solution of water and Na^+ and Cl^- is momentarily and locally released, concomitant with the lowering of the barriers to ion permeation and to osmotic water flow at the serosal cell surface. This occurs because cooperative multilayer polarization of water drastically reduces osmotic permeability but only moderately reduces diffusive permeability, while depolarization of water increases both. As a result, an essentially isotonic fluid containing Na^+ is excreted into the lumen of the "low-resistance" epithelia.

Solute and water transport may be rate-limited either by the frequency of the cycles of adsorption and desorption or by the mucosal surface permeability. The fact that anti-diuretic hormones applied to the outside surface of frog skin and the mucosal surface of toad bladder greatly increase the rate of Na^+ transport and the osmotic water permeability without a major effect on diffusional permeability (Curran *et al.*, 1963) suggests that this hormone may depolarize water at the external (skin) or mucosal (bladder) surface.

While the cyclic adsorption-desorption model can explain active coupled salt and water transport with only the serosal surface involved in polarization-depolarization cycling of permeability changes, there is no reason why in different tissues the cycling may not occur at the mucosal rather than the serosal surface, as is known or at least indicated in insect Malpighian tubules, insect midgut, choroid plexus, and gastric mucosa.

17.4.5. The Relation between "Homocellular" Regulation of Cell K^+ and Na^+ Composition and "Homoe epithelial" Na^+ Transport

In a review on "Transport across Small Intestine" Schultz said: "The data available at present cannot be readily reconciled with any model that invokes a close relation between transepithelial Na transport and the homocellular regulation of Na and K composition or with the notion that the epithelial cell can be adequately represented by a double membrane model" (S. G. Schultz, 1979, p. 769). I suggest that this problem is primarily the consequence of the application of the incorrect basic concepts of the membrane pump theory to active transport.

The AI model does not encounter any internal conflict between its theory of the mechanism of selective K^+ accumulation and Na^+ exclusion in epithelial cells (and algal cells) and its theory of transepithelial Na^+ transport. Indeed, the transepithelial Na^+ transport model is built on the foundation of the mechanism for "homocellular" K^+ accumulation and Na^+ exclusion outlined in Chapter 11.

17.4.6. Coupling of Na^+ Transport with Sugar and Amino Acid Transport

The cotransport of Na^+ and sugars and the cotransport of Na^+ and amino acids across epithelial systems are fascinating phenomena. The cotransport of Na^+ and amino acids was discussed in Section 12.6. Interpretations of this have generally relied on the concept that an electrochemical gradient of Na^+ exists between the mucosal fluid and the cytoplasm because cell Na^+ and water are free. This concept is now disproven (Chapters 8 and 9), so I will briefly recast some important findings in terms of the cyclic

adsorption-desorption model of transepithelial transport (Riklis and Quastel, 1958; Czaky and Thale, 1960; Crane *et al.*, 1961).

17.4.6.1. Surface Adsorption Sites

In the conventional view, the interdependency of Na^+ and sugar (or amino acids) in their rates of transepithelial transport is due to the formation of a ternary complex of Na^+ and sugar with a carrier for permeation into the cells (Crane, 1965; S. G. Schultz and Curran, 1970). If the carrier is coupled to Na^+ or to sugar alone, it is not able to permeate into the cell readily. The fact that the cell membrane physiological barrier is now known not to be due to phospholipid (Chapter 12) itself demands a new theoretical model.

Polarized water offers relatively strong resistance to the permeation of sugars or Na^+ . To enter many cells, these solutes must take the adsorption-desorption route via surface protein sites (Figs. 12.14 and 12.51). Normally the surface proteins have few specific adsorption sites for Na^+ or D-glucose. However, in the presence of both Na^+ and D-glucose, the surface proteins undergo a cooperative transformation to assume a new conformation with a new *c*-value profile which provides both anionic sites of the proper *c*-value for adsorption of Na^+ (Figs. 6.7 and 6.8) and a combination of a sterically suitable backbone and side chain sites for adsorption of D-glucose (Fig. 11.46). Subsequent entry will follow typically the adsorption-desorption route described for simple ion entry in Chapter 12. Since D-glucose and Na^+ adsorption are cooperative, desorption of one will facilitate the desorption of the other, hence the enhanced simultaneous entry of Na^+ and D-glucose.

17.4.6.2. Studies of Microvilli Isolated from Intestinal and Kidney Epithelia

The isolation of microvilli from intestinal mucosa provides an interesting model to study transport (Sacktor, 1977). The rate of D-glucose (but not L-glucose) or amino acid uptake is often increased if the external medium contains a high concentration of Na^+ and the microvilli contain a low concentration of Na^+ . Preincubation of the microvilli with a medium containing a high Na^+ concentration, the inclusion of phloridzin in the incubation medium, or the substitution of K^+ for Na^+ in the external medium will slow the initial uptake of the solute. Valinomycin added to K^+ -preloaded vesicles also accelerates D-glucose uptake. Addition of the uncoupler *p*-trifluoromethylcarbonylcyanidephenylhydrazine (FCCP) to proton-loaded microvilli produces an increase of the initial uptake of D-glucose as well. The conventional interpretation is that D-glucose uptake is driven by the Na^+ gradient, or, in the presence of valinomycin, the K^+ gradient, or, in the presence of FCCP, a proton gradient. The theoretical as well as experimental evidence against ion gradients as sources of energy for biological work performance has been extensively discussed in Chapter 15.

The accelerated uptake of D-glucose quickly reaches a peak (or "overshoot") in the microvilli and then declines until a much lower and steady level is reached. The relative height of this overshoot may give us some additional insight into the mechanism which maintains or controls the level of D-glucose. It is generally agreed that in the intestinal and kidney tubule epithelium the postulated pumps are located at the serosal surface

TABLE 17.1. Apparent Maximum Equilibrium Distribution Coefficients for D-Glucose, L-Glucose, L-Lactate, and L-Alanine in Isolated Microvilli from Intestinal and Renal Epithelia^{a,b}

Authors	Tissue source	Solute studied and concentration	ρ_{\max}	ρ_{eq}
Hopfer <i>et al.</i> (1973)	Rat intestine	D-Glucose 1 mM	0.15	0.15
Murer and Hopfer (1974)	Rat intestine	D-Glucose 1 mM	0.2	0.1
Aronson and Sacktor (1975)	Rabbit kidney	D-Glucose 50 μ M	2.5	0.24
Beck and Sacktor (1975)	Rabbit kidney	D-Glucose 50 μ M	0.5	0.15
Kinne (1975)	Rat kidney	D-Glucose 1 mM	1.25	0.45
		L-Lactate 1 mM	0.61	0.31
Kinne <i>et al.</i> (1975)	Rat kidney	D-Glucose 1 mM	0.58	0.16
Turner and Silverman (1977)	Human kidney (Na^+) (K^+ -val)	D-Glucose 1 mM	1.07	0.98
		D-Glucose 1 mM	0.94	0.55
		L-Glucose 1 mM		0.27
Fass <i>et al.</i> (1977)	Rabbit kidney (Na^+)	L-Alanine 20 μ M	0.14	0.09

^a ρ_{\max} is the apparent distribution at the peak of the overshoot; ρ_{eq} is the final equilibrium value.

^bFrom Ling (1981b), by permission of *Physiological Chemistry and Physics*.

and that there is no outward pump for Na^+ or sugars in the mucosal (microvillus) surface. The osmotic activity of the isolated microvilli shows that most of them are resealed at the broken end. Thus the isolated microvilli present a unique system that contains *no outward pump*. Following the logic of the conventional membrane pump theory, one would expect that the steady level of sugar reached in the microvilli must be equal to that in the bathing solution.

Table 17.1 shows data from the literature showing two sets of apparent equilibrium distribution coefficients, or ρ values, for L-,D-glucose, L-alanine, and L-lactate. The apparent distribution coefficient at the peak of the overshoot is expressed as ρ_{\max} . The apparent equilibrium distribution coefficient at the final equilibrium level is expressed as ρ_{eq} . The data were calculated on the assumption that the external concentration of the solute did not significantly differ from that given as the initial concentration of the medium, and that the microvilli contain 80% water. Table 17.1 shows that, while ρ_{\max} occasionally rose above unity, ρ_{eq} is always below unity and is more or less at the same level as in intact cells. These data are explained simply by the fact that the water in the cytoplasm in the microvilli exists in a state of polarized multilayers and as such has a reduced solubility for all solutes, including D-glucose, L-glucose, L-lactate, and L-alanine. It is most interesting that Mooseker (1976) reported that actin is the main protein of the brush borders. One recalls that actin may be one of the matrix proteins that polarize water in multilayers (Chapter 9).

The synergistic adsorption of Na^+ and D-glucose onto surface protein sites facilitates the entry of Na^+ and D-glucose into the microvilli. The overshoot is then a transient adsorption of D-glucose onto some cytoplasmic proteins. Several observations support this concept:

1. The apparent maximum ρ -value at the peak of the overshoot often exceeds unity, and this suggests selective adsorption or other forms of complex formation in the cytoplasm.

2. An overshoot does not occur in liposomes incorporating proteins extracted from microvilli (Crane *et al.*, 1976; Kinne and Faust, 1977). These vesicles are hollow rather than solid and lack the cytoplasmic proteins essential for the transient D-glucose and L-alanine adsorption.
3. The strong dependency of the overshoot on anions known to have strong affinity for cationic sites (e.g., SCN^- versus Cl^-) (Kinne and Faust, 1977; Crane *et al.*, 1976) suggests that the adsorption of D-glucose involves the unmasking of sites when Na^+ and SCN^- join in dissociating salt linkages, as in equations (17.1) and (17.2) from right to left.
4. The cell surface physiological barrier is not primarily lipid in nature, and valinomycin does not function as an ionophore but as a cardinal adsorbent, controlling the electronic and steric conformation of certain proteins that adsorb K^+ (Chapter 15). Similarly, FCCP acts as a cardinal adsorbent to bring anionic sites to a *c*-value suitable for H^+ binding (i.e., an increase of *c*-value).

Why the overshoot of increased adsorption is not sustained is less amenable to explanation. It may correspond to part of the cyclic change proposed or it may be a transient change of a deteriorating system. These and many other questions can only be answered by future studies.

17.5. Summary

Epithelial tissues and vacuolated plant cells perform true active transport—the creation of an asymmetric solute electrochemical gradient between two dilute aqueous solutions. The mechanism of active transport is a major current problem in physiology. In view of the evidence cited earlier in this book that the conventional concepts of cell membrane permeability and pumps are no longer tenable, a reevaluation of concepts of active transport by epithelia, which have been based on the membrane pump theory, is indicated.

Any theory of active transport must make a number of assumptions; one of the major ones is an inherent asymmetry in the properties of the cells involved, and that this inherent asymmetry somehow provides a “one-way valve.” Whether the asymmetry resides solely within the surface or surface membranes, or within parts of the cytoplasm, is not entirely clear. Nevertheless, the basic concepts of the association-induction hypothesis, established in Chapters 6–12 and applied to a variety of physiological phenomena and examples of biological work performance in Chapters 13–16, were used here to suggest a hypothesis of the mechanism of active transport.

In addition to the recognition of an inherent asymmetry in properties of the bifacial cell, it would seem that any theory of active transport also must assume a cyclic process and an alternation between high- and low-energy states. This alternation must somehow be linked to ATP and the ATPase, in order to achieve this kind of work. In this context, the cornerstone of the association-induction hypothesis of active transport is the concept of cyclic cooperative adsorption and desorption of the transported solute, coupled to polarization and depolarization of water, and triggered and restored alternately by ATP removal by the ATPase and ATP resynthesis and readsorption. As in the general con-

cept of biological work performance in the association-induction hypothesis (Chapter 10), the ATPase is a trigger, not a specific releaser of the energy required for active transport. In this view, the reason that epithelial tissues that transport Na^+ have high amounts of the ATPase is not because they need it to provide more "energy," but because they need to ensure a continuously high level of cyclic desorption and readsorption of ATP.

In this brief chapter, a few selected examples of experimental findings were presented within the context of the hypothesis of the mechanism of active transport. It is anticipated that the concepts presented may help guide future research in this field of physiology, in which there are many problems as yet unsolved.

V

A Tentative Approach to Some
Unsolved Problems in Biology and
Medicine

The Control of Protein Synthesis

The purpose of this chapter is to discuss some subjects of importance in the field of protein synthesis and to present an integrated interpretation of some of the key observations within the framework of the association-induction (AI) hypothesis.

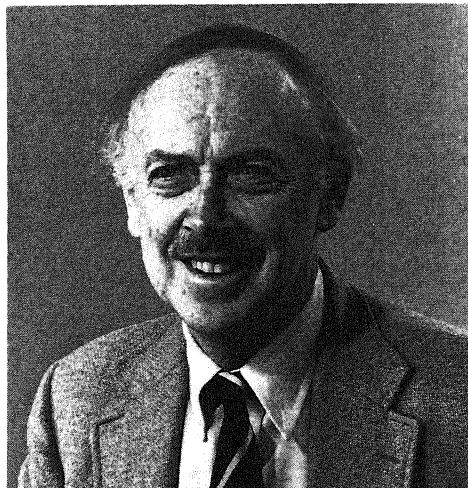
18.1. Transcription and Translation in Prokaryotes

18.1.1. The lac Operon and the Control of Gene Transcription

The brilliant investigations of *Escherichia coli* (*E. coli*) opened a new era in the progress of cell physiology (Watson, 1970). A major accomplishment was the elucidation of the molecular mechanisms by means of which *E. coli* adapts to its environment (Jacob and Monod, 1961a,b; Beckwith and Zipser, 1970). Thus, normal wild type *E. coli* prefer to have glucose as their energy source. Occasionally they find themselves in an environment containing lactose but not glucose. In response to this new environment, the cells will manufacture all the proteins essential to make use of lactose. They will not manufacture these proteins before the need arises, nor after lactose has disappeared from the environment or glucose has been added to it. Lactose, a β -galactoside and the potential energy source which induces *E. coli* to turn on this dormant capability, is called an inducer.

The inherent ability to use lactose lies in the possession, in the ringlike DNA chain common to microbes, of a segment called the *lactose operon*, or *lac operon*, which contains the base sequence coded for the synthesis of three proteins: β -galactosidase, coded by the Z gene; β -galactoside permease, coded by the Y gene; and β -galactoside acetylase, coded by the AC gene. These were illustrated in Fig. 5.1. All three genes are dormant in wild type *E. coli* living in a glucose-containing medium.

The first step in the awakening of the synthetic apparatus for the new proteins is the production of messenger RNAs (mRNAs). mRNA production is in turn initiated by the binding of an RNA polymerase to the stretch of DNA chain called the *promoter* (P in Fig. 5.1). When the *E. coli* is in a lactose-free environment, the initiation of the transcription of the lac operon is prevented by the binding of another protein called the



James D. Watson

repressor onto a region of the lac operon called the *operator* (O in Fig. 5.1). Since there is a partial overlap of the promoter and the operator regions, occupancy of the operator by the repressor protein inhibits the attachment of RNA polymerase and hence initiation of the transcription of the lac operon and the production of the mRNAs. This blockage is removed, however, when the repressor is made inactive by the binding of an inducer, e.g., transformed lactose (allolactose) or its analogues like the nonmetabolized isopropylthiogalactoside (IPTG). This type of control of gene transcription, in which the controlling agent, the repressor, acts to turn off transcription, is called *negative control*.

The behavior of the repressor is remarkable. Under normal conditions when no β -galactoside is present in the environment, the repressor binds tightly onto the operator. Indeed this binding is so tight that it persists even when the rest of the DNA molecule has been digested away. At least 10–12 bases are present in the operator to provide the binding site complex. One asks, How can the binding of a single inducer molecule onto the repressor promptly cause the peeling off of the repressor from the operator region of the DNA when there are so many individual linkages between these two macromolecules?

Before attempting to answer this question, it must be made clear that the simple sequence of lac operon transcription following the binding of the inducer occurs only in special mutants. In normal wild type *E. coli*, another requirement must also be fulfilled before transcription can take place: the absence of glucose in the environment. Lactose is not metabolized as long as there is glucose available. The absence of glucose is made known to the synthetic apparatus in an intricate way through the mediation of another protein called the *catabolite gene activator protein* (CAP). When glucose is present, the level of the omnipresent molecule cyclic AMP (cAMP) is low. When the levels of glucose and its catabolites fall, the concentration of cAMP rises. Under this condition cAMP binds onto CAP. For this reason, CAP is also called cAMP receptor protein. The cAMP-CAP complex thus formed then combines with a region of the DNA mol-

ecule further downstream from the promoter region called the CAP site, resulting in the facilitation of the initiation of RNA polymerase. This is an example of *positive control*, in which the controlling protein complex turns on transcription. Thus, for the transcription of the lac operon in wild type *E. coli*, not only must β -galactoside be present and bind to the repressor, but cAMP must also be present. Why the combination with cAMP enables CAP to bind to the CAP site and how the RNA polymerase action is facilitated by the binding of the cAMP-CAP protein are questions that have remained largely unanswered.

18.1.1.1. Molecular Mechanisms in Negative Control

Existing information clearly shows that the mechanism of negative control cannot be that of simple displacement of the repressor protein from its binding sites by the inducer. As mentioned earlier, at least 10–12 bases of the operator region must be bound to the repressor, and on each repressor there is only one or at most two inducer binding sites (W. Gilbert and Müller-Hill, 1966). The all-or-none severance of many bonds as a result of interaction of one or two inducer molecules is a striking phenomenon that bears resemblance to a host of other striking biological phenomena: the denaturation of ferri- and carbonyl-hemoglobin, where the binding of one H^+ leads to the unmasking of 36 H^+ binding sites (J. Steinhardt and Zaisser, 1951, 1953); the binding of one ATP to muscle proteins, which causes the adsorption of 10 or 50 K^+ (Fig. 11.39); and the binding of one molecule of the drug 48/80 to cat skin, which liberates “explosively” 70–80 molecules of histamine* (Feldberg and Paton, 1951). All of these phenomena follow a general pattern described in the AI hypothesis in terms of cardinal adsorbent control of autocooperative adsorption or association (Capability III, Section 7.4.4.2). One can apply the same theoretical interpretation illustrated in Fig. 7.13. The inducer IPTG here acts as a cardinal adsorbent. In this role, (1) IPTG must be strongly bound; (2) there must be alternative adsorbents displacing the repressor protein, and (3) the dissociation must be autocooperative, i.e., all-or-none.

Strong binding of IPTG to isolated repressor protein has long been known (W. Gilbert and Müller-Hill, 1966). Thus, at 4°C the IPTG binding constant is $1.67 \times 10^6 M^{-1}$ for the i^t mutant and $7.7 \times 10^5 M^{-1}$ for the wild type, corresponding to $-\Delta F$ of 7.88 and 7.45 kcal/mole, respectively.

Additional support for this interpretation came from the *in vitro* demonstration of the suppression of binding of the repressor protein to d lac DNA by IPTG (A. D. Riggs *et al.*, 1970) and the high sensitivity of the lac repressor-operator complex to KCl concentration. Thus, a tenfold increase in KCl concentration caused a 100-fold decrease in the association constant (Fig. 18.1). A. D. Riggs and Bourgeois (1968) also showed strong binding of lac repressor on phosphocellulose at neutral pH and that the bound lac repressor can also be dissociated by 0.3 M KCl, but not by lower concentrations of KCl, suggesting all-or-none autocooperativity in the dissociation process.

Several investigators seemed inclined to believe that the effect of salt ions is due to

*The effect of compound 48/80 cannot be due to destruction of the cells because histamine release can be brought about by a dose of 48/80 that does not liberate any K^+ from the skin. If cell lysis were the cause of histamine release, K^+ should be liberated (Paton, 1956, p. 68).

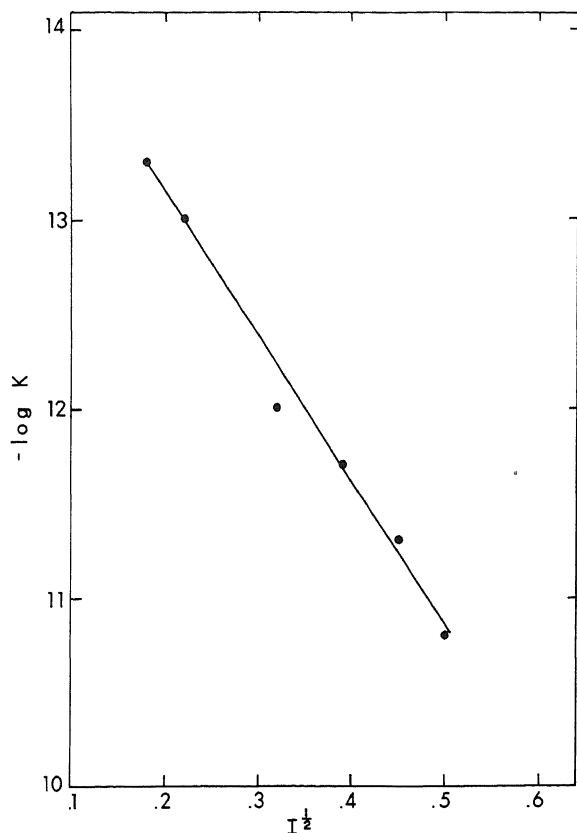
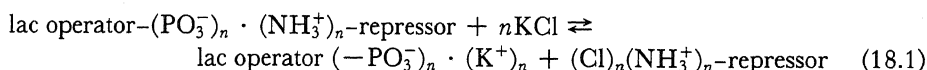


FIGURE 18.1. Effect of ionic strength of KCl solution on the dissociation constant of the lac repressor-operator complex. Complete binding curves in which repressor was varied were done at each ionic strength and the dissociation constant was calculated, usually from the one-half saturation point. [From A. D. Riggs *et al.* (1970), by permission of *Journal of Molecular Biology*.]

an "ionic strength effect" in which all the ions are fully dissociated and not adsorbed. I have pointed out that the assumption of full counterion dissociation at this level of ion concentration is theoretically not justifiable and experimentally counterindicated (see Section 6.2.1). A more reasonable assumption is that binding of the repressor on the lac operator is through salt linkages between anionic phosphate groups of the DNA and cationic ϵ -amino or guanidyl groups of lysine and arginine side chains of the repressor protein. The cardinal adsorbent, IPTG, causes the autocooperative dissociation of the repressor protein from DNA by KCl:



This reaction is diagrammatically illustrated in Fig. 18.2. Additional evidence that alkali metal ions are specifically adsorbed on DNA and not merely part of a diffuse ion cloud can be found in the work of Felsenfeld and Miles (1967) and the more recent work of Anderson and Bauer (1978) and of Bleam *et al.* (1980), all demonstrating specific ion binding to DNA. It is also interesting to note that de Haseth *et al.* (1977)

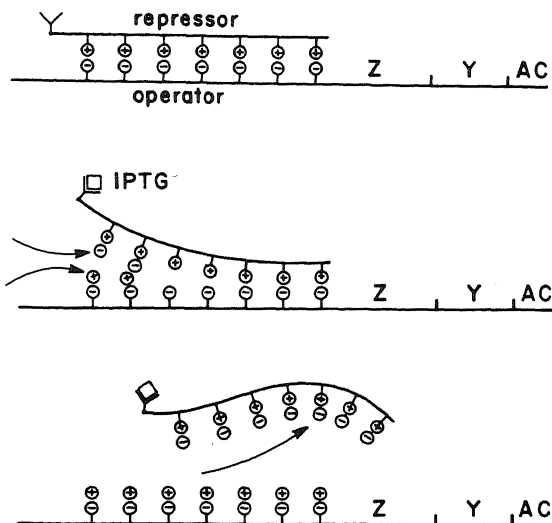


FIGURE 18.2. Diagrammatic illustration of the steps in the all-or-none peeling off of the repressor from the operator region of the lac operon by the binding of the cardinal adsorbent IPTG.

considered counterion release to play a key role in the interaction of lac repressor with DNA. Clearly a counterion must be "bound" or adsorbed before it can be released. If so, the difference between their view and that represented here is the causal relationship: de Haseth *et al.* considered counterion release as the driving force for the lac repressor-DNA binding; as part of an exchange adsorption phenomenon I consider that the driving force is provided by the adsorption or desorption of the cardinal adsorbent (e.g., IPTG or another inducer).

A simple Langmuir-type of adsorption exchange cannot theoretically predict the observed all-or-none nature of repressor detachment with IPTG binding. Here, auto-cooperativity with a relatively high nearest-neighbor interaction energy between near-neighbor binding sites is critically important. Evidence that the interaction of DNA with K^+ and other ions is autocoperative is also available in the literature. Hughes (1970), from conductance measurements, showed autocoperative K^+ binding to and release from DNA. The data of Felsenfeld and Huang (1961) are illustrated in Fig. 18.3. Having first established that the tetraamine, spermine, like polylysine or the dye acridine orange, binds stoichiometrically to the phosphate groups of nucleic acids, they then studied the displacement of H^+ from the phosphate group by increasing concentrations of spermine. Note the strongly sigmoidal autocoperative characteristic of the displacement of H^+ . These experiments show quite clearly a strong near-neighbor interaction between neighboring phosphate groups of the denatured DNA in the stoichiometric displacement of positively charged ions by other positively charged ions. In this connection it is interesting to note that Demmink (1962) demonstrated autocoperativity in the adsorption of K^+ versus Na^+ on the polyphosphates. Other extensive evidence of auto-cooperative adsorption on proteins was presented in Figs. 7.19-7.26.

It should be pointed out that, while K^+ plays a specific role here and the reaction is described by equation (18.1), in other cases, Na^+ salts may serve as the specific effective agent (see Section 18.2.2).

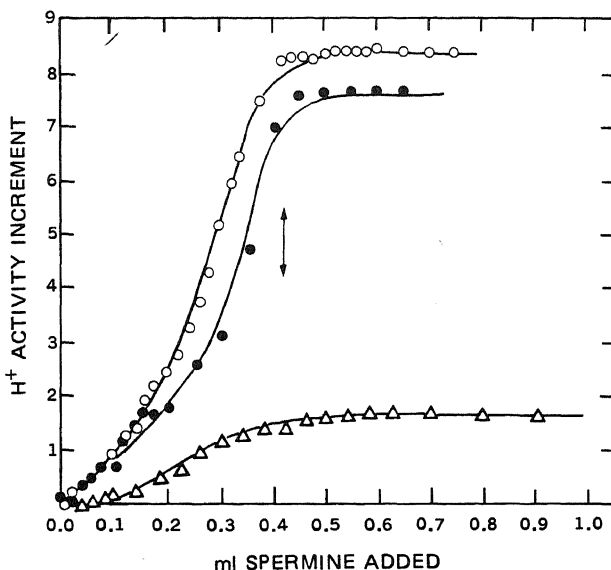


FIGURE 18.3. Increase in H⁺ activity when 1.25×10^{-3} M spermine tetrahydrochloride is added to denatured DNA dissolved in distilled water. Arrow indicates theoretical equivalence point, temperature 27°C. Initial pH values: ●—●, 6.31; ○—○, 5.40; △—△, 4.69. The scale for H⁺ is multiplied by 10^7 , 10^6 , and 10^5 respectively. [From Felsenfeld and Huang (1961), by permission of *Biochimica et Biophysica Acta*.]

18.1.1.2. Molecular Mechanisms in Positive Control

The basic scheme of the modulation of autocooperative association and dissociation by cardinal adsorbents to explain negative control can also be somewhat modified in order to explain positive control. Only a brief sketch will be given here of two specific subjects: why cAMP binding is essential for CAP protein attachment to the CAP site and how the binding of cAMP-CAP complex to CAP sites initiates synthesis of mRNA.

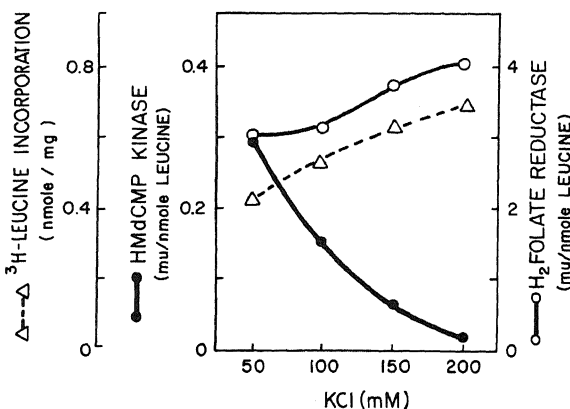
To explain its essential role, one regards cAMP as a cardinal adsorbent whose adsorption initiates an all-or-none preferential binding of the CAP protein to the CAP site, as illustrated in Fig. 7.13, but in the reverse direction. Similarly the facilitation of the initiation of RNA polymerase activity can be theoretically explained by assuming that the cAMP-CAP complex also acts as a cardinal adsorbent whose attachment initiates the autocooperative adsorption of the polymerase.

18.1.2. The Role of K⁺, Na⁺, Glycerol, and DMSO in DNA Transcription

In vitro, the transcription of bacterial and bacteriophage DNA with the aid of *E. coli* RNA polymerase has been shown to be influenced by the concentration of KCl or NaCl in the buffer medium, as has the binding of RNA polymerase (Hinkle and Chamberlin, 1972; Seeburg *et al.*, 1977; Strauss *et al.*, 1980), initiation (So *et al.*, 1967; Schäfer and Zillig, 1973), elongation (Bremer, 1970), and termination and reinitiation (Millette *et al.*, 1970).

Of particular importance is the strong differential effect of KCl concentration on

FIGURE 18.4. Effect of increasing KCl concentration on the *in vitro* transcription of T2 phage dihydrofolate reductase (O) and 5-hydroxymethyl-2'-deoxycytidylate (HMdCMP) kinase (●) mRNAs. The extent of protein synthesis was measured by [4,5-³H]leucine incorporation (Δ). [From Trimble and Maley (1975), by permission of *Archives of Biochemistry and Biophysics*.]



specific mRNA synthesis from T2 phage DNA by purified *E. coli* RNA polymerase *in vitro*. Thus the genes for dihydrofolate reductase and deoxynucleotide kinase were transcribed at 50 mM KCl, but at 200 mM KCl the synthesis of kinase mRNA was almost eliminated while that of reductase was increased (Fig. 18.4) (Trimble and Maley, 1975). Similar observations of differential promoter site selection by *E. coli* RNA polymerase were demonstrated by Dausse *et al.* (1976) using T7 DNA as a template (see also Nakanishi *et al.*, 1974; Miller and Burgess, 1978).

Of equal interest is the finding of Nakanishi *et al.* (1974), who showed that 2.5 M glycerol, ethylene glycol, dimethylsulfoxide (DMSO), 1,3-propanediol, or sucrose not only stimulates *in vitro* RNA synthesis (Table 18.1) but also can replace the requirement of cAMP and cAMP receptor protein (see also Crepin *et al.*, 1975). These authors interpreted their data on the basis of glycerol changing the conformation of DNA, bringing to mind the finding that glycerol, ethylene glycol, DMSO, and 1,3-propanediol all reduce the melting temperature of DNA (L. Levine *et al.*, 1963), an interpretation in general agreement with the theory of Schäfer *et al.* (1973). A possible new insight that

TABLE 18.1. Comparison of Effect of Various Solvents on RNA synthesis^{a,b}

Solvent	Total RNA (pmoles CMP)	gal RNA (pmoles CMP)
None	25.5	1.06
2.5 M Glycerol	63.4	8.18
2.5 M Ethylene glycol	60.2	6.54
2.5 M Dimethylsulfoxide	145.2	20.55
2.5 M 1,3-Propanediol	58.7	7.53
0.37 M Sucrose	50.4	5.97

^aA preincubation mixture containing the bacteriophage galP-211 and RNA polymerase was mixed at 0°C with the various solvents indicated in the first column. After a 10-min preincubation at 37°C, MgCl₂ and rifampin were added, and total RNA and gal RNA synthesized after a 10-min incubation at 37°C were measured. 2.5 M glycerol corresponds to 18.5% (v/v).

^bFrom Nakanishi *et al.* (1974), by permission of *Journal of Biological Chemistry*.

the AI hypothesis can offer here is that such agents as glycerol, ethylene glycol, and DMSO can promote DNA melting because in the melted state water is polarized in multilayers and these agents are the ones that fit in and stabilize this multilayered water (Chapter 9).

18.1.3. The Role of K^+ in mRNA Translation

A strain of *E. coli* low in K^+ content (B-207) was isolated by Lubin and Kessel (1960). If this *E. coli* is grown in a medium containing K^+ at a concentration well suited for the growth of wild type *E. coli*, cell division will stop. Growth resumes in a high- K^+ medium (Lubin, 1964). Indeed the growth rate of this mutant is quantitatively related to the concentration of K^+ in the medium in a saturable manner (Fig. 18.5). In a medium of low K^+ , cell K^+ is partly replaced by Na^+ and the rate of cell growth is low. Lubin and Kessel also showed that K^+ depletion primarily affects protein synthesis and has little or no effect on RNA synthesis. The inhibiting effect of K^+ depletion on protein synthesis lies in the initial step or *primary reaction* before the formation of poly-peptide bonds in the assembly of functional polyribosomes.

Lubin and Kessel adopted the conventional membrane pump model and attributed the genetic defect of B-207 *E. coli* to membrane leakage. In fact their own data provide interesting insight into the nature of the role of intracellular K^+ in regulating protein synthesis. First, the saturability (Fig. 18.5) and competition demonstrated in the effect

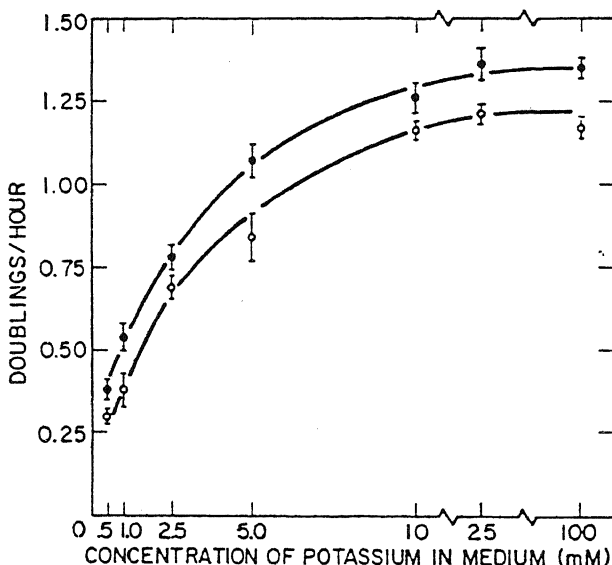


FIGURE 18.5. Dependence of rate of growth of strain B-207 on K^+ and Na^+ concentrations in medium ($37^\circ C$). In the usual growth medium the concentration of K^+ is 100 mM. At lower values of K^+ , Na^+ was substituted mole for mole. Bracket shows 1 SE of mean. O—O, Minimal medium; ●—●, medium supplemented with 0.1% casein hydrolysate. [From Lubin and Ennis (1964), by permission of *Biochimica et Biophysica Acta*.]

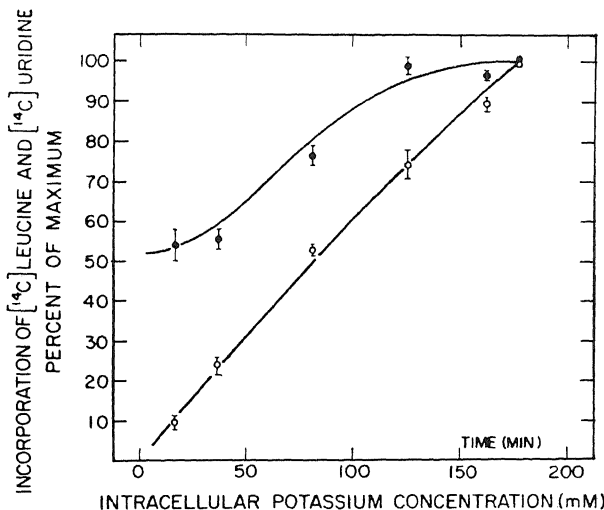


FIGURE 18.6. Incorporation of [^{14}C]leucine into protein ($\textcircled{\text{o}}$) and [^{14}C]uridine into RNA (\bullet) at various levels of intracellular K^+ in *E. coli* strain B-207. Each point shown represents a rate of synthesis. Bracket shows 1 SE of mean. All values expressed as percent of rate at highest K^+ level. [From Lubin and Ennis (1964), by permission of *Biochimica et Biophysica Acta*.]

of external K^+ suggest that the activity of K^+ shows adsorptive behavior. Figure 18.6 shows that the rate of protein synthesis, as measured by [^{14}C]leucine incorporation, is linearly related to intracellular K^+ concentration. The data in general agree with the AI hypothesis, suggesting that it is adsorbed K^+ that is required for the proper priming reaction of polysome assembly. Adsorption of Na^+ has little effect in promoting protein synthesis in this case, as indicated by [^{14}C]phenylalanine incorporation (Fig. 18.7).

18.2. The Control of Gene Function in Eukaryotes

An important difference between prokaryotic and eukaryotic cells is the control mechanism for gene transcription. The prokaryote *E. coli*, for example, in response to a change of environment, produces new proteins coded by the lac operon, and the daughter cells will continue to produce these proteins as long as there is galactoside but no glucose in the environment. In multicellular eukaryotes, such as mammals, widely different cell types share the same genome. Here the control of the specific genes transcribed in each cell type is dependent on the environment, and other factors at a critical moment in the development of the organism. Once set, however, the same gene transcription persists through generations of daughter cells and is, as a rule, stable toward their immediate environment. Since DNA itself is not basically different in *E. coli* and in mammals, what is the molecular basis for this profound difference in the pattern of gene transcription?

One of the factors that distinguishes prokaryotes and eukaryotes is the histones, which are found in all eukaryotes but not prokaryotes (Zubay and Watson, 1959).

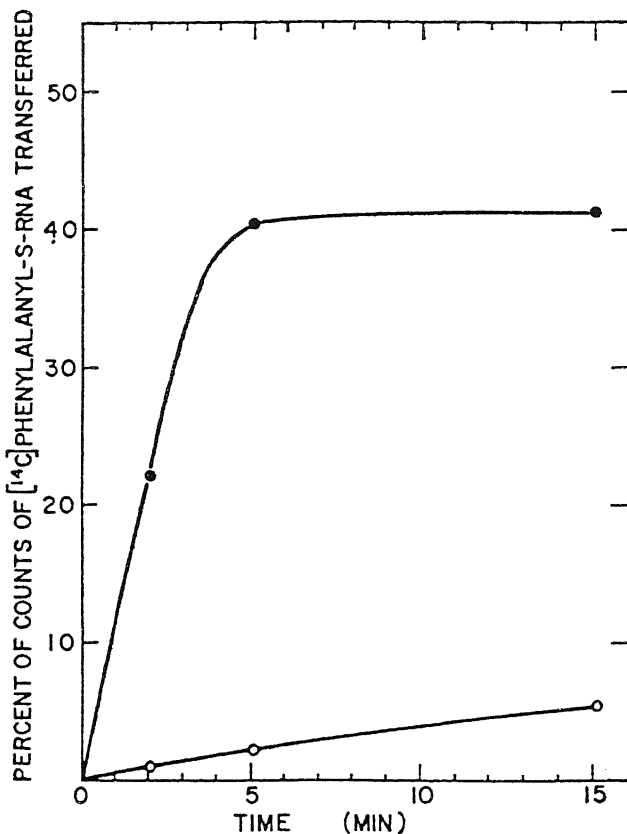


FIGURE 18.7. Kinetics of transfer of counts from L-[¹⁴C]phenylalanyl sRNA to trichloroacetic-acid-precipitable polypeptide (37°C). Each milliliter of reaction mixture contained Tris-HCl (pH 7.4), magnesium acetate, mercaptoethanol, sucrose, trisodium-GTP, disodium-ATP, disodium-creatine phosphate, creatine phosphokinase, polyuridylic acid, [¹⁴C]phenylalanyl-sRNA, S-30 fraction, and either KCl, 50 μmoles (●—●), or NaCl, 50 μmoles (○—○). [From Lubin and Ennis (1964), by permission of *Biochimica et Biophysica Acta*.]

Indeed, chromosomes of viruses and bacteria are simply pure DNA, often in a circular form, and mostly not complexed with proteins (Wilkins and Zubay, 1959). In eukaryotes, on the other hand, DNA is not free but is tightly bound to histones and to non-histone proteins in a complex called chromatin. A role for histone in gene regulation in eukaryotes was proposed long ago (Stedman and Stedman, 1950).

Histones are separable into four classes, and all contain large amounts of the basic amino acid residues lysine and arginine (Isenberg, 1979). As mentioned previously, there are reasons to believe that the positively charged ε-amino and guanidyl groups of the histones form salt linkages with the negatively charged phosphate groups of the DNA molecules, and that these salt linkages play important roles in the control of gene transcription. To what extent these histones and nonhistone proteins resemble the repressor protein of the lac operon of *E. coli* remains to be answered.

18.2.1. Gene Transcription

The salivary glands of the larvae of insects like the fruit fly, *Drosophila*, and the midge, *Chironomas*, are unusual in that duplication of the chromosome pairs is not followed by separation of the daughter chromosomes. Instead, the daughter pairs line up gene for gene with some 1000–2000 similar individual chromosomes in intimate and accurate opposition. These *polytene chromosomes* are so large that they are easily visible under the light microscope. Balbiani (1881), who first described them, noted their intestinelike appearance. Each of these giant chromosomes is distinguished by a sequence of highly characteristic bands, which have been recognized and correlated with specific genes from the studies of *Drosophila* mutants (Bridges, 1935).

The DNA content of a haploid unit of a polytene chromosome band is equivalent to 10^5 base pairs (Rudkin, 1965; Daneholt and Edström, 1967) and is thus enough to code for 30,000 amino acid residues or 100 proteins with an average molecular weight of 23,000 daltons. This is far too large a number to be handled by one single band. Clearly only a small fraction of this genetic information is actually utilized at any one time.

A remarkable behavior of the polytene chromosomes is that at a highly specified time in the life of the insect some bands lose their dense appearance and swell up into "puffs," only to become dense again some time later (Beermann, 1952; Pavan and Breuer, 1952). Puffing is an indication of regional gene activation.

The formation of a puff involves the decondensation or uncoiling of the DNA strand, thereby permitting its transcription. That mRNA is actively formed at the puffs was first demonstrated by Pelling (1959), who showed incorporation of radioactively labeled uridine at the puff site. Figure 18.8 reproduces a figure from Beermann and Clever (1964). Since uridine is only found in RNA, the radioactivity of the puffs in the squashed and fixed chromosomes establishes active mRNA synthesis at the puff. Addi-

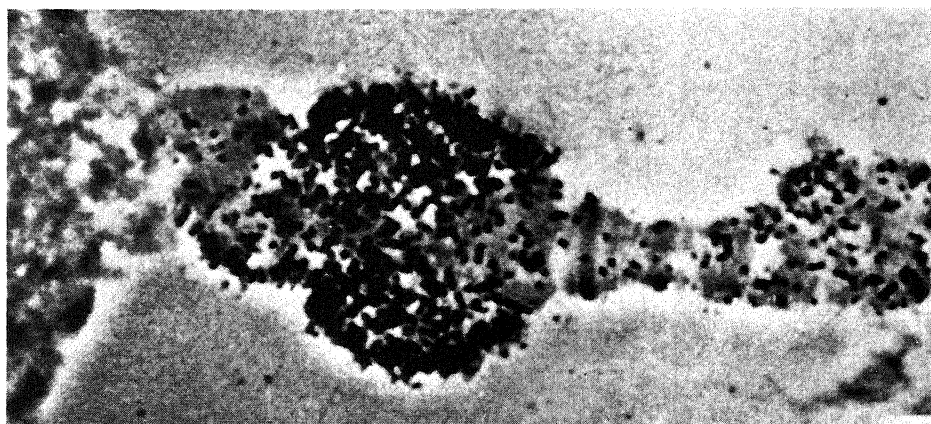


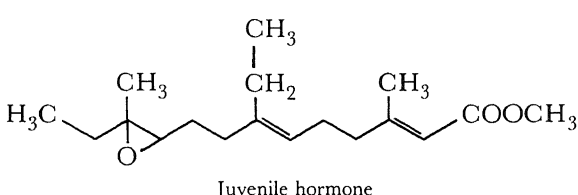
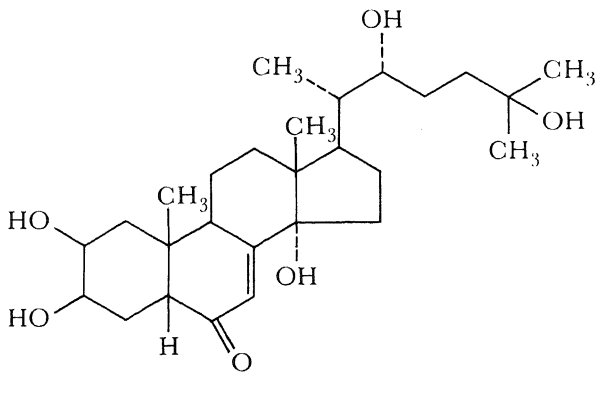
FIGURE 18.8. Inhibition of puffing and of RNA synthesis is accomplished by treatment with the antibiotic actinomycin D. Autoradiogram of a chromosome IV of *Ch. tentans* shows the incorporation of much radioactive uridine (black spots), which takes place during the production of RNA as explained in the text. [From Beermann and Clever (1964), by permission of *Scientific American*.]

tional evidence comes from the inhibiting effect on labeled uridine incorporation by actinomycin D, known to suppress DNA-dependent RNA synthesis (Ritossa and Pulitzer, 1963).

18.2.1.1. The Hormonal Control of Gene Transcription in Polytene Chromosomes

Since puffing indicates active transcription of a specific gene, puffing has been used successfully to probe the agents which initiate and terminate gene transcription. Toward this aim, the giant salivary gland chromosomes have provided marvelous experimental materials for study.

An insect larva on reaching a certain age metamorphoses into an adult or imago. A pair of key controlling agents is the steroid molting hormone, ecdysone, and the juvenile hormone.



Ecdysone is secreted by the ring (prothorax) gland of the insect. H. J. Becker (1962) ligated third instar *Drosophila melanogaster* larvae before the ring gland in such a way that the posterior half of the salivary gland became separated from the hormonal source. As a result, the nuclei of the anterior part of the gland showed a typical puffing pattern while the nuclei of the posterior half did not advance beyond the typical intermoult stage. Becker's work was later confirmed by Ashburner (1970).

Puffing of the polytene chromosomes of *Drosophila* salivary gland in the late larval and prepupal stages of development follows a time sequence. Some puffs appear while others disappear, all primarily controlled by the molting hormone, ecdysone. The pattern is at once intricate and perfectly orchestrated. Here I shall present a small part of

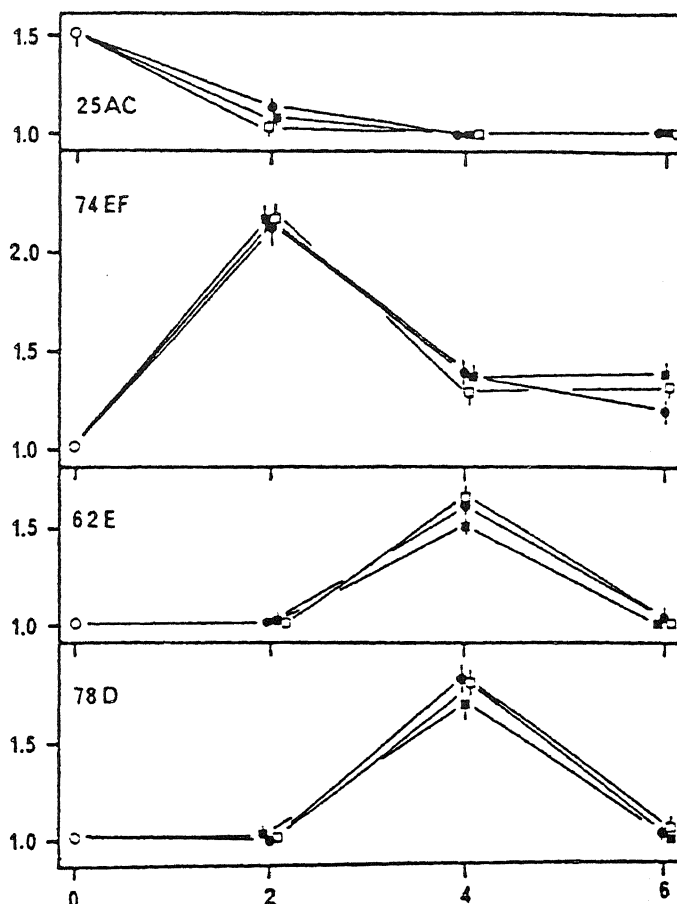


FIGURE 18.9. Response at chromosome regions 25AC, 74EF, 62E, and 78D in PS1 larval glands incubated for 2, 4, and 6 hr with (●) β -ecdysone (1.5×10^{-6} M), (■) β -ecdysone + ZR 515 (2.9×10^{-5} M), or (□) β -ecdysone + methylepoxyhexadecanoate (3.2×10^{-4} M). Ordinate, puff size; abscissa, hours of culture at 25°C. [From Richards (1978), by permission of *Developmental Biology*.]

the fine work from the laboratory of Ashburner and Richards (Ashburner, 1973; Ashburner and Richards, 1976; Richards, 1978).

The sequence of changes in puffing can be reproduced *in vitro* in isolated chromosomes (Fig. 18.9). If third instar larval glands are cultivated in β -ecdysone, there will follow the regression of some preexisting puffs (e.g., 25 AC, Fig. 18.9), the rapid induction of early puffs (e.g., 74EF), and the slower induction of late puffs (e.g., 62E). For a long time it was thought that juvenile hormone acts by antagonizing the action of ecdysone. Early efforts to prove this point failed until the function of juvenile hormone in puff induction was clarified by the work of Richards (1978). Exposure of the isolated chromosome to ecdysone led to sequential puffing and regression of puffing of different bands. However, simultaneous administration of the juvenile hormone ZR515 (isopro-

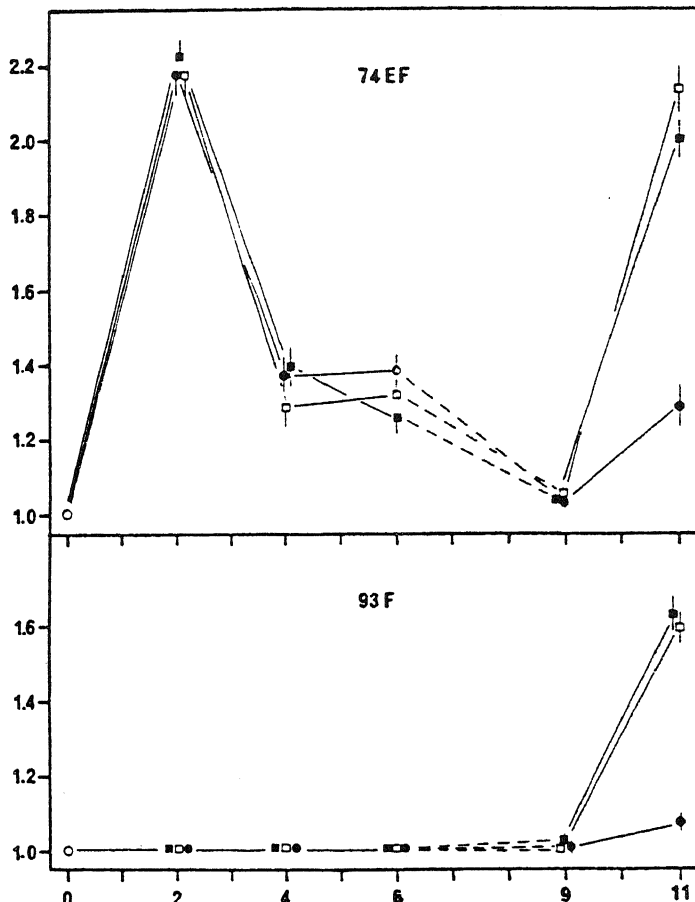


FIGURE 18.10. Responses at 74 EF and 93F in PS1 larval glands cultured for 6 hr in β -ecdysone (—), transferred for 3 hr to ecdysone-free medium (----), and then transferred for a final 2 hr to β -ecdysone (—). ■, Control series (no juvenile hormone); ●, all media contained ZR515 (2.9×10^{-5} M); □, all media contained 3.0×10^{-4} M methyl epoxide hexadecanoate, an inactive homologue of juvenile hormone. Ordinate, puff size; abscissa, hours of culture at 25°C. [From Richards (1978), by permission of *Developmental Biology*.]

pyl-11-methoxy-3,7,11-trimethyl-2,4-dodecadienoate) and ecdysone produced no noticeable additional effects. If on the other hand the culture was exposed first to ecdysone and ZR515 for 6 hr, followed by washing in a solution containing only ZR515 for 3 more hr, then exposure to ZR515 and ecdysone for 2 more hr suppressed puffing (Fig. 18.10). From these and other studies, Richards concluded that the function of juvenile hormone lies in modifying the development of a stage of responsiveness or "competence" (see Section 19.4.2) to ecdysone rather than in directly antagonizing ecdysone action. There is a critical period for the inhibition of the late prepupal response to ecdysone. This beautiful work is cited to provide a conceptual link between control of gene activation and embryology to be discussed in a later section.

18.2.1.2. Kroeger's Theory of Ionic Control of Gene Transcription

I have shown that gene transcription in *E. coli* depends on the concentration of KCl present, in agreement with the molecular mechanism described in equation (18.1). There is evidence that K⁺ and other alkali metal salts also play a significant role in the transcription of genes in eukaryotes. Working with isolated salivary glands of *Chironomus thummi*, Kroeger found that the puffing pattern may be made to revert back from one characteristic of a later stage to a more juvenile pattern by manipulating the ratio of Na⁺ and K⁺ in the culture medium (Kroeger, 1963). Thus one puff (III d 1), which could be induced by ecdysone, was also induced by exposure to a medium containing 120 mM K⁺ (and no ecdysone). This observation, according to Ashburner, was confirmed by Berendes (see Ashburner, 1970, p. 43). The activation of earlier puffs (e.g., III d ½; III d 1:1) was reported by Kroeger to be induced by exposure to a medium containing 100 mM Na⁺ (see also Rensing and Fischer, 1975).

Kroeger then proposed that the action of ecdysone was to alter Na⁺ pump activity in the nuclear membrane. The resulting changes in the K⁺ and Na⁺ concentrations in the nuclear sap then led to puffing or suppression of puffing. He also suggested that Na⁺ or K⁺ may cause puffing by displacing suppressive histone from its binding onto DNA. Table 18.2 taken from Lezzi and Gilbert (1970) shows the differential effects of

TABLE 18.2. Differential Effects of Monovalent Cations on Specific Chromosomal Regions in *Chironomus*^{a,b}

Cation	Chromosome region	Number of bands		Number of preexisting puffs unchanged
		Fading	Unchanged	
K ⁺	I-18-C	13 (2)	1	3
Na ⁺	I-18-C	0	12 (2)	5 (1)
K ⁺	I-19-A	0 (1)	3	15
Na ⁺	I-19-A	6 (4)	0	9 (1)

^aSalt solutions contained 150–200 mM KCl (or NaCl), 12 mM MgCl₂, and 50 mM Tris (pH 7.6). In most experiments the solutions also contained 2 mM glutathione and 1.9 mM CaCl₂, while in some studies RNA polymerase and the four ribonucleoside phosphates were added. These added substances did not influence the differential effects of added Na⁺. Numbers in parentheses indicate number of equivocal results.

^bFrom Lezzi and Gilbert (1970), by permission of *Journal of Cell Science*.

K^+ and Na^+ on the "fading" (i.e., activation) of specific bands I-18-C and I-19-A in the chromosomes of *Chironomas*. In support of Kroeger's theory, Lezzi (1970) cited the work of Latt and Sober (1967), who studied a model of histone, oligolysine polypeptide, that binds to different polynucleotides. Monovalent ions have different and specific effects on the oligolysine-polynucleotide interaction (Fig. 18.11). Thus Li^+ is 63.1 times more effective in displacing oligolysine from poly(I+C) than from poly(A+U), while K^+ is only 1.2 times more effective. Whether Kroeger's theory is entirely correct or not, Latt and Sober's finding pointed out the important role of the alkali metal ions in the control of gene transcription in eukaryotes.

The high degree of K^+ and Na^+ specificity in inducing puffing reported by Kroeger was not seen by Clever (1965), who attributed the effects to different osmotic activities of the salt solutions used.

Recently, Wuhrmann *et al.* (1979) measured with a K^+ -specific microelectrode the K^+ activity in the salivary glands of *Chironomas tentans*. They found that the measured K^+ activity increased by a factor of 2.6 as the oligopausing larvae developed into pre-

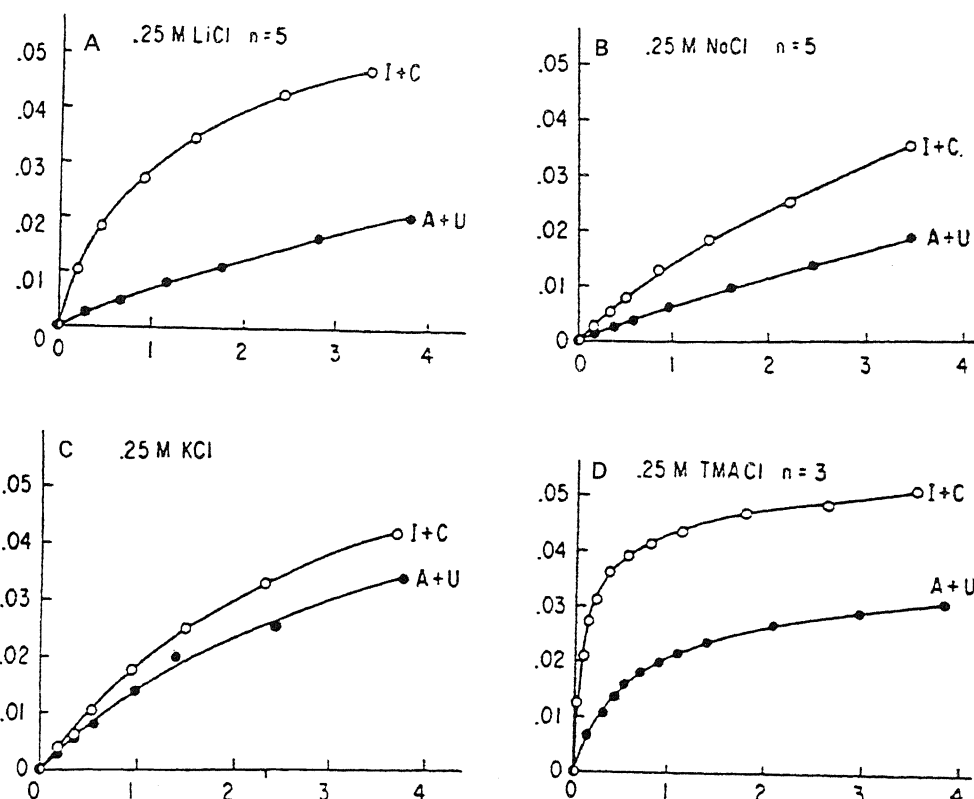


FIGURE 18.11. Effect of cations on ϵ -DNP-Lys(Lys)₅ binding to poly(I+C) and poly(A+U). Solutions were buffered at pH 7.0 by sodium cacodylate-cacodylic acid. Temperature was 4°C. Polynucleotide concentrations: A-C, 1.50; D, 1.33 mM. [From Latt and Sober (1967), by permission of *Biochemistry*.]

pupae, while bands of the chromosomes previously shown to respond to high K⁺ concentration underwent puffing. Wuhrman *et al.* also noted that, in contrast to the 2.6-fold increase of K⁺ activity, the total K⁺ in the salivary gland increased by only a factor of 1.5. They concluded that a large part of the nuclear K⁺ must be in a bound state.

In view of what we know now about nuclear membranes, which have permeability properties that can be matched by membranes with very large pores (Fry, 1970; Paine *et al.*, 1975), the high degree of leakiness makes a pump mechanism for regulating nuclear K⁺ and Na⁺ concentrations highly unlikely (Paine *et al.*, 1981). Nevertheless, the work of Kroeger, Lezzi, and others certainly emphasized once more the importance of alkali metal ions in the selective transcription of DNA. Kroeger and Müller's (1973) more recent publication seemed at once to support a specific ion effect, suggested by Kroeger, and an effect of osmotic activity, suggested by Clever. Thus, 100 mM Na⁺ induced puff III d 1:1 but not III d 1; 150 mM KCl induced III d 1 but not III d 1:1. However, if we take the whole "map" into consideration, clearly a lower *total* concentration of K⁺ or Na⁺, regardless of the proportion in which they are mixed, is more likely to induce puffing of III d 1:1 than III d 1. Different osmotic activity, of course, means different activity of water. Beermann's observation that puffing of the Balbiani rings Br₁ and Br₂ in *Chironomas* was affected by exposure to sucrose and other sugar solutions tends to support the effect of osmotic changes on puffing induction and repression (Beermann, 1973).

Returning to the theoretical models shown in Fig. 7.13 and Fig. 11.3, one may well expect that the autocooperative transition of proteins as well as the protein-nucleic acid system will depend not only on ions but also on water. Thus, taken as a whole, our knowledge about polytene chromosome activation is in harmony with the concepts outlined for DNA transcription in prokaryotes and described in Fig. 18.2 and equation (18.1).

18.2.1.3. Heat-Shock-Induced Puffing Changes

A double-stranded helix of DNA contains many H bonds between its base pairs, and each set of these H bonds entails an enthalpy of several kcal/mole. Yet it is well known that the separation of the duplex strands of DNA can be achieved by heating a solution of the native DNA to 75°C or somewhat higher followed by slow cooling. A rise of temperature from 37°C to 75°C involves an increase of the average kinetic energy from 0.615 to 0.694 kcal/mole, which is a very small amount of energy.

This kind of all-or-none transition produced by a small change in average kinetic energy is typical of the type of microscopic cooperative behavior we have already discussed, where clearly the existence of a positive nearest-neighbor interaction energy and of alternative H-bonding partners makes possible the maintenance of two discrete states and sharp transitions in macroscopic properties that occur with small changes in temperature (Chapters 7 and 11). The heat denaturation of proteins and DNA is an expression of this widely observed phenomenon. It is therefore not too surprising that exposure of intact living cells to quite modestly high temperatures can activate DNA transcription in eukaryotes—a phenomenon first reported by Ritossa in 1962 and now the subject of vigorous and fruitful research (see Ashburner and Bonner, 1979).

Ritossa (1962, 1964) showed that, after exposure to a temperature of 37°C, the

salivary glands of *Drosophila* showed puffing of a specific number of bands. *In vivo*, the induction of puffs by heat shock takes less than 1 min. It requires RNA but not protein synthesis. However, the first indication of uridine incorporation at a puff site occurs slightly later than another primary event occurring at the puff site: an increase in protein binding of anionic dyes such as acidic fast green, naphthol yellow S (acid yellow S) or bromphenol blue. This increased dye binding is observed after ecdysone treatment and after heat shock in sharply defined transverse bands and is indifferent to the protein synthesis inhibitors puromycin and cycloheximide.

There is strong evidence for migration of preexisting proteins, including RNA polymerase, into the puffs (Berendes, 1973). Nevertheless, the rapid and sharp increase in acidic dye binding should not, in my opinion, be entirely attributed to a gain of total protein. It may well also involve the sudden availability of cationic lysine and arginine residues of histone and/or nonhistone proteins in the puff region which will bind the acidic dyes. One recalls that deoxygenation of hemoglobin leads to a sudden increase of sites capable of binding bromthymol blue, another acidic dye closely related to bromphenol blue, even though in this case there is no net increase of protein content (Antonini *et al.*, 1963).

If during puffing the increase of acidic dye binding truly results from dissociation of histone (and/or nonhistone proteins) from DNA, and if histone binding is the cause of nontranscription of DNA (Stedman and Stedman, 1950), these concepts would provide explanations of the following interesting finding: (1) DNase I (Weintraub and Groudine, 1976) and DNase II (Gottesfeld *et al.*, 1974) preferentially attack those regions of interphase chromatin that are actively transcribed, and (2) *E. coli* RNA polymerase can recognize and transcribe DNA in the heat-shock-induced puffs (Biesmann *et al.*, 1978).

The heat-shock-induced puffing took on new significance and engendered wide interest after Tissières *et al.* (1974) demonstrated that heat shock did not just cause puffing but also induced the synthesis of a set of specific polypeptides, the number of which apparently correspond to the number of specific puffs induced (Ashburner and Bonner, 1979).

Two other sets of interesting phenomena connected with the heat-shock-induced polypeptide synthesis are these: (1) Exposure to metabolic poisons and other agents may induce similar sets of puffs, and (2) heat shock induces similar puffs in a variety of tissues of the animal. These subjects will be separately discussed in the following sections.

18.2.1.3a. Other Agents That Duplicate Puffing Patterns Produced by Heat Shock. Ashburner and Bonner (1979) showed that, while the number and kind of bands induced to puff by heat shock are quite well defined, heat shock is not the only means to induce puffing of this same set of bands. Other effective agents include the uncoupler of oxidative phosphorylation 2,4-dinitrophenol; the ionophores valinomycin and dinactin; the respiration inhibitors amytal and azide (but not cyanide); and also, paradoxically, recovery from anoxia but not anoxia itself. Iodoacetate, which reduces the ATP content of the salivary glands, did not induce heat-shock puffs; arsenite, which does not change the ATP content, does produce the puffs. However, externally applied ATP (and ITP) inhibit the induction of heat shock puffs (Leenders and Berendes, 1972; Behnall and Rensing, 1975).

Since so many different agents can produce the same set of puffs, it was suggested that they all act on an energy-producing system and cause it to make a single puff-producing agent. Indeed Sin and Leenders (1975) were able to demonstrate that isolated mitochondria from heat-shocked *Drosophila hydei* produce in the supernatant solution a nondialyzable, heat-labile agent which when injected into untreated salivary glands produced heat shock puffs.

The best reason for postulating a unitary cause for the induction of heat-shock puffs is that heat shock and the large variety of diverse agents all produce the same battery of puffs. It is somewhat ironic that Sin's mitochondrial agent, which offers the best support for a unitary hypothesis, did not elicit all the puffs induced by heat shock. It elicited only two puffs (36A and 48BC). Indeed a more careful reading of the literature shows that Sin's agent is by no means unique. There are other agents that produce less than the full battery of puffs induced by heat shock. Thus, colchicine and vitamin B₆ induce only puff 20 CD (Ashburner and Bonner, 1979). Under different conditions and at possibly different concentrations, vitamin B₆, alone or in combination with oligomycin, induces only puff 48C. Benzamide induces only puff 93D. Antimycin, oligomycin, and atracyloside or oligomycin and KCN induce all heat shock puffs except 81B. In this context, the findings of McKenzie, Bonner, Pardue, and others merit special attention.

McKenzie *et al.* (1975) and Spradling, Penman, and Pardue (1975) first succeeded in demonstrating, with an *in situ* hybridization technique, mRNA molecules in the cytoplasm of normal *Drosophila* cells, which hybridize with DNA at some 50 bands. When the cells were heat-shocked, activity of most of these 50 bands was shut off. Newly synthesized RNA then hybridizes with seven new bands not active in the normal control cells. J. J. Bonner and Pardue (1976), using the same technique, showed that heat shock produced essentially the same set of puffing in a variety of different tissues of the fly (Fig. 18.12). Invariably 93D and 87C showed intense labeling with [³H]uridine-labeled

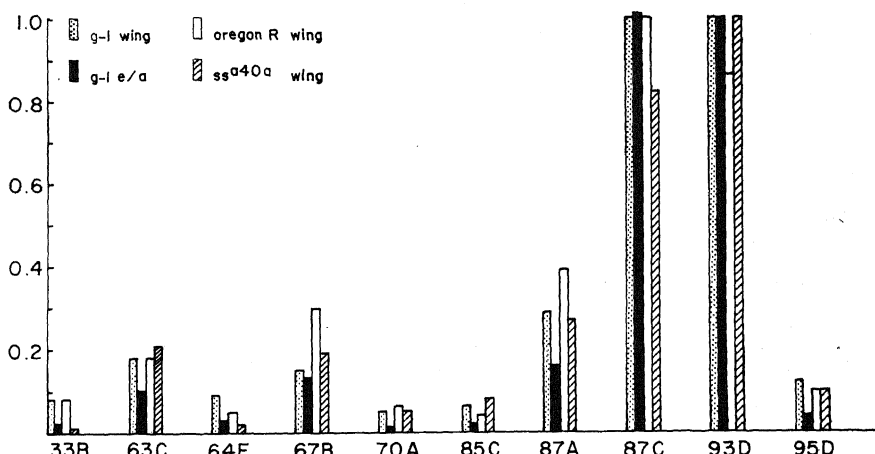


FIGURE 18.12. Comparison of heat shock response in different fly stocks and disc types. Samples are, left to right, g-1 wing discs, g-1 eye-antennal discs, oregon R wing discs, ss^{a40a} wing discs. Ordinate represents autoradiographic grain counts at different chromosomal loci owing to hybridization to [³H]uridine-labeled RNA produced in response to heat shock. [From J. J. Bonner and Pardue (1976), by permission of *Cell*.]

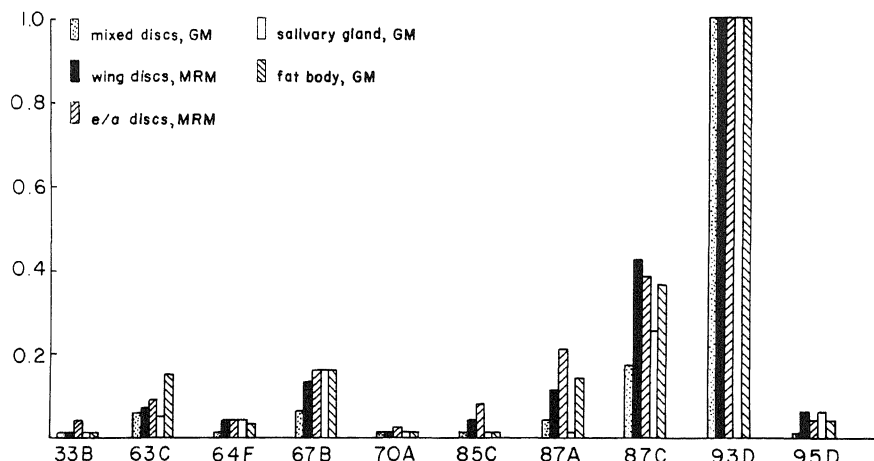


FIGURE 18.13. Effect of aged medium on different tissues. Samples are, left to right, wing leg and eye-antennal discs cultured in aged Grace's medium (GM), wing discs from aged minimum Robb's medium (MRM), eye-antennal discs from aged MRM, salivary glands from aged GM, and fat body from aged GM. All tissues are from g-1 larvae. For a further description of the figure see Fig. 18.12. [From J. J. Bonner and Pardue (1976), by permission of *Cell*.]

cytoplasmic heat shock RNA. The results of Fig. 18.12 were obtained from a standard freshly prepared minimal Robb's medium. Then Bonner and Pardue discovered something unexpected when, instead of the minimal Robb's medium, they used a different medium, Grace's medium, which had been stored at 4°C for 2 years before use. Now the gene activities were remarkably altered. (See also Leenders *et al.*, 1973, for an earlier similar observation). Bonner and Pardue found an excessive transcription of the 93D puff and failure of RNA synthesis at other active sites (Fig. 18.13). Again all the different tissues were similarly affected. Bonner and Pardue (1976) concluded from their data that heat-shock-induced puffing is not controlled by "a single sensing mechanism tied into the energy metabolism" but that different alterations affect different loci.

18.2.1.3b. The Uniformity of Different Tissues in Their Puffing Response to Heat Shock and Other Treatments. Figures 18.12 and 18.13 not only demonstrate the unusual effect of the aged Grace's medium in modifying heat-shock puff behaviors, they demonstrate another striking feature of gene activation induced by heat shock and other agents: a uniformity in response in diverse tissues. This uniformity may offer significant insight into the phenomenon of cancer, as will be discussed in Chapter 20. As Spradling *et al.* (1975) demonstrated, heat shock not only activated a new set of genes not active in each of the diverse normal tissues studied, but also shut off the normal protein synthesis. In Section 18.2.2.2 I shall discuss a similar shut-off phenomenon induced not by heat shock but by viral infection.

18.2.1.4. Ouabain-Induced Synthesis of Hemoglobin in Friend Erythroleukemic Cells

Cultured cell lines (Friend cells) originally derived from the spleens of Friend-virus-infected mice can be induced to synthesize hemoglobin (A. Bernstein *et al.*, 1976).

FIGURE 18.14. Induction of globin mRNA by ouabain. Cultures of ouabain-resistant mutant OUArc-22 containing 1.5% DMSO (●—●), 1 mM ouabain (□—□), or control cultures with no inducer (○—○) were seeded at 5×10^4 cells/ml and incubated for 96 hr at 37°C. Cellular RNA was prepared and hybridized to mouse globin [^{3}H]-cDNA. [From A. Bernstein *et al.* (1976), by permission of *Cell*.]

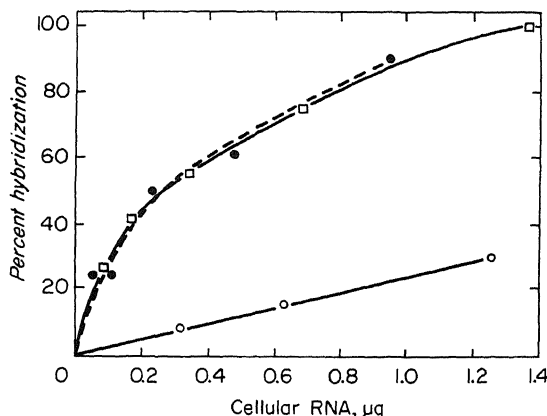


Figure 18.14 shows that untreated control cells contain a low level of globin mRNA that can hybridize with the globin cDNA probe. However, treatment of the cells with ouabain (1 mM) (or dimethylsulfoxide, another hemoglobin synthesis inducer) caused a marked increase in these hybridizable globin sequences. Figure 18.15, also taken from Bernstein *et al.* (1976), shows that an increase of external K⁺ concentration from 1.8

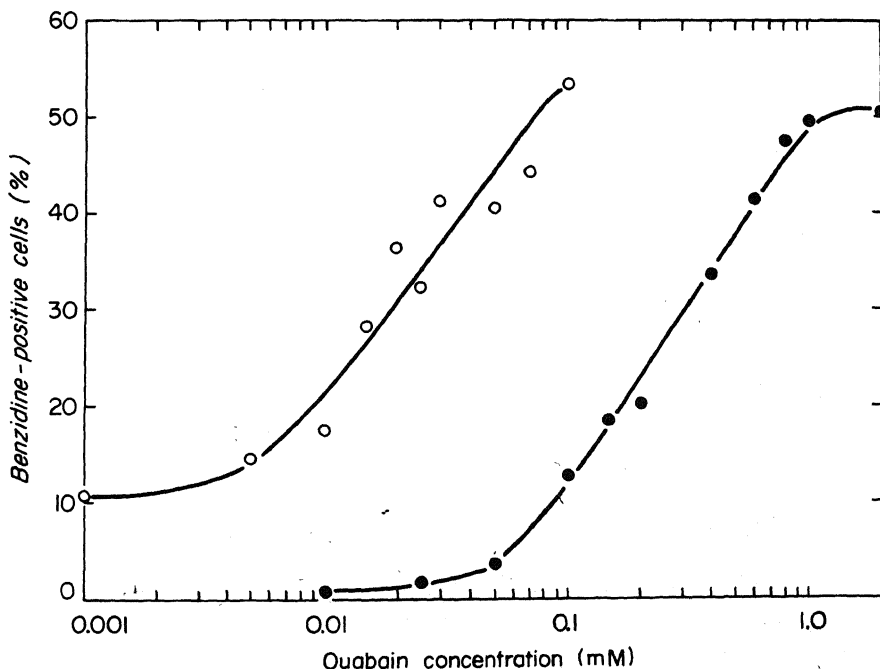


FIGURE 18.15. Dose-response curve for ouabain induction in low- or high-K⁺ medium. Cultures of OUArc-22, growing in either low-K⁺ medium (1.8 mM K⁺) (○—○) or high-K⁺ medium (6.8 mM K⁺) (●—●), were seeded at 5×10^4 cells/ml in various concentrations of ouabain as indicated and incubated at 37°C. The proportion of differentiated cells was determined 5 days later. [From A. Bernstein *et al.* (1976), by permission of *Cell*.]

mM to 6.8 mM increased the concentration of ouabain required to induce hemoglobin synthesis, here measured as percentage of cells that contain hemoglobin and can therefore be stained by the dye benzidine. Bernstein *et al.* concluded that "changes in the concentration of intracellular K⁺ ion may lead to the induction of hemoglobin synthesis."

Comparing the data of Fig. 18.14 with those of Fig. 11.32 shows that the interaction between ouabain level and external K⁺ concentration in affecting hemoglobin production bears a striking resemblance to the interaction between ouabain level and external K⁺ concentration in changing the intracellular K⁺ and Na⁺ concentrations in muscle and other cells (Section 11.2.4.1). Thus it would seem that the mechanism more directly involved in inducing the transcription of the globin gene may entail enhanced Na⁺ binding. In Section 18.1.1.1 I have already presented the view that the inducer activates protein synthesis in *E. coli* by promoting enhanced K⁺ binding.

18.2.2. mRNA Translation and Protein Synthesis

In eukaryotes, in contrast to prokaryotes, owing to the presence of a separate nucleus and the long lifespan of messenger RNA, translation (the process by which genetic information carried by mRNA dictates the specific amino acid sequence in the synthesis of a protein) is well separated from DNA transcription. Much about transcription is understood. I shall concentrate here on the role of K⁺ and Na⁺ ions and of water activity in gene translation and protein synthesis in eukaryotic cells.

18.2.2.1. Reversal of Inhibition of DNA, RNA, and Protein Synthesis by K⁺

We discussed in Section 18.1.2 how the concentrations of Na⁺ and K⁺ influence DNA transcription and translation, or more specifically the initiation of the translation of mRNA, in *E. coli*. Lubin (1967) showed a similar dependence of mRNA translation on K⁺ in mammalian cells. Indeed synthesis of proteins, RNA, and DNA was depressed when intracellular K⁺ was reduced in cancer cells (sarcoma 180) and L cells when these cells were treated with the fungicide amphotericin B (Fungizone®). This depression was substantially reversed by a high-K⁺ medium (Fig. 18.16), presenting yet another analogy to the ouabain–external K⁺ interaction just mentioned. Similarly, ouabain at relatively high concentration ($3\text{--}10 \times 10^{-4}$ M) reduced cell K⁺ and inhibited protein synthesis in sarcoma 180 cells. In terms of the AI hypothesis, protein synthesis depends on the maintenance of the living state: High external K⁺ can compensate for the change of $K_{\text{Na}^+ \rightarrow \text{K}}^{\text{o}}$ by poisons like ouabain (see also Fig. 11.32), or for depression by the fungicide of the supply of essential cardinal adsorbents, most probably ATP (see T. R. Riggs *et al.*, 1958).

Lubin (1967) discovered that, besides ouabain and amphotericin B, the addition of high levels of histone or polylysine reduced cell K⁺ (F. F. Becker and Green, 1960; Kornguth and Stahmann, 1961) and depressed protein synthesis. Protein synthesis can again be restored almost completely by increasing external K⁺ (Fig. 18.17). Similarly, [¹⁴C]thymidine incorporation, depressed by histone, could also be reversed by high K⁺, providing still another example of the agent–K⁺ concentration relation. This finding, potentially of importance in understanding the role of histones in the selective transcrip-

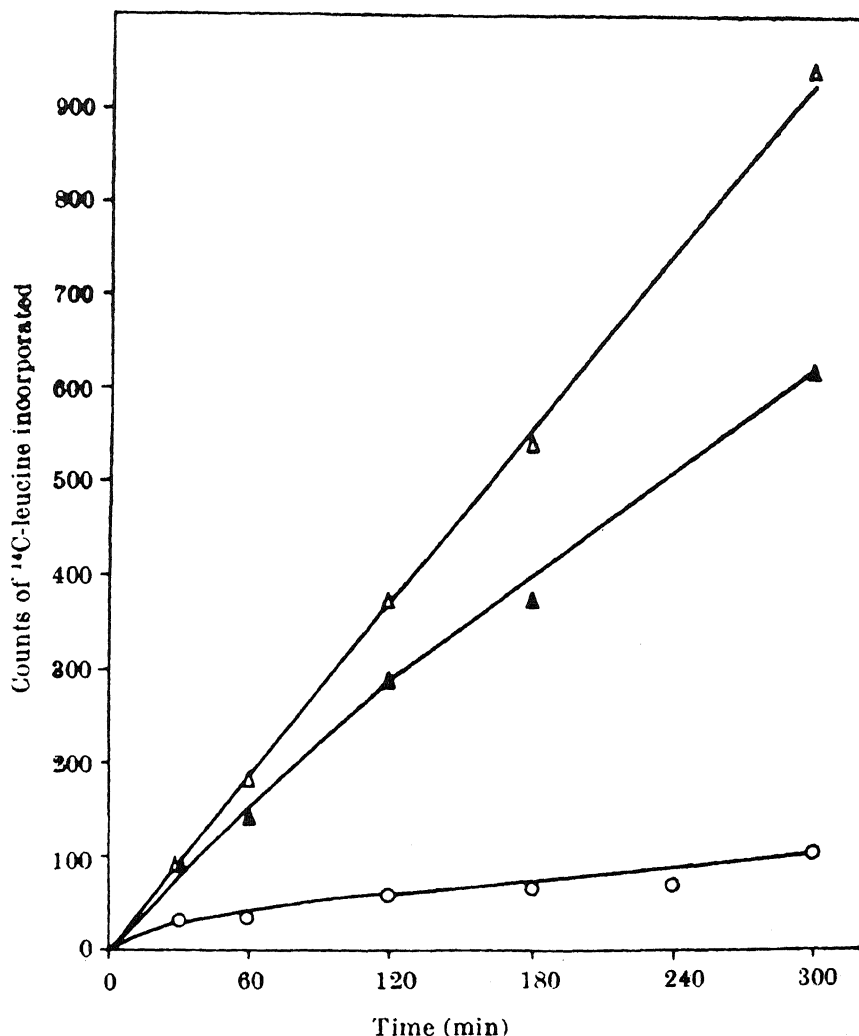


FIGURE 18.16. Effect of high- and low-K⁺ media on protein synthesis after amphotericin B. Δ , Control; \circ , incorporation in 5 mM potassium Eagle's medium, with 8.5 $\mu\text{g}/\text{ml}$ of amphotericin B; \blacktriangle , 8.5 $\mu\text{g}/\text{ml}$ of drug, but 100 mM potassium Eagle's medium. [From Lubin (1967), by permission of *Nature*.]

tion of eukaryotic genes (Stedman and Stedman, 1950), possibly involves autocooperative liberation of DNA phosphate groups from binding to cationic lysine or arginine side chains of histone, resembling reactions described in equation (18.1) for the negative control of the lac operon transcription.

18.2.2.2. Control of Translation of Host Cell and Viral mRNA

K^+ , Na^+ , and water, major constituents of the intra- and extracellular phases of the living cell, seem to play major roles in deciding what mRNA will be translated,

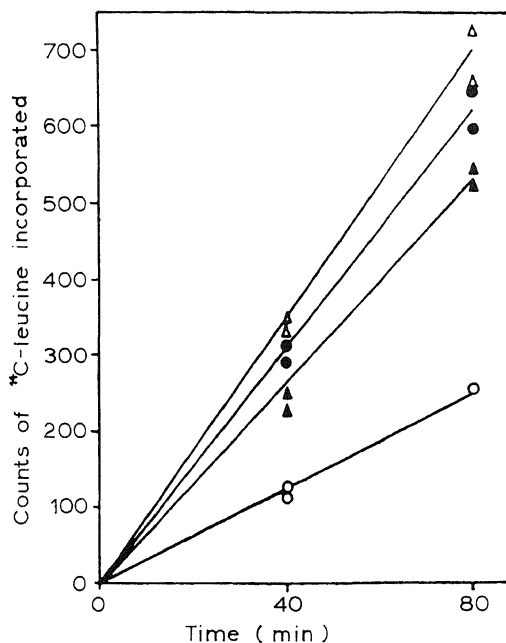


FIGURE 18.17. Inhibition of protein synthesis in sarcoma 180 cells by histone. Δ , Control, cells in 6 mM potassium Eagle's medium, no drug; ●, cells in 100 mM potassium Eagle's medium; ○, 5 mM potassium Eagle's medium plus 100 $\mu\text{g}/\text{ml}$ of histone; ▲, 100 mM potassium Eagle's medium plus 100 $\mu\text{g}/\text{ml}$ of histone. The histone used was the Sigma 3000 fraction. [From Lubin (1967), by permission of *Nature*.]

thereby producing proteins to maintain and replenish the cells. These constituents may also play roles in the proliferation of viruses within the host cells.

It has been known for some time that invasion of host cells by picornavirus leads to cessation of host cell protein synthesis (the shut-off phenomenon) (Franklin and Baltimore, 1962; Baltimore, 1969). Waite and her colleagues (Waite and Pfefferkorn, 1968, 1970; Waite *et al.*, 1972) found that, while lowering or raising the NaCl concentration in the culture medium had little effect on the production of the alphavirus-specified proteins, it inhibited host-specified proteins. Robbins *et al.* (1970) and Wengler and Wengler (1972) exposed cells to concentrated solutions of different kinds (including sucrose, NaCl, KCl, and MgCl₂) and showed that hypertonicity rather than a specific effect of Na⁺ or other ions produced the inhibition of the production of host cell protein. On the other hand, Saborio *et al.* (1974), in agreement with Waite and her associates, demonstrated that a medium containing a total NaCl concentration of 211 mM completely suppressed labeled methionine incorporation into HeLa cell protein, while 261 mM NaCl was required to stop protein synthesis of polio-virus-infected HeLa cells (England *et al.*, 1975).

In view of these facts, the frequent observations that viral infection leads to an increase of host cell permeability, and the fact that K⁺ has been found to be essential for mRNA translation (Lubin, 1967), Carrasco and Smith (1976, see also Carrasco, 1977) proposed a general theory for the mechanism of the shut-off phenomenon. They suggested that attachment of the virus to the cell membrane results in a change of membrane permeability, leading to an influx of Na⁺ and an efflux of K⁺, and the altered cell ionic environment thus created brings about a differential translation of the host and viral mRNA and the shut-off of host cell protein synthesis.

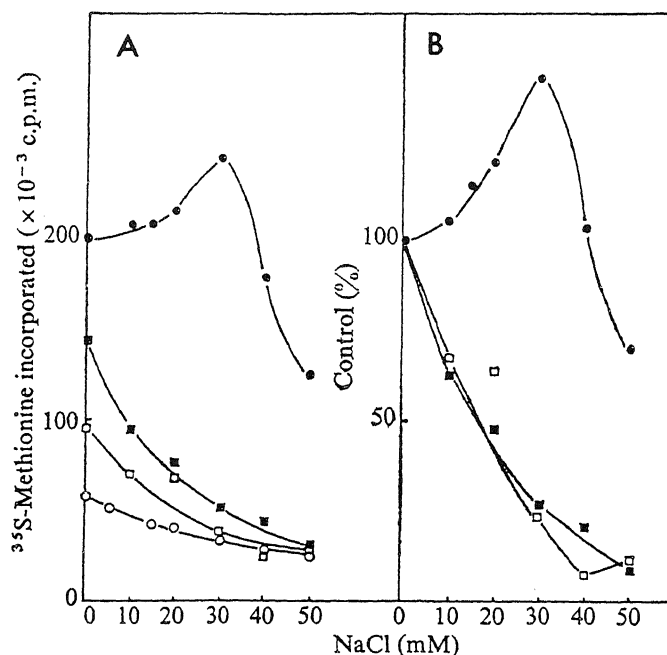


FIGURE 18.18. Effect of NaCl on cellular and viral protein synthesis. O, Endogenous protein synthesis; ●, plus encephalomyocarditis virus RNA; □, plus globin mRNA; ■, plus mouse cell poly(A)-containing RNA. (A) Incorporation of ^{35}S -methionine at different NaCl concentrations. (B) Results expressed as a percentage of incorporation in the incubation containing no added NaCl. [From Carrasco and Smith (1976), by permission of *Nature*.]

In support of this theory, Carrasco and Smith showed that, in a cell-free system, addition of increasing amount of NaCl to a basic medium containing 80 mM KCl causes a progressive decline in the synthesis of proteins directed by added globin mRNA or by mouse cell poly(A)-containing RNA. In contrast, the addition of NaCl (up to about 30 mM) actually stimulated synthesis of protein directed by RNA from encephalomyocarditis virus (Fig. 18.18).

The theory of Carrasco and Smith was tested by Francoeur and Stanners (1978), working with vesicular-stomatitis-virus-infected L cells, and by Stevely and McGrath (1978), working with herpesvirus-infected HeLa cells and BHK21 cells. Both groups of workers obtained negative results. Apparently, herpesvirus was no more resistant to NaCl than to KCl in these systems. Stevely and McGrath concluded that "herpesvirus provides an important exception to the hitherto described common effect of virus infection in conferring on protein synthesis increased resistance to hypertonic medium."

In the critical experiments of both Carrasco and Smith and Stevely and McGrath, two potentially separate factors had not been sorted out: the decreased water activity and the increased Na^+ concentration. Thus, Carrasco and Smith studied the effect of Na^+ by adding NaCl to a medium containing a constant concentration of KCl. As a result the increase of Na^+ went hand in hand with a decrease of water activity (i.e., hypertonicity). Stevely and McGrath's experiment involved a similar ambiguity.

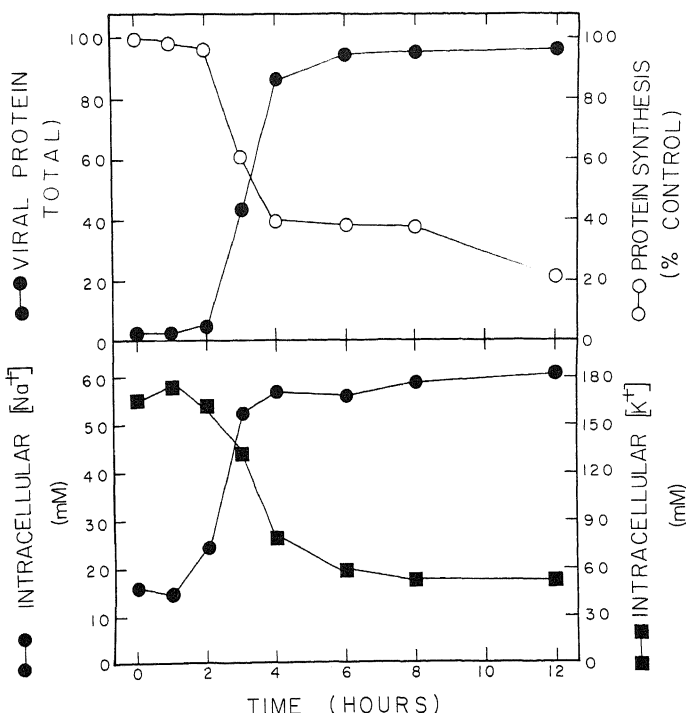


FIGURE 18.19. Changes in protein synthesis and Na^+ and K^+ concentrations in Sindbis-virus-infected chick embryo fibroblast (CEF) cultures. Infected and uninfected CEF cultures were labeled in triplicate with [^3H]leucine. Protein synthesis in infected cells (\circ) is expressed as a percentage of the incorporation in the uninfected cultures labeled at the same time. At each time interval, an additional infected culture was labeled with [^{35}S]methionine and the proteins were subjected to SDS-PAGE. Autoradiograms of the gels were analyzed in a densitometer. Bands corresponding to known alphavirus proteins ($\text{p} 130$, B , PE2 , E1 , E2 , and C) were cut from the tracings and weighed. Their percentage of the total label incorporated by the infected cells was determined (\bullet). Lower panel: At various times after infection of the CEF cultures with Sindbis virus, duplicate cultures were washed with double distilled, deionized H_2O . The amounts of intracellular Na^+ and K^+ were determined by atomic absorption. Protein, cell numbers, and cell volumes were determined in parallel cultures, and the intracellular cation concentrations were calculated. Symbols: \bullet , intracellular Na^+ concentrations; \blacksquare , intracellular K^+ concentration. [From Garry *et al.* (1979), by permission of *Virology*.]

The studies of Robbins *et al.* (1970) and of Wengler and Wengler (1972), however, were different. Their demonstration of a comparable effect produced by hypertonic solutions of sucrose and other solutes established that in these cases it was primarily the decreased water activity that brought about the inhibition of cell mRNA translation. In contrast, Waite's laboratory demonstrated in their system that the effect of Na^+ activity was specific, freed from a concomitant change in water activity, in support of the Carrasco-Smith theory (see also Alonso and Carrasco, 1981).

Garry *et al.* (1979) studied the effect of Sindbis virus infection on chick embryo fibroblasts grown in an unvarying normal minimal essential culture medium. Figure 18.19, taken from this paper, shows that, after a short delay, viral infection brought

about a gain of cell Na^+ and a loss of K^+ . At the time when the intracellular Na^+ reached 40 mM and the intracellular K^+ fell to 80 mM, translation of host mRNA ceased and the proteins synthesized became entirely those dictated by the virus. These authors concluded that the altered NaCl inhibited chick cell protein synthesis at the initiation of translation. Differences in the affinity of host cell and viral mRNA for ribosomes then produced the differential translation effect. Garry *et al.* suggested that most host mRNAs are low-affinity mRNAs (LAM), while viral RNAs as well as some host cell mRNAs are high-affinity mRNAs (HAM). In a following paper Garry and Waite (1979) varied NaCl concentration in the incubation medium and successfully simulated the effect of viral infection of chick embryo fibroblasts. In the presence of a high concentration of NaCl most host protein synthesis was inhibited. However, these cells continued to synthesize interferon. This led the authors to classify interferon as the product of a HAM.

18.2.2.3. Selective Translation of mRNA in Early Development of the Surf Clam

Rosenthal, Hunt, and Ruderman (1980) studied protein synthesis in developing eggs of surf clams (*Spisula solidissima*). Before fertilization, the oocytes synthesized one set of proteins (X, Y, Z of Fig. 18.20); after fertilization, the embryo synthesized a different set of proteins (A, B, C of Fig. 18.20). Yet oocytes and embryos contained mRNA for both sets of proteins, as shown by the simultaneous synthesis of both sets of proteins in a cell-free system containing phenol-extracted mRNA of both the eggs and the embryo. In unfertilized eggs one set of mRNA associates with the ribosomes; after fertilization the other set of mRNA associates with the ribosomes. These and other findings led the authors to conclude that the switching of protein synthesis is at the level of mRNA translation. More discussion of the complex chemical events accompanying egg fertilization will be offered in the following chapter. Some new insights may also be gained by examining mRNA in cell-free systems, as will be seen in the next section.

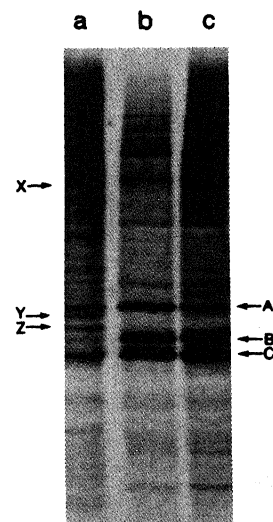


FIGURE 18.20. Fluorographs of proteins synthesized by oocytes and embryos labeled with [^{35}S]methionine. Lane a, oocytes labeled for 20 min; lane b, embryos labeled for 20 min after germinal vesicle breakdown; lane c, embryos labeled for 20 min after first cleavage. Exposures are adjusted to represent approximately equal cpm in each lane. A-C and X-Z are specific bands whose significance is discussed in the text. [From Rosenthal *et al.* (1980), by permission of *Cell*.]

18.2.2.4. Selective mRNA Translation in Cell-Free Systems

With the development of cell-free systems in which the transcription of different mRNAs can be studied, many workers noted that transcription was sensitive to the concentration of K^+ , Mg^{2+} , and anions (e.g., Cl^- , acetate) in the system. For each system, as a rule, there is an optimal concentration of K^+ and an optimal concentration of Mg^{2+} for maximal transcription of the mRNA (Figs. 18.21 and 18.22). However, in a similar cell-free wheat-germ-based medium the optimal K^+ concentration may be as low as 30 mM (Marcus *et al.*, 1968) or as high as 160 mM (Sonenshein *et al.*, 1976; Tuite *et al.*, 1980). The K^+ optimum is also highly sensitive to the nature of the anion present (Fig. 18.21).

Even more significant is the finding that the right concentration of K^+ needed to

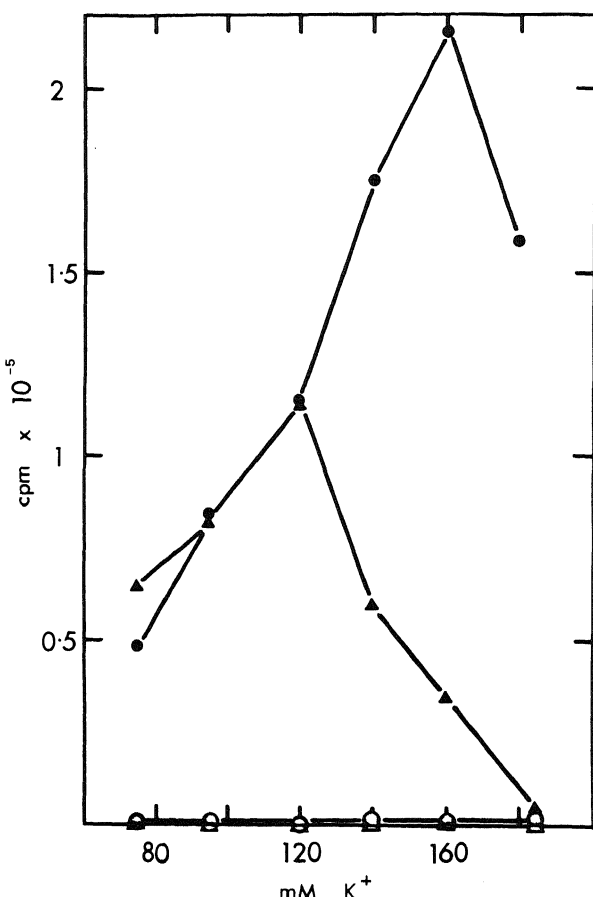


FIGURE 18.21. Influence of concentration of K^+ salts on the incorporation of $[^3H]$ leucine into protein in a yeast cell-free system programmed with yeast polysomal RNA (640 $\mu\text{g}/\text{ml}$). Either KCl (▲) or K(OAc) (●) was used at the source of K^+ . Incorporation in the absence of exogenous mRNA was measured in parallel incubations for both KCl (△) and K(OAc) (○). The K^+ concentration given includes 30 mM contributed by the S-100' lysate. [From Tuite *et al.* (1980), by permission of *Journal of Biological Chemistry*.]

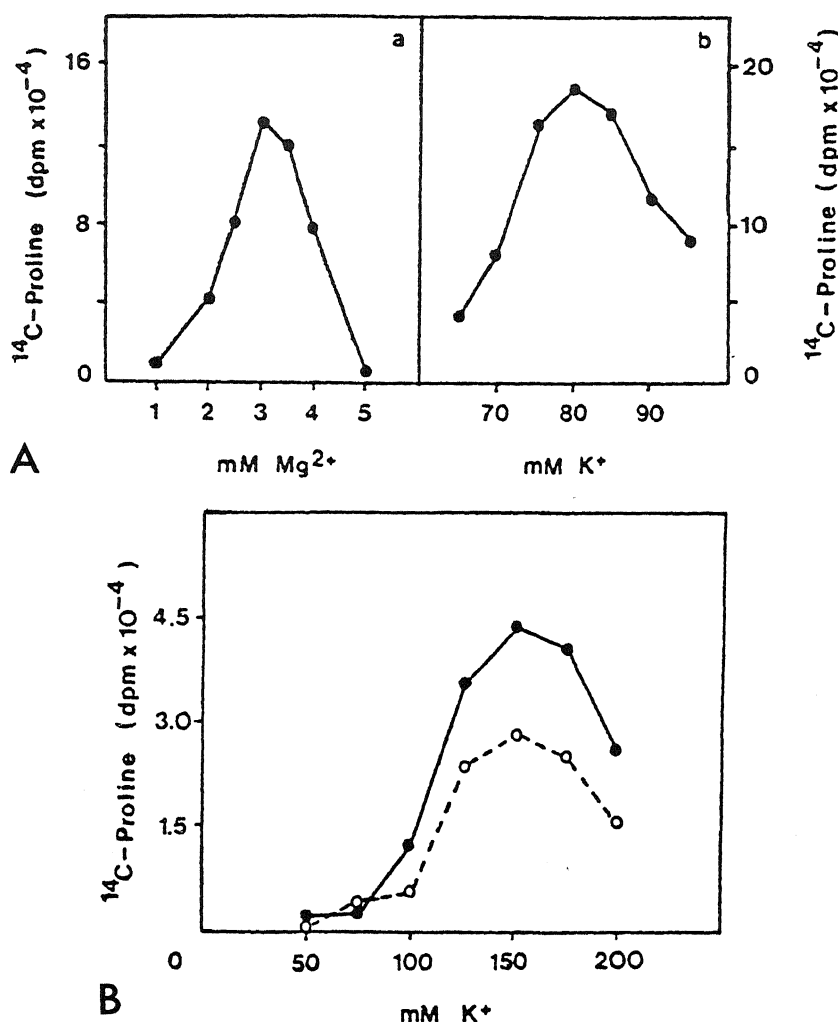


FIGURE 18.22. (A) Determination of optimal ionic conditions for the translation of tendon RNA. Protein synthesis assays containing 15 µg tendon RNA and 5 µCi [¹⁴C]proline were conducted for 60 min. (a) Influence of Mg²⁺ concentration at 80 mM K⁺. (b) Influence of K⁺ concentration at 3 mM Mg²⁺. (B) Influence of K⁺ concentration on the synthesis of collagenase-susceptible [¹⁴C]proline-labeled polypeptides. Protein synthesis assays containing 3 mM Mg²⁺, 15 µg tendon or cartilage RNA, 5 µCi [¹⁴C]proline, and increasing K⁺ concentrations were incubated for 60 min at 37°C. The sample was dialyzed exhaustively against water prior to collagenase digestion. Collagenous peptides were recovered after dialysis against two changes of 25 ml H₂O and the diffusate was concentrated and counted as described previously. ●—●, Tendon RNA; O---O, cartilage RNA. [From Harwood *et al.* (1975), by permission of FEBS Letters.]

translate one kind of mRNA may be quite different from that more suited for the translation of another mRNA, concomitantly present in the same system. Thus Sonenshein and Brawerman (1977) investigated a wheat germ cell-free system containing mRNA for different proteins. As the potassium acetate concentration increased, there was an absolute as well as a relative increase in the synthesis of albumin, despite a reduction of

TABLE 18.3. Effect of K⁺ Concentration on
Albumin Synthesis^{a,b}

KCl (mM)	Albumin synthesis (%)
30	1.6
45	2.0
60	3.2
75	3.8
90	6.0
105	9.6

^aThe relative amount of albumin synthesized by the total liver mRNA preparation was analyzed. At each K⁺ concentration, the radioactivity in the immunoprecipitate is expressed as a percent of the radioactivity in the total trichloroacetic-acid-precipitable material.

^bFrom Tse and Taylor (1977), by permission of *Journal of Biological Chemistry*.

[³⁵S]methionine incorporation by as much as 50% of that at a lower K⁺ concentration. Thus one or more unidentified mRNAs are translated at a much lower K⁺ concentration than is mRNA for albumin. In complete agreement with Sonenshein and Brawerman, Tse and Taylor (1977), also using the wheat germ cell-free system containing liver mRNA, showed that the relative proportion of albumin synthesized as a fraction of the total protein synthesized varied greatly with the K⁺ (and Mg²⁺) concentrations of the medium, as illustrated in Table 18.3. Like mRNA for albumin, specific resistance to high K⁺ concentration was also observed for the translation of mRNA for immunoglobulin light chain (Sonenshein and Brawerman, 1976). Harwood *et al.* (1975), using a similar wheat germ cell-free system, showed that the translation of mRNA for a collagenase-susceptible [¹⁴C]proline-labeled polypeptide reached a maximum at an external K⁺ concentration of 150 mM (Fig. 18.22B), while the optimal concentration for the translation of tendon RNA was 80 mM K⁺ (Fig. 18.22A).

Commenting on the different KCl or potassium acetate optimal concentrations for mRNA translation, L. A. Weber *et al.* (1977) concluded that the inhibiting effect of high K⁺ salt on translation was due to impairment of mRNA binding to ribosomes and that the binding of initiator Met-tRNA is only slightly inhibited by 150 mM KCl. These findings of different optimal K⁺ concentrations for the translation of mRNA for different proteins have been regarded with some curiosity, but so far no great significance has been attached to these phenomena. The indifference follows naturally from the almost universally held belief that all cell K⁺ is free and maintained essentially at a constant concentration. This belief has ruled out any consideration for a possible physiological counterpart *in vivo*. The establishment that in resting cells the bulk of cell K⁺ is not free (Chapter 8) but may become free during cellular activity (Chapters 14–16) thus offers a new vista for future understanding of the specificity in protein synthesis which can be under the control of different levels of K⁺ liberated at a specific time that suits the overall purpose and economy of the cell as an integral unit.

18.3. Summary

There is a considerable amount of evidence that salts in general, and K^+ and Na^+ in particular, play an important role in the control of the macromolecular interactions that lead to protein synthesis. The association-induction hypothesis offers a viewpoint from which some of the extensive data may be interpreted. Three of the major concepts of the association-induction hypothesis, developed earlier in this book, are of special importance here. These are: (1) the making and breaking of salt linkages between and within macromolecules (protein-protein, protein-DNA, protein-RNA, and DNA-RNA); (2) the autocooperative nature of changes in adsorption processes that include salt link formation and breakage; and (3) the influences of cardinal adsorbents on these processes.

In this view, the dissociation of the repressor from the lac operator region of DNA in *Escherichia coli* occurs as an autocooperative breakage of salt linkages, preferentially by KCl, potentiated by the action of the inducer (lactose or its analogue) as a cardinal adsorbent. The cAMP-CAP complex initiates RNA polymerase activity by acting as a cardinal adsorbent to promote the autocooperative adsorption of the polymerase to DNA. The different sensitivities of different RNA polymerases to KCl are due to different abilities of K^+ and/or of Cl^- to compete with their salt linkages with DNA.

In eukaryotes, the role of histones in the control of gene transcription is likely to involve their special role as positively charged elements in salt linkage with DNA. Similarly, studies with polytene chromosomes indicate that there is a differential sensitivity of salt linkages to different salts in their ability to potentiate the breakage of salt linkages that accompany the "puffing" of the chromosomes in regions of active gene transcription. There is evidence that viruses and their host cells may show different susceptibilities of their mRNA translation to activities of K^+ , Na^+ , and water. Finally, the optima noted in the effects of K^+ , Mg^{2+} , and other ions on translation from mRNAs in cell-free systems is in accord with these concepts of the hypothesis.

In the next chapter, a wealth of information will be reviewed that shows further the important roles of ions and water in growth and differentiation of cells and that suggests the role of macromolecular salt linkages in these processes.



Growth and Differentiation

19.1. Mosaic and Regulative Eggs

The physiology of individual organisms varies a great deal more than the physiology of individual cells, regardless of their origin. Thus a mouse can develop cancer; *E. coli* cannot. The highest order of coherence in the “society” of many different, or differentiated, cells of a multicellular organism begins with unequal cell divisions very early in the life history of the organism. Indeed in many organisms it begins with the very first cell division of the fertilized egg.

Most multicellular organisms exist briefly in their life histories as a single cell, the egg cell. In most echinoderms and vertebrates, the early divisions of the fertilized egg give rise to similar daughter cells whose future destinies have not yet been set. These are called *regulative eggs*; they become differentiated in a later stage of development. In contrast, eggs of most invertebrates, like worms and molluscs, are *mosaic eggs*, in which the first division after fertilization already gives rise to different daughter cells (J. Needham, 1950). Thus, studies of mosaic eggs offer insights into a better understanding of cell differentiation and may give us significant clues toward a better understanding of cell maldifferentiation, as in cancer (Chapter 20).

Since cell division leads to replication of the entire genome of the parent cell, the differences in the daughter cells of a mosaic egg seem more likely to originate from regional differences in the cytoplasm of the egg cell. Indeed in 1896 Herlitzka observed that, if the first cleavage of a mosaic egg happens to be vertical, the daughter cells or blastomeres will each develop into a complete embryo. On the other hand, if the first cleavage happens to be in the horizontal plane, only the top blastomere develops into a full embryo. Regional differences in the cytoplasm of a mosaic egg were also demonstrated by Conklin (1905, 1906). Centrifugation, which produces stratification of the cell contents into layers in both regulative and mosaic eggs, produces grossly disorganized, chaotic embryos only in a mosaic egg. Moreover, mosaic eggs show differentiation of the cytoplasm, revealed by asymmetric uptake of vital stains producing regions of different colors.

Spek (1930) studied the mosaic eggs of the polychaete worm, *Nereis dumerilii*,

which possess a natural indicator that is lemon yellow at alkaline pH and violet at acid pH. In a maturing egg, soon after the extrusion of the polar bodies, the endoderm-forming vegetal pole appears violet while the ectoderm-forming animal pole turns lemon yellow. The artificial vital dye neutral red indicates a more alkaline pH at the animal pole. These findings were confirmed by studies of eggs of other *Nereis* species and of the mollusc *Aplysia linacina* (Ries and Gersh, 1936). Why these important findings have not been extensively pursued can at least in part be attributed to the wide acceptance and teaching of an incorrect theory of the living cell. However, Heipel and Lansing-Taylor (1980) have recorded a difference of 0.4 pH unit at different parts of the same cell.

Thus, according to the membrane theory, water in the cell is normal. The existence of a persistent pH gradient within the same cell (and without a membrane barrier) presents a virtually insurmountable problem. Owing to the von Grothuss phenomenon (proton displacing proton in water molecules) the diffusion coefficient of H^+ is very high (Glasstone, 1946, p. 898). It can easily be shown that, even in a large egg cell 1 mm in diameter, the time for the two halves of the egg, initially with different pHs, to reach pH equilibrium is not longer than 1 min. There is no conceivable way to install pumps throughout the aqueous phases of the cytoplasm to counter the rapid back diffusion of H^+ and to maintain a standing pH gradient from one end of the cytoplasm to the other. Without walls, even the hypothetical Maxwellian demon cannot operate.

The difficulty is readily explained in terms of the association-induction hypothesis by the existence of a *q*-value gradient, i.e., water is polarized in multilayers to different degrees at the two poles. The alkalinity at the animal pole could simply mean that the *q*-value for H^+ (and its anion) is lower at the animal pole than the vegetal pole because water at the animal pole is more intensely polarized in multilayers. *Such a q-value gradient may then provide a possible mechanism for the differences of cytoplasmic environment that react with the identical daughter nuclei of the dividing mosaic egg to produce different daughter cells.*

19.2. Maturation of Amphibian Eggs

Most cells of higher animals and plants are in a *diploid* state, in which there are two identical copies of each chromosome, except the sex chromosomes. To maintain this diploid state, each chromosome is exactly duplicated before a cell divides. In this type of cell division, or *mitosis*, the two daughter cells are alike in both chromosome content and cell size. Sex cells, on the other hand, divide by a different mechanism, called *reduction division* or *meiosis*. As a result of this type of division, *haploid* eggs and spermatozoa are produced, in which only one copy of each chromosome is present. The diploid state is resumed when a haploid egg and a haploid spermatozoan are united during fertilization of the egg.

In most cells, chromosomes exist in a highly extended form and while in this form they duplicate. The onset of mitosis, called prophase, begins with the dissolution of the nuclear membrane, and the condensation of chromosomes into shorter and thicker bodies. In the next stage, called metaphase, the condensed chromosomes line up at the equa-

torial plane, and the centromeres holding the two daughter halves of the chromosomes together also divide. The two daughter chromosomes, now completely separated, move toward the opposite sides of the cell (anaphase). In the last phase, telophase, two new nuclei are formed, each with a nuclear membrane.

In meiosis, there are two divisions in succession. In prophase I, each chromosome of the sex cell pairs with its homologous chromosome and these chromosomes undergo condensation. In metaphase I the paired chromosomes line up at the equatorial phase. In anaphase I, the homologous chromosomes separate again and move to opposite poles of the cell. Telophase I completes the division. In the ensuing interphase II the once more elongated chromosomes divide and then condense again. Going through a similar prophase II and metaphase II, the two haploid daughter nuclei separate at anaphase II. Unlike in mitosis, each meiotic division of an egg cell is unequal. The first unequal division gives rise to the egg cell and one small polar body; the second division gives rise to a second small polar body. It is only after the extrusion of the second polar body that the egg nucleus, called the *pronucleus*, is ready for its union with a sperm pronucleus.

The female germ cells enter prophase I of meiosis when the parent organism is still at its fetal or larval stage. It is in this phase that the oocyte grows extensively. Growing oocytes have a very large nucleus called the *germinal vesicle* (GV). Its fuzzy or lampbrush chromosomes are actively engaged in RNA synthesis. As growth draws to an end, the lampbrush chromosomes regress and the egg or oocyte enters a stationary state from which it either matures or dies. *Maturation* usually accompanies ovulation and involves prominently the breakdown of the germinal vesicle (GVBD) and chromosomal condensation.

Maturation, defined by E. B. Wilson (1925), includes the extrusion of two polar bodies. Clearly the union of the female and male pronucleus can only follow in the wake of this event. The term *fertilization* refers to more than just the union of the pronuclei; it also encompasses events immediately following the penetration of the egg cell by the spermatozoan that are referred to as *activation*. Fertilization does not always follow maturation. Indeed, in different types of animals, fertilization may occur on various characteristic time schedules of its own, some before GVBD and others after the second polar body extrusion (Dalcq, 1957). Maturation and activation are clearly delineated separate events only in animals like the sea urchin, in which fertilization occurs after extrusion of the second polar body.

Although the phenomenon of maturation has been of interest to biologists throughout history, it is only in recent decades that major strides have been made in describing its physiological correlates. Most efforts are concentrated on the study of amphibian eggs and, to a lesser extent, starfish eggs. I shall concentrate here on amphibian oocytes. Fortunately, the work on amphibian oocytes and that on starfish oocytes corroborate and reinforce each other in many important aspects.

In amphibian oocytes, maturation is triggered indirectly by gonadotropin (Heilbrunn *et al.*, 1939), which stimulates ovarian follicular cells to secrete progesterone (Masui, 1967; Fortune *et al.*, 1975). There is evidence which strongly suggests that progesterone acts on the oocyte surface and not on the cytoplasm or GV (L. D. Smith and Ecker, 1971), as indicated by the fact that progesterone, at a dose level sufficient to induce GVBD on surface contact, will not do so if injected into the cells (Masui and

Markert, 1971). Furthermore, effective agents conjugated to a polymer too big to enter the oocytes can induce maturation just as the free agents do (Baulieu *et al.*, 1978; Shida and Shida, 1976). The sites reacting with progesterone seem more abundant at the animal pole than at the vegetal pole (Cloud and Schuetz, 1977). In terms of the AI model, there are cardinal sites for progesterone at the egg cell surface, especially at the animal pole. Next we shall examine the molecular events that immediately follow binding of progesterone onto these cardinal sites.

19.2.1. Ca^{2+} and the Depolarization of the Electrical Potential

Moreau *et al.* (1980) showed that exposure of amphibian oocytes to progesterone elicited a burst of free Ca^{2+} release in the cell, detected both by a Ca^{2+} -specific micro-electrode inserted into the cell and by light emitted by the Ca^{2+} -sensitive protein aequorin injected into the cell. Their figure, with an arrow pointing to the time of the occurrence of GVBD following exposure of *Ambystoma* oocytes to progesterone is reproduced as Fig. 19.1. Figure 19.2, taken from the same paper, shows a continuous recording from a single *Xenopus* oocyte. Here the concomitant depolarization of the resting potential following progesterone treatment was recorded side by side with the increase of intracellular free Ca^{2+} . In the inset of Fig. 19.2, these authors recorded the increase of free Ca^{2+} in the external solution bathing 50 *Xenopus* oocytes that had been exposed to progesterone. Based on these findings, as well as those from the study of starfish eggs, Moreau *et al.* (1978) concluded that the surge of free Ca^{2+} in the cell is not due to an increase of influx of external Ca^{2+} but is due to the release of Ca^{2+} from "intracellular stores." *In support they demonstrated that maturation proceeds normally in response to progesterone treatment when the external medium contained neither Ca^{2+} nor Mg^{2+} but a 10 mM concentration of the divalent ion chelator ethylenediaminetetraacetic acid (EDTA).**

Cast in the framework of the AI model, progesterone binds onto cardinal sites on the egg cell surface to bring about an autocooperative release of Ca^{2+} , in much the same way that the binding of ouabain releases K^+ from muscle cells (Section 11.2.4.1) or the binding of 48/80 releases histamine (Section 18.1.1.1). The released Ca^{2+} then acts as the next level of cardinal adsorption in a cascade of controlled physiological events.

That Ca^{2+} is involved in egg maturation has long been known. Injection of Ca^{2+} could elicit true meiosis without progesterone treatment (Wasserman and Masui, 1975; Moreau *et al.*, 1976). Similar techniques enabled Ziegler and Morrill (1977) to conclude that maturation occurs in response to Ca^{2+} injected to a depth of no more than 0.2 mm below the cell surface, i.e., Ca^{2+} acts only on the cortical layer of the oocyte.

*The conclusion of Moreau *et al.*, however, seemed in conflict with a sizeable collection of other data showing that in other animals, oocyte maturation fails to initiate in a Ca^{2+} free system (*Chaetopterus*, Brachet and Denis-Donini, 1977; *Spisula*, Schuetz, 1975; *Urechis caupo*, Johnston and Paul, 1977). This conflict may be only illusory. Thus different oocytes may have intracellular stores of Ca^{2+} that differ both in size and in exchangeability. Perhaps a large store of more tightly held intracellular Ca^{2+} exists in eggs of *Ambystoma*, *Xenopus*, *Pleurodeles*, and *Sabellaria* (Peaucellier, 1977) and starfish (Moreau *et al.*, 1978), whereas a smaller and/or less tightly held Ca^{2+} store exists in prematuration oocytes of *Chaetopterus*, *Spisula*, and *U. caupo*. Therefore deprivation of an external source of Ca^{2+} would not interfere with Ca^{2+} release in *Ambystoma* oocytes, but will do so in the oocytes of *Chaetoptera*.

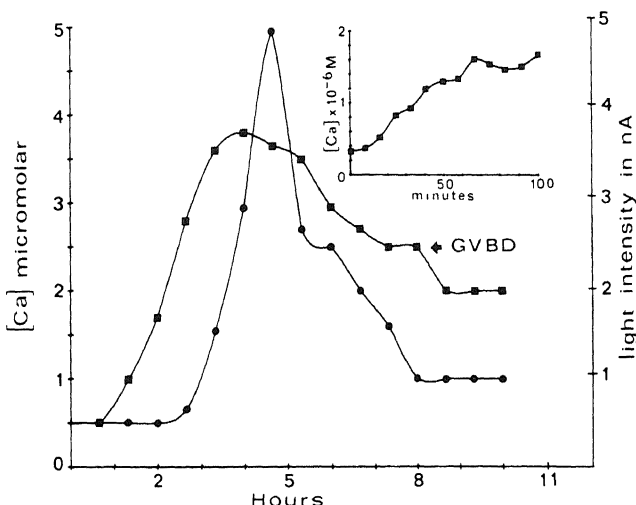


FIGURE 19.1. Progesterone-induced Ca^{2+} transients as recorded from a Ca^{2+} -sensitive microelectrode (■—■) and 25 aequorin-injected oocytes taken from the same *Ambystoma* (●—●). Maturation ratio was 14/25. Inset illustrates initial changes in Ca^{2+} activity as recorded with the electrode. Right ordinate indicates light intensity in nA. Left ordinate refers to Ca^{2+} activity changes as measured with the Ca^{2+} -sensitive electrode. Arrow indicates time of GVBD. [From Moreau *et al.* (1980), by permission of *Developmental Biology*.]

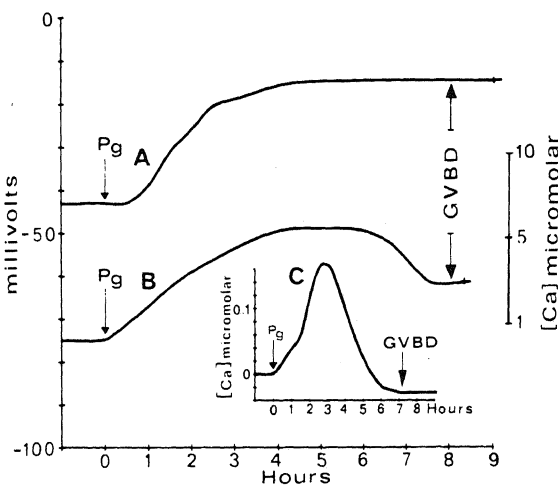


FIGURE 19.2. Ca^{2+} -sensitive electrode records. (A) Change in the resting potential (E_m) as recorded from a single *Xenopus* oocyte stimulated with progesterone at t_0 (Pg). (B) Simultaneous change in internal Ca^{2+} activity ($E_{\text{Ca}} - E_m$) as recorded by the Ca^{2+} -sensitive electrode. The right scale refers to the micromolar Ca^{2+} internal concentration. (C) Increase in the external Ca^{2+} concentration ($E_{\text{Ca}} - E_m$) recorded from 50 progesterone-stimulated oocytes (electrode in the external medium, 0.3 ml normal OR_2 culture solution). [From Moreau *et al.* (1980), by permission of *Developmental Biology*.]

19.2.2. Maturation-Promoting Factor

Following progesterone treatment, amphibian oocytes with or without a GV produce in their cytoplasm a non-species-specific heat-labile macromolecule. When injected into untreated oocytes, it induces GVBD, surface contraction, chromosome condensation, and polar body formation (Masui and Markert, 1971). According to Masui and Clarke (1979), this maturation-promoting factor (MPF) is a phosphoprotein that has a molecular weight of between 0.6 and 1.0×10^6 daltons. In further purifying MPF, Wu and Gerhart (1980) found that the factor may be more complex. Full elucidation of its composition must await further research.

The question arises, Is appearance of MPF related to the surge of Ca^{2+} ? Masui *et al.* (1977) showed that, whereas injection of the Ca^{2+} chelators EDTA or EGTA blocks GVBD, it fails to do so after the appearance of MPF in the cytoplasm. They concluded that Ca^{2+} release precedes and may initiate MPF production. On the basis of this, one may conclude that Ca^{2+} binding on the cardinal site of the second member of the maturation cascade releases MPF.

19.2.3. A Key Role of Adsorbed Na^+ in the Control of Maturation

In Chapter 8 I presented extensive evidence that the bulk of cell K^+ , as well as Na^+ displacing K^+ under nondeteriorating conditions, is adsorbed. I now suggest that the state in which egg K^+ is adsorbed resists maturation and that Na^+ adsorption is an important component of the maturation process. Evidence in harmony with this concept includes the following:

1. K^+ depletion causes replacement of adsorbed K^+ by adsorbed Na^+ (Table 8.4).
Vitto and Wallace (1976) found that K^+ depletion facilitated maturation.
2. Ouabain causes replacement of adsorbed K^+ by adsorbed Na^+ (Table 11.5).
Vitto and Wallace (1976) found that ouabain facilitated maturation.
3. An increase of external K^+ concentration decreases Na^+ adsorption (Fig. 11.32). Ecker and Smith (1971) found that increased external K^+ concentration inhibited maturation.
4. In isolated mitochondria, valinomycin increases K^+ adsorption (Fig. 15.16). Powers and Biggers (1976) found that valinomycin retards maturation.
5. Decreased external Na^+ concentration decreases Na^+ adsorption in the cell (Fig. 11.32). O'Connor, Robinson, and Smith (1977) found that reduction of external Na^+ concentration retards maturation.

In conclusion, the known published data support the concept that intracellular adsorbed Na^+ somehow promotes maturation. Our next question is, What does the adsorption of Na^+ do to promote maturation? In all cases mentioned GVBD was a major criterion of maturation. Thus we may question whether Na^+ adsorption is essential for GVBD.

There is increasing evidence that the integrity of the GV does not depend only on a confining membrane but that nuclear proteins accumulate in the GV owing to specific adsorption (Feldherr and Pomerantz, 1978). I would like to suggest that Na^+ facilitates the dissociation of salt linkages that provide much of the cohesive forces of the GV. As pointed out earlier (Sections 13.7 and 14.5), liberation of proteins and other macromol-

ecules from binding sites may reflect a state that underlies dissociative swelling. The key role of Na^+ in dissociative swelling has already been discussed in Section 13.6.

19.2.4. An Attempt to Provide a Consistent Theoretical Framework for Future Investigation

Masui and Clarke (1979, p. 232) noted that, despite the extensive observations of Ca^{2+} in egg maturation, "the mode of Ca^{2+} action is not fully understood." They also pointed out that, while much data suggested that maturation and electrical potential depolarization go hand in hand, other data indicate quite the contrary: Maturation can occur without depolarization or even with hyperpolarization (Doreé *et al.*, 1976). Masui and Clarke (1979) saw in these contradictions "the most serious challenge to the theory that assumes the existence of a strict causal relationship between changes in the membrane potential and the initiation of maturation" (p. 239).

Let us reiterate that the oocyte surface contains cardinal sites for progesterone. The regular sites which these cardinal sites dominate adsorb Ca^{2+} before progesterone binding. Progesterone adsorption onto the surface cardinal sites causes an all-or-none liberation of Ca^{2+} near the cell surface. This postulation is in harmony with evidence that the oocyte surface is the site of progesterone action and agrees with the facts that progesterone brings about a protein conformation change and that maturation can be brought about by agents other than progesterone, including trypsin, dithiothreitol, and mersalyl, all known to interact with proteins (Masui and Clarke, 1979).

As mentioned above, the finding of Masui *et al.* (1977) that an injected Ca^{2+} chelator blocks GVBD before but not after the appearance of MPF led these authors to conclude that Ca^{2+} action precedes and may indeed initiate MPF release. If this stipulation is correct, and if MPF is the third link in the cascade chain progesterone $\rightarrow \text{Ca}^{2+} \rightarrow \text{MPF}$, then a possible next step is MPF's action as a cardinal adsorbent to bring about a c -value change similar to that brought about by the action of ouabain or ATP depletion (see Section 11.2.4). That is to say, MPF would elicit a gain of relative affinity of the fixed anions for Na^+ in relation to that for fixed ϵ -amino groups or guanidyl groups. Dissolution of the salt linkages between fixed ionic sites in the GV causes it to dissolve.

Now I return to the question of the cellular electrical potential. The most useful degree of freedom provided by the AI hypothesis is that events determining the resting potential may parallel and yet not be causally related to similar events occurring in one or another part of the cytoplasm. Thus a shift of ξ of equations (7.20) and (14.8) to a lower value, as brought about by ouabain or change in $[\text{K}^+]_{\text{ex}}/[\text{Na}^+]_{\text{ex}}$, may cause Na^+ adsorption in the GV and thereby bring about both GVBD and a fall of ψ . The two events occur hand-in-hand but neither one is the cause of the other. Thus the occasional lack of accord between maturation and depolarization is easily understandable.

19.2.5. Other Cytoplasmic Factors in Maturing Oocytes: Cytostatic Factor and Chromosome-Condensing Activity

Oocyte maturation is generally arrested at metaphase I or II; meiosis resumes after fertilization. In these cases fertilization, or rather activation, overlaps with maturation. Masui and Markert (1971) injected unfertilized egg cytoplasm from *Rana pipiens*

oocytes into cells (blastomeres) of a two-cell embryo and found that mitosis of these also became arrested at metaphase. Furthermore, both the frequency and the duration of arrested mitosis correlated with the amount of cytoplasm injected. Masui and Markert postulated that this phenomenon is caused by a *cytostatic factor* (CSF), which appears shortly after GVBD and is sustained at a high level until activation. Further study by P. G. Meyerhof and Masui (1977) showed that a fresh oocyte extract contains a CSF that is stable in the presence of Mg^{2+} but that rapidly deteriorates in the presence of Ca^{2+} at concentrations as low as 10^{-5} M. This Ca^{2+} sensitivity of CSF is of significance in activation in the resumption of meiosis arrested by CSF and will be taken up again in Section 19.3.3.

Ziegler and Masui (1973, 1976) discovered the presence of another factor, called *chromosome-condensing activity* (CCA), which causes chromosome condensation of nuclei from adult frog brain when injected into progesterone-treated oocytes. This subject will be taken up further in Section 19.5.3.

19.3. Fertilization (or Activation) of Sea Urchin Eggs

Fertilization refers to a series of physiological events that begins with the penetration of a spermatozoon into an egg and culminates in the union of the egg pronucleus and the sperm pronucleus. The fertilized egg then divides and develops into an embryo. Events that precede and accompany this nuclear fusion are referred to as *activation*, and are illustrated by parthenogenetic activation without a spermatozoon.

In 1886 Tichomirov discovered the parthenogenetic activation of silkworm egg by sulfuric acid; he remarked on the similarity between parthenogenesis and nerve excitation, both elicited by a wide variety of stimuli seemingly unconnected to one another, including chemicals (Delage, 1910), temperature (Lillie, 1908, 1941), and exposure to hypertonicity (double strength saline).

Just as modern investigations of egg maturation have centered around the study of amphibian and starfish eggs, modern investigations of fertilization and parthenogenetic activation have centered around sea urchin eggs. These are fully mature, having given off two polar bodies before they are fertilizable.

As the following sections will reveal, egg activation involves a sequence of events that are very similar to those seen during egg maturation, including surface protein changes, Ca^{2+} release, Na^+ dependence, and electrical potential changes. Occurring at a later stage of development, activation releases the egg from an arrested state of maturation and initiates cell cleavage.

19.3.1. Alteration of Surface Proteins Accompanying Activation

In 1930, L. Loeb suggested that all parthenogenetic agents cause a cytolysis of the superficial layer of the egg. Mazia, Schattan, and Steinhardt (1975) found that in sea urchin eggs a variety of parthenogenetic agents (ammonia, isotonic glycerol, or urea) turn on chromosome replication and condensation. In addition, they cause elongation of microvilli of the cell surface, which the authors attributed to a loss of protein from the plasma membrane. Direct demonstration of parthenogenetically induced release of a

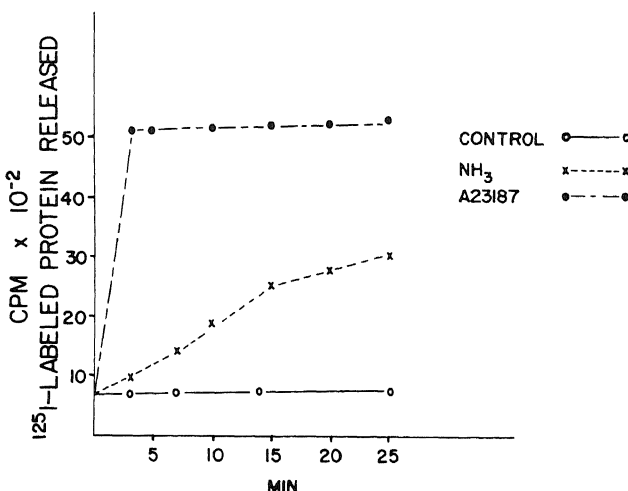


FIGURE 19.3. Time course of release of ^{125}I -labeled protein from egg surface after treatment with ionophore A23187 or ammonia. Iodinated eggs were treated with either 5 μM A23187 or 10 mM NH_4Cl , pH 8.0. [From Johnson and Epel (1975), by permission of *Proceedings of the National Academy of Sciences*.]

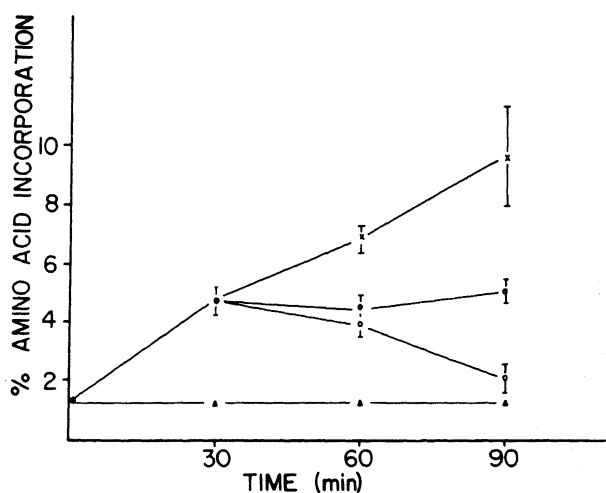


FIGURE 19.4. Suppression of protein synthesis by nondialyzable components released by eggs. A 0.2% suspension of eggs was incubated in 10 mM ammonia for 30 min, at which time a 2-ml sample of eggs was pulsed with [^3H]valine for 5 min. Eggs were then washed twice in filtered seawater, and separate groups were incubated in ammonia (X), filtered seawater (●), or components released by eggs (○). Controls remained in filtered seawater throughout (▲). Samples (2 ml) from each group were pulsed for 5 min with [^3H]valine beginning at 60 and 90 min. Error bars are SDs of five experiments. [From Johnson and Epel (1975), by permission of *Proceedings of the National Academy of Sciences*.]

protein component was provided by J. D. Johnson and Epel (1975). A 150,000-dalton glycoprotein is liberated from the sea urchin egg surface 45 sec and 120 sec following fertilization (Fig. 19.3). Furthermore, exposure of partially activated eggs to a concentrated and dialyzed solution of the released glycoprotein suppressed protein synthesis to a level occurring before fertilization (or parthenogenesis) (Fig. 19.4). These authors suggested that this glycoprotein is responsible for the normal suppression of the functional activation of the egg.

19.3.2. Electrical Potential Changes Accompanying Activation

In Section 14.4.4., Maeno's study of the resting potential of toad oocytes was briefly discussed (Maeno, 1959). The unfertilized egg has a K^+ -sensitive resting potential much like those of frog muscle and squid axon, with the inside negative by as much as 70 mV. Activation by microelectrode puncturing produces a Cl^- -dependent activation potential within 30 sec. The peak height reached in 1–2 min following activation shows an overshoot of 50 mV. Neither external K^+ nor external Na^+ exercises a significant effect on the activation potential. This sudden shift from a K^+ -sensitive electrical potential to a Cl^- -sensitive potential was explained in terms of the AI hypothesis as being due to a rather dramatic change of the cell surface protein. The result is that the β - and γ -carboxyl groups at or near the cell surface become neutralized by salt linkage formation and/or buried in a deeper non-potential-generating region of the cell surface. In place of the fixed anionic groups, cationic groups carried by lysine or arginine residues take up the superficial exposed positions, generating the anion-sensitive activation potentials.

In echinoderm eggs, fertilization or parthenogenetic stimulation also set in motion a complex change of the resting potential (R. A. Steinhardt *et al.*, 1971). Shen and Steinhardt (1978), observed that before fertilization there is a small resting potential of 5–10 mV, inside negative. This resting potential, contrary to that of toad eggs, is indifferent to external K^+ and Na^+ concentration but is Cl^- -sensitive. Upon fertilization, there is a depolarization so that the polarity of the potential is reversed, with the inside positive by some 10 mV (Fig. 19.5). It was found that this potential, which Steinhardt *et al.* named the *fertilization action potential*, is Na^+ -dependent, like the nerve and muscle action potentials. The fertilization action potential takes some 2 min to reach its peak and then gradually returns to its initial resting value in about 5 min (17° – 19° C). This whole cycle of change was referred to as phase I. In phase II, a steady potential of variable duration is observed, followed by a slow and profound hyperpolarization (phase III), at the end of which the potential attains a value of 60–70 mV. The electrical potential after phase III is fully K^+ -sensitive, with a corresponding increase of K^+ conductance.

In terms of the AI hypothesis, the surface of an unfertilized sea urchin egg has essentially fixed cationic sites to begin with, thus making the potential anion-sensitive. Fertilization in this case has produced a change opposite to that observed in toad eggs. Here, a masking of these surface fixed cationic sites is accompanied by the liberation and exposure of fixed anionic sites with a high *c*-value, making them Na^+ -selective (Figs. 6.7 and 6.8). Changes at phase III would represent essentially a slow fall of the *c*-value of the surface anionic sites to a lower value at which K^+ preference exceeds Na^+ preference.

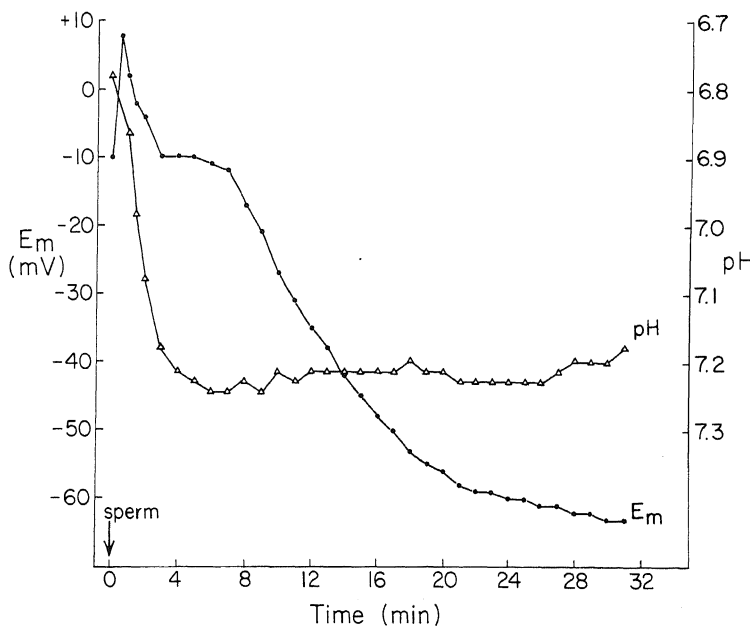


FIGURE 19.5. Continuous recording of membrane potential (E_m) (●) and intracellular pH (Δ) during fertilization of sea urchin egg. The conventional microelectrode was inserted into the egg, followed by the pH-sensitive microelectrode. [From Shen and Steinhardt (1978), by permission of *Nature*.]

The release of surface protein from 45 sec to 120 sec after insemination occurs in the early phase I. Thus, the major conformation change proposed here may well be initiated by the release of the surface glycoprotein. Whether this glycoprotein acts only as a cardinal adsorbent as suggested or actually offers cationic sites for the generation of a Cl^- -sensitive electrical potential remains to be answered.

19.3.3. Ca^{2+} Release Accompanying Activation

Early investigators came to the conclusion that Ca^{2+} plays a major role in egg activation (Mazia, 1937; Heilbrunn and Wilbur, 1937; Pasteels, 1938). Thus, Mazia in 1937 observed an increase of free Ca^{2+} in the ultrafiltrate of a homogenate of sea urchin eggs following fertilization. It was then widely believed that this release of Ca^{2+} results from an increase of membrane permeability to Ca^{2+} . When the divalent-ion-specific ionophore A23187 became available (Lardy *et al.*, 1967), its action on mature eggs was studied. It was theoretically anticipated that A23187 would induce parthenogenesis by transporting external Ca^{2+} into the egg through a lipid membrane barrier. In 1974 Steinhardt and Epel (see also E. L. Chambers, 1974) reported that A23187 did not induce parthenogenesis in this way; rather it caused the liberation of bound or sequestered Ca^{2+} from an intracellular source. *Thus A23187 can bring about a full parthenogenetic response, including an increase of DNA and protein synthesis (Table 19.1) and the development of the fertilization action potential, in the total absence of external*

TABLE 19.1. Protein Synthesis in Eggs
Activated with Sperm or Ionophore (5 μM) and
Impulsed for 5 min with [^3H]Valine 30 and 60
min Later^a

Activator and type of seawater (SW)	Percent incorporation at	
	30 min	60 min
Sperm, artificial SW	18.8	18.7
A23187, artificial SW	20.2	16.4
A23187, 0 Ca^{2+} SW	32.0	15.2
A23187, 0 Mg^{2+} SW	24.4	23.3
Unfertilized		1.5

^aData selected from R. A. Steinhardt and Epel (1974), by permission of *Proceedings of the National Academy of Sciences*.

Ca^{2+} . Both A23187 and fertilization brought about a marked increase in Ca^{2+} efflux, which the authors attributed to a release of intracellular Ca^{2+} . All these sound very similar to events in egg maturation (Section 19.2.1); apparently the same instrument is used to play a different tune for a different company.

The role of A23187 in inducing parthenogenesis closely parallels the role of progesterone in inducing egg maturation. Like progesterone, A23187 serves its physiological role as a cardinal adsorbent. That A23187 may act as a cardinal adsorbent rather than an ionophore has already been discussed in relation to oxidative phosphorylation of mitochondria (Section 15.5.3.2). One is reminded of the similar story of the behavior of K^+ during muscle contraction: Increased efflux of K^+ occurs as a result of desorption rather than an increase of K^+ permeability (Section 16.5.4.2).

Ca^{2+} release in the egg of the freshwater oriental killifish, medaka (*Oryzias latipes*), induced by A23187 or fertilization, was beautifully demonstrated by Gilkey *et al.* (1979) in the form of a traveling wave (Fig. 19.6) which starts at the animal pole where the sperm enters. This Ca^{2+} activity wave is, like the pulse of Ca^{2+} activity following progesterone, independent of external Ca^{2+} .

Having clearly demonstrated that egg activation, like egg maturation, involves a transient release of Ca^{2+} , the next problem is to understand what this liberation of Ca^{2+} does. Masui *et al.* (1977) pointed out that one of the main events triggered by activation is the release of metaphase I or of metaphase II from its arrest in a variety of eggs, including amphibian eggs. This arrest is attributed to the elaboration of CSF after GVBD (Section 19.2.5). Since CSF inactivates rapidly in the presence of low concentrations of Ca^{2+} , Masui *et al.* (1977) suggested that one of the functions of parthenogenetic release of Ca^{2+} is to break the CSF-induced meiosis arrest. While this theory is applicable to amphibian eggs and other eggs, it is not directly applicable to sea urchin eggs, since meiosis has passed beyond metaphase II before activation can occur. One wonders if in sea urchin eggs there might not be an earlier inactivation of CSF during the maturation release of Ca^{2+} . It is interesting to note that injection of the cytoplasm of progesterone-treated eggs into immature amphibian eggs brings maturation to its

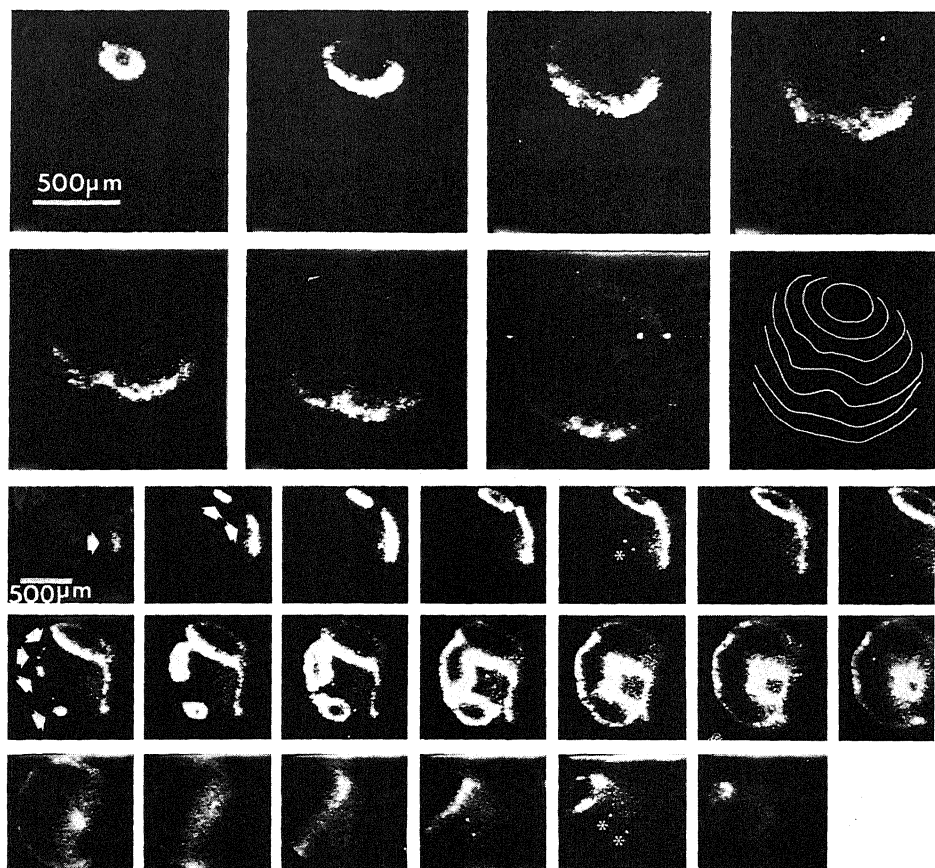


FIGURE 19.6. Ionophore-initiated Ca^{2+} waves in aequorin-injected medaka eggs. (Top) One initiation point. Five seconds elapsed between successive photographs. Egg with micropyle upward. (Bottom) Seven initiation points (indicated by arrows). Ion noise spots, e.g., those indicated by asterisks, can be readily distinguished from initiation sites in the original records by their failure to persist and grow as well as by their characteristically sharp outlines. Two seconds elapsed between photographs in the first two rows, whereas the photographs in the last row are 15 sec apart. Egg with micropyle upward. [From Gilkey *et al.* (1979), by permission of *Journal of Cell Biology*.]

completion with the production of two polar bodies, and is thus different from the usual metaphase II arrest seen in normal maturing eggs. Is this differentiation due to liberated Ca^{2+} in the injected cytoplasm?

19.3.4. Requirement of External Na^+ in Egg Fertilization

Following fertilization, sea urchin eggs divide. Chambers observed that this cell cleavage depends on the presence of Na^+ in the external medium within a period of from 0.5 to 10 min following normal fertilization or exposure to A23187 (E. L. Chambers, 1974, 1975; Chambers and Dimich, 1975). Figure 19.7 shows the stringent and

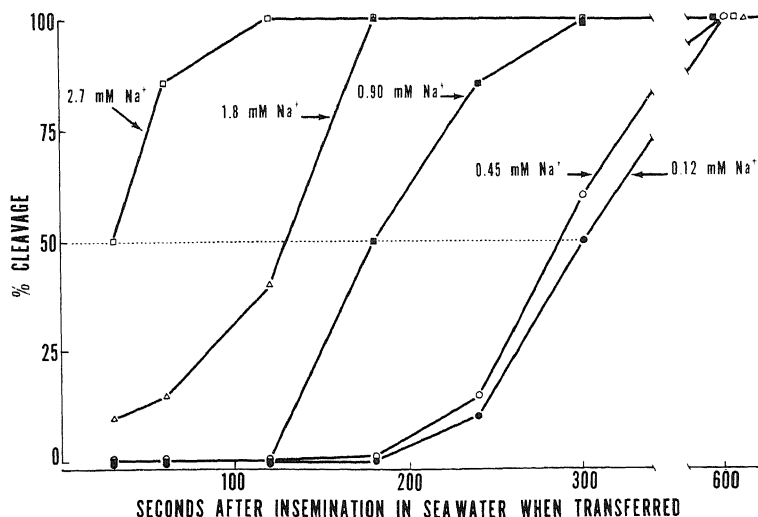


FIGURE 19.7. Dependence of cleavage of sea urchin (*Arbacia*) eggs on concentration of Na^+ in the external medium. [From E. L. Chambers (1976), by permission of *Journal of Experimental Zoology*.]

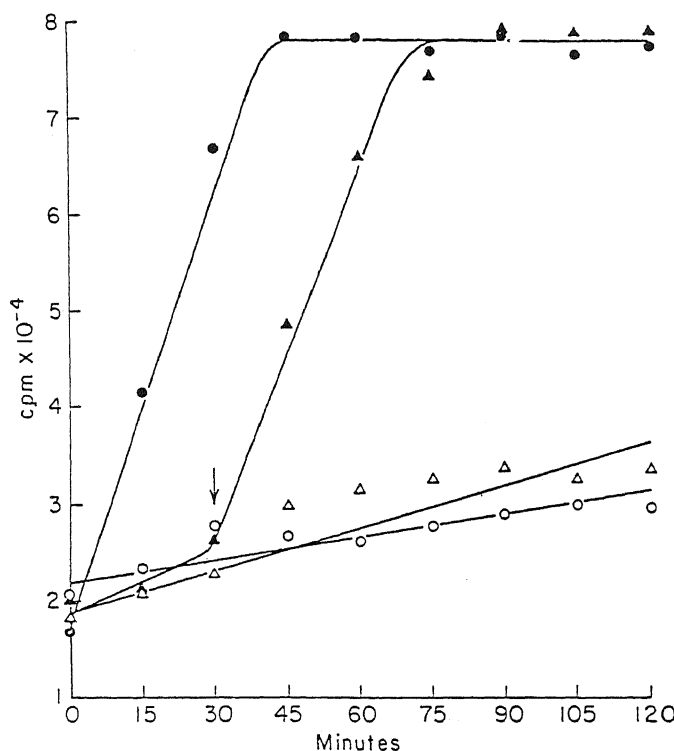


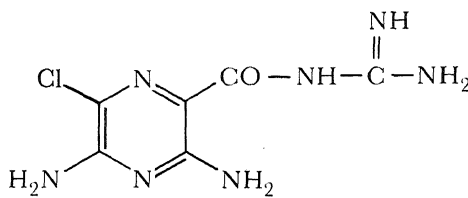
FIGURE 19.8. Cumulative incorporation of [^3H]leucine in preloaded sea urchin eggs. O—O, Unfertilized eggs in normal seawater; ●—●, fertilized eggs in normal seawater; Δ—Δ, ionophore-treated eggs in Na^+ -free seawater; ▲—▲, ionophore-treated eggs in Na^+ -free seawater to which 0.05 M NaCl is added at 30 min. [From Nishioka and McGwin (1980), by permission of *Journal of Experimental Zoology*.]

quantitative dependence of *Arbacia* egg cleavage on Na^+ , which cannot be replaced by tetramethylammonium, guanidium, Tris, K^+ , Rb^+ , Ca^{2+} , or Mg^{2+} . Li^+ alone can partially substitute for Na^+ . Figure 19.8, taken from Nishioka and McGwin (1980) shows a similar critical dependence on external Na^+ of protein synthesis in A23187-activated sea urchin eggs.

Egg fertilization is followed by acid liberation (Ashbel, 1929). Recently, J. D. Johnson, Epel, and Paul (1976) showed that about 80% of this acid release depends on external Na^+ . Indeed, the amount of acid released is directly related to the external Na^+ concentration. The rate of H^+ efflux, measured as an increment of pH per min, doubled with a doubling of external Na^+ concentration. Again Li^+ can substitute for Na^+ but is 50 times less effective.

In agreement with Chambers's original observation of the need for Na^+ for activation, Johnson *et al.* found that the Na^+ -dependent H^+ release occurs only within a narrow span of time, from 1 min until 6 min after fertilization. Comparing this now with the time course of the electrical potential change (Fig. 19.5), one notes that this is precisely the period of time referred to as phase I, when the electrical potential becomes Na^+ -sensitive. In terms of the AI hypothesis, the egg surface acquires at this time ionized β - and γ -carboxyl groups of high *c*-value. Since Na^+ entry by the adsorption-desorption route via the surface anionic sites requires a favorable *c*-value (Section 12.4.1), the increase of Na^+ permeation during this period of time is expected.

It is interesting that Johnson *et al.* also found that only during this period of time can the H^+ efflux from eggs in a Na^+ -containing medium be inhibited by the K^+ -sparing diuretic amiloride. I have cited, in discussing active transport in Chapter 17, evidence that those apical surfaces of bifacial cells like the outer surface of frog skin and the mucosal surface of intestinal epithelium have fixed anionic sites with high *c*-values and that amiloride competitively inhibits Na^+ entry only at this surface. Similarly the frog egg after fertilization takes on the characteristics of the apical surfaces of these bifacial cells for a transient period.



Amiloride

Amiloride is a guanidine derivative. At physiological pH, the guanidyl group becomes positively charged. It is likely that this cationic group combines with the high-*c*-value anionic sites which normally function as the adsorption-desorption route for entry and exit of Na^+ .

Johnson *et al.* (1976) also pointed out that, if the interior of the egg were totally unbuffered, then the amount of H^+ liberated from the egg (in exchange for Na^+), 6

μ moles of H^+ /ml of cell water, would make the pH of the cell interior at least as acid as pH 2.2. However, actual measurements showed that the pH of the cell interior is much less acidic than that, i.e., pH would rise from 6.8 before fertilization to 7.2 after fertilization (Fig. 19.5). These calculations left no doubt that the H^+ liberated in exchange for Na^+ could not be free to begin with but must also bind onto anionic sites. Johnson *et al.* attributed this buffering capacity to small molecules. If this is correct, it would be very difficult to see how there could be such a high degree of specificity in the requirement for Na^+ . Complexing of Na^+ of small molecules of biological origin is in general too weak and too nonspecific. On the other hand, large numbers of proteins are always present in cells and they are all endowed with aspartic and glutamic acid residues with pK values close to 4.6. The ability of these protein anionic sites to exhibit a strong selectivity among alkali metal ions (see Chapter 8) makes it much more likely that the H^+ is liberated by a Na^+ -for- H^+ exchange at specific anionic groups of cell proteins.

Since cell surfaces in general are not absolute barriers to Na^+ (Section 3.1) and since we know that the larger Ca^{2+} can traverse the cell surface with ease, the next question to answer is: What causes this exchange adsorption of Na^+ for H^+ ? Does A23187 serve the role of the cardinal adsorbent for this change? If so, it would be in accord with our conclusion from mitochondrial studies that A23187 acts as an electron-withdrawing cardinal adsorbent, lowering the c -value of anionic sites (Section 15.5.3.2) and resulting in a decrease of preference for H^+ and an increase of preference for Na^+ in some key protein sites. Where are these proteins? What are they? How do they promote cell cleavage? All these questions remain to be answered.

There is one more phenomenon that the AI model may help explain: the sustained higher pH in activated sea urchin eggs demonstrated by Shen and Steinhardt (1978) and shown in Fig. 19.5. It suggests a reduction of the q -value for H^+ as a result of enhanced polarization of the water in the activated egg.

19.4. Differentiation

Embryonic differentiation, through which a single fertilized egg transforms itself into a complex adult organism comprising many different cell types, each unerringly reproducing its own kind often for many years to come, is one of the most fascinating biological phenomena, and a complete understanding of it is still very far away. Continuing from our discussion of the amphibian egg, I shall focus attention on the specific subjects of amphibian egg differentiation, occasionally referring to the early development of echinoderm eggs.

19.4.1. Brief Historical Sketch

By mitosis, the fertilized egg divides into many cells aggregated in the shape of a solid ball called the *morula*. Further division produces a hollow *blastula* (Fig. 19.9). The eccentric cavity in the blastula, the *blastocoel*, separates the thinner layer of cells making up the dorsal, or animal pole from the thicker mass of larger yolk-laden cells of the vegetal pole. Eventually the animal pole forms the ectoderm and the vegetal cells form the endoderm. However, up to the end of the blastula stage, all cells, when isolated,

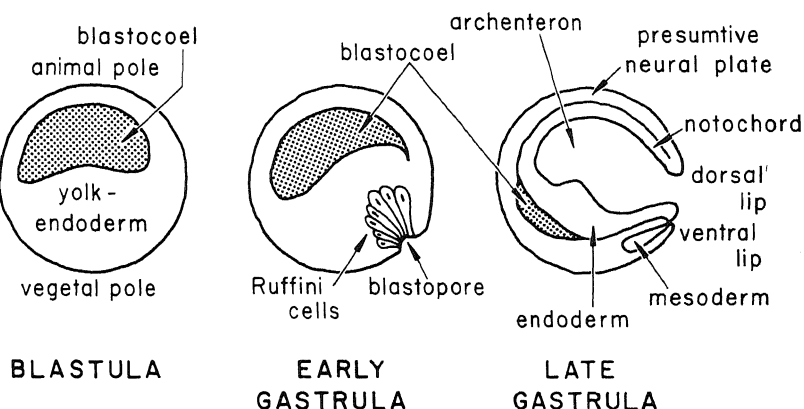


FIGURE 19.9. Diagrams of the early frog embryo at the blastula and gastrula stages.

develop into a spherical miniature whole embryo (Landström and Løvtrup, 1979). With further growth, the blastula becomes a gastrula (Fig. 19.9); the totipotency of the earlier embryo cells is then lost.

The gastrulation process is complex but largely the result of the rapid expansion of the dorsal ectoderm layer accompanied by a much more sluggish enlargement of the blastocoel. The expanding ectoderm eventually covers the entire gastrula. In the process, the original marginal zone between the ectoderm and endoderm, as well as the endoderm itself, becomes enclosed by a process of invagination which begins when a groove or blastopore is formed at the posterior surface of the egg. The formation of the blastopore creates two new structures, the dorsal lip and the ventral lip of the blastopore (Fig. 19.9).

Vogt (1925, 1929) painted the surface of an early gastrula with spots of dyes and followed the movements of these stained spots during gastrulation. From these studies he obtained a "fate map" (see Fig. 19.10A) which shows the destiny of the different surface areas of the early gastrula; one part will become the notochord (No), another part

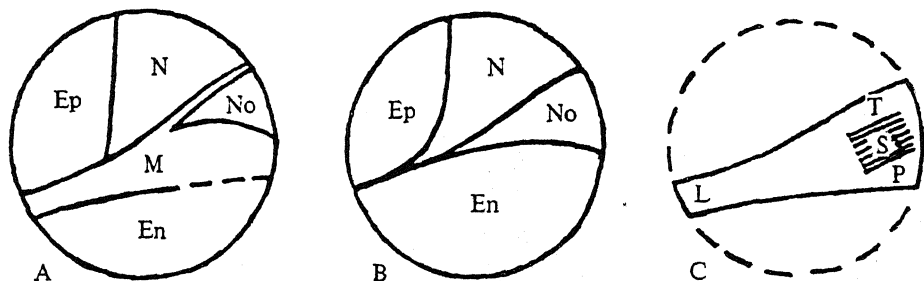


FIGURE 19.10. Fate maps of the urodelan blastula. (A) Vogt's fate map; (B) revised fate map for the ectoderm-endoderm; (C) revised fate map for the mesoderm, indicating that the cells in question are located beneath the embryonic surface. [From Landström and Løvtrup (1979), by permission of *Journal of Embryology and Experimental Morphology*.]

the neural plate (N), and still another part the skin (Ep). In recent times Landström and Løvtrop (1979) explained why, of the three germ layers, only the endoderm and ectoderm are initially at the embryo surface. The mesoderm is buried beneath them. Their revised fate map is reproduced as Fig. 19.10B,C.

19.4.2. Classical Transplantation Experiments of Spemann and Mangold

Hans Spemann (1918) showed in newt embryos that, up to a certain stage of gastrulation, all parts of the embryos are interchangeable. Thus a small piece of the ectoderm that would normally develop into skin (presumptive epidermis), when transplanted to the neural plate region, becomes, like the rest of the neural plate, part of the brain; presumptive neural plate when transplanted to the area of presumptive epidermis turns into skin. However, with further development, a drastic change occurs. In an older gastrula, if the dorsal lip of the blastopore is transplanted somewhere else, the transplant no longer becomes part of its new neighboring tissue. Instead, it begins to alter the fate of the new neighboring tissue in such a way that an additional full embryo is formed. Thus, the dorsal lip of the blastopore acts as a *primary organizer*. Figure 19.11, from Needham's (1950) reproduction of the figure of Bautzmann (1926), shows that in an early gastrula most of the presumptive mesoderm, and not just the dorsal lip, has the inductive power of a primary organizer.

In the normal embryo the dorsal lip of the blastopore acts as a primary organizer, dictating many of the main structures of a whole, organized embryo. The developmental fate of the embryo involves both the inductive power of the organizer and the "competence" of the target tissue to differentiate in a certain direction. Usually the organizer activity persists over a long period of time, while competence appears and disappears rapidly. Furthermore, the target tissue as a rule has its own induction power.



Hans Spemann

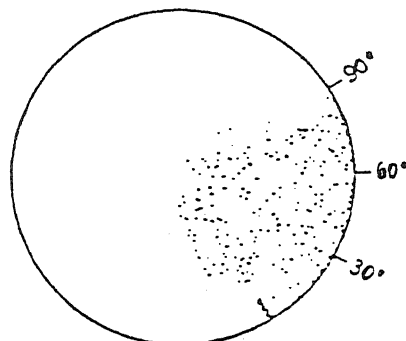


FIGURE 19.11. Boundaries of the primary organizer region. [From Needham's (1950) reproduction of Bautzmann's (1926) figure, by permission of Cambridge University Press.]

The complexity of these mutual interactions made early analytical investigations of causal relationships difficult. It was highly desirable to have a more neutral medium than that provided by parts of the same or other embryos. In response to this need Holtfreter produced two important contributions. First, in 1931 he formulated a simple salt solution in which an isolated piece of pure or mixed newt embryonic tissue could continue independent development (Table 19.2). Then, following his discovery that an increase of salt concentration in the artificial medium has profound effects on development, he developed a simple way [i.e., culture of blastula in a 0.35% salt solution (Holtfreter, 1933b)] of producing at will an extremely malformed embryo, the *exogastrula* (Fig. 19.12).

In this abnormal embryo, the expanding ectoderm does not turn inward at the dorsal lip, but turns outward, resulting in an exogastrula in which pure ectoderm cells become a solid mass separated and dangling from the rest of the embryo by a narrow thread of ectoderm. The ectoderm-free mesoderm and endoderm continue to develop into a highly ordered but bizarre embryo. Without direct contact with the mesoderm, the isolated ectoderm cells remain completely undifferentiated.

The total lack of differentiation of the ectoderm in an exogastrula provides proof that exposure to the underlying mesodermal cells is indispensable for its differentiation into neural tissues. In addition, the dependable production at will of a mass of easily isolated, undifferentiated ectodermal cells offered another new technique for the study of the induction phenomenon. There was evidence then that, even though the mesodermal tissue is quite able to induce and set the fate of ectodermal tissues fairly early in gastrular development, the fate of the mesoderm tissue itself remains plastic to the end of the gastrula stage. T. Yamada (1938) studied the behavior of isolated somite mesoderm *in vitro*. He found that, if somite mesoderm of a later gastrula is cultivated in Holtfreter's salt solution, it will develop only into muscle tissue. On the other hand, if the somite mesoderm is reimplanted into an isolated ectodermal ball, the somite mesoderm will develop into a pronephros. This ectoderm-induced transformation is prevented by the simultaneous presence of notochordal tissue.

Notochord, however, does not act as a simple inhibitor, for it too can induce muscle tissue from presumptive pronephros (Yamada, 1939a,b, 1940). Yamada further discovered that the relationship between presumptive muscle and pronephros is paralleled by a similar relationship between presumptive pronephros and presumptive blood from

TABLE 19.2. Ionic Composition of the Neutral Media for the Cultivation of Amphibian Embryonic Tissues^a

	Ionic concentration (mM)										Total osmotic equivalent (mM NaCl)	Total tonicity (mOsM)	
	Na ⁺	K ⁺	Ca ²⁺	Mg ²⁺	Cl ⁻	HCO ₃ ⁻	PO ₄ ³⁻	NO ₃ ⁻	SO ₄ ²⁻	Glucose			
Holtfreter (1931)	62.4	0.67	0.9		62.5	2.4						64.4	129
Niu and Twitty (1953) (urodeles)	58.2	0.67	0.39	0.8	58.9	2.4	0.91	0.78				63.0	126
Barth and Barth (1959) (anurans)	90.8	1.31	0.75	0.83	89.8	2.4	0.52	0.68		(0.1%)		93.5	187
Landström and Løvtrup (1979)	136	1.97	1.13	1.25	135	3.6	0.78	1.02				140.0	280
Ling's frog Ringer solution “731”	100	2.5	1.0	1.2	86.7	15.7	2.7	0.1	0.8	23.5		118	236

^aFrog Ringer solution “731” is included for comparison.

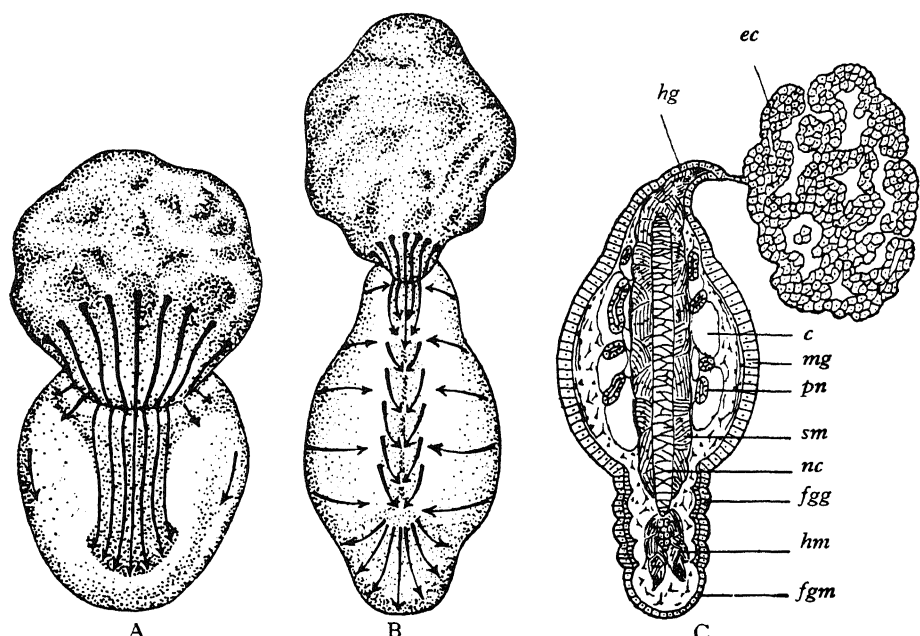


FIGURE 19.12. Diagram of three successive stages in the process of exogastrulation. c, Coelom; ec, ectoderm; fgg, foregut (gill region); fgm, foregut (mouth); hg, hindgut; hm, head mesoderm; mg, midgut; nc, notochord; pn, pronephros; sm, somite muscle. [From Needham (1950), by permission of Cambridge University Press.]

another mesodermal region. Thus, presumptive pronephros will form blood cells if isolated in an ectodermal ball but will develop into pronephros if notochord tissue is also present.

These fascinating findings led Needham (1950, p. 164) to suggest that these various morphogenetic effects may be the result of a quantitative variation of a single chemical substance, an *evocator*: At its weakest concentration, blood cells are induced; at an intermediate concentration, pronephros is formed; at its highest concentration, muscle is formed.

19.4.3. In Search of the Evocator

Spemann (1931) showed that the integrity of the cells of the organizer is not essential for its inductive effect. Like its intact counterpart, the crushed dorsal lip of the blastopore, when implanted into the blastocoel cavity, produced a secondary embryo. In the ensuing years, much effort was spent in attempts to assess the nature of the evocator.

Isolated dorsal lip of blastopore was subjected to various destructive treatments and the treated organizer was tested for its inductive power. The results showed that the evocator is remarkably stable. It is resistant to prolonged boiling or exposure to alcohol, ether, and even concentrated HCl. However, heating to 135°C diminishes its activity; heating to 150°C or ashing destroys it. This heat lability rules out inorganic substances

as the primary evocator. Holtfreter (1934a) showed that these noxious treatments did not destroy the inductive power of a living organizer, but that treatment with organic solvents, boiling, or freeze-drying can actually turn a noninducer (e.g., presumptive epidermis, yolk endoderm) into an active inducer. This discovery strongly suggests that the evocator is of wide occurrence but exists in a bound and dormant form. Severe treatments denature the protein binding the evocator, causing its liberation. Holtfreter (1933a, 1934b) then found that adult tissues of all phyla of the animal kingdom would produce a secondary embryo when implanted into the blastocoel cavity. Boiling was not essential. Quantitatively vertebrate tissues were more active than invertebrate tissues. A large number of plant tissues were also tested by Holtfreter (1934b); all gave negative results.

The burst of intensive effort that followed this initial brilliant work then slowed down, partly because of the outbreak of the Second World War and partly because of the bewilderingly large number of chemicals and agents that produce neural induction, including glycogen, fatty acids, cephalin, and nucleoproteins (see Needham, 1950). In some cases, a minute quantity of impurity might have produced the positive results; in other cases, the cell injury during transplantation might have liberated masked evocators. Above all, one cannot help recalling similar complaints and bewilderment expressed by other investigators researching an entirely different biological problem outlined earlier in this volume in the discussion of mitochondrial physiology (e.g., Section 15.5.3): Why should so many different unrelated agents all produce the same results? I suggest that it may indeed be the nature of the protoplasm and its ability to be triggered into another metastable state that is crucial. The trigger may be its normal cardinal adsorbent or agents that may appear to have no relevance to the phenomenon in question at all.



Lester G. Barth (1905-1979)



Lucena J. Barth

19.4.4. Barth and Barth's Experiments and Theory of Differentiation

In 1959 Lester G. Barth and Lucena J. Barth developed a new solution for the *in vitro* culture of frog embryo explants (Table 19.2). The tissue on which Barth and Barth devoted their next 15 years of research was small explants (125 cells) of the presumptive epidermis of the early gastrula. This choice was made with good reason. The presumptive epidermis is unusually stable. In an exogastrula, it remains undifferentiated, even though it shares the same bathing medium with the differentiating mesoderm and endoderm tissues of the abnormal embryo (Fig. 19.12).

The main conclusion of Barth and Barth from their early work was that the presumptive epidermis can be made to differentiate into different kinds of tissues in response to different courses of treatment with inorganic ions. The differences in the tissues thus induced (compare Fig. 19.13 with Fig. 19.14) seem to be related to the "intensity" of the inducing agents. The intensity is determined by both the concentration of the agent and the duration of exposure to the agent. Of great interest was their discovery of a mandatory sequential order in tissue induction. Each step in the sequence, motor nerves → ganglia nerve → pigment cells → astrocytes → neuroglia, was found to be necessary for the induction of the next cell type and each step was reversible within a 2- to 3-hr period (Barth and Barth, 1963, 1964).

The inducing substance can be CaCl_2 (2.4 mM) or MgSO_4 (12.8 mM), both found in the cell's natural environment, or "unnatural" agents like lithium or sucrose. Exposure to the inducer at high enough concentration for an adequate period of time and subsequent culture in the standard Barth and Barth solution (5 or more days) were by themselves not sufficient to bring on differentiation. These initial treatments must be

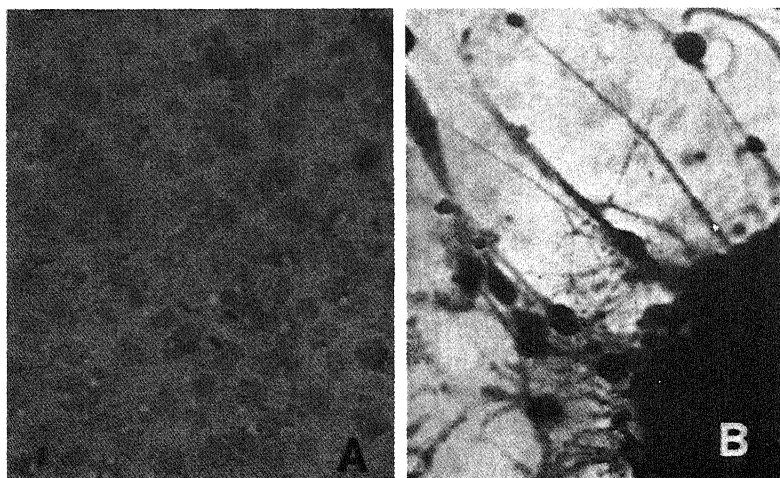


FIGURE 19.13. Presumptive epidermal cells without treatment with Li^+ or other inducing substances. (A) Epithelium type of cellular differentiation. The spherical aggregate has spread out into a sheet of cells, some of which are ciliated. (B) A 6-day culture of presumptive epidermis of Stage 11 with maximal proliferation of nerve fibers. High power. [From Barth and Barth (A, 1962; B, 1959), by permission of *Journal of Morphology* (A), and *Journal of Embryology and Experimental Morphology* (B).]

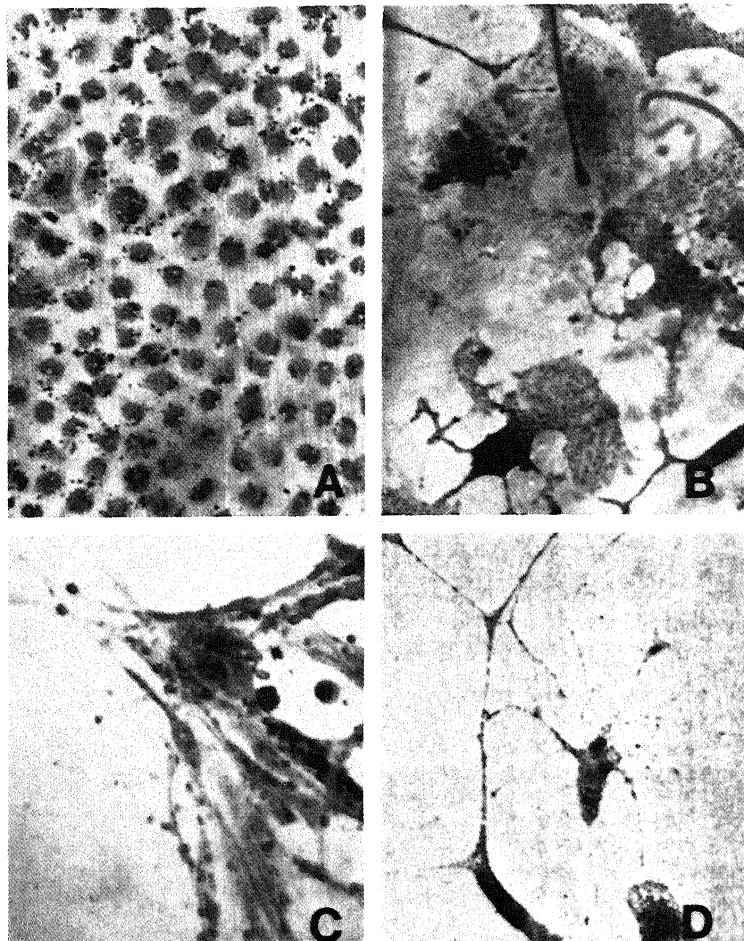


FIGURE 19.14. Various types of cells derived from presumptive epidermal cells following different Li^+ treatments. (A) Portion of a sheet of presumptive epidermis cells 6 days after a 2-hr treatment with 0.1 M LiCl administered to explants made from Stage 11. Cytoplasm does not stain; pigment rings and kidney-shaped nuclei are visible. Low power. (B) Vacuolization of pigmented cells in the process of becoming highly dendritic melanophores. Stage 11 presumptive epidermis was treated in 0.1 M LiCl for 4.5 hr. High power. (C) Five-day culture of muscle cells induced from presumptive epidermis cells by pre- and posttreatment with LiCl. Eggs were pretreated from 256-cell stage to Stage 10 with 0.1 M LiCl in 10% Ringer solution. Posttreatment for 3 hr was with standard medium from which NaCl had been omitted, with 4.2 mg/ml of LiCl substituted. Culture was in standard medium. Magnification 325 \times . (D) An "astrocyte" from a culture prepared by treating presumptive epidermis with a solution of 17.5 mM LiCl for 47 hr at 23°C. On return to standard solution the cell differentiated as large pigment ring cells and transformed into astrocytes, which tend to make contact with adjacent cells. [From Barth and Barth (A,B, 1959; C, 1962; D, 1963), by permission of *Journal of Embryology and Experimental Morphology* (A,B), *Journal of Morphology* (C), and *Biological Bulletin* (D).]

followed by exposure (lasting another 4–6 hr) to a solution containing Na^+ at a high enough concentration (88 mM) (Barth and Barth, 1974a). Without this exposure to Na^+ or with exposure to an insufficiently high Na^+ concentration, no differentiation occurs. All cells then remain as epithelial cells (Fig. 19.13A).

Exposure (2–3 hr) of presumptive epidermis explant to 71 mM Li^+ , followed by treatment in a standard solution containing 88 mM Na^+ and 1.3 mM K^+ (see Table 19.2) will produce nerve, muscle, and pigment cells (Fig. 19.14D,C,A, respectively). It was toward the ends of their careers that Barth and Barth (1974b) discovered that, if the K^+ concentration of the posttreatment solution was increased from 1.3 mM to 5.3 mM, instead of pigment cells and nerves, notochord tissue develops (Fig. 19.15A; compare with Fig. 19.15B).

Barth and Barth presented their theory of ionic regulation of amphibian differentiation in these words: “during the course of normal gastrulation, and later differentiation, release of cations from bound or sequestered states followed by binding at new sites within the embryo leads to conditions similar to those provided in cell culture and found effective in sustaining cells to a new type of differentiation” (Barth and Barth, 1974b, p. 313). In general support of this theory, Barth and Barth (1967) showed that, during the 2-hr period following either lithium or sucrose treatment, there is an increase of uptake of labeled Na^+ from the medium. This is also the period of time during which differentiation is Na^+ -dependent. While Barth and Barth used the conventional phraseology of increase of “membrane permeability” to Na^+ during the critical period, they recognized that this term might not be quite correct. Thus, a 24-hr exposure to $^{22}\text{Na}^+$ led to higher or equal uptake of the isotope than one four times longer (Barth and Barth, 1972, p. 24). These and similar observations suggested an increased rate of exchange of intracellular ions with external labeled Na^+ as a result of release from binding or sequestration.

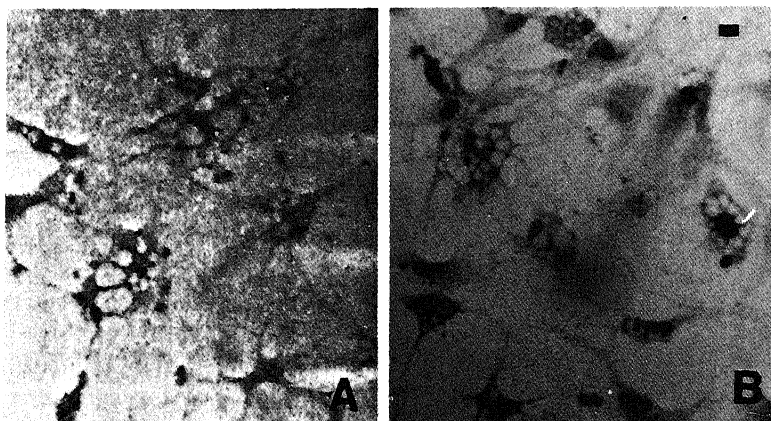


FIGURE 19.15. Comparison of Li^+,K^+ -transformed presumptive epidermal cells with normal notochord cells. (A) Li^+ treatment of presumptive epidermis cells for 4 hr in standard solution with 5.3 mM K^+ ; fusions among cells with large vacuoles. (B) Archenteron roof cells, removed at neural tube stage, were cultured in 5.3 mM K^+ in standard solution for 9 days. Scale bar: 20 μm . [From Barth and Barth (1974b), by permission of *Biological Bulletin*.]

19.4.5. Landström and Løvtrup's Work on Differentiation

While Barth and Barth investigated in depth the differentiation of frog presumptive epiderm, the Barth and Barth medium (Table 19.2) was used by Landström and Løvtrup (1979) in a broad study of differentiation of all amphibian tissues. Landström and Løvtrup isolated even smaller explants (15 cells). They also found that, for the small colonies of cells to survive, they had to increase the strength of the solution to $1.5 \times$ standard. Table 19.2 shows that, while original Barth and Barth solution is about 40 mOsM hypotonic, the Landström–Løvtrup modification is about 40 mOsM hypertonic when compared to frog Ringer solution (or frog plasma).

In this modified Barth and Barth solution, the cells spontaneously differentiate into three types: undifferentiated cells, which are spherical; “vegetal” cells, which are fibroblastlike Ruffini cells arising mostly from endodermal cells outside the vegetal pole; and “animal” cells, which are epidermal cells forming spherical aggregates with ciliated cells dispersed among nonciliated cells. If no other inducer is added, these cells will remain in one of the three categories with no further differentiation.

Since in classical experiments the dorsal lip of the blastopore is the primary organizer, and the Ruffini cells are located at the dorsal lip (Fig. 19.9), it was suggested that Ruffini cells embody the inductive agent. In agreement, it was found that, if a few vegetal cells were introduced into explants of ectodermal cells, the ectodermal cells eventually differentiated into mesenchyme cells, nerve cells, and pigment cells.

Landstrom and Løvtrup (1977) raised the question, Is heparin sulfate (HS) the agent of amphibian induction? From their studies they concluded that HS is at least one inducer when applied in the medium at a concentration of $0.1\text{--}1 \mu\text{g/ml}$. Owing to the variability of the molecular weight, this would correspond to a range of concentrations of from 5×10^{-10} to $1.6 \times 10^{-7} \text{ M}$, a very low concentration range indeed.

The vegetal cells are not strikingly affected by HS; in contrast, all cells from the ecto-mesodermal region are profoundly affected by HS. Thus equatorial ectoderm cells give rise to swollen hyaline cells (chondrocytes, presumably the notochord cells of Barth and Barth), while the remaining ectodermal cells fall into a differentiation pattern of the sequence mesenchyme cells, nerve cells, melanophores, and xanthophores. The free interior cells differentiate into muscle and elongated collagen-producing fibroblasts.

19.4.6. Concluding Remarks on Differentiation

The concordance between Barth and Barth's theory and the AI hypothesis should be quite evident. Their work, and a considerable amount of other observations, fit the notions first that the modulation of macromolecular salt linkages has a role in differentiation, just as it does specifically in protein synthesis (Chapter 18), and second, that part of the process of differentiation involves changes in the nature of protoplasm and its ability to be triggered into an alternative state. Ions may modulate the latter by their specific effect on the making and breaking of salt linkages in an autocooperative manner.

19.5. The Cell Cycle

Thus far we have seen how in meiosis of egg cells the divisions are unequal. In the case of mosaic eggs, even the first mitotic division creates two different daughter cells.

More equal mitotic divisions occur in the blastula and the early gastrula of regulative amphibian eggs. From a late gastrula stage on, mitotic divisions during embryonic differentiation tend to be unequal again. Once the embryonic stage is past, the greatest mass of adult higher animal and plant cells cease division. Only certain types of cells in normal adult organisms continue mitosis, including intestinal epithelial cells and bone marrow cells. Abnormal cancer cells, on the other hand, divide ceaselessly. In the following section I shall discuss when and how the cell divides, or does not divide, as the case may be.

Growth of most living tissue is achieved by mitosis. Recognition that the replication of DNA occurs only in a limited period within the mitotic interphase led to the division of the cell cycle into four periods (Fig. 19.16). G_1 represents the interlude between the completion of mitosis (M) and the onset of the period of DNA replication called the S phase, while G_2 represents the interlude between the completion of DNA replication and the onset of cell division. The termination of the M phase is followed by G_1 and the cycle repeats itself.

The concept of the cell cycle consisting of four discrete steps is a useful reference scheme, although many types of cells in uni- and multicellular organisms go through cell cycles without a demonstrable G_1 phase. By far the greatest number of the cells in a normal adult human being, including nerve, muscle, and liver cells, do not undergo cyclic division at all but are arrested in the G_1 phase indefinitely until death. Using the cell cycle concept as a basis, Baserga (1981) divided tissue cells into three classes: non-dividing cells, proliferative cells which undergo cyclic division continually, and G_0 cells. G_0 cells will not enter into DNA synthesis and cell division except under special conditions, e.g., liver cells will divide after partial hepatectomy, which triggers regeneration. Figure 19.16 is a diagram of the cell cycle which combines the features described by Prescott (1976) and Baserga (1981). An important trait of the cell cycle is the constancy of the length of time a cell spends in most of the phases: some 7 hr in S phase, 4 hr in G_2 phase, and 1 hr in M phase. On the other hand, the generation time, the time for a cell to complete one cycle, varies widely because the durations of the G_1 phase vary widely (Mitchison, 1971; Mazia, 1974; Prescott, 1976; Pardee *et al.*, 1978).

How can the cell so unerringly keep such good time? According to one theory, the *linear reading theory* (Watson, 1970), timing is based on a linear transcription along

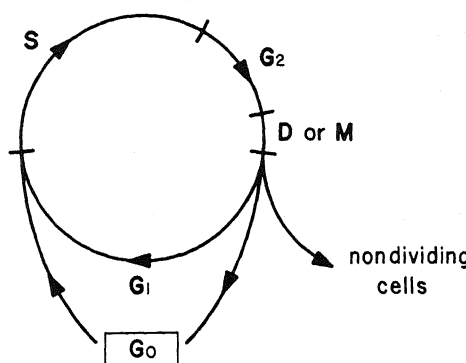


FIGURE 19.16. The cell cycle. D and M, division or mitosis.

the genome. The timing of the transcription is dependent on the movement of RNA polymerase molecules along the DNA chain. Such a theory may indeed be applicable to the more "determinate" part of the cycle that includes S, G₂, and M (Rudland and de Asua, 1979). However, the timing of the G₁ phase cannot be described by such a linear reading theory because this part of the cycle varies greatly and thus is indeterminate. The determinate portion of the cell cycle means that once the cell decides to replicate its DNA, thereby entering S, there is no holding back. Understanding this decision may be of critical importance because it may set apart normal cells from those that constantly divide, such as cancer cells (Chapter 20). To explain the timing of G₁ a different kind of theory has been presented, the *transition probability* model.

19.5.1. The Transition Probability Model

Burns and Tannock in 1970 presented the transition probability model of cell cycling. In the Prescott-Baserga scheme, shown in Fig. 19.16, the G₀ phase is represented as an outgrowth. In the Burns and Tannock model G₀ is a part of the cell cycle, interposed between M and "true" G₁. This G₀ phase is indeterminate and in this sense is different from the rest of the cycle. G₁, S, G₂, and M are collectively referred to as the determinate C phase (Fig. 19.17). The position of the true G₁ phase before or after G₀ is not yet clear, although in Fig. 19.17 G₀ is tentatively placed before true G₁. The point of the transition probability theory is that, after completing the prior division, the cells enter the G₀ phase. Cells enter the determinate (C) phase randomly following first-order transition kinetics. Thus, in a population of G₀ cells of the same kind under the same condition, their number N_{G0} declines with time by the simple relationship

$$\frac{dN_{G_0}}{dt} = \gamma N_{G_0} \quad (19.1)$$

This equation predicts that, in a synchronized population of cells, the logarithm of the proportion of cells remaining in the G₀ phase, when plotted against time *t*, should yield a straight line. Figure 19.18, taken from J. A. Smith and Martin (1973), shows that the remaining fraction of synchronized cells not yet entering S does logarithmically decline with time. All of these cells are of the rapidly proliferating type, most, if not all, neoplastic. However, the logarithmic decline does not begin immediately, as implied in equation (19.1). There is in every case a lag phase, the length of which varies with the cell type.

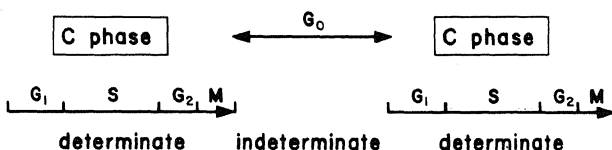


FIGURE 19.17. The Burns and Tannock scheme of the cell cycle.

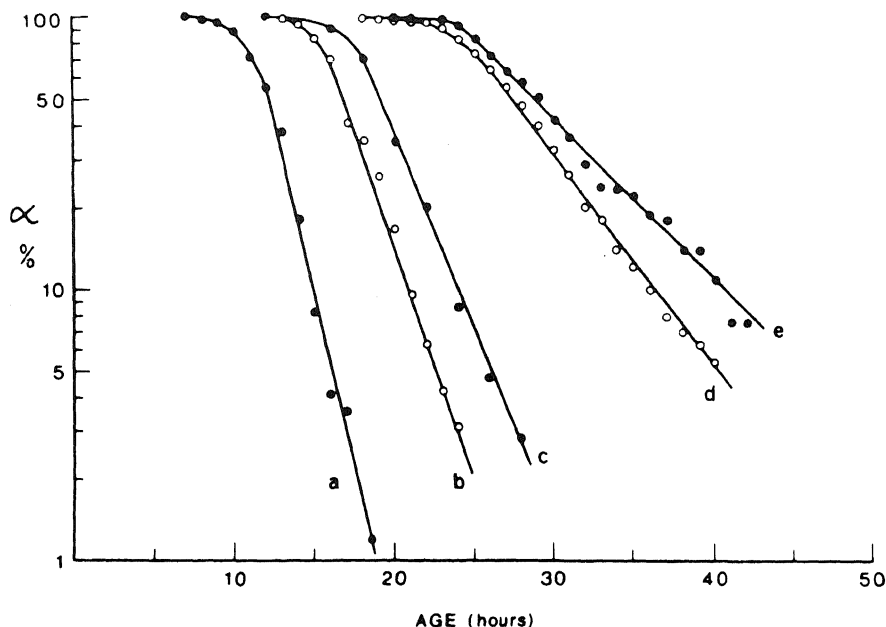


FIGURE 19.18. Distribution of generation times of various cell types in culture. α represents the proportion of the initial population of cells remaining at interphase. (a) Rat sarcoma; (b) HeLa S3; (c) mouse fibroblasts; (d) L5 cells; (e) HeLa. [From J. A. Smith and Martin (1973), by permission of *Proceedings of the National Academy of Sciences*.]

19.5.2. The Control of Entry into the C Phase

Evolution from the simple unicellular organism like *E. coli* to the extremely complex multicellular organism required the development of control mechanisms which determine when cells remain in the G_0 phase and when they enter the C phase (Fig. 19.17). We are still far from understanding these complex and intricate mechanisms, but some significant advances have been made in recent years.

19.5.2.1. Stimulation of DNA Synthesis in 3T3 Cells by Hormones

de Asua *et al.* (1977) studied the initiation of DNA replication in quiescent Swiss mouse 3T3.4 fibroblast cells in response to the prostaglandin F₂ (Fig. 19.19). In a plot of the percentage of unlabeled nuclei against time after the addition of the hormone, they found that the effect of the hormone is primarily to increase the value of γ in equation (19.1) (Fig. 19.20).

19.5.2.2. Stimulation of DNA Synthesis by Nuclear Transplantation and Cell Fusion

Using a technique described by A. Briggs and King (1952), Gurdon and his co-workers (Gurdon, 1962, 1967; C. F. Graham *et al.*, 1966; Gurdon and Brown, 1965)

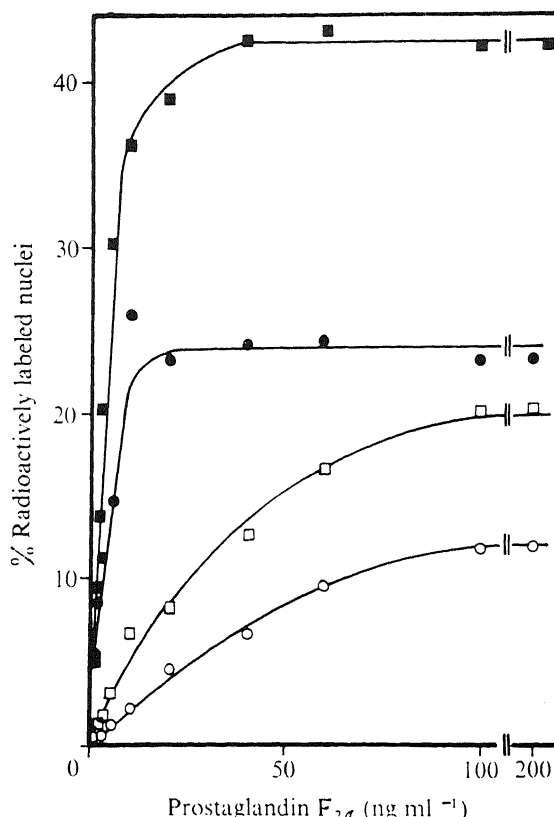


FIGURE 19.19. Effect of concentrations of prostaglandin $F_{2\alpha}$ ($PGF_{2\alpha}$) on the percentage of cells synthesizing DNA in 30 hr in Swiss mouse 3T3.4 fibroblasts. Increasing concentrations of $PGF_{2\alpha}$ were added to quiescent 3T3.4 cells in Dulbecco's modified Eagle's medium (DMEM) without (○—○) and with (●—●) 50 ng ml^{-1} insulin, or to quiescent cells in DMEM supplemented with low-molecular-weight nutrients without (□—□) and with (■—■) insulin. Fibroblasts were maintained in DMEM containing 100 units ml^{-1} penicillin, 100 ng ml^{-1} streptomycin, and 10% fetal calf serum. [From de Asua *et al.* (1977), by permission of *Nature*.]

published a series of important papers that offered insights into the key control mechanisms of the transition of nondividing cells into C phase.

As discussed in previous sections, a mature egg will develop into a full embryo after insemination by a spermatozoon. Gurdon (1962) showed that an enucleated mature egg which cannot continue development by itself can develop into a complete tadpole if the nucleus from a fully differentiated intestinal epithelial cell is transplanted into it. This finding shows that the nucleus of a fully differentiated cell retains the same totipotency

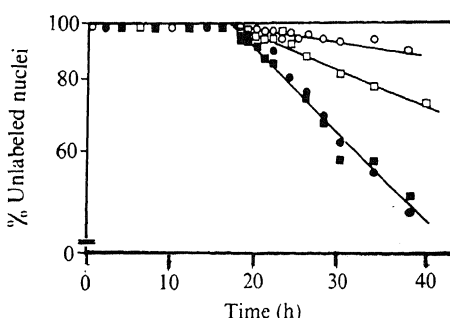


FIGURE 19.20. Fraction of cells remaining in G_1 after synchronous addition of $PGF_{2\alpha}$ and insulin, given as logarithm of percent of unlabeled cells against time in hours. ○—○, $PGF_{2\alpha}$, 30 $ng\ ml^{-1}$; ●—●, $PGF_{2\alpha}$, 30 $ng\ ml^{-1}$, insulin, 50 $ng\ ml^{-1}$; □—□, $PGF_{2\alpha}$, 300 $ng\ ml^{-1}$; ■—■, $PGF_{2\alpha}$, 300 $ng\ ml^{-1}$, insulin, 50 $ng\ ml^{-1}$. [From de Asua *et al.* (1977), by permission of *Nature*.]



John B. Gurdon

of the nucleus of a fertilized egg. Potentially, it is possible to make a large number of copies of the same animal just as it was possible to make a large number of copies of the same plant.

C. F. Graham, Arms, and Gurdon (1966) discovered that nuclei of fully differentiated adult *nondividing* cells—such as brain, liver, and blood cells—regain the power to synthesize DNA after being transplanted into the enucleated, mature, unfertilized egg of the frog *Xenopus laevis*. Clearly there is something in the egg cytoplasm that stimulates the quiescent nuclei of adult liver, brain, and red blood cells to go from G_0 into the C state.

In an equally brilliant piece of research, H. Harris, Watkins, Ford, and Schoefl (1966) discovered a general method which permits the fusion of differentiated cells (e.g., hen erythrocytes, rat lymphocytes) and undifferentiated cells (e.g., HeLa cells, Ehrlich ascites cells), when into a mixed culture of the cells of different types an inactivated Sendai virus is introduced. Using this technique Harris and co-workers showed that cells from different species of animals are quite compatible with one another when fused into a single unit, and that, in such *heterokaryons*, regulation of entry into the C state is always unilateral, that is, dormant nuclei are induced to resume synthesis of DNA and RNA. Thus fusion of proliferating HeLa cells and quiescent erythrocytes will induce the nondividing erythrocyte into active DNA synthesis. The fusion experiments confirmed and extended the transplantation experiment in showing that nondividing cells can be triggered into S phase by an agent (or agents) present in the cytoplasm of mature egg cells and in the cytoplasm of proliferating undifferentiated cells like HeLa cells. The search for this agent soon proved successful.

19.5.2.3. Stimulation of DNA Synthesis by Egg Cytoplasmic Extracts

In 1975 Benbow and Ford succeeded in demonstrating very convincingly the stimulation of nondividing adult liver cell nuclei into active DNA synthesis by incubation in

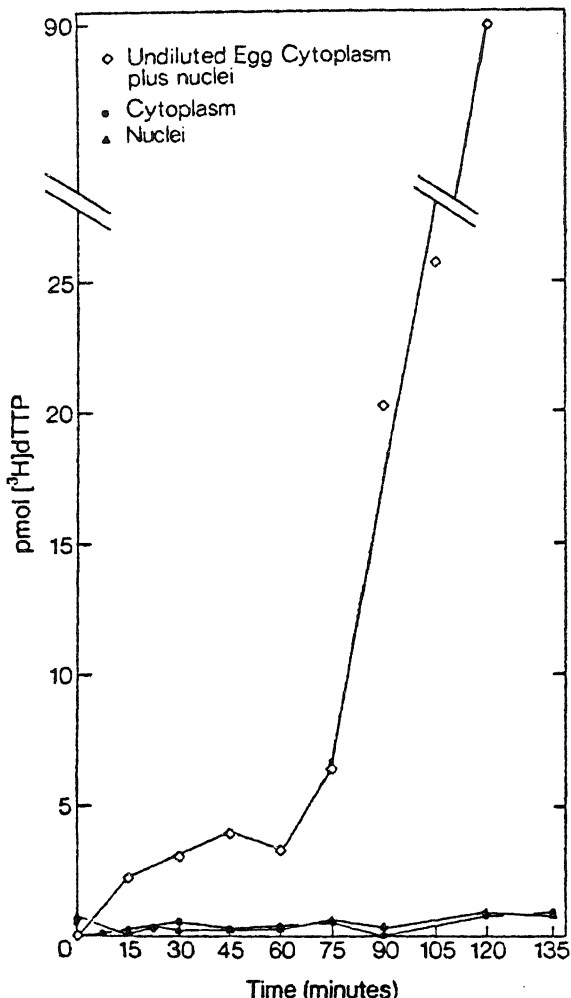


FIGURE 19.21. Incorporation of [^3H]-dTTP by isolated nuclei. Liver nuclei (1.0×10^7) were incubated with 3.0×10^3 egg equivalents of undiluted egg cytoplasm. Aliquots containing 8×10^5 nuclei were removed at various times, precipitated, filtered, and counted. Control assays contained homogenization buffer plus either nuclei or cytoplasm only. [From Benbow and Ford (1975), by permission of *Proceedings of the National Academy of Sciences*.]

an extract of the cytoplasm of mature eggs of *Xenopus* larvae (Fig. 19.21). The criteria that distinguished Benbow and Ford's experiment from many other reports of induced DNA synthesis included the following: (1) Benbow and Ford were dealing with liver nuclei that exhibited virtually no DNA synthesis before exposure to the egg cytoplasm. (2) They demonstrated by autoradiography that 99% of the treated liver nuclei incorporated [^3H]-dTTP. (3) Small replication eyes in DNA were induced by the cytoplasm extract (see Fig. 19.22). They showed further that the cytoplasmic factor causing DNA synthesis, the I factor, is present in the *Xenopus* egg only after maturation. The I factor of an extract of mature oocytes is not removed by high-speed centrifugation. Extracts of blastula and gastrula, which also can induce DNA synthesis in liver nuclei, show no activity after similar centrifugation. Benbow and Ford believe that the I factor is probably a protein with a molecular weight larger than 60,000 daltons.

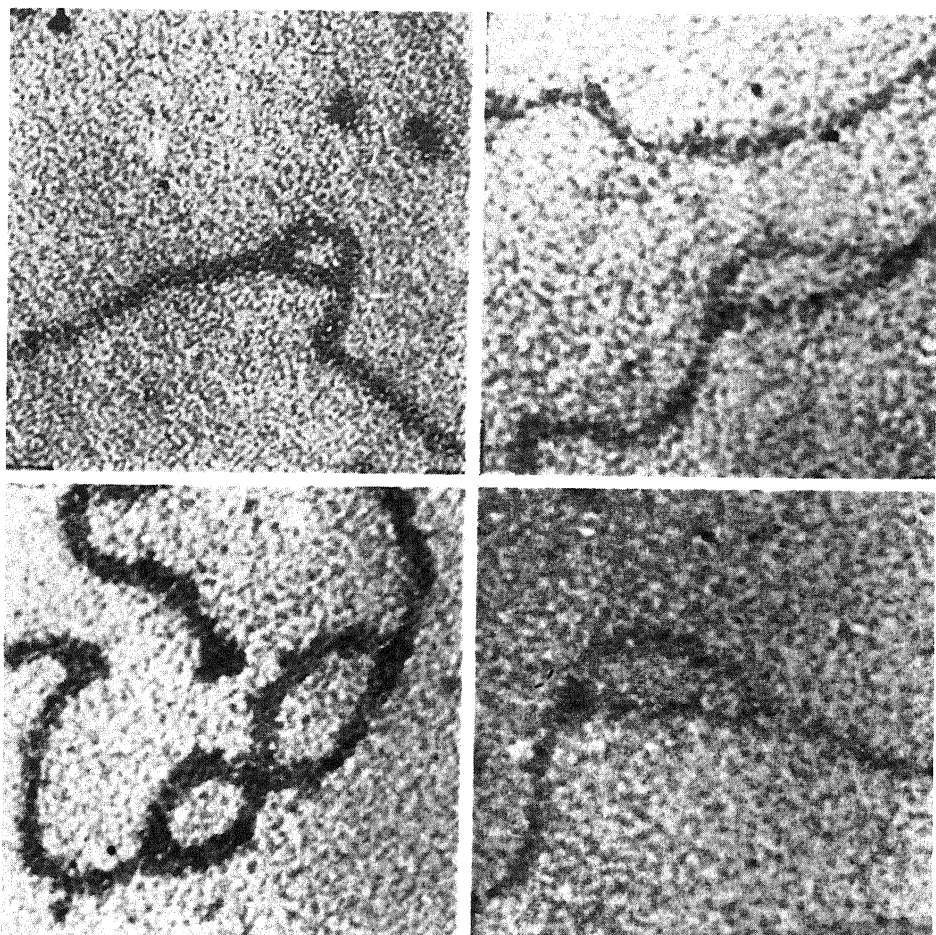


FIGURE 19.22. Replication "eyes." Frog liver nuclei (3.6×10^6) were incubated with or without $50 \mu\text{l}$ of P388 cell extract. [From Jazwinski *et al.* (1976), by permission of *Proceedings of the National Academy of Sciences*.]

A year after Benbow and Ford's publication, Jazwinski, Wang, and Edelman (1976) demonstrated replication of DNA in nuclei from adult frog spleen and liver cells, both nondividing cells, by exposure to extracts of various proliferating cells. Like Benbow and Ford, these authors used a battery of stringent criteria to establish that actual DNA replication (rather than, say, repair) was induced: Besides the demonstration by electron microscopy of a tenfold increase of replication eyes in response to the extract, they showed that [^3H]-dTTP incorporation depends on Mg^{2+} , ATP, and the four deoxyribonucleotide triphosphates: dATP, dGTP, dCTP, and dTTP. Moreover, the DNA replication process was discontinuous, which is known in eukaryotes to result initially in the formation of nascent S-55 fragments. They found the active factor in the extract to be heat-labile, nondialyzable, and destroyed by trypsin, and thus apparently a protein having a molecular weight larger than 50,000 daltons.

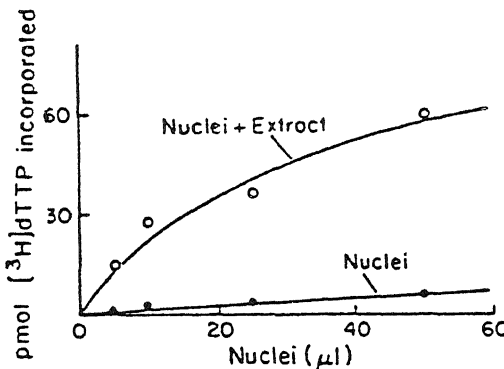


FIGURE 19.23. Dependence of [3 H]-dTTP incorporation on added nuclei and cell extract. Frog liver nuclei were at 6×10^7 /ml and 50 μ l of P385 cell extract was used. Incubation was for 60 min. [From Jazwinski *et al.* (1976), by permission of *Proceedings of the National Academy of Sciences*.]

Jazwinski *et al.* compared the effectiveness of the extracts of different cells in initiating DNA synthesis in liver and spleen nuclei. They found that adult mouse liver (and brain) cells were inactive, while fetal liver cells were active. Stationary normal 3T3 fibroblasts were ineffective, but transformed SV 3T3 cells were effective. Chicken embryo fibroblasts transformed by Rous sarcoma virus ts 68 (ts NY68 SRA) were ineffective at 41°C; they were active at 37°C. Nondividing mouse lymphoma P388 cells in a dense pellet (and thus suffering from contact inhibition) were relatively inactive, while logarithmically growing thin suspensions were more active.

Figure 19.23, taken from Jazwinski *et al.*, shows that, for a fixed concentration of the extract, the amount of [3 H]-dTTP incorporation into DNA shows saturation with

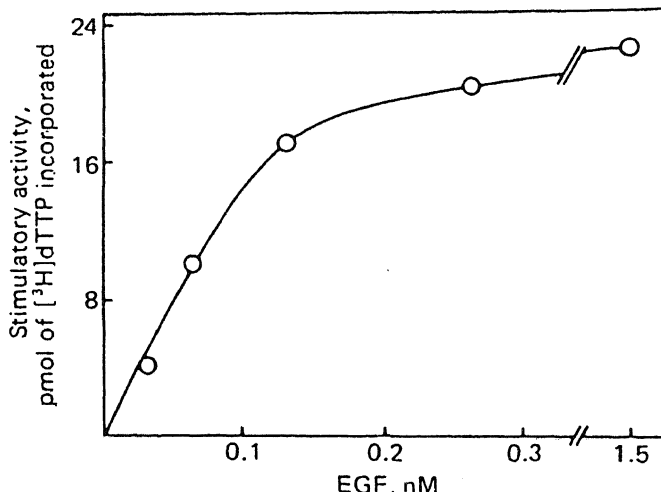


FIGURE 19.24. Dependence of the DNA-synthesis-stimulating effect on EGF concentration. Confluent density-inhibited cultures of 3T3 cells were incubated in the presence of the indicated concentrations of EGF. After a 20-hr incubation period, cytoplasmic extracts (1 ml per 10^7 cells) were prepared and then assayed for DNA synthetic stimulatory activity. [From Das (1980), by permission of *Proceedings of the National Academy of Sciences*.]

increasing number of nuclei added, suggesting that the proteinaceous factor binds to a limited number of sites which control DNA replication.

The experiments of Jazwinski *et al.* strongly suggest that, in the increased DNA synthesis during egg maturation, following release from contact inhibition, and in viral transformation, the key G₀-to-C transitions are all the result of the synthesis, liberation, or activation of a specific protein.

Another protein, in this case a hormone, that can induce DNA synthesis in 3T3 cells is the epidermal growth factor (EGF), which is an insulinlike peptide. Das (1980) recently showed that cytoplasmic extracts of 3T3 cells treated with EGF stimulated [³H]-dTTP incorporation into adult frog spleen nuclei. The extent of DNA synthesis induced is quantitatively related to the concentration of EGF used to treat the 3T3 cells (Fig. 19.24). As in the data in Fig. 19.23, DNA synthesis follows a curve (possibly autocooperative) showing saturation at high EGF concentration.

19.5.3. Control of Chromosome Condensation

As mentioned above, nuclei of a variety of adult, fully differentiated cells, when introduced by surgical transplantation into enucleated mature frog eggs, promptly undergo swelling and DNA synthesis. However, these nuclei do not undergo mitosis (C. F. Graham *et al.*, 1966). In contrast, in Sendai-virus-induced fusion of proliferating and nonproliferating cells, not only is DNA synthesis induced in the nonproliferating nuclei, but the nuclei also undergo mitosis. Furthermore, those nuclei from the different cells that enter mitosis together usually fuse together to form a mononuclear hybrid containing, in a single nucleus, chromosomal components from the different nuclei of the different species. Under favorable conditions the cells can carry on mitosis repeatedly over a period of many days (H. Harris *et al.*, 1966).

One major difference between nuclear transplantation and cell fusion lies in the prior destruction of the nucleus of the mature egg in transplantation while the nuclei of both "parents" are retained in fusion. Thus, the nuclei of the fused nonproliferating cells are exposed not only to the cytoplasm of the proliferating cells but also to the dividing nucleus of the proliferating cell. Nuclei transplanted into enucleated mature eggs are exposed only to the egg cytoplasm.

Gurdon (1967, 1968) first noted that, when a suspension of brain nuclei is injected into an ovarian oocyte, the animal hemisphere contains no intact nucleus but hundreds of asters and spindles attached to highly condensed chromosomes, which are in number far larger than those from the egg nucleus and must therefore be from the brain nuclei. However, these eggs with many chromosomes do not undergo cleavage.

Rao and Johnson (1970, 1971) showed that fusion of cells in the M phase with cells in the interphase creates dramatic but diverse effects on the interphase nuclei, depending on whether the interphase nuclei are in G₁, S, or G₂ (Fig. 19.25). Such a phenomenon, referred to as premature chromosome condensation (PCC), produces long, single chromosomes with only one chromatid in G₁ nuclei, a more condensed chromosome with a double chromatid in G₂ nuclei, and a fragmented and unevenly condensed chromosome in S nuclei. The pulverized chromosomes of female *Microtus agrestis* cells, along with the condensed chromosome of the HeLa cell in the heterokaryon, are shown in Fig. 19.25 on the pages following. Rao and Johnson also showed clearly that silver

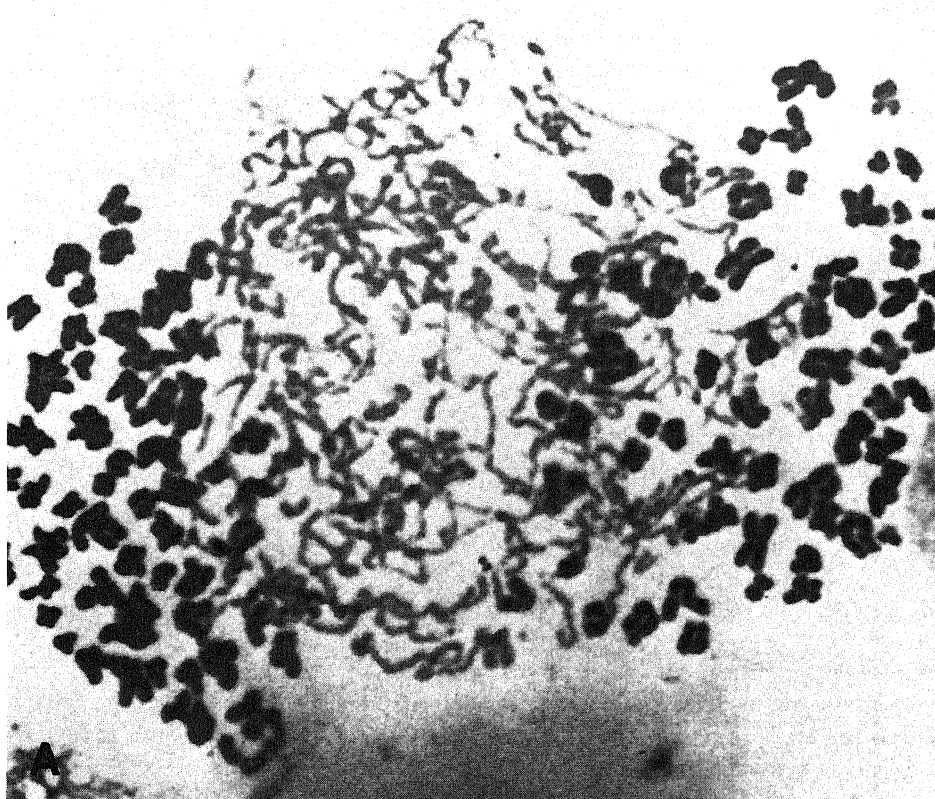
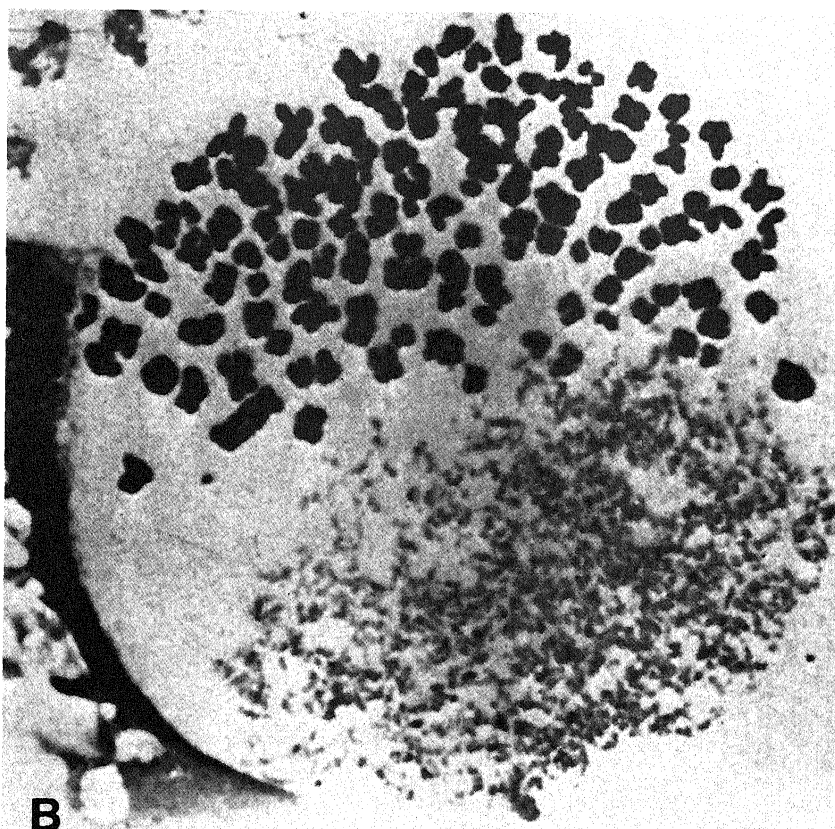


FIGURE 19.25. (A) Chromosome condensation can be forced on cells in other phases of the cycle by inducing fusion with a cell in the M phase. Here prematurely condensed chromosomes of a cell in the G₁ phase appear as strands of chromatin (center). Not having replicated, the strands are single, unlike the doubled chromosomes of the M phase cell (left and right). (B) Another kind of fusion, between an M phase cell and

silver granules, which correspond to [³H]thymidine incorporated into the newly synthesized DNA, are localized in the "pulverized" chromosomes of *Microtus* but not in the HeLa cell chromosomes.

Ziegler and Masui (1973) transplanted brain nuclei from adult *Rana pipiens* into *Rana pipiens* oocytes which were induced to mature *in vitro* by progesterone. As a result condensation of chromosomes from the brain nuclei was induced, which followed closely the condensation of the chromosomes of the egg nucleus following GVBD. Oocytes enucleated before GVBD failed to induce chromosome condensation. Nucleoplasm from oocytes that had not undergone GVBD injected into the cytoplasm of such enucleated eggs restored the condensation activity (CCA) if the oocyte had reached the stage of GVBD. Ziegler and Masui concluded that CCA has a dual origin, from both the germlinal vesicle and the cytoplasm of the mature egg.



a cell in the S phase, has a peculiar outcome. The prematurely condensed chromatin does not form strands, but instead is fragmented and pulverized (right). The experiments were conducted by P. N. Rao and R. T. Johnson. [From Mazia (1974), by permission of *Scientific American*.]

19.5.4. The Promotion of Differentiation of Enucleated Eggs by Nuclear Transplantation

At the blastula stage, the endodermal cells of the embryos of *Xenopus* and *Rana* are totally undifferentiated. When the nuclei of these endodermal cells are injected into enucleated eggs, these eggs develop into normal adult animals. The capacity of the endodermal cell nuclei to promote normal tadpole development decreases after gastrulation. Nevertheless, Gurdon (1962) found that in a small percentage of trials (1%), injection of fully differentiated intestinal cell nuclei into enucleated egg cells resulted in tadpoles.

Since then, success has been reported in transplantation of nuclei from nonciliated epithelial cells of hatching tadpoles (Kobel *et al.*, 1973), from erythroblasts (Brun, 1978), and from lymphocytes (DuPasquier and Wabl, 1977) into enucleated eggs (Fig.



FIGURE 19.26. Mosaic (4-nu) individual obtained after transplantation of albino blastula cells into wild type egg (bottom right). Note the pigmentless left eye. Top, wild type control; bottom left, albino control. [From du Pasquier and Wabl (1977), by permission of *Differentiation*.]

19.26). All of these cells are undifferentiated and/or engaged in some degree of proliferation. Nuclei of nondividing cells do not generally lead to development of enucleated eggs. However, there are exceptions. Thus, adult nondividing cell nuclei have been successfully manipulated so that development followed when they were finally transplanted into enucleated eggs (Fig. 19.27). Among those nondividing cells were epithelial cells (Gurdon and Laskey, 1970); adult somatic lung, skin, and kidney cells (Laskey and Gurdon, 1970); lens cells (Muggleton-Harris and Pezella, 1972); melanophores (Kobel *et al.*, 1973); and keratinized skin cells (Gurdon *et al.*, 1975). The secret of the successful manipulation lies in obtaining nuclei not directly from the donor animal (i.e., first transfer) but following serial nuclear transfers in tissue culture. To prove that the tadpole was truly the descendant of the donor nucleus and not of a surviving host nucleus, diploid donor nuclei with genetic markers 2-nu (2 nucleoli) and 1-nu (one nucleolus) were transplanted into 2-nu eggs, as for example in the successful experiment shown in Fig. 19.27.

What then are the benefits of serial nuclear transfer? Is it likely that the prolonged

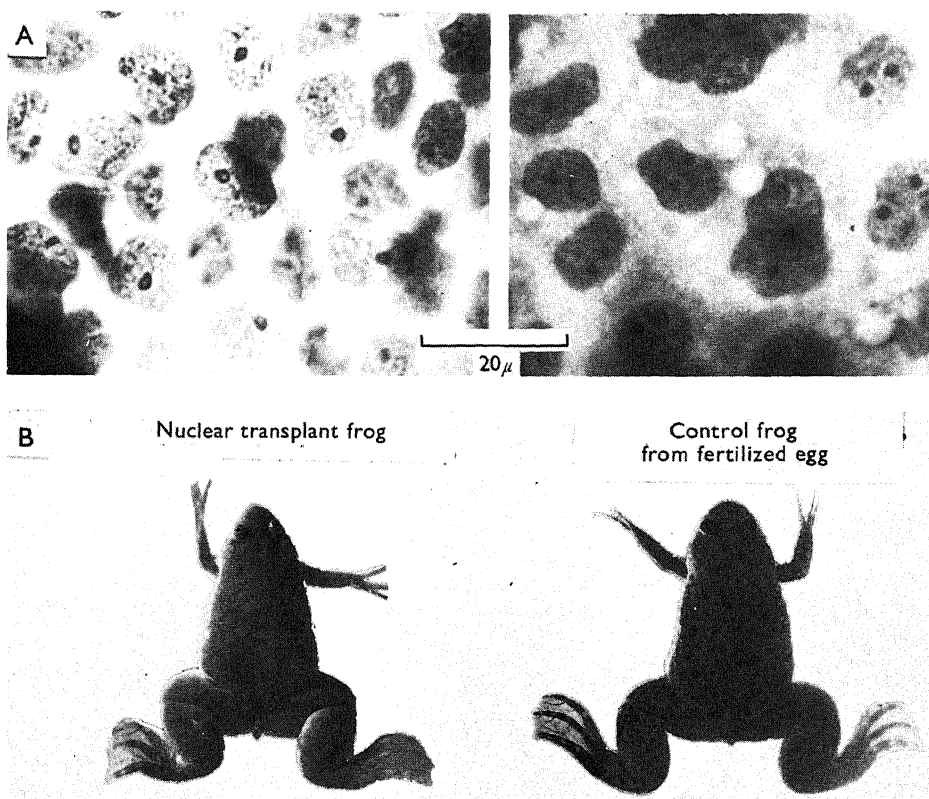


FIGURE 19.27. (A) 1-nu and 2-nu nuclei of epidermal cells of nuclear transplant tadpoles. Whole mounts of fixed tail fin. (B) Nuclear transplant and control frogs, 3 months after metamorphosis. [From Gurdon and Laskey (1970), by permission of *Journal of Embryology and Experimental Morphology*.]

stay in the tissue culture medium with its hormones and peptides makes the donor nuclei more suitable for full development? In general support of this view, Fig. 19.28 shows how the concentration of serum in the culture medium quantitatively determines the degree of dedifferentiation of neuroblastoma cells. A higher serum concentration increases both the rate of cell proliferation and the percentage of spherical undifferentiated cells (Schubert *et al.*, 1971). Serum, which is present in most culture media, has thus succeeded in pushing the nondividing cells toward a more undifferentiated state, more readily able to cause enucleated eggs to develop into an adult animal.

The simplifying assumption that a cell, having once started to replicate DNA, will follow a determinate time course in the C phase is clearly applicable to proliferative cells without major modification. Entry of nondividing cells into a DNA-replicating phase, as in the case of brain or erythrocyte nuclei in the cytoplasm of mature eggs, does not automatically lead to progression to G₂ and M phases. This apparently requires that other energy barriers be overcome, a process that may require the participation of other hormones or polypeptides, which in some cases must act over a long period of time.

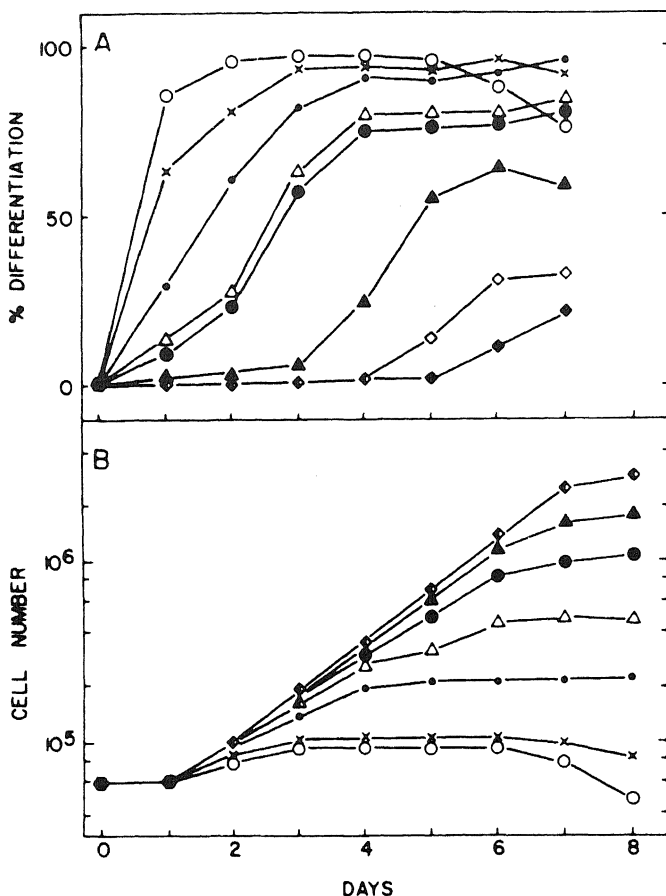


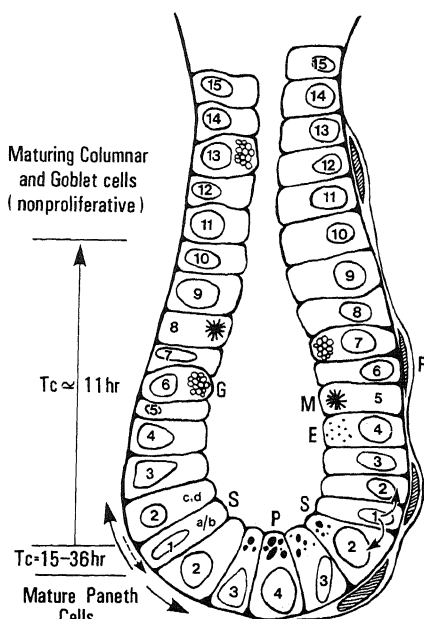
FIGURE 19.28. Relationship between differentiation of neuroblastoma cells and serum concentration. (A) Percent differentiation plotted as a function of time. (B) Viable cell number per dish plotted as a function of time. ○, Serum-free media; X, 0.5% serum; ●, 1% serum; △, 2% serum; ●, 3% serum; ▲, 5% serum; ◊, 10% serum; ◆, 20% serum. [From Schubert *et al.* (1971), by permission of *Developmental Biology*.]

19.6. The Stem Cells: “Immortal” Queen Bees of the Society of Renewing Cells

In the first few cell cycles, a fertilized regulative egg bears a resemblance, at least superficially, to prokaryotes like *E. coli*, producing fundamentally similar daughter cells with each division. In healthy adult animals, the greatest mass of cells, including muscle, brain, liver, and kidney cells, do not undergo division at all. A much smaller proportion of cells, however, do divide to replenish cells that have relatively short lifespans. These include blood cells; epithelium of intestine, skin, and tongue; and the testes.

While specific details vary in these proliferative tissues, in general they follow a similar pattern. Every unit structure of this type of tissue contains a few *stem cells*, each of which occupies a fixed position, or *niche* (see Cairne *et al.*, 1976). Stem cells divide

FIGURE 19.29. Schematic representation of a section of a mouse small intestinal crypt. The base of the crypt contains several mature Paneth cells (P) and some immature Paneth cells (e.g., cell position 2 on the left). Above this is a ring of about twenty cells that are cycling more slowly (cell position 1) than the majority of proliferating crypt cells (cell positions 2–10). At the top of the crypt there are several cell positions where no DNA synthetic activity can be detected. The crypt contains goblet cells (G), occasional enteroendocrine cells (E), and cells in mitosis (M) and is enclosed by a sheath of fibroblasts (F). Cell position 1 is the “anchored” stem cell position in steady state (a). S represents stem cells. Stem cells fall into shells a–d, increasing increasingly farther away from the niche and with increasing probability of differentiation and triggering into the cycle. [From Potten *et al.* (1979), by permission of *Biochimica et Biophysica Acta*.]



very slowly, spending long periods of time in G_0 ; they have pleuripotency and can greatly accelerate division, for example when the tissue is injured. Each division of a stem cell produces only one daughter stem cell; the other daughter cell is pushed out of the niche into the front of a series of positions of decreasing multipotency and increasing differentiation. It is these daughter cells pushed out of the niche that produce cells to replenish the dying blood, intestinal, and epithelial cells. Figure 19.29, taken from Potten *et al.* (1979), shows a section through a mouse small intestinal crypt. Cell position 1 is the “anchored” stem cell.

What sets the stem cells apart from other dividing cells is not fully known. Recent evidence suggests that it is the microenvironment at the niche (or focal point) that decides which daughter cell of the dividing stem cell takes the place of the parent stem cell (Trentin, 1976). The situation reminds one of the society of bees, in which a fertilized bee egg when given a special niche develops into a queen bee, but when raised outside the special niche develops into a worker bee.

Figure 19.30, also taken from Potten *et al.* (1979), illustrates a more specific scheme for cell replacement.

One recalls Gurdon's successful development of an adult frog from an enucleated frog egg into which the nucleus of a fully differentiated intestinal epithelial cell of a feeding tadpole had been transplanted. Could these successful transplants be from stem cell nuclei, and the unsuccessful ones from non-stem-cell nuclei? Unfortunately our knowledge about the stem cell is mostly derived from mammalian tissues. However, if one assumes that the stem cell generalization can directly apply to frog tissues, then clearly the less differentiated cells at the bottom of the intestinal folds (or trough cells) are more likely to contain the stem cells than the more differentiated cells at the top of

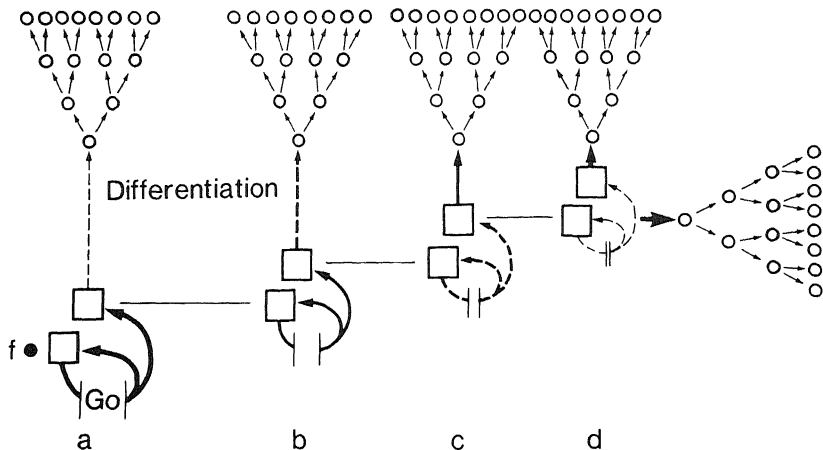


FIGURE 19.30. General scheme for cell replacement in the various tissues according to Potten *et al.* The stem cells at a hypothetical focal point (*f*) have a polarity imposed on them by the local tissue microenvironment which may result in an ability to selectively segregate older and newer DNA strands. In order to achieve this and possibly perform other genetic housekeeping tasks (e.g., repair of damage in the older strands) they require prolonged periods in G_0 . By virtue of their position they are shielded from differentiation initiation and thus have a low differentiation probability and a high self-replicative probability. Only one daughter at each division remains at the focal point; the other daughter is "pushed" into the first of a series of shells (*b-d*) of declining stem cell quality and increased differentiation probability. The length of the lines between cells and the length of the self-replicative lines are indicative of the cell cycle duration (G_0 duration); the thickness of the lines is an indication of probability. The boxes are stem cells and the circles are transit cells. Under normal steady-state conditions all stem cells but the "anchored" foci and stem cell will ultimately be lost by displacement and differentiation. [From Potten *et al.* (1979), by permission of *Biochimica et Biophysica Acta*.]

the folds (or crest cells) (Fig. 19.29). Surprisingly, McAvoy *et al.* (1975) found that the nuclei of crest cells and trough cells from adult *Xenopus* intestinal epithelium had similar developmental potentials when transplanted into enucleated mature *Xenopus* eggs. Both occasionally develop into feeding tadpoles.

The knowledge about stem cells also emphasizes that in an adult animal there is no totipotent cell, only multipotent stem cells which are themselves somewhat differentiated. However, since even adult fully differentiated nuclei of brain and red cells can become totipotent in the mature egg cytoplasm, perhaps one can argue that, just as the microenvironment at the niche specifies the multipotency of the stem cells, the microenvironment of the egg cytoplasm confers totipotency on any normal nucleus.

19.7. Some Molecular Mechanisms According to the AI Hypothesis

19.7.1. Migration of Proteins (and RNA) between the Nucleus and the Cytoplasm

There is now a wide range of evidence that traffic of proteins and RNA between the nucleus and the cytoplasm accompanies many major events associated with protein synthesis, chromosomal condensation, and the cell cycle (Goldstein, 1974). The most

dramatic example occurs during the early M phase, when the nuclear envelope fragments and releases into the cytoplasm a large quantity of nuclear macromolecules. These materials then return to the new daughter nuclei in later telophase and early interphase. The promptness and completeness of this return traffic is illustrated by the data of Prescott and Goldstein (1968). At least 90% of the nuclear proteins of the amoeba leave the nucleus during late prophase and all of these return to the postmitotic nucleus (Fig. 19.31). Most if not all nuclear proteins, including the histones, are synthesized in the cytoplasm (Pederson and Robbins, 1970; Goldstein, 1970) and enter the nucleus after completion of their synthesis.

The ability of the oocyte GV to accumulate proteins selectively has been investigated by Gurdon (1970) and W. M. Bonner (1975). Recently, de Robertis, Longthorne, and Gurdon (1978) cultured oocytes in [¹⁴C]-amino acid mixtures for 24 hr, after which the GV were manually isolated from the cytoplasm. A high-resolution, two-dimensional gel electrophoresis allowed identification of the nuclear and cytoplasmic proteins. A soluble preparation of [³⁵S]methionine-labeled GV protein was then injected into the oocyte cytoplasm in an amount equal to $\frac{1}{20}$ of the volume of a GV, and the cell was incubated for 24 hr at 10°C and then dissected. The separated GV and the cytoplasm were analyzed for the distribution of radioactivity in the protein fractions. The results show that the nuclear proteins are rapidly concentrated in the nucleus and not detectable in the cytoplasm. Actin, which is normally present in both the cytoplasm and the nucleus, becomes distributed in both phases. The autoradiograph of the injected egg shows uni-

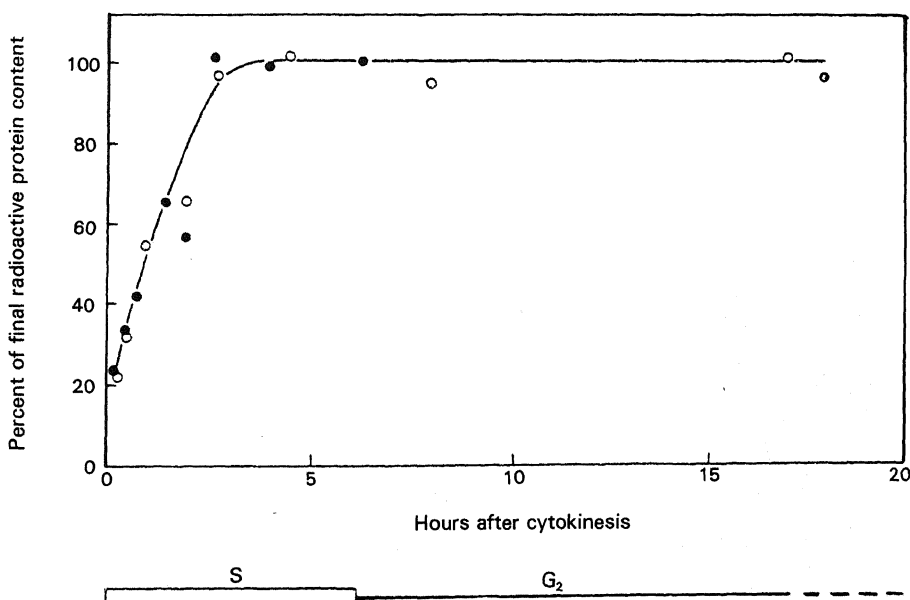


FIGURE 19.31. Return of labeled proteins to the nucleus of amoeba after mitosis. At least 90% of the nuclear proteins leave the nucleus during late prophase, and all of these return to the postmitotic daughter nuclei. Some protein has returned to daughter nuclei by the time of the first measurements in this experiment. [From Prescott and Goldstein (1968), by permission of *Journal of Cell Biology*.]

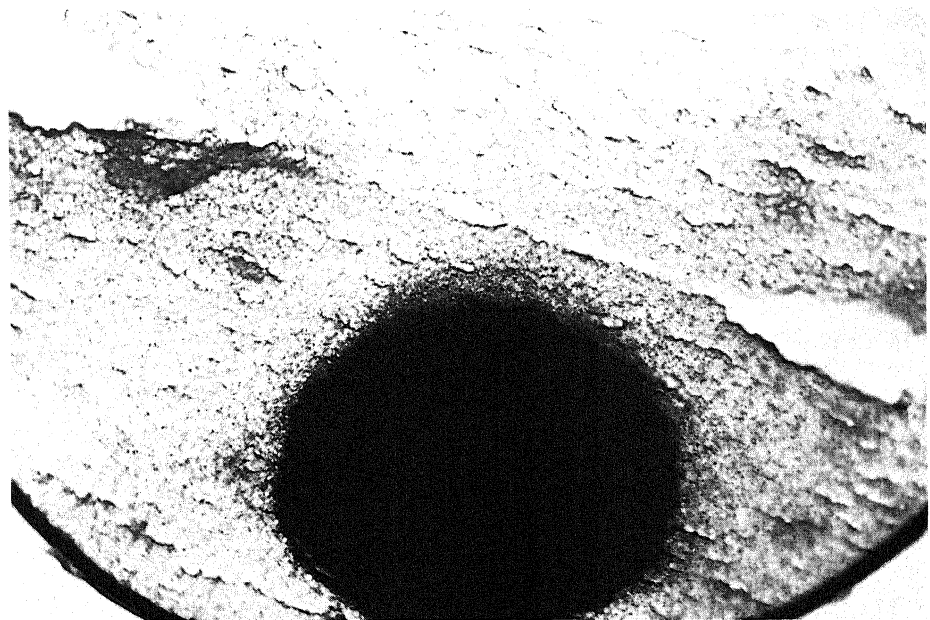


FIGURE 19.32. Autoradiograph of a sectioned *Xenopus laevis* oocyte the cytoplasm of which had been injected 24 hr previously with a soluble preparation of [³⁵S]methionine-labeled GV proteins. [From de Robertis *et al.* (1978), by permission of *Nature*.]

form distribution of radioactivity in the GV (Fig. 19.32). This led de Robertis *et al.* to conclude that most of the radioactivity is free in the nucleus and not bound to chromosomes and nucleoli. From these findings, the authors concluded that nuclear proteins contain in their molecular structure a signal that enables them to accumulate selectively in the nuclear compartment. Actin, on the other hand, lacks such a signal.

The AI hypothesis considers that the selective accumulation and exclusion of large macromolecules depends on the same general principle as does that of small molecules and ions: a combination of selective binding and variable exclusion from ordered cell water (Ling, 1969a). The distribution of the protein in a large or a small part of a living cell also can be described by the general equation for solute distribution in living cells [equation (11.5)]. More specifically, I suggest that all the proteins accumulate in the nucleus because each one of them is specifically adsorbed or complexed to the other macromolecular components of the nucleus. On the other hand, actin is found in both the cytoplasm and the nucleus because binding sites exist in both places.

The low level of nuclear proteins in the cytoplasm is attributed to a lack of such binding sites and the fact that cytoplasmic water exists in the state of polarized multi-layers, which exclude large molecules in general. There is evidence that water in the nucleus is less "polarized," with a higher *q*-value for sucrose* (Paine *et al.*, 1981). If this conclusion is correct, then theoretically a larger amount of protein can exist in the free state in the nucleus than in the cytoplasm, as de Robertis *et al.* suggested.

*This conclusion is now in serious doubt. See footnote on page 331.

This interpretation of protein distribution is more in harmony with the view of Feldherr and Pomerantz (1978) discussed in Section 19.2.3. It also agrees with the knowledge that histones are bound strongly, specifically, and cooperatively to DNA (Renz *et al.*, 1977), and that many of the nuclear histone and non-histone proteins play essential structural and regulatory roles (Pardee *et al.*, 1978).

Why is the nuclear autoradiograph reproduced in Fig. 19.32 so uniformly dark? I think this can be explained perhaps most easily by the more random distribution of DNA and interphase chromatin throughout the nucleoplasm, by the sections not being thin enough, and by ^{35}S being a fairly strong β emitter (0.167 MeV in comparison with an energy of β emission of ^1H of 0.018 MeV). In any case, with a nuclear membrane readily permeable to proteins with molecular weights of 120,000 daltons, it is difficult to conceive of a pump mechanism to keep these labeled nuclear proteins from staying in the cytoplasm into which they were injected (Paine *et al.*, 1981).

The nucleus does not, however, provide permanent binding sites for all its proteins and RNAs. Rather, the change in binding of these components must be the major event underlying the control mechanism. After all, the work of Benbow and Ford and of Jazwinski *et al.* has shown that it is a cytoplasmic protein that initiates DNA replication, and this clearly must involve its migration into the G_0 phase nucleus and specific binding to the specific DNA-protein complex.

19.7.2. Nuclear Swelling during DNA Replication

Gurdon (1964) showed that, when only one intestinal cell nucleus is transplanted into an egg, *it may swell 40 times in 40 min! Liver nuclei may increase in volume 25 times and brain and blood cell nuclei 60 times in 90 min* (Fig. 19.33). Figure 19.34, also taken from C. F. Graham *et al.* (1966), shows a close correlation between swelling and DNA synthesis. In those cases where some of the injected nuclei failed to swell, they remained unlabeled with $[^3\text{H}]$ thymidine. What could be the molecular mechanism involved in this enormous swelling?

The eggs were cultured in Elsdale's modified Barth solution (Table 19.2), which is isotonic with frog plasma; the adult intestinal, blood, liver, and brain cells were all freshly dissected from the frog. Therefore, transfer to egg cytoplasm should, in terms of the conventional membrane theory, involve no change in the osmotic activity of the environment.

The AI hypothesis offers the following explanation for the nuclear swelling:

1. The primary cause of the nuclear swelling is an increase in the amount of polarized water.
2. The cause of the increase in the amount of polarized water is the dissociation of DNA from nuclear proteins.
3. The dissociation of DNA and nuclear proteins may occur because of the loss of one polypeptide or the interaction with another polypeptide that functions as a cardinal adsorbent, presumably like those isolated by Benbow and Ford and by Jazwinski *et al.* and mentioned in Section 19.5.2.3.
4. The fixed cationic and anionic sites previously involved in DNA-protein and protein-protein salt linkages adsorb anions and cations that are present in the

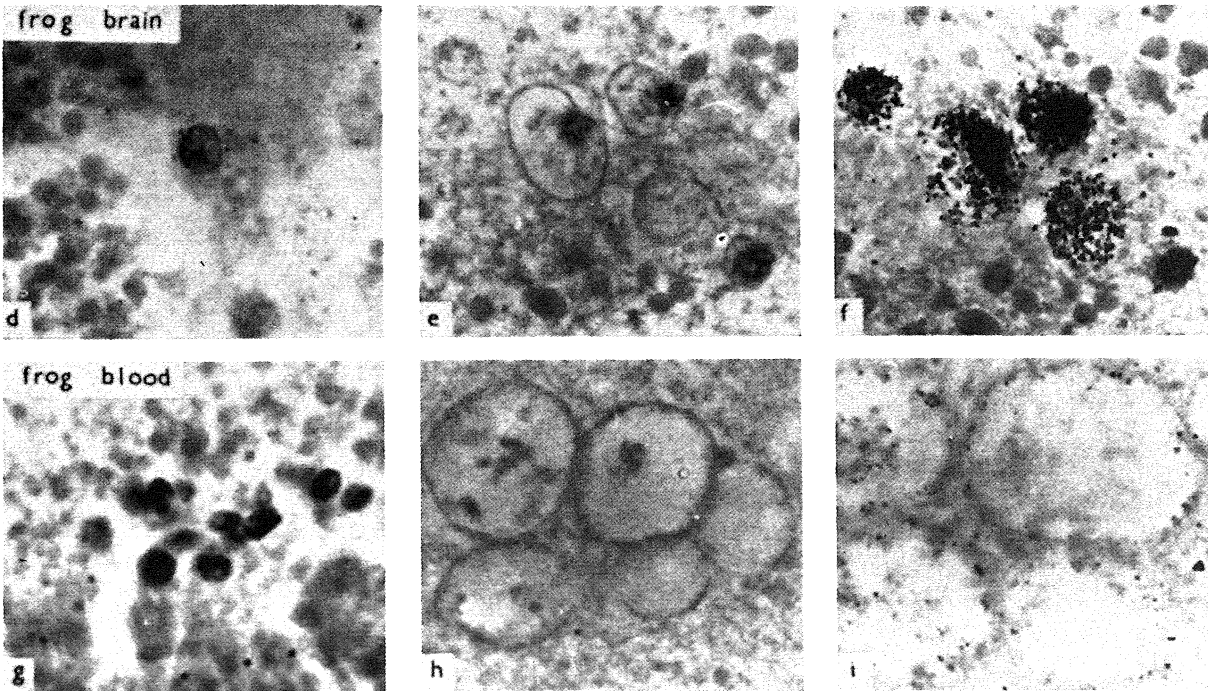


FIGURE 19.33. Nuclei from adult cells in sectioned eggs of *Xenopus laevis*. Left-hand column: Eggs fixed 30 min after injection of nuclei. Middle column: Eggs fixed 90 min after injection of nuclei. Right-hand column: Autoradiographs of the same nuclei shown in the middle column. The kinds of adult nuclei are indicated on the figure, and in each case these nuclei were considerably swollen after 90 min in egg cytoplasm. [From C. F. Graham *et al.* (1966), by permission of *Developmental Biology*.]

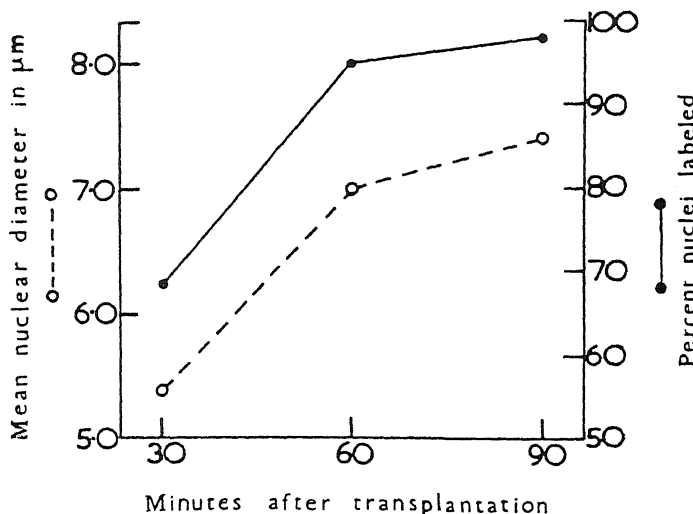


FIGURE 19.34. Increase in nuclear volume and in the proportion of nuclei labeled after injection of a crude preparation of *Xenopus* brain nuclei into unfertilized *Xenopus* eggs. [From C. F. Graham *et al.* (1966), by permission of *Developmental Biology*.]

cell. Moreover, salts present in the cell may in some cases potentiate the tendency to breakage of the macromolecular salt linkages, in a manner similar to that described in relation to the KCl- and NaCl-dependent swelling described in Chapter 13.

Known facts that are in harmony with this scheme include the following:

1. Isolated proteins, including histones, can hydrate deep layers of water (see Fig. 6.14).
2. DNA can hydrate deep layers of water and water so oriented has a low q -value for Cs^+ salts (see Section 9.2.2).
3. DNA and proteins (e.g., histones) interact to create a relatively dehydrated complex.
4. DNA (and protein) can be isolated from these complex nucleoproteins by an aqueous concentrated solution of NaCl.

Liberation of DNA from its association with histone and nonhistone proteins, and hence its repressed state, sets the stage for DNA replication, as discussed earlier in regard to polytene chromosome puffing, a phenomenon which also represents active RNA polymerase activity associated with intense hydration (Chapter 18).

19.8. Amphibian Metamorphosis

So far the subject matter of this chapter has centered around the development of frog eggs from maturation to the stage of feeding tadpoles. However, amphibian devel-

opment does not stop at the stage of feeding tadpoles but includes another major event: metamorphosis, the rapid transformation from an aquatic, herbivorous, tailed tadpole with no legs to a terrestrial, carnivorous, tailless, four-legged frog. In salamanders and newts (urodeles), metamorphosis converts the larval form to the terrestrial elf form, which lasts some 2–3 years before undergoing a second metamorphosis and returning to water in the final adult form (Wald, 1960).

19.8.1. Thyroid Hormones

Gudernatsch (1912) discovered that feeding tadpoles mammalian thyroid tissue induces precocious metamorphosis. When this occurred in young tadpoles, very tiny froglets were produced. In the normal life history of a frog, certain environmental changes are perceived by the nervous system, which then stimulates the anterior pituitary gland to produce thyrotropic hormone (TSH). TSH in turn activates the dormant thyroid gland to produce two thyroid hormones—L-thyroxine and 3,3,5-triiodo-L-thyronine (T_3)—which then act directly on the cells.

Metamorphosis is a many-faceted phenomenon. In one aspect, the growth of new tissues and new organs is akin to differentiation of embryonic tissues and must therefore involve sequential transcription and translation of genes. In another aspect, perfectly well developed and functional tissues must be eliminated or replaced by different kinds of tissues. Only two of the most outstanding examples of tissue replacement and elimination will be presented here.

19.8.1.1. Replacement of the Larval Visual Pigment, *Porphyropsin*, by the Adult Visual Pigment, *Rhodopsin*

Wilt, Ohtsu, and their co-workers (Wilt, 1959; Ohtsu *et al.*, 1964) showed that only the eye which has been treated with thyroxine undergoes visual pigment change. Thus thyroxine acts directly on the target cells.

19.8.1.2. Tail Resorption

Kollros (1942) discovered that only the part of the tadpole tail to which thyroxine was applied underwent lysis. Figure 19.35 shows that T_3 -induced regression of amputated tails of *Rana temporaria* tadpoles in organ cultures (c,d) depends on RNA synthesis. Thus actinomycin, which inhibits RNA synthesis, stops tail resorption. The author of this work, Tata (1966, 1971), provided evidence that this dependence on RNA synthesis is manifested by the production of a series of hydrolases whose activities cause the breakdown of the muscular tail tissue. Thus not only the growth of a new structure but also the destruction of an old structure depend on new protein synthesis.

19.8.2. Prolactin

In Section 18.2.1.1 we discussed the pair of insect hormones, ecdysone and juvenile hormone, and how juvenile hormone modifies the competence of target organs to respond to ecdysone during metamorphosis. In recent years, it has been discovered that in

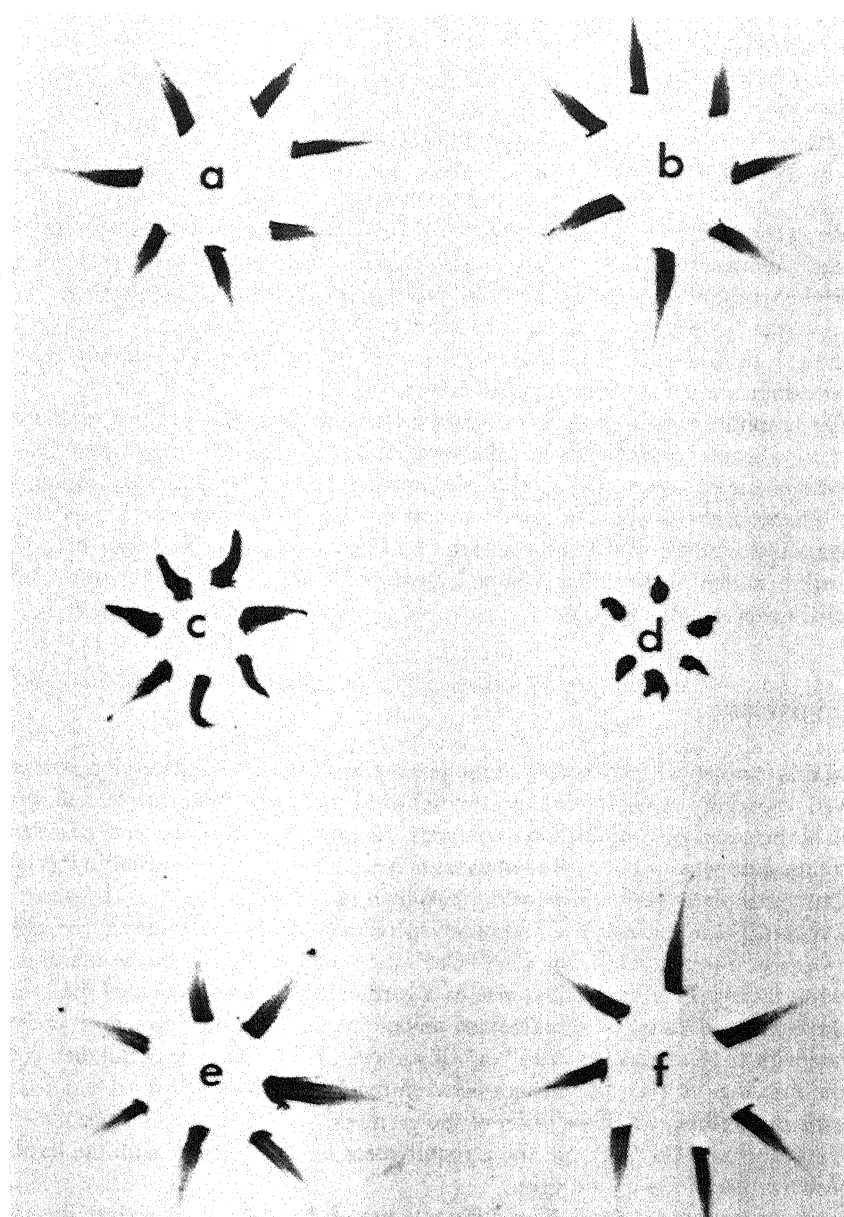


FIGURE 19.35. Triiodothyronine (T_3)-induced regression of amputated tails of *Rana temporaria* in organ culture. (a) Control samples on the first day of culture; (b) control, after 8 days of culture; (c) on the fourth day of culture in medium containing $1 \mu\text{g} T_3/\text{ml}$; (d) on the eighth day of culture with T_3 ; (e) the same as (c) but with $2.5 \mu\text{g}$ actinomycin D/ml; (f) the same as (d) but with $2.5 \mu\text{g}$ actinomycin D/ml. [From Tata (1966), by permission of *Developmental Biology*.]

amphibian metamorphosis the thyroid hormone is also "antagonized" by a "juvenilizing" factor, prolactin.

Salamanders and newts undergo primary metamorphosis in response to a hypothalamus–pituitary–thyroid chain like that in the frog and other anurans (Etkins, 1964). The land-dwelling elf form, however, undergoes a second metamorphosis, described as *water drive*, in response to prolactin, a pituitary hormone that prepares the animal to return to its watery environment as an adult (W. C. Grant and Grant, 1958). W. C. Grant and Cooper (1965) discussed the behavior of the adult newt, *Diemictylus*, in response to thyroxine and prolactin when this animal was kept in cages providing both an aquatic and a terrestrial environment. Animals injected with thyroxine preferred the terrestrial environment; those injected with prolactin preferred the aquatic environment. Thus, apparently just as thyroxine affects the amphibians' ability to adapt to a terrestrial environment, prolactin affects their ability to assume an aquatic habitat for, among other purposes, their annual spawning, which occurs only in water.

The amphibian primary and secondary metamorphoses are matters of great interest and significance to biologists because they represent nature's ontogenetic replay of the phylogenetic evolution that marked the invasion of land by originally aquatic life forms. There is also a personal aspect to this interest, as the metamorphosis of frog tadpoles was the subject of the first research that I undertook under Professor P. S. Tang while still a student in Kunming China. I await with eagerness more important developments in this tantalizing field.

19.9. Summary

In this chapter selected aspects of the phenomena of growth and development were reviewed, especially in regard to their physiological correlates and controls, and, in the context of the association–induction hypothesis, their modulation by cardinal adsorbents. Some of the data were reinterpreted in terms of mechanisms outlined earlier in this book.

One example is germinal vesicle breakdown in amphibian oocytes. Progesterone acts as a cardinal adsorbent, itself adsorbed specifically onto surface sites at the animal pole, to cause internal release of Ca^{2+} . Ca^{2+} then induces release of the maturation-promoting factor. This factor then acts as a cardinal adsorbent to change the *c*-value (i.e., the electron density) of specific fixed anionic sites so that they no longer prefer to associate with fixed cations but with Na^+ . If sufficient Na^+ is present, it can then potentiate the breakage of the salt linkages between the fixed anions and fixed cations, and this leads to swelling and dissolution of the germinal vesicle. A parallel phenomenon, which also includes Ca^{2+} release and a requirement for Na^+ , occurs with the fertilization or activation of sea urchin eggs.

Another example is amphibian differentiation. It has been known since the 1930s and 1940s that the differentiation of the blastula and gastrula can be manipulated by different salt solutions, and that differentiation into a specific tissue may be induced by a variety of apparently unrelated substances. Many years ago, Barth and Barth developed a theory, which is in general consistent with parts of the association–induction hypothesis, according to which release of cations from fixed sites and binding at new ones serve to promote specific tissue differentiation.

A number of phenomena—including germinal vesicle breakdown, the swelling of transplanted nuclei, and the puffing of polytene chromosomes—have as an underlying mechanism an increased polarization of water by macromolecules released from salt linkages with other macromolecules. Related to this is the concept of specific binding sites for specific nuclear proteins.

From the standpoint of the association-induction hypothesis, it is suspected once again that the common elements needed to understand growth and development, as well as the mechanism of protein synthesis in general, are the modulation of macromolecular salt linkages, and the concept of the coherent nature of protoplasm and its ability to be triggered into one or the other metastable state. In the following chapter, it will be suggested that this concept of the existence of alternative metastable states of the living cell may help in understanding the nature of cells that proliferate abnormally to form cancers.

Cancer

Cancer is one of the major sets of diseases whose control has on the whole eluded medical science. I have chosen to conclude this book with a brief discussion of cancer, and have done so for two basic reasons: First, it logically follows the previous chapter on growth and development. Second, I believe that an understanding of the cancer cell requires a correct knowledge of cells in general, and therefore a correct theory of cellular physiology.

20.1. General Theories of Cancer

20.1.1. The Somatic Mutation Theory: Historical Background

Long before the precise role of DNA in genetics had been elucidated, the idea was suggested that mutation, in the classical Darwinian sense, caused cancer (Boveri, 1914; Lockhart-Mummery, 1934; Haddow, 1937, 1938). This theory was not widely accepted. Most investigators writing on the subject believed that cancer was due not to mutation but to anomalous differentiation (Haldane, 1934; Needham, 1950) or viral infection (Oberling, 1952). The phenomenal progress made in the field of microbial genetics, however, paved the ground for a change of opinion and an intense growth in the popularity of the somatic mutation theory, which has by now become much specified in the sense that DNA is seen as the focal point of the defect (Burnet, 1957, 1974).

One of the pieces of evidence supporting the somatic mutation theory is the observation that chromosomal disorder is a regular feature of cancer cells (Knudsen, 1973). Another is the increasing incidence of cancer with aging. It is interesting that a little while ago this very age dependence was cited as evidence against the somatic mutation theory (Oberling, 1952). However, proponents of the somatic mutation theory now see the need for multiple lesions in carcinogenesis that would accumulate with age (Burnet, 1957, 1974).

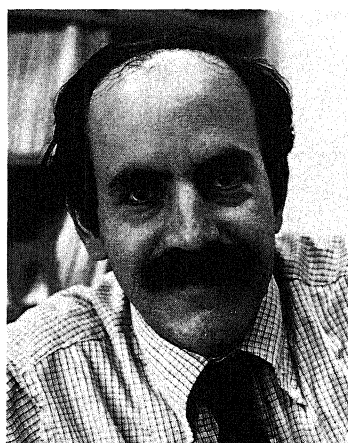
Perhaps the single most convincing set of evidence in favor of the somatic mutation theory is the fact that most strong carcinogens are also mutagens. Thus out of 174 car-

cinogens tested, 90% (156) were shown to be mutagens (McCann *et al.*, 1975) as demonstrated by the *Salmonella* test (Ames *et al.*, 1973). I suspect it is this kind of evidence that led reviewer Watson (1977, p. 646) to state, "There thus seems little doubt that much if not most carcinogenesis is the result of change in DNA"—even though Watson in the same review (1977, p. 644) remarked that there is no evidence for somatic mutation *per se*. I have pointed out this apparent contradiction because it probably reflects the somewhat troubled state of mind of many on this issue at the time (see Cairns, 1975).

20.1.2. Dramatic Recent Confirmation of the Somatic Mutation Theory

However, stimulated by the findings of Ames and McCann just mentioned, dramatic confirmations of the single-point somatic mutation theory have been reported in the last few years from studies of the effects of externally introduced DNA derived from cancer cells. Many capable scientists took part in this adventure, but Robert A. Weinberg (Weinberg, 1981), G. M. Cooper (1982), M. Wigler (see Goldfarb *et al.*, 1982), Mariano Barbacid (see Reddy *et al.*, 1982), and C. Shih (Shih *et al.*, 1979) played major roles.

Avery, MacLeod, and McCarty (1944) first successfully introduced biologically active DNA from one kind of bacteria into another. The method was successfully applied to mammalian cells (M. Hill and Hillock, 1971). In the recent studies of tumor DNA, the technique of F. L. Graham and van der Eb (1973) was often employed: In this method, the DNA is introduced in the form of a calcium phosphate coprecipitate into a monolayer culture of a nonneoplastic cell line (e.g., mouse fibroblast NIH-3T3). A relatively small percentage of the cancer DNAs produced a change in the morphology of the cell culture. In these successful cases, foci developed, with cells becoming hyper-refractile and growing over each other, thereby displaying a loss of contact inhibition. When cells in these foci were isolated and grown in mass culture, their DNA could also induce similar foci in other NIH-3T3 cell cultures.



Robert A. Weinberg



Mariano Barbacid

This type of study led to the belief that tumor cells contain *oncogenes*, i.e., genes that control cancer development. Many oncogenes have since been found (see Cooper, 1982). It was soon discovered that the oncogenes have their counterparts in the normal genome of the NIH-3T3 cells. These parts of the normal gene have been referred to as proto-oncogenes. Preliminary efforts could not detect any major differences between oncogenes and proto-oncogenes. Intensive efforts were then made to determine what, if any, small genetic alterations might be involved in the activation of the proto-oncogenes. In the following account I shall concentrate on the work of Reddy, Reynolds, Santos, and Barbacid (1982) in regard to the T24 human bladder carcinoma oncogen.

To find out which part of the gene had undergone alterations, Reddy *et al.* constructed a series of DNA fragments or plasmids in which the different parts of the normal gene were substituted by their oncogenic counterparts and vice versa. Figure 20.1 describes these plasmids and their respective transforming activities. From those plasmids with positive activity, the conclusion was drawn that the altered region in the oncogene is rather small and is restricted to a fragment ($\text{Sac I-K}_{pn}\text{ I}$) having a total of only 900 bases [or 0.9 kilobase (KB)], as illustrated in the bottom figure.

These authors then determined the nucleotide sequence of the 0.9-kb $\text{Sac I-K}_{pn}\text{ I}$ DNA fragment of the T24 oncogene and compared that with its normal homologue. The results are shown in Fig. 20.2. Out of 900 bases examined, there was only a single (nucleotide) difference (indicated in the box)—a clear indication of the involvement of a single-point mutation. More precisely, a guanosine residue in the normal allele was substituted by a thymidine. From the base sequence obtained the predicted amino acid sequence of the first functional segment or exon of the protein product was derived. Figure 20.3 shows that the normal glycine residue at position 12 of the p21 protein coded by the normal proto-oncogene (or, more specifically, the normal human *c-has/bas-1* gene) has been substituted by a valine residue. The rest of the proteins are identical. Figure 20.3 also shows that, in two kinds of mouse sarcoma viruses that also have trans-

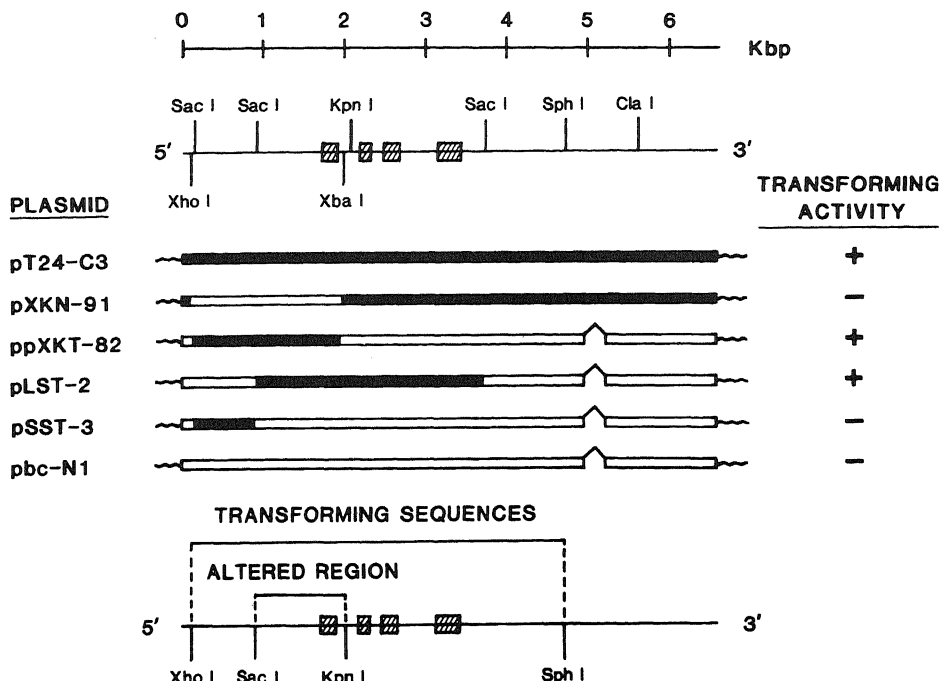


FIGURE 20.1. Location of the region of the *c-has/bas-1* gene that underwent the genetic alterations that led to the activation of the T24 oncogene. Hybrid plasmids containing sequences derived from pT24-C3 (■) and pbc-N1 (□) were tested for their biological activity. pT24-C3, pXKT-82, and pLST-2 transformed NIH-3T3 cells in transfection assays, with specific transforming activities. In contrast, pbc-N1, pXKN-91, and pSST-3 exhibited no transforming activity. The hatched boxes in the restricted endonuclease map shown in the top of the figure represent the predicted exons of the T24 oncogene and its normal homologue, the *c-has/bas-1* gene. Deletions (Δ) and plasmid sequences (~~) are also indicated in the diagram. [From Reddy *et al.* (1982), by permission of *Nature*.]

forming properties, displacements of the same glycine by other amino acids also occur at position 12 of the p21 transforming protein. The authors concluded that it is the loss of the specific glycine residue that has activated the proto-oncogene.

20.1.3. The Maldifferentiation Theory

That cancer is the result of faulty differentiation was proposed a long time ago (Fischer-Wasels, 1927; Haldane, 1934; Needham, 1950). In more recent years, with further major refinements, the statement has been reiterated by Pierce (1967), Markert (1968), Mintz (1978), Mintz and Fleischman (1981), and others. Early embryologists could cite much significant evidence in favor of this theory. One enlightening discovery from the Cambridge school was that synthetic carcinogens can also act as primary evocators in normal development of amphibian embryos (Needham, 1950; Waddington, 1938). Figure 20.4 reproduces the results of Shen (1939). The carcinogen 1:2:5:6-dibenzanthracene-endo- α - β -succinate implanted in the blastocoel of a frog embryo

FIGURE 20.2. Comparative sequence analysis of the Sac I-Kpn I DNA fragment of the T24 oncogene and its normal human homologue, *c-has/bas-1*. The upper line shows the sequence of the T24 oncogene. The corresponding sequence of the Sac I-Kpn I DNA fragment of *c-has/bas-1* has also been determined and found to be identical to that of the T24 oncogene with the exception of the nucleotide located at position 653, where a G instead of a T was detected. [From Reddy *et al.* (1982), by permission of *Nature*.]

induces neural tubes in more than 40% of embryos at an optimal concentration of 0.0125 μg per embryo. The existence of an optimum argues against the effect being produced by cell injury since injury by noxious agent as a rule increases with increasing concentration of the agent.

Three sets of experimental findings that provide some of the evidence that an epigenetic mechanism creates malignancy will be mentioned. The evidence relies essentially on the ability of certain cancers to be induced to form normal tissues.

20.1.3.1. Transformation of Plant Teratoma Cells into Normal Tobacco Plants (Braun)

Plant galls originate from the abnormal development of plant meristematic tissues as a result of injury sustained from insect parasites (for early work, see Ross and Hedicke, 1927; Needham, 1950). The typical crown gall tumor of plants resembles a malignant animal tumor. It represents permanently altered cells which reproduce true to type.

	1	2	3	4	5	6	7	8	9	10	11	12	13	14	15	16	17	18	19	20	21	22	23	24	25	26	27	28	29	30	31	32	33	34	35	36	37
Human c-bas/ras^H	M	T	E	Y	K	L	V	V	V	G	A	G	G	V	G	K	S	A	L	T	I	Q	L	I	Q	N	H	F	V	D	E	Y	D	P	T	I	E
T24 oncogene	M	T	E	Y	K	L	V	V	V	G	A	V	G	V	G	K	S	A	L	T	I	Q	L	I	Q	N	H	F	V	D	E	Y	D	P	T	I	E
BALB-MSV	M	T	E	Y	K	L	V	V	V	G	A	K	G	V	G	K	S	A	L	T	I	Q	L	I	Q	N	H	F	V	D	E	Y	D	P	T	I	E
Harvey-MSV	M	T	E	Y	K	L	V	V	V	G	A	R	G	V	G	K	S	A	L	T	I	Q	L	I	Q	N	H	F	V	D	E	Y	D	P	T	I	E
Kirsten-MSV	M	T	E	Y	K	L	V	V	V	G	A	S	G	V	G	K	S	A	L	T	I	Q	L	I	Q	N	H	F	V	D	E	Y	D	P	T	I	Q

FIGURE 20.3. Predicted amino acid sequence of the first exon of the normal human *c-has/bas-1* gene and its transforming allele, the T24 oncogene. Comparison with the first 37 amino acids predicted for the p21 proteins coded for by Harvey-MSV and Kirsten-MSV. The letter code for the amino acids is A, Ala; D, Asp; E, Glu; F, Phe; G, Gly; H, His; I, Ile; K, Lys; L, Leu; M, Met; N, Asn; P, Pro; Q, Gln; R, Arg; S, Ser; T, Thr; V, Val; and Y, Tyr. [From Reddy *et al.* (1982), by permission of *Nature*.]

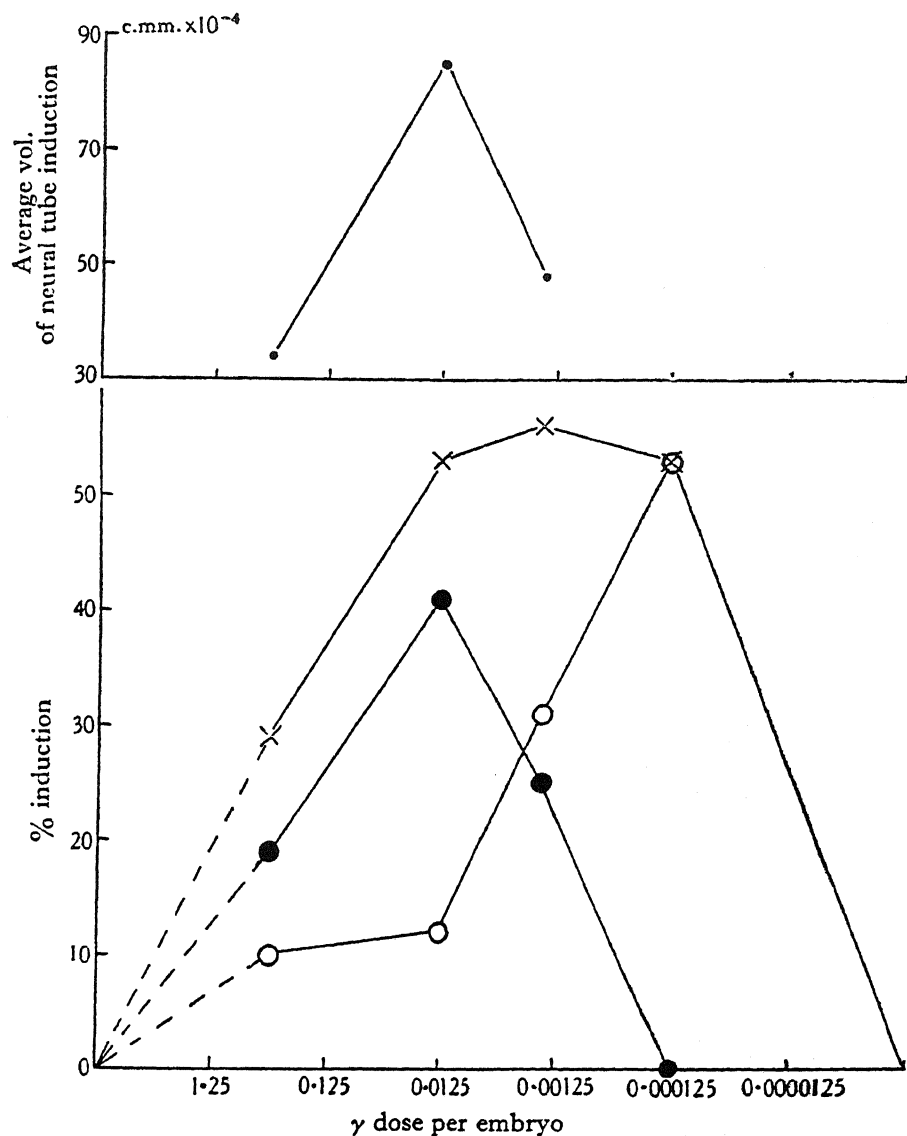


FIGURE 20.4. Effect of the carcinogen 1:2:5:6-dibenzanthracene-endo- α - β -succinate implanted in the blastocoel of a frog embryo. Relation between dosage and induction frequency (bottom) and size (top). X, All inductions; ●, neural tube induction; ○, palisade induction. [Figure taken from Needham (1950), data of Shen (1939), by permission of *Journal of Experimental Biology*.]

Braun argued that some as yet uncharacterized cytoplasmic entity or agent is responsible for the cell changes underlying the tumorous state of the crown gall disease, and that this cytoplasmic agent is self-duplicating but can be eliminated if the cells are forced to multiply rapidly, thereby diluting it. Since plant meristematic cells divide much more frequently than most crown gall tumor cells, it was argued and then experimen-



FIGURE 20.5. A normal tobacco plant of the type obtained by forcing morphologically abnormal shoots derived from teratoma tissue of single-cell origin into very rapid growth by means of a series of graftings to healthy plants. A complete recovery from the tumorous state has resulted from this procedure. [Photograph by J. A. Carlile. From Braun (1959), by permission of *Proceedings of the National Academy of Sciences*.]

tally confirmed that tumor buds forced into rapid growth by a series of grafts to healthy plants would gradually recover and become normal plants (Braun, 1953).

Braun's work was criticized on the ground that the crown gall teratoma tissue may not represent a single cell type but a stable mixture of normal and tumor cells (Gutheret, 1955). This question was resolved by Braun (1959) using a clone of tumor cells developed from a single tumor cell. Of 267 single teratoma cells isolated and raised *in vitro*, 5% grew and developed organized structure. Teratoma tissue of single-cell origin was grafted onto a second healthy plant and so on. Eventually the graft developed into normal plants (Fig. 20.5). Braun concluded that "these findings make somatic mutation at the nuclear gene end appear unlikely," believing that the findings favored an epigenetic origin of the tumor state.

20.1.3.2. Transformation of Frog Cancer Cells into Normal Swimming Tadpoles (McKinnel, Deggins, and Labat)

King and McKinnel (1960) first showed that nuclei of frog renal tumor cells when transplanted into an enucleated frog egg cell could develop into tadpoles. Their initial results were marred by a low rate of success and hence the possibility that the tadpoles were not guided by the tumor nuclei but resulted from inadvertently retained genetic material. However, a genetic marker for the tumor nuclei was obtained by incorporating the technique of creating frog tumors at will (Tweedell, 1967) and the technique of producing triploid embryos with hydrostatic pressure (Dasgupta, 1962). Thus armed, McKinnel, Deggins, and Labat (1969) implanted triploid frog tumor cell nuclei into diploid enucleated frog eggs and produced normal triploid swimming tadpoles (Fig. 20.6). The results again substantiated the authors' view that the development of the tumor involves an epigenetic mechanism.

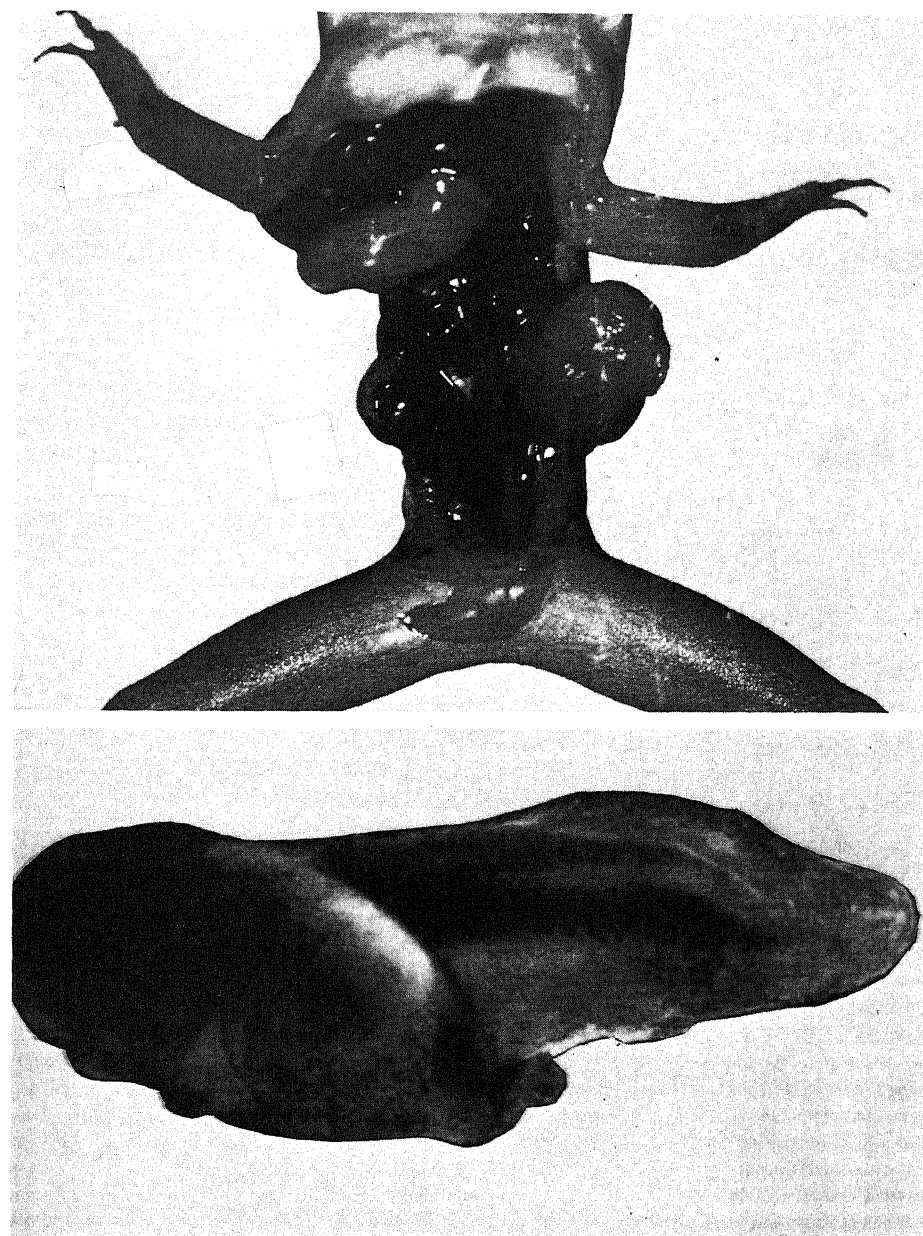


FIGURE 20.6. Formation of swimming triploid tadpole (B) by the implantation of nuclei from triploid renal tumor cells (A) into diploid activated and enucleated eggs. [From McKinnel *et al.* (1969), by permission of *Science*.]

20.1.3.3. Normal Mosaic Mice from Malignant Teratocarcinoma Cells (Mintz et al.)

Some teratocarcinomas or embryonic carcinomas of mice have been converted into an ascites form. In this form they are called "embryoid bodies" and consist of a "core" and a yolk sac epithelial "rind". When single cells isolated from the core are injected subcutaneously, they develop into tumors containing various types of chaotic tissue masses. Mintz and her co-workers (Mintz and Illmensee, 1975; Mintz, 1978; Mintz and Fleischman, 1981), in an elegant and interesting experiment, produced proof that these tumor cells possess complete developmental totipotency.

Core cells from "embryoid bodies" from solid teratomas of black 129 mice were microinjected into the blastocoel of early embryos (see Fig. 19.9) isolated from

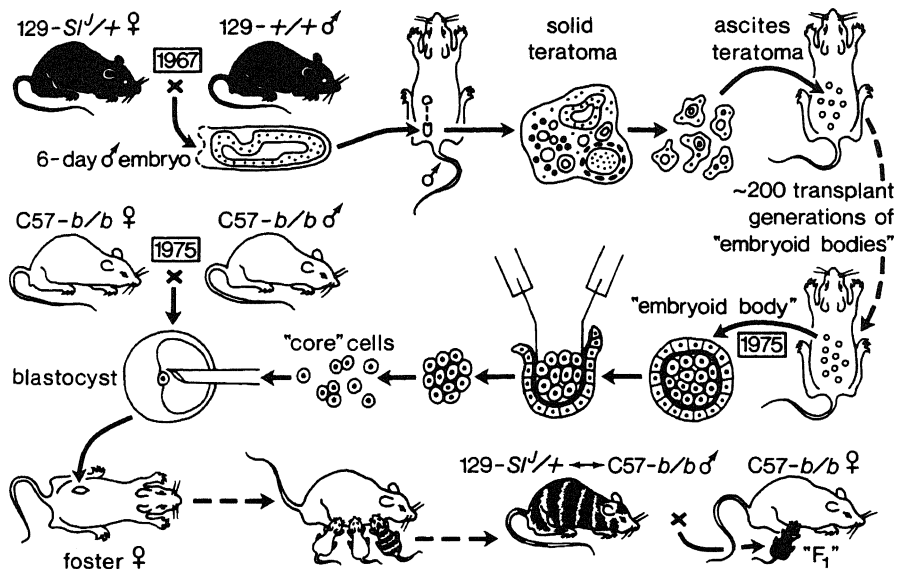


FIGURE 20.7. Eight-year history of the Mintz-Illmensee experiment, starting at the upper left. The OTT 6050 teratoma was experimentally produced in 1967 from a 6-day chromosomally male (X/Y) embryo of 129 strain (129/Sv Sv^l C P) agouti black parents. [Retrospectively, from the coat of mosaic mouse no. 1, this embryo and its mother were found to have had the steel ($Sv^l/+$) coat genotype; the father was wild-type (+/+).] The embryo was placed under a testis capsule, where it became disorganized, forming a teratoma which metastasized to a renal node. The primary tumor was minced and transplanted intraperitoneally; it became an ascites tumor of "embryoid bodies" with yolk sac "rinds" and teratocarcinoma (or embryonal carcinoma) "cores." In 1975, after almost 200 transplant generations in syngeneic hosts, the rinds of some embryoid bodies were peeled away and the malignant core cells were injected into blastocysts from parents of the nonagouti brown C57-b/b (C57 BL/6-b/b) strain. The blastocysts were transferred to the uterus of a pseudopregnant foster mother (mated to a sterile vasectomized male). Pregnancy ensued and live normal mice were born. Some had coat-color mosaicism (striped) and/or internal tissue contributions of the 129 tumor strain. At maturity, a mosaic male was test-mated to C57-b/b females. Production of " F_1 "-like offspring proved that he also had normal sperms derived from the teratocarcinoma cells; some progeny were $Sv^l/+$, some +/+. [From Mintz and Illmensee (1975), by permission of *Proceedings of the National Academy of Sciences*.]

FIGURE 20.8. Male mosaic mouse No. 1, produced as shown in Fig. 20.7. His coat is largely agouti and black, as in mouse strain 129, with an overall grayish dilution (especially visible on the feet) owing to the steel gene. Very narrow transverse stripes of agouti and nonagouti hair follicle clones appear on both flanks and the crown of the head. Abbreviated wide patches of brown melanoblast clones occur over the hindquarters, on each side of the head, and on the tail. [From Mintz and Illmensee (1975), by permission of *Proceedings of the National Academy of Sciences*.]



white C57-*b/b* parents and the isolated embryos were surgically transplanted into the uteri of white ICR mice that had just been mated to sterile vasectomized male ICR mice.

Of 183 blastocysts allowed to develop to full term, 48 mice were delivered alive. All fetuses appeared normal and showed no evidence of tumor. Of the six fetal and eight postnatal individuals extensively analyzed three of the postnatal animals proved to be genetic mosaics possessing features of both the teratocarcinoma cell strain and those of the "foster parent" C57 strain. The complete history illustrated by the author is reproduced in Fig. 20.7.

Figure 20.8 shows one of the mosaic mice thus produced, which has most of the coat characteristics (agouti, light-colored belly) of the 129 mice which gave rise to the teratocarcinoma. The red and white blood cells of this mouse are predominantly those of the 129-strain type and so is the hemoglobin produced. Other tests revealed 129-strain characteristics in many other tissues as well. This same (male) mouse had produced 61 offspring, all normal and all from sperm of 129 strain, as revealed by the production of F₁-like progeny for coat and other markers.

In conclusion, the authors wrote, "The results furnish an unequivocal example in animals of a non-mutational basis for transformation to malignancy and of reversal to normalcy."

Other evidence in favor of an epigenetic rather than a mutative etiology of cancer will be discussed in Sections 20.3 and 20.4 of this chapter.

20.2. Physiological Theories of Cancer

The significance of a correct theory needs no explanation; it becomes the structure and substance of our knowledge. The significance of an incorrect theory is rarely understood except in retrospect. Yet the bulk of this monograph demonstrates quite clearly that popular theories may prove wrong; theories that had long ago been discarded may be closer to the truth. The only harm from theories comes from their being ignored and left untested. I mention here two of the theories that approach cancer on a physiological basis.

20.2.1. Szent-Györgyi's Theory of Cancer

This theory of cancer is intimately tied up with Albert Szent-Györgyi's theory of the living state. This is altogether different from the living state as defined in the association-induction hypothesis (Section 6.1). Szent-Györgyi (1976, 1978) believed that there was life on earth before light and oxygen were available. Life then involved constant, unchecked proliferation, referred to as the α state. With the condensation of the opaque thick layer of water vapor, light and oxygen became extant. Life entered a β state in which the basic structural proteins of living systems acquired the characteristics of semiconductors by losing electrons to oxygen, thereby becoming free radicals, or multiradicals. Life in the β state can differentiate and produce increasingly complex structures.

In Szent-Györgyi's theory, dicarbonyls, such as methylglyoxal (MG), play a key role. It is believed that MG binds to the ϵ -amino group of the lysine residue of the protein and an ascorbic acid radical in turn binds itself onto MG, making MG a stronger electron acceptor. Folding of the lysine side chain permits contact of MG to desaturate the protein chain by taking away electrons by a charge-transfer mechanism. Since it is oxygen that converts ascorbic acid into ascorbic radical, the ultimate electron acceptor is oxygen. Much of the theory is based on studies of the electron spin resonance of model systems.

At a suitable concentration MG inhibits cell proliferation, but the active enzyme glyoxalase converts MG into ineffective lactic acid. Szent-Györgyi believes that glyoxalase is turned on by reduced glutathione, which thus acts as an on-off switch for cell proliferation.

Cancer cells are "stuck in the α state" somewhere between the α and β states. Factors which favor glyoxalase activity and disfavor the action of carbonyls favor carcinogenesis. Supporting this general concept, Szent-Györgyi showed that the structural portion of normal liver is brown, as is casein treated with glyoxal, indicative of its being in the free-radical β state. On the other hand the structural portion of Morris hepatoma 3524A (a fairly rapidly proliferating hepatoma) is colorless. However, after the addition of an electron acceptor, crotonaldehyde, the hepatoma also turns the same color as normal liver.

Although Szent-Györgyi's theory of cancer contains an admirable directness and simplicity that are characteristic of his many prior new ideas, it leaves many basic questions unanswered. Allosteric interaction with effective information transfer over a distance can be readily demonstrated in a pure protein, hemoglobin, without the intervention of any dicarbonyls. Moreover, muscle and nerve are well known nonproliferating tissues which according to Szent-Györgyi's theory should be opaque, but in fact single muscle fibers are transparent and essentially colorless. The complex layers of nerve tissues covering and separating impinging light and images on the rods and cones of the retina would make vision impossible if they were opaque. Nor has Szent-Györgyi provided a theoretical connection between the postulated role of the dicarbonyls and the fundamental role of ATP, which is fully capable of activating a glycerinated paramecium as well as a glycerinated rabbit psoas muscle—a technique which Szent-Györgyi himself pioneered.

20.2.2. Cone's Theory of Cancer

The observation that actively proliferating malignant cells in culture show a much lower resting potential during early G₁ (Cone, 1969) led Cone (1971) to suggest a theory of mitogenesis and oncogenesis. The basic idea is that the cellular resting potential and its associated intracellular ion levels act to regulate preparation for DNA synthesis and mitosis. The experimental findings that Cone cited in support of this theory include the demonstration of blockage of mitosis by substituting mannitol for NaCl in the culture medium; the demonstration of an acceleration as well as an improved synchrony of the cell cycle by exposing cells swollen in response to hyptonic solution to a pulse of hypertonic NaCl (0.17 M) (Cone, 1969); and the demonstration of a higher resting potential (ψ) in Chinese hamster ovary (CHO) and fibroblast (3T3) cells that had ceased proliferation (owing to contact inhibition when the cell culture became confluent) than in cells rapidly proliferating (Table 20.1).

In 1976 Cone and Cone cultured nonproliferative mature neurons of the avian central nervous system in medium containing ouabain (10^{-4} – 10^{-6} M), veratridine (5×10^{-5} M), or gramicidin (10^{-8} M), all of which are known to cause depolarization of the cell ψ and to increase the concentration of Na⁺ in the cells. In agreement with theory, all these agents caused an increase in DNA synthesis, as revealed by a nearly tenfold increase in [³H]thymidine uptake, an increase in mitotic activity, and a four- to sevenfold increase in the number of binucleated neurons, regarded as products of incomplete cell divisions.

Cone's theory is faulted by the acceptance of the membrane theory of cellular electric potentials, relating intracellular K⁺ and Na⁺ concentrations to ψ . This subject has been extensively discussed in Chapter 14. However, Cone's own data from proliferating (log phase) and nonproliferating (saturated) CHO and 3T3 cells (Table 20.1) once more show the disparity between ψ as measured and ψ as predicted on the basis of the Hodgkin-Katz equation [equation (3.11) or (14.1)] and the measured intracellular K⁺ and Na⁺ concentrations. The large differences of ψ are not accompanied by corresponding changes in intracellular K⁺ and Na⁺ concentrations. However, this weakness does not

TABLE 20.1. Demonstration of Higher Resting Potential (ψ) of Chinese Hamster Ovary (CHO) and 3T3 Fibroblast Cells When They Stopped Proliferation after Reaching the Saturated State Than When They Were in the Rapidly Proliferating Log Phase^a

	CHO		3T3	
	Log	Saturated	Log	Saturated
ψ (mV)	10.1 ± 0.8	61.3 ± 2.7	12.2 ± 1.4 ^b	65.7 ± 2.4
[Na ⁺] _{in}	15.3 ± 1.8	7.9 ± 2.1	17.6 ± 1.5	8.6 ± 0.8
[K ⁺] _{in}	186.1 ± 5.3	185.9 ± 6.2	204.5 ± 3.6	197.0 ± 9.8

^aData from Cone (1974).

^bValue given for cells nearest to the log phase (i.e., in active growth phase). [Na⁺]_{in} and [K⁺]_{in} are given in mmoles/liter of fresh cells.

rule out the possibility that either ψ or intracellular Na^+ and K^+ plays a major role in regulating or maintaining cell proliferation.

Cone's theory is far from being generally accepted. Thus Sachs *et al.* (1974) rejected the idea that ψ controls DNA synthesis and cell proliferation, even though Sachs *et al.* themselves confirmed Cone's observation of a cyclic change of ψ during the cell cycle. Orr *et al.* (1972) had found that increasing external K^+ to 0.114 M in baby hamster kidney cells promptly and reversibly stopped DNA synthesis. High external K^+ would most likely depolarize the cell and, according to Cone's theory, should have stimulated DNA synthesis. On the other hand, the 0.114 M K^+ used had completely replaced external Na^+ . If intracellular Na^+ is essential for DNA synthesis, as Cone contends, the data might confirm Cone's theory.

It bears mentioning that an essential role for Na^+ has already been discussed in egg maturation (Section 19.2.3) fertilization (Section 19.3.4), and tissue differentiation (Section 19.4.4). Na^+ influx was also found to be important in liver regeneration (Koch and Leffert, 1979) and in lens protein synthesis (Piatigorsky *et al.*, 1978). There is, therefore, no question that Na^+ is very important in the growth and differentiation of living cells; some specific mechanisms for the role of Na^+ in various aspects of growth have been discussed (Sections 18.1.1.1, 18.2.1.2, 18.2.2.2, 19.2.4, 19.3.4, 19.4.4, and 19.7.2).

If ouabain, veratridine, and gramicidin can indeed induce adult neurons into proliferation as Cone and Cone (1976, 1978) believed, it is a finding of great significance. As already mentioned (Section 18.2.1.4), ouabain stimulates Friend cells to synthesize hemoglobin. However, lymphocyte proliferation is inhibited by ouabain (Quastel and Kaplan, 1968). The techniques used by Cone and Cone, moreover, are fraught with difficulty. For example, Chalazonitis and Fishbach (1980) found that increasing external K^+ from 6 to 40 mM caused differentiation, not proliferation, of neurons in chick embryo cells. Clearly, one needs some more basic facts in order to evaluate the significance of these variable kinds of physiological phenomena.

20.3. What Distinguishes Cancer from Normal Tissues?

In his review in 1967, Knox listed three criteria that distinguish cancer from normal tissues: the morphological generalization, the Warburg generalization, and the Greenstein generalization. I shall begin with these three and continue with other new generalizations.

20.3.1. The Morphological Generalization

Normal living cells vary widely in shape, size, and other characteristics. Yet a competent pathologist can recognize cancer cells reliably. Cancer cells are proliferative and thus frequently show mitotic figures, which tend to vary greatly in size and shape, in contrast to the high degree of uniformity in the mitotic figures of normal cells. As a rule cancer cells have an enlarged and often misshapen nucleus and scanty cytoplasm. The nucleus tends to be hyperchromatic, with sharp boundaries but a dented or wrinkled shape. But above all, the nucleus of cancer cells shows irregular chromatin. Indeed, K.



Otto Warburg (1883–1970)

M. Graham (1972), in her treatise *The Cytology and Diagnosis of Cancer*, emphasized that “chromatin irregularity is the only reliable criterion for the diagnosis of cancer.” These irregularities usually involve clumping of darkly staining material interspersed among empty spaces and may result from extensive nuclear hydration like the transplanted nuclei of Gurdon (Section 19.7.2).

20.3.2. The Warburg Generalization

The Coris (Cori and Cori, 1925a,b) first observed that the consumption of glucose and release of lactate into the circulation by tumors was larger than that by normal tissues. However, Otto Warburg (1930) extensively compared the glycolytic activities of normal and neoplastic tissues. Warburg concluded that the lactate production of neoplastic tissues from glucose fell, within narrow limits, close to the higher values from normal tissues. Table 20.2, taken from part of the table compiled by Knox (1967), illustrates Warburg’s experimental basis for his conclusion, which was later confirmed by Dickens and Simer (1931). Weinhouse (1955) pointed out that this high rate of glycolysis could not be explained as being due to a disturbance of respiration in tumor cells (Warburg, 1930). Indeed, respiration of tumor cells appears quite comparable to that of normal tissues. Knox suggested that the increased glycolysis is due simply to the presence of more glycolytic enzymes in cancer cells.

20.3.3. The Greenstein Generalization

In an extensive comparative study of the enzyme contents of normal tissues and a large variety of cancer cells, Jesse Greenstein noted that as a rule wide variations in enzyme activity exist among different normal tissues. On the other hand, cancers from widely different tissues have closely similar enzyme contents. Figure 20.9 reproduces the summarizing figure of Greenstein (1956), whose concluding remarks read:

The more autonomous such cancerous tissues are, i.e., the more malignant, the more do they deviate from the chemical pattern of their tissue of origin and the closer do they approach an



Jesse Greenstein

TABLE 20.2. Lactate Formation in Normal and Neoplastic Tissues^{a,b}

	Slices (with glucose)		Homogenates (with fructose- 1,6- diphosphate)
	Aerobic	Anaerobic	
Normal tissues			
Thyroid	0	0.2	—
Liver	0.05	0.24	5.8
Intestinal mucosa	0.1	0.3 ^c	—
Diaphragm muscle (Long, 1961)	0.16	0.37	12.1
Kidney (Long, 1961)	0	0.38	7.3
Spleen	0.2	0.6	—
Testis	0	0.6	—
Thymus	0.05	0.6	—
Placenta	0.7	1.0	—
Brain	0.2	1.4	5.7
Embryo	0.4	1.7	—
Retina	3.4	6.6	—
Neoplasms			
Flexner-Jobling carcinoma	1.9	2.3	5.5
Jensen sarcoma	1.3	2.5	6.0
Walker 256 carcinosarcoma	—	—	5.0
Sarcoma 37 (mouse)	0.9	2.1	—
Spontaneous tumors (mouse)	0.6	1.9	—
Tar carcinoma (mouse)	1.1	1.9	—
Melanoma	0.4	1.2	—
Yale I tumor (mouse)	0.5	1.2	—
Bladder carcinoma (man)	1.8	2.7	—
Sarcoma (man)	1.2	2.1	—
Laryngeal carcinoma (man)	1.1	1.4	—

^aTissues are from rat unless specified. Values are in μ moles per minute per 100 mg dry tissue at 37°C.

^bFrom Knox (1967, by permission of *Advances in Cancer Research*.

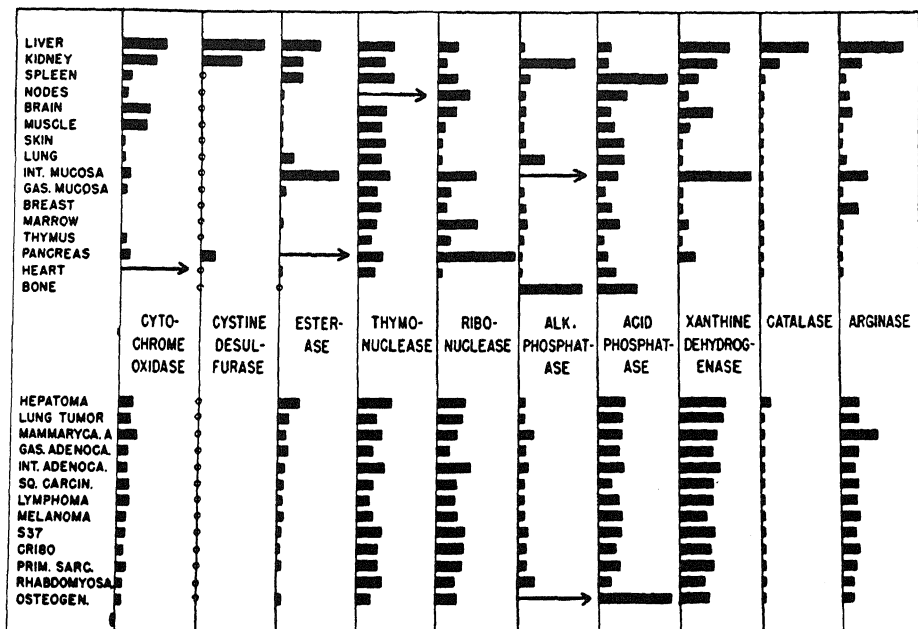


FIGURE 20.9. Levels of various enzyme activities in cell-free extracts of different normal and neoplastic tissues of mice. The relative activities for a given enzyme are indicated by the length of the horizontal bars in a column. The arrows denote a higher order of magnitude of activity. [From Greenstein (1956), by permission of *Cancer Research*.]

apparently functionally undifferentiated type of tissue presumably common to all. In this respect they resemble early embryonic tissue. [Greenstein, 1947, p. 367]

20.3.4. The Roberts-Frankel Generalization

Enzyme activities are not the only criteria that indicate the trend suggested. Another cell property known to be specific is free amino acid distribution patterns, which vary widely in different normal tissues, even though all are bathed in the same tissue fluid. In 1952 I suggested that the selective accumulation of amino acids, like that of K^+ , is the result of selective adsorption on protein sites (Ling, 1952). Cowie and Walton (1956) reached a similar conclusion in their studies of amino acid distribution in yeast-like *Toralopsis utilis*.

Figure 20.10 illustrates the generalization of E. Roberts and Frankel (1949) that, whereas free amino acid distribution patterns vary from normal tissue to normal tissue, in cancer cells of diverse origin the patterns appear to be similar. They all accumulate glycine, alanine, taurine, and glutamic acid (plus an unidentified "underglutamic acid") in roughly equal proportions.

20.3.5. The Damadian Generalization

Raymond Damadian (1971) first reported longer NMR relaxation times (T_1 and T_2) of the water proton in three rat malignant (solid) tumors than in six normal rat

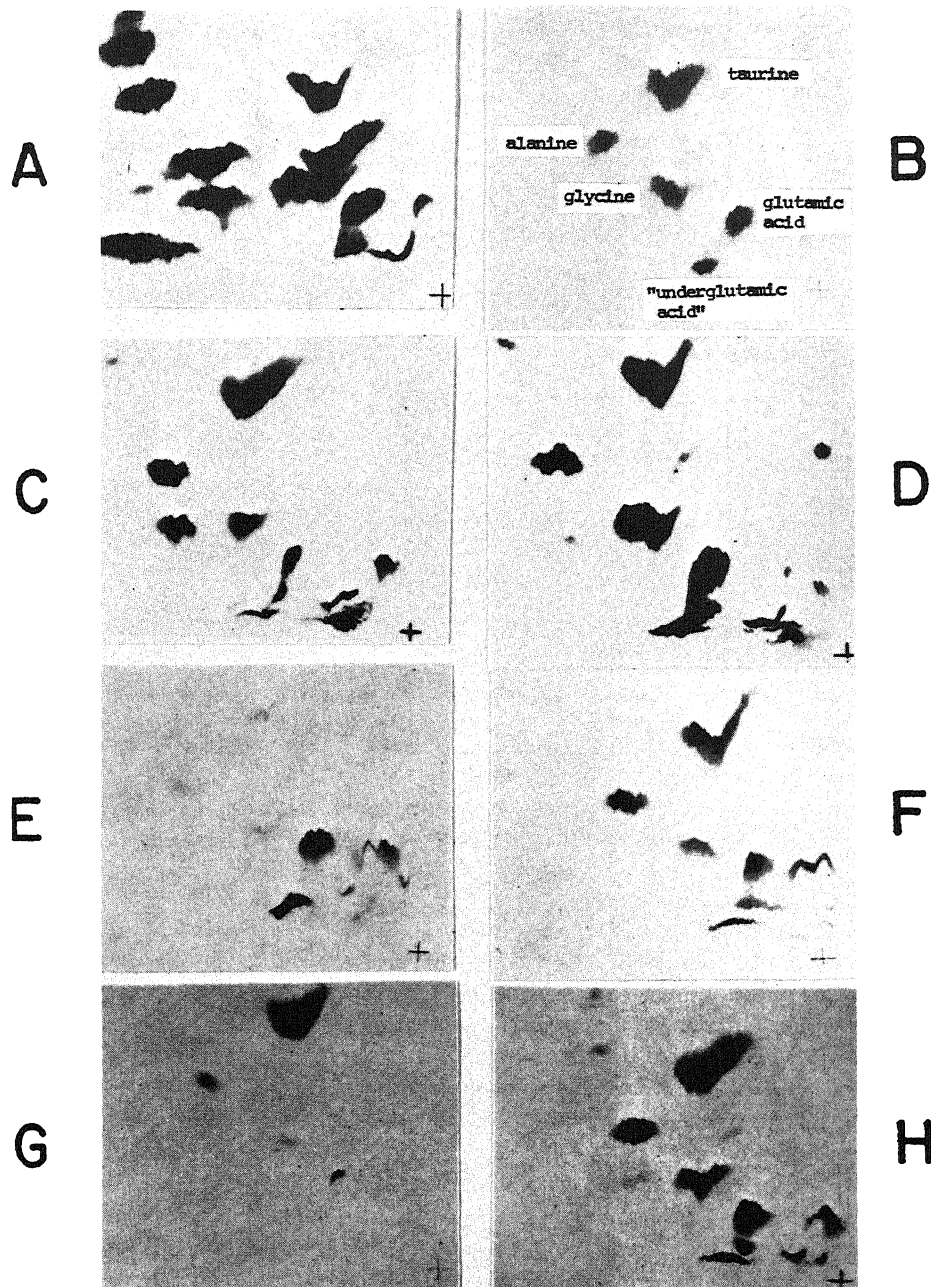
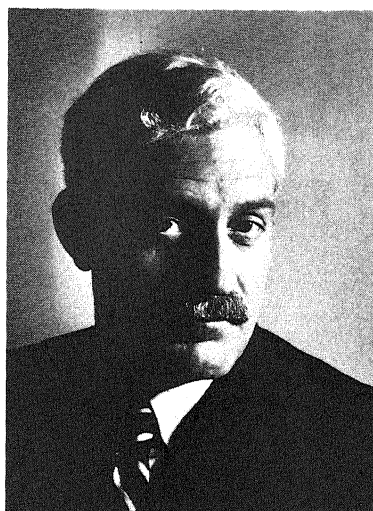


FIGURE 20.10. Comparison of the free amino acid distribution pattern in normal tissues (left) and cancer (right). (A) Normal epidermis, (B) tumor MA 387; (C) normal liver, (D) hepatoma; (E) normal testis, (F) interstitial cell tumor; (G) normal muscle, (H) rhabdomyosarcoma. [From E. Roberts and Frankel (1949), by permission of *Cancer Research*.]



Raymond Damadian

tissues (Table 20.3). He considered the data to agree with, first, Ling's polarized multilayer theory of cell water and, second, Albert Szent-Györgyi's suggestion that the cancer cell has less structured water (Szent-Györgyi, 1957). His initial report stimulated a great deal of interest. Subsequent workers, however, expressed the belief that the malignant tumors studied by Damadian and others simply had more water than normal tissues (Inch *et al.*, 1974; Eggleston *et al.*, 1978). It is well known that increasing the water content of a complex macromolecular system prolongs the NMR relaxation times.

In a recent paper, Ling and Tucker (1980) attempted to resolve the problem. Figure 20.11 shows that, if the percentage of extracellular water in an Ehrlich ascites cell suspension is varied, both T_1 and T_2 decrease. By extrapolation, T_1 and T_2 of pure cells without extracellular fluid could be obtained: $T_1 = 800$ msec and $T_2 = 60$ msec at an

TABLE 20.3. Spin-Lattice (T_1) and Spin-Spin (T_2) Relaxation Times of Normal and Malignant Tissues^a

Tissue	T_1 (sec)	T_2 (sec)
Normal		
Rectus muscle	0.538 ± 0.015	0.055 ± 0.005
Liver	0.293 ± 0.010	0.052 ± 0.003
Stomach	0.270 ± 0.016	
Small intestine	0.257 ± 0.030	
Kidney	0.480 ± 0.026	
Brain	0.595 ± 0.007	
Tumor		
Walker sarcoma	0.736 ± 0.022	0.100
Novikoff hepatoma	0.826 ± 0.013	0.118 ± 0.002

^aFrom Damadian (1971), by permission of *Science*.

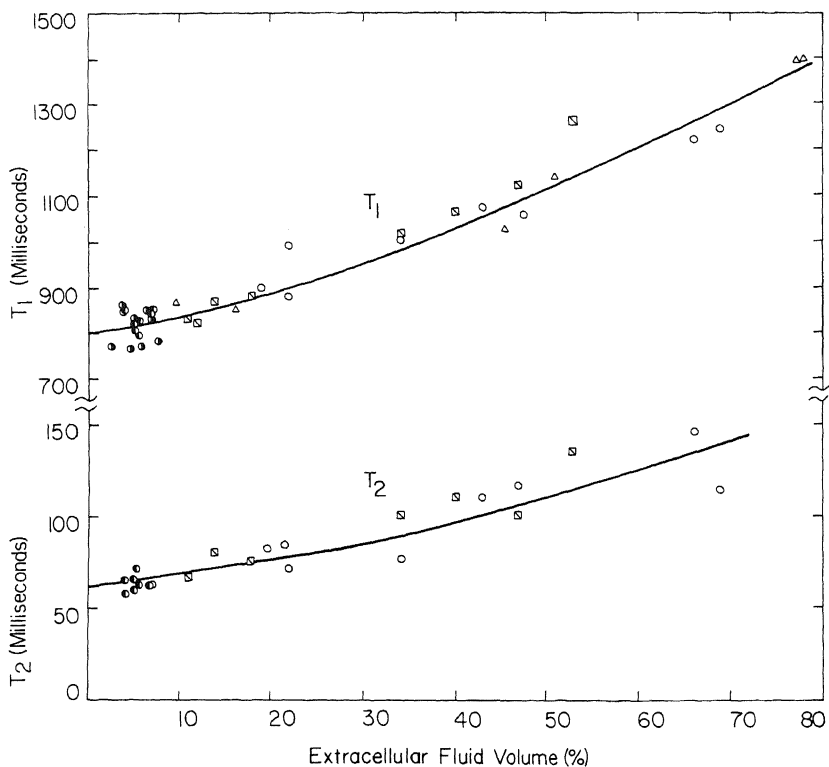


FIGURE 20.11. Variation of NMR relaxation times (T_1 and T_2) of water protons from suspensions of Ehrlich carcinoma cells with varying amounts of extracellular fluid volume. Different symbols represent various sets of experiments. [From Ling and Tucker (1980), by permission of *Journal of the National Cancer Institute*.]

NMR resonance frequency of 17.1 MHz. These values were not materially different from those of cell suspensions containing 5% extracellular space fluid as determined by centrifugation at 45,000g for 10 min. With this centrifugation technique, the water contents, T_1 and T_2 of three mouse and two rat ascites tumors were studied, and the results are shown in Table 20.4. The five strains of ascites tumors were mouse Ehrlich carcinoma which originated from mammary gland, mouse sarcoma 180 from polymorph cells, mouse Meth A (a fibrosarcoma), and rat Novikoff and AS-30D hepatomas. All five are transplanted once every week and are thus all "maximally deviated" (Potter, 1961). These cancer cells have water contents and NMR relaxation times within narrow ranges. In contrast, both parameters vary widely among the normal tissues studied and in "minimally deviated" Morris hepatomas (Hollis *et al.*, 1975).

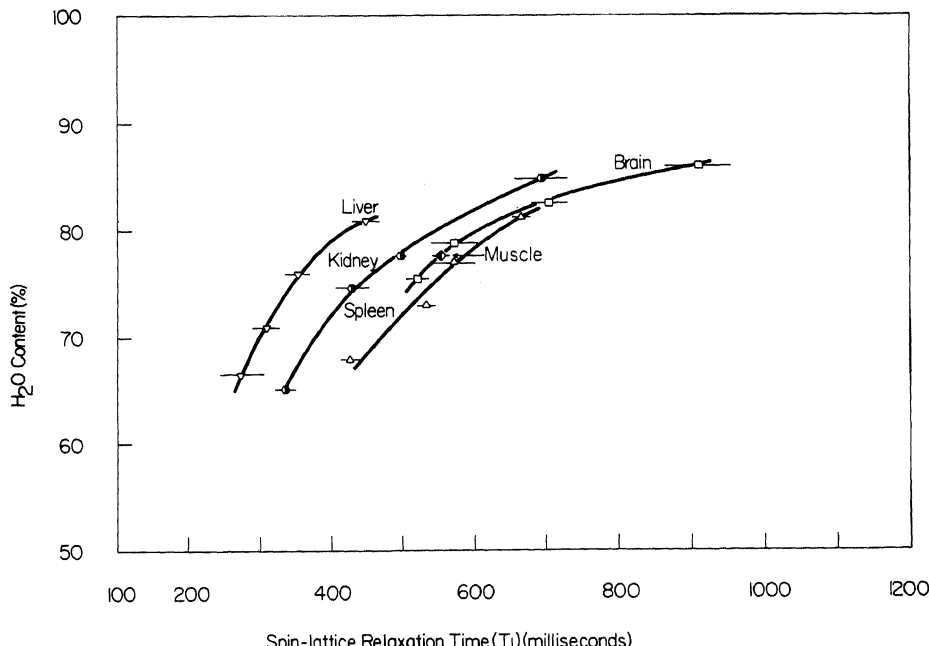
To show that it is not the water content (intra- plus extracellular) of the cancer cells that is the cause of the longer T_1 observed in cancer cells, Ling and Tucker manipulated the water contents of normal tissues and cancer cells by exposing them to normal Ringer solution and to Ringer solution containing either less NaCl or more sucrose than normal. The results are illustrated by the mouse data shown in Figs. 20.12 and 20.13,

TABLE 20.4. Water Contents, T_1 , and T_2 of Cancer Cells^{a,b}

Ascites tumor	Host	Mean water content \pm SE (%)	T_1 (msec)	T_2 (msec)
Ehrlich carcinoma	Mouse	80.8 \pm 0.34 (20)	815 \pm 7.07 (20)	61.6 \pm 1.87 (10)
Sarcoma 180	Mouse	81.7 \pm 1.6 (8)	802.5 \pm 15.5 (8)	86.3 \pm 3.20 (8)
Meth A fibrosarcoma	Mouse	80.8 \pm 0.49 (8)	805 \pm 10.4 (8)	68.2 \pm 1.31 (8)
Novikoff hepatoma	Rat	82.7 \pm 0.12 (4)	855 \pm 8.66 (4)	96.9 \pm 1.2 (4)
AS-30D hepatoma	Rat	81.3 \pm 0.3 (8)	843.6 \pm 16.4 (8)	80.6 \pm 2.13 (8)

^aNumbers in parentheses are number of measurements.^bFrom Ling and Tucker (1980), by permission of *Journal of the National Cancer Institute*.

in which T_1 is plotted against the water content of each tissue. The results clearly show that varying water content changes T_1 . But, at the same water content, each normal tissue has its own T_1 , different from the T_1 of other tissues. The T_1 s of all normal tissues are shorter than the T_1 s of all the cancer cells so far studied. Having excluded higher extra- and intracellular water content as the cause of the long T_1 observed in cancer cells, Ling and Tucker concluded that only two plausible sources of T_1 lengthening remain: Either cancer cells have fewer paramagnetic "contaminants" or cancer cell water is less structured.

FIGURE 20.12. T_1 of normal mouse tissues at varying water contents. [From Ling and Tucker (1980), by permission of *Journal of the National Cancer Institute*.]

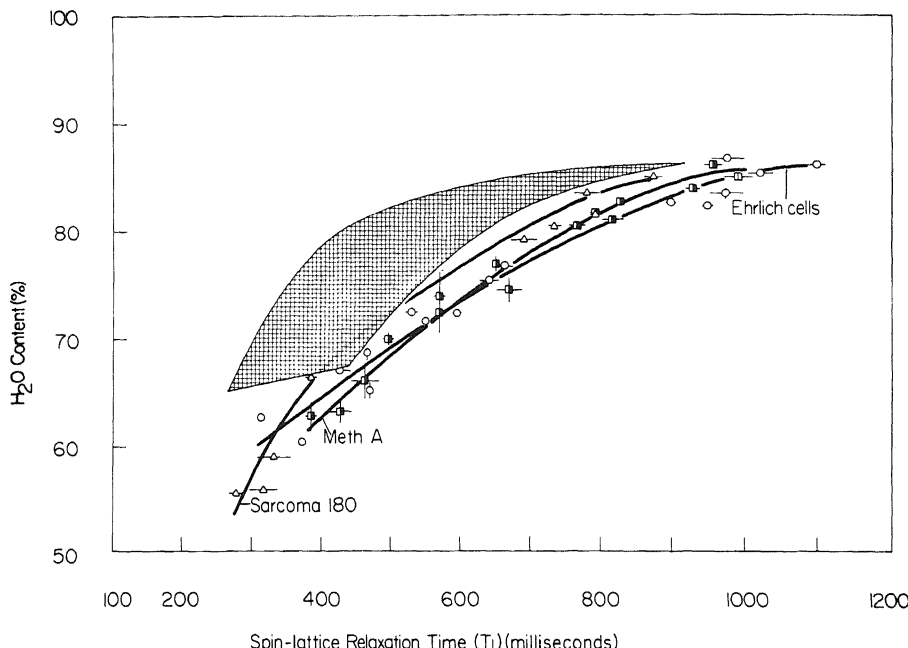


FIGURE 20.13. T_1 of three strains of mouse cancer cells with varying water contents. Hatched area covers the ranges of T_1 and water contents of normal tissues and is taken from Fig. 20.12. [From Ling and Tucker (1980), by permission of *Journal of the National Cancer Institute*.]

To help choose between these possibilities, one may recall that the degree of structuring of the polarized multilayered water in living cells and model systems can be studied with probe molecules, as discussed extensively in Chapter 7. Ling, Ochsenfeld, Tucker, and Murphy (1983) showed that the equilibrium distribution of seven pentoses (i.e., D- and L-arabinose, D- and L-lyxose and D-ribose) in all the maximally deviated cancer cells are all unity or very close to unity (Figs. 20.14 and 20.15). The rectilinearity of the distribution profiles and their indifference to specific steric structure are taken to indicate the existence of the probe molecules primarily in the cell water. These data together suggest that water in "maximally deviated" cancer cells may exist in a different physical state than that in normal cells and that it has a relatively weaker ability to exclude certain probe molecules. However, a difference in paramagnetic ion content and interactions is not ruled out.

20.3.6. The Ling-Murphy Generalization

Using sodium dodecyl sulfate gel electrophoresis, Ling and Murphy (1982b) studied the total protein content of 14 types of mouse cancer cells and 5 types of rat cancer cells. All 19 strains were maximally deviated, with transplantation time about one week (Potter, 1961). Ling and Murphy found that, in contrast to normal fully differentiated tissues with highly characteristic and different proteins within each animal species, the recognizable tumor proteins are similar in type as well as in quantity. The tentative

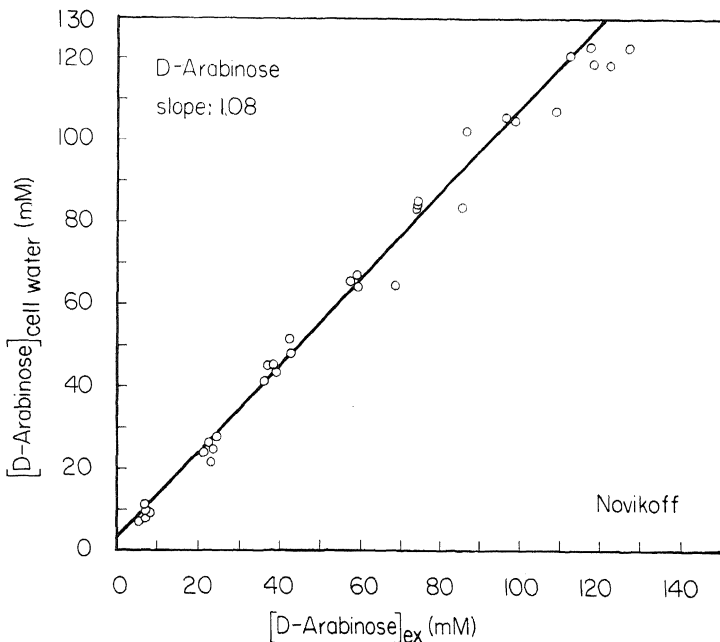


FIGURE 20.14. Equilibrium distribution of D-arabinose between the cell water of Novikoff hepatoma cells (ordinate) and the external solution (abscissa). Slope indicated was determined by the method of least squares. [From Ling *et al.* (1984), by permission of *Physiological Chemistry and Physics*.]

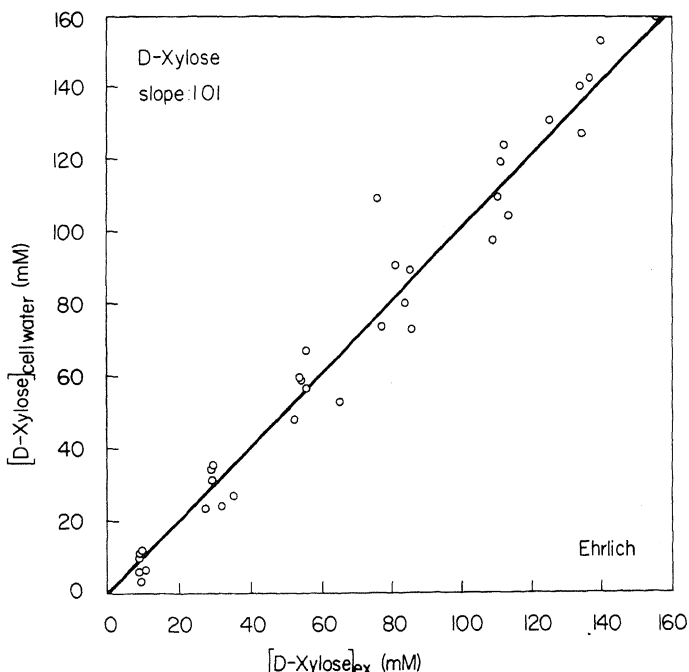


FIGURE 20.15. Equilibrium distribution of D-xylose between the cell water of Ehrlich ascites cells (ordinate) and the external solution (abscissa). Slope indicated was determined by the method of least squares. [From Ling *et al.* (1984), by permission of *Physiological Chemistry and Physics*.]

conclusion was drawn that, when maximally deviated, cancer cells not only are similar to one another in regard to metabolism (Warburg generalization), enzyme distribution (Greenstein generalization), free amino acid distribution (Roberts-Frankel generalization), and water proton NMR relaxation time (Damadian generalization) but are, in fact, either identical or highly similar as whole living cells. Since each of these generalizations refers to the properties or behaviors of some of the cell proteins, the Ling and Murphy findings, if fully confirmed, will in fact constitute a generalization of all the other generalizations previously cited.

20.4. Another Apparent Paradox and the Bright Future of Cancer Research

In the preceding chapters we have already described two apparent paradoxes (Sections 6.3.1.6 and 12.4.2.1). In the end, both sides of the seemingly irreconcilable dichotomies were in fact reconcilable because the subjects were more complex than previously assumed. Here, our knowledge about carcinogenesis appears to have created yet another paradox: The two opposing theories of carcinogenesis, the somatic mutation theory and the mal differentiation theory, are each becoming stronger as more supportive evidence for each accumulates. There is now no question that a single-point mutation produces an oncogene which turns nonneoplastic, contact-inhibited cells into neoplastic cells. Nor is there much doubt that the cancer genome has not been permanently altered by mutation and thus is widely divergent: From cancer cells, perfectly normal individuals can develop; all maximally differentiated cancers appear to be the same.

Perhaps the overall solution of this apparent paradox lies once more in the recognition that carcinogenesis is a complex phenomenon. Thus, somatic mutations may occur before and are a key step in the development of mal differentiation.

In fact this multistage model has already been suggested and accepted by many (Cairns, 1981; Tabin *et al.*, 1982). It was implied in the recognition that the NIH-3T3 cells used in the oncogene assays already have some of the properties of "transformed" cells (Littlefield, 1982) and might therefore have already completed the initial stage of carcinogenesis (Cooper, 1982). Similarly, the increasing evidence that cancers are associated with chromosomal abnormality led many to believe that chromosomal translocation may be another essential step in the production of cancer (Cairns, 1981; see Marx, 1982, for a recent review). G. Klein (1981) suggested that chromosome fragment translocation might lead to cancer by causing abnormal activation of normal cellular genes. In support of this view, one recalls that DNA from normal cells also can, though less effectively, transform NIH-3T3 cells (Cooper *et al.*, 1980).

Carcinogenesis and differentiation appear to represent similar processes, but which operate in opposite directions, and may share certain basic attributes. One common feature of cellular differentiation is the sequential nature of its various stages: Stage 1 must be accomplished before stage 2 can begin. Thus in the induction of notochord from frog ectodermal tissue *in vitro*, a prior exposure to K^+ must precede a subsequent exposure to Na^+ (Section 19.4.4). To bring about the *in vitro* activation of certain genes and inactivation of others in *Drosophila* chromosomes, prior exposure to juvenile hormone is essential for the effective action of the molting hormone (Section 18.2.1.1). Richards described the juvenile hormone as changing the "competence" of the polytene chromo-

somes. Indeed the very concept of competence in developmental biology (Needham, 1950) may well be an expression of the mandatory prior steps in sequential gene functions.

Recent findings of Lotem and Sachs (1982) are also highly cogent. Two kinds of macrophage- and granulocyte-inducing (MGI) proteins were discovered in myeloid cells. MGI-1 protein induces multiplication of normal myeloid precursor cells while MGI-2 induces differentiation. In normal cells MGI-1 also induces the production of MGI-2. Thus differentiation depends on a sequence of events. In leukemia cells, MGI-1 is required for growth, but MGI-1 is no longer able to induce the production of MGI-2. Here the inability to produce a differentiation-promoting protein apparently characterizes this particular form of cancer.

Sequential multistage events *per se* would not necessarily be so slow, as is well known in carcinogenesis: From 30 to 100 days of daily application of coal tar to the ears of rabbits by Yamagiwa and Ichigawa (1915, 1918) produced the first successful laboratory chemical induction of cancer. I believe that this slowness may be due to the auto-cooperative nature of each of the individual steps. As shown in the theoretical curves of Huang and Seitz (Section 12.4.2.6), autocooperative interaction involves lag periods. Experimentally lag periods have been demonstrated not only in the ion fluxes described in Section 12.4.2.6 but also in the induction of 3T3 cells to enter into the proliferative C phase by hormones (Section 19.5.2.1) and in other similar types of C-phase inductions.

Carcinogenesis having been characterized as a multistage event in one of the steps of which oncogenes play a key role, the above-mentioned Ling-Murphy finding, if and when fully confirmed, may offer a general direction for the multistage events. The singleness of the entire protein ensemble of all maximally deviated cancer cells, despite their widely different origins, makes it very attractive to speculate that these maximally deviated cells eventually return to the other well known unique (totipotent) stage in the history of all cells, the egg cell. This is by no means a new concept (see Greenstein, 1947, p. 367), but the Ling-Murphy findings add a new persuasiveness. If proven, it would mean that carcinogenesis is in fact a dedifferentiation, again an old concept.

But the question of whether or not the cancer cell will ultimately prove to be the same as the egg cell does not alter the fact that, from widely different origins, with widely different spectra of genes being transcribed in normal cells, one set of genes alone is being transcribed in cancer cells. This uniformity demands that in normal differentiated cells there must be a single controlling master agent (e.g., a master repressor protein) that directly or indirectly shuts off the expression of this collection of genes specifying the unique protein ensemble common to all maximally deviated cancer cells. In addition, this master controlling repressor protein must also open the door for other secondary agents or proteins to function, thereby bringing about differentiation into various tissues. The question is, Are the proto-oncogene and the p21 protein (with the right glycine residue at position 12) related to this postulated master repressor protein?

As of now, no one knows. However, witnessing how powerfully and efficiently scientists of different disciplines have so successfully resolved the highly complex oncogene problem, one can look forward with eagerness and certainty to the brilliant developments in cancer research soon to come.



Appendices

A

Nuclear Magnetic Resonance Spectroscopy

Nuclear magnetic resonance (NMR) spectroscopy is a new addition to the tools of biological research. F. Block *et al.* (1946) and E. M. Purcell *et al.* (1946) independently discovered ways to observe NMR signals of protons in water and in paraffin, respectively, for which they conjointly received the Nobel Prize for Physics in 1952. Since then, what was originally a subject of interest only to theoretical physicists has grown into one of the major pillars of methodology in organic chemistry. As of now, the applications of NMR to biology are impressive though often tentative. In the long run, one feels certain that NMR will be just as important a tool to biologists as it is already to chemists.

A.1. NMR Relaxation Time, T_1

In the early part of the century, physicists realized that atomic nuclei undergo rotation or spin. This spin generates an angular momentum and a magnetic moment. The angular momentum is quantized in levels separated by units of \hbar (Planck's constant h divided by 2π) and is a function of the nuclear spin quantum number, I , the nuclear spin quantum number, in turn, is the algebraic sum of contributions from the nuclear protons and the nuclear neutrons, each of which possesses a spin quantum number of $\frac{1}{2}$, either positive or negative. The magnetic moment N_1 is proportional to the angular momentum $I\hbar$ by a factor, γ , the magnetogyric ratio characteristic of each nuclide. ^{12}C and ^{16}O have no angular momentum or magnetic moment, because their spin quantum numbers, I , are zero; the positive spins exactly cancel out the negative spins. The H atom has only one proton and possesses a spin quantum number of $\frac{1}{2}$. It is the NMR spectrum of the H atom in water that is most extensively studied in NMR research on water in biological systems.

It is known that an atomic nucleus with a spin quantum number I has a total of $2I + 1$ energy levels. Interaction with an external magnetic field may cause the separation of the $2I + 1$ equally spaced energy levels (nuclear Zeeman effect). For the hydrogen atom, $I = \frac{1}{2}$ and $2I + 1 = 2$. Much NMR study deals with induced trans-

sitions between these separate energy levels by the absorption or emission of energy quanta.

Transitions between separated energy levels do not take place in a simple static field. That is to say, spontaneous transitions between the separated energy levels are negligible. However, if an oscillating electromagnetic field is applied at a direction perpendicular to that of the static magnetic field, the nuclear spin will interact with it. At a frequency matching the energy difference between the separated energy levels (the resonance or Larmor frequency) of the specific atomic nuclei in question, the nuclear spin will undergo a transition into the excited state. If the applied radiofrequency energy source is suddenly turned off, the nuclear spin system will return to equilibrium with its environment (i.e., the "lattice") following a first-order exponential time course. The time constant for this exponential decay, or relaxation, is called the *spin-lattice relaxation time*, or the *longitudinal relaxation time*, or simply T_1 . The rate of relaxation depends on the environment of the nucleus.

Hot water remains hot in a thermos; it cools rapidly when in contact with a good metallic conductor of large mass. The thermal energy in the heated water dissipates only when in contact with matter, like metal, that can readily absorb the thermal energy. An insulator cannot. Similarly, the dissipation of magnetic energy in the nuclear spin of the water proton will be fast or slow, with short or long T_1 , respectively, depending on the availability of a magnetic energy-accepting environment or lattice. The major mechanisms of magnetic energy dissipation are dipole-dipole interactions owing to the fluctuating magnetic field created by intramolecular oscillation (primarily rotational) and intermolecular motions of other magnetic nuclei in the sample (primarily translational) (Krynicki, 1966). Thus, the rate of spin-lattice relaxation (T_1^{-1}) has two components, $T_{1(\text{intra})}^{-1}$ and $T_{1(\text{inter})}^{-1}$:

$$T_1^{-1} \simeq T_{1(\text{intra})}^{-1} + T_{1(\text{inter})}^{-1} \quad (\text{A.1})$$

A third term, called the spin-rotational contribution, is insignificant for ambient temperature (see Krynicki, 1966).

Bloembergen, Purcell, and Pound (1948) derived an equation for $T_{1(\text{intra})}^{-1}$ which, in the form modified by Kubo and Tomita (1954), is as follows:

$$(T_{1(\text{intra})}^{-1})^{-1} = \frac{3\gamma^4 \hbar^2}{10b^6} \left[\frac{\tau_c}{1 + \omega_0^2 \tau_c^2} + \frac{4\tau_c}{1 + 4\omega_0^2 \tau_c^2} \right] \quad (\text{A.2})$$

where γ is the magnetogyric ratio, a characteristic property of each nuclide and equal to 5.585 for protons; \hbar is the Dirac h ($h/2\pi$, where h is the Planck constant); b is the interproton distance; and ω_0 is the Larmor frequency. τ_c is the rotational correlation time, the time for a local magnetic field to "lose memory" of a previous value, or more simply the time a molecule takes to turn through a radian. For normal liquid water, τ_c is 2.7×10^{-12} sec (20°C).

For the water proton with spin $\frac{1}{2}$, Abragam (1961, p. 302) derived a simplified equation for $T_{1(\text{inter})}^{-1}$

$$T_{1(\text{inter})}^{-1} = \frac{\pi}{5} \cdot \frac{N\gamma^4 \hbar^2}{aD} \quad (\text{A.3})$$

where N is the density of spins per cm^3 ; a is the radius of the hard sphere, used to approximate the water molecule in the Stokes formula; and D is the translational diffusion coefficient of the water molecule.

Abragam showed that, when τ_c is very much shorter than the Larmor period, $2\pi/\omega_0$,

$$T_{1(\text{intra})}^{-1} = \frac{3}{2} \cdot \frac{\gamma^4 \hbar^2}{b^6} \cdot \tau_c \quad (\text{A.4})$$

$$= 2\pi \frac{\gamma^4 \hbar^2}{b^6} \cdot \frac{a^3 \eta}{kT} \quad (\text{A.5})$$

where η is the viscosity; b is the distance between protons; and k and T have the usual meanings. Substituting (A.3) and (A.5) into (A.1), and rewriting, Abragam (1961, p. 326) showed that the full T_1 for both intramolecular (rotational) and intermolecular (translational) motions is described by the following equation:

$$T_1^{-1} = \left(\frac{a}{b} \right)^2 \left(\frac{\gamma^4 \hbar^2}{3Db^4} \right) \left(1 + \frac{3\pi}{5} \cdot \frac{Nb^6}{a^3} \right) \quad (\text{A.6})$$

Using values of $a = 1.74 \times 10^{-8} \text{ cm}$, $b = 1.58 \times 10^{-8} \text{ cm}$, $N = 6.75 \times 10^{22}$, and $D = 1.85 \times 10^{-5} \text{ cm}^2/\text{sec}$ (J. H. Simpson and Carr, 1958), equation (A.6) yields $T_1 = 3.7 \text{ sec}$, which is (probably fortuitously) close to the experimentally determined value of $3.6 \pm 0.2 \text{ sec}$ (Chiarotti and Guilotto, 1954). This calculation also shows that the translational (intermolecular) contribution to T_1^{-1} is one third the rotational (intramolecular) one. [However, $T_{1(\text{inter})}^{-1}$ makes up two fifths of the total T_1^{-1} , as estimated by Emsley *et al.* (1965) and Krynicki (1966).] Also worth noting is that the rotational correlation time, τ_c , is related to Debye's correlation time, τ_d [see equation (9.10)] by the formula

$$\tau_d = 3\tau_c \quad (\text{A.7})$$

While the fluctuating dipole-dipole interaction accounts for the T_1 of the water proton with spin $\frac{1}{2}$, in other magnetic nuclei with higher spin, additional interactions may contribute to the relaxation. Thus in Section 8.4.3.3 I referred to the quadrupolar interaction of ^{23}Na , since atoms of ^{23}Na contain an electric quadrupolar moment and therefore fluctuating electric field gradients contribute significantly to the T_1 of ^{23}Na . [For additional descriptions of relaxation mechanisms see Abragam (1961), D. Eisenberg and Kauzmann (1969), and Farrar and Becker (1971).]

A.2. Proton Resonance Spectrum, Linewidth, and T_2

As mentioned previously, the application of a uniform steady magnetic field, H_0 , produces in the proton a splitting of energy levels. The energy difference between these nuclear Zeeman levels is proportional to H_0 and to the nuclear moment. Under equilibrium conditions, there are more nuclei in the lower energy state than in the higher

energy state, according to Boltzmann's distribution. The application of a perpendicular oscillating radio-frequency (rf) electromagnetic field causes a transition to the higher energy state when the applied rf frequency matches the natural or Larmor frequency (ω_0) of the nucleus involved. The consequent absorption of the energy is recorded on the spectrum. Theoretically one might expect that the absorption creates an infinitely sharp line on the frequency spectrum corresponding to that of the Larmor frequency of the proton. In fact it is usually more complicated.

A.2.1. Chemical Shift

The application of a magnetic field induces an orbital motion of the electrons of the molecule. This orbital motion in turn creates a secondary magnetic field so that locally a nucleus does not "see" only H_0 but also a contribution from the local perturbations. Thus,

$$H_{\text{loc}} = H_0(1 - \sigma) \quad (\text{A.8})$$

where σ is called a screening constant. The effect of this screening constant, which varies with the nature of the chemical environment, is to bring the Zeeman levels closer together in a specific manner. As an example, protons in different chemical environments, such as those in an ethanol molecule, $\text{CH}_3\text{CH}_2\text{OH}$ (three in the methyl group, two in the methylene group, and one in the alcohol group), will resonate at somewhat different frequencies (Fig. A.1). The displacement of the signal owing to different chemical environments is called the *chemical shift* and is a property of great importance in the use of NMR spectroscopy for deciphering the structure of unknown organic compounds.

A.2.2. Linewidth and T_2

Each of the NMR signals is not infinitely thin but has a definite linewidth. Basically, this width is an expression of Heisenberg's uncertainty principle, and the linewidth measured on a frequency scale is of the order of T_1^{-1} .

In solids or highly viscous liquids, the linewidth may appear considerably wider than T_1^{-1} . Here the most outstanding cause of the additional widening is the different static magnetic fields experienced by different nuclei in the sample in respect to the more or less rigidly fixed magnetic dipoles of the neighboring nuclei. This difference creates

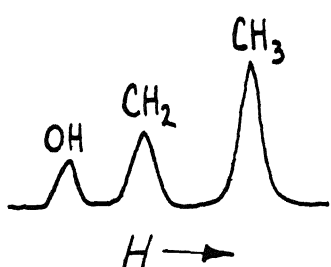


FIGURE A.1. Proton resonance spectrum of ethyl alcohol under low resolution. Arrow indicates direction of increasing field strength. Note that the intensities of the three peaks are roughly in the ratio 3:2:1, corresponding to the number of protons in each of the groupings. [Figure drawn after Pople *et al.* (1959).]

a variety of local magnetic fields and hence a variety of natural resonance frequencies. Thus, when the linewidth is larger than can be accounted for by T_1 , another relaxation time parameter, T_2 , is introduced,

$$T_2 = \frac{1}{\pi\nu_{1/2}} \quad (\text{A.9})$$

where $\nu_{1/2}$ is the linewidth at the half-maximum height of the signal. T_2 is also called the *transverse* or *spin-spin relaxation time*.

In many solids, the interaction between nuclear magnetic moments is the largest cause of broadening. In gases and liquids of low viscosity, the tumbling of molecules causes an averaging of local fields; as a result T_1 and T_2 tend to be equal (see Section A.3).

Often the measured T_2 may be affected by instrumental imperfections, e.g., inhomogeneity of the magnetic field, H_0 .

A.3. The Relation of T_1 and T_2 to the Rotational Correlation Time, τ_c

Bloembergen, Purcell, and Pound (1948) also presented an equation for T_2^{-1} , which in the form modified by Kubo and Tomita (1954) is as follows:

$$T_2^{-1} = \frac{3\gamma^4\hbar^3}{20b^6} \left[3\tau_c + \frac{5\tau_c}{1 + \omega_0^2\tau_c^2} + \frac{2\tau_c}{1 + 4\omega_0^2\tau_c^2} \right] \quad (\text{A.10})$$

Figure 9.24 shows the theoretically calculated relationship between T_1 , T_2 , and the correlation time τ_c based on equations (A.2) and (A.10). In the range of rapidly moving nuclei with τ_c shorter than 10^{-9} sec, $\omega_0\tau_c \ll 1$ and T_1 and T_2 are equal, both decreasing with increasing τ_c . However, with increase of τ_c to and beyond a certain critical value, equal to $(2\tau_c\omega_0)^{-1}$, T_1 begins to increase while T_2 continues to decrease until it reaches a limiting value, which is a measure of the dipole broadening of the nuclear resonance line for molecules rigidly fixed in a solid. Although equations (A.2) and (A.10) are highly useful and their predictions are of far-reaching significance, one might, nevertheless, regard the theoretically predicted relations with some reservations. Thus, for example, equations (A.2) and (A.10) took into account only the intramolecular interactions. As in the case of T_1^{-1} , the intermolecular interaction also plays a significant role here. With this in mind, one should note that the equality of T_1 and T_2 at $\omega_0\tau_c \ll 1$, indicated in Fig. 9.24, is not exact and thus, at a frequency of 31.6 MHz, T_1 of pure deoxygenated water is higher than T_2 , and the ratio T_1/T_2 is 25°C varied between 1.2 and 1.5 depending on pH (Meiboom *et al.*, 1957; see also Glick and Tewari, 1966).

A.4. Orientation-Dependent Doublet Structure on NMR Spectral Line Shape

In a solid, where all the atoms take fixed positions, a magnetic dipole does experience not only the applied magnetic field but also a local field due to its neighboring magnetic nuclei. A precessing magnetic nucleus generates a local magnetic field H_{loc} at

a distance r and an angle α between the external magnetic field and the line spanning the internuclear distance, so that the effective magnetic field at the position of the neighboring nucleus is

$$H_{\text{eff}} = H_0 \pm (\gamma\mu_n/2r^3)(3 \cos^2 \alpha - 1) \quad (\text{A.11})$$

where γ is the magnetogyric ratio and μ_n is the nuclear magneton, which is related to the charge and mass of the nuclide and for the proton is equal to 5.05×10^{-24} erg gauss $^{-1}$. Thus, the neighboring magnetic nucleus is in a magnetic field either a little greater or a little smaller than H_0 , the difference varying with the angle α . The result is that the NMR signal no longer appears as a single line but as two lines, i.e., a doublet. The appearance of a doublet signal is possible only in a solid and when the magnetic nuclei occur in closely situated pairs like the two protons in a water molecule. Other nuclei nearby may also modify the effective field, creating a general blurred line broadening. In the liquid state, the nuclei tumble about and the local field averages out. As a result only a single line is seen.

B

Infrared and Raman Spectra

When sunlight is examined through a spectroscope the spectrum contains many dark lines (called *Fraunhofer lines* after the Bavarian physicist Joseph von Fraunhofer). These dark lines are due to the absorption of light of certain characteristic wavelengths by elements present in the vapor envelope of the sun. Similarly if white light passes through the vapor of a pure element, an *absorption spectrum* consisting of many dark lines of different wavelengths is seen. On the other hand, if vapor of the same element is heated, bright lines at exactly the same wavelengths are seen and this type of spectrum is called an *emission spectrum*.

While the spectral lines in the spectra of pure elements are very sharp and narrow, a much broader kind of line or band is seen in the spectra of molecules. A closer look reveals that each of the broader lines consists of a series of very closely placed lines that are due to the vibrational sublevels, and that each vibrational sublevel in turn contains a number of still more closely placed lines due to the rotational sublevels. The energy difference between successive vibrational energy levels is from $\frac{1}{10}$ to $\frac{1}{100}$ of that between successive electronic levels, and that between successive rotational sublevels is about $\frac{1}{100}$ of that between vibrational sublevels.

The radiation accompanying purely vibrational changes appears in the near infrared (IR) region with wavelengths near 10 μm . Actually vibrational transition is always accompanied by rotational energy changes, and these vibration-rotation bands are in the range of 1–23 μm . Purely rotational transitions yield band spectra at far IR regions with wavelengths of about 200 μm . Another way to describe the atomic and molecular spectra is to use *wave numbers*, $\bar{\nu}$, given in units of cm^{-1} , which represent the number of wavelengths per centimeter. Thus a 10- μm near-IR band corresponds to a $\bar{\nu}$ of $1 \text{ cm}/10 \mu\text{m} = 1/0.001 = 100 \text{ cm}^{-1}$; a 200- μm band corresponds to a $\bar{\nu}$ of 50 cm^{-1} .

The vibrational levels are designated as 0, 1, 2, 3, and so on. When the vibrational energy changes from level 0 to level 1, the absorption band is called the *fundamental*; when it changes from level 0 to level 2, the *first overtone* band, and from 0 to level 3, the *second overtone* band.

To obtain good IR spectra is difficult, especially in the far IR region and in samples that are inhomogeneous and opaque. In the latter case, another kind of spectrum, called

the *Raman spectrum* (due to C. R. Raman), is often useful. When any substance, gas, liquid, or solid, is exposed to radiation of definite frequency, the light scattered at right angles contains frequency characteristics of the radiated substance. If $\bar{\nu}_i$ is the frequency of the incident light, and $\bar{\nu}_s$ that of scattered light, then the difference $\bar{\nu}_i - \bar{\nu}_s = \Delta\bar{\nu}$ is called the *Raman frequency*. The energy $hc\Delta\bar{\nu}$ is the energy difference between the initial and final state, where h is Planck's constant (6.625×10^{-27} erg · sec) and c is the velocity of light (2.998×10^{10} cm/sec). It has been shown that $hc\Delta\bar{\nu}$ is almost invariably equal to the change in rotational and vibrational energy levels of the molecule.

References

- Abbé Nollet, 1748, see Glasstone (1946, p. 651); Findlay (1919).
- Abelson, P. H., and Duryee, W. R., 1949, *Biol. Bull.* **96**:205.
- Abetsedarskaya, L. A., Miftakhutdinova, F. G., Fedotov, V. D., and Mal'tsev, N. A., 1967, *Mol. Biol.* **1**:451.
- Abetsedarskaya, L. A., Miftakhutdinova, F. G., and Fedotov, V. D., 1968, *Biofizika* **13**:630 [Russian], *Biophysics* [English transl.] **13**:750.
- Abragam, A., 1961, *The Principles of Nuclear Magnetism*, Oxford University Press, London.
- Addanki, S., Cahill, F. D., and Sotos, J. F., 1968, *J. Biol. Chem.* **243**:2337.
- Adelman, W. J., and Senft, J. P., 1966, *J. Gen. Physiol.* **50**:279.
- Adelstein, R. S., and Eisenberg, E., 1980, *Annu. Rev. Biochem.* **49**:921.
- Adrian, R. H., 1956, *J. Physiol.* **133**:631.
- Adrian, R. H., 1969, *Prog. Biophys. Mol. Biol.* **19**:341.
- Aebi, H., 1952, *Helv. Physiol. Pharmacol. Acta* **10**:184.
- Aithal, H. N., and Toback, F. G., 1978, *Lab. Invest.* **39**:186.
- Akedo, H., and Christensen, H. N., 1962, *J. Biol. Chem.* **237**:118.
- Allen, R. D., and Kamiya, N., 1964, *Primitive Motile Systems in Cell Biology*, Academic Press, New York.
- Alonso, M. A., and Carrasco, L., 1981, *J. Virol.* **37**:535.
- Ames, B. N., Lee, F. D., and Durston, W. E., 1973, *Proc. Natl. Acad. Sci. USA* **70**:782.
- Ananthanarayanan, V. S., and Hew, C. L., 1977, *Nature* **268**:560.
- Anderson, P., and Bauer, W., 1978, *Biochemistry* **17**:594.
- Andreoli, T. E., Tieffenberg, M., and Tosteson, D. C., 1967, *J. Gen. Physiol.* **50**:2527.
- Anson, M. L., 1941-1942, *J. Gen. Physiol.* **25**:355.
- Antonini, E., Wyman, J., Moretti, R., and Rossi-Fanelli, A., 1963, *Biochim. Biophys. Acta* **71**:124.
- Antonini, E., Wyman, J., Belleli, L., Ruman, N., and Siniscalco, M., 1964, *Arch. Biochem. Biophys.* **105**:404.
- Araki, T., and Otani, T., 1955, *J. Neurophysiol.* **18**:472.
- Araku, Y., 1968, *J. Biol. Chem.* **243**:3128.
- Ariëns, E. J., 1964, *Molecular Pharmacology: The Mode of Action of Biologically Active Compounds*, Vol. 1, Academic Press, New York.
- Ariëns, E. J., Simonis, A. M., and de Groot, W. M., 1954, *Arch. Int. Pharmacodyn. Ther.* **100**:298.
- Ariëns, E. J., Van Rossum, J. M., and Simonis, A. M., 1957, *Pharm. Rev.* **9**:218.
- Armstrong, C. M., 1971, *J. Gen. Physiol.* **58**:413.
- Armstrong, C. M., 1975, in: *Membranes: A Series of Advances*, Vol. III (G. Eisenman, ed.), Academic Press, New York, p. 325.
- Aronson, P. S., and Sacktor, B., 1975, *J. Biol. Chem.* **250**:6032.
- Arrhenius, S., 1887, *Z. Physik. Chem.* **1**:631.
- Asakura, S., Kasai, M., and Oosawa, F., 1960, *J. Polym. Sci.* **44**:35.
- Ashbel, R., 1929, *Boll. Soc. Ital. Biol. Sper.* **4**:492.

- Ashburner, M., 1970, *Adv. Insect Physiol.* 7:1.
- Ashburner, M., 1973, *Dev. Biol.* 35:47.
- Ashburner, M., and Bonner, J. J., 1979, *Cell* 17:241.
- Ashburner, M., and Richards, G., 1976, *Dev. Biol.* 54:241.
- Avery, O. T., MacLeod, C. M., and McCarty, M., 1944, *J. Exp. Med.* 79:137.
- Azzone, G. F., and Azzi, A., 1966, *Biochim. Biophys. Acta* 7:332.
- Bagshaw, C. R., Eccleston, J. F., Eckstein, F., Goody, R. S., Gutfreund, H., and Trentham, D. R., 1974, *Biochem. J.* 141:351.
- Bagshaw, J. C., and Warner, A. H., 1979, *Biochemistry of Artemia Development* University Microfilms International, Ann Arbor, Michigan, p. 239.
- Bailey, K., 1946, *Nature* 157:368.
- Bailey, K., 1948, *J. Biochem.* 43:271.
- Baker, P. F., Hodgkin, A. L., and Shaw, T. I., 1961, *Nature* 190:885.
- Baker, P. F., Foster, R. F., Gilbert, D. S., and Shaw, T. I., 1971, *J. Physiol.* 219:487.
- Balbiani, E. G., 1881, *Zool. Anz.* 1:637 and 662.
- Baltimore, D., 1969, in: *Biochemistry of Viruses* (H. B. Levy, ed.), Marcel Dekker, New York.
- Barnford, C. H., Elliott, A., and Hanby, W. E., 1956, *Synthetic Polypeptides*, Academic Press, New York.
- Banks, B. E. C., and Vernon, C. A., 1970, *J. Theor. Biol.* 29:301.
- Barnes, H., 1954, *J. Exp. Biol.* 31:582.
- Barnes, T. C., and Beutner, R., 1949, *Nature* 164:109.
- Barth, L. G., and Barth, L. J., 1959, *J. Embryol. Expt. Morphol.* 7:210.
- Barth, L. G., and Barth, L. J., 1962, *J. Morphol.* 110:347.
- Barth, L. G., and Barth, L. J., 1963, *Biol. Bull.* 124:125.
- Barth, L. G., and Barth, L. J., 1964, *Biol. Bull.* 127:413.
- Barth, L. G., and Barth, L. J., 1967, *Biol. Bull.* 133:495.
- Barth, L. G., and Barth, L. J., 1972, *Biol. Bull.* 28:18.
- Barth, L. G., and Barth, L. J., 1974a, *Dev. Biol.* 39:1.
- Barth, L. G., and Barth, L. J., 1974b, *Biol. Bull.* 146:313.
- Baserga, R., 1981, *N. Engl. J. Med.* 304:453.
- Bauereisen, E., 1962, *Physiologist* 5:293.
- Baulieu, E. E., Godeau, F., Shorderet, M., and Schorderet-Slatkine, S., 1978, *Nature* 275:593.
- Baur, E., 1913, *Z. Elektrochem.* 19:590.
- Baur, E., and Kronmann, S., 1917, *Z. Phys. Chem.* 92:81.
- Bautzmann, H., 1926, *Arch. Entwicklungsmech. (Roux's)* 108:283.
- Bayliss, W. M., 1918, *Principles of General Physiology*, 2nd ed., Longmans, Green, London and New York.
- Bayliss, W. M., 1927, *Principles of General Physiology*, 4th ed., Longmans, Green, London and New York.
- Beck, J. C., and Sacktor, 1975, *J. Biol. Chem.* 250:8874.
- Becker, F. F., and Green, H., 1960, *Exp. Cell Res.* 19:361.
- Becker, H. J., 1962, *Chromosoma* 13:341.
- Beckwith, J., and Zipser, D., 1970, *The Lactose Operon*, Cold Spring Harbor Laboratory, Cold Spring Harbor, New York.
- Beermann, W., 1952, *Chromosoma* 5:139.
- Beermann, W., 1973, *Chromosoma* 41:297.
- Beermann, W., and Clever, J., 1964, *Sci. Am.* 210:50.
- Behnel, J., and Rensing, L., 1975, *Exp. Cell Res.* 91:119.
- Belton, P. S., Jackson, R. R., and Packer, K. J., 1972, *Biochim. Biophys. Acta* 286:16.
- Benbow, R. M., and Ford, C. C., 1975, *Proc. Natl. Acad. Sci. USA* 72:2437.
- Bendall, J. R., 1951, *J. Physiol.* 114:71.
- Bendall, J. R., 1969, *Molecules and Movements: An Essay in the Contraction of Muscle*, American Elsevier, New York.
- Benesch, R. E., and Benesch, R., 1962, *Biochemistry* 1:735.
- Benesch, R. and Benesch, R. E., 1969, *Nature* 221:618.
- Benesch, R., Benesch, R. E., and Rogers, W. I., 1954, in: *Glutathione* (S. Colowick, ed.), Academic Press, New York, p. 31.

- Benson, S. W., and Ellis, D. A., 1948, *J. Am. Chem. Soc.* **70**:3563.
Benson, S. W., and Ellis, D. A., 1950, *J. Am. Chem. Soc.* **72**:2095.
Benson, S. W., Ellis, D. A., and Zwanzig, R. W., 1950, *J. Am. Chem. Soc.* **72**:2102.
Berendes, H. D., 1973, *Int. Rev. Cytol.* **35**:61.
Berendsen, H. J. C., and Edzes, H. T., 1973, *Ann. N.Y. Acad. Sci.* **204**:459.
Berger, M., 1957, *Biochim. Biophys. Acta* **23**:504.
Bernal, J. D., and Fankuchen, I., 1941, *J. Gen. Physiol.* **25**:111.
Bernstein, A., Hunt, D. M., Crichley, V., and Mak, T. W., 1976, *Cell* **9**:375.
Bernstein, J., 1902, *Pflügers Arch. Ges. Physiol.* **92**:521.
Bernstein, J., 1905, *Pflügers Arch. Ges. Physiol.* **109**:323.
Bernstein, J., 1908, *Pflügers Arch. Ges. Physiol.* **122**:129.
Bernstein, J., 1912, *Elektrobiologie*, F. Vieweg und Sohn, Braunschweig.
Bernstein, R. E., 1954, *Science* **120**:459.
Berthelot, M., and Jungfleisch, H., 1872, *Ann. Chim. Phys.* **26**:396.
Best, C. H., and Taylor, N. B., 1945, *The Physiological Basis of Medical Practice*, 4th ed., Williams and Wilkins, Baltimore.
Bethe, A., and Toropoff, T., 1914, *Z. Phys. Chem.* **88**:686.
Bethe, A., and Toropoff, T., 1915, *Z. Phys. Chem.* **89**:597.
Beutner, R., 1914, *Z. Phys. Chem.* **87**:385.
Beutner, R., 1920, *Die Entstehung elektrischer Ströme in lebenden Geweben und ihre künstliche Nachahmung durch synthetische organische Substanzen*, Enke, Stuttgart.
Beutner, R., 1944, in *Medical Physics*, Vol. I (O. Glasser, ed.), Year Book Publishers, Chicago.
Bezanilla, F., and Armstrong, C. M., 1972, *J. Gen. Physiol.* **60**:588.
Biesmann, H., Beatrizlevy, W., and McCarthy, B. J., 1978, *Proc. Natl. Acad. Sci. USA* **75**:759.
Bjerrum, N., 1923, *Z. Phys. Chem.* **106**:219.
Blanchard, K. C., 1940, *Cold Spring Harbor Symp. Quant. Biol.* **8**:1.
Bleam, N. L., Anderson, C. F., and Record, M. T., 1980, *Proc. Natl. Acad. Sci. USA* **77**:3085.
Blicharska, B., Florkowski, Z., Hennel, J. W., Held, G., and Noack, F., 1970, *Biochim. Biophys. Acta* **207**:381.
Blinks, L. R., 1930, *J. Gen. Physiol.* **13**:495.
Block, F., Hansen, W. W., and Packard, M., 1946, *Phys. Rev.* **70**:474.
Bloembergen, M., Purcell, E. M., and Pound, R. V., 1948, *Phys. Rev.* **73**:679.
Blondin, G. A., and Green, D. E., 1967, *Proc. Natl. Acad. Sci. USA* **58**:612.
Bodemann, H. H., and Hoffman, J. F., 1976, *J. Gen. Physiol.* **67**:497.
Bodemann, H. H., and Passow, H., 1972, *J. Membr. Biol.* **8**:1.
Bone, S., Cascoyne, P. R. C., and Pethig, R., 1977, *J. Chem. Soc. Faraday Trans.* **73**:1605.
Bonner, J. J., and Pardue, M. L., 1976, *Cell* **8**:43.
Bonner, O. D., 1978, *Physiol. Chem. Phys.* **10**:399.
Bonner, W. M., 1975, *J. Cell Biol.* **64**:421.
Bonninger, M., 1909, *Z. Exp. Pathol.* **7**:556.
Bonting, S. L., 1970, in: *Membranes and Ion Transport*, Vol. 1 (E. E. Bittar, ed.), Wiley-Interscience, New York, p. 257.
Bonting, S. L., and Caravaggio, L. L., 1963, *Arch. Biochem. Biophys.* **101**:37.
Born, M., 1920, *Z. Phys.* **1**:221.
Botts, J., and Morales, M. F., 1951, *J. Cell. Comp. Physiol.* **37**:27.
Boveri, T., 1914, *Zur Frage der Entstehung maligner Tumoren*, Fischer, Jena [English translation by M. Boveri, Baltimore, 1929].
Bowen, W. J., and Mandelkern, L., 1971, *Science* **173**:239.
Boyer, P. D., 1965, in: *Oxidase and Related Redox Systems* (T. E. King, H. S. Mason, and M. Morrison, eds.), Wiley, New York, p. 994.
Boyer, P. D., Cross, R. L., Chude, O., Dahms, A. S., and Kanazawa, T., 1972, in: *Biochemistry and Biophysics of Mitochondrial Membranes* (G. F. Azzone, E. Carafoli, A. L. Lehninger, E. Qualierello, and N. Siliprandi, eds.), Academic Press, New York, p. 343.
Boyle, P. J., and Conway, E. J., 1941, *J. Physiol.* **100**:1.
Bozler, E., 1953, *Am. J. Physiol.* **168**:760.

- Brachet, J., and Denis-Donini, S., 1977, *C. R. Acad. Sci. Ser. D* **284**:1091.
- Bradley, S., 1936, *J. Chem. Soc.* **1936**:1467.
- Bragg, W. L., and Williams, E. J., 1934, *Proc. R. Soc. London Ser. A* **145**:699.
- Branch, G. E. K., and Calvin, M., 1941, *The Theory of Organic Chemistry: An Advanced Course*, Prentice Hall, Englewood Cliffs, New Jersey.
- Brand, J. C. D., and Speakman, J. C., 1960, *Molecular Structure: The Physical Approach*, Edward Arnold, London.
- Bratton, L. B., Hopkin, A. L., and Weinberg, J. W., 1965, *Science* **147**:738.
- Braun, A. C., 1953, *Bot. Gaz.* **114**:363.
- Braun, A. C., 1959, *Proc. Natl. Acad. Sci. USA* **45**:932.
- Bregman, J. I., 1953, *Ann. N. Y. Acad. Sci.* **57**:125.
- Bremer, K., 1970, *Cold Spring Harbor Symp. Quant. Biol.* **35**:109.
- Brenner-Holzach, O., and Raafaub, J., 1954, *Helv. Physiol. Pharmacol. Acta* **12**:242.
- Bresler, S. E., 1949, *Biokhimiya* **14**:180.
- Bridges, C. B., 1935, *J. Hered.* **26**:60.
- Brierly, G. P., Jurkowitz, M., 1976, *Biochem. Biophys. Res. Commun.* **68**:82.
- Brierly, G. P., Jurkowitz, M., Scott, K. M., and Merda, J., 1970, *J. Biol. Chem.* **245**:5405.
- Briggs, D. R., 1932, *J. Phys. Chem.* **36**:367.
- Briggs, R., and King, T. J., 1952, *Proc. Natl. Acad. Sci. USA* **38**:455.
- Brinley, F. J., and Mullins, L. J., 1968, *J. Gen. Physiol.* **52**:181.
- Brooks, S. C., 1937, *Trans. Faraday Soc.* **33**:1002.
- Brooks, S. C., 1939, *J. Cell. Comp. Physiol.* **11**:383.
- Brooks, S. C., 1940, *Cold Spring Harbor Symp. Quant. Biol.* **8**:171.
- Brooks, S. C., and Brooks, M. M., 1941, *The Permeability of Living Cells* (J. W. Edwards, transl.), University of Michigan Press, Ann Arbor.
- Brues, A. M., Wesson, L. G., and Cohn, W. E., 1946, *Anat. Rec.* **94**:451.
- Brun, R. B., 1978, *Dev. Biol.* **65**:271.
- Brunauer, S., Emmett, P. H., and Teller, E., 1938, *J. Am. Chem. Soc.* **60**:309.
- Buchanan, T. J., Haggis, G. H., Hasted, J. B., and Robinson, B. G., 1952, *Proc. R. Soc. London Ser. A* **213**:379.
- Buchthal, F., 1947, *Annu. Rev. Physiol.* **9**:119.
- Buck, B., and Goodford, P. J., 1966, *J. Physiol.* **183**:551.
- Buckley, C. E., Whitney, P. L., and Tanford, C., 1963, *Proc. Natl. Acad. Sci. USA* **50**:827.
- Bugarszky, S., and Liebermann, L., 1898, *Arch. Ges. Physiol.* **72**:51.
- Buij, K., and Choppin, G. R., 1940, *J. Chem. Phys.* **8**:63.
- Bull, H., 1944, *J. Am. Chem. Soc.* **66**:1499.
- Bull, H. B., 1946, *Q. Bull. Northwest Univ. Med. Sch.* **20**: 175.
- Bull, H. B., and Breese, K., 1968a, *Arch. Biochem. Biophys.* **128**:488.
- Bull, H. B., and Breese, K., 1968b, *Arch. Biochem. Biophys.* **128**:497.
- Bunch, W. H., and Kallsen, G., 1969, *Science* **164**:1178.
- Bungenberg de Jong, H. G., 1932, *Protoplasma* **15**:110.
- Bungenberg de Jong, H. G., 1949, in: *Colloid Science*, Vol. II (H. R. Kruyt, ed.), Elsevier, New York, p. 287.
- Bungenberg de Jong, H. G., and Kruyt, H. R., 1929, *K. Ned. Akad. Wet.* **32**:849.
- Burawoy, A., 1959, in: *Hydrogen Bonding* (D. Hadzi and H. W. Thompson, eds.), Pergamon Press, New York, p. 259.
- Burdon-Sanderson, J. S., and Gotch, F., 1891, *J. Physiol.* **12**:XLIII.
- Burnet, F. M., 1957, *Br. Med. J.* **1**:779 and 841.
- Burnet, F. M., 1974, in: *Chromosomes and Cancer* (J. German, ed.), Wiley, New York, p. 21.
- Burns, F. J., and Tannock, I. F., 1970, *Cell Tissue Kinet.* **3**:321.
- Burnstock, G., 1958, *J. Physiol.* **143**:183.
- Buser, W., Graf, P., and Grutter, W. F., 1955, *Chimia* **9**:73.
- Bütschli, O., 1894, *Investigation on Microscopic Foams and on Protoplasm* (E. A. Minchin, transl.), Black, London.

- Bystrov, G. S., Romanenko, G. I., Nikolaev, N. I., Grigoreva, G.N.A., and Atamanchuk, L., 1972, *Bio-physics USSR* 17:649.
- Cabantchik, Z. I., Balshin, M., Breuer, W., and Rothstein, A., 1975, *J. Biol. Chem.* 250:5130.
- Caillé, J. P., and Hinke, J. A. M., 1974, *Can. J. Physiol. Pharmacol.* 52:814.
- Cairnie, A. B., Lala, P. K., and Osmond, D. G., 1976, *Stem Cells of Renewing Cell Populations*, Academic Press, New York.
- Cairns, J., 1975, *Nature* 255:197.
- Cairns, J., 1981, *Nature* 289:353.
- Caldwell, P. C., 1954, *J. Physiol. (London)* 126:169.
- Caldwell, P. C., 1968, *Physiol. Rev.* 48:1.
- Caldwell, P. C., and Keynes, R. D., 1959, *J. Physiol.* 148:8P.
- Caldwell, P. C., Hodgkin, A. L., Keynes, R. D., and Shaw, T. I., 1960, *J. Physiol.* 152:561.
- Calhoun, J. A., and Harrison, T. R., 1931, *J. Clin. Invest.* 10:139.
- Cannon, C. G., 1955, *Mikrochim. Acta* 2-3:555.
- Caputo, C., 1966, *J. Gen. Physiol.* 50:129.
- Cardon, J. W., and Boyer, P. D., 1978, *Eur. J. Biochem.* 92:443.
- Carey, J. J., and Conway, E. J., 1954, *J. Physiol.* 125:232.
- Carpenter, D. O., Hovey, M. M., and Bak, A. F., 1973, *Ann. N. Y. Acad. Sci.* 204:502.
- Carrasco, L., 1977, *FEBS Lett.* 76:11.
- Carrasco, L., and Smith, A. E., 1976, *Nature* 264:807.
- Carvalho, A. P., and Leo, B., 1967, *J. Gen. Physiol.* 50:1327.
- Cavatorta, F., Fontana, M. P., and Vecchi, A. R., 1976, *J. Chem. Phys.* 65:3635.
- Cereijido, M., and Rotunno, C. A., 1967, *J. Physiol. (London)* 190:481.
- Cereijo-Santalo, R., 1970, in: *Membranes and Ion Transport*, Vol. 2 (E. E. Bittar, ed.), Wiley-Interscience, New York, p. 229.
- Chalazonitis, A., and Fishbach, G. D., 1980, *Dev. Biol.* 78:173.
- Chambers, E. L., 1974, *Biol. Bull.* 147:471.
- Chambers, E. L., 1975, *J. Cell Biol.* 67:60a.
- Chambers, E. L., 1976, *J. Exp. Zool.* 197:149.
- Chambers, E. L., and Dimich, R. A., 1975, *J. Gen. Physiol.* 66:9a.
- Chambers, R., and Chambers, E. L., 1961, *Explorations into the Nature of the Living Cell*, Harvard University Press, Cambridge, Massachusetts.
- Chambers, R., and Hale, H. P., 1932, *Proc. R. Soc. London Ser. B* 110:336.
- Chambers, R., and Höfler, K., 1931, *Protoplasma* 12:338.
- Chambers, R., and Kao, C. Y., 1952, *Exp. Cell Res.* 3:564.
- Chance, B., 1964, *Fed. Proc.* 22:404.
- Chance, B., and Williams, G. R., 1956, *Adv. Enzymol.* 17:65.
- Chance, B., and Yoshioka, T., 1966, *Arch. Biochem. Biophys.* 117:451.
- Chance, B., Williams, G. R., and Hollunger, G., 1963, *J. Biol. Chem.* 238:439.
- Chandler, W. K., and Meves, H., 1965, *J. Physiol.* 180:788.
- Chang, D. C., and Woessner, D. E., 1978, *J. Magn. Reson.* 30:185.
- Chang, D. C., Hazlewood, C. F., Nichols, B. L., and Rorschach, H. E., 1972, *Nature* 235:170.
- Chang, D. C., Rorschach, H. E., Nichols, B. L., and Hazlewood, C. F., 1973, *Ann. N.Y. Acad. Sci.* 204:434.
- Chanutin, A., and Curnish, R. R., 1964, *Arch. Biochem. Biophys.* 106:433.
- Chanutin, A., and Curnish, R. R., 1967, *Arch. Biochem. Biophys.* 121:96.
- Chapman, G., and McLaughlan, K. A., 1967, *Nature* 215:391.
- Chapman, N. B., and Shorter, J. (eds.), 1972, *Advances in Linear Free Energy Relationships*, Plenum Press, New York.
- Chappell, J. B., 1964, *Biochem. J.* 90:237.
- Chappell, J. B., and Crofts, A. R., 1965, *Biochem. J.* 95:393.
- Charmasson, R., 1981, *Physiol. Chem. Phys.* 13:11.
- Chiang, M. C., and Tai, T. C., 1963, *Sci. Sin.* 12:785.
- Chiariotti, G., and Giulotto, L., 1954, *Phys. Rev.* 93:1241.

- Chimadzhev, Y. A., Muler, A. L., and Markin, V. S., 1972, *Biofizika* **17**:1012.
- Chock, S. P., Chock, P. B., and Eisenberg, E., 1979, *J. Biol. Chem.* **254**:3244.
- Chou, P. Y., and Fasman, G. D., 1974, *Biochemistry* **13**:211.
- Christensen, H. N., 1970, in: *Membranes and Ion Transport*, Vol. 1 (E. E. Bittar, ed.), Wiley-Interscience, New York, p. 365.
- Christensen, H. N., and Liang, M., 1966, *J. Biol. Chem.* **241**:5542, 5552.
- Christensen, H. N., Riggs, T. R., Fischer, H., and Palatine, I. M., 1952, *J. Biol. Chem.* **198**:1.
- Christian, J. H. B., and Walther, J. A., 1962, *Biochim. Biophys. Acta* **65**:506.
- Christie, G. S., Ahmed, K., McLean, A. E. M., and Judah, J. D., 1965, *Biochim. Biophys. Acta* **94**:432.
- Civan, M. M., and Shporer, M., 1972, *Biophys. J.* **12**:404.
- Civan, M. M., and Shporer, M., 1974, *Biochim. Biophys. Acta* **343**:399.
- Civan, M. M., McDonald, G. G., Pring, M., and Shporer, M., 1976, *Biophys. J.* **16**:1385.
- Clark, A. J., 1926, *J. Physiol. (London)* **61**:547.
- Clark, A. J., 1933, *The Mode of Action of Drugs on Cells*, 3rd. ed., Edward Arnold, London.
- Clegg, J. S., Szwarnowski, S., McClean, V. E. R., Scheppard, R. J., and Grant, E. H., 1982, *Biochim. Biophys. Acta* **721**:458.
- Cleveland, G. G., Chang, D. C., Hazlewood, C. F., and Rorschach, H. E., 1976, *Biophys. J.* **16**:1403.
- Clever, U., 1965, *Chromosoma* **17**:309.
- Cloud, J. G., and Schuetz, A. W., 1977, *Dev. Biol.* **60**:359.
- Cockrell, R. S., Harris, E. J., and Pressman, B. C., 1967, *Nature* **215**:1487.
- Cohen, G. N., and Monod, J., 1957, *Bacteriol. Rev.* **21**:169.
- Cohn, W. E., and Cohn, E. T., 1939, *Proc. Soc. Exp. Biol. Med.* **41**:445.
- Colacicco, G., 1965, *Nature* **207**:936.
- Cole, K. S., 1932, *J. Cell. Comp. Physiol.* **1**:1.
- Cole, K. S., 1949, *Arch. Sci. Physiol.* **3**:253.
- Cole, K. S., and Cole, R. H., 1941, *J. Chem. Phys.* **9**:341.
- Cole, K. S., and Curtis, H. J., 1938-1938a, *J. Gen. Physiol.* **22**:37.
- Cole, K. S., and Curtis, H. J., 1938-1939b, *J. Gen. Physiol.* **22**:649.
- Cole, K. S., and Hodgkin, A. L., 1938-1939, *J. Gen. Physiol.* **22**:671.
- Collander, R., 1937, *Trans. Faraday Soc.* **33**:985.
- Collander, R., 1959, in: *Plant Physiology*, Vol. 2 (F. C. Steward, ed.), Academic Press, New York, p. 3.
- Collander, R., and Bärlund, H., 1933, *Acta Bot. Fenn.* **11**:1.
- Cone, C. D., 1969, *Trans. N.Y. Acad. Sci.* **31**:404.
- Cone, C. D., 1971, *J. Theor. Biol.* **30**:151.
- Cone, C. D., 1974, *Ann. N.Y. Acad. Sci.* **238**:420.
- Cone, C. D., and Cone, C. M., 1976, *Science* **192**:155.
- Cone, C. D., and Cone, C. M., 1978, *Exp. Neurol.* **60**:41.
- Conklin, E. G., 1905, *J. Exp. Zool.* **2**:185.
- Conklin, E. G., 1906, *Arch. Entwicklungsmech. (Roux's)* **21**:727.
- Constantin, L. L., and Taylor, S. R., 1971, *J. Physiol. (London)* **218**:13P.
- Conway, E. J., 1946, *Nature* **157**:715.
- Conway, E. J., 1955, *Int. Rev. Cytol.* **4**:377.
- Conway, E. J., and Duggan, F., 1958, *Biochem. J.* **69**:265.
- Conway, E. J., Kernan, R. P., and Zadunaisky, J. A., 1961, *J. Physiol.* **155**:263.
- Cooke, E., 1898, *J. Physiol. (London)* **23**:137.
- Cooke, R., and Kuntz, I. D., 1974, *Annu. Rev. Biophys. Bioengin.* **3**:95.
- Cooke, R., and Wien, R., 1971, *Biophys. J.* **11**:1002.
- Cookson, B. A., and Wiercinski, F., 1949, *Biol. Bull.* **97**:226.
- Coombs, J. S., Eccles, J. C., and Fatt, P., 1955, *J. Physiol.* **130**:291.
- Cooper, G. M., 1982, *Science* **217**:801.
- Cooper, G. M., Okenquist, S., and Silverman, L., 1980, *Nature* **284**:418.
- Cope, F. W., 1967, *J. Gen. Physiol.* **50**:1353.
- Cope, F. W., 1969, *Biophys. J.* **9**:303.
- Cope, F. W., 1970a *Biophys. J.* **10**:843.
- Cope, F. W., 1970b, *Physiol. Chem. Phys.* **2**:545.

- Cope, F. W., and Damadian, R., 1970, *Nature* **228**:76.
- Cope, F. W., and Damadian, R., 1974, *Physiol. Chem. Phys.* **6**:17.
- Corabœuf, E., and Weidemann, S., 1954, *Helv. Physiol. Acta* **12**:32.
- Cori, C. F., and Cori, G. T., 1925a, *J. Biol. Chem.* **64**:11.
- Cori, C. F., and Cori, G. T., 1925b, *J. Biol. Chem.* **65**:397.
- Costello, D. P., 1932, *Protoplasma* **17**:239.
- Cowie, D. B., and Walton, B. P., 1956, *Biochim. Biophys. Acta* **21**:211.
- Crane, R. K., 1960, *Physiol. Rev.* **40**:789.
- Crane, R. K., 1962, *Fed. Proc.* **21**:891.
- Crane, R. K., 1965, *Fed. Proc.* **24**:1000.
- Crane, R. K., Miller, D., and Bihler, I., 1961, in: *Membrane Transport and Metabolism* (A. Kleinzeller and A. Kotyk, eds.), Academic Press, London, p. 439.
- Crane, R. K., Malathi, P., and Preiser, H., 1976, *FEBS Lett.* **67**:214.
- Crank J., 1956, *The Mathematics of Diffusion*, Clarendon Press, Oxford.
- Creese, R., Hashish, S. E. E., and Scholes, N. W., 1958, *J. Physiol. (London)* **143**:307.
- Cremer, M., 1906, *Z. Biol.* **47**:562.
- Crepin, M., Cukierka, R., and Cros, R., 1975, *Proc. Natl. Acad. Sci. USA* **72**:333.
- Crompton, M., Capano, M., and Carafoli, E., 1976, *Biochem. J.* **154**:735.
- Cuny, H., 1965, *Ivan Pavlov: The Man and His Theories* (P. Evans, transl.), Souvenir Press, London.
- Curran, P. F., and McIntosh, J. R., 1962, *Nature* **193**:347.
- Curran, P. F., Herrera, K. C., and Flanigan, W. J., 1963, *J. Gen. Physiol.* **46**:1011.
- Curtin, N. A., and Woledge, R. C., 1975, *J. Physiol. (London)* **246**:737.
- Czaky, T. Z., and Thale, M., 1960, *J. Physiol. (London)* **151**:59.
- Czarnetzky, E. J., and Schmidt, C. L. A., 1931, *J. Biol. Chem.* **92**:453.
- Czeisler, J. L., and Swift, T. J., 1973, *Ann. N.Y. Acad. Sci.* **204**:261.
- Czeisler, J. L., Fritz, O. G., Jr., and Swift, T. J., 1970, *Biophys. J.* **10**:260.
- Dalcq, A., 1957, *Introduction to General Embryology*, Oxford University Press, Oxford.
- Dalton, R. W., McClanahan, J. L., and Maatman, R. W., 1962, *J. Colloid Sci.* **17**:207.
- Damadian, R., 1971, *Science* **171**:1151.
- Damadian, R., and Cope, F. W., 1973, *Physiol. Chem. Phys.* **5**:511.
- Daneholt, B., and Edström, J. E., 1967, *Cytogenetics* **6**:350.
- Das, M., 1980, *Proc. Natl. Acad. Sci. USA* **77**:112.
- Dasgupta, S., 1962, *J. Exp. Zool.* **151**:105.
- Daszkiewicz, O. K., Hennel, J. W., Lubas, B., and Szczepkowski, T. W., 1963, *Nature* **200**:1006.
- Dausse, J. P., Sentenac, A., and Fromageo, P., 1976, *Eur. J. Biochem.* **65**:387.
- Davson, H., and Danielli, J. F., 1943, *The Permeability of Natural Membranes*, 2nd ed., Cambridge University Press, London.
- Dean, P. M., and Matthews, E. K., 1970, *J. Physiol.* **210**:265.
- Dean, R. B., 1940, *J. Cell. Comp. Physiol.* **15**:189.
- Dean, R. G., 1941, *Biol. Symp.* **3**:331.
- de Asua, L. J., O'Farrell, M., Bennett, D., Clingan, D., and Rutland, P., 1977, *Nature* **265**:151.
- de Boer, J. H., and Zwikker, C., 1929, *Z. Phys. Chem. Abt. B* **3**:407.
- Debye, P., 1929, *Polar Molecules*, Dover, New York.
- Debye, P., and Hückel, W., 1923, *Phys. Z.* **24**:185.
- de Haseth, P. L., Lohman, T. M., and Record, M. T., Jr., 1977, *Biochemistry* **16**:4783.
- Dehmelt, H. G., and Krüger, H., 1950, *Naturwissenschaften* **37**:111.
- Delage, Y., 1910, in: *Verhandlungen des VIII. International Kongress der Zoologie, Graz*, p. 100.
- DeLong, J., and Civan, M. M., 1978, *J. Membr. Biol.* **42**:19.
- DeLong, J., and Civan, M. M., 1979, *Colloq. Inst. Natl. Santé Rech. Med.* **85**:221.
- DeLong, J., and Civan, M. M., 1980, *Curr. Top. Membr. Transp.* **13**:93.
- Del Re, G., 1958, *J. Chem. Soc.* **1958**:4031.
- Demmink, H. W., 1962, *De Lekkage en de Opname van Kaliumionen bij de Gistcel Drukkerij Luctor et Emergo*, Leiden.

- de Phillips, H. A., 1965, Ph.D. Thesis, Department of Chemistry, Northwestern University [cited in Klotz, I., 1965, *Fed. Proc.* **24**:S24].
- Derick, C. G., 1911, *J. Am. Chem. Soc.* **33**:1152.
- de Robertis, E. M., Longthorne, R. F., and Gurdon, J. B., 1978, *Nature* **272**:254.
- Devaux, H., 1904-1916, *P. V. Séances Soc. Sci. Phys. Nat. Bordeaux*, January 7, 1904; January 27, 1916; February 10, 1916.
- de Vries, A. L., Komatsu, S. K., and Fenney, R. E., 1970, *J. Biol. Chem.* **245**:2901.
- de Vries, A. L., and Wohlschlag, D. E., 1969, *Science* **163**:1073.
- de Vries, H., 1871, *Arch. Neerl. Sci.* **6**:117.
- de Vries, H., 1885, *Jahrb. Wiss. Bot.* **16**:465.
- de Vries, H., 1888a, *Z. Phys. Chem.* **2**:415.
- de Vries, H., 1888b, *Bot. Z.* **46**:229.
- Diamond, J. M., and Bossert, W. H., 1967, *J. Gen. Physiol.* **50**: 2061.
- Dick, D. A. T., and McLaughlin, S. G., 1969, *J. Physiol. (London)* **205**:61.
- Dickens, F., and Simer, F., 1931, *Biochem. J.* **25**:985.
- Dirkin, M. N., and Mook, H. W., 1931, *J. Physiol. (London)* **73**:349.
- Dodge, J. T., Mitchell, C., and Hanahan, D. J., 1963, *Arch. Biochem. Biophys.* **100**:119.
- Dole, M., and Faller, I. L., 1950, *J. Am. Chem. Soc.* **72**:414.
- Donnan, F. G., 1911, *Z. Elektrochem.* **17**:572.
- Donnan, F. G., 1924, *Chem. Rev.* **1**:73.
- Dorée, M., Guerrier, P., and Moreau, J., 1976, *Colloq. Int. CNRS* **251**:199.
- Dorsey, N. F., 1940, *Properties of Ordinary Water Substance*, ACS Monograph 81, American Chemical Society, New York.
- Doty, P., and Gratzer, W. B., 1962, in: *Polyamino Acids, Polypeptides and Proteins* (M. A. Stahmann, ed.), University of Wisconsin Press, Madison, p. 111.
- Dowben, R. M., 1969, *General Physiology: A Molecular Approach*, Harper and Row, New York.
- Dragomir, C. T., 1970, *J. Theor. Biol.* **27**:343.
- Drahota, Z., Carafoli, E., Rossi, C. S., Gamble, R. L., and Lehninger, A. L., 1965, *J. Biol. Chem.* **240**:2712.
- Draper, M. H., and Hodge, A. J., 1949, *Nature* **163**:576.
- Draper, M. H., Friebel, H., and Karzel, K., 1963, *Med. Exp.* **8**:242.
- Drouin, H., and The, R., 1969, *Pflügers Arch. Ges. Physiol.* **313**:80.
- DuBois-Reymond, E., 1843, *Ann. Phys. Chem.* **58**:1.
- DuBois-Reymond, E., 1848-1849, *Untersuchungen über Tierische Elektrizität*, Vols. I and II, Reimer, Berlin.
- Dujardin, F., 1835, *Ann. Sci. Nat. Zool. Ser. 2* **4**:343.
- Dunham, E. T., and Glynn, I. M., 1961, *J. Physiol. (London)* **156**:274.
- Dünwald, H., and Wagner, C., 1934, *Z. Phys. Chem.* **B24**:53.
- DuPasquier, L., and Wabl, M. R., 1977, *Differentiation* **8**:9.
- Durst, R. A., 1974, in: *Ion-Selective Microelectrodes* (H. J. Berman and N. C. Hebert, eds.), Plenum Press, New York, p. 13.
- Dutrochet, R. H. H., 1827, *Ann. Chim. Phys.* **34**:393.
- Eaton, B. L., 1976, *Science* **192**:1337.
- Eavenson, E., and Christensen, H. N., 1967, *J. Biol. Chem.* **242**:5386.
- Ebashi, S., 1960, *J. Biochem.* **48**:150.
- Ebashi, S., 1961, *J. Med. Sci. (Tokyo)* **69**:65.
- Ebashi, S., 1965, in: *Molecular Biology of Muscle Contractionn*(S. Ebashi, F. Oosawa, T. Sekine, and Y. Tonomura, eds.), Igaku Shoin, Tokyo, p. 197.
- Ebashi, S., and Ebashi, F., 1964, *J. Biochem.* **55**:604.
- Ebashi, S., and Endo, M., 1968, *Prog. Biophys. Mol. Biol.* **18**:123.
- Ebashi, S., and Kodama, A., 1965, *J. Biochem.* **58**:107.
- Ebashi, S., and Kodama, A., 1966, *J. Biochem.* **59**:425.
- Ebashi, S., and Lipmann, F., 1962, *J. Cell Biol.* **14**:389.
- Ebashi, S., Ebashi, F., and Kodama, A., 1967, *J. Biochem.* **62**:137.
- Ecker, R. E., and Smith, L. D., 1971, *J. Cell. Physiol.* **77**:61.
- Eddy, A. A., Mulcahy, M. F., and Thomson, P. J., 1967, *Biochem. J.* **103**:863.

- Edelmann, L., 1973, *Ann. N.Y. Acad. Sci.* **204**:534.
Edelmann, L., 1977a, *J. Microsc.* **12**:243.
Edelmann, L., 1977b, *Physiol. Chem. Phys.* **9**:313.
Edelmann, L., 1978, *Microsc. Acta Suppl.* **2**:166.
Edelmann, L., 1980a, *Histochemistry* **67**:233.
Edelmann, L., 1980b, *Physiol. Chem. Phys.* **12**:509.
Edelmann, L., 1981, *Fresenius Z. Anal. Chem.* **308**:218.
Edelmann, L., 1983, *Physiol. Chem. Phys.* **15**(4) (in press).
Edelmann, L., and Baldauf, J. H., 1971, *1st Eur. Biophys. Cong.*, Baden **3**:243.
Edelmann, L., Pfeifer, K., and Matt, K. H., 1971, *Biophysik* **7**:181.
Edsall, J. T., and Blanchard, M. H., 1933, *J. Am. Chem. Soc.* **55**:2337.
Edzes, H. T., and Berendsen, H. J. C., 1975, *Ann. Rev. Biophys. Bioeng.* **4**:265.
Edzes, H. T., and Samulski, E. T., 1977, *Nature* **265**:521.
Edzes, H. T., Ginzburg, M., Ginzburg, B. Z., and Berendsen, H. J., 1977, *Experientia* **33**:732.
Ege, R., 1922, *Biochem. Z.* **130**:99.
Eggleston, J. C., Saryan, L. A., and Hollis, D. P., 1978, *Cancer Res.* **35**:1326.
Eggleton, M., and Eggleton, P., 1933, *Q. J. Exp. Physiol.* **23**:391.
Eggleton, P., and Eggleton, G. P., 1927, *J. Biol. Chem.* **21**:190.
Ehrenberg, W., and Spear, W. E., 1951, *Proc. Phys. Soc.* **64**:67.
Ehrensvard, G., and Sillen, L. G., 1938, *Nature* **141**:788.
Eigen, M., and Schwarz, G., 1957, *J. Colloid. Sci.* **12**:181.
Eisenberg, D., and Kauzmann, W., 1969, *The Structure and Properties of Water*, Oxford University Press, Oxford.
Eisenberg, E., and Greene, L. E., 1980, *Annu. Rev. Physiol.* **42**:293.
Eisenberg, E., and Moos, C., 1968, *Biochemistry* **7**:1486.
Eisenberg, E., and Moos, C., 1970, *J. Biol. Chem.* **245**:2451.
Eisenman, G., 1962, *Biophys. J. Suppl.* **2**:259.
Eisenman, G., 1967, in: *Glass Electrodes for Hydrogen and Other Cations* (G. Eisenman, ed.), Marcel Dekker, New York, p. 268.
Eisenman, G., Rudin, D. O., and Casby, J. U., 1957, *Science* **126**:831.
Eisenstadt, M., and Friedman, H. L., 1966, *J. Chem. Phys.* **44**:1407.
Elliott, G. F., 1967, *J. Gen. Physiol.* **50**:171.
Elliott, G. F., 1973, *Ann. N.Y. Acad. Sci.* **24**:564.
Elliott, G. F., Lowy, J., and Millman, B. M., 1967, *J. Mol. Biol.* **25**:31.
Elliott, G. F., Rome, E. M., and Spencer, M., 1970, *Nature* **226**:417.
Embden, G., Hirsch-Kaufmann, H., Lehnartz, E., and Deuticke, H. J., 1926, *Hoppe-Seylers Z. Physiol. Chem.* **151**:209.
Emsley, J. W., Feeney, J., and Sutcliffe, L. H., 1965, *High Resolution Nuclear Magnetic Resonance Spectroscopy*, Vol. I, Pergamon Press, London.
Englehardt, V. A., 1946, *Adv. Enzymol.* **6**:147.
Englehardt, V. A., and Ljubimova, M. N., 1939, *Nature* **144**:668.
Engelhardt, V. A., and Ljubimova, M. N., 1942, *Biokhimiya* **7**:205.
Englemann, T. W., 1873, *Pflügers Arch. Ges. Physiol.* **7**:155.
Englemann, T. W., 1906, *Preuss. Akad. Wiss.* **39**:694.
England, J. M., Howett, M. K., and Tan, K., B., 1975, *J. Virol.* **16**:1101.
Epstein, E., 1956, *Annu. Rev. Plant Physiol.* **7**:1.
Epstein, E., and Hagen, C. E., 1952, *Plant Physiol.* **27**:457.
Ernst, E., 1963, *Biophysics of the Striated Muscle*, Publishing House of the Hungarian Academy of Science, Budapest.
Ernst, E., and Scheffer, L., 1928, *Pflügers Arch. Ges. Phys.* **220**:655.
Ernster, L., and Kuhlenstierna, B., 1970, in: *Membranes of Mitochondria and Chloroplasts* (E. Racker, ed.), Van Nostrand Reinhold, New York, p. 191.
Ernster, L., Lee, C. P., and Janda, S., 1967, in: *Biochemistry of Mitochondria* (E. C. Slater, Z. Kaniuge, and J. L. Wojtezak, eds.), Academic Press, New York, p. 29.
Estrada-O, S., and Gomez-Lojero, C., 1971, *Biochemistry* **10**:1598.
Estrada-O, S., Graven, S. N., and Lardy, H. A., 1967, *J. Biol. Chem.* **242**:2925.

- Etkins, W., 1964, in: *Physiology of the Amphibian* (J. A. Moore, ed.), Academic Press, New York, p. 427.
- Etzler, F. M., and Drost-Hansen, W., 1979, in: *Cell-Associated Water* (W. Drost-Hansen and J. Clegg, eds.), Academic Press, New York, p. 125.
- Fahr, G., 1909, *Z. Biol.* **52**:72.
- Falcone, A. B., and Hadler, H. I., 1968, *Arch. Biochem. Biophys.* **124**:91.
- Falk, G., and Gerard, R. W., 1954, *J. Cell. Comp. Physiol.* **43**:393.
- Falk, M., Poole, A. G., and Goymour, C. G., 1970, *Can. J. Chem.* **48**:1536.
- Farrar, T. C., and Becker, E. D., 1971, *Pulse and Fourier Transform NMR: Introduction to Theory and Methods*, Academic Press, New York.
- Fass, S. J., Hammermann, M. R., and Sacktor, B., 1977, *J. Biol. Chem.* **252**:583.
- Fatt, P., and Katz, B., 1953, *J. Physiol. (London)* **120**:171.
- Feeley, R. E., and Yeh, Y., 1978, *Adv. Protein Chem.* **32**:191.
- Feldberg, W., and Paton, W. D. M., 1951, *J. Physiol. (London)* **114**:490.
- Feldherr, C. M., and Pomerantz, J., 1978, *J. Cell Biol.* **78**:168.
- Felsenfeld, G., and Huang, S. L., 1961, *Biochim. Biophys. Acta* **51**:19.
- Felsenfeld, G., and Miles, H., 1967, *Annu. Rev. Biochem.* **36**: 407.
- Fenn, W. O., 1930, *Am. J. Physiol.* **93**:124.
- Fenn, W. O., 1931, *Am. J. Physiol.* **97**:635.
- Fenn, W. O., 1936, *Physiol. Rev.* **16**:450.
- Fenn, W. O., and Cobb, D. M., 1934, *J. Gen. Physiol.* **17**:629.
- Fenn, W. O., Cobb, D. M., and Marsh, B. S., 1934, *Am. J. Physiol.* **110**:261.
- Ferry, J. D., 1948, *Adv. Protein Chem.* **4**:1.
- Fessard, A., and Tauc, L., 1957, *J. Physiol. Pathol. Gen.* **49**:162.
- Few, A. V., Ottewill, R. H., and Parreira, H. C., 1955, *Biochim. Biophys. Acta* **18**:136.
- Fick, A., 1893, *Pflügers Arch. Ges. Physiol.* **53**:606.
- Finch, E. D., and Homer, L. D., 1974, *Biophys. J.* **14**:907.
- Finch, E. D., Harmon, J. F., and Muller, B. H., 1971, *Arch. Biochem. Biophys.* **147**:299.
- Findlay, A., 1919, *Osmotic Pressure*, 2nd ed., Longman, Green, London.
- Fischer, A., 1899, *Fixierung, Färbung und Bau des Protoplasmas*, Fischer Verlog, Jena.
- Fischer, M. H., 1908, *Pflügers Arch. Ges. Physiol.* **124**:69.
- Fischer, M. H., 1909, *Trans. Coll. Physicians Philadelphia* **31**:457.
- Fischer, M. H., 1921, *Oedema and Nephritis: A Critical Experimental and Chemical Study of the Physiology and Pathology of Water Absorption by the Living Organism*, 3rd ed., Wiley, New York.
- Fischer, M. H., and Moore, G., 1907, *Am. J. Physiol.* **20**:330.
- Fischer, M. H., and Suer, W. J., 1935, *Arch. Pathol.* **20**:683.
- Fischer, M. H., and Suer, W. J., 1938, *Arch. Pathol.* **26**:51.
- Fischer, M. H., and Suer, W. J., 1939, *Arth. Pathol.* **27**:811.
- Fischer-Wasels, B., 1927, in: *Handbuch der Nom. und Pathol. Physiol.* **14**:1211.
- Fischer, H. F., 1965, *Biochim. Biophys. Acta* **109**:544.
- Fishman, S. N., Khodorov, B. I., and Volkenschtein, M. V., 1971, *Biochim. Biophys. Acta* **225**:1.
- Fiske, C. H., and Subbarow, Y., 1929, *J. Biol. Chem.* **81**:629.
- Fleischer, S., Fleischer, B., and Stoeckenius, W., 1967, *J. Cell Biol.* **32**:193.
- Fleming, D., 1954, *William H. Welch and the Rise of Modern Medicine*, Little, Brown, Boston.
- Flemming, W., 1882 *Zellsubstanz: Kern- und Zellteilung*, Vogel, Leipzig.
- Fletcher, W. M., 1902, *J. Physiol. (London)* **28**:474.
- Fletcher, W. M., and Brown, G. M., 1914, *J. Physiol. (London)* **48**:177.
- Fletcher, W. M., and Hopkins, F. G., 1907, *J. Physiol. (London)* **35**:247.
- Flexner, S., and Flexner, J. T., 1941, *William Henry Welch and the Heroic Age of American Medicine*, Viking Press, New York.
- Florini, J. R., and Vestling, C. S., 1957, *Biochim. Biophys. Acta* **25**:575.
- Fordham, S., and Tyson, J. T., 1937, *J. Chem. Soc.* **1937**:483.
- Fortune, J. E., ConCannon, P. W., and Hansel, W., 1975, *Biol. Reprod.* **13**:561.
- Foster, K. R., Bidinger, J. M., and Carpenter, D. O., 1976, *Biophys. J.* **16**:991.
- Foster, K. R., Schepps, J. L., Stoy, R. D., and Schwan, H. P., 1979, *Phys. Med. Biol.* **24**:1177.
- Foster, K. R., Schepps, J. L., and Schwan, H. P., 1980, *Biophys. J.* **29**:271.

- Fowler, R. H., and Guggenheim, E. A., 1939, *Statistical Thermodynamics*, Cambridge University Press, London.
- Fox, S. W., 1965, *Nature* **205**:328.
- Fox, S. W., 1973, *Naturwissenschaften* **60**:359.
- Fox, S. W., and Dose, K., 1977, *Molecular Evolution and the Origin of Life*, Marcel Dekker, New York.
- Francoeur, A. M., and Stanners, C. P., 1978, *J. Gen. Virol.* **39**:551.
- Frank, M., and Horowitz, S. B., 1975, *J. Cell Sci.* **19**:127.
- Franke, H., Malyusz, M., and Weiss, C., 1975, in: *Current Problems in Clinical Biochemistry*, Vol. 4 (S. Angielski and U. C. Dubach, eds.), Huber, Berne, p. 169.
- Frankenhaeuser, B., 1957, *J. Physiol. (London)* **137**:245.
- Frankenhaeuser, B., and Hodgkin, A. L., 1957, *J. Physiol. (London)* **137**:218.
- Franklin, R. M., and Baltimore, D., 1962, *Cold Spring Harbor Symp. Quant. Biol.* **27**:175.
- Freedman, J. C., 1973, Control of solute distribution by erythrocytes during *in vitro* incubation, Ph.D. Thesis, Department of Biology, University of Pennsylvania, Philadelphia.
- Freedman, J. C., 1976, *Biochim. Biophys. Acta* **455**:989.
- Fricke, H., and Curtis, A. T., 1934, *Nature* **133**:651.
- Fricke, H., and Morse, S., 1926, *J. Gen. Physiol.* **9**:153.
- Friedman, A. M., and Kennedy, J. W., 1955, *J. Am. Chem. Soc.* **77**:4499.
- Fritz, O. G., and Swift, T. J., 1967, *Biophys. J.* **7**:675.
- Fröhlich, H., 1958, *Theory of Dielectrics: Dielectric Constant and Dielectric Loss*, 2nd ed., Clarendon Press, Oxford.
- Frumento, A. S., 1965, *Science* **147**:142.
- Fry, D. J., 1970, in: *Membranes and Ion Transport*, Vol. 2 (E. E. Bittar, ed.), Wiley-Interscience, New York, p. 259.
- Fujita, A., 1926, *Biochem. Z.* **170**:18.
- Fujita, K., 1954, *Folia Pharmacol. Japan* **50**:183.
- Fuller, M. E., and Brey, W. S., Jr., 1968, *J. Biol. Chem.* **243**:274.
- Fung, B. M., 1975, *Science* **190**:800.
- Fung, B. M., and McGaughy, T. W., 1974, *Biochim. Biophys. Acta* **343**:663.
- Fung, B. M., Ryan, L. M., and Gerstein, B. C., 1980, *Biophys. J.* **29**:299.
- Gaddum, J. H., 1957, *Pharm. Rev.* **9**:211.
- Galvani, L., 1953, *Commentary on the Effects of Electricity on Muscular Motion* (M. G. Foley, transl.), Norwalk, Connecticut.
- Gamble, J. L., 1957, *J. Biol. Chem.* **228**:955.
- Gamble, J. L., and Hess, R. C., 1966, *Am. J. Physiol.* **210**:765.
- Garcia-Diaz, J. F., and Armstrong, W., 1980, *J. Membr. Biol.* **55**:213.
- Garcia-Diaz, J. F., O'Doherty, J., and Armstrong, W., 1978, *Physiologist* **21**:41.
- Gardos, G., 1960, *J. Neurochem.* **5**:199.
- Garrahan, P. J., and Glynn, I. M., 1967, *J. Physiol. (London)* **192**: 237.
- Garry, R. F., and Waite, R. F., 1979, *Virology* **96**:121.
- Garry, R. F., Bishop, J. M., Parker, S., Westbrook, K., Lewis, G., and Waite, M. R. F., 1979, *Virology* **96**:108.
- Gary-Bobo, C. M., and Lindenberg, A. B., 1969, *J. Colloid Interface Sci.* **29**:702.
- Gear, A. R. L., and Lehninger, A. L., 1968, *J. Biol. Chem.* **243**:3953.
- Gellhorn, E., 1931, *Lehrbuch der allgemeinen Physiologie*, Georg Thieme, Leipzig.
- Genevois, L., 1930, *Protoplasma* **10**:478.
- George, P., and Rutman, R. J., 1960, *Prog. Biophys. Biophys. Chem.* **10**:1.
- George, P., Witonsky, R. J., Trachtman, M., Wu, C., Dorwart, W., Richman, L., Richman, W., Shurayh, F., and Lentz, B., 1970, *Biochim. Biophys. Acta* **223**:1.
- Gerard, R. W., 1940, *The Unresting Cell*, Harper, New York.
- Gergeley, J., 1950, *Fed. Proc.* **9**:176.
- Gersh, I., 1938, *Anat. Rec.* **70**:311.
- Geyer, R. P., Sholtz, K. I., and Bowie, E. J., 1955, *Am. J. Physiol.* **182**:487.
- Gibbs, J. H., and DiMarzio, E. A., 1958, *J. Chem. Phys.* **28**:1247.
- Giese, W., and Rekowski, 1970, *Zentralbl. Veterinaermed. Reihe A* **11**:198.

- Giguère, P. A., and Harvey, K. B., 1956, *Can. J. Chem.* **34**:798.
- Gilbert, C., Kretzschmar, K. M., Wilkie, D. R., and Woledge, R. C., 1971, *J. Physiol. (London)* **213**:163.
- Gilbert, I. G. F., 1972, *Eur. J. Cancer* **8**:99.
- Gilbert, W., and Müller-Hill, B., 1966, *Proc. Natl. Acad. Sci. USA* **56**:1891.
- Gilkey, J. C., Jaffe, L. F., Ridgway, E. B., and Reynolds, G. T., 1979, *J. Cell. Biol.* **76**:448.
- Giulian, D., and Diacumakos, E. G., 1977, *J. Cell Biol.* **72**:86.
- Glasstone, S., 1946, *Textbook of Physical Chemistry*, 2nd ed., Van Nostrand, New York.
- Glasstone, S., Laidler, K. J., and Eyring, H., 1941, *The Theory of Rate Processes*, McGraw-Hill, New York, p. 555.
- Glauber, R. J., 1963, *J. Math. Phys.* **4**:294.
- Glick, R. E., and Tewari, K. C., 1966, *Nature* **211**:739.
- Glueckauf, E., 1952, *Proc. R. Soc. London Ser. A* **214**:207.
- Glynn, I. M., 1954, *J. Physiol. (London)* **126**:35P.
- Glynn, I. M., and Lewis, V. L., 1970, *J. Physiol.* **207**:393.
- Goldfarb, M., Shimizu, K., Perucho, M., and Wigler, M., 1982, *Nature* **296**:404.
- Goldin, S. M., and Tong, S. W., 1974, *J. Biol. Chem.* **249**:5907.
- Goldman, D. E., 1943, *J. Gen. Physiol.* **27**:37.
- Goldstein, L., 1970, *Adv. Cell Biol.* **1**:187.
- Goldstein, L., 1974, in: *The Cell Nucleus*, Vol. I (H. Busch, ed.), Academic Press, New York, p. 387.
- Gomez-Puyou, A., Sandoval, F., Tuena, M., Pena, A., and Chavez, E., 1969, *Biophys. Biochem. Res. Commun.* **36**:316.
- Gomez-Puyou, A., Sandoval, F., Chavez, E., and Tuena, M., 1970, *J. Biol. Chem.* **245**:5239.
- Goody, R. S., Holmes, K. C., Mannherz, H. G., Barrington-Leigh, J., and Rosenbaum, G., 1975, *Biophys. J.* **15**:687.
- Goody, R. S., Hofmann, W., and Mannherz, H. G., 1977, *Eur. J. Biochem.* **78**:317.
- Gordon, A. M., and Godt, R. E., 1970, *J. Gen. Physiol.* **55**:254.
- Gordon, A. M., Huxley, A. F., and Julian, F. J., 1966, *J. Physiol.* **184**:170.
- Gordy, W., and Stanford, S. C., 1941, *J. Chem. Phys.* **9**:204.
- Gorter, E., and Grendel, F., 1925, *J. Exp. Med.* **41**:439.
- Gortner, R. A., 1929, *Outline of Biochemistry*, Chapman and Hall, London.
- Gortner, R. A., 1930, *Trans. Faraday Soc.* **26**:678.
- Gortner, R. A., and Gortner, W. A., 1949, *Outline of Biochemistry*, 3rd ed., Wiley, New York.
- Gottesfeld, J. M., Garrard, W. T., Bagi, G., Wilson, R. F., and Bonner, J., 1974, *Proc. Natl. Acad. Sci. USA* **71**:2193.
- Graham, C. F., Arms, K., and Gurdon, J. B., 1966, *Dev. Biol.* **14**:349.
- Graham, F. L., and van der Eb, A. J., 1973, *Virology* **52**:456.
- Graham, J., and Gerard, R. W., 1946, *J. Cell. Comp. Physiol.* **28**:99.
- Graham, R. M., 1972, *The Cytologic Diagnosis of Cancer*, 3rd ed., Saunders, Philadelphia.
- Graham, T., 1861, *Philos. Trans. R. Soc. London* **151**:183.
- Grant, E. H., 1966, *J. Mol. Biol.* **19**:133.
- Grant, W. C., and Cooper, G., 1965, *Biol. Bull.* **129**:510.
- Grant, W. C., and Grant, J. A., 1958, *Biol. Bull.* **114**:1.
- Graven, S. N., Lardy, H. A., and Rutter, A., 1966, *Biochemistry* **5**:1735.
- Greaser, M. L., and Gergely, J., 1971, *J. Biol. Chem.* **246**:4226.
- Greenberg, D. M., and Cohn, W. E., 1934, *J. Gen. Physiol.* **18**:93.
- Greene, L. E., and Eisenberg, E., 1978, *Proc. Natl. Acad. Sci. USA* **75**:54.
- Greene, L. E., and Eisenberg, E., 1980, *J. Biol. Chem.* **255**:543.
- Greenstein, J. P., 1947, *Biochemistry of Cancer*, Academic Press, New York.
- Greenstein, J. P., 1956, *Cancer Res.* **16**:641.
- Greenstein, J. P., and Edsall, J. T., 1940, *J. Biol. Chem.* **133**:397.
- Gregor, H. P., 1948, *J. Am. Chem. Soc.* **70**:1293.
- Gregor, H. P., 1951, *J. Am. Chem. Soc.* **73**:642.
- Gregor, H. P., and Bregman, J. I., 1951, *J. Colloid Sci.* **6**:323.
- Gregor, H. P., Hamilton, M. J., Becher, J., and Berstein, F., 1955, *J. Phys. Chem.* **59**:874.
- Gregor, H. P., Hamilton, M. J., Oza, R. J., and Bernstein, F., 1956, *J. Phys. Chem.* **60**:263.

- Griffith, D. E., 1976, in: *Mitochondria, Bioenergetics, Biogenesis and Membrane Structures* (L. Packer and A. Gomez-Puyou, eds.), Academic Press, New York, p. 269.
- Grundfest, H., Kao, E. Y., and Altamirano, M., 1954, *J. Gen. Physiol.* **38**:245.
- Gudernatsch, J. F., 1912, *Arch. Entwicklungsmech. Org.* **35**:457.
- Guggenheim, E. A., 1950, *Thermodynamics: An Advanced Treatment for Chemists and Physicists*, 2nd ed., North-Holland/Interscience, New York.
- Gulati, J., 1973, *Ann. N.Y. Acad. Sci.* **204**:337.
- Gulati, J., and Jones, A. W., 1971, *Science* **172**:1358.
- Gulati, J., and Reisin, I. L., 1972, *Science* **176**:1139.
- Gurdon, J. B., 1962, *J. Embryol. Exp. Morphol.* **10**:622.
- Gurdon, J. B., 1964, *Adv. Morphog.* **4**:1.
- Gurdon, J. B., 1967, *Proc. Natl. Acad. Sci. USA* **58**:545.
- Gurdon, J. B., 1968, *J. Embryol. Exp. Morphol.* **20**:401.
- Gurdon, J. B., 1970, *Proc. R. Soc. London Ser. B* **176**:303.
- Gurdon, J. B., and Brown, D. D., 1965, *J. Mol. Biol.* **12**:27.
- Gurdon, J. B., and Laskey, R. A., 1970, *J. Embryol. Exp. Morphol.* **24**:227.
- Gurdon, J. B., Laskey, R. A., and Reeves, O. R., 1975, *J. Embryol. Exp. Morphol.* **34**:93.
- Gustavsson, H., Siegel, G., Lindman, B., and Fransson, L., 1978, *FEBS Lett.* **86**:127.
- Gutheret, R. J., 1955, *Rev. Gen. Bot.* **62**:5.
- Gutknecht, J., Hastings, D. F., and Bisson, M. A., 1978, in: *Membrane Transport in Biology*, Vol. 3 (G. Giebisch, D. C. Tosteson, and H. H. Ussing, eds.), Springer, New York, p. 125.
- Guzman-Barron, E. S., 1951, *Adv. Enzymol.* **11**:201.
- Gylkhandanyan, A. V., Evtodienko, Yu. V., Zhabotinsky, A. M., and Kondrashova, M. N., 1976, *FEBS Lett.* **66**:44.
- Haber, F., 1908, *Ann. Phys.* **26**:927.
- Haber, F., and Klemensiewicz, Z., 1909, *Z. Phys. Chem.* **67**:385.
- Haber, F., and Klemensiewicz, Z., 1911, *Z. Phys. Chem.* **78**:228.
- Hackenbrock, C. R., 1968, *Proc. Natl. Acad. Sci. USA* **61**:598.
- Haddow, A., 1937, *Acta Int. Union Against Cancer* **2**:376.
- Haddow, A., 1938, *Acta Int. Union Against Cancer* **3**:342.
- Haggis, G. H., Buchanan, T. J., and Hasted, J. B., 1951, *Nature* **167**:607.
- Hagiwara, S., and Saito, N., 1959, *J. Physiol.* **148**:161.
- Hagiwara, S., 1960, in: *Electrical Activity of Single Cells* (Y. Katsuki, ed.), Igaku Shoin, Tokyo, p. 145.
- Hagiwara, S., Chichibu, S., and Naka, K. I., 1964, *J. Gen. Physiol.* **48**:163.
- Hagiwara, S., Fukuda, J., and Eaton, D. C., 1974, *J. Gen. Physiol.* **63**: 564.
- Hahn, L. A., Hevesy, G. Ch., and Rebbe, O. H., 1939, *Biochem. J.* **33**:1549.
- Haldane, J. B. S., 1934, *J. Pathol. Bacteriol.* **38**:507.
- Hall, T. S., 1969, *Ideas of Life and Matter*, University of Chicago Press, Chicago.
- Hallet, J., 1965, *Fed. Proc. Symp.* **24**:34.
- Hamaker, H. C., 1946, Discussion at the Meetings of the American Chemical Society, Chicago, September, 9–13 [cited in Ferry, 1948].
- Hamburger, H. J., 1889, *Z. Biol.* **26**:214.
- Hamburger, H. J., 1904, *Osmotische Druck- und Ionenlehre*, Vol. 3, Bergmann, Wiesbaden.
- Hammett, L. P., 1970, *Physical Organic Chemistry*, 2nd ed., McGraw-Hill, New York.
- Hanahan, D. J., and Ekholm, J. E., 1974, in: *Methods of Enzymology*, Vol. 31 (S. Fleischer and L. Packer, eds.), Academic Press, New York, p. 168.
- Hanson, J., and Huxley, H. E., 1953, *Nature* **172**:530.
- Hanson, J., and Huxley, H. E., 1955, *Proc. Soc. Exp. Biol.* **9**:228.
- Hansson-Mild, H., James, T. L., and Gillen, K. T., 1972, *J. Cell Physiol.* **80**:155.
- Hardt, A., and Fleckenstein, A., 1949, *Naunyn-Schmiedebergs Arch. Exp. Pathol. Pharmakol.* **207**:39.
- Hardy, W. B., 1899, *J. Physiol. (London)* **24**:158.
- Harrington, W. F., and Schellman, J. A., 1956, *C. R. Trav. Lab. Carlsberg Ser. Chim.* **30**:21.
- Harris, E. J., 1950, *Trans. Faraday Soc.* **46**:872.
- Harris, E. J., 1966, *Biochem. J.* **99**:200.

- Harris, E. J., and Burn, G. P., 1949, *Trans. Faraday Soc.* **45**:508.
 Harris, E. J., and Maisels, M., 1951, *J. Physiol. (London)* **113**:506.
 Harris, E. J., Catlin, G., and Pressman, B.C., 1967, *Biochemistry* **6**:1360.
 Harris, E. J., Al-Shalkhaly, M., and Baum, H., 1979, *Biochem. J.* **182**:455.
 Harris, F. E., and Rice, S. A., 1956, *J. Chem. Phys.* **24**:1258.
 Harris, H., Watkins, J. F., Ford, C. E., and Schoeft, G. I., 1966, *J. Cell Sci.* **1**:1.
 Harris, J. F., 1941, *J. Biol. Chem.* **141**:570.
 Harris, R. A., Penniston, J. T., Asai, J., and Green, D. E., 1968, *Proc. Natl. Acad. Sci. USA* **39**:830.
 Hartree, W., and Hill, A. B., 1921, *Biochem. J.* **15**:379.
 Hartshorne, D. J., and Müller, A., 1968, *Biochem. Biophys. Res. Commun.* **31**:647.
 Harvey, E. N., and Collander, R., 1932, *J. Franklin Inst.* **1**:214.
 Harvey, E. N., and Danielli, J. F., 1939, *Usp. Sovrem. Biol.* **10**:471.
 Harvey, S. C., and Hoekstra, P., 1972, *J. Phys. Chem.* **21**:2987.
 Harwood, R., Grant, M. E., and Jackson, D. S., 1975, *FEBS Lett.* **57**:47.
 Haselgrove, J. C., 1973, *Cold Spring Harbor Symp. Quant. Biol.* **37**:341.
 Hashimoto, T., and Yoshikawa, H., 1963a, *Biochim. Biophys. Acta* **75**:135.
 Hashimoto, T., and Yoshikawa, H., 1963b, *J. Biochem. (Tokyo)* **54**:468.
 Hasselbach, W., 1953, *Z. Naturforsch.* **8**E:449.
 Hasselbach, W., and Makinose, M., 1960, *Pflügers Arch. Ges. Physiol.* **272**:45.
 Hasselbach, W., and Makinose, M., 1961, *Biochem. Z.* **333**:518.
 Hasselbach, W., and Schneider, G., 1951, *Biochem. Zeitschr.* **321**:462.
 Hastings, D. F., and Gutknecht, J., 1976, *J. Membr. Biol.* **28**:263.
 Haugaard, G., 1941, *J. Phys. Chem.* **45**:148.
 Haurowitz, F., 1938, *Z. Physiol. Chem.* **254**:266.
 Hayashi, T., and Rosenbluth, R., 1952, *J. Cell. Comp. Physiol.* **40**:495.
 Hazlewood, C. F., 1973, *Ann. N.Y. Acad. Sci.* **204**:1.
 Hazlewood, C. F., 1979, in: *Cell-Associated Water* (W. Drost-Hansen and J. Clegg, eds.), Academic Press, New York, p. 165.
 Hazlewood, C. F., Nichols, B. L., and Chamberlain, N. F., 1969, *Nature* **222**:747.
 Hazlewood, C. F., Chang, D. C., Nichols, B. L., and Woessner, D. E., 1974, *Biophys. J.* **14**:583.
 Hazlewood, C. F., Singer, D. B., and Beall, P., 1979, *Physiol. Chem. Phys.* **11**:181.
 Hearst, J. E., and Vinograd, J., 1961, *Proc. Natl. Acad. Sci. USA* **47**:1005.
 Heckmann, K., 1953, *Naturwissenschaften* **40**:478.
 Hedin, S. G., 1897, *Pflügers Arch. Ges. Physiol.* **68**:229.
 Heilbrunn, L. V., 1928, *The Colloid Chemistry of Protoplasm*, Gebruder Borntraeger, Berlin.
 Heilbrunn, L. V., 1937, *An Outline of General Physiology*, Saunders, Philadelphia.
 Heilbrunn, L. V., and Wilbur, K. M., 1937, *Biol. Bull.* **75**:557.
 Heilbrunn, L. V., Dougherty, K., and Wilbur, K. M., 1939, *Physiol. Zool.* **12**:97.
 Heiple, J. M., and Lansing-Taylor, D., 1980, *J. Cell Biol.* **86**:885.
 Held, G., Noack, F., Pollak, V., and Melton, B., 1973, *Z. Naturforsch.* **28C**:59.
 Helfferich, F., 1962, *Ion Exchange Equilibria*, McGraw-Hill, New York.
 Hellam, D. C., and Podolsky, R. J., 1969, *J. Physiol. (London)* **200**:807.
 Hellerman, L., Chinard, F. P., and Deitz, V. R., 1943, *J. Biol. Chem.* **147**:443.
 Henmiker, J. C., and McBain, J. W., 1948, *The Depth of the Surface Zone of a Liquid*, Technical Report No. 5 N60 ri-154-T. 0 II, Stanford Research Institute, Stanford, California.
 Heppel, L. A., 1939, *Am. J. Physiol.* **127**:385.
 Heppel, L. A., 1940, *Am. J. Physiol.* **128**:449.
 Herlitzka, A., 1896, *Arch. Entwicklungsmech. (Roux's)* **4**:624.
 Hermann, L., 1867, *Untersuchungen über den Stoffwechsel der Muskeln*, Horschwald, Berlin.
 Hermann, L., 1879, *Handbuch der Physiologie*, Vol. 1, F. C. W. Vogel Verlag, Leipzig, p. 1.
 Herskovitz, T. T., Gadegbeku, B., and Jaille, H., 1970, *J. Biol. Chem.* **245**:2588.
 Hild, W., and Tasaki, I., 1962, *J. Neurophysiol.* **25**:277.
 Hilden, S., Rhee, H. M., and Hokin, L. E., 1974, *J. Biol. Chem.* **249**:7432.
 Hill, A. E., 1975, *Proc. R. Soc. London Ser. B* **190**:115.
 Hill, A. V., 1910, *J. Physiol.* **40**:iv.

- Hill, A. V., 1926, *Muscular Activity*, Williams and Wilkins, Baltimore.
- Hill, A. V., 1930, *Proc. R. Soc. London Ser. B* **106**:477.
- Hill, A. V., 1932, *Physiol. Rev.* **12**:56.
- Hill, A. V., and Kupalov, P. S., 1930, *Proc. R. Soc. London Ser. B* **106**:445.
- Hill, A. V., and Parkinson, J. L., 1931, *Proc. R. Soc. London Ser. B* **108**:148.
- Hill, D. K., 1960, *J. Physiol.* **153**:433.
- Hill, D. K., 1962, *J. Physiol.* **164**:31.
- Hill, M., and Hillova, J., 1971, *C. R. Acad. Sci. (Paris) Ser. D* **272**:3094.
- Hill, R., and Wolvekamp, H. P., 1936, *Proc. R. Soc. London Ser. B* **120**:484.
- Hille, B., 1968, *J. Gen. Physiol.* **51**:221.
- Hille, B., 1972, *J. Gen. Physiol.* **59**:637.
- Hille, B., 1975, *Fed. Proc.* **34**:1318.
- Hinke, J. A. M., 1959, *Nature* **184**:1257.
- Hinke, J. A. M., 1961, *J. Physiol. (London)* **156**:314.
- Hinke, J. A. M., and Gayton, D. C., 1971, *Can. J. Physiol. Pharmacol.* **49**:312.
- Hinkle, D. C., and Chamberlin, M. J., 1972, *J. Mol. Biol.* **70**:187.
- Hirata, H., Altendorf, K., and Harold, F. M., 1974, *J. Biol. Chem.* **249**:2939.
- Hitchcock, S. E., 1977, *J. Cell Biol.* **74**:1.
- Hoagland, D. R., and Broyer, T. C., 1936, *Plant Physiol.* **11**:471.
- Hoagland, D. R., and Broyer, T. C., 1942, *J. Gen. Physiol.* **25**:865.
- Hoagland, D. R., Hibbard, P. L., and Davis, A. R., 1926, *J. Gen. Physiol.* **10**:121.
- Höber, R., 1906, *Physikalische Chemie der Zellen und der Gewebe*, 2nd ed., Englemann, Leipzig, Berlin.
- Höber, R., 1912, *Pflügers Arch. Ges. Physiol.* **148**:189.
- Höber, R., 1913, *Pflügers Arch. Ges. Physiol.* **150**:15.
- Höber, R., 1914, *Physikalische Chemie der Zellen und der Gewebe*, 4th ed., Englemann, Leipzig, Berlin.
- Höber, R., 1945, *Physical Chemistry of Cells and Tissues*, Blakiston, Philadelphia.
- Hodge, A. J., and Schmidt, F. O., 1960, *Proc. Natl. Acad. Sci. USA* **46**:186.
- Hodgkin, A. L., 1951, *Biol. Rev.* **26**:339.
- Hodgkin, A. L., 1958, *Proc. R. Soc. London Ser. B* **148**:1.
- Hodgkin, A. L., 1971, *The Conduction of the Nervous Impulse*, Liverpool University Press, Liverpool.
- Hodgkin, A. L., and Horowicz, P., 1957, *J. Physiol. (London)* **136**:17P.
- Hodgkin, A. L., and Horowicz, P., 1960, *J. Physiol. (London)* **153**:404.
- Hodgkin, A. L., and Huxley, A. F., 1939, *Nature* **144**:710.
- Hodgkin, A. L., and Huxley, A. F., 1945, *J. Physiol. (London)* **104**:176.
- Hodgkin, A. L., and Huxley, A. F., 1952a, *J. Physiol. (London)* **116**:449.
- Hodgkin, A. L., and Huxley, A. F., 1952b, *J. Physiol. (London)* **116**:473.
- Hodgkin, A. L., and Huxley, A. F., 1952c, *J. Physiol. (London)* **116**:497.
- Hodgkin, A. L., and Huxley, A. F., 1952d, *J. Physiol. (London)* **117**:500.
- Hodgkin, A. L., and Katz, B., 1949a, *J. Physiol. (London)* **108**:37.
- Hodgkin, A. L., and Katz, B., 1949b, *J. Physiol. (London)* **109**:240.
- Hodgkin, A. L., and Keynes, R. D., 1953, *J. Physiol. (London)* **119**:513.
- Hodgkin, A. L., and Keynes, R. D., 1955a, *J. Physiol. (London)* **128**:28.
- Hodgkin, A. L., and Keynes, R. D., 1955b, *J. Physiol. (London)* **128**:61.
- Hodgkin, A. L., and Keynes, R. D., 1956, *J. Physiol. (London)* **131**:592.
- Hodgkin, A. L., Huxley, A. F., and Katz, B., 1952, *J. Physiol. (London)* **116**:424.
- Hodgman, C. D., Weast, R. C., and Selby, S. M., 1961, *Handbook of Chemistry and Physics*, 43rd ed., Chemical Rubber Publishing Company, Cleveland, Ohio.
- Höfer, M., and Pressman, B. C., 1966, *Biochemistry* **5**:3919.
- Hoff, H. E., 1936, *Ann. Sci.* **1**:157.
- Hoffman, J. F., and Kregenow, F. M., 1966, *Ann. N.Y. Acad. Sci.* **137**:566.
- Hofmann, W., and Goody, R. S., 1978, *FEBS Lett.* **89**:169.
- Hofmeister, W., 1867, *Handbuch der Physiologischen Botanik*, Vol. I, Engelmann, Leipzig.
- Hofmeister, F., 1891, *Arch. Exp. Pathol. Pharmakol.* **28**:210.
- Hogeboom, G. H., Schneider, W. C., and Palade, G. E., 1948, *J. Biol. Chem.* **172**:619.
- Holleman, L. W., Bungenberg de Jong, H. G., and Modderman, R. S. T., 1934, *Kolloid Beih.* **39**:334.

- Hollis, D. P., Saryan, L. A., Eggleston, J. C., and Morris, H. P., 1975, *J. Natl. Cancer Inst.* **54**:1469.
- Holtfreter, J., 1931, *Arch. Entwicklungsmech. (Roux's)* **124**:404.
- Holtfreter, J., 1933a, *Naturwissenschaften* **21**:766.
- Holtfreter, J., 1933b, *Arch. Entwicklungsmech. (Roux's)* **129**:669.
- Holtfreter, J., 1934a, *Arch. Entwicklungsmech. (Roux's)* **132**:225.
- Holtfreter, J., 1934b, *Arch. Entwicklungsmech. (Roux's)* **132**:307.
- Homsher, E., and Kean, C. J., 1978, *Annu. Rev. Physiol.* **40**:93.
- Hooke, R., 1665, *Micrographia, or Some Physiological Descriptions on Minute Bodies by Magnifying Glasses*, London.
- Hoover, S. R., and Mellon, E. F., 1950, *J. Am. Chem. Soc.* **72**:2562.
- Hopfer, Y., Nelson, K., Perrotto, J., and Isselbacher, K. J., 1973, *J. Biol. Chem.* **248**:25.
- Hori, T., 1956, *Low Temp. Sci. A* **15**:34.
- Horovitz, K., 1923, *Z. Phys.* **15**:369.
- Horowitz, P., and Gerber, C. J., 1965, *J. Gen. Physiol.* **48**:515.
- Horowitz, S. B., 1972, *J. Cell Biol.* **54**:609.
- Horowitz, S. B., and Moore, L. C., 1974, *J. Cell Biol.* **60**:405.
- Horowitz, S. B., and Paine, P. L., 1979, *Biophys. J.* **25**:45.
- Horowitz, S. B., Paine, P. L., Tluczek, L., and Reynhout, J. K., 1979, *Biophys. J.* **25**:33.
- Höser, N., Dargel, R., Dawczyhski, H., and Winnefield, K., 1976, *FEBS Lett.* **72**:193.
- Howarth, J. V., 1958, *J. Physiol. (London)* **144**:167.
- Hsi, E., and Bryant, R. G., 1977, *Arch. Biochem. Biophys.* **183**:588.
- Huang, H. W., 1977, *J. Theor. Biol.* **67**:557.
- Huang, H. W., 1979, *J. Chem. Phys.* **70**:2390.
- Huang, H. W., and Negendank, W., 1980, *J. Chem. Phys.* **73**:4136.
- Huang, H. W., and Seitz, W. A., 1980, in: *Cooperative Phenomena in Biology* (G. Karreman, ed.), Pergamon Press, New York, p. 71.
- Huang, H. W., Hunter, S. H., Warburton, W. K., and Moss, S. C., 1979, *Science* **204**:191.
- Hubbard, D., 1946, *Bur. Stand. (U.S.) J. Res.* **37**:223.
- Hubbard, P. S., 1970, *J. Chem. Phys.* **53**:985.
- Hucho, F., and Schiebler, W., 1977, *Mol. Cell. Biochem.* **18**:151.
- Hückel, W., 1925, *Phys. Z.* **26**:93.
- Hughes, F., 1928, *J. Chem. Soc.* **131**:491.
- Hughes, F., 1970, *Biophys. J.* **10**:679.
- Hukuda, K., 1931, *J. Physiol. (London)* **72**:438.
- Hunter, D. R., Howorth, R. A., and Southard, J. H., 1976, *J. Biol. Chem.* **251**:5069.
- Hunter, F. E., and Ford, L., 1955, *J. Biol. Chem.* **216**:357.
- Hutter, O. F., and Padsha, S. M., 1959, *J. Physiol. (London)* **146**:117.
- Huxley, A. F., 1957, *Prog. Biophys. Biophys. Chem.* **7**:255.
- Huxley, A. F., 1974, *J. Physiol.* **243**:1.
- Huxley, A. F., and Niedergerke, R., 1954, *Nature* **173**:971.
- Huxley, A. F., and Simmons, R. M., 1971, *Nature* **233**:533.
- Huxley, A. F., and Straub, R. W., 1958, *J. Physiol. (London)* **143**:408.
- Huxley, A. F., and Taylor, R. E., 1958, *J. Physiol. (London)* **144**:426.
- Huxley, H. E., 1951, *Disc. Faraday Soc.* **11**:148.
- Huxley, H. E., 1953a, *Biochim. Biophys. Acta* **12**:387.
- Huxley, H. E., 1953b, *Proc. R. Soc. London Ser. B* **141**:59.
- Huxley, H. E., 1957, *J. Biophys. Biochem. Cytol.* **3**:631.
- Huxley, H. E., 1968, *J. Mol. Biol.* **37**:507.
- Huxley, H. E., 1969, *Science* **164**:1356.
- Huxley, H. E., 1971, *Proc. R. Soc. London Ser. B* **178**:131.
- Huxley, H. E., 1973, *Cold Spring Harbor Symp. Quant. Biol.* **37**:361.
- Huxley, H. E., and Brown, W., 1967, *J. Mol. Biol.* **30**:383.
- Huxley, H. E., and Hanson, J., 1954, *Nature* **173**:973.
- Huxley, H. E., Faruqi, A. R., Bordas, J., Koch, M. H. J., and Milch, J. R., 1980, *Nature* **284**:140.
- Huxley, H. E., Simmons, R. M., Faruqi, A. R., Kress, M., Bordas, J., and Koch, M. H. J., 1981, *Proc. Natl. Acad. Sci. USA* **78**:2297.

- Huxley, T. H., 1853, *Br. and Foreign Med. Chir. Rev.* **12**.
- Huxley, T. H., 1880, *The Crayfish: An Introduction to the Study of Zoology*, Kegan Paul, London, p. 186.
- Inch, W. R., McCredie, J. A., Knispel, R. R., Thompson, R. T., and Pintar, M. M., 1974, *J. Natl. Cancer Inst.* **52**:353.
- Infante, A. A., Klaupiks, D., and Davies, R. E., 1964, *Science* **144**:1577.
- Infante, A. A., Klaupiks, D., and Davies, R. E., 1965, *Biochim. Biophys. Acta* **94**:504.
- Ingold, C. K., 1953, *Structure and Mechanism in Organic Chemistry*, Cornell University Press, Ithaca, New York.
- Inoue, I., Ishida, N., and Kobatake, Y., 1973a, *Biochim. Biophys. Acta* **330**:37.
- Inoue, I., Ueda, T., and Kobatake, Y., 1973b, *Biochim. Biophys. Acta* **298**:653.
- Inoue, I., Ishida, N., and Kobatake, Y., 1974, *Biochim. Biophys. Acta* **367**:24.
- Inoue, I., Pant, H. C., Tasaki, I., and Gainer, H., 1976, *J. Gen. Physiol.* **68**:385.
- International Critical Tables*, Vol. VI, 1929, p. 230.
- Isenberg, I., 1979, *Ann. Rev. Biochem.* **48**:159.
- Ishima, Y., Przybylski, A., and Fox, S. W., 1981, *BioSystems* **13**:243.
- Ising, E., 1925, *Z. Phys.* **31**:253.
- Ives, D. J. G., and Janz, G. J., 1961, *Reference Electrodes*, Academic Press, New York.
- Iwasa, K., Tasaki, I., and Gibbons, R. C., 1980, *Science* **210**:338.
- Iwazumi, T., 1970, A New Field Theory of Muscle Contraction, Ph.D. Thesis, Department of Bioengineering, University of Pennsylvania, Philadelphia.
- Jacob, F., and Monod, J., 1961a, *Cold Spring Harbor Symp. Quant. Biol.* **26**:193.
- Jacob, F., and Monod, J., 1961b, *J. Mol. Biol.* **3**:318.
- Jacobson, B., 1955, *J. Am. Chem. Soc.* **77**:2919.
- Jaffé, H. H., 1953, *Chem. Rev.* **53**:191.
- Jain, M. K., 1972, *The Bimolecular Lipid Membrane: A System*, Van Nostrand Reinhold, New York.
- James, H. M., and Coolidge, A. S., 1933, *J. Chem. Phys.* **1**:825.
- Jangendorf, A. T., and Uribe, E., 1966, *Proc. Natl. Acad. Sci. USA* **55**:170.
- Jardetzky, O., and Wertz, J. E., 1956, *Am. J. Physiol.* **187**:608.
- Jardetzky, O., and Wertz, J. E., 1960, *J. Am. Chem. Soc.* **82**:318.
- Jay, A. W. L., and Burton, A. C., 1969, *Biophys. J.* **9**:115.
- Jazwinski, S. M., Wang, J. L., and Edelman, G. M., 1976, *Proc. Natl. Acad. Sci. USA* **73**:2231.
- Jellinek, H. H. G., and Fok, S. Y., 1967, *Kolloid Z. Z. Polym.* **220**:122.
- Jenerick, H. P., and Gerard, R. W., 1953, *J. Cell. Comp. Physiol.* **42**:79.
- Jenin, P. C., and Schwan, H. P., 1980, *Biophys. J.* **30**:285.
- Jewell, B. R., and Rüegg, J. C., 1966, *Proc. R. Soc. London Ser. B* **164**:428.
- Jirgensons, B., 1972, *Makromol. Chem.* **158**:1.
- Jöbsis, F. F., and O'Connor, M. J., 1966, *Biochem. Biophys. Res. Commun.* **25**:246.
- Johnson, J. D., and Epel, D., 1975, *Proc. Natl. Acad. Sci. USA* **72**:4474.
- Johnson, J. D., Epel, D., and Paul, M., 1976, *Nature* **262**:661.
- Johnson, K. A., and Taylor, E. W., 1978, *Biochemistry* **17**:3432.
- Johnson, S. L., and Woodbury, J. W., 1964, *J. Gen. Physiol.* **47**:827.
- Johnston, R. N., and Paul, M., 1977, *Dev. Biol.* **57**:364.
- Johnstone, R. M., and Scholefield, P. G., 1965, *Biochim. Biophys. Acta* **94**:130.
- Jones, A. W., 1970, *Physiol. Chem. Phys.* **2**:151.
- Jones, A. W., 1973, *Ann. N.Y. Acad. Sci.* **204**:379.
- Jones, A. W., and Karreman, G., 1969, *Biophys. J.* **9**:910.
- Jones, I. D., and Gortner, R. A., 1932, *J. Phys. Chem.* **36**:387.
- Jordan-Lloyd, D., and Moran, T., 1934, *Proc. R. Soc. Ser. A* **147**:382.
- Jordan-Lloyd, D., and Phillips, H., 1933, *Trans. Faraday Soc.* **29**:132.
- Jordan-Lloyd, D., and Shore, A., 1938, *The Chemistry of Proteins*, 2nd ed., J. A. Churchill, London.
- Jost, W., 1960, *Diffusion in Solids, Liquids and Gases*, Academic Press, New York.
- Judah, J. D., McLean, A. E. M., Almed, K., and Christie, G. S., 1965, *Biochim. Biophys. Acta* **94**:441.

- Kaatze, U., Göttmann, O., Podbielski, R., Pottel, R., and Terveer, U., 1978, *J. Phys. Chem.* **82**:1.
- Kaback, H. R., 1976, *J. Cell Physiol.* **89**:575.
- Kalckar, H. M., 1942, *Biol. Rev.* **17**:28.
- Kalk, A., and Berendsen, H. J. C., 1976, *J. Magn. Reson.* **24**:343.
- Kamb, B., 1972, in: *Structure and Transport Processes in Water and Aqueous Solutions* (R. A. Horne, ed.), Wiley-Interscience, New York, p. 9.
- Kamnev, I. Ye., 1938, *Arkh. Anat. Gistol. Embriol.* **19**:145.
- Kanazawa, T., 1972, *Seikagaku* **44**:323.
- Kanazawa, T., and Boyer, P. D., 1973, *J. Biol. Chem.* **248**:3165.
- Kanazawa, T., Yamada, S., and Tonomura, Y., 1970, *J. Biochem. (Tokyo)* **68**:593.
- Kao, C. Y., 1956, *Biol. Bull.* **111**:292.
- Karreman, G., 1971, *Bull. Math. Biophys.* **33**:483.
- Karreman, G., 1973, *Ann. N.Y. Acad. Sci.* **204**:393.
- Katchalski, E., Bichowski-Slommitzki, L., and Volcani, B. E., 1953, *Biochem. J.* **55**:671.
- Katchalsky, A., 1949, *Experientia* **5**:319.
- Katchalsky, A., Danon, D., Nevo, A., and deVries, A., 1959, *Biochim. Biophys. Acta* **33**:120.
- Katz, B., 1948, *Proc. R. Soc. London Ser. B* **135**:506.
- Katz, B., 1949, *Arch. Sci. Physiol.* **3**:285.
- Katz, B., 1966, *Nerve, Muscle, and Synapse*, McGraw-Hill, New York.
- Katz, J. A., 1896, *Pflügers Arch. Ges. Physiol.* **63**:1.
- Katz, J. R., 1919, *Kolloid Beih.* **9**:1.
- Katz, Y., and Diamond, J. M., 1974, *J. Membr. Biol.* **17**:87.
- Kawahara, H., Kirshner, A. G., and Tanford, C., 1965, *Biochemistry* **4**:1203.
- Kell, D. B., 1979, *Biochim. Biophys. Acta* **549**:55.
- Kendrick-Jones, J., Szentkiralyi, E. M., and Szent-Györgyi, A. G., 1976, *J. Mol. Biol.* **104**:747.
- Kent, M., 1970, *J. Phys. (D)* **3**:1275.
- Kent, M., 1972, *J. Phys. (D)* **5**:394.
- Kerkut, G. A., and Thomas, R. C., 1965, *Comp. Biochem. Physiol.* **14**:167.
- Kern, W., 1938, *Z. Phys. Chem. Abt. A* **181**:249.
- Kern, W., 1939, *Z. Phys. Chem. Abt. A* **184**:197.
- Kern, W., 1948, *Makromol. Chem.* **2**:279.
- Kernan, R. P., 1962, *Nature* **193**:986.
- Kernan, R. P., 1970, in: *Membranes and Ion Transport*, Vol. 1 (E. E. Bittar, ed.), Wiley-Interscience, New York, p. 399.
- Keyes, F. G., and Marshall, M. J., 1927, *J. Am. Chem. Soc.* **49**:156.
- Keynes, R. D., 1954, *Proc. R. Soc. London Ser. B* **142**:359.
- Keynes, R. D., and Maisel, G. W., 1954, *Proc. R. Soc. London Ser. B* **142**:383.
- Keynes, R. D., and Martins-Ferreira, H., 1953, *J. Physiol. (London)* **119**:315.
- Keynes, R. D., and Swan, R. C., 1959, *J. Physiol. (London)* **147**:626.
- Khuri, R. N., Agulian, S. K., and Bogharian, K., 1974, *Pflügers Arch. Ges. Physiol.* **346**:319.
- Khuri, R. N., Hajjar, J. J., Agulian, S. K., Bogharian, K., Kalloghlian, A., and Biari, H., 1972a, *Pflügers Arch. Ges. Physiol.* **338**:73.
- Khuri, R. N., Agulian, S. K., and Kalloghlian, A., 1972b, *Pflügers Arch. Ges. Physiol.* **335**:297.
- Kielley, W. W., and Meyerhof, O., 1950, *J. Biol. Chem.* **183**:391.
- Kimmich, R., and Noack, F., 1970, *Z. Naturforsch.* **25A**:1680.
- Kimmich, R., and Noack, F., 1971, *Ber. Bunsenges. Phys. Chem.* **75**:269.
- Kimmich, G. A., and Rasmussen, H., 1967, *Biochim. Biophys. Acta* **131**:413.
- Kimura, G., and Fujimoto, M., 1977, *Jpn. J. Physiol.* **27**:291.
- Kimura, G., Urakabe, S., Yuasa, S., Miki, S., Takamitsu, Y., Orita, Y., and Abe, H., 1977, *Am. J. Physiol.* **232**:F196.
- King, L. S., 1963, *J. Hist. Med.* **18**:257.
- King, T., and McKinnel, R., 1960, in: *Cell Physiology of Neoplasia*, University of Texas Press, Austin, p. 591.
- Kinne, R. K. H., 1975, *Symp. Renal Metab. Med. Clin. N. Am.* **59**:615.
- Kinne, R., 1979, in: *Membrane Transport in Biology*, Vol. 4B (G. Giebisch, D. C. Tosteson, and H. H. Ussing, eds.), Springer, New York, p. 529.

- Kinne, R. K. H., and Faust, R. G., 1977, *Biochem. J.* **168**:311.
Kinne, R. K. H., Murer, H., Kinne-Saffran, E., Thees, M., and Sachs, G., 1975, *J. Membr. Biol.* **21**:375.
Kite, G. L. 1913, *Biol. Bull.* **25**:1.
Klebs, G., 1887, *Ber. Dtsch. Bot. Ges.* **5**:181.
Klein, G., 1981, *Nature* **294**:313.
Klein, M. P., and Phelps, D. E., 1969, *Nature*, **224**:70.
Kleinzeller, A., Knotkova, A., and Nedvidko, J., 1968, *J. Gen. Physiol.* **51**:S326.
Klotz, I. M., 1958, *Science* **128**:815.
Knowles, A. F., and Racker, E., 1975, *J. Biol. Chem.* **250**:1949.
Knox, W. E., 1967, *Adv. Cancer Res.* **10**:117.
Knudsen, A. G., 1973, *Adv. Cancer Res.* **17**:317.
Kobel, H. R., Brun, R. B., and Fischberg, M., 1973, *J. Embryol. Exp. Morphol.* **29**:539.
Koch, K. S., and Leffert, H. L., 1979, *Cell* **18**:153.
Koefoed-Johnson, V., and Ussing, H. H. 1958, *Acta Physiol. Scand.* **42**:298.
Koenig, S. H., and Schillinger, W. E., 1969, *J. Biol. Chem.* **244**:3283.
Koeppe, H., 1897, *Pflügers Arch. Ges. Physiol.* **67**:189.
Koketsu, K., 1971, *Adv. Biophys.* **2**:77.
Koketsu, K., and Kimura, Y., 1960, *J. Cell. Comp. Physiol.* **55**:239.
Kolber, A. R., and Stein, N. D., 1966, *Nature* **209**:691.
Kollros, J. J., 1942, *J. Exp. Zool.* **89**:37.
Koppenhofer, E., 1974, *Pflügers Arch. Ges. Physiol.* **347**:R36.
Kornguth, S. E., and Stahmann, M. A., 1961, *Cancer Res.* **21**:907.
Korr, I. M., 1939, *Cold Spring Harbor Symp. Quant. Biol.* **7**:74.
Kossiakoff, A., and Harker, D., 1938, *J. Am. Chem. Soc.* **60**:2047.
Krall, A. R., Wagner, M., and Gozansky, D., 1964, *Biochem. Biophys. Res. Commun.* **16**:77.
Kraus, K. A., Marcinkowsky, A. E., Johnson, J. S., and Shor, A. J., 1966, *Science* **151**:194.
Kroeger, H., 1963, *Nature* **200**:1234.
Kroeger, H., and Müller, G., 1973, *Exp. Cell Res.* **82**:89.
Kromphardt, H., Grobecker, H., Ring, K., and Heinz, E., 1963, *Biochim. Biophys. Acta* **74**:549.
Krynicki, K., 1966, *Physica* **32**:167.
Kubo, R., and Tomita, K., 1954, *J. Phys. Soc. Jpn.* **9**:888.
Kuhn, W., 1949, *Experientia* **5**:318.
Kühne, W., 1864, *Untersuchungen über das Protoplasma und Contractilität*, Englemann, Leipzig, p. 1.
Kumagai, H., Ebashi, S., and Takeda, F., 1955, *Nature* **176**:166.
Kunitz, M., 1927, *J. Gen. Physiol.* **10**:811.
Kuntz, I. D., Brassfield, T. S., Law, G. D., and Purcell, G. V., 1969, *Science* **163**:1329.
Küntzel, A., 1944, in: *Handbuch der Gerbereichemie*, Vol. 1 (W. Grassmann, ed.), Springer, Vienna, p. 602.
Küntzel, A., and Schwank, M., 1940, *Collegium* **12**:489.
Kuroda, K., 1964, in: *Primitive Motile Systems in Cell Biology* (R. D. Allen and N. Kamiya, eds.), Academic Press, New York, p. 3.
Kushmerick, M. J., 1979, *Trends Biochem. Sci. Lett. Ed.* **3**:N210.
Kushmerick, M. J., and Podolsky, R. J., 1969, *Science* **166**:1297.
Kushmerick, M. J., Larson, R. E., and Davies, R. E., 1969, *Proc. R. Soc. London Ser. B* **174**:293.

Landström, U., and Løvtrop, S., 1977, *Acta Embryol. Exp.* **1977**:171.
Landström, U., and Løvtrop, S., 1979, *J. Embryol. Exp. Morphol.* **54**:113.
Langmuir, I., and Waugh, D. F., 1938, *J. Gen. Physiol.* **21**:745.
Lansdowne, D., Potter, L. T., and Tarrar, D. A., 1975, *Annu. Rev. Physiol.* **37**:485.
Lant, A. F., Priestland, R. N., and Whitam, R., 1970, *J. Physiol. (London)* **207**:291.
Lardy, H., 1951, in: *Phosphorus Metabolism*, Vol. I (W. D. McElroy and B. Glass, eds.), Johns Hopkins University Press, Baltimore, p. 31.
Lardy, H. A., and Graven, S. N., 1965, *Fed. Proc.* **24**:424.
Lardy, H. A., Graven, S. N., and Estrada-O., S., 1967, *Fed. Proc.* **26**:1355.

- Lark-Horovitz, K., 1931, *Nature* **127**:440.
- Larsson, K. E., 1965, in: *Thermal Neutron Scattering* (P. E. Eglestaff, ed.), Academic Press, New York.
- Laskey, R. A., and Gurdon, J. B., 1970, *Nature* **228**:1332.
- Lassen, U. V., and Sten-Knudsen, O., 1968, *J. Physiol. (London)* **199**:681.
- Lassen, U. V., Nielsen, A. M. T., Pape, L., and Simonsen, L. O., 1971, *J. Membr. Biol.* **6**:269.
- Lassen, U. V., Pape, L., Vestergaard-Bogind, B., and Bengtson, O., 1974, *J. Membr. Biol.* **18**:125.
- Latimer, W. M., and Rodebush, W. H., 1920, *J. Am. Chem. Soc.* **42**:1419.
- Latt, S. A., and Sober, H. A., 1967, *Biochemistry* **6**:3307.
- Lauffer, M. A., 1943, *J. Am. Chem. Soc.* **65**:1793.
- Lee, C. O., and Armstrong, W., 1972, *Science* **175**:1261.
- Lee, C. P., and Ernster, L., 1968, *Eur. J. Biochem.* **3**:391.
- Lee, J. C., and Timasheff, S. N., 1977, *Biochemistry* **16**:1754.
- Leenders, H. J., and Berendes, H. D., 1972, *Chromosoma* **37**:433.
- Leenders, H. J., Derkens, J., Mass, P. M. J. M., and Berendes, H. D., 1973, *Chromosoma* **41**:447.
- Lehnninger, A. L., 1964, *The Mitochondrion*, Benjamin, Menlo Park, California.
- Lehnninger, A. L., 1967, *Adv. Enzymol.* **29**:259.
- Lehnninger, A. L., 1975, *Biochemistry*, 2nd ed., Worth, New York.
- Lehnninger, A. L., Ray, B. L., and Scheider, M., 1957, *J. Biophys. Biochem. Cytol.* **5**:97.
- Lehnninger, A. L., Vercesci, A., and Bababonmi, E. A., 1978, *Proc. Natl. Acad. Sci. USA* **75**:1690.
- Lengyel, B., and Blum, E., 1934, *Trans. Faraday Soc.* **30**:461.
- Leonis, J., 1956, *Arch. Biochem. Biophys.* **65**:182.
- Lepeschkin, W. W., 1924, *Biol. Gen.* **1**:368.
- Lepeschkin, W. W., 1928, *Science* **68**:45.
- Lepeschkin, W. W., 1930, *Protoplasma* **9**:269.
- Lepeschkin, W. W., 1936, *Biodynamica* **19**:1.
- Lev, A. A., 1964, *Nature* **201**:1132.
- Lev, A. A., and Buzhinsky, E. P., 1961, *Cytology (USSR)* **3**:614.
- Levi, H., and Ussing, H. H., 1948, *Acta Physiol. Scand.* **16**:232.
- Levine, L., Gordon, J. A., and Jencks, W., 1963, *Biochemistry* **2**:168.
- Levine, R., and Goldstein, M. S., 1955, *Rec. Prog. Horm. Res.* **11**:343.
- Levine, S., 1939, *Proc. R. Soc. London Ser. A* **170**:145.
- Levintow, L., and Meister, A. H., 1954, *J. Biol. Chem.* **209**:265.
- Lewis, G. N., 1916, *J. Am. Chem. Soc.* **38**:762.
- Lewis, G. N., 1923, *Valence and the Structure of Atoms and Molecules*, Chemical Catalogue, New York.
- Lezzi, M., 1970, *Int. Rev. Cytol.* **29**:127.
- Lezzi, M., and Gilbert, L. I., 1970, *J. Cell Sci.* **6**:615.
- Li, C. L., Bak, A. F., and Parker, L. O., 1968, *Exp. Neurol.* **20**:544.
- Lillie, R. S., 1908, *J. Exp. Zool.* **5**:375.
- Lillie, R. S., 1923, *Protoplasmic Action and Nervous Action*, University of Chicago Press, Chicago.
- Lillie, R. S., 1941, *Physiol. Zool.* **14**:239.
- Lindblom, G., 1971, *Acta Chem. Scand.* **25**:2767.
- Lineweaver, H., and Burk, D., 1934, *J. Am. Chem. Soc.* **56**:658.
- Lineweaver, H., and Schwimmer, S., 1941, *Enzymologia* **10**:81.
- Ling, G. N., 1951, *Am. J. Physiol.* **167**:806.
- Ling, G. N., 1952, in: *Phosphorus Metabolism*, Vol. II (W. D. McElroy and B. Glass, eds.), Johns Hopkins University Press, Baltimore, p. 748.
- Ling, G. N., 1953, in: *Proceedings of the 19th International Physiological Congress*, Montreal, p. 566.
- Ling, G. N., 1955, *Fed. Proc.* **14**:93.
- Ling, G. N., 1957, *Fed. Proc.* **16**:81.
- Ling, G. N., 1959, *Fed. Proc.* **18**:371.
- Ling, G. N., 1960, *J. Gen. Physiol.* **43**:149.
- Ling, G. N., 1962, *A Physical Theory of the Living State: The Association-Induction Hypothesis*, Blaisdell, Waltham, Massachusetts.
- Ling, G. N., 1964a, *Biopolymers* (Biophysical Symposium Issue) **1**:91.
- Ling, G. N., 1964b, *Tex. Rep. Biol. Med.* **22**:244.
- Ling, G. N., 1965a, *Fed. Proc.* **24**:S103.

- Ling, G. N., 1965b, *Persp. Biol. Med.* **9**:87.
Ling, G. N., 1965c, *Ann. N.Y. Acad. Sci.* **125**:401.
Ling, G. N., 1966a, *Fed. Proc.* **25**:958.
Ling, G. N., 1966b, *Ann. N.Y. Acad. Sci.* **137**:837.
Ling, G. N., 1967a, in: *Thermobiology* (A. Rose, ed.), Academic Press, New York, p. 5.
Ling, G. N., 1967b, in: *Glass Electrodes for Hydrogen and Other Cations* (G. Eisenman, ed.), Marcel Dekker, New York, p. 284.
Ling, G. N., 1967c, *Naturwiss. Rundsch.* **20**:415.
Ling, G. N., 1969a, *Int. Rev. Cytol.* **26**:1.
Ling, G. N., 1969b, *Nature* **221**:386.
Ling, G. N., 1970a, *Proc. Natl. Acad. Sci. USA* **67**:296.
Ling, G. N., 1970b, *Int. J. Neurosci.* **1**:129.
Ling, G. N., 1971, in: *Die Zelle*, 2nd ed. (H. Metzner, ed.), Wissenschaftliche Verlag, Stuttgart, p. 314.
Ling, G. N., 1972a, in: *Water and Aqueous Solutions: Structure, Thermodynamics and Transport Processes* (A. Horne, ed.), Wiley-Interscience, New York, p. 663.
Ling, G. N., 1972b, in: *Water Structure at the Water-Polymer Interface* (H. H. G. Jellinek, ed.), Plenum Press, New York, p. 4.
Ling, G. N., 1972c, *Physiol. Chem. Phys.* **4**:199.
Ling, G. N., 1973a, *Physiol. Chem. Phys.* **5**:295.
Ling, G. N., 1973b, *Biophys. J.* **13**:807.
Ling, G. N., 1974, *Physiol. Chem. Phys.* **6**:285.
Ling, G. N., 1977a, *J. Mol. Cell. Biochem.* **15**:159.
Ling, G. N., 1977b, *Physiol. Chem. Phys.* **9**:217.
Ling, G. N., 1977c, *Physiol. Chem. Phys.* **9**:301.
Ling, G. N., 1977d, *Physiol. Chem. Phys.* **9**:319.
Ling, G. N., 1977e, *Science* **198**:1281.
Ling, G. N., 1978a, *J. Physiol.* **280**:105.
Ling, G. N., 1978b, *Physiol. Chem. Phys.* **10**:353.
Ling, G. N., 1978c, *Bioelectrochem. Bioenerg.* **5**:411.
Ling, G. N., 1979a, *Physiol. Chem. Phys.* **11**:59.
Ling, G. N., 1979b, in: *The Aqueous Cytoplasm* (A. D. Keith, ed.), Marcel Dekker, New York, p. 23.
Ling, G. N., 1979c, *Trends Biochem. Sci. Lett. Ed.* **4**:N134.
Ling, G. N., 1980a, in: *Cooperative Phenomena in Biology* (G. Karreman, ed.), Pergamon Press, New York, p. 39.
Ling, G. N., 1980b, *Physiol. Chem. Phys.* **12**:215.
Ling, G. N., 1981a, *Physiol. Chem. Phys.* **13**:29.
Ling, G. N., 1981b, *Physiol. Chem. Phys.* **13**:356.
Ling, G. N., 1982, *Physiol. Chem. Phys.* **14**:47.
Ling, G. N., 1983a, *Physiol. Chem. Phys.* (in preparation).
Ling, G. N., 1983b, in: *Structure and Function of Excitable Cells* (D. S. Chang, I. Tasaki, W. J. Adelman, Jr., and H. R. Leuchtag, eds.), Plenum Press, New York, p. 365.
Ling, G. N., 1983c, *Physiol. Chem. Phys.* **15**:155.
Ling, G. N., and Balter, M., 1975, *Physiol. Chem. Phys.* **7**:529.
Ling, G. N., and Bohr, G., 1969, *Physiol. Chem. Phys.* **1**:591.
Ling, G. N., and Bohr, G., 1970, *Biophys. J.* **10**:519.
Ling, G. N., and Bohr, G., 1971a, *Physiol. Chem. Phys.* **3**:431.
Ling, G. N., and Bohr, G., 1971b, *Physiol. Chem. Phys.* **3**:573.
Ling, G. N., and Brady, M., 1983, *Physiol. Chem. Phys.* (in preparation).
Ling, G. N., and Cope, F. W., 1969, *Science* **163**:1335.
Ling, G. N., and Ferguson, E., 1970, *Physiol. Chem. Phys.* **2**:516.
Ling, G. N., and Fisher, A., 1983, *Physiol. Chem. Phys.* **15** (in press).
Ling, G. N., and Gerard, R. W., 1949a, *J. Cell. Comp. Physiol.* **34**:383.
Ling, G. N., and Gerard, R. W., 1949b, *J. Cell. Comp. Physiol.* **34**:397.
Ling, G. N., and Gerard, R. W., 1949c, *J. Cell. Comp. Physiol.* **34**:413.
Ling, G. N., and Gerard, R. W., 1949d, *Fed. Proc.* **8**:97.

- Ling, G. N., and Gerard, R. W., 1950, *Nature* **165**:113.
- Ling, G. N., and Graham, D. A., 1983, *Physiol. Chem. Phys.* (in preparation).
- Ling, G. N., and Kromash, H. M., 1967, *J. Gen. Physiol.* **50**:677.
- Ling, G. N., and Kwon, Y., 1983, *Physiol. Chem. Phys.* **15** (in press).
- Ling, G. N., and Murphy, R., 1982a, *Physiol. Chem. Phys.* **14**:209.
- Ling, G. N., and Murphy, R., 1982b, *Physiol. Chem. Phys.* **14**:213.
- Ling, G. N., and Murphy, R., 1983, *Physiol. Chem. Phys.* **15**:137.
- Ling, G. N., and Negendank, W., 1970, *Physiol. Chem. Phys.* **2**:15.
- Ling, G. N., and Negendank, W., 1980, *Persp. Biol. Med.* **23**:215.
- Ling, G. N., and Ochsenfeld, M. M., 1965, *Biophys. J.* **5**:777.
- Ling, G. N., and Ochsenfeld, M. M., 1966, *J. Gen. Physiol.* **49**:819.
- Ling, G. N., and Ochsenfeld, M. M., 1970, *Physiol. Chem. Phys.* **2**:189.
- Ling, G. N., and Ochsenfeld, M. M., 1973a, *Science* **181**:78.
- Ling, G. N., and Ochsenfeld, M. M., 1973b, *Ann. N.Y. Acad. Sci.* **204**:325.
- Ling, G. N., and Ochsenfeld, M. M., 1976, *Physiol. Chem. Phys.* **8**:389.
- Ling, G. N., and Ochsenfeld, M. M., 1977a, *Physiol. Chem. Phys.* **9**:405.
- Ling, G. N., and Ochsenfeld, M. M., 1977b, *Physiol. Chem. Phys.* **9**:427.
- Ling, G. N., and Ochsenfeld, M. M., 1983a, *Physiol. Chem. Phys.* **15**:127.
- Ling, G. N., and Ochsenfeld, M. M., 1983b, *Physiol. Chem. Phys.* (in preparation).
- Ling, G. N., and Ochsenfeld, M. M., 1983c, *Physiol. Chem. Phys.* (in preparation).
- Ling, G. N., and Ochsenfeld, M. M., 1983d, *Physiol. Chem. Phys.* (in preparation).
- Ling, G. N., and Palmer, L., 1972, *Physiol. Chem. Phys.* **4**:517.
- Ling, G. N., and Peterson, K., 1977, *Bull. Math. Biol.* **39**:721.
- Ling, G. N., and Sobel, A. M., 1975, *Physiol. Chem. Phys.* **7**:415.
- Ling, G. N., and Tucker, M., 1980, *J. Natl. Cancer Inst.* **64**:1199.
- Ling, G. N., and Tucker, M., 1983, *Physiol. Chem. Phys.* (in press).
- Ling, G. N., and Walton, C. L., 1975a, *Physiol. Chem. Phys.* **7**:215.
- Ling, G. N., and Walton, C. L., 1975b, *Physiol. Chem. Phys.* **7**:501.
- Ling, G. N., and Walton, C. L., 1976, *Science* **191**:293.
- Ling, G. N., and Will, S., 1969, *Physiol. Chem. Phys.* **1**:263.
- Ling, G. N., Will, S., 1976, *Physiol. Chem. Phys.* **8**:115.
- Ling, G. N., and Woodbury, J. W., 1949, *J. Cell. Comp. Physiol.* **34**:407.
- Ling, G. N., and Zodda, D., 1983, *Physiol. Chem. Phys.* (in press).
- Ling, G. N., Kalis, K., and Gale, M., 1964 [cited in Ling, G. N., 1964a, *Biopolymers* **1**:91].
- Ling, G. N., Ochsenfeld, M. M., and Karreman, G., 1967, *J. Gen. Physiol.* **50**:1807.
- Ling, G. N., Neville, M. C., Shannon, P., and Will, S., 1969a, *Physiol. Chem. Phys.* **1**:42.
- Ling, G. N., Neville, M. C., Will, S., and Shannon, P., 1969b, *Physiol. Chem. Phys.* **1**:85.
- Ling, G. N., Will, S., and Shannon, P., 1969c, *Physiol. Chem. Phys.* **1**:355.
- Ling, G. N., Miller, C., and Ochsenfeld, M. M., 1973, *Ann. N.Y. Acad. Sci.* **204**:6.
- Ling, G. N., Walton, G., and Ling, M. R., 1979, *J. Cell. Physiol.* **101**:261.
- Ling, G. N., Ochsenfeld, M. M., Walton, C., and Bersinger, T. J., 1980a, *Physiol. Chem. Phys.* **12**:3.
- Ling, G. N., Walton, C., and Bersinger, T. J., 1980b, *Physiol. Chem. Phys.* **12**:111.
- Ling, G. N., Walton, C. L., and Ochsenfeld, M. M., 1981, *J. Cell. Physiol.* **106**:385.
- Ling, G. N., Baxter, J., and Leitman, M., 1983, *Physiol. Chem. Phys.* **15** (in press).
- Ling, G. N., Ochsenfeld, M. M., Tucker, M., and Murphy, R., 1984, *Physiol. Chem. Phys.* (in preparation).
- Lipmann, F., 1941, *Adv. Enzymol.* **1**:99.
- Littlefield, J. W., 1982, *Science* **218**:214.
- Lockhart-Mummery, J. P., 1934, *The Origin of Cancer*. Churchill, London.
- Locy, W. A., 1908, *Biology and Its Makers*, 3rd ed., Holt, New York.
- Loeb, J., 1897, *Pflügers Arch. Ges. Physiol.* **69**:1.
- Loeb, J., 1905, *The Decennial Publication* (University of Chicago) **2**:450.
- Loeb, J., 1913, *Science* **37**:427.
- Loeb, J., 1920-1921a, *J. Gen. Physiol.* **3**:247.
- Loeb, J., 1920-1921b, *J. Gen. Physiol.* **3**:667.
- Loeb, L., 1930, *Physiol. Rev.* **10**:547.

- Lohmann, K., 1931, *Biochem. Z.* **233**:460.
Lohmann, K., 1935, *Biochem. Z.* **282**:120.
Long, C., 1961, *Biochemist's Handbook*, Spon, London.
Lorenz, R., 1920, *Z. Elektrochem.* **26**:424.
Lorente de Nò, R., 1947, *Stud. Rockefeller Inst.* **13**:106.
Lorkovic, H., and Tomanek, R. J., 1977, *Am. J. Physiol.* **232**:C109.
Lotem, J., and Sachs, L., 1982, *Proc. Natl. Acad. Sci. USA* **79**:4347.
Lowey, S., and Luck, S. M., 1969, *Biochemistry* **8**:3195.
Lowy, J., and Hanson, J., 1962, *Physiol. Rev.* **42**(Suppl. 5):34.
Lubin, M., 1964, *Fed. Proc.* **23**:994.
Lubin, M., 1967, *Nature* **213**:451.
Lundsgaard, E., 1930, *Biochem. Z.* **227**:51.
Lundsgaard, E., 1938, *Annu. Rev. Biochem.* **7**:377.
Luxoro, M., Cannessa, M., and Vargas, F., 1965, *Proceedings of the International Union of Physiological Sciences, XXIIId International Congress, Tokyo, 1965, Lectures and Symposium*, Volume 5.
Luyet, B., Tanner, J., and Rapatz, G. L., 1962, *Biodynamica* **9**:21.
Lynn, R. W., and Taylor, E. W., 1971, *Biochemistry* **10**:4617.

McAvoy, J. W., Dixon, K. E., and Marshall, J. A., 1975, *Dev. Biol.* **45**:330.
McBain, J. W., and Kellogg, F., 1928, *J. Gen. Physiol.* **12**:1.
McBain, J. W., and Peaker, C. R., 1930, *J. Phys. Chem.* **34**:1033.
Macallum, A. B., 1905, *J. Physiol. (London)* **32**:95.
Macallum, A. B., 1911, *Ergeb. Physiol.* **11**:599.
McCann, J., Choi, E., Yamasaki, E., and Ames, B. N., 1975, *Proc. Natl. Acad. Sci. USA* **72**:5135.
MacDonald, J. S., 1900, *Proc. R. Soc. London* **67**:310.
MacDonald, J. S., 1909, *Q. J. Exp. Physiol.* **2**:1.
McDonald, R. E., and Lanyi, J. K., 1975, *Biochemistry* **14**:2882.
McDougall, W., 1897, *J. Anat. Physiol.* **32**:187.
McFarlane, A. S., McFarlane, M. G., Amies, C. R., and Eagles, G. H., 1939, *Br. J. Exp. Pathol.* **20**:485.
McFarlane, M. G., and Spencer, A. G., 1953, *Biochem. J.* **54**:569.
McKenzie, S. L., Henikoff, S., and Meselson, M., 1975, *Proc. Natl. Acad. Sci. USA* **72**:1117.
McKinley, D., and Meissner, G., 1977, *FEBS Lett.* **82**:47.
McKinnel, R. G., Deggins, B. A., and Labat, D. D., 1969, *Science* **165**:394.
McLaren, A. D., and Rowen, J. W., 1951, *J. Polym. Sci.* **7**:289.
McLaughlin, S. G. A., and Hinke, J. A. M., 1966, *Can. J. Physiol. Pharmacol.* **44**:837.
McLaughlin, S. G. A., and Hinke, J. A. M., 1968, *Can. J. Physiol. Pharmacol.* **46**:247.
MacLeod, J., and Ponder, E., 1936, *J. Physiol.* **86**:147.
Maddrell, S. H. P., 1978, in: *Membrane Transport in Biology*, Vol. 3 (G. Giebisch, D. C. Tosteson, and H. H. Ussing, eds.), Springer, New York, p. 239.
Maeno, T., 1959, *J. Gen. Physiol.* **43**:139.
Makino, M., and Hasselbach, W., 1971, *FEBS Lett.* **12**:271.
Maloff, B. L., Scordilis, S. P., Reynolds, C., and Tedeschi, H., 1978, *J. Cell Biol.* **78**:199.
Mannherz, H. G., Schenck, H., and Goody, R. S., 1974, *Eur. J. Biochem.* **48**:287.
Manning, G. S., 1978, *Q. Rev. Biophys.* **11**:179.
Manwell, C., 1958, *Science* **127**:592.
Marchesi, V. T., and Palade, G. E., 1967, *J. Cell. Biol.* **35**:385.
Marcus, A., Luginbill, B., and Feeley, 1968, *Proc. Natl. Acad. Sci. USA* **59**:1243.
Margoliash, E., Barlow, G. H., and Byers, V., 1970, *Nature* **228**:723.

- Margolit, S., and Schejter, A., 1974, *Eur. J. Biochem.* **46**:387.
- Margossian, S. S., and Lowey, S., 1978, *Biochemistry* **17**:5431.
- Markert, C. L., 1968, *Cancer Res.* **28**:1908.
- Marmont, G., 1949, *J. Cell. Comp. Physiol.* **34**:351.
- Marsh, B. B., 1952, *Biochim. Biophys. Acta* **9**:247.
- Marsh, D. J., De Bruin, S. H., and Gratzer, W. B., 1977, *Biochemistry* **16**:1738.
- Marsh, G., 1935, *J. Plant Physiol.* **10**:681.
- Marston, S. B., Rodger, C. D., and Trigeau, R. T., 1976, *J. Mol. Biol.* **104**:263.
- Martinez, D., Silvidi, A. A., and Stokes, R. M., 1969, *Biophys. J.* **9**:1256.
- Marx, J. L., 1982, *Science* **218**:983.
- Massari, S., Balboni, E., and Azzone, G. F., 1972, *Biochim., Biophys. Acta* **283**:16.
- Masszi, G., 1972, *Acta Biochim. Biophys. Acad. Hung* **7**:349.
- Masszi, G., and Örkényi, J., 1967, *Acta Biochim. Biophys. Acad. Sci. Hung.* **2**:131.
- Masszi, G., Szijártó, Z., and Gróf, P., 1976, *Acta Biochim. Biophys. Acad. Sci. Hung* **11**:129.
- Masuda, H., and de Meis, L. D., 1973, *Biochemistry* **12**:4581.
- Masui, Y., 1967, *J. Exp. Zool.* **166**:365.
- Masui, Y., and Clarke, H. J., 1979, *Int. Rev. Cytol.* **57**:185.
- Masui, Y., and Markert, C. L., 1971, *J. Exp. Zool.* **177**:129.
- Masui, Y., Meyerhof, P. G., Miller, M. A., and Wasserman, W. I., 1977, *Differentiation* **9**:49.
- Matsubara, I., and Elliott, G. F., 1972, *J. Mol. Biol.* **72**:657.
- Matsui, H., Hayashi, Y., Homareda, H., and Kimimura, M., 1977, *Biochem. Biophys. Res. Commun.* **75**:373.
- Matteucci, M. C., 1841, *C. R. Acad. Sci.* **13**:540.
- Mazia, D., 1937, *J. Cell. Comp. Physiol.* **10**:291.
- Mazia, D., 1974, *Sci. Am.* **230**:54.
- Mazia, D., Schattan, G., and Steinhardt, R., 1975, *Proc. Natl. Acad. Sci. USA* **72**:4469.
- Meiboom, S., Lutz, Z., and Gill, D., 1957, *J. Chem. Phys.* **27**:1411.
- Meigs, E. G., 1912, *J. Exp. Zool.* **13**:497.
- Meigs, E. G., and Ryan, L. A., 1912, *J. Biol. Chem.* **11**:401.
- Mellon, E. F., Korn, A. H., and Hoover, S. R., 1948, *J. Am. Chem. Soc.* **70**:3040.
- Menten, M. L., 1908, *Trans. Can. Inst.* **8**:403.
- Menz, L. J., and Luyet, B. J., 1961, *Biodynamica* **8**:261.
- Meryman, H. T., 1958, *Biodynamica* **8**:69.
- Metuzals, J., 1969, *J. Cell Biol.* **43**:480.
- Metuzals, J., and Izzard, C. S., 1969, *J. Cell Biol.* **43**:456.
- Meyer, K. H., 1901, *Arch. Exp. Pathol. Pharmakol.* **46**:358.
- Meyer, K. H., and Mark, H., 1930, *Der Aufbau des Hochpolymeren organischen Naturstoffe auf Grund Molekular-morphologischer Betrachtungen*, Leipzig, pp. 232 and 243.
- Meyer, K. H., and Pickens, L. E. R., 1937, *Proc. R. Soc. London Ser. B* **124**:29.
- Meyer, K. H., and Sievers, J. F., 1936a, *Helv. Chim. Acta* **19**:649.
- Meyer, K. H., and Sievers, J. F., 1936b, *Helv. Chim. Acta* **19**:665.
- Meyerhof, O., and Hill, A. V., 1923, *Ergeb. Physiol.* **22**:299.
- Meyerhof, P. G., and Masui, Y., 1977, *Dev. Biol.* **61**:214.
- Michaelis, L., 1925, *J. Gen. Physiol.* **8**:33.
- Michaelis, L., 1926, *Naturwissenschaft* **15**:33.
- Michaelis, L., and Fujita, A., 1926, *Biochem. Z.* **161**:47.
- Michaelis, L., and Menten, M. L., 1913, *Biochem. Z.* **49**:333.
- Michaelis, L., and Perlzweig, W. A., 1927, *J. Gen. Physiol.* **10**:575.
- Michaelis, L., and Rona, P., 1908, *Biochem. Z.* **14**:476.
- Mihalyi, E., 1950, *Enzymologia* **14**:224.
- Mihalyi, E., and Szent-Györgyi, A. G., 1953, *J. Biol. Chem.* **201**:189.
- Miller, C., 1974, *Biochim. Biophys. Acta* **339**:71.
- Miller, C., and Ling, G. N., 1970, *Physiol. Chem. Phys.* **2**:495.
- Miller, J. S. L., and Burgess, R. R., 1978, *Biochemistry* **17**:2054.
- Millette, R., Trotter, C. D., Herrlich, P., and Schweiger, M., 1970, *Cold Spring Harbor Symp. Quant. Biol.* **35**:135.

- Mills, R., 1961, *Rev. Pure Appl. Chem.* **11**:78.
Mills, R., 1973, *J. Phys. Chem.* **77**:685.
Mills, R., and Kennedy, J. W., 1953, *J. Am. Chem. Soc.* **75**:5696.
Mines, G. R., 1913, *J. Physiol.* **46**:11.
Minkoff, L., and Damadian, R., 1973, *Biophys. J.* **13**:167.
Minkoff, L., Abramowitz, J., and Damadian, R., 1976, *Physiol. Chem. Phys.* **8**:167.
Mintz, B., 1978, *Harvey Lect.* **71**:193.
Mintz, B., and Fleischman, R. A., 1981, *Adv. Cancer Res.* **34**:211.
Mintz, B., and Illmensee, K., 1975, *Proc. Natl. Acad. Sci. USA* **72**:3585.
Mitchell, P., 1961, *Nature* **191**:144.
Mitchell, P., 1966, *Chemiosmotic Coupling in Oxidative and Photosynthetic Phosphorylation*, Glynn Research, Bodmin, Cornwall, England.
Mitchell, P. H., Wilson, J. N., and Stanton, R. E., 1922, *J. Gen. Physiol.* **4**:141.
Mitchison, J. M., 1971, *The Biology of the Cell Cycle*, Cambridge University Press, New York.
Miyake, M., Inoue, I., and Kobatake, Y., 1973, *Biochim. Biophys. Acta* **323**:367.
Mizushima, S., 1954, *Structure of Molecules and Internal Rotation*, Academic Press, New York.
Mizushima, S., Nakagawa, I., Schmelz, J. J., Curran, C., and Quagliano, J. V., 1958, *Spectrochim. Acta* **13**:31.
Mond, R., 1927, *Pflügers Arch. Ges. Physiol.* **217**:618.
Mond, R., and Amson, K., 1928, *Pflügers Arch. Ges. Physiol.* **20**:69.
Mond, R., and Hoffmann, F., 1928, *Pflügers Arch. Ges. Physiol.* **220**:194.
Mond, R., and Netter, H., 1930, *Pflügers Arch. Ges. Physiol.* **224**:702.
Monoi, H., 1976, *Biophys. J.* **16**:1349.
Moore, B., 1906, in: *Recent Advances in Biochemistry* (L. Hill, ed.), Arnold, London, p. 139.
Moore, B., and Roaf, H. E., 1908, *Biochem. J.* **3**:55.
Moore, B., Roaf, H. E., and Webster, A., 1912, *Biochem. J.* **6**:110.
Moore, C., and Pressman, B. C., 1964, *Biochem. Biophys. Res. Commun.* **15**:562.
Moore, T. S., and Winnill, T. F., 1912, *J. Chem. Soc.* **101**:1635.
Mooseker, M. S., 1976, *J. Cell Biol.* **71**:417.
Morales, M., and Botts, J., 1952, *Trans. Faraday Soc.* **11**:5867.
Morales, M., and Botts, J., 1953, *Disc. Faraday Soc.* **13**:125.
Morales, M., Botts, J., Blum, J. J., and Hill, T. L., 1955, *Physiol. Rev.* **35**:475.
Moran, T., 1926, *Proc. R. Soc. London Ser. A* **112**:30.
Moreau, M., Dorée, M., and Guerriere, P., 1976, *J. Exp. Zool.* **197**:443.
Moreau, M., Guerriere, P., Dorée, M., and Ashley, C. C., 1978, *Nature* **272**:251.
Moreau, M., Vilain, J. P., and Guerriere, P., 1980, *Dev. Biol.* **78**:201.
Morel, F., 1961, in: *Proceedings of the 1st International Congress of Nephrology*, Karger, Basel, p. 16.
Morowitz, H. J., and Terry, T. M., 1969, *Biochim. Biophys. Acta* **183**:276.
Mozhayeva, G. N., 1969, *Biophysics* **14**:68.
Muggleton-Harris, A. L., and Pezzella, K., 1972, *Expt. Gerontol.* **7**:427.
Muirhead, H., Cox, J. M., Mazzarella, L., and Perutz, M. F., 1967, *J. Mol. Biol.* **28**:117.
Müller, P., 1975, *Ann. N.Y. Acad. Sci.* **264**:97.
Müller, P., Rudin, D. O., Tien, H. T., and Wescott, W. C., 1962, *Nature* **194**:979.
Müller, P., Rudin, D. O., and Tien, T., 1963, *J. Phys. Chem.* **67**:534.
Mullins, L. J., 1942, *Biol. Bull.* **83**:326.
Mullins, L. J., 1959, *J. Gen. Physiol.* **42**:817.
Mullins, L. J., and Brinley, F. J., 1969, *J. Gen. Physiol.* **53**:704.
Mullins, L. J., and Noda, K., 1963, *J. Gen. Physiol.* **47**:117.
Murcray, H., and Hopfer, U., 1974, *Proc. Natl. Acad. Sci. USA* **71**:484.
Murray, J. M., and Weber, A., 1974, *Sci. Am.* **230**:59.
Mysels, K. J., and McBain, J. W., 1948, *J. Colloid Sci.* **3**:45.

Nachmansohn, D., 1928, *Biochem. Z.* **196**:73.
Nagai, T., Makino, M., and Hasselbach, W., 1960, *Biochim. Biophys. Acta* **43**:223.
Nagel, W., Garcia-Diaz, J. F., and Armstrong, W. McD., 1981, *J. Membr. Biol.* **61**:127.
Naitoh, Y., and Kaneko, H., 1972, *Science* **176**:523.

- Nakanishi, S., Adhya, S., Gottesman, M., and Pastan, I., 1974, *J. Biol. Chem.* **249**:4050.
- Nakao, M., Nakao, T., Yamazoe, S., and Yoshikawa, H., 1961, *J. Biochem. (Tokyo)* **49**:487.
- Nakazawa, T., Asami, K., Suzuki, H., and Yukawa, O., 1973, *J. Biochem. (Tokyo)* **73**:397.
- Napolitano, L., Le Baron, F., and Scaletti, J., 1967, *J. Cell Biol.* **34**:817.
- Narahara, H. T., Ozand, P., and Cori, C. F., 1960, *J. Biol. Chem.* **235**:3370.
- Narahashi, T., 1960, in: *Electrical Activities of Single Cells* (Y. Katsuki, ed.), Igaku Shoin, Tokyo, p. 119.
- Nasonov, D. N., 1962, *Local Reaction of Protoplasm and Gradual Excitation* (Y. S. Halpern, transl.), Israel Program for Scientific Translations, Jerusalem [available from Office of Technical Services, U.S. Department of Commerce, Washington, D.C.].
- Nasonov, D. N., and Aleksandrov, V. Ya., 1944, *Usp. Sovrem. Biol.* **17**:1.
- Nathansohn, A., 1904, *Jahrb. Wiss. Bot.* **39**:607.
- Natori, R., 1954, *Jikeikai Med. J.* **1**:18.
- Natori, R., 1955, *Jikeikai Med. J.* **2**:1.
- Needham, D. M., 1937, in: *Perspectives in Biochemistry* (J. Needham and D. E. Green, eds.), Cambridge University Press, Cambridge, p. 201.
- Needham, D. M., 1971, *Machina Carnis: The Biochemistry of Muscular Contraction in Its Historical Development*, Cambridge University Press, Cambridge.
- Needham, J., 1950, *Biochemistry and Morphogenesis*, Cambridge University Press, Cambridge.
- Negendank, W., and Collier, C. R., 1976, *Exp. Cell Res.* **101**:31.
- Negendank, W., and Karreman, G., 1979, *J. Cell. Physiol.* **98**:107.
- Negendank, W., and Shaller, C., 1979a, *J. Cell. Physiol.* **98**:95.
- Negendank, W., and Shaller, C., 1979b, *J. Cell. Physiol.* **98**:539.
- Negendank, W., and Shaller, C., 1980a, *J. Cell. Physiol.* **103**:87.
- Negendank, W., and Shaller, C., 1980b, *J. Cell. Physiol.* **104**:443.
- Negendank, W., and Shaller, C., 1981, *Biochim. Biophys. Acta* **640**:368.
- Negendank, W., and Shaller, C., 1982a, *Biochim. Biophys. Acta* **688**:316.
- Negendank, W., and Shaller, C., 1982b, *Biochim. Biophys. Acta* **694**:123.
- Nernst, W., 1889, *Z. Phys. Chem.* **4**:129.
- Nernst, W., 1891, *Z. Phys. Chem.* **8**:110.
- Nernst, W., 1892, *Z. Phys. Chem.* **9**:137.
- Nesterov, V. P., and Tigyi-Sebes, A., 1965, *Acta Physiol. Acad. Sci. Hung.* **28**:97.
- Netter, H., 1928, *Pflügers Arch. Ges. Physiol.* **220**:107.
- Neuschloss, S. M., 1925, *Pflügers Arch. Ges. Physiol.* **207**:27.
- Neuschloss, S. M., 1926, *Pflügers Arch. Ges. Physiol.* **213**:19, 40, and 47.
- Neville, M. C., 1962, quoted in Ling, 1962, p. 280.
- Neville, M. C., 1973, *Ann. N.Y. Acad. Sci.* **204**:538.
- Neville, M. C., Paterson, C. A., Rae, J. L., and Woessner, D. E., 1974, *Science* **184**:1072.
- Newton, R., and Gortner, R. C., 1922, *Bot. Gaz.* **74**:442.
- Nicolksky, B. P., 1937, *Acta Physicochim.* **7**:595.
- Nielsen, J. M., Adamson, A. W., and Cobble, J. W., 1952, *J. Am. Chem. Soc.* **74**:446.
- Nishioka, D., and McGwin, N. F., 1980, *J. Exp. Zool.* **212**:215.
- Niu, M. C., and Twitty, W., 1953, *Proc. Natl. Acad. Sci.* **39**:985.
- Noack, F., 1971, *NMR: Basic Principles and Progress* **3**:83.
- Nobel Foundation, New York, 1965, *Nobel Lectures, 1922–1941*, Vol. II.
- Noonan, T. R., Fenn, W. O., and Haege, L., 1941, *Am. J. Physiol.* **132**:612.
- Nutting, P. G., 1927, *J. Phys. Chem.* **31**:531.
- Oberling, C., 1952, *The Riddle of Cancer*, revised ed. (W. H. Woglom, transl.), Yale University Press, New Haven, and Oxford University Press, London.
- O'Connor, C. M., Robinson, K. R., and Smith, L. D., 1977, *Dev. Biol.* **61**:28.
- Odeblad, E., 1957, *Ann. N.Y. Acad. Sci.* **83**:189.
- Odeblad, E., Bhar, B. N., and Linström, G., 1956, *Arch. Biochem. Biophys.* **63**:221.
- Ohtsu, K., Naito, K., and Wilt, F. H., 1964, *Dev. Biol.* **10**: 216.
- Oikawa, T., Spyropoulos, C. S., Tasaki, I., and Teorell, I., 1961, *Acta Physiol. Scand.* **52**:195.
- Okada, Y., Ogawa, M., Aoki, N., and Izutsu, K., 1973, *Biochim. Biophys. Acta* **291**:116.

- Oncley, J. L., 1953, in: *Proteins, Amino Acids and Peptides* (E. J. Cohn and J. T. Edsall, eds.), Reinhold, New York, Chapter 22.
- Oosawa, F., and Kasai, M., 1971, in: *Subunits in Biological Systems* (S. N. Timasheff and G. Fasman, eds.), Marcel Dekker, New York, p. 261.
- Opit, L. J., and Charnock, J. S., 1965, *Biochim. Biophys. Acta* **110**:9.
- Orr, C. W., Yoshikawa-Fukuda, M., and Ebert, J. D., 1972, *Proc. Natl. Acad. Sci. USA* **69**:243.
- Osterhout, W. H., 1936, *Bot. Rev.* **2**:283.
- Ostwald, W., 1890, *Z. Phys. Chem.* **6**:71.
- Outhred, R. K., and George, E. P., 1973, *Biophys. J.* **13**:97.
- Overton, E., 1895, *Vierteljahrsschr. Naturforsch. Ges. Zürich* **40**:159.
- Overton, E., 1899, *Vierteljahrsschr. Naturforsch. Ges. Zürich* **44**:88.
- Overton, E., 1902a, *Pflügers Arch. Ges. Physiol.* **92**:115.
- Overton, E., 1902b, *Pflügers Arch. Ges. Physiol.* **92**:346.
- Overton, E., 1907, in: *Handbuch der Physiologie des Menschen*, Vol. II (W. Nagel, ed.), Vieweg, Braunschweig, p. 744.
- Owe-Berg, T. G., 1965, *Ann. N.Y. Acad. Sci.* **125**:298.
- Oxender, D. L., and Christensen, H. N., 1963, *J. Biol. Chem.* **238**:3686.
- Packer, L., Utsumi, K., and Mustafa, M., 1966, *Arch. Biochem. Biophys.* **117**:381.
- Page, D. I., 1972, in: *Water: A Comprehensive Treatise*, Vol. 1 (F. Franks, ed.), Plenum Press, New York, p. 333.
- Page, E., and Storm, S. R., 1965, *J. Gen. Physiol.* **48**:957.
- Paine, P. L., Moore, L. C., and Horowitz, S. B., 1975, *Nature* **254**:109.
- Paine, P. L., Pearson, T. W., Tluczek, L. J. M., and Horowitz, S. B., 1981, *Nature* **291**:258.
- Pallansch, M. J., and Briggs, D. R., 1954, *J. Am. Chem. Soc.* **76**:1396.
- Palmer, L. G., and Gulati, J., 1976, *Science* **194**:521.
- Palmer, L. G., Century, T. J., and Civan, M. M., 1978, *J. Membr. Biol.* **40**:25.
- Panet, R., and Selinger, Z., 1972, *Biochem. Biophys. Acta* **255**:34.
- Pant, H. C., Terakawa, S., Baumgold, J., Tasaki, I., and Gainer, H., 1978, *Biochim. Biophys. Acta* **513**:132.
- Pardee, A. B., Dubrow, R., Hamlin, J. L., and Kletzien, R. F., 1978, *Annu. Rev. Biochem.* **47**:715.
- Park, C. R., Bornstein, J., and Post, R. L., 1955, *Am. J. Physiol.* **182**:12.
- Passow, H., 1969, *Prog. Biophys. Mol. Biol.* **19**:425.
- Pasteels, J., 1938, *Bull. Acad. R. Med. Belg.* **24**:721.
- Patlak, C. S., Goldstein, D. A., and Hoffman, J. F., 1963, *J. Theor. Biol.* **5**:426.
- Paton, W. D. M., 1956, in: *Histamine: Ciba Foundation Symposium* (G. E. W. Wolstenholme and G. M. O'Connor, eds.), Little, Brown, Boston, p. 59.
- Pauli, W., and Rona, P., 1902, *Beitr. Chem. Physiol. Pathol.* **1902**:114.
- Pauli, W., and Samec, M., 1909, *Biochem. Z.* **17**:235.
- Pauling, L., 1945, *J. Am. Chem. Soc.* **67**:555.
- Pauly, H., and Schwan, H. P., 1964, *IEEE Trans. Biomed. Eng.* **BME-11**(3):103.
- Pauly, H., and Schwan, H. P., 1966, *Biophys. J.* **6**:621.
- Pavan, C., and Breuer, M. E., 1952, *J. Hered.* **43**:150.
- Peachey, L. D., 1965, *J. Cell. Biol.* **25**:209.
- Peaucellier, G., 1977, *C. R. Acad. Sci. Ser. D* **285**:913.
- Pederson, T., and Robbins, E., 1970, *J. Cell Biol.* **45**:509.
- Pelling, G., 1959, *Nature* **184**:655.
- Pennock, B. E., and Schwan, H. P., 1969, *J. Phys. Chem.* **73**:2600.
- Perry, S. V., and Grey, T. C., 1956, *Biochem. J.* **64**:184.
- Perutz, M. F., 1978, *Science* **201**:1187.
- Perutz, M. F., 1979, *Annu. Rev. Biochem.* **48**:327.
- Perutz, M. F., Muirhead, H., Cox, J. M., Goaman, L. C. G., Mathews, F. S., McGandy, E. L., and Webb, L. E., 1968, *Nature* **219**:29.
- Peschel, G., and Belouschek, P., 1979, in: *Cell Associated Water* (W. Drost-Hansen and J. S. Clegg, eds.), Academic Press, New York, p. 3.

- Peters, J. P., 1935, *Body Water—The Exchange of Fluids in Man*, Thomas, Springfield, Illinois.
- Pezolet, M., Pigeon-Gosselin, M., Savoie, R., and Caille, J., 1978, *Biochim. Biophys. Acta* **544**:394.
- Pfeffer, W. F., 1877, *Osmotische Untersuchungen: Studien zur Zell-Mechanik*, Englemann, Leipzig.
- Pfeffer, M. F., 1881, *Pflanzenphysiologie*, Vol. 1, Englemann, Leipzig, p. 26.
- Pfeffer, W. F., 1897, *Pflanzenphysiologie*, 2nd ed., Vol. 1, Englemann, Leipzig, p. 116.
- Pfeffer, W. F., 1921, *Osmotische Untersuchungen: Studien zur Zell-Mechanik*, 2nd ed., Englemann, Leipzig.
- Pfeiffer, D. R., and Lardy, H. A., 1976, *Biochemistry* **15**:935.
- Pfeiffer, P., 1913, *Ann. Chem.* **398**:137.
- Philippson, M., 1920, *C. R. Soc. Biol. (Paris)* **83**:1399.
- Phillips, R. C., George, S. J. P., and Rutman, R. J., 1966, *J. Am. Chem. Soc.* **88**:2631.
- Piatigorsky, J., Fukvi, H. N., and Kinoshita, J. H., 1978, *Nature* **274**:558.
- Pierce, G. B., 1967, *Curr. Top. Dev. Biol.* **2**:223.
- Podolsky, R. J., 1959, *Ann. N.Y. Acad. Sci.* **72**:522.
- Podolsky, R. J., and Kitzinger, C., 1955, *Fed. Proc.* **14**:115.
- Podolsky, R. J., and Morales, M. F., 1956, *J. Biol. Chem.* **218**:945.
- Polanyi, M., 1920, *Biochem. Z.* **104**:237.
- Pollak, J. L., 1975, *Biochem. J.* **150**:477.
- Pollak, J. K., 1977, *Biochem. Soc. Trans.* **5**:341.
- Pollard, T. D., and Weihing, R. R., 1974, *Crit. Rev. Biochem.* **2**:1.
- Ponder, E., 1948, *Hemolysis and Related Phenomena*, Grune and Stratton, New York.
- Ponder, E., 1951, *J. Exp. Med.* **28**:567.
- Popple, J. A., Schneider, W. G., and Bernstein, H. J., 1959, *High-Resolution Nuclear Magnetic Resonance*, McGraw-Hill, New York.
- Porter, K. R., and Bonneville, M. A., 1968, *Fine Studies of Cells and Tissues*, 3rd ed., Lea and Febiger, Philadelphia.
- Porter, K. R., and Palade, G. E., 1957, *J. Biophys. Biochem. Cytol.* **3**:269.
- Post, R. L., Merritt, C. R., Kinsolving, C. R., and Albright, C. D., 1960, *J. Biol. Chem.* **235**:1796.
- Post, R. L., Toda, G., Kume, S., and Taniguchi, K., 1975, *J. Supramol. Struct.* **3**:479.
- Potten, C. S., Schofield, R., and Lajtha, L. G., 1979, *Biochim. Biophys. Acta* **560**:281.
- Potter, V. R., 1961, *Cancer Res.* **21**:1331.
- Powers, R. D., and Biggers, J. D., 1976, *J. Cell. Biol.* **7**:352a (article 1054).
- Prescott, D. M., 1976, *Reproduction of Eukaryotic Cells*, Academic Press, New York.
- Prescott, D. M., and Goldstein, L., 1968, *J. Cell Biol.* **39**:404.
- Pressman, B. C., 1965, *Proc. Natl. Acad. Sci. USA* **53**:1076.
- Pressman, B. C., and Lardy, H. A., 1952, *J. Biol. Chem.* **197**:547.
- Procter, H. R., 1914, *J. Chem. Soc.* **105**:313.
- Procter, H. R., and Wilson, J. A., 1916, *J. Chem. Soc.* **109**:307.
- Prusch, R. D., and Dunham, P. B., 1972, *J. Exp. Biol.* **56**:551.
- Pryor, M. G. M., 1950, *Prog. Biophys. Biophys. Chem.* **1**:216.
- Przybylski, A. T., Stratten, W. P., Syren, R. M., and Fox, S. W., 1982, *Naturwissenschaften* **69**:561.
- Purcell, E. M., Torrey, H. C., and Pound, R. V., 1946, *Phys. Rev.* **69**:37.
- Purkinje, J. E., 1840; *Über die Analogien in den Strukturelementen des pflanzlichen und tierischen Organismus. Übersicht der Arbeiten und Veränderungen der schlesischen Gesellschaft für vaterländische Kultur im Jahre*, Dresden.
- Quastel, M. R., and Kaplan, J. G., 1968, *Nature* **219**:198.
- Quinke, G., 1898, *Ann. Physik.* **64**:618.
- Rajewsky, B., 1938, in: *Ergebnisse Biophysikalischer Forschungen Ultra Kurzwellen* (B. Rajewsky, ed.), Georg Thieme, Leipzig.
- Ramachandran, G. N., 1967, in: *Treatise on Collagen*, Vol. 1 (G. N. Ramachandran, ed.), Academic Press, New York, p. 103.
- Ramsey, R. W., and Street, S. F., 1940, *J. Cell. Comp. Physiol.* **15**:11.
- Rangachari, P. K., Paton, D. M., and Daniel, E. E., 1972, *Biochim. Biophys. Acta* **274**:462.

- Rao, P. N., and Johnson, R. T., 1970, *Nature* **225**:159.
- Rao, P. N., and Johnson, R. T., 1971, *J. Cell. Physiol.* **78**:217.
- Rapatz, G., and Luyet, B., 1959, *Biodynamica* **8**:121.
- Raventos, J., 1937, *Q. J. Exp. Physiol.* **26**:361.
- Reddy, E. P., Reynolds, R. K., Santos, E., and Barbacid, M., 1982, *Nature* **300**:149.
- Reed, N., and Fain, J. N., 1968, *J. Biol. Chem.* **243**:6077.
- Reedy, M. K., Holmes, K. C., and Tregear, R. T., 1965, *Nature* **207**:1276.
- Reichenberg, D., 1966, in: *Ion Exchange: A Series of Advances*, Vol. 1 (J. A. Marinsky, ed.), Marcel Dekker, New York, p. 227.
- Reid, R. A., Moyle, J., and Mitchell, P., 1966, *Nature* **212**:257.
- Reiser, A., 1959, in: *Hydrogen Bonding* (D. Hadzi and H. W. Thompson, eds.), Pergamon Press, New York, p. 446.
- Reisin, I. L., and Gulati, J., 1973, *Ann. N.Y. Acad. Sci.* **204**:358.
- Reisin, I. L., and Ling, G. N., 1973, *Physiol. Chem. Phys.* **5**:183.
- Reisin, I. L., Rotunno, C. A., Corchs, L., Kowalewski, V., and Cerejido, M., 1970, *Physiol. Chem. Phys.* **2**:171.
- Reisin, I. L., Gulati, J., and Ling, G. N., 1971, *Fed. Proc.* **30**:331.
- Rensing, L., and Fischer, M., 1975, *Cell Differ.* **4**:209.
- Renz, M., Nehls, P., and Holzier, J., 1977, *Proc. Natl. Acad. Sci. USA* **74**:1879.
- Reznikoff, P., and Chambers, R., 1925, *Proc. Soc. Exp. Biol. Med.* **22**:386.
- Rich, S. A., and Estes, J. E., 1976, *J. Mol. Biol.* **104**:777.
- Richards, G., 1978, *Dev. Biol.* **66**:32.
- Ridgeway, E. B., and Ashley, C. C., 1967, *Biochem. Biophys. Res. Commun.* **29**:229.
- Ries, E., and Gersch, M., 1936, *Pubbl. Stn. Zool. Napoli* **15**:223.
- riggs, A. D., and Bourgeois, S., 1968, *J. Mol. Biol.* **34**:361.
- riggs, A. D., Suzuki, H., and Bourgeois, S., 1970, *J. Mol. Biol.* **48**:67.
- riggs, T. R., Walker, L. M., and Christensen, H., 1958, *J. Biol. Chem.* **223**:1479.
- Riklis, E., and Quastel, J. H., 1958, *Can. J. Biochem. Physiol.* **36**:347.
- Riseman, J., and Kirkwood, J. G., 1948, *J. Am. Chem. Soc.* **70**:2820.
- Ritossa, F., 1962, *Experientia* **18**:571.
- Ritossa, F., 1964, *Exp. Cell. Res.* **35**:601.
- Ritossa, F., and Pulitzer, J. F., 1963, *J. Cell Biol.* **19**:60a.
- Rizzino, A. A., Barouch, W. W., Eisenberg, E., and Moos, C., 1970, *Biochemistry* **9**:2402.
- Robbins, E. A., and Boyer, P. D., 1957, *J. Biol. Chem.* **224**:121.
- Robbins, E. A., Pederson, T., and Klein, P., 1970, *J. Cell Biol.* **44**:400.
- Roberts, E., and Frankel, S., 1949, *Cancer Res.* **9**:231 and 645.
- Roberts, I. Z., and Wolffe, E. L., 1951, *Arch. Biochem. Biophys.* **33**:165.
- Roberts, R. B., Roberts, I. Z., and Cowie, D. B., 1949, *J. Cell. Comp. Physiol.* **34**:259.
- Robertson, J. D., 1960, *Prog. Biophys. Biophys. Chem.* **10**:343.
- Rogus, E., and Zierler, K. L., 1970, *Fed. Proc.* **29**:455.
- Rome, E., 1967, *J. Mol. Biol.* **27**:591.
- Rome, E., 1968, *J. Mol. Biol.* **37**:331.
- Rorschach, H. E., 1984, in: *Water and Ions in Biological Systems* (V. Vasilescu, ed.), Plenum Press, New York (in preparation).
- Rose, B., and Loewenstein, W. R., 1975, *Science* **190**:1204.
- Rosenthal, E. T., Hunt, T., and Ruderman, J. V., 1980, *Cell* **20**:487.
- Ross, H., and Hedicke, H., 1927, *Die Pflanzengallen*, Fischer, Jena.
- Rossi, C. S., and Lehninger, A. L., 1964, *J. Biol. Chem.* **239**:3971.
- Rossi, C., Azzi, A., and Azzone, G. F., 1967, *J. Biol. Chem.* **242**:951.
- Rossi, E., and Azzone, G. F., 1970, *Eur. J. Biochem.* **12**:319.
- Rossi-Fanelli, A., Antonini, E., and Caputo, A., 1959, *Nature* **183**:827.
- Rossi-Fanelli, A., Antonini, E., and Caputo, A., 1964, *Adv. Protein Chem.* **19**:73.
- Rothechuh, K. E., 1957, *Klin. Wochenschr.* **35**:605.
- Rothechuh, K. E., 1963, in: *Essays on the History of Italian Neurology* (G. Belloni, ed.), CEDAM, Milan, p. 117.

- Rothschuh, K. E., 1973, *History of Physiology* (G. Risse, transl.), Robert E. Krieger Publishing, Huntington, New York.
- Rothstein, A., Cabantchik, Z. I., and Knauf, P., 1976, *Fed. Proc.* **35**:3.
- Rottenberg, H., 1970, *Eur. J. Biochem.* **15**:22.
- Rouayre, J. F., and Travers, F., 1981, *Eur. J. Biochem.* **116**:73.
- Rubin, R. L. L., and Moudrianakis, E. N., 1972, *J. Mol. Biol.* **67**:361.
- Rubner, M., 1922, *Abh. Preuss. Akad. Wiss.* 1:1.
- Rüdel, R., and Taylor, S. R., 1973, *J. Physiol.* **233**:5P.
- Rudkin, G. T., 1965, *Genetics* **52**:665.
- Rudland, P. S., and Asua, L. J., 1979, *Biochim. Biophys. Acta* **560**:91.
- Ruhland, W., 1908, *Ber. Dtsch. Bot. Ges.* **26**:772.
- Ruhland, W., 1912, *Jahrb. Wiss. Bot.* **51**:376.
- Ruhland, W., 1913, *Kolloid Z.* **12**:113.
- Ruhland, W., and Hoffman, C., 1925, *Planta* 1:1.
- Ruzyllo, W., and Vick, R. L., 1974, *J. Mol. Cell. Cardiol.* **6**:27.
- Ryan, L. A., 1912, *J. Biol. Chem.* **11**:401.
- Saborio, J. L., Pong, S. S., and Koch, G., 1974, *J. Mol. Biol.* **85**:195.
- Sachs, H. G., Stambrook, P. J., and Ebert, J. D., 1974, *Exp. Cell Res.* **83**:362.
- Sacktor, B., 1977, *Curr. Top. Bioenerg.* **6**:39.
- Saladino, A. J., Bentley, P. J., and Trump, B. F., 1969, *Am. J. Pathol.* **54**:421.
- Sandor, K., and Pollak, J. K., 1976, *Biochem. Soc. Trans.* **4**:1122.
- Sanger, F., 1952, *Adv. Protein Chem.* **7**:1.
- Satir, P., 1974, *Sci. Am.* **231**:44.
- Schäfer, R., and Zillig, W., 1973, *Eur. J. Biochem.* **33**:215.
- Schäfer, R., Zillig, W., and Zechel, K., 1973, *Eur. J. Biochem.* **33**:207.
- Schatzmann, H. J., 1953, *Helv. Physiol. Pharmacol. Acta* **11**:346.
- Schauf, C. L., and Davis, F. A., 1976, *J. Gen. Physiol.* **67**:185.
- Schellman, J. A., 1955, *C. R. Trav. Lab. Carlsberg Ser. Chim.* **29**:15.
- Schoenheimer, R., 1942, *The Dynamic State of Body Constituents*, Harvard University Press, Cambridge, Massachusetts.
- Scholander, P. F., Van Dam, L., Kanwisher, J. W., Hammel, H. T., and Gordon, M. S., 1957, *J. Cell. Physiol.* **49**:5.
- Schramm, G., and Weber, H. H., 1942, *Kolloid Z.* **100**:242.
- Schubert, D., Humphreys, S., de Vitry, F., and Jacob, R., 1971, *Dev. Biol.* **25**:514.
- Schuetz, A. W., 1975, *J. Exp. Zool.* **191**:433.
- Schultze, R. D., and Asunmaa, S. K., 1969, *Recent Prog. Surface Sci.* **3**:291.
- Schultz, S. G., 1979, in: *Membrane Transport in Biology*, Vol. 4B (G. Giebisch, D. C. Tosteson, and H. H. Ussing, eds.), Springer, New York, p. 749.
- Schultz, S. G., and Curran, P. F., 1970, *Physiol. Rev.* **50**:637.
- Schultze, M., 1863, *Das Protoplasma der Rhizopoden unter der Pflanzenzelle: Ein Beitrag zur Theorie der Zelle*, Engelmann, Leipzig.
- Schwan, H. P., 1965, *Ann. N.Y. Acad. Sci.* **125**:344.
- Schwan, H. P., and Foster, K. R., 1977, *Biophys. J.* **17**:193.
- Schwindewolf, U., 1953, *Naturwissenschaften* **40**:435.
- Scott, G. T., and Hayward, H. R., 1993a, *J. Gen. Physiol.* **36**:659.
- Scott, G. T., and Hayward, H. R., 1953b, *Biochim. Biophys. Acta* **12**:401.
- Seeburg, P. H., Nusslein, C., and Shaller, H., 1977, *Eur. J. Biochem.* **74**:107.
- Segal, S., and Crawhall, J. C., 1968, *Proc. Natl. Acad. Sci. USA* **59**:231.
- Sewall, H., 1923, *Science* **58**:187.
- Seymour, J., and O'Brien, E. J., 1980, *Nature* **283**:680.
- Shanes, A. M., 1958, *Pharmacol. Rev.* **10**:59.
- Shaw, F. H., and Simon, S. E., 1955, *Aust. J. Exp. Biol. Med. Sci.* **3**:153.
- Shaw, F. H., Simon, S. E., and Johnstone, B. M., 1956, *J. Gen. Physiol.* **40**:1.
- Shaw, T. I., 1954, Sodium and Potassium Movements in Red Cells, Ph.D. Thesis, Department of Physiology, Cambridge University.

- Shen, S. S., 1939, *J. Exp. Biol.* **16**:143.
Shen, S. S., and Steinhardt, R. A., 1978, *Nature* **272**:253.
Shida, H., and Shida, M., 1976, *Nature* **263**:77.
Shih, C., Shilo, B., Goldfarb, M. P., Dannenberg, A., and Weinberg, R., 1979, *Proc. Natl. Acad. Sci. USA* **76**:5714.
Shikama, K., 1971, *Arch. Biochem. Biophys.* **147**:311.
Shporer, M., and Civan, M. M., 1972, *Biophys. J.* **12**:114.
Shporer, M., and Civan, M. M., 1974, *Biochim. Biophys. Acta* **354**:291.
Shporer, M., and Civan, M. M., 1979, *Curr. Top. Membr. Transp.* **9**:1.
Shporer, M., Haas, M., and Civan, M. M., 1976, *Biophys. J.* **16**:601.
Shull, C. A., 1913, *Bot. Gaz.* **56**:169.
Shull, C. A., 1924, *Ecology* **5**:230.
Siliprandi, D. A., Toninello, A., Zoccarato, F., and Bindoli, A., 1975a, *FEBS Lett.* **51**:15.
Siliprandi, D. A., Toninello, A., Zoccarato, F., Rugolo, M., and Siliprandi, N., 1975b, *Biochem. Biophys. Res. Commun.* **66**:956.
Siliprandi, D. A., Toninello, A., Zoccarato, F., Rugolo, M., and Siliprandi, N., 1979, *J. Bioenerg. Biomembr.* **10**:1.
Simpson, J. H., and Carr, H. Y., 1958, *Phys. Rev.* **111**:1201.
Simpson, R. B., and Kauzmann, W., 1953, *J. Am. Chem. Soc.* **75**:5139.
Sin, Y. T., and Leender, H. J., 1975, *Insect Biochem.* **5**:447.
Singer, C., 1959, *A History of Biology to About the Year 1900: A General Introduction to the Study of Living Things*, Abelard-Schuman, London, New York.
Singer, S. J., and Nicolson, G. L., 1972, *Science* **175**:720.
Singwi, K. S., and Sjölander, A., 1960, *Phys. Rev.* **119**:863.
Sjöstrand, F. S., 1964, *Nature* **201**:45.
Sjöstrand, F. S., 1978, *J. Ultrastruct. Res.* **64**:217.
Sjöstrand, F. S., and Bernhard, W., 1976, *J. Ultrastruct. Res.* **56**:233.
Skou, J. C., 1957, *Biochim. Biophys. Acta* **23**:394.
Skou, J. C., 1960, *Biochim. Biophys. Acta* **42**:6.
Skulachev, V. P., 1971, *Curr. Top. Bioenerget.* **4**:127.
Slater, E. C., 1953, *Nature* **172**:975.
Slater, E. C., 1971, *K. Ned. Akad. Wet. Versl. Gewone Vergad. Afd. Natuurkd.* **80**:122.
Slayman, C. L., 1965, *J. Gen. Physiol.* **49**:93.
Smith, J. A., and Martin, L., 1973, *Proc. Natl. Acad. Sci. USA* **70**:1263.
Smith, L. D., and Ecker, R. E., 1971, *Dev. Biol.* **25**:232.
Smith, T. and Adams, R., 1977, *J. Membr. Biol.* **35**:57.
So, G., Davie, E. W., Epstein, R., and Tissieres, A., 1967, *Proc. Natl. Acad. Sci. USA* **58**:1739.
Sobell, H. M., 1974, *Sci. Am.* **231**:82.
Sokolove, P. M., and Marsho, T. V., 1979, *FEBS Lett.* **100**:179.
Sollner, K., 1949, *J. Phys. Colloid. Chem.* **53**:1211.
Sollner, K., Abrams, I., and Carr, C. W., 1941a, *J. Gen. Physiol.* **24**:467.
Sollner, K., Abrams, I., and Carr, C. W., 1941b, *J. Gen. Physiol.* **25**:7.
Solomon, A. K., 1952, *J. Gen. Physiol.* **36**:57.
Somlyo, A. V., Shuman, H., and Somlyo, A. P., 1977, *J. Cell Biol.* **74**:828.
Somlyo, A. V., Gonzalez-Serratos, H., Shuman, H., McClellan, G., and Somlyo, A. P., 1981, *J. Cell Biol.* **90**:577.
Sonenschein, G. E., and Brawerman, G., 1977, *Biochemistry* **16**:5445.
Sonenschein, G. E., Geoghegan, T. E., and Brawerman, G., 1976, *Proc. Natl. Acad. Sci. USA* **73**:3088.
Spanswick, R. M., 1968, *Nature* **218**:357.
Speakman, J. B., and Hirst, M. C., 1931, *Nature* **128**:1073.
Speakman, J. B., and Hirst, M. C., 1933, *Trans. Faraday Soc.* **29**:148.
Spector, W. G., 1953, *Proc. R. Soc. London Ser. B* **141**:268.
Spek, F., 1930, *Arch. Entwicklungsmech.* **9**:370.
Spemann, H., 1918, *Arch. Entwicklungsmech.* **43**:448.
Spemann, H., 1931, *Verhand. Dtsch. Zool. Ges. (suppl. to Zool. Anz.)* **34**:129.
Spiro, K., 1903, *Beitr. Chem. Physiol. Pathol.* **iv**:300.

- Sponsler, O. L., Bath, J. D., and Ellis, J. W., 1940, *J. Phys. Chem.* **44**:996.
- Spradling, A., Penman, S., and Pardue, M. L., 1975, *Cell* **4**:395.
- Spring, K. R., and Giebisch, G., 1977, *J. Gen. Physiol.* **70**:307.
- Springer, T., 1972, *Springer Tracts in Modern Physics*, Vol. 64, Springer, New York.
- Stanbury, S. W., and Mudge, G. H., 1953, *Proc. Soc. Exp. Biol. Med.* **82**:675.
- Stedman, E., and Stedman, E., 1950, *Nature* **166**:780.
- Stein, L. A., Schwartz, R. P., Jr., Boon Chock, P., and Eisenberg, E., 1979, *Biochemistry* **18**:3895.
- Steinbach, B., 1940a, *J. Biol. Chem.* **133**:695.
- Steinbach, B., 1940b, *Cold Spring Harbor Symp. Quant. Biol.* **8**:242.
- Steinhardt, J., and Zaiser, E. M., 1951, *J. Biol. Chem.* **190**:197.
- Steinhardt, J., and Zaiser, E. M., 1953, *J. Am. Chem. Soc.* **75**:1599.
- Steinhardt, J., Fugitt, C. H., and Harris, M., 1941, *Natl. Bur. Stand. (U.S.) J. Res.* **26**:293.
- Steinhardt, R. A., and Epel, D., 1974, *Proc. Natl. Acad. Sci. USA* **71**:1915.
- Steinhardt, R. A., Lundin, L., and Mazia, D., 1971, *Proc. Natl. Acad. Sci. USA* **68**:2426.
- Stevely, W. S., and McGrath, B. M., 1978, *FEBS Lett.* **87**:308.
- Steward, F. C., 1932, *Protoplasma* **15**:29.
- Steward, F. C., and Harrison, J. A., 1939, *Ann. Bot.* **3**:427.
- Stiasny, E., 1931, *Gerbereichemi*, Steinkopf, Dresden, p. 173.
- Stiasny, E., and Scotti, H., 1930, *Ber. Dtsch. Chem. Ges.* **63**:2977.
- Stillman, I. M., Gilbert, D. L., and Robbins, M., 1970, *Biochim. Biophys. Acta* **203**:338.
- Stillman, I. M., Gilbert, D. L., and Lipicky, R. J., 1971, *Biophys. J.* **11**:55a.
- Stone, F. W., and Stratta, J. J., 1967, in: *Encyclopedia of Polymer Science and Technology*, Vol. 6, Wiley, New York, p. 103.
- Stoner, C. D., and Sirak, H. D., 1973, *J. Cell. Biol.* **56**:51.
- Straub, F. B., 1942, *Stud. Inst. Med. Chem. Chiv. Szeged.* **2**:3.
- Straub, F. B., 1943, *Stud. Inst. Med. Chem. Chiv. Szeged.* **3**:23.
- Strauss, H. S., Burgess, R. R., and Record, M. T., Jr., 1980, *Biochemistry* **19**:3496.
- Swift, T. J., and Barr, F. M., 1973, *Ann. N.Y. Acad. Sci.* **204**:191.
- Szent-Györgyi, A., 1941–1943, *Stud. Inst. Med. Chem. Szeged.*, Vol. 1 (1941–1942), Vol. 2 (1942), Vol. 3 (1943), Karger, Basel.
- Szent-Györgyi, A., 1947, *Chemistry of Muscular Contraction*, Academic Press, New York.
- Szent-Györgyi, A., 1951, *Chemistry of Muscular Contraction*, 2nd ed., Academic Press, New York.
- Szent-Györgyi, A., 1957, *Bioenergetics*, Academic Press, New York.
- Szent-Györgyi, A., 1976, *Electronic Biology and Cancer: A New Theory of Cancer*, Marcel Dekker, New York.
- Szent-Györgyi, A., 1978, *The Living State and Cancer*, Marcel Dekker, New York.
- Szent-Györgyi, A. G., 1960, in: *Structure and Function of Muscle*, Vol. II, (G. H. Bourne, ed.), Academic Press, New York.
- Szentkiralyi, E. M., and Oplatka, A., 1969, *J. Mol. Biol.* **43**:551.
- Tabin, C. J., Bradley, S. M., Bargmann, C. I., Weinberg, R. A., Papageorge, A. G., Scolnick, E. M., Dhar, R., Lowy, D. R., and Chang, E. H., 1982, *Nature* **300**:143.
- Tables Annuelles de Constantes et Données Numericales*, 1930, Vol. X, Part 2.
- Taft, R. W., 1953, *J. Am. Chem. Soc.* **75**:4231.
- Taft, R. W., 1956, in: *Steric Effects in Organic Chemistry* (M. S. Newman, ed.), John Wiley, New York, Chapter 13.
- Taft, R. W., and Lewis, I. C., 1958, *J. Am. Chem. Soc.* **80**:2436.
- Tanford, C., 1962, *Adv. Protein Chem.* **17**:69.
- Tanford, C., and Wagner, M. L., 1954, *J. Am. Chem. Soc.* **76**:3331.
- Taniguchi, K., and Post, R. L., 1975, *J. Biol. Chem.* **250**:3010.
- Tasaki, I., 1963, *J. Gen. Physiol.* **46**:755.
- Tasaki, I., 1968, *Nerve Excitation: A Macromolecular Approach*, Thomas, Springfield, Illinois.
- Tasaki, I., 1982, *Physiology and Electrochemistry of Nerve Fibers*, Academic Press, New York.
- Tasaki, I., and Takenaka, T., 1963, *Proc. Natl. Acad. Sci. USA* **50**:619.
- Tasaki, I., and Takenaka, T., 1964, *Proc. Natl. Acad. Sci. USA* **52**:804.

- Tasaki, I., Luxoro, M., and Ruarte, A., 1965, *Science* **150**:899.
- Tasaki, I., Takenaka, T., and Yamagishi, 1968, *Am. J. Physiol.* **215**:152.
- Tata, J. R., 1966, *Dev. Biol.* **13**:77.
- Tata, J. R., 1971, *Curr. Top. Dev. Biol.* **6**:79.
- Tawada, K., and Oosawa, F., 1969, *J. Mol. Biol.* **44**:309.
- Taylor, E. W., 1979, *Crit. Rev. Biochem.* **6**:103.
- Tedeschi, H., 1980, *Biol. Rev.* **55**:171.
- Teorell, T., 1953, *Prog. Biophys. Biophys. Chem.* **3**:305.
- Terner, C., Eggleton, L. V., and Krebs, M. A., 1950, *Biochem. J.* **47**:139.
- Teunissen, P. H., and Bungenberg de Jong, H. G., 1939, *Kolloid Beih.* **48**:33.
- Thames, M. D., Teichholz, L. E., and Podolsky, R. J., 1974, *J. Gen. Physiol.* **63**:509.
- Thoenes, F., 1925, *Biochem. Z.* **157**:174.
- Thomas, R. C., 1972, *Physiol. Rev.* **52**:563.
- Thompson, M. R., 1932, *Natl. Bur. Stand. (U.S.) J. Res.* **9**:833.
- Thomson, D. L., 1928, *J. Physiol.* **65**:214.
- Tichomirov, A., 1886, *Arch. Anat. Physiol. (Meckel's)* **1886**(Suppl.):35.
- Tigyi, J., Kallay, N., Tigyi-Sebes, A., and Trombitas, K., 1981, in: *International Cell Biology, 1980-1981* (H. G. Schweiger, ed.), Springer, Berlin, p. 925.
- Tigyi-Sebes, A., 1962, *Acta Physiol. Hung.* **22**:243.
- Tilney, L. G., 1975, in: *Molecules and Cell Movement* (S. Inoue and R. E. Stephens, eds.), Raven Press, New York, p. 339.
- Tilney, L. G., 1976, *J. Cell Biol.* **69**:73.
- Tilney, L. G., Hatano, S., Ishikawa, H., and Mooseker, M. S., 1973, *J. Cell Biol.* **59**:109.
- Tilney, L. G., Bonder, E. M., and DeRosier, D. J., 1981, *J. Cell Biol.* **90**:485.
- Tissières, A., Mitchell, H. K., and Tracy, U. M., 1974, *J. Mol. Biol.* **84**:389.
- Tobias, J. M., 1950, *J. Cell. Comp. Physiol.* **36**:1.
- Tombs, M. P., and Peacocke, A. R., 1974, *The Osmotic Pressure of Biological Macromolecules*, Clarendon Press, Oxford.
- Tonomura, Y., Nakamura, H., Konoshita, N., Onishi, H., and Shigekawa, M., 1969, *J. Biochem.* **66**:509.
- Tosteson, D. C., 1955, *J. Gen. Physiol.* **39**:55.
- Tosteson, D. C., 1959, *Acta Physiol. Scand.* **46**:19.
- Tosteson, D. C., Shea, E., and Darling, R. C., 1952, *J. Clin. Invest.* **31**:406.
- Tosteson, D. C., Andreoli, T. E., Tifenberg, M., and Cook, P., 1968, *J. Gen. Physiol.* **61**:373S.
- Trachenberg, M. C., and Pollen, D. A., 1970, *Science* **167**:1248.
- Trantham, E. C., Rorschach, H. E., Clegg, J. S., Hazlewood, C. F., Nicklow, R. M., and Wakabayashi, N., 1983, *Biophys. J.* (in press).
- Traube, M., 1867, *Arch. Anat. Physiol. Wiss. Med.* **87**:128, 129-165.
- Trentin, J. J., 1976, in: *Stem Cells of Renewing Cell Populations* (A. B. Cairnie, P. K. Lala, and D. G. Osmond, eds.), Academic Press, New York, p. 255.
- Trimble, R. B., and Maley, F., 1975, *Arch. Biochem. Biophys.* **167**:377.
- Trombitas, C., and Tigyi-Sebes, A., 1979, *Acta Physiol. Acad. Sci. Hung.* **14**:271.
- Troshin, A. S., 1951a, *Byull. Eksp. Biol. Med.* **31**:180.
- Troshin, A. S., 1951b, *Byull. Eksp. Biol. Med.* **31**:285.
- Troshin, A. S., 1951c, *Byull. Eksp. Biol. Med.* **32**:162.
- Troshin, A. S., 1951d, *Byull. Eksp. Biol. Med.* **32**:228.
- Troshin, A. S., 1951e, *Biokhimiya* **16**:164.
- Troshin, A. S., 1952, *Byull. Eksp. Biol. Med.* **34**:59.
- Troshin, A. S., 1966, *Problems of Cell Permeability* (M. G. Hall, transl.) (W. F. Widdas, ed.), Pergamon Press, London.
- Tse, T. P. H., and Taylor, J. M., 1977, *J. Biol. Chem.* **252**:1272.
- Tsuboi, M., 1952, *Bull. Chem. Jpn.* **25**:60.
- Tsuboi, M., 1951, *J. Chem. Soc. Jpn.* **72**:146.
- Tuite, M. F., and Plesset, J., Moldave, K., and McLaughlin, C. S., 1980, *J. Biol. Chem.* **255**:8761.
- Tupper, J. T., 1973, *Dev. Biol.* **32**:140.
- Tupper, J. T., and Maloff, B. L., 1973, *J. Exp. Zool.* **185**:133.

- Tupper, J. T., and Tedeschi, H., 1969a, *Proc. Natl. Acad. Sci. USA* **63**:370.
 Tupper, J. T., and Tedeschi, H., 1969b, *Proc. Natl. Acad. Sci. USA* **63**:713.
 Tupper, J. T., and Tedeschi, H., 1969c, *Science* **166**:1539.
 Turner, R. J., and Silverman, M., 1977, *Proc. Natl. Acad. Sci. USA* **74**:2825.
 Tweedell, K. S., 1967, *Cancer Res.* **27**:2042.
- Ueda, T., Muratsugu, M., Inoue, I., and Kobatake, Y., 1974, *J. Membr. Biol.* **18**:177.
 Ullrick, W. C., 1967, *J. Theor. Biol.* **15**:53.
 Urano, F., 1908, *Z. Biol.* **51**:483.
 Urban, F., and Steiner, A., 1931, *J. Phys. Chem.* **35**:3058.
 Ussing, H. H., and Leaf, A., 1978, in: *Membrane Transport in Biology*, Vol. 3 (G. Giebisch, D. C. Tosteson, and H. H. Ussing, eds.), Springer, New York, p. 1.
- van Hove, L., 1954, *Phys. Rev.* **95**:249.
 van Loon, R., and Finsey, R., 1975, *J. Phys. D* **8**:1232.
 van Rossum, J. M., and Ariëns, B. J., 1958, *Arch. Int. Pharmacodyn.* **118**:393.
 Veis, A., 1964, *The Macromolecular Chemistry of Gelatin*, Academic Press, New York.
 Verworn, M., 1922, *Allgemeine Physiologie*, 7th ed., Jena, Fischer, p. 284.
 Vidaver, G. A., 1964, *Biochem. Z.* **3**:662.
 Villegas, R., Blei, M., and Villegas, G. M., 1965, *J. Gen. Physiol.* **48**:41.
 Vitto, A., Jr., and Wallace, R. A., 1976, *Exp. Cell. Res.* **97**:56.
 Voegeli, K. K., O'Keefe, D., Whitmarsh, J., and Dilley, R. A., 1977, *Arch. Biochem. Biophys.* **183**:333.
 Vogt, W., 1925, *Arch. Entwickelungsmech. (Roux's)* **106**:542.
 Vogt, W., 1929, *Arch. Entwickelungsmech. (Roux's)* **120**:385.
 Von Helmholtz, H., 1881, in: *Vorträge und Reden*, Volume II: *Die Neue Entwicklung von Faraday über Elektrizität, Vortrag zu Faradays Gedächtnisfeier vor den Chemischen Gesellschaft zu London*, 5 April.
 Von Korösy, K., 1914, *Z. Physiol. Chem.* **93**:154.
 Von Mohl, H., 1846, *Bot. Z.* **4**:73.
 Von Muralt, A. L., and Edsall, J. T., 1930, *J. Biol. Chem.* **89**:351.
 Von Nägeli, C., 1855, *Pflanzenphysiologische Untersuchungen*, Schulthess, Zurich.
- Waddington, C. H., 1938, *Proc. R. Soc. London Ser. B* **125**: 365.
 Waite, M. R. F., and Pfefferkorn, E. R., 1968, *J. Virol.* **2**:759.
 Waite, M. R. F., and Pfefferkorn, E. R., 1970, *J. Virol.* **5**:60.
 Waite, M. R. F., Brown, D. T., and Pfefferkorn, E. R., 1972, *J. Virol.* **10**:537.
 Wakabayashi, T., Huxley, H. E., Amos, L. A., and Klug, A., 1975, *J. Mol. Biol.* **93**:477.
 Wald, G., 1960, *Circulation* **21**:916.
 Walker, J. L., and Brown, H. M., 1977, *Physiol. Rev.* **57**:729.
 Walrafen, G. E., 1968, in: *Hydrogen-Bonded Solvent Systems* (A. K. Covington and P. Jones, eds.), Taylor and Francis, London, p. 9.
 Walter, H., 1923, *Jahrb. Wiss. Bot.* **62**:145.
 Walter, J. A., and Hope, A. B., 1971, *Aust. J. Biol. Soc.* **24**:497.
 Walton, H. F., 1943, *J. Phys. Chem.* **47**:371.
 Wang, J. H., Robinson, C. V., and Edelman, I. S., 1953, *J. Am. Chem. Soc.* **75**:466.
 Warburg, O., 1930, *Metabolism of Tumors* (F. Dickens, transl.), Constable Press, London.
 Wasserman, W. J., and Masui, Y., 1975, *J. Exp. Zool.* **193**:369.
 Watson, J. D., 1970, *Molecular Biology of the Gene*, Benjamin, New York, p. 528.
 Watson, J. D., 1977, *Molecular Biology of the Gene*, 3rd ed., Benjamin, Menlo Park, California.
 Weber, A., 1959, *J. Biol. Chem.* **234**:2764.
 Weber, A., and Winicur, S., 1961, *J. Biol. Chem.* **236**:3198.
 Weber, H. H., 1925, *Biochem. Z.* **158**:443 and 473.
 Weber, H. H., 1934, *Pflügers Arch Ges. Physiol.* **235**:205.
 Weber, H. H., and Portzehl, H., 1952, *Adv. Protein Chem.* **7**:161.
 Weber, L. A., Hickey, E. D., Maroney, P. A., and Baglioni, C., 1977, *J. Biol. Chem.* **252**:4007.
 Webster's New Collegiate Dictionary, 1977, G. & C. Merriam, Springfield, Massachusetts.
 Wehrle, J. P., and Pedersen, P. L., 1979, *J. Biol. Chem.* **254**:7269.

- Weidmann, S., 1951, *J. Physiol.* **114**:372.
Weidmann, S., 1955, *J. Physiol.* **129**:568.
Weidemann, S., 1971, in: *Research in Physiology* (F. F. Kao, K. Koizumi, and M. Vassale, eds.), Aulo Gaggi, Bologna, p. 3.
Weinberg, R. A., 1981, *Biochim. Biophys. Acta* **651**:25.
Weinhouse, S., 1955, *Adv. Cancer Res.* **3**:269.
Weintraub, H., and Groudine, M., 1976, *Science* **193**:848.
Weismann, O., 1938, *Protoplasma* **31**:27.
Wengler, G., and Wengler, G., 1972, *Eur. J. Biochem.* **27**:162.
White, J. F., 1976, *Am. J. Physiol.* **231**:1214.
Wiggins, P. M., 1975, *Clin. Exp. Pharmacol. Physiol.* **2**:171.
Wilbrandt, W., 1940, *Pflügers Arch. Ges. Physiol.* **243**:519.
Wilde, W. S., and O'Brien, J. M., 1953, in: *Proceedings of the 19th International Physiological Congress, Montreal*, p. 889.
Wilde, W. S., O'Brien, J. M., and Bay, I., 1956, in: *Proceedings of the 1st International Conference on Peaceful Uses of Atomic Energy, Geneva 1955*, Vol. 12, p. 318 (U.N. Publication IX.1).
Wilkins, M. H. F., and Zubay, G., 1959, *J. Biophys. Biochem. Cytol.* **5**:55.
Wilson, E. B., 1925, *The Cell in Development and Heredity*, Macmillan, New York.
Wilson, J. A., and Wilson, W. H., 1918, *J. Am. Chem. Soc.* **40**:886.
Wilt, F. H., 1959, *Dev. Biol.* **1**:199.
Woessner, D. E., and Snowden, B. S., 1973, *Ann. N.Y. Acad. Sci.* **204**:113.
Wohl, K., and James, W. O., 1942, *New Physiol.* **41**:230.
Wohlisch, E., 1940, *Naturwissenschaften* **28**:305 and 326.
Wolcott, R. G., and Boyer, P. D., 1974, *Biochem. Biophys. Res. Commun.* **57**:709.
Wolfenden, R., 1978, *Biochemistry* **17**:201.
Wolvekamp, H. P., 1961, in: *Functions of the Blood* (R. G. MacFarlane and A. H. T. Robb-Smith, eds.), Academic Press, New York, p. 36.
Wood, E. H., and Moe, G. K., 1938, *Am. J. Physiol.* **123**:219.
Wood, E. H., Collins, D. A., and Moe, G. K., 1940, *Am. J. Physiol.* **128**:635.
Woodhull, A. M., 1973, *J. Gen. Physiol.* **61**:687.
Woodrum, D. T., Rich, S. A., and Pollard, T. D., 1975, *J. Cell Biol.* **67**:231.
Woolley, D. W., 1946, *Adv. Enzymol.* **6**:129.
Wu, M., and Gerhart, J. C., 1980, *Dev. Biol.* **79**:465.
Wuhrmann, P., Ineichen, H., Riesen-Will, U., and Lezzi, M., 1979, *Proc. Natl. Acad. Sci. USA* **76**:806.
Wyman, J., Jr., 1939, *J. Biol. Chem.* **127**:1.
Wyman, J., Jr., 1964, *Adv. Protein Chem.* **19**:223.

Yagi, K., Nakata, T., and Sakakiba, I., 1965, *J. Biochem.* **58**:236.
Yamada, S., and Tonomura, Y., 1973, *J. Biochem. (Tokyo)* **74**:1091.
Yamada, T., 1938, *J. Fac. Sci. Imp. Univ. Tokyo* **5**:133.
Yamada, T., 1939a, *Folia Anat Jpn.* **18**:565 and 569.
Yamada, T., 1939b, *Jpn. J. Zool.* **8**:265.
Yamada, T., 1940, *Folia Anat. Jpn.* **19**:131.
Yamagiwa, K., and Ichikawa, K., 1915, *Tokyo Igaku Zasshi* **15**:295.
Yamagiwa, K., and Ichikawa, K., 1918, *J. Cancer Res.* **3**:1.
Yang, Y. Z., Gordon, D. J., Korn, E. D., and Eisenberg, R., 1977, *J. Biol. Chem.* **252**:3374.
Yeh, H. J. C., Brinley, F. J., and Becker, E. D., 1973, *Biophys. J.* **13**:56.
Yoshioka, T., Pant, H. C., Tasaki, I., Baumgold, J., Matsumoto, G., and Gainer, H., 1978, *Biochim. Biophys. Acta* **538**:616.
Young, J. Z., 1938, *J. Exp. Biol.* **15**:170.
Yount, R. G., Ojala, D., and Babcock, D., 1971, *Biochemistry* **10**:2490.
Yu, L. C., Dowben, R. M., and Kornacker, K., 1970, *Proc. Natl. Acad. Sci. USA* **66**:1199.

Zeuthen, T., 1978, *J. Membr. Biol.* **39**:185.
Zeuthen, T., and Monge, C., 1974, in: *International Workshop on Ion-Selective Electrodes in Biology and*

- Medicine* (M. Kessler, L. C. Clark, Jr., D. M. Lübbers, I. A. Silver, and W. Simon, eds.), Urban and Schwarzenberg, Munich, p. 345.
- Zief, J., and Edsall, J. T., 1937, *J. Am. Chem. Soc.* **59**:2245.
- Ziegler, D. H., and Masui, Y., 1973, *Dev. Biol.* **35**:283.
- Ziegler, D. H., and Masui, Y., 1976, *J. Cell Biol.* **68**:620.
- Ziegler, D. H., and Morrill, G. A., 1977, *Dev. Biol.* **60**:318.
- Zierler, K. L., 1972, *Scand. J. Clin. Lab. Invest.* **29**:343.
- Zimm, B. H., and Bragg, J. K., 1958, *J. Chem. Phys.* **28**:1246.
- Zimmerman, J. R., and Brittin, W. E., 1957, *J. Phys. Chem.* **61**:1328.
- Zubay, G., and Watson, M. R., 1959, *J. Biophys. Biochem. Cytol.* **5**:51.

Abbreviations

The number in brackets following each definition is that of the page on which the abbreviation first appears.

Å	Angstrom, a unit of length equal to 10^{-8} cm [79]
AIB	α -Amino isobutyric acid [340]
AMINOW	Apparent minimal nonsolvent water [179]
AP	Action potential [72]
BET	Brunauer, Emmett, and Teller's theory of multilayer gas condensation [163]
cAMP	Cyclic AMP [604]
CAP	Catabolite gene activator protein
CCA	Chromosome-condensing activity [642]
DB	Double-barrel microelectrode (one electrode records the electrical potential (ψ) and the other records both ψ and the ion potential) [255]
DMSO	Dimethyl sulfoxide [305]
DNA	Deoxyribonucleic acid [287]
ecs	Extracellular space [326]
EDC	Electron-donating cardinal adsorbent [528]
EM	Electron microscope [231]
EMOC	Effectively membrane (pump)-less open-ended cell [133]
EP	Phosphoenzyme [517]
ES	Enzyme-substrate complex [98]

esf	Extracellular space fluid [139]
EWC	Electron-withdrawing cardinal adsorbent [528]
FCCP	<i>p</i> -Trifluoromethoxyphenylhydrazone [533]
GEDTA	Glycoetherdiamine-tetraacetic acid [562]
GV	Germinal vesicle [637]
GVBD	Germinal vesicle breakdown [637]
Hz	Herz, a unit of frequency equal to one cycle per second [292]
HMM	Heavy meromyosin [557]
IAA	Iodoacetate [58]
K	Degree kelvin of absolute temperature [11]
IPTG	Isopropylthiogalactoside [604]
LAMMA	Laser microprobe mass spectrometric analysis [237]
LFCH	Ling's fixed-charge hypothesis [94]
LIE	Liquid ion exchange electrode [255]
LMM	Light meromyosin [557]
MC	Methylcellulose [174]
MPF	Maturation-promoting factor [640]
NAD, NADH	Nicotinamide adenine dinucleotide (or diphosphopyridine nucleotide) and its reduced form [503, 504]
NMR	Nuclear magnetic resonance [257]
PEO	Polyethylene oxide [174]
PMF	Protomotive force [510]
PVME	Polyvinylmethylether [174]
PVP	Polyvinylpyrrolidone [174]
RNA	Ribonucleic acid [609]
RP	Resting potential [82]
	Reference phase [331]
	Ringer phosphate solution, a solution including Na^+ , K^+ , Ca^{2+} , PO_4^{2-} , Cl^- and used for short-term culture of isolated tissues [344]
SAM	Surface adsorption model [473]
SDS	Sodium dodecyl sulfate [177]

SR	Sarcoplasmic reticulum [416, 558]
TEA	Tetraethylammonium [152]
TMA	Tetramethylammonium [152]
TMV	Tobacco mosaic virus [573]
TSH	Thyrotropic hormone [682]
<i>c</i> -value	A displacement in Å of the unit negative charge carried by the oxygen atom of an oxyacid group, either away (negative <i>c</i> -value) or toward (positive <i>c</i> -value) the interacting cation, so that the net interaction with the cation matches the cumulative action of the inductive effects exerted by the rest of the molecule. The <i>c</i> -value is a measure of the pK_a value of the acid. [156]
F-effect	Combined direct electrostatic (D) and inductive (I) effect. [184]
<i>q</i> -value	Equilibrium distribution coefficient of a solute between two separate phases in contact. [170]
<i>ρ</i> -value	Apparent equilibrium distribution coefficient of a solute between a phase under study and a contiguous reference phase, usually water or a sample solution. If there is no adsorption or complexing of this solute in the studied phase, the <i>ρ</i> -value equals the <i>q</i> -value of the solute. [274]
Z line	Cross-section of the dislike structure (Z-disc) separating adjacent sarcomeres in a voluntary muscle fiber [229]

Notation List

The number in brackets following each definition is that of the page on which the symbol is first used in the context of that definition.

a	A constant, equal to the number of "places" available in the solid phase [106]
	A constant [85]
a_1, a_2	Activities of two species of ions, 1 and 2 [106]
A	Concentration of fixed anion in the membrane [32]
	Concentration of adsorbed solute [85]
	A constant [299, 397]
	A constant, equal to $\mu_2 K_1 / \mu_1 K_2$ [106]
A_∞	A constant, equal to the limit of adsorption [85]
A/V	Ratio of the surface area (A) to the volume (V) of cells [404]
$a_{K^+}^I/a_{K^+}^{II}$	Ratio of the activity of K^+ in phase I to that in phase II [28]
$a_{Cl^-}^{II}/a_{Cl^-}^I$	Ratio of activity of Cl^- in phase II to that in phase I [28]
$[a_{C_i}]^I, [a_{C_i}]^{II}$	Activity of the i th cation in phases I and II, respectively [28]
$[a_{A_j}]^I, [a_{A_j}]^{II}$	Activity of the j th anion in phases I and II, respectively [28]
a_K^{app}	Apparent activity of K^+ [253]
a_i^I, a_i^{II}	Activity of the i th solute in phases I and II, respectively [171]
b	Nonsolvent volume [44]
c	Total ionic concentration in the external solution [34]
	A constant [163]
C	Cardinal adsorbent [326]

C	Membrane capacity [78] Concentration of the solute dissolved in the water of the coacervate [85]
C_1, C_2	Concentration of the two ions present in the solution [106]
$C_{\text{in}}, C_{\text{ex}}$	Concentration of the salt inside and outside the cell, respectively [22]
C_c	Concentration of a solute in the coacervate [85]
C_s	Concentration of a solute in the solution phase [85]
C_x	Equivalent capacity [250]
$[C]_{\text{ad}}$	Concentration of adsorbed cardinal adsorbent C [220]
$C_{\text{I}}^i, C_{\text{II}}^i$	Concentration of the i th solute in phases I and II, respectively [171]
C_K, C_{Na}	Concentrations of K^+ and Na^+ , respectively [253]
C_K^c, C_{Na}^c	Concentrations of cytoplasmic K^+ and Na^+ , respectively [334]
C_K^n, C_{Na}^n	Concentrations of nuclear K^+ and Na^+ , respectively [334]
$C_K^{\text{RP}}, C_{\text{Na}}^{\text{RP}}$	Concentrations of K^+ and Na^+ in the reference phase, respectively [334]
$C_{\text{KCNS, oil}}, C_{\text{NaCl, oil}}$	Concentrations in the oil phase of KCNS and NaCl, respectively [24]
D	Diffusion coefficient [114] Dielectric displacement [292]
$dn/dt, dm/dt, dh/dt$	Rate of change with time of n , m , and h , respectively [78]
D_K, D_{Na}	Self-diffusion coefficients of K^+ and Na^+ , respectively [139, 245]
e	Excess of diffusible ion in the protein-containing phase [29]
E	Free enzyme [98]
E	Field strength of periodically fluctuating field [291] Efficiency [541]
E_0	Time-independent component of the fluctuating field strength [291]
E_{Na}	Na^+ concentration potential [62]
f	Frequency of the alternating current [297]
$[f]$	Concentration of adsorption sites [208]

$[f_0]$	Total concentration of sites f_0 [201]
f^+	Fixed cations [445]
f^-	Fixed anions [445]
f^+f^-	Salt linkage formed between a fixed cation and a fixed anion [445]
\mathcal{F}	Faraday constant [22]
F_{inw}	Inward flux [404]
F_{outw}	Outward flux [61]
g_K, g_{Na}	Conductances of K^+ and Na^+ , respectively [76]
$\bar{g}_K, \bar{g}_{\text{Na}}$	Constants equal to the maximum conductances of K^+ and Na^+ , respectively [78]
h	Probability of a single CP'_{Na} moving in the blocking position [78]
	Heat [580]
	Planck constant [714]
\hbar	Dirac \hbar , equal to Planck constant divided by 2π [714]
$[\text{H}^+]_{\text{I}}, [\text{H}^+]_{\text{II}}$	H^+ concentration in phases I and II, respectively [23]
i_{\pm}	Effects of charges on atoms [187]
I	Inductive effect [185]
$[\text{I}]$	Concentration of the competing ion I [99]
j	Designation of a specific reaction different from the i reaction [184]
k	Boltzmann's constant or the molecular gas constant [405]
k_1, k_2	Constants [21]
k_1, k_2, k_3, k_4	Rate constants of four reactions 1–4 [98]
k_{ij}	Rate of equilibrium constant of a reaction [184]
k_{oj}	Equilibrium constant for the reaction j in the absence of any substituent i [184]
k_{outw}	Outward exchange constant [62]
K	Equilibrium constant for the exchange of ion 1 for ion 2 [107] “Coefficient of proportionality characteristic of the aqueous phase of the coacervate as a solvent” [85] Dissociation constant of the galactoside-permease complex [117]

	Acid dissociation constant for the substituted acid XCH_2COOH in an aqueous solution at 25°C [185]
K_0	Acid dissociation constant of acetic acid in an aqueous solution at 25°C [185]
K_1, K_2	“Integration constants in the expression for the thermodynamic potential of the ions present in the solid phase-solution tension” [105]
K_2, K_1	Functions of the field of the sorptive polar groups and the dipole moment and polarizability of the polar gas [164]
K_4	A constant under specified conditions [164]
$K_{B/A}$	Equilibrium constant [159]
K_i	Adsorption constant of the i th solute [322]
K_j	Adsorption constant of the j th solute [397]
K_s, K_i	Michaelis constants for the ion-carrier complexes of the ion s and a competing ion i , respectively [99]
K_K, K_{Na}	Adsorption constants of K^+ and Na^+ on the surface β - and γ -carboxyl groups [109]
$K_{Na^+}^{K^+}$	Selectivity coefficient equal to $[K^+]_i/[Na^+]_e/[K^+]_e[Na^+]_i$ [275]
$K_{j \rightarrow i}^{00}$	Intrinsic equilibrium constant of exchange of j for i [208, 321]
$K_{(j \rightarrow i)C}^{00}$	Intrinsic equilibrium constant of the j th-to- i th exchange in a gang with its cardinal site occupied by the cardinal adsorbent C [222]
$K_{(j \rightarrow i)0}^{00}$	Intrinsic equilibrium constant of the j th-to- i th solute in a gang in which the cardinal site is not occupied [222]
$[K^+]_{in}, [K^+]_{ex}$	Intracellular and extracellular K^+ concentrations, respectively [22, 110]
m	Probability that a single CP _{Na} occupies position B [78]
$M_{inside}, M_{outside}$	Alkali-metal ions inside and outside the cell membrane [98]
MR	Unstable carrier-ion complex [98]
MR_D	Molar refraction coefficient [16]
n	The Hill coefficient, an empirical constant [211] Probability that a single CP _K moves from position C to position D in the cell membrane [78]
$n_{K,Na}, n_{K,Rb}$	Hill's coefficients of K-to-Na exchange adsorption and for K-to-Rb adsorption, respectively [353]
N	Negative site [169]

NP-NP, NO-NO	Checkerboard of negative (N) sites alternating with positive (P) or vacant (O) sites [169]
NP-NP-NP, NO-NO-NO	Matrix of chains carrying negative (N) sites alternating with positive (P) or vacant (O) sites [169]
N_K, N_A	Passage numbers of a membrane [32]
$[Na^+]_{ex}$	Extracellular Na^+ concentration [110]
$([Na^+]_{ex}/[Na^+]_{in})_t$	Extracellular/intracellular Na^+ concentration gradient at time t [124]
O	Neutral or vacant site [169]
p_i	i th solute [321]
$[p_i]_{ad}$	Concentration of the i th adsorbed solute [208]
$[p_i]_{cw}$	i th solute dissolved in cell water [321]
$[p_i]_{ex}, [p_j]_{ex}$	Concentration of the i th and j th solutes in free solutions [208]
pK_a	Negative logarithm of the acid dissociation constant [198]
p	Vapor pressure of a gas [163] Specific resistance [250]
p_0	Vapor pressure of a gas at saturation [163]
P	Positive site [169]
$\sim P$	High-energy phosphate bond [59]
$-P$	Ordinary low-energy phosphate bond [59]
P_{O_2}	Partial pressure of oxygen in the gas phase [211]
PO-PO	Checkerboard of alternatingly positive (P) and neutral or vacant (O) sites [169]
PO-PO-PO	Matrix of chains carrying positive (P) sites alternating with vacant (O) sites [169]
P	Membrane permeability constants in the Hodgkin-Katz-Goldman equation [66]
P_i	Probability of water in a specific environment [300]
P_i	Probability that the nuclei under discussion are found in the i th environment [300]
q_i	Equilibrium distribution coefficient of the i th solute between two separate phases in contact [321]
$-Q_1$	Heat given off by an engine at a lower temperature T_1 [541]

Q_2	Heat absorbed by an engine at a higher temperature T_2 [541]
r	Equilibrium distribution ratio of an ion according to Donnan's theory (the Donnan ratio) [28]
	Bond length [187]
	Coupling factor in a postulated electrogenic pump [468]
r'_1, r'_2	Covalent radii of the charged atoms [187]
r_{BA}	Bond length of the bond BA [187]
R	Chemical state of a metabolically produced carrier [98]
R, R'	Different chemical states of the metabolically produced carrier [98]
R	Gas constant, equal to $1.987 \text{ cal deg}^{-1} \text{ mol}^{-1}$ [12]
S	Substrate [99]
$[S]$	Substrate concentration [99]
t	Time [123, 405]
$t_{1/2}$	Half-time of exchange [61]
t_K, t_{Na}	Durations of the experiments on K^+ diffusion and Na^+ diffusion, respectively [139]
T	Absolute temperature [11]
T_1	Longitudinal or spin-lattice relaxation time [299]
T_2	Transverse or spin-spin relaxation time [259]
T_i	Relaxation time of the nuclei in the i th phase [300]
T_{obs}	Observed relaxation time [300]
u	Mobility of a cation
v	Mobility of an anion [22]
	Rate of ionic permeation [99]
V	Volume of a solution containing 1 mole of dissolved solute [11]
	Membrane potential in the Hodgkin-Huxley theory [76]
V_{max}	Maximum value of ionic permeation [99]
V_i	Rate of entry of the i th ion [397]
V_i^{max}	Maximum rate of entry of the i th ion [397]
V_K	Rate of entry of labeled K^+ into cells [402]
V_{Na}	Rate of entry of labeled Na^+ into cells [402]
W	Work performed [580]

x	Concentrations of external H^+ or Cl^- in Procter and Wilson's theory of swelling [29]
X_A, X_B	Equivalent fractions of ions A and B in the external solution phase [159]
\bar{X}_A, \bar{X}_B	Equivalent fractions of ions A and B in the ion exchange resin phase [159]
$X_{\xi}^{f_0}$	Mole fraction of fixed sites, f_0 , occupied by the specific adsorbent ξ [204]
$X_{\xi}^{f_0}[f_0]$	Mole fraction of the enzymatically active sites adsorbing the substrate ξ , which forms the activated complex [204]
y	Concentration of free H^+ in the protein-containing phase in the Procter-Wilson theory of swelling [29]
	Mole fraction of sites binding oxygen [211]
Z_i	Valence of the i th ion [114]
α	Water content in liters per kilogram of fresh cells [321]
	Rate constant in the Hodgkin-Huxley theory [78]
α, α'	Ionization constants of KCNS and NaCl in the oil phase [24]
$1/\alpha$	Loss of inductive effect in transmission through one atom [187]
β	Rate constant in the Hodgkin-Huxley theory [78]
$-\gamma/2$	Free energy of the nearest-neighbor interaction [208]
$-(\gamma_c/2), -(\gamma_0/2)$	Nearest-neighbor interaction energies for the gang controlled by the cardinal adsorbent and for the one not controlled by the cardinal adsorbent, respectively [222]
$-\gamma^{ij}$	Twice the free energy of nearest-neighbor interaction between adsorption sites [321]
$-\gamma_L^{ij}$	Twice the free energy of nearest-neighbor interaction between the L th type of adsorption sites [321]
γ_{K^+}	Activity coefficient of K^+ [252, 253]
$-(\Gamma/2)$	Nearest-neighbor interaction energy between cardinal adsorbents [222]
δ	Polarity index [187]
δ_{BA}	Polarity index of the bond BA [187]
δ/r	Intensity index [187]

ΔE	Theoretically required minimal energy for the Na^+ pump [123]
ΔE_{K^+}	K^+ concentration potential [255]
ΔF	Free energy of hydrolysis [60]
$\Delta F_{j \rightarrow i}^{00}$	Intrinsic free energy of the j th to i th solute exchange on the adsorption site [208]
$-\Delta F_{\text{Na} \rightarrow \text{K}}^{00}$	Intrinsic free energy of the Na^+ -to- K^+ exchange on the adsorption sites [347]
$-\Delta G^\circ$	Standard (Gibbs) free energy change at pH 7.0 [313]
ΔH	Enthalpy change [59]
$\Delta H'$	Apparent heat of ionization [197]
ΔH_i	Molar enthalpy change in the i th reaction [580]
ΔH^0	Difference in standard enthalpy of the solute in two contiguous phases [172]
$\Delta \bar{\mu}_{\text{Na}}$	Electrochemical potential difference between the intra- and extracellular phases [62]
ΔS	Entropy change [60, 312]
ΔS^0	Difference in standard entropy in two contiguous phases [172]
$\Delta \psi$	Membrane potential [255]
ϵ^*	Complex dielectric constant [293]
ϵ'	Dielectric constant [295]
ϵ''	Dielectric loss [295]
ϵ_1	Dielectric constant [292]
ϵ_2	Dielectric loss [293]
ϵ_∞	Dielectric constant at a frequency of infinity [292]
ϵ_s	Dielectric constant [293]
λ	Ionic conductance [114]
λ_+, λ_-	Ionic conductance of the cation and anion, respectively [114]
μ	Mobility of a cation [22]
	Ionic mobility [114]
μ_1, μ_2	Mobilities of the two species of ions in the solid phase [105]
μ_+, μ_-	Mobilities of cation and anion, respectively [114]

μ_K, μ_A	Mobilities of free cation and anion, respectively [32]
μ^0	Gibbs standard chemical potential [171]
μ_I^0, μ_{II}^0	Standard chemical potentials of a solute in liquid phases I and II, respectively [170]
$\mu_{i(I)}^0, \mu_{i(II)}^0$	Standard chemical potential of the i th solute in liquid phases I and II, respectively [171]
ν_0	Larmor precession frequency in units of hertz [299]
ν_p	Larmor precession frequency [303]
ξ	A parameter representing the ratio of the concentrations of the two solutes in the surrounding medium multiplied by the intrinsic equilibrium constant of their exchange adsorption [208]
ξ_i	Magnitude of change of the i th reaction in muscle contraction [580]
ξ^{ij}	ξ for the i th and j th solutes [321]
ξ_L^{ij}	ξ^{ij} that occurs on the L th type of site [321]
π	Osmotic pressure [11]
π_{KCNS}, π_{NaCl}	Electrical potential differences at the interfaces separating the oil phase and the aqueous phases containing KCNS and NaCl, respectively [24]
$4\pi a/\omega$	A calibration factor [250]
ρ_{eq}	Apparent equilibrium distribution coefficient at final equilibrium level [597]
ρ_j	Reaction constant [184]
ρ_{max}	Apparent distribution coefficient at peak of overshoot [597]
σ	Hammett's constant [191]
σ_i	Empirical constant specific for the i th substituent [184]
τ	Transmissivity constant [323]
	Time constant, equal to the time for the level of a substance or condition to fall to $1/e$ of its initial value, where $e = 2.718$ [404]
τ_c	Correlation time, or rotational correlation time [265, 299]
τ_{c1}	One of the correlation times present in a complex system [265]
τ_{c2}	Another correlation time present in a complex system [265]

τ_d	(Debye) dielectric relaxation time [293]
τ_{BA}	Bond length of the bond BA [187]
ϕ	Factor describing the number of H^+ ions released or taken up in phosphate hydrolyses [312]
Φ	Rate of enzyme activity [201] Intensity or rate of a physiological effect [201] Phase shift or loss angle [292]
ψ	Normal resting potential [22]
ψ_0	Electrical potential measured before salt solution was applied [21]
ψ_{inj}	Diffusion potential at the injured cell surface [22]
ψ_n	Electrical potential measured in the presence of a salt of concentration [p_n] [21]
$\psi_{(t)}$	Resting potential at time t [123]
ω	2π times the frequency in cycles per second (Hz) of an applied AC field [293]
ω_0	Larmor angular frequency [299]
$+ -$ $- +$	Diagrammatic illustration of a quadruple charge distribution [263]

Index

- A23187, 530, 533, 643–647, 650
A bands, 228–240, 539, 541, 549, 552
Absorption spectrum, 721
AC genes, 116, 603
Acetyl-coenzyme, 504
Acid dissociation constants, 195
from the inductive indices, 197
Acid liberation, 649
Actin, 597, 677
filaments, 549
polymerization, 570
profilamentous, 568, 582
state of in resting muscle cells, 568
Action potential, 20, 74, 77, 465–467, 477, 494, 498, 500; *see also* Resting potential
fertilization, 644
Activation, 642
electrical potential changes in, 644
selective ion sensitivity, 644
surface protein change in, 642
Active transport, 64, 585
epithelial tissues and giant algal cells, 64
Activity, ATPase, 118, 557
Activity coefficients of K^+ and Na^+ , 494
Activity of K^+ and Na^+ , ion-specific
microelectrode study, 115
Acto-HMM complex, 558, 574
Acto-S1 complex, 558
Actomyosin, 399, 544
 Ca^{2+} chelator effect on, 560
superprecipitation of Ca^{2+} on, 560
Adenosine diphosphate: *see* ADP
Adenosine triphosphate: *see* ATP
ADP (adenosine diphosphate), 507, 534
Adsorbed K^+ , 549
Adsorbed solutes, control by cardinal adsorbents, 323
Adsorption
Langmuir-type, 607
negative, 84
positive, 85
Adsorption and desorption, cyclic, 591
Adsorption-desorption route, 397, 492
entry of amino acids, 434
Adsorption isotherm
Langmuir, 85
Yang-Ling cooperative, 208
Adsorption of K^+
in living tissue, 347
nearest-neighbor interaction in, 347
simultaneous accumulation of K^+ , Rb^+ , and Na^+ , 353
uniformity of, 347
Adsorption sites
for Cl^- , 447
for Cs^+ , 454
for K^+ , 454
for Rb^+ , 454
surface, 596
AI hypothesis: *see* Association-induction hypothesis
Alanine
accumulation, 431
entry into cells, 431
Alkali-metal ions, 327, 619
All-or-none responses, 213
Allosteric effect, 589
 α (alpha) state, 698
Alphavirus-specified proteins, 626
Alteration theory of cell potential, 20, 41
Amiloride, 649
Amino acid
free, 340
selective distribution, 319

- Amino acid permeation, 428
 dependence on external Na^+
 nonsaturable fractions, 428
 saturable fractions, 428
- ϵ -Amino groups, 93, 403, 445, 606
- ϵ -Amino groups and guanidyl groups, 93
- Ammonium ion, as prototype
 of ϵ -amino groups, 445
 of guanidyl groups, 445
- AMP-PNP, 580
- Amphibian eggs, 331, 636
- Amphibian metamorphosis, 681
- Amphibian oocytes, 637
- Amphotericin B, 456
- Anaerobiosis, 529
- Anchored stem cell, 675
- Animal cells, 660
- Animal electricity, 20
- Animistic (or vitalistic) view, 4
- Anions and cations, mobilities of, 22
- Anoxia, 58
- Antidiuretic hormones, 595
- Antifreeze proteins, 280
- Antimycin A, 506
- Apical (or mucosal) surface, 589
- Aplysia linacina*, 636
- Aquatic habitat, 684
- L-Arabinose, 340
- Arginine phosphate, 503
- Ascites cells, mouse Ehrlich, 398
- Ascorbic acid, 698
- Association, 183
- Association-induction (AI) hypothesis, 145, 147, 183, 317, 548
- Atomic sieve theory, 11, 17, 377
- ATP (adenosine triphosphate), 58, 93, 97, 126, 311–313, 455–459, 489, 503, 513–516, 521, 525, 534, 544, 549, 555, 558, 564, 570, 571, 580, 583, 591, 641
 in biological work performance, 503
 as cardinal adsorbent, 363, 578
 depletion, 455–459, 641
 causes cell swelling, 455–459
 increases Na^+ preference 455–459
 functions as intact adsorbed molecular ion, 97
 inhibits salt linkage formation, 97
 interaction with intracellular proteins, 93
 nonhydrolytic function of, 97
 sources, 503
 transport, 521
- ATP analogues, 580
- ATP binding
 cardinal site, 571
 myosin, 558
- ATP hydrolysis
 enthalpy, 126
 free energy charge, 312
 ΔH , 312, 313
 $-\Delta S$, 312, 313
 $\phi RT \ln H^+$, 312, 313
- ATP regeneration, 591
- ATP synthesis, 503, 513
- ATP synthesis and ion gradient, 513
 role of ATPase, 515, 516
 in chloroplasts, 513
 in erythrocytes, 514
 in sarcoplasmic reticulum, broken SR, 514
- ATPase, 118, 510, 557, 574, 589
- ATPase activity, correlation with ion transport, 118
- ATPase site, 557
- Autocooperative dissociation, 606
- Autocooperative interaction, between surface anionic sites, 481
- Autocooperative ion adsorption, oxidation-reduction control, 520
- Autocooperative linkage, 518
- Autocooperative shift, Na^+ state, 591
- Autocooperative transition
 protein-nucleic acid system, 619
 proteins, 619
- Autocooperativity, 607
 in K^+ uptake, 346
- Backbone NHCO groups, 569
- Barley roots, Rb^+ entry into, 98
- Barth and Barth solution, 654, 657
- Base pairs, 619
- Basolateral (or serosal) surface, 589
- Beggiaota mirabilis*, 17
- Bernstein, J., 21, 541
 membrane theory of, 541
- β State, 698
- Bifacial cells, 585, 586
- Biological work performance: *see* Energy sources
- Bladder, pig, 81
- Blastocysts, 697
- Blastopore, 655
- Blastula, 651, 661
- Blood cells, 665
- Blood, presumptive, 653
- Bohr effect, 519
- Bound K^+ , 46
 significance for electrical potential, 469
- Bound water, 8, 43
 demonstration of, 45
- Bovine serum albumin
 dodecyl sulfate binding, 216
 dodecyltrimethylammonium bromide, 214

- Boyle's law, 12
 Boyle-van't Hoff Law, 12
 Bradley's theory of polarized multilayers, 164
 Brain, 88, 665
 Breakdown of the germinal vesicle, 637, 640, 670
 Bromthymol blue binding, 620
Bryopsis plumosa, 36
 Bulk phase cell water, 569
 Bulk-phase-limited diffusion, 387
 Bulk phase theories, 47–50
 cell water, 48
 bound, 50
 free, 49, 50
 K⁺ free in muscle, 49
- C phase, 673
 c-Value, 155, 158, 161, 330, 496
 calculated association energy, relation to, 158
 definition, 155
 variation with DVB content, 161
 versus salt linkages, 163
 c-Value profile, 596
 Calcium, 265, 337, 362, 365, 525, 570, 582, 583, 638, 639, 645, 646
 binding, 582
 cardinal adsorbent, 362, 367, 570, 583
 distribution, 265, 338, 365
 ATP control, 365
 release, 582, 638, 645, 646
 in medaka, 646
 role of A23187, 645
 cAMP (cyclic AMP), 604
 Cancer, 635, 661, 687, 694–696, 698, 699, 700–703, 708, 710
 and aging, 687
 Cone's theory, 699
 distinctive features, 700
 Damadian generalization, 708
 Greenstein generalization, 701–703
 Ling-Murphy generalization, 708
 morphological generalization, 701
 Roberts-Frankel generalization, 703
 Warburg generalization, 701
 mechanism, apparent paradox, 710
 Szent-Györgyi's theory, 698
 Cancer cells, 694–696
 development into normal mice, 696
 maximally deviated, 708
 transformation into normal tadpoles, 694, 695
 CAP (catabolite gene activator protein), 608
 Capacity current, 74
 Carbon dioxide, 504
 Carbonylhemoglobin, acid titration, 216
 β- and γ-carboxyl groups, 93, 302, 319, 445, 491, 492, 579, 583
 Carcinogenesis, 710
 Carcinogens, 687
 synthetic, 690
 Cardiac glycosides, 358
 as cardinal adsorbents, 358
 Cardiac Purkinje muscle fibers, 480
 Cardinal adsorbents, 220, 323, 525
 Cardinal site, 492
 Carnosine, 88
 Carrier model, 98, 398
 Carriers: *see* Electron carriers
 Cat skin, 605
 Catabolite gene activator protein (CAP), 608
 Cations and anions, mobilities, 22
 CCA (chromosome-condensing activity), 670
 Cell, 5, 7, 585, 586, 660, 665, 675
 anchored stem, 675
 animal, 660
 bifacial, 585, 586
 blood, 88, 665
 egg, 635
 lens, 672
 maximally deviated cancer, 708
 myeloid, 711
 neuroblastoma, 674
 nondividing, 661, 665
 pigment, 659
 Ruffini, 651, 660
 stem, 674–676
 3T3, 663
 hormone control of DNA synthesis in, 663
 teratoma, 691
 vegetal, 660
 Cell cycle, 660
 Cell fusion, 665
 by inactivated Sendai virus, 665
 of differentiated and undifferentiated cells, 665
 Cell K⁺, adsorbed, 475
 Cell membrane, 437
 resistance, 378
 Cell potentials
 general equation, 493
 protoplasmic droplets, 498, 499
 Cell surface, semipermeable, 392
 Cellular electrical potentials, 18, 641
 Cellulose acetate sheets
 active layer, 391
 diameter of pores, 394
 Centrifugation-extractable fluid, 437
 Centrifugation extraction, of extracellular Na⁺, 412
 Centromeres, 637
 Cesium, 328
 replacing K⁺ in frog muscles, 32
 CG electrode: *see* Collodion-coated glass electrode

- Channels
 K^+ , 77
 Na^+ , 77
- Charged pores, 17
- Chemical coupling hypothesis, 507
- Chemical shift, 716
- Chemiosmotic hypothesis, 503, 509
critique of, 511
evidence against, 510
- Chiang and Tai's theory, 185
- Chironomas*, 338, 618
- Chloride
competing for f^+ , 445
permeability of, 33
relation to ψ , 475
- Chloride conductance, higher than K^+
conductance, 463
- Chloride efflux, in KCl-treated muscle, 447, 450–453
- Chloroplasts, 513
- Chromatin, 612
- Chromosomal disorder, 687
- Chromosome condensation, 642
- Chromosome-condensing agent (CCA), 641, 669, 670
- Chromosomes, lamp-brush, 637
- Cilia, 563
- C=O bond, 192
- Coacervates
cells as, 84
engulf solid particles, 42
protoplasm as, 41
- Coal tar, 711
- Coenzyme, 518
- Collagen, phenol binding, 214
- Collodion, 17
fixed ionic sites on, 109
oxidized, 398
- Collodion-coated glass (CG) electrode
insensitivity to divalent ions, 471
polylysine-treated (PCG)
sensitivity to anions, 471
sensitivity to monovalent ions, 470
- Collodion membranes, 17, 22, 25–27, 31
diffusion rate of H^+ , K^+ , and Cl^- through dried, 26
- Michaelis's theory of cation-permeable, 25
mobilities of cations in dried, 26
permeability to H^+ of fully dried, 27
- Colloidal chemistry, 8
- Colloidal condition of matter, 8
- Colloids, 8
- Competence, 617, 652
- Competition, in ion permeability, 100
- Conductivity
in *Aplysia* neurons, 249
in cells, 244
in squid axons, 249
- Cone's theory of cancer, 699
- Conformation coupling hypothesis, 509
- Contact inhibition, 688
- Contractile force, 574
- Contractions, 58, 544, 570
control mechanism, 558
velocity, 574
- Cookson and Wiercinski, observations, 566
- Cooling protects cells against metabolic poisons, 111
- Cooperative adsorption, 480
diagnostic criteria, 213
on proteins, 211
- Cooperative adsorption–desorption model, 588
- Cooperative adsorption isotherm, 208, 220
- Cooperative interaction
basic traits, 222
potential capabilities, 223
- Cooperative shift
due to cardinal adsorbent, 212
due to a change in concentration of adsorbents, 212
nondirectional, 222
- Cooperative states, discrete, control of shifts, 219
- Cooperative transition, 489
- Cooperativity, 345
in controlled and coordinated physiological activities, 204
- Copper ferrocyanide, 9, 10
- Copper ferrocyanide membrane, 17, 22
X-ray studies, 377
- Coupling
ion and water transport, 493
mechanism, 517
between respiratory chain centers and ATPase, 518
- Coupling of transport
between Na^+ and amino acid, 595
between Na^+ and sugar, 595
- Creatine kinase, 59, 504
- Creatine phosphate, 58, 125, 503
- Cross-bridges, 555, 570, 583
formation and breakage, 565
- Cross-correlation, 300
- Cross-linking agent (DVB), 160
- Crown gall teratoma, 694
- Crystalloids, 8
- CSF (cytostatic factor), 641–642, 646
- Cyclic adsorption–desorption model, 595
- Cyclic AMP (cAMP), 604

- Cycloheximide, 620
 Cytochromes, 518, 520
 Cytoplasmic extracts, 665
 Cytoplasmic proteins, 589
 Cytostatic factor (CSF), 641–642, 646
- D-effect, 184
 Damadian generalization, 703
 de Boer and Zwikker's theory, 163
 Brunauer, Emmett, and Teller critique of, 163
 Debye and Hückel theory for very dilute solutions, 113
 Dehydrogenases
 flavin-linked, 506
 NAD-linked, 504
 Demarcation current, 20
 considered as a concentration cell, 21
 Demarcation potential, 20, 22
 Deoxygenated state, 519
 Depolarization swelling, 460
 Determinate C phase, control of entry into, 663
 Dielectric dispersion of water
 of bound water, 293
 of free water, 293
 in ice, 293
 Dielectric saturation, 95
 Differentiation, 635, 650, 660, 671, 710
 Differentiation-inducing agents
 Ca^{2+} , Mg^{2+} , 657
 “intensity” of, 657
 Li^+ , 657
 Na^+ , 659
 sucrose, 657
 Diffusion
 exchange, 63
 facilitated, 398
 ionic, through the membrane, 24
 surface-limited, 387
 Diffusion coefficients
 K^+ , Na^+ , Ca^{2+} , SO_4^{2-} , sorbital, sucrose, ATP, 115
 in muscle cytoplasm, 115
 translational, 715
 Diffusion potential, 21, 22
 Diffusional permeability, 595
 Dimethyl sulfoxide (DMSO), 305, 609, 623
 2,4-Dinitrofluorobenzene (DNFB; Sanger reagent), 504
 Diploid state, 636
 Direct F-effect, 198
 Discrete cooperative states, control of shifts, 219
 Discrete states, 619
 Dissociation of DNA from nuclear proteins, 679
- Dissolved solutes, control by cardinal adsorbents, 326
 Distinctive features of cancer: *See* Cancer
 Distribution, non-Donnan, of permeant solutes, 88
 Divinylbenzene (DVB), as cross-linking agent, 160
 DMSO (dimethyl sulfoxide), 305, 609, 623
 DNA, 603, 619, 665–669
 melting temperature, 609
 replication, 661
 DNA synthesis, 665–669
 control
 by intracellular Na^+ , 669
 by resting potential, 699
 stimulation
 by EGF, 669
 by egg extract, 665–668
 by gramicidin, 699
 by ouabain, 699
 by veratridine, 699
 DNFB (2,4-dinitrofluorobenzene; Sanger reagent), 504
 Donnan membrane equilibrium, 365
 K^+ (and H^+) distribution, 33
 Donnan potential, 465
 Donnan ratio (r), 28, 53
 Donnan system, 32
 Donnan theory, 28, 30
 cell volume, 34
 ion distribution, 56
 resting potential, 34
 Dorsal lip, 652, 655
 Drosophila, 613, 614
 DVB (divinylbenzene), as cross-linking agent, 160
 Dynamic equilibrium, 57
- β -Ecdysone, 614, 615, 620
 EDC (electron-donating cardinal adsorbents), 528
 EDTA (ethylenediaminetetraacetic acid), 638
 Effectively membrane (pump)-less open-ended muscle cell (EMOC), 133
 EGF (epidermal growth factor), 669
 Egg, 635; *see also* Fertilization of eggs; Mosaic eggs; Regulative eggs
 Egg cytoplasmic extracts, 665
 Electrical potential, 30, 463, 644
 fixed-charge theory, 109
 general equation, 493
 of mitochondria *in vitro*, 510, 512
 of mitochondria *in vivo*, 510, 512
 of nucleus *in vivo*, 511
 of protoplasmic droplets, 498, 499
 Electrical resistance, 378

- Electrode
 CG, 470, 471
 glass, 104, 153, 470, 471
 Horovitz studies, 104
 mechanism of, 23
 Electrogenic Na^+ pump, 467, 481
 coupling factor, in 468
 definition by Kernan, 468
 Electromotive molecules, 20
 Electron acceptor, 698
 Electron carriers, 506
 oxidation-reduction states of, 506
 Electron diffraction studies, 11
 of copper ferrocyanide gel, 377
 Electron-donating cardinal adsorbents (EDC), 528
 Electron transport-oxidative phosphorylation system, 504
 Electron-withdrawing cardinal adsorbents (EWC), 528
 Electrostatic repulsive forces, 573
 Elongation of protein chain, 608
 Elsdale's modification of Barth's solution, 679
 Embryoid bodies, 696
 Emission spectrum, 721
 EMOC [effectively membrane (pump-)less open-ended muscle cell], 133
 ouabain-sensitive accumulation of K^+ over Na^+ in, 133
 Encephalomyocarditis virus, 627
 Endosmosis, 9
 Energy, 145, 580
 Energy barrier, 56
 Energy sources, 125
 for active transport, 493
 for biological work performance, 311
 according to the AI hypothesis, 314
 cyclic work performance, 315
 immediate, 314
 in muscle contraction, 578
 Engelmann, T. W., 540
 Enthalpy, distribution of Mg^{2+} , 337
 Entropy
 distribution of Mg^{2+} , 337
 gain during polymerization, 569
 Entry of water, rate-limiting step into living cells, 386
 Enzyme contents, 701
 Epidermal growth factor (EGF), 669
 Epidermis, presumptive, 657
 Epithelia, intestinal, 585
 Equatorial X-ray diagram of live muscle, 553
 Equilibrium, dynamic, 57
 Equilibrium potentials, 465
Escherichia coli, 603
 K^+ accumulation in, 88
 Ethylene glycol, 509
 Ethylenediaminetetraacetic acid (EDTA), 638
 Evocator
 activation of inactive, 656
 primary, 690
 stability to acid, 655
 stability to heat, 655
 EWC (electron-withdrawing cardinal adsorbents), 528
 Exchange diffusion, 63
 evidence against, 126
 Exchange resin: *see* Ion exchange resin
 Excitation, 493-497, 544
 channel inactivation, 497
 evidence of *c*-value change during, 496
 molecular events underlying, 489
 nonspecific permeability increase during, 495
 permeability change during, 493
 transient local swelling in nerves during, 497
 Excitation phenomena, 480
 Exclusion of macromolecules from nuclei, 678
 Exogastrula, 653
 Exogastrulation, 655
 Exosmosis, 9
 Extracellular space, 81
 F-actin, 569, 571
 F-effect, 184, 477
 direct, 198
 indirect, 206
 Facilitated diffusion, 398
 Facilitation of ion entry, 399
 Fate map, 651
 FCCP (*p*-Trifluoromethylcarbonylcyanidephenylhydrazine), 596
 Fermentation, 504
 Fertilization action potential, 644
 Fertilization of eggs, 642
 acid liberation during, 649
 amiloride action in, 649
 role of external Na^+ in, 647, 648
 Fertilized egg, 635
 Fick, A., 651
 Filaments
 tangling, 565
 mechanism preventing, 572
 thick, 522
 thin, 552
 First overtone band, 721
 Fixed amino groups, affinities for anions, 446
 Fixed-charge systems, 148
 labile amphoteric, 96

- Fixed charges, 17
in membranes
 in Meyer and Sievers's theory of ion permeability, 95
on pore walls of model membranes, 95
- Fixed ions
 association with counterions, 95
 surface, and their counterions, electrostatic field, 101
- Fixed negative sites, 588
- Flagella, 563
- Fraunhofer lines, 721
- Free amino acids, 340
 selective distribution, 319
 in normal and cancer tissues, 703, 705
- Free Ca^{2+} distribution, 337, 365, 366
 restricted, 338
- Freezing patterns of water in living cells
 in contracted muscle, 283
 in relaxed muscle, 282
- Freezing points of water, 45, 50, 51, 278, 282
 between AgCl plates, 279
 between glass surfaces, 279
 in blood of antarctic fish, 280
 in gelatin solution, 280
 in PVP solution, 280
- Frog, 587
 muscles, 327, 398
 total heat output of poisoned, 125
 vapor equilibrium, 443
 skin, 387, 588
- Fundamental band, 721
- G_0 cells, 661
- G_0 phase, 662
- G_1 , 661
- G_2 , 661, 673
- $G \rightarrow F$ transformation, 569
- β -Galactosidase, 603
- β -Galactoside
 acetylase, 603
 permease, 603
- Gangs
 of heterogeneous population, 216
 of homogeneous population, 214
- Gastrula, 651, 661
- Gating current, 70, 79
- Gay-Lussac's law, 12
- Gelatin, 17
 reduction of solubility of water for Na_2SO_4 , 84, 85, 175
- Gelatin as NP-NP-NP system, 175
- Gelée vivante, 7
- Gene function, control of, in eukaryotes, 611
- Gene transcription, 613
- Genes
 Y, 371, 603
 Z, 603
- Genetic marker, 694
- Genome, 611
- Germlinal vesicle (GV), 677
 breakdown of (GVBD), 637, 640, 670
- Ghosts; *see also* Red blood cell ghosts
 Freedman method of preparing, 131
 Marchesi-Palade method of preparing, 130
- Giant algal cells, 65, 591
- Giant axons, squid, 67, 120, 121, 127; *see also* Nerve
- Glass electrodes, 104, 153, 470, 471; *see also* Collodion-coated glass electrode
 hard Jena, 23
 soft Thüringer, 23
- Glass membrane, 22
- Glycerol, 609
- Glycine, 340
 accumulation in cells, 431
 K^+ effect, 433
 rate of entry into cells, 431
 K^+ and Na^+ effect, 432
- Glycolysis, 504, 701
 anaerobic, 58
- Glycolytic activities, 701
- Glycoprotein, 644
- Glycosides, 358
- Gonadotropin, 637
- Grace's medium (aged), 622
- Greenstein generalization, 701
- Gregor's theory, 96, 148, 264
- Growth, 635, 661
- Growth factor, epidermal (EGF), 669
- Guanidyl groups, 445, 606
 of arginine residues, 403
- Guinea pig heart muscle, 398
- GV (germlinal vesicle), 677
- GVBD (germlinal vesicle breakdown), 637, 640, 670
- H-bonding, 191; *see also* Hydrogen bonds
- H-bonds: *see* Hydrogen bonds
- Half-time of isotopic exchange, 56
- Halobacterium, 260, 267, 268
- HAM (high-affinity mRNAs), 629
- Hammett's constant, σ
 inductive (I) component, 184
 resonance (R) or mesomeric (M) component, 184
- Hammett's equation, 184
- Haploid, 636

- Heat engine theory, 311, 540
 Heavy meromyosin, 557
 Heme–heme interaction, 519
 Hemoglobin, 520, 588
 binding of oxygen by, 214
 crystals, 193
 influenced by cooperative binding of oxygen, 222
 influenced by 2,3-diphosphoglycerate, 222
 influenced by inositol hexaphosphate, 222
 oxygenated and deoxygenated, 519
 synthesis induced by ouabain, 621
 T and R structure, 519
 Hemolysis, 13, 129
 Heparin sulfate in amphibian induction, 660
 Herpesvirus, 627
 High-affinity mRNAs (HAM), 629
 High-energy phosphate bonds, 59, 503
 concept, 311
 serious doubts, 312
 in ATP, 119
 reassessment, 126
 High-energy resting relaxed state, 578
 High-energy state
 and association of components, 146
 versus equilibrium state, 146
 Hill, A. V., 542
 coefficient, 345, 350
 equation, relation to the Yang–Ling isotherm, 211
 Histones, 611, 681
 binding, cause of nontranscription of DNA, 620
 in gene regulation, 612
 Hodgkin–Huxley theory, 74
 Hodgkin–Katz equation, 65, 66, 464, 699
 Hodgkin–Katz–Goldman equation, 65, 66, 464, 465, 468, 475
 Hofmeister's series, 31
 Holtfreter solution, 654
 Homocellular regulation of cell K^+ and Na^+ , 595
 Homoepithelial Na^+ transport, 595
 Hormones
 antidiuretic, 595
 juvenile, 614, 615, 617
 thyroid, 682
 thyrotropic (TSH), 682
 Hybridization, 621
 Hydration shell, 17
 Hydration water, 305
 Hydrogen atoms, 36, 504
 Hydrogen bonds, 619
 strengths
 influenced by an inductive effect, 190
 influencing α -helical content, 191
 Hydrogen ion, ionic mobility of, 23
 Hydrolases, 682
 Hydrostatic pressure, 694
 Hypertonic medium, 627
 Hypertonic solution, 438
 Hypotheses
 association-induction (AI), 548
 chemical coupling, 507
 chemiosmotic, 503, 509–511
 critique, 511
 evidence against, 510
 conformation coupling, 509
 Ling's fixed-charge, 91
 I-bands, 539
 water in, 566
 I-effect, 184
 Imbibition pressure, 44
 Impedance, transient drastic decrease, 72
 Inactivated Sendai virus, 665
 Inactivation, 77, 497
 Independence principle, violations, 469
 Indeterminate phase (G_0), 662
 Indirect F-effect, 206
 Inducer, 605
 Inducing agents, 657
 Induction theory of G. N. Lewis, 183
 Inductive–associative coupling, 517
 Inductive effect, 193, 655
 functional groups affected, 190
 Inductive index, 186
 Inductive mechanism, 519
 Influx of ions, 397
 Influx profile, 387
 Infrared and Raman spectra, 721–722
 vibrational levels
 fundamentals, 721
 overtones, 721
 Infrared spectra, 721
 of water associated with DNA, 291
 Initiation of RNA polymerase activity, 608
 Injury current and potential, 20
 Insulin as cardinal adsorbent, 367
 Intactness of cell membrane
 not required for swelling, 437, 438
 Interfacial tension, 18
 Intestinal epithelia, 585
 Invertebrates, 635
 125 Iodine-labeled protein, 643
 Ions
 accumulation in mitochondria, affected by ionophores, 526, 528
 association
 experimental models, 150
 theoretical basis, 148, 149
 dissociation energies calculated, 157
 distribution, 323

- Ions (*cont.*)
efflux, 404
profile, 387
standard technique, 405
entry, 265, 399
exchange, 97
fixed
association with one counterion, 95
surface, and their counterions (electrostatic field), 101
gradients, 503
influx, 397
linear model adsorption, 155
mobility, of adsorbed, 243
selective distribution, 319
selectivity ratios, reversal, 159
Ion exchange resin, 113, 261–263
ion permeation into, 102, 398
theories
experimental testing, 152
of Gregor, 95, 148, 264
of Harris and Rice, 95
of Ling, 95, 103, 150
Ionic association, high degree of as the basis for ionic selectivity, 95
Ionic current, 74
Ionic mobility in cells, 244
Ionic permeation
nonsaturable fraction, 397
saturable fraction, 397
Ionophores, 512, 525, 528, 530
 K^+ -specific, 379
Iron-sulfur proteins, 518
Ising model
kinetics of, 423
one-dimensional, 417
Juvenile hormone, 614, 615, 617
Keratinized skin cells, 672
Kidney cells, 672
Kroeger's theory of gene activation control, 617
lac operon, 603
Lactic acid, 539
Lactose operon, 603
LAM (low-affinity mRNAs), 629
LAMMA (laser microprobe mass spectrometric analysis), 237
Lampbrush chromosomes, 637
Landström and Løvtrup solution, 660
Langmuir-type of adsorption, 607
Larmor frequency, 299, 714
Laser microprobe mass spectrometric analysis (LAMMA), 237
Length-tension relation in frog muscle, 556
Lens cells, 672
LFCH: *see* Ling's fixed-charge hypothesis
Light meromyisin, 557
Linear reading theory, 661
Linewidth, 715
broadening, 267
Ling's fixed-charge hypothesis (LFCH), 91, 381
of cell permeability, 99
selective accumulation of K^+ over Na^+ , 94, 95
Lipid membrane analysis, missing water content of, 381
Lipoidal membrane theory, 15, 16, 377
evidence against, 379
Lipoprotein films, 378
Liposomes, 598
Lithium chloride ($LiCl$), 456
Lithium ion (Li^+), 330, 658, 659
Liver, 665
Living state, definition according to the AI hypothesis, 147
Living systems, major components, 147
Lohmann reaction, 59, 504
Long-range attribute, 95
Longitudinal relaxation time, 261, 268, 299–303, 306, 307, 713, 716; *see also* T_1
Low-affinity mRNAs (LAM), 629
Ludwig, Carl, 4, 541
Lung, 672
M phase, 661, 673, 677
MacDonald's theory, 541
McDougall's theory, 541
Macromolecules in nuclei
accumulation, 678
exclusion, 678
Magnesium, 331, 333, 336, 525
enthalpy, distribution of, 337
entropy, distribution of, 337
Magnetic moment, 713
Magnetogyric ratio, 713
Malldifferentiation theory, 690
Malpighian tubule, 592
Marsh factor, 559
Maturation, 636, 637
role of Na^+ , K^+ , 640
Maturation-promoting factor (MPF), 640
Maximally deviated cancer cells, 708
Medaka, 646
Meiosis, 636
Melanophores, 672
Membrane
cell, 437
collodion, 17, 22, 31; *see also* Collodion membranes

- Membrane (*cont.*)

copper ferrocyanide gel, 17, 22

Donnan equilibrium, 33

glass, 22

nuclear, 619, 637

oil, 472, 473

RBC ghosts, 129

resistance, 378

semipermeable, 17, 395
- Membrane permeability; *see also* Permeability

change during action potential, 72

increase of, 22

Nitella, 72

squid giant axon, 72

transient increase, 72
- Membrane pores

sievelike property, 33

size, 33, 394
- Membrane potential, Donnan model, 28; *see also* Potential
- Membrane pump, 53
- Membrane pump theory

Boyle-Conway theory, 53

evidence supporting, 113
- Membrane theory, 12, 18, 699

Bernstein, J., 21, 64, 541

cellular electrical potential, 64, 463

equilibrium, 53

erythrocytes, 53

ionic distribution, 32

Nasonov's opposition, 40
- Membrane vesicles, 128

mechanism of ion diffusion, triplet formation, 399
- Meromyosin

heavy, 557

light, 557
- Mesoderm, inducing power, 653
- Metamorphosis, 682
- Metaphase, 636
- Methylcellulose, 176
- Methylglyoxal (MG), 698
- MGI (macrophage- and granulocyte-inducing) proteins, of myeloid cells, 711
- Microelectrode

 Ca^{2+} -sensitive, 639

glass capillary, Gerard-Graham-Ling (GGL) type, 68

 H^+ -sensitive intracellular, 116

ion-specific, 253-256
- Microspheres

electrical potentials, 498

from proteinoid materials, 385
- Microvilli, 588

isolated, 596
- Migration of proteins

between nucleus and cytoplasm, 676, 677

return to daughter nuclei, 677
- Migration of RNA, 676
- Missing energy in muscle contraction, 580
- Mitochondria

inner membrane, 381

lipid removal, 382

outer membrane, 381
- Mitochondrial physiology, 521
- Mitogenesis, 699
- Mitosis, 661
- Mobility of adsorbed ions, 243
- Molar refraction, 17
- Molecular sieve, 17
- Molecules

electromotive, 20

hydrogen, xxv

myosin, 557
- Molluscs, 635
- Morphological generalization of cancers, 700
- Mosaic eggs, cytoplasm

original difference in, 635

pH gradient in, 636

q-value gradient in, 636
- Mosaic membrane, 16

theory, 17
- Mosaic mice, 696
- Mouse Ehrlich ascites cells, 398
- MPF (maturation-promoting factor), 640
- mRNA, 603, 609

high-affinity, 629

low-affinity, 629

translation, 624, 629-633
- Mucosal or apical surface, 589
- Muscle

activity, acid produced during, 23

contraction, 539, 563

adenosine triphosphate in, 58

A-lactic acid, 57

failure in hypertonic solution, 572

iodoacetic acid effect on, 57

key role of cell water in, 572

lactic acid role in, 57

missing energy, 580

reversible loss of K^+ during, 574

contraction force, source versus osmotic force, 582
- fibers

cardiac Purkinje, 480

permeability and impermeability to ions, 32
- frog, 54, 327, 398

length-tension relation, 556
- guinea pig heart, 398

presumptive, 653

in rigor, 554

- Muskelstrom*, 20
Mutagens, 687
Mutations
 single-point, 710
 somatic, 710
Myeloid cells, macrophage- and granulocyte-inducing (MGI) proteins, 711
Myosin
 ADP binding on, 580
 ATP binding on, 580
 ATPase activity, dependence on Ca^{2+} , 560
 contains enough free β - and γ -carboxyl groups, 94
 filaments, 549
 head, 557
 molecule, 557
 state of in resting muscle cells, 568
- Natori's technique, effect of pCa on skinned muscle fiber, 561
Necturus kidney cells, 592
Negative control, 604
 molecular mechanisms of, 605
Negative Schwankung (negative variation), 20
Negative sites, 588
Nereis dumerilii, 635
Nerve, 497, 659; *see also* Giant axons, squid
Neuroblastoma cells, 675
Neutralization of fixed anionic sites, 93
Newts, 682
NH bond, 192
NHCO groups (backbone), 569
Niche, 675
Nicolsky's glass electrode potential equation, 106
Nicolsky's solute distribution equation, 321
NIH-3T3 cells, 688, 689
Nitella, 6, 53, 591
Niu and Twitty solution, 654
NMR (nuclear magnetic resonance), 257, 267, 298, 307, 715
NMR relaxation times, 715; *see also* T_1 ; T_2
 in living cells, 257
 of $^{39}\text{K}^+$, in living cells and ion exchange resins, 257
 of $^7\text{Li}^+$, $^{39}\text{Rb}^+$, $^{133}\text{Cs}^+$, 267
 of $^{23}\text{Na}^+$, in living cells and ion exchange resins, 257
 of water protons, 298
 in solutions of polyethylene oxide (PEO), polyvinylpyrrolidone (PVP), and polyvinylmethyl ether (PVME), 307
NMR signal
 quadrupolar splitting of Na^+ , 263, 720
 selective modulation, 265
- NMR studies of water
 in living cells, 301
 in solutions of native globular proteins, 301
NMR theories
 Bloembergen-Purcell-Pound, 299, 716, 719
 Kubo-Tomita, 299, 716, 719
 Zimmerman-Brittin, 299
NO, 169
NO-NO-NO, 169
Nondividing cells, 661, 665, 667
Nonsaturable fraction of ions, rapid exchanging fractions, corresponding to, 414
Nonsolvent volume, 44
Notochord tissue, 659
NP-NP-NP system, 169
N-P surfaces, 169
Nuclear fusion, 665
Nuclear magnetic resonance: *see* NMR
Nuclear membrane, 619, 637
Nuclear spin quantum number, 715
Nuclear transplantation
 promotion of differentiation, 671
 of nondividing cells, 672
 of undifferentiated cells, 672
 stimulation of DNA synthesis, 663
 in nondividing cells, 665
 by prostaglandin, 664
Nuclear Zeeman effect, 715
Nucleus, egg, 416
- Oil, 107
layers, 22
 effect of CTAB, 473
 effect of SDS, 473
 as models of cell potential, 472
Oligolysine-polynucleotide interaction, 618
Olive oil/water partition coefficients, 16
Oncogenes, 689
Oncogenesis, 699
One-receptor-site system for competitive interaction, 201
One-way valve in active transport, 589
Oocyte activation
 activation potential
 dependence on Cl^- , 489
 effect of puncturing, 488-490
 dependence on Ca^{2+} , 488, 489
Operator, protein, 117
Ordered bulk phase water, arguments against, 302
Organ physiology, 5
Oscillatory changes
 ATPase-dependent, 589
 synchronous, 534
Osmosis, 9

- Osmotic activity, 438, 570, 619
 increase, 577
- Osmotic behavior of living cells, 83, 442
- Osmotic pressure, 9
- Osmotic water permeability, 595
- Ouabain, 358, 481, 623, 641, 699
- Overshoot, 73, 588, 596
- Overton's lipidal membrane theory, 377, 395, 526
- Overton's rules, 15
- Oxidation of pyruvate, 594
- Oxidation-reduction potential theory of cell electrical potential, 64
- Oxidative phosphorylation, 503
 theories, 507, 517
- Oxidized collodion, 398
- Oxygen accumulation in erythrocytes, 345
- Oxygenated state, 519
- $\sim P$, 59
- p21 protein, 689
- PCC (premature chromosome condensation), 669
- PCG (polylysine-treated collodion-coated glass) electrode, 471
- P_i burst, 558
- pK_a, 402
 substituted ethyl ammonium ion, 197
 substituted n-propionic acid, 197
- Paradox, 404
 in cancer mechanism, 710
- Parchment paper, 10, 17
- Parthenogenetic activation, 642
- Partition coefficient, 24
- Passage numbers, of a membrane, 32
- Paucimolecular theory of cell membrane, 18
- Pentose distribution, 340
- PEO (polyethylene oxide), 176
- Permeability, 72, 377
 charge-selective, Meyer and Sievers's formulation, 31
 Cl⁻, 88
 during excitation
 role of Ca²⁺, 490
 transient increase, 490
 of hydroxylic compounds, 394
 increase, transient, 493
 of ions, 396
 membrane: *see* Membrane permeability selective, 17
 molecular mechanism of, 97
 of water, 394
- Permeability constants, 16
- Permeability rates, 13
- Permeases
 genetic control of, 115
 as insulinlike cardinal adsorbents, 371
 as sugar pumps, 371
- Permeation
 glycine, 329
²⁴Na⁺, 54
 neutral amino acids, 429
- pH gradient, 510, 636
- Phase boundary, 24
- Phlogiston, 4
- Phloridzin, 596
- Phosphate bonds: *see* High-energy phosphate bonds
- Phosphocreatine, 58, 125, 503
- Phylogenetic evolution, 684
- Physiological activities
 control and modulation, 200
 inductive effect in, 183
 molecular mechanism for, 198
- Physiological theories of cancer
 Cone's theory, 699
 Szent-Györgyi's theory, 698
- Picornavirus, 626
- Pig bladder, 17
- Pigment cells, 639
- Plasma membrane, 13, 15
- Plasmolysis, 13
- Plasticizing action, 578, 579
- PO, 169
- PO-PO-PO system, 169
- Polarity index (δ), 185
- Polarization theory, Hoover and Mellon's application, 164
- Polarized multilayer theory of cell water, 305, 396
 solvent properties of water, 272
 testing in model systems, 172
- Polarized multilayer theory of de Boer and Zwicker, 163
- Polarized multilayers of water molecules, effect of charge site distribution on stability of, 168
- Polarized water, 438
 as semipermeable, selective permeability barrier, 391
- Polyethylene oxide (PEO), 176
- Polylysine-treated collodion-coated glass (PCG) electrode, 471
- Polymethacrylate, polystyrene sulfonate, 149
- Polytene chromosomes, 613
- Polyvinylmethylether (PVME), 176
- Polyvinylpyrrolidone (PVP)
 high water adsorption, 176
 as NO-NO-NO systems, 176
- Popcorn model of K⁺, Na⁺ permeation, 407
- Pores, 16
 charged, 17
 negatively charged, 33
- Porphyropsin, 682
- Positive control of gene transcription, 605
 molecular mechanisms of, 608

- Potassium
 accumulation, 526
 failure to demonstrate, in squid axon membrane sac, 127
 in muscle, activity coefficient of, 252
activity in cells, 250
adsorbing sites of, 492
adsorption, 437, 574
 autocooperative, 607
 implications, 238
 muscle, 288
content, 610
desorption, 574
diffusion
 in muscle, 114, 245
 in squid axon, 114, 242
distribution, 33
efflux, dependence on external K⁺ concentration, 407
homocellular regulation, 595
influx, Na⁺ efflux coupling to, 417
liberation, 570, 574
 in living cells, 345
mobility
 in frog muscle cells, 245
 in giant axon of cuttlefish, 113
 in living cells, 242
 relation to diffusion coefficient, 114
physical state in living cells, 227
release, 577
smaller than (hydrated), 33
state of, 569
in synthesis of
 DNA, 624
 protein, 624
 RNA, 624
volume regulation, 33
X-ray absorption edge fine structure, 241
Potassium- and Na⁺-activated ATPases, ionic pumps as, 128
Potassium channels, Armstrong's model, 79
Potassium chloride, 544, 605
 differential effect on DNA transcription, 608
Potassium electrode, 492
Potassium gate (Na⁺ gates), opening and closing, 468
Potassium ion, 624
Potassium localization, 228
 autoradiographic demonstration, 231
 electron microscopic demonstration, 230
 by LAMMA, 237
 by X-ray microprobe analysis, 235
Potassium permeability, 33
 of frog egg, no effect of K⁺ ionophore on, 380
 of frog muscle, no effect of K⁺ ionophore on, 380
- Potassium permeability (*cont.*)
 of mitochondrial membrane, no effect of valinomycin on, 380
 of red cell membrane, effect of K⁺ ionophore on, 380
 of squid axon membrane, no effect of monactin on, 380
Potassium-precipitating reagent sodium coboltinitrite, 228
Potassium reagent, 229
Potassium-specific microelectrode, 618
Potential; *see also* Action potential; Electrical potential; Resting potential; Surface potential
 cellular electrical, 18, 641
Donnan, 465
electrical, 463, 644
equilibrium, 465
fertilization action, 644
Potential and permeability, relation between, 27
Potential energy, 539
Precipitation membrane, 10
Preexistence theory, 20
Premature chromosome condensation (PCC), 669
Presumptive blood, 653
Presumptive epidermis, 657
Presumptive muscle, 653
Primary evocators, 690
Primary organizer, 652, 653
Primers for sugar accumulation, steric requirements, 371
Profilamentous actin, 568, 582
Progesterone, 637, 638
Prokaryotes, 611
 translation and transcription in, 603
Prolactin, 682
Promoter, 603
Pronephros, 653, 655
Pronucleus, 637
Propagated inductive effect, 206
1,3-Propanediol, 609
Prophase, 636
Protein
 antifreeze, 280
 catabolite gene activator (CAP), 604
 cytoplasmic, 589
 ¹²⁵I-labeled, 643
 repressor, 605
 SDS-denatured, 177
 surface, 605
 release, 645
 urea-denatured, 177
Protein hydration
 Jordan-Lloyd's theory of, 165
 Pauling's theory of, 165
 resolution of a paradox in, 166

- Protein synthesis, 624
 control of, 603
 Proton gradient, 510
 Protomotive force, 510
 Proto-oncogenes, 689
 Protoplasm, 6, 7, 592
 Bütschli's foam theory, 38
 Flemming's fibrillar theory, 38
 isolated, 37
 living state, 147
 naked, osmotic activity of, 36
 structural substance, 36
 Protoplasm doctrine, 8
 Protoplasmic droplets, swelling and shrinkage, 36
 Puffing, 613
 heat-shock-induced, 619, 620
 poison-induced, 620
 Pumping mechanism, 591
 Pumps, 585
 Puromycin, 620
 PVME (polyvinylmethylether), 176
 PVP (polyvinylpyrrolidone)
 high water adsorption, 176
 as NO-NO-NO-system, 176
 Pyridine nucleotide, 518
 Pyruvate oxidation, 594
- q*, 442
 q_K , 331, 494
 q_{Na} , 331, 494
q-value, 319, 340, 636, 678
 for Ca^{2+} , 365
 definition, 170
 determinations
 enthalpy mechanism, 171
 entropy mechanism, 171
 for pentoses in cancer cells, 708, 709
 relation to molecular size, 172
- Quadrupolar effect, 261
 Quadrupolar moment, 715
 Quasielastic neutron scattering
 in brine shrimp cysts, 309
 in 36% PEO, 309
- Quellungsdruck*
 of dried gelatin, 44
 of dried pig's bladder, 44
 of seed of plant, *Xanthium glabratum*, 44
- Quellungswasser*, 44
- Radioautograph, $^{22}Na^+$, 416
 Raman spectra, 721–722; *see also* Infrared and
 Raman spectra of water associated with
 DNA, 291
 Rate of ion entry into ion exchange resin, 265
 Rate of Na^+ efflux at 0°C in poisoned muscle, 123
- Reactivity of sulphydryl groups, 519
 Receptor site, for valinomycin, 528
 Red blood cell ghosts, 128
 are solid, 129
 ATP-induced ^{86}Rb uptake, 129
 correlation between net K^+ uptake and dry solid
 content, 132
 Na^+ extrusion and K^+ accumulation, 129
 Red blood cells, 88
 Reduction division, 636
 Reference phase, 331
 Regulation mechanism of muscle contraction, 562
 Regulative eggs, 635, 661, 674
 Reinitiation of DNA transcription, 608
 Relation between external Cl^- and ψ , 475
 Relaxation of muscle, 544, 571
 Relaxation times of water proton, multiple
 fractions, 304
 Relaxed (R) structure of hemoglobin, 519
 Replication "eyes", 666, 667
 Replication of DNA, 667
 Repressor, 604
 inactivation, 117
 Repressor protein, 605
 Resin: *see* Ion exchange resin
 Resistance of cell membranes, 378
 Respiration, 518, 529
 State 3, 507
 State 5, 507
 Respiratory chain, 504
 Respiratory control, 507
 Resting and action potential
 molecular mechanisms, 477
 new equation, 477
 confirmation, 478
 Resting potential, 22, 323, 639, 699
 as Cl^- potential in erythrocytes, 465
 Edelmann's experiment, 473
 as equilibrium potential, 465
 control, cardinal adsorbents, 481
 dependence on absolute temperature, 68
 external K^+ concentration, 69
 intracellular K^+ concentration, 69
- of frog muscle
 in adrenaline, 484, 485
 in azide, 484
 as K^+ potential, 465
 at low external K^+ , 478–480
 in ouabain, 483
- historical models: glass, oil, and collodion, 104
 indifference to Cl^- , 463
 lack of, in *Fundulus* eggs, 466, 467
 of oocytes
 dependence on Ca^{2+} , 485, 487
 dependence on Mg^{2+} , 487
 dependence on $[K^+]_{ex}$, 484

- Resting potential (*cont.*)
 relation to intracellular K^+ , 465, 466
 relation to intracellular Na^+ , 466
 role of new interface, 475
 surface adsorption theory of, 104
- Resting state
 general concept, 147
 models of, 147
- Retina, 88
- Reversible loss of K^+ from contracting muscle, 76
- ρ -value
 definition, 170
 for D-glucose, L-alanine, and L-lactate, 597
 for Na_2SO_4 and Na-citrate
 in gelatin, 174, 176
 in native globular protein, 174
 in PEO, PVP, MC, 174, 176
 in SDS-denatured protein, 177
 in urea-denatured protein, 178
 for urea, 177
- Rhodnius*, 592
- Rhodopsin, 682
- Rigid (T) structure of hemoglobin, 519
- RNA: *see* Translation control
- RNA polymerase, 605, 608, 620
- Roberts-Frankel generalization of cancer, 703
- Rotation correlation time (τ_c), 299, 716
- Rubidium, 328
 inhibits K^+ permeation, 103, 398
 NMR relaxation times, 260
 permeation into cells, 100
 facilitated by K^+ , 399
 permeation into models, 401
 replaces K^+ in cells, 32, 233, 265, 328, 331, 354
- Ruffini cells, 651, 660
- S phase, 661
- Salamanders, 682
- Salivary glands, 614
 cells, 338
Drosophila, 620
- Salt linkages, 454, 579, 641
 dissociation
 in KCl-induced cell swelling, 445
 in mitochondrial swelling, 524, 530
 by NaCl in swelling of injured cells, 455
 in nerve swelling during action potential, 497
 in oscillating mitochondrial swelling and
 shrinkage, 536
- formation
 as cause for K^+ liberation, 548, 574
 to form cross-bridges, 574
 in muscle contraction, 547, 570
 relation to ATP level, 93, 548
 prevent K^+ , Na^+ adsorption in protein, 93, 163
 versus c -value, 163
- Saltatory route, 397
- Sanger reagent (2,4-dinitrofluorobenzene; DNFB), 504
- Sarcode, 7
- Sarcolemma, 416
- Sarcoplasmic reticulum, 416, 558, 559
- Saturable fraction of ion efflux, 430
 slowly exchanging fraction, corresponding to, 414
- Saxitoxin, 79
- Scatchard plot, 214
 binding of K^+ on the Na^+, K^+ -activated ATPase, 216
- Second overtone band, 721
- Selective ionic permeability, 17
 molecular mechanisms of, 97, 398, 402
- Semipermeability, 11, 377
- Semipermeable cell surface, 392
- Semipermeable membranes, 17
 models, 395
- Sendai virus, inactivated, 665
- Serosal (or basolateral) surface, 589
- Serum, promoting differentiation, 673
- SH reactivity
 influenced by oxygenation, 519
 influenced by urea, 200
- Sheep's wool, 398
 ion permeation into, 102
- Shrinkage, 437; *see also* Salt linkages
- Shut-off phenomenon
 role of K^+ , Na^+ , 626-628
 theory of Carrasco and Smith, 626
- Sindbis virus, 628
- Single-point mutation, 710
- Site
 cardinal, 492
 definition, 213
 receptor for valinomycin, 528
 surface adsorption, 596
- Skin, 672
 frog, 587, 588
 potential, 587
- Skinned muscle fiber
 effect of pCa, 561
 Natori's, 561
- Sliding filament model, 555, 583
- Sodium, 319, 330, 333, 647
 adsorption, evidence for in muscle cells, 257-265, 267
- efflux
 cardiac glycoside effect on, 418
 coupling to inward K^+ pumping, 120
 in dying muscles, 412
 nonpumping mechanisms, 126
 in poisoned muscles at 0°C, 91
 K^+ influx, coupling to, 417

- Sodium
 efflux (*cont.*)
 rate, 124
 rate-limiting steps, fast fractions, 411
 single muscle fibers, 412
 $t_{1/2}$, 62
 Sodium channels, 77
 Hille's model, 79
 Sodium gates, 77
 opening and closing, 468
 Sodium gradient hypothesis of active transport
 of amino acids, 588
 of sugars, 588
 Sodium- and K^+ -activated ATPase, 588
 Sodium pump, 617
 Conway's version, 64
 electrogenic, 467
 coupling factor in, 468
 definition by Kernan, 468
 energy
 balance sheet in frog sartorius muscles, 124
 consumption, 63
 insufficiency, 45, 122
 requirement, 64
 theory, evidence in support of, 64
 Solute
 accumulation, 84
 adsorption, 345
 dissolved, control by cardinal adsorbents, 326
 distribution, 585
 control by cardinal adsorbents, 358
 equation, 321
 general theory, 319
 temperature, 353
 exclusion, 84
 Solvent properties of water
 in biopolymers and viruses, 275
 in living cells, 277
 in polymer PVME, 273
 in silica gel, 273
 in sulfonate ion exchange resin, 272
 Somatic mutations, 710
 Sorption of water in living cells
 comparison with DNA, 287
 comparison with gelatin, 287, 288
 comparison with ion exchange resin, 288
 Sorption theory of Troshin, 319
 Source of energy
 for active transport, 593
 for cyclic work performance, 315
 immediate, 314
 in muscle contraction, 578
 Spawning, 684
 Spin diffusion, 300
 Spin-lattice relaxation time (T_1), 716
 Spin-spin relaxation time (T_2), 716
Spirogyra, 53
 SR, 560, 570
 Standing osmotic gradient theory, 588
 States
 discrete, 519
 discrete cooperative control of shifts between,
 219
 Stem cells, 674–676
 Steric blocking theory, 579
 Stimulation, 577
 Subfragments 1 and 2, 557
 Sugar
 distribution, 71
 permeation, control by insulin, 426
 selective distribution, 319
 test for adsorption, 338
 Sugar alcohols, test for adsorption, 338
 Sulfhydryl groups, reactivity, 519
 Superprecipitation of actomyosin, 544
 Ca^{2+} chelator effect on, 560
 Ca^{2+} effect on, 560
 Surface adsorption sites, 596
 Surface adsorption theory of cellular resting
 potentials, evidence, 470
 Surface anionic sites in frog muscle, nature of,
 402
 Surface cationic sites in erythrocytes, 403
 Surface-limited diffusion, 387
 Surface potential
 of *Nitella* protoplasm, 476
 no sensitivity to external Mg^{2+} , 492
 sensitivity to Cl^- , 492
 Surface proteins, 642
 release, 645
 Surface tension, 18
 Swelling, 18, 437
 acid-induced
 characteristics, 30
 Boyle and Conway's theory of, 33
 depressing effect of neutral salts, 30, 39
 desorptive (Type 3), 460
 dissociative (Type 2), 460
 of dying cells, 455
 role of Cl^- , 456
 role of Li^+ , 456
 role of Na^+ , 456–458
 fibrin, 39
 of frog muscle
 in KCl , 433, 446
 gelatin, 39
 gelatin gel and collagen, 29
 Loeb's studies of, 30
 of nucleus during DNA synthesis, 679
 osmotic (Type 1), 460

- Swelling (cont.)**
- and shrinkage
 - role of ATP, 521
 - role of Ca^{2+} , Mg^{2+} , 523
 - theory of Procter and Wilson, 29
- Swelling pressure**, 44
- Synchronous oscillatory changes**, 534
- Synthetic carcinogens**, 690
- Szent-Györgyi's theory of cancer**, 698
- T_1** , 716; *see also* Longitudinal or Spin-lattice relaxation time
 - of the water proton, 703, 706
- T_2** , 717, 719; *see also* Transverse or Spin-spin relaxation time
 - of the water proton, 703, 706
- T_3 (3,3,5-triiodo-L-thyronine)**, 682
- 3T3 cells**, 663
 - hormone control of DNA synthesis in, 663
- Taft's equation**, 185
- Tail resorption**, induction by T_3 , 682, 683
- Tangling of filaments**, 565
 - mechanism preventing, 572
- Telophase**, 637
- Temperature**
 - effect on solute distribution, 326
 - transition in solvent properties of cell water, 357
- Teratocarcinomas**, 696
- Teratoma cells**, 691
- Termination of DNA transcription**, 608
- Tetanus**, 582
- Tetrodotoxin**, 79
- Theory**
 - Bernstein's membrane theory, 21, 64, 541
 - Boyle and Conway's theory, 53
 - Bradley's theory of polarized multilayers of dipolar gases, 164
 - Bütschli's foam theory, 38
 - cancer
 - Cone's theory, 699
 - mal differentiation theory, 690
 - somatic mutation theory, 687
 - Szent-Györgyi's theory, 698
 - Carrasco and Smith's theory, 626
 - Chiang and Tai's theory, 185
 - Clark's theory of drug action, 201
 - deBoer and Zwikker's polarized multilayer theory, 163
 - Debye and Hückel's theory, 113
 - fixed-charge theory, 109
 - Flemming's fibrillar theory, 38
 - Gregor's theory, 96
 - heat engine theory, 311
 - Hermann's theory, 41
 - Hodgkin and Huxley's theory, 74
- Theory (cont.)**
- Jordan-Lloyd's theory of protein hydration sites, 165
 - Kroeger's theory of ionic control, 617
 - Lewis's induction theory, 183
 - linear reading theory, 661
 - lipoidal membrane theory, 379
 - Michaelis and Menten's theory of enzyme action, 201
 - mosaic theory, 17
 - muscle contraction
 - actin-myosin association theory, 543
 - active relaxation theory, 545
 - association-induction theory
 - early, 546
 - updated, 566
 - electrostatic hydrolic theory, 564
 - electrostatic theory, 564
 - heat engine theory, 540
 - lactic acid theory, 541
 - osmotic theory, 541
 - NMR
 - Bloembergen-Purcell-Pound theory, 299
 - Kubo-Tomita theory, 299
 - Zimmerman-Brittin theory, 299
 - Pauling's polar side chain theory, 165
 - pericellular pump theory, 588
 - polarization theory, Hoover and Mellon's
 - application to adsorption of water vapor by polymers, 164
 - preexistence theory, 20
 - Procter-Wilson theory, 29
 - sliding filament theory, 555
 - Sponsler-Bath-Ellis theory of hydration, 165
 - standing osmotic gradient theory, 588
 - steric blocking theory, 579
 - surface adsorption theory, 470
 - Troshin's sorption theory, 319
 - two-membrane theory, 586
 - zwitterion theory, 17
 - Thick filaments, 552
 - Thin filaments, 552
 - Thiol reagents, 533
 - Threshold, 213
 - Thyroid hormones, 682
 - Thyrotropic hormone (TSH), 682
 - L-Thyroxine, 682
 - Toad bladder epithelium, 456
 - Tobacco mosaic virus, 573
 - Tobacco plants, 691
 - Tonoplast, 13, 54
 - Total heat output, poisoned frog muscles, 125
 - Totipotency, 651
 - Transcription, 604
 - ionic control, Kroeger's theory of, 617

- Transepithelial transport, 596
 Transition probability model, 662
 Translation control
 of host cell RNA, 625
 of viral RNA, 625
 Translation of mRNA
 in cell-free system, 630
 role of K^+ , Mg^{+} , 630–633
 in development of surf clam, 629
 Translation versus transcription in prokaryotes, 603
 Translational diffusion coefficient, 715
 Transmissivity constant, 323
 Transmissivity factor, 189
 Transplantation, classical experiment of Spemann, 652
 Transport
 amino acid, 588
 sugar, 588
 transepithelial, 596
 Transverse relaxation time: *see* Spin–spin relaxation time
 Tricarboxylic acid cycle, 504
 p -Trifluoromethylcarbonylcyanidephenylhydrazine (FCCP), 596
 3,3,5-Triiodo-L-thyronine (T_3), 682
 Triplet mechanism, 389
 of ion diffusion, 249
 of ion permeation, 402
 Tropomyosin, 561, 583
 Troponin, 561, 583
 binds Ca^{2+} , 561
 subunits, 562
 Troshin equation, 85
 TSH (thyrotropic hormone), 682
 Two-membrane theory, 586
 Two-receptor-site system for noncompetitive facilitation and inhibition, 203
 Ubiquinone, 518
 Uncouplers, 525, 528, 530
 Unifacial, 585
 Unmasking, 605
 Urea
 activates functional groups in proteins, 193
 activates simple (monomeric) amino acids, 193
 in muscle cell, 227
 Urodeles, 682
Urschleim, 6, 7
 Vacuolization, in coacervates, 42
 Valinomycin, 489, 630, 698
 affecting mitochondrial potential, 511
 as cardinal adsorbent, 513
 and mitochondrial permeability, 512, 513
 uncoupler, 510
Valonia, 585
 van't Hoff equation, 442
 Vapor equilibrium of frog muscles, 443
 Vapor sorption isotherms of water
 in frog muscle, 289
 in gelatin, 286, 288
 in ion exchange resin, 288
 in living protoplasm, 286
 in solution of albumin, 286
 in solution of DNA, 287
 in solution of hemoglobin, 286
 Vegetal cells, 660
 Vegetal pole, 638
 Veratridine, 699
 Vibration–rotation bands, 719
 Virus
 herpes, 627
 Sendai inactivated, 665
 Sindbis, 628
 tobacco mosaic, 573
 Vitalistic or animistic view, 4
 Voltage clamp method, 74
 Volume control, 437
 Volume regulation, 441
 Warburg generalization of cancer, 701
 Water, 568
 activity, lowering, 439
 association, 163
 intracellular macromolecules, 271
 with monomeric tubulin, 569
 osmotic activity change with tubulin polymerization, 569
 bound, 8, 43
 demonstration of 45
 drive, 684
 entry, rate-limiting step into living cells, 386
 freezing patterns in living cells
 contracted muscle, 283
 relaxed muscle, 282
 freezing points
 between AgCl plates, 279
 in gelatin solution, 280
 between glass surfaces, 279
 in PVP solution, 280
 hydration, 305
 liberation, 572
 in living cells, physical state, 271
 molecules, released during polymerization, 569
 osmotically inactive, 443
 polarized, 438, 610
 semipermeable, selective permeability barrier, 391
 polarized multilayer theory, 167
 polarized multilayers, 573, 591
 relaxation times, multiple fractions, 304

- Water (*cont.*)
in solutions of denatured protein, 178
solvent properties
in biopolymers and viruses, 275
in living cells, 277
in silica gel, 273
in sulfonate ion exchange resin, 272
sorption, in agreement with Bradley adsorption isotherm
in gelatin, 288
in ion exchange resin, 288
in living muscle, 289
sorption, in living cells
comparison with DNA, 287
comparison with gelatin, 287, 288
comparison with ion exchange resin, 288
state of in resting muscle cells, 568
vapor sorption isotherms, 283
- Wave numbers, 719
- Weber-Edsall solution, 539
- Work, osmotic, 59
- Worms, 635
- X ray, 11
equatorial diagram of living frog sartorius muscle, 553
X-ray absorption edge fine structure of K⁺, 241
X-ray diffraction pattern of muscle, 554
X-ray microprobe analyses, 416
X-ray studies of the copper ferrocyanide gel membrane, 377
Xenopus oocyte, 638
L-Xylose, 340
- Y gene, 371, 603
Yang-Ling cooperative adsorption isotherm, 208
relation to Hill equation, 211
- Yeast, 398
- Z gene, 603
Zeeman effect, 713
Zwitterion theory, 17

